ISSN 0021-9673

UBLISHED
VEEKLY

VOL. 239 APRIL 30, 1982
COMPLETE IN ONE ISSUE

Advances in Chromatography 1982
Las Vegas, NV, April 5–8, 1982
and Tokyo, April 15–18, 1982

JOURNAL OF CHROMATOGRAPHY

INTERNATIONAL JOURNAL ON CHROMATOGRAPHY, ELECTROPHORESIS AND RELATED METHODS

ELSEVIER SCIENTIFIC PUBLISHING COMPANY
AMSTERDAM

JOURNAL OF CHROMATOGRAPHY

Scope. The *Journal of Chromatography* publishes papers on all aspects of chromatography, electrophoresis and related methods. Contributions consist mainly of research papers dealing with chromatographic theory, instrumental development and their applications. The section *Biomedical Applications,* which is under separate editorship, deals with the following aspects: developments in and applications of chromatographic and electrophoretic techniques related to clinical diagnosis (including the publication of normal values); screening and profiling procedures with special reference to metabolic disorders; results from basic medical research with direct consequences in clinical practice; combinations of chromatographic and electrophoretic methods with other physicochemical techniques such as mass spectrometry. In *Chromatographic Reviews,* reviews on all aspects of chromatography, electrophoresis and related methods are published.

Submission of Papers. Papers in English, French and German may be submitted, in three copies. Manuscripts should be submitted to: The Editor of *Journal of Chromatography,* P.O. Box 681, 1000 AR Amsterdam, The Netherlands, or to: The Editor of *Journal of Chromatography, Biomedical Applications,* P.O. Box 681, 1000 AR Amsterdam, The Netherlands. Review articles are invited or proposed by letter to the Editors and will appear in *Chromatographic Reviews* or *Biomedical Applications*. An outline of the proposed review should first be forwarded to the Editors for preliminary discussion prior to preparation. Submission of an article is understood to imply that the article is original and unpublished and is not being considered for publication elsewhere. For copyright regulations, see below.

Subscription Orders. Subscription orders should be sent to: Elsevier Scientific Publishing Company, P.O. Box 211, 1000 AE Amsterdam, The Netherlands. The *Journal of Chromatography* and the *Biomedical Applications* section can be subscribed to separately.

Publication. The *Journal of Chromatography* (incl. *Biomedical Applications, Chromatographic Reviews* and *Cumulative Author and Subject Indexes, Vols. 221–230, 231–240* and *241–250*) has 25 volumes in 1982. The subscription prices for 1982 are:

J. Chromatogr. (incl. *Chromatogr. Rev.* and *Cum. Indexes Vols. 221–230, 231–240 and 241–250*) + *Biomed. Appl.* (Vols. 227–251):
Dfl. 3625.00 plus Dfl. 500.00 (postage) (total *ca.* US$ 1650.00)

J. Chromatogr. (incl. *Chromatogr. Rev.* and *Cum. Indexes Vols. 231–240* and *241–250*) only (Vols. 234–251):
Dfl. 2826.00 plus Dfl. 360.00 (postage) (total *ca.* US$ 1274.50)

Biomed. Appl. (incl. *Cum. Indexes Vols. 221–230*) only (Vols 227–233):
Dfl. 1050.00 plus Dfl. 140.00 (postage) (total *ca.* US$ 476.00).

Journals are automatically sent by airmail to the U.S.A. and Canada at no extra costs, and to Japan, Australia and New Zealand, with a small additional postal charge. Back volumes of the *Journal of Chromatography* (Vols. 1 through 226) are available at Dfl. 173.00 (plus postage). Claims for issues not received should be made within three months of publication of the issue. If not, they cannot be honoured free of charge. For customers in the U.S.A. and Canada, wishing additional bibliographic information on this and other Elsevier journals, please contact Elsevier Science Publishing Company Inc., Journal Information Center, 52 Vanderbilt Avenue, New York, NY 10017. Tel: (212) 867-9040.

Abstracts/Contents Lists published in Analytical Abstracts, Biochemical Abstracts, Biological Abstracts, Chemical Abstracts, Chemical Titles, Current Contents/Physical, Chemical & Earth Sciences, Current Contents/Life Sciences, Index Medicus, Mass Spectrometry Bulletin, and Science Citation Index.

See page 3 of cover for Publication Schedule, Information for Authors, and information on the News Section and Advertisements.

Printed in The Netherlands

For contents see p. VII

Reagents

MERCK

TLC pre-coated plates and HPTLC pre-coated plates for nano-TLC

Greater sharpness of separation

Higher number of samples per plate through smaller applied volumes

Shorter analysis times

Higher sensitivity

Achievement of hitherto unattainable reproducibilities

Please ask for our special brochure

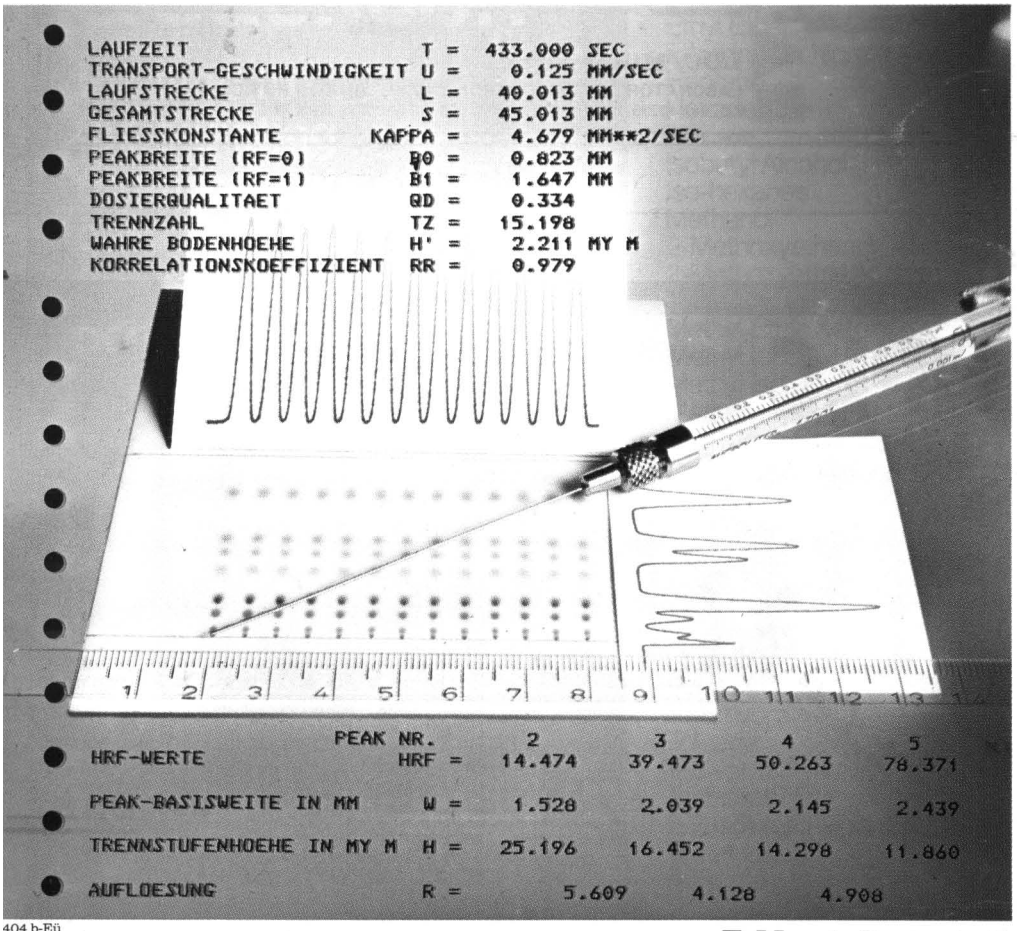

404 b-Eü

E. Merck, Darmstadt
Federal Republic of Germany

SIEMENS

New horizons in GC

You would welcome a step forward in GC? We give you 6!

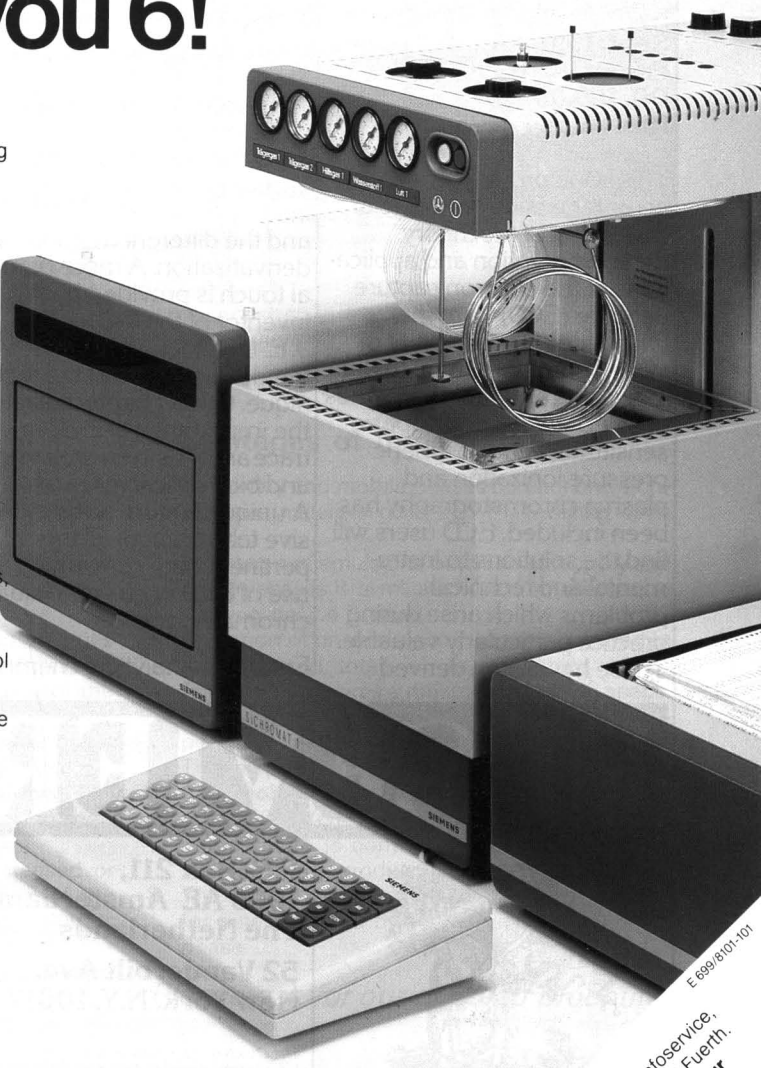

More, analyses, higher demands, new tasks call for analysis equipment offering greater speed, accuracy and flexibility.

The Siemens SiCHROMAT® meets these demands – a gas chromatograph that has been recast in every detail to give you these vital advantages:

1) free access to the oven from three sides through self-adjusting, fully lowerable mantle – an original, exclusive concept
2) shorter analysis times, better detection limits through valveless column switching on the "live" principle
3) great flexibility through the modular design of 3 injectors and 5 detectors, suitable for all columns
4) dynamic range through 9 orders of magnitude by microprocessor control and evaluation
5) two analysis chambers in one device with the twin-oven version
6) automatic feed-in of up to 200 samples with the new Autosampler 200.

For a detailed description of these decisive features of the new Siemens SiCHROMAT, ask for our 24-page brochure now.

Easier handling, greater speed and precision with the Siemens SiCHROMAT

E 699/8101-101

To: Siemens AG, Infoservice,
Postfach 156, D-8510 Fuerth.
Please send me your 24-page SiCHROMAT brochure
1234

Electron Capture – Theory and Practice in Chromatography

edited by A. ZLATKIS, *Houston, TX, USA and* C.F. POOLE, *Detroit, MI, USA*

JOURNAL OF CHROMATOGRAPHY LIBRARY – Volume 20

Sept. 1981 xii + 418 pages
Price: US $76.50/
Dfl. 180.00
ISBN 0-444-41954-3

This book provides the first comprehensive coverage of all aspects of the theory, design, operation and applications of the electron capture detector (ECD) from the chromatographer's point of view. In addition, an up-to-date look at the ancillary techniques of selective electron-capture sensitization, atmospheric pressure ionization and plasma chromatography has been included. ECD users will find the solutions to instrumental and technical problems which arise during practice particularly valuable. These have been derived from the experiences of the internationally distinguished team of authors.

Each chapter has been prepared by experts in their field and provides an in-depth coverage of its topic. The basic theory of the mechanisms of electron capture detection is included. Practical sections form the bulk of the book and are devoted to such topics as the construction and operating principles of the detector, including the establishment of instrument design criteria, and the different methods of derivatization. A more personal touch is provided by the inventor of the ECD, J.E. Lovelock, in his review of the development of the technique. Other chapters illustrate the importance of ECD in trace analysis in environmental and biomedical research. A unique feature is the extensive tabulation of all the pertinent data concerning the use of ECD in gas and liquid chromatography.

For those analytical chemists who use chromatography in their research, this book should become a standard text.

CONTENTS: Chapter 1. The electron-capture detector – A personal odyssey *(J.E. Lovelock)*. 2. The design and operation of the electron-capture detector *(C.F. Poole and A. Zlatkis)*. 3. Theory of electron capture *(W.E. Wentworth and E.C.M. Chen)*. 4. Selective electron-capture sensitization *(F.C. Fehsenfeld, P.D. Goldan, M.P. Phillips and R.E. Sievers)*. 5. Oxygen-doping of the carrier gas in electron-capture detection *(E.P. Grimsrud)*. 6. Wide-range calibration of electron-capture detectors *(R.E. Kaiser and R.I. Rieder)*. 7. Response of the electron-capture detector to compounds with natural electrophores *(J. Vessman)*. 8. Sensitive derivatives for the determination of organic compounds by electron-capture gas chromatography *(C.F. Poole and A. Zlatkis)*. 9. The detection of inorganic and organometallic compounds by electron-capture gas chromatography *(C.F. Poole and A. Zlatkis)*. 10. Environmental applications of the electron-capture detector – pesticides *(W.P. Cochrane and R.B. Maybury)*. 11. Environmental applications of the electron-capture detector – dioxins *(F. Bruner)*. 12. The electron-capture detector as a monitor of halocarbons in the atmosphere *(P.G. Simmonds)*. 13. Biomedical applications of the electron-capture detector *(J. Vessman)*. 14. Negative ion atmospheric pressure ionization mass spectrometry and the electron-capture detector *(E.C. Horning, D.I. Carroll, I. Dzidic and R.N. Stillwell)*. 15. Electron-capture process and ion mobility spectra in plasma chromatography *(F.W. Karasek and G.E. Spangler)*. 16. The electron-capture detector as a detector in liquid chromatography *(J.A. Th. Brinkman)*. Subject index.

ELSEVIER

P.O. Box 211,
1000 AE Amsterdam
The Netherlands

52 Vanderbilt Ave.
New York, N.Y. 10017

The Dutch guilder price is definitive. US $ prices are subject to exchange rate fluctuations.

EYELA TOKYO RIKAKIKAI CO., LTD.

)ROPLET COUNTERCURRENT ;HROMATOGRAPH

)CC-300

OR LIQUID-LIQUID ARTITION HROMATOGRAPHY

)ecial feature of Model DCC-300:)u may choose the most suitable pe of column to meet with your search since four (4) different types columns can be optionally installed the cabinet of the DCC-300

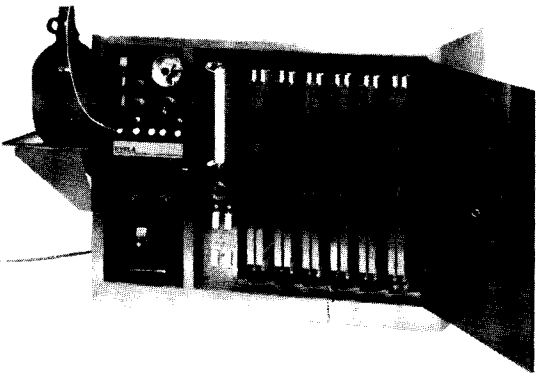

Droplet Countercurrent Chromatograph DCC-300

dvantages of the Method

Sample is quantitatively recovered since there is no solid support which may cause non-specific irreversible adsorption.

Several grams of sample can be applied due to the large volume and solubility of the stationary phase.

Separations are reproducible. Elution volumes are based entirely on partition coefficients and are not affected (within limits) by the purity of the sample.

Depending on the partition coefficients, either phase may be used as the mobile phase.

The operation is simple and straightforward. It requires only an understanding of partition coefficients to assure success.

The number of columns can be increased or decreased depending on the difficulty of the separation. Increasing the number of columns increases the number of theoretical plates.

Total volume of mobile phase required is comparatively small.

Advantages of the Equipment

1 Stationary and mobile phases contact only non-corrosive materials–glass and PTFE–during operation.
2 Formation of emulsions between stationary and mobile phases is eliminated since no mechanical shaking device is used.
3 Oxidation of unstable compounds is avoided in the degassed, totally enclosed system.
4 Equipment requires a minimum of bench space.
5 If operating pressures exceed a preset level, the pumping system will shut down.
6 The reciprocating pump assures steady flow for both mobile and stationary phases at pressures up to 60 kg/cm² (850 psi).
7 Temperature is controlled to maintain system stability and reproducibility.
8 The system can easily be cleaned and prepared for a new sample by flushing it with stationary phase.

Please ask for our detailed brochure!

TOKYO RIKAKIKAI CO., LTD.
No. 2 (Toei Bldg. 10F) 4-chome
Muromachi Nihonbashi, Chuo-ku, TOKYO
Japan, Tel.: (03) 245-0481
Cable: EYELARIKA, Telex: 02228135J

Shodex® GPC KF-800

SHOWA DENKO

A New Series of Packed Columns

Developed by Showa Denko K.K., the packed columns of the Shodex® GPC KF-800 series enable high speed and high resolution chromatography with 70,000 theoretical plates per meter.

We recommend the new series to you for high performance separation of oligomers and organic substances by molecular size.

Separation of standard polystyrenes and benzene

Column: KF-802, 300 mm
Mobile phase: THF; 1 ml / min
Samples:
1. Polystyrene, Mw: 42,800
2. Polystyrene, Mw: 2,800
3. Polystyrene, Mw: 300
4. Benzene

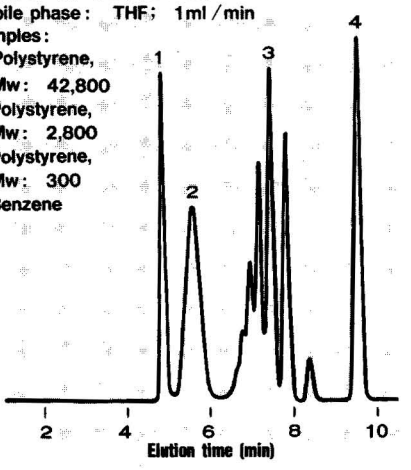

Separation of phthalates and benzene

Column: KF-801, 300 mm
Mobile phase: THF; 2 ml / min
Samples:
1. DOP
2. DBP
3. DEP
4. DMP
5. Benzene

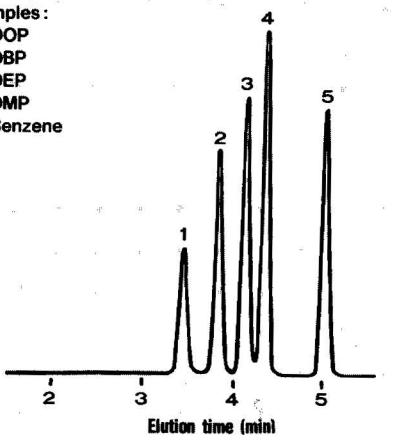

Nomenclature	Specifications			
	Theoretical plates	Exclusion limit (Polystyrene)	Size	In-column eluent
GPC KF-801	16,000 minimum	1.5×10^3	8mmϕ × 300mm	THF
KF-802	〃	5×10^3	〃	〃
KF-802.5	〃	2×10^4	〃	〃
KF-803	〃	7×10^4	〃	〃
KF-800P	Protective column for KF-801 to KF-803		4.6mmϕ × 10mm	〃

A number of other high-quality Shodex® devices are also available. They include Shodex® GPC A-800(THF), AC-800($CHCl_3$) and AD-800(DMF) series, packed columns for GPC with water used as mobile phase and for partition and adsorption chromatography and a refractive index detector.

Contact us for further information.

SHOWA DENKO AMERICA, INC.

27th Floor, West Building
280 Park Avenue
New York, N.Y.10017, U.S.A.
Telephone: 212-687-0773
Telex: 23423898

SHOWA DENKO K.K.
Instrument Products Department

13-9, Shiba Daimon 1-chome,
Minato-ku, Tokyo 105, Japan
Telephone: (03)432-5111
Telex: J26232
Cable: SECIC TOKYO

DÜSSELDORF REPRESENTATIVE OFFICE
4000 Düsseldorf, Charlottenstr. 51
Federal Republic of Germany
Telephone: (0211)362037
Telex: 8587649 SDK D

FOXY matches fractions to your chromatogram.

Not to the clock.

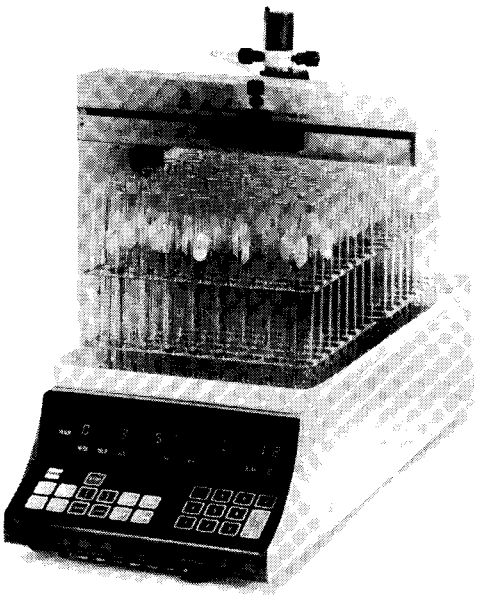

FOXY, the Fraction-Optimizing X-Y fraction collection from ISCO. Microprocessor control permits collection by time, counted drops, pump revolutions, or volumetric dispenser. Test tube and fraction size can be varied during the run. FOXY rejects void volumes and isolates peaks identified by elution times or located by an ISCO UV detector. And it stops flow between tubes and at the end of the run.

FOXY takes practically any size test tube, 28 mm scintillation vials, and even 500 ml bottles. It holds up to 288 tubes in minimal bench space.

You can add FOXY to your staff for only $2795. To learn more, call toll free: [**800**] **228-4250** (continental USA except NE). ISCO, Box 5347, Lincoln, Nebraska 68505.

506v

ISCO **Instruments with a difference**

kipp analytica

GAS CHROMATOGRAPHY SYSTEM 8200

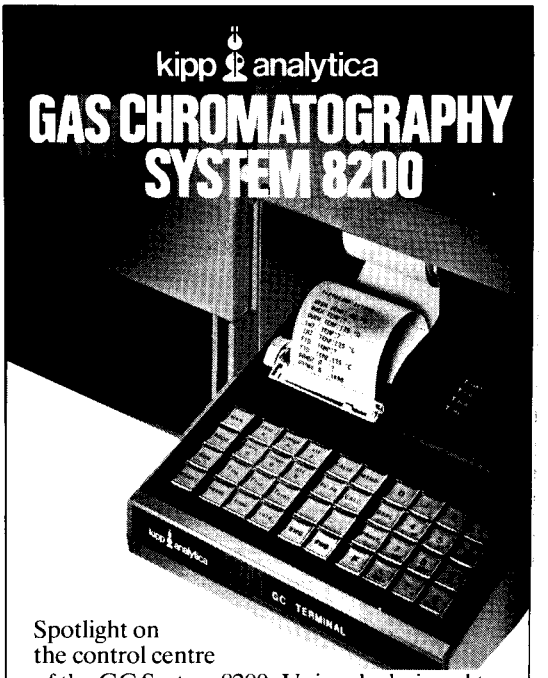

Spotlight on the control centre of the GC System 8200. Uniquely designed to give excellent performance and flexibility, featuring:

- Complete micro computer control
- High performance column oven
- Dedicated injection system, for capillary and packed columns, as well as gas samples
- Choice of control terminals
- Expandability in data handling and BASIC-programming
- Time programming of all functions and parameters

If you like to know more about this powerful Gas Chromatography System contact your local dealer or Kipp Analytica.

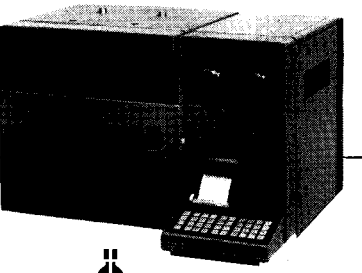

kipp analytica

Phileas Foggstraat 24, P.O. Box 620.
7800 AP Emmen, Netherlands.
Phone: (0) 5910-14640. Telex: 77094.

504 V

use this card for more information on advertisements and news items

Reader service card

JOURNAL OF

CHROMATOGRAPHY

INTERNATIONAL JOURNAL ON CHROMATOGRAPHY, ELECTROPHORESIS AND RELATED METHODS

I would like to receive, without any obligation, further information on

News items: _____

Advertisements: _____

I am especially interested in the fields as indicated below:

- ☐ 6040 Analytical Chemistry
- ☐ 6050 Chromatography
- ☐ 6150 Mass Spectrometry
- ☐ 6140 Spectroscopy
- ☐ 6240 Pharmaceutical Chemistry
- ☐ 6241 Medicinal Chemistry
- ☐ 6242 Clinical Chemistry
- ☐ 6260 Environmental Chemistry

Name: _____

Position: _____

Address: _____

_____

please use envelope; mail as printed matter

ELSEVIER SCIENCE PUBLISHERS

Advertising department

P.O. BOX 211,

1000 AE AMSTERDAM – THE NETHERLANDS

please use envelope; mail as printed matter

ELSEVIER SCIENCE PUBLISHERS

Advertising department

P.O. BOX 211,

1000 AE AMSTERDAM – THE NETHERLANDS

Reader service card

JOURNAL OF
CHROMATOGRAPHY
INTERNATIONAL JOURNAL ON CHROMATOGRAPHY, ELECTROPHORESIS AND RELATED METHODS

use this card for more information on advertisements and news items

I would like to receive, without any obligation, further information on
News items: _____
Advertisements: _____

I am especially interested in the fields as indicated below:

- ☐ 6040 Analytical Chemistry
- ☐ 6050 Chromatography
- ☐ 6150 Mass Spectrometry
- ☐ 6140 Spectroscopy
- ☐ 6240 Pharmaceutical Chemistry
- ☐ 6241 Medicinal Chemistry
- ☐ 6242 Clinical Chemistry
- ☐ 6260 Environmental Chemistry

Name: _____

Position: _____

Address: _____

_____

c acid glacial
ıne
ınitrile
ıne
yl alcohol
ın tetrachloride
oform (stabilized
ımylene)
oform (stabilized with
alcohol)
exane
ylenedioxide
yl ether
acetate
alcohol
ıtane
ane
l alcohol
lene chloride
lized with amylene)
lene chloride
lized with ethyl alcohol)
lethylketone
ctane
pyl alcohol
opyl alcohol
ıydrofuran
ne
(in preparation)

SOLVENTS RS FOR HPLC

TO EXTEND THE LIFE
AND IMPROVE THE
PERFORMANCE OF YOUR
HPLC COLUMNS,
A LINE OF SPECIALLY
PURIFIED AND CONTROLLED
SOLVENTS FOR HPLC
IS AVAILABLE

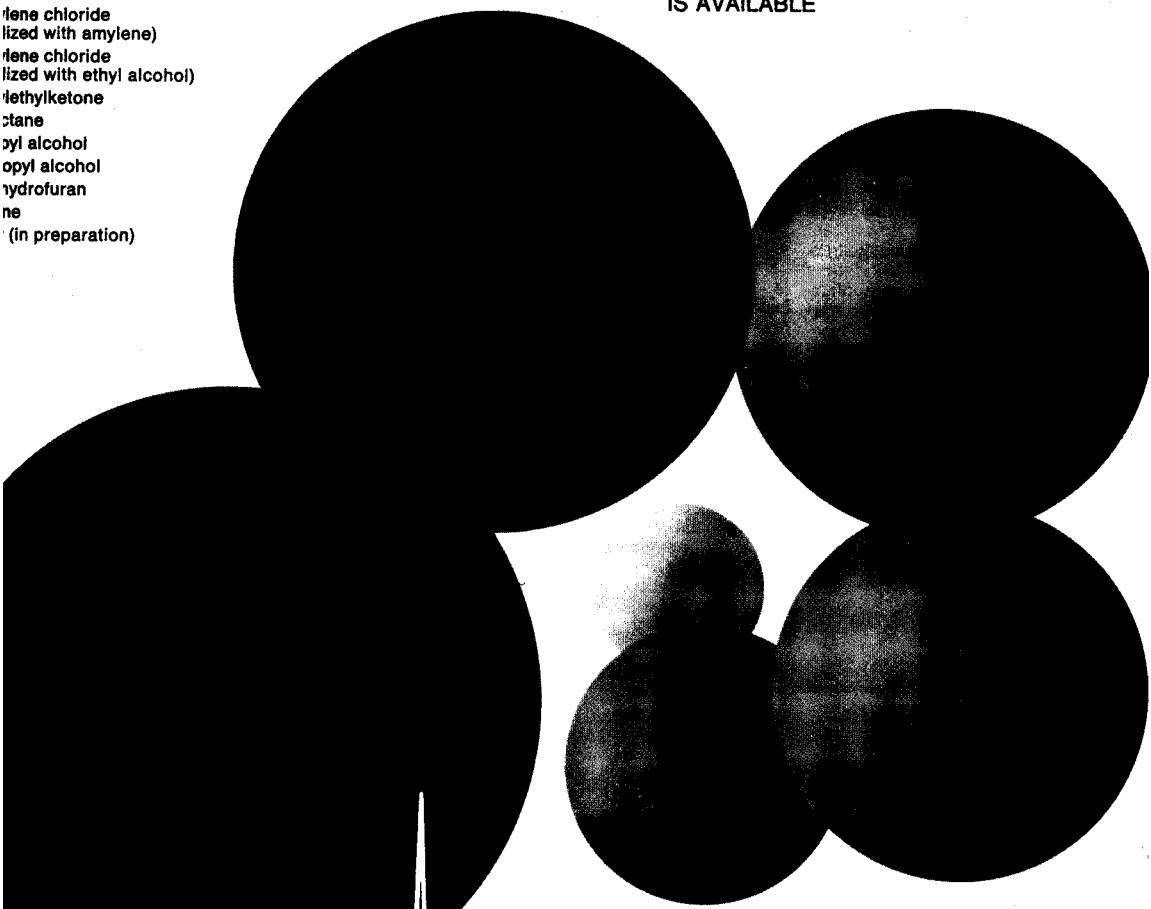

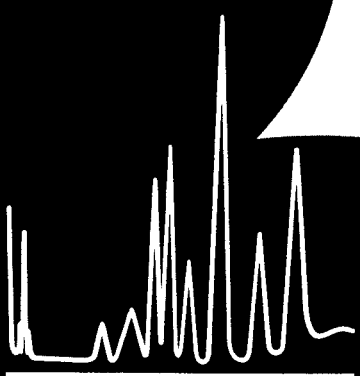

FARMITALIA CARLO ERBA

ANALYTICAL DIVISION / REAGENTS / 20159 Milano / Via C. Imbonati 24

MONTEDISON GROUP

High resolution is not enough! High fidelity is also necessary to assess quantitative sample composition.

For further information in Europe and USA please contact our local Subsidiary or Distributor.

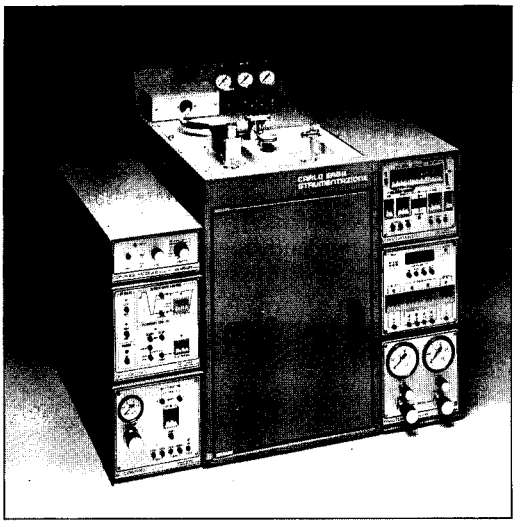

Unique
Specially cooled, automatic, non-vaporizing septum-less on-column injector allowing true:
non-discriminating
non-destructive
non-contaminating
sampling into capillary column.
Automatic split-splitless injector.

Innovative
Zero dead volume, true all-glass system.
New accurate all-metal pneumatic system.
Constant flow/constant pressure option for carrier gas.
Ultra-rapid amplifier.
Wide range of easily interchangeable detectors.

These are only some of the most advanced features making the

Fractovap 4160 Series the only real answer for true quantitation in capillary gas chromatography.

CARLO ERBA STRUMENTAZIONE

FARMITALIA CARLO ERBA SUBSIDIARY montedison GROUP

More and more primary literature? Less and less time to read it?

take TrAC

trends in analytical chemistry

A monthly publication of short, critical reviews and news on trends and developments in analytical chemistry

How much better informed you could be if only you had the time to keep up with the latest developments.

Time we cannot give you, but we can give you concise, critical information on what is going on in the analytical sciences. Every month, as it happens.

It's all in TrAC – Trends in Analytical Chemistry – new for the 1980's from Elsevier and yours now at a low introductory rate.

Introductory Offer

SIXTEEN ISSUES FOR THE PRICE OF TWELVE!

Volume 1 – 1981/82 – of **Trends in Analytical Chemistry** will have sixteen issues: March 1981 and monthly from October 1981 to December 1982.

Personal Edition

US $42.50 (USA and Canada), £20.00 (UK), 91.50 Dutch guilders (Europe), 95.50 Dutch guilders (elsewhere).

Library Edition

for US $133.25 or 260.00 Dutch guilders throughout the world.

All issues of both editions are sent by air worldwide.

*) *The Dutch guilder price is definitive.*

Take just a minute to order either edition now – you will enjoy the time it saves you later.

ELSEVIER

TrAC is your opportunity to learn from researchers in related fields, to get first-hand, detailed reports on important developments in methodology and instrumentation. **TrAC** brings you current information on trends and techniques from laboratories all over the world.

Lab managers will find in **TrAC** evaluations of new methods and techniques which will enable them to make better-informed purchasing decisions. As a training aid **TrAC** is more up-to-date than any textbook.

TrAC is written in clear, jargon-free language, avoiding highly specialized terminology and provides you with a working knowledge of related methodology and techniques.

In every issue you will find:

- short critical reviews written for an interdisciplinary audience
- feature articles
- insights into the function, organization and operation of industrial, government or research laboratories
- news on topics of general interest
- teaching aids – TrAC is more up-to-date than any textbook
- articles on the history of analytical chemistry
- reports on meetings and book reviews

Trends in Analytical Chemistry comes in either the monthly **Personal Edition** or the special **Library Edition** which includes the monthly issues plus a hardbound volume containing all the review articles published over the year and indexed for easy retrieval.

Order Form

Special Introductory Offer for the Personal Edition valid until December 31, 1981

To **ELSEVIER Dept. TrAC AP**

P.O. Box 330
1000 AH Amsterdam
The Netherlands

52 Vanderbilt Avenue
New York, NY 10017

US residents may call (212) 867-9040 and charge their American Express, Master Charge or Visa/Bankamericard account.

Yes! Please enter my subscription now – Volume 1 – 1981/82

☐ Personal Edition ☐ Library Edition

I enclose my ☐ personal cheque ☐ bankcheque

Orders from individual subscribers must be prepaid.

☐ Please send me a free sample copy first.

Name: _____ Position: _____ Date: _____

Address: _____

_____

City: _____ State: _____ Postal Code _____

ELECTROPHORESIS

A SURVEY OF TECHNIQUES AND APPLICATIONS

Part A: Techniques

Z. DEYL, Czechoslovak Academy of Sciences, Prague (editor)
F. M. EVERAERTS, Z. PRUSÍK, and P. J. SVENDSEN (co-editors)

JOURNAL OF CHROMATOGRAPHY LIBRARY 18

This first volume in a two part set, deals with the principles, theory and instrumentation of modern electromigration methods. The second volume will be concerned with details of applications of electromigration methods to diverse categories of compounds, although a few applications are already discussed in Part A.

Some electromigration methods have become standard procedures because of their extensive use in analytical and preparative separations. These are discussed together with newer developments in the field. Hints are included to help the reader to overcome difficulties frequently arising from the lack of suitable equipment. Adequate theoretical background of the individual techniques is included. A theoretical approach to the deteriorative processes is presented in order to facilitate further development of a particular technique and its application to a special problem.

In each chapter practical realizations of different techniques are discussed and examples are presented to demonstrate the limits of each method. The mathematical and physicochemical background is arranged so as to make it as coherent as possible for both non-professionals such as post-graduate students, and experts using electromigration techniques.

CONTENTS: Preface. Foreword. Introduction. Chapters: 1. Theory of electromigration processes. 2. Classification of electromigration methods. 3. Evaluation of the results of electrophoretic separation. 4. Molecular size and shape in electrophoresis. 5. Zone electrophoresis (except gel-type techniques and immunoelectrophoresis). 6. Gel-type techniques. 7. Quantitative immunoelectrophoresis. 8. Moving boundary electrophoresis in narrow-bore tubes. 9. Isoelectric focusing. 10. Analytical isotachophoresis. 11. Continuous flow-through electrophoresis. 12. Continuous flow deviation electrophoresis. 13. Preparative electrophoresis in gel-media. 14. Preparative electrophoresis in columns. 15. Preparative isoelectric focusing. 16. Preparative isotachophoresis. 17. Preparative isotachophoresis on the micro scale. List of frequently occurring symbols. Subject index.

1979 xvi + 492 pages US $83.00/Dfl. 170.00 ISBN: 0-444-41721-4

"The Editor, aided by an eminent team of Co-editors, has produced an impressive and worthwhile book. The overall conclusion must be, "I like it."

The Analyst

ELSEVIER

P.O. Box 211,
1000 AE Amsterdam
The Netherlands

52 Vanderbilt Ave
New York, N.Y. 10017

The Dutch guilder price is definitive. US $ prices are subject to exchange rate fluctuations.

7153A

YOURS FOR THE ASKING...

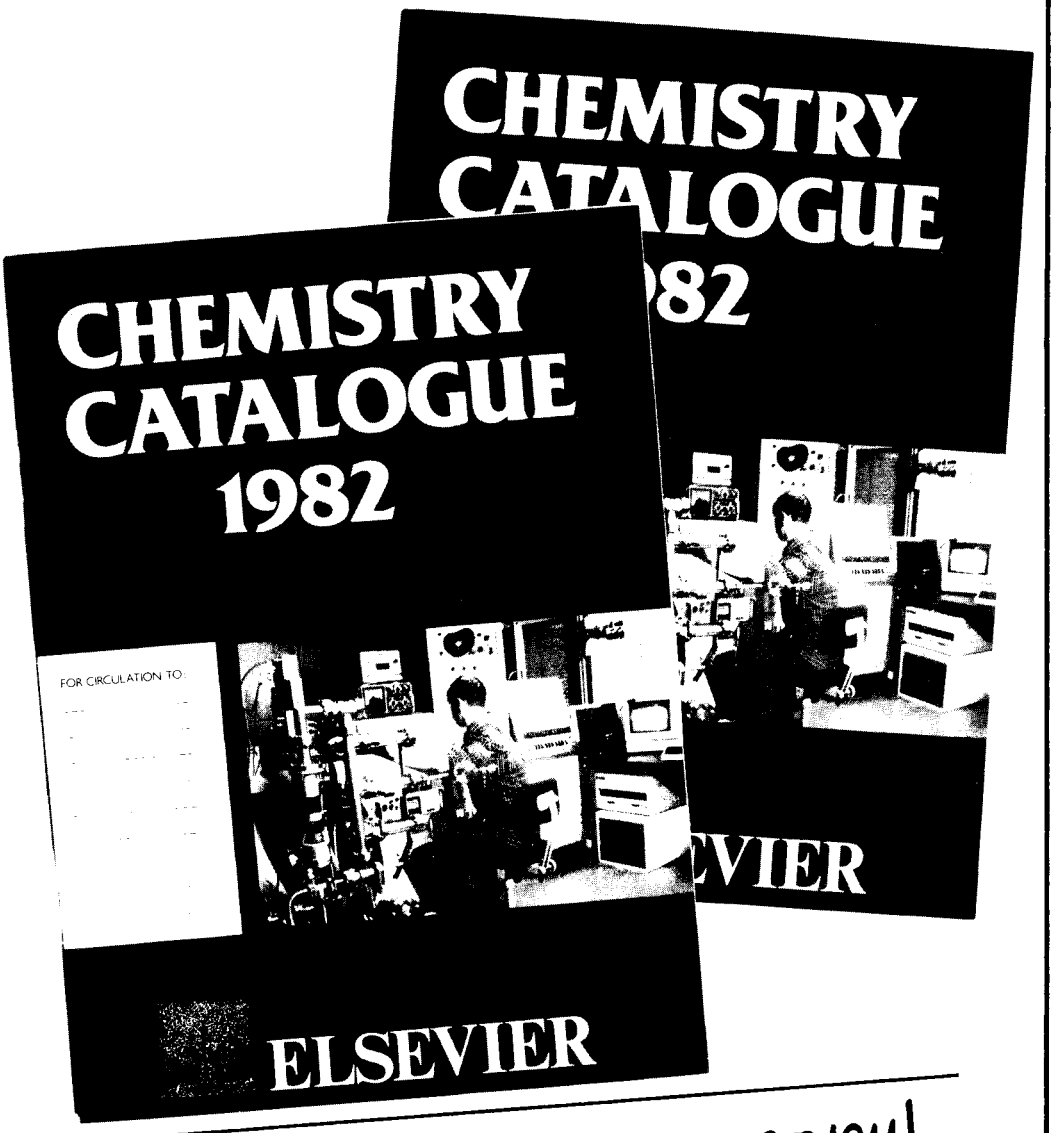

Write now for your copy!

Elsevier Scientific Publishing Company

P.O. Box 330
1000 AH Amsterdam
The Netherlands
Tel: (20) 5803-449

52 Vanderbilt Avenue
New York, NY 10017
U.S.A.
Tel: (212) 867-9040

7239

JOURNAL OF ANALYTICAL AND APPLIED PYROLYSIS

JOURNAL OF CHROMATOGRAPHY

VOL. 239 (1982)

JOURNAL *of* CHROMATOGRAPHY

INTERNATIONAL JOURNAL ON CHROMATOGRAPHY,
ELECTROPHORESIS AND RELATED METHODS

ELSEVIER SCIENTIFIC PUBLISHING COMPANY
AMSTERDAM

J. Chromatogr., Vol. 239 (1982)

Printed in The Netherlands

SPECIAL VOLUME

ADVANCES IN CHROMATOGRAPHY 1982

17th International Symposium, Las Vegas, NV, April 5–8, 1982
and
18th International Symposium, Tokyo, April 15–18, 1982

CONTENTS

ADVANCES IN CHROMATOGRAPHY 1982: 17TH INTERNATIONAL SYMPOSIUM, LAS VEGAS, NV, APRIL 5–8, 1982, AND 18TH INTERNATIONAL SYMPOSIUM, TOKYO, APRIL 15–18, 1982.

Preface
by M. Lederer XIII

Adsorption from liquid mixtures and liquid chromatography
by F. Riedo and E. sz. Kováts (Lausanne, Switzerland) 1

Multi-component analyses of human body fluids and tissues in health and disease using capillary gas chromatography–mass spectrometry and high-resolution two-dimensional electrophoresis
by E. Jellum (Oslo, Norway) 29

Optimization of liquid phase mixtures
by D. F. Ingraham, C. F. Shoemaker and W. Jennings (Davis, CA, U.S.A.) 39

Peroxide-initiated *in situ* curing of silicone gums for capillary column gas chromatography
by L. Blomberg, J. Buijten, K. Markides and T. Wännman (Stockholm, Sweden) 51

Performance of different types of cross-linked methyl polysiloxane stationary phases on fused-silica glass capillary columns
by S. R. Lipsky and W. J. McMurray (New Haven, CT, U.S.A.) 61

Analysis of picomolar concentrations of 6-oxo-prostaglandin $F_{1\alpha}$ in biological fluids
by S. E. Barrow, K. A. Waddell, M. Ennis, C. T. Dollery and I. A. Blair (London, Great Britain) 71

Simultaneous analysis of imipramine and its metabolite desipramine in biological fluids
by J. C. Craig, L. D. Gruenke and T.-L. Nguyen (San Francisco, CA, U.S.A.) 81

Measurement of endogenous leucine enkephalin in canine thalamus by high-performance liquid chromatography and field desorption mass spectrometry
by D. M. Desiderio and S. Yamada (Memphis, TN, U.S.A.) 87

Gram quantity synthesis and chromatographic assessment of 3,3′,4,4′-tetrachlorobiphenyl
by K. Nakatsu, J. F. Brien, H. Taub, W. J. Racz and G. S. Marks (Kingston, Canada) . 97

A split system applicable as a gas chromatographic–mass spectrometric interface and as effluent splitter for specific gas chromatographic detectors
by E. Wetzel, Th. Kuster and H.-Ch. Curtius (Zurich, Switzerland) 107

Detection of carbon monoxide at ambient levels with an N_2O-sensitized electron-capture detector
by C. D. Pfaffenberger and A. J. Peoples (Miami, FL, U.S.A.) 115

Evidence for more than one response mechanism in pulsed electron-capture detectors
by W. A. Aue and K. W. M. Siu (Halifax, Canada) 127

Selective electron-capture sensitization of water, phenols, amines and aromatic and heterocyclic compounds
by M. A. Wizner, S. Singhawangcha, R. M. Barkley and R. E. Sievers (Boulder, CO, U.S.A.) 145

Volatile constituents of the produced water effluent from the Buccaneer Gas and Oil Field
by B. S. Middleditch (Houston, TX, U.S.A.) 159

Distribution of PCDDs and other toxic compounds generated on fly ash particulates in municipal incinerators.
by F. W. Karasek, R. E. Clement and A. C. Viau (Waterloo, Canada) 173

Plasma emission spectral detection for high-resolution gas chromatographic study of group IV organometallic compounds
by S. A. Estes, P. C. Uden and R. M. Barnes (Amherst, MA, U.S.A.) 181

Characterization of dihydroarenediols and related compounds by gas chromatography–mass spectrometry: Comparison of derivatives
by C. J. W. Brooks, W. J. Cole, J. H. Borthwick and G. M. Brown (Glasgow, Great Britain) 191

Long-term variation study of blood plasma levels of chloroform and related purgeable compounds
by C. D. Pfaffenberger and A. J. Peoples (Miami, FL, U.S.A.) 217

Gas chromatographic enantiomer separation of chiral alcohols
by W. A. König, W. Francke and I. Benecke (Hamburg, G.F.R.) 227

Microanalysis of brassinolide and its analogues by gas chromatography and gas chromatography–mass spectrometry.
by S. Takatsuto, B. Ying, M. Morisaki and N. Ikekawa (Tokyo, Japan) 233

Gas chromatographic and mass spectrometric studies on the metabolism and pharmacokinetics of Δ^1-tetrahydrocannabinol in the rabbit
by D. J. Harvey, J. T. A. Leuschner and W. D. M. Paton (Oxford, Great Britain) 243

Unidimensional, sequential separation of PTH-amino acids by high-performance thin-layer chromatography
by S. A. Schuette and C. F. Poole (Detroit, MI, U.S.A.) 251

Quantitative determination of lecithin and sphingomyelin at nanogram levels by high-performance thin-layer chromatography using fluorescence. Preliminary results
by L. Zhou, H. Shanfield and A. Zlatkis (Houston, TX, U.S.A.) 259

Automated qualitative and quantitative metabolic profiling analysis of urinary steroids by a gas chromatography–mass spectrometry–data system
by J. J. Vrbanac, W. E. Braselton, Jr., J. F. Holland and C. C. Sweeley (East Lansing, MI, U.S.A.) 265

Simultaneous determination of glyceryl trinitrate and its principal metabolites, 1,2- and 1,3-glyceryl dinitrate, in plasma by gas chromatography–negative ion chemical ionization–selected ion monitoring
by H. Miyazaki, M. Ishibashi, Y. Hashimoto, G. Idzu and Y. Furuta (Tokyo, Japan) . . 277

Gas chromatographic–mass spectrometric analysis of endogenous levels of estradiol in plasma and in cytosol from rat uterus
by M. Tetsuo, H. Eriksson and J. Sjövall (Stockholm, Sweden) 287

Compilation of gas chromatographic retention indices of 163 metabolically important organic acids, and their use in detection of patients with organic acidurias
by K. Tanaka and D. G. Hine (New Haven, CT, U.S.A.) 301

Determination of tocainide in human plasma by gas chromatography with nitrogen-selective detection after Schiff base formation
by L. Johansson and J. Vessman (Mölndal, Sweden) 323

Determination of picomole amounts of choline and acetylcholine in blood by gas chromatography–mass spectrometry equipped with a newly improved pyrolyzer
by Y. Hasegawa, M. Kunihara and Y. Maruyama (Gunma, Japan) 335

Quantification of endogenous aliphatic alcohols in serum and urine
by H. M. Liebich, H. J. Buelow and R. Kallmayer (Tübingen, G.F.R.) 343

Determination of the pore size distribution, by exclusion chromatography, of ion-exchange polymers which swell in water
by T. Crispin and I. Halász (Saarbrücken, G.F.R.) 351

Computerized auto-control of on-line processes or laboratory gas and liquid chromatographs
by C. L. Guillemin (Aubervilliers, France) 363

Chromatographic analysis of aromatic polyhydrazides, oxalyl arylene polyhydrazides and aromatic poly(amide–hydrazides) after alkali fusion
by J. K. Haken and J. A. Obita (Kensington, Australia) 377

Prediction of retention times for aromatic acids in liquid chromatography
by T. Hanai, K. C. Tran and J. Hubert (Montréal, Canada) 385

Spacial distribution of ions and electrons within ^{63}Ni ionization cells
by E. P. Grimsrud and M. J. Connolly (Bozeman, MT, U.S.A.) 397

Adsorption of polar solutes on liquid-modified supports
by M. I. Selim, J. F. Parcher and P. J. Lin (University of Mississippi, MS, U.S.A.) . . . 411

High-performance displacement chromatography of corticosteroids. Scouting for displacer and analysis of the effluent by thin-layer chromatography
by H. Kalász and Cs. Horváth (New Haven, CT, U.S.A.) 423

Quantitative computer resolution of severely overlapping liquid chromatographic peaks
by N. J. D'Allura and R. S. Juvet, Jr. (Tempe, AZ, U.S.A.) 439

Resolution of optical isomers of Dns-amino acids by high-performance liquid chromatography with L-histidine and its derivatives in the mobile phase
by S. Lam and A. Karmen (Bronx, NY, U.S.A.) 451

Total amino acid analysis using pre-column fluorescence derivatization
by H. Umagat, P. Kucera and L.-F. Wen (Nutley, NJ, U.S.A.) 463

A simple high-performance liquid chromatographic pre-column technique for investigation of drug metabolism in biological fluids
by W. Voelter and T. Kronbach (Tübingen, G.F.R.) and K. Zech and R. Huber (Konstanz, G.F.R.) 475

Prediction of molecular structures of thiols and sulphides by retention indices
by F. Morishita, H. Murakita, Y. Takemura and T. Kojima (Kyoto, Japan) 483

Gas chromatographic determination of optical isomers of some carboxylic acids and amines with optically active stationary phases
by N. Ôi, T. Doi, H. Kitahara and Y. Inda (Hyogo-ken, Japan) 493

Liquid crystals as stationary phases in gas chromatography. V. Adsorption behaviour of aliphatic alcohols and their esters on an electric field liquid crystal column
by K. Watabe, T. Hobo and S. Suzuki (Tokyo, Japan) 499

Packed microcapillary liquid chromatography with reduced I.D. columns
by T. Tsuda, I. Tanaka and G. Nakagawa (Nagoya, Japan) 507

Application of the streaming current detector to the analysis of individual bile acids
by S. Terabe, K. Yamamoto and T. Ando (Kyoto, Japan) 515

Hydrophobicity and chromatographic behaviour of aromatic acids found in urine
by T. Hanai and J. Hubert (Montréal, Canada) 527

Ion chromatography with an ion-exchange membrane suppressor
by Y. Hanaoka, T. Murayama, S. Muramoto, T. Matsuura and A. Nanba (Tokyo, Japan) 537

High-performance liquid chromatography of human serum lipoproteins. Selective detection of triglycerides by enzymatic reaction
by I. Hara, K. Shiraishi and M. Okazaki (Ichikawashi, Japan) 549

Separation and determination of naproxen enantiomers in serum by high-performance liquid chromatography
by J. Goto, N. Goto and T. Nambara (Sendai, Japan) 559

Two-dimensional separation system for analysis of proteins employing isoelectric focusing and high-performance liquid chromatography
by K. Kojima, T. Manabe, T. Okuyama, T. Tomono, T. Suzuki and E. Tokunaga (Tokyo, Japan) 565

Characterization of bile acid methyl ester acetate derivatives of rat bile using solventless glass capillary gas chromatography and electron impact and ammonia chemical ionization mass spectrometry
by T. Murata, S. Takahashi, S. Ohnishi, K. Hosoi, T. Nakashima, Y. Ban and K. Kuriyama (Kyoto, Japan) 571

Determination of captopril and its disulphide in biological fluids
by Y. Matsuki, T. Ito, K. Fukuhara, T. Nakamura, M. Kimura and H. Ono (Kanagawa, Japan) and T. Nambara (Sendai, Japan) 585

Microdetermination of prostaglandins and thromboxane B_2 by gas chromatography using an electron-capture detector
by H. Miyazaki, M. Ishibashi, K. Yamashita and I. Ohguchi (Tokyo, Japan), H. Saitoh, H. Kurono and M. Shimono (Kyoto, Japan) and M. Katori (Kanagawa, Japan) 595

Determination of β-adrenergic blocking drugs as cyclic boronates by gas chromatography with nitrogen-selective detection
by T. Yamaguchi, Y. Morimoto, Y. Sekine and M. Hashimoto (Osaka, Japan) 609

Chemiluminescent nitrogen detector–gas chromatography and its application to measurement of atmospheric ammonia and amines
by N. Kashihira, K. Makino, K. Kirita and Y. Watanabe (Tokorozawa, Japan) 617

"Buffer memory" technique for the combination of micro-high-performance liquid chromatography and infrared spectrometry
by K. Jinno and C. Fujimoto (Toyohashi, Japan) and D. Ishii (Nagoya, Japan) 625

High-back-pressure liquid chromatography. II. Development of a post-column-controlled flow system
by T. Takeuchi and D. Ishii (Nagoya, Japan) 633

A new centrifugal counter-current chromatograph and its application
by W. Murayama, T. Kobayashi, Y. Kosuge, H. Yano, Y. Nunogaki and K. Nunogaki (Kyoto, Japan) 643

High-speed high-resolution gel permeation chromatography of small molecules and oligomers
by S. Ishiguro, Y. Inoue and T. Hosogane (Tokyo, Japan) 651

Solvent dependence of gel chromatographic retention of low-molecular-weight compounds of polystyrene–divinylbenzene gel
by K. Saitoh, E. Ozaki and N. Suzuki (Miyagi, Japan) 661

Reversed-phase liquid chromatographic resolution of underivatized D,L-amino acids using chiral eluents
by N. Nimura, A. Toyama, Y. Kasahara and T. Kinoshita (Tokyo, Japan) 671

Silica gel liquid–liquid chromatography using aqueous binary phase systems. High-efficiency extraction and resolution of phenols and carboxylic acids
by S. Hara, Y. Dobashi and K. Oka (Tokyo, Japan) 677

Ternary solvent system design for liquid–solid chromatography
by S. Hara (Tokyo, Japan), K. Kunihiro and H. Yamaguchi (Hiroshima, Japan) and E. Soczewiński (Lublin, Poland) 687

Liquid chromatography with crown ether-containing mobile phases. II. Retention behaviour of β-lactam antibiotics in reversed-phase high-performance liquid chromatography
by T. Nakagawa, A. Shibukawa and T. Uno (Kyoto, Japan) 695

Determination of blood transketolase by high-performance liquid chromatography (a preliminary note)
by M. Kimura and Y. Itokawa (Kyoto, Japan) 707

Determination of prednisone and prednisolone in human serum by high-performance liquid chromatography —especially on impaired conversion of corticosteroids in patients with chronic liver disease
by T. Ui, M. Mitsunaga, T. Tanaka and M. Horiguchi (Tokyo, Japan) 711

Determination of 5′-nucleotidase activity in human erythrocytes and plasma using high-performance liquid chromatography
by T. Sakai, S. Yanagihara and K. Ushio (Tokyo, Japan) 717

Pre-column labelling for high-performance liquid chromatography of amino acids with 7-fluoro-4-nitrobenzo-2-oxa-1,3-diazole and its application to protein hydrolysates
by Y. Watanabe and K. Imai (Tokyo, Japan) 723

Analysis of body functions using a clinical liquid chromatograph
by H. Miyagi, J. Miura, Y. Takata, S. Kamitake, S. Ganno and H. Yamagata (Ibaraki, Japan) 733

Preparation of affinity adsorbents with Toyopearl gels
by I. Matsumoto, Y. Ito and N. Seno (Tokyo, Japan) 747

Adsorption chromatography of proteins on siliconized porous glass
by T. Mizutani and T. Narihara (Nagoya, Japan) 755

Effect of stationary phase structure on retention and selectivity in reversed-phase liquid chromatography
by N. Tanaka, Y. Tokuda, K. Iwaguchi and M. Araki (Kyoto, Japan) 761

Separation and determination of bile acids by high-performance liquid chromatography using immobilized 3α-hydroxysteroid dehydrogenase and an electrochemical detector
by S. Kamada, M. Maeda, A. Tsuji and Y. Umezawa (Tokyo, Japan) and T. Kurahashi (Kyoto, Japan) 773

Author Index 784

PREFACE

ADVANCES IN CHROMATOGRAPHY

17th International Symposium, Las Vegas, NV, U.S.A., April 5–8, 1982, and 18th International Symposium, Tokyo, Japan, April 15–18, 1982.

This volume contains 74 of the 140^{+} manuscripts that were read at these two symposia. The papers published here were received in time to be refereed and revised by January 1st, 1982. Some papers that were received late will be published in subsequent issues. A large number of papers were not submitted to us at all (about 50% of the total), and will presumably appear elsewhere.

The papers are arranged here in chronological order, *i.e.*, first the Las Vegas Symposium and then the Tokyo Symposium and within each symposium they are in the order in which they appear in the programme.

Sils-Maria
January 1st, 1982.

MICHAEL LEDERER

Journal of Chromatography, 239 (1982) 1–28
Elsevier Scientific Publishing Company, Amsterdam — Printed in The Netherlands

CHROM. 14,663

ADSORPTION FROM LIQUID MIXTURES AND LIQUID CHROMATOGRAPHY*

FRANÇOIS RIEDO and ERVIN sz. KOVÁTS*
Laboratoire de Chimie Technique de l'École Polytechnique Fédérale de Lausanne, CH-1015 Lausanne (Switzerland)

SUMMARY

It is shown that retention volumes can be calculated in terms of the total material content in the chromatographic column as transported by the eluent, termed the "column capacity". With the aid of this retention equation, of general validity, the necessary link is established between Gibbs' description of adsorption at a liquid–solid interface and the theory of retention in liquid-solid chromatography. Relationships are given for the correct interpretation of retention volumes and for the chromatographic determination of adsorption isotherms of the components in a binary liquid mixture.

INTRODUCTION

In the mathematical treatment of multi-component chromatography by De Vault[1], retention volumes are found to be the eigenvalues of a matrix, the elements of which are the partial derivatives of the partition isotherms with respect to the concentration in the mobile phase. Baylé and Klinkenberg[2] and Mangelsdorf[3] pointed out very clearly that conclusions drawn from this model can be considered valid only if it can be shown that the matrix has real, positive eigenvalues. At present there is no thermodynamic proof of general validity; a demonstration was given only for some special cases by Mangelsdorf[3] and Helfferich and Klein[4]. Perhaps it is because of this basic difficulty that the results of this treatment were never applied to a quantitative evaluation of experiments. Further, the link was never obvious between the theory of adsorption from liquid mixtures and that of liquid–solid chromatography. This question has already been treated by De Vault[1] and later by Schay[5], but the application of their theoretical results to experiment is not without difficulties, as it is shown by several more recent papers[6–15] on the determination of hold-up volumes and composite adsorption isotherms.

In this paper we propose an interpretation of experimental data in liquid chromatography that is coherent with the theory of adsorption. Restrictions had to be introduced for the general validity of the conclusions; they are in relation to the lack

* Based on the doctoral thesis of F. Riedo.

0021-9673/82/0000–0000/$02.75

of a solution of the fundamental eigenvalue problem. Also, an experimental method for the determination of composite isotherms in binary liquid mixtures is discussed.

RETENTION IN THE CHROMATOGRAPHIC COLUMN UNDER ANALYTICAL CONDITIONS

In the *classical model of the chromatographic process* a solute is distributed between two homogeneous phases of well defined boundary and extent, one of which is mobile and the other stationary. The identification of such phases in different types of chromatography is not always obvious. For example, in liquid–solid chromatography with a mixture as the eluent there exists in the liquid, normal to the eluent–solid interface, a concentration gradient. Experimental evidence shows that far enough from the interface there is liquid of homogeneous composition but no definite boundary can be established between the homogeneous portion inside the liquid and the certainly non-homogeneous surface phase. In the dynamic chromatographic system there arises a further boundary problem, namely that between the mobile part of the eluent (supposedly of homogeneous composition) and the stationary layer near the surface. A final problem is the identification of an eluent in the sense of a "carrier of solutes". Actually, in this respect there is no difference between components of the eluent and those of the sample; in the column every compound is once part of the carrier and then part of the stationary layer. Liquid–solid chromatography is a typical example of "multi-component chromatography with interference" as defined by Helfferich and Klein[4]. It can be concluded that in these instances the classical model is not adequate to describe the chromatographic process because the identification of a homogeneous stationary phase is not possible. Obviously, concepts intimately related to this model such as partition coefficient and hold-up volume also have no evident interpretation.

In the following, a *new approach* is proposed and it will be shown that it is possible to describe the chromatographic process with the aid of a function called the "*column capacity*" and by only supposing that there is a homogeneous mobile phase (referred to by the subscript μ) which has a material content greater than zero. It will be shown that in the general case the exact value of this material content (and of the corresponding volume) can be left unspecified. If useful or necessary it can be determined from case to case on the basis of a model (*e.g.*, gas–liquid chromatography) or a convention (*e.g.*, liquid–solid chromatography).

For the *definition of the column capacity* let us consider an infinite amount of a fluid m-component mixture (liquid or gas) of the composition $\vec{x}_\beta$, where the subscript β refers to this bulk. The composition is designated by an $m-1$-dimensional vector with the individual molar fractions, $x_{\beta,i}$, as components:

$$\vec{x}_\beta = (x_{\beta,\mathrm{a}}, \ldots, x_{\beta,i}, \ldots, x_{\beta,\mathrm{m}-1}) \tag{1}$$

(the composition can also be given in terms of mass fractions, $\vec{p}_\beta$, or volume fractions, $\vec{\varphi}_\beta$). Let us also imagine a rigid tube filled with a well defined amount of a non-volatile powder absolutely insoluble in the aforementioned fluid. The nature of the powder is left unspecified. The tube closed at the ends by membranes permeable to the fluid is now considered as the system to be characterized. It is placed into the fluid mixture at temperature T and pressure P. After equilibrium is established the fluid is completely

emptied from the tube and the mass, composition and nature of the fluid yield are determined. This result expressed in terms of number of moles is deemed the "molar capacity vector of the tube", $\vec{n}_\kappa$. One of the components of this vector is the "molar component capacity", *i.e.*, the total amount of a compound contained in the tube. At constant temperature and pressure these m functions depend on the composition of the fluid mixture:

$$n_{\kappa,i} = n_{\kappa,i}(\vec{x}_\beta) \tag{2}$$

They are equilibrium properties of the tube and as such characterize its equilibrium state. Equivalently, the total molar capacity

$$n_{\kappa,\text{tot}} = \sum_{i=a}^{m} n_{\kappa,i} \tag{3}$$

together with the composition vector of the yield, $\vec{x}_\kappa$, also define the equilibrium state of the tube. In non-trivial cases $\vec{x}_\kappa \neq \vec{x}_\beta$.

It will be now shown that if this tube is used as a *chromatographic column* where any compound admitted in the chromatographic process (including the sample, eluent, etc.) was included in the set of m substances then the m functions $n_{\kappa,i}(\vec{x}_\beta)$ determine unequivocally the retention properties of the column under the following conditions:

(a) The process must be considered to proceed through states of equilibrium (instantaneous equilibrium at any point inside the column) because the value of the column capacity refers to equilibrium. Any other knowledge about the retention, *e.g.*, retention mechanism, is not necessary.

(b) The hypothesis of the existence of a homogeneous mobile phase of non-zero and positive material content must be admissible and plausible. It will be identified as part of the fluid mixture from the foregoing experiment; consequently, the column capacity will refer to the composition of this phase. However, the extent of the volume of the mobile phase need not be specified.

So far, the model as presented has been very general. For proper mathematical treatment it is necessary to specify further the chromatographic system. The *idealized chromatographic column* which will be referred to (see Fig. 1) has a uniform cross-section at any distance, z, from the inlet ($z = 0$) to the outlet ($z = L$). It is filled with a quasi-continuum of a porous column material with pores uniformly and microscopically distributed. It is not necessary at this stage to specify the material and composition of the column filling (solid, solid support coated with a liquid, solid with chemically modified surface, etc.). A fluid m-component mixture is made to flow through the column at constant temperature, T_c. It experiences no flow resistance, and consequently the pressure in the column is uniform, $\bar{P}_c$ (mean column pressure). In this dynamic situation the composition of the mobile phase becomes a function of distance along the column and time, $\vec{x}_\mu(z,t)$. The interface separating the eluent and the column material has a total area S. The mobile phase advances through the column with a piston flow profile. As previously noted, it has a positive volume but the exact value will be left unspecified. A detector is placed at the column outlet to measure the composition $[\vec{x}_\mu(z=L,t)]$ of the mobile phase. In order to simplify the

description of the dynamic behaviour of the system, the usual assumptions are introduced: instantaneous equilibrium in each cross-section and no axial diffusion. The only novel hypothesis to be made is that within any cross-section that part of the fluid mixture which has a different composition from that of the mobile phase $x_\mu(z,t)$ remains stationary. For such a column the column capacity is an intensive function if referred to unit column length, $\vec{n}_\kappa/L$.

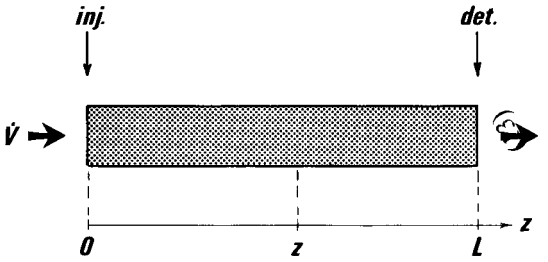

Fig. 1. Scheme of the chromatographic column filled with a quasi-continuum of a porous powder.

We now address the usual problem encountered in elution chromatography, *i.e.*, that of the *retention volume*, $V_{R,i}$, of a concentration signal introduced at the beginning of the column but in terms of the vector function

$$\vec{n}_\kappa = \vec{n}_\kappa(\vec{x}_\mu) \tag{4}$$

Within any cross-section the material content can only change through material transport by the eluent. Therefore for compound i, the material balance in the section from the column inlet to distance z is given by the equation

$$\underbrace{\int_0^z \{[n_{\kappa,i}(\vec{x}_\mu(z,t))]/L\}\,\mathrm{d}z}_{\text{Material content in the section } (0-z) \text{ at time } t} = \underbrace{\int_0^z \{[n_{\kappa,i}(\vec{x}_\mu(z,0))]/L\}\,\mathrm{d}z}_{\text{Material content in the section at time } t=0} + \underbrace{\int_0^t [\dot{V}(0,t)x_{\mu,i}(0,t)/v_\mu(\vec{x}_\mu(0,t))]\,\mathrm{d}t}_{\text{Amount of compound } i \text{ which entered at } z=0} - \underbrace{\int_0^t [\dot{V}(z,t)x_{\mu,i}(z,t)/v_\mu(\vec{x}_\mu(z,t))]\,\mathrm{d}t}_{\text{Amount of compound } i \text{ which left the section at } z} \tag{5}$$

$i = a, \ldots, m$, where the term $\dot{V}(z,t)$ represents the flow-rate considered to be a function of z and t and v_μ is the mean molar volume of the mobile phase. Partial differentiation of eqn. 5 first with reference to time and then to length gives the differential equation of the material balance as follows:

$$(1/L)\frac{\partial}{\partial t}[n_{\kappa,i}(\vec{x}_\mu(z,t))] = -\frac{\partial}{\partial z}[\dot{V}(z,t)x_{\mu,i}(z,t)/v_\mu(\vec{x}_\mu(z,t))] \tag{6}$$

With suitable initial and boundary conditions, this set of m partial differential equa-

tions determines the m functions in question: $m - 1$ composition functions, $x_{\mu,i}(z,t)$, for the components $a, \ldots, i, \ldots, (m-1)$ and the mth function, the flow-rate, $\dot{V}(z,t)$. It is shown in the Appendix that, by an appropriate change of variables, the system can be reduced to a set of $m - 1$ equations for the components of the unknown composition vector $\vec{x}_\mu(z,t)$.

Seeking a specific solution for *analytical chromatography under isothermal and isocratic* conditions, appropriate initial conditions are now given as follows. Prior to chromatography the column is equilibrated with the eluent which is an N-component mixture of the composition $\vec{x}_\mu^0$ with components designated by capital letters A, ..., J, ..., N. The superscript zero refers to the time $t = 0$ when the column is ready for injection and eluent of identical composition will enter at the inlet ($z = 0$) and leave at the outlet ($z = L$), suggesting that this is also the composition of the mobile phase throughout the column:

$$\vec{x}_\mu(z,t=0) = \text{constant} = \vec{x}_\mu^0 \tag{7}$$

At the time $t = 0$ the composition of the incoming mixture is modified by injection of an infinitesimal sample. This will introduce a composition change in a small section of the column. As the signal is infinitesimal, only the case of one solute will be treated, as at infinite dilution the solutes do not interact and their retention volumes are independent of one another (see also Appendix). The vector $\vec{x}_\mu = \vec{x}_\mu(z,t)$ is the composition vector of the eluent also containing a solute, $\vec{x}_{\mu,su}$. For reasons of uniformity and (as will be seen later) of simplicity, the molar fraction of one of the components of the eluent will always be considered as the dependent variable $\vec{x}_\mu = (x_{\mu,A}, \ldots, x_{\mu,J}, \ldots, x_{\mu,N-1}, x_{\mu,su})$. Even by considering only infinitesimal perturbations of the composition, the complete solution of the mathematical problem is only possible if the eluent contains not more than two components (*i.e.*, the eluent is a binary mixture). In this case the retention volume of an infinitesimal perturbation of the concentration vector is given by

$$V_{R,i} = v_\mu^0 \left[\left(\frac{\partial n_{\kappa,i}}{\partial x_{\mu,i}} \right)_{\vec{x}_\mu^0} - x_{\mu,i}^0 \left(\frac{\partial n_{\kappa,\text{tot}}}{\partial x_{\mu,i}} \right)_{\vec{x}_\mu^0} \right] \tag{8}$$

where $v_\mu^0 = v_\mu(\vec{x}_\mu^0)$ is the mean molar volume of the eluent and all other symbols are as previously defined. If i is a solute, its initial concentration $x_{\mu,i}^0 = 0$ and eqn. 8 yields the retention volume in the usual sense. If a small sample of one of the components, A or B, of the binary eluent is injected, the resulting peak is called the "concentration peak" and its retention volume is designated as $V_{R,cc}$. As the composition of the binary eluent is given by only one independent variable [*i.e.*, $\vec{x}_\mu^0 = (x_{\mu,A}^0)$ as $x_{\mu,B} = 1 - x_{\mu,A}$] there will be only one concentration peak. In general, the injection of a solute will also perturb the concentration of the mixture, and therefore two peaks will appear: the peak of the solute and that of the concentration perturbation, as illustrated in Fig. 2.

With binary mixtures as eluent *eqn. 8 is a retention equation of general validity* for isothermal, isocratic analytical chromatography and the solution is independent of the retention mechanism. For the retention volume of solutes it is also valid in any

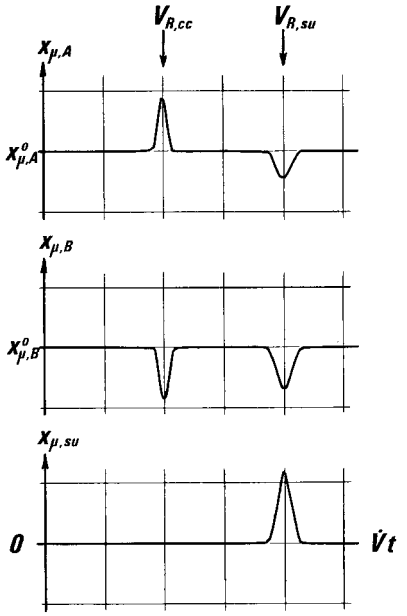

Fig. 2. Trace of a detector capable of measuring the concentration, $\vec{x}_\mu(L,t)$ (molar fraction), after injection of a solute, su, in an eluent composed of a binary mixture with components A and B. Composition of the eluent before injection is designated by $\vec{x}^0_\mu$; $V_{R,cc}$ is the retention volume of the perturbation of the eluent composition; $V_{R,su}$ is that of the solute; $\dot{V}$ is the (constant) flow-rate of the eluent; and t is time. Note that $x_{\mu,A} + x_{\mu,B} + x_{\mu,su} = 1$.

N-component eluent. Its application to liquid–solid chromatography will be shown in a separate section.

In order to demonstrate its versatility, eqn. 8 will now be applied to a well known case: gas–liquid chromatography with a mobile phase composed of a mixture of two ideal gases; component S is soluble in the liquid stationary phase whereas component I is insoluble. The volume of the gas phase in the chromatographic column will be designated by V_μ. Further, it is supposed that the liquid film on the inert solid support has the same density, d_σ, as that of the bulk. Therefore, the volume of the stationary phase can be calculated as $V_\sigma = w_\sigma/d_\sigma$, where w_σ is the mass of the stationary liquid in the column. The column capacity is then calculated as

$$n_{\kappa,J} = V_\mu c_{\mu,J} + V_\sigma c_{\sigma,J} = V_\mu x_{\mu,J}/v_\mu + V_\sigma c_{\sigma,J} \tag{9}$$

where v_μ is the molar volume of the gas phase and J refers to one of the components of the mobile phase (I or S). The gas phase will always behave as a mixture of ideal gases such that $v_\mu(\vec{x}^0_\mu) = v_\mu(\vec{x}_\mu) = RT_c/\bar{P}_c$. Also, as component I is insoluble in the stationary phase, the column capacity is

$$n_{\kappa,tot} = V_\mu/v_\mu + V_\sigma c_{\sigma,S} \tag{10}$$

Eqn. 11 results from the use of eqns. 9 and 10 in eqn. 8 to calculate the retention volume:

$$V_{R,J} = V_\mu + V_\sigma(1 - x^0_{\mu,J})\, v_\mu \left(\frac{\partial c_{\sigma,J}}{\partial x_{\mu,J}}\right)_{x^0_{\mu,J}} \tag{11}$$

This same result was found by Valentin and Guiochon[16] in their discussion of the "step and pulse method" for the determination of equilibrium isotherms (the "method of minor disturbance" in ref. 17). The reasoning used by these authors is, in principle, the same as that presented here, with the restriction that their treatment applies only to the specific case of gas chromatography.

Eqn. 11 gives the same retention volume for the perturbation of the eluent composition by the injection of a very small amount of S or I ("concentration peak", cc):

$$V_{R,cc} = V_\mu + V_\sigma\, v_\mu\, (1 - x^0_{\mu,S}) \left(\frac{\partial c_{\sigma,S}}{\partial x_{\mu,S}}\right)_{x^0_{\mu,S}} \tag{12}$$

expressed with $x_{\mu,S}$ as the independent variable. Of course, the polarity of the detector signal will be inverted depending on whether S or I was injected. Eqn. 11 may be further applied to two special situations. In the first case, the concentration of the soluble gas, $x^0_{\mu,S}$, is diminished to a small value, small enough that $(1 - x^0_{\mu,S}) \approx 1$ but much higher than the concentration perturbation introduced by a sample. For the injection of an "infinitesimal" amount of the insoluble carrier eqn. 12 gives the following for the retention volume of the "vacancy peak" (subscript vp; a special case of the concentration peak):

$$V_{R,vp} = V_\mu + V_\sigma v_\mu \left(\frac{\partial c_{\sigma,S}}{\partial x_{\mu,S}}\right)_{\sim 0} = V_\mu + k_S^{(id*)}\, V_\sigma$$

where $k_S^{(id*)}$ is the partition coefficient in the classical sense of the soluble gas, S, at ideal dilution, but, as the asterisk indicates, referring to a stationary phase saturated with the gas S. At these low concentrations eqn. 13 may be generalized. If the gas S is a mixture of n components, $S_a, \ldots, S_j, \ldots, S_n$, but the total concentration of the soluble gases remains small, then the injection of an even smaller amount of the insoluble carrier will provoke a "vacancy chromatogram" as a series of "negative" peaks[18]. Eqn. 13 is valid for the retention volume of every component, S_j, in this chromatogram. In the second special case there is only an insoluble carrier ($x^0_{\mu,S} = 0$) and the soluble carrier is injected as solute, su $\equiv$ S. Eqn. 12 simplifies to

$$V_{R,su} = V_\mu + V_\sigma v_\mu \left(\frac{\partial c_{\sigma,S}}{\partial x_{\mu,S}}\right)_0 = V_\mu + k_S^{(id)}\, V_\sigma \tag{14}$$

and gives the classical relationship for partition chromatography as presented by Martin and Synge[19]. Eqn. 14 can also be generalized for an n-component sample of solutes. Comparing eqns. 13 and 14 it is seen that a "vacancy chromatogram" is the mirror image reflected through the baseline of that made in the normal mode if $k^{(id*)} = k^{(id)}$.

In summary, this section has shown that the chromatographic process can be described in terms of the column capacities, $\vec{n}_\kappa$, and the composition of the mobile phase, $\vec{x}_\mu$. The composition vector is known and its deviation around the constant eluent composition, $\vec{x}^0_\mu$, is measured by a detector subsequent to the chromatographic column. On the other hand, for the measurement of the unknown column capacity only a non-chromatographic method was available, namely to empty the mobile phase from the column and then determine amount and composition of the column yield.

CHROMATOGRAPHIC DETERMINATION OF THE COLUMN CAPACITY

Let us imagine a solute, J*, which is in every respect identical with component J of the eluent with the exception of one property permitting its detection. Obviously the two compounds are inseparable and the same molar ratio will be found everywhere in any system. In the chromatographic column, the following holds true:

$$\frac{n_{\kappa,J*}}{n_{\kappa,J}} = \frac{x_{\mu,J*}}{x_{\mu,J}} \left(= \frac{p_{\mu,J*}}{p_{\mu,J}} = \frac{\varphi_{\mu,J*}}{\varphi_{\mu,J}} \right) \tag{15}$$

The retention volume of the labelled component J* can be calculated with eqn. 8 by substituting the partial derivative computed with the aid of eqn. 15. This results in

$$V_{R,J*} = v^0_\mu \left(\frac{\hat{c} n_{\kappa,J*}}{\hat{c} x_{\mu,J*}} \right)_{\vec{x}^0_\mu} = v^0_\mu n^0_{\kappa,J} / x^0_{\mu,J} \tag{16}$$

Rearrangement of eqn. 16 gives the relationship between molar component capacity, total molar eluent capacity and retention volumes of the labelled components as follows:

$$n^0_{\kappa,J} = x^0_{\mu,J} V_{R,J*} / v^0_\mu \tag{17}$$

$$n^0_{\kappa,tot} = \sum_{J=A}^{N} (x^0_{\mu,J} V_{R,J*} / v^0_\mu) \tag{18}$$

Eqn. 18 gives the method of determination of the molar total eluent capacity of the column.

Following the suggestion of Knox and co-workers, for chromatographic purposes labelled solutes can best be approximated by compounds containing radioactive carbon[8]. Less satisfactory but much easier to work with regarding handling and detection are deuterated compounds proposed in ref. 20 and used by McCormick and Karger[6,7]. The best solution might be the use of a series of compounds with a different degree of deuteration. In general there is a small change in physical properties with the degree of deuteration from non-deuterated to fully deuterated compounds. To a first approximation, this change may be considered to be linear. Therefore, retention volumes of compounds deuterated to different degrees, *e.g.*, 50 and 100%, could be extrapolated to 0% to give retention volumes of "labelled but not deuterated compounds".

ADSORPTION AT A LIQUID–SOLID INTERFACE

In the *classical experiment* demonstrating adsorption at a liquid–solid interface, a total of $n_{\tau,\mathrm{tot}}$ moles of an N-component liquid mixture of known composition $\vec{x}_\tau$ is brought into contact with a solid of surface area S. After equilibration there remains a liquid phase, the composition of which is determined at a point far enough from the interface to give $\vec{x}_\beta$ (β refers to the bulk). Any difference between the molar fraction of a component before and after contact, $\Delta x_\mathrm{J} = x_{\tau,\mathrm{J}} - x_{\beta,\mathrm{J}}$, is interpreted to be the effect of adsorption of the components of the mixture at the liquid–solid interface. It is concluded that there is a surface phase in which material is retained with a composition different from that of the bulk but it is now realized that the information, $n_{\tau,\mathrm{tot}}$, $\vec{x}_\tau$ and $\Delta\vec{x}$, is not sufficient to calculate the amount and composition of the adsorbed substance. Therefore, surface concentrations cannot be given.

Let us recall *Gibbs' proposal* to find the way out of this dilemma. For the description of the adsorption system in equilibrium a volume with a boundary parallel to the plane (not curved) interface, $V_{\beta/\mathrm{CX}}$, is chosen for the liquid bulk by some well defined "convention X" (referred to by the subscript "CX"). The plane placed parallel to the interface to limit the bulk is normally termed the "Gibbs dividing plane". It is assumed that material in this volume has the bulk composition, $\vec{x}_\beta$. Volume and composition determine the material content of the bulk $n_{\beta,\mathrm{J}}$, and as the total amount of component J in the system, $n_{\tau,\mathrm{J}}$, is known, the adsorbed material, $n_{\sigma,\mathrm{J}}$, can be calculated as in eqn. 19a. Further, being proved by experiment that the imbalance of the composition is proportional to the surface area of the solid, the following material balance can be written for each component:

$$n_{\sigma,\mathrm{J}} = S\Gamma_{\mathrm{J/CX}} = n_{\tau,\mathrm{J}} - x_{\beta,\mathrm{J}}\, V_{\beta/\mathrm{CX}}/v_\beta(\vec{x}_\beta) \quad (\mathrm{J} = \mathrm{A,B,\ldots,N}) \tag{19a}$$

The *surface concentration*, $\Gamma_{\mathrm{J/CX}}$, as defined by eqn. 19a and given in units of moles per unit surface area, clearly depends on the choice of the bulk volume and *can be positive or negative.*

Analogous reasoning can be applied in describing the adsorption process in terms of mass m and mass fraction p, resulting in surface concentrations Π, expressed in units of mass/surface area. The resulting material balance can also be obtained by multiplication of eqn. 19a with the molar mass, M_J, of component J, giving

$$m_{\sigma,\mathrm{J}} = n_{\sigma,\mathrm{J}}M_\mathrm{J} = S\Pi_{\mathrm{J/CX}} = m_{\tau,\mathrm{J}} - p_{\beta,\mathrm{J}}\, V_{\beta/\mathrm{CX}}/\tilde{v}_\beta(\vec{p}_\beta) \tag{19b}$$

where $\tilde{v}_\beta(\vec{p}_\beta) = v_\beta(\vec{x}_\beta)/M_\beta$ is the specific volume of the mixture in the bulk at the composition $\vec{p}_\beta$ (M_β is the mean molar mass of the bulk).

Multiplication of eqn. 19a by the partial molar volume, $v_\mathrm{J}(\vec{x}_\beta)$, of component J results in a similar material balance in terms of volume, V, volume fraction, φ, and surface concentration, Ψ, in units of volume/surface area given by eqn. 19c:

$$V_{\sigma,\mathrm{J}} = v_\mathrm{J}(\vec{\varphi}_\beta)n_{\sigma,\mathrm{J}} = S\Psi_{\mathrm{J/CX}} = V_{\tau,\mathrm{J}}(\vec{\varphi}_\beta) - \varphi_{\beta,\mathrm{J}}\, V_{\beta/\mathrm{CX}} \tag{19c}$$

The language of eqn. 19c is unusual in application of Gibbs' procedure. Its basic drawback lies in the fact that partial volumes, being functions of the composition,

pressure and temperature, are also different in an adsorbed state. The value of a partial volume will change with the concentration gradient generated by the force field near the interface and its (average) value in the surface phase will not be known. In the adsorption system only the bulk has a well defined composition and there is no other choice but to refer to a partial volume at the bulk composition after the adsorption process ($\bar{x}_\beta$). In conclusion, all disadvantages of this language originate from the "non-ideality" of fluid mixtures. Concerning volumes, however, the laws of ideal mixtures are in general good approximations for non-ionic liquid mixtures. Therefore, apart from some drawbacks, this language has several advantages. Surface concentrations expressed as volume per unit surface area are easy to visualize. In Figs. 3–5 these units are chosen to illustrate the principle of Gibbs' procedure. With the example of a binary (ideal) liquid mixture it is illustrated in Fig. 3 that surface concentrations depend directly on the position of the dividing plane, *i.e.*, on the volume attributed to the bulk.

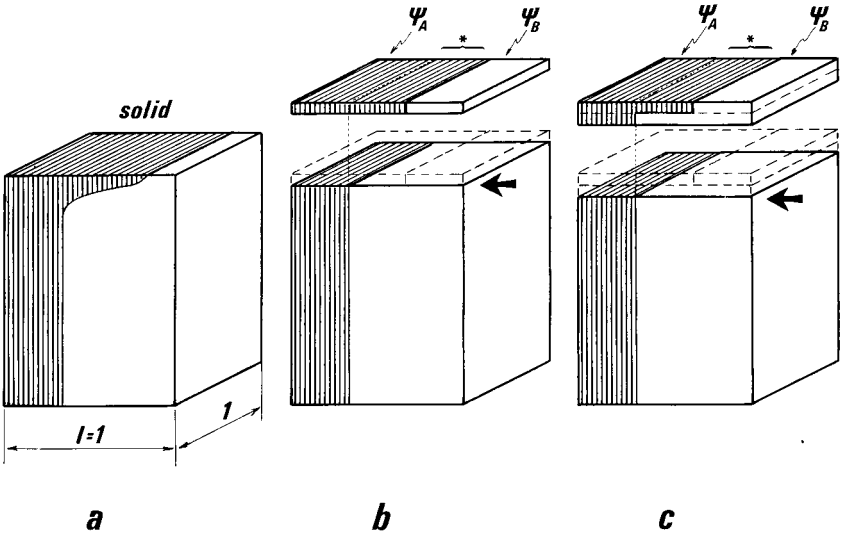

Fig. 3. Illustration of the adsorption in a binary liquid mixture at the interface in contact with a solid (above the liquid, not shown). (a) Near the interface there is a concentration gradient. (b), (c) A plane is placed parallel to the surface at two different positions chosen by purely arbitrary conventions. The portion cut off is considered as the surface phase accounting for the whole concentration difference near the surface. The bulk has now a well defined volume, V_β, and, being homogeneous, a well defined material content, $V_\beta (c_{\beta,A} + c_{\beta,B})$. The position of the plane (arrow) determines also the volumes of A and B left in the surface phase which, projected to the surface area of the dividing plane, give surface concentrations in units of volume/surface area. Note that the surface concentration of components Ψ_A and Ψ_B strongly depend on the position of the dividing plane. For the volume designated by an asterisk, see caption to Fig. 4.

The question now arises of how to fix the position of the Gibbs' dividing plane, and more specifically, how to fix it by an internal convention. Internal conventions are those which refer to the adsorption process itself. In the present treatment surface concentrations will only be referred to "classical" internal conventions. For an N-component mixture there are N conventions stating that component "J is not ad-

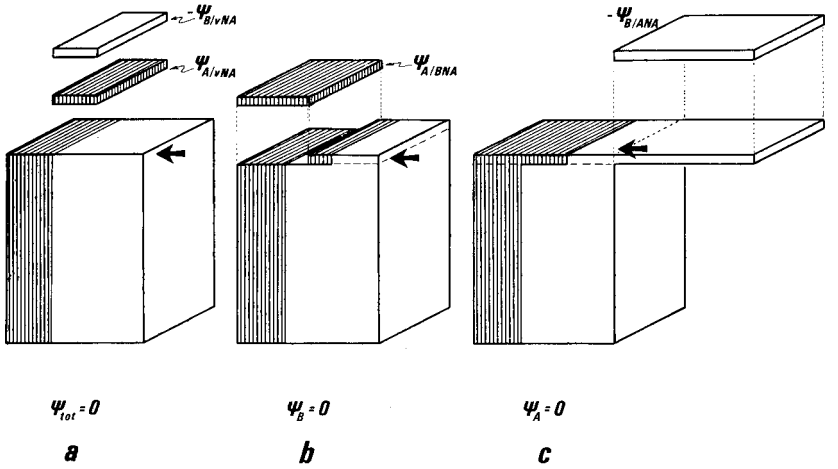

Fig. 4. Illustration of the surface concentration of adsorbed components, Ψ (volume/surface area), for three of the "classical" conventions to fix the position of the Gibbs dividing plane at the liquid–solid interface of a binary liquid mixture. The solid is above the liquid (not shown, as in Fig. 3). The component A is the more strongly adsorbed component while B exhibits a weaker adsorption. Note that for the sake of demonstration, the additional volume is not spread over the liquid surface (as it should be), extending the homogeneous liquid column up to the dividing plane the approximate position of which is marked by arrow. The excess concentration referring to the *v*NA convention is also identified in Fig. 3 (see in Fig. 3 the volume designated by an asterisk).

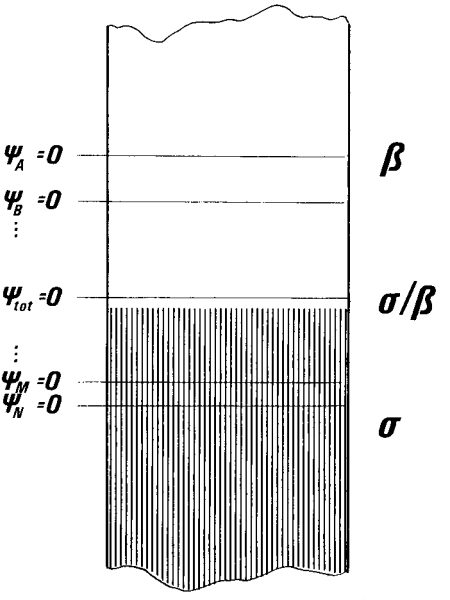

Fig. 5. "Classical" positions of the Gibbs dividing plane at the solid–liquid (σ/β) interface of an N-component liquid mixture defined by the conditions indicated. Concentration of components in the surface phase, $\Psi_A, \ldots, \Psi_N$, are given in units of volume/surface area. The component adsorbed weakest is A and adsorption strength is increasing to N. The bulk volume is largest (exceeding into the solid) if the plane is placed with the convention that the strongest adsorbed component is considered to be non adsorbed ($\Psi_N = 0$) and smallest with the condition $\Psi_A = 0$. Note that with the condition that as an overall effect there is no adsorbed volume ($\Psi_{tot} = 0$), the dividing plane is near the physical interface.

TABLE I

SUMMARY OF THE RELATIONSHIPS (A) FOR THE INTERPRETATION OF RETENTION VOLUMES IN LIQUID-SOLID CHROMATOGRAPHY WITH AN *N*-COMPONENT LIQUID MIXTURE AS THE ELUENT AND (B) FOR THE DETERMINATION OF ADSORPTION ISOTHERMS AT THE LIQUID-SOLID INTERFACE OF BINARY LIQUID MIXTURES BY THE CHROMATOGRAPHIC METHOD

The symbols Γ, Π and Ψ represent surface concentrations in units of mol m^{-2}, g m^{-2} and ml m^{-2}, respectively, and x, p and φ are the corresponding dimensionless bulk concentrations: molar fraction, mass fraction and volume fraction. Lower-case Greek letters refer to material transported by the eluent being in the mobile phase, μ, in the stationary phase, σ, or referring to the total capacity of the column ($\kappa = \mu + \sigma$); in the static adsorption system σ has the same meaning and β refers to the bulk ($\tau = \beta + \sigma$). Capital J or K refers to components of the eluent, su to a solute and cc to a concentration perturbation of the eluent. The symbols n, m and v represent the number of moles, mass and volume, respectively; v is the partial molar volume and $\tilde{v}$ is the partial specific volume. An example for the interconversion of surface concentrations: $\Gamma_{J/n\mathrm{NA}}$ is to be converted to $\Pi_{J/m\mathrm{NA}}$: calculate first $\Gamma_{J/n\mathrm{NA}} M_J = \Pi_{J/n\mathrm{NA}}$ (mass concentration but with the incoherent convention) and substitute this into eqn. 24b. Interconversion in the JNA convention is simple, *e.g.*, $\Pi_{K/\mathrm{JNA}} = M_K \Gamma_{K/\mathrm{JNA}}$.

Convention		*Gibbs' conventions for the adsorption from an N-component liquid mixture at the liquid–solid interface; static system*				*Relationships for the interpretation of retention volumes in liquid–solid chromatography. Eluent: N-component mixture (see eqn. 4)*	
Definition	*CY*	*Equations for the calculation and interconversion of surface concentrations referring to a "classical" convention*		*Volume of the bulk,* $V_{\beta/CY}$		*Exptl. detn. of* $V_{\mu/CY}$	
$\Gamma_J = \Pi_J = \Psi_J = 0$	JNA (20)	$\Gamma_{K/\mathrm{JNA}} = \Gamma_{K/CX} - (x_{\beta,K}/x_{\beta,J})\,\Gamma_{J/CX}$	(22)	$n_{\tau,J} v_\beta / x_{\beta,J}$	(26)	$V_{R,J*}$	(32)
$\Gamma_{tot} = 0$	nNA (23a)	$\Gamma_{J/n\mathrm{NA}} = \Gamma_{J/CX} - x_{\beta,J} \sum_{K=A}^{N} \Gamma_{K/CX}$	(24a)	$v_\beta \sum_{K=A}^{N} n_{\tau,K}$	(27a)	$\sum_{K=A}^{N} x^0_{\mu,K} V_{R,K*}$	(38a)
$\Pi_{tot} = 0$	mNA (23b)	$\Pi_{J/m\mathrm{NA}} = \Pi_{J/CX} - p_{\beta,J} \sum_{K=A}^{N} \Pi_{K/CX}$	(24b)	$\tilde{v}_\beta \sum_{K=A}^{N} m_{\tau,K}$	(27b)	$\sum_{K=A}^{N} p^0_{\mu,K} V_{R,K*}$	(38b)
$\Psi_{tot} = 0$	vNA (23c)	$\Psi_{J/v\mathrm{NA}} = \Psi_{J/CX} - \varphi_{\beta,J} \sum_{K=A}^{N} \Psi_{K/CX}$	(24c)	$\sum_{K=A}^{N} n_{\tau,K} v_K$	(27c)	$\sum_{K=A}^{N} \varphi^0_{\mu,K} V_{R,K*}$	(38c)

* Note that $\Pi_{K/\mathrm{JNA}} = M_K \Gamma_{K/\mathrm{JNA}}$ and $\Psi_{K/\mathrm{JNA}} = v_K \Gamma_{K/\mathrm{JNA}}$.

** Valid for ideal mixtures only. For real mixtures see eqn. 94 in the Appendix.

sorbed". This JNA convention, as introduced, is independent of the units used, contrary to a further "nothing is adsorbed" NA convention. In this further case it is construed to fix the total amount adsorbed as zero in terms of number of moles (n) or mass (m) or volume (v). Consequently, there will be only one JNA convention but three different NA conventions: nNA, mNA and vNA.

In order to show that these conventions allow the calculation of well defined surface concentrations, let us suppose that surface concentrations referring to an

Experimental determination of points on the isotherm of A in a binary mixture, A + B

Const. of eqn. 43, ν_μ	*Peak propagation resistivity,* $\chi_{i,CY}$ *in eqn. 43*				*Concentration peak* $\chi_{cc/CY}$		*Isotherm of A:* Γ_A, Π_A *and* Ψ_A *from experiment*	
	Labelled K		*Solute*					
v_μ^0	$\left(\frac{\Gamma^0_{K/JNA}}{x_{\mu,K}}\right)$	(33)	$\left(\frac{\partial \Gamma_{su/JNA}}{\partial x_{\mu,su}}\right)_{\vec{x}_\mu^0}$	(34)	$\left(\frac{\partial \Gamma_{A/BNA}}{\partial x_{\mu,A}}\right)_{x^0_{\mu,A}}$	(35)	$x^0_{\mu,A} V_{N,A*}/S v^0_\mu$	(33)
v_μ^0	$\left(\frac{\Gamma^0_{K/nNA}}{x_{\mu,K}}\right)$	(36a)	$\left(\frac{\partial \Gamma_{su/nNA}}{\partial x_{\mu,su}}\right)_{\vec{x}_\mu^0}$	(39a)	$\left(\frac{\partial \Gamma_{A/nNA}}{\partial x_{\mu,A}}\right)_{x^0_{\mu,A}}$	(40a)	$\frac{(V_{R,A*} - V_{R,B*})\, x^0_{\mu,A} x^0_{\mu,B}}{S v^0_\mu}$	(45a)
$\tilde{v}_\mu^0$	$\left(\frac{\Pi^0_{K/mNA}}{p_{\mu,K}}\right)$	(36b)	$\left(\frac{\partial \Pi_{su/mNA}}{\partial p_{\mu,su}}\right)_{\vec{p}_\mu^0}$	(39b)	$\left(\frac{\partial \Pi_{A/mNA}}{\partial p_{\mu,A}}\right)_{p^0_{\mu,A}}$	(40b)	$\frac{(V_{R,A*} - V_{R,B*})\, p^0_{\mu,A} p^0_{\mu,B}}{S \tilde{v}^0_\mu}$	(45b)
1	$\left(\frac{\Psi^0_{K/vNA}}{\varphi_{\mu,K}}\right)$	(36c)	$\left(\frac{\partial \Psi_{su/vNA}}{\partial \varphi_{\beta,su}}\right)_{\vec{\varphi}_\mu^0}$	(39c)	$\left(\frac{\partial \Psi_{A/vNA}}{\partial \varphi_{\mu,A}}\right)^{\star\star}_{\varphi^0_{\mu,A}}$	(40c)	$\frac{(V_{R,A*} - V_{R,B*})\, \varphi^0_{\mu,A} \varphi^0_{\mu,B}}{S}$	(45c)

arbitrary convention, CX, are known. For a first example, it is presumed that

$$\Gamma_J = 0 \; (= \Pi_J = \Psi_J) \tag{20}$$

implementing the JNA convention in the n–x–Γ language. The link between surface concentrations referring to the CX and JNA conventions is formed by applying eqn. 19a successively to calculate $\Gamma_{K/CX}$, $\Gamma_{K/JNA}$ and $\Gamma_{J/JNA}$ (= 0). Combination of the

resulting expressions gives, after rearrangement, eqn. 21,

$$\Gamma_{K/JNA} = \Gamma_{K/CX} - (x_{\beta,K}/x_{\beta,J})\,[n_{\tau,J} - x_{\beta,J} V_{\beta/CX}/v_\beta(\vec{x}_\beta)]S \tag{21}$$

Comparison of eqn. 21 with eqn. 19a reveals that the coefficient of $(x_{\beta,K}/x_{\beta,J})$ is the surface concentration $\Gamma_{J/CX}$ and so

$$\Gamma_{K/JNA} = \Gamma_{K/CX} - (x_{\beta,K}/x_{\beta,J})\,\Gamma_{J/CX} \tag{22}$$

Eqn. 22 can be multiplied by M_K, the molar mass of component K, or by its partial molar volume, $v_K(\vec{x}_\beta)$, to give analogous expressions in terms of the variables p, Π and φ,Ψ without changing the convention.

To give "excess adsorption" or "reduced adsorption" in terms of number of moles the convention "nothing is adsorbed" (nNA convention) is given by

$$\Gamma_{tot} = \sum_{J=A}^{N} \Gamma_J = 0\ (\neq \Pi_{tot} \neq \Psi_{tot}) \tag{23a}$$

Similar reasoning to that leading to eqn. 22 gives, by using eqn. 23a in 19a, the surface concentration of component J:

$$\Gamma_{J/nNA} = \Gamma_{J/CX} - x_{\beta,J} \sum_{K=A}^{N} \Gamma_{K/CX} = \Gamma_{J/CX} - x_{\beta,J}\,\Gamma_{tot/CX} \tag{24a}$$

Analogous equations in terms of the variables m–p–Π and v–φ–Ψ with the conventions "mNA" and "vNA" are listed in Table I (eqns. 24b and c). Eqns. 24a, b and c imply that surface concentration and NA convention should be coherent meaning that the convention should be stated in units coherent with that of the surface concentration. Consequently, only $\Gamma_{J/nNA}$, $\Pi_{J/mNA}$ and $\Psi_{J/vNA}$ are *surface concentrations with coherent conventions*. Incoherent surface concentrations are obtained in equations of the following type:

$$\Gamma_{J/nNA}\, M_J = \Pi_{J/nNA} \tag{25}$$

where M_J is the molecular mass of J. Obviously, the mass surface concentration in eqn. 25 refers to the nNA convention and can be substituted into eqn. 24b to be converted to $\Pi_{J/mNA}$ with the coherent convention if the surface concentrations of all components are known in the nNA convention. Sometimes incoherent surface concentrations are encountered in the literature (see, *e.g.*, $\Gamma_{J/vNA}$ in refs. 7 and 11).

Surface concentrations defined in eqns. 24 and 26 are independent of the position of the Gibbs dividing plane. Alternatively, these surface concentrations are true surface concentrations for a particular position of the dividing plane fixed by the convention which is characterized by the condition stated in the convention (*e.g.*, $\Gamma_J = 0$ for the JNA convention or $\Psi_{tot} = 0$ for the vNA convention, etc.). Fig. 4 illustrates the three "classical" positions of the Gibbs dividing plane for a binary mixture and Fig. 5 the N+1 positions of this plane for an N-component mixture where conventions are stated in terms of concentrations expressed in v–φ–Ψ units. It can be seen

that the dividing plane is inside the liquid mixture if the adsorption is expressed relative to that of the weaker adsorbed substance and inside the solid if the stronger adsorbed substance is the standard. For the following discussion note that in practice the plane corresponding to the vNA convention is very near to the physical surface of the liquid.

The calculation of the bulk volume corresponding to a given convention is straightforward. For an example, applying the JNA convention expressed in eqn. 20 to eqn. 19a gives

$$V_{\beta/\mathrm{JNA}} = v_\beta(\vec{x}_\beta)\, n_{\tau,\mathrm{J}}/x_{\beta,\mathrm{J}} \tag{26}$$

where $V_{\beta/\mathrm{JNA}}$ designates the value of the bulk phase volume with reference to the convention. The bulk volume corresponding to the nNA convention is obtained by summing eqn. 19a over all components in the system to give, after rearrangement

$$V_{\beta/n\mathrm{NA}} = v_\beta(\vec{x}_\beta) \sum_{\mathrm{J=A}}^{\mathrm{N}} n_{\tau,\mathrm{J}} \tag{27a}$$

where the symbol $V_{\beta/n\mathrm{NA}}$ stands for the volume of the bulk with reference to this specific convention and the units used to introduce the convention. Bulk volumes referring to other conventions are listed in Table I.

In summarizing Gibbs' procedure, let us emphasize three points before applying the results to liquid–solid chromatography:

(a) Surface concentrations $\Gamma_{\mathrm{J/CX}}$, $\Pi_{\mathrm{J/CX}}$ and $\Psi_{\mathrm{J/CX}}$ are intensive equilibrium properties of the adsorption system and so at a given temperature and pressure they are functions of the bulk composition only:

$$\Gamma_{\mathrm{J/CX}} = \Gamma_{\mathrm{J/CX}}(\vec{x}_\beta) \qquad \text{(mol/surface area)} \tag{28a}$$

$$\Pi_{\mathrm{J/CX}} = \Pi_{\mathrm{J/CX}}(\vec{\rho}_\beta) \qquad \text{(mass/surface area)} \tag{28b}$$

$$\Psi_{\mathrm{J/CX}} = \Psi_{\mathrm{J/CX}}(\vec{\varphi}_\beta) \qquad \text{(volume/surface area)} \tag{28c}$$

As already mentioned, units for convention and surface concentration should be coherent and should refer to one of the three systems: the n–x–Γ system of molar units (referred to by the subscript n), the m–p–Π system of mass units (m) or the v–φ–Ψ system of volume units (v).

(b) Bulk volume, $V_{\beta/\mathrm{CX}}$, has the dimensions of volume but is a convention and has no physical meaning. Its value depends on the total number of moles, $\vec{n}_\tau$, and on the composition of the bulk if the convention is internal.

(c) There is an important difference between the system in the classical adsorption experiment and that determined by the chromatographic column; in the latter case the overall volume of the liquid–solid system is imposed.

LIQUID–SOLID ADSORPTION CHROMATOGRAPHY

By identifying the composition of the "mobile phase" ($\vec{x}_\mu$) in the chromatographic model with that of the "bulk liquid" ($\vec{x}_\beta$), and the capacity vector of the chro-

matographic column ($\vec{n}_\kappa$) with the vector of total number of moles in the adsorption system ($\vec{n}_\tau$) the retention volume in liquid–solid chromatography is easy to calculate by use of eqn. 8. This derivation will be demonstrated by applying units related to number of moles, n (for analogous derivations in other units, see Appendix and Table I).

The molar component capacity of the column for any substance, i, is calculated using eqn. 19a ($\beta \rightarrow \mu$; $\tau \rightarrow \kappa$) to give, after rearrangement:

$$n_{\kappa,i} = x_{\mu,i} V_{\mu/\mathrm{CX}} / v_\mu(\vec{x}_\mu) + S\Gamma_{i/\mathrm{CX}} \tag{29}$$

By summing eqn. 29 over all components in the system, the molar total capacity is given by

$$n_{\kappa,\mathrm{tot}} = V_{\mu/\mathrm{CX}} / v_\mu(\vec{x}_\mu) + S\Gamma_{\mathrm{tot/CX}} \tag{30}$$

Using eqns. 29 and 30 in eqn. 8, the retention volume of component i is calculated as

$$V_{\mathrm{R},i} = V_{\mu/\mathrm{CX}}(\vec{x}^0_\mu) + S\, v^0_\mu \left[\left(\frac{\partial \Gamma_{i/\mathrm{CX}}}{\partial x_{\mu,i}} \right)_{\vec{x}^0_\mu} - x^0_{\mu,i} \left(\frac{\partial \Gamma_{\mathrm{tot/CX}}}{\partial x_{\mu,i}} \right)_{\vec{x}^0_\mu} \right] \tag{31}$$

Let us now apply eqn. 31 to the three cases important for analytical chromatography: the retention volume of labelled components of the eluent, of the concentration peak (binary eluent) and of solutes.

With the convention "J is not adsorbed" (J is a component of the eluent), eqn. 31 gives for labelled J:

$$V_{\mathrm{R,J}*} = V_{\mu/\mathrm{JNA}} \tag{32}$$

giving the experimental method for the determination of $V_{\mu/\mathrm{JNA}}$. For labelled K, the following equation results;

$$V_{\mathrm{R,K}*} = V_{\mu,\mathrm{JNA}} + S\, v^0_\mu \left(\frac{\Gamma^0_{\mathrm{K/JNA}}}{x^0_{\mu,\mathrm{K}}} \right) \tag{33}$$

For a solute the following equation results:

$$V_{\mathrm{R,su}} = V_{\mu/\mathrm{JNA}} + S\, v^0_\mu \left(\frac{\partial \Gamma_{\mathrm{su/JNA}}}{\partial x_{\mu,\mathrm{su}}} \right)_{\vec{x}^0_\mu} \tag{34}$$

Injection of a solute always perturbs the eluent concentration, and therefore the peak given in eqn. 34 will always be accompanied by (one or more) concentration peaks (probably there will be $N-1$ concentration peaks[4]). In a binary eluent, eqn. 31 gives for the perturbation of the concentration (J ≡ B) "a concentration peak"[17,21] with the retention volume given by eqn. 35:

$$V_{\mathrm{R,cc}} = V_{\mu/\mathrm{BNA}} + S\, v^0_\mu \left(\frac{\partial \Gamma_{\mathrm{A/BNA}}}{\partial x_{\mu,\mathrm{A}}} \right)_{\vec{x}^0_{\mu,\mathrm{A}}} \tag{35}$$

With the convention "nothing is adsorbed" eqn. 31 reduces to a particularly simple form. Considering that by definition $\Gamma_{\mathrm{tot}/n\mathrm{NA}} = 0$, eqn. 31 is transformed into

$$V_{\mathrm{R},i} = V_{\mu/n\mathrm{NA}} + S\, v_{\mu}^{0} \left(\frac{\partial \Gamma_{i/n\mathrm{NA}}}{\partial x_{\mu,i}} \right)_{\vec{x}_{\mu}^{0}} \tag{36a}$$

For labelled J eqn. 36 gives

$$V_{\mathrm{R,J}*} = V_{\mu/n\mathrm{NA}} + S\, v_{\mu}^{0} \left(\frac{\Gamma_{\mathrm{J}/n\mathrm{NA}}^{0}}{x_{\mu,\mathrm{J}}^{0}} \right) \tag{37}$$

Multiplication of eqn. 37 by $x_{\mu,\mathrm{J}}$ and summing the N equations gives the experimental method for the determination of the volume, $V_{\mu/n\mathrm{NA}}$, referring to this convention:

$$V_{\mu/n\mathrm{NA}} = \sum_{\mathrm{J=A}}^{\mathrm{N}} x_{\mu,\mathrm{J}}^{0}\, V_{\mathrm{R,J}*} \tag{38a}$$

Application of eqn. 36 to a solute gives

$$V_{\mathrm{R,su}} = V_{\mu/n\mathrm{NA}} + S\, v_{\mu}^{0} \left(\frac{\partial \Gamma_{\mathrm{su}/n\mathrm{NA}}}{\partial x_{\mu,\mathrm{su}}} \right)_{\vec{x}_{\mu}^{0}} \tag{39a}$$

Finally, the retention volume of a concentration peak in a binary mixture is given by

$$V_{\mathrm{R,cc}} = V_{\mu/n\mathrm{NA}} + S\, v_{\mu}^{0} \left(\frac{\partial \Gamma_{\mathrm{A}/n\mathrm{NA}}}{\partial x_{\mu,\mathrm{A}}} \right)_{x_{\mu,\mathrm{A}}^{0}} \tag{40a}$$

The derivations followed in eqns. 31–36–40 were repeated, *mutatis mutandis*, with the *p*NA and *t*NA conventions. The results are listed in Table I.

The general form of the equation for liquid–solid chromatography is

$$V_{\mathrm{R},i} = V_{\mu/\mathrm{CX}}\,(\vec{x}_{\mu}^{0}) + S\, v_{\mu}\, \chi_{i/\mathrm{CX}} \tag{41}$$

where v_{μ} is a property of the eluent and $\chi_{i/\mathrm{CX}}$ will be referred to as the *peak propagation resistivity* of the stationary phase in question for compound *i*.

It is interesting to compare this expression with the "classical" equation for the retention volume in partition chromatography given in eqn. 14. The first term in eqn. 41 is independent of the solute and therefore it will be interpreted as a "hold-up volume by convention". The second term is proportional to the surface area of the adsorbent, S, which has the same role as the volume of the stationary phase, V_{σ}, and finally the coefficient of S is analogous to the partition coefficient. Let us emphasize that these analogies are purely formal with the exception of that between S and V_{σ}. The hold-up volume is the result of a convention and therefore it has no physical meaning. Further, a partition coefficient can never become negative and $\chi_{i/\mathrm{CX}}$ in eqn. 41 can. However, it is right to designate the peak propagation resistivity of a solute as a Henry coefficient. It is now clear that "net retention volumes" can be defined by

analogy with classical partition chromatography as

$$V_{N,i/CX} = V_{R,i} - V_{\mu/CX} \tag{42}$$

but they will depend on the convention. Specific retention volumes should be referred to unit surface area of the adsorbent;

$$V_{S,i/CX} = V_{N,i/CX}/S = v_{\mu}\,\chi_{i/CX} \tag{43}$$

Equations listed in Table I give all the information necessary to determine the hold-up volume experimentally and to interpret retention volumes correctly with reference to a given convention.

It was repeatedly stressed that hold-up volumes are based purely upon conventions but the question now arises as to which hold-up volume is nearest to the "geometrical interstitial volume" of the column. Although at first sight real to some extent, this volume is also an undefined quantity, having no special convention to fix exactly the position of the dividing plane. Actually, the volume eluent capacity of the column measured with a pure liquid would be the geometrical interstitial volume if the density (specific volume) of the liquid in question was the same in the bulk and adsorbed state and if the boundary between liquid and solid was independent of the nature of the liquid. If these two conditions are fulfilled, the proposition of refs. 22 and 23 to calculate this volume from the weight difference of the column filled with two liquids and using the density of the pure non-adsorbed liquid in the calculations would result in the correct answer. An additional condition should be fulfilled if mixtures are used for its determination: the partial molar volumes of the components should remain the same at the composition of the surface phase as they are in the bulk. In practice, in non-ionic mixtures, partial molar volumes can be considered to be independent of composition to within 3%. It is therefore expected that the volume eluent capacity will also be a constant within these limits if the pore size of the solid is such that exclusion effects may be ignored.

DETERMINATION OF THE ADSORPTION ISOTHERM IN BINARY LIQUID MIXTURES

In the case of a binary eluent, composed of A and B, derivation of the necessary equations for the determination of the "composite isotherm" is straightforward.

In binary eluents there is only one independent variable of composition and points on this isotherm can easily be calculated from retention data of labelled A and B. For example, in the case of the molar "nothing is adsorbed" convention the sum of $\Gamma_{A/nNA}$ and $\Gamma_{B/nNA}$ is zero, and therefore

$$\Gamma_{B/nNA} = -\Gamma_{A/nNA} \tag{44}$$

Eqn. 37 applied to solutes A* and B* and the combination of the results with eqn. 44 produces, after rearrangement

$$\Gamma_{A/nNA}(x^0_{\mu,A}) = (V_{R,A*} - V_{R,B*})x^0_{\mu,A}\,x^0_{\mu,B}/S\,v^0_{\mu} \tag{45a}$$

By injection of labelled A or B a concentration peak is also produced, its net retention volume providing the first derivative of the isotherm as further information. Combination of eqns. 40 and 42 gives

$$\left(\frac{\partial \Gamma_{A/nNA}}{\partial x_{\mu,A}}\right)_{x^0_{\mu,A}} = V_{N,cc/nNA}/v^0_\mu S \tag{46}$$

Complete information is given for isotherms expressed in other units in Table I.

The relationship of the retention volumes of labelled compounds and of the concentration perturbation to the composite isotherm in a binary mixture is illustrated in Fig. 6. The retention volumes were calculated for the two possible shapes of the composite isotherm, U- and S-shaped, using the volume/surface language and the convention $\Psi_{tot} = 0$.

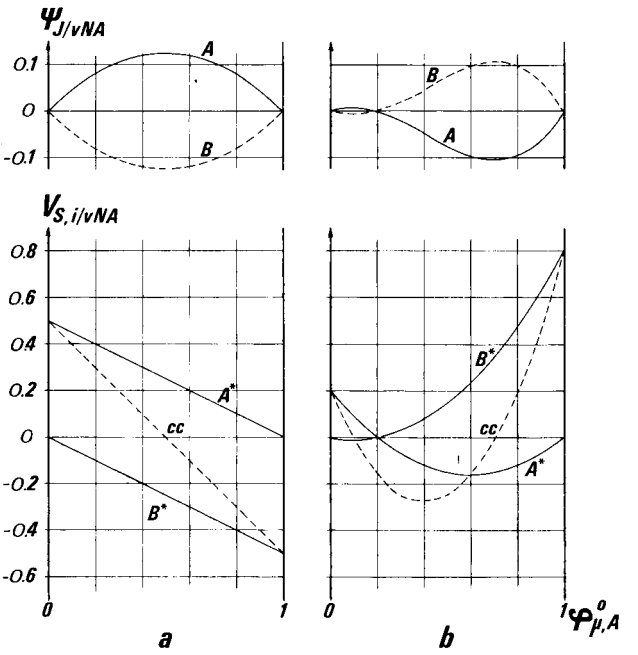

Fig. 6. Relationship between the composite isotherm of component A of a binary liquid mixture, $\Psi_{A/nNA}$, and the specific retention volumes of the labelled components, A* and B*, and the perturbation of the concentration, cc, if the ideal mixture of A and B is used as the eluent. The specific retention volume, designated by $V_{S,i/nNA}$, is the net retention volume referred to 1 m^2 of adsorbent surface and to the specific condition $\Psi_{tot} = 0$. The example constructed employs arbitrary units but in practice figures of similar order of magnitude are obtained if expressing the data in units of $\mu l\ m^{-2}$ (= nm). (a) The equation used for the U-shaped isotherm is $\Psi_{A/vNA} = \varphi^0_{\mu,A}\varphi^0_{\mu,B}/2$; (b) the equation for the S-shaped isotherm is $\Psi_{A/nNA} = \varphi^0_{\mu,B}(0.2 - \varphi^0_{\mu,A})$.

CONCLUSION

The results of this discussion may be important in two areas. The first concerns the experimental determination of composite adsorption isotherms. By the classical

method, a given amount of a liquid mixture of known composition is equilibrated with a given amount of adsorbent and a point on the adsorption isotherm is calculated from the composition change. Experimentally, this method is relatively easy with powders with high-energy surfaces where the wetting angle is zero or very nearly so. Even in this case, equilibrium times of several hours are common. The chromatographic method might considerably reduce the time of the determination of the twenty or more experimental points necessary to describe the isotherm. Concerning hydrophobic, low-energy surfaces, this could be the only method for the determination of composite adsorption isotherms at surfaces not wettable by the liquid. Inspite of wetting angles of up to 100° (water on paraffinic surfaces)[24], even small mesopores would be completely filled at the pressures usually applied in liquid chromatography to establish the necessary contact between the liquid and the whole surface of the low-energy solid. For the calculation of isotherms, the experimental points must be evaluated in the coherent language of units and of a specific convention. Of course, one could create new conventions; the composite isotherm symbolized by $\Gamma_{J/vNA}$ is given in units of mol m^{-2} but the position of the Gibbs dividing plane is determined by the requirement that the total adsorbed volume is zero and not the total adsorbed number of moles, and consequently $\Sigma \Gamma_{J/vNA} \neq 0$. Isotherms with such unusual conventions are described in refs. 7 and 11.

The second area is liquid–solid chromatography. Retention data have a definite meaning only if the hold-up volume is determined in the "self-consistent field" of the logic of the adsorption process. Of course, it would be desirable for data to be interconvertible. Actually they are, but only if detailed knowledge is available about the properties and adsorption behaviour of the components of the eluent, *i.e.*, if all the $N-1$ independent isotherms are known. For the recording and publication of liquid chromatographic data there appears to be a serious problem of communication and two related questions must be asked: (a) what is the best language to be applied in the calculation of hold-up volumes?, and (b) what is the net retention volume in liquid chromatography?

The hold-up volume, $V_{\mu/vNA}$, has already been proposed and by Knox and coworkers[8] for general use. Indeed, in practice a hold-up volume that is easy to model would be advantageous and an approximately constant hold-up volume would be preferable in approximate calculations. These arguments point very strongly towards the convention "nothing is adsorbed" in terms of volume, $V_{\mu/vNA}$. Further, as already mentioned, this hold-up volume is nearest to some sort of geometrical interstitial volume in the column and it can also be approximated by the weighing method of refs. 22 and 23 if adsorbents of low surface energy are used, as in reversed-phase chromatography. On the other hand, theoretical arguments are in favour of the relative adsorption language with the "J is not adsorbed" convention, because in the Gibbs equation for adsorption from mixtures the decrease in the interfacial tension is proportional to this surface concentration.

An experimental verification of the results presented in this paper and further information on this subject will be published in the near future[25].

APPENDIX

Solution of the mass balance equation (eqns. 6–8)

The law of mass conservation was expressed by a system of m partial differen-

tial equations (eqn. 6). Replacement of the mth of these equations by the sum of all equations gives the set

$$\frac{\partial}{\partial t}(n_{\kappa,i}/L) = -\frac{\partial}{\partial z}(\dot{V}x_{\mu,i}/v_\mu) \quad (i = a, \ldots, m-1)$$

$$\frac{\partial}{\partial t}(n_{\kappa,\mathrm{tot}}/L) = -\frac{\partial}{\partial z}(\dot{V}/v_\mu) \tag{47}$$

In order to solve this system of equations, it is convenient to perform a change of variables, replacing the pair (z,t) by a new set of independent variables $[z, q(z,t)]$ by using the following rules:

$$\left(\frac{\partial}{\partial t}\right)_z = \left(\frac{\partial q}{\partial t}\right)_z \left(\frac{\partial}{\partial q}\right)_z$$

$$\left(\frac{\partial}{\partial z}\right)_t = \left(\frac{\partial}{\partial z}\right)_q + \left(\frac{\partial q}{\partial z}\right)_t \left(\frac{\partial}{\partial q}\right)_z \tag{48}$$

where the subscripts indicate in which set of variables the partial differentiations are performed. The new variable, q, is defined as

$$q(z,t) = \int_0^t (\dot{V}/v_\mu)\mathrm{d}t \tag{49}$$

Eqn. 49 gives, after partial differentiation,

$$\left(\frac{\partial q}{\partial t}\right)_z = \dot{V}/v_\mu \tag{50}$$

The last equation of the set 47 can now be written as

$$\frac{\partial}{\partial t}(n_{\kappa,\mathrm{tot}}/L) = -\frac{\partial^2 q}{\partial z \partial t} \tag{51}$$

As by definition $q(z, t=0) = 0$ for all z (see eqn. 49), integration of eqn. 51 with respect to time gives

$$\left(\frac{\partial q}{\partial z}\right)_t = (n^0_{\kappa,\mathrm{tot}} - n_{\kappa,\mathrm{tot}})/L \tag{52}$$

where the superscript zero indicates that the function is taken at the initial time ($t = 0$):

$$n^0_{\kappa,\mathrm{tot}} \equiv n_{\kappa,\mathrm{tot}}(z,t=0) \tag{53}$$

The new variable q may be interpreted as a "local time", given at each distance, z,

from the column inlet as the total number of moles having flowed through the cross-section from the beginning of the process ($t=0$) to time t. The transformation of variables indicated in eqn. 48 applied to the first $m-1$ equations of system 47, combined with eqns. 50 and 51, leads, after rearrangement, to

$$\frac{1}{L}\left[\frac{\partial}{\partial q}(n_{\kappa,i} - x_{\mu,i}\, n_{\kappa,\mathrm{tot}}) + n^0_{\kappa,\mathrm{tot}} \cdot \frac{\partial x_{\mu,i}}{\partial q}\right] = -\frac{\partial x_{\mu,i}}{\partial z} \quad (i = a, \ldots, m-1) \tag{54}$$

As previously noted, the molar capacities, $n_{\kappa,i}$, depend only on the mobile phase composition $\vec{x}_\mu$:

$$n_{\kappa,i} = n_{\kappa,i}\,[\vec{x}_\mu(z,q)] \tag{55}$$

The system of $m-1$ differential equations (eqn. 54) can now be written in the form

$$\frac{1}{L}\sum_{l=a}^{m-1}\left[\frac{\partial}{\partial x_{\mu,l}}(n_{\kappa,i} - x_{\mu,i}\, n_{\kappa,\mathrm{tot}}) + \delta_{il} n^0_{\kappa,\mathrm{tot}}\right]\frac{\partial x_{\mu,l}}{\partial q} = -\frac{\partial x_{\mu,i}}{\partial z} \quad (i = a, \ldots, m-1) \tag{56}$$

where the Kronecker symbol, δ_{il}, is defined as usual ($\delta_{il} = 0$ if $i \neq l$ and $\delta_{ii} = 1$ for all i). With vector notation, the set of eqn. 56 becomes

$$\boldsymbol{A} \cdot \frac{\partial \vec{x}_\mu}{\partial q} = -\frac{\partial \vec{x}_\mu}{\partial z} \tag{57}$$

where $\boldsymbol{A}$ is the $(m-1) \times (m-1)$ matrix with the elements a_{il}:

$$a_{il}(\vec{x}_\mu) = \frac{1}{L}\left[\frac{\partial}{\partial x_{\mu,l}}(n_{\kappa,i} - x_{\mu,i}\, n_{\kappa,\mathrm{tot}}) + \delta_{il}\, n^0_{\kappa,\mathrm{tot}}\right] \quad (i,l = a, \ldots, m-1) \tag{58}$$

If at time $t = 0$ the composition of the mobile phase is uniform along the column, then

$$\vec{x}_\mu(z,\, t=0) = \vec{x}^0_\mu \tag{59}$$

and if only infinitesimal perturbations of the concentration are considered, the matrix $\boldsymbol{A}$ can be taken as constant, its elements being $a_{il}(\vec{x}^0_\mu)$. Under the same assumptions, also the molar volume of the mobile phase is constant:

$$v_\mu\,(z,q) = v_\mu\,(x^0_\mu) \equiv v^0_\mu \tag{60}$$

In this case the local time, q, is proportional to the volume having flowed through the cross-section, as follows from eqn. 49:

$$v^0_\mu\, q(z,t) = \int_0^t \dot{V}\, \mathrm{d}t \tag{61}$$

Let us now look for solutions of the system of eqns. 57 having the following particular form:

$$\vec{x}_\mu(z,q) = \mathrm{f}_\lambda\,(\lambda z - q)\,\vec{x}_\mu^\lambda \tag{62}$$

where f_λ is any differentiable function and $\vec{x}_\mu^\lambda$ is a constant vector. The calculation of partial derivatives of eqn. 62 is straightforward and gives

$$\frac{\partial \vec{x}_\mu}{\partial q} = \frac{\partial \mathrm{f}_\lambda}{\partial q}\cdot\vec{x}_\mu^\lambda$$

$$\frac{\partial \vec{x}_\mu}{\partial z} = \frac{\partial \mathrm{f}_\lambda}{\partial z}\cdot\vec{x}_\mu^\lambda = -\lambda\,\frac{\partial \mathrm{f}_\lambda}{\partial q}\cdot\vec{x}_\mu^\lambda \tag{63}$$

Introduction of eqn. 63 into the differential system 57 transforms it to an eigenvalue problem:

$$\boldsymbol{A}\vec{x}_\mu^\lambda = \lambda\,\vec{x}_\mu^\lambda \tag{64}$$

An expression having the form of eqn. 64 is a solution of the differential problem if λ is an eigenvalue of the matrix $\boldsymbol{A}$ and $\vec{x}_\mu^\lambda$ is the corresponding eigenvector. If the matrix $\boldsymbol{A}$ has $(m-1)$ distinct eigenvalues $(\lambda_a, \ldots, \lambda_{m-1})$, the set of the corresponding eigenvectors $(\vec{x}_\mu^a, \ldots, \vec{x}_\mu^{m-1})$ is a basis of the vector space of the $\vec{x}_\mu$. In this case the general solution of the differential problem may be written as a linear combination of the eigenvectors:

$$\vec{x}_\mu(z,q) = \sum_{i=a}^{m-1} \mathrm{f}_i(\lambda_i z - q)\,\vec{x}_\mu^i \tag{65}$$

The coefficients f_i have to be determined from the boundary condition at the inlet of the column:

$$\vec{x}_\mu(z=0,q) = \vec{y}(q) \tag{66}$$

where $\vec{y}(q)$ describes the composition of the mixture entering in the column as a function of the "local time", $q(z=0,t)$.

The form of eqn. 65 shows that, for any differentiable boundary condition (eqn. 66), the general solution is a superposition of $m-1$ concentration signals, each travelling without deformation along the column with constant velocity (the inverse of the eigenvalue) with respect to the local time. Taking into consideration eqn. 61, the corresponding retention volumes are given as

$$V_{\mathrm{R},i} = v_\mu^0\,\lambda_i\,L \qquad (i = a, \ldots, m-1) \tag{67}$$

Let us now examine the question of the existence of the eigenvalues of the matrix $\boldsymbol{A}$, restricting the discussion to the case of a binary mixture as eluent, but allowing any number of solutes. Let a and m be the components of the eluent. For

each other substance in the system, the initial value of the molar fraction is zero by hypothesis:

$$x^0_{\mu,b} = x^0_{\mu,c} = \ldots = x^0_{\mu,m-1} = 0 \tag{68}$$

It is evident that if a substance has zero concentration in the mobile phase, its molar capacity in the column also disappears:

$$n_{\kappa,i}(\vec{x}_\mu) = 0 \tag{69}$$

if $x_{\mu,i} = 0$, whatever is the value of the other components of the vector $\vec{x}_\mu$. As a consequence the following rule is valid:

$$\left(\frac{\partial n_{\kappa,i}}{\partial x_{\mu,l}}\right)_{\vec{x}^0_\mu} = 0 \tag{70}$$

if $i = b, c, \ldots, m-1$ and $l \neq i$. The matrix A thus takes a triangular form, all elements a_{il} with $l < i$ being zero; in fact, by eqn. 58 we have for $i = b, \ldots, m$-1 and $l < i$:

$$a_{il} = \frac{1}{L}\left[\frac{\partial}{\partial x_{\mu,l}}(n_{\kappa,i} - x_{\mu,i}\, n_{\kappa,\mathrm{tot}})\right]_{\vec{x}^0_\mu} = 0 \tag{71}$$

The eigenvalues of a triangular matrix are the diagonal elements. If these eigenvalues are all distinct and positive. the signal observed at the outlet of the column will be a superposition of $m-1$ signals characterized by the retention volumes given by eqn. 67:

$$V_{\mathrm{R},i} = v^0_\mu\left[\left(\frac{\partial}{\partial x_{\mu,\mathrm{i}}}(n_{\kappa,i} - x_{\mu,i}\, n_{\kappa,\mathrm{tot}})\right)_{\vec{x}_0} + n^0_{\kappa,\mathrm{tot}}\right]$$

$$= v^0_\mu\left[\left(\frac{\partial n_{\kappa,i}}{\partial x_{\mu,i}}\right)_{\vec{x}^0_\mu} - x^0_{\mu,i}\left(\frac{\partial n_{\kappa,\mathrm{tot}}}{\partial x_{\mu,i}}\right)_{\vec{x}^0_\mu}\right] \quad (i = a, \ldots, m-1) \tag{72}$$

It should be noted that, depending on the boundary condition, some of these concentration signals may have a zero amplitude. It is easy to show that eqn. 72 (identical to eqn. 8) is also valid in an eluent composed of more than two components if i is a solute (i.e., if $x^0_{\mu,i} = 0$).

Retention equations for liquid–solid chromatography in terms of different units; transformations of eqn. 31

Mass language: m-p-Π (mass, mass fraction, mass per unit surface area). For a solute su ($x^0_{\mu,\mathrm{su}} = 0$ or equivalently, $p^0_{\mu,\mathrm{su}} = 0$), eqn. 31 reduces to

$$V_{\mathrm{R,su}} = V_{\mu/\mathrm{CX}} + S\cdot\frac{v^0_\mu}{M_{\mathrm{su}}}\left(\frac{\partial \Pi_{\mathrm{su/CX}}}{\partial x_{\mu,\mathrm{su}}}\right)_{\vec{x}^0_\mu} \tag{73}$$

By definition $p_{\mu,i} = M_i x_{\mu,i}/M_\mu$, so for a solute

$$\left(\frac{\partial p_{\mu,\mathrm{su}}}{\partial x_{\mu,\mathrm{su}}}\right)_{\vec{x}^0_\mu} = M_{\mathrm{su}}/M^0_\mu \tag{74}$$

On the other hand, $\Pi_{\mathrm{su/CX}}$ is identically zero if $p_{\mu,\mathrm{su}} = 0$, and thus

$$\left(\frac{\partial \Pi_{\mathrm{su/CX}}}{\partial x_{\mu,l}}\right)_{\vec{x}^0_\mu} = 0 \tag{75}$$

for $l \neq$ su. Consequently, for solutes eqn. 76 holds true:

$$V_{\mathrm{R,su}} = V_{\mu/\mathrm{CX}} + S\,\tilde{v}^0_\mu \left(\frac{\partial \Pi_{\mathrm{su/CX}}}{\partial p_{\mu,\mathrm{su}}}\right)_{\vec{p}^0_\mu} \tag{76}$$

For the concentration peak, the derivation is restricted to the case of a binary mixture (A and B) as eluent. Eqn. 31 gives for the retention volume

$$V_{\mathrm{R,cc}} = V_{\mu/\mathrm{CX}} + S\,\tilde{v}^0_\mu \left[\frac{x^0_{\mu,\mathrm{B}}}{M_\mathrm{A}}\left(\frac{\mathrm{d}\Pi_{\mathrm{A/CX}}}{\mathrm{d}x_{\mu,\mathrm{A}}}\right)_{x^0_{\mu,\mathrm{A}}} - \frac{x^0_{\mu,\mathrm{A}}}{M_\mathrm{B}}\left(\frac{\mathrm{d}\Pi_{\mathrm{B/CX}}}{\mathrm{d}x_{\mu,\mathrm{A}}}\right)_{x^0_{\mu,\mathrm{A}}}\right] \tag{77}$$

Differentiation of the expression $p_{\mu,\mathrm{A}} = M_\mathrm{A} x_{\mu,\mathrm{A}}/(M_\mathrm{A} x_{\mu,\mathrm{A}} + M_\mathrm{B} x_{\mu,\mathrm{B}})$ gives

$$\left(\frac{\mathrm{d}p_{\mu,\mathrm{A}}}{\mathrm{d}x_{\mu,\mathrm{A}}}\right)_{x^0_{\mu,\mathrm{A}}} = M_\mathrm{A} M_\mathrm{B}/(M^0_\mu)^2 \tag{78}$$

Introduction of eqn. 78 into eqn. 77 gives, after rearrangement,

$$V_{\mathrm{R,cc}} = V_{\mu/\mathrm{CX}} + S\,\tilde{v}^0_\mu \left[\left(\frac{\mathrm{d}\Pi_{\mathrm{A/CX}}}{\mathrm{d}p_{\mu,\mathrm{A}}}\right)_{p^0_{\mu,\mathrm{A}}} - p^0_{\mu,\mathrm{A}}\left(\frac{\mathrm{d}\Pi_{\mathrm{tot,CX}}}{\mathrm{d}p_{\mu,\mathrm{A}}}\right)_{p^0_{\mu,\mathrm{A}}}\right] \tag{79}$$

In particular, in the convention mNA ($\Pi_{\mathrm{tot}\,m\mathrm{NA}} = 0$) eqn. 79 simplifies to give

$$V_{\mathrm{R,cc}} = V_{\mu/m\mathrm{NA}} + S\,\tilde{v}^0_\mu \left(\frac{\mathrm{d}\Pi_{\mathrm{A}/m\mathrm{NA}}}{\mathrm{d}p_{\mu,\mathrm{A}}}\right)_{p^0_{\mu,\mathrm{A}}} \tag{80}$$

Volume language: v-φ-Ψ (volume, volume fraction, volume per unit surface area). For a solute su ($x^0_{\mu,\mathrm{su}} = 0$ or equivalently $\varphi^0_{\mu,\mathrm{su}} = 0$), eqn. 31 gives

$$V_{\mathrm{R,su}} = V_{\mu/\mathrm{CX}} + S\left[\frac{v^0_\mu}{v^0_{\mathrm{su}}}\left(\frac{\partial \Psi_{\mathrm{su/CX}}}{\partial x_{\mu,\mathrm{su}}}\right)_{\vec{x}^0_\mu} - \Gamma_{\mathrm{su/CX}}(\vec{x}^0_\mu)\left(\frac{\partial v_{\mathrm{su}}}{\partial x_{\mu,\mathrm{su}}}\right)_{\vec{x}^0_\mu}\right] =$$

$$V_{\mu/\mathrm{CX}} + S \cdot \frac{v^0_\mu}{v^0_{\mathrm{su}}}\left(\frac{\partial \Psi_{\mathrm{su/CX}}}{\partial x_{\mu,\mathrm{su}}}\right)_{\vec{x}^0_\mu} \tag{81}$$

as $\Gamma_{su/CX}(\vec{x}_\mu^0) = 0$. By definition $\varphi_{\mu,i} = v_i x_{\mu,i}/v_\mu$ (v_i is for the partial molar volume and v_μ for the mean molar volume of the eluent), and so for a solute

$$\left(\frac{\partial \varphi_{\mu,su}}{\partial x_{\mu,su}}\right)_{\vec{x}_\mu^0} = v_{su}/v_\mu^0 \tag{82}$$

Considering that $\Psi_{su/CX}$ is identically zero if $\varphi_{\mu,su} = 0$,

$$\left(\frac{\partial \Psi_{su/CX}}{\partial \varphi_{\mu,l}}\right)_{\vec{\varphi}_\mu^0} = 0 \tag{83}$$

for $l \neq$ su. Eqn. 81 can now be written as

$$V_{R,su} = V_{\mu/CX} + \left(\frac{\partial \Psi_{su/CX}}{\partial \varphi_{\mu,su}}\right)_{\vec{\varphi}_\mu^0} \tag{84}$$

The derivation for the concentration peak is restricted to a binary system. Eqn. 31 can be written in the following form:

$$V_{R,cc} = V_{\mu/CX} + S\left[v_\mu^0 x_{\mu,B}^0 \left(\frac{d\Gamma_{A/CX}}{dx_{\mu,A}}\right)_{x_{\mu,A}^0} + v_\mu^0 x_{\mu,A} \left(\frac{d\Gamma_{B/CX}}{dx_{\mu,B}}\right)_{x_{\mu,A}^0}\right] \tag{85}$$

Let us now recall two basic properties of the molar volumes in a binary mixture:

$$\frac{dv_\mu}{dx_{\mu,A}} = v_A - v_B \tag{86}$$

$$\frac{dv_A}{dx_{\mu,A}} = x_{\mu,B} \cdot \frac{d^2 v_\mu}{dx_{\mu,A}^2} \tag{87}$$

and that the volume fraction $\varphi_{\mu,A}$ is given by

$$\varphi_{\mu,A} = x_{\mu,A} v_A/v_\mu \tag{88}$$

By using eqns. 86 and 87 the derivative of the volume fraction with respect to the molar fraction can now be expressed as follows:

$$\frac{d\varphi_{\mu,A}}{dx_{\mu,A}} = \frac{v_A v_B}{v_\mu^2} + \frac{x_{\mu,A} x_{\mu,B}}{v_\mu} \cdot \frac{d^2 v_\mu}{dx_{\mu,A}^2} \tag{89}$$

As by definition $\Psi_{A/CX} = v_A \Gamma_{A/CX}$, the first term of the coefficient of S in eqn. 85 can be written as

$$v_\mu x_{\mu,B} \cdot \frac{d\Gamma_{A/CX}}{dx_{\mu,A}} = \frac{v_\mu x_{\mu,B}}{v_A}\left(\frac{d\Psi_{A/CX}}{d\varphi_{\mu,A}} \cdot \frac{d\varphi_{\mu,A}}{dx_{\mu,A}} - \Gamma_{A/CX} \cdot \frac{dv_A}{dx_{\mu,A}}\right) \tag{90}$$

Using eqns. 86, 87 and 88, the following expression is obtained after tedious manipulations:

$$v_\mu x_{\mu,B} \cdot \frac{d\Gamma_{A/CX}}{dx_{\mu,A}} = \varphi_{\mu,B}(1+\alpha) \cdot \frac{d\Psi_{A/CX}}{d\varphi_{\mu,A}} - \alpha \cdot \frac{\varphi_{\mu,B}}{\varphi_{\mu,A}} \cdot \Psi_{A/CX} \tag{91}$$

where the parameter α is

$$\alpha = (x_{\mu,A}x_{\mu,B}\, v_\mu / v_A v_B) \frac{d^2 v_\mu}{dx_{\mu,A}^2} \tag{92}$$

The value of α remains unchanged if the subscripts A and B are interchanged. For reasons of symmetry a relation analogous to eqn. 91 is valid for the second term of the coefficient of S in eqn. 85:

$$v_\mu x_{\mu,A} \cdot \frac{d\Gamma_{B/CX}}{dx_{\mu,B}} = \varphi_{\mu,A}(1+\alpha) \cdot \frac{d\Psi_{B,CX}}{d\varphi_{\mu,B}} - \alpha \cdot \frac{\varphi_{\mu,A}}{\varphi_{\mu,B}} \cdot \Psi_{B/CX} \tag{93}$$

Introduction of eqns. 91 and 93 into eqn. 85 gives the desired retention volume. Its form becomes particularly simple if the vNA convention is chosen for the adsorption. Considering eqn. 44, the expression for the retention volume becomes

$$V_{R,cc} = V_{\mu/vNA} + S\left[\frac{d\Psi_{A/vNA}}{d\varphi_{\mu,A}} + \alpha\left(\frac{d\Psi_{A/vNA}}{d\varphi_{\mu,A}} + \frac{\varphi_{\mu,A} - \varphi_{\mu,B}}{\varphi_{\mu,A}\varphi_{\mu,B}} \cdot \Psi_{A/vNA}\right)\right]_{\varphi^0_{\mu,A}} \tag{94}$$

If the mixture is ideal (*i.e.*, the molar volume is a linear function of $x_{\mu,A}$), the coefficient α is zero (see eqn. 92), and eqn. 94 takes the simple form given in Table I.

SYMBOLS

Symbols

c (mol l^{-1}), concentration; d (g cm^{-3}) $= 1/\tilde{v}$, density; Γ (mol m^{-2}), surface concentration; φ (—) $= p\tilde{v}/\tilde{v}_\mu = xv/v_\mu$, volume fraction; k (—) $= c_\sigma/c_\mu$, partition coefficient; χ (mol m^{-2} or g m^{-2} or ml m^{-2}), peak propagation resitivity; L (cm), column length; m (g), mass of eluent or solute; m (—), number of components in a fluid mixture; M (g mol^{-1}), molar mass; n (mol), number of moles of eluent or solute; N (–): number of components in the liquid mixture (in particular, eluent); v (ml mol^{-1} or ml g^{-1} or no units), constant in eqn. 45; p (—), mass fraction; $\bar{P}$ (bar), mean pressure; Π (g m^{-2}), surface concentration; Ψ (ml $m^{-2} \approx \mu m$), surface concentration; S (m^2), surface area of a solid; t (min), time; T (°K), temperature; v (ml mol^{-1}), (partial) molar volume; $\tilde{v}$ (ml g^{-1}), (partial) specific volume; V (ml), volume; $\dot{V}$ (ml min^{-1}), flow-rate; V_R (ml), retention volume; V_N (ml), net retention volume; V_S (μl m^{-2}), surface specific retention volume; V_g (ml g^{-1}), specific retention volume; w (g), mass referring to the stationary phase; x (—), molar fraction; z (cm), distance in the column.

Subscripts

A, ..., J, ..., N, components of the eluent; cc, peak due to concentration per-

turbation; su, solute; i, either J, cc or su; c, column; β, bulk of the liquid; CX, convention X (GLC, model for gas–liquid chromatography or one of the conventions JNA, nNA, mNA and vNA); κ, column capacity (total of a component in the column transported by the mobile phase); μ, mobile phase; σ, [two meanings], (i) of the stationary phase and (ii) material adsorbed or absorbed in the stationary phase; S, unit surface area; tot, sum over all components present; τ, total amount in (or of) a mixture before adsorption.

Superscripts

0, before the beginning of the chromatographic process; (id), ideal dilution.

ACKNOWLEDGEMENTS

The authors thank Dr. D. F. Fritz for discussions and D. Mazzo for correction of the English. This work is a report on part of a project supported by the Fonds National Suisse de la Recherche Scientifique.

REFERENCES

1 D. de Vault, *J. Amer. Chem. Soc.*, 62 (1940) 1583.
2 G. G. Baylé and A. Klinkenberg, *Rec. Trav. Chim. Pays-Bas*, 73 (1954) 1037.
3 P. C. Mangelsdorf, Jr., *Anal. Chem.*, 38 (1966) 1540.
4 F. Helfferich and G. Klein, in J. C. Giddings and R. A. Keller (Editors), *Multicomponent Chromatography —Theory of Interference*, Marcel Dekker, New York, 1970.
5 G. Schay, *Ber. Bunsenges. Phys. Chem.*, 77 (1973) 184.
6 R. M. McCormick and B. L. Karger, *J. Chromatogr.*, 199 (1980) 259.
7 R. M. McCormick and B. L. Karger, *Anal. Chem.*, 52 (1980) 2249.
8 J. H. Knox and R. Kaliszan, to be published, but cited in J. H. Knox, R. Kaliszan and G. J. Kennedy, *Faraday Symposium No. 15, Brighton, 1980*, Royal Society of Chemistry, London, 1980, p. 113.
9 J. H. Knox and E. sz. Kováts, discussion contribution, *Faraday Symposium No. 15, Brighton, 1980*, Royal Society of Chemistry, London, 1980, p. 177.
10 C. L. de Ligny, discussion contribution, *Faraday Symposium No. 15, Brighton, 1980*, Royal Society of Chemistry, London, 1980, p. 171.
11 E. H. Slaats, W. Markovski, J. Fekete and H. Poppe, *J. Chromatogr.*, 207 (1981) 299.
12 E. H. Slaats, *Doctoral Thesis*, University of Amsterdam, 1980.
13 M. Jaroniec, B. Oscik-Mendyk, A. Dabrowski and H. Kolodziejczyk, *J. Liquid Chromatogr.*, 4 (1981) 277.
14 G. E. Berendsen, P. J. Schoenmakers, L. de Galan, G. Vigh, Z. Varga-Puhony and J. Inczédy, *J. Liquid Chromatogr.*, 3 (1980) 1669.
15 P. Fini, F. Brusa and L. Chiesa, *J. Chromatogr.*, 210 (1981) 326.
16 P. Valentin and G. Guiochon, *J. Chromatogr. Sci.*, 14 (1976) 56 and 132.
17 J. F. K. Huber and R. G. Gerritse, *J. Chromatogr.*, 58 (1971) 137.
18 A. A. Zhukhovitskii, *Gaz Khromatogr. Akad. Nauk. S.S.S.R. Tr. Vtoroi, Vses. Konf., Moskow*, (1962) 5; *C.A.*, 62 (1965) 5868. See also in A. Goldup (Editor), *Gas Chromatography 1964*, Institute of Petroleum, London, 1965, p. 161.
19 A. J. P. Martin and R. L. M. Synge, *Biochem. J.*, 35 (1941) 1358.
20 K. Karch, I. Sebestian, I. Halász and H. Engelhardt, *J. Chromatogr.*, 122 (1976) 171.
21 A. W. J. de Jong, J. C. Kraak, H. Poppe and F. Nooitgedacht, *J. Chromatogr.*, 193 (1980) 181.
22 J. L. M. van de Venne, *Doctoral Thesis*, University of Eindhoven, Eindhoven, 1979.
23 E. H. Slaats, J. C. Kraak, W. J. T. Brugman and H. Poppe, *J. Chromatogr.*, 149 (1978) 255.
24 G. Körösi and E.sz. Kováts, *Coll. Surf.*, 2 (1981) 315.
25 Ngoc Le Ha, *Doctoral Thesis*, École Polytechnique Fédérale de Lausanne, Lausanne, in preparation.

Journal of Chromatography, 239 (1982) 29–37
Elsevier Scientific Publishing Company, Amsterdam — Printed in The Netherlands

CHROM. 14,502

MULTI-COMPONENT ANALYSES OF HUMAN BODY FLUIDS AND TISSUES IN HEALTH AND DISEASE USING CAPILLARY GAS CHROMATOGRAPHY–MASS SPECTROMETRY AND HIGH-RESOLUTION TWO-DIMENSIONAL ELECTROPHORESIS

EGIL JELLUM
Institute of Clinical Biochemistry, Rikshospitalet, University of Oslo, Oslo 1 (Norway)

SUMMARY

Glass capillary gas chromatography–mass spectrometry and high resolution two-dimensional electrophoresis have been used in combination to achieve multi-component analyses of human serum, urine, cerebrospinal fluid and various tumours. The analytical system covers both low- and high-molecular-weight constituents, that is, metabolites and proteins. Over 1000 compounds can be separated in a single sample of a few milligrams. The techniques have been used to study changes in the biochemical composition of body fluids and tissues in different human diseases: metabolic disorder, neurological disorders and certain types of cancer. The new multi-component analytical approach, now in its early stages, may have considerable potential in biomedical research and diagnosis.

INTRODUCTION

During the past decade much attention has been paid to "metabolic profiling" of human body fluids and tissues using gas chromatography (GC) and mass spectrometry (MS)[1–3]. This type of technique is suitable for the diagnosis and study of a number of metabolic disorders[2–4], as many of these often result in easily recognizable changes in the pattern of metabolites. Other diseases, *e.g.*, various types of cancer, seem to lead only to small changes in the metabolic profiles. Useful information may nevertheless be extracted, particularly when advanced multivariate data analyses are used to handle the analytical results. Thus, using capillary GC and the SIMCA pattern recognition method[5], we have shown that it is possible to differentiate between various brain tumours based solely upon differences in their chromatographic profiles[6].

Only compounds of low molecular weight (up to about 1000) may be analysed by GC–MS methods. Recent advances in high-performance liquid chromatography (HPLC) may extend the molecular weight range considerably, and may bridge the gap between GC–MS and a new multi-component analytical technique for proteins: high-resolution two-dimensional electrophoresis. The latter method was described by O'Farrell[7] in 1975 and later modified by Anderson and Anderson[8,9] to handle many samples in parallel.

0021-9673/82/0000–0000/$02.75

In our laboratory we now use GC–MS and high-resolution two-dimensional electrophoresis to study body fluids and tissues in health and disease. The results, some of which are presented in this paper, indicate that this new multi-component analytical approach may have considerable potential in biomedical research and diagnosis.

EXPERIMENTAL

Materials

Solvents were redistilled before use. The silylating reagent, bistrimethylsilyltrifluoroacetamide (BSTFA), was obtained from Supelco (U.S.A.). N-Nitrosomethylurea for diazomethane production was obtained from ICN Pharmaceuticals (New York, U.S.A.). Glass capillary columns for gas chromatography were products of LKB (Stockholm, Sweden), Chrompack (Middelburg, The Netherlands) or Hewlett-Packard (U.S.A.) (fused-silica columns). The columns were 25–50 m long, coated with SE-30 or SP-1000.

Acrylamide, bisacrylamide and sodium dodecyl sulphate (SDS) were products of Bio-Rad Labs. (U.S.A.) or Serva (Heidelberg, G.F.R.). Ampholytes for isoelectric focusing were either Ampholines (LKB) or Servalyt (Serva).

All other chemicals were commercially available products of analytical-reagent grade.

Methods

The capillary GC–MS procedures were as described earlier[10–12]. The instruments used where either a Varian 112 GC–MS with Spectrosystem 100 MS computing system (Varian-MAT, Bremen, G.F.R.) or a Finnigan 4021C GC–MS with an Incos/Nova 4 computer (Finnigan-MAT, U.S.A., G.F.R.).

The equipment for high-resolution two-dimensional electrophoresis was obtained from Electro-Nucleonics (Oak Ridge, TN, U.S.A.) and was based on the apparatus constructed and described by Anderson and Anderson[8,9]. The analytical procedures were as developed by Andersons group at Argonne National Laboratory (*e.g.*, refs. 8, 9, 13 and 14). In principle, the two-dimensional electrophoresis is based on isoelectric focusing in one dimension followed by SDS electrophoresis in a gradient polyacrylamide gel in the second dimension. All proteins (or rather polypeptide chains, as the protein was treated with 9 *M* urea and mercaptoethanol) are therefore separated according to electrical charge and size (molecular weight). Staining of the separated proteins was achieved with Coomassie Brilliant Blue R-250 (Bio-Rad Labs.).

RESULTS AND DISCUSSION

Our combined multi-component analytical system covers both low- and high-molecular-weight constituents, *i.e.*, metabolites and proteins. At this early stage of our work with the system, we have attempted to gain some experience with various body fluids and tissues both from normals and from selected patients.

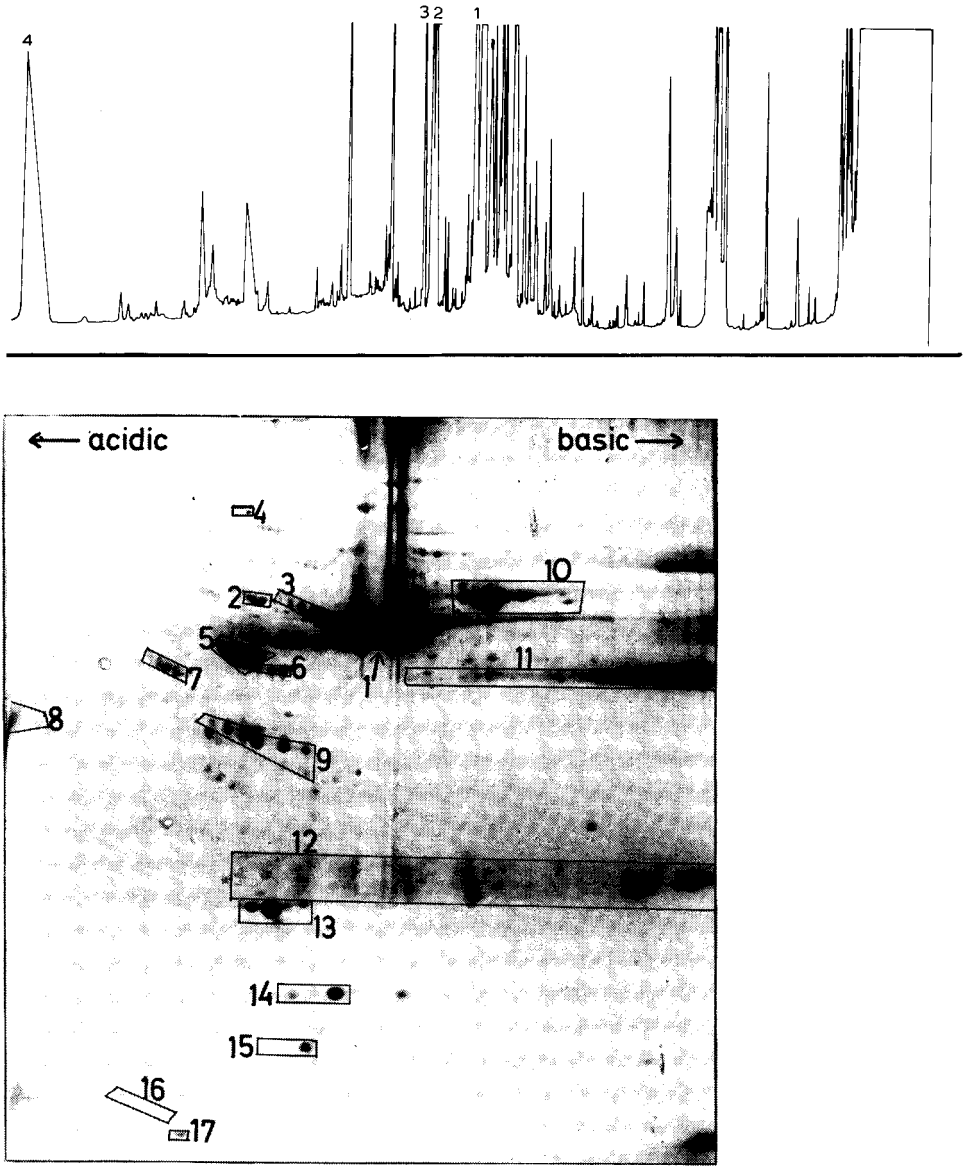

Fig. 1. Metabolic profile of normal serum (top) and protein pattern of the same serum (bottom). The serum (0.3 ml) was evaporated to dryness and refluxed with anhydrous methanol–hydrochloric acid overnight to complete methanolysis. After removal of the solvent and silylation with BSTFA, the compounds were separated in a 25-m SE-30 glass capillary column coupled to a Varian 112 mass spectrometer. The identities of some of the major peaks are: 1 = palmitic acid, 2 = oleic acid, 3 = stearic acid, 4 = cholesterol. High-resolution two-dimensional electrophoresis as described in the text was used to separate the proteins. The identities of some of the proteins are: 1 = albumin; 2 = α_1-B-glycoprotein; 3 = hemopexin; 4 = α_1-antitrypsin dimer; 5 = α_1-antitrypsin; 6 = Gc-globulin; 7 = α_2-SH-glycoprotein; 8 = α_1-acid-glycoprotein; 9 = haptoglobin β-chain; 10 = transferrin; 11 = IgG γ-chain; 12 = IgG light chains; 13 = Apo A-I lipoprotein (HDL); 14 = haptoglobin α^2-chain; 15 = prealbumin; 16 = lipoprotein (LDL); 17 = Apo A-II lipoprotein (HDL) (see ref. 13).

Serum

Typical multi-component patterns of low- and high-molecular-weight constituents of a normal serum sample are shown in Fig. 1. About 30–40 proteins have been identified by Anderson and Anderson[13]. Our studies[15] and those of Latner *et al.*[16,17] on sera from patients with various myelomas have added new information. We now know the position of all the main immunoglobulin types.

Fig. 2 shows the protein pattern of serum from a patient suffering from cancer of the colon. The first serum sample was collected during an early stage of his disease and a second sample when the patient's condition had deteriorated. Some proteins (marked with arrows) appear as the disease progresses. The clinical interpretation of these changes must, however, await further studies on larger number of patients.

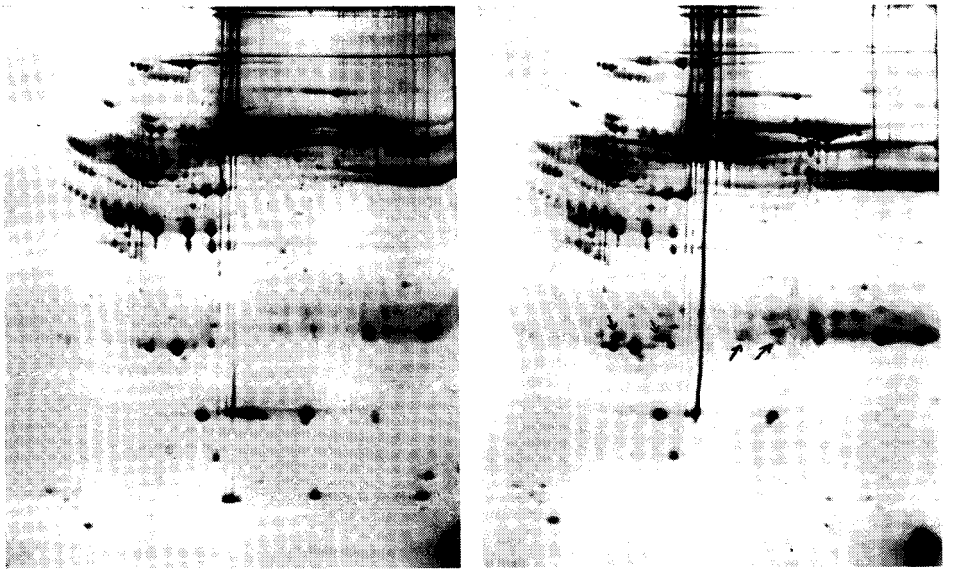

Fig. 2. Two-dimensional pattern of serum proteins from a patient with cancer of the colon. Left: serum collected during an early stage of disease. Right: serum collected 6 months later. Some spots appearing in the light chain region are marked with arrows.

Also the low-molecular-weight pattern may change with development of cancer, although it is our experience (unpublished results) that changes in the GC–MS profiles are small. An example of this is shown in Fig. 3, which shows the organic acid profile of serum collected from the same person several months before and immediately after diagnosis (but before treatment) of cancer mammae. Many more patients and controls, however, are required before one can attribute any significance to the observed, small changes in the metabolic profile.

The question remains of whether it is possible to detect changes in the metabolic profile and protein pattern of serum prior to clinical recognition of cancer. For this purpose the JANUS collection[18] of sera might prove to be of great value. In the JANUS project, sponsored by the Norwegian Cancer Society, serum samples from 64,000 people are collected at 1–3 year intervals, and stored at −25°C. Since this

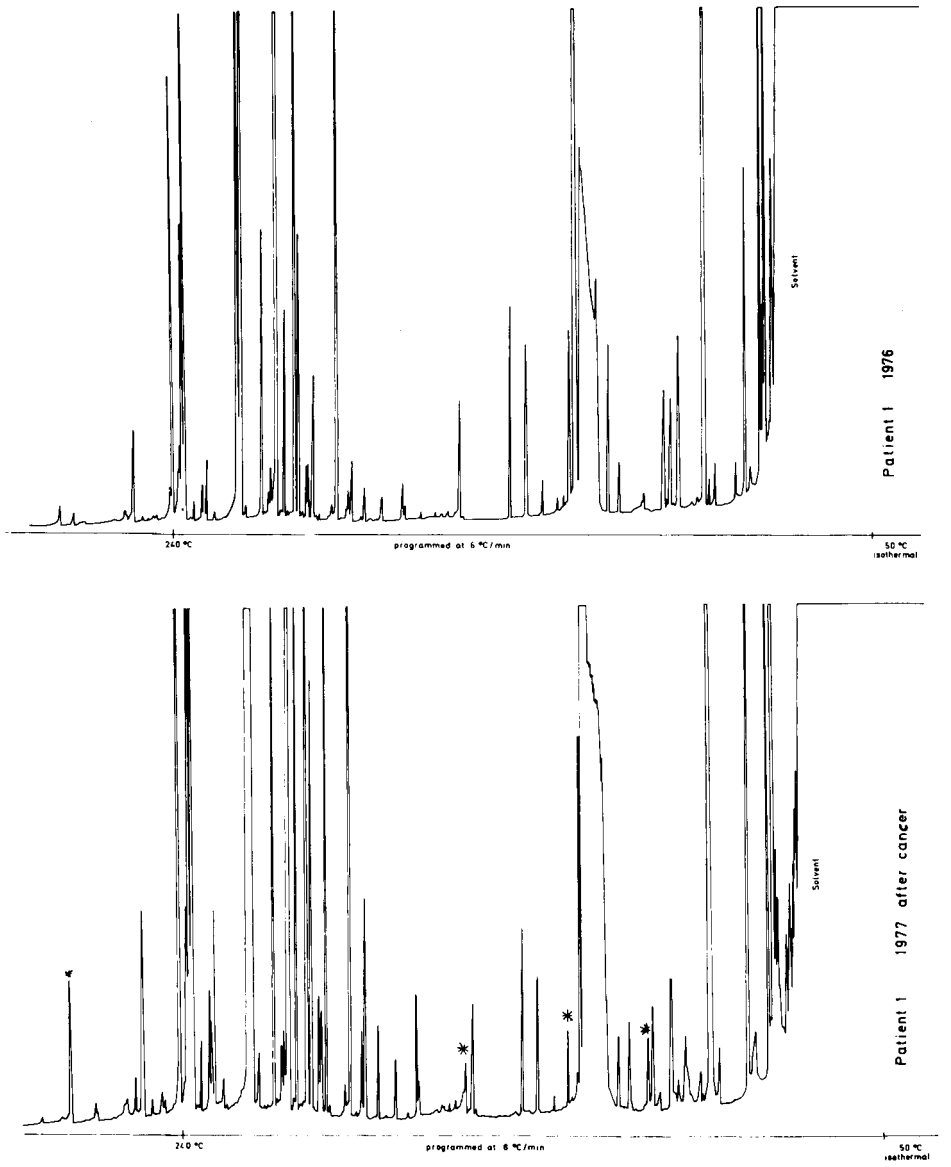

Fig. 3. Organic acid profile of serum from a patient with breast cancer. Top: sample collected 8 months prior to the recognition of the cancer. Bottom: sample collected after diagnosis, but before treatment. The sera were treated with ethanol (final concentration 80%) to precipitate the proteins. After removal of the ethanol *in vacuo*, the residue was acidified and extracted with diethyl ether and methylated with diazomethane. A 25-m SE-30 glass capillary column, programmed from 80 to 250°C, was used to separate the organic acids. Differences are marked with asterisks.

work began in 1973 over 1000 originally healthy persons have developed cancer, and sera obtained 1–8 years prior to recognition of their disease are available. The protein pattern in some of these sera have been examined in a preliminary investigation. Some changes were observed, but a serious problem became evident, namely the

dominance of albumin (*e.g.*, see Fig. 1). Selective removal of this protein and perhaps of some of the other dominant serum proteins prior to the two-dimensional electrophoresis seems to be a necessity. Larger amounts of albumin-free serum may then be applied to the gels, facilitating the detection of less abundant proteins. The chances of detecting tumour-produced proteins in serum may then increase.

Urine

The GC–MS profiles of, *e.g.*, organic acids in urine have been studied in a variety of clinical cases and in many different laboratories[1–4]. An example of such a profile is shown in Fig. 4. The urine appears to contain at least 500 organic acids[19].

After a 1000-fold concentration of urine and analysis of urinary proteins by high-resolution two-dimensional electrophoresis as described by Anderson and coworkers[20,21], several hundred spots are seen. Thus, by combining the two multicomponent analytical techniques, information on a large number of urinary constituents can be obtained. With the experience already gained with the metabolic profiles during the last 15 years, it seems reasonable to expect additional diagnostic information to be obtained by incorporating the protein pattern.

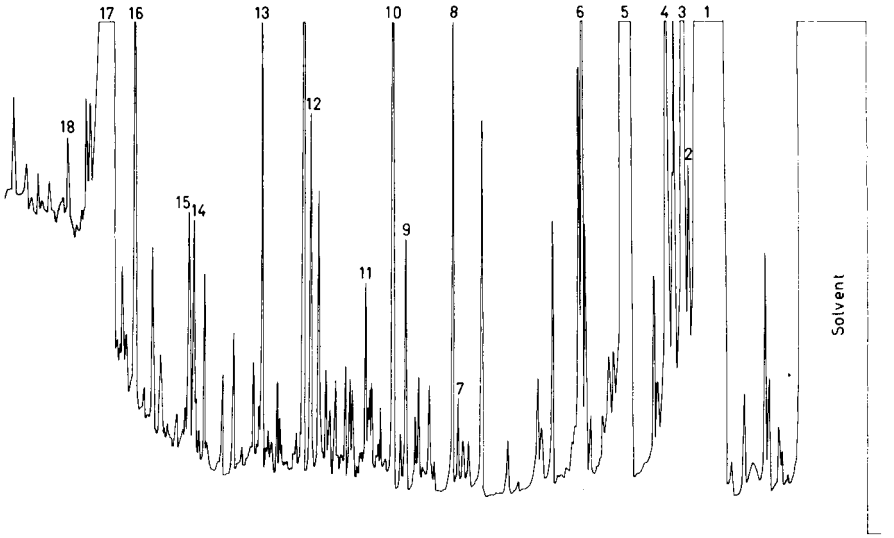

Fig. 4. Profile of urinary organic acids in a patient with ketoacidosis. The urine was acidified, extracted with diethyl ether and methylated with diazomethane. Separation and identification of the methyl esters were effected in an SP-1000 glass capillary column (25 m) coupled to a Varian 112 GC–MS instrument. Peaks: 1 = lactic acid; 2 = 3-hydroxyisovaleric acid; 3 = 2-hydroxybutyric acid; 4 = acetoacetic acid; 5 = 3-hydroxybutyric acid; 6 = 3-hydroxyisobutyric acid; 7 = adipic acid; 8 = methyladipic acid; 9 = dimethyladipic acid; 10 = eicosan (internal standard); 11 = *p*-cresol; 12 = 2,5-furandicarboxylic acid; 13 = citric acid; 14 = metabolite from Fenemal; 15 = homovanillic acid + furoylglycine; 16 = *p*-hydroxyphenylacetic acid; 17 = hippuric acid; 18 = coffeine.

Cerebrospinal fluid (CSF)

Two-dimensional electrophoresis of CSF has been described by Merril and coworkers[22,23]. Using a highly sensitive silver staining technique, only a four-fold concentration of the liquid was required. In our studies we use Sartorius Colloid Bags

(Sartorius, Göttingen, G.F.R.) to concentrate the CSF 100-fold. To illustrate differences that may occur in various neurological conditions, the protein patterns in a case of meningoencephalitis and a case of multiple sclerosis are shown in Fig. 5. Although one does not know at the present stage, it may turn out that the two-dimensional protein patterns of CSF carry valuable diagnostic information.

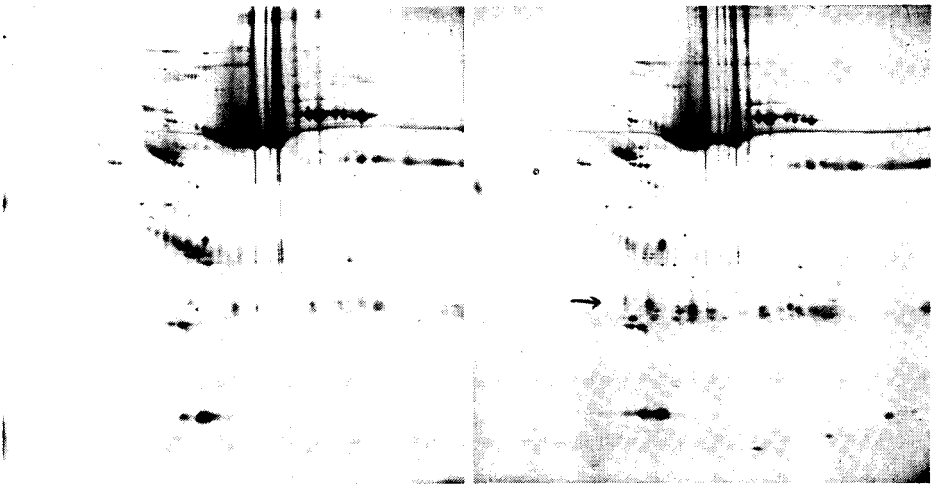

Fig. 5. Two-dimensional protein pattern of cerebrospinal fluid from a patient with meningoencephalitis (left) and from a patient with multiple sclerosis (right). Note marked changes especially in the light chain region (arrow).

Tissue analyses

The great advantage from the analytical point of view with tissues is that there is no single component, such as albumin in serum, that totally dominates the picture. Because of this, many more protein spots are seen in the electrophoresis method, and also the GC–MS profiles of low-molecular-weight constituents give true multi-component analytical results.

One of our main projects, in collaboration with scientists and surgeons of the Norwegian Radium Hospital and the Norwegian Cancer Society, is to search for tumour-produced metabolites and proteins. For this purpose both GC–MS and high-resolution two-dimensional electrophoresis are used. A biopsy of the tumour and of control tissue (cells from which the tumour originated) and serum from each patient are analysed. By comparing the multi-component analytical data of the tumour with the control tissue, it is possible to detect tumour-characteristic proteins and metabolites and also to examine for the presence of these compounds in serum. Sera collected in earlier years (JANUS collection[18]) may then be analysed to detect at what time prior to clinical diagnosis the cancer metabolites and/or proteins appear. To exemplify the complexity of the patterns, Fig. 6 shows the protein patterns of a biopsy from breast cancer, of a brain tumour and the capillary GC profile of the latter. With all these analytical data available, there is at least a possibility that new information on cancer may be obtained.

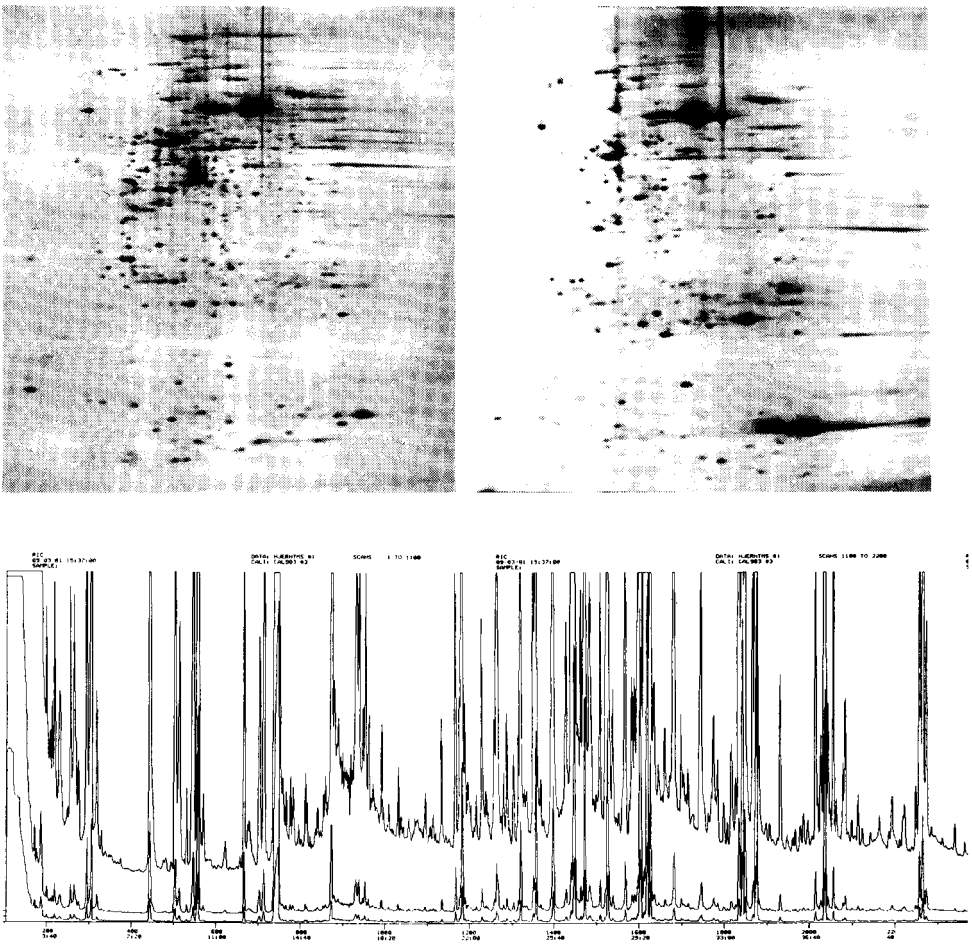

Fig. 6. Two-dimensional protein pattern and metabolic profile of biopsies from breast cancer and brain tumour. Top left, breast cancer; top right, pituitary tumour; bottom, GC–MS profile of the pituitary tumour. Experimental condition as in Fig. 1, except that a Finnigan 4021C GC–MS with an Incos/Nova 4 data system was used to record the profile of the metabolites. No attempts were made to identify the constituents.

ACKNOWLEDGEMENTS

The author is indebted to Per Helland, Gro Guldal, Ingun Bjørnson, Live Horn and Anne Karine Thorsrud for technical assistance. This work was supported by the Norwegian Cancer Society.

REFERENCES

1 E. C. Horning and M. G. Horning, *J. Chromatogr. Sci.*, 9 (1971) 129.
2 E. Jellum, *J. Chromatogr.*, 143 (1977) 427.
3 B. Halpern, *CRC Critical Reviews in Analytical Chemistry*, CRC Press Inc., Boca Raton, Florida, 1981.

4 S. I. Goodman and S. P. Markey, *Diagnosis of Organic Acidemias by Gas Chromatography-Mass Spectrometry*, Alan R. Liss Inc. New York, and Heyden, London 1981.
5 S. Wold and M. Sjøstrøm, in B. R. Kowalski (Editor), *Chemometrics, Theory and Application*, Symposium Series No. 52, American Chemical Society, Washington, DC, 1977, p. 243.
6 E. Jellum, I. Bjørnson, R. Nesbakken, E. Johanssen and S. Wold, *J. Chromatogr.*, 217 (1981) 231.
7 P. H. O'Farrell, *J. Biol. Chem.*, 250 (1975) 4007.
8 N. G. Anderson and N. L. Anderson, *Anal. Biochem.*, 85 (1978) 331.
9 N. L. Anderson and N. G. Anderson, *Anal. Biochem.*, 85 (1978) 341.
10 E. Jellum, P. Størseth, J. Alexander, P. Helland, O. Stokke and E. Teig, *J. Chromatogr.*, 126 (1976) 487.
11 C. Jacobs, E. Solem, J. Ek, K. Halvorsen and E. Jellum, *J. Chromatogr.*, 143 (1977) 31.
12 S. I. Goodman, P. Helland, A. Flatmark, O. Stokke and E. Jellum, *J. Chromatogr.*, 142 (1977) 497.
13 N. L. Anderson and N. G. Anderson, *Proc. Nat. Acad. Sci. U.S.A.*, 74 (1977) 5421.
14 C. S. Giometti, N. G. Anderson and N. L. Anderson, *Clin. Chem.*, 25 (1979) 1877.
15 A. K. Thorsrud, H. F. Haugen and E. Jellum, in B. J. Radola (Editor), *Electrophoresis' 79*, Walter de Gruyter, Berlin, New York, 1980, p. 425.
16 A. L. Latner, T. Marshall and M. Gambie, *Clin. Chim. Acta*, 103 (1980) 51.
17 A. L. Latner, T. Marshall and M. Gambie, *Electrophoresis*, 1 (1980) 82.
18 E. Jellum, H. Ørjaseter, S. Harvei, L. Theodorsen and A. Pihl, *Cancer Detection and prevention*, Vol. 3, No. 1, 1980, Abstract 143.
19 M. Spiteller and G. Spiteller, *J. Chromatogr.*, 164 (1979) 253.
20 N. G. Anderson, N. L. Anderson, S. L. Tollaksen, H. Hahn, F. Giere and J. Edwards, *Anal. Biochem.*, 95 (1979) 48.
21 N. G. Anderson, N. L. Anderson and S. L. Tollaksen, *Clin. Chem.*, 25 (1979) 1199.
22 C. R. Merril, R. C. Switzer and M. L. van Keuren, *Proc. Nat. Acad. Sci. U.S.A.* 76 (1979) 4335.
23 D. Goldman, C. R. Merril and M. H. Ebert, *Clin. Chem.*, 26 (1980) 1317.

Journal of Chromatography, 239 (1982) 39–50
Elsevier Scientific Publishing Company, Amsterdam — Printed in The Netherlands

CHROM. 14,660

OPTIMIZATION OF LIQUID PHASE MIXTURES*

D. F. INGRAHAM**, C. F. SHOEMAKER and W. JENNINGS*
Department of Food Science and Technology, University of California, Davis, CA 95616 (U.S.A.)

SUMMARY

The concept of window diagrams has been used to predict what lengths of dissimilar fused-silica capillaries should be serially coupled to achieve the optimum separation of two "real world" samples whose separation on a single column has not yet been reported. Complicating factors, including the role of the solute partition ratio and the velocity gradient of the carrier gas, are discussed. Separations of mixtures of (a) volatiles produced by yeast fermentation, and (b) solvents used in the preparation of food packaging films, were achieved in single passes on properly configured serially coupled columns composed of two precise lengths, one coated with polymethylsiloxane, and the other with polyethylene glycol.

INTRODUCTION

The optimization of gas chromatographic (GC) parameters such as separation and analysis time must logically be predicated on the use of open tubular capillary columns, because of their inherent superiority over packed columns with respect both to the above parameters[1] and to their increased inertness, greater convenience and lower overall cost[2]. The degree to which two given solutes are separated by a GC system at some given temperature is a function of (a) the breadth of the solute bands (which is influenced both by the width of the starting band or injection efficiency, and by band broadening or column efficiency), and (b) their relative retention, *i.e.*, liquid phase selectivity. While one well chosen liquid phase is best for separating two solutes, it does not always have the selectivity to adequately separate a mixture of three or more solutes. To predict what ratio of two liquid phases yields the best separation of three or more solutes, Maier and Karpathy[3] proposed a method based on the fact that the retention behavior of a solute in a liquid phase mixture could be predicted from a knowledge of its retention behavior in the pure liquid phases, and the relative amounts of those liquid phases in that mixture (all other things being constant). They suggested that the desired proportions of the two liquid phases could be

* Portions of this paper are from a thesis submitted by the senior author in partial fulfillment of the requirements for the Ph.D. degree in Agricultural and Environmental Chemistry.

** Present address: Research Department, Philip Morris Research Center, P.O. Box 26583, Richmond, VA 23261, U.S.A.

0021-9673/82/0000–0000/$02.75

realized by (1) series coupling predetermined lengths of columns packed with support coated (separately) with the two liquid phases, (2) packing the column with two differently coated solid supports that had been intimately mixed in the proper proportions and (3) packing the column with a solid support that had been coated with the appropriate mixture of the two liquid phases. They observed the best separation of a hydrocarbon mixture for case (3), but because it demanded ideal solution behavior, they removed it from further consideration. A very similar method was subsequently proposed by Laub and Purnell (*e.g.*, ref. 4); most of these examples employed packed columns whose efficiencies were sufficiently low that more selective liquid phases were required to affect separation. Most of the mixtures employed in those investigations can be completely resolved by a single liquid phase in a more efficient capillary system. Purnell *et al.*[5] recently employed a coupled capillary column and constructed a "window diagram" (see below) of the relative retentions of the solutes *vs.* the length fraction of one of the columns. The method of determining the length fraction was not specified, but apparently it involved a direct relationship between α and the length fraction. Although they were able to achieve a slightly shorter analysis time on the coupled capillary columns as contrasted to their packed column, resolution was not improved. They attributed this to their inexperience in the preparation of capillary columns. It should be noted that determining the appropriate length fraction is not as trivial as it might seem, as would surely have been demonstrated by a more challenging separation.

Two advantages are offered by the use of serially coupled columns to achieve liquid phase mixtures: it obviates the danger of non-ideal solution behavior that may occur with liquid phase mixtures (although this is rarely demonstrated), and because the preparation of highly efficient capillary columns is not a trivial matter, it is often preferable to be able to employ lengths of commercially manufactured columns.

On the other hand, the relationship between ϕ and the length fraction is rarely simple and direct. There are several complicating factors, of which the most serious is (usually) the velocity gradient in the column. Because of this, the second column in the series must always operate at higher linear gas velocities than does the first; the first column will contribute more (and the second column will contribute less) to the separation that would be implied by its length fraction alone. This complication will be discussed in more detail later.

If the effect of the velocity gradient is ignored and both columns have the same phase ratios, the length of column containing liquid phase A (L_A) is related to the length of column containing liquid phase B (L_B) by the equation

$$L_A = \phi_A(L_A + L_B) = \phi_A L \tag{1}$$

where the total length, L, is equal to L_A plus L_B. If the phase ratios of the two columns differ, then

$$\frac{L_A}{\beta_A} = \frac{\phi_A L}{\beta} \tag{2}$$

where β_A and β_B are the phase ratios of columns A and B, respectively, and β is the average phase ratio of the coupled column, given by the relationship:

$$\beta = (L_A\beta_A + L_B\beta_B)/L \tag{3}$$

Substituting eqn. 3 into eqn. 2, the length of either segment can be calculated:

$$\frac{L_A}{\beta_B} = \frac{\phi_A L^2}{L_A\beta_A} + (L - L_A)\beta_B \tag{4}$$

Rearranging yields an equation that is second order with respect to L_A and L:

$$(\beta_A - \beta_B)\, L_A^2 + \beta_B L L_A - (\phi_A\beta_B)L^2 = 0 \tag{5}$$

Application of the quadratic equation yields

$$L_A = \frac{-L\beta_B \pm [L^2\beta_B^2 + 4(\beta_A - \beta_B)\phi_A L^2\beta_A]^{1/2}}{2(\beta_A - \beta_B)} \tag{6}$$

or

$$L = \frac{-\beta_B L_A \pm [L_A^2\beta_B^2 + 4(\beta_A - \beta_B)\phi_A\beta_A]^{1/2}}{2(\phi_A\beta_A)} \tag{7}$$

Either equation can be employed, depending on whether a certain total column length is desired (eqn. 6), or whether one wishes to use an existing column of length L_A (eqn. 7).

The concept of window diagrams, proposed by Laub and Purnell and their co-workers (*e.g.*, refs. 4,5) is based on the fact that

$$K_{D(A+B)} = K_{D(A)}\phi_A + K_{D(B)}\phi_B \tag{8}$$

where the subscripts A and B denote the liquid phase for that distribution constant in question, and $\phi_{A,B}$ represents the volume fraction of the specified liquid phase. Inasmuch as ϕ_A plus ϕ_B equals 1:

$$K_{D(A+B)} = K_{D(B)} + \phi_A(K_{D(A)} - K_{D(B)}) \tag{9}$$

From this it is apparent that a plot of $K_{D(A,B)}$ *vs.* ϕ_A must be linear; *i.e.*, the distribution constant of a solute in that mixture is a linear function of the amount of either of the liquid phases comprising that mixture.

The present study, an offshoot of our recycling work[6], was directed toward using these principles in a more efficient system to achieve the separation of two "real world" mixtures that have plagued a number of investigators.

EXPERIMENTAL

Test mixtures

Test mixture I was composed of solutes produced by alcoholic fermentation, whose separation is of considerable industrial interest. At least two separate columns

are traditionally employed to separate these components; their separation in a single chromatographic column has not yet been reported. Solutes, listed in Table I, were present in roughly equal amounts, with the exception of ethanol, which amounted to 30% of the mixture. The industrial importance of this separation was drawn to our attention by Liddell[7]. Test mixture II was composed of solvents (Table II) used in a variety of food packaging films. Determination of residual solvent in these films and in the packaged food is of obvious interest, both to regulatory agencies and to segments of the food processing industry. The mixture was suggested to us by Kolb[8], who had previously worked with this mixture[9].

Gas chromatography

GC separations employed a Varian 3700 gas chromatograph equipped with an inlet splitter and make up gas adaptor, both from J & W Scientific, Fused-silica capillary columns were obtained from the same source. The DB-1 polymethylsiloxane bonded phase (equivalent to SE-30) was 14 m × 0.32 mm I.D. with a liquid phase film thickness of 1.0 μm. Two polyethylene glycol (Carbowax) columns were employed, differing only in length (31 m and 21 m). Both were 0.25 mm I.D. with liquid phase film thicknesses of 0.25 μm. All columns were operated at 60°C and at average linear carrier gas velocities of 8–50 cm/sec with helium carrier gas.

The window diagrams were generated with BASIC computer programs on an Apple II plus computer, using a Paper Tiger 460G graphics printer (Integral Data Systems, Milford, NH, U.S.A.). The graphics printer routines were from Computer Stations (Granite City, IL, U.S.A.). These will be published separately.

For the purposes of testing the window diagrams using capillary columns, 15–20 cm of thin walled heat shrink PTFE tubing (0.025-in. expanded I.D., 0.010-in. recovered I.D., 0.004-in. wall; Zeus Industrial Products) was used to connect columns. Shrinking was accomplished with a heat gun at a maximum temperature of about 350°C.

RESULTS

Chromatograms of test mixture I run on pure DB-1 and pure Carbowax are shown in Figs. 1 and 2. An analysis temperature of 60°C was chosen because of the high volatility of the solutes and the lower operating temperature limit of Carbowax. Fig. 1 shows that the DB-1 column failed to separate methanol and acetaldehyde, while in Fig. 2 it can be seen that the Carbowax column failed to separate 2-methylbutanol from 3-methylbutanol. The method of Laub and Purnell[4] was used to estimate the optimum mixture of these two liquid phases. The distribution constant of each solute was determined at 60°C on columns of known phase ratio, coated with pure polyethylene glycol or DB-1 (Table I). The two points (for each solute) were then connected by a straight line, producing a plot of the volume fraction of DB-1, *vs.* K_D (Fig. 3). This plot also reveals the elution order of those solutes as functions of the volume ratios of those two liquid phases at that temperature. The relative retention (α = larger K_D/smaller K_D) of every possible solute pair as a function of the liquid phase volume ratio is calculated; larger values (which would not be separation-limiting) are rejected by the computer, and those that are on-scale are plotted as in Fig. 4. The highest "window" in such a plot indicates what volume ratio of those liquid phases

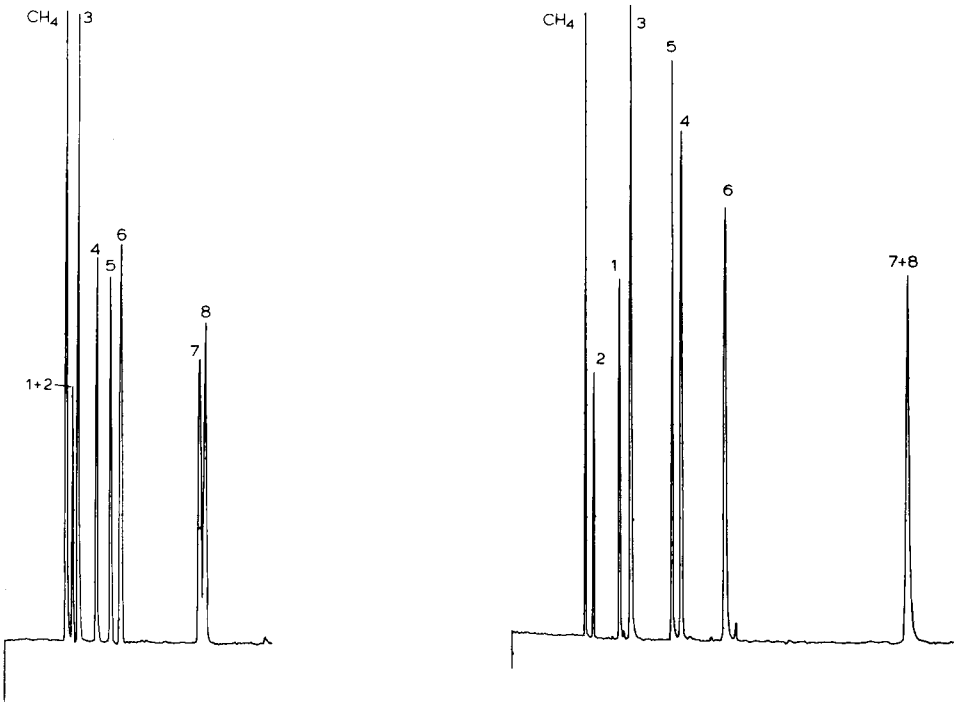

Fig. 1. Chromatogram of test mixture I on an 11 m × 0.32 mm fused-silica capillary, coated with 1.0-μm bonded film of polymethylsiloxane (DB-1); split injection (*ca.* 1:100), 60°C isothermal, u = 26 cm/sec. See Table I for compound identification.

Fig. 2. Chromatogram of test mixture I on a 30 m × 0.25 mm fused-silica capillary, coated with a 0.25-μm film of polyethylene glycol (Carbowax); 60°C, u = 30 cm/sec. See Table I for compound identification.

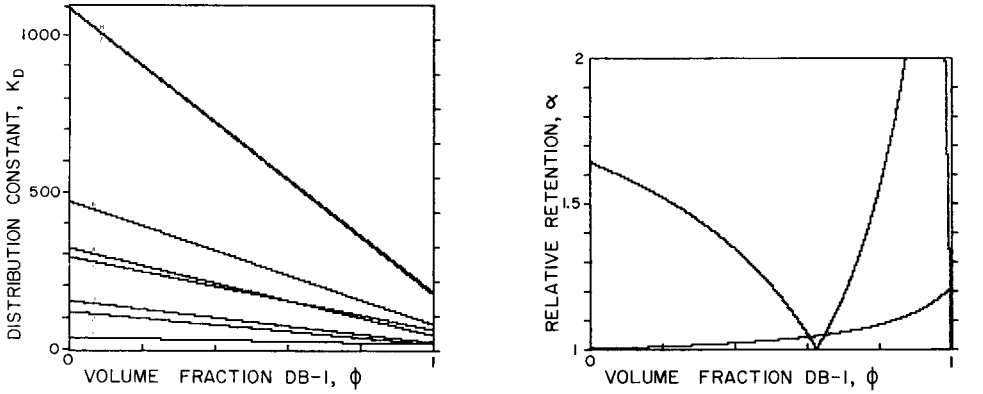

Fig. 3. Computer plot of the distribution constants (K_D) of the individual solutes *versus* the volume fraction of DB-1 (ϕ) for test mixture I. See Table I for compound identification.

Fig. 4. Computer plot of the relative retentions of separation-limiting solute pairs *versus* the volume fraction of DB-1 for test mixture I.

TABLE I

K_D VALUES (60°C) FOR SOLUTES OF TEST MIXTURE I

Solute	*Peak No.**	*DB-1*	*Carbowax*
Methanol	1	8	117
Acetaldehyde	2	8	30
Ethanol	3	16	153
n-Propanol	4	39	324
sec.-Butanol	5	57	294
Isobutanol	6	71	475
3-Methylbutanol	7	172	1099
2-Methylbutanol	8	178	1099

* As used in Figs. 1, 2 and 6.

produces the highest relative retentions for those limiting solutes at that temperature. In this particular case, the relative retention of acetaldehyde and methanol rapidly approaches unity as the last traces of Carbowax are removed from the system, and the optimum window would appear to be at *ca.* 99.5% DB-1 and 0.5% Carbowax.

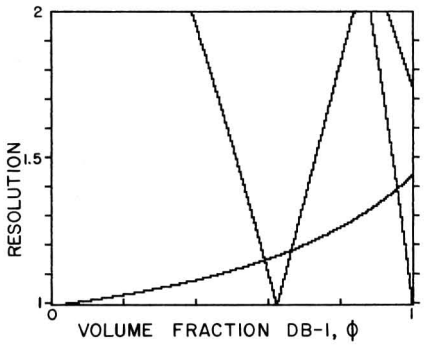

Fig. 5. Computer plot of resolution (*Rs*) *versus* volume fraction of DB-1 (ϕ) for test mixture I. See text for details.

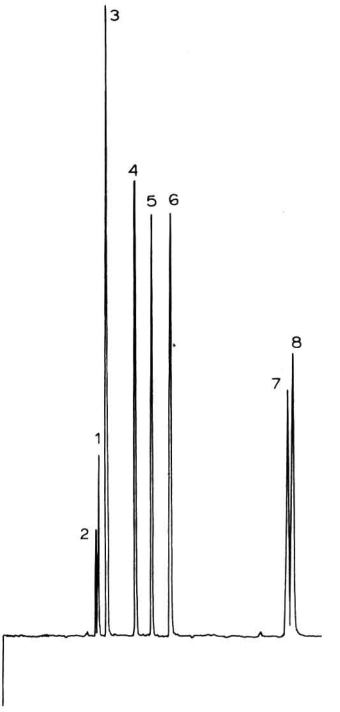

Fig. 6. Chromatogram of test mixture I on a serially coupled column composed of a 3.7 m × 0.25 mm section coated with a 0.25-μm film of polyethylene glycol (Carbowax), followed by a 28.5 m × 0.32 mm section coated with a 1.0-μm bonded film of polymethylsiloxane (DB-1); split injection, 60°C, u = 28 cm/sec. See Table I for compound identification.

Using lengths calculated according to eqn. 7, a column of these proportions was assembled; separation differed from that obtained on pure DB-1 only in that a slight shoulder was noticeable on the first peak (acetaldehyde plus methanol). This poor separation was attributable to the fact that these two solutes exhibit very small partition ratios, *ca.* 0.2, at that window. Although these proportions of the two liquid phases produced the highest relative retentions for the overall mixture, separation was less than adequate, in that resolution is also affected by the partition ratio, k.

A plot of resolution *vs.* ϕ confirmed this (Fig. 5); the best resolution window occurs at 95% DB-1 and 5% Carbowax. Utilizing eqn. 7, a column was constructed of 28.5 m DB-1 (thick film, wide bore) plus 3.7 m Carbowax. With the Carbowax segment connected to the inlet, methanol and acetaldehyde exhibited a resolution of 1.72 (Fig. 6); when the DB-1 segment was connected to the inlet, the resolution of these two solutes was 1.09. On the other hand, the resolution of the two methylbutanol isomers was 1.45 in the first configuration, and 1.59 in the second.

Fig. 7 shows test mixture II run on a column coated with pure DB-1, on which acetone and isopropanol, and methyl acetate and dichloromethane coeluted, and Fig. 8 shows the mixture on a column coated with pure Carbowax, where 2-butanone,

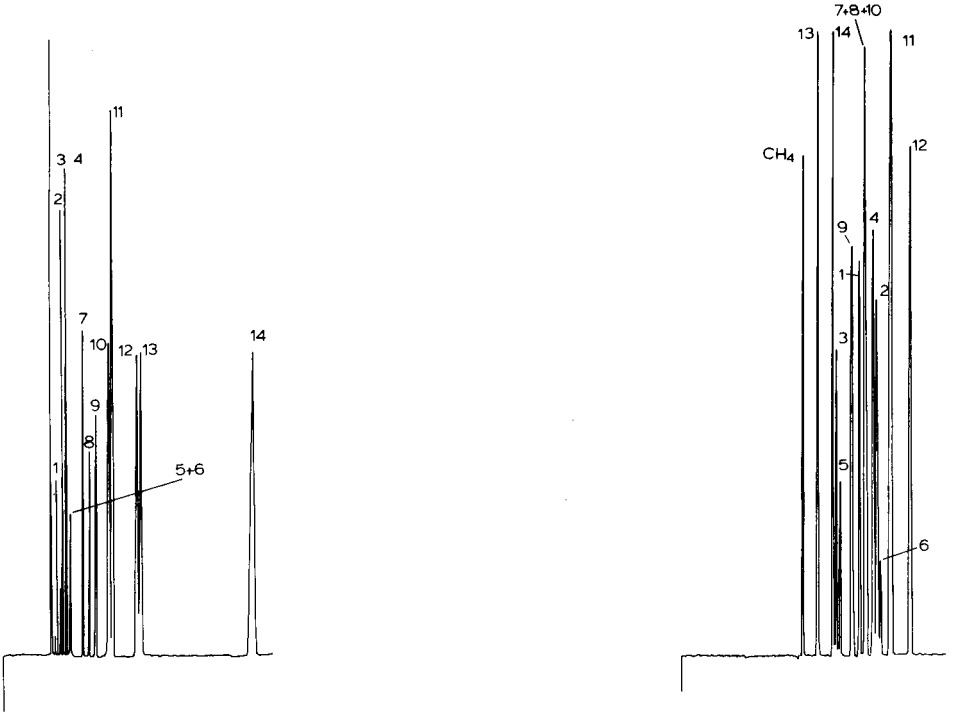

Fig. 7. Chromatogram of test mixture II on an 11 mm × 0.32 mm fused-silica capillary, coated with 1.0-μm bonded film of polymethylsiloxane (DB-1); split injection, 60°C isothermal, u = 26 cm/sec. See Table II for compound identification.

Fig. 8. Chromatogram of test mixture II on a 30 m × 0.25 mm fused-silica capillary, coated with a 0.25-μm film of polyethylene glycol (Carbowax); 60°C, u = 28 cm/sec. See Table II for compound identification.

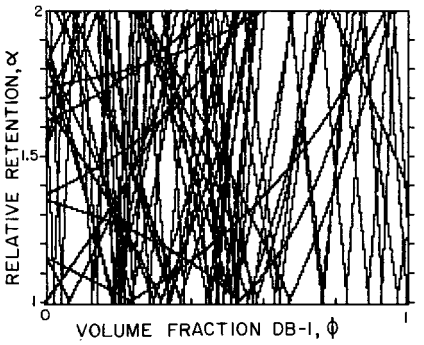

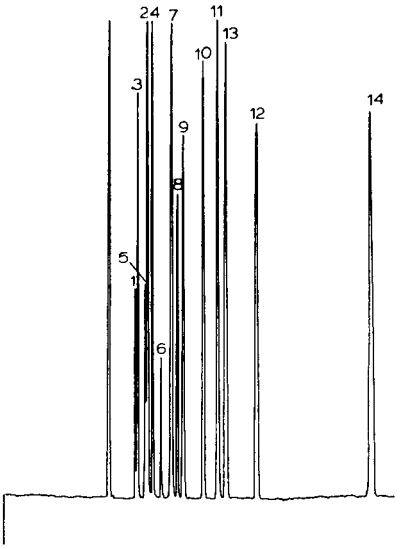

Fig. 9. Computer plot of relative retentions (α) of individual pairs of solutes in test mixture II, *versus* the volume fraction of DB-1 (ϕ). See text for details.

Fig. 10. Chromatogram of test mixture II on a serially coupled column composed of a 14.0 m × 0.32 mm section coated with a 1.0-μm bonded film of polymethylsiloxane (DB-1), followed by a 23.1 m × 0.25 mm section coated with a 0.25-μm film of polyethylene glycol (Carbowax); split injection, 60°C, u = 30 cm/sec. See Table II for compound identification.

ethyl acetate and isopropyl acetate eluted as a single peak. The distribution constants are listed in Table II.

A window diagram of α *vs.* ϕ is shown in Fig. 9, which indicates two approximately equal windows, one at 80% DB-1, and the other at 86% DB-1. Using

TABLE II

K_D VALUES (60°C) FOR SOLUTES IN TEST MIXTURE II

Compound	*Peak No.**	*DB-1*	*Carbowax*
Methanol	1	8	118
Ethanol	2	16	153
Acetone	3	21	70
Isopropanol	4	23	145
Methyl acetate	5	32	78
Dichloromethane	6	31	162
2-Butanone	7	53	130
Ethyl acetate	8	63	128
Tetrahydrofuran	9	75	102
Isopropyl acetate	10	96	130
Benzene	11	102	183
n-Propyl acetate	12	144	224
n-Heptane	13	149	30
n-Octane	14	336	63

* As used in Figs. 7, 8, 10, 11 and 13.

eqn. 7, 14 m of the DB-1 column were joined to 23.1 m of Carbowax. The resultant chromatogram (with the DB-1 segment connected to the inlet) is shown in Fig. 10, where it can be seen that the most difficult solutes to resolve are methanol–acetone, and methyl acetate–ethanol. Since the calculated column lengths can only approximate the desired ratios of the two liquid phases (largely because of the carrier gas velocity gradient discussed earlier), short lengths of column were removed by trial and error until the optimum resolution of all solutes was achieved. This resulted in a column composed of 13.35 m of DB-1 and 23.1 m Carbowax. The chromatogram obtained with this column is shown in Fig. 11, and resulted in a resolution of 1.12 for methanol and acetone, and 1.19 for methyl acetate and ethanol.

To determine the optimum average carrier gas velocity for this particular separation, a Van Deemter plot was generated, which indicated that the optimum was 30–40 cm/sec under these conditions. At a velocity of 35 cm/sec however, methyl acetate and ethanol co-eluted. Plots of resolution of these two solvent pairs *vs.* the average linear carrier gas velocity are shown in Fig. 12. Although all of these solutes exhibited optimum velocities of *ca.* 35 cm/sec, resolution between methanol and ethyl acetate was maximum somewhere below 7 cm/sec, while that between acetone and methanol is best at a velocity of *ca.* 40 cm/sec. It seems probable that this is due to the carrier gas velocity gradient operating in the column.

To test this hypothesis, the column was reversed and the Carbowax end connected to the inlet. By comparing the elution order of the solutes to those indicated by

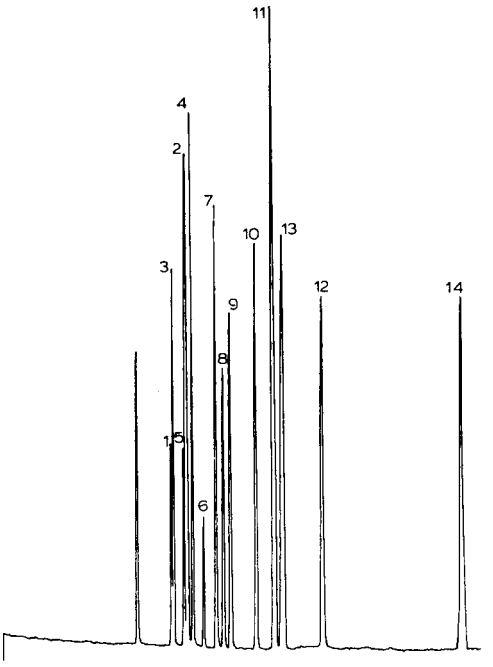

Fig. 11. Chromatogram of test mixture II on a serially coupled column composed of a 13.35 m × 0.32 mm section coated with a 1.0-μm bonded film of polymethylsiloxane (DB-1), followed by a 23.1 m × 0.25 mm section coated with a 0.25-μm film of polyethylene glycol (Carbowax); split injection, 60°C, u = 30 cm/sec. See Table II for compound identification.

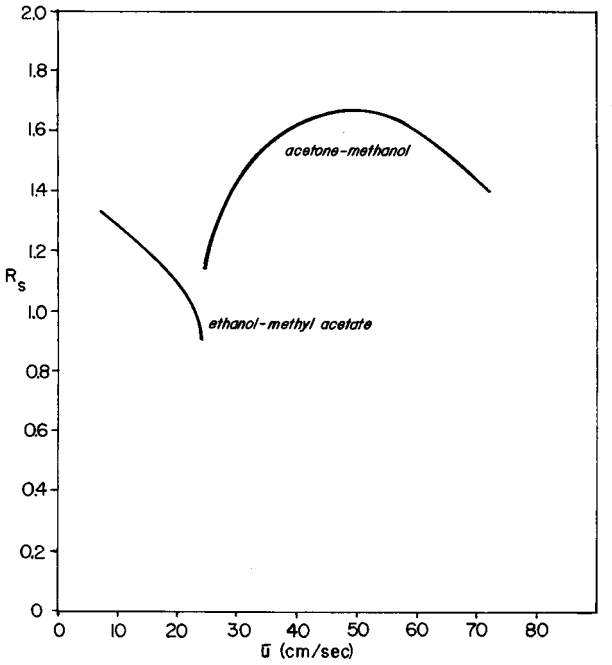

Fig. 12. Plot of resolution (R_s) *vs.* u for ethanol–methyl acetate, and acetone–methanol on a serially coupled column composed of a 13.35 m × 0.32 mm section coated with a 1.0-μm bonded film of polymethylsiloxane (DB-1), followed by a 23.1 m × 0.25 mm section coated with a 0.25-μm film of polyethylene glycol (Carbowax); split injection, 60°C.

plotting the values in Table II (as was done in Fig. 3 for the values in Table I), it was determined that because the gas velocity at the inlet end is lower than the average and that at the outlet end is higher than the average, the "apparent" liquid phase mixture in this configuration (Carbowax preceding DB-1) approximated 66% DB-1 instead of the 80% desired. Small segments of the Carbowax column were removed by trial and error until the correct elution order was observed. This resulted in a column composed of 13.35 m of DB-1 and 13.1 m of Carbowax. A chromatogram run on this column is shown in Fig. 13.

DISCUSSION

Window analysis seems well suited to predicting binary phase mixtures that can achieve the separation of complex mixtures that resist separation even on high resolution columns coated with a single liquid phase. Both test mixtures investigated fall into this category, and both were resolved using coupled capillary columns to achieve the desired ratio of the two liquid phases.

Calculation of the requisite column lengths is complicated by the carrier gas velocity gradient operating in the column. While the velocity gradient itself is well understood (*e.g.*, refs. 10–13), the matter is further complicated by the fact that the velocity gradient and the column length are interdependent. Neither is it readily apparent which column parameter is most closely related to ϕ.

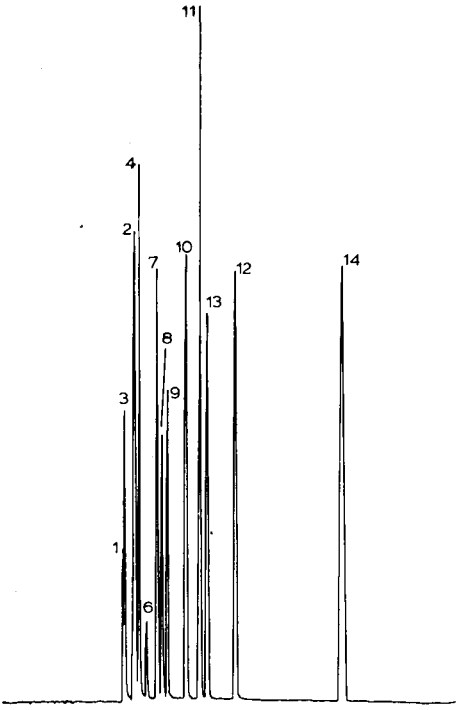

Fig. 13. Chromatogram of test mixture II on a serially coupled column composed of a 13.1 m × 0.25 mm section coated with a 0.25-μm film of polyethylene glycol (Carbowax), followed by a 13.35 m × 0.32 mm section coated with a 1.0-μm bonded film of polymethylsiloxane (DB-1); split injection, 60°C, u = 40 cm/sec. See Table II for compound identification.

In practice, however, excellent results can be achieved by using the window diagram concept to approximate the proper liquid phase mixture; the required lengths of column are then calculated using eqn. 6 or 7, as appropriate. The calculated lengths usually require some modification, because the section which is first in sequence (*i.e.*, the inlet end) will need to be shorter than that calculated, and/or the second segment (that connected to the detector) will need to be longer than that calculated. Which of these choices is best will depend on the lengths of column available, and their inner diameters. For example, the DB-1 column employed with test mixture II was a wide-bore column (0.32 mm I.D.). When this was first, only a small adjustment (−64 cm) was required; when the Carbowax segment (0.25 mm I.D.) was first, a larger adjustment (−900 cm) was necessary to achieve the same results.

Columns coated with premixed liquid phase mixtures offer another possibility. There have been some notable successes in the coating of fused-silica capillaries with premixed liquid phases[14,15]. It is probable that column suppliers will soon offer commercial columns coated with liquid phases premixed to the analyst's specifications and designed for the optimal separation of specific mixtures.

An alternate approach to minimizing the velocity gradient would be to place a restriction at the detector outlet and operate at higher average column pressures[16]. Neither of these possibilities was investigated in the present study.

The observed partition ratio exhibited by any solute is the sum of the times spent in the two liquid phases, quantity divided by the time spent in the gas phase. Hence in series coupled columns coated with dissimilar liquid phases, the apparent partition ratio is affected by the carrier gas velocity, a situation that is not encountered with columns coated with a pure (or homogeneously mixed) liquid phase. It should be possible to set the length of the second column segment so that the linear velocity is optimized with respect to resolution.

REFERENCES

1 W. Jennings, *Gas Chromatography with Glass Capillary Columns*, Academic Press, New York, San Francisco, London, 2nd ed., 1980.
2 W. Jennings, *Comparisons of Fused Silica and Other Glass Columns for Gas Chromatography*, Huethig Verlag, Heidelberg, New York, 1981.
3 H. J. Maier and O. C. Karpathy, *J. Chromatogr.*, 8 (1962) 308.
4 R. J. Laub and J. H. Purnell, *Anal. Chem.*, 48 (1976) 799.
5 J. H. Purnell, P. S. Williams and G. A. Zabierek, in R. E. Kaiser (Editor), *Proc. 4th International Symposium on Capillary Gas Chromatography, Hindelang, May 4–7, 1981*, Huethig Verlag, Heidelberg, New York, 1981.
6 W. Jennings, J. A. Settlage, R. J. Miller and O. G. Raabe, *J. Chromatogr.*, 186 (1979) 189.
7 P. A. P. Liddell, personal communication, 1981.
8 B. Kolb, personal communication, 1981.
9 B. Kolb, P. Pospisil and M. Auer, *J. Chromatogr.*, 204 (1981) 371.
10 J. C. Giddings, L. S. Spencer, L. R. Stucki and G. H. Stewart, *Anal. Chem.*, 32 (1960) 867.
11 J. C. Giddings, *Anal. Chem.*, 34 (1962) 314.
12 J. C. Giddings, *Anal. Chem.*, 35 (1963) 353.
13 J. C. Giddings, *Anal. Chem.*, 36 (1964) 741.
14 P. Sandra and M. van Roelenbosch, *Chromatographia*, 14 (1981) 345.
15 R. Jenkins, personal access to unpublished results, 1981.
16 D. H. Desty, personal communication, 1981.

Journal of Chromatography, 239 (1982) 51–60
Elsevier Scientific Publishing Company, Amsterdam — Printed in The Netherlands

CHROM. 14,593

PEROXIDE-INITIATED *IN SITU* CURING OF SILICONE GUMS FOR CAPILLARY COLUMN GAS CHROMATOGRAPHY

L. BLOMBERG*, J. BUIJTEN, K. MARKIDES and T. WÄNNMAN
Department of Analytical Chemistry, University of Stockholm, Arrhenius Laboratory, S-106 91 Stockholm (Sweden)

SUMMARY

The combination of leaching, silanization with cyclic siloxanes and peroxide-initiated *in situ* vulcanization of silicone stationary phases for gas chromatography gives capillary columns that show very high efficiencies, very low adsorptivity as reflected by stringent tests and very high stability, *e.g.*, low bleeding rates. Such columns have been prepared using AR-glass and fused silica as the supports and SE-30, SE-52, SE-54 and polar OV-215 as stationary phases. The versatility of these columns is demonstrated by the analysis of underivatized drugs, barbiturates and tricyclic antidepressants. The separation of aqueous solutions is also described.

INTRODUCTION

The *in situ* preparation of bonded silicone stationary phases applied to capillary columns for gas chromatography (GC) was first described by Rigaud *et al.*[1], and since then several papers dealing with refinements of the method have been published[2–5]. The preparation of columns coated with bonded silicone phases was also investigated in our laboratory when we attempted instead to combine bonding with the introduction of a slight degree of cross-linking in the polymer[6–10]. The cross-linking was accomplished by addition of tri- or tetrachlorosilanes to the so-called pre-polymer. Madani and co-workers[1–5] prepared polymers from dichlorosilanes only, which makes cross-linking impossible unless some siloxanes able to undergo tri- or tetrafunctional reaction were formed during the *in situ* polymerization.

Earlier endeavours to combine experimentally bonding and cross-linking of the stationary phase in capillary columns were made by Grob[11] with polybutadiene phases and by Bossart[12] with silicones.

When a stationary phase film has been fixed by cross-linking, it can withstand various strains. The column thus retains its good chromatographic properties also at elevated temperatures and there is no risk of stationary phase rearrangements or deterioration of performance due to poor wettability. Further, as the phase is insoluble in commonly used solvents, the stationary phase film is resistant to the relatively large amounts of liquid solvent passing the first column coils upon on-column injection. Moreover, the insolubility of the phase makes possible the rinsing out of

0021-9673/82/0000–0000/$02.75

non-volatile material from a used column, thus regenerating the column[10]. Another advantage is that an immobilized phase can withstand water[13], the analysis of aqueous solutions thus being feasible. A further application would be that with a supercritical fluid as carrier[14].

Cross-linking of a stationary phase would in general result in impaired chromatographic performance[15]. Our silicones probably contain relatively few cross-links, and according to our experience these do not seem to have an adverse effect on the chromatographic properties[10].

In our earlier work, cross-linking was obtained through Si–O–Si bonds[6–10]. Recently, immobilization of stationary phases by means of Si–C–C–Si bonds has been described by Grob and co-workers[16,17], Sandra *et al.*[13] and the present authors[18]. This type of cross-linking is a radical reaction, the radicals being formed by decomposition of organic peroxides[19]. Peroxide curing of silicones was first reported in 1948[20], and the method has since been used extensively in the rubber industry[21]. Several types of peroxides are useful, see *e.g.* refs 22 and 23, but we chose to use dicumyl peroxide, which has proved to be effective in the rubber industry, especially when the polymer contains some vinyl groups[21]. Further, relatively inactive ketones are formed on decomposition of dicumyl peroxide[24]. Some peroxides, *e.g.*, benzoyl peroxide, form organic acids on decomposition, which might be a drawback, as the hydrolysis of siloxanes is catalysed by acids[24].

Radical-initiated cross-linking can also be effected by other methods, *e.g.*, with high-energy radiation[19]. For glass capillary columns, a low-temperature plasma has been used[25]. Air-curing of SE-52 columns has been reported to result in increased column stability; such an effect can also be attributed to cross-linking[26].

Compared with our earlier methods, the peroxide-initiated cross-linking is simpler to perform and, in addition, the necessary chemicals are readily available. The columns prepared according to the two methods have, however, different properties.

In this paper, we describe the preparation of capillaries coated with *in situ* cured stationary phases. AR-glass and fused silica capillaries have been used as supports and SE-30, SE-52, SE-54 and OV-215 as stationary phases. Further, some properties of peroxide-cured columns and $SiCl_4$-cured columns are compared.

EXPERIMENTAL

AR-glass (Glaswerk Wertheim, Wertheim am Main, G.F.R.) capillaries were drawn on a Brechbühler (Schlieren, Switzerland) glass-drawing machine. Fused silica capillaries were obtained from Hewlett-Packard (Avondale, PA, U.S.A.).

The AR-glass capillaries were leached with 18 % hydrochloric acid, principally according to Grob *et al.*[27], *i.e.*, heat treatment overnight at 140°C. The hydrochloric acid was then displaced by two capillary lengths of dilute hydrochloric acid solution (pH 3), this solution being in turn displaced by two capillary lengths of methanol. The methanol was flushed out and the capillary placed in an oven, the temperature of which was programmed from 60 to 250°C at 10°C/min, then held at 250°C for 2 h. This dehydration step was accomplished under a low carrier gas flow. Dehydration could also be carried out by heating for 30 min at 230°C. Both ends of the capillary were then connected to a vacuum.

Some fused silica capillaries were treated with hydrochloric acid in the same

way as AR-glass capillaries, with the exception that they were heated at 100°C and then rinsed with several capillary lengths of hydrochloric acid of pH 3, followed by methanol.

Silanization was performed with octamethylcyclotetrasiloxane[28,29] and 3,3,3-trifluoropropyl(methyl)cyclosiloxane[30]. For AR-glass, reaction was effected by heating at 400°C for 15 h, and for fused silica, at 350°C for 15 h. During the heat treatment, the polyimide of the fused silica capillary was protected by an atmosphere of nitrogen.

Curing procedure

Solutions for static coating of capillaries were prepared using methylene chloride as solvent for all phases except OV-125, for which diethyl ether–ethyl acetate (4:1) was used. For phases containing vinyl groups, the amount of dicumyl peroxide (Merck, Darmstadt, G.F.R.) added to the solution was 0.1–0.5% (w/w) of the amount of stationary phase; for other phases 0.5–1.0% was used. The solutions were dried over calcium sulphate and, when stored in the dark, remained stable for at least 1 week. Before use, the solutions were centrifuged.

Capillaries were statically coated using the prepared solutions. After coating, the capillaries were flushed with dry nitrogen for 1 h at room temperature. The capillary was then evacuated by attaching both ends to vacuum and sealing with a micro-flame. To seal fused silica capillaries, a micro-flame gas-welding torch was used. The closed capillary was placed in the oven of a gas chromatograph, the temperature of which was rapidly raised to 140°C and maintained at this temperature for 30 min (for OV-215 only for 5 min). The oven was then rapidly cooled, and the column flushed with dry nitrogen at room temperature. Finally, the columns were rinsed with 5 ml of methylene chloride. The rinsing should be performed slowly; 5–6 h are suitable. Before testing, the columns were conditioned at 300°C (270°C for OV-215) for 1 h.

Testing procedure

The columns were tested by injection of a Grob text mixture[31] and also by test mixtures suggested by Schomburg *et al.*[32]. The amount of each test substance injected on the column was *ca.* 1 ng.

RESULTS AND DISCUSSION

The leaching of AR-glass has four purposes. First, metal ions, especially sodium ions, are removed from the glass surface. Second, a dense layer of silica xerogel is formed, which is presumed to counteract further diffusion of sodium ions from the bulk to the surface. The properties of such a layer are, however, dependent on how the gel has been formed. Silica hydrogel shrinks upon drying and is converted to a silica xerogel. The degree of shrinkage is, however, reduced if the gel water is displaced by an organic liquid before drying[33]. Third, the number of surface silanol groups is increased, and thus the surface is prepared for the following silanization. Fourth, leaching might level off differences between different glass batches.

Some fused silica capillaries were "leached" in order to increase the number of surface silanol groups. For the silanizing agents used here, however, such "leaching"

had little effect on silanization. We think that "leaching" of fused silica deserves to be further investigated.

Cyclic siloxanes were used for the silylation of AR-glass and fused silica capillaries. The reagents were chosen to give properties to the glass that facilitate wetting with stationary phases. For this purpose, a silylating agent was selected that contained the same functional side-groups as the phase to be coated, *e.g.*, for coating with silicone gum OV-215, the glass surface was silanized with cyclic siloxanes having (methyl)trifluoropropyl side-groups. The silylation procedure thus provides both deactivation and wettability[29,30].

In our opinion, it is very important that the stationary phase is deposited as an even film upon coating. This film is fixed in position on cross-linking, and no improvement of the film can be obtained after fixation. The pre-treatment of the capillaries gives the necessary wettability, and a carefully performed static coating results in the formation of even films. High column efficiencies were obtained (Table I).

TABLE I

CHARACTERISTICS OF SOME TYPICAL CAPILLARY COLUMNS

Column No.	*Column diameter (mm)*	*Type of capillary*	*Stationary phase*	d_f *(μm)*	*Coating efficiency (%)*	*HETP for naphthalene (mm)*	*Kováts retention index at 90 °C*	
							Octanol	*Naphthalene*
1	0.28	AR-glass	SE-30	0.34	107	0.25	1051	1153
2	0.20	Fused silica	SE-30	0.25	93	0.19	1054	1156
3	0.28	AR-glass	SE-52	0.34	99	0.24	1066	1184
4	0.26	AR-glass	SE-54	0.32	90	0.25	1069	1191
5	0.20	Fused silica	SE-54	0.25	96	0.19	1069	1184
6	0.26	AR-glass	OV-215	0.32	86	0.28	1244	1436
7	0.26	AR-glass	OV-215*	0.32	87	0.25	1242	1429

* Not cross-linked.

Peroxide concentration, reaction time and temperature are inter-related, the peroxide decomposition rate increasing rapidly with increase in temperature. At 140°C, the half-life of dicumyl peroxide in benzene is 30 min and at 160°C it is 3 min[34]. We have found that for the preparation of non-polar columns, the reaction conditions are not particularly critical, and highly inert columns are obtained [Figs. 1, 2(2) and 2(3)] (peaks in all figures represent an amount of sample of *ca.* 1 ng). The curing is performed in a closed system at a relatively low temperature, which we believe, facilitates control of the reaction, and thereby reproducibility. One can, of course, use higher temperatures combined with smaller amounts of peroxide, but too intense curing leads to stationary phase films that are unsuitable for chromatographic purposes, *e.g.*, adsorption of hydrocarbons occurs. Dicumyl peroxide shows a higher reactivity with vinyl groups than with methyl groups, and therefore a smaller amount of peroxide can be used for vinyl-containing siloxanes than for methylsiloxanes[24]. With polar phases, column adsorptivitiy is a problem, but when using short curing times (5 min) for OV-215, well deactivated columns are obtained also with this phase [Fig. 2(1)]; a certain amount of amine adsorption is evident, however.

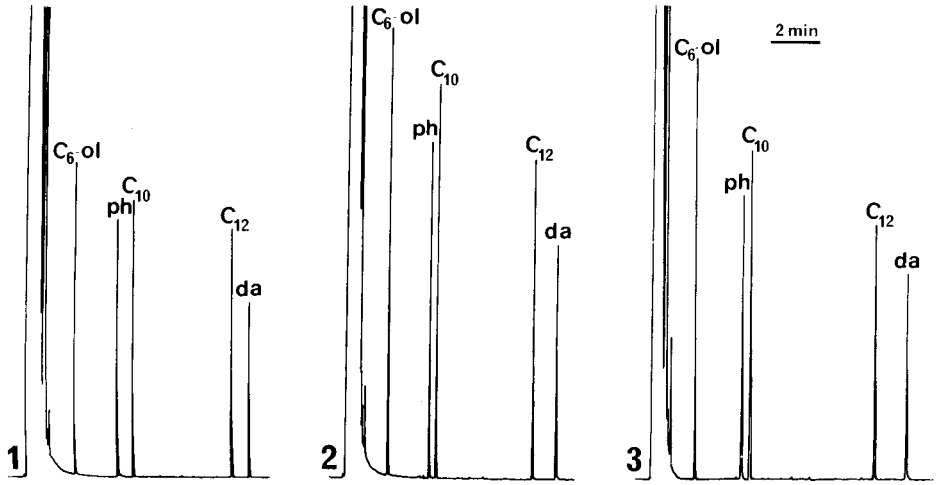

Fig. 1. Gas chromatograms [with flame-ionization detector (FID)] of a test mixture on different AR-glass capillary columns, D_4-deactivated and dicumyl peroxide cured. Initial temperature, 40°C for chromatograms 1 and 2, programmed at 7°C/min; 50°C for chromatogram 3, programmed at 5°C/min. Stationary phases: (1) SE-30; (2) SE-52; (3) SE-54. Peaks: C_6-ol = cyclohexanol; ph = phenol; C_{10} = decane; C_{12} = dodecane; da = decylamine.

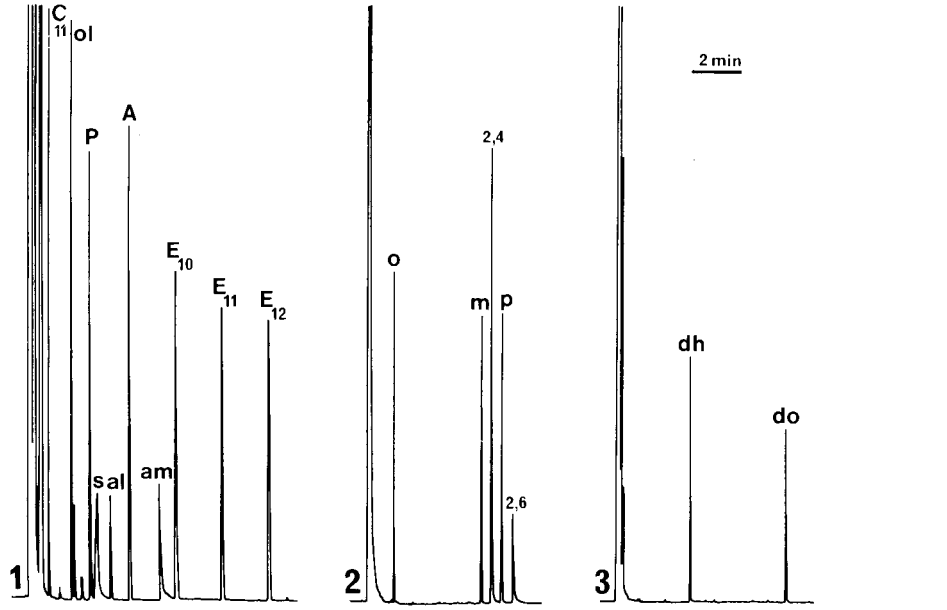

Fig. 2. Gas chromatograms (FID) of test mixtures on AR-glass capillary columns. (1) Grob test mixture on OV-215. Initial temperature 70°C, programmed at 5°C/min. Peaks: C_{11} = undecane; ol = octanol; P = 2,6-dimethylphenol; s = 2-ethylhexanoic acid; al = nonanal; A = 2,6-dimethylaniline; am = dicyclohexylamine; E_{10}, E_{11} and E_{12} = C_{10}, C_{11} and C_{12}-acid methyl esters. (2) Nitrophenol test on SE-52. Initial temperature 100°C, programmed at 7°C/min. Peak assignment: *o*, *m*, *p* = *ortho*, *meta*, *para*-nitrophenol; 2,4, 2,6 = 2,4-dinitrophenol and 2,6-dinitrophenol. (3) Diamine test on SE-30. Initial temperature 60°C, programmed at 7°C/min. Peaks: dh = 1,6-diaminohexane; do = 1,8-diaminooctane.

For all columns listed in Table I, extraction with methylene chloride led to a decrease in k values of only *ca.* 5%, as established by comparison with columns coated with non-cured stationary phases.

Column polarity, as reflected by the Kováts retention indices for octanol and naphthalene, is not much affected by vulcanization (columns 6 and 7 in Table I).

Fused silica columns have some acidic properties[32], which lead to a certain adsorptivity for amines (Fig. 3). Substances having a slightly basic character can, however, be chromatographed; the separation of some underivatized drugs is thus equally good on fused silica and AR-glass capillaries (Fig. 4). On the other hand, AR-glass has a basic character, which can be reduced by careful leaching. The separation of some underivatized barbiturates, slightly acidic in character, is thus very similar on fused silica and AR-glass capillaries (Fig. 5). The alkaline properties of AR-glass become evident on increasing the amount of sample, AR-glass columns being thus overloaded by *ca.* 20 ng of a barbiturate. The separation of some underivatized barbiturates has been demonstrated earlier[35].

The separation of underivatized tricyclic antidepressants is a new application at our laboratory. Separations achieved on fused silica capillaries coated with cross-linked SE-54 are shown in Fig. 6. The columns are so temperature stable and inert that even high-boiling, polar compounds such as opipramol can be chromatographed [Fig. 6(3)].

Separation of aqueous solutions

The GC separation of aqueous solutions on capillary columns can in some instances be an alternative to separation by high-performance liquid chromatography

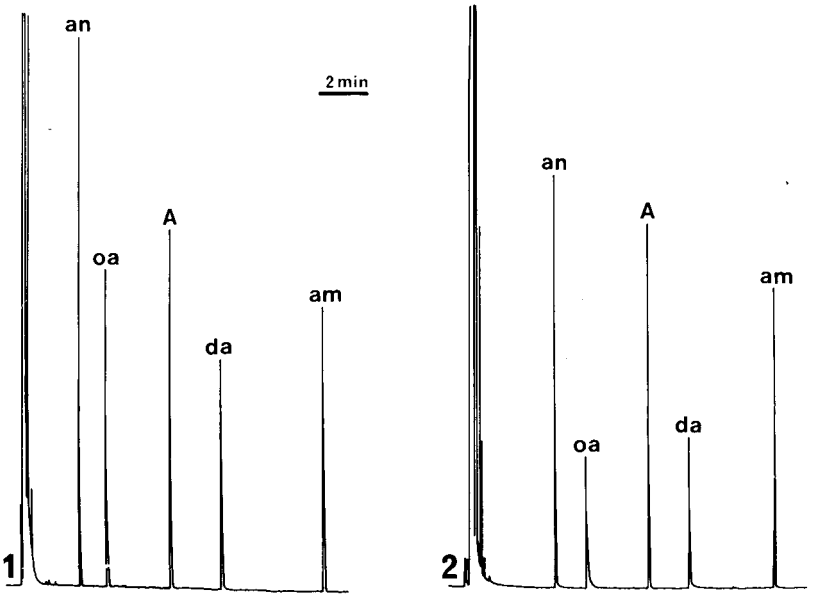

Fig. 3. Gas chromatograms (FID) of an amine test mixture on capillary columns coated with SE-54. (1) AR-glass. Initial temperature 60°C, programmed at 5°C/min. (2) Fused silica. Initial temperature 60°C, programmed at 7°C/min. Peaks: an = aniline; oa = octylamine; A = 2,6-dimethylaniline; da = decylamine; am = dicyclohexylamine.

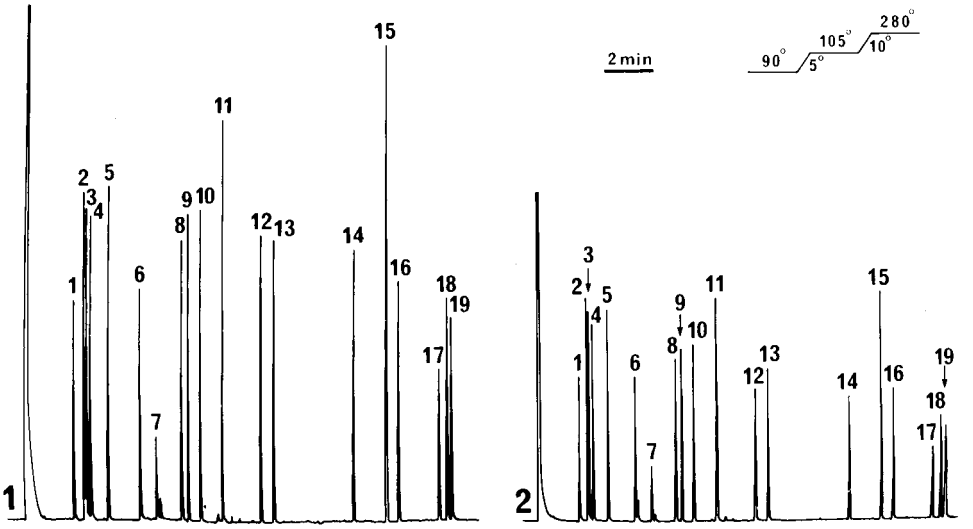

Fig. 4. Gas chromatograms (FID) of drug standard mixtures on capillary columns coated with SE-54. Temperature programme as shown. (1) AR-glass; (2) fused silica. Substances: 1 = Amphetamine; 2 = phentermine; 3 = propylhexedrine; 4 = methamphetamine; 5 = ethylamphetamine; 6 = propylamphetamine; 7 = ephedrine; 8 = phenmetrazine; 9 = phendimetrazine; 10 = amfepramone; 11 = benzocaine; 12 = phenacetin; 13 = methyl phenidate; 14 = procaine; 15 = methaqualone; 16 = cocaine; 17 = codeine; 18 = ethylmorphine; 19 = morphine.

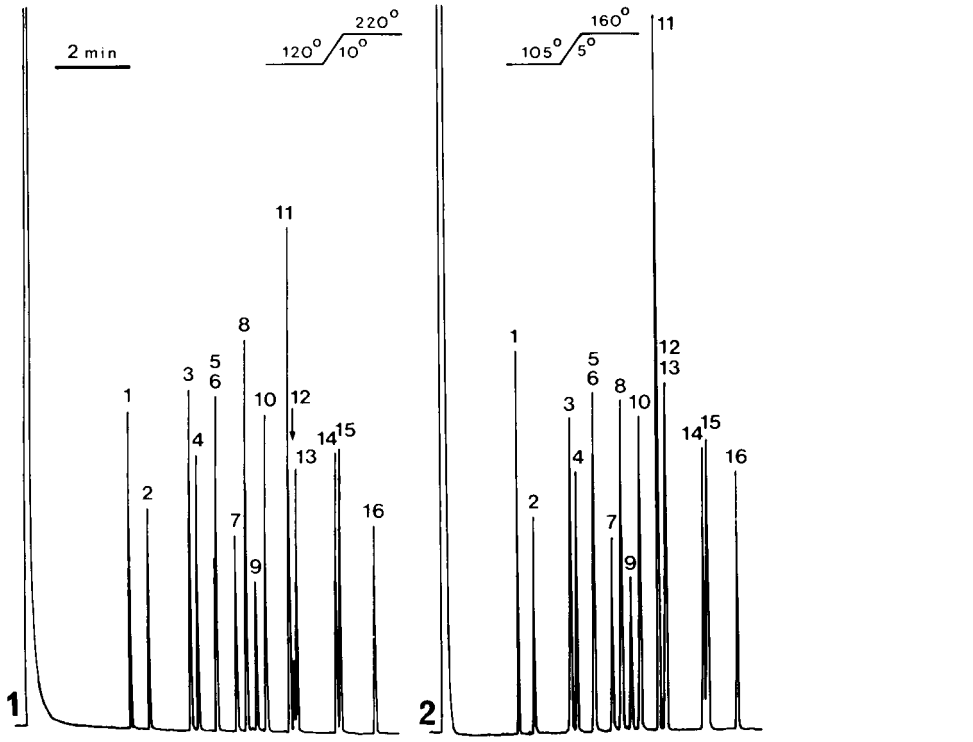

Fig. 5. Gas chromatograms (FID) of barbiturate standard mixtures on capillary columns coated with SE-54. Temperature programme as shown. (1) Fused silica; (2) AR-glass. Substances: 1 = Metharbital; 2 = barbital; 3 = allobarbital; 4 = aprobarbital; 5 = butethal; 6 = butalbital; 7 = amobarbital; 8 = pentobarbital; 9 = vinbarbital; 10 = secobarbital; 11 = glutethimide; 12 = brallobarbital; 13 = hexobarbital; 14 = phenobarbital; 15 = cyclobarbital; 16 = heptabarbital.

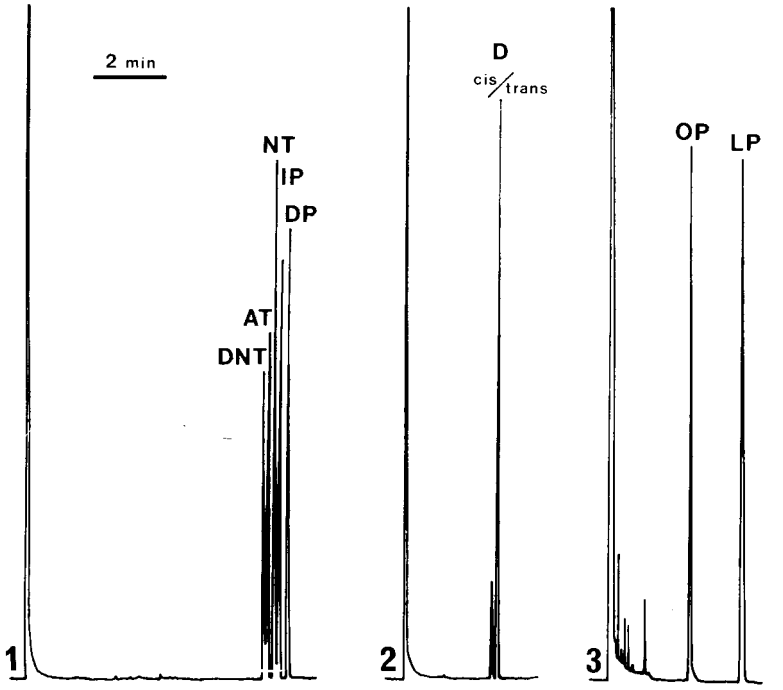

Fig. 6. Gas chromatograms (FID) of tricyclic antidepressant test mixtures on fused silica capillary columns coated with SE-54. (1) Initial temperature 180°C, programmed at 7°C/min. Peaks: DNT = desmethylnortriptyline; AT = amitriptyline; NT = nortriptyline; IP = imipramine; DP = desipramine. (2) Temperature: isothermal at 240°C. Separation of D = doxepine, *cis* and *trans*. (3) Temperature: isothermal at 320°C. Peaks: OP = opipramol; LP = lofepramine.

(HPLC), the grounds for this being that capillary columns have a much higher separation power. Moreover, sensitive detection can often be achieved without derivatization of the sample. Good separations of some aqueous test solutions on Carbowax-coated capillary GC columns have been demonstrated by Bastian *et al.*[36].

We consider that peroxide-cured silicone columns are suitable for such samples. The immobilized stationary phase cannot be displaced from the capillary surface by water, and non-volatile material deposited in the column upon injection can be rinsed out, provided, of course, that it is soluble. One must, however, be aware of the fact that injection of acids and bases together with water can lead to hydrolysis of the stationary phase; this problem also occurs in HPLC when silanized silica is used. The separation of a test mixture injected by an on-column technique is demonstrated in Fig. 7. Column activity as reflected by the elution of octanol was not influenced by 50 on-column injections at 110°C of 0.4 μl of aqueous solution.

Comparison of cross-linking techniques

Two types of cross-linked bonded silicones are now available. The cross-linking is based, in an earlier type, on Si–O–Si bonds and in a newer type on Si–C–C–Si bonds. The two types of columns do not have identical properties. We have shown in a previous paper[10] that silicone phases, where the cross-linking is based on Si–O–Si

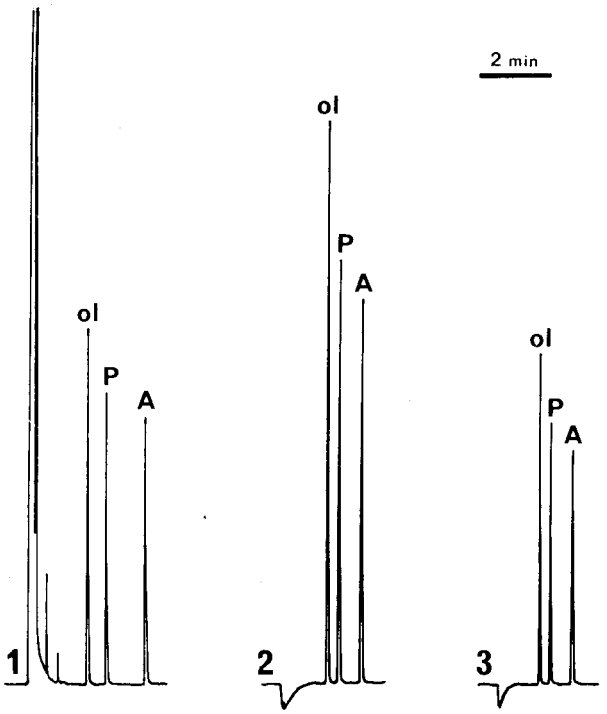

Fig. 7. Gas chromatograms (FID) of a polarity text mixture on an AR-glass capillary column coated with SE-54. On-column injection, 0.4 μl injected. (1) Temperature: isothermal at 100°C. Solvent: heptane. (2) Temperature: isothermal at 110°C. Solvent: water. (3) Conditions as in (2), but after 50 on-column injections of the aqueous test solution.

bonds, have much lower bleeding rates than corresponding conventional phases, especially at temperatures above 350°C. For peroxide-cured silicones, however, we obtain bleeding rates in the same range as for commercially available phases. A special merit of the earlier column types is their outstanding capability for the separation of polycyclic aromatic hydrocarbons[6–10]. We attribute this to a slight residue of silanol groups in the phase. Further, it is possible to prepare columns coated with cyanopropylsilicones when using the earlier curing method. The peroxide-cured columns are, on the other hand, easier to prepare, and show higher efficiencies and better deactivation. We consider that the two methods are complementary to each other.

ACKNOWLEDGEMENTS

This investigation was kindly supported by the Swedish Natural Science Research Council and by the Department of Analytical Chemistry of the University of Stockholm. We thank Dr. R. G. Jenkins for helpful discussions and B. Holm for reading the manuscript.

REFERENCES

1 M. Rigaud, P. Chebroux, J. Durand, J. Maclouf and C. Madani, *Tetrahedron Lett.*, (1976) 3935.

2 C. Madani, E. M. Chambaz, M. Rigaud, J. Durand and P. Chebroux, *J. Chromatogr.*, 126 (1976) 161.
3 C. Madani, E. M. Chambaz, M. Rigaud, P. Chebroux, J. C. Breton and F. Berthou, *Chromatographia*, 10 (1977) 466.
4 C. Madani and E. M. Chambaz, *Chromatographia*, 11 (1978) 725.
5 C. Madani and E. M. Chambaz, *J. Amer. Oil Chem. Soc.*, 58 (1981) 63.
6 L. Blomberg, J. Buijten, J. Gawdzik and T. Wännman, *Chromatographia*, 11 (1978) 521.
7 L. Blomberg and T. Wännman, *J. Chromatogr.*, 168 (1979) 81.
8 L. Blomberg and T. Wännman, *J. Chromatogr.*, 186 (1979) 159.
9 L. Blomberg, K. Markides and T. Wännman, *J. Chromatogr.*, 203 (1981) 217.
10 L. Blomberg, J. Buijten, K. Markides and T. Wännman, *J. Chromatogr.*, 208 (1981) 231.
11 K. Grob, *Helv. Chim. Acta*, 51 (1968) 718.
12 C. J. Bossart, *U.S. Pat.*, 3,514,925 (1970).
13 P. Sandra, G. Redant, E. Schacht and M. Verzele, *J. High Resolut. Chromatogr. Chromatogr. Commun.*, 4 (1981) 411.
14 M. L. Lee, P. A. Peaden, B. W. Wright, D. W. Later and J. C. Fjeldsted, in R. E. Kaiser (Editor), *Proceedings of the Fourth International Symposium on Capillary Chromatography, Hindelang*, Huethig, Heidelberg, 1981, p. 229.
15 M. B. Evans, M. J. Kawar and R. Newton, *Chromatographia*, 14 (1981) 398.
16 K. Grob, G. Grob and K. Grob, Jr., *J. Chromatogr.*, 211 (1981) 243.
17 K. Grob and G. Grob, *J. Chromatogr.*, 213 (1981) 211.
18 L. Blomberg, J. Buijten, K. Markides and T. Wännman, *J. High Resolut. Chromatogr. Chromatogr. Commun.*, 4 (1981) 578.
19 W. Noll, *Chemistry and Technology of Silicones*, Academic Press, New York, 1968.
20 G. Wright and C. S. Oliver, *U.S. Pat.*, 2,448,565 (1948).
21 J. A. Brydson, *Rubber Chemistry*, Applied Science Publ., Barking, 1978.
22 C. S. Sheppard and V. R. Kamath, *Polym. Eng. Sci.*, 19 (1979) 597.
23 C. J. Dyball, R. B. Gallagher, V. R. Kamath and S. E. Stromberg, *Plast. Des. Process*, 20 (1980) No. 1, 41 and No. 2, 38.
24 K. E. Polmanteer, *J. Elastoplast.*, 2 (1970) 165.
25 Y. Masada, K. Hashimoto, T. Inoue, Y. Simuda, T. Kishi and Y. Suwa, *J. High Resolut. Chromatogr. Chromatogr. Commun.*, 2 (1979) 400.
26 R. G. Sinclair, E. R. Hinnenkamp, K. A. Boni, D. A. Berry, W. H. Schuller and R. V. Lawrence, *J. Chromatogr. Sci.*, 9 (1971) 126.
27 K. Grob, G. Grob and K. Grob, Jr., *J. High Resolut. Chromatogr. Chromatogr. Commun.*, 2 (1979) 677.
28 T. J. Stark, R. D. Dandeneau and L. Mering, *Pittsburgh Conference, Atlantic City, 1980.*
29 L. Blomberg, K. Markides and T. Wännman, in R. E. Kaiser (Editor), *Proceedings of the Fourth International Symposium on Capillary Chromatography, Hindelang*, Huethig, Heidelberg, 1981, p. 73.
30 L. Blomberg, K. Markides and T. Wännman, *J. High Result. Chromatogr. Chromatogr. Commun.*, 3 (1980) 527.
31 K. Grob, Jr., G. Grob and K. Grob, *J. Chromatogr.*, 156 (1978) 1.
32 G. Schomburg, H. Husmann and H. Behlau, *Chromatographia*, 13 (1980) 321.
33 K. S. W. Sing, in S. Modrý and M. Svatá (Editors), *Pore Structure and Properties of Materials, Proceedings of the International Symposium Rilem/IUPAC, Part 1*, Academia, Prague, p. B-5.
34 H. R. Simonds and J. M. Church (Editors), *The Encyclopedia of Basic Materials for Plastics*, Reinhold, New York, 1967, p. 315.
35 P. Sandra, M. Van den Broeck and M. Verzele, *J. High Resolut. Chromatogr. Chromatogr. Commun.*, 3 (1980) 196.
36 E. Bastian, H. Behlau, H. Husmann, F. Weeke and G. Schomburg, in R. E. Kaiser (Editor), *Proceedings of the Fourth International Symposium on Capillary Chromatography, Hindelang*, Huethig, Heidelberg, 1981, p. 465.

Journal of Chromatography, 239 (1982) 61–69
Elsevier Scientific Publishing Company, Amsterdam – Printed in The Netherlands

CHROM. 14,533

PERFORMANCE OF DIFFERENT TYPES OF CROSS-LINKED METHYL POLYSILOXANE STATIONARY PHASES ON FUSED-SILICA GLASS CAPILLARY COLUMNS

S. R. LIPSKY* and W. J. McMURRAY
Section of Physical Sciences, Department of Laboratory Medicine, Yale University School of Medicine, New Haven, CT 06510 (U.S.A.)

SUMMARY

The chromatographic properties of two distinctly different types of silicone polymers, utilized as stationary phases and rendered insoluble on fused-silica glass capillary tubing by different methods involving the *in situ* cross-linking with either tetrachlorosilane or a variety of peroxides, were assessed. Columns showing excellent efficiency, thermal stability, and resistance to certain solvents were prepared from both classes of polymers having either Si–O–Si or Si–C–C–Si cross-linkages. The process of vulcanization of the silicone gums with certain of the peroxides frequently appeared to give rise to signs of renewed surface activity on fused silica columns previously rendered inert. This effect was either minimal or absent when reactive prepolymers were cross-linked with tetrachlorosilane.

INTRODUCTION

During the past six years, considerable progress has been made in the field of gas chromatography by Madini *et al.*[1–4] and Blomberg and Wännman[5,6] by pioneering the development of methods for the *in situ* production of efficient, thermally stable, insoluble silicone polymeric stationary phases from α,ω-hydroxypolymethylsiloxane type prepolymers on the treated surfaces of either sodalime or borosilicate glass capillary tubes. Film stability, the exceedingly low level of "bleeding" phenomena at elevated temperatures, the imperviousness of cross-linked stationary phases to exposure to large volumes of solvent, the ability to rinse away residual sample and film debris by appropriate solvents, and the relative ease by which thick films could be fabricated, were considered by these investigators to be the outstanding advantages of this technique.

More recently, in an attempt to achieve similar goals, Grob and co-workers[7,8] and Sandra *et al.*[9] utilizing methods well known in the field of silicone polymer chemistry used peroxides to insolubilize certain high-molecular-weight polydimethylsiloxane gums commonly employed as stationary phases for glass capillary columns. Both of these groups were impressed with the relative ease by which their preliminary attempts to cross-link these non-polar silicone phases succeeded in producing satis-

0021-9673/82/0000–0000/$02.75

factory capillary columns. Interestingly, Grob and Grob[8] who carried out his cross-linking experiments on regular glass capillary column surfaces which were first subjected to persilanization[10], readily obtained well deactivated columns. In contrast, in a similar study, Sandra *et al.*[9], using fused-silica glass capillary tubing which was first deactivated either by octamethylcyclotetrasiloxane[11] or by the polysiloxane technique of Schomburg *et al.*[12], failed to offer results which could provide one with information concerning the status of activity or lack thereof on these surfaces after cross-linking under the conditions of their experiments.

When we sought to modify the methods of Madani and co-workers[1-4] and Blomberg and Wännman[5,6] as well as those of Grob and co-workers[7,8] and Sandra *et al.*[9], in early attempts[13,14] to insolubilize non-polar silicone polymers on fused-silica glass capillary surfaces, several problems were encountered.

These primarily centered around (a) the residual surface activity that remained following vulcanization and (b) the erratic wettability of these surfaces by polymeric solutions containing certain peroxides. In an effort to overcome these and other technical problems that developed under these circumstances, we then studied in detail the various factors that affected cross-linking, uniform film formation, thermal stability, and surface deactivartion. These on-going investigations, some of which are now described below, also extended into the utilization of other reactions which involved the use of one- or two-component systems in the presence of appropriate catalysts for the cross-linking of various types of silicone polymer at room or elevated temperatures.

At the outset, it was also recognized that the cross-linking reactions that occurred with the type of silicone polymer produced by the methods described by Madani and co-workers[1-4] and Blomberg and Wännman[5,6], differed significantly from that brought about by the action of free radicals formed during the thermal decomposition of various peroxides upon those silicone gum phases usually employed in gas chromatography.

As seen from the structure depicted in Fig. 1, in the former instance, mild cross-linking involves the silicon oxygen (Si–O–Si) bond in the polymer chain. This siloxane moiety, found also in the vitreous silica glasses and sand, is known to contribute to the outstanding high-temperature characteristics of certain of the silicones[15]. On the other hand, as noted from the structure seen in Fig. 2, when peroxides are heated to their decomposition temperatures in the presence of high-molecular-weight silicone gums or fluids, free radicals readily evolve which then react with and remove hydrogen atoms from the methyl groups of adjacent linear molecules, to form an elastic

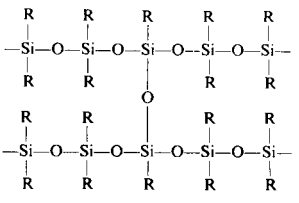

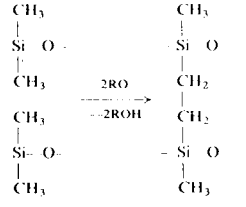

Fig. 1. Room temperature cross-linking (mild) of polyxiloxane diol polymer by tetrachlorosilane. Note Si–O–Si linkage.

Fig. 2. High temperature cross-linking of polysiloxane polymer by peroxides. Note Si–C–C–Si linkage.

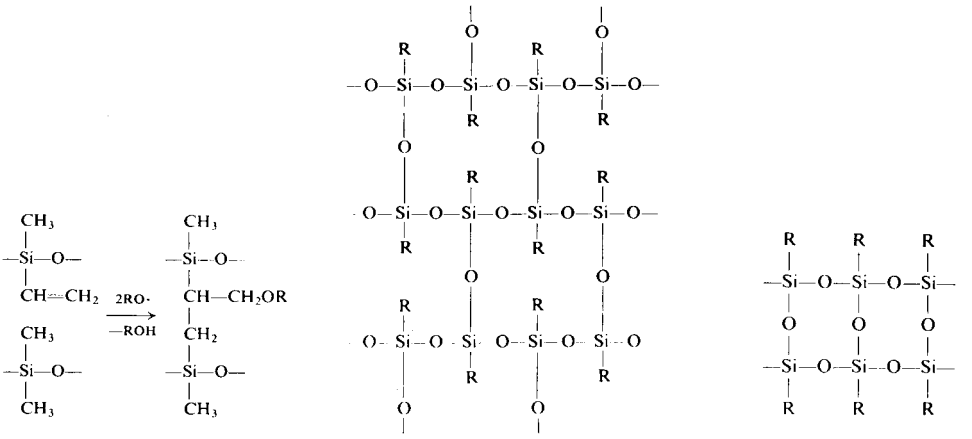

Fig. 3. High-temperature cross-linking of polysiloxane polymer containing vinyl side-chain. Note attack at the double bond and the Si–C–C–Si linkage.

Fig. 4. A "moderately" cross-linked polysiloxane polymer involving Si–O–Si linkages.

Fig. 5. A "highly" cross-linked polysiloxane polymer involving S–O–Si linkages.

(elastomeric) silicone rubber. In contrast to that observed in Fig. 1, the linkage here is of the Si–C–C–Si type. Similarly, when vinyl groups are present in the silicone polymer as in SE-54, the free radicals in this instance readily attack at the double bond (Fig. 3), permitting rapid and efficient cross-linking reactions to occur.

Under ordinary conditions, it is thought that silicone elastomers may have from 20 to 50 cross-links per polymer chain, spaced some 200–500 siloxy units apart[15]. If care is not taken to control the extent of the reactions, more extensive cross-linking induces physical and chemical changes which result in glassy, brittle polymers which are totally unsuitable for use as stationary phases in gas chromatography. Examples of moderate and extensive cross-linking involving Si–O–Si bonding are shown in Figs. 4 and 5.

From all of this, it was of great interest to also ascertain whether or not each of the two types of cross-linked polymer produced notable differences in chromatographic properties when used as insolubilized stationary phases on fused-silica glass capillary tubing.

EXPERIMENTAL

The fused-silica glass capillary tubing used in these studies had an outer polyimide coating capable of withstanding temperatures up to 400°C. All the surfaces were vigorously deactivated either by modifications of the procedure described by Stark *et al.*[11] utilizing octamethylcyclotetrasiloxane or by slight variations of the Schomburg *et al.*[12] polysiloxane method. In the latter instance, care was also taken to employ chemical moieties which bore a close structural relationship to the stationary phase used in the final preparation of the capillary column.

TABLE I*

DATA CONCERNING THE PEROXIDES USED

Peroxide	*1 h $T_{\frac{1}{2}}$ (°C)***	*10 h $T_{\frac{1}{2}}$ (°C)*	*Active oxygen (% by wt.)*
Benzoyl peroxide (a)	91	73	6.5
Dicumyl peroxide (b)	135	115	5.8
tert.-Butyl peroxide (c)	149	126	10.8

Decomposition products: (a) benzoic acid derivatives; (b) methane, acetophenone, cumyl alcohol; (c) acetone, *tert.*-butyl alcohol

* Data derived from Bulletins from Pennwalt Co., New York, NY, U.S.A.

** The half-life of a peroxide in a specific solvent (usually 0.2 *M* benzene) at any specified temperature is the time required at that temperature to affect a loss of 50% of the active oxygen content of the peroxide. The reactivities of the various peroxides can be rated by comparing the temperature at which the half-lives are 1 h and 10 h.

Cross-linking with tetrachlorosilane

The α,ω-hydroxypolymethylsiloxane prepolymers were obtained by slight modifications of the methods described by Blomburg and Wännman[5,6] and Lewis and Martin[16]. Those used in this study were relatively free-flowing liquids, readily soluble in pentane or methylene chloride. They provided one with remarkably uniform films when deposited by either the static or dynamic coating technique on previously deactivated fused-silica capillary tubing. Vulcanization with $SiCl_4$ in the vapor phase was then carried out at room temperature[5,6] on the prepared columns.

Cross-linking with peroxides

Three different peroxides were used in this aspect of the study. These were benzoyl peroxide (BP), dicumyl peroxide (DCUP), and di-*tert.*-butyl peroxide (DTBP). Pertinent data concerning their relative reactivities at certain temperatures are given in Table I.

(1) Benzoyl peroxide or dicumyl peroxide, in concentrations of 0.1–0.8% (w/w) of the silicone polymer (SE-30 or SE-54), was added to the coating solution[8]. Film deposition was carried out by the static method. Following this, a gentle stream of nitrogen was passed through the columns for 3 h. At this point, with the flow of nitrogen reduced to 0.2–0.4 ml/min, the columns were placed for 1 h in an oven whose temperature was raised to 130°C (for BP) or to 150°C (for DCUP). After this, the columns were cooled down to room temperature with the low flow-rate of nitrogen being maintained for an additional 2 h. They were then placed in a gas chromatograph, where they were temperature programmed for 1–2 h at 225°C and then tested. If statisfactory results were obtained, the columns were slowly programmed to 280–300°C and then conditioned overnight at these temperatures and then retested in the morning. They were then removed from the instrument and then rinsed slowly with 4–6 column volumes of either pentane or methylene chloride. The solvent was then completely removed by a stream of nitrogen. The column was again placed in the gas chromatograph and slowly programmed to 300–325°C where it remained for 8–12 h.

(2) Another set of fused-silica columns were similarly coated with solutions of stationary phase containing either BP or DCUP. However, after the coating pro-

cedure was finished, the column ends were sealed and the columns placed in an oven at 130°C (BP) or 150°C (DCUP) for 1 h. They were then allowed to cool down for an additional hour, after which time the ends were opened and the columns were flushed with nitrogen for an additional 2 h. They were then placed in gas chromatographs and conditioned, tested, and rinsed with solvents in a manner described above.

(3) A third set of deactivated fused-silica glass capillary columns were routinely coated with SE-30 without the addition of the individual peroxides to the coating solution. The columns were then conditioned and tested for efficiency and thermal stability. Following this, the columns were placed in an oven in a manner whereby 12–18 in. of the inlet and outlet ends of the column remained outside the oven proper. The inlet end of the column was placed through the silicone-teflon seal of a 25-ml vial which was filled with 3–5 ml of *tert.*-butyl peroxide. The outlet end was placed in a small flask containing vermiculite. The vial was then gently pressurized with nitrogen. Since the boiling point of this peroxide is 40°C at 55 mmHg, the peroxide vapor was very carefully allowed to flow slowly into the column for 30 min at room temperature. The temperature of the oven was then raised to 150°C and the flow of gaseous peroxide was allowed to continue for an additional 30 min. The column ends outside the oven were then sealed, and the column remained in the oven for an additional 30 min at 150°C. These columns were then processed as described in paragraph (2). Because of the high flammability of the DTBP vapors, this particular procedure should be carried out in a hood and approached with extreme caution! Only very small amounts of DTBP should be used at one time.

RESULTS AND DISCUSSION

Cross-linking with tetrachlorosilane (Si–O–Si linkages)

Excellent results were readily obtained with the reactive diol polymers produced by a modification of methods similar to that described either by Blomberg and Wännman[5,6] or Lewis and Martin[16]. The outstanding virtue of this procedure is the ability to pretest the column for uniformity of coating (*i.e.* efficiency), film thickness, and activity, prior to cross-linking. Moreover, it was noted that cross-linking with tetrachlorosilane (vapor phase) overnight at room temperature[6] was mild and effective. The columns obtained by this procedure (Fig. 6) were very inert, had excellent efficiencies (well over 3000 plates/m) and outstanding thermal stability in the 300–350°C range. After rinsing with solvent, the loss of phase, as measured by changes in the capacity factor (k'), averaged from 10–15%. Interestingly, in contrast to that usually noted with the cross-linking procedures carried out on the polysiloxane gums with the various peroxides, there was no discernible effect here on the deactivation procedures used to neutralize the residual silanol groups[14,17] found on the fused-silica glass capillary tubing.

Cross-linking with peroxides (Si–C–C–Si linkages)

Considerable differences in column quality were noted when the various peroxides were used in the *in situ* cross-linking of the non-polar silicone stationary phases on deactivated fused-silica capillary tubing.

Benzoyl peroxide. Droplet formation and all its consequences were occasionally seen following the application of the coating solutions containing this compound.

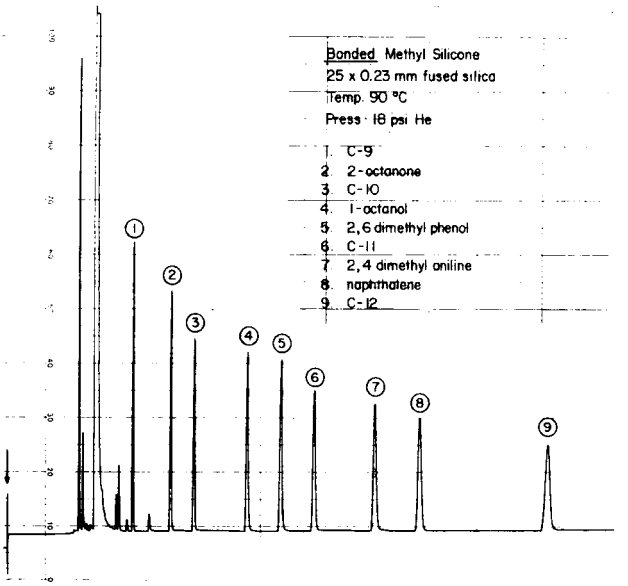

Fig. 6. Chromatogram obtained from fused-silica capillary column coated with a polysiloxane polymer cross-linked with tetrachlorosilane. Chart speed, 2 cm/min. Note complete absence of "tailing" of polar components.

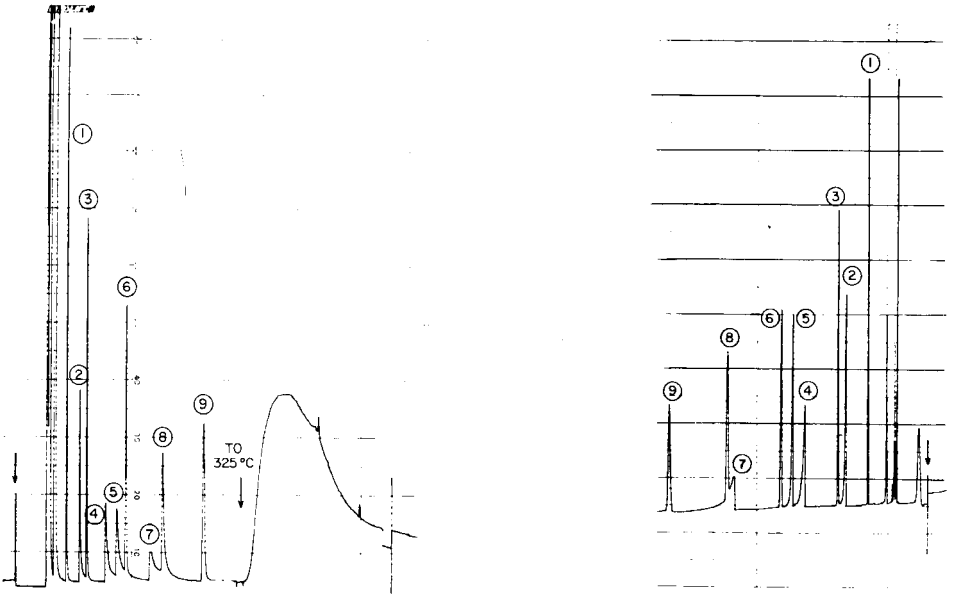

Fig. 7. Chromatogram obtained from a fused-silica capillary column (25 × 0.23 mm), coated with SE-30 cross-linked with benzoyl peroxide (closed system). Temperature, 90°C; pressure, 18, p.s.i. helium. Peaks: 1 = C_9 hydrocarbon; 2 = 2-octanone; 3 = C_{10} hydrocarbon; 4 = 1-octanol; 5 = 2,6-dimethylphenol; 6 = C_{11} hydrocarbon; 7 = 2,4-dimethylaniline; 8 = naphthalene; 9 = C_{12} hydrocarbon.

Fig. 8. As Fig. 7 except that cross-linking with benzoyl peroxide was carried out in an open system. Conditions and peaks as in Fig. 7.

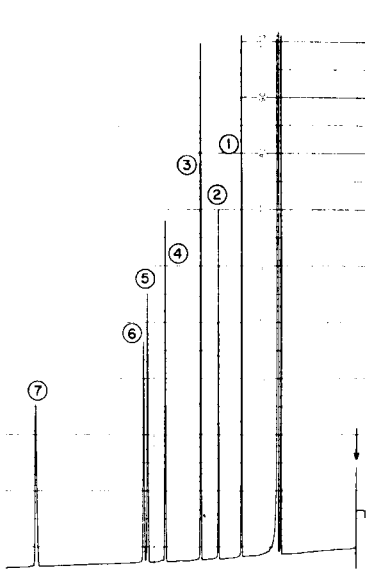

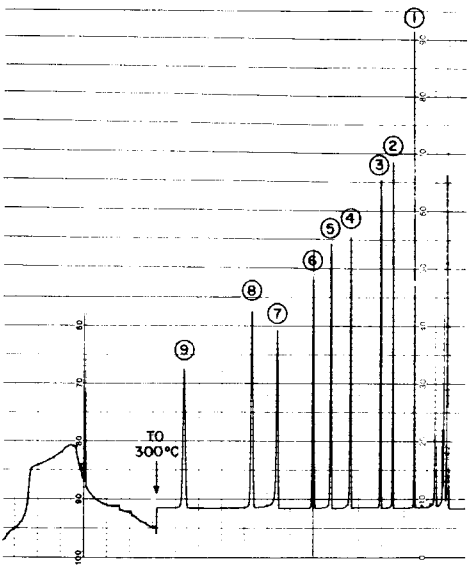

Fig. 9. Chromatogram obtained from a fused-silica capillary column (25 m × 0.009 in.) coated with 5% SE-54 cross-linked with dicumyl peroxide. Temperature, 110°C; pressure 14 p.s.i. helium. Peak 7, 3835 theoretical plates/m at $k' = 4.8$. Peaks: 1 = 2-octanone; 2 = 1-octanol; 3 = 2,6-dimethylphenol; 4 = 2,4-dimethylaniline; 5 = naphthalene; 6 = C_{12} hydrocarbon; 7 = C_{13} hydrocarbon.

Fig. 10. Chromatogram obtained from a fused-silica capillary column coated with SE-30 cross-linked with dicumyl peroxide. Note very slight "tails" on peak 4 (octanol) and 7 (dimethylaniline). Conditions and peaks as in Fig. 7.

An increase in activity (Figs. 7 and 8) was frequently observed with both the open- and closed-column reaction techniques. It is difficult to determine at this time whether or not this is due to the persistance of by-products formed during the reaction or due to some chemical interaction with the particular surface deactivation procedure. Prolonged conditioning and/or solvent rinsing did not ameliorate the situation. The degree of cross-linking (90–95%) was excellent as was the thermal stability. Different concentrations of the reagent maintained at slightly different temperatures did not significantly after the results here.

Dicumyl peroxide. Of all of the peroxides used in this study, on average, DCUP usually produced the most inert, efficient, cross-linked films, particularly when used in conjunction with the vinyl-containing SE-54 (Fig. 9). If SE-54 itself was initially employed in the polysiloxane deactivation procedure[12], surface activity was absent. Here too, the degree of cross-linking was high (> 90%) and the thermal stability in the 300–350°C range was outstanding.

Similar results were seen when SE-30 was cross-linked with DCUP. On occasion, very small residual surface activity was noted here (Fig. 10).

Tert.-butyl peroxide. This compound provided us with very interesting results when it was used in its gaseous state to cross-link silicone stationary phase films that were previously coated onto the fused-silica glass capillary tubing. Under these circumstances, *prior to cross-linking*, as with the diol polymers[5,6,15], one had the opportunity here to test and condition the coated columns and select only those that

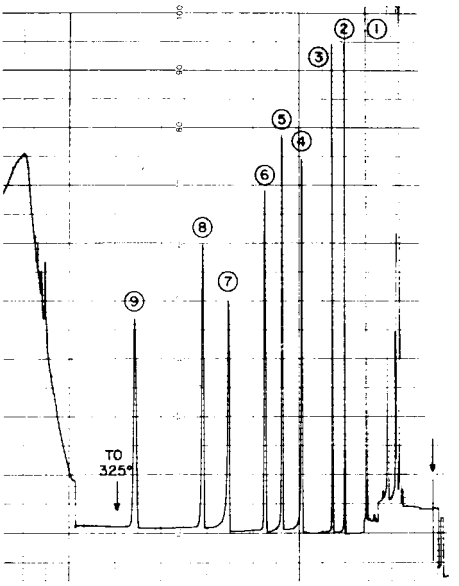

Fig. 11. Chromatogram obtained from a fused-silica capillary column coated with SE-30 cross-linked with di-*tert.*-butyl peroxide. Note slight "tails" on polar components 4 (octanol), 5 (dimethylphenol) and 7 (dimethylaniline). Conditions and peaks as in Fig. 7.

displayed very inert surfaces, appropriate film thicknesses, and very high efficiencies. Despite this outstanding advantage, in the beginning it was quite difficult to determine the optimal flow-rate, the time of exposure, and the optimal decomposition temperature for free radical formation, in order to achieve the required degree of cross-linking. Once these parameters were adequately determined, fewer failures were noted (insufficient vulcanization) and very efficient, thermally stable, cross-linked columns were produced (Fig. 11). Very slight surface activity was noted here since several of the polar components of the test mixture showed some signs of "tailing" (Fig. 11). Again, as mentioned previously, at this point it is difficult to determine the source of this activity since on pre-testing, prior to the institution of the cross-linking step, these columns appeared to be very inert. Accordingly, it has to be attributed to reactions occurring during the vulcanization procedure with peroxides which interfere directly or indirectly with the surface deactivation. The precise cause awaits further work in this area.

From the data thus far available from this study, it is difficult to discern any major chromatographic differences when cross-linked silicone polymers with either Si–O–Si or Si–C–C–Si linkages are properly prepared *in situ* on deactivated fused-silica glass capillary tubing. Obviously, vulcanization of the silicone gums, particularly the vinyl-containing SE-54, with peroxides is a much shorter and more straightforward procedure. However, once a significant amount of an appropriate molecular-weight, reactive linear polysiloxane-diol prepolymer is at hand, cross-linking of this material with tetrachlorosilane provided one with very efficient, thermally stable, capillary columns. The previously deactivated surfaces here usually remained totally unaffected by the procedure and continued to exhibit a very high degree of inertness.

Very good fused-silica glass capillary columns containing silicone stationary phases cross-linked by certain of the peroxides, in particular DCUP and *tert.*-butyl peroxide (in the gas phase), were also produced. However, difficulties were frequently encountered here in maintaining the well deactivated surfaces under conditions of the experiment. This is in contrast to the results obtained by Grob *et al.*[7] using borosilicate glass deactivated by persilanization[10], a process which we find to be not nearly as effective on fused-silica glass.

The maximum optimal temperatures for these columns appear to be in the range 300–325°C when operated isothermally, and 325–350°C when temperature programmed. Interestingly, when certain of the columns were heated for 18 h at 350°C, a considerable increase in surface activity was noted. However, the k' values and the efficiency essentially remained unaltered.

ACKNOWLEDGEMENT

This work was supported in part by a Contract DE-AC02-76EV02958 A006 from the Department of Energy.

REFERENCES

1 C. Madani, E. M. Chambaz, M. Rigaud, J. Durand and P. Chebroux, *J. Chromatogr.*, 126 (1976) 161.
2 C. Madani, E. M. Chambaz, M. Rigaud, P. Chebroux, J. C. Breton and F. Berthou, *Chromatographia*, 10 (1977) 466.
3 C. Madani and E. M. Chambaz, *Chromatographia*, 11 (1978) 725.
4 C. Madani and E. M. Chambaz, *J. Amer. Oil Chem. Soc.*, 58 (1981) 63.
5 L. Blomberg and T. Wännman, *J. Chromatogr.*, 168 (1979) 81.
6 L. Blomberg and T. Wännman, *J. Chromatogr.*, 186 (1979) 159.
7 K. Grob, G. Grob and K. Grob Jr., *J. Chromatogr.*, 211 (1981) 243.
8 K. Grob and G. Grob, *J. Chromatogr.*, 213 (1981) 211.
9 P. Sandra, G. Redant, E. Schacht and M. Verzele, *J. High Resolut. Chromatogr. Chromatogr. Commun.*, 4 (1981) 411.
10 K. Grob and G. Grob, *J. High Resolut. Chromatogr. Chromatogr. Commun.*, 2 (1980) 493.
11 T. Stark, R. Dandeneau and L. Mering, *Pittsburgh Conference on Analytical Chemistry and Applied Spectroscopy, Atlantic City, NJ, March 1980.*
12 G. Schomburg, H. Husmann and H. Borwitzky, *Chromatographia*, 12 (1979) 651.
13 S. R. Lipsky and W. J. McMurray, *Expo Chem II, Houston, TX, Sept. 1981.*
14 S. R. Lipsky and W. J. McMurray, *J. Chromatogr.*, 217 (1981) 3.
15 W. Lynch, *Handbook of Silicone Rubber Fabrication*, Van Nostrand-Reinhold, New York, 1978.
16 R. Lewis and E. Martin, *U.S. Pat.* 4,066,680 (1978).
17 S. R. Lipsky and W. J. McMurray, M. Hernandez, J. E. Purcell and R. A. Billeb, *J. Chromatogr. Sci.*, 18 (1980) 1.

Journal of Chromatography, 239 (1982) 71–80
Elsevier Scientific Publishing Company, Amsterdam – Printed in The Netherlands

CHROM. 14,543

ANALYSIS OF PICOMOLAR CONCENTRATIONS OF 6-OXO-PROSTAGLANDIN $F_{1\alpha}$ IN BIOLOGICAL FLUIDS

SUSAN E. BARROW*, KEITH A. WADDELL, MADELEINE ENNIS, COLIN T. DOLLERY and IAN A. BLAIR

Department of Clinical Pharmacology, Royal Postgraduate Medical School, Ducane Road, London W12 0HS (Great Britain)

SUMMARY

A highly sensitive and specific assay for the quantitation of 6-oxo-prostaglandin $F_{1\alpha}$, the stable hydrolysis product of prostacyclin, is described. The method involves the addition of [3,3′,4,4′-$^2H_4$]-6-oxo-prostaglandin $F_{1\alpha}$ as internal standard, extraction from biological fluids using μBondapak C_{18} reversed-phase Sep-Paks, and preliminary purification by normal-phase chromatography. Following conversion to the methoxime, tris-trimethylsilyl, pentafluorobenzyl derivative, samples were analysed using combined capillary column gas chromatography negative ion chemical ionisation mass spectrometry. Fragment ions at m/z 614 (^1H) and 618 (^2H) $[M - C_7H_2F_5]^-$ were monitored for quantitation. This method was used for the measurement of endogenous levels of 6-oxo-prostaglandin $F_{1\alpha}$ in human urine and for the determination of prostacyclin release from rat peritoneal mast cells and from rat aortic rings incubated in human plasma.

INTRODUCTION

Prostacyclin (PGI_2), a product of the cyclooxygenase pathway of fatty acid metabolism, is a potent inhibitor of platelet aggregation and a powerful vasodilator[1]. It has been the subject of numerous investigations designed to define its physiological role more fully. Such studies rely heavily on the availability of an assay capable of quantitating relatively low concentrations contained in a complex biological matrix.

PGI_2 is unstable and is hydrolysed non-enzymically to 6-oxo-prostaglandin $F_{1\alpha}$ (6-oxo-$PGF_{1\alpha}$) which is biologically inactive. As a result, physicochemical methods of analysis are dependent upon the measurement of 6-oxo-$PGF_{1\alpha}$ to provide a reflection of PGI_2 concentration. Current techniques for the quantitation of 6-oxo-$PGF_{1\alpha}$ in biological fluids include radioimmunoassay (RIA)[2], electron-capture gas chromatography (GC)[3] and GC–mass spectrometry (MS)[4,5].

It is generally accepted that GC–MS provides the most sensitive and specific methodology available. Nevertheless, extensive mass-spectral fragmentation in the electron impact (EI) mode limits the sensitivity of such assays. In addition, biological fluids tend to contain other endogenous prostanoids which are not easily separated from 6-oxo-$PGF_{1\alpha}$ on packed columns.

0021-9673/82/0000–0000/$02.75

We report a novel assay for 6-oxo-$PGF_{1\alpha}$ based on combined capillary column GC–negative ion chemical ionisation (NICI) MS. This method is capable of providing both the specificity and sensitivity required to measure picomolar concentrations in biological fluids. We have applied this method to a number of studies in our laboratories and in this paper, we describe the determination of endogenous levels of 6-oxo-$PGF_{1\alpha}$ in human urine. This investigation was carried out with a view to using the method in future studies concerning the role of PGI_2 in the kidney[6]. In addition, we have used this method to analyse samples obtained from incubations of rat peritoneal mast cells and rat aortic rings.

EXPERIMENTAL

Reagents

Analytical grade reagents were used at all times and solvents were redistilled immediately before use. μBondapak C_{18} and silica Sep-Pak cartridges are proprietry products manufactured by Waters Assoc. (Northwich, Great Britain). Silica thin-layer chromatography (TLC) plates (Merck) were purchased from BDH (Enfield, Great Britain). Sephadex LH-20 was obtained from Pharmacia (Uppsala, Sweden). Methoxyamine hydrochloride was obtained from Eastman (Rochester, NY, U.S.A.) and was recrystallised from ethanol containing *ca.* 1% concentrated hydrochloric acid before use. Pentafluorobenzyl bromide (PFBB) was purchased from Fluorochem (Glossop, Great Britain) and used without further purification. Bis-(trimethylsilyl)-trifluoroacetamide (BSTFA) was purchased from Pierce (Rockford, IL, U.S.A.). N-Methyl-N-nitroso-*p*-toluenesulfonamide (Diazald), for diazomethane generation, was supplied by Aldrich (Milwaukee, WI, U.S.A.). 6-Oxo-$PGF_{1\alpha}$ and [3,3′,4,4′-$^2H_4$]-6-oxo-$PGF_{1\alpha}$ standards were kindly supplied by Dr. J. Pike, Upjohn (Kalamazoo, MI, U.S.A.), and [5,8,9,11,12,14,15(N)^{3}H]-6-oxo-$PGF_{1\alpha}$ (sp.act. = 120 Ci mmole^{-1}) was purchased from New England Nuclear (Southampton, Great Britain). Compound 48/80, a basic histamine releaser (a polymeric condensation product of N-methyl-*p*-methoxyphenethylamine with formaldehyde) was a gift from Dr. A. N. Payne of Wellcome Research Laboratories (Beckenham, Great Britain).

Instrumentation

GC–MS. A Finnigan 4000 quadrupole gas chromatograph–mass spectrometer interfaced with a 6110 data system, was used in this study. The system had been modified with a Finnigan PPNICI package to permit monitoring of negative ions in the chemical ionisation mode.

Chromatography was carried out using fused silica capillary columns. An SP 2100 column (25 m × 0.2 mm I.D. × 0.11 μm coating thickness) was obtained from Hewlett-Packard (Wokingham, Great Britain), and an SE-54 column (30 m × 0.3 mm I.D. × 0.3 μm coating thickness) was purchased from GC^2 (Chromatography) (Northwich, Great Britain). Helium was used as a carrier gas at an inlet pressure of 100–140 kPa. Samples were injected using a Grob-type splitless injector set at 270°C and the column temperature programmed from 100°C at 20°C min^{-1}.

For NICI-MS, methane was used as reagent gas with an ion source pressure of 27 Pa. The operating conditions were ioniser temperature, 200°C; electron energy, 100 eV; electron multiplier voltage, 1100–1300 V; conversion dynode voltage ±3 kV; and emission current, 0.33 mA.

In the EI mode, operating conditions were modified to give an ioniser temperature, 210°C; electron impact energy, 25 eV; and ion source pressure <1 Pa.

Selective ion monitoring (SIM) was performed using a four-channel multiple ion monitor operating at a pre-amplifier gain of 10^{-8} AV^{-1}.

Radiochromatogram scanner. A Packard Model 7201 Scanner System was used to monitor standard [^{3}H]6-oxo-PGF$_{1\alpha}$ on TLC plates.

Biological samples

Urine was collected from normal, healthy volunteers and used immediately or frozen and stored at -20°C. Aliquots of 1 ml were taken for analysis.

Rat peritoneal mast cells were obtained as described previously[7] and purified to 88–93% by centrifugation in a bovine serum albumin density gradient by a modification of the method of Sullivan *et al.*[8].

Aliquots of cells ($2.6–3.5 \cdot 10^5$ ml^{-1}) were incubated in Tyrodes buffer at 37°C for 30 min either in the presence of compound 48/80 (1 μg ml^{-1}) or in control buffer. Aliquots (1 ml) of the supernatants were analysed for 6-oxo-PGF$_{1\alpha}$. % Histamine release was determined as described previously[7].

Rat aortic rings were prepared and incubated in human plasma as described previously[9]. Aliquots (200 μl) of the plasma were analysed for 6-oxo-PGF$_{1\alpha}$.

Extraction and purification procedure

Biological samples were made up to 20 ml with distilled water and equilibrated with [3,3′,4,4′-$^2H_4$]6-oxo-PGF$_{1\alpha}$ (10 ng or 2 ng in 10 μl ethanol) at 0°C for 30 min and acidified to pH 3.0–3.5 with 2 *M* HCl. A typical extraction was carried out using a μBondapak C_{18} reversed-phase Sep-Pak which had been preconditioned with methanol (5 ml) followed by distilled water (5 ml). The sample was applied using a polypropylene syringe at a flow-rate of <30 ml min^{-1}. The Sep-Pak was washed with distilled water (10 ml) to remove highly polar components originating from the biological matrix. 6-Oxo-PGF$_{1\alpha}$ was eluted with ethyl acetate (7 ml) and collected into a glass pointed tube. A small amount of water (*ca.* 0.5 ml) was allowed to settle out.

Initial sample clean up was achieved by application of the upper organic layer to a normal-phase silica Sep-Pak which had been prewashed with methanol (5 ml) and ethyl acetate (5 ml). The Sep-Pak was washed with ethyl acetate (5 ml) to remove components of relatively low polarity and 6-oxo-PGF$_{1\alpha}$ was eluted with methanol (5 ml).

Solvent was removed at ambient temperature under a stream of nitrogen and the residue transferred with methanol to a small vial. This furnished a crude prostanoid extract.

Preparation of derivatives

Methoximation. The methoxime derivative of 6-oxo-PGF$_{1\alpha}$ was prepared by treating the residue with 100 μl methoxyamine hydrochloride in anhydrous pyridine (5 mg ml^{-1}). The sample was allowed to stand overnight at ambient temperature and the pyridine was then removed *in vacuo*.

Esterification. The 6-oxo-PGF$_{1\alpha}$–methoxime derivative was converted to a pentafluorobenzyl (PFB) ester by adding acetonitrile (30 μl), 35% PFBB in acetonitrile (10 μl) and diisopropylethylamine (10 μl) and heating at 40°C for 30 min. Alter-

natively, the methyl ester was prepared using an alcoholic ethereal solution of diazomethane prepared according to the method of Fales *et al.*[10]. The residue was first dissolved in methanol (200 μl) and the diazomethane solution (0.5 ml) added and allowed to stand for 5 min. In both cases, samples were evaporated to dryness under a stream of nitrogen at ambient temperature.

Sephadex LH-20. Electron-capturing impurities and excess derivatising reagents were removed using a short column of pre-swollen Sephadex LH-20 (30 × 5 mm I.D.). The ester residue was taken up in dichloromethane (200 μl), applied to the column and eluted with dichloromethane (2 ml). The sample was taken to dryness under a stream of nitrogen.

Trimethylsilylation. All samples were converted to tris-trimethylsilyl (tris-TMS) derivatives by adding BSTFA (125 μl) and allowing to stand overnight at ambient temperature. The samples were transferred to small vials, evaporated under dry nitrogen and immediately reconstituted in BSTFA (25 μl). Generally, aliquots (2.5 μl) were analysed by GC–MS immediately but it was possible to store samples for up to 3 weeks in a desiccator at −20°C.

TLC Purification

It was necessary to include an additional purification step for the urine extracts. Preparative TLC was carried out on the residue obtained after the methoximation step. Typically, a sample was taken up in methanol (60 μl) and applied to the preconcentration zone of a precoated silica gel 60 TLC plate (200 × 50 × 0.25 mm thickness). The sample was developed using the organic phase obtained from a mixture of ethyl acetate–acetic acid–hexane–water (54:12:25:60). The band corresponding to the methoxime derivative of 6-oxo-$PGF_{1\alpha}$ was located by comparison with a tritiated standard. A sample of the methoxime derivative (2 ng) containing its ^3H analogue (*ca.* $4 \cdot 10^5$ dpm) was applied to a separate TLC plate. After development alongside the biological extracts, the appropriate band was located by radiochromatogram scanning. Under these conditions, the R_F value was 0.19.

The corresponding zone for 6-oxo-$PGF_{1\alpha}$–methoxime, in the urinary extracts, was scraped off the TLC plate and eluted with methanol (2 × 2 ml). The combined eluates were evaporated to dryness under a stream of nitrogen and the residue transferred to a small reagent vial. Esterification and trimethylsilylation was carried out as described above.

GC–MS Quantitation

Standard curves were prepared for 6-oxo-$PGF_{1\alpha}$ in the range 0–20 ng. Appropriate concentrations of 6-oxo-$PGF_{1\alpha}$ and either 10 ng or 2 ng of [$^2H_4$]6-oxo-$PGF_{1\alpha}$ were added to Krebs buffer (pH 7.4). These standard solutions were then processed through the relevant assay procedure. Quantitative SIM analyses were performed in the NICI mode using the fragment ions at m/z 614 (^1H) and 618 (^2H). Quantitation was based on peak area ratios ($^1H/^2H$) which for the standard mixtures were plotted against the known weights of 6-oxo-$PGF_{1\alpha}$.

Curves were obtained using an unweighted least squares linear-regression analysis. Using the parameters obtained, unknown levels of 6-oxo-$PGF_{1\alpha}$ could be determined.

RESULTS

The recovery through the entire assay procedure, including TLC purification, was determined using 5 urine samples spiked with [^{3}H]6-oxo-$PGF_{1\alpha}$ ($4 \cdot 10^5$ dpm) and [$^2H_4$]6-oxo-$PGF_{1\alpha}$ (10 ng). The recovery was 51.4 ± 7.4% (mean ± S.D.). The recovery through the procedure where no TLC step was included was determined using 5 aqueous samples spiked as above. In this case, the recovery was 90.5 ± 6.9% (mean ± S.D.).

Retention data for the capillary-column GC separation of the methoxime, methyl ester, tris-trimethylsilyl (MO–Me–TMS) and the methoxime, PFB ester, tris-trimethylsilyl (MO–PFB–TMS) derivatives of 6-oxo-$PGF_{1\alpha}$ are given in Table I.

TABLE I

CAPILLARY COLUMN GC RETENTION DATA FOR THE DERIVATIVES OF 6-OXO-$PGF_{1\alpha}$

Column	*Temperature programme*	*Inlet pressure (kPa)*	*Retention times (min)*	
			MO–Me–TMS derivative	*MO–PFB–TMS derivative*
SE-54	100–290 °C (20 °C min^{-1})	100	8.4	12.0
SP-2100	100–280 °C (20 °C min^{-1})	140	10.9	16.5

Analyses were carried out on an SP-2100 or an SE-54 capillary column. The latter column was more convenient as shorter run times could be employed with little loss of resolution. No separation of *syn* and *anti* isomers was observed on either column.

The EI mass spectrum of the MO–Me–TMS derivative of 6-oxo-$PGF_{1\alpha}$ is shown in Fig. 1. Extensive fragmentation of the molecule occurs but SIM quantitation could be carried out using the fragment ion at *m/z* 508 $[M–TMSOH–MeO]^+$ for the ^{1}H form and *m/z* 512 for the ^{2}H form. The limit of detection of a standard sample was set at 500 pg injected on column. This corresponded to a signal-to-noise ratio of 3:1. It was not possible to use the fragment ions at *m/z* 378 (^{1}H) and *m/z* 382 (^{2}H) for quantitative analysis because of substantial interference in this lower mass range.

The NICI mass spectrum of the MO–PFB–TMS derivative of 6-oxo-$PGF_{1\alpha}$ is shown in Fig. 2. The inclusion of the PFB ester group enhanced the electron-capturing ability of the molecule and allowed efficient negative ion chemical ionisation. The base peak at *m/z* 614 $[M - C_7H_2F_5]^-$ for the ^{1}H form and *m/z* 618 for the ^{2}H analogue were used for quantitation. A limit of detection when employing a 10 ng internal standard was set at 2 pg injected on column. This amount could be detected with a signal-to-noise ratio of 10:1 and provided a peak area ratio which was twice the value obtained for the intercept on the standard curve. The enhanced sensitivity and specificity provided by NICI–MS, was employed in subsequent analyses.

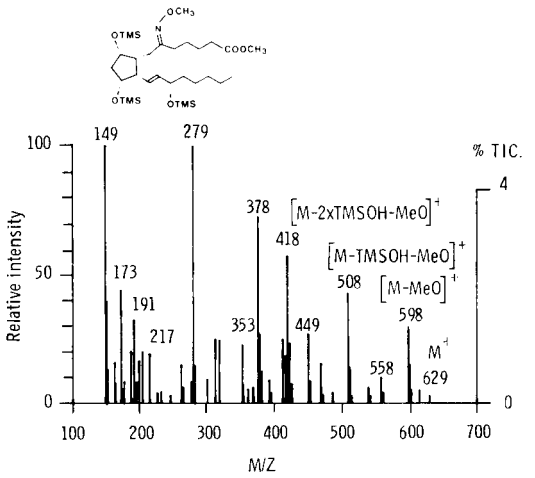

Fig. 1. EI mass spectrum of 6-oxo-$PGF_{1\alpha}$ as MO–Me–TMS derivative.

The standard curve for the range 0–10 ng using 10 ng internal standard gave a regression line of $y = 0.0103 + 0.1347x$; $r^2 = 0.997$. For the range 0–20 ng when 2 ng internal standard was used, a regression line of $y = 0.0099 + 0.6877x$; $r^2 = 0.994$ was obtained.

Endogenous levels of 6-oxo-$PGF_{1\alpha}$ in human urine were detected using this assay. A typical limited mass chromatogram is illustrated in Fig. 3. In this example, the concentration of 6-oxo-$PGF_{1\alpha}$ was found to be 46 pg ml^{-1}. This assay has also been used to investigate the generation of prostaglandins by mast cells in response to an immunological stimulus. Fig. 4 shows an SIM analysis of the medium in which purified rat peritoneal mast cells had been stimulated using compound 48/80. In this case, no TLC purification of the fluid was necessary and thromboxane B_2 (TxB_2) in addition to 6-oxo-$PGF_{1\alpha}$ was identified on the chromatogram. This compound has

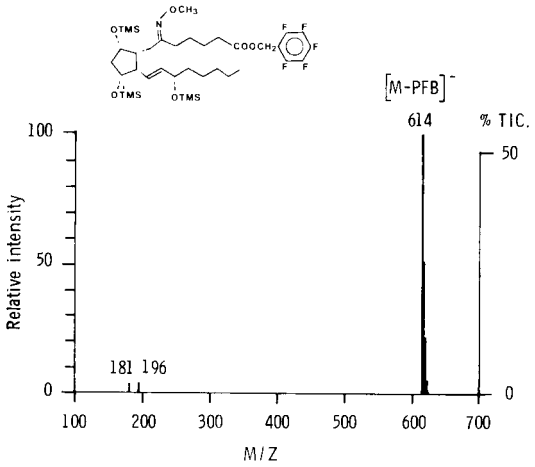

Fig. 2. NICI mass spectrum of 6-oxo-$PGF_{1\alpha}$ as MO–PFB–TMS derivative.

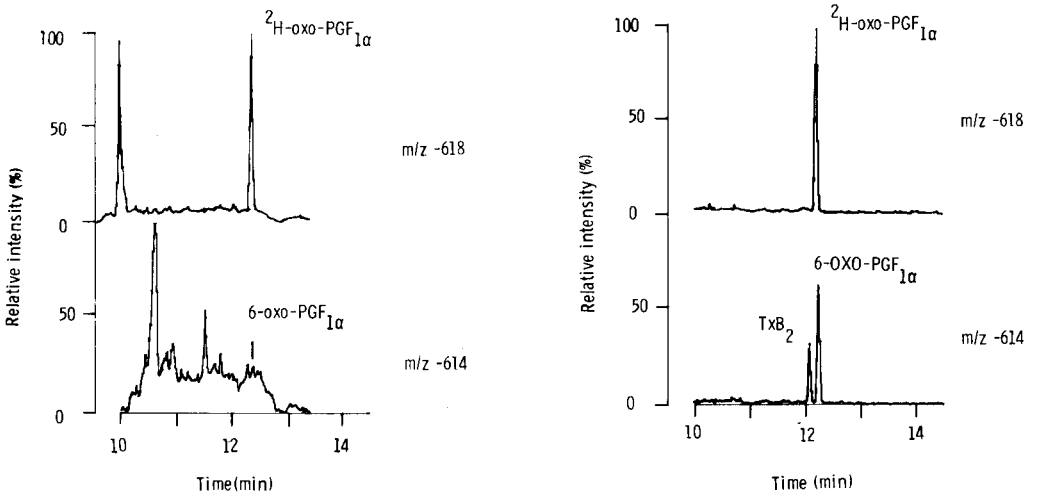

Fig. 3. Limited mass chromatogram of 6-oxo-PGF$_{1\alpha}$ and [3,3',4,4'-^{2}H$_4$]6-oxo-PGF$_{1\alpha}$ extracted from human urine.

Fig. 4. Limited mass chromatogram of 6-oxo-PGF$_{1\alpha}$ extracted from mast cell incubation medium after stimulation with compound 48/80.

the same molecular weight as 6-oxo-PGF$_{1\alpha}$ and similar gas chromatographic properties. Fig. 5 illustrates the NICI mass spectrum of the MO–PFB–TMS derivative of TxB_2 which can be only distinguished from that of 6-oxo-PGF$_{1\alpha}$ by the additional fragment ion at m/z 582 [M − $C_7H_2F_5$ − MeOH]$^-$. Concentrations of 6-oxo-PGF$_{1\alpha}$ determined in this example for cells incubated in the presence of compound 48/80 and in control buffer were 12.5 ng per 10^6 mast cells and 11.6 ng per 10^6 mast cells respectively. Values of 63 % and 6 % of total histamine release were obtained for these incubates.

A limited mass chromatogram of 6-oxo-PGF$_{1\alpha}$ obtained from an incubation of rat aortic rings in human plasma is shown in Fig. 6. In the example illustrated an

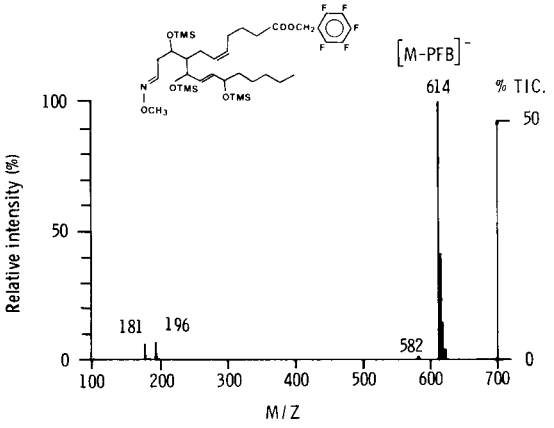

Fig. 5. NICI mass spectrum of TxB_2 as MO–PFB–TMS derivative.

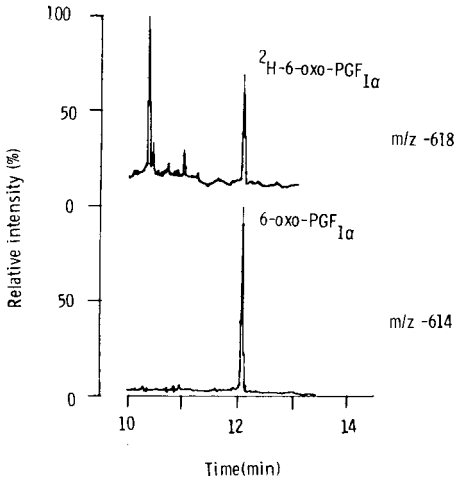

Fig. 6. Limited mass chromatogram of 6-oxo-PGF$_{1\alpha}$ and [3,3′,4,4′-^{2}H$_4$]6-oxo-PGF$_{1\alpha}$ extracted from human plasma after incubation with rat aortic rings. The internal standard chromatogram (−618) has been multiplied by a factor of five.

internal standard of 2 ng rather than 10 ng was used and the concentration of 6-oxo-PGF$_{1\alpha}$ in the plasma incubate was determined by GC–MS as 6.37 ng/100 μl.

DISCUSSION

The extraction, purification and quantitation of 6-oxo-PGF$_{1\alpha}$ from biological fluids, outlined in this paper, offers several advantages over methods described previously. μBondapak Sep-Pak cartridges provided a very quick and simple extraction procedure using small volumes of organic solvents. Silica Sep-Pak cartridges were incorporated into the method to provide a simple clean-up step. For fluids obtained from mast cell and aortic ring incubations, no additional sample purification was necessary prior to derivatisation and GC–MS analysis. Recovery through the assay was virtually quantitative.

It was necessary to include an additional clean up step in the assay of urine samples. In this case, contaminants can overshadow the relatively low concentrations of 6-oxo-PGF$_{1\alpha}$ present. If these contaminants are not removed, or at least minimised, suppression of ionisation in the source of the mass spectrometer can result in a dramatic decrease in sensitivity.

In our initial studies, preparative TLC was carried out on samples prior to methoximation. However, we found that no 6-oxo-PGF$_{1\alpha}$ could be detected by GC–MS following derivatisation unless a borate back extraction was included. TLC residues were dissolved in borate buffer at pH 8.5 which was extracted with ethyl acetate (discarded); the aqueous layer was acidified to pH 3.0 and 6-oxo-PGF$_{1\alpha}$ recovered by a second extraction with ethyl acetate. Even using this method, recoveries were rather variable. As an alternative, we investigated the TLC properties of the methoxime derivative of 6-oxo-PGF$_{1\alpha}$ and found that this compound gave a sharp band on TLC which could be eluted with consistently good recovery. It was not

necessary to include any additional extraction procedure following TLC and residual silica in the samples did not interfere with subsequent derivative formation.

We have speculated that 6-oxo-$PGF_{1\alpha}$ may be converted to a ketal or hemiketal[11] on TLC plates and such structures are not then accessible to methoximation. It is possible that by including a borate back extraction[4], or by just partitioning the TLC residue between an aqueous and organic phase[5], the ketal formation is reversed so that methoximation proceeds smoothly. In the method described in this paper, the possibility of ketal formation is avoided by trapping the ketone functionality as a methoxime prior to TLC purification.

The specificity of this assay was aided by the use of capillary column GC. This is illustrated by the baseline separation of the MO–PFB–TMS derivatives of TxB_2 and 6-oxo-$PGF_{1\alpha}$ derived from incubations of rat peritoneal mast cells. These compounds are not fully resolved on packed columns. Previous investigators have resorted to a TLC separation prior to GC–MS analysis when both these compounds have been present in a biological fluid. Using capillary columns this was not necessary.

Other GC–MS methods used to quantitate 6-oxo-$PGF_{1\alpha}$ have relied on EI-MS. In this mode, considerable fragmentation of the molecule leaves few ions suitable for sensitive SIM. We reasoned that a softer form of ionisation might reduce such fragmentation and provide an ion of sufficiently high intensity and high mass to give increased sensitivity and selectivity over EI-MS. Positive ion chemical ionisation (PICI) gives minimal fragmentation but poor efficiency of ionisation. For NICI-MS, it was necessary to enhance the electron capturing ability of the 6-oxo-$PGF_{1\alpha}$ molecule. This was achieved by esterification with PFBB[15]. Using this derivative and monitoring the fragment ion at m/z 614, it was possible to improve the limit of sensitivity from 500 pg (EI-MS) to 2 pg (NICI-MS) injected on column. This method of quantitation should be applicable to the full range of prostaglandins where in each case the carboxylic acid functionality can be converted to an electron-capturing ester.

The observation that PGI_2 is the major prostanoid produced by the renal cortex[6] prompted us to attempt quantitation of 6-oxo-$PGF_{1\alpha}$ in urine. Infused PGI_2 and 6-oxo-$PGF_{1\alpha}$ can be recovered as 6-oxo-$PGF_{1\alpha}$ in the urine of human subjects[12]. There is only one report of quantitation of endogenous 6-oxo-$PGF_{1\alpha}$ in human urine and no methodological detals or concentrations were given[13]. Modification of the present assay to include a chromatographic separation step permits routine determinations of urinary 6-oxo-$PGF_{1\alpha}$. The assay is currently being employed to investigate a possible renal role for PGI_2 in man.

This assay was also used in a preliminary study to measure levels of 6-oxo-$PGF_{1\alpha}$ released from mast cells. We found that both stimulated and unstimulated rat peritoneal mast cells were capable of synthesizing PGI_2 (measured as 6-oxo-$PGF_{1\alpha}$). However, no significant increase in the concentration of 6-oxo-$PGF_{1\alpha}$ was observed after stimulation with compound 48/80. This contrasts with the work of Roberts *et al.*[14] who reported very variable elevations of 6-oxo-$PGF_{1\alpha}$ levels after stimulation with the ionophore A 23187. This may reflect differences in the mode of mast cell activation by these agents. Work is now in progress to compare the release of prostaglandins by a range of different releasors. The chromatographic resolution of 6-oxo-$PGF_{1\alpha}$ from TxB_2 will allow quantitation of the latter prostanoid in future studies.

ACKNOWLEDGEMENTS

We thank the Upjohn Company for generous gifts of 6-oxo-$PGF_{1\alpha}$ and [$^2H_4$]6-oxo-$PGF_{1\alpha}$, Ms. Cherry Whyte for technical assistance, Dr. J. Ritter and Ms. M. Orchard for carrying out the aortic ring incubation. This work was supported by a programme grant from the Medical Research Council.

REFERENCES

1 S. Moncada, R. Gryglewski, S. Bunting and J. R. Vane, *Nature (London)*, 263 (1976) 663.
2 J. A. Salmon, *Prostaglandins*, 15 (1978) 383.
3 F. A. Fitzpatrick, D. A. Stringfellow, J. Maclouf and M. Rigaud, *J. Chromatogr.*, 177 (1979) 51.
4 C. N. Hensby, G. A. Fitzgerald, L. A. Friedman, P. J. Lewis and C. T. Dollery, *Prostaglandins*, 18 (1979) 731.
5 M. Claeys, C. van Hove, A. Duchateau and G. A. Herman, *Biomed. Mass Spectrom.*, 7 (1980) 544.
6 A. R. Whorton, M. Smigel, J. A. Oates and J. C. Frolich, *Biochim. Biophys. Acta*, 529 (1978) 176.
7 G. Atkinson, M. Ennis and F. L. Pearce, *Brit. J. Pharmacol.*, 65 (1979) 395.
8 T. J. Sullivan, K. L. Parker, W. Stenson and C. W. Parker, *J. Immunol.*, 114 (1975) 1473.
9 J. M. Ritter, M. A. Orchard, I. A. Blair and P. J. Lewis, *Biochem. Pharmacol.*, in press.
10 H. M. Fales, T. M. Jaouni and J. F. Babashak, *Anal. Chem.*, 45 (1973) 2302.
11 K. C. Nicolaou, W. F. Barnette and R. L. Magolda, *J. Chem. Res. (M)*, (1979) 2444.
12 B. Rosenkranz, C. Fischer, K. E. Weimer and J. C. Frolich, *J. Biol. Chem.*, 255 (1980) 10194.
13 J. C. Frolich, B. Rosenkranz, W. Kitajuna, C. Fischer and L. Walker, in P. J. Lewis and J. O'Grady (Editors), *Clinical Pharmacology of Prostacyclin*, Raven Press, New York, 1981, p. 53.
14 L. J. Roberts II, R. A. Lewis, J. A. Oates and K. F. Austen, *Biochim. Biophys. Acta*, 575 (1979) 185.
15 B. H. Min, J. Pao, W. A. Garland, J. A. F. de Silva and M. Parsonnet, *J. Chromatogr.*, 183 (1980) 411.

Journal of Chromatography, 239 (1982) 81–86
Elsevier Scientific Publishing Company, Amsterdam — Printed in The Netherlands

CHROM. 14,674

SIMULTANEOUS ANALYSIS OF IMIPRAMINE AND ITS METABOLITE DESIPRAMINE IN BIOLOGICAL FLUIDS

J. CYMERMAN CRAIG*, LARRY D. GRUENKE and TRONG-LANG NGUYEN
Department of Pharmaceutical Chemistry, School of Pharmacy, University of California, San Francisco, CA 94143 (U.S.A.)

SUMMARY

A method for the simultaneous quantitation of imipramine and its N-demethylated metabolite desipramine at the nanogram level in a single gas chromatograph peak is presented, utilizing gas chromatography–mass spectrometry with selected ion recording. The assay is specific and quantitation is achieved using [$^2H_4$]imipramine as the internal standard.

The method involves the *in situ* methylation of desipramine with [$^2H_2$]formaldehyde and sodium borohydride to give [$^2H_2$]imipramine. Quantitation is then achieved by selected ion recording at *m/z* 280, 282 and 284, whence the ratio of the ion currents at 280/284 and at 282/284 gives the quantities of imipramine and desipramine respectively.

INTRODUCTION

The four most widely used tricyclic antidepressants are imipramine and amitriptyline and their N-demethylated analogues (and metabolites) desipramine and nortriptyline, and recent studies indicate a relationship between blood levels of these drugs and therapeutic response[1]. Because of wide interpatient differences in the hepatic elimination of tricyclic antidepressants, the lack of response observed in about 30–40 % of patients[2,3] may be due to non-therapeutic plasma levels, and sensitive and specific analytical methods for both the tertiary drugs and their secondary metabolites are required in order to measure their low (nanogram range) plasma or cerebrospinal fluid concentrations for pharmacokinetic studies with single doses or for clinical evaluation.

A number of drug assay procedures have been developed using thin-layer chromatography[4], spectrophotometry with fluorometric techniques[5–7], radioisotopic derivatization methods[8,9], and radioimmunoassay[10,11]. Gas chromatography (GC) with electron-capture or nitrogen-specific flame-ionization detectors has been used[12–14], as has high-performance liquid chromatography[15,16], but (like most of the other methods) is prone to problems of sensitivity and–or lack of specificity, mainly due to interference from coeluting compounds. The use of combined GC–mass spectrometry (MS) made it possible to obtain the required specificity by monitoring the identity of the peaks as they eluted from the gas chromatograph, and selected ion

0021-9673/82/0000–0000/$02.75

recording brought the sensitivity into the 5–10 ng/ml range using *e.g.* promazine as the internal standard for quantitation[17,18]. A further improvement was achieved by the use of the deuterated drugs as internal standards, whereby the internal standard was the actual drug itself in the form of an isotopic variant[19–22]. For maximum sensitivity and reproducibility of the assay, the secondary amine drugs had to be acylated to the N-acetyl, N-trifluoroacetyl, or N-heptafluorobutyryl derivatives[19–24].

This report describes a simple and convenient method for the simultaneous measurement of imipramine and desipramine in a *single* GC peak. The assay involves the *in situ* methylation of desipramine with [$^2H_2$]formaldehyde and sodium borohydride to give [$^2H_2$]imipramine. Quantitation is then achieved by selected ion recording at the molecular ions of imipramine and [$^2H_2$]imipramine, using [$^2H_4$]imipramine as an internal standard in a single GC peak. Imipramine N-oxide, a known metabolite of imipramine[25,26] is not reduced to imipramine by this methylation procedure. The same method has been applied successfully to the conversion of nortriptyline to amitriptyline to achieve the simultaneous measurement of these two drugs in a single GC peak[27].

EXPERIMENTAL

Standard solutions and reagents

Standard solution A (5.92 nmoles [$^2H_4$]imipramine per μl) was prepared by dissolving 9.5 mg of [$^2H_4$]imipramine · HCl (KOR Isotopes; 98% $^2H_4$, 2% $^2H_3$ by electron impact MS analysis of the molecular ion) in 5.00 ml of degassed water. This solution was stored in an amber hypovial (Pierce) under nitrogen for several months at 4°C without noticeable decomposition.

Standard solution B (1.022 nmoles per μl of imipramine (Ciba-Geigy) and 1.093 nmoles per μl of desipramine (Geigy Pharmaceuticals) was made by dissolving 32.4 mg of imipramine · HCl and 33.1 mg of freshly recrystallized desipramine · HCl in 100.0 ml of degassed water. This solution was stored in a standard hypovial under nitrogen at 4°C. After one month there was a noticeable loss (about 5%) of desipramine.

A 37% solution of [$^2H_2$]formaldehyde-d_2 in ^2H_2O was prepared by placing 195 mg of perdeuterioparaformaldehyde (98% ^2H, Stohler Isotope Chemicals) and 500 μl of ^2H_2O (99.8% D. Stohler Isotope Chemicals) in a 1-ml reaction vial and heating at 100°C for 3 h.

Extraction procedure

To a 2 ml of sample of human plasma in a silanized (dimethylchlorosilane) 8-ml glass culture tube fitted with a Teflon® lined screw cap was added 5.00 μl of standard solution A (27.6 nmoles of [$^2H_4$]imipramine), 4 drops of 1 *N* aqueous sodium hydroxide (to adjust the plasma to pH 10) and 3 ml of 1.5% isoamyl alcohol (aldehyde free) in *n*-pentane. The sample was extracted by Vortex mixing for 10 min. The organic layer was removed and a second extraction of the plasma with 3 ml of isoamyl alcohol–pentane (1.5:98.5) was carried out. The combined organic extracts were evaporated to dryness at room temperature under a stream of nitrogen and the residue was submitted to the methylation procedure described below.

Methylation procedure

To the above residue was added 250 μl of methanol and 3 μl of [$^2H_2$]formaldehyde solution (37% in ^2H_2O, 35 μmoles). After 5 min at room temperature, 3.2 mg of sodium borohydride (100 μmoles) in 150 μl of water was added. The mixture was allowed to stand for 15 min and was then extracted with 2 ml of dichloromethane. The dichloromethane extract was shaken for 2 min with 1.5 ml of 0.1 *N* sulfuric acid in order to back-extract the organic bases. The acidic aqueous layer was removed, brought to pH 10 with 10 drops of 15% KOH, and extracted with 1 ml of dichloromethane. The sample was reduced to 10 μl under a stream of nitrogen and was then ready for GC–MS analysis.

Extent of conversion of desipramine to imipramine

A mixture containing 27.5 μg (86.9 nmoles) of imipramine · HCl and 28.1 μg (29.9 nmoles) of desipramine · HCl was subjected to the methylation procedure described above and the product was analyzed by direct insertion electron impact MS. The peak height ratios of the ion currents at *m/z* 282 and *m/z* 280 were determined by five repetitive scans, and when corrected for the (M + 2) isotopic abundance from natural imipramine, gave the yield for the conversion of desipramine to [$^2H_2$]imipramine. Five separate methylation experiments were carried out in this manner and gave values of 95.5 ± 1% for the conversion of desipramine to [$^2H_2$]imipramine.

Extent of conversion of imipramine N-oxide to imipramine

To each of four tubes containing 1 ml of water was added 25 μl of standard solution A (148 nmoles of [$^2H_4$]imipramine) and 32.5 μg (97.6 nmoles) of imipramine N-oxide · HCl (Dumex) in 25 μl of water. The solutions were made alkaline to pH 10 with 2 drops of 1 *N* sodium hydroxide, extracted with 1 ml of dichloromethane, and the extracts were evaporated at room temperature under a stream of nitrogen. Samples 1 and 2 were immediately subjected to thin-layer chromatography (Analtech silica gel GF plates) using benzene–isopropanol–conc. aq. ammonium hydroxide (90:10:1) as solvent, while samples 3 and 4 were subjected to the methylation procedure described above and then to thin layer chromatography. The imipramine bands (UV visualization) were scraped off from each plate (R_F value 0.65 for imipramine and 0.04 for imipramine N-oxide) and extracted with methanol–dichloromethane (1:1). The extracts were reduced to 50 μl volume under a stream of nitrogen at room temperature and the ratio of imipramine to [$^2H_4$]imipramine determined by GC–MS by monitoring the ions at *m/z* 280 and *m/z* 284. Samples 3 and 4 showed a ratio 1.55 ± 0.08% higher than samples 1 and 2, indicating that 98% of the imipramine N-oxide had remained unaffected by the methylation procedure.

Instrumentation

An Infotronics 2400 gas chromatograph coupled to an AEI (Kratos) MS-12 mass spectrometer via a single-stage ceramic frit molecular separator was used for all GC–MS work. A PDP 8I computer using the DS-30 software was used to record magnetically scanned mass spectra and a specially constructed accelerating voltage alternator was used to obtain selected ion records[28]. For imipramine ions at *m/z* 284, *m/z* 282, and *m/z* 280 were recorded using either a 1.3 m × 2 mm I.D. glass column

with 2% Dexyl 400 on Gas-Chrom Q (100–120 mesh) at 235°C (retention time 4 min) or a 2 m × 2 mm I.D. glass column with 1% SP 2250 on Supelcoport (100–120 mesh) at 235°C (retention time 3.5 min). The mass spectrometer was operated at a nominal accelerating voltage of 8 kV with 500 μA of trap current, an ionization potential of 50 eV and a source temperature of 250°C.

RESULTS AND DISCUSSION

In the mild reductive methylation procedure, desipramine is first treated with [$^2H_2$] formaldehyde and subsequently (after 5 min) sodium borohydride is added (when the order of addition was reversed, the unreduced secondary amine was recovered). Using imipramine as internal standard, the time course of the reaction was followed by electron impact MS at the molecular ions and showed that the reductive methylation was essentially complete in 5 min; additional samples taken at 10, 15 and 30 min showed no further changes in the *m/z* 282 to *m/z* 280 ratio. The conversion to [$^2H_2$]imipramine proceeded to 95.5 ± 1% completion in trials. It was also found that the reaction could be carried out with the same efficiency by using sodium cyanoborohydride as reducing agent and methyl cyanide as solvent under the same experimental conditions.

In contrast, imipramine N-oxide remained unaffected by the methylation procedure, only <2% of imipramine N-oxide being converted to imipramine in duplicate experiments.

Table I gives the results for the standard durve obtained for the analysis of desipramine and imipramine in human plasma over the therapeutic range of concentrations (0–200 ng/ml). [$^2H_4$]Imipramine is used as the internal standard for both drugs and the analysis is thus carried out on a single GC peak resulting from a single injection. A least-squares analysis shows excellent linearity of the data with slopes close to unity and correlation coefficients of 0.997 and 0.998.

TABLE I

STANDARD CURVE DATA FOR THE SIMULTANEOUS ANALYSIS OF IMIPRAMINE AND DESIPRAMINE IN PLASMA

Mole ratio (%) (Concentration in ng/ml)		*Ratio (%) of the ion currents**	
Desipramine [$^2H_2$]/[$^2H_4$]	*Imipramine* [$^2H_0$]/[$^2H_4$]	*At m/z 282 to m/z 284***	*At m/z 280 to m/z 284****
0.00 (0.0)	0.00 (0.0)	1.38 ± 0.01	0.49 ± 0.01
0.37 (14)	0.34 (14)	1.64 ± 0.11	0.96 ± 0.12
0.91 (36)	0.85 (36)	2.20 ± 0.06	1.43 ± 0.09
2.74 (108)	2.56 (106)	4.43 ± 0.04	3.46 ± 0.06
5.48 (216)	5.12 (213)	6.99 ± 0.27	5.98 ± 0.42

* Average observed value (triplicate injections) obtained from 3 samples ± standard deviation between samples.

** Calculation of a regression line gives $y = 1.34 + 1.048x$ with $r^2 = 0.997$.

*** Calculation of a regression line gives $y = 0.56 + 1.072x$ with $r^2 = 0.998$.

TABLE II

STANDARD CURVE DATA FOR THE SIMULTANEOUS ANALYSIS OF IMIPRAMINE AND DESIPRAMINE, USING LABELED AND UNLABELED DERIVATIZATION*

Mole ratio (%) vs [$^2H_4$]-impramine		*Ratio (%) of the ion currents***		*Ratio of the ion currents**** (%)
Desipramine	*Imipramine*	*At m/z 282 to m/z 284*[§], *desipramine*[§§]	*At m/z 280 to m/z 284*[§], *imipramine*[§§§]	*At m/z 280 to m/z 284*[§], *total drug*[†]
0.00	0.00	2.10 ± 0.15	0.86 ± 0.10	0.83 ± 0.07
1.34	1.26	3.81 ± 0.28	2.54 ± 0.17	3.83 ± 0.12
3.36	3.14	6.27 ± 0.33	5.26 ± 0.11	8.81 ± 0.12
14.8	13.8	19.1 ± 0.75	19.7 ± 0.21	36.5 ± 0.46
36.9	34.5	47.3 ± 3.3	47.4 ± 0.51	92.9 ± 0.81

* Using mixtures of standard solutions containing 42 μg [$^2H_4$]imipramine as internal standard.

** Experiment using [$^2H_2$]formaldehyde in the methylation step.

*** Experiment using unlabeled formaldehyde in the methylation step.

§ Average value (triplicate injections) obtained from 3 samples ± standard deviation between samples.

§§ Calculation of a regression line gives $y = 1.96 + 1.220x$ with $r^2 = 0.9993$.

§§§ Calculation of a regression line gives $y = 0.94 + 1.349x$ with $r^2 = 0.9999$.

† Calculation of a regression line gives $y = 0.41 + 2.672x$ with $r^2 = 0.9998$.

Table II gives data for two standard curves run under identical conditions except that unlabeled formaldehyde was used in the methylation step for one standard curve while [$^2H_2$]formaldehyde was used for the other. It is possible to calculate from the known weight ratio of desipramine to imipramine the expected increase in the slope of the line obtained for imipramine alone when total drug is measured. The slope of the regression line for the last column in Table II is in fact 96% of the theoretical value. Thus the use of the methylation procedure to obtain total drug by a single GC measurement from a single injection is not likely to fall short of the true value by more than a few percent. It would be possible to avoid this error entirely by carrying out a GC measurement of imipramine *before* and *after* methylation, using the appropriate standard curves.

In conclusion, the method described in this paper allows the simultaneous determination of imipramine and desipramine in a single GC peak, using a simple and rapid *in situ* methylation reaction.

REFERENCES

1 L. F. Gram, *Clin. Pharmacokinetics*, 2 (1977) 237; and references cited therein.
2 A. H. Glassman, M. Shostak, S. J. Kantor and J. M. Perel, *Psychopharmacol. Bull.*, 14 (1975) 27.
3 A. H. Glassman, J. M. Perel, M. Shostak, S. J. Kantor and J. L. Fleiss, *Arch. Gen. Psychiatry*, 34 (1977) 197.
4 A. Nagy and L. Treiber, *J. Pharm., Pharmacol.*, 18 (1973) 599.
5 J. V. Dingell, F. Sulser and J. R. Gillette, *J. Pharmacol. Exp. Ther.*, 143 (1964) 14.
6 J. P. Moody, A. C. Tait and A. Todrick, *Br. J. Psychol.*, 113 (1967) 183.
7 J. P. Moody, S. F. Whyte and G. J. Naylor, *Clin. Chim. Acta*, 43 (1973) 355.
8 W. M. Hammer and B. B. Brodie, *J. Pharmacol. Exp. Ther.*, 157 (1967) 503.

9 J. E. Wallace, H. E. Hamilton, L. K. Goggin and K. Blum, *Anal. Chem.*, 47 (1975) 1516.
10 S. Spector, N. L. Spector and M. P. Almeida, *Psychopharmacol. Communications*, 1 (1975) 421.
11 K. P. Maguire, G. D. Burrows, T. R. Norman and B. A. Scoggins, *Clin. Chem.*, 24 (1978) 549.
12 R. A. Braithwaite and B. Widdop, *Clin. Chim. Acta*, 35 (1971) 461.
13 O. Borgå and M. Garle, *J. Chromatogr.*, 68 (1972) 77.
14 N. Bailey and P. I. Jatlow, *Clin. Chem.*, 22 (1976) 1697.
15 I. D. Watson and M. J. Stewart, *J. Chromatogr.*, 132 (1977) 155; 134 (1977) 182.
16 F. L. Vandemark, R. F. Adams and G. J. Schmidt, *Clin. Chem.*, 24 (1978) 87.
17 A. Frigerio, G. Belvedere, F. De Nadai, R. Fanelli, C. Pantarotto, E. Riva and P. L. Morselli, *J. Chromatogr.*, 74 (1972) 201.
18 G. Belvedere, L. Burti, A. Frigerio and C. Pantarotto, *J. Chromatogr.*, 111 (1975) 313.
19 W. A. Garland, *J. Pharm. Sci.*, 66 (1977) 77.
20 M. Claeys, G. Muscettola and S. P. Markey, *Biomed. Mass Spectrom.*, 3 (1976) 110.
21 H. A. Heck, N. W. Flynn, S. E. Butrill, R. L. Dyer and M. Anbar, *Biomed. Mass Spectrom.*, 5 (1978) 250.
22 J. T. Biggs, W. H. Holland, S. Chang, P. P. Hipps and W. R. Sherman, *J. Pharm. Sci.*, 65 (1976) 261.
23 O. Borga, L. Palmer, A. Linnarson and B. Holmstedt, *Anal. Lett.*, 4 (1971) 837.
24 J. P. Dubois, W. Kund, W. Theobald and B. Wirz, *Clin. Chem.*, 22 (1976) 892.
25 A. Nagy and T. Hansen, *Acta Pharmacol. Toxicol.*, 42 (1978) 58.
26 W. Rapp, B. Noren and F. Pedersen, *Acta Psychiat. Scand.*, 49 (1973) 77.
27 L. D. Gruenke and J. C. Craig, in preparation.
28 L. D. Gruenke, J. C. Craig and D. M. Bier, *Biomed. Mass Spectrom.*, 7 (1980) 381.

Journal of Chromatography, 239 (1982) 87–95
Elsevier Scientific Publishing Company, Amsterdam — Printed in The Netherlands

CHROM. 14,648

MEASUREMENT OF ENDOGENOUS LEUCINE ENKEPHALIN IN CANINE THALAMUS BY HIGH-PERFORMANCE LIQUID CHROMATOGRAPHY AND FIELD DESORPTION MASS SPECTROMETRY

DOMINIC M. DESIDERIO* and SHIGETO YAMADA
Department of Neurology and Stout Neuroscience Mass Spectrometry Laboratory, University of Tennessee Center for the Health Sciences, 800 Madison Avenue, Memphis, TN 38163 (U.S.A.)

SUMMARY

A combination of high-performance liquid chromatography and field desorption mass spectrometry is used to quantify endogenous amounts of leucine enkephalin in canine thalamus tissue. Reversed-phase high-performance liquid chromatography effects rapid high resolution of brain neuropeptides using a triethylamine formate buffer. An internal standard, ^{2}Ala-leucine-enkephalin, is used. Field desorption mass spectra of neuropeptides generally display only protonated molecular ions. $(M+H)^+$ ion currents of endogenous leucine enkephalin and internal standard were integrated by field desorption mass spectral-selected ion monitoring techniques. The ratio of the two integrated ion currents was used to calculate endogenous amount of leu-enkephalin in thalamus tissue extracts. Leucine enkephalin was determined in this structurally unambiguous fashion in canine thalamus tissue at 50 ng/g thalamus tissue, or the 50 part per billion level.

INTRODUCTION

The objective of this research is to quantify in a structurally unambiguous manner the endogenous amount of an opioid peptide, leucine enkephalin (LE), in a selected canine brain region, the thalamus. This objective is accomplished with a combination of two instrumental methods, high-performance liquid chromatography (HPLC) and field desorption mass spectrometry (FD-MS).

The long-term objective of this laboratory is two-pronged: utilize mass spectrometry in elucidating the structure of unknown peptides[1] and measurement of endogenous amounts of bioactive peptides in biologic tissue[2]. Use of FD, chemical ionization (CI), electron ionization (EI), fast atom bombardment (FAB), and any other appropriate mass spectral ionization technique followed by collision activation (CA), link-scanning (*e.g.*, B/E), and any other analysis technique to produce sequence ions is the mechanism to obtain the amino acid sequence of an unknown peptide. Once the structure of the biologically active peptide is elucidated, the second phase is to quantify, with optimal structural specificity, endogenous amounts of this peptide in biologic fluids and tissues. Biologic matrix effects demand an internal standard for

0021-9673/82/0000–0000/$02.75

quantification of each peptide and metabolite of interest. Biologic matrix effects are ill-defined, but are the sum of peptide–protein, –lipid, –saccharide plus other unknown interactions that cause the observed difference between measurement of a pure solution and a biologic extract.

Whenever endogenous amounts of neuropeptides are measured by utilizing fluorescence, electrochemical, ultraviolet, or other detection methods following HPLC separation, then that one parameter (fluorescence quantum yield, half-wave potential of an electroactive species, UV absorbance, etc.) and not structure is determined at that specific HPLC retention time. On the other hand, many laboratories utilize radioimmunoassay (RIA) for quantification[3] of neuropeptides because of facile production of antibodies to a neuropeptide, short measurement time, low cost per measurement, and high sensitivity. An objective of RIA measurement is to have total molecular specificity so that chromatographic separation is not necessary. This criterion has not always been met[4,5]. The presence of metabolic enzymic apparatus for rapid and massive release of opioid peptides during certain metabolic events (death[6], pain, euphoria, etc.) implies ready availability of precursor molecules[7]. On the other hand, the extremely rapid metabolism of potent endogenous opioid peptides that is required in neural events implies the presence of metabolizing enzymes with high turnover number. Both metabolic situations provide precursors and metabolites which may have indistingishable RIA activity *vis-a-vis* the bioactive neuropeptide. RIA measurements of somatostatin, Leu-enkephalin, and bradykinin demonstrate this point. A molecular parameter is needed (mass of molecule or specific sequence-related ion) for quantification of a particular neuropeptide in a complex biologic extract.

This laboratory has developed volatile HPLC buffer systems[8], internal standards, extraction schemes, methods to avoid catabolism and metabolism, and FD-MS measurements of neuropeptides[8] in biologic tissue including canine caudate nucleus[9], hypothalamus[10], and tooth pulp[11]. Triethylamine–formate (TEAF) has been used as the HPLC buffer to quantify femtomole (fmol) amounts of somatostatin[8]. Picomole amounts of synthetic Leu-enkephalin solutions were quantified by FD-MS[12]. No other laboratory has reported on quantifying underivatized endogenous peptides by FD-MS.

MATERIALS AND METHODS

Tissue procurement

Dogs under pentobarbital anesthesia are exsanguinated via a femoral artery. The cranium is opened and brain removed. Caudate nuclei, hippocampus, pituitary, cerebellum, hypothalamus, cortex, spinal cord, olfactorum tubercle, pons, thalamus, etc. are excised and placed into liquid nitrogen within 4 min. Samples are stored at $-70°C$. Tissue weights are wet weight.

Internal standard and spiking

A 200-μg amount of internal standard (^{2}Ala-LE) (Bachem, Torrance, CA, U.S.A.) per gram of tissue in 20 ml Tris buffer (pH 7.4) is added to the homogenization flask. A 200–250 ng "spike" of LE is added, as indicated below (Fig. 2).

Sample preparation

Samples (2 g) are defrosted, mixed with 3 ml of 1.0 *M* acetic acid and homogenized for 3 min at 0°C with a VirTis 23 (Gardiner, New York, NY, U.S.A.) or Polytron homogenizer. This pH disrupts any peptide tissue protein complexes. Cell membranes in this solution are disrupted with a Kontes (Evanston, IL, U.S.A.) ultrasonic generator (300 W, 3 min) with a 4.5-in. probe.

Tracer

Homogenate is diluted ten-fold with either 1.0 *M* acetic acid or acetone–0.01 *M* HCl and transferred to a polypropylene centrifuge tube. Tritiated LE (tyrosyl-[3,5-^{3}H]Gly_2-Phe-Leu) (0.1 μCi, New England Nuclear, Cambridge, MA, U.S.A.) is added. Samples equilibrate overnight at 4°C[13].

Protein precipitation

Proteins are precipitated with ten volumes of acetone–0.01 *M* HCl (80:20) and removed after centrifugation at 15,000 *g* for 20 min at 0–5 C (Beckman J-21, Palo Alto, CA, U.S.A.). Supernatant is removed, five volumes of acetone–0.01 *M* HCl (60:40) are added and recentrifuged[14]. Supernatant is carefully removed and evaporated in a gentle stream of nitrogen. Residue is centrifuged at 3000 *g* for 5 min.

Porous polystyrene–divinylbenzene (PD) columns

Sample is dissolved in 4 ml of Tris–HCl buffer at pH 7.4 and placed on a PD column (0.5 g of Biobeads SM2 per g of tissue, Bio-Rad Labs, Richmond, CA, U.S.A., 20–50 μm mesh). PD column material is a 50:50 copolymer of polystyrene and divinylbenzene. Columns are 100 × 10 mm. A peptide fraction containing enkephalins is eluted with 6 ml of methanol in 2 ml fractions instead of a total of 0.9 ml as mentioned by other workers[15].

Octadecylsilica (ODS) mini-columns

ODS minicolumns are commercially available (Sep-Paks, Waters Assoc., Milford, MA, U.S.A.) prepackaged columns (0.4 g) used for reversed-phase (RP) chromatography[16]. An octadecyl group is chemically bound to the silica. The ODS minicolumn is prepared by washing with 4 ml of methanol, 4 ml of water, 4 ml of methanol, then 8 ml of trifluoroacetic acid (TFA, 0.5%)[17]. Sample is dissolved in 4 ml of 0.5% TFA and placed on the minicolumn. A peptide fraction is removed with 2 ml of acetonitrile–0.15% TFA (80:20).

Radioactivity counting

Radiolabeled enkephalin is determined by counting radioactivity (Hewlett-Packard Tri-Carb 460C) during several purification steps to determine recovery yield: protein precipitation, before and after P-D and ODS columns, and at the end of HPLC separation.

High-performance liquid chromatography

A Waters HPLC apparatus is used and consists of a U6K injector, guard column packed with Corasil B (30–50 μm diameter), two μBondapak C_{18} (10 μm diameter) reversed-phase analytical stainless-steel columns (30 cm × 4 mm I.D.) in series,

two Model 6000A solvent delivery pumps, a Model 600 solvent programmer, and a Model 450 variable-wavelength UV detector[8]. Analogue signals are recorded on a Houston potentiometric recorder.

A volatile HPLC buffer is used for resolution of peptides in biologic extracts. Dilute formic acid (0.04 *M*) is titrated to pH 3.15 with distilled triethylamine to form TEAF buffer[8]. Aqueous solutions are filtered and degassed with filters (0.45 μm pore diameter, HAWP 04700, Millipore, Bedford, MA, U.S.A.). Organic solutions are treated similarly (FHIP 04700, 0.5 μm pore diameter).

The peptide bond absorbance at 190–200 nm was monitored to optimize sensitivity of detection[9]. For example, HPLC of synthetic somatosatin solutions with TEAF at 190 nm yielded femtomole sensitivity[8].

Lyophilized biologic extracts are dissolved in TEAF (100 μl). After HPLC resolution into individual components, fractions are collected in non-silylated "reacti-vials" by switching the "waste–recycle–collect" valve to "collect". Collected volumes of solvent (several millilitres) are reduced with a gentle stream of nitrogen, then lyophilized. Use of non-silylated glassware is mandatory during this process to avoid shifts in mass values during FD-MS.

Field desorption mass spectrometry

A Finnigan (Varian) MAT 731 (Bremen, G.F.R.) mass spectrometer of Mattauch–Herzog double-focusing geometry outfitted with a field desorption–field ionization–electron ionization combination source is used. Static resolution is 1000; source temperature, 90°C; emitter potential, +8 kV; counterelectrode, −3 kV. Emitters are fabricated in our laboratory from 10 μm diameter tungsten wire by activation at high temperature in a benzonitrile atmosphere under influence of a high electric field. Carbon microneedle growth on the emitter wire surface extended to a length of *ca.* 30 μm. The instrument is focused on the FI spectrum of acetone.

Lyophilized HPLC fractions are dissolved in 100 μl of methanol to wash sides of the reacti-vial, and a gentle stream of nitrogen reduces sample volume to less than 10 μl. Sample is carefully transferred to the emitter with assistance from a microsyringe–micromanipulator–stereomicroscope ensemble[9].

FD emitters display no difficulty during desorption of synthetic peptide solutions. However, biologic matrix effects are manifested at this stage of analysis by a "stickiness" of the extract on the emitter. Due to the multi-step chromatographic procedures used, this "stickiness" may be due to the RP-ODS-HPLC column material, lipids, or other biologic matrix material. Care must be exercised during emitter heating to avoid mechanical breakage of the emitter.

The peak matching unit is set to scan alternately $(M+H)^+$ ions of LE at *m/z* 556 and ^{2}Ala-LE at 570. The emitter heating current is increased manually to 16 mA where enkephalins desorb optimally[9–12]. An oscillographic recording is obtained manually of the entire desorption envelope as peak switching continues. The entire process is monitored on an oscilloscope. Individual ion currents of the two $(M+H)^+$ ions are integrated manually by summing respective peak heights. Mass spectral ion signals are corrected for cross contributions due to isotopes and to fragmentation (contribution of 570 to 556 is 2% and 556 to 570 is 0.3%).

RESULTS

Fig. 1 contains the RP-HPLC chromatogram of unspiked canine thalamus tissue (2 g) containing internal standard. A second sample was spiked with 200 ng of LE per gram of tissue. Experimental chromatographic conditions are shown in the figure. The retention times for LE (7.1 min) and internal standard (10.6 min) are known and reproducible. A mixture of synthetic peptide standards was injected before biologic sample to accurately verify retention times.

Fig. 2 contains an outline of the scheme used to calculate endogenous amount of LE in brain tissue. A known amount of tissue is divided into two equal parts. One-half is subjected to Sep-Pak, Bio-Beads SM2, another Sep-Pak, HPLC, then FD-MS measurement. The other half is spiked with 200 ng of LE per gram of tissue and subjected to the same sequence of chromatography.

FD-MS measurement yields a ratio (R) of integrated $(M+H)^+$ ion currents due to LE and internal standard. The R_1 value is linearly proportional (slope = a) to endogenous amount of LE (x ng per g of tissue) in the unspiked sample. Preliminary data (not published) indicate that the intercept of this straight line equals zero. Whenever sample is spiked, the straight line shifts to the right 200 ng on the abscissa and the equation $a(x + 200) = R_2$ is used. The a and x values remain the same as in the unspiked analysis, while R_2 becomes the new ratio determined by FD-MS. Solution of the two equations with two unknowns yields an x value of ng LE per g of tissue. Use of spiked sample increases accuracy.

Data in Fig. 3 were obtained to determine the level of sensitivity achievable

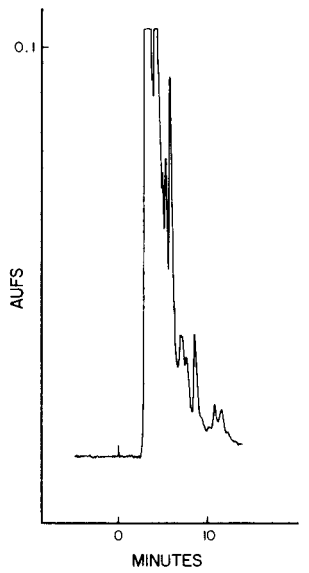

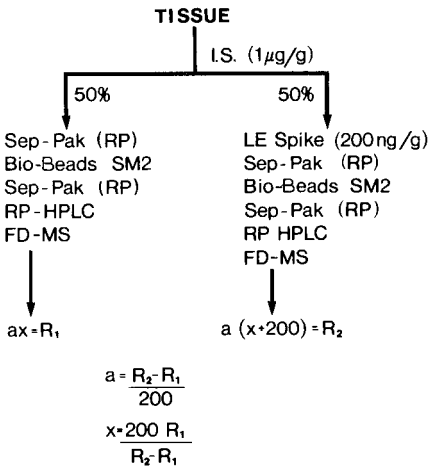

Fig. 1. RP-HPLC chromatogram of thalamus tissue extract. Two C_{18} columns; solvent, acetonitrile–TEAF (30:70), 1.5 ml/min; detection at 200 nm.

Fig. 2. Scheme used to calculate endogenous LE in spiked and unspiked thalamus tissue extracts.

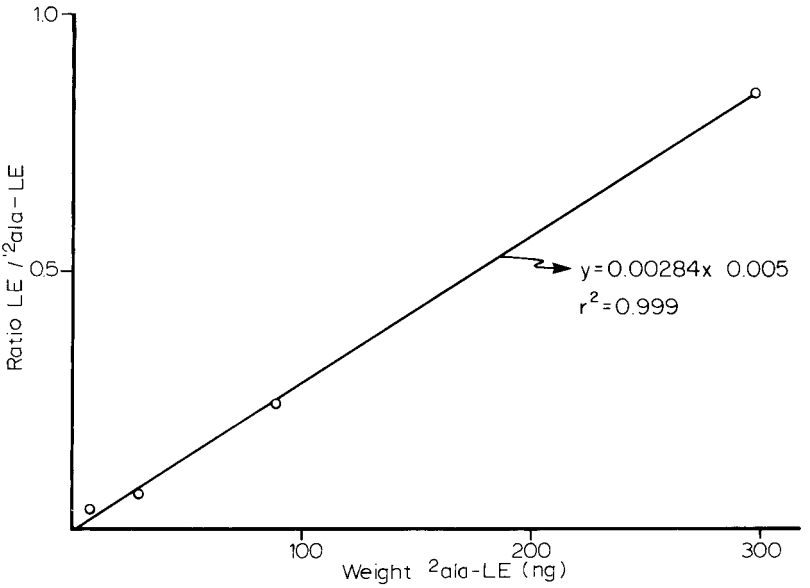

Fig. 3. Calibration curve of FD-MS measurement of synthetic LE/I.S. solutions.

with the combination of HPLC and FD-MS measurement of synthetic solutions of opioid peptides. Four samples were prepared where each sample contained 300 ng of internal standard, ^{2}Ala-LE. To each one of these four samples, successively lower amounts (300, 100, 30 and 10 ng) of LE were added to produce solutions with ratios of 1:1, 3:1, 10:1 and 30:1, LE to IS, respectively. FD-MS measurement of these four synthetic mixtures yielded data shown in Fig. 3. It can be clearly seen that down to 30 ng (60 pmol) LE can be measured. It must be remembered that all aspects of this measurement are done manually. Experience in our laboratory indicates that biologic matrix effects play a role in measurement of peptides in biological samples and the 30 ng level is not routinely obtained for biologic samples.

Field desorption (selected ion monitoring) measurement of LE in tissue extract

TABLE I

MEASUREMENT OF LE/IS ION CURRENT RATIOS (R) IN SPIKED AND UNSPIKED THALAMUS TISSUE EXTRACTS

	Sample				*Mean*
	1	*2*	*3*	*4*	
Unspiked	0.0528	0.0572	0.0587	–	0.0561
Spiked	0.1609	0.2785	0.3288	0.3202	0.2721

$ax = 0.0561$
$a(x + 200) = 0.2721$
$x = 51.92$ ng LE/g thalamus tissue

from canine thalamus was performed on HPLC fractions and data are collected in Table I. The data yield a value for amount of endogenous LE equal to 51.92 ng/g tissue or 52 ppb.

DISCUSSION

Leucine enkephalin is measured in canine thalamus tissue by a combination of instrumental analytical techniques in an effort to preserve molecular specificity of the measurement. HPLC efficiently and rapidly resolves Leu-enkephalin from a biologic tissue extract with high resolution. FD-MS of chemically underivatized LE efficiently provides a protonated molecular ion $(M+H)^+$ from picomole amounts of that neuropeptide and retains molecular structure information. Measurement of $(M+H)^+$ provides confidence that quantification of only that compound of interest is being performed. The sensitivity of this novel HPLC–FD-MS measurement is at the 50 ng LE/g tissue (50 ppb), or picomole amounts.

Other workers have measured brain peptides by RIA, and is some cases, preliminary chromatography was done. Variability in published methods of handling tissue and the time elapsed[18] following tissue procurement but before measurement are two highly variable and critical parameters that must be understood and controlled. Recent research indicates endogenous tissue proteinases, peptidases[19], enkephalinases[20], and synthetases are all present in tissue extracts. For that reason, rapid tissue procurement, temperature lowering, and protein precipitation to destroy all enzyme activity are important preliminaries to measure biologic peptides of interest to reflect accurately amounts of that specific peptide originally present in the biologic tissue.

Tissue is procured in a very rapid manner in our study and a specific method of handling that tissue was developed in this laboratory and applied to various brain tissues. Within minutes of neurosurgery, neuroanatomic identification of specific brain regions was followed by rapid excision of these individual brain regions and placement of tissue into liquid nitrogen followed by storage at $-70°C$. Enzyme activity of enkephalinases, proteinases, peptidases, and synthetases were minimized or completely abolished. Specific RP chromatographic techniques were utilized to take advantage of chromatographic hydrophobic properties of individual peptide:buffer molecular complexes. For example, for enkephalins, a polystyrene–divinylbenzene minicolumn[15] was utilized because of this column's propensity to retain enkephalins. Most other peptides are retained by ODS RP packing, and these minicolumns are utilized followed by ODS RP-HPLC columns.

Biologic matrix effects observed with brain and tooth-pulp tissue demand that an internal standard be used for each neuropeptide quantified. Higher homologs have been used with success in this study. Stable isotope-labeled internal standards are also possible.

Recovery studies were performed with tritiated peptide (LE) tracers to determine accurately recovery of individual peptides. Close scrutiny of the Materials and Methods sections in many published papers failed to reflect accurately what is the overall recovery of a peptide from biologic tissue. Many workers do not equilibrate IS with tissue overnight[13]. We equilibrate tracer and IS overnight to ensure optimal penetration into biologic matrix and mixing of endogenous peptide with exogenous tracer.

The most important parameter obtained by methods outlined here include the molecular parameter demanded for any accurate measurement of an endogenous biologically active peptide or metabolite in biologic tissue or fluid. FD-MS produces a protonated molecular ion $(M+H)^+$ which relates to the total molecular information of the molecule being quantified. Fast atom bombardment is another ionization method[21]. For further increased molecular specificity, other instrumental techniques (collision activation, linked scanning, and high-resolution MS) can be utilized[22]. A microprocessor system is being fabricated to control emitter heating current and ion current integration. Microprocessor-controlled data acquisition will reduce errors and increase sensitivity.

Analytic measurements of LE in thalamus tissue described here are compatible with our previously published RP-HPLC–FD-MS measurements of LE and Met-enkephalin in brain tissue (caudate nucleus and hypothalamus[10]) and tooth pulp[11]. Current measurements extend our experience to achieve our goal to quantify several neuropeptides in several brain regions. Furthermore, the results from RP-HPLC indicate that other peptides remain to be sequenced and quantified. Sequencing is required in an effort to (a) determine all bioactive peptides in these tissues, (b) provide a "metabolic profile" to describe normal and pathological conditions, and (c) describe the biosynthetic precursors and metabolic products of active neuropeptides. Having been sequenced, individual peptides can then be quantified.

ACKNOWLEDGEMENTS

The authors acknowledge typing assistance of D. Cubbins, technical assistance of G. Fridland, and financial assistance from NIH (GM NS 26666).

LIST OF ABBREVIATIONS

B/E	link scanning
CA	collision activation
CI	chemical ionization
EI	electron ionization
FAB	fast atom bombardment
FD-MS	field desorption-mass spectrometry
fmol	femtomole (10^{-15} mole)
HPLC	high-performance (pressure) liquid chromatography
LE	leucine-enkephalin (Tyr-Gly-Gly-Phe-Leu)
mA	milliampere
m/z	mass-to-charge ratio of an ion
$(M+H)^+$	protonated molecular ion
ODS	octadecylsilica
ppb	parts per billion
PD	polystyrene–divinylbenzene
pmol	picomole
RIA	radioimmunoassay
RP	reversed-phase
TEAF	triethylamine–formic acid
TFA	trifluoroacetic acid

REFERENCES

1 R. Burgus, T. Dunn, D. M. Desiderio, D. Ward, W. Vale and R. Guillemin, *Nature (London)*, 226 (1970) 321.
2 D. M. Desiderio, S. Yamada, F. S. Tanzer, J. Horton and J. Trimble, in A. Zlatkis (Editor), *Advances in Chromatography 1981*, Department of Chemistry, University of Houston, Houston, TX, 1981, pp. 475–490.
3 B. N. Jones, A. S. Stern, R. V. Lewis, S. Kimura, S. Stein, S. Udenfriend and J. E. Shively, *Arch. Biochem. Biophys.*, 204 (1980) 392.
4 R. Carraway, R. A. Hammer and S. W. Leeman, *Endocrinol.*, 107 (1980) 400.
5 E. Granstrom and H. Kindahl, *Advan. Prostag. Thrombox. Res.*, 5 (1978) 119.
6 D. B. Carr, *Lancet*, i (1981) 390.
7 R. V. Lewis, A. S. Stein, S. Kimura, J. Rossier, S. Stein and S. Udenfriend, *Science*, 208 (1980) 1459.
8 D. M. Desiderio and M. D. Cunningham, *J. Liquid Chromatogr.*, 4 (1981) 721–722.
9 D. M. Desiderio, S. Yamada, F. S. Tanzer, J. Horton and J. Trimble, *J. Chromatogr.*, 217 (1981) 437.
10 S. Yamada and D. M. Desiderio, *Anal. Biochem.*, submitted for publication.
11 F. S. Tanzer, D. M. Desiderio and S. Yamada, in D. H. Rich and E. Gross (Editors), *Peptides Synthesis, Structure, and Function*, Pierce Publishers, Rockford, IL, in press.
12 D. M. Desiderio, S. Yamada, J. Z. Sabbatini and F. S. Tanzer, *Biomed. Mass Spectrom.*, 8 (1981) 10.
13 A. M. Lawson, D. K. Lim, W. Richmond, D. M. Samson, K. D. R. Setchell and A. C. S. Thomas, in A. M. Lawson, D. K. Lim and W. Richmond (Editors), *Current Developments in the Clinical Application of HPLC, GC, and MS*, Academic Press, New York, 1980, pp. 144–145.
14 H. Ueda, H. Shiomi and H. Takagi, *Brain Res.*, 198 (1980) 460.
15 E. Peralta, H.-Y. T. Yang, J. Hong and E. Costa, *J. Chromatogr.*, 190 (1980) 43.
16 H. P. J. Bennett, C. A. Browne and S. Solomon, *Biochemistry*, 20 (1981) 4530.
17 M. J. Fasco, M. J. Cashin and L. S. Kaminsky, *J. Liquid Chromatogr.*, 2 (1979) 656.
18 P. C. Emson, A. Arregui, V. Clement-Jones, B. E. B. Sandberg and M. Rossor, *Brain Res.*, 199 (1980) 147.
19 L. B. Hersh, *Biochemistry*, 20 (1981) 2345.
20 G. Patey, S. de la Baume, J.-C. Schwarz, C. Gros, B. Roques, M.-C. Fournie-Zaluski and E. Soroca-Lucas, *Science*, 212 (1981) 1153.
21 M. Barber, R. S. Bordoli, R. D. Sedgwick, A. N. Tyler and E. T. Whalley, *Biomed. Mass Spectrom.*, 8 (1981) 337.
22 D. M. Desiderio and J. Z. Sabbatini, *Biomed. Mass Spectrom.*, in press.

Journal of Chromatography, 239 (1982) 97–106
Elsevier Scientific Publishing Company, Amsterdam — Printed in The Netherlands

CHROM. 14,501

GRAM QUANTITY SYNTHESIS AND CHROMATOGRAPHIC ASSESSMENT OF 3,3′,4,4′-TETRACHLOROBIPHENYL

K. NAKATSU*, J. F. BRIEN, H. TAUB, W. J. RACZ and G. S. MARKS
Department of Pharmacology, Queen's University, Kingston, Ontario K7L 3N6 (Canada)

SUMMARY

3,3′,4,4′-Tetrachlorobiphenyl (TCBP) was synthesized by diazotization of 3,3′-dichlorobenzidine followed by chlorination with cuprous chloride and hydrochloric acid. Purification of crude TCBP was conducted by alumina column chromatography and two recrystallizations from ethanol. The composition of the product during purification was assessed by gas–liquid chromatography with electron-capture detection and high-performance liquid chromatography with UV absorption detection. TCBP with greater than 99% purity (dioxin- and furan-free) was obtained with a yield of 40–44%. The identity of the major synthetic product was confirmed by gas chromatography–mass spectrometry (electron ionization) and nuclear magnetic resonance spectroscopy. The major impurity, a trichlorobiphenyl, constituted 0.37% of the final product. It is concluded that this synthetic product can be used to produce reliable results in toxicological studies.

INTRODUCTION

Industrial polychlorinated biphenyls (PCBs), which have been identified as important environmental hazards, are mixtures of several chlorinated biphenyl compounds that contain variable amounts of chlorinated dioxin and furan contaminants. In order to determine the mechanism of toxicity of each individual compound, it is necessary to prepare pure individual compounds for study. The syntheses of individual PCBs have been described[1–5]. However, it is recognized that many of the synthetic routes to PCBs result in the contamination of the final product with small amounts of material (*e.g.* chlorinated dioxins and furans), which may have a toxic potential several orders of magnitude greater than the PCB under study[6–9]. Thus, to assess the toxicity of individual PCB isomers, it is imperative to determine the purity of the compounds studied and to elucidate the chemical nature of impurities contained in the PCB sample. A review of the synthetic procedures employed for PCB synthesis gives insufficient information to allow careful assessment of the purity of the PCB synthesized and employed in toxicological studies. In this study, we have utilized a variety of current techniques to define the purity of the PCB during the course of its synthesis and purification on a preparative scale. This report is also intended to assist other investigators in the preparation of individual PCB isomers with respect to the purity, amount and economy required for large-scale *in vivo* toxicity studies.

0021-9673/82/0000–0000/$02.75

MATERIALS AND METHODS

Reagents and solvents

For use as a reference standard 3,3′,4,4′-tetrachlorobiphenyl (TCBP) was obtained with a purity of 99% and chlorinated dibenzo-*p*-dioxin (CDD) and dibenzofuran free from RFR (Hope, RI, U.S.A.). For the present synthesis, the starting material, 3,3′-dichlorobenzidine dihydrochloride, was purchased from Sigma (St. Louis, MO, U.S.A.). Cuprous chloride, analytical reagent, 97% pure, was obtained from BDH (Toronto, Canada). The following chemicals were purchased from Fisher (Whitby, Canada) as ACS grade: sodium nitrite crystals, 98.2%; A-950 alumina, neutral, Brockman activity 1, 80–200 mesh; anhydrous sodium carbonate; methylene chloride; carbon tetrachloride; hydrochloric acid; sulfuric acid; and glacial acetic acid. Hexane, ethyl acetate and acetone were obtained from Caledon (Georgetown, Canada) as HPLC grade. The water utilized in these studies was passed through a Barnstead Nanopure® apparatus (Canlab, Toronto, Canada). Melting points were determined on a Thomas Hoover Capillary melting point apparatus (A.H. Thomas, Philadelphia, PA, U.S.A.) and are uncorrected.

Synthesis of 3,3′,4,4′-tetrachlorobiphenyl

3,3′,4,4′-TCBP was prepared by the method of Cain[10] as modified by Van Roosmalen[3]. 3,3′-Dichlorobenzidine was converted into the corresponding diazonium salt, and two chlorine atoms were introduced by treatment with cuprous chloride and concentrated HCl. 3,3′-Dichlorobenzidine dihydrochloride (0.01 mole; 3.26 g) was suspended in concentrated HCl (0.06 mole; 5 ml) to which was added 5 ml of water, and the reaction flask was kept on ice. An aqueous solution of sodium nitrite (0.028 mole; 8.3 ml) was added dropwise to the mixture, which was stirred vigorously under nitrogen. To verify the presence of excess nitrous acid at the completion of the reaction, the reaction mixture was tested with potassium iodide-starch paper. Cuprous chloride (0.024 mole; 2.38 g) was dissolved in concentrated HCl (12 ml), and 10 ml of this solution were added dropwise to the stirred reaction mixture over a period of *ca.* 40 min. A frothy slurry resulted due to the liberation of free nitrogen gas. After 1 h at room temperature, a yellowish crude complex was obtained by filtration and dried overnight in a vacuum dessicator (yield of crude product was 4.3 g). For large batches, the amount of the starting material and reagents was increased 10-fold.

Alumina column chromatography purification

The purification of 3,3′,4,4′-TCBP was based on the procedures of Goldstein *et al.*[5], Parkinson *et al.*[11] and Kamops *et al.*[12]. Individual 1-g portions of the yellowish, crude TCBP dissolved in 100 ml of acetone were added to 6 g of alumina which had been activated overnight at 130°C, and the contents were stirred for several hours. The solvent was then removed by evaporation using a stream of nitrogen. The alumina containing the TCBP was then loaded onto a glass column (67 cm × 1.1 cm I.D.) which was dry-packed with 60 g of alumina. The column had a medium-porosity glass frit and a teflon stopcock. The TCBP was eluted with hexane, and 100-ml fractions were collected. The progress of the elution of the TCBP was monitored by gas–liquid chromatography with electron-capture detection (GLC–ECD). The frac-

tions were subsequently pooled and after removal of solvent on a rotary evaporator under reduced pressure, a white crystalline material remained.

Recrystallization

The white crystalline product was recrystallized twice from ethanol; *ca.* 400 ml of ethanol were required for 1 g of the TCBP.

Gas chromatography–mass spectrometry (GC–MS)

The identification of the synthetic product and the characterization of the minor contaminants were conducted using a Hewlett-Packard Model 5985B gas chromatograph–mass spectrometer. The apparatus was interfaced with a HP Model 2648A graphics terminal and data station. The GC conditions were: coiled glass column (1.8 m × 2 mm I.D.), containing 3% OV-101 on 80–100 mesh Chromosorb W HP (Chromatographic Specialties, Brockville, Canada); helium flow-rate, 30 ml/min; injection port temperature, 250°C; column temperature, 220°C. The mass spectrometer was operated in the electron ionization mode (70 eV); ion source temperature, 250°C; mass range, 40–500 a.m.u.

High-resolution MS was done on a CEC Model 21-110B mass spectrometer.

Nuclear magnetic resonance spectroscopy (NMR)

The samples were prepared by dissolving 40 mg of TCBP in 1 ml of C^2HCl_3. Proton spectra were recorded at 60 and 200 MHz on a Brucker Model instrument. All chemical shifts are reported as δ values with respect to the internal standard, tetramethylsilane.

Gas–liquid chromatography

Electron-capture detection. The chemical purity of the TCBP was assessed by GLC–ECD using a Hewlett-Packard Model 5730A gas chromatograph equipped with a ^{63}Ni electron capture detector, a 1 mV potentiometric recorder and Hewlett-Packard Model 3390A electronic integrator. A coiled glass column (1.8 m × 2 mm I.D.) was washed in sequence with distilled water, methanol, acetone, methylene chloride and hexane, dried with a stream of nitrogen and silanized with 10% Surfasil® (Chromatographic Specialties) in toluene for 1 h. The column was heated at 100°C for 30 min, cooled, rinsed with methanol and dried with a stream of nitrogen. The silanized column was packed with 3% OV-1 on 80–100 mesh Chromosorb 750 (Chromatographic Specialties), and conditioned for at least 15 h at 250°C using argon–methane (95:5) carrier gas at a flow-rate of 5 ml/min. The operating conditions were: injection port temperature, 250°C; column temperature, 220°C; detector temperature, 300°C; carrier gas flow-rate, 22 ml/min.

To prepare a standard curve, known amounts of pure 3,3′,4,4′-TCBP were prepared in hexane (10 pg–1000 ng in 1–5 μl) and analyzed by GLC–ECD. The absolute peak area of the chromatographic signal was measured by electronic integration and plotted against TCBP content.

Nitrogen–phosphorus detection. In order to check for the presence of nitrogen-containing contaminants in the TCBP synthetic product, the above analysis was repeated using a Hewlett-Packard Model 5710A gas chromatograph equipped with a nitrogen–phosphorus detector (NPD). All chromatographic conditions were as de-

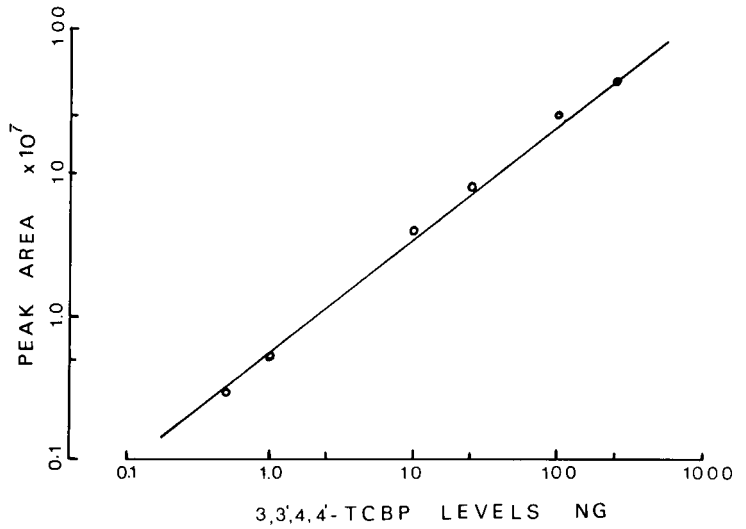

Fig. 1. GLC–ECD standard curve for 3,3′,4,4′-TCBP. Note linearity over three orders of magnitude.

scribed above, except that the carrier gas flow-rate was 30 ml/min; hydrogen and air flow-rates were 3 and 50 ml/min, respectively.

High-performance liquid chromatography–ultraviolet absorption detection (HPLC–UV)

The chemical purity of the synthesized TCBP was assessed by HPLC–UV. The liquid chromatographic system consisted of the following components: solvent me-

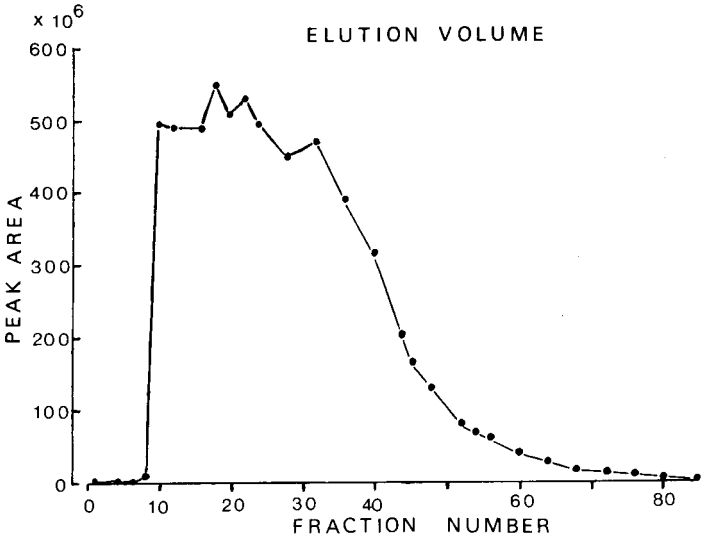

Fig. 2. Hexane elution profile of 10 g of TCBP on an alumina column. A 10-g portion of crude product was adsorbed onto 60 g of alumina and subsequently applied to a large glass column (100 cm × 24 cm I.D.) dry-packed with 150 g of alumina. Hexane elution fractions (100 ml) were collected and a 1-μl sample of each fraction was analyzed by GLC–ECD. The peak areas of the chromatograms were determined by electronic integration.

tering pump (Model 110A Beckman, Fullerton, CA, U.S.A.); injection valve with a 20-μl injection loop (Valco, Houston, TX, U.S.A.); UV detector with a 8-μl microflow cell and 254-nm filter (Model 153, Altex, Berkeley, CA, U.S.A.); strip chart recorder (Fisher). The stainless-steel column (20 cm $\times$ 4 mm I.D.) was packed with 5 μm silica gel (Partisil 5; Whatman, Clifton, NJ, U.S.A.). The eluting solvent was degassed hexane, and the flow-rate was 1.0 ml/min. Peak height measurements were used for quantitation.

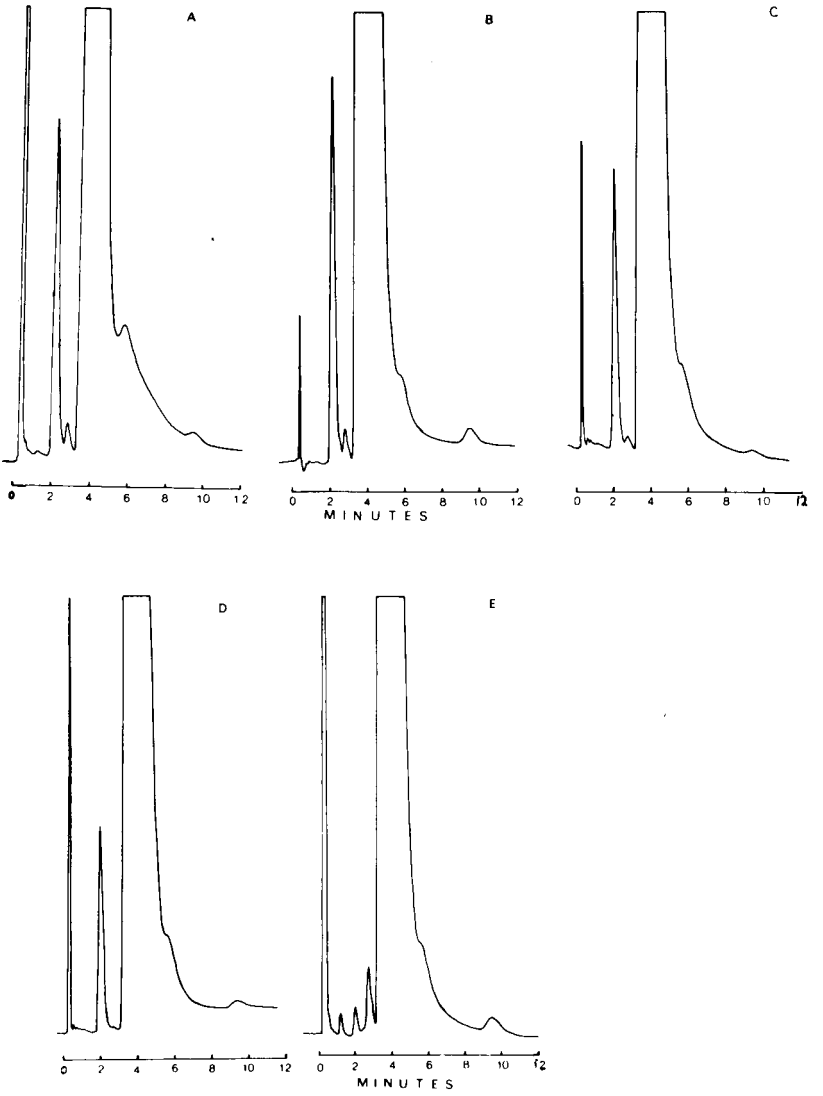

Fig. 3. GLC–ECD chromatograms of 3,3′,4,4′-TCBP in the course of purification. A, Crude product; B, post alumina; C, one ethanol crystallization; D, two ethanol crystallization; E, RFR 3,3′,4,4′-TCBP (99% CDD-free).

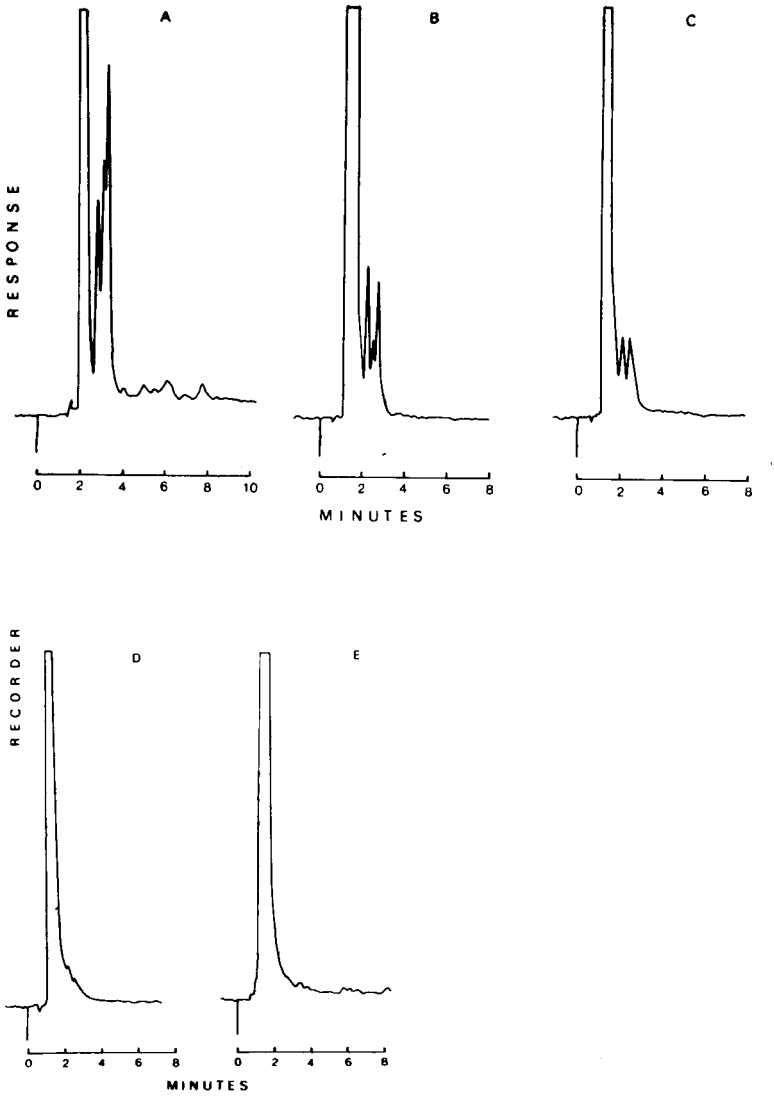

Fig. 4. HPLC–UV chromatograms of 3,3′,4,4′-TCBP in the course of purification. A–E as in Fig. 3.

RESULTS AND DISCUSSION

Data regarding the yield of product at each step were obtained by GLC–ECD with reference to the 3,3′,4,4′-TCBP standard curve (Fig. 1). The calibration curve was linear over the range from 500 pg to 500 ng of 3,3′,4,4′-TCBP, and the amounts injected for yield analysis were between 1 and 100 ng.

The crude synthetic product was yellowish brown and had a melting point of 152–155°C. The first step in the purification was alumina column chromatography, which was based on available procedures[5,11,12]. The recovery of compound from the

TABLE I

PURITY OF 3,3′,4,4′-TETRACHLOROBIPHENYL BY GLC–ECD FOLLOWING ALUMINA COLUMN CHROMATOGRAPHY AND REPEATED ETHANOL RECRYSTALLIZATION

Peak areas are expressed as percentage of total area of the chromatogram as determined by electronic integration

Retention time (min)	*Peak area (%)*				
	Crude product (A)	*Post column (B)*	*First ethanol recrystallization (C)*	*Second ethanol recrystallization (D)*	*Commercial reference standard (E)*
1.24	0.008	0.003	0.002	0.002	0.027
2.15	1.086	0.972	0.526	0.368	0.053
2.97	0.109	0.088	0.079	*	0.155
3.85	98.553	98.836	99.296	99.550	99.632
6.28	0.202	*	*	*	*
10.50	0.043	0.102	0.097	0.080	0.132

* Signal present but non-measurable by electronic integration.

column after application of 1–10 g amounts ranged from 78 to 87%. Elution through the column removed all the coloured impurity and upon removal of the eluent, a white residue, m.p. 173–176°C, was obtained. A typical profile for a 10-g load of crude material on a alumina column with elution by hexane is shown in Fig. 2. Preliminary studies revealed that florisil or silica gel column chromatography did not provide satisfactory purification. However, the use of alumina or alumina/Florisil column chromatography resulted in improved purification. Since the adsorptivity of florisil was reported to differ from lot to lot[12,13], alumina alone was added as the matrix. Comparison by GLC–ECD of the product before and after alumina chromatography (Figs. 3A and B, Table I) and by HPLC–UV (Figs. 4A and B) illustrates the reduction in the amount of contamination.

The second step in the purification procedure was recrystallization from ethanol, which produced a white crystalline solid. The overall yield of purified material ranged from 40 to 44% (4.0–4.4 mmole). Considerable purification was achieved by this means, and the melting points were 176–177°C after one recrystallization and 177–177.5°C after two recrystallizations. However, the melting point for 3,3′,4,4′-TCBP has been reported to be 177–178°C[2], 172°C[3,10] and 173°C[1]. In a separate experiment, recrystallization from glacial acetic acid produced a brown-coloured crystalline solid, m.p. 171–173°C. Thus the discrepancy amongst the reported melting points may be related to the mode of recrystallization and/or the presence of a chromophore. Analysis by GLC–ECD (Figs. 2C and D, Table I) and HPLC–UV (Figs. 4C and 1D) of the ethanol-recrystallized product illustrates the successive purification with each recrystallization. The final product had a purity of greater than 99.5% by GLC–ECD, which compares favourably with the commercially available 3,3′,4,4′-TCBP reference standard (Fig. 3E, Table I). Analysis by HPLC–UV gave comparable values. The identity of the final product is supported by retention times (t_R) from GLC–ECD (Fig. 3) and HPLC–UV (Fig. 4), mass spectra and NMR spectra.

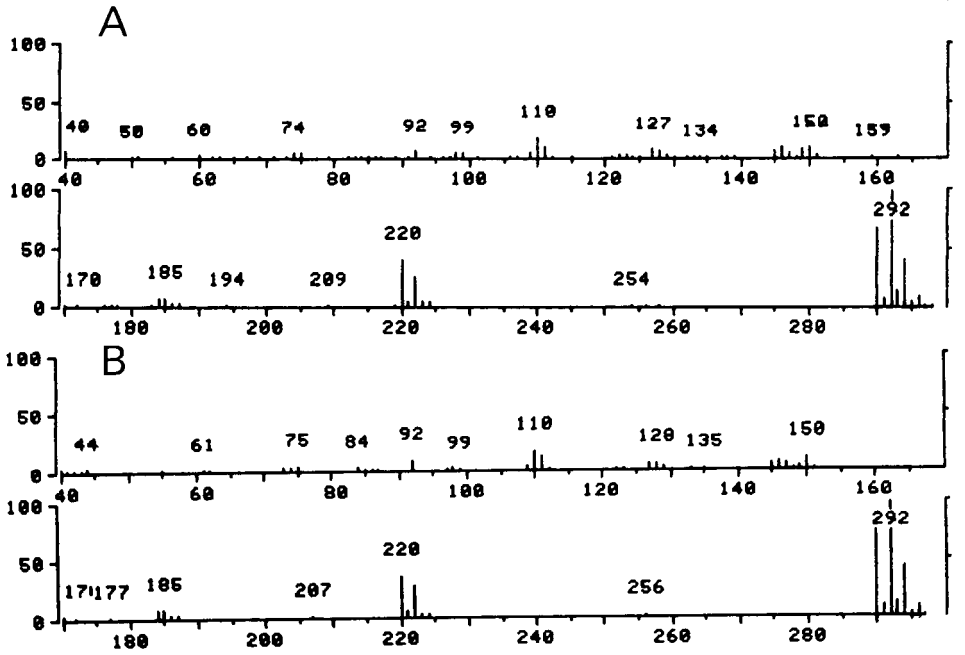

Fig. 5. Mass spectra of commercial 99% pure and CDD-free, 3,3′,4,4′-TCBP, reference standard (A) and the purified TCBP (B).

The mass spectrum of the synthetic product (GLC t_R 3.85 min) was indistinguishable from that for the commercial reference product (Figs. 5A and B). Electron ionization produced an abundant molecular ion at *m/z* 290 (relative intensity of 75% compared with the base ion, 292 *m/z*) with characteristic chlorine isotope peaks. The fragmentation pattern (Fig. 5) is consistent with TCBP and is identical with the pattern reported by the Environmental Protection Agency (Washington, DC, U.S.A.) for 3,3′,4,4′-TCBP[14]. The molecular nature of the three minor impurities, corresponding to GLC–ECD signals at t_R 2.15, 2.97 and 10.5 min, was tentatively identified (Fig. 6). The mass spectrum of the major contaminant (t_R 2.15) had a molecular ion at *m/z* 256 (Fig. 6a) with the characteristic trichloro-isotopic fragmentation pattern and is consistent with 3,4,4′-trichlorobiphenyl. The GLC–ECD signal at t_R 2.97 min was tentatively identified as being due to a tetrachlorobiphenyl (possibly 2,3′,4,4′-tetrachlorobiphenyl) (Fig. 6b). The unidentified material at t_R 10.5 min is *not* chlorinated (Fig. 6c). A further search for dioxins and furans by GC–MS indicated no detectable amounts of either potential contaminant. Moreover, GLC–NPD analysis failed to detect the presence of nitrogen-containing components. Our 3,3′,4,4′-TCBP product had more contamination with the trichlorobiphenyl (0.37%) but considerably less contamination with the tetrachlorobiphenyl (0.05%) when compared with the commercially available reference standard (0.05 and 0.155%, respectively). High-resolution MS indicated that the mass of the molecular ion was 289.9204, which compares well with the theoretical mass of 289.9224 for $C_{12}H_6Cl_4$ (TCBP).

NMR data of the purified 3,3′4,4′-TCBP were in good agreement with those reported by Hutzinger *et al.*[13]. There was a multiplet, δ 7.06–7.60, at 60 MHz and a

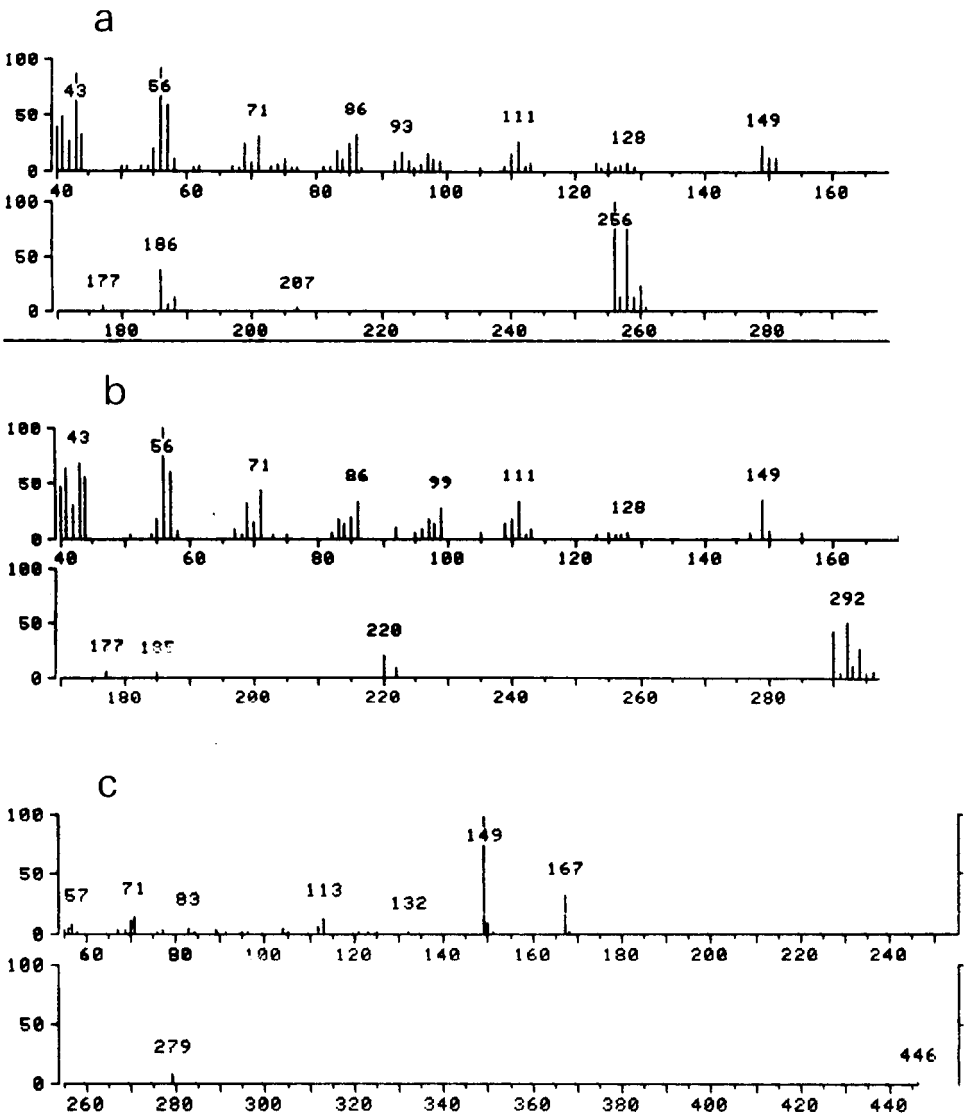

Fig. 6. Mass spectra of minor contaminants of the 3,3′,4,4′-TCBP synthetic product. The spectra were obtained for contaminants with GLC t_R 2.15 min (a), 2.97 min (b) and 10.5 min (c).

multiplet, δ6.90–7.56, at 200 MHZ, relative to the internal standard, tetramethylsilane, when dissolved in C^2HCl_3.

Thus, we have shown that 3,3′,4,4′-TCBP can be synthesized in large amounts and purified by one alumina chromatographic step followed by two recrystallizations from ethanol. The product, which is greater than 99.5% pure, is dioxin- and furan-free and contains a trichlorobiphenyl contaminant as the major impurity (0.37%). We believe that this product can be used to produce reliable results in toxicological studies.

ACKNOWLEDGEMENTS

This work was supported by the Natural Sciences and Engineering Research Council of Canada. High-resolution MS was done by Mr. Fred Montgomery in the laboratory of Dr. Evan Horning, Institute for Lipid Research, Baylor College of Medicine, Houston, TX, U.S.A. The assistance of Dr. R. A. Whitney, Department of Chemistry, Queen's University, in the interpretation of the NMR spectra is acknowledged. We also acknowledge the technical assistance of Mr. D. Zelt who was supported by Queen's University. The Hewlett-Packard mass spectrometer is maintained by a grant from the Medical Research Council of Canada. We thank Mrs. D. Browne who typed this manuscript and Mr. R. Roscher and Ms. B. Gillespie who did the graphics.

REFERENCES

1 O. Hutzinger, S. Safe and V. Zitko, *Bull. Environ. Contam. Toxicol.*, 6 (1971) 209.
2 G. Sundstrom, *Acta Chem. Scand.*, 27 (1973) 600.
3 F. L. W. Van Roosmalen, *Rec. Trav. Chim.*, 53 (1934) 359.
4 J. I. G. Cadogan, *J. Chem. Soc.*, (1962) 4257.
5 J. A. Goldstein, P. Hickman, H. Bergman, J. D. McKinney and M. P. Walker, *Chem.-Biol. Interact.*, 17 (1977) 69.
6 J. A. Goldstein, J. R. Hass, P. Linko and D. J. Harvan, *Drug Metab. Dispos.*, 6 (1978) 258.
7 A. Poland and E. Glover, *Mol. Pharmacol.*, 13 (1977) 924.
8 A. Poland, W. F. Greenlee and A. S. Kende, *Ann. N.Y. Acad. Sci.*, 320 (1979) 214.
9 J. D. McKinney, K. Chae, B. N. Gupta, J. A. Moore and J. A. Goldstein, *Toxicol. Appl. Pharmacol.*, 36 (1976) 65.
10 J. C. Cain, *J. Chem. Soc.*, 85 (1904) 7.
11 A. Parkinson, R. Cockerline and S. Safe, *Chem.-Biol. Interact.*, 29 (1980) 277.
12 L. R. Kamops, W. J. Trotter, S. J. Young, A. C. Smith, J. A. G. Roach and S. W. Page, *Bull. Environ. Contam. Toxicol.*, 23 (1979) 51.
13 O. Hutzinger, S. Safe and V. Zitko, in *The Chemistry of PCBs*, CRC Press, Cleveland, 1974, p. 197.
14 S. R. Heller and G. W. A. Milne, in *EPA/NUH Mass Spectal Data Base*, Vol. 3, U.S. Government Printing Office, Washington, DC, 1978, p. 2143.

Journal of Chromatography, 239 (1982) 107–114
Elsevier Scientific Publishing Company, Amsterdam — Printed in The Netherlands

CHROM. 14,518

A SPLIT SYSTEM APPLICABLE AS A GAS CHROMATOGRAPHIC–MASS SPECTROMETRIC INTERFACE AND AS EFFLUENT SPLITTER FOR SPECIFIC GAS CHROMATOGRAPHIC DETECTORS

E. WETZEL, Th. KUSTER* and H.-Ch. CURTIUS
Division of Clinical Chemistry, Department of Pediatrics, University of Zurich, Steinwiesstrasse 75, CH-8032 Zurich (Switzerland)

SUMMARY

An interface is described which allows the open split mode and direct coupling operation to be used. The transfer line consists of a fused silica tube which leads from the end of the column to the mass spectrometer. This device is suitable for various applications in gas chromatography alone and in gas chromatography–mass spectrometry work. The advantages are (1) the possibility of suppressing unwanted peaks, such as those due to solvents and bulk impurities; (2) dead volume-free connections through a transfer line which does not show any active sites; (3) cheap and easy to replace; (4) atmospheric pressure at the column end, so that chromatograms are exactly comparable with previous runs; and (5) easy change of columns without affecting the ion source conditions or flushing and activating the transfer line with air. Examples of applications are given for pterins and steroids.

INTRODUCTION

Since the introduction of capillary columns into gas chromatography–mass spectrometry (GC–MS), various types of coupling devices have been constructed in order to retain the excellent separation characteristics of these columns. Nowadays, the most widely used interfaces are classified into two types: (i) direct connection of the GC column to the MS system, and (ii) open split coupling.

Direct coupling, first described by Ten Noever de Brauw and Brunnée[1] and Henneberg and Schomburg[2], has the advantage of a 100% yield, lack of dead volumes and, therefore, no reduction of the resolving power; on the other hand, the vacuum at the end of the column may affect retention times. The main disadvantage arises from the fact that all of the eluate reaches the ion source. In trace analysis, especially with on-column injection, amounts of up to 5 μl are applied to the column and the solvent and bulk impurities such as derivatizing reagents contaminate the ion source and can diminish the sensitivity severely.

These difficulties can be circumvented by the use of an open split connection, introduced by Henneberg *et al.*[3]. The features of such a device are as follows. As the end of the column is at atmospheric pressure, the separation characteristics (resolving

0021-9673/82/0000–0000/$02.75

power, retention times, flow through the column) are not affected and the chromatograms are easily comparable with chromatograms obtained with flame-ionization detection (FID). The possibility of using the split device allows the cut-off of unwanted peaks, conditioning of the column without contaminating the ion source with column bleed and rapid changing of columns without flushing the system with air so that oxygen cannot activate the transfer line.

Concerning the material of the transfer line, four types can be used: platinum[3–6], glass-lined steel tubes[7,8], glass[9–13] and flexible quartz capillaries[14].

Platinum capillaries exhibit good mechanical stability, but there is no conformity of the catalytic effects of this material. Grob[15] showed this metal to be responsible for various problems arising in the analysis of some critical classes of substances, whereas Etzweiler[6] could not detect such phenomena. We ourselves would agree with Grob[15], as we had severe problems when measuring hawkinsin[16] and we were not able to determine pterins in amounts below 20 ng*.

Glass-lined tubes are mechanically unproblematical; their drawback arises from the fact that the amount of metal ions in the glass is high, and they cannot be deactivated efficiently. Also, it is not possible to check their condition optically.

Of increasing importance are glass transfer lines. If they consist of the same type of glass as the capillary column and are deactivated in the same way[18], they give excellent results[11]. One must, however, have some expertise when handling them.

The introduction of fused silica capillaries offers some attractive features for connecting a GC to an MS system: flexibility, good mechanical properties, inactivity and cheapness[14].

Our demands for a GC–MS interface which led to a do-it-yourself type of system may be summarized as follows:

(1) The separation characteristics of the capillary column must be fully retained (dead volume-free connection and homogeneous heating).

(2) Substance losses due to catalytic decomposition of labile compounds and adsorption should be minimal (chemically inert material, no contact sites with metal parts).

(3) Possibility of cutting off of solvent and parts of the chromatogram by a multi-timer system.

(4) Ease of handling and replacing the transfer line.

(5) Rapid column changing without affecting the ion source conditions.

(6) The device should also be applicable to GC work alone.

EXPERIMENTAL

Instrumentation

Gas chromatographs. A Carlo Erba Fractovap 2101, equipped with an FID, and a Carlo Erba Fractovap 2900, reconstructed for GC–MS, were used. The carrier gas was helium.

* It seems that these problems arise only when analysing special and critical substances and are not observed when testing the material with alkanes. For a detailed study concerning the adsorption of pterins, see Grob *et al.*[17].

Transfer line. A 300 × 0.12 (I.D.) × 0.24 mm (O.D.) fused silica tube was used.

Coupling capillary. 20 × 0.12 (I.D.) × 0.24 mm (O.D.) fused silica capillaries were obtained from ICT-Handelsgesellschaft (Frankfurt, G.F.R.). Graphpack high-temperature connections for glass and fused silica capillaries were supplied by: Fa. Gerstel (Mülheim/Ruhr, G.F.R.).

Pressure controllers. A precision micro pressure controller, type ND, was obtained from Siemens (Karlsruhe, G.F.R.).

Mass spectrometer. A micromass 16-F instrument with an electron energy of 40 eV (nominal) and an ion source temperature of 220°C was used.

Interface

Construction. The principle of the interface is shown in Fig. 1. The GC-column (14) is connected to the transfer line (1) via the coupling capillary (7), both consisting of fused silica. As there was no coupling capillary available with dimensions suitable for positioning it in the transfer line (1), we used a "guiding tube" (6) to bring both capillaries as near as possible together. For splitting purposes, we adapted the principle introduced by Deans[19]. Further constructional details are given elsewhere[20].

Direct coupling mode. The outlet C in Fig. 1 is closed. Two streams of helium, through A and B (flow-rate 0.1–0.2 ml/min each), guide the eluate from the GC column directly into the transfer line (1). This mode corresponds to a fixed connection, as for instance with a platinum capillary. Therefore, the pressure at the end of the GC column is a function of the flow through the column. The flow of scavenger gas through A and B allows the system to be dead volume-free.

Open split coupling mode. The outlet C is now open and at atmospheric pres-

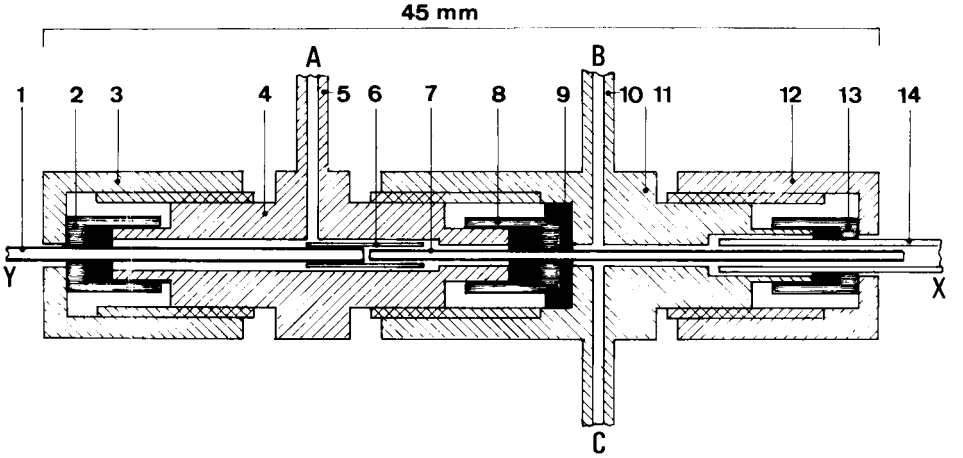

Fig. 1. Schematic diagram of the interface system. 1 = Transfer line (fused silica), I.D. 0.12 mm, O.D. 0.24 mm; 2, 8, 13 = metal sleeves and graphite packings; 3, 12 = nuts; 4, 11 = stainless-steel blocks; 6 = guiding tube (fused silica), I.D. 0.32 mm, O.D. 0.5 mm; 7 = coupling capillary (fused silica), I.D. 0.12 mm, O.D. 0.24 mm; 9 = graphite vespel seal; 5, 10 = stainless-steel tubes, I.D. 0.5 mm, O.D. 1.6 mm; 14 = gas chromatographic column; A = scavenger gas (helium) inlet; B = scavenger gas (helium) inlet; C = scavenger gas (helium) outlet; C = scavenger gas (helium) outlet; Y = to mass spectrometer or detector; X = GC column.

sure. At A, there is a flow-rate of 0.1–0.2 ml/min. In order to prevent air entering through C, the pressure at B is higher (0.5 ml/min). The result is atmospheric pressure at the column end, independent of the flow through the column, which varies when working with a temperature programme. Hence retention times obtained are identical with those obtained with a GC detector.

Cut mode. In instances where unwanted peaks have to be suppressed, C is open and the flow at A is increased to 3–4 ml/min. There is now a stream of helium opposite to the flow from the GC column (flow from Y to X *versus* flow from X to Y). Therefore, the whole eluate is split off through outlet C and does not reach the transfer line and the mass spectrometer.

RESULTS

To test the performance of the interface, we used the Grob test mixture[21]. A comparison of chromatograms obtained with an FID and total ion current (TIC) is shown in Figs. 2 and 3. The separation characteristics of the capillary column are fully retained and no peak broadening or tailing can be seen. The differences in the relative intensities of the peaks should not be overestimated, because the various substances show different responses with an FID and an electron impact detector. The good

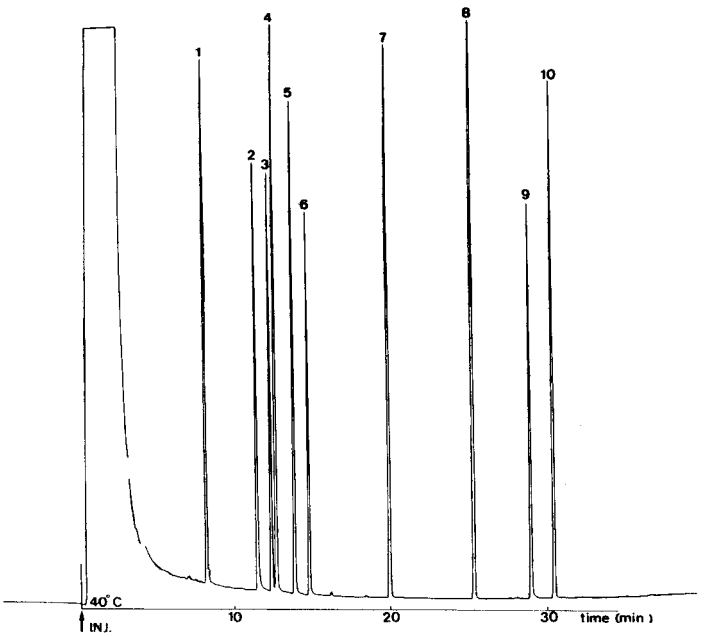

Fig. 2. Gas chromatogram (flame-ionization detection) of the Grob test mixture[21] consisting of (1) decane (5.7 ng), (2) 1-octanol (7.1 ng), (3) 2,6-dimethylphenol (6.4 ng), (4) nonanal (8.0 ng), (5) undecane (5.7 ng), (6) 2,6-dimethylaniline (6.4 ng), (7) C_{10}-acid methyl ester (8.5 ng), (8) C_{11}-acid methyl ester (8.3 ng), (9) dicyclohexylamine (6.3 ng) and (10) C_{12}-acid methyl ester (8.0 ng) in hexane. (the peak for 2,3-butanediol elutes with the solvent and is therefore not visible; 2-ethylhexanoic acid was not added to the mixture). Column, 20 m × 0.3 mm, OV-1; carrier gas, helium, 1.2 bar; Temperature programme, from 40°C (2 min isothermal) to 140°C at 2°C/min.

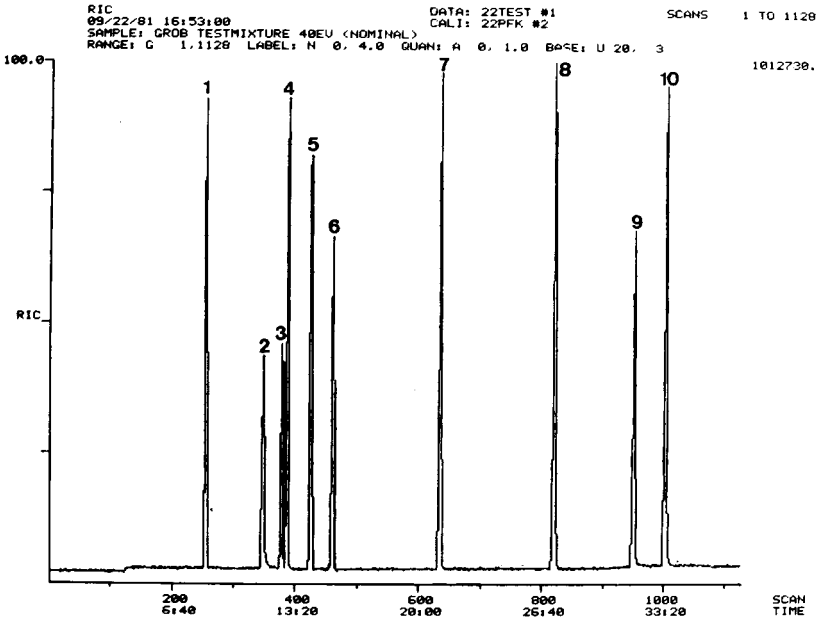

Fig. 3. Total ion current chromatogram of the Grob test mixture[21]. For peak identification and conditions, see Fig. 2.

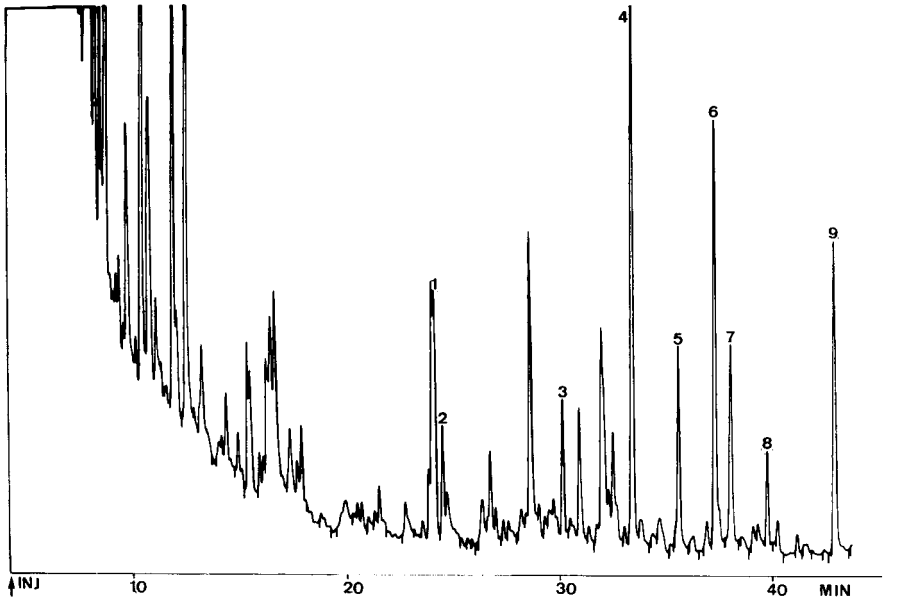

Fig. 4. Chromatogram (FID) of a urine steroid fraction. Peaks: 1 = androsterone (3α-hydroxy-5α-androstane-17-one); 2 = etiocholanolone (3α-hydroxy-5β-androstane-17-one); 3 = pregnanediol (3α,20α-dihydroxy-5β-pregnane); 4 = pregnanetriol (3α,17α,20α-trihydroxy-5β-pregnane); 5 = pregnanetriolone (3α,17α,20α-trihydroxy-5β-pregnane-11-one); 6 = cholesterin; 7 = tetrahydrocortisone (3α,17α,21-trihydroxy-5β-pregnane-11,20-dione); 8 = cortolone (3α,17α,20α,21-tetrahydroxy-5β-pregnane-11-one); 9 = internal standard (cholesteryl butyrate). Derivatives: Methoxime trimethylsilyl ethers; for details, see ref. 23. Column, 20 m × 0.3 mm, OV-1; carrier gas, helium, 0.8 bar; temperature programme, 10 min at 160°C, then increased to 260°C at 3°C/min.

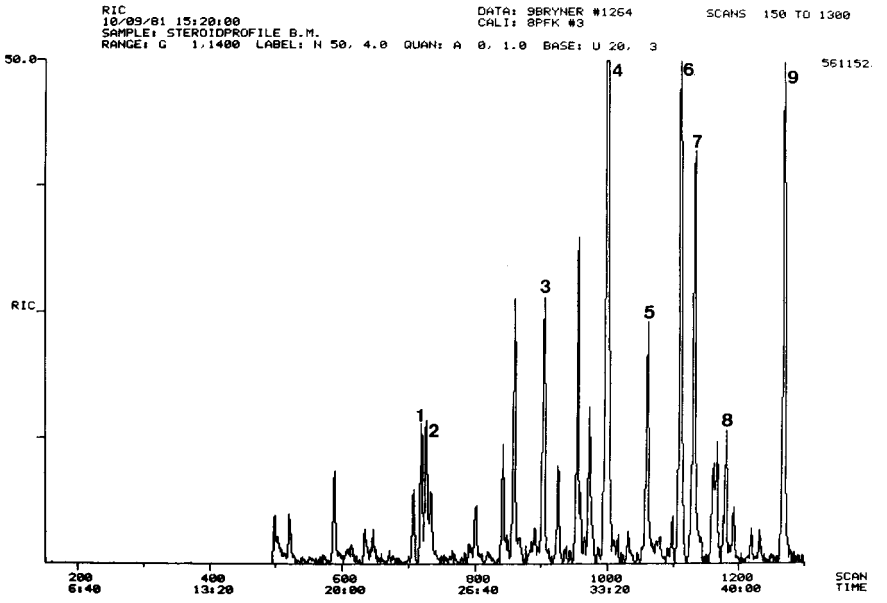

Fig. 5. Total ion current chromatogram of the same urine fraction as in Fig. 4. During the first 17 min the interface splitter was open, in order to cut off the unwanted part of the chromatogram. For peak identification and conditions, see Fig. 4.

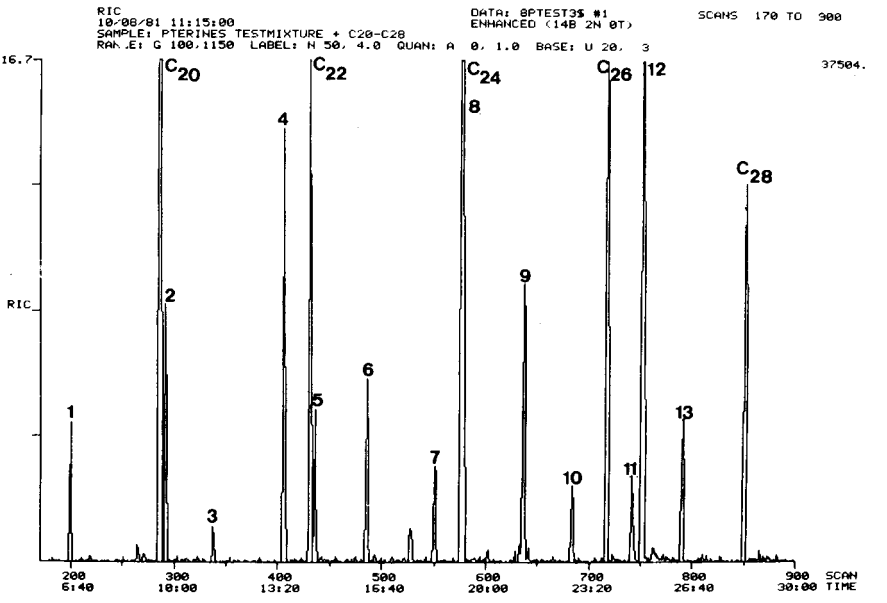

Fig. 6. Total ion current chromatogram of a pterin test mixture. Peaks: 1 = lumazine; 2 = pterin; 3 = 6-methylpterin; 4 = isoxanthopterin; 5 = xanthopterin; 6 = leukopterin; 7 = 6-hydroxymethylpterin; 8 = deoxysepiapterin; 9 = biopterin; 10 = sepiapterin; 11 = monapterin; 12 = neopterin; 13 = 3-hydroxysepiapterin. C_{20}–C_{28} alkanes. Derivatives: Trimethylsilyl ethers; for details see ref. 22. Column: 20 m × 0.3 mm, SE52; carrier gas, helium, 1.4 bar; temperature programme, from 150 to 270°C at 3°C/min.

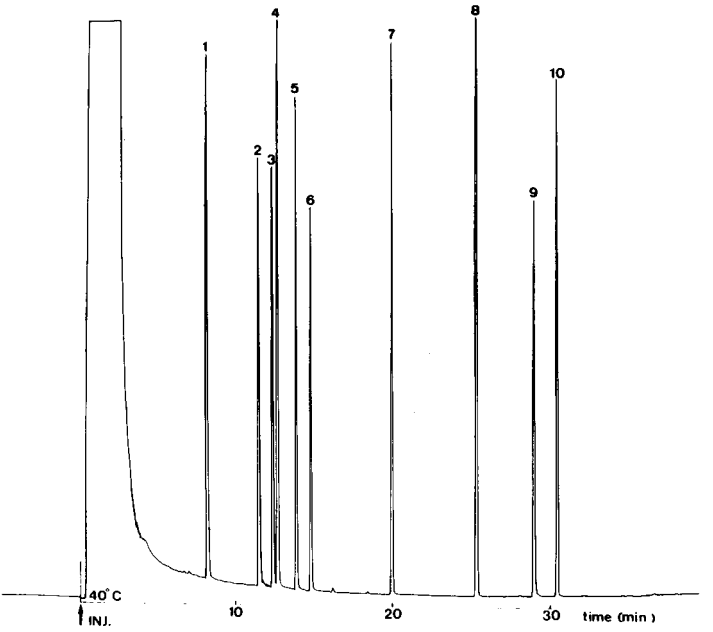

Fig. 7. Chromatogram (FID) of the Grob text mixture. Interface mode (A).

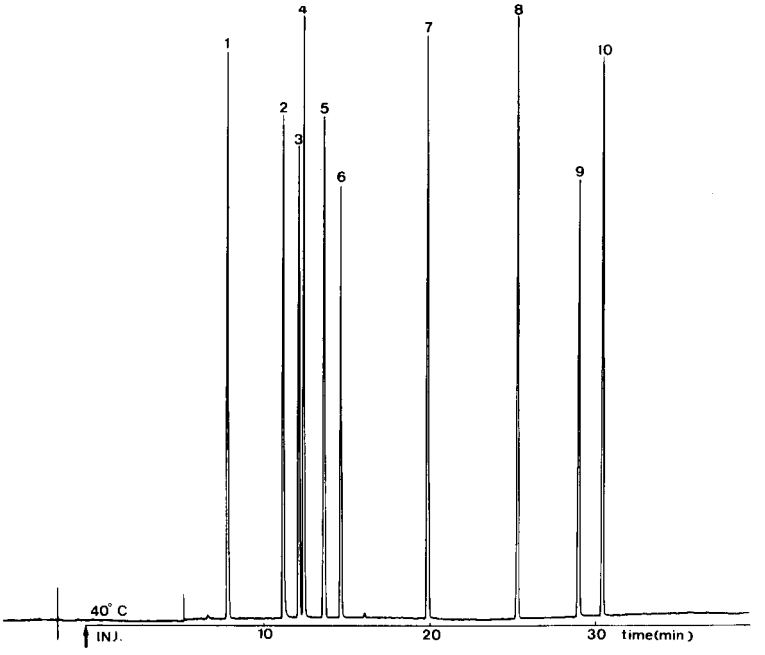

Fig. 8. Chromatogram (FID) of the Grob test mixture. Interface mode (C) to cut off the solvent peak. Conditions as in Fig. 2.

stability of the baseline arises from the constant carrier gas flow-rate into the ion source, independent of the flow through the column. The comparison of the two chromatograms also confirms the absence of dead volumes in the system, as we found equal separation numbers under GC and GC–MS conditions.

Fig. 4 shows a steroid profile obtained during a routine run in our laboratory. The first part of the chromatogram up to 20 min is not relevant to the analysis, as it consists mainly of derivatizing agents, fatty acids and other impurities. When confirming anomalous metabolic patterns with GC–MS, we cut off this part with the splitting facilities (mode C) of the interface and the result is shown in Fig. 5, where only the interesting steroid peaks are visible.

Fig. 6 shows the chromatogram of a pterin test mixture[22]. The amount of each of the substances lies in the range 5–10 ng, levels which we were not able to analyse with the platinum or glass-lined tube transfer line. Fig. 6 confirms the results obtained with the test mixture, as there is no loss of sensitivity or resolving power due to adsorption or catalytic decomposition.

Figs. 7 and 8 show how this interface can be applied to GC work alone. When performing analyses at trace levels, the detector is very sensitive towards contamination (this holds especially for an electron-capture detector). In such instances, it is highly desirable to split off the solvent and/or impurities originating from the derivatizing agent. This is possible when operating the system in the cut-off mode (C). Fig. 8 shows how the solvent peak in the Grob test mixture is suppressed totally. In a similar way, parts of the chromatogram can be split off when the desired time intervals are set by a multi-timer system.

REFERENCES

1 M. C. ten Noever de Brauw and C. Brunnée, *Z. Anal. Chem.*, 229 (1967) 321.
2 D. Henneberg and G. Schomburg, *Z. Anal. Chem.*, 221 (1964) 55.
3 D. Henneberg, U. Henrichs and G. Schomburg, *Chromatographia*, 8 (1975) 449.
4 K. Grob and H. Jaeggi, *Anal. Chem.*, 45 (1973) 1788.
5 N. Neuner-Jehle, F. Etzweiler and G. Zarske, *Chromatographia*, 6 (1973) 211.
6 F. Etzweiler, *J. Chromatogr.*, 167 (1978) 133.
7 G. A. Thome and G. W. Young, *Anal. Chem.*, 48 (1976) 1423.
8 U. Rapp, U. Schröder, S. Meier and H. Elmenhorst, *Chromatographia*, 8 (1975) 474.
9 H. W. Dürbeck, I. Büker and W. Leymann, *Chromatographia*, 11 (1978) 295.
10 H.-J. Stan and B. Abraham, *Anal. Chem.*, 50 (1978) 2161.
11 P. P. Schmid, M. D. Müller and W. Simon, *J. High Resolut. Chromatogr. Chromatogr. Commun.*, 2 (1979) 31.
12 W. Blum and W. J. Richter, *J. Chromatogr.*, 132 (1977) 249.
13 D. Henneberg, U. Henrichs, H. Husmann and G. Schomburg, *J. Chromatogr.*, 167 (1978) 139.
14 W. D. Koller and G. Tressl, *J. High Resolut. Chromatogr. Chromatogr. Commun.*, 3 (1980) 359.
15 K. Grob, *Chromatographia*, 9 (1976) 509.
16 A. Niederwieser, A. Matasović, F. Neuheiser and E. Wetzel, *J. Chromatogr.*, 146 (1978) 207.
17 K. Grob, G. Grob, B. Brechbühler and P. Pichler, *J. Chromatogr.*, 205 (1981) 1.
18 K. Grob, G. Grob and K. Grob, Jr., *J. High Resolut. Chromatogr. Chromatogr. Commun.*, 2 (1979) 31.
19 D. R. Deans, *Chromatographia*, 1 (1968) 18.
20 E. Wetzel and Th. Kuster, *J. High Resolut. Chromatogr. Chromatogr. Commun.*, submitted for publication.
21 K. Grob Jr., G. Grob and K. Grob, *J. Chromatogr.*, 156 (1978) 1.
22 A. Niederwieser and Th. Kuster, in preparation.
23 Th. Kuster, M. Zachmann and B. Zagalak, in press.

Journal of Chromatography, 239 (1982) 115–126
Elsevier Scientific Publishing Company, Amsterdam — Printed in The Netherlands

CHROM. 14,556

DETECTION OF CARBON MONOXIDE AT AMBIENT LEVELS WITH AN N_2O-SENSITIZED ELECTRON-CAPTURE DETECTOR

PAUL D. GOLDAN* and FRED C. FEHSENFELD*
Aeronomy Laboratory, National Oceanic and Atmospheric Administration, Boulder, CO 80303 (U.S.A.)
and
MICHAEL P. PHILLIPS**
Aeronomy Laboratory, National Oceanic and Atmospheric Administration, Boulder, CO 80303, and Department of Chemistry, University of Colorado and Cooperative Institute for Research in the Environmental Sciences, University of Colorado/NOAA, Boulder, CO 80309 (U.S.A.)

SUMMARY

It is observed that the response of the electron-capture detector (ECD) for carbon monoxide can be dramatically increased by the addition of N_2O to the nitrogen carrier gas. In this way a detection limit for carbon monoxide in air of $3.4 \cdot 10^{11}$ molecules (16 pg) has been achieved. This detection limit compares favorably with that obtained using other state-of-the-art CO detectors. A mechanism to explain the observed enhancement of the N_2O-doped ECD is proposed. The implication of the present results for the N_2O-doping technique and the application of this method to detection of CO in the atmosphere are discussed.

INTRODUCTION

Carbon monoxide is produced in the earth's atmosphere as a byproduct of the oxidation of hydrocarbons from both natural and anthropogenic sources. In turn, CO is an active participant in the chemistry of atmospheric minor constituents. The oxidation of CO by OH is an important reaction in the atmospheric odd-hydrogen chemistry[1] and initiates a sequence of reactions, which in the presence of NO provides a mechanism for ozone production in "clean" air[2]. Since the concentration of carbon monoxide in the atmosphere reflects the reaction sequences which produce and destroy it, considerable effort has been expended to measure CO as a function of time, latitude and altitude[3–6].

The instruments developed for measurement of CO in air may be generally classified as colorimetric, mass spectrometric (MS), infrared (IR) absorption and gas chromatographic (GC) techniques. The colorimetric techniques which have been described[7,8] are suitable only for CO mole fractions of several ppm or greater and are thus inapplicable to background atmospheric sampling without sample enrichment. The use of MS for the detection of CO in whole air samples is severely hampered by

* Fellow of the Cooperative Institute for Research in the Environmental Sciences (CIRES), University of Colorado/NOAA, Boulder, CO 80309, U.S.A.
** Present address: Rocky Mountain Analytical Laboratory, Arvada, CO, U.S.A.

the extremely small mass difference between CO and N_2 (0.01123 a.m.u.). Ions of these two species can be distinguished only by high-resolution MS.

Because of these difficulties, most of the measurements to date have been made using optical absorption and GC techniques. Typical commercially available instruments for the measurement of CO in air, relying on either dispersive IR absorption or non-dispersive IR photometry, have sensitivities yielding detection limits of approximately 10 ppm (v/v) and 0.5 ppm (v/v), respectively. Both of these methods suffer from interference from H_2O and CO_2. Long path IR absorption spectrometry using laser sources and an absorption path length of some 25 m has significantly lowered these detection limits and demonstrated a capability of measuring CO at ambient background concentrations (0.05–0.5 ppm, v/v) under favorable conditions[9]. This method still suffers from interference from H_2O, CO_2 and O_3 limiting its usefulness. Efforts to reduce the effects of such interferences have led to the development of a non-dispersive IR gas filter correlation instrument[10]. The noise equivalent CO mixing ratio for this instrument is approximately 20 ppb (v/v)*. This reasonably low detection limit, wide dynamic range (up to 100 ppm, v/v) and rapid response make it suitable for microscale studies where rapid variations are important, but its relative complexity makes it unattractive as a general monitoring instrument.

A completely different spectroscopic technique for the measurement of CO takes advantage of the chemical reaction between CO and HgO to produce CO_2 and Hg in the gas phase. The resulting mercury vapor is measured by absorption of resonance radiation at 2537 Å provided by a mercury lamp[11–13]. Although providing very low detection limits for CO (some 2–3 ppb, v/v), this technique is also sensitive to other reducing gases such as H_2, SO_2 and olefins and aldehydes that also reduce hot HgO and can cause erroneously high CO readings if not removed prior to analysis.

Since GC columns are readily available which separate CO from other potentially interfering species in atmospheric samples, attention has been drawn to the development of sensitive detectors to be used in conjunction with these columns. Currently the most widely used gas chromatographic CO detector is the flame ionization detector (FID), which measures the CH_4 produced by the catalytic conversion of CO[14–18]. Using a molecular sieve column to separate the CO in an air sample and under ideal laboratory conditions, the amount of CO required to produce a signal-to-noise ratio of 2 in the FID is some $4 \cdot 10^{11}$ molecules (18 pg), corresponding to a mole fraction of 15 ppb for a 1 standard cm^3 air sample. Helium ionization detectors that utilize the energetic, long-lived excited states of atomic and molecular helium to produce detectable secondary ionization in analyte gases of lower ionization potential[19] have been successfully used for the detection of atmospheric CO (ref. 3). Unfortunately this detector is also sensitive to N_2, and the CO appears as a small shoulder on a large tailing N_2 peak, making quantitation difficult at ambient CO levels in air[20].

We previously reported that the sensitivity of an electron-capture detector (ECD) to non-electron attaching compounds and to compounds, such as vinyl chloride, that attach electrons only weakly can be enhanced by the addition of N_2O to the carrier gas stream of a gas chromatograph[21–23]. In the present study we find that the detection limit for carbon monoxide in air is $3.4 \cdot 10^{11}$ molecules (16 pg) using this

* Throughout this article, the American billion (10^9) is meant.

enhancement technique. This detection limit corresponds to a CO mole fraction of 13 ppb for a 1 standard cm^3 air sample and is achieved with no sample enrichment. This detection limit is comparable to, or better than, that achieved under optimal conditions using the detection methods mentioned above. The combination of sensitivity, simplicity and freedom from interfering species using the GC technique makes it an attractive option for the measurement of carbon monoxide in clean air.

EXPERIMENTAL

The gas chromatograph used in this study was designed and built in collaboration with Valco Instruments (Houston, TX, U.S.A.). Entirely contained in a 60 × 40 × 20 cm aluminum "suitcase", it is equipped with a cylindrical ECD with a 10-mCi ^{63}Ni foil lining the 0.63-cm^3 detector volume. Sample inlet and current collector are axially symmetric within the detector, which is operated at 350°C in a fixed frequency variable current mode. The entire system plumbing: multiport gas injection valve, columns, oven and detector, are housed in a sealed chamber which is flushed with the nitrogen carrier gas so that gas composition, temperature and pressure surrounding these elements can be controlled[24].

Two columns, both packed in 1/8-in. stainless-steel tubing, are used with a nitrogen carrier flow of approximately 40 cm^3/min. The first, a precut column, is 2.4 m long, packed with Porapak Q (100–120 mesh), and operated at the ambient box temperature of approximately 55°C. The second, analytical, column is 2.8 m long, packed with molecular sieve 5A (100–120 mesh), and operated at 80°C. A schematic diagram of the plumbing arrangement is shown in Fig. 1. When the valve is in the load position, sample is introduced into the sample loop by a flush and fill technique. When the valve is rotated to the inject position, as shown in Fig. 1, the sample passes first through the Porapak Q column where relatively heavy chlorinated species to which the ECD is extremely sensitive such as CF_2Cl_2, $CFCl_3$, C_2HCl_3 and CCl_4 are retarded while the H_2, O_2, CH_4 and CO contained in the sample pass quickly into the molecular sieve column. As soon as these latter species have passed into the molecular sieve column (approximately 2 min after injection), the valve is returned to the sample

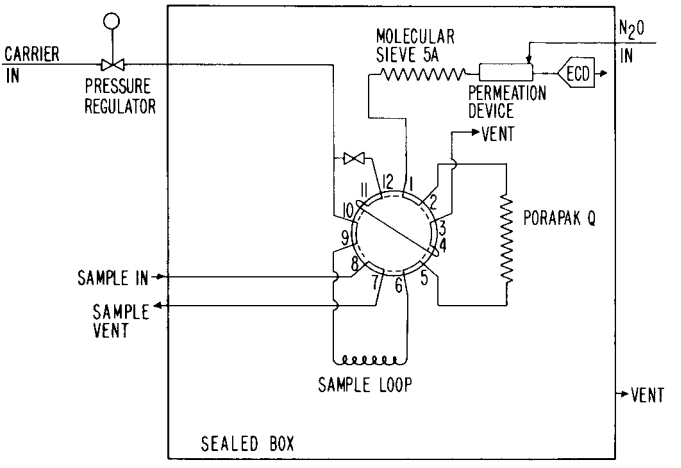

Fig. 1. Schematic diagram of gas chromatograph gas handling system.

load position allowing the H_2, O_2, CH_4 and CO to be separated on the analytical column while the remaining air sample components are dumped from the precut column. A restrictor supplants the precut column when the valve is in the load position so that the carrier gas flow through the detector is independent of the valve position, thus avoiding switching transients. Dumping the unwanted species from the precut column allows repetitive sampling on a 15-min basis.

Nitrous oxide at a mole fraction of approximately 30 ppm (v/v) is introduced into the carrier gas stream between the analytical column and detector by means of a permeation device which has been previously described[23]. The N_2O source used is a 250-cm^3 stainless-steel cannister which was evacuated and filled with "electronic grade" N_2O to a pressure of approximately 400 kPa. The N_2O consumption is quite small, being typically 300 standard cm^3 per year for continuous operation.

In order to remove CO and other impurities from the commercial grade N_2 used as carrier gas before it enters the chromatograph, it is passed through a Hopcalite (Mine Safety Appliances Company, Pittsburgh, PA, U.S.A.) trap followed by a molecular sieve 13X trap, both of which are used at room temperature. The Hopcalite serves to oxidize CO to CO_2 which is subsequently removed along with H_2O, hydrocarbons and other impurities by the molecular sieve. Both traps are activated by heating for 10–12 h; the Hopcalite to 150–200°C and the molecular sieve to 300–350°C, with a nitrogen flow of 40–60 standard cm^3/min.

Carbon monoxide standards were prepared by static dilution with "zero air"* of a previously calibrated mixture containing a CO mole fraction of 1.6 ppm (v/v) in "zero air". The diluted standards at a CO mole fraction of approximately 270 ppb (v/v) were then checked against the 1.6 ppm (v/v) standard using the flame ionization technique described earlier. All sensitivities and detection limits quoted are with respect to these diluted secondary standards.

RESULTS

A chromatogram of a whole air sample obtained using the sealed chromatograph with N_2O doping in the carrier gas is shown in Fig. 2. Because of the precut column configuration described in the Experimental section, the chromatogram consists of only four peaks, *i.e.*, those due to H_2, O_2, CH_4 and CO. The sample size is 2.2 standard cm^3 and the concentration of the components are 20% (v/v) O_2, 0.6 ppm (v/v) H_2, 1.67 ppm (v/v) CH_4 and 390 ppb (v/v) CO. All of these compounds are easily detected at these levels using this technique. However, with no N_2O in the carrier gas, only the O_2 is detectable in this system and the CO detection limit increases to greater than 10^2 μg per sample.

The signal-to-noise ratio of the N_2O doped ECD for CO is essentially independent of the N_2O mole fraction between the doping levels of 16 and 70 ppm (v/v), so that the N_2O concentration need only be set at some convenient level in this range. Slow reduction of the N_2O level due to decreasing pressure in the N_2O cannister at a rate of approximately 3 kPa per month has little effect upon the system performance. The detector response to CO as a function of detector temperature is similar to that

* "Zero air" refers to a synthetic mixture of 80% N_2, 20% O_2 and no detectable levels of any other gas of consequence in the present study.

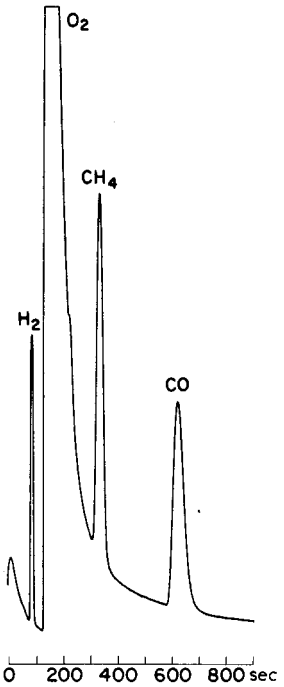

Fig. 2. Chromatogram of a 2.2 standard cm^3 air sample with pre-cut obtained with the N_2O-sensitized ECD.

reported for several other gases[21–23]. That is, the response is greatest at the maximum operating temperature of the detector, 350°C, and decreases by approximately a factor of 10 as the detector temperature is lowered to 200°C.

The response of the N_2O-doped ECD to CO has been found to be linear within the 2% precision of the measurement from the CO detection limit of $3.4 \cdot 10^{11}$ molecules (16 pg) per sample up to $1.7 \cdot 10^{13}$ molecules (790 pg) per sample. Departures from linearity do not exceed 10% up to $5.3 \cdot 10^{13}$ molecules per sample, corresponding to a mole fraction of 2 ppm for a 1 standard cm^3 sample. Quantitation outside this range can be accomplished by the use of appropriate calibration data.

DISCUSSION

The sensitivity of the N_2O-enhanced ECD to CO can be explained in the following way. In the ECD, free electrons are in an N_2O-induced reactive steady state with O^- through the reactions

$$e + N_2O \xrightarrow{k_1} O^- + N_2 \quad (1)$$

$$O^- + N_2O \xrightarrow{k_2} NO^- + NO \quad (2)$$

$$NO^- + M \xrightarrow{k_3} NO + M + e \quad (3)$$

where M is any collision partner and k_1, k_2 and k_3 are the reaction rate constants for the corresponding reactions. This mechanism is discussed in detail in our previous publications[21–23]. Any compound that reacts with O^- to form a stable negative ion will interrupt this reaction cycle causing a reduction in the electron density and thus a detector response.

According to this scheme, however, the N_2O-sensitized ECD should have no intrinsic sensitivity to CO since CO does not directly react with O^- to form a stable negative ion. Rather, it seems that the observed response results from the oxidation of CO to CO_2 within the ECD with subsequent reaction of CO_2 with O^-[21]. Although there are several possible mechanisms for the oxidation of CO to CO_2 in or near the ECD, it seems most likely that this oxidation takes place on the hot detector walls. Strong support for this speculation is provided by recent findings that an N_2O-oxidized polycrystalline platinum surface at about 350°C rapidly converts CO to CO_2[25]. It seems most likely that the gold, nickel and stainless steel surfaces within the ECD at 350°C in the presence of N_2O will effectively oxidize CO, *i.e.*

$$CO + N_2O/_{wall} \xrightarrow{\tau_w} CO_2 + N_2/_{wall} \tag{4}$$

with τ_w being the associated time constant. Further support for this contention is gained from the observations that although the CO sensitivity of an N_2O-doped ECD may decrease after long use or after injection of "dirty" samples, it can be restored by passing H_2 for several hours through the detector while it is kept at 350°C. Presumably the hydrogen strips impurities which inhibit reaction 4 from the internal surfaces of the detector. Following reaction 4, the CO_2 reacts with O^- causing the ECD response:

$$O^- + CO_2 + M \xrightarrow{k_5} CO_3^- + M \tag{5}$$

The rate equations which describe eqns. 1–5 are

$$\partial[e]/\partial t = S - k_1\,[e]\,[N_2O] + k_3\,[NO^-]\,[N_2] - L\,[e] \tag{6}$$

$$\partial[O^-]/\partial t = k_1\,[e]\,[N_2O] - k_2\,[O^-]\,[N_2O] - k_5\,[O^-]\,[CO_2]\,[N_2] \tag{7}$$

$$\partial[NO^-]/\partial t = k_2\,[O^-]\,[N_2O] - k_3\,[NO^-]\,[N_2] \tag{8}$$

$$\partial[CO_2]/\partial t = [CO]/\tau_w - (k_5\,[O^-]\,[N_2] + 1/\tau_R)\,[CO_2] \tag{9}$$

$$\partial[CO]/\partial t = Q_{CO}\,(t)/V_D - (\tau_R^{-1} + \tau_w^{-1})\,[CO] \tag{10}$$

where S is the ionization source rate associated with the radioactive source lining the detector walls (electron–ion pairs per $cm^3 \cdot sec$), L is the net electron loss due to diffusion, recombination with positive ions, attachment to impurities in the carrier gas, ventilation, etc. which are not explicitly stated in eqn. 6, and $[N_2]$ as the most likely collision partner has been substituted for [M]. $Q_{CO}(t)$ is the time dependent

influx rate of CO molecules (molecules per sec), V_D is the detector volume, τ_R is the mean residence time of the sample within the detector and τ_w has been defined in eqn. 4.

For the column and operating conditions specified in the Experimental section, and listed for convenience in Table I, the CO peak is roughly Gaussian in shape with a width at half maximum of approximately 30 sec, a time long compared to $\tau_R \approx 0.7$ sec. Thus, during the passage of the CO peak through the detector, the chemistry approaches a steady state and the remainder of the discussion deals with the steady state solutions to eqns. 6–10 with the pertinent reaction rate constants listed in Table II.

TABLE I

ELECTRON-CAPTURE DETECTOR PARAMETERS AND SYMBOLS USED IN THE TEXT

Detector internal volume, V_D	0.65 cm^3
Carrier gas flow, Q_{N_2}	$\approx$40 standard cm^3/min
Pressure in the detector (ambient pressure at 1600 m), P	$\approx$0.8 atm
Gas residence time in the detector, $\tau_R = V_D P/Q_{N_2}$	$\approx$0.7 sec
^{63}Ni foil activity (67·keV β-rays), R	10 mCi = $3.7 \cdot 10^8$ sec^{-1}
Foil area, A_f	2.55 cm^2
Ionizing flux from foil, $j = R/4\pi A_f$	$1.2 \cdot 10^7$ cm^{-2} sec^{-1} steradian^{-1}
Effective ionizing flux density, $J = 3\pi j$*	$1 \cdot 10^8$ cm^{-2} sec^{-1}
Ionization rate per unit path length (67 keV β-rays in 625 Torr N_2), γ_β	$5 \cdot 10^2$ electron–ion pairs per cm^3[26]
Volume ionization rate, $S = J\gamma_\beta$	$5 \cdot 10^{10}$ electron–ion pairs per $cm^3 \cdot$ sec
Detector temperature, T_D	350°C
Detector pulse repetition rate, f	10^3 Hz
In the absence of analyte in the detector (see text)	
Detector current, I_0	$1 \cdot 10^{-9}$ A
Electron density, $[e]_0 = I_0 (qfV_D)^{-1}$	$\approx 10^7$ cm^{-3}
Electron loss rate, $L = S([e]_0)^{-1}$	$\approx 5 \cdot 10^3$ sec^{-1}
Atomic oxygen negative ion density, $[O^-]_0$	$\approx 1.5 \cdot 10^6$ cm^{-3}

* Because of the short cylinder geometry, a typical point inside the detector is exposed to the ionizing radiation over only 3π steradians.

TABLE II

REACTION RATE CONSTANTS AT 350°C

Reaction	*Rate constant*	*Ref.*
1	$k_1 = 3.3 \cdot 10^{-11}$ cm^3/sec	27, 28
2	$k_2 = 2.2 \cdot 10^{-10}$ cm^3/sec	29, 30
3	$k_3 \approx 10^{-11}$ cm^3/sec*	
5	$k_5 = 3 \cdot 10^{-28}$ cm^6/sec	32

* Estimated from results in ref. 31.

In the absence of CO,

$$[e] = [e]_0 = S/L \tag{11}$$

and

$$[O^-]_0 = k_1[e]_0/k_2 \tag{12}$$

At 350°C $k_1/k_2 \approx 0.15$[21]. For the pulsed ECD, assuming all the electrons within the detector are collected during each pulse, the detector standing current is

$$I_0 = qf \int [e]_0 dV \approx qf [e]_0 V_D \tag{13}$$

where q is the charge on the electron and f is the pulse frequency of the detector. The approximate values calculated for $[e]_0$, $[O^-]_0$, S and L in the absence of CO for typical operating conditions are listed in Table I.

In the N_2O-enhanced ECD, we observe a sensitivity for CO approximately equal to that observed for CO_2. To be consistent with our understanding of the enhancement process this implies that a majority of the CO is converted to CO_2 in or before the CO reaches the detector. Undoubtedly this conversion proceeds most rapidly at the highest temperatures[25] which in the present system is in the electron capture detector. The efficiency required for this conversion process is limited by the residence time $\tau_R \approx 0.7$ sec. This time must suffice for most of the CO to contact the hot walls and for the chemical conversion to be accomplished.

Transport of CO to the detector walls does not represent a limitation as this will occur in a time short compared to τ_R. In cylindrical geometry, the diffusion time constant, τ_D, in the fundamental mode is

$$\tau_D \approx R^2/D_{CO}\,(2.4)^2 \approx 0.036 \text{ sec} \tag{14}$$

where D_{CO} is the diffusion constant for CO in N_2 at atmospheric pressure, R is the cylinder radius and 2.4 is the first zero of $J_0(x)$, the zeroth order Bessel function of the first kind. This represents an upper limit to the actual diffusion time constant since end effects, diffusion to the central electron collector electrode and turbulent mixing in the detector will all contribute to reducing τ_D.

The remaining uncertainty involves the efficiency with which CO is converted to CO_2 on the detector walls. If diffusional transport to the walls is much more rapid than the wall oxidation process, then the CO density will be approximately uniform inside the detector and, according to simple kinetic theory, the loss rate of CO will be given by

$$\frac{\partial[CO]}{\partial t} = \frac{1}{4}\bar{v}\,[CO]\,\gamma A_D/V_D = [CO]/\tau_w^* \tag{15}$$

where $\bar{v}$ is the mean thermal speed of CO, A_D is the surface area involved and γ is the fraction of wall collisions leading to CO oxidation. The time constant, τ_w^*, for the present detector geometry and temperature is:

$$\tau_w^* \approx 10^{-5}/\gamma \tag{16}$$

If $\gamma > 2 \times 10^{-5}$, $\tau_R > \tau_w^* \gg \tau_D$, diffusion is not a significant limitation as stated above and a sizable fraction of the CO introduced into the detector will be converted to CO_2. For comparison, Adlhoch *et al.*[25] found that for a polycrystalline platinum surface at about 350°C, $\gamma \approx 4 \times 10^{-3}$. It is certainly possible that clean metal surfaces within the detector will have oxidation efficiencies at least 1% of that ob-

served for platinum. It should be noted that as γ increases the rate of oxidation at the wall is finally limited by the rate of transport, τ_D, so that the actual wall oxidation time constant τ_w is always greater than or equal to τ_D.

The steady state solution to eqns. 6–10, neglecting τ_w/τ_R and $\tau_R k_5 [O^-] [N_2] \leqslant 0.004$ with respect to 1, and with CO present yield:

$$[CO] = Q_{CO}(t)\,\tau_w/V_D \tag{17}$$

$$[CO_2] = \tau_R [CO]/\tau_w \tag{18}$$

$$[e] = [e]_0 \left\{ 1 + \frac{k_1 k_5 [N_2]\, Q_{CO}(t)\tau_R}{V_D k_2 L \left(1 + \frac{k_5 [N_2]\, Q_{CO}(t)\tau_R}{V_D k_2 [N_2O]} \right)} \right\}^{-1} \tag{19}$$

In the limit as $Q_{CO}(t) \to 0$

$$[e] = [e]_0 \left\{ 1 - \frac{k_1 k_5 [N_2]\, Q_{CO}(t)\,\tau_R}{V_D k_2 L} \right\} \tag{20}$$

and the electron density and therefore the detector current become linearly dependent on $Q_{CO}(t)$, the CO influx rate.

Furthermore, from eqn. 19 and 20 we may calculate the fractional change in current expected from the injection, into the gas chromatograph, of a sample containing a given number of CO molecules. For a Gaussian peak with width parameter σ, the total number of CO molecules passing through the detector is

$$N_{CO} = Q_{CO}(t_0) \int_{-\infty}^{\infty} \exp - [(t - t_0)^2/\sigma^2]\,dt = \sqrt{\pi}\,\sigma\, Q_{CO}(t_0) \tag{21}$$

where t_o is the arrival time of the peak maximum. Substituting this result in eqn. 20 yields at peak maximum:

$$1 - \frac{[e]}{[e]_0} = \frac{k_1 k_5 [N_2]\,\tau_R N_{CO}}{V_D k_2 L \sqrt{\pi}\,\sigma} \tag{22}$$

Numerical values from Table I substituted into eqn. 22 predict that the peak fractional change in electron density, and therefore the fractional change in detector current, should be approximately $3 \times 10^{-15} N_{CO}$ for values of N_{CO} sufficiently small so that eqn. 20 is valid. For $N_{CO} = 1.45 \cdot 10^{13}$ molecules (2 standard cm^3 sample with a CO mole fraction of 270 ppb), eqn. 22 predicts a fractional change in current of 4%. This is to be compared with the experimentally observed value of 4.0%. Although the agreement is obviously fortuitous considering the uncertainties in the ECD parameters, the gas phase reaction rate constants and the approximations used to formulate and solve eqns. 6–10, this agreement supports the correctness of the arguments presented above.

Application and comparison

As may be seen from the chromatogram of the whole air sample shown in Fig. 2, H_2, CH_4 and CO are readily quantitated at clean air levels. It should be mentioned that the simultaneous measurement of atmospheric concentrations of CO, CH_4 and H_2 cannot be achieved with the other detectors currently used for *in situ* atmospheric CO measurement.

Atmospheric mixing ratios of CO are currently being monitored at an atmospheric sampling site west of Boulder that is jointly maintained by the National Oceanic and Atmospheric Administration and the University of Colorado. Located on Niwot Ridge at an altitude of 3050 m (longitude 105° 32′, latitude 40° 30′), the site is usually swept by the prevailing winds which blow from west to east. Under these conditions the concentrations of minor atmospheric constituents represent clean, continental, rural air. Occasionally, "upslope" conditions exist during which winds from the east transport pollution from the Denver metropolitan area to the Niwot Ridge site.

Carbon monoxide mixing ratios found during the onset of such an episode on September 22, 1980 are shown in Fig. 3. The morning was overcast, foggy and calm. At about 1:00 p.m. MST the cloud cover broke and a slight breeze from the southeast developed. By 2:00 p.m. the wind was from the east at 5–10 mph and a strong "upslope" easterly wind condition existed. Fig. 3 clearly shows the increase in CO mole fraction from about 250 ppb (v/v) to more than 400 ppb (v/v) during this period. Concurrent measurements showed that the ozone concentration doubled, increasing from 31 ppb (v/v) to 59 ppb (v/v), during the same period.

Carbon monoxide mixing ratios have been monitored intermittently at this site with the N_2O-sensitized ECD technique since August 2, 1980. From August 2 to September 22 the concentration ranged from 160 to 473 ppb (v/v), with mixing ratios in excess of 300 ppb (v/v) being observed only during the strong "upslope" on September 22. Analysis of these data showed a CH_4 mole fraction of 1.7 ppm (v/v) and an average H_2 mole fraction of 0.6 ppm (v/v).

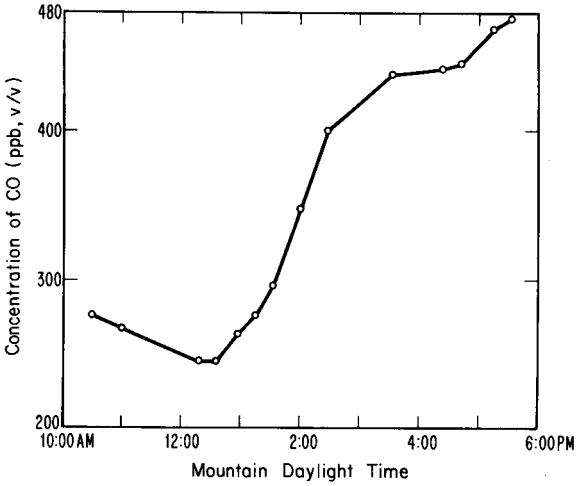

Fig. 3. CO mixing ratio over a 7-h period at Niwot Ridge, Colorado.

During this period the results obtained with the N_2O-sensitized ECD technique were compared with similar measurements made using an FID with catalytic conversion of CO to CH_4 (Baseline Industries, Model 1030A) and an HgO-reduction, resonance-absorption instrument (Trace Analytical Company, Model RDG-1). The N_2O-sensitized ECD achieved approximately equal sensitivity to the HgO-reduction technique and considerably better than the FID. In terms of quantifying atmospheric concentrations of CO (relatively high CO levels in a multicomponent gas mixture), the N_2O-sensitized ECD was as free of interferences, as dependable and somewhat more linear than the other instruments.

The detection limits for CO using FID with catalytic converter, HgO reduction, and helium ionization detection were reported[3] in connection with a measurement program intended to determine vertical profiles of CO, as well as several other trace gases, in the mid-latitude atmosphere. This intercomparison indicated detection limits for helium ionization detectors of 15 ppb (v/v), nickel catalysis-FID of 5 ppb (v/v) and HgO reduction detection of 1 ppb (v/v). Since the sample size used in these measurements was not specified, the quoted detection limits are somewhat nebulous. However, using a 20-cm^3 sample at atmospheric pressure, the N_2O-sensitized ECD configured as it is in the present GC has a detection limit comparable to the HgO reduction detector quoted above.

CONCLUSIONS

The N_2O-sensitized ECD exhibits remarkable sensitivity for carbon monoxide. This sensitivity is explained by the catalytic conversion of CO to CO_2 in the presence of N_2O on the hot detector walls. The effect is stable and reproducible. Although the data reported here were obtained using a specially designed nitrogen purged instrument, comparable results have been obtained using a standard Perkin-Elmer instrument equipped with an ECD. Detectors which have been subjected to "dirty" samples, and occasionally new detectors which have been improperly cleaned, do not exhibit the reported sensitivity to CO, but these may be restored to adequate sensitivity by purging with H_2 at 350°C for several hours.

To our knowledge this is the first quantitative observation of catalytic gas conversion in these detectors, although such processes have often been suspected, and it is certainly the first use of such a process in a practical instrument. The N_2O-sensitized ECD coupled with a gas chromatograph is currently our method of choice for the *in situ* measurement of CO in the atmosphere. For such use, however, care must be taken to remove trace CO impurities contained in the carrier gas. This is of considerable consequence since CO is a very common impurity in gases pressurized in steel cylinders.

ACKNOWLEDGEMENTS

This work was supported in part by an American Chemical Society, Division of Analytical Chemistry Fellowship awarded to M. P. P. and sponsored by the Procter and Gamble Company.

REFERENCES

1 C. J. Howard, in A. C. Aiken (Editor), *Proc. NATO Advanced Study Institute on Atmospheric Ozone: Its Variation and Human Influences, Algarve, Oct. 1–13, 1979; FAA Rep. FAA-EE-80-20*, U.S. Department of Transportation, Washington, DC, 1980, pp. 409–427.
2 P. J. Crutzen, *Annu. Rev. Earth Planetary Sci.*, 7 (1979) 443–472.
3 P. Fabian, R. Borschers, K. H. Weiler, U. Schmidt, A. Volz, D. H. Ehhalt, W. Seiler and F. Müller, *J. Geophys. Res.*, 84 (1979) 3149–3154.
4 C. B. Farmer, O. F. Raper, B. D. Robbins, R. A. Toth and C. Muller, *J. Geophys. Res.*, 85 (1980) 1621–1632.
5 A. Goldman, D. G. Murcray, F. H. Murcray, W. J. William, J. N. Brooks and C. M. Bradford, *J. Geophys. Res.*, 78 (1973) 5273–5283.
6 W. Seiler, *Tellus*, 26 (1974) 116–135.
7 *Methods of Air Sampling and Analysis*, Intersociety Committee, American Public Health Association, Washington, DC, 1972.
8 J. L. Lambert and R. E. Wiens, *Anal. Chem.*, 46 (1974) 929–930.
9 B. M. Golden and E. S. Yeung, *Anal. Chem.*, 47 (1975) 2132–2135.
10 L. W. Chaney and W. A. McClenny, *Environ. Sci. Technol.*, 11 (1977) 1186–1190.
11 R. C. Robbins, K. M. Borg and E. J. Robinson, *Air Pollut. Control Assn.*, 18 (1968) 106.
12 L. A. Cavanagh, C. F. Schadt and E. J. Robinson, *Environ. Sci. Technol.*, 3 (1969) 251–257.
13 W. Seiler and C. Junge, *J. Geophys. Res.*, 75 (1970) 2217–2226.
14 F. W. Hightower and A. H. White, *Ind. Eng. Chem.*, 20 (1928) 10.
15 K. Porter and D. H. Volman, *Anal. Chem.*, 34 (1962) 748–749.
16 F. W. Williams, F. J. Woods and M. E. Umstead, *J. Chromatogr. Sci.*, 10 (1972) 570–572.
17 L. Dubois and J. L. Monkman, *Anal. Chem.*, 44 (1972) 74–76.
18 A. Volz, D. H. Ehhalt, L. E. Heidt and W. Pollock, *Proc. Joint Symp. Atmos. Ozone, Dresden, 1976.*
19 R. L. Grob, *Modern Practices of Gas Chromatography*, Wiley, New York, 1977.
20 F. Bruner, P. Ciccioli and R. Rastelli, *J. Chromatogr.*, 77 (1973) 125–129.
21 M. P. Phillips, R. E. Sievers, P. D. Goldan, W. C. Kuster and F. C. Fehsenfeld, *Anal. Chem.*, 51 (1979) 1819–1825.
22 R. E. Sievers, M. P. Phillips, R. M. Barkley, M. A. Wizner, M. J. Bollinger, R. S. Hutte and F. C. Fehsenfeld, *J. Chromatogr.*, 186 (1979) 3–14.
23 P. D. Goldan, F. C. Fehsenfeld, W. C. Kuster, M. P. Phillips and R. E. Sievers, *Anal. Chem.*, 52 (1980) 1751–1754.
24 W. C. Kuster, P. D. Goldan and F. C. Fehsenfeld, *J. Chromatogr.*, 205 (1981) 271–279.
25 W. Adlhoch, R. Kohler and H. G. Lintz, *Z. Phys. Chem. (Wiesbaden)*, 120 (1980) 111–118.
26 *American Institute of Physics Handbook*, McGraw-Hill, New York, NY, 2nd ed., 1963, p. 8–313.
27 J. M. Warman, R. W. Fessenden and G. Bakale, *J. Chem. Phys.*, 57 (1972) 2702.
28 W. E. Wentworth, F. Chen and R. Freeman, *J. Chem. Phys.*, 55 (1971) 2075.
29 R. Marx, G. Mauclaire, F. C. Fehsenfeld, D. B. Dunkin and E. E. Ferguson, *J. Chem. Phys.*, 58 (1973) 3267.
30 D. A. Parks, *J. Chem. Soc., Farad. Trans. I*, (1972) 2103.
31 M. McFarland, D. B. Dunkin, F. C. Fehsenfeld, A. L. Schmeltekopf and E. E. Ferguson, *J. Chem. Phys.*, 56 (1972) 2358.
32 F. C. Fehsenfeld and E. E. Ferguson, *J. Geophys. Res.*, 78 (1973) 1699.

Journal of Chromatography, 239 (1982) 127–144
Elsevier Scientific Publishing Company, Amsterdam — Printed in The Netherlands

CHROM. 14,755

EVIDENCE FOR MORE THAN ONE RESPONSE MECHANISM IN PULSED ELECTRON-CAPTURE DETECTORS*

WALTER A. AUE* and K. W. MICHAEL SIU**
5637 Life Sciences Building, Dalhousie University, Halifax, Nova Scotia B3H 4J1 (Canada)

SUMMARY

Evidence has been found for two distinct response modes operating in a laboratory-made and a commercial pulse-driven electron-capture detector. These modes are speculatively associated with a classical "neutralization" process and a recently proposed "space charge" mechanism.

INTRODUCTION

There is little doubt that the electron-capture detector (ECD) rightfully bears its name: Quite a variety of techniques have shown analyte molecules to produce negative ions. Their further fate, however, is less well known: How they make the detector respond has been the subject of some recent debate.

To understand the mechanism of response may be interesting and perhaps even useful for most analytical work. But it becomes essential when physico-chemical data are to be extracted, or when this detector is to be used in an "absolute" measurement such as gas phase coulometry[1–8]. In this technique, the response must accurately reflect the moles of electrons initially captured.

Interestingly enough, one of the pioneer authors that described responses coulometric[1] had actually found one hypercoulometric[9]. This is interesting because the classical ECD mechanism[10] implies a limit: Not more than one electron should appear to be captured by any molecule capable of doing so. Yet, apparent electron molecule ratios as high as 50 F/mol have been measured —even if only under d.c. fields and elevated pressures[11,12].

These surprising ratios called for an explanation and prompted us to speculate on an "alternative" response mechanism for d.c.-ECDs[13]. It portrays response as the effect of migrating anions upon the cation–electron recombination rate. In other words, the recorder signal serves no longer as a quantitative measure of initial electron capture, and hypercoulometric behavior becomes possible. Certain predictions of this theory have since been confirmed[14–16].

* Taken from the doctoral thesis of K.W.M.S. (Dalhouse University, September 1981).

** Present address: National Research Council, Division of Chemistry, Montreal Road, Ottawa, Ontario, Canada.

0021-9673/82/0000–0000/$02.75

To breach the coulometric limit, however, did not necessarily violate the classical ECD theory. The latter had maintained all along that only "field-free" conditions —*i.e.* a pulse regime of short pulse widths and long pulse intervals— could be trusted to provide reliable data. Other regimes, especially d.c., could lead to "erroneous and anomalous responses"[17].

Although hypercoulometric response has not been unknown to pulsed systems[9,13,18–20], there always remained the question how closely conditions had approached the field-free ideal; and whether relatively small effects could not have been due to, say, some electron-capturing products of the initial sample[21] or a recycling species[22]. Furthermore, conditions such as cell geometry and radioactive range[13] have a bearing on whether or not hypercoulometric behaviour can be observed —quite apart from the question whether or not the latter does indeed occur on a molecular level. Thus the choice (or happenstance) of detector construction and operation may have been responsible for the presence or absence of hypercoulometric response.

Recently we designed a detector in which the classical ECD response mechanism —the gas-phase neutralization of an analyte-derived anion— could be excluded at will. Under those conditions and in the d.c. mode, the detector exhibited good response[16]. A newer, more versatile model behaved likewise[23]. Since it could be easily switched between the two configurations that included or excluded the classical cation–anion neutralization, it appealed to us as a potential tool for probing the existence of more than one response mechanism. The probe was not directed at the mechanism of the initial capture of an electron (associative, dissociative, etc.), but at the way in which this initial reaction was translated inside the cell to "response"— *i.e.* the electrical measurement that finally appears as a peak on the recorder chart.

Some of our earlier d.c. experiments seemed to indicate that, even with the classical mechanism allowed, it was the alternative space charge mechanism that produced most of the response[14,16]. On a formal basis one could even imagine that the two mechanisms opposed one another in their competition for the analyte-derived anion: A neutralized anion no longer contributes to the space charge, while an anion migrating through the unipolar region can no longer find a cation for neutralization. (The d.c. detector in this case is presumed large enough to exhibit bipolar and unipolar regions.)

Obviously these d.c. experiments invited extension to the pulse regime. With the classical mechanism disallowed, would a pulse-driven ECD fail where a d.c.-powered one had worked so well? That seemed unlikely. And, indeed, "clean" conditions —*e.g.* pulses of 1 μsec width, 360 μsec period and 60 V amplitude— produced subpicogram responses. That seemed to settle the matter.

However, this was a matter of some importance and so we felt obliged to examine the full range of pulse conditions available to us. That turned out to be a lucky decision because it produced evidence (where before there had been only conjecture) of more than one response mechanism at work.

EXPERIMENTAL

The laboratory-made ECD used in this study is shown in Fig. 1. It can operate at high temperatures[23] and resembles an earlier, low-temperature model[16].

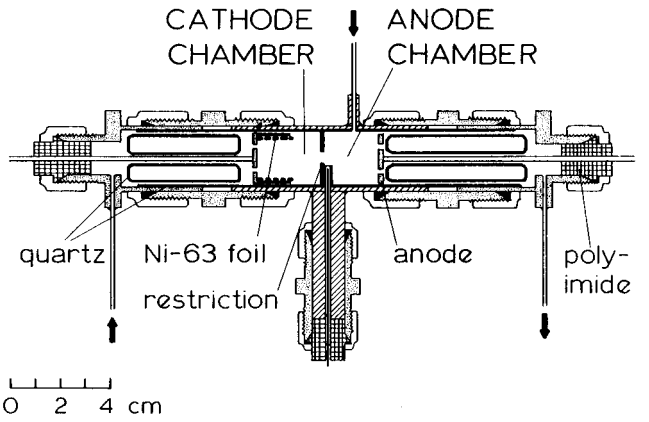

Fig. 1. Two-chamber electron-capture detector for "separated" and "conventional" mode operation.

Repeated here for reader's convenience, this type of ECD uses a restriction that formally divides the detector into cathode chamber (housing the radioactive foil) and anode chamber. The distinguishing feature of this construction is that the column effluent can be routed either to the cathode or to the anode chamber. In the former, "conventional" mode, column effluent and purge gas flow through the whole detector (in Fig. 1 all the way from the left to the right past the blocked central inlet); while in the latter, "separated" mode, the column effluent enters the anode chamber via this central inlet, and meets a fast stream of purge gas sweeping across the restriction from the cathode chamber. In either case, all gases exit at the far right end of the anode chamber. According to arguments made earlier[16], the separated mode prevents the contact of cations with solute-derived anions, thereby precluding the classical neutralization mechanism.

A conventional Tracor ECD pulsing unit (part of the Model 550 electrometer) was used initially. If required, its output was amplified by a laboratory-made circuit. Nominal settings of the pulse power supply were ignored in favor of direct measurements by oscilloscope. Later, a Phillips PM 5705 pulse generator was used in conjunction with the laboratory-made inverting and amplifying circuit shown in Fig. 2. This

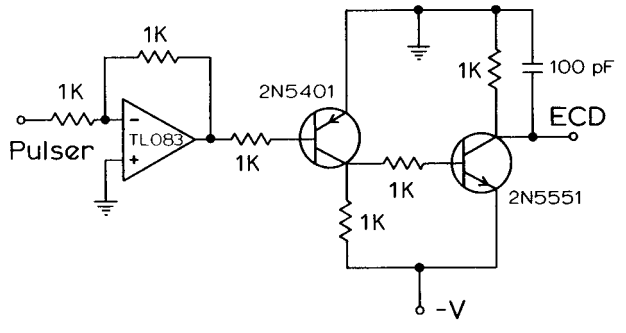

Fig. 2. Inverting and amplifying circuit. K = kΩ.

allowed variation of the pulse width from less than 1 μsec to values approaching the pulse period, *i.e.* d.c. Electrometers were of the varactor type supplied with the Tracor 550 gas chromatograph.

Responses were recorded for lindane (γ-hexachlorocyclohexane) and on occasion 2,4,6-trinitrotoluene (TNT) at different concentrations, different temperatures, and different flows of nitrogen; at different settings of pulse width, period, and amplitude; and in separated and sometimes in conventional mode (see above) —but these measurements were made on a selective rather than on an exhaustive basis.

RESULTS AND DISCUSSION

Similar to the "voltage profile" of the d.c. regime, the "pulse profile" —that is a plot of baseline current over a range of pulse widths— is often considered diagnostic for the state of an ECD. It will tell an experienced analyst how clean the ECD is, what settings to use and what performance to expect.

At first sight, the pulse profiles of this study did not bode any unusual responses. They rose more or less steadily and finally leveled off at long pulse width. The corresponding response curves, however, were most surprising: They clearly exhibited *two* maxima.

This unexpected behavior is illustrated in Fig. 3 for the separated mode. Response peaks strongly in two separate regions, but between these it drops down to rather low levels. For purpose of subsequent referral, we shall name the sharp maximum on the left "A", the broader one on the right "B".

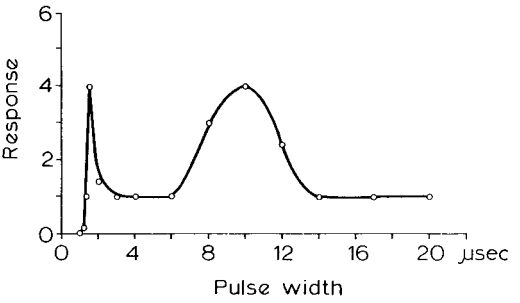

Fig. 3. Typical response maxima in the separated mode. Sample: 10 pg lindane. Column: 3% OV-101 on Carbowax 20M-modified Chromosorb W at 175°C. Flow-rates: column 14, detector purge 200 ml/min. Detector: 280°C, aperture diameter 8 mm. Pulses applied to cathode: amplitude −30 V, period 360 μsec.

These two humps emerged from many measurements, although often in not as pronounced a form. Fig. 4 shows a comparable run in the conventional mode, and includes data taken off a commercial (Tracor) detector. It suggests that the presence of two response maxima is a fairly general phenomenon and not dependent on the use of the separated mode or a particular laboratory-made ECD. One must add, however, that other commercial detectors have not been investigated in this context and that these, if of a different and perhaps smaller geometry, may not produce similarly obvious effects. But that, of course, is speculative.

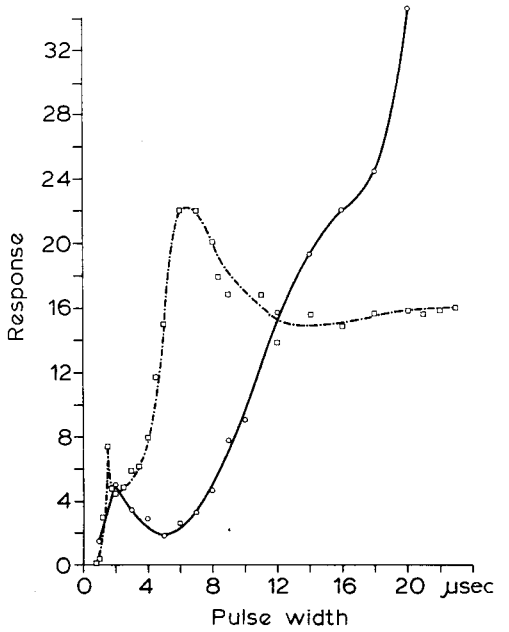

Fig. 4. Response maxima of the conventional mode on the laboratory-made detector (□) and on a commercial (Tracor) ECD (○). Laboratory-made ECD: −60 V pulse amplitude, 360 μsec period. Tracor ECD: column 17, purge 43 ml/min; 280°C; −30 V pulse amplitude, 360 μsec period. Other conditions as in Fig. 3.

A larger number of experiments were performed to follow the behavior of the two response maxima when subjected to a variation of detector parameters. The separated mode was used almost exclusively, since the induced changes were clearer and could therefore be measured over a wider range of operating conditions.

Changing the pulse width was not expected to change the nature of the process in which an electron is initially captured. From that point on, however, it is not clear whether there are two (or more) distinct response mechanisms at work, or whether one and the same response mechanism somehow produces two response maxima owing to, say, the peculiarities of detector geometry. To complicate matters further, one must be aware that the initial electron capture reaction may be similar in nature, but not in extent, at conditions corresponding to the two response maxima: The number of available electrons may be quite different at the two settings.

These caveats noted, it is still reasonable to expect that the behavior of the two response maxima under varying detector conditions would reflect the response mechanism(s) at work: If there was only one, the induced changes would be similar; but with two mechanisms operating, at least some of the changes should be dissimilar. The task then is to look for consonant or dissonant shifts in amplitude and position of the two response maxima.

In regard to the first parameter, the *absolute* response amplitude may not be the best measurement to plot, since it can be influenced by a variety of extraneous factors such as column bleed. The *relative* size of the two maxima, however, should suffer much less from such effects. It is the ratio of response maxima A and B, therefore, which is shown in Fig. 5. Clearly, this ratio varies considerably with circumstances, suggesting that different response mechanisms are at work.

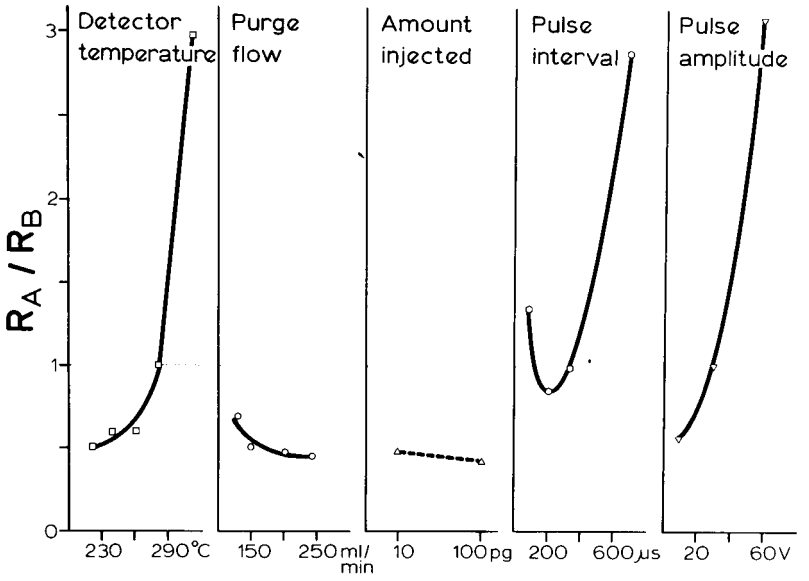

Fig. 5. Relative response (ratio of peak heights) at the two maxima for various experimental conditions.

This appears also indicated by the response profiles of Fig. 6, showing the peak heights for lindane and TNT in conventional mode. It should be added, however, that there appeared very little difference between the two compounds when tested in separated mode, and that no further studies with different compounds were done.

It should also be noted that the *position* of the maxima on the pulse width axis was essentially the same for the two compounds. This is in agreement with information from earlier studies, in which the position of response maxima was generally independent of solute structure.

While the nature of the solute did not appear to influence the position of the response maxima, a variety of detector conditions did. Rather than to present these measurements as mere numbers in a table, the response profile format was chosen to convey the full range of available information.

Fig. 7 presents the profiles of lindane at three different temperatures. Here, as in some other correlations, the measurements were repeated after some weeks in order to confirm the validity of initially established trends. Aside from the shift in relative amplitude discussed earlier, Fig. 7 shows response maximum A shifting to shorter pulsewidths as the temperature is raised, while response maximum B appears to remain more or less stationary.

This is a matter of some interest. The temperature dependence of response has been used as a kinetic probe almost since the ECD's inception. For this and other physico-chemical purposes, the choice at what conditions to measure may have a significant bearing on the results. This is particularly important should there be *two* response mechanisms operating; perhaps in unknown and, during the course of the experiment, changing proportions.

The effects of a change in temperature may be complex. Beyond its influence on the initial capture of the electron, *i.e.* the reaction of much primary interest, tempera-

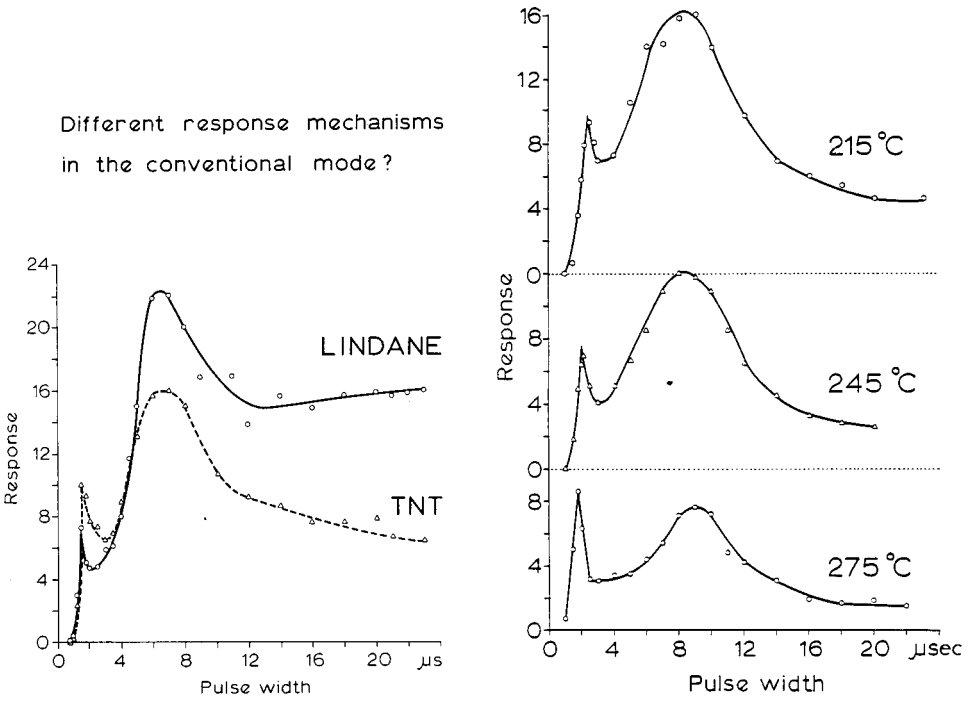

Fig. 6. Simultaneously measured response profiles for lindane and TNT in the conventional mode. Other conditions as in Fig. 4.

Fig. 7. Variation of lindane response profile with temperature in separated mode. Other conditions as in Fig. 3.

ture can be expected to affect several processes that alter response. For instance, cation–electron recombination is temperature dependent[24,25], as is cation–anion neutralization. Furthermore, the cation composition, even in the pure carrier purge gas of the separated mode, may change with temperature. In real-life ECD operation, cations will also arise from carrier gas contamination, stationary-phase bleed and the solute itself. The different equilibria one would expect to exist are again subject to temperature dependence. The formation of various clusters[26,27] influences not only the distribution of positive charge among several species, but also its overall mobility[28,29]. A similar argument can be made for anions. One process that has been discussed repeatedly and in different ECD contexts, is the strongly temperature-dependent equilibrium $O_2 + e^- \rightleftharpoons O_2^-$ (refs. 30–33).

Even if one disregards the effects of typical carrier gases, the mobilities —hence concentrations— of charged particles must change with temperature due to the corresponding density change. It may be noted in this context that theoretical predictions of ion mobility are not always consistent with empirical data[34,35]. The changes in the density of the carrier gas also lead to a different linear flow value and a different range of β radiation, whereby the latter can be strongly influenced by confined detector geometries[36].

And then there is always the chance of variable detector cleanliness (*e.g.* outgassing effects) and premature analyte decomposition. The latter is particularly dif-

ficult to evaluate and, perhaps for this reason, often ignored. While this is justified under some conditions, under others —*e.g.* when polyhalogenated species are detected at high temperatures, using a catalytically active ^{63}Ni foil and traces of hydrogen in the carrier gas— the temperature dependence of solute degradation may become the subject of legitimate concern. If and to what extent such processes do influence the finally observed response, remains in most cases unresolved.

The paragraphs above discussed at some length the possibly complex meaning of a seemingly simple experimental result. This was done, *inter alia*, to stress that an observed divergence of two response maxima should be taken only as an indicator, but not as a proof, of two disparate response mechanisms at work. A similar argument applies to later discussions.

In separated mode, the cathode chamber with its radioactive foil is purged by pure nitrogen. The flow of purge gas exerts considerable influence on whether or not two response maxima can be observed: While the latter are completely merged at low values, a high purge flow will make them move apart. Perhaps this has something to do with the change in solute concentration due to dilution by the purge gas, or perhaps the high flow raises the pressure inside the detector. Whatever the reason, it is clear from Fig. 8 that response maximum A moves to lower, but response maximum B to higher pulsewidths as the flow of purge gas is increased.

If solute dilution was responsible for this dissonant shift in the position of the maxima, a similar effect should be observed for changes in analyte concentration. And indeed it is, as can be seen in Fig. 9.

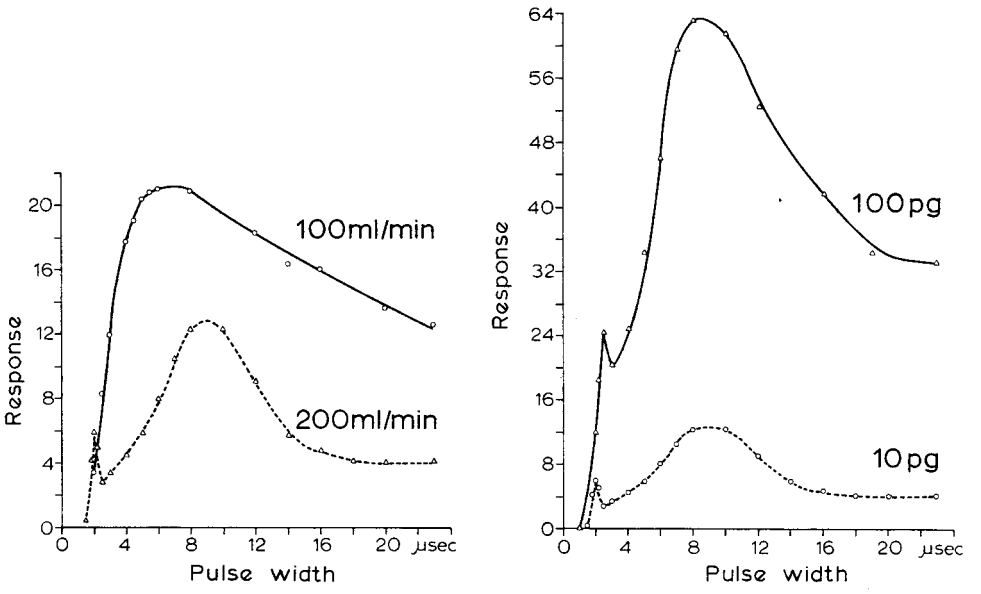

Fig. 8. Variation of response profile with purge flow-rate. Detector temperature 215°C, other conditions as in Fig. 3.

Fig. 9. Variation of response profile with analyte concentration. Detector temperature 215°C, other conditions as in Fig. 3.

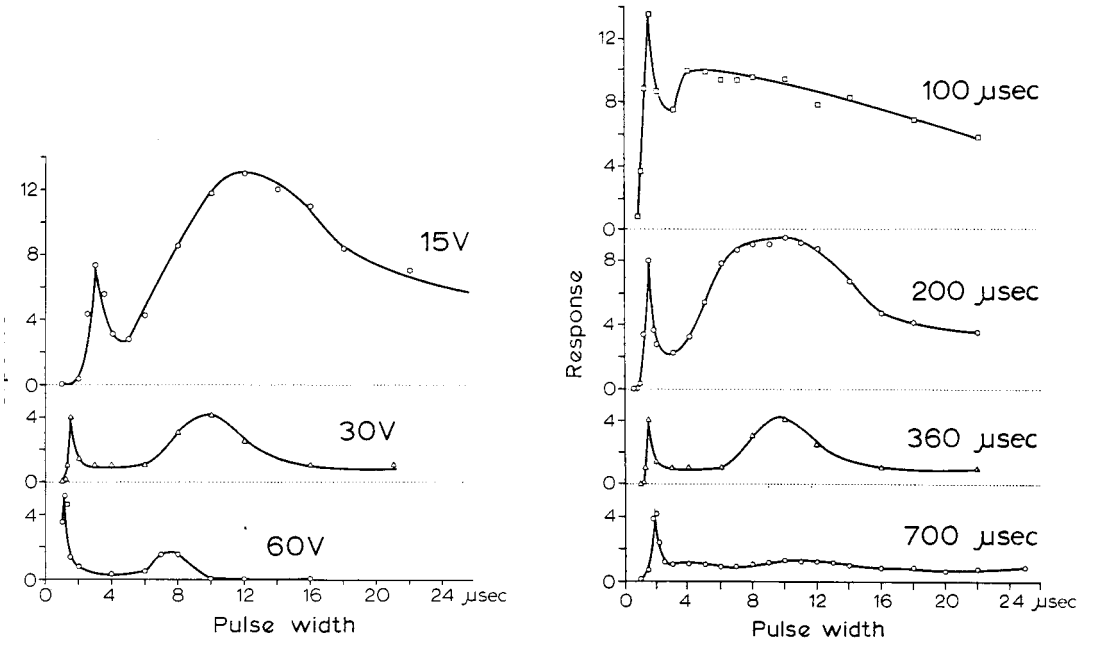

Fig. 10. Variation of response profile with pulse amplitude. Other conditions as in Fig. 3.
Fig. 11. Variation of response profile with pulse period. Other conditions as in Fig. 3.

Perhaps the effects easiest to predict are those induced by changes in pulse height, duration or interval. If we assume that transport of charged species is involved in producing response, then the crucial parameter, within limits, should be the "effective voltage". This parameter would in the simplest case be the product of pulse amplitude, width and frequency. Not surprisingly, the actual situation is not that simple. The reaction kinetics in the ECD are mostly second order, local field gradients are more or less influenced by space charges, and the pulses can remove charged reagent species in a non-linear fashion. Still, a qualitative relationship of the suggested sort is evident.

For instance, Fig. 10 shows both maxima moving to longer pulse width as the pulse amplitude is decreased. Note that this is a "consonant" shift as opposed to earlier "dissonant" ones. At high amplitudes, the two maxima become very well separated and the valley between them moves close to zero response.

Fig. 11 presents the effects of increasing the pulse interval. It is interesting to note how peak B recedes so that, at low frequencies, peak A becomes the most prominent feature. This happens at conditions close to the field-free ideal.

From the viewpoint of two distinct response mechanisms, it is interesting to compare calibration curves run at the two maxima. To do this, conditions were chosen at which the maxima appeared well separated and maximum A —weaker under most conditions— was considerably larger than maximum B. The fairly predictable results are shown in Fig. 12: maximum A yields a more sensitive analysis but with a shorter linear range. This is a consequence of the very low baseline (about 6 to

7% of the maximum available one): It means decreased fluctuations and a smaller capacity of the information-carrying current; in other words one notices less noise and an earlier cut-off.

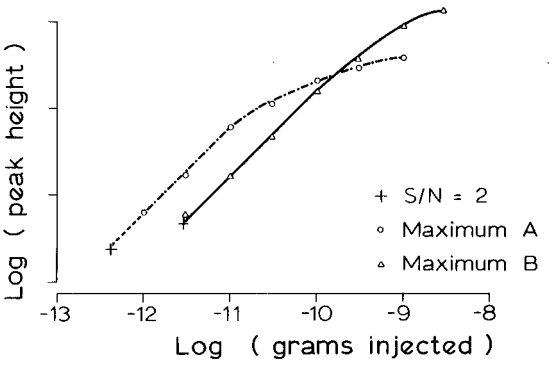

Fig. 12. Calibration plots of lindane. Pulse conditions: amplitude −60 V, period 360 μsec, width 1 μsec for maximum A and 7.5 μsec for maximum B. Other conditions as in Fig. 3. S/N = Signal-to-noise ratio.

If the observation of the two response *maxima* was surprising, the assumption of two response *mechanisms* may be disturbing. It was for this reason that our experiments returned to the pulse profile; in order to be sure that no possibly important clue had been overlooked.

Following a common ECD routine, pulse profiles had been run from time to time alongside response profiles. There is a close correlation between baseline and response curves in various modes of electron capture detection; the former are often used as diagnostic tools for the latter.

Given this fact, it seemed highly unusual that (as reported earlier on) the pulse profiles should contain no feature whatsoever correlating with response maximum A. After all, the baseline current carries some continuous "response" (to impurities in the carrier gas, for instance) and, in a manner of speaking, it consists of electrons potentially available for capture.

Very careful measurements were therefore made of the pulse profile I_b, shown as the top trace of Fig. 13. Below it is the response profile R, and the fat arrows pinpoint the precise positions of the two response maxima. A slight distortion may be noticed in I_b at the position of the first maximum. To have a closer look, the slope of the pulse profile, $\Delta I_b/\Delta$ pulse width (p.w.), is plotted at the bottom of Fig. 13. It establishes beyond doubt that the position of response maximum A corresponds to the maximum slope, *i.e.* the point of inflection, of the pulse profile. Maximum B, on the other hand, corresponds to the "knee" position of the pulse profile and that is nothing unusual. Operating at this position often provides the best performance in conventional ECD practice (suggesting that such practice may rely primarily on response mechanism B).

Conventional ECD analysis hardly uses pulse widths beyond those of Fig. 13; yet, the rather unusual circumstances of this study made it advisable to probe further.

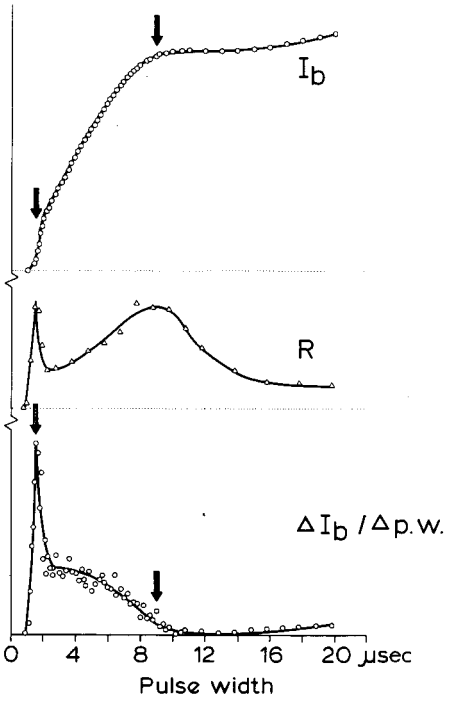

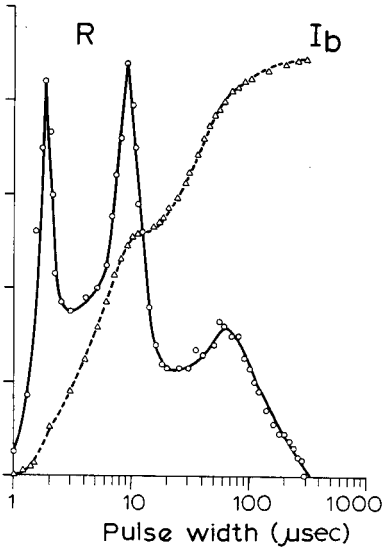

Fig. 13. Correlation of pulse profile (I_b) and response profile (R). Other conditions as in Fig. 3. Bottom trace: Slope of pulse profile. Arrows show the precise position of response maxima. All scales linear.

Fig. 14. Extended response and pulse profiles of lindane. Other conditions as in Fig. 3. Ordinate linear, abscissa logarithmic. Ordinate units are different for different curves.

The results are shown in the (now semi-logarithmic) plot of Fig. 14. Beyond the two strong response maxima, a third, weak one shows up, duly matched by another "knee" in the pulse profile. The size of the maximum was close to the experimental error limit and therefore (besides taking note of this interesting phenomenon) nothing further was done about it.

Still, it appears quite clear that a correlation between the pulse and response profiles does exist. This is also supported by the fact that, when conditions change, respective features of the two profiles move in unison. Of course, it could be argued on a formal basis that this is to be expected since both the baseline current and its temporary decrease known as response, are effects of charge transport processes which, in turn, are influenced by the same geometries and operating conditions.

However, that does not really explain why response maximum A takes a relatively large fraction out of a rather small current, and why, again relatively speaking, the pulse profile shows but a small warp (which was not even noticed the first time around). Judging from the pulse profile —as well as from common sense— there is no reason to assume that the initial electron-capture reaction, while high at positions A and B, but would somehow fail to function between the two maxima. Rather, this appears to be another case where the electron capture proper is improperly represented by the observed response (*cf.*, ref. 15).

When we combined the evidence from all the experiments discussed above, it

seemed to us to constitute reasonable evidence of two (or more) response mechanisms at work. Yet, we could not completely discount the possibility that we had seen but a simple mechanism being split into various maxima by the pecularities of detector construction.

If the experiments indeed indicate more than one response mechanism at work, the obvious question arises as to the nature of these mechanisms. At this point the question can be answered only by engaging in outright speculation. Before so doing, however, it may be profitable to make some rough estimates of certain transport processes. What one would like to know are the approximate migration rates of charged particles inside the ECD, as brought about by carrier gas flow, diffusion and the electrical field, in order to use them for interpreting pulse and response profiles.

Some estimates

The detector operates generally at 280°C and ambient pressure. If one assumes that anions such as Cl^-, with a reduced mobility K_0 of 2.5 $cm^2\ V^{-1}\ sec^{-1}$ (ref. 37), are created near the restriction, and, while drifting 2 cm to the anode, pass through a potential difference of 15 V, and if one furthermore neglects space charges, surface charges and field inhomogeneities, the ionic drift speed turns out to be 38 cm/sec during a 30 V rectangular pulse. To take the example of Fig. 3, the pulse is "on" *ca.* 1.5 μsec and *ca.* 10 μsec —out of a 360 μsec period— for response maxima A and B, respectively. Therefore the ion would need 13 sec or $3.5 \cdot 10^4$ pulses to reach the anode in the first case, 2 sec or $5.3 \cdot 10^3$ pulses in the second case. This means rather long periods of time and rather many pulses. Furthermore, the estimate ignores effects of coulombic forces such as the "floating-back" of oppositely charged ions during the field-free period.

The average, *i.e.* time-integrated, ion drift speeds are 0.2 and 1 cm/sec for response maxima A and B; somewhat lower than the average gas flow of 2.0 cm/sec (200 ml external) through the anode chamber.

In order to compare these numbers with diffusion effects, a number of simplifying assumptions have again to be made. A rigorous treatment is impossible since the areas of creation, transformation and neutralization of ions would have to be known, not to mention the influence of the detector's peculiar geometry. Pretending diffusion to take place from an infinite plane and taking σ as the distance travelled, one may apply the Einstein equation.

$$\sigma^2 = 2Dt$$

where σ^2 is the variance of a Gaussian distribution and t is the time span of the process[38]. The diffusion coefficient D may be calculated from the mobility K for the linear regime[39] from

$$K/D = 1.16 \cdot 10^4/T$$

and turns out to be 0.24 cm^2/sec (T = absolute temperature). Thus the "distance that ions travelled" during 1 sec is calculated as 0.7 cm.

Since drift, flow and diffusion rates turn out to be of the same order of magnitude, the situation is much more complex here than in prior experiments using the d.c.

regime[16]. For instance, it is no longer possible to assume, as could be done confidently for d.c. conditions, that cations never enter the anode chamber.

One of the major premises of the classical mechanism is that all free electrons are collected by each pulse (*e.g.*, ref. 40). This is reasonable if one assumes negligible charge interactions, small cell dimensions and strong pulses. Our experiments do not fit these assumptions; thus it becomes necessary to estimate, in analogy to earlier treatments of ionic speed and subject to similar assumptions, the velocities of electrons.

For 30 V/3 cm and ambient pressure, an extrapolation of the measurements by Pack and Phelps[41] to 280°C shows electrons drifting in nitrogen at speed $v = 9 \cdot 10^4$ cm/sec. To traverse the interelectrode distance of *ca.* 3 cm, electrons would need, very roughly, 22 pulses or a total of 8 msec at maximum A, and 3 pulses or 1 msec at maximum B. The fact that the number of pulses is greater than unity even for the second case, is quite interesting.

The gas flow does not play a role in the movement of electrons, but diffusion might. If it is assumed that the mobility equation

$$K = v/E$$

is applicable at $E/p = 10^{-2}$ V cm^{-1} mmHg^{-1} (ref. 42) and K is used as has been done above for ions, D turns out to be 430 cm^2/sec (E = electric field gradient; p = pressure). From the Einstein equation it can then be estimated that to diffuse 1 cm takes electrons about 1 msec. This compares with drift speeds of about 3 and 0.4 cm/msec. It should be noted in this context that different estimates of diffusion coefficients have been used in the ECD literature, *e.g.* Siegel and McKeown[22] assumed values of 0.05 and 50 cm^2/sec for positive ions and electrons.

Despite the oversimplifications inherent in our estimates, the results are taken to present a qualitatively accurate picture. Perhaps the most important conclusion is that more than one pulse is needed to collect unimpeded electrons. While the underlying calculations may be subject to doubt, the experimental pulse profiles (*e.g.* that of Fig. 13) support this conclusion.

To see why, one may start by remembering the classical concept of the baseline current (*e.g.*, ref. 43). A pulse profile, in idealized form, exhibits two distinct regions. The initial steep current rise indicates that pulses are too short to clear the cell of electrons. As pulses become wider, most electrons will eventually be removed by a single pulse. From then on, the current rise becomes very shallow, reflecting the collection of electrons generated while the pulse is still on. The transition region between the steep and shallow slopes, the "knee", is therefore supposed to indicate a pulse more or less wide enough to empty the cell of electrons. Off-hand, this does not seem to agree even with calculations for maximum B (located in the knee region) which suggest that not one but three pulses are necessary for an electron to traverse the cell.

However, the calculations are really quite compatible with the experimental data, as the following reasoning will show.

First, the measured pulse profile represents integrated current values. The pulse width at which, say, 50% of the maximum current is collected and the one at which 50% of available electrons are swept from the cell, are not identical: The

former is shorter than the latter. This can be demonstrated by following a train of short pulses, each of which removes the same percentage of electrons from the cell. The residual electrons from the last period are added to the ones newly generated, and imposing the (commonly assumed) second-order recombination rate in an iterative procedure then completes a simulation that supports the argument above.

Second, and perhaps easier to appreciate, is the question what constitutes a "cell" in the present context. If cell means the whole detector volume, then the picture tacitly assumes a "stirred reactor" system, *i.e.* an essentially homogeneous charge environment. However, should the detector contain bipolar and unipolar regions, *i.e.* should cations populate only part of the detector, then a pulse needs to sweep electrons out of only that region —not out of the whole detector— in order to make them escape recombination.

Reality is a bit more complex than this simple picture suggests. Primary ionization decreases in a roughly exponential manner from the radioactive foil. Furthermore, the effects of recombination, not to mention flow and diffusion, need to be considered for a closer definition of the steady-state charge density distribution. Yet, it is quite obvious from recently measured beta ranges[36] that most initial ionization occurs within a few mm of the foil. Fig. 1 shows the cylindrical foil occupying about one third of the detector length. Once electrons have escaped this area they have escaped recombination. Now the electrical field gradient is *not* linear (because of the detector geometry and the differences between bipolar and unipolar regions) but as a qualitative description arrived at in hindsight, it seems not unreasonable to look at Fig. 1 and expect electrons to escape the plasma region in about one third of the time it takes them to get all the way across the detector to the anode. If so, the theoretical estimate and the experimental observation are in essential agreement.

The notion that the knee of the pulse profile (and response maximum B) occur in a region where it takes several pulses to transport electrons from the point of generation to the collecting anode, is at first a surprising one. However, it makes sense not only in terms of the baseline current, as discussed above, but also in terms of response.

In the separated configuration, electrons can meet electron-capturing analyte molecules in the anode chamber only. If, however, these electrons are swept through the chamber by a single pulse, electron capture can occur only during a few microseconds out of (if we take the most commonly used pulse period) 360 μsec. Since response, in whichever mechanistic hypothesis, depends on the initial occurrence of electron capture, it would turn out to be severely depressed under such a condition. On the other hand, the initial electron-capture reaction (though not necessarily response) would clearly attain its highest rate at the highest possible electron concentration in the anode chamber. That would occur at a pulse just wide enough to remove most electrons from recombination in the cathode chamber, but short enough to make these electrons stay for one or perhaps more pulse periods in the anode chamber and be available for capture. Considering these two situations together jives with the experimental observation that response in the separated mode drops off fairly quickly at pulse widths longer than those characteristic of maximum B and the knee position.

In the conventional configuration, on the other hand, electrons may be captured by analyte molecules in both cathode and anode chambers. In fact, under conditions where the pulse width is long enough to sweep electrons all the way

through the anode chamber and restrict capture there to the fraction of time when the pulse is on, capture in the cathode chamber —which is free to occur all of the time— will be the major source of response. From this point of view, response in the conventional mode beyond maximum B and the knee position will drop off much less than in the separated mode. A comparison of the respective modes shown in Figs. 4 and 3 demonstrates that this is indeed the case.

All this, while reasonable, does not yet explain why two response maxima occur and what mechanisms do produce them. At the moment, the only explanation possible is a purely speculative one and the following paragraphs should be viewed in that light.

Some speculations

It is perhaps best to start not with the two response maxima but with the valley between them, taking again the separated mode shown in Fig. 3 as an example. That this valley exists in so pronounced a form is even more surprising than the occurrence of maxima, for there is no doubt that electrons *were* available for capture. As can be seen from the pulse profile, electrons were indeed collected by the anode at pulse widths where the valley occurred; consequently, they must have traversed the anode chamber and met analyte molecules. If there was electron capture, why was there little or no response?

Electron capture results in the formation of an anion, which will drift toward the anode. If detector geometry, flow and effective voltage prevent its contact with a cation —as was mostly the case here— the negative charge cannot be neutralized but must reach the anode. If so, there is no change in current, *i.e.* no response. In other words, the classical response mechanism of neutralization is precluded. But why did the alternative space charge mechanism[13] also fail to respond?

A qualitative answer, given after the fact, could be as follows: The space charge mechanism relies, obviously, on high charge densities[14]. In contrast, the situation here involves a very low electron input into a large-volume chamber flushed by a fast carrier flow. The anion density must therefore be very low and the space charge effect minimal.

If pulse width is increased, however, more electrons are pushed into the anode chamber and become available for capture, and denser space charges form in closer defined regions. As space charges build up, it becomes more difficult to transport anions to the cathode and so the electrical gradient during the pulse steepens in the anode chamber and softens in the cathode chamber. There, cations and electrons now drift slower and their concentration, hence their second-order recombination rate, increases. Thus the detector produces the decrease in current commonly known as electron capture response.

This suggests that maximum B represents a space charge effect. As far as experimental observations are relevant in this context, they tend to support this assignment. In an earlier, d.c.-based study, it was suggested that response increases with higher pressure, lower temperature and a lower voltage gradient, *i.e.* all factors that slow down anion migration[13]. In analogy, response maximum B in this pulsed system also increases when anions travel slower and are more concentrated; be it through lower temperature (= higher density), lower flow, or lower pulse amplitude as shown in Figs. 7, 8 and 10, respectively.

The position of maximum B on the pulse width axis would thus be determined by two factors: On one hand, by the number of electrons available in the anion chamber for capture —a number that first rises, then falls with increasing pulse width; on the other hand, by the relative concentration (inversely related to drift speed) of anions —a number that decreases with increasing pulse width. It is reasonable that this interplay should result in a response maximum situated at the knee of the pulse profile.

In this context it may be interesting to note that commercial pulsed systems often work at or close to the knee position. To consider, furthermore, the fact that in the comparable conventional mode of this study, maximum B is the predominant response (compare Fig. 4 with Fig. 3), raises the question whether a space charge mechanism may not also dominate some commercial pulse-driven ECDs. However, to answer that question is beyond our present means and intentions.

Before moving on to a discussion of maximum A, another possibly controversial matter should be shortly mentioned: Why had we not considered the possible occurrence of ambipolar diffusion (*cf.*, ref. 22)? It is well established that one can estimate the largest possible electron/cation concentration from pulse profiles over a range of frequencies. This limiting value, in our system, is close to $3 \cdot 10^7$ electrons. For, say, the cathode chamber of approximately 8 cm^3 volume, our average limiting electron density of $0.4 \cdot 10^7/cm^3$ may be compared to a range of 10^7 to $10^8/cm^3$ quoted by McDaniel for the onset of ambipolar diffusion[44]. Now, an ECD plasma is not homogeneous, but that quoted range would apply only to a layer very close to the radioactive foil, and hence we feel justified in neglecting ambipolar diffusion in the present context.

Response maximum A is undoubtedly the most difficult object of speculation. It occurs at pulse conditions so weak that few electrons are pulled out of the plasma, and the ones that are need several pulses to do it. If one increases pulse width, the baseline current duly increases but response drops, in contrast to any reasonable expectation (*cf.*, Figs. 3 and 13).

A number of scenarios were considered in attempts to explain this unusual behavior, but none was totally convincing. That one that follows is —to stress it again— born of outright speculation.

At the very weak pulse regime of maximum A, as earlier suggested, the nominal ionic drift speed is slower than gas flow or diffusion effects. Not too much can be made of these numbers since they are based on simplifying assumptions and disregard local geometry. However, they are good enough to allow consideration of a scenario in which a limited number of cations would reach the restriction and be carried through it into the anion chamber.

If pulse width is increased, there must come a point where the field is strong enough to hold cations —against diffusion and gas flow— inside the cathode chamber. This change-over from a bipolar to a unipolar anode chamber should be accompanied by some characteristic feature of the pulse profile, since there ought to occur changes in recombination rate, changes in surface charges at the restriction, etc. Fig. 13 does indeed show an undulation in the pulse profile, which coincides with maximum A of the response profile.

Since the detector is in separated configuration, analyte molecules are available only in the anode chamber, and only there can anions be formed. As long as cations

are also able to enter, charge recombination may occur. Although such conditions are not really comparable to those of ECDs described in the literature, the response mechanism suggested here is, in fact, the classical one of enhanced cation–anion neutralization. Incidentally, the electron/molecule ratio for maximum A, about 0.5 F/mol, falls safely below the coulometric limit. Additionally, the presence of slow anions may help to attract nearby cations across the restriction.

As increasing pulse widths prevent cations from reaching the anode chamber, the classical mechanism must cease to operate and response drops to the valley seen in Fig. 3. Response does not drop all the way to zero, but that is reasonable given the diffuse nature of the plasma and the likelihood that some contribution from the space charge mechanism is already present. In conventional configuration, where the classical mechanism is allowed at any pulsewidth, the valley becomes much less pronounced (Fig. 4).

So, taking Fig. 3 as an example, the position of maximum A is on its left side established by the available information-carrying current —current must be collected in order for response to be observed— and on its right side limited by cations receding back into the cathode chamber. To a certain extent, measurements support this assignment. The position of maximum A on the pulse width axis should shift to the right when it becomes more difficult to keep cations, by way of the electric field, inside the cathode chamber. That should occur at lower temperature (*i.e.* higher density), lower pulse amplitude, longer pulse interval, and faster purge flow. Except for the last parameter, the changes are in the predicted direction, as shown in Figs. 7, 10, 11 and 8, respectively. However, the observed changes are small and offer qualified support at best for the proposed scenario.

CONCLUSIONS

The two response maxima seen in particular, pulse-driven ECDs have been speculatively associated with response mechanisms of the "neutralization" and "space charge" type. In doing so, emphasis was placed on transport processes rather than, as usual, on chemical reactions. Obviously it would be interesting to prove or disprove these concepts, and to find out whether and to what extent they operate in more commonly used ECDs. However, this is beyond our means and intentions. That two pronounced maxima appeared in our initial experiments may have been a stroke of luck: As can be seen from several of the figures, these maxima merge or come close to merging under a variety of conditions. "Merged maxima" may also exist under typical operating conditions in some commercially available ECDs. If our speculation linking experimental maxima with theoretical mechanisms is correct, such detectors would translate the initial electron-capture reactions via two or more concurrent response mechanisms into the peaks seen on the chromatogram. That, however, would likely go unnoticed.

ACKNOWLEDGEMENTS

This study was supported by NSERC grant A-9604 and a Killam Scholarship for one of us (K.W.M.S.).

REFERENCES

1 J. E. Lovelock, R. J. Maggs and E. R. Adlard, *Anal. Chem.*, 43 (1971) 1962.
2 D. Lillian and H. B. Singh, *Anal. Chem.*, 46 (1974) 1060.
3 H. B. Singh, D. Lillian and A. Appleby, *Anal. Chem.*, 47 (1975) 860.
4 S. O. Farwell and R. A. Rasmussen, *J. Chromatogr. Sci.*, 14 (1976) 224.
5 E. P. Grimsrud and S. H. Kim, *Anal. Chem.*, 51 (1979) 537.
6 E. P. Grimsrud and S. W. Warden, *Anal. Chem.*, 52 (1980) 1842.
7 E. Broś and F. M. Page, *J. Chromatogr.*, 126 (1976) 271.
8 J. Rosiek, I. Śliwka and J. Lasa, *J. Chromatogr.*, 137 (1977) 245.
9 E. R. Adlard, in L. S. Ettre and A. Zlatkis (Editors), *75 Years of Chromatography —A Historical Dialogue* (*Journal of Chromatography Library*, Vol. 17), Elsevier, Amsterdam, Oxford, New York, 1979, p. 8.
10 E. D. Pellizzari, *J. Chromatogr.*, 98 (1974) 323.
11 W. A. Aue and S. Kapila, *J. Chromatogr.*, 112 (1975) 247.
12 S. Kapila and W. A. Aue, *J. Chromatogr.*, 118 (1976) 233.
13 W. A. Aue and S. Kapila, *J. Chromatogr.*, 188 (1980) 1.
14 S. Kapila, C. R. Vogt and W. A. Aue, *J. Chromatogr.*, 195 (1980) 17.
15 S. Kapila, C. R. Vogt and W. A. Aue, *J. Chromatogr.*, 196 (1980) 397.
16 W. A. Aue and K. W. M. Siu, *J. Chromatogr.*, 203 (1981) 237.
17 J. E. Lovelock, *Anal. Chem.*, 35 (1963) 474.
18 D. C. Leggett, *J. Chromatogr.*, 133 (1977) 83.
19 C. Vidal-Madjar, F. Parey, J.-L. Excoffier and S. Békássy, *J. Chromatogr.*, 203 (1981) 247.
20 P. Ciccioli, P. H. Hammer and J. M. Hayes, *13th International Symposium on Chromatography, Cannes, July 1980*, Abstract H5-1.
21 S. Kapila and W. A. Aue, *J. Chromatogr.*, 148 (1978) 343.
22 M. W. Siegel and M. C. McKeown, *J. Chromatogr.*, 122 (1976) 397.
23 K. W. M. Siu and W. A. Aue, in preparation.
24 M. A. Biondi, in M. H. Bortner and T. Baurer (Editors), *Reaction Rate Handbook*, U.S. Defense Nuclear Agency, Santa Barbara, CA, 2nd ed., 1972, Table 16-1.
25 V. L. Tal'Rose and G. V. Karachevtsev, in M. Venugopalan (Editor), *Reactions under Plasma Conditions*, Vol. 2, Wiley-Interscience, New York, 1971, pp. 111–115.
26 J. L. Franklin and P. W. Harland, *Ann. Rev. Phys. Chem.*, 25 (1974) 485.
27 P. Kebarle, in J. L. Franklin (Editors), *Ion–Molecule Reactions*, Vol. 1, Plenum Press, New York, 1972, pp. 315–360.
28 J. L. Pack and A. V. Phelps, *J. Chem. Phys.*, 45 (1966) 4316.
29 S. H. Kim, K. R. Betty and F. W. Karasek, *Anal. Chem.*, 50 (1978) 2006.
30 H. J. van de Wiel and P. Tommassen, *J. Chromatogr.*, 71 (1972) 1.
31 P. Kebarle, M. Arshadi and J. Scarborough, *J. Chem. Phys.*, 49 (1968) 817.
32 F. W. Karasek and D. M. Kane, *Anal. Chem.*, 45 (1973) 576.
33 E. P. Grimsrud and R. G. Stebbins, *J. Chromatogr.*, 155 (1978) 19.
34 E. A. Mason, H. O'Hara and F. J. Smith, *J. Phys. B*, 5 (1972) 169.
35 E. W. McDaniel, *Collision Phenomena in Ionized Gases*, Wiley, New York, 1964, Ch. 9.
36 K. W. M. Siu and W. A. Aue, *Can. J. Chem.*, in preparation.
37 F. W. Karasek, *Anal. Chem.*, 46 (1974) 710A.
38 B. L. Karger, L. R. Snyder and C. Horváth, *An Introduction to Separation Science*, Wiley, New York, 1973, p. 67.
39 E. W. McDaniel, *Collision Phenomena in Ionized Gases*, Wiley, New York, 1964, p. 491.
40 J. E. Lovelock and A. J. Watson, *J. Chromatogr.*, 158 (1978) 123.
41 J. L. Pack and A. V. Phelps, *Physical Rev.*, 121 (1961) 798.
42 E. W. McDaniel, *Collision Phenomena in Ionized Gases*, Wiley, New York, 1964, pp. 428, 488–491 and 536.
43 W. E. Wentworth, E. Chen and J. E. Lovelock, *J. Phys. Chem.*, 70 (1966) 445.
44 E. W. McDaniel, *Collision Phenomena in Ionized Gases*, Wiley, New York, 1964, p. 512.

Journal of Chromatography, 239 (1982) 145–157
Elsevier Scientific Publishing Company, Amsterdam — Printed in The Netherlands

CHROM. 14,595

SELECTIVE ELECTRON-CAPTURE SENSITIZATION OF WATER, PHENOLS, AMINES AND AROMATIC AND HETEROCYCLIC COMPOUNDS

M. A. WIZNER, S. SINGHAWANGCHA, R. M. BARKLEY and R. E. SIEVERS*
Department of Chemistry and Cooperative Institute for Research in Environmental Sciences, University of Colorado, Campus Box 449, Boulder, CO 80309 (U.S.A.)

SUMMARY

A survey of signal enhancements for various classes of compounds was made using selective electron-capture sensitization (SECS) with nitrous oxide-doping. This technique was used to aid in the identification of five phenolic compounds in a complex oil shale waste water fraction. The three-fold difference in the enhancements found for *ortho*- and *para*-toluidine and the twenty-fold difference for benzo[*a*]pyrene and benzo[*e*]pyrene indicate that SECS can be valuable for identifying these isomers. Enhancement factors are presented for other aromatic and heterocyclic compounds. The signal from water was enhanced 260-fold, allowing trace determinations at part-per-million concentrations.

INTRODUCTION

The sensitivity of an electron-capture detector (ECD) to a variety of compounds that do not rapidly attach electrons can be enhanced markedly by the addition of nitrous oxide to the carrier gas stream of a gas chromatograph. The basis of this enhancement is the application of ion-molecule chemistry to reduce electron density in the cell indirectly. For the case when N_2O is added, the reactive ion is O^- (ref. 1). Signal enhancement is observed when the rate of the reaction between O^- and an analyte is faster than direct attachment of electrons. A similar sensitization has been observed by Grimsrud and co-workers[2,3] when O_2 is added to the carrier gas. In that case, O_2^-, which is in equilibrium with neutral O_2 and free electrons, is the reactant with analytes.

The sensitivity of an ECD toward carbon dioxide, carbon monoxide, hydrogen and hydrocarbons can be enhanced by the addition of N_2O to the nitrogen carrier gas stream and we have termed the technique selective electron-capture sensitization (SECS)[4,5]. It has also been shown that SECS with N_2O can lead to an improved sensitive analysis of vinyl chloride in air[6]. In the present paper, we report data for nitrous oxide-induced signal enhancements for various other classes of compounds. Because the magnitude of signal enhancement appears to be quite reproducible for a given compound and varies greatly from one compound to another, these data could

0021-9673/82/0000–0000/$02.75

aid in the qualitative identification of compounds in complex matrices. Analysis of phenolic compounds in an oil shale waste water sample exemplifies this type of application. Studies of aromatic amines and polynuclear aromatic hydrocarbons (PAHs) show substantially differing sensitivities for closely related positional isomers, which, when coupled with comparing retention indices, can be very helpful in confirming isomer identifications. Marked improvement in the detection limit for water by N_2O doping will be demonstrated. Additionally, anomalous responses sometimes occurring in the ECD operated in the SECS mode will be discussed.

EXPERIMENTAL

Instruments

Most of the experiments were carried out with Hewlett-Packard (HP) Models 5730 and 5713 gas chromatographs with 15 mCi ^{63}Ni constant-current ECDs. The Model 5730 gas chromatograph with dual flame ionization detectors (FIDs) and single ECD was equipped with a Grob-type split/splitless capillary injector[7]. The effluent from the ECD was passed through a heated 25 cm × 1/8 in. O.D. stainless-steel tube which was connected to one of the FIDs. This aided in confirming the identity of peaks by allowing simultaneous recording of the ECD and FID responses[8]. The Model 5713 gas chromatograph, equipped with a single ^{63}Ni ECD, a Grob-type capillary injector, and a 10-port Valco gas sampling valve, was also used in these experiments. Both ECDs on these instruments are identical in design and performance. A Tracor Model 560 gas chromatograph equipped with a ^{63}Ni ECD and a Tracor capillary injection system was used for some experiments. The Tracor ECD has a coaxial design with a considerably larger cell volume than the pin-in-cup design of the Hewlett-Packard detector. The Tracor detector also has the capability to be operated at 400°C, compared to a temperature limit of 350°C for the Hewlett-Packard ECD. The higher temperature capability constitutes a definite advantage for SECS experiments with N_2O owing to the temperature sensitivity of the formation of O^- (ref. 4).

The detector pulsing rate of all ECDs was monitored with a frequency counter connected to the detector pulse circuitry. Frequency measurements provide an indication of the relative cleanliness of the electron-capture cell and help determine whether the system is operating properly[9].

Gas purification and mixing

USP grade nitrogen (General Air, Denver, CO, U.S.A.) was used for carrier gas and make-up gas. Electronic grade nitrous oxide (Scientific Gas Products, South Plainfield, NJ, U.S.A.) was added to the carrier gas. Before use, all gases were passed through 3/8 in. O.D. copper tubing containing molecular sieve 13X which had been activated by passing nitrogen through the sieves while heating at 350°C. The nitrogen carrier gas was passed through an oxygen scrubber composed of 3/8 in. copper tubing packed with R3-11 (Chemical Dynamics, South Plainfield, NJ, U.S.A.), a copper-containing catalyst, before it entered the molecular sieve cartridge. This catalyst must be activated by passing hydrogen through the catalyst while heating to 150°C[11].

Two different devices were used to introduce nitrous oxide into the carrier gas. The first device[10] was a 0.25 mm I.D., type 316 stainless-steel capillary tube that was

crushed nearly flat with a vice and twisted 3 complete turns over a length of approximately 5 cm (see Fig. 1). This flow restricting twisted capillary device was connected to both the HP 5713 and the Tracor instruments through a stainless-steel tee placed in the carrier gas line before it enters the gas chromatograph.

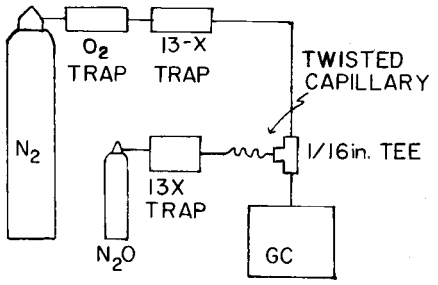

Fig. 1. Twisted capillary method for the addition of N_2O.

A permeation device similar to one used by Goldan *et al.*[6] was constructed by sealing the end of a 1.5 mm O.D., 0.5 mm I.D. PTFE tube by melting the end of the tube in the heated tip of a sealed disposable glass pipet. The sealed end of the PTFE tube extends about 2 cm into a tee interposed into the carrier gas line. This particular permeation device was used with the HP 5730 chromatograph.

The column flow-rate for all packed-column analyses was either 30 or 40 ml min^{-1}; the N_2O level was approximately 20 ppm.

Chemicals

All chemicals analyzed were obtained either from Chem Service (West Chester, PA, U.S.A.) or Aldrich (Milwaukee, WI, U.S.A.). Solvents used for preparing standards were of the highest purity available. Distilled-in-glass hexane and toluene were purchased from Burdick & Jackson (Muskegon, MI, U.S.A.) and Nanograde cyclohexane was obtained from Mallinckrodt (St. Louis, MO, U.S.A.). For those analytes with boiling points less than 120°C, it was necessary to redistill these solvents to remove compounds that produced interfering peaks in the solvent chromatograms[12].

When N_2O was present in the carrier gas, all the analyses performed with the HP gas chromatographs were at 350°C, the detector temperature of maximum sensitivity[5]. Under normal electron-capture mode, most analyses were carried out at 350°C with the exception of the PAHs for which the detector temperatures were either 250 or 350°C. Identifications of compounds were confirmed by retention time analysis using an FID.

Calculations

A signal enhancement value was calculated by dividing the response of the detector in the SECS mode by the response observed with normal electron capture for the same amount of compound.

$$\text{Signal enhancement} = \frac{\text{Peak height with } N_2O}{\text{Peak height without } N_2O}$$

This value reflects the rate of reaction for the analyte with O^- relative to normal electron-capture mechanisms. It is most useful in detector response ratioing or in identification of unknown peaks in the chromatogram.

When 20 ppm N_2O was present in the carrier gas, the noise level normally increased to approximately 4 to 5 times that during normal operation without nitrous oxide addition. To reflect the true improvement in detection limits attainable with N_2O doping, a signal-to-noise (S/N) enhancement must be calculated.

$$\text{Signal-to-noise enhancement} = \frac{\text{S/N with } N_2O}{\text{S/N without } N_2O}$$

RESULTS AND DISCUSSION

Identification of phenols in oil shale waste water

The signal enhancement that is observed when nitrous oxide is added to the carrier gas of an ECD can be used to assist in identifying the compounds giving rise to particular chromatographic peaks in very complex matrices. This approach was used to help identify five phenolic compounds in a waste water sample derived from the pyrolysis of oil shale.

A sample of waste water was obtained from a Colorado oil shale retorting process. This water was steam distilled and the distillate components extracted into hexane with a Nielsen–Kryger apparatus as the condensed steam passed through a layer of this solvent. After removal of most of the hexane by roto-evaporation, 2 μl of the condensed sample were injected (split injection technique) into a gas chromatograph for analysis. A 25-m long fused-silica capillary column (0.25 mm I.D.) coated with Carbowax 20M (Hewlett-Packard, Avondale, PA, U.S.A.) was used to separate the components with the Model 5730 chromatograph. Fig. 2 depicts the analysis of this sample with an ECD operating in the normal and sensitized modes. The complex nature of this sample, even after fractionation, can be seen in both chromatograms. Although the resolution of the capillary column was excellent, there was still a large number of unresolved peaks. Identification of these peaks is ordinarily very difficult without an expensive gas chromatography–mass spectrometry (GC–MS) system. Even with a GC–MS system one may have problems with sensitivity and isomer identification with such a complex sample containing so many overlapping peaks. Indeed, attempts to analyze the sample by GC–MS failed to identify the phenolic components in this sample because of their low concentration and the complexity of the mixture. However, it was possible to identify these components by GC–MS in a different sample (toluene fraction of liquid–liquid extraction) in which the phenols were present in higher concentration than in the distillate.

The identification of the GC peaks by ECD was carried out in a number of ways. Addition of N_2O to the carrier gas produced a large increase in size of a number of peaks in the chromatogram. This allowed more ready location of these peaks from one chromatogram to another. A number of compounds that could possibly be present in this sample were obtained in their pure form and retention times measured in a search for compounds that would match the enhanced sample peaks. When several possible matches were found, each compound was tested to see whether and how much the signal for it was enhanced by SECS (Table I). Finally, a small amount

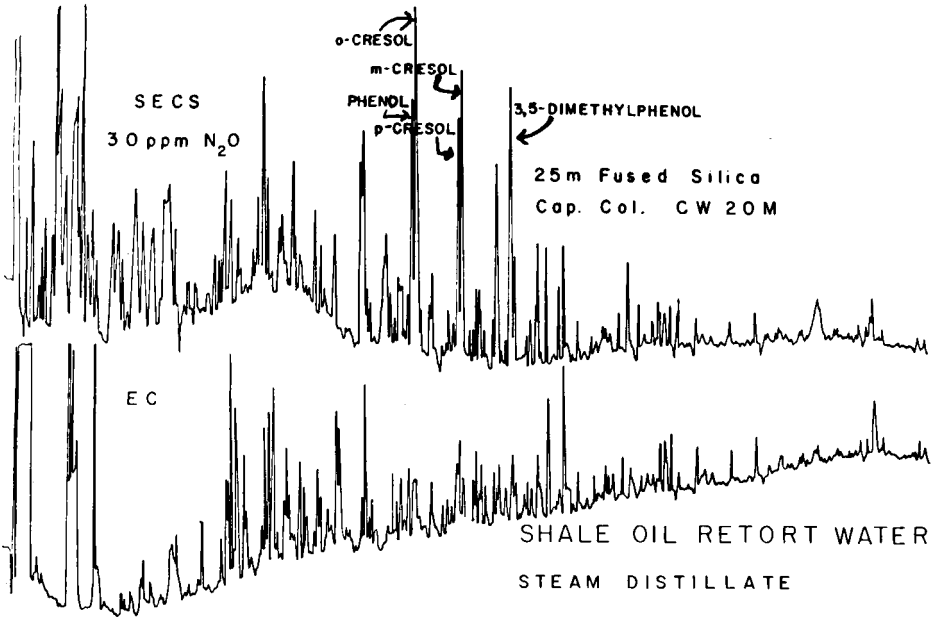

Fig. 2. Identification of phenols in shale oil waste water. 2-μl split injection, temperature program: 50–200 °C at 2 °C min^{-1} make-up flow-rate, detector temperature 350 °C. Top, SECS with 30 ppm N_2O in N_2 carrier gas stream. Bottom, same sample analyzed by ordinary (ECD) without N_2O.

of the pure compound corresponding to each suspected analyte was added to the original hexane sample and the analysis re-run to confirm the identifications. This allowed identification of the peaks with a relatively high degree of certainty. Even higher levels of certainty can be attached if the degree of enhancement matches that of authentic samples. This constitutes a form of signal ratioing. The presence of phenolic components in a sample related to oil shale is not unusual[13], but the identification of these compounds in a very complex matrix at levels too low to be detected with a GC–MS system is significant.

This analysis of an oil shale waste water fraction exemplifies the use of SECS enhancement to identify compounds in a very complex sample. Because only certain compounds were enhanced, only some peaks showed large changes, making the identification of these compounds much simpler.

TABLE I

SECS ENHANCEMENT OF PHENOLS

Compound	*Signal enhancement*	*S/N enhancement*
Phenol	7	2
o-Cresol	14	4.5
m-Cresol	12	4
p-Cresol	5	1.5
2.6-Dimethylphenol	6	2
3.4-Dimethylphenol	12	4
3.5-Dimethylphenol	12	4

Aromatic amines

The SECS detector response produced by a number of aromatic amines was investigated. For these analyses a 30-m fused-silica capillary column coated with SP-2100 (J & W Scientific, Orangevale, CA, U.S.A.) was used with the HP 5713 gas chromatograph. Samples of 1–100 ng of the amines in hexane were injected (splitless). At low nanogram levels, there appeared to be some irreversible adsorption of aromatic amines in this system. This may be due to the intrinsic acidic nature of the fused-silica surface or to the activity of the wall of the silanized glass injection port insert. Attempts to solve the adsorption problem led us to investigate two other columns: a 2 m × 2 mm I.D. glass column packed with 4% Carbowax 20M + 0.8% KOH on Carbopack B (Supelco) and a 2 m × 2 mm I.D. glass column packed with 5% KOH on Chromosorb 102. Both of these had earlier been reported to be very satisfactory for analysis of amines[14,15]. Due to excessive column bleed and appearance of various ghost peaks from both columns, even after one week of conditioning, we were unable to use these columns for analyses of amines.

All six of the amines studied showed large enhancements and exhibited some interesting isomeric effects. Table II contains the observed signal enhancement values.

TABLE II

SECS ENHANCEMENT OF AMINES

Compound	*Signal enhancement*	*S/N enhancement*	*Boiling point (°C)*
Aniline	70	20	184
N-Methylaniline	46	12	196
N,N-Dimethylaniline	38	9	194
o-Toluidine	100	25	200
m-Toluidine	35	9	203
p-Toluidine	35	9	200

The differences in the toluidine signal enhancements presented an excellent example of how SECS could be a valuable tool for isomer identification. *Ortho-* and *para*-toluidine have the same boiling points, but they can be separated with some columns. The three isomers of toluidine exhibit different enhancement values so these data can be used together with retention data to confirm the identifications. The addition of N_2O to the carrier gas of an ECD makes it possible to determine relative response factors for each analyte. Comparison of these values with values obtained from standards allows ready identification of which isomer is present or indicates that a peak consists of a mixture of two or more compounds.

Polynuclear aromatic hydrocarbons

PAHs were studied to determine whether SECS could be used as a tool to aid in the identification of these compounds. It was also of interest to compare results using N_2O doping with those obtained by the O_2-doping technique of Grimsrud and Miller[16] and Miller *et al.*[17].

Several workers[18,19] have shown that PAH molecules capture thermal electrons in a non-dissociative manner and therefore larger responses for these com-

pounds could be obtained by operating the electron capture detector at lower detector temperatures. For this reason, the responses for PAHs when N_2O is added to an ECD at 350°C have also been compared to the normal ECD responses at 250°C. This is a more realistic measure of the improvement in sensitivity of this new method over one currently in use. The detector temperature, 250°C, was chosen to maintain a detector temperature 50°C above the maximum column temperature.

The results for seventeen PAHs are shown in Table III. These compounds were analyzed with a 1 m × 2 mm I.D. glass column packed with 3% OV-17 on Gas-Chrom Q, that was installed in the Model 5713 chromatograph. The carrier gas was 25 ppm N_2O in nitrogen at a flow-rate of 30 ml min^{-1}. Samples ranging from 1 to 50 ng of PAH per injection were prepared by dilution with toluene.

TABLE III

SECS ENHANCEMENT FOR POLYNUCLEAR AROMATIC HYDROCARBONS

Compound	*Detector temperature 250°C**		*Detector temperature 350°C*	
	Signal enhancement	*S/N enhancement*	*Signal enhancement*	*S/N enhancement*
Anthracene	3.2	0.8	6.3	1.6
9-Methylanthracene	1.5	0.4	5.9	1.5
Phenanthrene	9.7	2.4	8.1	2.0
Tetracene	1.4	0.4	1.6	0.4
1,2-Benzanthracene	1.3	0.3	3.2	0.8
Chrysene	5.5	1.4	6.5	1.6
Triphenylene	9.5	2.4	17	4.3
Pyrene	6.8	1.7	11	2.8
Benzo[*a*]pyrene	0.6	0.2	1.7	0.4
Benzo[*e*]pyrene	3.5	0.9	34	8.5
Perylene	3.2	0.8	6	1.5
Acenaphthene	4.0	1.0	4.0	1.0
Fluorene	1.2	0.3	1.5	0.4
Dibenzofuran	17	4.3	29	7.3
Dibenzothiophene	18	4.5	25	6.3
Carbazole	3.2	0.8	8.4	2.1
Acridine	3.7	0.9	14.4	3.6

* SECS response at a detector temperature of 350 C divided by the ECD response at 250°C.

The signal enhancements observed for many of these compounds were relatively small. However, there were substantial differences in enhancement factors for a few of the fused ring systems. The most notable effect of structural variation is illustrated in the case of benzo[*e*]pyrene contrasted with benzo[*a*]pyrene, for which the signal enhancement values differed by a factor of twenty. This may be due partly to the fact that at 350°C the normal EC response of benzo[*e*]pyrene is significantly smaller than that of benzo[*a*]pyrene. The enhancement for triphenylene was also significantly larger than those for the other compounds containing four fused aromatic rings. Overall, the more linear fused ring systems tended to exhibit smaller enhancements. Therefore, for certain compounds, it would be possible to use relative enhancement values to differentiate isomers in a difficult analysis of PAHs. This is particularly significant because the mass spectra of isomers of PAHs are very similar, and not of much use in assessing which isomer(s) are present.

Dibenzofuran, dibenzothiophene, carbazole and acridine are heterocyclic molecules in which oxygen, nitrogen or sulfur are included in the ring system. The signal enhancement values differ widely, from 1.5 for fluorene to 28.5 for dibenzofuran. All heterocyclic compounds exhibited much larger enhancements than fluorene, the carbon analog.

From a comparison of our signal enhancements with those reported by Miller *et al.*[17] several interesting features can be noted. Triphenylene and dibenzothiophene exhibited relatively large enhancements with N_2O addition, although they were among the least enhanced compounds when O_2 was added. Substitution of a methyl group at the 9-position of anthracene decreased signal enhancement slightly with N_2O, while the response enhancement values increased by a factor of two with O_2.

For determination of actual improvement in detection limits of PAHs, the SECS response was compared to the response from the ECD operating normally without N_2O at 250°C. The increased noise levels resulting from the addition of N_2O must also be taken into account. The noise level when N_2O was present is approximately four times that without N_2O. The best signal to noise enhancement from our data was achieved with dibenzothiophene, for which the detection limit could be lowered by a factor of 4.5. Of the seventeen PAHs studied, there are only six compounds with signal-to-noise enhancements greater than one. Signal-to-noise enhancement values less than one are actually degradations in sensitivity that are only useful to aid in the identification of compounds if detector-ratioing schemes are employed.

Cyclic heteroatomic compounds

The effect of the presence of a hetero atom on the observed enhancement was investigated further by examining the detector responses for a number of cyclic compounds containing a sulfur, nitrogen or oxygen atom (Table IV). These analyses were performed with the HP 5730 instrument using a 25-m fused-silica capillary column coated with SE-54. Whenever possible, splitless injections were used for sample introduction. For thiophene and other compounds with boiling points below 110°C it was necessary to use split injections under isothermal conditions in order to obtain adequate separation of the analyte from the hexane solvent tail. Furan and tetrahydrofuran proved particularly difficult to resolve from hexane. In the case of furan, it was necessary to use toluene as the solvent and measure the furan response before the solvent was eluted. For tetrahydrofuran, it was necessary to use a 10 ft. × 2 mm I.D. glass column packed with 100–120 mesh Supelcoport with a 10% loading of SP-2250. The last analysis was performed using the Tracor instrument, raising the possibility that the enhancement observed may not be strictly comparable to the results for the other compounds measured with the HP instrument. However, in most cases the responses of the Tracor chromatograph were very similar, if not essentially identical, to those obtained with the HP instrument. It should be noted that the enhancement values reported here are not necessarily a constant for a given compound, but are dependent on detector design and cleanliness and may be dependent on other factors. It is necessary to determine these factors for a given instrument on a periodic basis as detector cleanliness changes.

Examination of the first five entries in the Table IV reveals that responses of all nitrogen-containing compounds were enhanced to a certain extent. The responses of the first four compounds demonstrate that the detection of aromatic compounds was

TABLE IV

SECS ENHANCEMENT FOR HETEROATOMIC COMPOUNDS

Compound	*Signal enhancement*	*S/N enhancement*
Pyrrole	75	15
Pyrrolidine	20	4
Pyridine	45	11
Piperidine	5	1
Quinoline	7.5	2
Furan	−*	–
Tetrahydrofuran	800	120**
2.5-Dimethylfuran	0.8	0.3
p-Dioxane	7	1.5
Thiophene	1.8	0.3
Tetrahydrothiophene	25	5

* Response to 100 ng of furan without and with N_2O = +88 mm peak height.

** Analysis performed with Tracor 560 gas chromatograph at a detector temperature of 400°C; all other measurements made with HP 5730 gas chromatograph at 350°C.

enhanced to a greater degree than that of their saturated analogues. Addition of one or two benzene rings to pyrrole or pyridyl moieties resulted in smaller enhancements. The response enhancements for quinoline, acridine and carbazole demonstrated that the nitrogen-compounds had improved responses over those of the carbon analogues, naphthalene, anthracene and fluorene.

The oxygen-containing compounds produced more unusual responses. Furan produced a small positive response with normal electron capture, but addition of N_2O to the N_2 carrier gas resulted in a large negative response when furan is eluted. This negative response increased with the concentration of furan in the solvent, asymptotically approaching a limit determined by an injection of neat furan. The signal for dimethylfuran was always positive, although not enhanced by N_2O. Tetrahydrofuran displayed a large signal enhancement with N_2O when the Tracor chromatograph was operated with the detector temperature at 400°C. Dibenzofuran exhibits a much larger signal enhancement than that of furan. This effect was the reverse of that observed with the analogous nitrogen heterocycles, carbazole and pyrrole.

The signals produced for SECS of sulfur-containing compounds appear to be intermediate in magnitude to those for the nitrogen- and oxygen-containing compounds. The enhancement of the thiophene signal was very small, but this could be considered intermediate between the negative response for furan and the large enhancement observed for pyrrole. The tetrahydrothiophene signal exhibits an enhancement less than the aromatic analogue thiophene, the reverse of the trend observed for nitrogen compounds. However, the value was greater than that of pyrrolidine and less than that of tetrahydrofuran.

Aromatic compounds

Analyses of aromatic compounds were done on a 3 m × 2 mm I.D. glass column packed with 10% SP-2250 on Supelcoport. Examination of signal enhancement values of these compounds indicates that addition of N_2O to the ECD improved

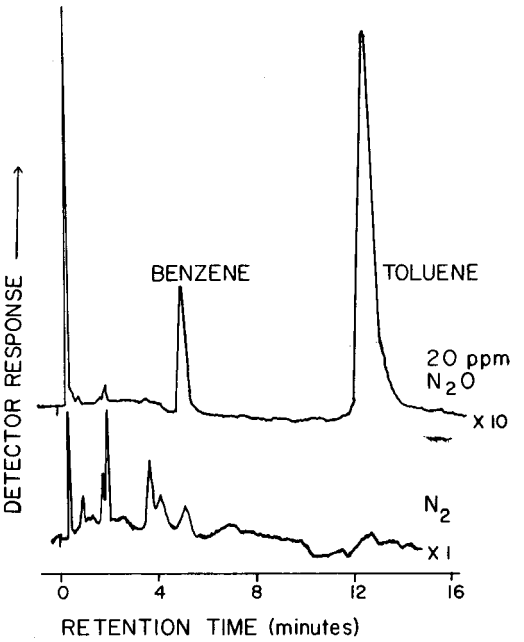

Fig. 3. Response enhancement of benzene and toluene with and without N_2O. Tracor gas chromatograph. 3 m × 2 mm I.D. glass column packed with 10% SP-2250 on 100–120 mesh Supelcoport at 40°C with 45 ml min^{-1} carrier flow, detector temperature 400°C. The sample contained 100 ng each of benzene and toluene.

these responses significantly (see Table V). The detector response for benzene and toluene with and without N_2O in the carrier gas is depicted in Fig. 3.

All aromatic compounds studied produced somewhat unusual responses with the ECD. Benzene signals appeared to be extremely sensitive to impurities in the carrier gas. Under some circumstances, it exhibited negative response with normal electron capture[5]. Styrene, however, always produces a negative response with normal electron capture and positive response when N_2O is added. Biphenyl and naphthalene sometimes produce a "W"-shaped peak, which will be discussed in the section on anomalous responses.

Although the detector responses to all these compounds were increased when N_2O was present, their sensitivities were not superior to those obtainable with an

TABLE V

SECS ENHANCEMENT FOR AROMATIC COMPOUNDS

Compound	*Signal enhancement*	*S/N enhancement*
Benzene	50	10
Toluene	150	30
Naphthalene	9.4	2.4
Biphenyl	44	11
p-Methylbiphenyl	17	43
m-Dimethoxybenzene	26	8.5

FID. However, because SECS makes it possible to detect both *n*-alkanes and aromatic compounds used as retention index standards, this may facilitate compound identification based on retention indices when ECDs are used.

Water

Water exhibited a relatively large enhancement factor, 260 (Fig. 4), and can be sensitively detected with SECS. Unfortunately, the Porapak Q column operating at 110°C exhibited a substantial level of bleed, resulting in a high baseline when N_2O was present in the carrier gas. Therefore, signal-to-noise enhancement with the Porapak column was only a factor of 21. The major problem with the chromatography of water is poor column performance. Porapak Q has been the most common column packing used for GC determination of water; however, recent evidence indicates that these columns cannot be used for the determination of water in most solvents because the solvent can displace the small amount of water adsorbed on the surface of the styrene–divinylbenzene polymeric beads[20]. This could create false peaks if the solvent were eluted before the water. To avoid solvent displacement of water, a 100-μl gas sample loop was constructed from 1/16 in. O.D. PTFE tubing to introduce gas samples containing water. A flowing gas system consisting of a bubbler filled with distilled water, thermostated at 30°C, and a tee to add dry make-up gas (air) was connected to the gas sample loop with 1/4 in. O.D. PTFE tubing. In this way a gas stream saturated with water vapor at 30°C could be diluted to desired levels with dry air. It appears that, with suitable low-bleed columns that give sharp peaks without tailing for water,

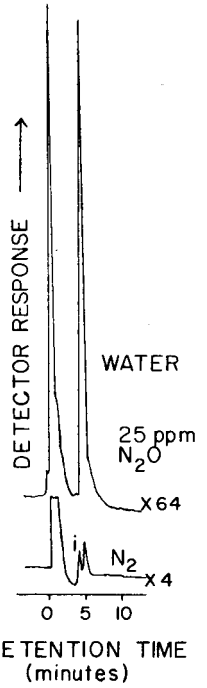

Fig. 4. Response enhancement of water with and without N_2O. Sample was 3 ng of water, 1.8 m × 2 mm I.D. glass column packed with Porapak Q at 110°C. The peak labelled "i" was an impurity.

it should be possible to measure water sensitively by SECS. As a corollary, attention must be paid to drying the carrier gas carefully.

Anomalous responses

The fact that SECS can enhance the detector signal for a compound to which the ECD does not respond has led to the study of many compounds that would not normally be analyzed by electron capture. Some compounds have produced unusual detector responses. The requirement that the detector be operated at a relatively high temperature (350°C) when N_2O is added to the carrier gas has also led to some interesting signals for other compounds that are normally analyzed at much lower detector temperatures with normal electron capture.

A good example of this is the negative response observed for some PAHs and aromatic hydrocarbons. This negative response was not simply an inverted peak, as Grimsrud and Miller[16] have reported, but rather a "W"-shaped peak. The leading edge of the negative response was very sharp, but the bottom of the peak was generally rounded and the return to the baseline was very slow. As more of the compound was injected, a positive peak would appear, superimposed on the negative component of the peak. The mirror image (positive peak) would appear to tail very badly. If a very large amount of analyte were injected, the negative component would appear as a slight drop in the baseline just before the large positive peak. The negative component was observed with pure nitrogen and sometimes with N_2O in the carrier gas and when using either packed or capillary columns. The size of the negative peak seemed to be influenced largely by the cleanliness of the septum and the amount of column bleed. Therefore, avoidance of negative and other anomalous responses depends in part on maintaining as clean a chromatographic flow system as possible. It appeared that whenever a compound produced a very poor detector response, there was a strong possibility of observing negative peaks.

For the purpose of estimating enhancements, only the positive component of the peak was used. The peak height was measured from the base of the negative signal to the top of the sharp positive peak.

A second type of negative peak was observed for olefin compounds. This was truly a negative peak, reasonably symmetrical, similar to that recorded for hydrogen at low detector temperature[4]. There was no positive component, and the magnitude of the peak increases in the negative direction (decreasing frequency) with increasing amount of analyte injected. Hexene and octene are examples of compounds that produce such negative peaks with or without N_2O present in the carrier gas.

ACKNOWLEDGEMENTS

Support for this research was provided by AFOSR under Grant No. 80-0011 and by DOE under contract DE-EV10298.

REFERENCES

1 R. Marx, G. Mauclaire, F. C. Fehsenfeld, D. B. Dunkin and E. E. Ferguson, *J. Chem. Phys.*, 58 (1973) 3267.
2 E. P. Grimsrud and D. A. Miller, *Anal. Chem.*, 50 (1978) 1141.
3 E. P. Grimsrud and R. G. Stebbins, *J. Chromatogr.*, 155 (1978) 19.

4 M. P. Phillips, P. D. Goldan, W. C. Kuster, R. E. Sievers and F. C. Fehsenfeld, *Anal. Chem.*, 51 (1979) 1819.
5 R. E. Sievers, M. P. Phillips, R. M. Barkley, M. A. Wizner, M. J. Bollinger, R. S. Hutte and F. C. Fehsenfeld, *J. Chromatogr.*, 186 (1979) 3.
6 P. D. Goldan, F. C. Fehsenfeld, W. C. Kuster, M. P. Phillips and R. E. Sievers, *Anal. Chem.*, 52 (1980) 1751.
7 K. Grob and K. Grob, Jr., *J. High Resolut. Chromatogr. Chromatogr. Commun.*, 1 (1978) 57.
8 A. Södergren, *J. Chromatogr.*, 160 (1978) 271.
9 C. Burgett, *Hewlett-Packard Service Note 5700A-6, Gas Purity Check and Standing Frequency Measurement*, Hewlett-Packard, Avondale, PA, 1972.
10 V. Pretorius, *J. High Resolut. Chromatogr. Chromatogr. Commun.*, 2 (1979) 10078.
11 *Technical leaflet on BASF Catalyst R3-11*, Chemical Dynamics Corp., South Plainfield, NJ, 1971.
12 W. D. Bowers, M. L. Parsons, R. E. Clements, G. A. Eiceman, F. W. Karasek, *J. Chromatogr.*, 206 (1981) 279.
13 J. S. Stanley, *Investigation of Trace Elements and Organic Ligands in Oil Shale Waste, Ph.D. Thesis*, University of Colorado, Boulder, CO, 1981.
14 F. Raulin, P. Price and C. Ponnamperuma, *Amer. Lab.*, 12 (1980) 45.
15 K. Kazuhiro, Y. Yamazaki and M. Uebori, *Anal. Chem.*, 52 (1980) 1980.
16 E. P. Grumsrud and D. A. Miller, *J. Chromatogr.*, 192 (1980) 117.
17 D. A. Miller, K. Skogerboe and E. P. Grimsrud, *Anal. Chem.*, 53 (1981) 464.
18 J. E. Lovelock, A. Zlatkis and R. S. Becker, *Nature (London)*, 84 (1962) 540.
19 W. E. Wentworth and R. S. Becker, *J. Amer. Chem. Soc.*, 84 (1962) 4263.
20 C. P. M. G. A'Campo, S. M. Lemkowitz, P. Verbrugge and P. J. van den Berg, *J. Chromatogr.*, 203 (1981) 271.

Journal of Chromatography, 239 (1982) 159–171
Elsevier Scientific Publishing Company, Amsterdam — Printed in The Netherlands

CHROM. 14,582

VOLATILE CONSTITUENTS OF THE PRODUCED WATER EFFLUENT FROM THE BUCCANEER GAS AND OIL FIELD*

BRIAN S. MIDDLEDITCH
Department of Biochemical and Biophysical Sciences, University of Houston, Houston, TX 77004 (U.S.A.)

SUMMARY

The volatile constituents of the effluent are concentrated on Tenax-GC using an automated purge-and-trap device and are then examined by combined gas chromatography–mass spectrometry. Some 200 compounds are resolved using a bonded-phase fused-silica column, and they are characterized with the aid of several data manipulation techniques. While the *n*-alkanes are the individual compounds found in highest concentration, the alkylaromatic hydrocarbons comprise a significant proportion of the total hydrocarbons.

INTRODUCTION

Between 1975 and 1980, the Bucanneer Gas and Oil Field, located in the nortwestern Gulf of Mexico (50 km south of Galveston, Texas), was studied extensively by 25 research groups working under the aegis of the National Marine Fisheries Service and the Environmental Protection Agency (EPA)[1]. Two components of this study focused on the hydrocarbon constituents of the effluents and their distribution in the environment. Brooks *et al.*[2] examined "gaseous" (C_1–C_5) and "volatile liquid" (C_6–C_{14}) hydrocarbons, while Middleditch and co-workers[3–11] concentrated on the "high-molecular-weight" (C_{14}+) hydrocarbons. The latter group also performed some analyses of the volatile liquid hydrocarbons[11].

Although it had earlier been demonstrated that detailed analyses for volatile liquid hydrocarbons could be performed in the research laboratory by preconcentration on Tenax-GC followed by gas chromatography–mass spectrometry (GC–MS) with glass or metal capillary columns[12], these procedures were time-consuming and impractical for the routine analysis of large numbers of samples. Accordingly, Brooks *et al.* employed the gas chromatographic procedure described by Sauer *et al.*[13]. They reported only eighteen C_6–C_{14} hydrocarbons in effluents and 30 in seawater[2]. Middleditch and co-workers used the GC–MS procedure mandated by the EPA for organic priority pollutants[14], and characterized 31 volatile constituents of effluents[11].

With the expectation that improved analytical techniques might subsequently be developed, representative samples from the Buccaneer field were archived by the various investigators. We have used some of these samples to develop a procedure for the examination of some 200 volatile liquid hydrocarbons in effluents.

* Dedicated to Professor E. C. Horning on the occasion of his 65th birthday.

0021-9673/82/0000–0000/$02.75

EXPERIMENTAL

Samples

The effluent discharged from the production platforms in the Buccaneer field consists of small droplets of oil suspended in brine. Thus, the hydrocarbon composition of the effluent is very similar to that of the light oil which floats to the surface in the separator tanks which comprise the final stage of effluent treatment prior to discharge. Samples of separator tank oil were collected from production platform 296-B in the Buccaneer field on January 14, 1979.

Instrument

The gas chromatograph–mass spectrometer employed for these analyses was a modified Finnigan 1020/OWA instrument. Preconcentration of the volatile hydrocarbons was performed using a Hewlett-Packard 7675A automated purge-and-trap device. The effluent tube from this device was connected in place of the carrier gas line to the sample splitter of the gas chromatograph. The gas chromatograph was equipped with a 30 m × 0.32 mm I.D. DB-5 bonded-phase fused-silica capillary column (J&W Scientific). The outlet of this column was connected directly into the ion source of the mass spectrometer.

Procedure

A 1-μl volume of the separator tank oil was added to 5 ml of prepurged water in a 15-ml centrifuge tube attached to the purge-and-trap device. The sample was purged with helium for 5 min, and the volatiles collected in the trap containing Tenax-GC. The trap was heated to 200°C for a further 5 min to desorb the volatiles into the gas chromatograph. During the desorption stage, three 5-cm diameter coils of the column (close to the inlet end) were immersed in liquid nitrogen in a polystyrene cup. When the desorption was complete, the liquid nitrogen was removed and the GC–MS analysis was initiated. The column was programmed from 0 to 250°C at 5°C/min. Spectra were scanned from m/z 40 to 500 every 0.5 sec, and were stored on a magnetic disc.

RESULTS AND DISCUSSION

When an automated purge-and-trap device is used with a packed gas chromatographic column, the sample would normally be desorbed onto the column at room temperature. This is impractical with capillary columns, where it is essential that the sample be introduced to the column in a sharp "plug" to preserve the resolution. Since the fused-silica columns are flexible, it was quite convenient to immerse three tights coils of the column in liquid nitrogen during the desorption step. It is possible that the capacity of a small number of coils might be inadequate to contain a large sample, so that break-through and "ghosting" might occur, but we have not encountered this problem. However, this phenomenon was occasionally a problem when, during earlier experiments, we concentrated the sample by freezing a loop of the transfer line between the purge-and-trap device and the gas chromatograph.

Tenax-GC is hydrophobic so that, theoretically, hydrocarbons and related compounds are collected in the trap while water vapor passes through it during the purge cycle. In practice, however, a small amount of water is usually retained in the

trap and is subsequently desorbed into the column along with the volatiles. Repeated use of a purge-and-trap device with columns containing water-sensitive stationary phases (such as silicones) leads to their degradation. This is a particular problem with capillary columns coated with silicone stationary phases. Accordingly, the procedure mandated by the EPA for the analysis of volatile organic priority pollutants employs a packed column containing Carbopack coated with Carbowax.

We have found that a bonded-phase fused-silica column can be used repeatedly with an automated purge-and-trap devide without loss of gas chromatographic resolution. Figs. 1–4 show a reconstructed ion chromatogram for an analysis of separator tank oil. The column employed for this analysis had been in almost constant use for 4 months, yet the resolution obtained was still quite adequate.

The high resolution attainable with the bonded-phase fused-silica column dictates that the repetitive mass spectra scans be very fast. With 1-sec scans, it was not possible to reconstruct chromatograms with any degree of fidelity. Even with 0.5-scans, we were usually only able to acquire three to four scans per component.

Not all of the components of the sample were fully resolved, but the Finnigan data system provided assistance in the characterization of partially resolved pairs of compounds.

One method for detecting partially resolved components relies upon the use of the Biller–Biemann algorithm[15]. This procedure indicates scan numbers at which four or more m/z values achieve maximum intensity. This technique is illustrated in Figs. 5–7 for benzene and cyclohexane. The reconstructed ion chromatogram (Fig. 1) contained a peak which maximized at scan 382. The Biller–Bieman algorithm indicated that this peak contained two components, maximizing at scans 381 and 384, respectively. These two spectra are reproduced as Figs. 5 and 6. The spectrum in Fig. 5 is that of cyclohexane, with a molecular ion of m/z 84 and prominent ions of m/z 41, 56, and 69. Fig. 6 gives the spectrum of benzene, with a molecular ion and base peak of m/z 78. Even though these compounds are not resolved, their spectra are remarkably "clean". There is only a small peak of m/z 78 in Fig. 5 and, conversely, only a small peak of m/z 84 in Fig. 6. The Finnigan "spectral enhancement" routine removes these contaminating ions completely. Fig. 7 shows a portion of the reconstructed ion chromatogram along with mass chromatograms for m/z 78 and 84, to illustrate further the degree of resolution between these compounds.

The Biller–Biemann algorithm fails to detect compounds with fewer than four intense ions in their spectra. In such cases reconstructed mass chromatograms can be examined in a search for additional compounds. For example, the algorithm revealed the presence of 2-methylnaphthalene at scan 2810, but gave no indication of the presence of 1-methylnaphthalene. The two most intense ions in the spectra of the methylnaphthalenes are the molecular ion and the $[M-1]^+$ ion, at m/z 142 and 141, respectively. Appropriate mass chromatograms showed that these two ions maximized at scan 2865, and an enhanced spectrum matched with that of 1-methylnaphthalene. This compound coeluted with *n*-tridecane (scan 2869).

Other pairs of unresolved compounds defy deconvolution. *m*-Xylene and *p*-xylene coelute at scan 1195 and have very similar spectra. It is impossible to determine the relative concentrations of these compounds from the data obtained in this analysis. Such analyses will have to await the development of more polar bonded-phase fused-silica columns.

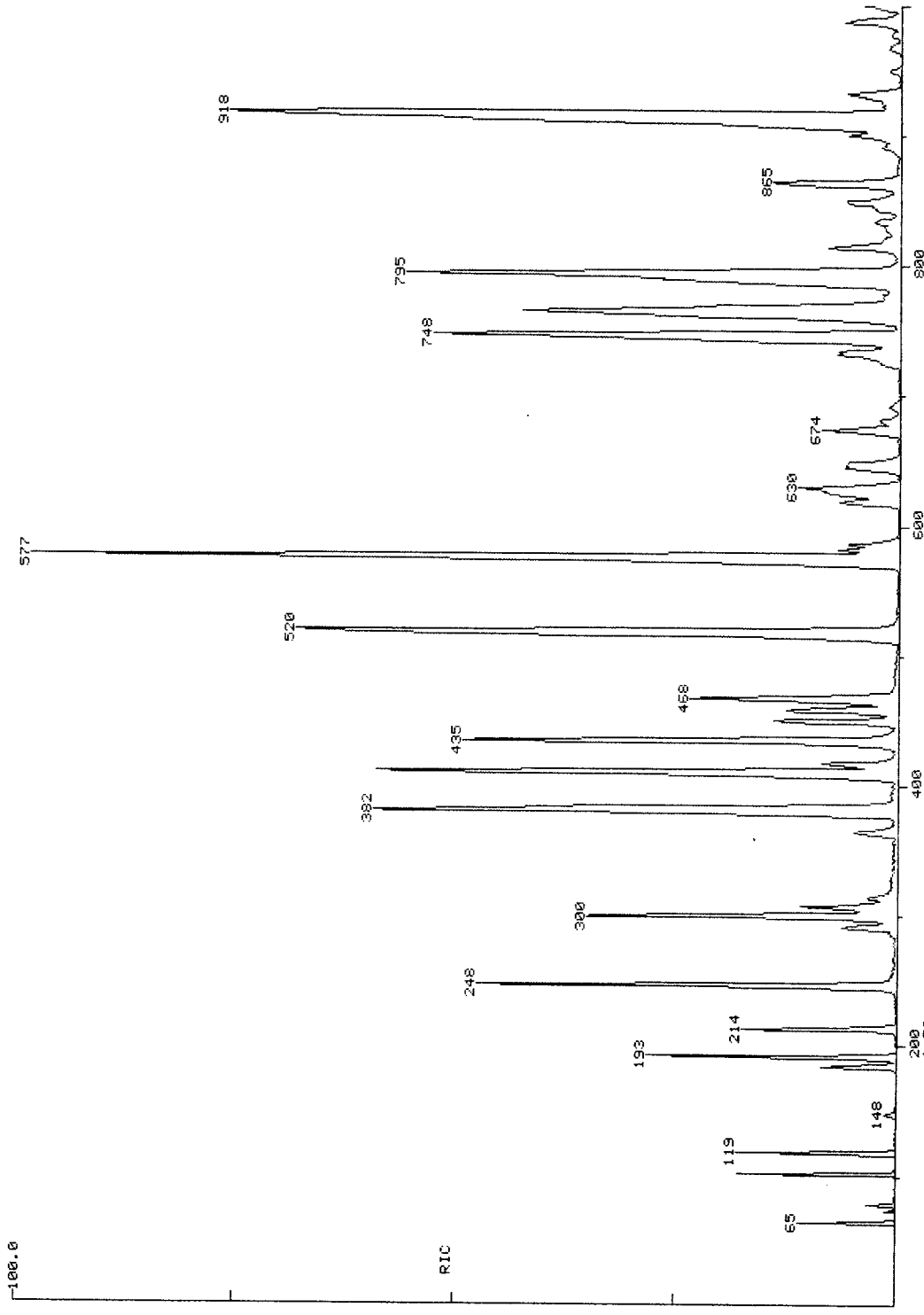

Fig. 1. Reconstructed ion chromatogram of separator tank oil (scans 1–1001).

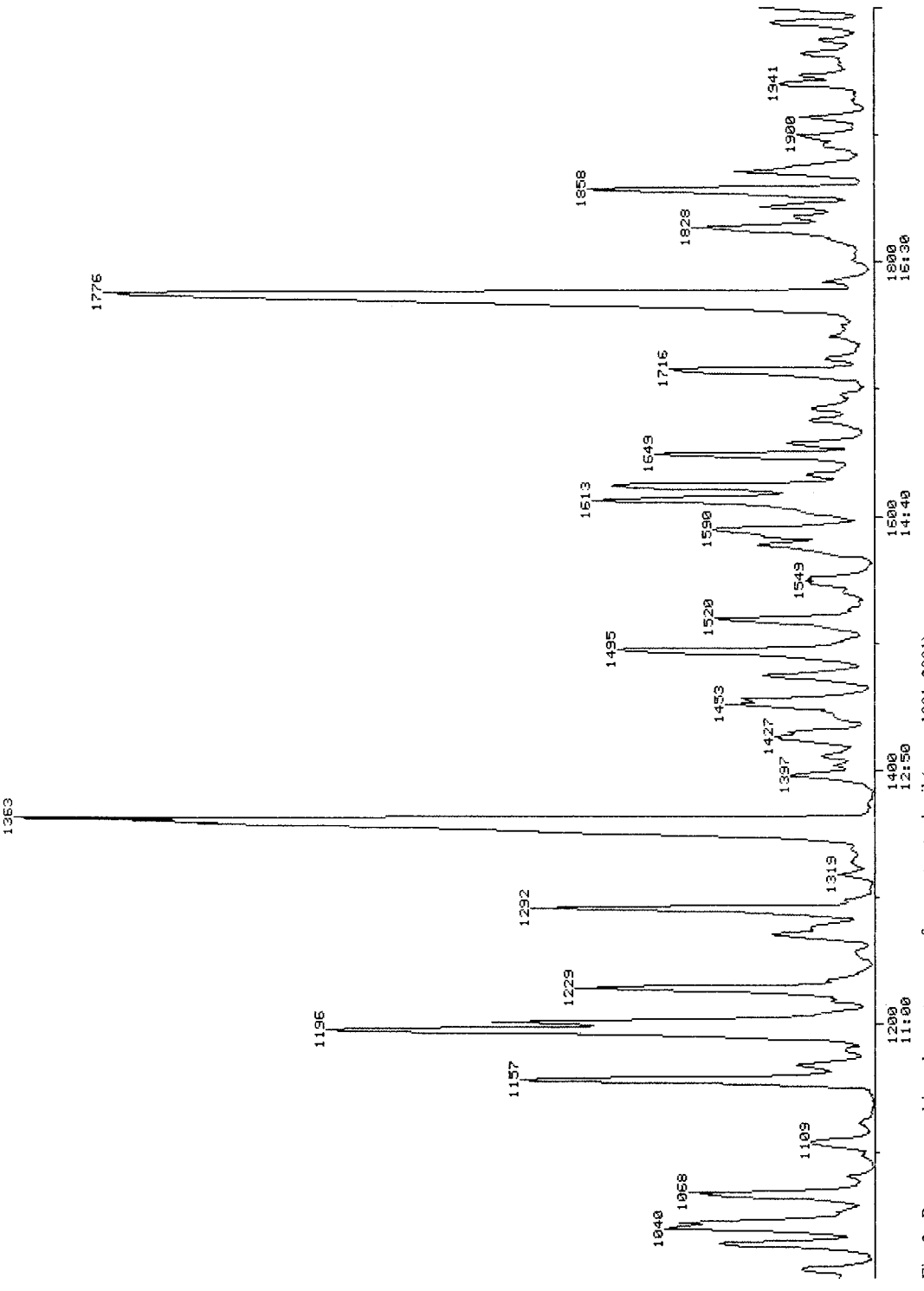

Fig. 2. Reconstructed ion chromatogram of separator tank oil (scans 1001–2001).

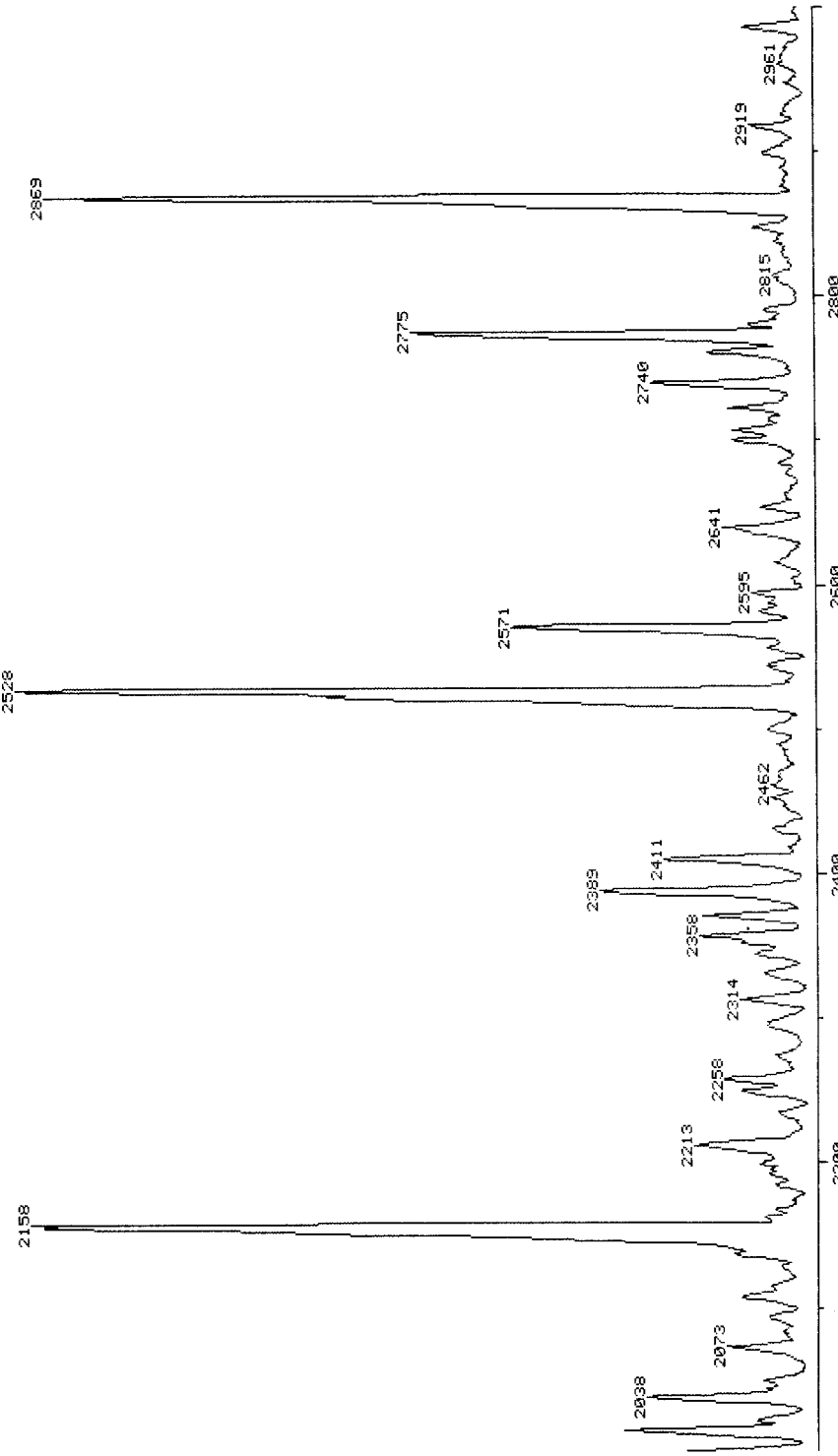

Fig. 3. Reconstructed ion chromatogram of separator tank oil (scans 2001–3001).

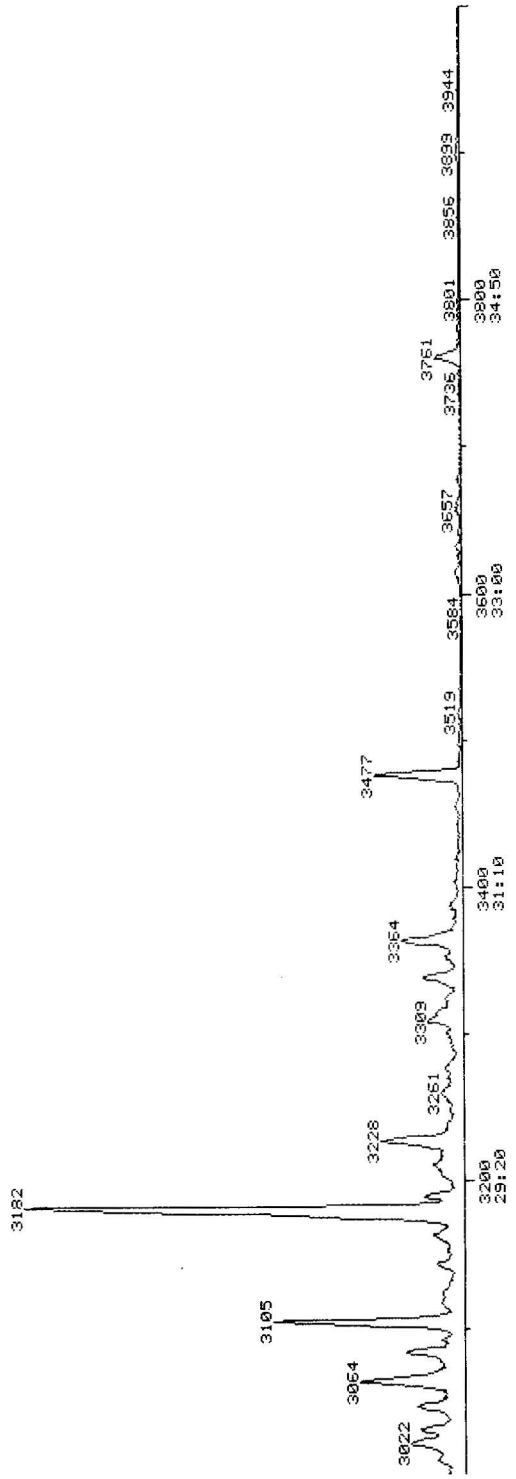

Fig. 4. Reconstructed ion chromatogram of separator tank oil (scans 3001–4001).

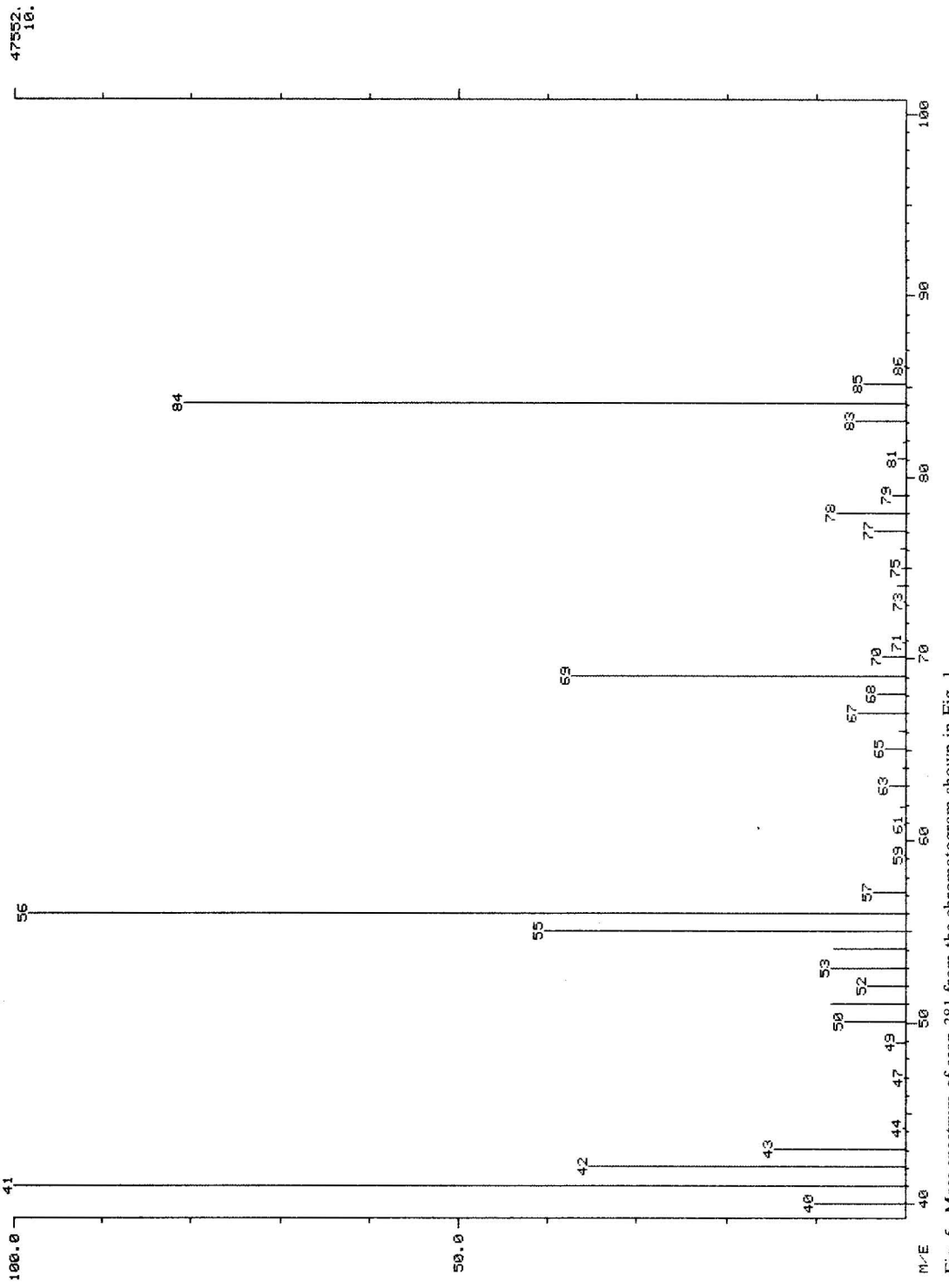

Fig. 5. Mass spectrum of scan 381 from the chromatogram shown in Fig. 1.

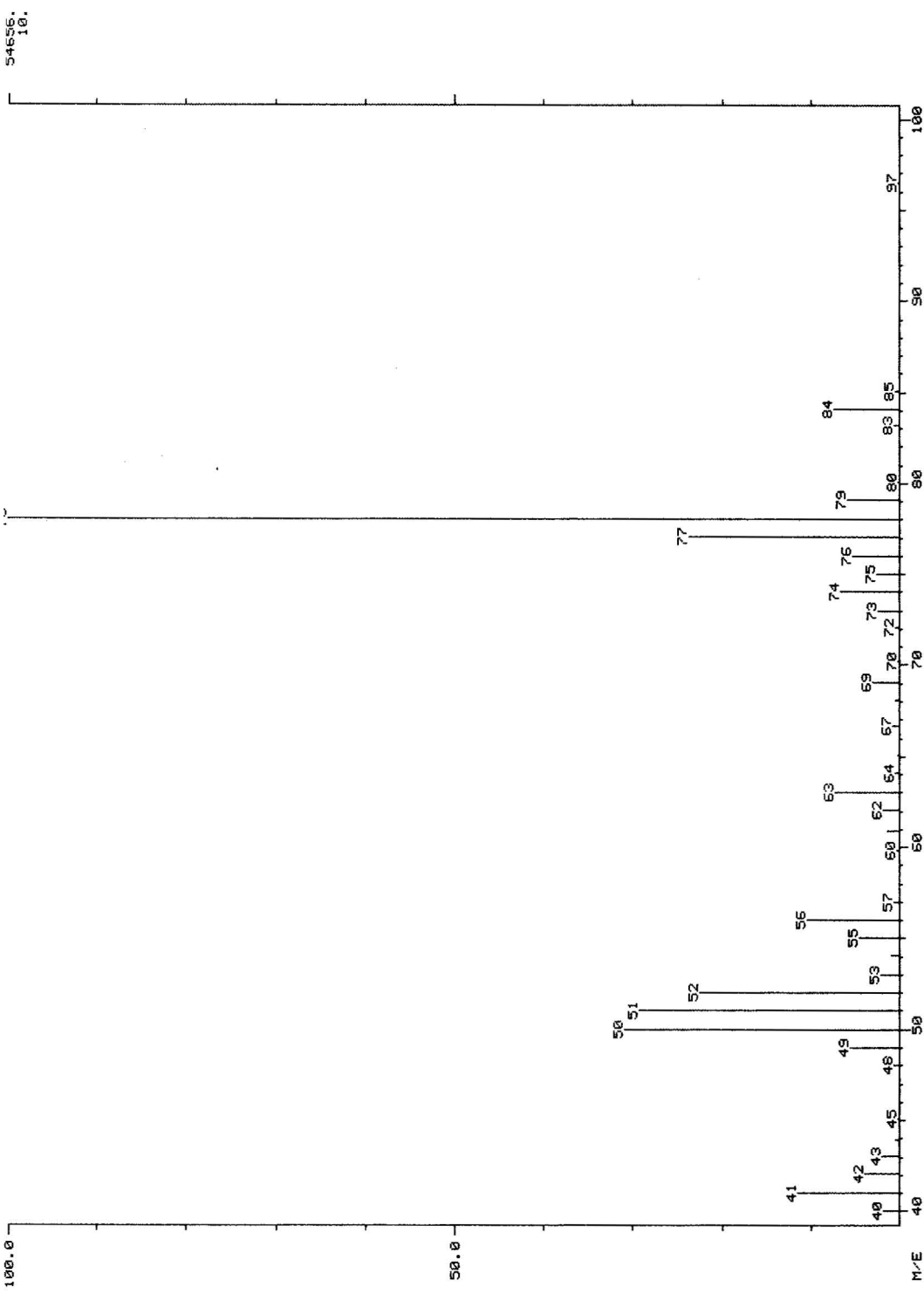

Fig. 6. Mass spectrum of scan 384 from the chromatogram shown in Fig. 1.

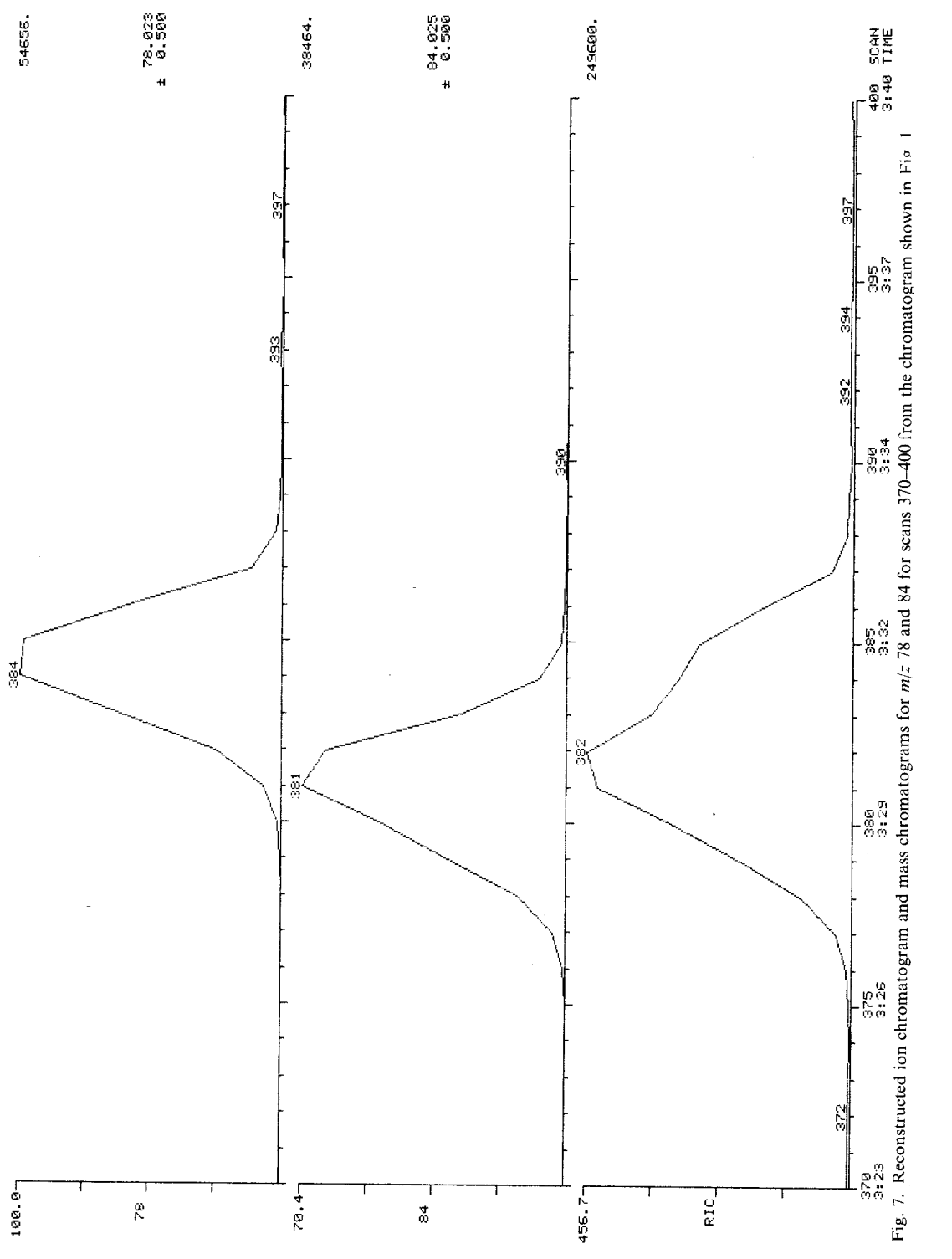

Fig. 7. Reconstructed ion chromatogram and mass chromatograms for *m/z* 78 and 84 for scans 370–400 from the chromatogram shown in Fig. 1

TABLE I

VOLATILE CONSTITUENTS OF OIL FROM SEPARATOR TANK

Scan	*Formula*	*Identity*	*Scan*	*Formula*	*Identity*
65	CO_2	Carbon dioxide	978	C_8H_{16}	?
74	C_4H_{10}	2-Methylpropane	988	C_9H_{20}	Alkane
79	C_4H_{10}	*n*-Butane	1002	C_8H_{16}	*cis*-1,2-Dimethylcyclohexane
103	C_5H_{12}	2-Methylbutane	1008	C_9H_{20}	2,4-Dimethylheptane
119	C_5H_{12}	*n*-Pentane	1028	C_8H_{16}	Ethylcyclohexane
148	C_6H_{14}	2,2-Dimethylbutane	1039	C_9H_{20}	2,6-Dimethylheptane
185	C_6H_{14}	2,3-Dimethylbutane	1045	C_9H_{18}	1,1,3-Trimethylcyclohexane
193	C_6H_{14}	2-Methylpentane	1068	C_9H_{20}	3,5-Dimethylheptane
214	C_6H_{14}	3-Methylpentane	1081	C_9H_{20}	Alkane
248	C_6H_{14}	*n*-Hexane	1109	C_9H_{18}	Trimethylcyclohexane
292	C_7H_{16}	2,2-Dimethylpentane	1123	C_9H_{18}	Trimethylcyclohexane
300	C_6H_{12}	Methylcyclopentane	1157	C_8H_{10}	Ethylbenzene
308	C_7H_{16}	2,4-Dimethylpentane	1170	C_8H_{14}	?
315	C_7H_{16}	Alkane	1181	C_9H_{20}	Alkane
365	C_7H_{16}	3,3-Dimethylpentane	1196	C_8H_{10}	*m*- + *p*-Xylene
381	C_6H_{12}	Cyclohexane	1203	C_9H_{20}	2-Methyloctane
384	C_6H_6	Benzene	1229	C_9H_{20}	3-Methyloctane
411	C_7H_{16}	2-Methylhexane	1258	$C_{10}H_{20}$	?
418	C_7H_{14}	1,1-Dimethylcyclopentane	1271	C_9H_{20}	1-Ethyl-4-methylcyclohexane
435	C_7H_{16}	3-Methylhexane	1277	C_9H_{20}	Ethylmethylcyclohexane
451	C_7H_{14}	?	1292	C_8H_{10}	*o*-Xylene
459	C_7H_{14}	?	1319	C_9H_{16}	?
468	C_7H_{14}	*cis*-1,2-Dimethylcyclopentane	1339	$C_{11}H_{22}$	Diethylmethylcyclohexane
520	C_7H_{16}	*n*-Heptane	1363	C_9H_{20}	*n*-Nonane
577	C_7H_{14}	Methylcyclohexane	1397	C_9H_{16}	?
587	C_8H_{18}	Alkane	1405	C_9H_{18}	Isopropylcyclohexane
619	C_7H_{14}	Ethylcyclopentane	1427	$C_{10}H_{22}$	Alkane
626	C_8H_{18}	Alkane	1431	C_9H_{12}	Ethylmethylbenzene
631	C_8H_{18}	2,4-Dimethylhexane	1452	C_9H_{18}	*n*-Propylcyclohexane
646	C_8H_{16}	1,2,4-Trimethylcyclopentane	1457	$C_{10}H_{22}$	Alkane
649	C_8H_{18}	Alkane	1476	$C_{10}H_{22}$	Alkane
674	C_8H_{16}	?	1495	$C_{10}H_{22}$	Alkane
682	C_8H_{18}	Alkane	1520	$C_{10}H_{22}$	Alkane
692	C_8H_{18}	Alkane	1549	$C_{10}H_{22}$	Alkane
725	C_8H_{14}	?	1553	C_9H_{12}	*n*-Propylbenzene
733	C_8H_{18}	2,3-Dimethylhexane	1578	$C_{10}H_{22}$	Alkane
748	C_7H_8	Toluene	1590	C_9H_{12}	Ethylmethylbenzene
765	C_8H_{18}	2-Methylheptane	1613	$C_{10}H_{22}$	Alkane
789	C_8H_{16}	Dimethylcyclohexane	1616	C_9H_{12}	1,2,4-Trimethylbenzene
795	C_8H_{18}	Alkane	1624	$C_{10}H_{22}$	2-Methylnonane
815	C_8H_{16}	*cis*-1,3-Dimethylcyclohexane	1633	$C_{10}H_{22}$	Alkane
835	C_8H_{16}	Ethylmethylcyclopentane	1649	$C_{10}H_{22}$	3-Methylnonane
850	C_8H_{16}	4-Octene	1658	C_9H_{12}	Ethylmethylbenzene
865	C_8H_{16}	*trans*-1,2-Dimethylcyclohexane	1676	$C_{10}H_{20}$	Methylpropylcyclohexane
892	C_9H_{18}	?	1686	$C_{10}H_{20}$	?
901	C_8H_{16}	Dimethylcyclohexane	1716	C_9H_{12}	Trimethylbenzene
918	C_8H_{18}	*n*-Octane	1724	$C_{10}H_{20}$	Methylpropylcyclohexane
950	C_8H_{16}	?	1771	$C_{10}H_{14}$	Butylbenzene
968	C_9H_{20}	Alkane	1776	$C_{10}H_{22}$	*n*-Decane

(Continued on p. 170)

TABLE 1 *(continued)*

Scan	*Formula*	*Identity*	*Scan*	*Formula*	*Identity*
1786	$C_{10}H_{14}$	Methylpropylbenzene	2462	$C_{13}H_{28}$	Alkane
1828	C_9H_{12}	Ethylmethylbenzene	2472	$C_{12}H_{18}$	Trimethylpropylbenzene
1836	$C_{10}H_{14}$	Methylisopropylbenzene	2490	$C_{12}H_{24}$	Methylpentylcyclohexane
1844	$C_{10}H_{14}$	Methylisopropylbenzene	2500	$C_{12}H_{20}$	?
1858	$C_{11}H_{24}$	Alkane	2528	$C_{12}H_{26}$	*n*-Dodecane
1871	$C_{10}H_{20}$	Butylcyclohexane	2542	$C_{12}H_{16}$	?
1897	$C_{10}H_{14}$	Butylbenzene	2557	$C_{13}H_{28}$	Alkane
1900	$C_{11}H_{24}$	Alkane	2571	$C_{13}H_{28}$	Alkane
1915	$C_{11}H_{24}$	Alkane	2582	$C_{13}H_{28}$	Alkane
1940	$C_{10}H_{18}$	Decalin?	2588	$C_{12}H_{18}$	Dimethylbutylbenzene
1947	$C_{10}H_{14}$	Methylpropylbenzene	2595	$C_{13}H_{28}$	Alkane
1964	$C_{10}H_{14}$	Butylbenzene	2605	$C_{12}H_{18}$	Dipropylbenzene
1975	$C_{10}H_{14}$	Ethyldimethylbenzene	2616	$C_{13}H_{28}$	Alkane
1988	$C_{11}H_{24}$	Alkane	2641	$C_{12}H_{24}$	Hexylcyclohexane
2000	$C_{11}H_{24}$	Alkane	2655	$C_{13}H_{28}$	Alkane
2002	$C_{10}H_{14}$	Methylpropylbenzene	2663	$C_{13}H_{28}$	Alkane
2015	$C_{11}H_{24}$	2-Methyldecane	2678	$C_{12}H_{18}$	Butylethylbenzene
2022	$C_{11}H_{24}$	Alkane	2685	$C_{13}H_{28}$	Alkane
2038	$C_{11}H_{24}$	3-Methyldecane	2701	$C_{13}H_{28}$	Alkane
2044	$C_{10}H_{14}$	Methylpropylbenzene	2708	$C_{13}H_{28}$	Alkane
2050	$C_{10}H_{14}$	Methylpropylbenzene	2710	$C_{12}H_{18}$	Dimethylbutylbenzene
2073	$C_{10}H_{14}$	Methylpropylbenzene	2715	$C_{13}H_{28}$	Alkane
2084	$C_{10}H_{14}$	Methylpropylbenzene	2723	$C_{13}H_{28}$	Alkane
2094	$C_{10}H_{14}$	Methylpropylbenzene	2740	$C_{13}H_{28}$	2-Methyltridecane
2108	$C_{11}H_{18}$	?	2762	$C_{13}H_{28}$	Alkane
2115	$C_{11}H_{22}$	Pentylcyclohexane	2775	$C_{13}H_{28}$	3-Methyltridecane
2136	$C_{11}H_{16}$	Isobutyltoluene	2781	$C_{14}H_{30}$	Alkane
2148	$C_{10}H_{14}$	Ethyldimethylbenzene	2791	$C_{14}H_{30}$	Alkane
2158	$C_{11}H_{24}$	*n*-Undecane	2810	$C_{11}H_{10}$	2-Methylnaphthalene
2163	$C_{12}H_{20}$	?	2815	$C_{13}H_{26}$	?
2168	$C_{12}H_{26}$	Alkane	2848	$C_{13}H_{26}$	?
2186	$C_{10}H_{14}$	Diethylbenzene	2865	$C_{11}H_{10}$	1-Methylnaphthalene
2194	$C_{11}H_{16}$	Dimethylpropylbenzene	2869	$C_{13}H_{28}$	*n*-Tridecane
2200	$C_{10}H_{14}$	Methylpropylbenzene	2899	$C_{14}H_{30}$	Alkane
2213	$C_{11}H_{20}$	Methyldecalin	2919	$C_{14}H_{30}$	Alkane
2236	$C_{12}H_{26}$	Alkane	2961	$C_{14}H_{26}$	?
2250	$C_{12}H_{26}$	Alkane	2987	$C_{13}H_{26}$	Heptylcyclohexane
2258	$C_{11}H_{22}$	Pentylcyclohexane	3022	$C_{14}H_{30}$	Alkane
2262	$C_{11}H_{16}$	Ethylpropylbenzene	3032	$C_{14}H_{30}$	Alkane
2268	$C_{11}H_{16}$	Dimethylpropylbenzene	3047	$C_{14}H_{30}$	Alkane
2275	$C_{12}H_{26}$	Alkane	3064	$C_{14}H_{30}$	2-Methyltetradecane
2295	$C_{11}H_{16}$	Ethylpropylbenzene	3084	$C_{14}H_{30}$	Alkane
2298	$C_{12}H_{26}$	Alkane	3105	$C_{14}H_{30}$	1-Methyltetradecane
2314	$C_{10}H_{14}$	Tetramethylbenzene	3163	$C_{12}H_{12}$	Dimethylnaphthalene
2330	$C_{11}H_{16}$	Isobutyltoluene	3182	$C_{14}H_{30}$	*n*-Tetradecane
2345	$C_{11}H_{18}$	?	3210	$C_{12}H_{12}$	Dimethylnaphthalene
2358	$C_{12}H_{26}$	Alkane	3221	$C_{12}H_{12}$	Dimethylnaphthalene
2372	$C_{12}H_{26}$	Alkane	3228	$C_{15}H_{28}$	?
2389	$C_{12}H_{26}$	2-Methylundecane	3309	$C_{14}H_{28}$	Octylcyclohexane
2407	$C_{12}H_{18}$	Dimethylbutylbenzene	3340	$C_{15}H_{28}$	?
2411	$C_{12}H_{26}$	3-Methylundecane	3364	$C_{15}H_{32}$	2-Methylpentadecane
2420	$C_{10}H_8$	Naphthalene	3477	$C_{15}H_{32}$	*n*-Pentadecane
2448	$C_{12}H_{18}$	Dimethylbutylbenzene	3761	$C_{16}H_{34}$	*n*-Hexadecane

CONCLUSIONS

Some 200 components of produced water effluent from the Buccaneer field have now been characterized, considerably more than were previously identified. The most abundant single compounds are tne *n*-alkanes, while alkylaromatic hydrocarbons are also present in a relatively high aggregate concentration.

The use of bonded-phase fused-silica columns allows one to examine effluent samples by combining an automated purge-and-trap device with a gas chromatograph–mass spectrometer. The sample is loaded into the purge tube and the operation of the device is initiated. Further operator intervention is only required when the desorption is complete: the cooled portion of the column is removed from the liquid nitrogen and data acquisition is initiated. Thus, the procedure is amenable to repetitive analyses.

While it has been demonstrated that some 200 components of an effluent can be resolved and characterized, it is unlikely that such detailed analyses would be needed repetitively. Manipulation of the data to provide target compound analyses for selected compounds could be performed simultaneously with data acquisition for subsequent samples if, as in the Finnigan instrument, the data system can be used in the foreground/background mode with priority interrupt.

ACKNOWLEDGEMENTS

The Buccaneer Gas and Oil Field Study was sponsored by the Environmental Protection Agency and Department of Commerce, National Oceanic and Atmospheric Administration, National Marine Fisheries Service, Southeast Fisheries Center, Galveston Laboratory under Interagency Agreement EPA-IAG-D5-E693-EO. This additional investigation was supported by the University of Houston Energy Laboratory.

REFERENCES

1 B. S. Middleditch (Editor), *Environmental Effects of Offshore Oil Production: The Buccaneer Gas and Oil Field Study*, Plenum Press, New York, 1981, 446 pp.
2 J. M. Brooks, E. L. Estes, D. A. Wiesenburg, C. R. Scwab and H. A. Abdel-Reheim, in W. B. Jackson and E. P. Wilkens (Editors), *Environmental Assessment of Buccaneer Gas and Oil Field in the Northwestern Gulf of Mexico, 1975-1980; NOAA Technical Memorandum NMFS-SEFC-47*, available from NTIS, Springfield, VA, 89 pp.
3 B. S. Middleditch, B. Basile and E. S. Chang, *J. Chromatogr.*, 142 (1977) 777.
4 B. S. Middleditch, B. Basile and E. S. Chang, *Bull. Environ. Contam. Toxicol.*, 20 (1978) 59.
5 B. S. Middleditch, B. Basile and E. S. Chang, *J. Chromatogr.*, 158 (1978) 449.
6 B. S. Middleditch, B. Basile and E. S. Chang, *Bull. Environ. Contam. Toxicol.*, 21 (1979) 413.
7 B. S. Middleditch, E. S. Chang and B. Basile, *Bull. Environ. Contam. Toxicol.*, 21 (1979) 421.
8 B. S. Middleditch, E. S. Chang, B. Basile and S. R. Missler, *Bull. Environ. Contam. Toxicol.*, 22 (1979) 249.
9 B. S. Middleditch, E. S. Chang and B. Basile, *Bull. Environ. Contam. Toxicol.*, 23 (1979) 6.
10 B. S. Middleditch, B. Basile and E. S. Chang, *Bull. Environ. Contam. Toxicol.*, in press.
11 B. S. Middleditch, in B. S. Middleditch (Editor), *Environmental Effects of Offshore Oil Production: The Buccaneer Gas and Oil Field Study*, Plenum Press, New York, 1981, p. 15.
12 A. Zlatkis and H. Shanfield, in B. S. Middleditch (Editor), *Practical Mass Spectrometry: A Contemporary Introduction*, Plenum Press, New York, 1979, p. 151.
13 T. C. Sauer, W. M. Sackett and L. M. Jeffrey, *Mar. Chem.*, 7 (1978) 1.
14 B. S. Middleditch, S. R. Missler and H. B. Hines, *Mass Spectrometry of Priority Pollutants*, Plenum Press, New York, 1981, 308 pp.
15 J. E. Biller and K. Biemann, *Anal. Lett.*, 7 (1974) 515.

Journal of Chromatography, 239 (1982) 173–180
Elsevier Scientific Publishing Company, Amsterdam — Printed in The Netherlands

CHROM. 14,447

DISTRIBUTION OF PCDDs AND OTHER TOXIC COMPOUNDS GENERATED ON FLY ASH PARTICULATES IN MUNICIPAL INCINERATORS

F. W. KARASEK*, R. E. CLEMENT and A. C. VIAU
Guelph-Waterloo Centre for Graduate Work in Chemistry, University of Waterloo, Waterloo, Ontario N2L 3G1 (Canada)

SUMMARY

A bulk fly ash sample from a municipal incinerator located in France has been separated into different particle size fractions by manual sieving using standard screens. Average particle sizes varied from 30 μm to over 850 μm. Separated fractions were extracted by ultrasonic agitation using benzene and analyzed by gas chromatography (GC) and gas chromatography–mass spectrometry (GC–MS) for polychlorinated dibenzo-*p*-dioxins, *n*-alkanes, phthalates, and selected polynuclear aromatic hydrocarbons. Differences were observed in the relative distribution of organics on the fly ash size fractions from the French incinerator and the distributions which were observed in fly ash from an Ontario (Canada) incinerator. No tetrachlorinated dibenzo-*p*-dioxins were detected on the French fly ash size fractions at a detection limit of 100 pg/g, although the concentration of octachlorodibenzo-*p*-dioxin was 120 ng/g for the 30-μm particles.

INTRODUCTION

There has been an increased interest in the use of municipal refuse incineration as a means of energy production. This is especially attractive since energy recovery facilities can be situated near large urban centres where fuel is readily available and there is a demand for energy. However, it has been shown that fly ash generated during this incineration contains hazardous organic compounds such as polynuclear aromatic hydrocarbons (PAHs) and polychlorinated dibenzo-*p*-dioxins (PCDDs)[1–4].

Most fly ash is collected by electrostatic precipitators or wet scrubbers and disposed of in landfill sites. About 1 to 5% of the fly ash particles remains uncollected and enters the environment with the stack gases. Knowledge of the distribution of hazardous organic compounds on different sized particles is important to estimate the transport of these substances in the environment and because particles of less than 30 μm are directly respirable by humans.

It has been demonstrated that PAHs are highly concentrated on the respirable fraction of atmospheric particulate matter[5,6]. Concentrations of PAHs for coke oven emissions also varied with particle size[7]. Recent data obtained on samples of fly ash from a Canadian municipal incinerator have shown that concentrations of various

0021-9673/82/0000–0000/$02.75

PCDD congeners varied with the different size fractions[8]. The results show that tetrachlorinated dibenzo-*p*-dioxins and pentachlorinated dibenzo-*p*-dioxins were more highly concentrated on the larger particles (550 μm), while octachlorodibenzo-*p*-dioxin was more concentrated on the smaller particles (30 μm). In this study, fly ash from a municipal incinerator located in France is separated into different size fractions as in the previous investigation. Concentrated extracts of each fraction containing the organic compounds are analyzed by gas chromatography (GC) and gas chromatography–mass spectrometry (GC–MS). A comparative study of the patterns of total organics, PAHs and PCDDs between French and Ontario fly ash size fractions is presented. These studies are necessary to increase our understanding of the generation of toxic organic compounds during the combustion of municipal refuse.

EXPERIMENTAL

Sample collection and storage

A large grab-sample of fly ash was taken under one of the electrostatic precipitator hoppers in a municipal incinerator located in the south of Paris, France. The incinerator temperature at the top of the furnace was 950°C and the primary air-flow was 45,000 m^3/h. The sample was stored in glass jars at ambient temperature and was protected from light. After extraction, sample extracts were stored in a freezer at about −15°C.

Fractionation of fly ash

Six size fractions of fly ash were obtained using five Tyler sieves (W. S. Tyler, St. Catherines, Canada). The brass sieves had metal screens with openings of 850 μm, 250 μm, 150 μm, 106 μm and 63 μm. All sieves, including the top and bottom collector were cleaned by ultrasonic agitation using an aqueous solution of Alconox detergent for approximately 15 min. This was followed by rinsing with tap water, deionized water, methanol and then air drying. Hand sieving was performed and all fractions were stored in polypropylene containers equipped with polypropylene screw caps that had first been rinsed with small portions of benzene, then air dried.

Sample extraction and concentration

Extraction was performed by ultrasonic agitation using benzene[8,9]. Samples of 10 g were added to individual flasks with 100 ml of benzene and agitated for 1 h. After initial extraction the fly ash was allowed to settle and the benzene was decanted into fresh flasks through porous glass frits. This procedure was repeated two additional times with 50 ml of fresh benzene added each time and ultrasonic agitation for 30 min. After the third extraction cycle, the fly ash was transferred to the glass frit and rinsed three times with 10-ml portions of fresh benzene.

Extracts were concentrated to 100 μl by rotary evaporation under aspirator vacuum and stored in 1.0 ml reacti-vials equipped with screw caps and PTFE liners as described previously[8]. All glassware, including reacti-vials and pipets, was cleaned by ultrasonic agitation for 30 min with Alconox detergent. After thorough rinsing with tap water and deionized water, glassware was then placed in an oven at 250°C for at least 1 h. All equipment was at ambient temperature before use. Solvents were "distilled-in-glass" grade (Caledon Labs., Georgetown, Canada). A 200-ml amount of benzene solvent was carried through the entire process as a procedure blank.

GC analysis

A Hewlett-Packard 5830A GC with flame ionization detector was equipped with a 2 m × 2 mm I.D. glass column packed with Aue packing[10]. A temperature program of 90°C initial temperature to 250°C final temperature at 4°C/min was employed for all sample extracts. Injection temperature was 250°C; detector temperature, 275°C; and the carrier gas flow-rate 37 ml/min, measured at 90°C. A slope sensitivity of 0.1 mV/min was used for peak detection.

For calculation of retention indices, a normal hydrocarbon standard mixture was analyzed periodically. Retention indices were calculated by the Fortran program RICALC[11]. GC peaks were displayed as bar-graph plots using a Zeta plotter by the program GCPLOT[11].

GC–MS analysis

Selected PAH and various PCDD congeners were analyzed by a Hewlett-Packard 5992A GC/MS/Calculator using selected ion monitoring (SIM). The ions monitored for the tetrachlorinated dibenzo-*p*-dioxins were 319.9 and 321.9. The ions selected for penta- through octachlorinated dibenzo-*p*-dioxins were 355.9, 389.8, 425.8 and 459.7, respectively. Chromatographic conditions were as described previously.

The series of congeners were quantified using a solution of 1,2,3,4-tetrachlorodibenzo-*p*-dioxin (1,2,3,4-TCDD) and octachlorodibenzo-*p*-dioxin (OCDD) standards. The intermediate congeners were quantified by using a linear interpolation of response factors between those of 1,2,3,4-TCDD and OCDD. Quantification of PAHs was performed by monitoring the ions 166.1, 202.1, 178.1 and 202.1 from a reference solution containing fluorene, fluoranthene, anthracene and pyrene. Six ions were monitored during each SIM analysis with a dwell time of 166 msec per ion. SIM areas were used for quantification. Normal alkanes and phthalate esters were determined by monitoring the ions 85.1 and 149.1.

Mass spectra were obtained by scanning from 500 to 50 a.m.u. at 330 a.m.u./sec. Spectra taken at the top of the eluting GC peaks were saved on floppy disk in addition to those at the lowest valley between peaks for later background subtraction. A user-developed program called Dual-Mode was employed which allowed storage of total ion abundances and mass chromatograms in addition to mass spectra[12]. Before operating in either scanning or SIM mode, the mass spectrometer was tuned daily by the manufacturer supplied program AUTOTUNE using a perfluorotributylamine calibration standard.

RESULTS AND DISCUSSION

Results of GC analyses of concentrated extracts of the different size fractions are shown in Fig. 1. This plot, termed GCPLOT, is a bar graph display of estimated GC peak concentrations *versus* Kovats' retention indices. The estimates are based on GC peak areas and an average organic compound response factor of 400 area counts per ng determined from previous work. The full-scale value is shown in the upper right hand corner of each plot. Any peak plotted to full-scale is estimated to have a concentration greater than or equal to the full-scale value. Visual comparison of plots for different size fractions indicates that the 30 μm and 80 μm size fractions contain

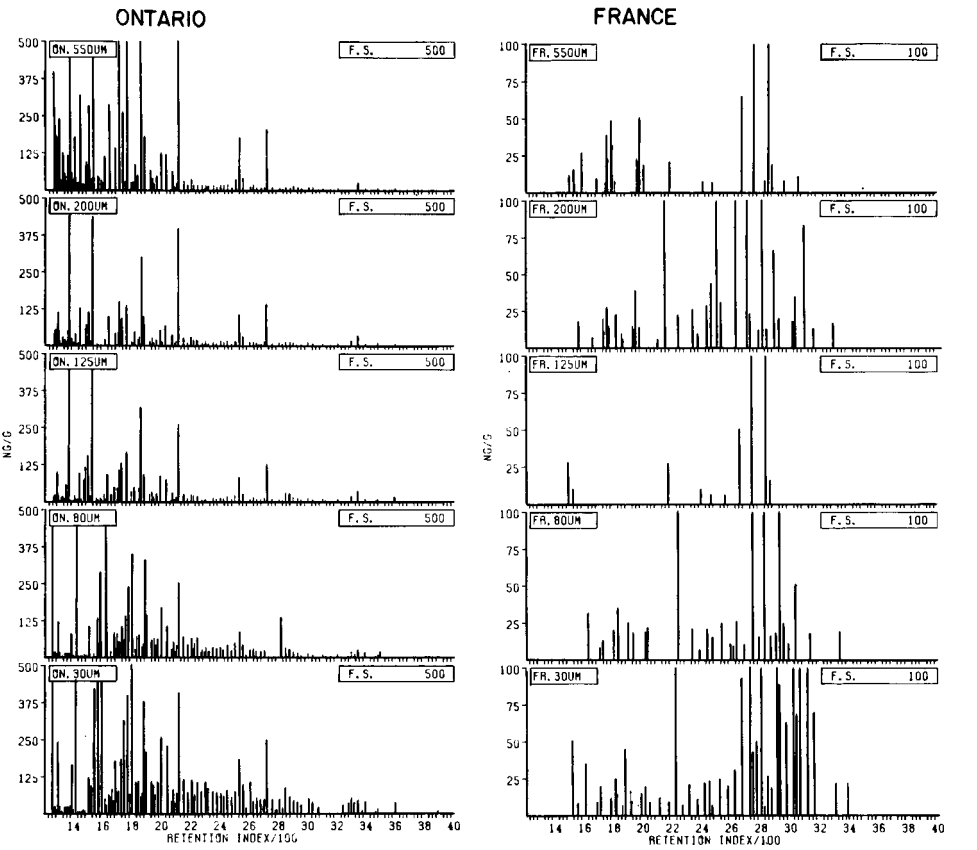

Fig. 1. GCPLOT comparison of chromatographic data from concentrated extracts of French and Ontario fly ash size fractions. Chromatograms are stacked in order of 550 μm size fraction (top of plot) to 30 μm size fraction (bottom of plot). All GC peak areas were converted to estimated concentrations (ng/g) before plotting.

the greatest numbers of components and in higher concentrations than the larger size fractions. The total organic compounds was estimated by using the average response factor of 400 area counts per ng and the sum of the GC integration values between retention indices 1100 and 4000. Estimates of total organic material extracted from the different size fractions for the French and Canadian fly ash samples are given in Table I. Procedure blanks included in these analyses showed contamination from two peaks at retention indices 2750 and 2850. These were identified by GC–MS analysis combined with computerized library search as dioctyl phthalate and farnesyl cyanide. The Ontario fly ash has more components than the French fly ash for each size fraction. Total concentrations of these components are also greater in the Ontario fly ash on each size fraction for the early eluting compounds. However, a greater number of later eluting compounds were detected in the French size fractions than in corresponding Ontario size fractions. Concentrations of the major identified components from each size fraction are given in Table II. These comprise more than 60% of the

TABLE I

ESTIMATED TOTAL ORGANIC MASS ON DIFFERENT SIZE FRACTIONS FOR FRENCH AND CANADIAN FLY ASH

Average particle size (μm)	*France (ng/g)*	*Ontario (ng/g)*
30	2500	97000
80	1600	64000
125	630	23000
200	1600	23000
550	900	55000
>850	22000	(1) 75000*
		(2) 3100

* The Ontario fly-ash large fraction consisted of two distinct types of particles; (1) black ash particles identical in appearance to those from the French fly-ash, and (2) large agglomerate particles.

TABLE II

CONCENTRATIONS (ng/g) OF MAJOR ORGANIC COMPONENTS IN CONCENTRATED ORGANIC EXTRACTS OF FRENCH FLY ASH SIZE FRACTIONS

	Average particle size (μm)					
	30	*80*	*125*	*200*	*550*	*>850*
Butyl benzyl phthalate	240	–	–	–	65	1300
Dibutyl phthalate	190	190	10	100	21	820
Dioctyl phthalate	–	–	300	190	110	5500
Total alkanes	620	510	120	440	190	3300
Farnesyl cyanide	340	160	170	240	290	2600
Total	1400	860	600	970	680	14000
Per-cent of total estimated organic mass	56	54	95	61	76	64

total extracted organic mass. Butylbenzyl phthalate was found in the French ash but not in the Ontario ash. In the previous study, the large Ontario particles (>850 μm) were observed to consist of two distinct fractions, light ash and agglomerate ash[8]. The corresponding French fly ash size fraction was homogeneous in composition and was more concentrated in total organic material than any of the other French size fractions.

The concentrations of PCDDs for each size fraction are given in Table III. No tetrachlorodibenzo-*p*-dioxins (TCDDs) were detected in any size fractions of the French fly ash. The detection limits under the given experimental conditions were determined to be 100 pg/g for 1,2,3,4-TCDD and 200 pg/g for OCDD. The total PCDD concentration decreases with increasing particle size, unlike the Ontario sample in which this trend is reversed. This is illustrated in Fig. 2. It can be observed that there is a skewed pattern among the congeners towards the OCDD in the French

TABLE III

PCDD CONCENTRATIONS (ng/g) IN FRENCH FLY ASH SIZE FRACTIONS

ND = Not detected.

Mean particle size (μm)	*Total*	*T_4CDD*	*P_5CDD*	*H_6CDD*	*H_7CDD*	*OCDD*
30	160	ND	5	8	30	120
85	67	ND	0.8	8	20	39
125	25	ND	1	4	8	12
200	6	ND	0.6	1	ND	4.1
550	4	ND	0.4	0.8	0.4	2.3
>850	13	ND	ND	ND	4	8.4

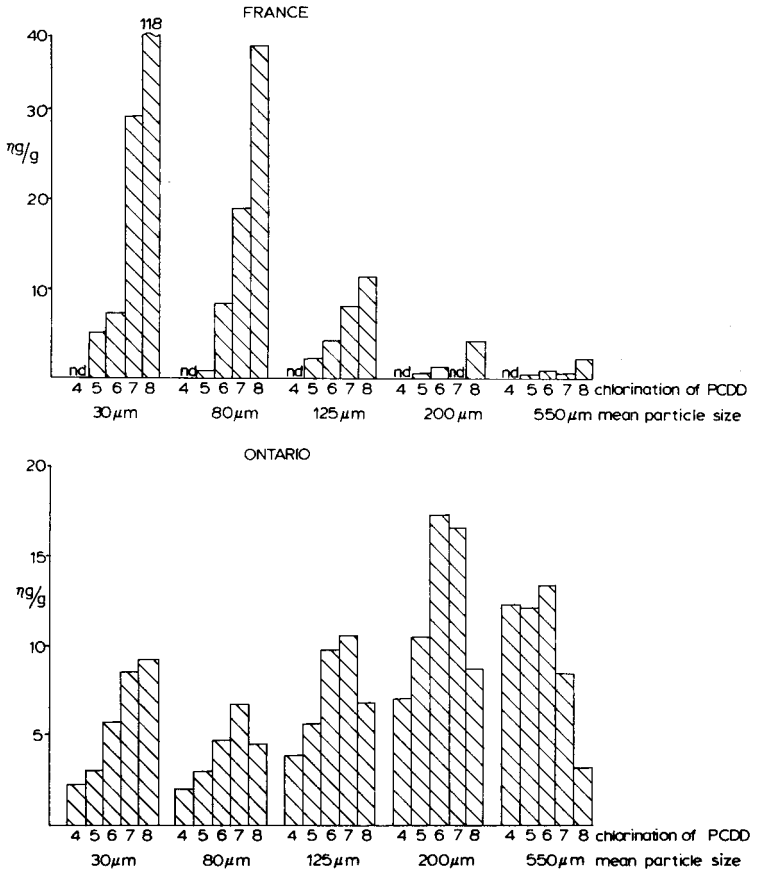

Fig. 2. Chlorinated dioxin concentrations on Ontario and French fly ash size fractions.

size fractions. This also differs from the Ontario sample, where there is a skewing towards OCDD in the smaller particles; but the larger sized particles are skewed towards TCDD. Additionally, the highest concentration of PCDD lies on the larger

particles of the Ontario sample. These differences may reflect the different incinerator conditions and designs as well as differences between France and Canadian incinerator feedstock.

Concentrations of selected PAHs for each particle size fraction are given in Table IV. Fluorene was not detected in these fractions, contrary to those of the Ontario fly ash study[8]. Anthracene is more concentrated on the 850 μm size particles. Pyrene and fluoranthene concentrations were observed to decrease with increasing particle size. No trend was observed in the Ontario sample.

TABLE IV

CONCENTRATIONS (ng/g) OF SELECTED PAHs IN FRENCH FLY ASH SIZE FRACTIONS

ND = Not detected.

Mean particle size (μm)	*Total*	*Fluorene*	*Pyrene*	*Fluoranthene*	*Anthracene*
30	5.9	ND	3.0	2.9	ND
85	8.1	ND	1.9	1.7	4.5
125	3.4	ND	0.9	1.3	1.2
200	1.3	ND	0.8	0.5	ND
550	4.6	ND	0.7	1.0	2.9
>850	15	ND	3.4	1.7	10

The total PCDDs, PAHs and estimated total organic compounds are compared in Fig. 3. The PCDDs and total organic carbon (TOC) are most concentrated on the 30 μm size fraction which contains respirable particle sizes. A moderate amount of PAH is also associated with this fraction. The general pattern of the TOC is similar as that reported for the Ontario fly ash. However, for total PCDDs and PAHs greater concentrations were found on the larger particle sizes of the Ontario fly ash. These results suggest that no universal distribution of PCDDs is evident at the source and that the pathway of formation is variable. Previously it has been reported that constant ratios of PCDDs were not evident on whole fly ash[13]. It is apparent that this is also the case when fly ash is size-fractionated. In the previous study, matched patterns between the levels of pyrene and fluorene with total organic compounds were observed, while anthracene did not follow this trend[13]. These trends are also consistent with the size-fractionated particles in this study. Not only does the organic composition of the bulk fly ash differ between incinerators, but also the relative distributions of the organics on various size fractions. Many models could be hypothesized to explain these differences. However, there is insufficient data presented here to determine the most important factors. Further studies which include detailed records of incinerator operating conditions and estimates of bulk feedstock composition are needed. These data indicate that there are considerable differences between fly ash from different incinerators and only suggest areas of further exploration to provide understanding of the process of organic compound formation during combustion.

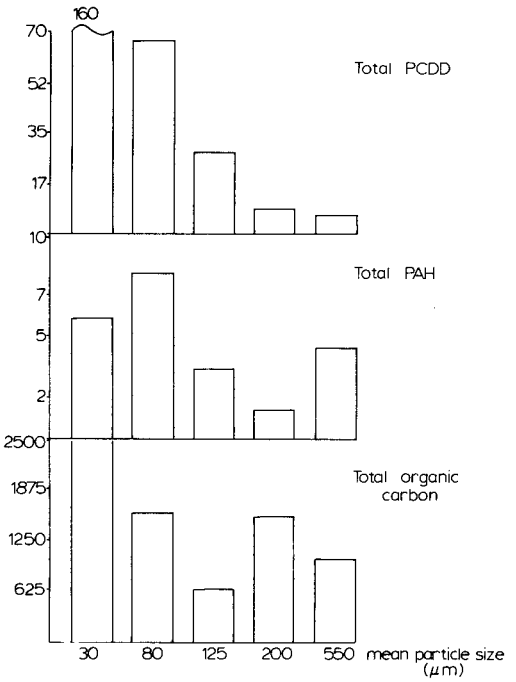

Fig. 3. Comparison of total PCDDs, total PAHs and estimated total organic carbon for French fly ash size fractions.

ACKNOWLEDGEMENTS

This work was supported by the Natural Sciences and Engineering Research Council of Canada and Imperial Oil, Limited.

REFERENCES

1 K. Olie, P. L. Vermeulen and O. Hutzinger, *Chemosphere*, 8 (1977) 455.
2 H. R. Buser, H. P. Bosshardt and C. Rappe, *Chemosphere*, 9 (1978) 165.
3 M. D. Erickson, E. D. Pellizzari, *Bull. Environ. Contam. Toxicol.*, 22 (1979) 688.
4 G. A. Eiceman, R. E. Clement and F. W. Karasek, *Anal. Chem.*, 51 (1979) 2343.
5 L. Van Vaeck and K. Van Cauwenberghe, *Atmos. Environ.*, 12 (1978) 2229.
6 L. Van Vaeck, G. Brooklin and K. Van Cauwenberghe, *Environ. Sci. Technol.*, 13 (1979) 1494.
7 G. Broddin, L. Van Vaeck and K. Van Cauwenberghe, *Atmos. Environ.*, 11 (1977) 1061.
8 R. E. Clement and F. W. Karasek, *J. Chromatogr.*, 234 (1982) 395.
9 G. A. Eiceman, A. C. Viau and F. W. Karasek, *Anal. Chem.*, 52 (1980) 1492.
10 W. A. Aue, C. R. Hastings and S. Kapila, *J. Chromatogr.*, 77 (1973) 299.
11 R. E. Clement, *M.Sc. Thesis*, University of Waterloo, Waterloo, Ontario, 1976.
12 L. C. Dickson, R. E. Clement, K. R. Betty and F. W. Karasek, *J. Chromatogr.*, 190 (1980) 311.
13 G. A. Eiceman, R. E. Clement and F. W. Karasek, *Anal. Chem.*, 53 (1981) 955.

Journal of Chromatography, 239 (1982) 181–189
Elsevier Scientific Publishing Company, Amsterdam — Printed in The Netherlands

CHROM. 14,642

PLASMA EMISSION SPECTRAL DETECTION FOR HIGH-RESOLUTION GAS CHROMATOGRAPHIC STUDY OF GROUP IV ORGANOMETALLIC COMPOUNDS

SCOTT A. ESTES, PETER C. UDEN* and RAMON M. BARNES
Department of Chemistry, GRC Towers, University of Massachusetts, Amherst, MA 01003 (U.S.A.)

SUMMARY

Specific element detection for fused-silica capillary column gas chromatography of germanium, tin and lead tetraalkyl organometallics is carried out by means of microwave-induced and sustained helium plasma atomic emission spectroscopy utilizing the TM_{010} cavity. Representative redistribution reactions are monitored and quantitative determinations made of individual products. Different distributions of tetraalkyllead compounds are quantitatively measured in various gasolines.

INTRODUCTION

In any mode of chromatographic separation, when components of interest contain an element not otherwise present in the sample matrix, detection responsive solely to that element gives significant simplification since species containing that element need be resolved only from each other and not from other matrix components.

Atomic emission spectroscopy as a chromatographic detection mode has the inherent advantage of simultaneous multi-element capability with wide dynamic range. The advent of various plasma sources for atomic emission and high-resolution monochromators to minimize spectral interferences has prompted increasing interest in atomic emission chromatographic detection. Microwave-induced and sustained plasmas[1–5], the argon d.c. plasma[6,7] and inductively coupled argon plasmas[8,9] have all been successively employed for gas chromatographic and/or liquid chromatographic applications.

The major advantages of such interfacing are as follows. (a) The ability to perform speciation, with regard to elemental content, either before or within the chromatographic column for many metals and non-metals; application may either be direct or by derivatization. (b) The ability to tolerate non-ideal chromatographic conditions and elution characteristics; incomplete resolution can be tolerated, a factor of great importance in complex matrixes. Elemental selectivity is here a primary concern. (c) The sensitivity of plasma emission detection which in many cases gives detection at or below the pg/sec level. (d) The potential simultaneous multi-element capacity of plasma emission. (e) The compatibility with chromatographic systems by simple interfacing.

0021-9673/82/0000–0000/$02.75

In general, plasma emission spectral detection has been much more widely used in gas chromatography than in liquid chromatography, where the many problems associated with solvent background and selectivity still remain to be addressed.

High-resolution gas chromatography (GC) makes heavy demands on detector design, since rapid quantitative response to match capillary column peak dimensions is needed in addition to the usual objectives of optimal detection and wide linear response range. Post-column band broadening must always be minimized, an aim which has been greatly simplified by the advent of flexible inert fused-silica capillary columns which can be routed directly into detection devices with minimal transfer volume. We have reported a detailed study of the characteristics of fused silica and glass capillary column interfaces to the Beenakker TM_{010} resonance cavity[10,11] for GC–microwave-induced and sustained plasma emission applications[12,13]. The present paper addresses the application of this system to the specific element detection of redistribution products of alkyl groups on germanium, silicon and lead atoms and to the quantitation of tetraalkyl-lead compounds in gasolines.

The scrambling of alkyl groups on tetraalkyl compounds of Group IVA elements has been studied by various workers[14,15]. We reported packed-column GC studies on scrambling between pairs of Group IVA elements utilizing the d.c. argon plasma as an element-specific detector[16]. Now considered are representative scrambling reactions for mixtures of the type $(R_1)_4M$ and $(R_2)_4M$ where M is germanium, tin or lead and R_1 and R_2 are ethyl, *n*-propyl and *n*-butyl groups. Such reactions yield five redistribution products for each metal center, with quantitative proportions as follows: $(R_1)_4M$, 6.25%, $(R_1)_3R_2M$, 25%, $(R_1)_2(R_2)_2M$, 37.5%, $R_1(R_2)_3M$, 25%, $(R_2)_4M$, 6.25%, assuming equivalent stoichiometric proportions of the starting tetraalkyl compounds.

A partical demonstration of such distributed tetraalkyl organometallic compounds is seen in the various mixtures of tetraethyl–tetramethyl redistributed lead compounds present in different gasolines. Here specific element lead detection serves to resolve these species from the predominant hydrocarbon background.

EXPERIMENTAL

Gas chromatographic systems

Varian 1200 (Walnut Creek, CA, U.S.A.) and Shimadzu Mini-2 (Columbia, MD, U.S.A.) gas chromatographs were used with SP-2100 fused-silica wall-coated open tubular (WCOT) capillary columns (12.5 m × 0.3 mm O.D. × 200 μm I.D.) (Hewlett-Packard, Avondale, PA, U.S.A.). Combination injection port liner splitters were designed for each gas chromatograph, consisting of quartz injection port liners attached to 1/4 in. to 1/16 in. brass Swagelok reducers. The reducers had 1/16 in. holes drilled through their sides into which a piece of 12 in. by 1/16 in. O.D. stainless-steel tubing was silver soldered. A Nupro brass fine-metering valve fitted to the end of the stainless-steel tubing served to adjust the injection split ratio.

Details of the spectrometer (Heath 703, McPherson Instruments, Acton, MA, U.S.A.), microwave power train and interface have been published elsewhere[12]. In the study described herein, the fused-silica capillary column was passed through a heated interface without any end-column splitting and terminated within 1–5 mm of the external wall of the Beenakker TM_{010} microwave cavity (Fig. 1). An alternative

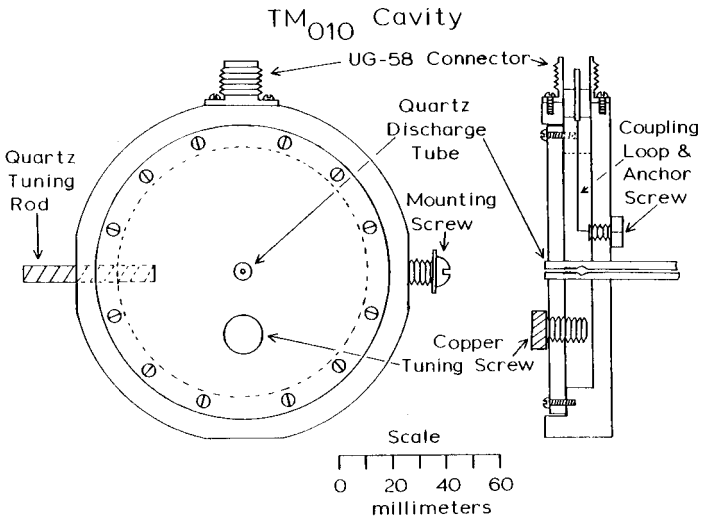

Fig. 1. Diagram of the TM_{010} cylindrical resonance cavity used to sustain the atmospheric pressure helium plasma.

system allowing for solvent venting and/or effluent splitting was described in detail[12]. The essentials of the TM_{010} microwave cavity configuration are shown in Fig. 1.

Materials

Tetra-*n*-propyltin, tetraethyltin, tetraethylgermanium, tetra-*n*-butylgermanium, and tetra-*n*-butyllead were obtained from Ventron Corporation (Beverly, MA, U.S.A.). Tetraethyllead was obtained from ROC/RIC Chemical Corporation (Sun Valley, CA, U.S.A.) and gasoline samples were purchased from local retail stations. Helium carrier gas and plasma gas was purified by passage through anhydrous calcium chloride and molecular sieve 3A traps.

Operational parameters

The operational parameters of the GC–microwave plasma emission system are given in Table I.

Redistribution reaction procedure

A total volume of 100 μl of liquid sample mixtures was placed in a 2-ml screw-capped glass vial. A 5–10-mg piece of resublimed anhydrous aluminum chloride was added and the vial immediately closed with an aluminum foil lined screw-cap. The vial was placed on a hot plate at 100–120°C, its top being cooled by a forced air draft from a hood to prevent rupture while under reflux. After 30 min, heating was stopped and the product liquid diluted with hexanes. Dilution ratios were adjusted (between 20:1 and 100:1) to give chromatographic peaks containing from 1 ng to 10 ng for microbore fused-silica capillary column analysis.

RESULTS AND DISCUSSION

The redistribution of representative examples of the mixture type $(R_1)_4M$ and

TABLE I

GC–MED OPERATING PARAMETERS

Chromatographic				
Column				
packing	SP-2100 WCOT			
material	Fused silica (Carbowax pretreated)			
dimensions	12.5 m × 300 μm O.D. × 200 μm I.D.			
Injection				
split	100:1 110:1			
volume	0.10 μl			
Carrier gas flow-rate (helium)	1 ml/min			
Temperatures				
column program	40°C to 140°C at 5°C/min and 80°C to 134°C, 176°C or 186°C at 6°C/min			
injector	210°C to 215°C			
transfer block	170°C to 220°C			
interface oven	160°C to 220°C			
Spectroscopic				
Entrance and exit slit				
width	25 μm			
height	12 mm			
PMT tube and voltage	RCA 1P28, 700 V			
Recorder	1.0 V full scale input, 1.0 cm/min			
Picoammeter time constant	0.10 sec			
Element	C(I)	Ge(I)	Sn(I)	Pb(I)
Wavelength observed nanometers	247.86	265.16	284.0	283.3
Total plasma flow-rate, helium (ml/min)	70	341	341	100
Microwave input power	75	58	58	75
Picoammeter gain (A)				
5 V full scale output	$3 \cdot 10^{-6}$	$3 \cdot 10^{-7}$	$1 \cdot 10^{-6}$	$1 \cdot 10^{-7}$
Hydrogen doping				
0.5–1.0 ml/min	no	yes	yes	yes

$(R_2)_4M$ is shown in Figs. 2, 3 and 4 for the compound pairs tetraethyl- and tetra-*n*-butylgermanium, tetraethyl- and tetra-*n*-propyltin and tetraethyl- and tetra-*n*-butyllead, respectively. For each of the product mixtures it is seen that qualitative redistribution of alkyl groups had occurred. The sensitivity of the Beenakker TM_{010} microwave detector towards germanium, tin and lead is evident from the elemental detection levels for individual compounds indicated in the chromatograms. Quantitation for the starting compounds was by peak area measurement calibration, while that for intermediate compounds was by interpolation with an accuracy estimated at $\pm 3\%$ relative. The absence of observed solvent response and background indicates the high selectivities of these elements over carbon under the conditions employed.

In Table II are shown the detection limits, selectivities and linear dynamic ranges of response for the three elements. All detection limits are in the low or sub picogram range with selectivities over carbon in the region of 100,000.

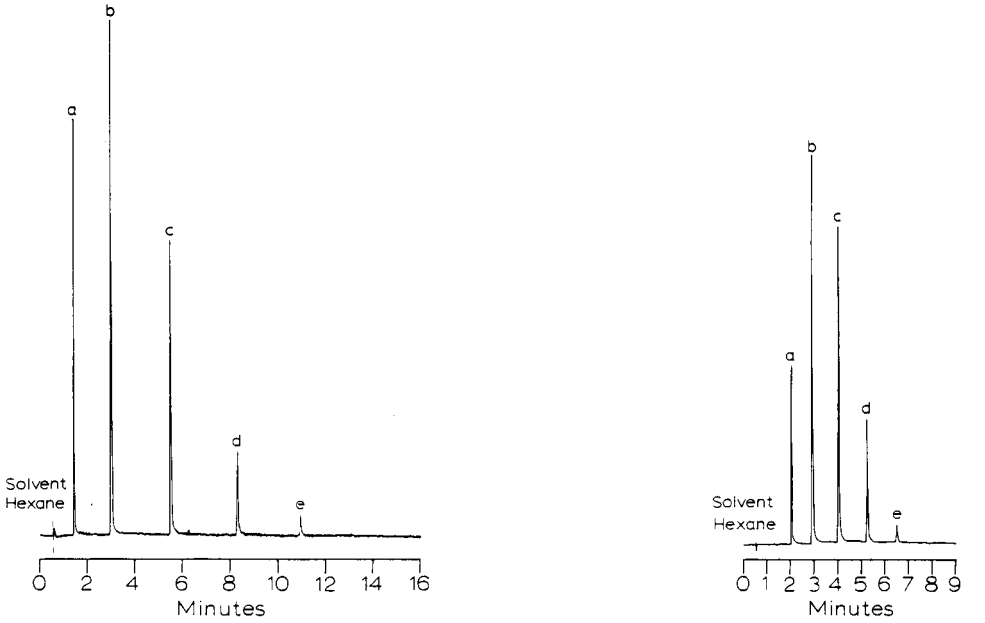

Fig. 2. Gas chromatogram of the alkyl redistribution products between tetraethylgermanium and tetra-*n*-butylgermanium. The microwave emission detector (MED) monitoring Ge(I) 265.16 nm. Column 12.5 m SP-2100 WCOT fused-silica capillary. Temperature program from 80 at 6°C/min. Injection 0.10 μl, split 110:1. Peaks: a = $(CH_3CH_2)_4$ Ge, 494 pg Ge; b = $(CH_3CH_2)_3$ (*n*-$CH_3CH_2CH_2CH_2$) Ge, 722 pg Ge; c = $(CH_3CH_2)_2$ (*n*-$CH_3CH_2CH_2CH_2)_2$ Ge, 509 pg Ge; d = (CH_3CH_2) (*n*-$CH_3CH_2CH_2CH_2)_3$ Ge 145 pg, Ge; e = (*n*-$CH_3CH_2CH_2CH_2)_4$ Ge, 32 pg Ge. Hydrogen bleed 0.5–1 ml/min.

Fig. 3. Gas chromatogram of alkyl redistribution products between tetraethyltin and tetra-*n*-propyltin. MED at Sn(I) 284.00 nm; column and conditions as in Fig. 2, except temperature program from 80 to 134°C at 6°C/min and split 100:1. Peaks: a = $(CH_3CH_2)_4$Sn, 0.78 ng Sn; b = $(CH_3CH_2)_3$(*n*-$CH_3CH_2CH_2$)Sn, 2.17 ng Sn; c = $(CH_3CH_2)_2$(*n*-$CH_3CH_2CH_2)_2$ Sn, 2.70 ng Sn; d = (CH_3CH_2)(*n*-$CH_3CH_2CH_2)_3$ Sn, 0.82 ng Sn; e = (*n*-$CH_3CH_2CH_2)_4$ Sn, 0.12 ng Sn.

Quantitative theoretical and attained redistribution of the mixtures is given in Table III, the data indicating that each mixture has moved towards the theoretical extent of rearrangement but has not attained it. Examination of the absolute levels of each element measured in the chromatograms, taking into account an initial dilution of 100:1, an injection volume of 0.10 μl and an injection split of 100:1 or 110:1, indicates that for lead and germanium a considerable amount of the element is not longer present as tetraalkyl species after reaction. In all cases 5–10 ng of metal should be present in the cumulative peak total for each redistribution chromatogram. The tin redistribution approaches this criterion and is the only chromatogram where an approach is seen to theoretical and quantitative scrambling.

The loss of tetraalkyllead compounds through chlorination by the aluminum chloride has been observed[16]; a larger, less polar alkyl group should be more easily replaced with a chloride, than would be a smaller, more polar alkyl group. Hence chlorination should be to the disadvantage of butyl groups in the redistribution, as is seen in the calculated molar ratio of 2.14 seen for ethyl to butyl groups as eluting. The loss of germanium, although less evident than for the lead system is clearly apparent.

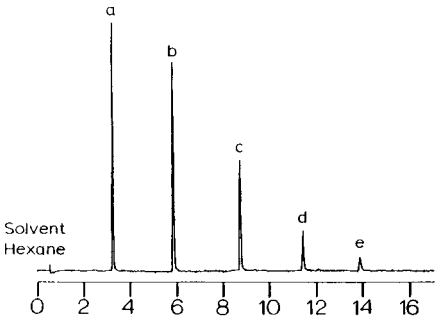

Fig. 4. Gas chromatogram of the alkyl redistribution products between tetraethyllead and tetra-*n*-butyllead. MED at Pb(I) 283.3 nm; column and conditions as in Fig. 2, except temperature program from 80 to 182°C at 6°C/min and split 100:1. Peaks: a = $(CH_3CH_2)_4$ Pb, 180 pg Pb; b = $(CH_3CH_2)_3(n\text{-}CH_3CH_2CH_2CH_2)$ Pb, 189 pg Pb; c = $(CH_3CH_2)_2(n\text{-}CH_3CH_2CH_2CH_2)_2$ Pb, 162 pg Pb; d = $(CH_3CH_2)(n\text{-}CH_3\text{-}CH_2CH_2CH_2)_3$ Pb, 62 pg Pb; e = $(n\text{-}CH_3CH_2CH_2CH_2)_4$ Pb, 21 pg Pb.

Although possibly attributable to chlorination, some decomposition may give rise to the unidentified rust-colored precipitate observed in this reaction. Again a higher proportion of butyl groups is no longer present as tetraalkyls, as is seen from the ethyl:butyl molar ratio of 2.28. Ethyl substituents are more strongly covalently bound to germanium than butyl groups.

The employment of hydrogen doping of the helium plasma to improve the characteristics of elements such as germanium, tin and lead has been reported earlier[13]. In general it doubles or triples the elemental signal for hydride-forming elements such as boron, aluminium, germanium, tin, lead, phosphorus and arsenic and is absolutely necessary for the GC–microwave emission analysis of volatile boron compounds[17]. The addition of hydrogen to the helium discharge also improves the ability of the plasma to resist "overload" by germanium, tin and lead at throughput rates of more than 1–2 ng/sec in the plasma. The "overload" is defined as that amount of mass flow-rate of element which causes metal to deposit on the discharge tube walls. The deposited element, which rests on the walls of the tube immediately after the hottest portion of the discharge, slowly vaporizes off causing the tailing which can be noticed in Fig. 3 for tin compounds and slightly in Fig. 2 for the largest peaks of germanium. In Fig. 4, overloading is not seen for lead compounds since levels are well below the overload condition.

TABLE II

DETECTION LIMITS, SELECTIVITIES AND LINEAR DYNAMIC RANGES

Element and emission wavelength (nm)	*Absolute detection limits (pg)*	*Detection limit (pg/sec)*	*Selectivity vs. C*	*Linear dynamic range*
Ge(I) 265.1	3.9	1.3	$7.57 \cdot 10^4$	10^3
Sn(I) 284.0	6.1	1.6	$3.58 \cdot 10^5$	10^3
Pb(I) 283.3	0.71	0.17	$2.46 \cdot 10^5$	10^3

TABLE III

CALCULATED AND EXPERIMENTAL VALUES FOR THE PROPORTIONS OF REDISTRIBUTION PRODUCTS FROM FRIEDEL–CRAFTS CATALYZED REACTIONS

Reachtion (A): tetraetylgermanium and tetra-*n*-butylgermanium. Reaction (B): tetraethyltin and tetra-*n*-propyltin. Reaction (C): tetraethyllead and tetra-*n*-butyllead.

Compound	$(R_1)_4M$	$(R_1)_3R_2M$	$(R_1)_2(R_2)_2M$	$R_1(R_2)_3M$	$(R_2)_4M$
Theoretical (%)	6.25	25.00	37.50	25.00	6.25
Reaction A					
Germanium alkyls	Et_4Ge	Et_3Bu^nGe	$Et_2Bu^n_2Ge$	$EtBu^n_3Ge$	Bu^n_4Ge
Experimental (%)	26.0	37.9	26.7	7.6	1.7
Ethyl:butyl molar ratio = 2.28					
Reaction B					
Tin alkyls	Et_4Sn	Et_3Pr^nSn	$Et_2Pr^n_2Sn$	$EtPr^n_3Sn$	Pr^n_4Sn
Experimental (%)	13.0	36.2	35.2	13.7	2.0
Ethyl:propyl molar ratio = 1.51					
Reaction C					
Lead alkyls	Et_4Pb	Et_3Bu^nPb	$Et_2Bu^n_2Pb$	$EtBu^n_3Pb$	Bu^n_4Pb
Experimental (%)	29.3	30.7	26.4	10.2	3.4
Ethyl:butyl molar ratio = 2.14					

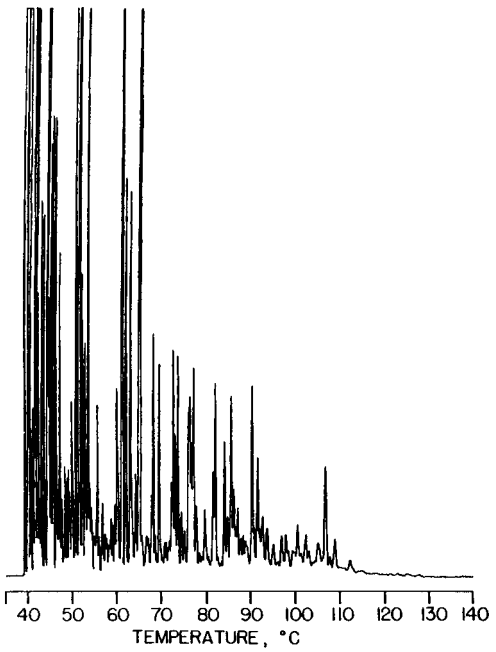

Fig. 5. Gas chromatogram of Super Shell leaded gasoline. MED at C(I) 247.86 nm. Column as in Fig. 2. Temperature program from 40 to 140°C at 5°C/min. Injection 0.10 μl, split 100:1.

Characterization of tetraalkylleads in leaded gasoline

The high complexity of gasoline is seen in the fused-silica capillary chromatogram shown in Fig. 5, where the microwave plasma detector is set to the 247.9 nm (C(I) emission line and is used similarly to a flame ionization detector to acquire a total organic compound assessment of a mixture. Leaded gasolines contain different alkylleads, typically the methyl-:ethyllead redistribution mixture. Figs. 6 and 7 depict gasoline tetraalkyllead profiles, monitoring the 283.3 nm Pb(I) emission line. Chromatographic separation and spectral resolution of lead over carbon background are well demonstrated. Patterns showed reproducibility of greater than 2.5 % relative standard deviation. Super Shell and Amoco gasolines contain mixed methyl-/ethylleads in differing proportions, while Exxon contains primarily tetraethyllead with some triethyllead chloride also present[12]. The microwave plasma emission system is clearly applicable to such gasoline characterizations, similar applications having been demonstrated by other workers with GC–plasma[18] and GC–atomic absorption analysis[19].

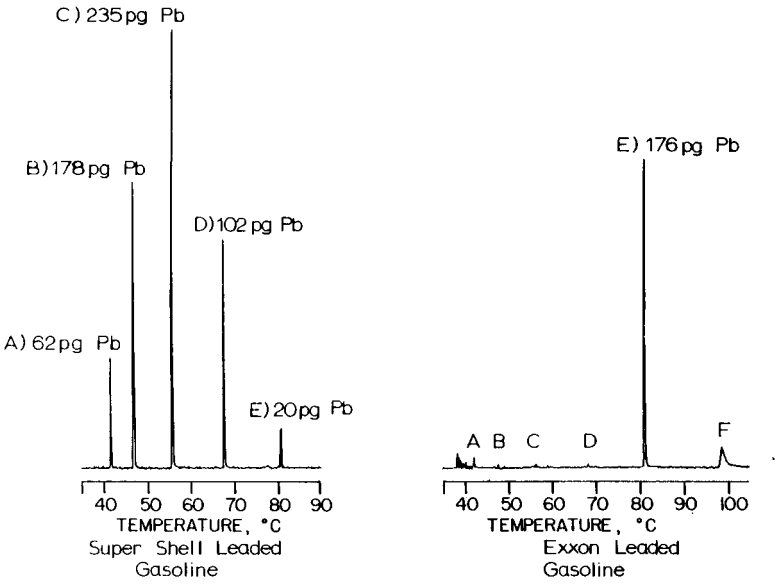

Fig. 6. Gas chromatograms of Super Shell and Exxon leaded gasolines. MED at Pb(I) 283.3 nm; column and conditions as in Fig. 5, except temperature program from 40 to 100°C at 5°C/min. Peaks: A = $(CH_3)_4$ Pb; B = $(CH_3)_3(CH_3CH_2)$Pb; C = $(CH_3)_2(CH_3CH_2)_2$ Pb; D = $(CH_3)(CH_3CH_2)_3$ Pb; E = $(CH_3CH_2)_4$ Pb; F = $(CH_3CH_2)_3$ PbCl.

ACKNOWLEDGEMENTS

This work was supported in part by the Ethyl Corporation, Ferndale, MI, U.S.A., by the U.S. Department of Energy through contract DE-AC02-077EV4320, and by a National Institutes Biomedical Sciences Research Grant to the University of Massachusetts. We also thank Bruce D. Quimby and the Hewlett-Packard Corporation, Avondale, PA, U.S.A. for provision of the fused-silica capillary column. We

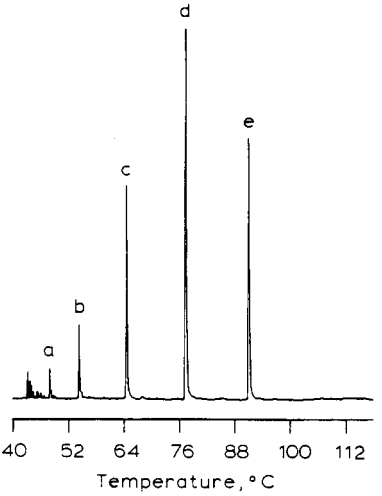

Fig. 7. Gas chromatogram of Amoco leaded gasoline. Detector, column and conditions as in Fig. 5. Gain $3 \cdot 10^{-7}$ A. Peaks: a = $(CH_3)_4$ Pb, 10 pg Pb; b = $(CH_3)_3$ (CH_3CH_2) Pb, 30 pg Pb; c = $(CH_3)_2(CH_3CH_2)_2$ Pb, 96 pg Pb; d = (CH_3) $(CH_3CH_2)_3$ Pb, 169 pg Pb; e = $(CH_3CH_2)_4$ Pb, 131 pg Pb.

thank the American Chemical Society, Analytical Division for provision of Fellowship Support (SEA) awarded by the Proctor and Gamble Company, Cincinnatti, OH, U.S.A.

REFERENCES

1 A. J. McCormack, S. C. Tong and W. D. Cooke, *Anal. Chem.*, 37 (1965) 1470.
2 W. R. McLean, D. L. Stanton and G. E. Penketh, *Analyst (London)*, 98 (1973) 432.
3 B. D. Quimby, P. C. Uden and R. M. Barnes, *Anal. Chem.*, 50 (1978) 2112.
4 B. D. Quimby, M. F. Delaney, P. C. Uden and R. M. Barnes, *Anal. Chem.*, 51 (1979) 875.
5 K. J. Mulligan, J. A. Caruso and F. L. Fricke, *Analyst (London)*, 105 (1980) 1060.
6 R. J. Lloyd, R. M. Barnes, P. C. Uden and W. G. Elliott, *Anal. Chem.*, 50 (1978) 2025.
7 P. C. Uden, R. M. Barnes and F. P. DiSanzo, *Anal. Chem.*, 50 (1978) 852.
8 D. Sommer and K. Ohls, *Z. Anal. Chem.*, 295 (1979) 337.
9 D. L. Windsor and M. B. Denton, *J. Chromatogr. Sci.*, 17 (1979) 492.
10 C. I. M. Beenakker, *Spectrochim Acta*, 31B (1976) 483.
11 C. I. M. Beenakker, *Spectrochim Acta*, 32B (1977) 173.
12 S. A. Estes, P. C. Uden and R. M. Barnes, *Anal. Chem.*, 53 (1981) 1336.
13 S. A. Estes, P. C. Uden and R. M. Barnes, *Anal. Chem.*, 53 (1981) 1829.
14 G. Calingaert and H. A. Beatty, *J. Amer. Chem. Soc.*, 61 (1939) 2748.
15 F. H. Pollard, G. Nickless and P. C. Uden, *J. Chromatogr.*, 19 (1965) 28.
16 S. A. Estes, C. A. Poirier, P. C. Uden and R. M. Barnes, *J. Chromatogr.*, 196 (1980) 265.
17 L. G. Sarto, Jr., S. A. Estes, P. C. Uden, S. Siggia and R. M. Barnes, *Anal. Lett.*, 14(A3) (1981) 205.
18 D. C. Reamer, W. H. Zoller and T. C. O'Haver, *Anal. Chem.*, 50 (1978) 1449.
19 J. C. van Loon, *Amer. Lab.*, 13(5) (1981) 47.

Journal of Chromatography, 239 (1982) 191–216
Elsevier Scientific Publishing Company, Amsterdam — Printed in The Netherlands

CHROM. 14,499

CHARACTERIZATION OF DIHYDROARENEDIOLS AND RELATED COMPOUNDS BY GAS CHROMATOGRAPHY–MASS SPECTROMETRY: COMPARISON OF DERIVATIVES

C. J. W. BROOKS*, W. J. COLE, J. H. BORTHWICK and G. M. BROWN
Chemistry Department, University of Glasgow, Glasgow G12 8QQ (Great Britain)

SUMMARY

Gas chromatographic and mass spectrometric properties are reported for some dihydrodiols and tetrahydrodiols, and for their diacetates, di(trimethylsilyl) ethers and cyclic alkaneboronates. The diols studied include typical metabolites formed via epoxidation of arylalkenes (indene, acenaphthylene) and arenes (anthracene, phenanthrene). The results confirm that trimethylsilylation is the most satisfactory general procedure for the protection of "metabolic" diols and for their analysis by combined gas chromatography–mass spectrometry. The formation of cyclic alkaneboronate esters is practicable from *cis*-diols and (somewhat less readily) from certain *trans*-diols of sufficiently flexible conformations. Where they can be formed, cyclic methaneboronates afford the advantages of short retention times, low mass increments and, generally, informative mass spectra with abundant molecular ions.

INTRODUCTION

One of the most important modes of metabolism of alkenes and arenes is their oxidation (by formal addition of the elements of H_2O_2) to vicinal dihydrodiols. The first such metabolite, 1,2-dihydroanthracene-1,2-diol, was isolated in 1935 from the urine of rats treated with anthracene[1]. The analogous dihydrodiol from naphthalene[2], and three positionally isomeric dihydrophenanthrenediols from phenanthrene (the preponderant metabolite being the 9,10-isomer) were also characterised in early work[2,3]. Typically, the dihydroarenediols of mammalian metabolism have *trans*-configurations[4,5], and Boyland's postulate[6] of the intermediacy of arene epoxides in dihydrodiol formation has been amply confirmed by the extensive studies of the N.I.H. group, following the isolation of 1,2-naphthalene epoxide as a microsomal metabolite of naphthalene[7]. Dihydroarenediols of *cis*-configuration are encountered particularly in the microbial metabolism of aromatic hydrocarbons via the action of dioxygenases[8,9]. Metabolism of the olefinic bond in conjugated benzocycloalkenes affords both *cis*- and *trans*-dihydrodiols, as was first observed for indene[10].

The characterisation of dihydrodiols in extracts of metabolites has been aided by the application of combined gas chromatography–mass spectrometry (GC–MS). Since the free dihydrodiols are susceptible to elimination of the elements of water by

0021-9673/82/0000–0000/$02.75

thermal or catalytic action (especially in the case of dihydroarenediols which thereby afford highly stable phenols), derivatives are generally employed for GC–MS. Trimethylsilyl (TMS) ethers have been used, for example, in the analysis of mixtures of naphthalene metabolites, including the preponderant dihydrodiol, extracted from rat urine after hydrolysis[11]. Dihydrodiols formed by microsomal metabolism of the carcinogen 7,12-dimethylbenz(*a*)anthracene, and separated by high-performance liquid chromatography (HPLC), have also been trimethylsilylated for analysis by GC–MS[12]. Protection of suitably constituted vicinal diols in the form of cyclic derivatives is also possible: thus indane-*cis*-1,2-diol was included in the first study of the value of cyclic boronate derivatives in GC–MS[13], and cyclic methaneboronates have since been applied to the analysis of metabolic dihydrodiols, *e.g.*, from naphthalene[11] and iminostilbene[14].

The aim of this paper is to compare the properties, in respect of GC–MS, of various types of dihydro- and tetrahydrodiols in their free forms and as their acetates, trimethylsilyl ethers and (where practicable) cyclic alkaneboronates.

MATERIALS AND METHODS

Solvents and reagents

Ethyl acetate (Nanograde) was obtained from Mallinckrodt (St. Louis, MO, U.S.A.). Pyridine (AnalaR: BDH, Poole, Great Britain) was dried over KOH pellets and redistilled prior to use. Acetic anhydride (AnalaR) and *p*-toluenesulphonic acid were supplied by BDH. 2,2-Dimethoxypropane (Fluka, Buchs, Switzerland) was obtained from Fluorochem (Glossop, Great Britain). Hexamethyldisilazane (HMDS), trimethylchlorosilane (TMCS), N,O-bis(trimethylsilyl)acetamide (BSA), N,O-bis(trimethylsilyl)trifluoroacetamide (BSTFA) and methaneboronic acid were obtained from Pierce and Warriner (Chester, Great Britain). 1-Butaneboronic acid was supplied by Ventron (Karlsruhe, G.F.R.).

Diols and other reference compounds

The compounds are denoted below by the numbers shown in Figs. 1 and 18 (chiral compounds were racemic except for No. 10). Compounds 1, 2, 6 and 7 were available from earlier work[10,15]; compounds 3, 4 and 8–18 were donated by the late Prof. J. D. Loudon and were synthetic samples, with the exception of compound 10, which had been isolated by Prof. E. Boyland from the urine of rabbits dosed with anthracene. Compound 5 was purchased from Alfred Bader Chemicals (Aldrich, Gillingham, Dorset, Great Britain), and compound 19 (Nadolol: SQ 11725) was donated by E. R. Squibb and Sons (Princeton, NJ, U.S.A.).

Gas–liquid chromatography

Gas–liquid chromatography (GLC) was carried out with a Perkin-Elmer (Beaconsfield, Great Britain) F-11 gas chromatograph (used for packed column studies) and a Pye Model 104 gas chromatograph (Pye Unicam, Cambridge, Great Britain) equipped with a falling needle injection system (used for open-tubular GLC). Silanized glass columns (1.8 m × 4 mm I.D.) were packed with 1% OV-1 or 1% OV-17 on Gas-Chrom Q, 100–120 mesh (Pierce and Warriner, Chester, Great Britain); the nitrogen carrier gas flow-rate was 40 ml/min. Open-tubular GLC was performed on a

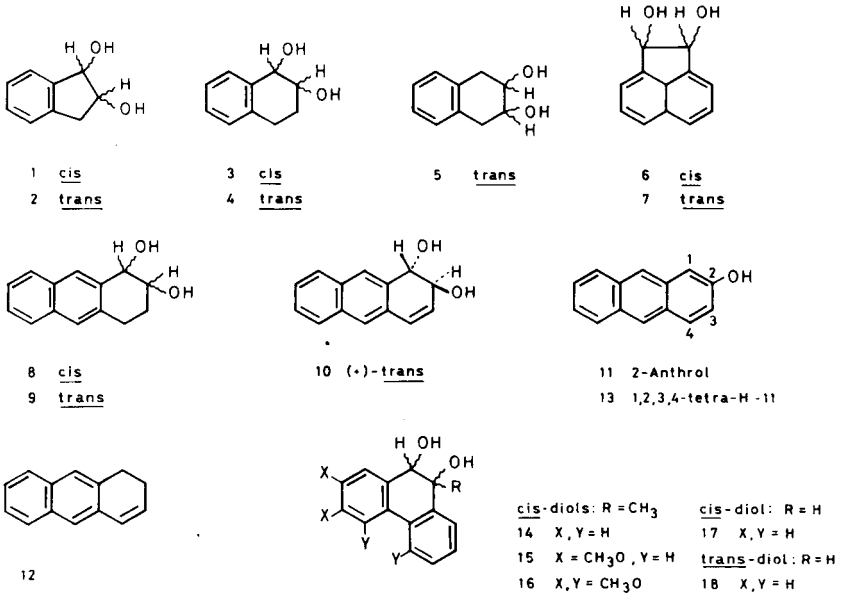

Fig. 1. Structures of dihydrodiols, tetrahydrodiols, and related compounds. 1 = Indane-*cis*-1,2-diol; 2 = indane-*trans*-1,2-diol; 3 = 1,2,3,4-tetrahydronaphthalene-*cis*-1,2-diol; 4 = 1,2,3,4-tetrahydronaphthalene-*trans*-1,2-diol; 5 = 1,2,3,4-tetrahydronaphthalene-*trans*-2,3-diol; 6 = acenaphthene-*cis*-1,2-diol; 7 = acenaphthene-*trans*-1,2-diol; 8 = 1,2,3,4-tetrahydroanthracene-*cis*-1,2-diol; 9 = 1,2,3,4-tetrahydroanthracene-*trans*-1,2-diol; 10 = 1,2-dihydroanthracene-*trans*-1,2-diol; 11 = 2-anthrol; 12 = 1,2-dihydroanthracene; 13 = 1,2,3,4-tetrahydroanthracen-2-ol; 14 = 9-methyl-9,10-dihydrophenanthrene-*cis*-9,10-diol; 15 = 2,3-dimethoxy-9-methyl-9,10-dihydrophenanthrene-*cis*-9,10-diol; 16 = 2,3,4,5-tetramethoxy-9-methyl-9,10-dihydrophenanthrene-*cis*-9,10-diol; 17 = 9,10-dihydrophenanthrene-*cis*-9,10-diol; 18 = 9,10-dihydrophenanthrene-*trans*-9,10-diol.

flexible fused silica column (12 m × 0.25 mm I.D.) coated with OV-1 (Hewlett-Packard, Altrincham, Great Britain); the helium carrier gas flow-rate was 2 ml/min. Both instruments employed hydrogen flame-ionization detectors.

Gas chromatography–mass spectrometry

Gas chromatography–mass spectrometry (GC–MS) was carried out on an LKB 9000 instrument fitted with a silanized glass column (1.8 m × 4 mm I.D.) packed with 1 % OV-1 on Gas-Chrom Q, 100–120 mesh; the helium carrier gas flow-rate was 30 ml/min. Mass spectra (20 eV) were recorded under electron-impact conditions: accelerating voltage, 3.5 kV; trap current, 60 μA; source and separator temperatures, 260°C.

Preparation of derivatives

Methaneboronate esters. Methaneboronic acid (1.1 mol proportion) in dry pyridine was added to the diol (100 μg) (compounds 1–3, 5–8 and 10–17) and the mixture heated at 60°C for 30 min. After removal of solvent under nitrogen the residue was redissolved in ethyl acetate (100 μl) for GLC; compounds 4 and 9 required 2.2 mol proportions of methaneboronic acid to effect complete derivative formation. Compounds 18 and 19 (100 μg), however, were dissolved in 2,2-dimethoxypropane and

TABLE I

KOVÁTS RETENTION INDICES (*I*) AND INCREMENTS FOR DERIVATIVE FORMATION (ΔI) FOR INDANE-, TETRAHYDRONAPHTHALENE- AND ACENAPHTHENEDIOLS

Stationary phase	*Derivative*	*Compound no.*													
		1		*2*		*3*		*4*		*5*		*6*		*7*	
		*I***	ΔI	*I***	ΔI	*I***	ΔI	*I***	ΔI	*I****	ΔI	*I*§*	ΔI	*I*§§*	ΔI
OV-1	Diol	1400		1440		1515		1535		1550		1790		1830	
	Diacetate (a)*	1610	+210	1610	+170	1710	+195	1705	+170	1730	+180	1990	+200	1975	+145
	Di-TMS (b)	1580	+180	1610	+170	1660	+145	1650	+115	1675	+125	1925	+135	1965	+135
	Me boronate (c)	1295	−105	–	–	1400	−115	1445	−90	1415	−135	1670	−120	–	–
	Bu boronate (d)	1565	+165	–	–	1680***	+165	1730***	+195	1730	+180	1935§§	+145	–	–
OV-17	Diol	1670		1710		1790		1820		1850		2145		2245	
	Diacetate (a)	1890	+220	1880	+170	2005	+215	2010	+190	2030	+180	2345	+200	2335	+90
	Di-TMS (b)	1685	+15	1695	−15	1770	−20	1760	−60	1770	−80	2100	−45	2120	−125
	Me boronate (c)	1500	−170	–	–	1620	−170	1640	−180	1640	−210	1965	−180	–	–
	Bu boronate (d)	1780	+110	–	–	1920***	+130	1950***	+130	1950	+100	2260§§	+115	–	–

* Letters denote derivative types.
** 120°C.
*** 140°C.
§ 150°C.
§§ 170°C.

heated at 60°C for 30 min in the presence of methaneboronic acid (2.2 mol proportion). The resultant solution was diluted with 2,2-dimethoxypropane (40 μl) and used directly for GLC analysis (1 μl).

n-Butaneboronate esters. Compounds 1–3, 5–8 and 10–17 (100 μg) were treated with *n*-butaneboronic acid (1.1 mol proportion) and heated at 60°C for 30 min. After removal of solvent under nitrogen, the residue was redissolved in ethyl acetate (100 μl) and used for GLC (1 μl). Compounds 4, 9 and 18, however, required 2.2 mol proportions of the boronic acid for complete derivative formation.

Trimethylsilyl ethers. For non-hindered hydroxyl groups, the compound (100 μg) was dissolved in BSA (BSTFA for compound 19) and heated at 60°C for 30 min. The reagent was removed in a stream of nitrogen and the product redissolved in EtOAc (100 μl), an aliquot (1 μl) being used for GLC. For hindered hydroxyl groups, the compound (100 μg) was heated with BSA–HMDS–TMCS (10:10:5 μl) in a Reactivial at 90°C for 24 h. After solvent removal the residue was taken up in ethyl acetate (100 μl) and analysed by GLC (1 μl).

Acetylation. Compounds 1–15, 17 and 18 (100 μg) were treated with acetic anhydride (20 μl) and pyridine (10 μl) and heated at 60°C for 30 min. After reagent removal under nitrogen the product was taken up in ethyl acetate (100 μl) and used for GLC (1 μl). Compound 16 required heating for 24 h at 90°C together with the reagents in a Reactivial to effect full derivative formation. Nadolol (100 μg) required heating with the reagents at 60°C for 48 h in the presence of *p*-toluenesulphonic acid as catalyst to effect complete acetylation.

RESULTS

The compounds studied are grouped (*cf.* Fig. 1) broadly in order of molecular size. Unless otherwise stated, diacetates and di-TMS ethers were readily formed from the diols. The comments on derivative formation therefore refer chiefly to the more selective process of cyclic boronate preparation.

Indanediols, tetrahydronaphthalenediols and acenaphthenediols (compounds 1–7)

The conformational rigidity of substituents in the five-membered rings of indane and acenaphthene renders the *trans*-diols incapable of forming simple cyclic esters, but leads to the ready formation from the *cis*-diols of exceptionally stable cyclic boronates[13]. In the case of the six-membered ring diols (compounds 3–5) derived from tetrahydronaphthalenes, cyclic boronates were afforded by the 1,2-*cis*-diol, by the 2,3-*trans*-diol and (incompletely) by the 1,2-*trans*-diol. It is well known that both *cis*- and *trans*-cyclohexane-1,2-diol yield cyclic boronates[16], but the virtually planar ring-fused portions of the cyclohexenoids 3–5 make it difficult for the *trans*-diols (especially at the 1,2-position) to accommodate the conformations required in cyclic ester formation.

Gas chromatographic data for derivatives of diols 1–7 are cited in Table I. The free diols usually gave unsatisfactory "tailing" peaks, but their retention index values are included to facilitate consideration of the increments attending derivative formation. The most noteworthy feature is the marked decrement in retention time ($\Delta I \approx -120$), on the OV-1 phase, for the conversion of a diol to its cyclic methaneboronate. The satisfactory nature of the latter derivative for acenaphthene-*cis*-1,2-diol is il-

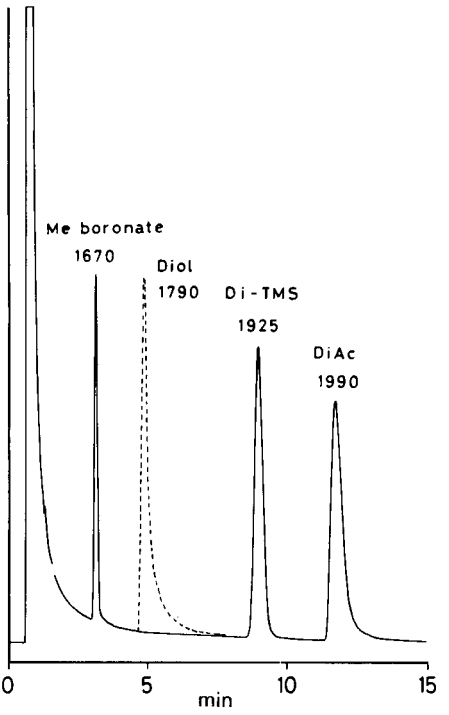

Fig. 2. Gas chromatographic separation of the methaneboronate (6c) di-TMS ether (6b) and diacetate (6a) of acenaphthene-*cis*-1,2-diol (with the peak obtained separately for the free diol superimposed). Column, 1% OV-1 (1.8 m × 4 mm I.D.); column temperature, 150°C; nitrogen flow-rate, 40 ml/min.

lustrated by the gas chromatogram in Fig. 2: the sequence of elution of the di-TMS ether and diacetate derivatives is typical of the whole group of diols.

Some salient features of the mass spectra of diols 1–7 and their derivatives are summarised in Table II. It is clear that the di-TMS ethers, which are the most generally useful derivatives for GLC, yield satisfactory molecular ions only for the indane and acenaphthene diols, while only one of the diacetates in the group affords an abundant molecular ion, because of the preponderance of eliminations of acetic acid and ketene. The methaneboronates yield abundant molecular ions, which are a little less prominent in butaneboronates: here the larger alkyl group offers additional pathways of fragmentation, and also appears to promote readier loss of the elements of alkaneboronic acid —a process affording the base peaks of m/z $(M-100)$ from the butaneboronates of indanediol[13] and acenaphthenediol. The fragmentations of typical derivatives are further illustrated with respect to acenaphthene-*cis*-1,2-diol (6) in Figs. 3 and 4. Each spectrum contains a clear molecular ion (preponderant only in the methaneboronate) and an ion of m/z 168 formally representing the acenaphthenone or epoxyacenaphthene ion. A fragment of m/z 152 (acenaphthylene ion) resulting from loss of both oxygen substituents is prominent only in the free diol spectrum. The relatively lower abundance of molecular ions in the spectra of the diacetate and di-TMS ether of the *trans*-diol (7) (*cf.* Table II) is of diagnostic and mechanistic interest: both the loss of Me_3SiOH by *cis*-elimination to give $(M-90)$ and, more unexpect-

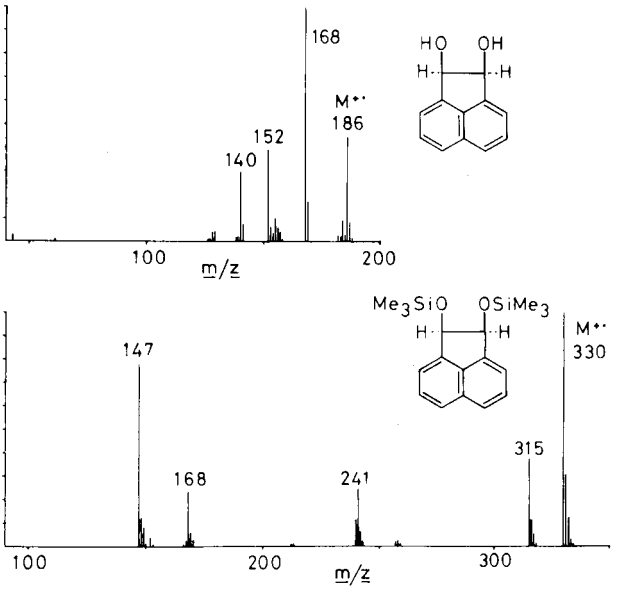

Fig. 3. Mass spectra (20 eV) of acenaphthene-*cis*-1,2-diol (6) and di-TMS ether (6b) measured on an LKB 9000 gas chromatograph–mass spectrometer. Column, 1% OV-1 (1.8 m × 4 mm I.D.); column temperatures as in Table I; helium flow-rate, 30 ml/min; accelerating voltage, 3.5 kV; source temperature, 260°C; trap current, 60 μA.

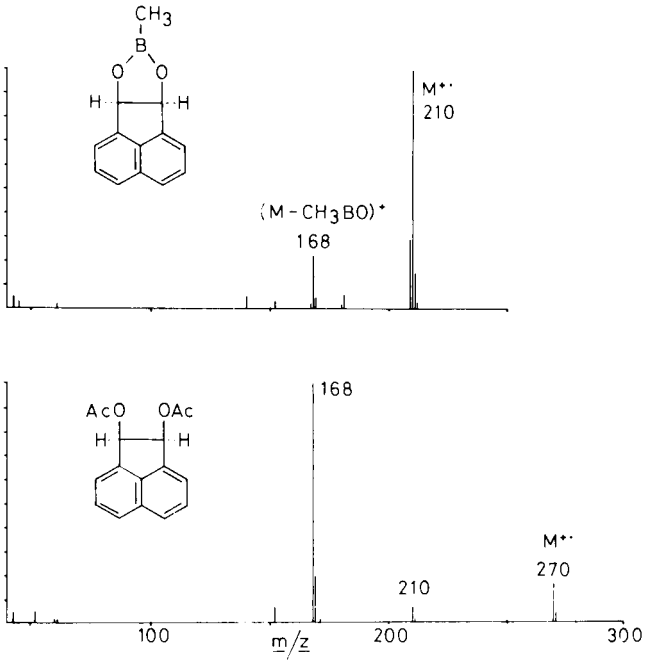

Fig. 4. Mass spectra (20 eV) of acenaphthene-*cis*-1,2-diol methaneboronate (6c) and diacetate (6a). GC–MS conditions as in Fig. 3.

TABLE II

BASE PEAKS AND RELATIVE ABUNDANCE OF MOLECULAR IONS IN THE MASS SPECTRA OF INDANEDIOLS, TETRAHYDRONAPHTHALENEDIOLS, ACENAPHTHENEDIOLS AND THEIR DERIVATIVES

Diol	*Free*			*Diacetate*			*Di-TMS ether*			*Me boronate*			*Bu boronate*		
	M		*Base peak*	*M*		*Base peak*	*M*		*Base peak*	*M*		*Base peak*	*M*		*Base peak*
	m/z	%	*m/z*	*m/z*	%	*m/z*	*m/z*	%	*m/z*	*m/z*	%	*m/z*	*m/z*	%	*m/z*
1	150	5	104 ($M - 46$)	234	0	132 ($M - 102$)	294	62	147*	174	100	174 (M)	216	7	116 ($M - 100$)
2	150	6	104 ($M - 46$)	234	0	132 ($M - 102$)	294	17	147*	Not formed			Not formed		
3	164	0	146 ($M - 18$)	248	0	146 ($M - 102$)	308	0	192 ($M - 116$)	188	95	128 ($M - 60$)	230	20	128 ($M - 102$)
4	164	5	104 ($M - 60$)	248	0	146 ($M - 102$)	308	0	192 ($M - 116$)	188	29	160 ($M - 28$)	230	25	202 ($M - 28$)
5	164	24	146 ($M - 18$)	248	0	128 ($M - 120$)	308	1	218 ($M - 90$)	188	100	188 (M)	230	40	139 ($M - 91$)
6	186	60	168 ($M - 18$)	270	15	168 ($M - 102$)	330	100	330 (M)	210	100	210 (M)	252	50	152 ($M - 100$)
7	186	7	168 ($M - 18$)	270	0.2	168 ($M - 102$)	330	26	147*	Not formed			Not formed		

* Ion $Me_2Si{=}\dot{O}SiMe_3$, typical of diol di-TMS ethers.

edly, the loss of $Me_3SiOSiMe_3$ to give $(M-162)$ appear to be enhanced in the *trans*-diol derivative as compared with the *cis*-isomer.

Figs. 5 and 6 provide a simple demonstration of the complementary value of di-TMS ethers and cyclic boronate esters in structural diagnosis. Both derivatives easily distinguish the tetrahydronaphthalene *cis*-1,2- and *trans*-2,3-isomers; however, for the former isomer (3) the *retro*-Diels–Alder fragment of *m/z* 192, strongly promoted by the dual α-cleavage of the di-TMS ether, is characteristic. The cyclic boronate group bridging the 1,2-positions suppresses the *retro*-Diels–Alder fragmentation. Conversely, the parent 2,3-diol structure (5) is indicated much more clearly from its methaneboronate spectrum (Fig. 6), by a pair of ions of *m/z* 91 ($C_7H_7^+$) and 97 ($C_4H_6BO_2^+$) formed by cleavage of the tetrahydro ring. The *retro*-Diels–Alder ion of *m/z* 104 is also more prominent in the latter spectrum than in that of the corresponding di-TMS ether.

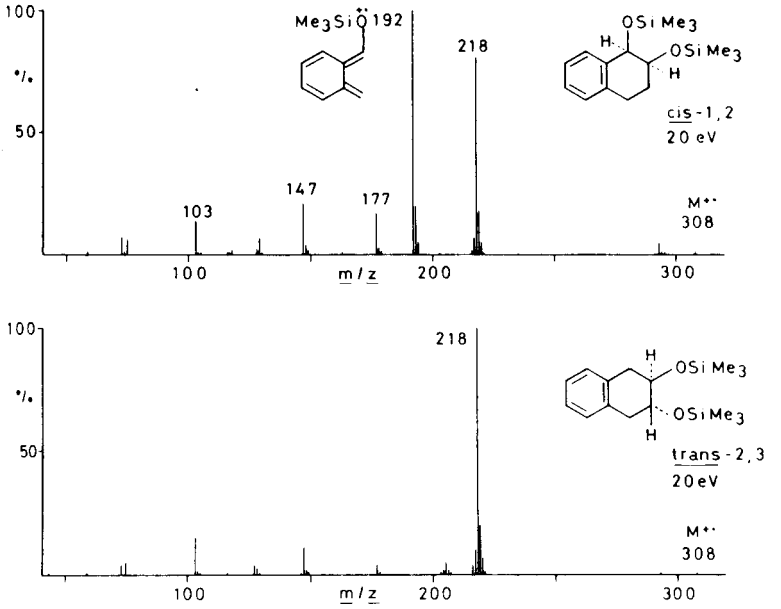

Fig. 5. Mass spectra (20 eV) of 1,2,3,4-tetrahydronaphthalene-*cis*-1,2-diol di-TMS ether (3b) and 1,2,3,4-tetrahydronaphthalene-*trans*-2,3-diol di-TMS ether (5b). GC–MS conditions as in Fig. 3.

Tetrahydroanthracenediols and a dihydroanthracenediol (compounds 8–10)

The tetrahydroanthracene-*cis*- and *trans*-1,2-diols, like their naphthalene analogues, both formed cyclic boronates, the *trans*-esters being produced incompletely even with a considerable excess of reagent. It proved impracticable to form a cyclic boronate from the cyclohexadienediol grouping in the anthracene metabolite, 1,2-dihydroanthracene-*trans*-1,2-diol (10). Inspection of molecular models suggests that such a cyclic ester would be highly strained (*cf.* however, the boronates of compound 18, described below).

In the tetrahydro series, the methaneboronates have the shortest retention times on OV-1 phase, as illustrated for the *cis*-diol in Fig. 7. [The additional small

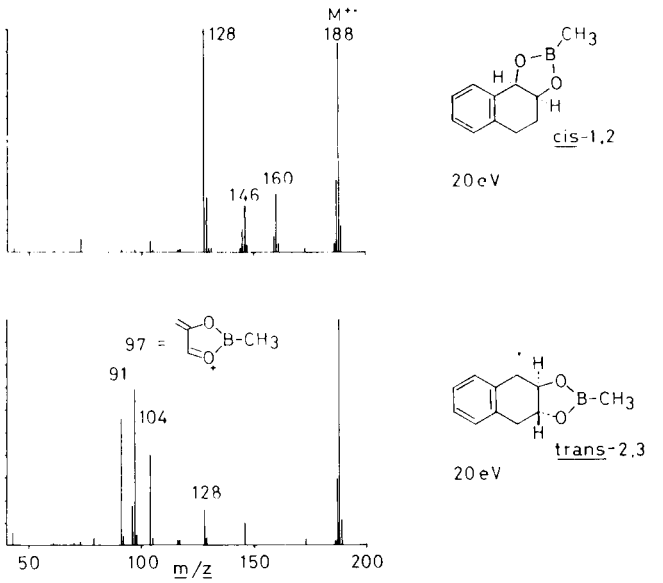

Fig. 6. Mass spectra (20 eV) of 1,2,3,4-tetrahydronaphthalene-*cis*-1,2-diol methaneboronate (3c) and 1,2,3,4-tetrahydronaphthalene-*trans*-2,3-diol methaneboronate (5c). GC–MS conditions as in Fig. 3.

peaks appear to have arisen from an impurity of octahydroanthracenediol present in the parent diol.] GLC data summarised in Table III show that the cyclic boronates afford the largest differences in retention index between the *cis*- and *trans*-tetrahydrodiols, an effect attributable to the fixation of distinctive conformations by ring formation. The stability of the metabolic diol, 1,2-dihydroanthracene-*trans*-1,2-diol, towards GLC was confirmed by comparison with its dehydration product, 2-anthrol (11) and their derivatives. The data included for tetrahydroanthracen-2-ol (13) show

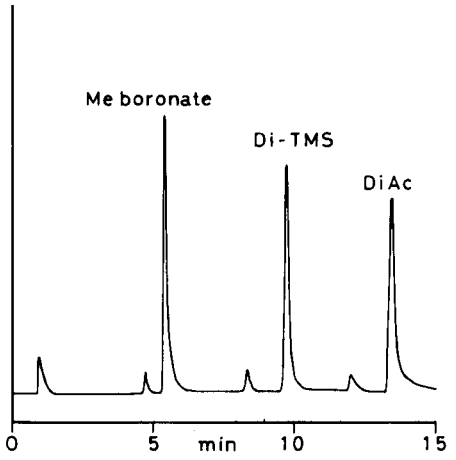

Fig. 7. Gas chromatographic separation of the methaneboronate (8c), di-TMS ether (8b) and diacetate (8a) of 1,2,3,4-tetrahydroanthracene-*cis*-1,2-diol. Column, WCOT OV-1 (12 m × 0.25 mm I.D.); column temperature, 190°C; helium flow-rate, 2 ml/min.

TABLE III

KOVÁTS RETENTION INDICES (*I*) FOR TETRAHYDRO- AND DIHYDROANTHRACENEDIOLS AND DERIVATIVES, AND RELATED COMPOUNDS

Stationary phase	*Derivative*	*Compound no.*		
		*8***	*9***	*10****
OV-1	Diol	2085	2095	2135
	Diacetate (a)*	2250****	2250****	2255
	Di-TMS (b)	2150	2140	2215
	Me boronate (c)	1960	1990	–
	Bu boronate (d)	2235	2290	–
OV-17	Diol	2540§	2550§	§§§
	Diacetate (a)	2700§§	2690§§	§§§
	Di-TMS (b)	2340§	2330§	§§§
	Me boronate (c)	2290	2310	–
	Bu boronate (d)	2570	2615	–
		Compound no.		
		*11***	*12*†	*13****
OV-1	Parent compound	2100	1700	1905
	Acetate (e)	2165	–	2035
	TMS (f)	2135	–	2000
OV-17	Parent compound	2485	1955	2300††
	Acetate (e)	2520	–	2410††
	TMS (f)	2390	–	2230††

* Letters denote derivative types.
** 175°C.
*** 200°C.
§ 210°C.
§§ 230°C.
§§§ Not examined.
† 150°C.
†† 190°C.

that the retention increments for introduction of the 1-hydroxy group are of the expected order ($\Delta I \approx 180$ on OV-1 phase).

The base peaks and molecular ion abundances in the mass spectra of diols 8–10 and their derivatives are summarised in Table IV. Mass spectra of the tetrahydroanthracenediol series, shown in Figs. 8–11, are of limited value in differentiating between the *cis*- and *trans*-isomers. The free diols (Fig. 8) give strong $[M]^{+\cdot}$ and $([M-H_2O]^{+\cdot})$ ions, together with $[M-44]^{+\cdot}$ (loss of vinyl alcohol by a *retro*-Diels–Adler process) and $[M-60]^{+\cdot}$ (m/z 154.0785 from diol 8) resulting from elimination of ethenediol (C-1 + C-2). The mass spectra of the diacetates (Fig. 9) are dominated by ions resulting from losses of acetic acid and ketene. In both the free diols and diacetates, the relative intensities of the common ions, though different for the *cis*- and *trans*-isomers, are of little discriminatory value in view of the similar retention times.

TABLE IV

BASE PEAKS AND RELATIVE ABUNDANCE OF MOLECULAR IONS IN THE MASS SPECTRA OF DIHYDRO- AND TETRAHYDROANTHRACENEDIOLS AND THEIR DERIVATIVES

Diol	*Free*			*Diacetate*			*Di-TMS ether*			*Me boronate*			*Bu boronate*		
	M		*Base peak*	*M*		*Base peak*	*M*		*Base peak*	*M*		*Base peak*	*M*		*Base peak*
	m/z	%	*m/z*	*m/z*	%	*m/z*	*m/z*	%	*m/z*	*m/z*	%	*m/z*	*m/z*	%	*m/z*
8	214	95	196 ($M - 18$)	298	13	178 ($M - 120$)	358	10	268 ($M - 90$)	238	75	178 ($M - 60$)	280	47	178 ($M - 102$)
9	214	100	214 (M)	298	3	196 ($M - 102$)	358	11	268 ($M - 90$)	238	100	238 (M)	280	100	280 (M)
10	212	1	194 ($M - 18$)	296	0.2	194 ($M - 102$)	356	7	191 ($M - 165$)	Not formed			Not formed		

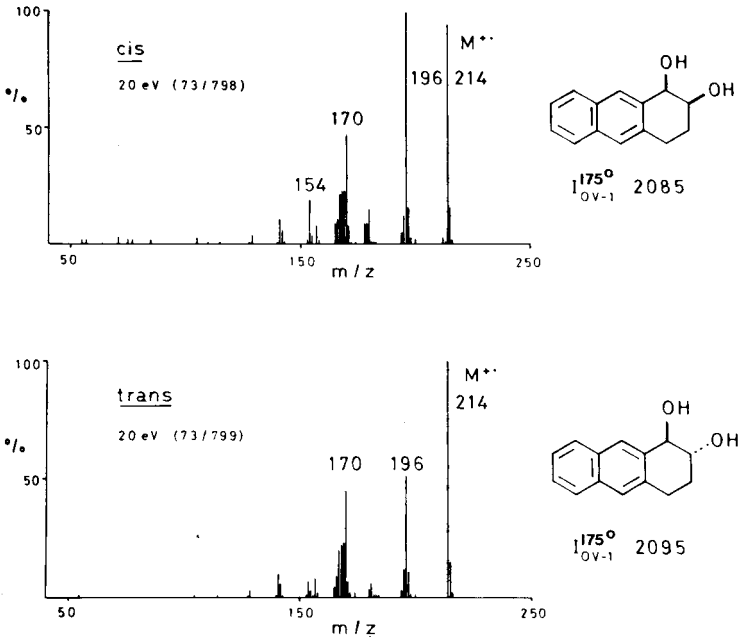

Fig. 8. Mass spectra (20 eV) of 1,2,3,4-tetrahydroanthracene-*cis*-1,2-diol (8) and -*trans*-1,2-diol (9). GC–MS conditions as in Fig. 3, except that column temperatures were as in Table III.

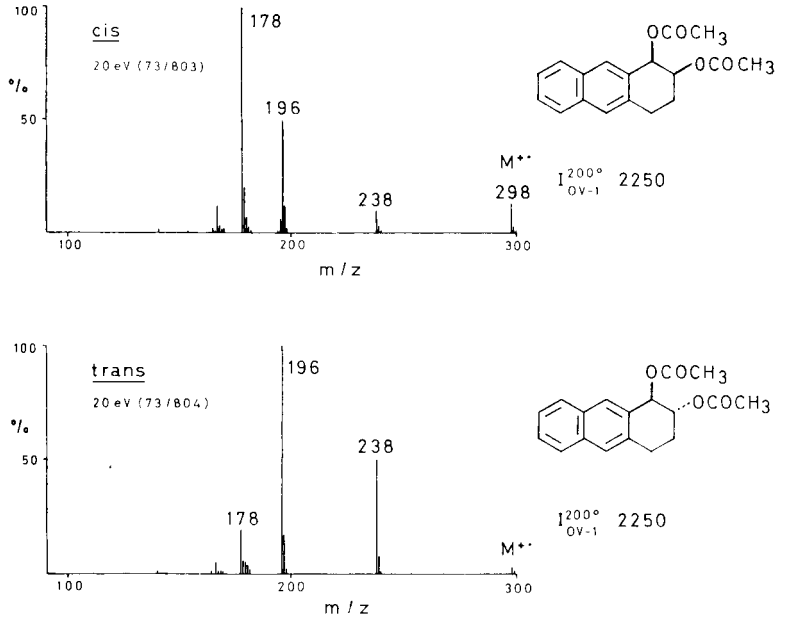

Fig. 9. Mass spectra (20 eV) of 1,2,3,4-tetrahydroanthracene-*cis*-1,2-diol diacetate (8a) and -*trans*-1,2-diol diacetate (9a). GC–MS conditions as in Fig. 8.

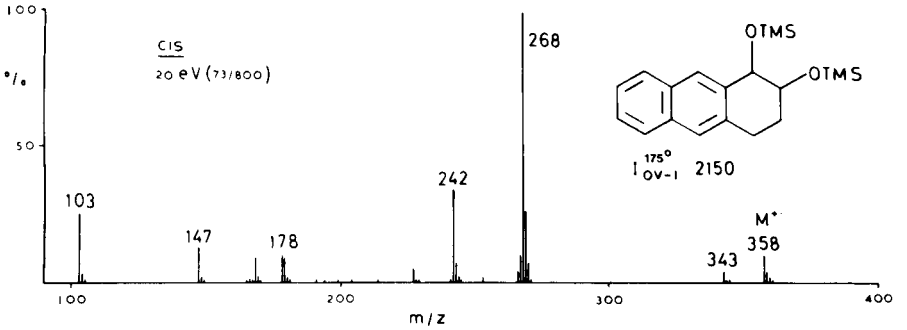

Fig. 10. Mass spectrum (20 eV) of 1,2,3,4-tetrahydroanthracene-*cis*-1,2-diol di-TMS ether (8b). GC–MS conditions as in Fig. 8.

In the case of the di-TMS ethers, the mass spectra are virtually identical, and that of the *cis*-diol derivative (Fig. 10) is sufficiently depictive of both. As in the naphthalene analogue (Fig. 5), major peaks are due to a *retro*-Diels–Alder process and to the elimination of trimethylsilanol moieties, while "rearrangement" ions of *m/z* 147 and 103 appear in the lower mass range. Finally, the spectra of the methaneboronates, shown in Fig. 11, are notable for the ions $[M-28]^{+\cdot}$ which are distinctly more abundant in the *trans*-isomer spectrum then in the *cis*: this regularity holds too for the butaneboronates, and is even more marked for the corresponding tetrahydronaphthalenediols (*cf.* Table II). Accurate mass measurement shows the ion $[M-28]^{+\cdot}$ to result from loss of C_2H_4, doubtless from C-3 + C-4: presumably the greater strain in the tetrahydro rings of cyclic boronates derived from *trans*-diols leads to a readier elimination of ethene resulting formally in a benzo- or naphthocyclobutenediol bo-

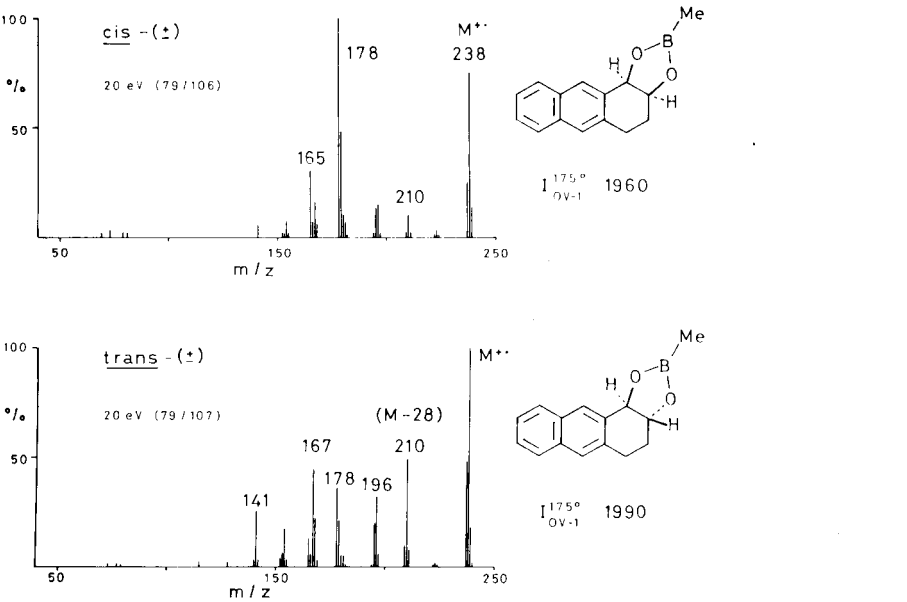

Fig. 11. Mass spectra (20 eV) of 1,2,3,4-tetrahydroanthracene-*cis*-1,2-diol methaneboronate (8c) and -*trans*-1,2-diol methaneboronate (9c). GC–MS conditions as in Fig. 8.

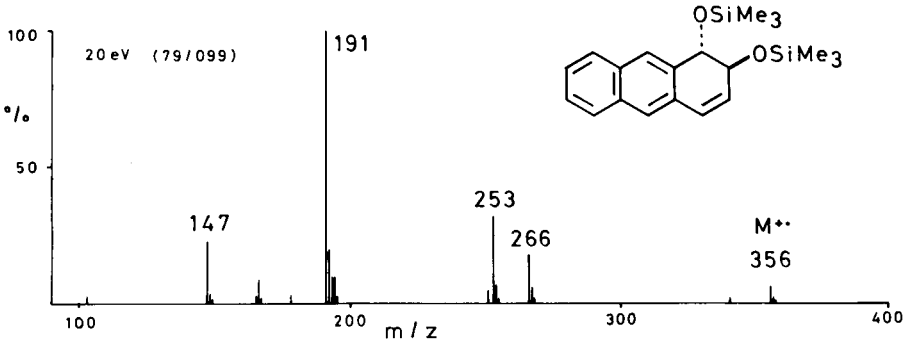

Fig. 12. Mass spectrum (20 eV) of 1,2-dihydroanthracene-*trans*-1,2-diol di-TMS ether (10b). GC–MS conditions as in Fig. 8.

ronate ion. A second regular distinction between the *cis*- and *trans*-tetrahydrodiol boronate spectra is the greater abundance of $[M-RBO_2H_2]^{+\cdot}$ ions from the *cis*-isomers.

The mass spectrum of 1,2-dihydroanthracene-*trans*-1,2-diol di-TMS ether (10b) shown in Fig. 12 includes clear, though small, $[M]^{+\cdot}$ and $[M-15]^{+\cdot}$ ions, together with the typical rearrangement ions of *m/z* 147 ($Me_3Si\overset{+}{O}=SiMe_2$), 191 ($MeSiOCH=\overset{+}{O}SiMe_3$) and 253 ($[M-CH_2OSiMe_3]^+$).

Dihydrophenanthrenediols (compounds 14–18)

Preparation of derivatives, including cyclic boronates, from the four *cis*-diols

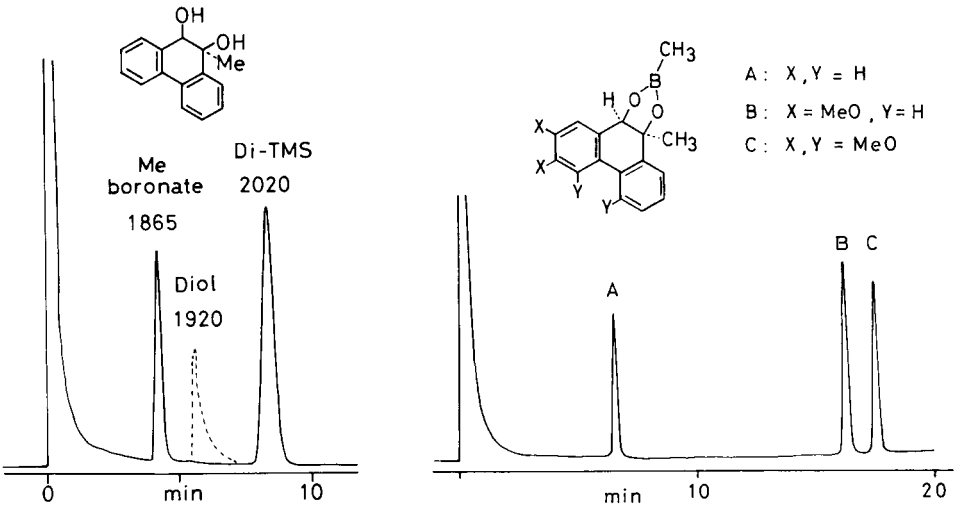

Fig. 13. Gas chromatographic separation of the methaneboronate (14c) and di-TMS ether (14b) of 9-methyl-9,10-dihydrophenanthrene-*cis*-9,10-diol (with the peak obtained separately for the free diol superimposed). Column, 1% OV-1 (1.5 m × 4 mm I.D.); column temperature, 180°C; nitrogen flow-rate, 40 ml/min.

Fig. 14. Gas chromatographic separation of methaneboronates (14c, 15c and 16c, respectively) of 9-methyl-9,10-dihydrophenanthrene-*cis*-9,10-diol and its 2,3-dimethoxy- and 2,3,4,5-tetramethoxy-derivatives. Column, 1% OV-17 (1.8 m × 4 mm I.D.); column temperature, programmed from 165 to 250°C at 4°C/min; nitrogen flow-rate, 40 ml/min.

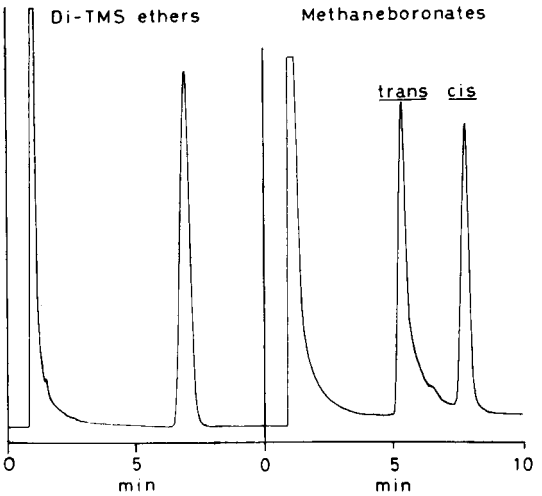

Fig. 15. Gas chromatograms of derivatives of 9,10-dihydrophenanthrene-*cis*- and -*trans*-9,10-diol: (i), di-TMS ethers (17b, 18b); (ii), methaneboronates (17c, 18c). Column, 1% OV-17 (1.8 m × 4 mm I.D.); column temperature, 180°C; nitrogen flow-rate, 40 ml/min.

(14–17), proceeded without difficulty. Formation of cyclic boronates from the *trans*-diol (18) required the use of 2.2 molar proportions of reagent (this diol was early reported not to yield an acetonide under conditions suitable for the corresponding derivative of the *cis*-diol[17]).

Gas chromatograms (Figs. 13–15) exemplify the utility of the methaneboronates in this series. The invariably lower retention indices (on OV-1) of these deriva-

TABLE V

KOVÁTS RETENTION INDICES (*I*) FOR DIHYDROPHENANTHRENE *cis*- AND *trans*-DIOLS AND DERIVATIVES

Stationary phase	*Derivative*	*Compound no.*				
		*14***	*15****	*16****	*17***	*18****
OV-1	Diol	1920	2350	2460	1980	2020
	Diacetate (a)*	2200	2630	2735	2120	2115
	Di-TMS (b)	2020	2360	2440	2015	2020
	Me boronate (c)	1865	2285	2340	1920	1880
	Bu boronate (d)	2125*****	2540§	2575§	2180	2165
OV-17	Diol	2275	2815	2930	2365	2430
	Diacetate (a)	2570	3100	3245	2525	2535
	Di-TMS (b)	2195	2625	2725	2225	2230
	Me boronate (c)	2170	2710	2780	2260	2155
	Bu boronate (d)	2455*****	2985§	3045§	2525	2450

* Letters denote derivative types.
** 180°C.
*** 200°C.
§ 220°C.

tives than those of the parent diols are illustrated for the 9-methyldiol in Fig. 13. The analogous 2,3-dimethoxy- and 2,3,4,5-tetramethoxy-9-methyldiols are equally conveniently studied as methaneboronates, which give very satisfactory peaks, even on a packed column (Fig. 14). With respect to the distinction between *cis*- and *trans*-isomers, Fig. 15 shows that the di-TMS ether peaks are unresolved under conditions whereby the methaneboronates are clearly separated, the *trans*-isomer being eluted first. The greater degree of tailing of the *trans*-diol ester peak reflects the strained nature of the cyclohexadienediol boronate ring, which probably undergoes partial cleavage and reclosure during GLC: the small additional peak may be due to a pyroboronate derivative, but the mass spectrum provided no evidence thereof. Gas chromatographic retention indices for all the derivatives of diols 14–18 on OV-1 and OV-17 phases are listed in Table V.

The mass spectra of all the 9,10-dihydrophenanthrene-9,10-diols and derivatives studied (Table VI) are noteworthy for the general occurrence of molecular ions (absent only for the diacetates of compounds 14 and 15) so that, for example, the di-TMS ethers of this group of diols are quite satisfactory for defining molecular masses. The base peaks from all the diacetates correspond to the phenanthrol fragments arising from elimination of acetic acid and ketene ($[M-102]^{+\cdot}$). Nine out of the ten cyclic boronates listed yield molecular ions as base peaks: in the exceptional case (compound 14d) the abundance of $[M]^{+\cdot}$ is 76% of a base peak ascribable to the fluorenyl ion (*m/z* 165) resulting from rearrangements and loss of the boronate group together with a two-carbon fragment.

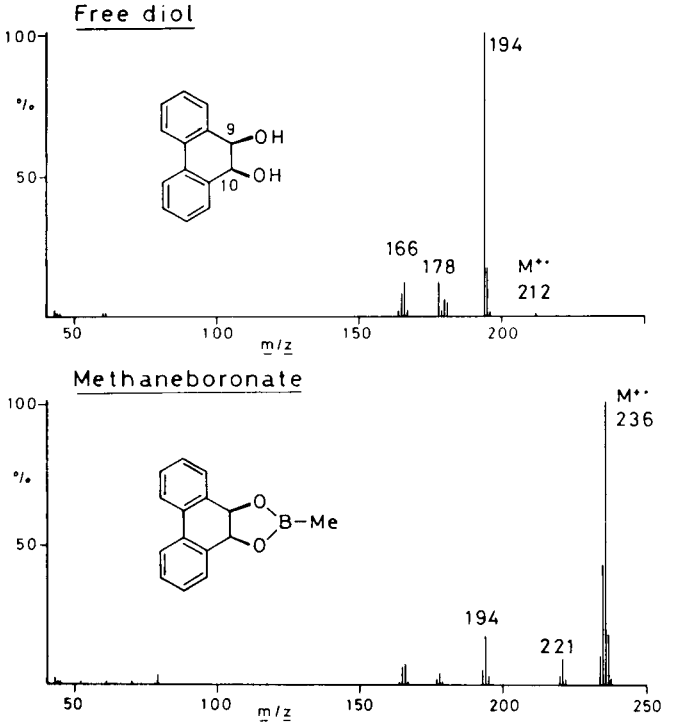

Fig. 16. Mass spectra (20 eV) of 9,10-dihydrophenanthrene-*cis*-9,10-diol (17) and its methaneboronate (17c). GC–MS conditions as in Fig. 3, except that column temperature was 180°C.

TABLE VI

BASE PEAKS AND RELATIVE ABUNDANCE OF MOLECULAR IONS IN THE MASS SPECTRA OF 9,10-DIHYDROPHENANTHRENEDIOLS AND THEIR DERIVATIVES

Diol	*Free*			*Diacetate*			*Di-TMS ether*			*Me boronate*			*Bu boronate*		
	M		*Base peak*	*M*		*Base peak*	*M*		*Base peak*	*M*		*Base peak*	*M*		*Base peak*
	m/z	%	*m/z*	*m/z*	%	*m/z*	*m/z*	%	*m/z*	*m/z*	%	*m/z*	*m/z*	%	*m/z*
14	226	100	226 (*M*)	310	0	208 (*M* − 102)	370	67	267 (*M* − 103)	250	100	250 (*M*)	292	76	165 (*M* − 127)
15	286	26	268 (*M* − 18)	370	0	268 (*M* − 102)	430	100	430 (*M*)	310	100	310 (*M*)	352	100	352 (*M*)
16	346	22	328 (*M* − 18)	430	5	328 (*M* − 102)	490	100	490 (*M*)	370	100	370 (*M*)	412	100	412 (*M*)
17	212	1	194 (*M* − 18)	296	5	194 (*M* − 102)	356	22	147*	236	100	236 (*M*)	278	100	278 (*M*)
18	212	6	196 (*M* − 18)	296	0.5	194 (*M* − 102)	356	28	147*	236	100	236 (*M*)	278	100	278 (*M*)

* Ion $Me_2Si{=}\overset{+}{O}SiMe_3$.

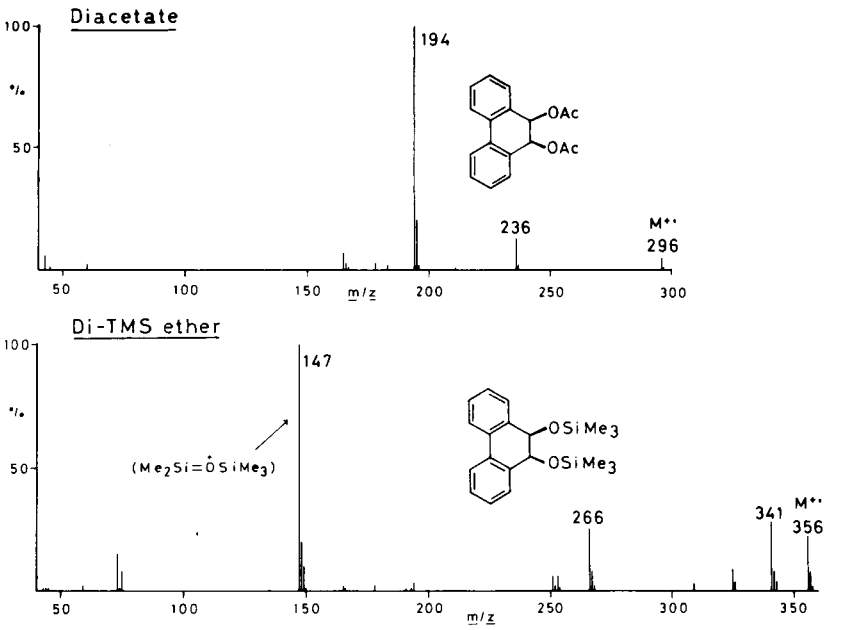

Fig. 17. Mass spectra (20 eV) of 9,10-dihydrophenanthrene-*cis*-9,10-diol diacetate (17a) and di-TMS ether (17b). GC–MS conditions as in Fig. 16.

Full mass spectra are shown in Figs. 16 and 17 for 9,10-dihydrophenanthrene-*cis*-9,10-diol (17) and three of its derivatives. [The spectra of the *trans*-series are very similar, emphasizing the importance of a chromatographic distinction as noted above.] Elimination of H_2O_2 to give a phenanthrene ion (*m/z* 178) is marked in the free diol spectrum, which also contains *m/z* 194 ($[M-H_2O]^{+\cdot}$) as base peak, and ions of fluorene and fluorenyl character (*m/z* 166, 165). In the methaneboronate (Fig. 16) the preferred fragmentation via loss of MeBO again yields a phenanthrol-type ion of *m/z* 194. Fig. 17 shows the preponderance of the similar ion in the diacetate spectrum, and the occurrence of the corresponding phenanthrol TMS fragment (*m/z* 266) in the mass spectrum of the di-TMS ether: the latter spectrum is, however, dominated by the rearrangement ion of *m/z* 147.

Nadolol (Fig. 18)

During the course of our work, the compound Nadolol (19) was introduced by E. R. Squibb & Sons as an antihypertensive agent. As it was unusual among drugs in

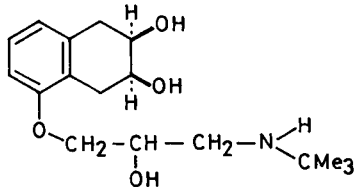

Fig. 18. Structure of Nadolol [5-(3-*tert.*-butylamino-2-hydroxypropoxy)-1,2,3,4-tetrahydronaphthalene-*cis*-2,3-diol] (19).

TABLE VII

KOVÁTS RETENTION INDICES (*I*) AND MASS SPECTROMETRIC DATA (20 eV) FOR NADOLOL (19) DERIVATIVES

Derivative	$I^{OV\text{-}1}_{225\,°C}$	$I^{OV\text{-}17}_{225\,°C}$	*M*		*Base peak*	*Other principal ions: m/z (intensities relative to base peak in parentheses)*						
Tetraacetate	3030	3005	477	(–)	98	420 (2)	417 (4)	403 (7)	361 (7)	343 (3)	301 (67)	259 (13)
						241 (67)	227 (9)	214 (52)	200 (81)	183 (20)	160 (52)	158 (91)
						144 (95)	128 (14)	100 (25)	84 (24)	72 (25)	56 (91)	
Tri-TMS ether	2505	2605	525	(0.3)	86	510 (1)	409 (1)	309 (0.3)	307 (0.2)	283 (0.2)	250 (0.3)	232 (0.3)
						217 (0.2)	203 (0.3)	184 (0.5)	144 (0.5)	128 (0.5)	116 (0.3)	112 (0.3)
						107 (0.3)	103 (0.6)					
Bismethaneboronate	2355	2680	357	(9)	342	300 (3)	289 (1)	246 (2)	244 (1)	217 (2)	204 (12)	162 (2)
						154 (3)	144 (5)	138 (5)	120 (20)	112 (7)	98 (8)	96 (5)
						86 (40)	70 (9)	57 (20)	56 (22)			

possessing a tetrahydronaphthalene-*cis*-2,3-diol group, some derivatives were examined as outlined below. Acid-catalysed acetylation afforded the N,O,O,O-tetraacetate, whereas the product of trimethylsilylation appeared to be the O,O,O-tri-TMS ether, the sterically hindered NH-*tert.*-Bu group remaining unreacted. As expected, the reaction with methaneboronic acid, which is hardly subject to steric hindrance, occurred with both the 2,3-*cis*-diol and side-chain β-hydroxyamine groups, although the unfavourable equilibria known to prevail in the formation of 1,3,2-oxazaborolidines made it necessary to use 2,2-dimethoxypropane as a scavenger of water produced in the reaction.

Gas chromatographic and mass spectrometric data for the three Nadolol derivatives are collected in Table VII. The tetraacetate had inconveniently long retention times, but the bismethaneboronate and tri-TMS ether were both satisfactory for GLC, as exemplified in Fig. 19.

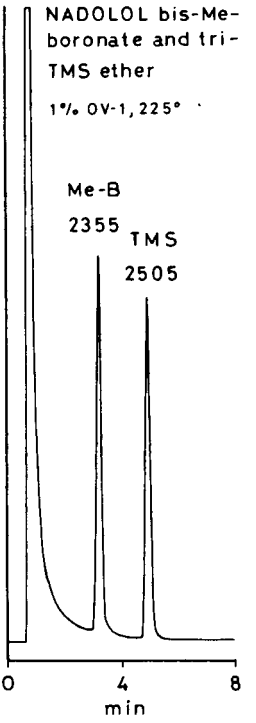

Fig. 19. Gas chromatographic separation of Nadolol bismethaneboronate (19c) and tri-TMS ether (19b). Column, 1% OV-1 (1.8 m × 4 mm I.D.). Column temperature, 225°C; nitrogen flow-rate, 40 ml/min.

Strikingly different mass spectra were observed for the three Nadolol derivatives. The tri-TMS ether spectrum (Table VII)[28] contained as base peak the ion from α-cleavage, $CH_2=NH$-*tert.*-Bu (*m/z* 86), with no other fragment ions at more than 1% relative abundance. The ion of *m/z* 86 has been used in the determination of serum Nadolol[28]. The bismethaneboronate and tetraacetate spectra are depicted in Fig. 20. The former spectrum shows as base peak the ion of *m/z* 342 ($[M-CH_3]^+$), which carries 20% of the total ion current, and could be of value in selective ion monitoring;

the only other prominent high-mass ions are $[M]^{+\cdot}$ and m/z 204 (tetrahydronaphthalene-2,3,5-triol methaneboronate fragment). In contrast, the tetraacetate spectrum shows no detectable molecular ion, but includes many fragment ions in substantially similar abundance, the origins of which are largely apparent. The tetraacetate is thus a very suitable derivative for characterisation of isolated samples of Nadolol, by virtue of its structurally informative mass spectrum.

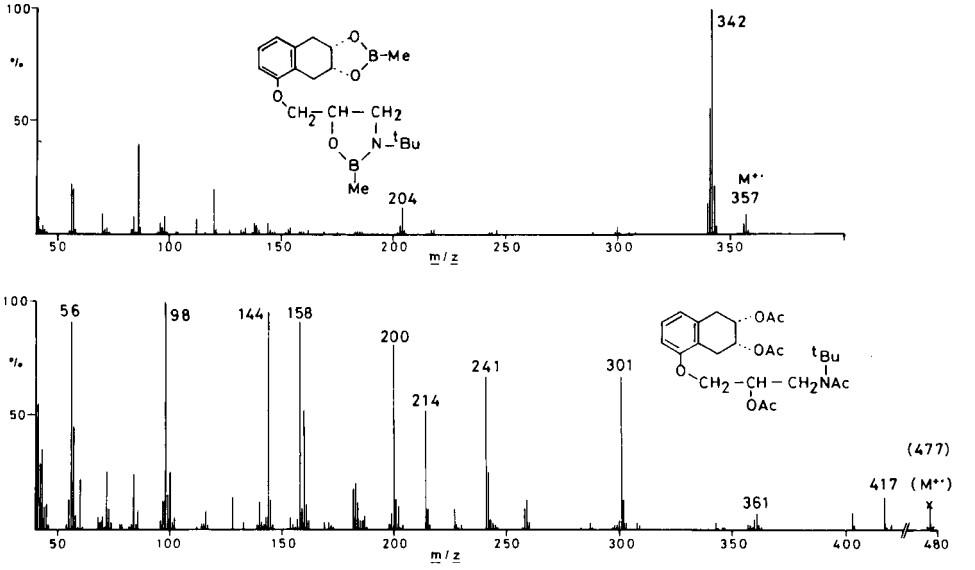

Fig. 20. Mass spectra (20 eV) of Nadolol bismethaneboronate (19c) and tetraacetate (19a). GC–MS conditions as in Fig. 3, except that column temperature was 225°C.

DISCUSSION

Attention is focused here principally upon those dihydrodiols that have been isolated as metabolites, and also (in the naphthalene and anthracene groups) upon the corresponding tetrahydrodiols. The latter compounds have not only been greatly used in the indirect characterisation of the less stable dihydrodiols, but they are also related to metabolic tetrahydrodiols such as the 1,2,3,4-(hydroxy/methylthio) derivatives of tetrahydronaphthalene recently identified as urinary metabolites of naphthalene in the rat[11,18]. One of these, a 1,3-di(methylthio)-1,2,3,4-tetrahydronaphthalene-2,4-diol, as its di-TMS ether, gave the informative *retro*-Diels–Alder fragment[11,18] analogous to that in Fig. 5; but the methaneboronate of the 2,4-diol grouping (apart from indicating it to be a *cis*-diol) did not yield a particularly useful mass spectrum except for an abundant molecular ion[11]. In their early work on the biogenesis of 1,2-naphthalene oxide and its conversion into the dihydrodiol, Jerina *et al.*[19] noted that mass spectra of the dihydrodiol did not yield evidence as to the location of ^{18}O in the diol group: accordingly, the diol was dehydrated to a mixture of 1- and 2-naphthol for mass spectrometry. It is clear that in 1,2,3,4-tetrahydroarene-1,2-diols (and 1,3-diols[11]) obtained as metabolites or by hydrogenation of dihy-

drodiols, distinction between the oxygen atoms is readily made via the *retro*-Diels–Alder fragmentation: although this is often prominent in the mass spectra of the free diols[20] (*cf.* Fig. 8), the higher mass of the ions from di-TMS ethers is often advantageous. The mass spectra of tetrahydronaphthalene-*cis*-1,2-diol and some related compounds were largely interpreted in an earlier investigation[20], though the fragmentation mode affording the ion at m/z $(M-60)$, mentioned above for the tetrahydroanthracenediols, was not discussed.

In the characterization of metabolic dihydrodiols and dihydrodiol epoxides derived from arenes of higher molecular weight such as benzpyrenes, mass spectrometry has been used mainly via direct probe sampling of fractions isolated by liquid chromatography[21,22]. However, as mentioned in the Introduction, GC–MS has been applied in studies of the *trans*-5,6-dihydrodiol and *trans*-8,9-dihydrodiol of 7,12-dimethylbenzanthracene[12]: the mass spectrum of the di-TMS ether of the 5,6-diol was characterised by the prominent rearrangement ions of m/z 191 and $(M-103)$ analogous to those from the 1,2-dihydroanthracenediol derivative (Fig. 12). Similar results have been reported in a study by GC–MS of the metabolites of phenanthrene in the coalfish[23]. The major dihydrodiol produced in that species, in contrast with the rat, was found to be a 1,2-diol, with very minor amounts of the 9,10-diol: the mass spectral data for the di-TMS ether of the latter isomer (presumably a *trans*-diol) are in good agreement with our observations on the reference samples (Table VI and Fig. 17). Brief data on the mass spectra of 1,2-dihydrophenanthrene-*trans*-1,2-diol, and of the corresponding *cis*-1,2-diol (as diacetate) have been reported[24].

One group of dihydrodiols to which GC–MS has been more extensively applied are those arising from metabolic oxidation of the olefinic bond in drugs derived from dibenzocycloheptene, dibenzoazepine[14] and related tricyclic structures. The flexibility of the seven-membered ring in many of these metabolites allows the formation of certain cyclic derivatives from both *cis*- and *trans*-diols (just as in the case of the 9,10-dihydrophenanthrene-9,10-diol groupings), and butaneboronates have been employed in the characterisation by GC–MS of 10,11-dihydro-10,11-diols among the metabolites of protriptyline[25], dibenzocycloheptadiene[26], carbamazepine[27] and related tricyclic drugs.

In the light of the above survey, it is clear that the range of derivatives studied in this paper includes the most generally useful types for the study of metabolic dihydrodiols and tetrahydrodiols by GC–MS. For those compounds which are not amenable to GC, the derivatives are still of value in mass spectrometry. The principal conclusions that can be drawn from our results, in combination with other published work, are briefly summarised below.

Gas chromatography

1. Trimethylsilyl ethers and acetates are both effective derivatives for stabilising dihydrodiols towards GC, but the TMS ethers have the advantage of shorter retention times, especially on the more polar OV-17 phase.

2. Cyclic alkaneboronates represent a selective type of derivative. *cis*-Dihydrodiols of rigid conformation and narrow dihedral angle, such as indane-*cis*-1,2-diol and acenaphthene-*cis*-1,2-diol, form especially stable cyclic boronates, while the equally rigid *trans*-isomers cannot form comparable derivatives. In other instances, where the diol groupings have enough conformational flexibility, cyclic boronates can

be formed from both *cis*- and *trans*-diols. We have observed that these derivatives provide the most satisfactory means of distinguishing between the *cis*- and *trans*-isomers by virtue of their different retention times. This is an important feature, because the di-TMS ethers and diacetates usually afford little distinction between retention data for *cis*- and *trans*-diols: moreover, mass spectra do not distinguish the isomers satisfactorily.

3. Cyclic methaneboronates are of special value in yielding retention times markedly shorter than those of the free diols and (on OV-1) those of any of the other derivatives studied. This allows diols of comparatively higher molecular weight, such as 2,3,4,5-tetramethoxy-9-methyl-9,10-dihydrophenanthrene-*cis*-9,10-diol (16) (Figs. 1 and 14) to be studied by GC–MS without the need for excessively high column temperatures or long retention times. A similar advantage arises for compounds such as Nadolol where four functional groups can be protected as a bismethaneboronate (Fig. 19).

Mass spectrometry

1. For the determination of molecular ions, the di-TMS ethers were effective for all but two of fifteen diols examined, whereas only seven of the diacetates gave detectable molecular ions. In those instances (twelve diols) where cyclic boronates could be formed they invariably afforded molecular ions at least 10% as abundant as the base peak, and usually constituting the base peak (Table VIII). In the particular case of Nadolol, the bismethaneboronate was the best derivative for establishing the molecular ion (the peak intensity at $M-1$ conforming with the presence of two boron atoms).

TABLE VIII

MOLECULAR ION ABUNDANCES FOR DIOLS AND DERIVATIVES RELATIVE TO RESPECTIVE BASE PEAKS (20 eV EI): DATA FROM TABLES II, IV AND VI

Derivative	*Number of examples*			
	0% abundance	*< 10% abundance*	*10–99% abundance*	*100% abundance*
Diols	1	6	6	2
Diacetates	8	5	2	0
Di-TMS ethers	2	3	7	3
Methaneboronates*	0	0	3	9
Butaneboronates*	0	0	4	8

* Three of the *trans*-diols did not yield boronates.

2. None of the particular derivative types examined was uniformly the best for the elucidation of structure from fragmentation modes. On the whole, the diacetates were the least useful in this respect, because of the prevalence of elimination of acetate and ketene moieties: however, in the exceptional case of Nadolol (Fig. 20) the moderating effect of the N-acetyl group on the α-cleavage reaction led to a good balance of informative fragmentations. More generally, the complementary use of di-TMS ethers and methaneboronates was found to be of great value because of the distinctive

differences in their modes of fragmentation, outlined in this paper and exemplified in Figs. 3/4, 5/6, 10/11 and 16/17. One such difference is the tendency for the cyclic esters to yield ions retaining the boronate group, which may also be accompanied by complementary fragment ions (*cf.* Fig. 6 in which the latter is a tropylium ion).

3. While high-resolution mass spectrometry is the most appropriate technique for establishing ion composition and for deducing fragmentation pathways, it is nevertheless possible to secure useful provisional data from low-resolution measurements. In this respect, the comparison of closely related derivatives (such as TMS and $[^2H_9]$TMS ethers) is a well established procedure. For the cyclic boronates, deuterium-labelled reagents are not conveniently accessible, but the comparative use of methane- and butaneboronates is practicable, as the latter derivatives (for a single diol grouping) have only slightly longer retention times than the di-TMS ethers and their mass spectrometric fragmentations largely parallel those of methaneboronates.

The mass spectrometric characteristics of the derivatives studied in this paper will be reported in more detail elsewhere.

ACKNOWLEDGEMENTS

We thank the late Prof. J. D. Loudon for generous gifts of diols, Dr. A. J. Baker for samples from the collection donated by the late Sir James Cook, Dr. R. P. Hopkins for acenaphthenediols and Mr. S. J. Lucania (E. R. Squibb and Sons) for Nadolol. Mr. A. Ritchie kindly provided high-resolution mass spectrometric measurements. The LKB 9000 instrument was provided by SRC grants Nos. B/SR/2398 and B/SR/8471.

REFERENCES

1 E. Boyland and A. A. Levi, *Biochem. J.*, 29 (1935) 2679.
2 L. Young, *Biochem. J.*, 41 (1947) 417.
3 E. Boyland and G. Wolf, *Biochem. J.*, 47 (1950) 64.
4 J. Booth and E. Boyland, *Biochem. J.*, 44 (1949) 361.
5 J. W. Cook, J. D. Loudon and W. F. Williamson, *J. Chem. Soc.*, (1950) 911.
6 E. Boyland, *Symp. Biochem. Soc.*, No. 5 (1950) 40.
7 D. M. Jerina, J. W. Daly, B. Witkop, P. Zaltzman-Nirenberg and S. Udenfriend, *J. Amer. Chem. Soc.*, 90 (1968) 6525.
8 D. T. Gibson, *CRC Crit. Rev. Microbiol.*, 1 (1971) 199.
9 R. V. Smith and J. P. Rosazza, *J. Pharm. Sci.*, 64 (1975) 1737.
10 C. J. W. Brooks and L. Young, *Biochem. J.*, 63 (1956) 264.
11 W. G. Stillwell, O. J. Bouwsma, J.-P. Thenot, M. G. Horning, G. W. Griffin, K. Ishikawa and M. Takaku, *Res. Commun. Chem. Pathol. Pharmacol.*, 20 (1978) 509.
12 Lan K. Wong, Chih-Lueh A. Wang and F. B. Daniel, *Biomed. Mass Spectrom.*, 6 (1979) 305.
13 C. J. W. Brooks and J. Watson, *Chem. Commun.*, (1967) 952.
14 C. Pantarotto, L. Cappellini, A. De Pascale and A. Frigerio, *J. Chromatogr.*, 134 (1977) 307.
15 R. P. Hopkins, C. J. W. Brooks and L. Young, *Biochem. J.*, 82 (1962) 457.
16 H. C. Brown and G. Zweifel, *J. Org. Chem.*, 27 (1962) 4708.
17 J. Booth, E. Boyland and E. E. Turner, *J. Chem. Soc.*, (1950) 1188.
18 W. G. Stillwell, O. J. Bouwsma and M. G. Horning, *Res. Commun. Chem. Pathol. Pharmacol.*, 22 (1978) 329.
19 D. M. Jerina, J. W. Daly, B. Witkop, P. Zaltzman-Nirenberg and S. Udenfriend, *Biochemistry*, 9 (1970) 147.
20 P. Perros, J. P. Morizur, J. Kossanyi and A. M. Duffield, *Bull. Soc. Chim. Fr.*, (1973) 2105.

21 K. M. Straub, T. Meehan, A. L. Burlingame and M. Calvin, *Proc. Nat. Acad. Sci. U.S.*, 74 (1977) 5285.
22 D. R. Thakker, W. Levin, A. W. Wood, A. H. Conney, T. A. Stoming and D. M. Jerina, *J. Amer. Chem. Soc.*, 100 (1978) 645.
23 J. E. Solbakken, K. H. Palmork, T. Neppelberg and R. R. Scheline, *Acta Pharm. Toxicol.*, 46 (1980) 127.
24 D. M. Jerina, H. Selander, H. Yagi, M. C. Wells, J. F. Davey, V. Mahadevan and D. T. Gibson, *J. Amer. Chem. Soc.*, 98 (1976) 5988.
25 V. Rovei, G. Belvedere, C. Pantarotto and A. Frigerio, *J. Pharm. Sci.*, 65 (1976) 810.
26 C. Pantarotto, L. Cappellini, P. Negrini and A. Frigerio, *J. Chromatogr.*, 131 (1977) 430.
27 G. Belvedere, C. Pantarotto and A. Frigerio, *Res. Commun. Chem. Pathol. Pharmacol.*, 11 (1975) 221.
28 P. T. Funke, M. F. Malley, E. Ivashkiv and A. I. Cohen, *J. Pharm. Sci.*, 67 (1978) 653.

Journal of Chromatography, 239 (1982) 217–226
Elsevier Scientific Publishing Company, Amsterdam — Printed in The Netherlands

CHROM. 14,503

LONG-TERM VARIATION STUDY OF BLOOD PLASMA LEVELS OF CHLOROFORM AND RELATED PURGEABLE COMPOUNDS

CARL D. PFAFFENBERGER* and ANITA J. PEOPLES
Department of Epidemiology and Public Health, Chemical Epidemiology Division, University of Miami School of Medicine, 15655 S.W. 127th Avenue, Miami, FL 33177 (U.S.A.)

SUMMARY

Values for circulating plasma chloroform of 25 white adult females were monitored for 6 months during the first phase of a four-phase long-term variation study. The data suggested four major exposure categories. Category I (20%) had average chloroform levels < 10 ppb* and variation ranges ⩽ 10 ppb. Category II (24%) had average levels of 10–25 ppb and ranges of ⩽ 10 ppb. Category III (20%) had average levels of 10–25 ppb and ranges > 20 ppb. Category IV (28%) had average chloroform levels of > 25 ppb and variation ranges > 20 ppb. Although the participants had been carefully screened to exclude incidents of occupational and recreational exposure, three subjects in category IV experienced obvious incidences of acute exposure to either chloroform or a chloroform precursor. In these situations circulating plasma chloroform levels were between 1655 ppb and 4000 ppb.

INTRODUCTION

Countless articles have been published concerning the presence of trihalomethanes in public drinking water supplies (for representative articles, see ref. 1), but very few reports have been made of the levels of these compounds in human tissues. This is not surprising in that the bulk of volatile halogenated organic compounds are readily expired, and most of the brominated species are effective alkylating agents which form non-volatile complexes with several blood components. Nevertheless, in 1979 Peoples *et al.*[2] published an analytical method by which volatile halogenated hydrocarbons can be purged from both human adipose tissue and blood plasma. The method, based on the purge/trap/desorb procedure of Bellar and Lichtenberg[3], has not been applied to many adipose tissue samples but has been used to analyze hundreds of blood samples in an effort to determine if a correlation exists between blood chloroform levels and the amount of chloroform found in the drinking water of individuals. Some correlation has been demonstrated[4] in that on the average, individuals who use finished water sources high in chloroform content do tend to have

* Throughout this article, the American billion (10^9) is meant.

0021-9673/82/0000–0000/$02.75

significantly higher plasma chloroform levels. However, to date, no report has been made of how plasma chloroform levels vary with time, and if the levels remain rather constant or scatter considerably over time for the same individual.

This report summarizes Phase I of a four-phase project (described below) concerned with determining long-term variations of human blood-plasma chloroform levels. Twenty-five white females were monitored over 6 months. Their average plasma chloroform levels and concentration ranges have been determined, categorized and reported herein.

EXPERIMENTAL

The apparatus and experimental conditions employed in this investigation have been previously reported[2].

RESULTS AND DISCUSSION

Analytical findings

Between five and seven values were obtained for each of the participants, and 92% of the subjects fell into one of four categories, as indicated in Table I. Values for four individuals from each category have been included in Figs. 1–4. Fig. 5 includes three special subjects who form subset IV-E within category IV.

TABLE I

CATEGORIZATION OF PLASMA CHLOROFORM LEVELS

Category	*Average $CHCl_3$ (ppb)**	*$CHCl_3$ range (ppb)*	*Specific examples*	*Percentage subjects***
I	<10	≤10	D, E, G, J, L	20
II	10–25	≤10	B, F, I, R, T, Y	24
III	10–25	≥20	H, M, O, U, W	20
IV	>25	≥20	A, K, N, P, S, V, X	28

* ppb = μg/l, or parts of chloroform per billion parts of plasma.

** One subject had an average $CHCl_3$ level of 10–25 ppb and a $CHCl_3$ range of 10–20 ppb; another had a level of >25 ppb and a range of ≤10 ppb.

Category I represents, from a health perspective, the best possible situation: consistently low exposure to chloroform as evidenced by low levels of circulating $CHCl_3$ or $CHCl_3$-precursor (discussed below) in the bloodstream; 20% of the participants fell into this category. Values for subjects D, E, J and L appear in Fig. 1. Subject L was remarkably consistent in that over a 5-month period she exhibited a total range of only 4 ppb, fluctuating only 1 ppb below and 3 ppb above an average chloroform level of 5 ppb. Subject G (not shown) was the most variable in this group and yet only fluctuated 3 ppb below and 5 ppb above an average $CHCl_3$ level of 9 ppb.

Category II represents the more usual levels of circulating chloroform in the bloodstream. It does not contain examples of acute exposure inasmuch as the fluctuation range is 10 ppb or less; 24% of the participants fell in this category. Values for

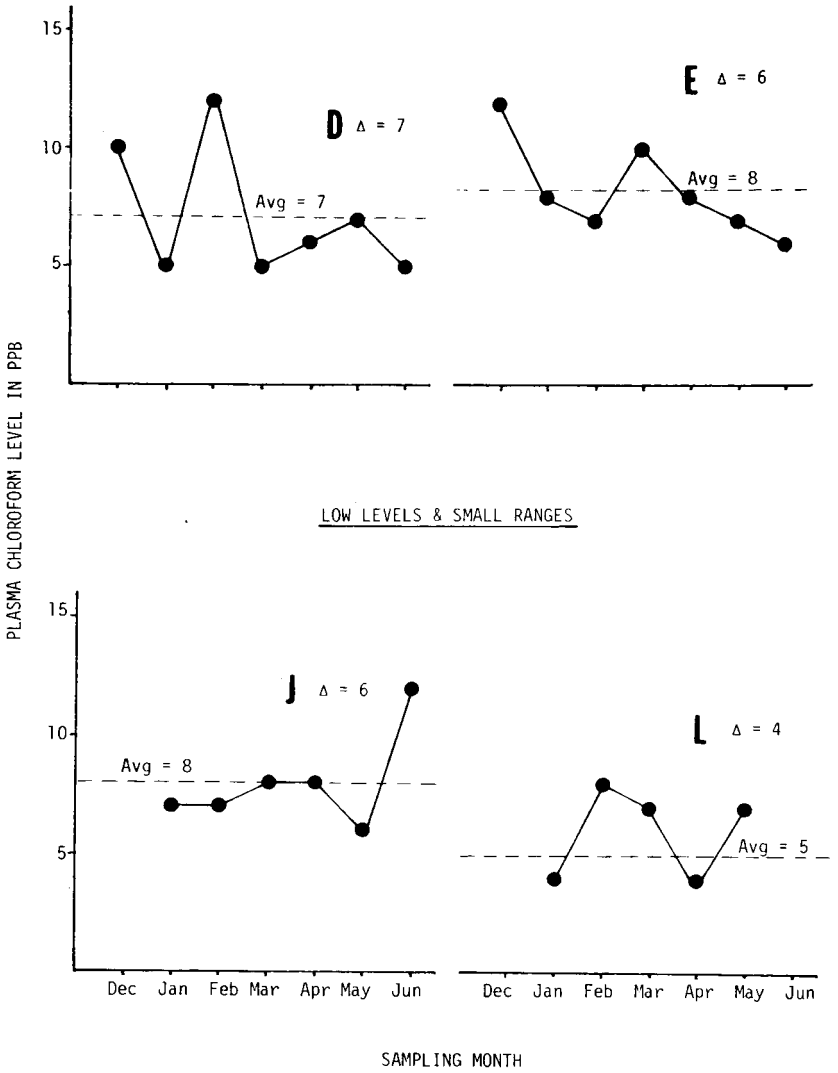

Fig. 1. Examples of values for category I participants. Plasma $CHCl_3$ levels are in parts per billion; ranges of $CHCl_3$ values are designated by $\triangle$. Averages are represented by broken lines; subject identities, by capital letters which cross-reference with the text.

subjects B, R, T and Y appear in Fig. 2. Subject I (not shown) was remarkably consistent in that over a 6-month period she had a total range of only 4 ppb, fluctuating above and below an average value of 10 ppb $CHCl_3$ by only 2 ppb. Subjects F and Y also had consistently constant levels; their fluctuations ranged over only 5 ppb.

Category III contained 20% of the participants, and represents exposure levels of 10–25 ppb of circulating chloroform and large fluctuation ranges. Values for subjects H, O, U and W appear in Fig. 3. Within categories I and II, ratios of the maximum level of $CHCl_3$ to the minimum level (max/min) were generally 2 or less. In

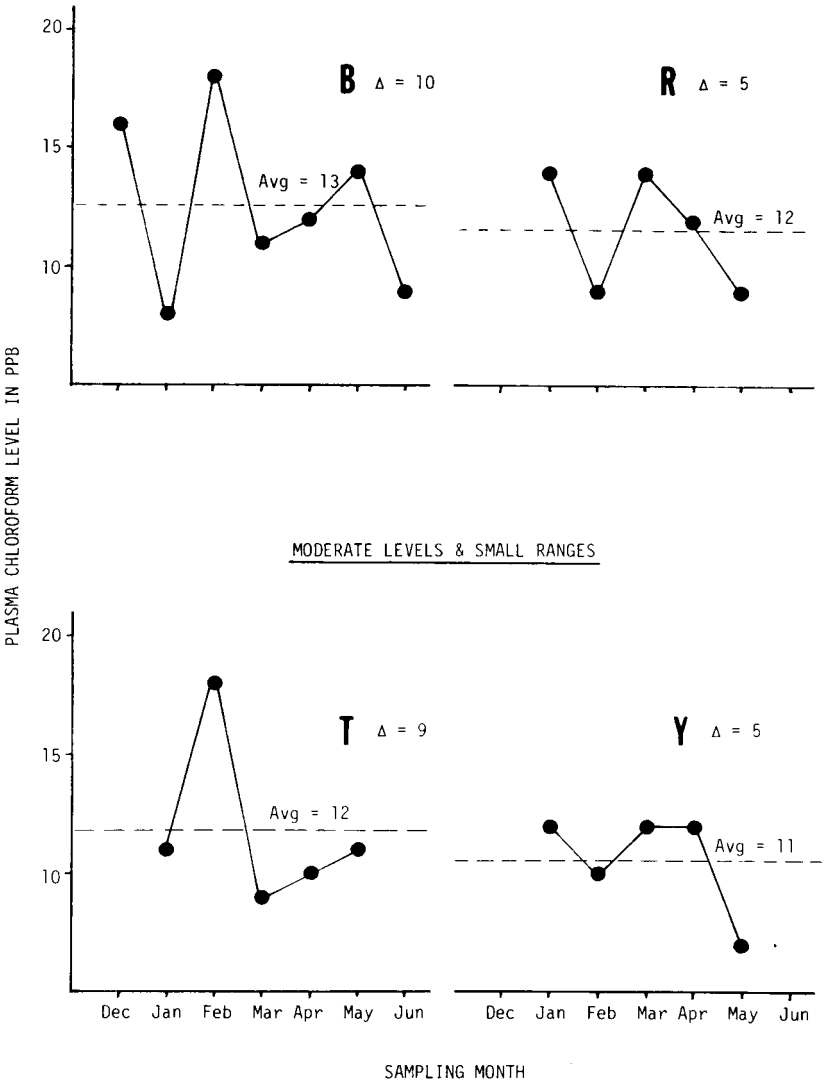

Fig. 2. Values for some category II participants. See Fig. 1 for further explanation.

category III, this ratio often exceeded 3, probably indicating some inconsistent exposure although not of a highly acute nature. Subject H appears to have passed through a sustained period of increasing chronic exposure. Subject O represents an almost consistent, cyclic fluctuation in this category.

Subject U was remarkably constant over a 4-month interval, varying only between 5 and 6 ppb, a 1-ppb range. The somewhat high level for subject U during January may be the down-side of a truly acute exposure situation. Subject W also exhibited an almost cyclic fluctuation of values which did not quite reach the three-fold difference for (max/min) obtained for the other members of this category.

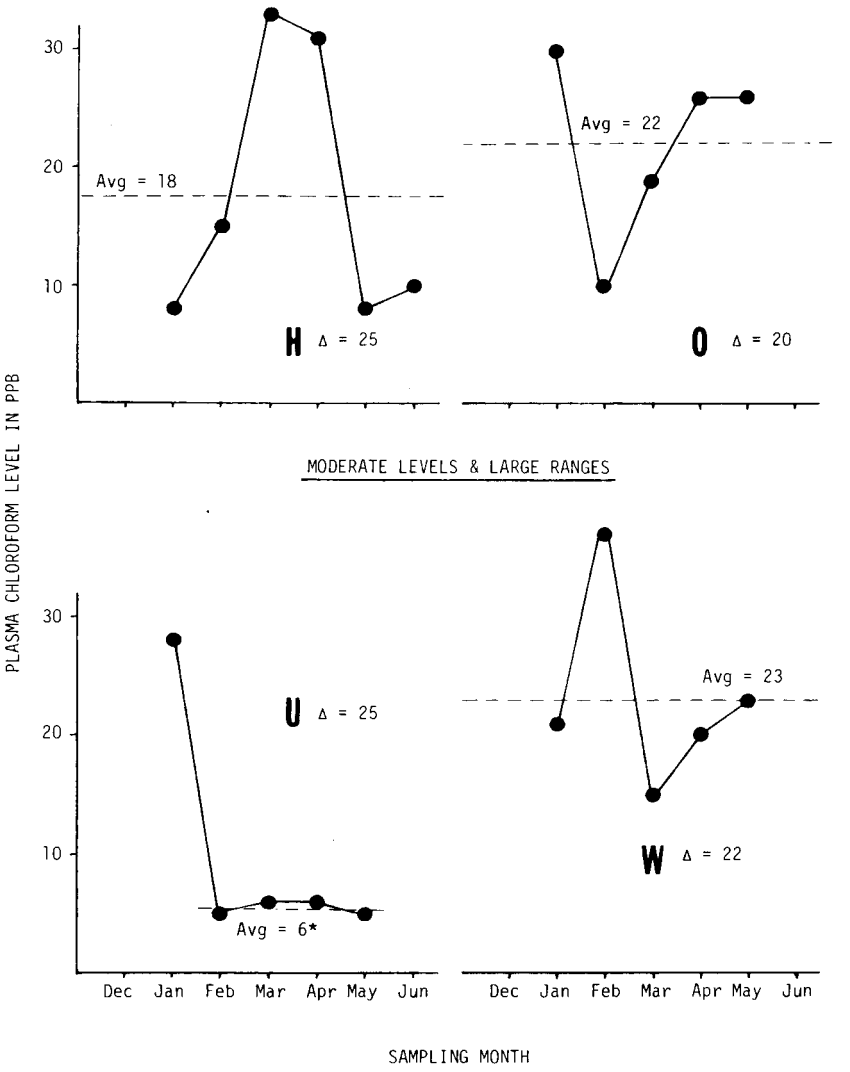

*First point omitted in average

Fig. 3. Values for some category III participants. See Fig. 1 for further explanation.

Category IV contains some examples of sustained high levels of circulating chloroform (above 25 ppb) and high fluctuation of these levels (above 20 ppb). Consequently it includes examples of both sub-acute exposure (Fig. 4; subjects K, N, S and X) and acute exposure (category IV-E; Fig. 5; subjects A, P and V); 25% of the participants were in this category.*

Participants K, N (borderline), S and X probably do not represent acute ex-

* To graph the values in category IV, the y-co-ordinate axis was, in most cases, changed from the usual range of 0–30 ppb $CHCl_3$ to as large as 0–4000 ppb.

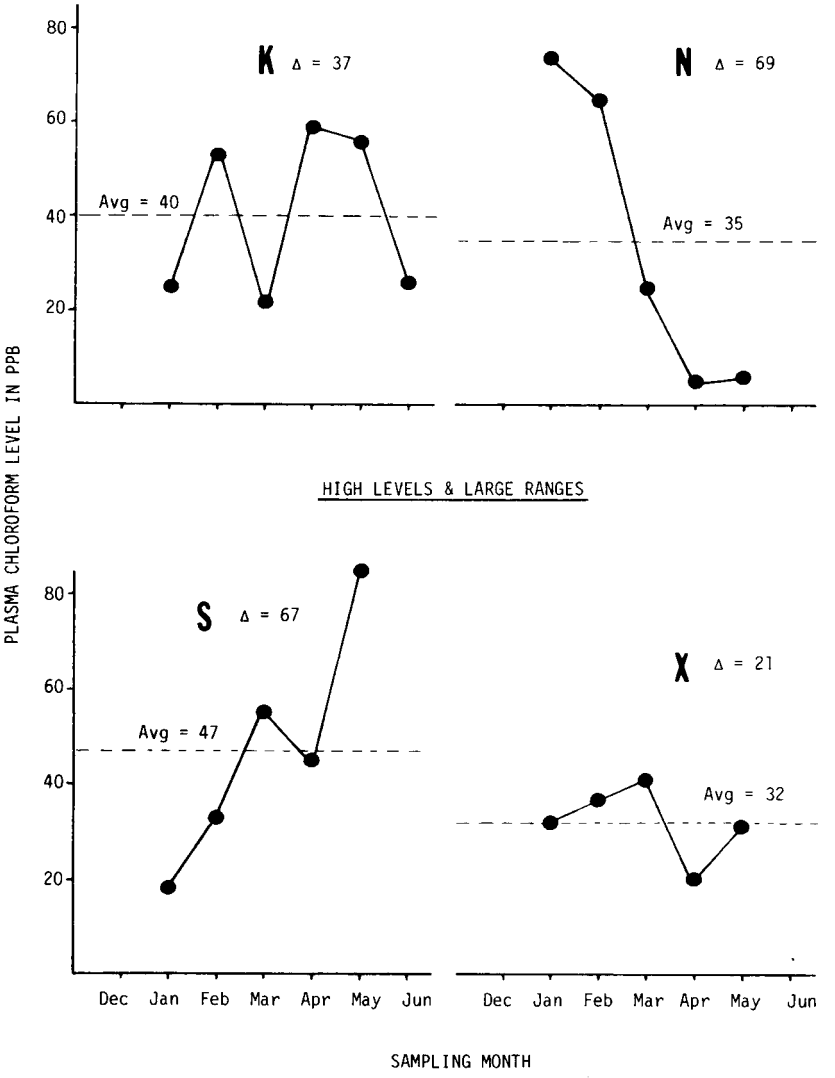

Fig. 4. Values for some category IV participants (non-acutely exposed). See Fig. 1 for further explanation.

posure situations inasmuch as their (max/min) ratios range from 2 to 5. They are, however, good examples of how widely $CHCl_3$ levels can fluctuate.

Subject K, which has an average chloroform value of 40 ppb, fluctuated between 22 and 59 ppb and actually passed through two cycles during the 6-month sampling period. Subject X was similar, with an average $CHCl_3$ value of 32 ppb and a range of 20–41 ppb. Only one cycle is evident for this individual.

Subject S, which averaged 47 ppb of $CHCl_3$, indicated a rather steady increase in $CHCl_3$ level from 18–85 ppb. Participant N showed a steady decrease from 74 to 5–6 ppb. The (max/min) value was 15.

Undoubtedly subjects A, P and V represent acute exposure situations (Fig. 5).

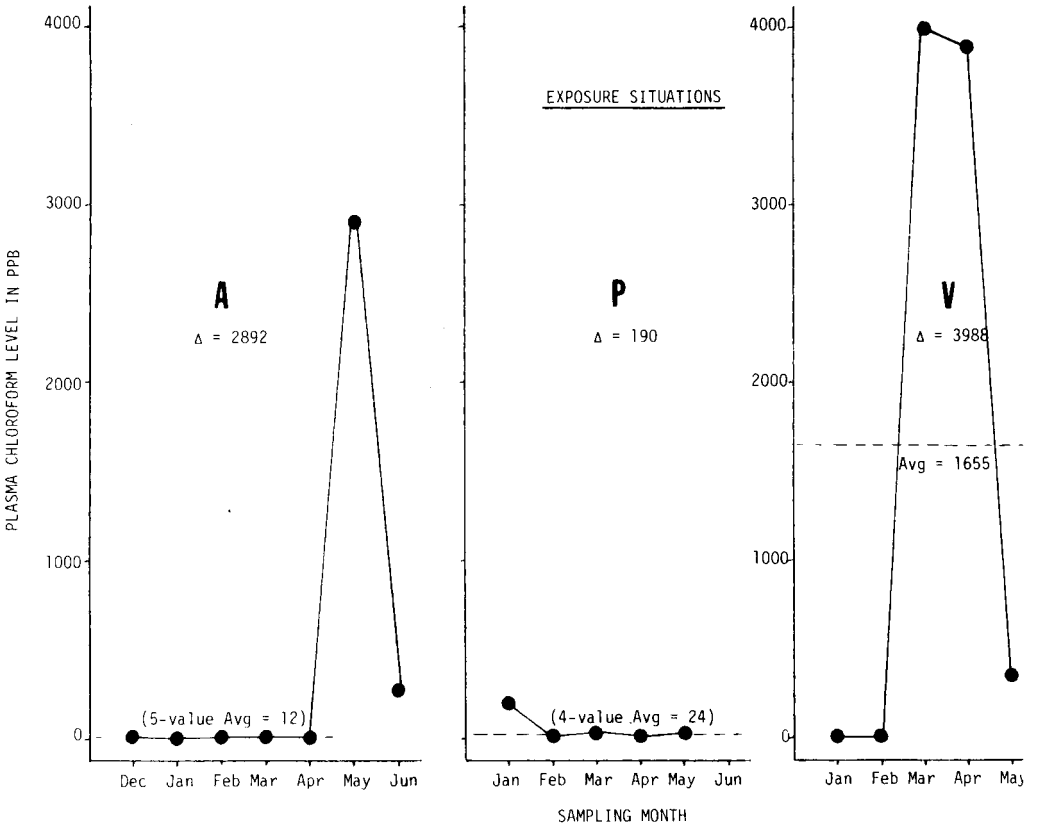

Fig. 5. Values for a subset of category IV participants (IV-E) who where acutely exposed to either $CHCl_3$ or a precursor thereof. Note the extreme change in the values along the y-coordinate axis. See Fig. 1 for further explanation.

For 5 months participant A exhibited a chloroform level of 8–18 ppb with an average value of 12 ppb. During May and June, however, the respective values were 2900 and 275 ppb. This subject had the highest (max/min) value observed, 363. Participant V was almost as high with a ratio of 333. After having $CHCl_3$ levels of 12 and 14 ppb for two successive months, levels of 4000, 3900 and 350 were obtained for the period March–May.

Subject P exhibited a rather constant level of chloroform, between 15 and 30 ppb (average 24 ppb) after an initial elevated value of 205 ppb. The (max/min) value was 14.

The extreme values found during Phase I work included: (1) chloroform levels from 4 to 4000 ppb (or 350 ppb if three values above 350 are excluded); (2) average chloroform levels from 5 to 1655 ppb (or 47 ppb if three values above 47 are excluded); and (3) total spread ($\triangle$) of chloroform values from 4 to 3988 ppb (or 69 ppb if three values above 69 ppb are excluded).

To arrive at the values reported in the table and figures, each of the 153 samples was analyzed in triplicate. Values for any one sample usually agreed within 15%, even when different instruments were used. A solution of known concentrations of seven

components: chloroform, methyl chloroform, trichloroethylene, bromodichloromethane, tetrachloroethylene, ethylene dichloride and chlorobenzene, was analyzed after every three analyses for use as an external reference for quantitation purposes. No other volatile halocarbon was detected above 1 ppb during this investigation. For those samples in which the $CHCl_3$ level exceeded 20 ppb, gas chromatographic–mass spectrometric (GC–MS) confirmation of the material was made based on the fragment ions appearing at 83, 85 and 87 atomic mass units.

Expanded definition of circulating chloroform

Throughout this discussion the term "circulating chloroform" has been used without comment. During analysis of blood plasma by this procedure[2], trichloroacetic acid (TCA) is thermally decomposed to yield $CHCl_3$, sometimes referred to as "derived chloroform". TCA results from the metabolism of trichloroethylene (3TCE) and tetrachloroethylene (4TCE), solvents used in dry-cleaning and degreasing industries, and is believed to be the primary source of derived $CHCl_3$.

Each participant chosen for this study was carefully screened; anyone with knowledge of exposure to tri- or tetrachloroethylene was not accepted. Other recognized sources of volatile halocarbons include: drinking water (trihalomethanes, 4TCE); soft drinks and reconstituted juices (trihalomethanes; 4TCE); margarine (chloroform, bromodichloromethane, trichloroethane and 3TCE); cigarette smoke (chloroform); and decaffeinated coffee (3TCE, 4TCE, methylene chloride). Cough syrup and dentifrice sources have been off the U.S. market for a number of years.

It must be emphasized that the participants in this study were encouraged to continue their usual lifestyles. Only individuals who would have had known vocational and/or recreational exposure to $CHCl_3$, 3TCE or 4TCE were excluded. The investigation was designed to study usual fluctuations and ranges of values within a group of subjects.

It turns out that plasma chloroform, no matter what the source, is one of the few reliable indices known to assess chronic exposure to volatile halogenated hydrocarbons. Apparently brominated analogues are too reactive, as mentioned earlier. In previously reported rodent work, Pfaffenberger *et al.*[5] observed comparatively little bromodichloromethane (BDCM) residue in the blood of rats dosed with relatively high amounts of BDCM, up to 5 mg/kg body weight for up to 25 days. Even when the animals were sacrificed 1 h after dosing, serum BDCM levels were low compared to chlorocarbon levels obtained for rats dosed with equivalent amounts of chlorinated volatile hydrocarbons and sacrificed after the same interval of time. The bulk of most ingested, absorbed or inhaled volatile organic compounds is rapidly eliminated via respiration. Apparently volatile halocarbons are not very highly sequestered by adipose tissue[2,5] as are the chlorinated pesticides and polychlorinated biphenyls.

Future studies

The results reported here comprise Phase I of a four-phase project. Fig. 6 presents hypothetical results similar to the type we anticipate obtaining over the next 18 months. During Phase II the only change in the sampling procedure will be a requirement that each participant ingests 15 fluid ounces of her usual drinking water 1 h prior to having her blood sampled. This may result in slightly higher averages for plasma $CHCl_3$ levels. The trihalomethane content of the ingested water will also be determined. A modest average increase of perhaps 10% is anticipated.

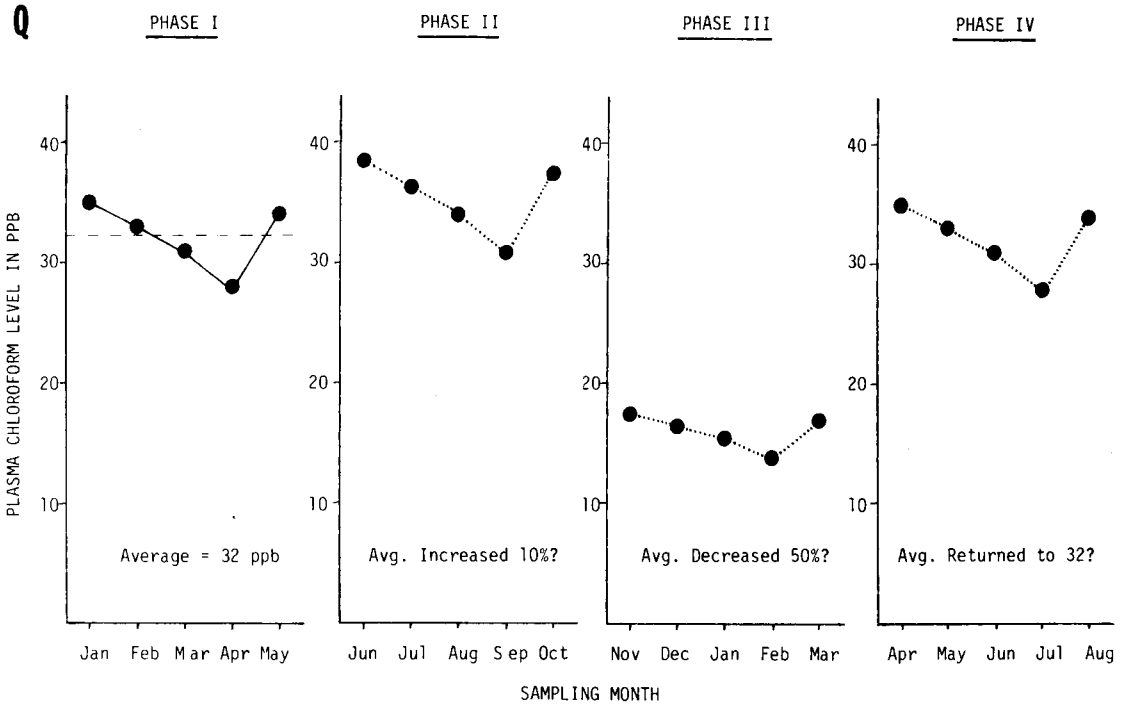

Fig. 6. Hypothetical results anticipated for subject Q during Phases II–IV of continued investigation. See Fig. 1 for further explanation and text for details.

During Phase III, the subjects will drink and cook with only pure bottled water containing no volatile halogenated organic compound. A significant average decrease of perhaps 50 % is anticipated under these circumstances. Phase IV will be a repeat of Phase I to determine if initial average values for plasma chloroform levels are re-attained.

ACKNOWLEDGEMENTS

This paper is a small contribution to a rather large symposium held in honor of Professor Evan C. Horning. C.D.P. should like to recognize the generous and lasting contributions Dr. Horning has made to his continuing scientific career.

The authors also gratefully acknowledge the helpful advice of Leland J. McCabe, Frederick M. Kopfler and Robert D. Lingg; the GC–MS confirmatory analyses of Thomas V. Briggle; and the financial support of the U.S. Environmental Protection Agency through Copperative Agreement CR-807714-01.

REFERENCES

1 R. L. Jolley, H. Gorchev, D. H. Hamilton, W. A. Brungs, R. B. Cumming and V. A. Jacobs (Editors), *Water Chloration: Environmental Impact and Health Effects*, Vols. 1–3, Ann Arbor Sci. Publ., Ann Arbor, MI, 1975, 1977 and 1979.

2 A. J. Peoples, C. D. Pfaffenberger, T. M. Shafik and H. F. Enos, *Bull. Environ. Contamin. Toxicol.*, 23 (1979) 244.
3 T. A. Bellar and J. J. Lichtenberg, *J. Amer. Water Works Assoc.*, 66 (1974) 739.
4 C. D. Pfaffenberger, K. P. Cantor, A. J. Peoples and H. F. Enos in R. L. Jolley, W. A. Brungs, R. B. Cumming and V. A. Jacobs (Editors), *Water Chlorination: Environmental Impact and Health Effects*, Vol. 3, Ann Arbor Sci. Publ., Ann Arbor, MI, 1979, pp. 1059–1074.
5 C. D. Pfaffenberger, A. J. Peoples and H. F. Enos, in A. Zlatkis (Editor), *Advances in Chromatography 1979*, Chromatography Symposium, Houston, TX, 1979, pp. 639–652.

Journal of Chromatography, 239 (1982) 227–231
Elsevier Scientific Publishing Company, Amsterdam — Printed in The Netherlands

CHROM. 14,516

GAS CHROMATOGRAPHIC ENANTIOMER SEPARATION OF CHIRAL ALCOHOLS

WILFRIED A. KÖNIG*, WITTKO FRANCKE and INGRID BENECKE
Institut für Organische Chemie und Biochemie der Universität, D-2000 Hamburg 13 (G.F.R.)

SUMMARY

A micro-scale procedure for the gas chromatographic enantiomer separation of chiral aliphatic, aromatic and monoterpene alcohols on glass capillary columns coated with XE-60–*S*-valine-*S*-α-phenylethylamide is described. By the formation of stable isopropyl urethanes in a facile derivatization step, the polarity of alcohols and their enantioselective intermolecular interaction with the chiral stationary phase is sufficiently enhanced to result in enantiomer separation with moderate retention times.

INTRODUCTION

The gas chromatographic separation of enantiomers has been achieved by the use of chiral stationary phases employing high stereoselectivity towards many polar compounds. After the fundamental work of Gil-Av and his associates[1], many groups have contributed to the improvement of the technique and to the understanding of stereoselective molecular interactions. Our recent investigations with novel monomeric and polymeric chiral stationary phases have dealt with the enantiomer separation of hydroxy acids[2–4], amino alcohols[4–6] and carbohydrates[4,6–8]. Few examples of the direct enantiomer separation of alcohols have been demonstrated. Ôi and coworkers[9,10] have used various low-molecular-weight chiral stationary phases which clearly show stereoselectivity for alcohols, but the retention times are very long.

We report here a more general procedure for the enantiomer separation of alcohols using isopropyl urethane derivatives and XE-60–*S*-valine-*S*-α-phenylethylamide as a very temperature stable polymeric stationary phase of outstanding enantioselectivity.

EXPERIMENTAL

Formation of derivatives

Some of the alcohols were kindly supplied by E. Ziegler (Aromachemie, Aufsess, G.F.R.). Samples of 0.5 mg or less of racemic mixtures of alcohols were dissolved in 200 μl of dichloromethane and 100 μl of isopropyl isocyanate (Fluka, Neu-

0021-9673/82/0000–0000/$02.75

Ulm, G.F.R.) were added. The mixture was heated in a screw-capped vial at 100°C for 20 min. Excess of reagent was removed with a stream of dry nitrogen and the derivatives were dissolved in 0.5 ml of dichloromethane for gas chromatography.

Gas chromatography

Glass capillary columns were drawn from Pyrex glass tubes with a Hupe & Busch capillary drawing machine and coated by the static procedure as described earlier[11]. The preparation of the chiral stationary phase XE-60–*S*-valine-*S*-α-phenylethylamide* has also been described previously[4,7]. Gas chromatography was performed in Carlo Erba Model 2101 gas chromatographs with hydrogen as the carrier gas.

RESULTS AND DISCUSSION

Most of our previous attempts to separate the enantiomers of alcohols on stationary phases derived from amino acids, amines or hydroxy acids have failed[2]. The lack of enantioselectivity of these phases for alcohols may be attributed to the fact that only one polar functional group is available for interaction with the stationary phase. We therefore introduced a second polar group by the reaction of alcohols with isopropyl isocyanate to form the corresponding urethanes. A similar approach has been described by Pereira *et al.*[12], who introduced a second chiral centre to form diastereoisomers by using N-(+)-α-phenylethyl isocyanate. The reaction with isopropyl isocyanate seems to proceed quantitatively even with tertiary alcohols in only 20 min with 50–100 molar excess of reagent in dichloromethane solution at 100°C. The excess of reagent (boiling point 74°C) can easily be removed with a stream of nitrogen. The volatility of the urethane derivatives is adequate for many chiral alcohols for elution from a 40-m glass capillary column within a reasonable retention time at temperatures between 70 and 180°C. The stationary phase is derived from commercially available polysiloxane XE-60 and exhibits the highest α-values for chiral alcohol derivatives of all stationary phases of this type that we have synthesized, including XE-60–*S*-valine-*R*-α-phenylethylamide, XE-60–*S*-phenylalanine-*S*-α-phenylethylamide, OV-225–*S*-valine-*R*-α-phenylethylamide and OV-225–*S*-valine-*S*-α-phenylethylamide.

As shown in Figs. 1–3 and Table I, aliphatic, aromatic and monoterpene alcohol enantiomers are separated. For 2-octanol, ipsdienol (1), *trans*-verbenol (2) and menthol (3) the (+)-enantiomers have the longer retention times; for terpinen-4-ol (4) the (+)-enantiomer is eluted first.

Chiral alcohols are important components of the pheromone systems in many insect species. They occur either in optically pure form or defined mixtures of enantiomers[13]. In many instances the "wrong" enantiomers proved to be biologically inactive or showed a repellent effect[14] and species specificity of chemical messages as well as interspecific competition for food and breeding places may well be based on pheromones of opposite chirality[15].

2-Heptanol and 3-octanol are widespread alarm pheromones in the mandibular gland secretions of different ant species[16]. One of the aggregation pheromones of elm bark beetles of the genus *Scolytus* is 4-methyl-3-heptanol[17], the natural com-

* Fused-silica columns with this phase are available from Chrompack, Middelburg, The Netherlands.

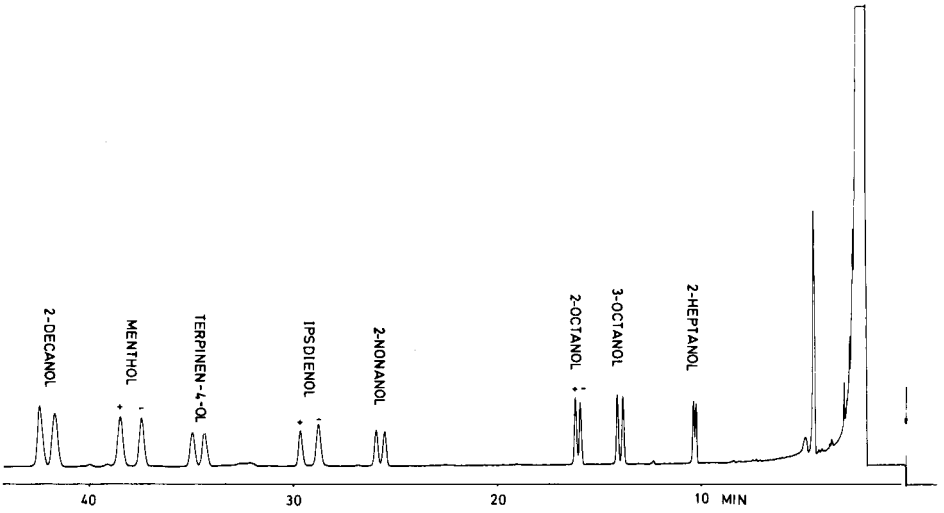

Fig. 1. Enantiomer separation of the isopropyl urethanes of chiral alcohols on a 40-m Pyrex glass capillary column coated with XE-60–*S*-valine-*S*-α-phenylethylamide. Column temperature, 120°C (isothermal).

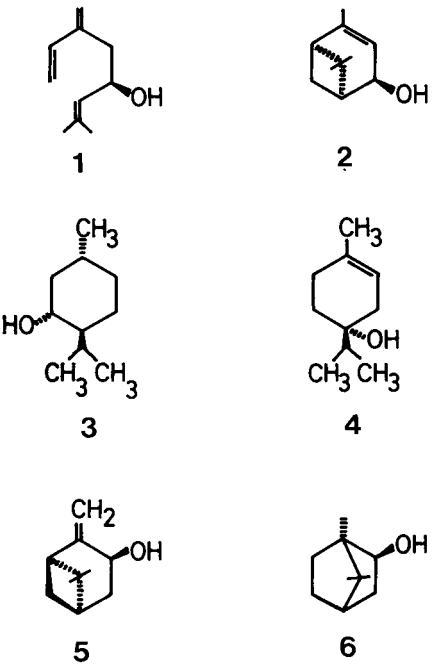

Fig. 2. Structures of some chiral monoterpene alcohols, separated as isopropyl urethanes. 1 = Ipsdienol; 2 = *trans*-verbenol; 3 = menthol; 4 = terpinen-4-ol; 5 = *trans*-pinocarveol; 6 = isoborneol.

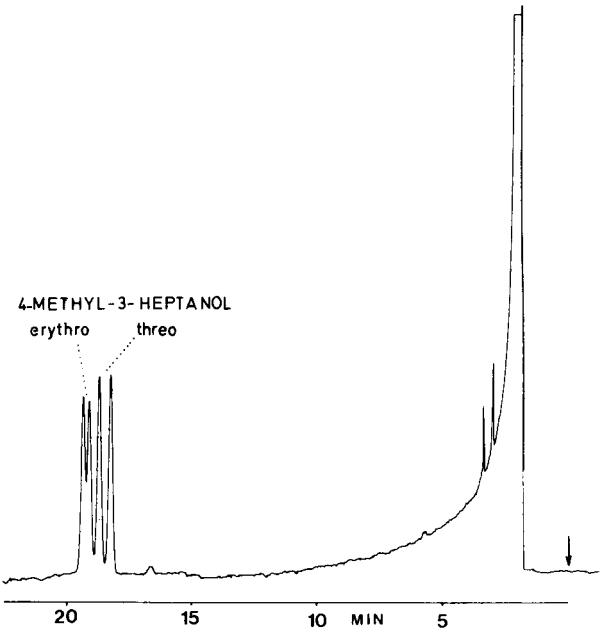

Fig. 3. Enantiomer separation of the four stereoisomers of 4-methyl-3-heptanol as isopropyl urethanes. Column temperature, 115°C; column as in Fig. 1.

TABLE I

SEPARATION FACTORS (α) AND OPERATING TEMPERATURES FOR ENANTIOMER SEPARATION OF CHIRAL ISOPROPYL URETHANES ON A 40-m GLASS CAPILLARY COLUMN COATED WITH XE-60-*S*-VALINE-*S*-α-PHENYLETHYLAMIDE

Racemate	*α-value*	*Column temperature (°C)*
2-Heptanol	1.014	120
2-Octanol	1.017	120
3-Octanol	1.025	120
4-Methyl-3-heptanol (*threo*)	1.024	120
4-Methyl-3-heptanol (*erythro*)	1.012	120
2-Nonanol	1.017	120
2-Decanol	1.019	120
2-Tetradecanol	1.016	170
1-Phenylethanol	1.040	120
1-Phenyl-1-propanol	1.049	120
Menthol	1.030	120
Isoborneol	1.020	140
Ipsdienol	1.033	120
Terpinen-4-ol	1.019	120
trans-Pinocarveol	1.039	140
trans-Verbenol	1.015	140
Sulcatol	1.011	120

pound having (3*S*,4*S*)-configuration[18]. The separation of all four stereoisomers of 4-methyl-3-heptanol is shown in Fig. 3.

trans-Verbenol (2) has been identified as a component of the aggregation pheromone in several bark beetles of the genus *Dendroctonus*[19], while *cis*-verbenol and ipsdienol (1) are important aggregation pheromones among certain *Ips* and *Pityokteines* species[20]. The verbenols are probably oxygenation products of the host terpene α-pinene, ipsdienol is produced from myrcene. *trans*-Pinocarveol (5), another constituent of the odour bouquet of bark beetles, especially *Crypnalus piceae*, may be derived from β-pinene[21].

Terpinen-4-ol (4) was found in several bark beetle species[22] and is the main compound in the aggregation pheromone of *Polygraphus poligraphus*[23]. 6-Methyl-5-hepten-2-ol (sulcatol) is the aggregation pheromone of male ambrosia beetles of the genus *Gnathotrichus*[24].

These examples demonstrate only part of the broad potential of applications of this new procedure for configurational analysis. We also expect that this method will be applied to the investigation of flavour and fragrance constituents and to the control of asymmetric syntheses.

REFERENCES

1 E. Gil-Av, B. Feibush and R. Charles-Sigler, in A. B. Littlewood (Editor), *Gas Chromatography 1966*, Institute of Petroleum, London, 1967, p. 227.
2 W. A. König and S. Sievers, *J. Chromatogr.*, 200 (1980) 189.
3 W. A. König, S. Sievers and U. Schulze, *Angew. Chem.*, 92 (1980) 935; *Angew. Chem., Int. Ed. Engl.*, 19 (1980) 910.
4 W. A. König, S. Sievers and I. Benecke, in R. E. Kaiser (Editor), *Proceedings of the IVth International Symposium on Capillary Chromatography, Hindelang, 1981*, Institut für Chromatographie, Bad Dürkheim, and Hüthig, Heidelberg, 1981, p. 703.
5 W. A. König and I. Benecke, *J. Chromatogr.*, 209 (1981) 91.
6 W. A. König, I. Benecke and H. Bretting, *Angew. Chem.*, 93 (1981) 688; *Angew. Chem., Int. Ed. Engl.*, 20 (1981) 693.
7 W. A. König, I. Benecke and S. Sievers, in A. Zlatkis (Editor), *Advances in Chromatography, 1981*, Elsevier, Amsterdam, 1981, p. 65; *J. Chromatogr.*, 217 (1981) 71.
8 I. Benecke, E. Schmidt and W. A. König, *J. High Resolut. Chromatogr. Chromatogr. Commun.*, 4 (1981) 553.
9 N. Ōi, T. Doi, H. Kitahara and Y. Inda, *J. Chromatogr.*, 208 (1981) 404.
10 N. Ōi, H. Kitahara, Y. Inda and T. Doi, *J. Chromatogr.*, 213 (1981) 137.
11 W. A. König, K. Stölting and K. Kruse, *Chromatographia*, 10 (1977) 444.
12 W. Pereira, V. A. Bacon, W. Patton and B. Halpern, *Anal. Lett.*, 3 (1970) 23.
13 E. L. Plummer, T. E. Stewart, K. Byrne, G. T. Pearce and R. M. Silverstein, *J. Chem. Ecol.*, 2 (1976) 307.
14 J. P. Vité, D. Klimetzek, G. Loskant, R. Hedden and K. Mori, *Naturwissenschaften*, 63 (1976) 582.
15 D. M. Light and M. C. Birch, *Naturwissenschaften*, 66 (1979) 159.
16 R. M. Crewe, M. S. Blum and C. A. Collingwood, *Comp. Biochem. Physiol. B*, 43 (1972) 703.
17 G. T. Pearce, W. E. Gore, R. M. Silverstein, J. W. Peacock, R. A. Cuthbert, G. N. Lanier and J. B. Simeone, *J. Chem. Ecol.*, 1 (1975) 115.
18 K. Mori, *Tetrahedron*, 33 (1977) 289.
19 G. B. Pitman, J. P. Vité, G. W. Kinzer and A. F. Fentiman, Jr., *J. Insect Physiol.*, 15 (1969) 363.
20 R. M. Silverstein, J. O. Rodin and D. L. Wood, *Science*, 154 (1966) 509.
21 W. Francke, unpublished results; D. Klimetzek and W. Francke, *Experientia*, 36 (1980) 1343.
22 W. Francke, P. Sauerwein, J. P. Vité and D. Klimetzek, *Naturwissenschaften*, 67 (1980) 147.
23 W. Francke, B. Brümmer, C. Lauze and A. Bakke, *Naturwissenschaften*, in press.
24 J. H. Borden, J. R. Handley, J. A. McLean, R. M. Silverstein, L. Chong, K. N. Slessor, B. D. Johnston and H. R. Schuler, *J. Chem. Ecol.*, 6 (1980) 445.

Journal of Chromatography, 239 (1982) 233–241
Elsevier Scientific Publishing Company, Amsterdam — Printed in The Netherlands

CHROM. 14,515

MICROANALYSIS OF BRASSINOLIDE AND ITS ANALOGUES BY GAS CHROMATOGRAPHY AND GAS CHROMATOGRAPHY–MASS SPECTROMETRY

SUGURU TAKATSUTO, BAIPING YING, MASUO MORISAKI and NOBUO IKEKAWA*
Department of Chemistry, Tokyo Institute of Technology, Ohokayama, Meguro-ku, Tokyo 152 (Japan)

SUMMARY

The microanalysis of brassinolide, a new plant growth promotor, was investigated using gas chromatography (GC) and gas chromatography–mass spectrometry (GC–MS). Bismethaneboronate was found to be a suitable derivative for analysis of brassinolide and its analogues by gas-phase analysis. GC and GC–MS analysis of the derivative are useful for identification and screening of brassinolide in plants.

INTRODUCTION

Recently a new plant growth-promoting steroid, brassinolide, has been isolated from rape pollen (*Brassica napus* L.). The structure was determined by mass spectrometry (MS) and X-ray crystallography as (22*R*,23*R*,24*S*)-2α,3α,22,23-tetrahydroxy-24-methyl-6,7-seco-5α-cholestano-6,7-lactone (1)[1]. Brassinolide is especially noteworthy because it is the first natural steroid containing a seven-membered *B*-ring lactone and an α_F configuration at the C_{22} position. The synthesis of brassinolide has been achieved by us[2] and by Siddall *et al.*[3] and its analogues have also been synthesized by three groups[4–6]. Brassinolide promotes both cell elongation and cell division, resulting in curvature, swelling and, more dramatically, splitting of the internode in the bean second-internode bioassy[1] and shows a strong activity in the lamina inclination assay at very low concentration[7]. Brassinolide also exhibits a broad spectrum of biological activities, compared with the known plant hormones[8,9]. The presence of brassinolide-like substances has been demonstrated in other pollens[10] and also in the leaves of *Distylium racemosum*[11].

The remarkable biological activities and the very small amounts contained in plants prompted us to develop a microanalysis and a screening method for brassinolide and its analogues. Thus we investigated analysis by gas chromatography (GC) and GC–MS.

EXPERIMENTAL

Samples and reagents

The following standard samples were synthesized in this laboratory: brassi-

0021-9673/82/0000–0000/$02.75

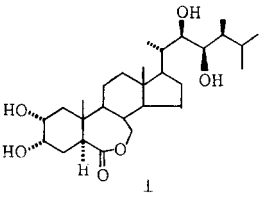

1

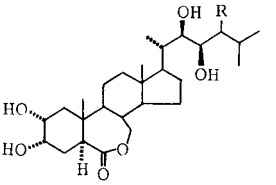

2 R = β-CH_3

3 R = α-C_2H_5

4 R = H

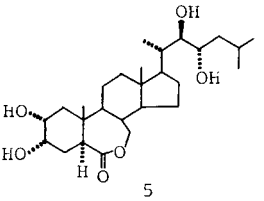

5

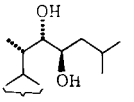

6

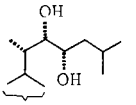

7

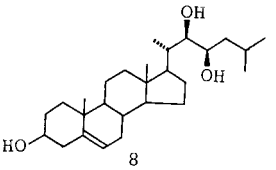

8

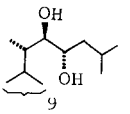

9

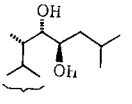

10

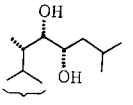

11

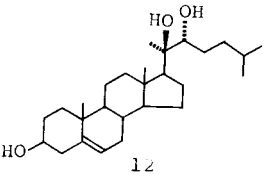

12

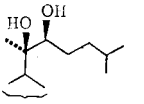

13

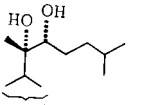

14

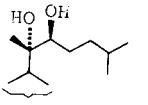

15

nolide (1)[2]; 24-epibrassinolide (2)[4]; (22*R*,23*R*)- (4); (22*R*,23*S*)- (5), (22*S*,23*R*)- (6) and (22*S*,23*S*)-28-norbrassinolide (7)[6]; (22*R*,23*R*)- (8), (22*R*,23*S*)- (9), (22*S*,23*R*)- (10) and (22*S*,23*S*)-dihydroxycholesterol (11)[6]; (20*R*,22*R*)- (12), (20*R*,22*S*)- (13), (20*S*,22*R*)- (14) and (20*S*,22*S*)-dihydroxycholesterol (15)[13]. (22*S*,23*S*)-28-Homobrassinolide (3)[5] was supplied by Dr. Wada, Nagoya University.

Methaneboronic acid was obtained from Alfa Products, Ventron Corporation, and trimethylsilylimidazole was from Tokyo Kasei.

Derivatization

Bismethaneboronate. Methaneboronic acid (100 μg) was dissolved in 50 μg of dry pyridine and this solution was added to 100 μg of brassinolide. The mixture was heated at 60°C for 30 min. Several microlitres of this solution were injected into the gas chromatograph.

Methaneboronate trimethylsilyl ether. The triol (100 μg) was converted into monomethaneboronate as described above. To this reaction mixture 30 μl of trimethylsilylimidazole were added and, after allowing to stand at room temperature for 30 min, several μl of this solution were injected into the gas chromatograph.

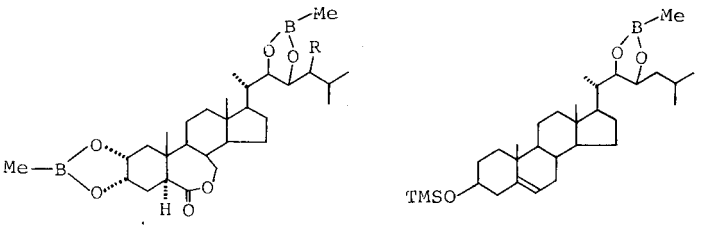

GC analysis

A Shimadzu Model GC-7A chromatograph equipped with dual hydrogen flame-ionization detector was employed. A glass capillary column coated with OV-17 (SCOT column) (40 m × 0.25 mm) was used at 270°C. The carrier gas (nitrogen) flow-rate was 0.4 ml/min, and the split ratio was 100:1. A U-shaped column packed with 2% OV-17 on Chromosorb W (80–100 mesh) (150 cm × 4 mm I.D.) was also used.

GC–MS analysis

A Shimadzu GC–MS 6020 gas chromatograph–mass spectrometer with electron impact (EI), chemical ionization (CI) sources and a SCAP-1123 was used. For GC–EI-MS a column packed with 2% OV-17 on Chromosorb W (80–100 mesh) (0.5 m × 2 mm I.D.) was used at 290°C; the carrier gas (helium) flow-rate was 30 ml/min; electron energy, 20 eV; electron current, 60 μA; acceleration high voltage, 3.5 kV; ion source temperature 290°C. For GC–CI-MS the same packed column was used; the reagent gas was isobutane; carrier gas (helium) flow-rate was 30 ml/min; electron energy, 150 eV; box current, 150 μA; acceleration high voltage, 3.5 kV; ion source temperature 250°C.

RESULTS AND DISCUSSION

GC analysis

Since brassinolide has two vicinal diols in the side chain and A-ring, a methaneboronate[12] seems to be the best derivative for GC analysis. The bismethaneboronate of brassinolide and its analogues exhibited sharp peaks and the derivatives can be separated as shown in Fig. 1. Brassinolide and its 24-epimer can also be separated by glass capillary column (Fig. 2). The compounds can be analysed using a packed column, but a capillary column afforded better resolution and sharper peak. It was

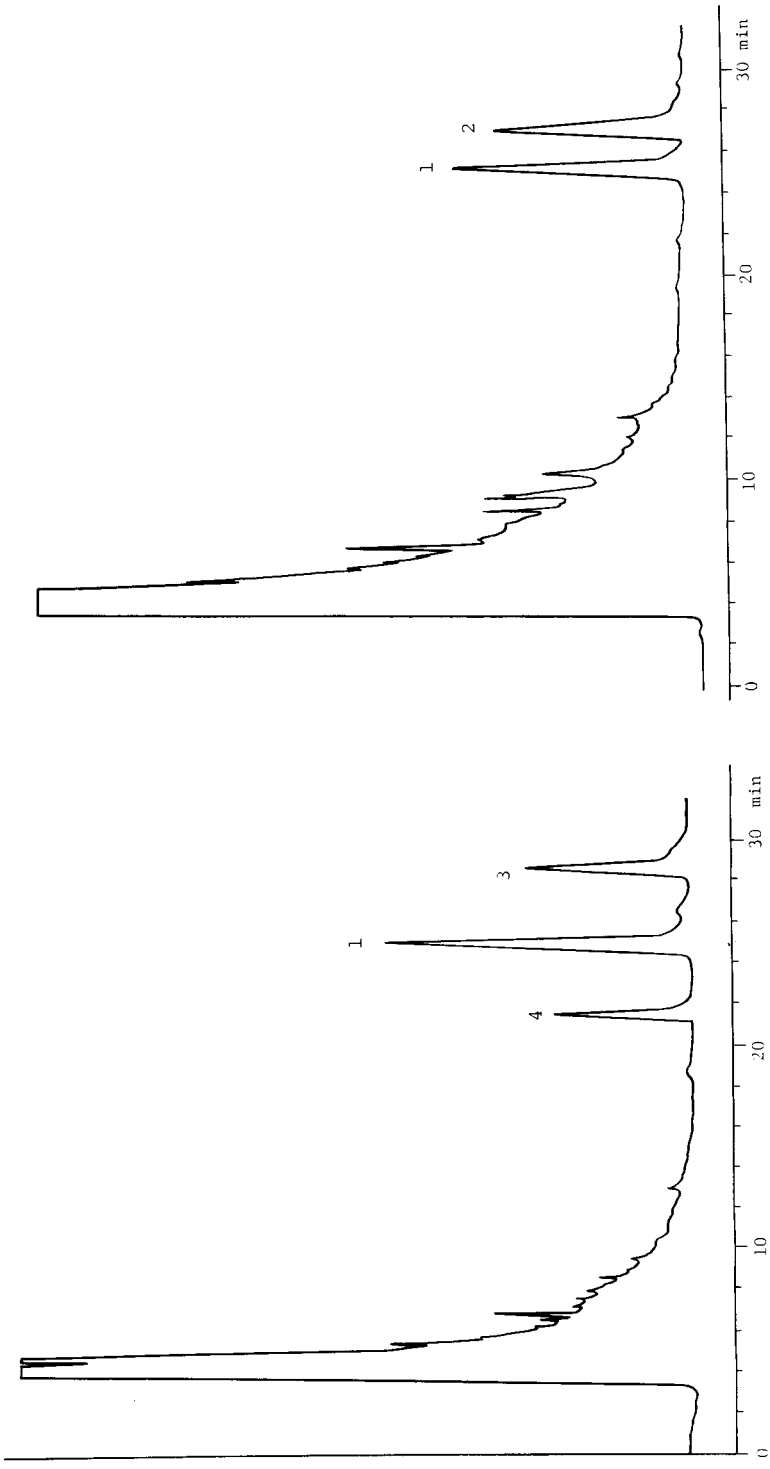

Fig. 1. Separation of a mixture of brassinolide (1), norbrassinolide (4) and homobrassinolide (3) bismethaneboronates.

Fig. 2. Separation of a mixture of brassinolide (1) and 24-epibrassinolide (2) bismethaneboronates.

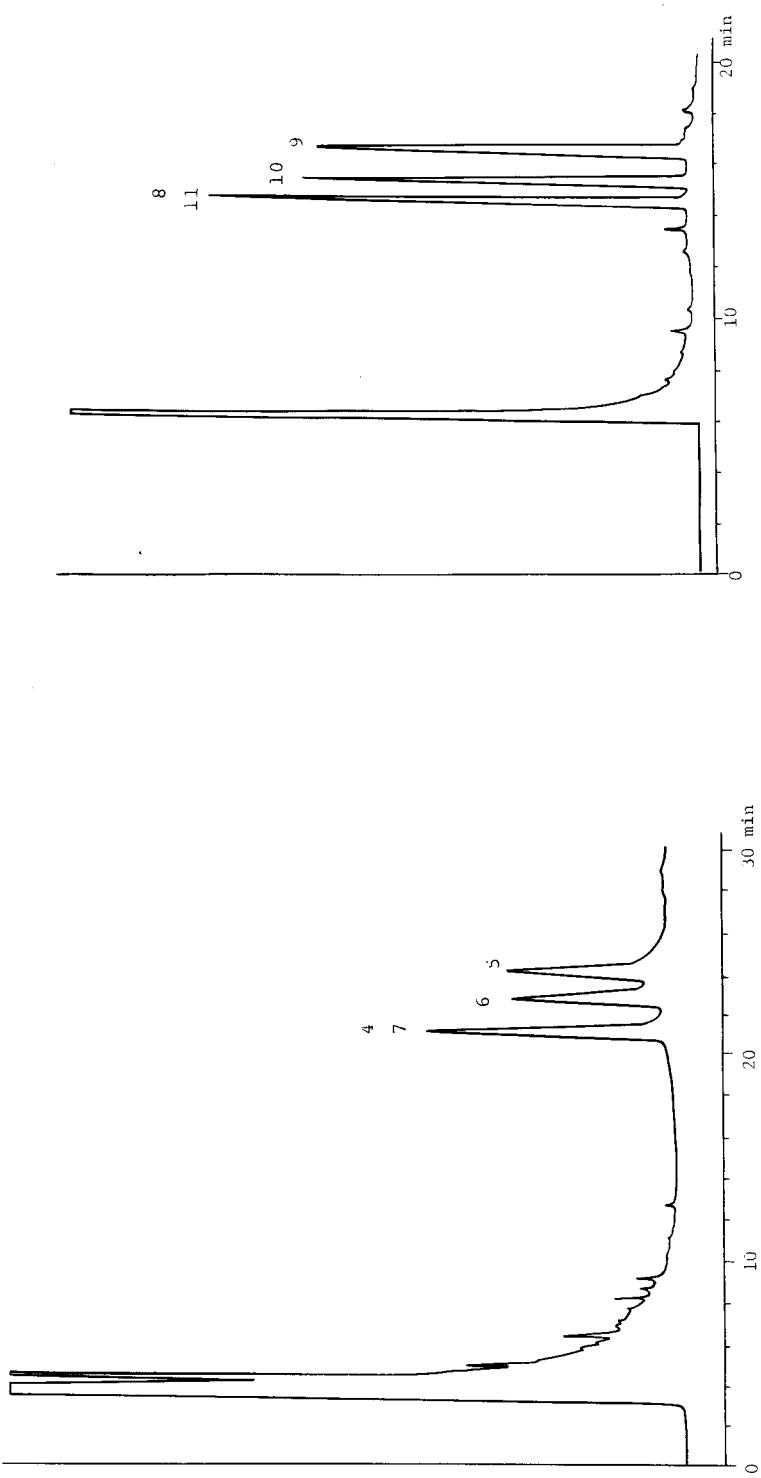

Fig. 3. Separation of four isomers of norbrassinolide bismethaneboronate.

Fig. 4. Separation of four isomers of 22,23-dihydroxycholesterol methaneboronate trimethylsilyl ether.

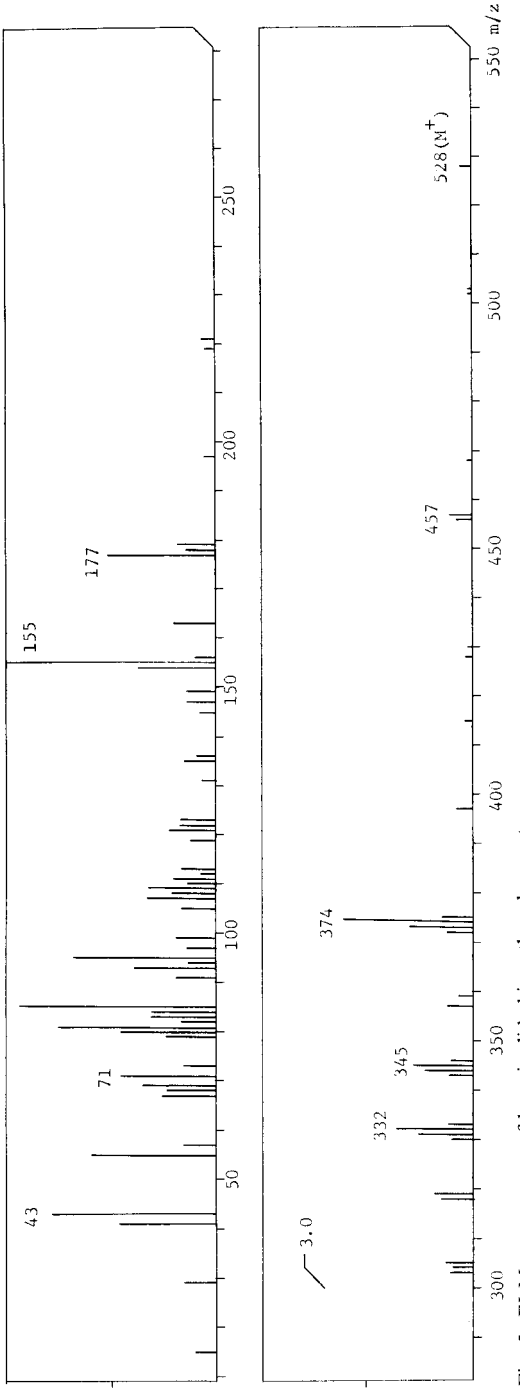

Fig. 5. EI Mass spectrum of brassinolide bismethaneboronate.

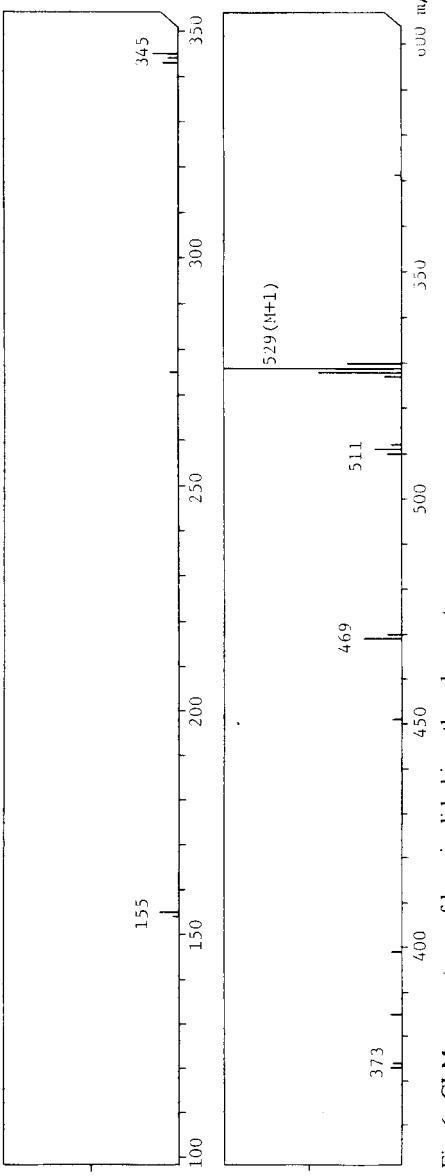

Fig. 6. CI Mass spectrum of brassinolide bismethaneboronate.

TABLE I

RETENTION TIMES OF DERIVATIVES OF BRASSINOLIDE AND ITS ANALOGUES

Compound	*Packed column (min)*	*Capillary column (min)*
Bismethaneboronate		
Brassinolide (1)	24.5	24.67
24-Epibrassinolide (2)	27.0	26.50
Homobrassinolide (3)	29.0	28.08
(22*R*,23*R*)-Norbrassinolide (4)	20.5	20.90
(22*R*,23*S*)-Norbrassinolide (5)	24.0	23.84
(22*S*,23*R*)-Norbrassinolide (6)	22.5	22.48
(22*S*,23*S*)-Norbrassinolide (7)	20.5	20.90
Methaneboronate trimethylsilyl ether		
(22*R*,23*R*)-Dihydroxycholesterol (8)		14.41
(22*R*,23*S*)-Dihydroxycholesterol (9)		16.46
(22*S*,23*R*)-Dihydroxycholesterol (10)		15.17
(22*S*,23*S*)-Dihydroxycholesterol (11)		14.41
(20*R*,22*R*)-Dihydroxycholesterol (12)		15.94
(20*R*,22*S*)-Dihydroxycholesterol (13)		15.49
(20*S*,22*R*)-Dihydroxycholesterol (14)		15.07
(20*S*,22*S*)-Dihydroxycholesterol (15)		15.94
Column	1.5% OV-17	OV-17
Column temperature (°C)	290	270
Nitrogen flow-rate (ml/min)	40	0.4

clear that the methaneboronate was a better derivative than the trimethylsilyl ether for GC analysis.

Separation of the four possible isomers at the C_{22} and C_{23} positions of norbrassinolide was investigated. Although (22*R*,23*S*)- (5) and its (22*S*,23*R*)-isomer (6) can be separated, (22*R*,23*R*)- (4) and its (22*S*,23*S*)-isomer (7) have very close retention times, as shown in Fig. 3. Similar behaviour was observed in the analysis of the four isomers of 22,23-dihydroxycholesterol (8–11) as their methaneboronate trimethylsilyl derivatives (Fig. 4). In the case of 20,22-dihydroxycholesterols (12–15), the (20*R*,22*S*)- (13), (20*R*,22*R*)- (12) and (20*S*,22*R*)-isomers (14) could be separated, but the (20*S*,22*S*)-isomer (15) had a retention time close to that of the (20*R*,22*R*)-isomer (12) (all as their boronate trimethylsilyl derivatives). The retention times of these derivatives on packed and capillary columns are listed in Table I.

GC–MS analysis

The EI mass spectrum of bismethaneboronate of brassinolide is shown in Fig. 5. The derivatives of brassinolide (1), homobrassinolide (3) and norbrassinolide (4) afforded molecular ions at *m/z* 528, 542 and 514, respectively, an ion at *m/z* 457 resulting from C_{23}–C_{24} fission and a strong ion at *m/z* 345 resulting from C_{17}–C_{20} fission. Thus, the fragment ions *m/z* 457, 374, 345 and 177 are common peaks for brassinolide skeleton. The peak at *m/z* 374 was accompanied by hydrogen transfer. The ions at *m/z* 155, 169 and 141 corresponding to the side-chain cleavage are base peaks in those spectra. The derivatives afforded characteristic ions for a *B*-ring lac-

TABLE II

CHARACTERISTIC FRAGMENT IONS OF BRASSINOLIDE BISMETHANEBORONATE (EI-MS)

Compound (bismethaneboronate)	M^+	C_{23}–C_{24} *fission*	C_{20}–C_{22} *fission*	C_{17}–C_{20} *fission*	*B-ring lactone*
Brassinolide (1)	528 (1.8)	457 (4.0)	374* (20.9) 155 (100)	345 (9.6)	332 (12.4) 177 (53.0)
Norbrassinolide (4)	514 (2.5)	457 (0.83)	374* (10.4) 141 (100)	345 (5.8)	318 (27.9) 177 (57.5)
Homobrassinolide (3)	542 (0.90)	457 (6.3)	374* (22.5) 169 (100)	345 (16.2)	346 (5.9) 177 (47.3)

* H-Transfer.

tone at *m/z* 332, 346 and 318, respectively. These characteristic ions may be useful for structural determination of brassinolide analogues.

The CI mass spectrum of the derivative of brassinolide is shown in Fig. 6. The ions corresponding to $M + 1$ at 529, 543 and 515 are base peaks for brassinolide (1), homobrassinolide (3) and norbrassinolide (4), respectively. These derivatives also gave side-chain cleavage ions at *m/z* 345 (C_{17}–C_{20} fission), and *m/z* 155, 169 and 141, together with ions at *m/z* 373 (C_{20}–C_{22} fission). The ions at *m/z* 345 and 373 are common for the brassinolide skeleton. These ions are useful for selected ion monitor-

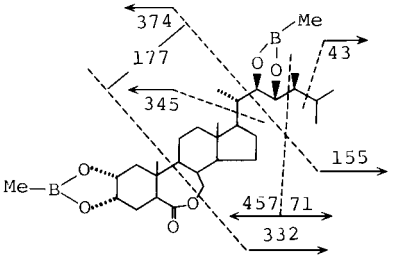

EI-MS

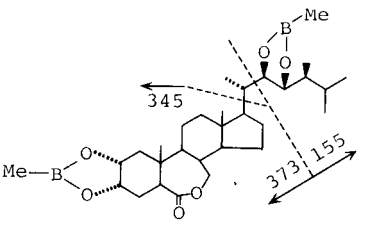

CI-MS

TABLE III

CHARACTERISTIC FRAGMENT IONS OF BRASSINOLIDE BISMETHANEBORONATE (CI-MS)

Compound (bismethaneboronate)	$M + 1$	$M + 1 - 18$	$M + 1 - 60$	C_{20}–C_{22} *fission*	C_{17}–C_{20} *fission*
Brassinolide (1)	529 (100)	511 (15.7)	469 (21.4)	373 (5.7) 155 (10.0)	345 (14.3)
Norbrassinolide (4)	515 (100)	497 (17.1)	455 (32.8)	373 (5.7) 141 (7.1)	345 (11.4)
Homobrassinolide (3)	543 (100)	525 (12.0)	483 (28.6)	373 (8.6) 169 (21.4)	345 (21.4)

ing for screening of brassinolide analogues. Thus, picogram amounts of brassinolide can be detected in plants by means of GC–CI-MS. The characteristic fragment ions of brassinolide derivatives are listed in Tables II and III. The mass spectra of free brassinolide and its analogues will be discussed in a future paper.

ACKNOWLEDGEMENTS

The authors are grateful to Dr. Masami Matsui, Mr. Takaharu Kitsuwa and Miss Masako Asai, Shimadzu Seisakusho Co. Ltd., for their technical assistance. This work was supported by research grants from the Ministry of Education of Japan.

REFERENCES

1 M. D. Grove, G. F. Spencer, W. K. Rohwedder, N. Mandava, J. F. Worley, J. D. Warthen, Jr., G. L. Steffens, J. L. Flippen-Anderson and J. Cook, Jr., *Nature (London)*, 281 (1979) 216.
2 M. Ishiguro, S. Takatsuto, M. Morisaki and N. Ikekawa, *J. Chem. Soc., Chem. Commun.*, (1980) 962.
3 S. Fung and J. B. Siddall, *J. Amer. Chem. Soc.*, 102 (1980) 6580.
4 M. J. Thompson, N. Mandava, J. L. Flippen-Anderson, J. F. Worley, S. R. Dutky, W. E. Robbins and W. Lusby, *J. Org. Chem.*, 44 (1979) 5002.
5 K. Mori, *Agr. Biol. Chem.*, 44 (1980) 1211.
6 S. Takatsuto, B. Ying, M. Morisaki and N. Ikekawa, *Chem. Pharm. Bull.*, 29 (1981) 903.
7 K. Wada, S. Marumo, N. Ikekawa, M. Morisaki and K. Mori, *Plant Cell Physiol.*, 22 (1981) 323.
8 J. H. Yopo, D. Ladd, D. Jaques and N. Mandava, *Abstracts of the 10th International Conference of Plant Growth Substances, Madison, WI, 1979*, p. 25.
9 W. J. Meudt, J. F. Worley, L. E. Gregory, N. Mandava, J. G. Buta, G. L. Steffens and M. J. Thompson, *Abstracts of the 10th International Conference of Plant Growth Substances, Madison, WI, 1979*, p. 25.
10 N. Mandava and J. F. Worley, *Abstracts of the 10th International Conference of Plant Growth Substances, Madison, WI, 1979*, p. 49.
11 S. Marumo, H. Hattori, H. Abe, Y. Nonoyama and K. Munakata, *Agr. Biol. Chem.*, 32 (1968) 528.
12 C. J. W. Brooks, W. J. Cole and H. B. McIntyre, *Lipids*, 15 (1980) 745.
13 M. Morisaki, S. Sato and N. Ikekawa, *Chem. Pharm. Bull.*, 25 (1977) 2576.

Journal of Chromatography, 239 (1982) 243–250
Elsevier Scientific Publishing Company, Amsterdam — Printed in The Netherlands

CHROM. 14,655

GAS CHROMATOGRAPHIC AND MASS SPECTROMETRIC STUDIES ON THE METABOLISM AND PHARMACOKINETICS OF Δ^1-TETRAHYDROCANNABINOL IN THE RABBIT

D. J. HARVEY*, J. T. A. LEUSCHNER and W. D. M. PATON
University Department of Pharmacology, South Parks Road, Oxford OX1 3QT (Great Britain)

SUMMARY

Gas chromatography–mass spectrometry has been used to investigate the *in vivo* hepatic metabolism of Δ^1-tetrahydrocannabinol (Δ^1-THC) in the New Zealand white rabbit. Sixteen metabolites were identified and shown to be present in different relative amounts compared with the hepatic metabolites of Δ^1-THC produced by other species. The metabolic profile was also different from that reported from rabbit urine particularly with regard to the lower relative concentrations of acidic metabolites in the liver. The pharmacokinetics of Δ^1-THC has been studied in the rabbit using the recently developed GC–MS method based on metastable ion monitoring. This revealed a terminal plasma Δ^1-THC half life ranging from 34.16 to 59.30 h (mean 46.75 h) after a single dose and a THC fat/plasma ratio of 10^3–10^4:1.

INTRODUCTION

The metabolism of Δ^1-tetrahydrocannabinol (Δ^1-THC, 1), the major psychoactive principle of *Cannabis sativa* L. is complex and shows considerable species variability[1–3]. Major sites of attack are the allylic positions, 6 and 7 and the aliphatic carbons of the pentyl side-chain. The resulting hydroxy compounds are readily oxidized to aldehydes, ketones and acids and these can be excreted either free or as glucuronide conjugates[4]. Previous studies from this laboratory have concentrated on the structural determination of metabolites in tissues, particularly liver[3,5] rather than those in excreta as this gives a better measure of the molecular species present at the site of action of the drug. The results of these studies in mice, guinea pigs and rats have shown considerable species variation particularly with regard to the initial site of metabolic attack[6,7]. Comparative studies on hepatic metabolites in the rabbit are lacking even though this species has been used for teratological[8–10] and pharmacokinetic studies of Δ^1-THC[11]. In this paper we examine the hepatic metabolites of the drug in the New Zealand white rabbit using gas chromatographic–mass spectrometric (GC–MS) techniques comparable to those used in the early studies. Plasma and tissue

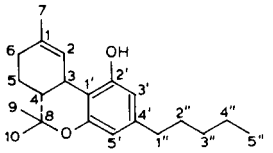

1, Δ^1-THC

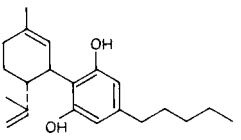

2, CBD

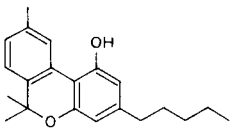

3, CBN

0021-9673/82/0000–0000/$02.75

levels of the drug are also reported. These are studied by GC–MS using metastable ion monitoring[12].

Previous studies of the metabolism and excretion of Δ^1-THC by the rabbit have shown that the urinary route is preferred to the faecal route[13] in contrast to excretion by most other species where faecal elimination is usually dominant. Further studies have shown that these urinary metabolites are mainly acids, diacids and hydroxy acids with metabolic attack at C-6, C-7 and in the side-chain[14–17]. Nilsson *et al.*[18] have reported that 7-hydroxy-Δ^1-THC is a major metabolite formed by rabbit liver homogenates and further studies by Ben-Zvi and Burstein[19] on the same system have revealed the additional presence of 6α,7-dihydroxy-Δ^1-THC and hexahydrocannabinol-1α,2α-epoxide. The disposition of radiolabelled Δ^1-THC and some of its metabolites has recently been studied by Law[20] but the metabolites were not identified.

EXPERIMENTAL

Materials

Δ^1-THC was obtained from the National Institute on Drug Abuse. "Cannabis tincture" was obtained from W. Ransom (Hitchin) and its cannabinoid content was determined by gas–liquid chromatography (GLC) as described below.

Examination of the cannabis sample

The sample of "cannabis tincture" was evaporated to dryness (nitrogen stream) and converted into trimethylsilyl derivatives by reaction with N,O-bis(trimethylsilyl)trifluoroacetamide (BSTFA) and trimethylchlorosilane (TMCS) in acetonitrile (2:1:2) for 10 min at 60°C. 5α-Cholestane was used as the internal standard.

Quantitation of cannabinoids in the cannabis extract was performed by GLC using a Varian 2440 dual-column gas chromatograph fitted with flame ionization detectors and two 2 m × 2 mm I.D. glass columns packed with 3% SE-30 on 100–120 mesh Gas-Chrom Q (Applied Science Labs., State College, PA, U.S.A.). The carrier gas was nitrogen at 30 ml min^{-1}, the column oven was temperature programmed from 150 to 300°C at 4°C min^{-1} and the injector and detector temperatures were 300°C.

Metabolism studies

Δ^1-THC (98% pure by GLC), suspended in Tween 80 and physiological saline were administered intraperitoneally to rabbits (male, New Zealand white, 2 kg) at a dose of 100 mg kg^{-1}. The animals were killed 1 h later, and the livers were removed and frozen. Metabolites were extracted from the homogenized livers with ethyl acetate and separated from neutral lipids by chromatography on Sephadex LH-20 (Table I), and converted into TMS, [$^2H_9$]TMS[21], methyl ester–TMS derivatives as described previously[5]. In addition, aliquots were reduced with lithium aluminium deuteride[22,23] and the resulting alcohols were examined by GC–MS as their TMS derivatives.

GC–MS of metabolites

GC–MS data from the metabolites were recorded with a VG Micromass 12B mass spectrometer interfaced to a VG 2040 data system and via a glass jet separator to a Varian 2440 gas chromatograph. The columns were 2 m × 2 mm glass packed with either 3% SE-30 or OV-17 on 100–120 mesh Gas-Chrom Q. Operating con-

TABLE I

FRACTIONATION OF THE CANNABINOIDS AND THEIR METABOLITES ON SEPHADEX LH-20

Fraction	*Solvent*	*Volume (ml)*	*Contents*
1	Chloroform	18	Triglycerides, cholesterol
2	Chloroform	8	Unchanged cannabinoids
3	Chloroform	10	Fatty acids, some CBN
4	Chloroform	35	Monohydroxy, ketohydroxy metabolites
5	Chloroform methanol (4:1)	50	Polar metabolites

ditions were: column oven, temperature programmed from 150 to 300°C at 2°C min^{-1}; injector, separator and ion source temperatures, 300, 290 and 260°C, respectively; carrier gas, helium at 30 ml min^{-1}; electron energy 25 eV; trap current, 100 μA; accelerating voltage 2.5 kV; scan, 3 sec $decade^{-1}$, exponential.

Treatment of animals for pharmacokinetic studies

Δ^1-THC in Tween 80 and sterilized physiological saline was administered into the marginal ear vein of female New Zealand White rabbits (2 kg) at a dose of 1 or 0.1 mg kg^{-1}. Blood was collected into heparinized tubes from the other ear at intervals until Δ^1-THC could no longer be detected. This was centrifuged to obtain the plasma which was stored at −30°C until required. Two rabbits were also treated with 1.0 and 0.1 mg kg^{-1} Δ^1-THC equivalent of cannabis tincture. One month later the animals were treated again with the same dose daily for 8 days. One animal was treated for 22 days (1 mg kg^{-1}). Blood samples were collected as before commencing after the last dose.

Quantitation of Δ^1-THC in plasma and fat

[1″,1″,2″,2″-$^2H_4$]CBN was added to the plasma sample, the cannabinoids were extracted 3 times with hexane, blown to dryness, allowed to stand with ethereal diazomethane for 2 min and were converted into TMS derivatives using BSTFA. Full details have been published[12]. THC levels were measured using metastable ion monitoring as described below. For the measurement of levels in fat, the hexane extract was reconstituted in chloroform and chromatographed twice on Sephadex LH-20 in chloroform. The fraction eluting between 19 and 36 ml (fractions 2 and 3, Table I) was collected and derivatized as described above.

Metastable ion monitoring

This was performed with a VG Micromass 70-70F mass spectrometer interfaced via a glass jet separator to a Varian 2440 gas chromatograph fitted with a 2 m × 2 mm 3% SE-30 column as described above. Operating conditions were: column oven, 220°C; injector, separator and ion source temperatures, 300, 290 and 260°C, respectively; carrier gas, helium at 30 ml min^{-1}; electron energy, 70 eV; trap current, 1 mA; accelerating voltage, 4.16 kV; magnet set to record m/z 371.

RESULTS AND DISCUSSION

Techniques such as GLC and MS are ideal for studies of the metabolism and disposition of lipophilic drugs such as Δ^1-THC as they do not require isolation of the

metabolites prior to examination. The low concentrations of the compounds present in animal fluids and tissues, together with the presence of a relatively large number of compounds having similar structures, makes isolation impractical for all but the most abundant metabolites. The extraction method adopted for the present studies was designed to obtain metabolic fractions containing the largest possible range of metabolites with the minimum of "clean-up"; GLC was then used to separate these compounds and GC–MS was used for identification.

Extraction of the metabolites from 2-g samples of liver was achieved as described above. Spectra of the metabolites were compared with those of authentic samples where available (see Table II) and with published data. Functional groups were identified by the preparation of group-specific derivatives such as methyl esters for carboxylic acids and correlations between metabolites in different oxidation states (acids and ketones) were made by reduction with lithium aluminium deuteride[22,23]. The 16 metabolites identified are listed in Table II. All of these compounds have been

TABLE II

METABOLITES OF Δ^1-THC EXTRACTED FROM RABBIT LIVER

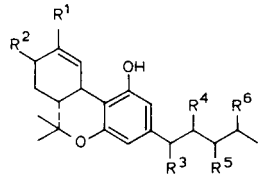

Metabolite	R^1	R^2	R^3	R^4	R^5	R^6	*Abundance**	*Lit. ref. for spectrum*
1″-OH-Δ^1-THC	H	H	OH	H	H	H	+	24, 25
3″-OH-Δ^1-THC	H	H	H	H	OH	H	+	24, 25
6α-OH-Δ^1-THC**	H	α-OH	H	H	H	H	+	25, 26
6β-OH-Δ^1-THC**	H	β-OH	H	H	H	H	+	25, 26
7-OH-Δ^1-THC**	CH_2OH	H	H	H	H	H	+ + +	25, 26
2″,7-di-OH-Δ^1-THC	CH_2OH	H	H	OH	H	H	+	26
3″,7-di-OH-Δ^1-THC	CH_2OH	H	H	H	OH	H	+	26
6α,7-di-OH-Δ^1-THC**	CH_2OH	α-OH	H	H	H	H	+	26
6β,7-di-OH-Δ^1-THC**	CH_2OH	β-OH	H	H	H	H	+	26
Δ^1-THC-7-oic acid**	COOH	H	H	H	H	H	+ + +	25, 26
6α-OH-Δ^1-THC-7-oic acid	COOH	α-OH	H	H	H	H	+	27, 28
2″-OH-Δ^1-THC-7-oic acid	COOH	H	H	OH	H	H	+	27, 28
3″-OH-Δ^1-THC-7-oic acid	COOH	H	H	H	OH	H	+ +	27, 28
4″-OH-Δ^1-THC-7-oic acid	COOH	H	H	H	H	OH	+ +	29

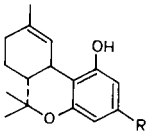

Metabolite	*R*	*Abundance**	*Lit. ref. for spectrum*
4″,5″-bis,nor-Δ^1-THC-3″-oic acid	C_2H_4COOH	+ +	2, 30
		+	31
2″,3″,4″,5″-tetrakis,nor-Δ^1-THC-1″-oic acid	COOH		

* + = trace metabolite; + + = intermediate concentration; + + + = major metabolite. Accurate concentrations were not measured because of the lack of suitable standards.

** Authentic sample available.

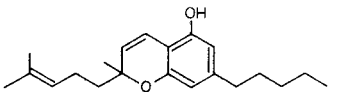

4, CBC

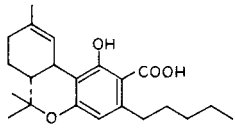

5, Δ^1-THC acid

observed as metabolites of Δ^1-THC in other species and the profile was intermediate between that observed for the mouse and guinea-pig. 7-Hydroxylation and oxidation to Δ^1-THC-7-oic acid was the major metabolic route in contrast to the results obtained by Nordqvist and co-workers[16,17] who have reported that in rabbit urine, 4″,5″-bis,nor-Δ^1-THC-3″-oic acid is the major metabolite. This is probably a reflection of the extent to which the 3″-acid is excreted into the urine rather than a difference in the overall profile. In our liver fractions, the 3″-oic acid was observed, but in much lower concentration than the 7-oic acid. It was accompanied by the 2″,3″,4″,5″-tetrakis,nor-Δ^1-THC-1″-oic acid. Other side-chain acids and their hydroxy and carboxy substituted derivatives reported by Nordqvist and co-workers were not observed in the liver, possibly as the result of their low concentration. In other respects the profiles were similar to those found by the other workers. Thus 6β-hydroxylation was preferred to 6α-hydroxylation although the amount of each metabolite was much lower than in the guinea-pig (Fig. 1). 6-Ketones were not detected. Hydroxylation of the side-chain was observed to a limited extent at positions 1″, 2″, 3″, and 4″. Table III shows a comparison of the *in vivo* hepatic metabolites of Δ^1-THC produced by the rabbit with those observed previously from mouse, rat and guinea pig.

Measurement of Δ^1-THC and its metabolites in plasma and tissues is difficult because of the low levels encountered and the presence of co-extracted lipid ma-

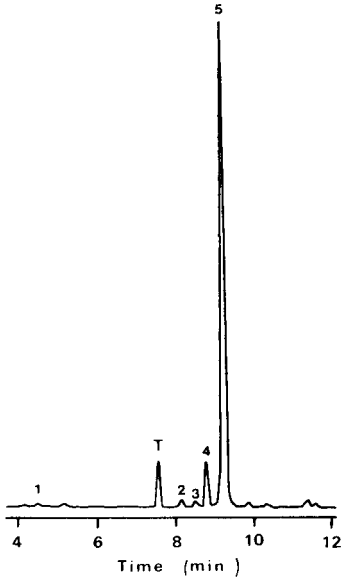

Fig. 1. Computer reprocessed total ion chromatogram [38] of the monohydroxy metabolite-containing fraction (fraction 4, Table I) from the livers of rabbits treated with Δ^1-THC. Peaks: 1 = 1″-hydroxy-Δ^1-THC; 2 = 6α-hydroxy-Δ^1-THC; 3 = 3″-hydroxy-Δ^1-THC; 4 = 6β-hydroxy-Δ^1-THC; 5 = 7-hydroxy-Δ^1-THC; T = tissue constituent.

TABLE III

SUMMARY OF THE MAJOR METABOLIC ROUTES FOR Δ^1-THC SHOWN BY FOUR SPECIES

+ → + + +, Increasing importance of metabolic route; −, not detected.

Metabolic route	*Mouse*	*Rat*	*Guinea-pig*	*Rabbit*
7-Hydroxylation	+ + +	+ + +	+ + +	+ + +
6α-Hydroxylation	+ +	+ +	+	+
6β-Hydroxylation	+	+	+ + +	+ +
1″-Hydroxylation	−	+	+	+
2″-Hydroxylation	+ +	+	+	+
3″-Hydroxylation	+ +	+ +	+	+
4″-Hydroxylation	+ +	+ +	+ +	+
7-Acid formation	+ + +	+ + +	+	+ + +
6-Ketone formation	+	+	+	−
β-Oxidation	+	+	+ + +	+ +

terial[32,33]. We have developed a rapid GC–MS assay for Δ^1-THC as its TMS derivative based on metastable ion monitoring of the $[M]^+$ (m/z 386) → $[M-CH_3]^+$ (m/z 371) transition using a double focussing mass spectrometer[12], as described in the experimental section. The method can measure Δ^1-THC to 5 pg/ml of plasma and has now been used to study the pharmacokinetics of Δ^1-THC in rabbits. Experiments were performed as described above and some typical results are presented in Fig. 2. These are in agreement with earlier results based on GLC and radiolabelling which indicate that Δ^1-THC accumulates extensively in the body[34,35]. Following a single 0.1 mg kg^{-1} dose, Δ^1-THC could be monitored for 4 days after administration. After an 8-day treatment with daily injections of the same dose, the drug could be monitored in plasma for 12 days and after a 22-day treatment with 1 mg kg^{-1} per day the drug could be monitored for 26 days. Terminal half lives were calculated using non-linear least squares regression analysis and ranged from 34.16 to 59.30 h (mean 46.75 h, n = 5) following a single dose and 77.94 to 120.02 h (mean 94.63 h, n = 5) following multiple doses. As this type of behaviour is typical of drugs which accumulate in

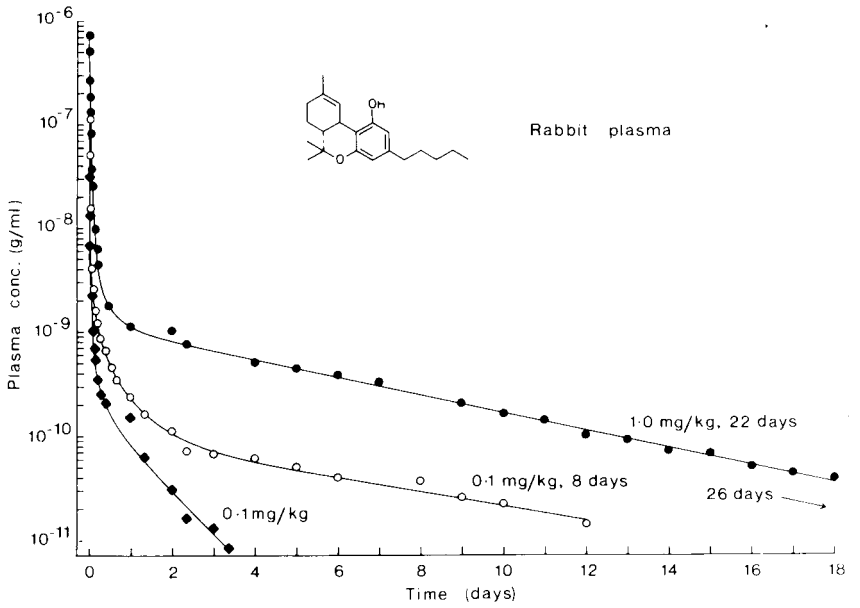

Fig. 2. Semi-logarithmic plot of the plasma levels of Δ^1-THC: time for rabbits dosed with: ◆, 0.1 mg kg^{-1}; ○, 0.1 mg kg^{-1} daily for 8 days; ●, 1.0 mg kg^{-1} daily for 22 days.

adipose tissue, the concentration of Δ^1-THC in fat was measured. Because of the large amount of triglyceride in the samples, these were chromatographed twice on Sephadex LH-20 prior to derivative formation. Concentrations in the region of 10^3 to 10^4 times the plasma concentration were found at various times after dosing and the decline in concentration matched the decline of the plasma Δ^1-THC levels. The concentration of Δ^1-THC in fat at 28 h after dosing with 1 mg/kg was 1161.0 ng/g and this fell to 36.4 ng/g at 240 h. In use, Δ^1-THC is usually present with other cannabinoids such as cannabidiol (CBD) and cannabinol (CBN) and the presence of these compounds could affect both the metabolism and distribution of the drug. Previous studies on the metabolism of a crude mixture of cannabinoids from "cannabis tincture" in the mouse suggests that the effects of the additional cannabinoids on the profile of hepatic metabolites is minimal[3]. The plasma levels of Δ^1-THC have now been measured in the rabbit treated with 1.0 an 0.1 mg/kg Δ^1-THC in cannabis tincture but no significant differences were found over the results from rabbits treated with pure Δ^1-THC. This is consistent with results recently obtained in other laboratories[36,37]. The composition of the "cannabis tincture" used in these experiments was determined by GLC and is shown in Table IV.

TABLE IV

CONCENTRATIONS OF THE MAJOR CANNABINOIDS PRESENT IN CANNABIS TINCTURE AS MEASURED BY GLC

Cannabinoid	*Quantity (mg/ml)*	*Relative amount (Δ^1-THC = 100)*
Pr-CBD	0.285**	20
Pr-Δ^1-THC	0.48	34
Pr-CBN	0.135	9.6
CBD	1.26	90
CBC*	0.28	20
Δ^1-THC	1.40	100
CBN	0.40	29

* Cannabichromene.

** Response factors of the propyl (Pr) cannabinoids were based on those of the pentyl homologues because of the lack of suitable standards.

CONCLUSIONS

GC–MS has proved to be a valuable method for analysis of cannabinoids and their metabolites. Identification of the metabolites can be accomplished at the microgram level by a combination of the use of group-specific derivatives, deuterium labelling and various GLC columns. The profiles obtained are complex and vary considerably with the animal species in which metabolism is studied. GC–MS using metastable ion monitoring has also provided the most sensitive method yet for the analysis of Δ^1-THC in body fluids and tissues and has enabled the pharmacokinetics of this compound to be elucidated. Results from these measurements have shown that despite its extensive metabolism, the psychoactive Δ^1-THC appears to be stored as such in a fatty reservoir, and to be slowly released over a prolonged period in a manner corresponding to its fat–water partition coefficient.

ACKNOWLEDGEMENTS

We thank the Medical Research Council for a Programme Research Grant and

the Wellcome Trust for additional financial support. We also thank Dr. M. C. Braude for supplies, through the MRC, of Δ^1-THC. Thanks are also due to Miss J. Hughes and Mr. D. Perrin for expert technical assitance.

REFERENCES

1 C. G. Turner, M. A. Elsohly and E. G. Boeren, *J. Nat. Prods.*, 43 (1980) 169.
1 R. Mechoulam, N. K. McCallum and S. Burstein, *Chem. Rev.*, 76 (1976) 75.
2 L. J. King, J. D. Teale and V. Marks in J. D. P. Graham (Editor), *Cannabis and Health*, Academic Press, London, 1976, p. 77.
3 D. J. Harvey, B. R. Martin and W. D. M. Paton, in G. G. Nahas and W. D. M. Paton (Editors), *Marihuana: Biological Effects*, Pergamon, Oxford, 1979, p. 45.
4 P. L. Williams and A. C. Moffat, *J. Pharm. Pharmacol.*, 32 (1980) 445.
5 D. J. Harvey, B. R. Martin and W. D. M. Paton, *J. Pharm. Pharmacol.*, 29 (1977) 482.
6 D. J. Harvey, B. R. Martin and W. D. M. Paton, in A. Frigerio and E. L. Ghisalberti (Editors), *Mass Spectrometry in Drug Metabolism*, Plenum, New York, 1977, p. 403.
7 D. J. Harvey, B. R. Martin and W. D. M. Paton, in A. Frigerio (Editor), *Recent Developments in Mass Spectrometry in Biochemistry and Medicine*, Vol. 1, Plenum, New York, 1978, p. 161.
8 D. D. Cozens, R. Clark, A. K. Palmer, N. Hardy, G. G. Nahas and D. J. Harvey, in G. G. Nahas and W. D. M. Paton (Editors), *Marihuana: Biological Effects*, Pergamon, Oxford, 1979, p. 469.
9 D. D. Cozens, D. J. Harvey, N. Hardy and G. G. Nahas, *Fed. Proc., Fed. Amer. Soc. Exp. Biol.*, 39 (1980) 849.
10 D. D. Cozens, G. G. Nahas, D. J. Harvey, N. Hardy and E. Wolff, *Bull. Acad. Nat. Méd.*, 164 (1980) 276.
11 D. J. Harvey, J. T. A. Leuschner and W. D. M. Paton, *Brit. J. Pharmacol.*, 74 (1981) 771P.
12 D. J. Harvey, J. T. A. Leuschner and W. D. M. Paton, *J. Chromatogr.*, 202 (1980) 83.
13 S. Agurell, I. M. Nilsson, A. Ohlsson and F. Sandberg, *Biochem. Pharmacol.*, 19 (1970) 1333.
14 S. Burstein, J. Rosenfeld and T. Wittstruck, *Science*, 176 (1972) 422.
15 M. Nordqvist, S. Agurell, M. Binder and I. M. Nilsson, *J. Pharm. Pharmacol.*, 26 (1974) 471.
16 M. Nordqvist, J.-E. Lindgren and S. Agurell, *J. Pharm. Pharmacol.*, 31 (1979) 231.
17 M. Nordqvist, S. Agurell, M. Rydberg, L. Falk and T. Ryman, *J. Pharm. Pharmacol.*, 31 (1979) 238.
18 I. M. Nilsson, S. Agurell, J. L. G. Nilsson, A. Ohlsson, F. Sandberg and M. Wahlqvist, *Science*, 168 (1970) 1228.
19 Z. Ben-Zvi and S. Burstein, *Biochem. Pharmacol.*, 24 (1975) 1130.
20 F. C. P. Law, *Drug Metab. Dispos.*, 6 (1978) 154.
21 J. A. McCloskey, R. N. Stillwell and A. M. Lawson, *Anal. Chem.*, 40 (1968) 233.
22 D. J. Harvey and W. D. M. Paton, in A. Frigerio (Editor), *Recent Developments in Mass Spectrometry in Biochemistry and Medicine*, Vol. 2, Plenum, New York, 1979, p. 127.
23 D. J. Harvey and W. D. M. Paton, *Advan. Mass Spectrom.*, 8 (1980) 1194.
24 M. Binder, S. Agurell, K. Leander and J.-E. Lindgren, *Helv. Chim. Acta*, 57 (1974) 1626.
25 D. J. Harvey, *Biomed. Mass Spectrom.*, in press.
26 M. E. Wall and D. R. Brine, in G. G. Nahas (Editor), *Marihuana: Chemistry, Biochemistry and Cellular Effects*, Springer, New York, 1976, p. 51.
27 D. J. Harvey and W. D. M. Paton, in G. G. Nahas (Editor), *Marihuana: Chemistry, Biochemistry and Cellular Effects*, Springer, New York, 1976, p. 93.
28 D. J. Harvey and W. D. M. Paton, *Res. Commun. Chem. Pathol. Pharmacol.*, 13 (1976) 585.
29 D. J. Harvey and W. D. M. Paton, *Res. Commun. Chem. Pathol. Pharmacol.*, 21 (1978) 435.
30 B. R. Martin, D. J. Harvey and W. D. M. Paton, *J. Pharm. Pharmacol.*, 28 (1976) 773.
31 D. J. Harvey, B. R. Martin and W. D. M. Paton, *J. Pharm. Pharmacol.*, 32 (1980) 267.
32 R. E. Willette (Editor), *Cannabinoid Assays in Humans, Res. Monogr. Ser. No. 7*, NIDA, Rockville, MD, 1976.
33 J. A. Vinson (Editor), *Cannabinoid Assays in Physiological Fluids, ACS Symposium Series No. 98*, American Chemical Society, New York, 1979.
34 D. S. Kreuz and J. Axelrod, *Science*, 179 (1973) 391.
35 E. R. Garrett and C. A. Hunt, *J. Pharm. Sci.*, 66 (1977) 395.
36 S. Agurell, S. Carlsson, J.-E. Lindgren, A. Ohlsson, H. Gillespie and L. Hollister, *Experientia*, 37 (1981) 1090.
37 C. A. nunt, R. T. Jones, R. I. Horning and J. Bachman, *J. Pharmacokinetics, Biopharmaceut.*, 9 (1981) 245.
38 P. Powers, M. J. Wallington, J. A. V. Hopkinson and G. L. Kearns, *23rd Annual Conference on Mass Spectrometry and Allied Topics, Amer. Soc. for Mass Spectrom., Houston, TX, May 25–30, 1975*, Abstr. p. 499.

Journal of Chromatography, 239 (1982) 251–257
Elsevier Scientific Publishing Company, Amsterdam — Printed in The Netherlands

CHROM. 14,568

UNIDIMENSIONAL, SEQUENTIAL SEPARATION OF PTH-AMINO ACIDS BY HIGH-PERFORMANCE THIN-LAYER CHROMATOGRAPHY

SHEILA A. SCHUETTE and COLIN F. POOLE*
Department of Chemistry, Wayne State University, Detroit, MI 48202 (U.S.A.)

SUMMARY

Eighteen of the twenty common protein PTH-amino acids derivatives are separated by continuous multiple development high-performance thin-layer chromatography. The separation is performed on silica gel plates using five development steps with four changes in mobile phase. The derivatives are identified by scanning densitometry, and the total analysis requires less than 1 h. The unseparated derivatives of alanine and tryptophan are baseline resolved in an alternative solvent system. Thus, all twenty of the common PTH-amino acid derivatives may be identified with the proposed method. By using the unidimensional method of development, the high sample capacity of the high-performance thin-layer chromatographic plate is preserved; samples and standards can be run simultaneously to improve the accuracy of identification. The detection limit for the PTH-amino acid derivatives determined by *in situ* reflectance scanning densitometry at 270 nm was found to be *ca.* 0.5 ng per spot.

INTRODUCTION

A major advance in analytical biochemistry was the development of automated sequential analyzers for the determination of the amino acid sequence of peptides and proteins. Although various reaction schemes may be used, one of the most popular methods is the Edman degradation reaction. In this process, the N-terminal amino acid, as its phenylthiohydantoin (PTH) derivative, is cleaved from the peptide chain at the conclusion of each cycle of the sequenator. The determination of the structure of a mammalian peptide or protein requires a support analytical method to identify which amino acid is produced at the end of each cycle of the sequenator. For this purpose gas–liquid chromatography (GLC), high-performance liquid chromatography (HPLC), thin-layer chromatography (TLC) or mass spectrometry are used. However, no single analytical technique has established itself as the method of choice for the identification of the PTH-amino acids. The literature describing new separation schemes or modifications to existing procedures has remained buoyant over the last decade and has been reviewed comprehensively[1–4].

Recent advances in the practice of TLC have led to its wider acceptance as a powerful analytical tool for the quantitative analysis of complex mixtures. This

0021-9673/82/0000–0000/$02.75

changed role and accompanying expectations have spawned a new expression "high-performance thin-layer chromatography" (HPTLC). The performance breakthrough in TLC was not a result of any specific advance in instrumentation or materials, but was rather a culmination of improvements in practically all of the operations of which TLC is comprised. For the separation of the PTH-amino acids, it was expected that HPTLC would provide a significant increase in separation efficiency and detection sensitivity approaching one order of magnitude, shorter analysis times, and an increase in the number of samples and standards which can be analyzed per plate compared to conventional TLC[5,6].

That HPTLC could be used with advantage for the separation of the PTH-amino acids was recognized by Bucher[7] and Yang[8]. However, neither author was able to demonstrate an adequate separation of all 20 common protein PTH-amino acids and some sample overlaps remained in all solvent systems investigated. The position of the PTH-amino acids in the chromatogram was made by eye or photographic means which is not the most accurate or appropriate method for this purpose. In this paper we have used the method of continuous multiple development to separate the PTH-amino acids a few components at a time and precision scanning densitometry for the accurate measurement of spot location at each step in the development sequence. In this way, a complete separation of the mixture at any one point in time becomes unnecessary and more selective solvents can be used to maximize the resolution of those components separated in each development sequence. Changes in the developing solvent can be made at the conclusion of any development sequence to create a step-wise mobile phase gradient. Also, each time the solvent front transverses the plate a natural spot reconcentration phenomenon occurs whereby the bottom half of the spot is pushed into the top and the axis of the spot becomes compressed in the direction of migration[9]. This spot reconcentration mechanism works in opposition to the normal spot broadening process occurring during migration and results in an improvement in sample resolution.

EXPERIMENTAL

The PTH derivatives of the common protein amino acids were obtained in kit form from Sigma (St. Louis, MO, U.S.A.). Standard solutions were prepared by dissolving 4.5–5.0 mg of the PTH-amino acid derivatives in 2.0 ml of ethyl acetate or methanol. Standard mixtures at the same concentration as the above were prepared for all twenty PTH-amino acid derivatives, for fifteen non-polar and moderately polar derivatives (ALA, ASP, GLU, GLY, ISL, LEU, LYS, MET, PHE, PRO, SER, THR, TRP, TYR and VAL), for seven moderately polar and polar derivatives (ARG, ASN, ASP, CM-CYS, GLN, GLU, and HIS) and for the pair ALA/TRP. The standard mixtures were used for identification purposes and in the optimization studies. When not in use the standard solutions are stored under refrigeration.

Chromatography was performed on 10 cm × 10 cm HPTLC plates coated with silica gel 60 (E. Merck, Darmstadt, G.F.R.). The plates were precleaned by a single development with acetonitrile. All solvents were distilled in glass, chromatography grade from Burdick & Jackson (Muskegon, MI, U.S.A.).

Standard solutions were applied to the plate using a 200-nl Pt–Ir micropipette (Antech, Bad Durkheim, G.F.R.) attached to an EVA-Chrom applicator (W & W

Electronic Instrument, Basel, Switzerland). The spots were applied in a line 0.5 cm apart and 0.5 cm from the lower edge. The plates were developed in a short-bed continuous development chamber (Regis, Morton Grove, IL, U.S.A.). Position 2, plate length 3.5 cm or position 4, plate length 7.5 cm were used as indicated in the text.

In situ scanning of the HPTLC plates was performed with a Shimadzu CS-910 scanning densitometer (Shimadzu, Columbia, MA, U.S.A.). All measurements were made in the reflectance mode, single beam operation, at a wavelength of 270 nm. The scanning speed and recorder speed were 48 mm min^{-1}. The slit width was 4.6 mm and slit height 0.46 mm.

RESULTS AND DISCUSSION

The method used is summarized in Table I. It provides a separation of eighteen of the twenty PTH-amino acid derivatives in well under 1 h. ALA and TRP are not separated in this scheme, but a second solvent system is available for their resolution.

The first development is made with methylene chloride for 5 min at position 2 in the short-bed continuous development chamber. The function of this development step is to provide an initial ordering of the derivatives in the region of the origin, thereby improving the resolution of the mixture in subsequent development steps (Fig. 1). The least polar of the amino acid derivatives, PTH-proline, can be identified at this stage. In fact, its migration properties are so different from the other PTH-amino acid derivatives that it remains baseline resolved in each of the first four development steps.

After the methylene chloride has been evaporated from the plate, it is re-developed for 10 min in methylene chloride–isopropanol (99:1) in position 4 of the short-bed chamber. Position 4 corresponds to a plate length of 7.5 cm. At this development stage any of the residues PRO, LEU, ILE, VAL and PHE can be identified (Fig. 2).

The third development sequence is a repeat of step 2. It provides a better separation of the peaks resolved in step 2 as well as enabling MET, ALA/TRP, GLY,

TABLE I

OPTIMUM EXPERIMENTAL CONDITIONS FOR THE SEPARATION OF THE PTH-AMINO ACIDS BY CONTINUOUS MULTIPLE DEVELOPMENT HPTLC

Development step	*Mobile phase composition*	*Plate length (cm)*	*Time (min)*	*PTH-amino acid derivative identified*
1	CH_2Cl_2	3.5	5	PRO
2	CH_2Cl_2–$(CH_3)_2CHOH$ (99:1)	7.5	10	PRO, LEU, ILE, VAL, PHE
3	CH_2Cl_2–$(CH_3)_2CHOH$ (99:1)	7.5	10	PRO, LEU, ILE, VAL, PHE MET, ALA/TRP, GLY, LYS, TYR, THR
4	CH_2Cl_2–$(CH_3)_2CHOH$ (97:3)	7.5	10	PRO, MET, LYS, TYR, THR, SER, GLU
5	$C_2H_5OOCCH_3$–CH_3CN–CH_3COOH (74.3:25:0.7)	7.5	10	ASN, GLU/GLN, ASP, CM-CYS, HIS, ARG

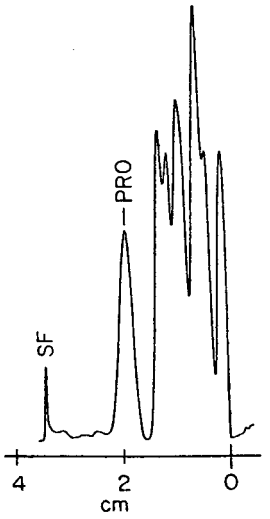

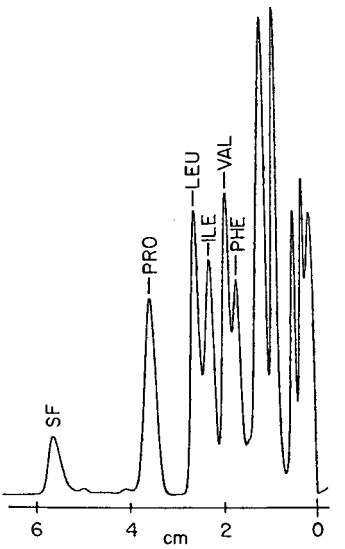

Fig. 1. First continuous multiple development. Methylene chloride, position 2, 5 min.

Fig. 2. Second continuous multiple development. Methylene chloride–isopropanol (99:1), position 4, 10 min.

LYS, TYR, THR residues to be identified (Fig. 3). TRP often appears as a shoulder on the side of the ALA peak, but it is not resolved adequately for identification purposes. ALA and TRP are separated almost to baseline by a 10-min development in hexane–tetrahydrofuran (9:1) in position 2 of the short-bed continuous development chamber (Fig. 4).

The mobile phase is changed to methylene chloride–isopropanol (97:3) for the fourth development step of 10 min in position 4. The separation between LYS, TYR and THR is improved and SER and GLU can be identified in addition (Fig. 5). The small satellite peaks accompanying the labelled peaks in this chromatogram are impurities in the original standards and not artifacts of the development process. Fig. 5 also illustrates the advantage of being able to make measurements with the densitometer at any stage in the sequence. The separation of LYS, TYR, THR, SER and GLU is to baseline at this stage and their identification is easily achieved. However, LEU/ILE, VAL/PHE and TRP/ALA/GLY have started to merge together and could not be determined individually, although well separated in earlier steps.

The very polar PTH-amino acid derivatives remain essentially unresolved in the region of the origin. A much more polar mobile phase is selected for their resolution in the fifth and final development step. A 10-min development in position 4 with ethyl acetate–acetonitrile–glacial acetic acid (74.3:25:0.7) separates all the remaining PTH-amino acid derivatives except GLU/GLN (Fig. 6). However, GLU is separated from GLN in the fourth development step so that the two are easily differentiated from each other.

The improved separating power and shorter analysis times provided by HPTLC technology in combination with the continuous multiple development mode

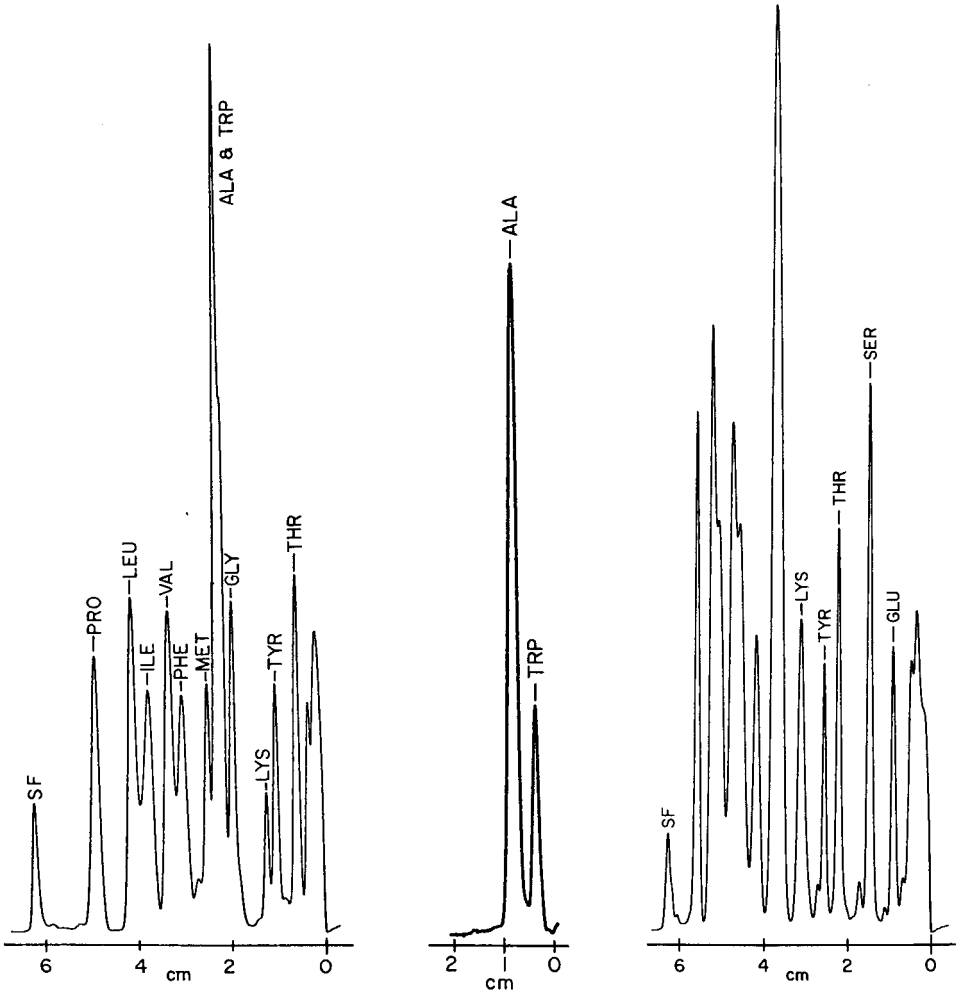

Fig. 3. Third continuous multiple development. Methylene chloride–isopropanol (99:1), position 4, 10 min.

Fig. 4. Separation of ALA and TRP by continuous development in hexane–tetrahydrofuran (9:1), position 2, 10 min.

Fig. 5. Fourth continuous multiple development. Methylene chloride–isopropanol (97:3), position 4, 10 min.

of separation have met our original goal of a fast and efficient method for the identification of the PTH-amino acid derivatives. An important advantage of this HPTLC method is that eighteen samples and standards can be separated simultaneously. Compared to closed-bed techniques such as HPLC, internal calibration can be used for improved identification. Also, on a per sample basis, the analysis time is reduced to the time required for one separation divided by the number of samples on the plate. Some additional time is required to scan each track but this is short compared to the time for development. Consequently, for multiple samples HPTLC is much faster

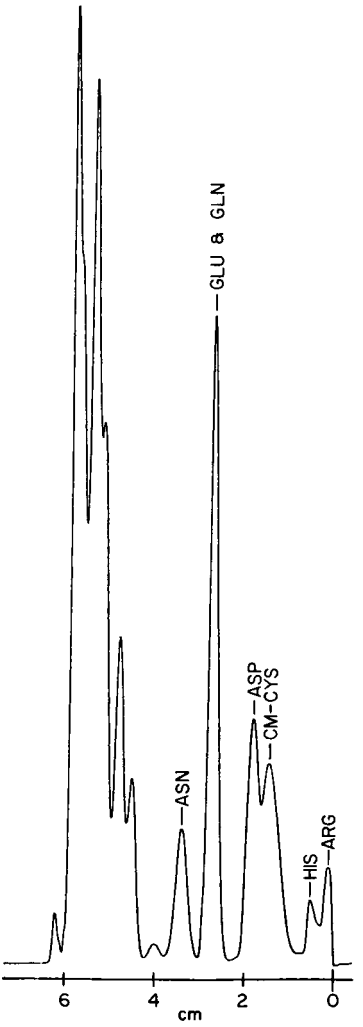

Fig. 6. Fifth continuous multiple development. Ethyl acetate–acetonitrile–glacial acetic acid (74.3:25:0.7), position 4, 10 min.

than HPLC, which relies on elution chromatography and can separate only one sample at a time.

CONCLUSIONS

The method described for the identification of the PTH-amino acids represents a considerable improvement over the results found using conventional TLC practices. Sample resolution is better and the analysis time reduced. Two-dimensional development is not necessary to enhance resolution so that the method preserves all the advantages expected of unidimensional development; namely, high sample capacity (eighteen samples on a 10 × 10 cm HPTLC plate) and the ability to separate samples and standards simultaneously to improve the certainty of derivative identification.

ACKNOWLEDGEMENTS

Work in the authors' laboratory is supported by the Camille and Henry Dryfus Foundation, the Research Corporation and the donors to the Petroleum Research Fund of the American Chemical Society.

REFERENCES

1 C. F. Poole and A. Zlatkis, *J. Chromatogr.*, 184 (1980) 99.
2 L. R. Croft, *Handbook of Protein Sequence Analysis*, Wiley, New York, 1980.
3 Z. Deyl, *J. Chromatogr.*, 127 (1976) 91.
4 J. Rosmus and Z. Deyl, *J. Chromatogr.*, 70 (1972) 221.
5 A. Zlatkis and R. E. Kaiser (Editors), *High Performance Thin-Layer Chromatography*, Elsevier, Amsterdam, 1977.
6 W. Bertsch, S. Hara, R. E. Kaiser and A. Zlatkis (Editors), *Instrumental HPTLC*, Huthig, Heidelberg, 1980.
7 D. Bucher, *Chromatographia*, 10 (1977) 723.
8 C.-Y. Yang, *Hoppe-Seyler's Z. Physiol. Chem.*, 361 (1980) 1599.
9 T. H. Jupille and J. A. Perry, *J. Amer. Oil Chem. Soc.*, 54 (1976) 179.

Journal of Chromatography, 239 (1982) 259–264
Elsevier Scientific Publishing Company, Amsterdam — Printed in The Netherlands

CHROM. 14,606

Note

Quantitative determination of lecithin and sphingomyelin at nanogram levels by high-performance thin-layer chromatography using fluorescence

Preliminary results

L. ZHOU, H. SHANFIELD* and A. ZLATKIS
University of Houston, Chemistry Department, Houston, TX 77004 (U.S.A.)

The use of inorganic acid vapors to induce fluorescence in a variety of compounds has been recently reported by Zhou *et al.*[1] for high-performance thin-layer chromatographic (HPTLC) use. The potentially high sensitivity of the method was noted, but quantitative separations were not carried out. The work reported here deals with the use of HPTLC, together with HNO_3 vapors as part of a fluorescence-inducing procedure, to carry out quantitative analysis of sphingomyelin (S) and lecithin (L) at nanogram levels.

The choice of HNO_3 as the fluorogenic agent was prompted by the observation that its vapors result in the lowest chromatoplate background, while still giving rise to significant fluorescence in the test compounds of many kinds[1].

Interest in sphingomyelin and lecithin was stimulated in part by observations made by Shanfield *et al.*[2] in which fluorescence was readily induced in these compounds by electrical discharge. In addition, there is the well-known lecithin/sphingomyelin (L/S) ratio as a diagnostic tool for assessing infant respiratory distress syndrome, through amniotic fluid analysis[3]. A recent paper by Blass and Ho[4] reported on a fluorescent visualization technique for lecithin and sphingomyelin arising from the incorporation of a fluorescent dye in the solvent system. They established the applicability of their technique for the visualization and quantitation of microgram amounts of lecithin and sphingomyelin. They also concluded that the detection limits of the fluorophores of these compounds were below 0.1 μg. The intensity of fluorescence was observed to decrease slightly over 12 h and quite dramatically over 24 h (without, however, affecting the L/S ratio).

The procedure utilized in the work to be described here, together with HPTLC, is a practical quantitation technique at the level of tens of nanograms. The limit of detection is *ca.* 3 ng for each compound. Finally, the fluorescence is stable for at least 2 weeks (stored in a closed, opaque container).

EXPERIMENTAL

Compounds, solvents, and nitric acid

The sphingomyelin (from bovine brain, Type 1) and lecithin (from egg yolk) employed in these experiments were obtained from Sigma (St. Louis, MO, U.S.A.).

The sphingomyelin was supplied as a solid and the lecithin as a solution (1 g/10 ml of chloroform–methanol (9:1)). Both were stored below 0°C in the course of these experiments. Solutions of each of these compounds were made with ethanol as solvent to provide the range of concentrations investigated. All solvents utilized in this work were of analytical, spectral, or HPLC grade. Nitric acid vapors were derived at room temperature from standard strength HNO_3 (70%) of analytical grade.

Thin-layer chromatoplates

Quantitative calibration data for sphingomyelin and lecithin were obtained on HPTLC silica gel 60 plates (Merck, Darmstadt, G.F.R.). In order to minimize fluorescent background, heating at 260°C for 4 h prior to use was generally sufficient, a procedure which has been previously described[1]. These same HPTLC chromatoplates were used in experiments where sphingomyelin and lecithin were separated chromatographically.

Test procedures

A series of ethanol solutions of sphingomyelin was made ranging in concentration from 50 mg/l to 1 g/l. These stock solutions were then used to spot heat-treated HPTLC chromatoplates with sphingomyelin in amounts from 3 ng to 200 ng. A similar series of lecithin solutions (in ethanol) was prepared (20 mg/l to 660 mg/l) to spot this compound in similar amounts.

Following solvent evaporation of the spotted compounds at room temperature, the chromatoplates were exposed to HNO_3 vapors (also at room temperature) for 10 min. They were then removed and heated in an oven (air) at 180°C for an additional 10 min. The spots were then scanned at 365 nm with a Zeiss KM3 Scanning Densitometer (Carl Zeiss, New York, NY, U.S.A.) without the use of the microoptic accessory. Both peak signal values and peak area values were recorded and plotted graphically against absolute amounts of each compound.

A sphingomyelin–lecithin mixture (100 ng: 52 ng) was spotted on an HPTLC chromatoplate and developed using dichloromethane–ethanol–water (100:25:3) solvent mixture. A continuous development chamber (Regis, Morton Grove, IL, U.S.A.) was utilized for this purpose, and 20 min were required for this separation phase. Subsequently, the plate was subjected to the HNO_3 vapor–air heating cycle previously described, and scanned with the Zeiss instrument.

Excitation spectra were taken of sphingomyelin and lecithin which had been rendered fluorescent by the same procedure. Exciting radiation wavelengths ranged from 260 nm to slightly above 400 nm.

In all the test procedures described, fluorescence was evaluated during the same day of the experiment. However, the measured intensity of fluorescence did not alter noticeably over a period of two weeks of storage in a closed, opaque container.

RESULTS AND DISCUSSION

Quantitative relation between fluorescence and amount

Fig. 1 illustrates the peak signal (mV) *versus* amount of sphingomyelin (365 nm excitation wavelength). The signal increases approximately in linear fashion for sphingomyelin levels from 10 ng to nearly 100 ng. Fig. 2 shows similar data for

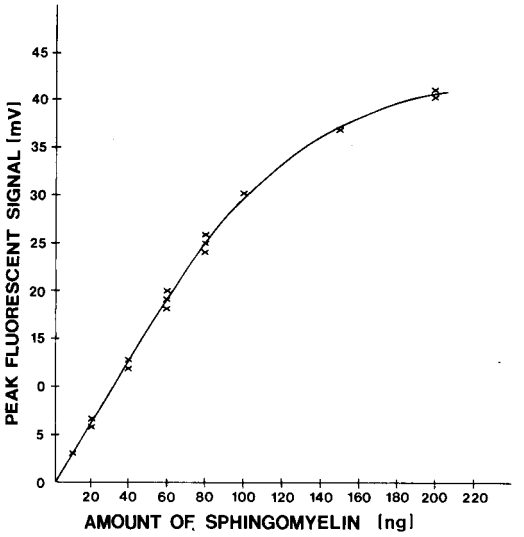

Fig. 1. Quantitative data for sphingomyelin based on peak signal value (mV). Excitation wavelength, 365 nm.

lecithin. Here linearity extends from *ca.* 3 ng to *ca.* 50 ng. Fig. 3 depicts peak area (mV sec) *versus* amount for the same experiments. Here the range of linearity is about the same as for peak signals alone. Thus, for levels of up to a few tens of nanograms, peak signal intensity or peak area appear to be of equal utility from the viewpoint of quantitative linearity. Table I compares a selected L/S ratio to the corresponding ratios of the peak signals obtained at various lecithin (and sphingomyelin) levels. Thus, for the selected ratio of 1.0, the ratio of the corresponding peak signal in-

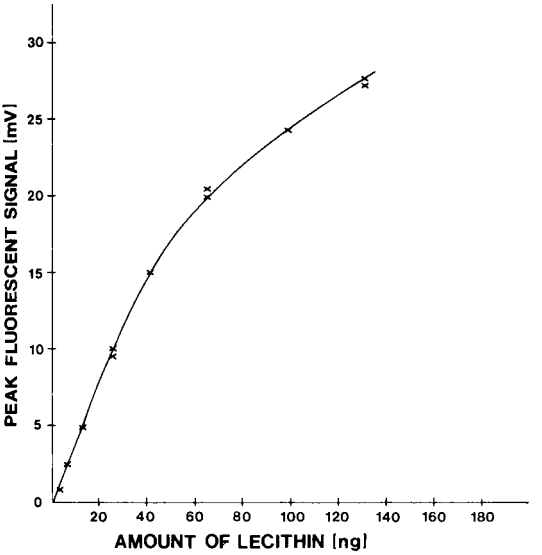

Fig. 2. Quantitative data for lecithin based on peak signal value (mV). Excitation wavelength, 365 nm.

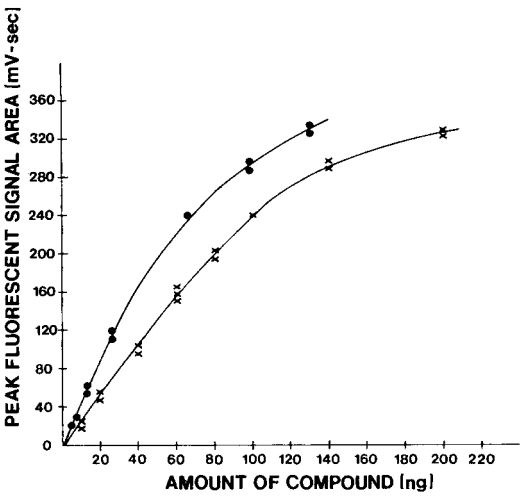

Fig. 3. Quantitative data for lecithin (●) and sphingomyelin (X) based on peak signal area (mV sec). Excitation wavelength, 365 nm.

tensities (taken from the data of Fig. 1) is roughly constant in the linear portion and diminishes slightly in the non-linear regions. Constancy of L/S ratio over a very wide range of L and S amounts would represent an analytical convenience, since the L/S ratio is considered the significant diagnostic factor in antenatal assessment of infant respiratory distress syndrome[3], rather than the absolute levels of lecithin and sphingomyelin.

Chromatographic separation of lecithin and sphingomyelin

Fig. 4 shows the results obtained in scanning (365 nm) an HPTLC chromatoplate on which lecithin and sphingomyelin were separated chromatographically (52 ng lecithin, 100 ng sphingomyelin), using dichloromethane–ethanol–water (100:25:3) solvent system, and rendered fluorescent by the HNO_3 procedure. The L/S ratio obtained from peak heights (0.57) is close to that of the original mixture (0.52). Some impurities appear to be present, adjacent to the sphingomyelin peak.

TABLE I

LECITHIN/SPHINGOMYELIN (L/S) RATIO CALCULATED FROM PEAK FLUORESCENT SIGNAL

Quantitative L/S ratio, 1.0.

Amount of lecithin (= Sphingomyelin) (ng)	*L/S ratio calculated from peak signal values*
20	1.1
40	1.1
60	1.0
80	0.9
100	0.8
120	0.8

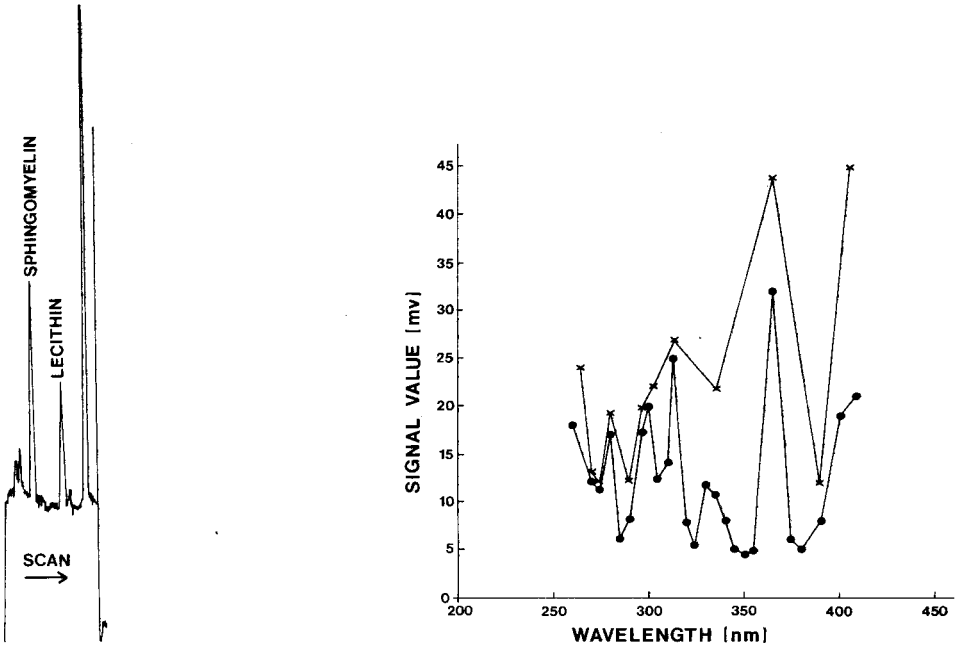

Fig. 4. Results of scanning HPTLC-separated sphingomyelin/lecithin (100 ng/52 ng) after being rendered fluorescent. Scanning wavelength, 365 nm.

Fig. 5. Excitation spectra of fluorescent products of sphingomyelin (X) and lecithin (●).

Excitation spectra of sphingomyelin and lecithin (fluorescent products)

Fig. 5 shows the excitation spectra for the fluorescent products of sphingomyelin and lecithin. For each compound, a distinct strong response occurs near 365 nm, and an additional peak occurs for sphyngomyelin just above 400 nm. Above 414 nm, strong absorption takes place. The peak response at 365 nm for these compounds which have been made fluorescent through the acid vapor treatment, closely duplicates the results obtained by other fluorogenic means previously reported, *e.g.* the NH_4HCO_3–heat cycle reported by Segura and Gotto[5] and the electrical discharge treatment reported by Shanfield *et al.*[2]. This probably reflects a strong commonality of fluorescent chemical structure produced by diverse means.

CONCLUSIONS

We have concluded the following, based on the work described here.

(1) The HNO_3 vapor technique for inducing fluorescence in sphingomyelin and lecithin on HPTLC chromatoplates is a relatively simple and rapid technique, which provides a detection limit of *ca.* 3 ng for each compound.

(2) The fluorescent derivatives of these compounds are stable in intensity for a period of at least two weeks.

(3) A moderately good linear relationship is obtained between either peak fluorescent signal or peak area *versus* amount (up to 100 ng for S and up to 50 ng for

L). The L/S ratio diminishes slightly (compared with the quantitative value) in going from the linear to the non-linear portions of the calibration data.

(4) Excitation spectral data show a peak response at *ca.* 365 nm for each compound, which corresponds closely to results obtained with structurally unrelated compounds, using other fluorescence-inducing procedures.

ACKNOWLEDGEMENT

We thank the Texas Research Institute of Mental Sciences for making available to us the Carl Zeiss KM3 scanning densitometer.

REFERENCES

1 L. Zhou, H. Shanfield, F.-S. Wang and A. Zlatkis, *J. Chromatogr.*, 217 (1981) 341.
2 H. Shanfield, K. Y. Lee and A. J. P. Martin, *J. Chromatogr.*, 142 (1977) 387.
3 L. Gluck, M. V. Kulovich, R. C. Borer and W. N. Keidel, *Amer. J. Obstet. Gynecol.*, 120 (1974) 142.
4 K. G. Blass and C. S. Ho, *J. Chromatogr.*, 208 (1981) 170.
5 R. Segura and A. M. Gotto, Jr., *J. Chromatogr.*, 99 (1974) 643.

Journal of Chromatography, 239 (1982) 265–276
Elsevier Scientific Publishing Company, Amsterdam — Printed in The Netherlands

CHROM. 14,678

AUTOMATED QUALITATIVE AND QUANTITATIVE METABOLIC PROFILING ANALYSIS OF URINARY STEROIDS BY A GAS CHROMATOGRAPHY–MASS SPECTROMETRY–DATA SYSTEM

J. J. VRBANAC
Departments of Biochemistry and Pharmacology and Toxicology, Michigan State University, East Lansing, MI 48824 (U.S.A.)
W. E. BRASELTON, Jr.
Department of Pharmacology and Toxicology, Michigan State University, East Lansing, MI 48824 (U.S.A.)
and
J. F. HOLLAND and C. C. SWEELEY*
Department of Biochemistry, Michigan State University, East Lansing, MI 48824 (U.S.A.)

SUMMARY

A computer system (MSSMET), using methylene unit retention indices for an off-line reverse library search analysis of selected ion chromatograms from gas chromatography–mass spectrometry data, has been applied to the qualitative and quantitative determination of urinary steroids. Several published methods for the isolation and derivatization of urinary steroids were evaluated for reproducibility using fused silica capillary column gas chromatography. Using a procedure that gave the greatest reproducibility, MSSMET analyses of urinary steroids were evaluated with packed (3-m 3% OV-101) and capillary (50-m OV-101 WCOT fused silica) columns. Most urinary steroids could be accurately quantitated using the packed column. However, urinary steroids with similar mass spectra and retention behavior on a packed column (*i.e.*, androsterone and etiocholanolone, or 3α,11β,17α,21-tetrahydroxy-5β-pregnane-20-one and 3α,11β,17α,21-tetrahydroxy-5α-pregnane-20-one) were completely separated using the capillary column and could be reproducibly quantitated with a 2-sec scan cycle time (10–15 data points across a peak) but not with a longer scan cycle time. Overloading was the major problem encountered with the fused silica capillary column.

INTRODUCTION

The concept that individuals have distinct metabolic patterns reflected by the constituents of their biological fluids (*i.e.*, urine, blood, amniotic fluid, cerebrospinal fluid, sweat, etc.) originated with the work of Williams[1]. By utilizing the technique of paper chromatography Williams showed convincingly that the patterns for a variety of compounds found in urine varied greatly from one individual to another but were relatively constant for any given individual. Williams' concept was not employed by others until the late 1960's when liquid and gas chromatographic (GC) techniques had become sufficiently refined for studies of this type. The phrase most often used to describe multicomponent analyses of biological fluids, "metabolic profiling", was

0021-9673/82/0000–0000/$02.75

defined by Horning and Horning[2,3] as "multicomponent GC analyses that define or describe metabolic patterns for a group of metabolically or analytically related metabolites". The Hornings also suggested that "profiles may prove to be useful for characterizing both normal and pathologic states, for studies of drug metabolism, and for human development studies".

Although metabolic profiling analysis of biological mixtures is a relatively new technology, the analytical techniques are well known. They include paper chromatography, thin-layer chromatography, column chromatography (GC) and gas chromatography–mass spectrometry (GC–MS). Of these techniques, the most versatile and useful is GC–MS with computer-assisted analysis of the data (DS). Indeed, most current research in the area of metabolic profiling analysis uses the technique of computer reconstructed ion chromatograms from arrays of complete mass spectra[4].

Metabolic profiling of human urinary steroids has attracted much more attention in the past 10 years, mostly from investigators in Europe, and the volume of literature on this subject is large. Among the more obvious applications of this technique in the steroid field are studies of individuals with defects in steroid metabolism (*i.e.*, Cushing's syndrome, adrenal carcinoma, pituitary tumors, 21-hydroxylase deficiency, 17α-hydroxylase deficiency, etc.) and many examples of steroid profiles have appeared in the literature[5–11]. Steroid metabolic profiles have also been studied in pregnancy[12,13], in newborns and infants[14,15], and in conditions of emotional stress and physical exertion[10]. Steroid metabolic profiles of neutral and acidic steroids have also been obtained for blood, amniotic fluid, bile and feces[16,17].

Metabolic profiling analysis of urinary steroids originated with the work of Gardiner and Horning[18], who demonstrated that most of the major urinary steroids could be separated in a single GC run as the methoxime-trimethylsilyl ether derivatives. The major advances since this time have involved improvements in the methods for isolation of steroids from urine, serum, or tissue[19–24], the use of wall-coated open-tubular (WCOT) glass capillary columns[5–7,25,26], and the use of computer-assisted GC–MS analysis of steroid profiles[27–31].

Automated analysis of steroid profiles by GC–MS–DS involves three stages of analysis: (1) preparation of derivatized samples; (2) GC–MS analysis and (3) computer analysis of the data. Extraction of steroids from urine, serum or tissues can be either general, or specific groups of steroids can be selectively isolated and purified. Introduction of the Amberlite XAD-2 extraction procedure by Bradlow[22] greatly simplified the extraction of polar steroids and steroid conjugates. Various procedures for general extraction of steroids from tissues and body fluids using solids and non-polar solvents have appeared in the literature[19,21,22,24]. Selective isolation procedures for estrogens, 3-keto steroids, synthetic steroids possessing an ethynyl group, free steroids, steroid glucuronides, steroid sulfates and steroid disulfates using column liquid chromatography and solvent extraction procedures have appeared in the literature[23,24,32–35]. Sjovall, Axelson and co-workers have done much of the pioneering research on these purification procedures[23,24,28,33] and on automated analysis using a forward library search technique for the qualitative identification of individual components of mixtures of steroids[23,29,36].

This report concerns the development in our laboratory of a suitable procedure for the analysis of steroids from urine with a previously described GC–MS computer system for automated qualitative and quantitative analysis by a reverse library search technique[37–39].

EXPERIMENTAL

Materials

All solvents were redistilled in glass. Enzymes used were β-glucuronidase from *Helix pomatia* [activity: 62880 Fishman units (F.U.) per vial, with one F.U. defined as that activity which will hydrolyze 1.0 mg of phenolphthalein glucuronide per hour at pH 5.0, 37°C; Calbiochem, La Jolla, CA, U.S.A.]. Amberlite XAD-7 (polystyrene non-ionic adsorbent; Mallinckrodt, Paris, KY, U.S.A.) was washed with ten volumes of methanol, acetone, methanol–distilled water (1:1), ethanol and finally distilled water. O-Methoxyamine hydrochloride and Sylon BTZ [N,O-bis(trimethylsilyl)trifluoroacetamide (BSTFA)–trimethylchlorosilane (TMCS)-trimethylsilylimidazole, 3:2:3] were purchased from Supelco (Bellefonte, PA, U.S.A.). Reference steroids were purchased from Steraloids (Wilton, NH, U.S.A.). Lipidex-5000 was purchased from Packard Instruments (Downers Grove, IL, U.S.A.).

Preparation of standards

Each steroid standard (2–5 mg) was weighed into a 2-dram screw-top vial with a PTFE cap liner. Methanol was then added to make a 1.0 μg/μl solution. Samples which contained undissolved steroids were diluted with an equal volume of dimethylsulfoxide (DMSO), making a 0.5 μg/μl solution. An aliquot (250 μl) of each stock solution (500 μl for those with DMSO added, making a total of 250 μg per sample) was placed in a 10-ml test-tube with a screw-top cap (PTFE-lined) and the solvent was evaporated with a stream of nitrogen at ambient temperature. Methoxime-trimethylsilyl (MO-TMS) derivatives were prepared as follows: 50 μl of a 100 μg/μl solution of O-methoxyamine hydrochloride in dry, redistilled pyridine were added and this mixture was heated at 60°C for 1 h. Following removal of excess reagent under a stream of nitrogen, 250 μl of Sylon BTZ were added and the samples were heated at 80°C for 18 h. Samples were placed in glass capillaries which had previously been sealed at one end and then sealed with a flame. Retention indices (*i.e.*, methylene units) for each MO-TMS derivative were determined on a 25-m SP-2100 wall-coated open tubular capillary (WCOT) column (0.2 mm I.D.) and on a 3-m, 3% OV-101 [Supelcoport 80–100 mesh, 2 mm I.D.] packed column by co-injection of straight-chain saturated hydrocarbons. Each sample was also injected separately to insure that the derivatization procedure was quantitative (*i.e.*, only one peak was observed).

Isolation of steroids

Amberlite XAD-7 was packed in 1.0-cm I.D. glass columns to a height of 4 cm. Each column had a 100-ml reservoir. Columns were washed with 30 ml of distilled water before being used. Urine samples (20 ml each) were pipetted onto the columns. The loaded columns were washed with 2 × 5 ml of distilled water. Steroids were eluted with 3 × 5 ml of absolute ethanol, at a constant flow-rate (0.5–1.0 ml/min). Ethanol was evaporated from the eluate by aspiration using a rotary evaporator in a water-bath at 37°C. A sodium acetate buffer (0.5 *M*, pH 4.55) was added (3 ml, plus 1 ml to wash) and the samples were transferred to small erlenmeyer flasks. Cholesteryl butyrate was added (1 μg/μl; 20 μl per sample) as an internal standard. β-Glucuronidase, derived from mollusk (Calbiochem) by adding 3 ml of distilled water to each vial, was added (300 μl) to each sample. After incubation for 48 h in a 37°C water-

bath, sodium chloride (1.5 g) was added. Liberated steroids and steroid sulfates were extracted by shaking with 25 ml of ethyl acetate for 60 min. The ethyl acetate layer was removed by pipet, and the aqueous phase was re-extracted two more times with 5-ml aliquots of ethyl acetate. The pH of the aqueous phase was adjusted to 1.0 with concentrated HCl and the solution was extracted again with ethyl acetete. The combined organic phases were heated at 45°C for 18 h and then combined with the first extraction phase. The recombined ethyl acetate phase was washed with 2 × 5 ml of 8% aqueous sodium bicarbonate then transferred to a small round-bottom flask (washing the aqueous phase three times with 2-ml aliquots of ethyl acetate). Steroids lost in the aqueous phase were recovered by XAD-7 extraction and elution with ethanol, as described above.

The combined ethyl acetate and ethanol phases were evaporated by aspiration using a rotary evaporator and a water-bath at 37°C. The samples were resuspended in 3 ml of ethanol and transferred to small screw-top test-tubes (washing with 2 × 1 ml ethanol). Samples were then dried under a stream of nitrogen at 60°C, and 50 μl of a solution of O-methoxyamine hydrochloride (100 μg/μl) in dry pyridine, plus 100 μl of dry pyridine, were added to the dry residue. This solution was heated for 60 min at 60°C, excess pyridine was removed under nitrogen at 60°C, 100 μl of Sylon BTZ were added, and the sample was heated for 18 h at 80°C.

Excess silylation reagents and compounds with polarities similar to those of steroids were separated from the steroid fraction on a Lipidex-5000 column (70 × 4 mm) containing hexane–hexamethyldisilazane–pyridine–2,2-methoxypropane (97:1:2:10, v/v). The sample was transferred to the top of the column by adding 400 μl of the solvent, which was also passed through the column. For rapid filtration nitrogen pressure was applied, resulting in a flow of 3 ml/min. Solvent (3.5 ml) was passed through the column to recover the derivatized compounds. Solvents were then evaporated under nitrogen at 60°C and the sample was redissolved in 1 ml of hexane containing 2% BSTFA.

Gas chromatography

Gas chromatography was performed on a Hewlett-Packard 5840A equipped with a split and splitless capillary column injection port and a flame ionization detector. Aliquots (1 μl) of the trimethylsilylation reaction mixture were chromatographed on a SP-2100 wall-coated open tubular (WCOT) fused silica capillary column (25 m × 0.2 mm I.D.). Conditions of analysis were as follows: injection port temperature, 280°C; initial temperature, 180°C; temperature programming at 2°C/min to a final temperature of 280°C; 50 min isothermal period at the end of the run; detection signal attenuation, 1; hydrogen flow, 30 ml/min; and air flow, 200 ml/min; split ratio, 20:1.

Mass spectrometry

Mass spectral data were obtained on an LKB-2091 gas chromatograph–mass spectrometer with a dual Digital Equipment PDP-8e based foreground–background data system[12]. The gas chromatograph contained a coiled glass column (3 m × 2 mm I.D.) packed with 3% OV-101 on Supelcoport (80–100 mesh), a 50-m OV-101 WCOT fused silica capillary column (0.3 mm I.D.) or a 25 m SP-2100 WCOT fused silica capillary column (0.2 mm I.D.). Conditions of operation were as follows: GC oven temperature programming from 180 to 280°C at 2°C/min; ion source temperature,

280°C; GC injection port, 280°C; electron multiplier voltage, 1500 V; scans at 4-sec intervals at scan speed 3 (m/z 50–730) or 2-sec intervals at scan speed 2 (m/z 50–600); accelerating voltage, 3.5 kV; trap current, 50 μA; filament current, approximately 4 A; and ionizing voltage, 70 eV. Calibration of nominal mass was against reference ions of perfluorokerosene and instrumental performance was evaluated each day by inspection of reconstructed mass chromatograms. The GC column was pre-treated by two injections of BSTFA–TMCS silylation mixture at 280°C. An aliquot (0.5 μl) of a mixture of eight straight-chain saturated hydrocarbons (20, 22, 24, 26, 28, 30, 32 and 34 carbon atoms) in hexane was co-injected with each sample. After samples were analyzed under the above conditions, each run was validated by brief manual inspection of a few selected ion chromatograms and the data were then transferred to a PDP 11/40 computer (Digital Equipment) for subsequent analysis and storage on magnetic tape. The PDP 11/40 system consisted of a 16-bit, 124 K-word memory minicomputer with two 1.2 million word removable disks, one CDC-9766 300 Mega byte disk, a seven-track magnetic tape drive, DEC writer, Tektronix 4010 scope display unit, and a Tektronix 4610 hard copy unit.

RESULTS AND DISCUSSION

Various methods for the isolation and derivatization of urinary steroids were investigated for reproducibility. The aim of these investigations was to establish the simplest "general" extraction procedure that would give a high degree of reproducibility. The first procedure we investigated used an XAD-2 extraction, followed by enzymatic hydrolysis and finally extraction of the steroids a second time with XAD-2. Trimethylsilylimidazole was used to derivatize the extracted steroids. We were unable to obtain a reproducible capillary column GC trace with or without a Lipidex-5000 "clean-up" step (see Experimental) using this procedure. Leunissen and Thijssen[19] reported overall recoveries of 90% or better of the radioactivity when human subjects were administered labeled androstenedione, estrone, 3β-hydroxy-5-androstene-17-one (DHEA) and DHEA sulfate. They also reported a high degree of precision, which we have confirmed (Fig. 1). Our investigations have also confirmed that the alkali wash and purification of the silylation mixture are important steps for obtaining reproducible GC chromatograms. The precision of this method was about the same with or without the solvolysis step. However, although we only found very small amounts of liberated steroids in the solvolysis phase in two different urine samples, this step was included in the procedure to minimize the effect of variations in enzyme activity from one batch to another, and because the sulfatases isolated from *Helix pomatia* reportedly are not able to hydrolyze 3α-OH sulfate conjugates in 5α-steroids and 17- and 20-hydroxyl sulfate conjugates[19].

Quantitative metabolic profiling of volatile derivatives of steroids isolated from tissues or body fluids by GC–MS analysis using the repetitive scanning technique can of course be accomplished using packed or capillary columns. Capillary columns offer two distinct advantages over packed columns, increased resolution and decreased sample loss due to adsorption during chromatography. The major disadvantage of capillary columns is the necessity for shorter repetitive scan cycle times to establish a sufficient number of data points in reconstructed mass chromatograms. Quadrupole mass filters offer sufficiently short repetitive scan cycle times and have

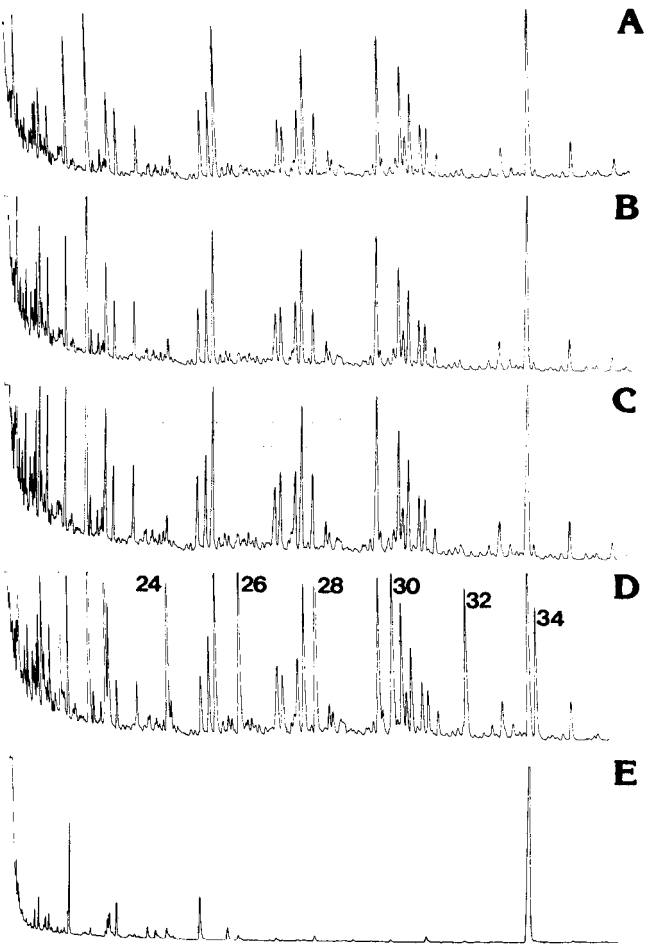

Fig. 1. Urinary steroid metabolic profile of a post-puberal pre-menopausal female, obtained by capillary column GC with flame ionization detection. The top three traces (A, B and C) are for three separate preparations of the same urine sample and demonstrate the overall excellent precision of the method. The lower recordings are of sample plus a mixture of straight-chain hydrocarbons (D), and of a sample blank, using distilled water (E). Conditions of analysis are given in the text.

been used in the analysis of steroid profiles by capillary column GC–MS[30,31]. However, magnetic sector instruments have the disadvantage of slower repetitive scan cycle times. One way to circumvent partially this problem is to shorten the mass range over which the magnet is scanned. For example, Axelson and Sjovall[33] reported using a 4-sec scan cycle time over m/z 250–480 in the analysis of steroids isolated from plasma.

Optimum qualitative and quantitative conditions for automated GC–MS–DS analysis of urinary steroids were established with a 3-m, 3% OV-101 packed column. Although it was known that many of the steroids do not separate satisfactorily by packed column chromatography, selected ion chromatograms were examined for their potential in quantitating poorly-resolved GC peaks. Fig. 2 is a GC–MS total ion

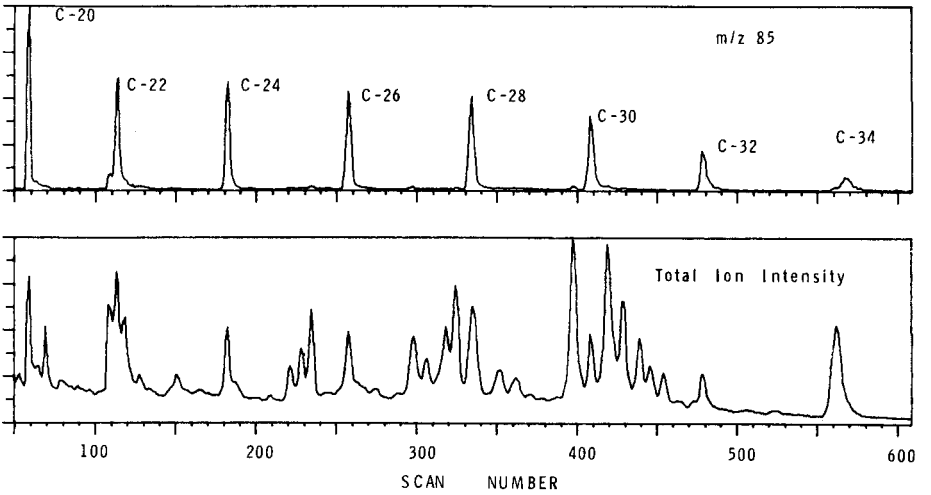

Fig. 2. GC–MS analysis of urinary steroids using a 3-m, 3% OV-101 packed column. Shown are the total ion intensity and the ion chromatogram for *m/z* 85 which shows where the co-injected hydrocarbons elute. Conditions of analysis are given in the text.

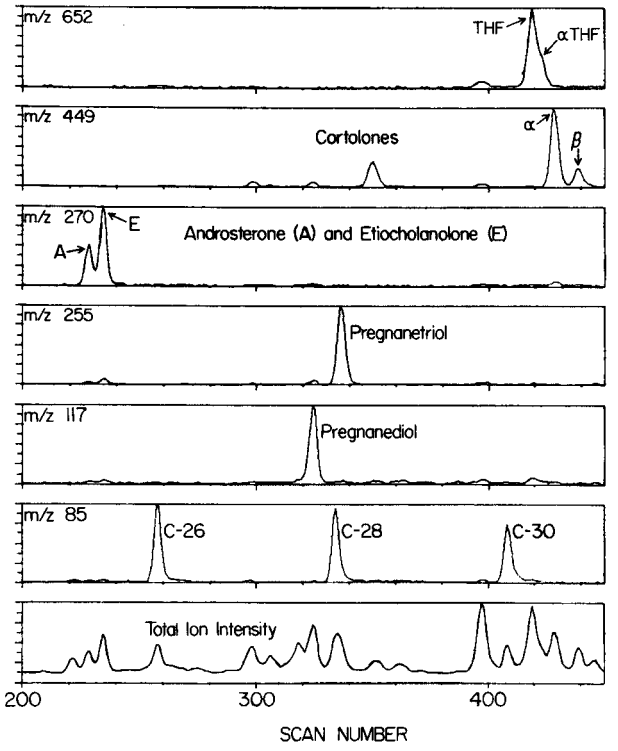

Fig. 3. GC–MS analysis of urinary steroids using a 3-m, 3% OV-101 packed column. Shown are the total ion intensity and an ion chromatogram of a characteristic ion for each of several steroids found in human urine. Conditions of analysis are given in the text.

intensity trace of a sample of urinary steroids separated on the 3-m OV-101 packed column. Conditions of analysis are given in the Experimental. The selected ion chromatogram at *m/z* 85 shows where the co-injected hydrocarbons eluted. Fig. 3 demonstrates that many urinary steroids can be easily quantitated by selected ion chromatography when packed columns are used, while poorly-resolved steroids, which have nearly identical mass spectra, cannot be adequately analyzed by this approach. These results were anticipated from previous work by other investigators.

An alternative approach, using capillary columns for the automated GC–MS–DS analysis of urinary steroids, was then investigated. To quantitate accurately the sharper capillary column peaks the scan cycle time was shortened. Using a 25-m SP-2100 WCOT fused silica capillary column (0.2 mm I.D.) the ability of 1-, 2-, and 3-sec repetitive scan cycle times to reproducibly quantitate the much sharper capillary column peaks using reconstructed ion chromatograms was investigated. Both 1- and 2-sec repetitive scan cycle times gave the desired reproducibility. A 3-sec cycle time was inadequate except when the amount of sample injected was sufficient to overload the column. Fig. 4 shows the total ion intensity obtained using a 2-sec scan cycle time (*m/z* 50–600). The top of Fig. 5 shows the region between C_{24} and C_{30}. Characteristic selected ion chromatograms of the co-injected hydrocarbons, androsterone, etiocholanolone, pregnanediol, pregnanetriol and 3α,17α,21-trihydroxy-5β-pregnane-11,20-dione (THE) are displayed. It is important to understand that these steroids are identified not only by their characteristic ion currents, but also by their characteristic retention indices.

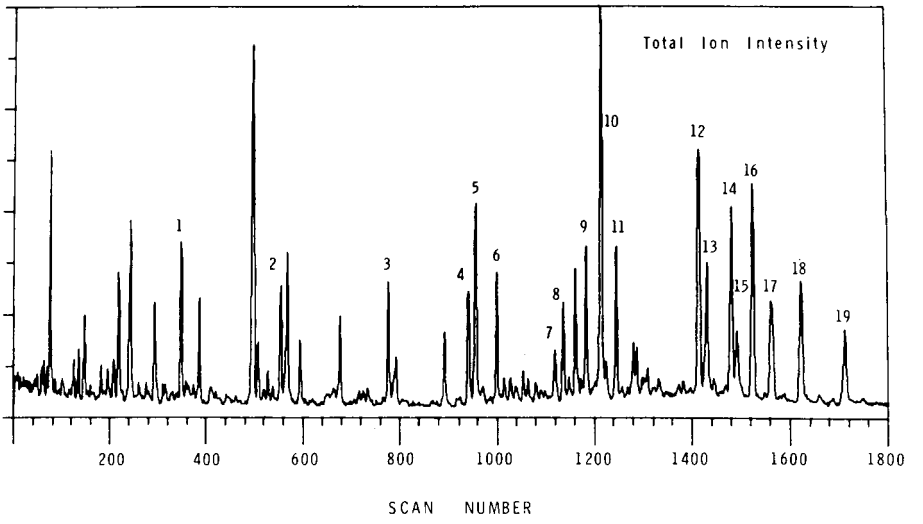

Fig. 4. GC–MS analysis of urinary steroids using a 50-m (0.3 mm I.D.) OV-101 WCOT fused silica capillary column. Shown is the total ion intensity. Three μl of the sample were injected along with 1 μl of a mixture of straight-chain saturated hydrocarbons (0.5 μg/μl). A 5:1 splitting ratio was used. Identity of peaks: 1 = C_{20} hydrocarbon; 2 = C_{22} hydrocarbon; 3 = C_{24} hydrocarbon; 4 = androsterone; 5 = etiocholanolone; 6 = C_{26} hydrocarbon; 7 = 11β-hydroxyandrosterone; 8 = 11β-hydroxyetiocholanolone; 9 = 16α-hydroxydehydroepiandrosterone; 10 = pregnanediol and C_{28} hydrocarbon; 11 = pregnanetriol; 12 = THE; 13 = C_{30} hydrocarbon; 14 = 3α,11β,17α,21-tetrahydroxy-5β-pregnane-20-one (THF); 15 = 3α,11β,17α,21-tetrahydroxy-5α-pregnane-20-one (α-THF); 16 = α-cortolone; 17 = β-cortolone and β-cortol; 18 = α-cortol; 19 = C_{32} hydrocarbon.

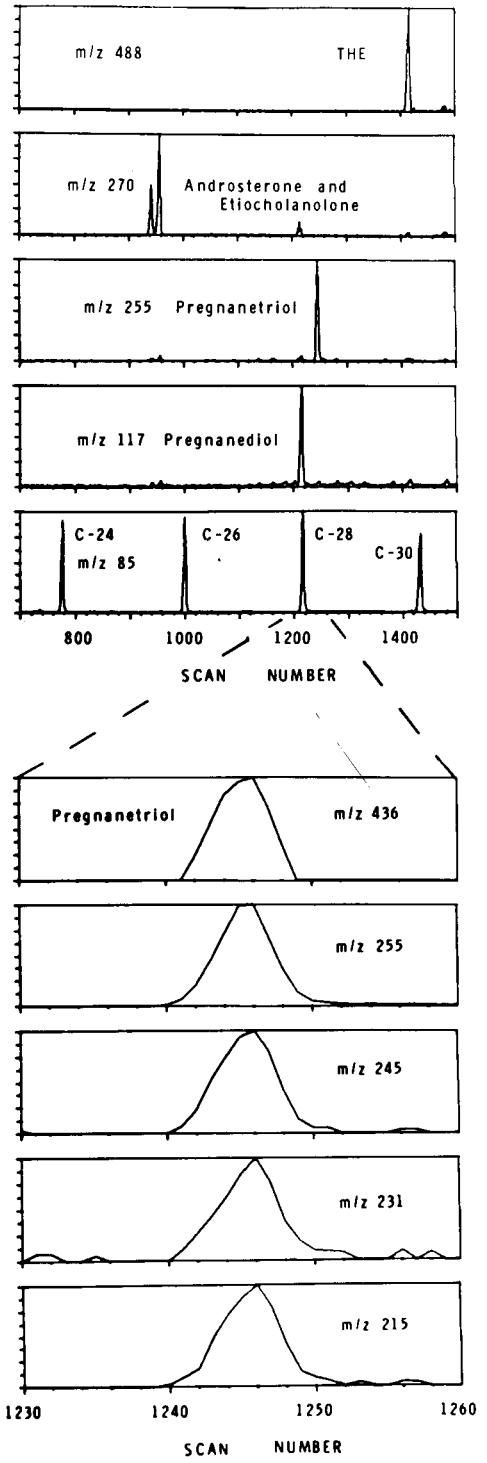

Fig. 5. GC–MS analysis of urinary steroids using a 50-m OV-101 WCOT fused silica capillary column. Shown are characteristic ion chromatograms for the co-injected hydrocarbons, androsterone, etiocholanolone, pregnanediol, pregnanetriol and THE. The bottom graph shows the set of ions for pregnanetriol that the MSSMET program uses to identify and quantitate this compound. Conditions of analysis are given in the text. A *K*-factor (refs. 37 and 39) was determined for pregnanetriol and the amount injected was calculated to be 18 ng.

During the past 5–6 years, a system has been developed at the MSU/NIH Mass Spectrometry Facility for automated simultaneous qualitative and quantitative analysis of complex organic mixtures by GC–MS–computer systems[37,38]. This technique uses methylene unit retention indices for the time dimension and an off-line reverse library search of the data obtained from GC–MS runs for qualitative and quantitative analysis of complex biological mixtures. The system is abbreviated as MSSMET (mass spectral metabolite program).

The bottom of Fig. 5 shows the set of ions for pregnanetriol that the MSSMET program used to identify and quantitate this compound. For each compound searched for by the MSSMET program, one ion that is both characteristic and intense is used for quantitative purposes and the presence and relative intensities of a few other ions produced during fragmentation are used to confirm the identity of the compound in question. Retention index as well as good ion statistics on the designate and confirming ions are crucial in the identification of each compound. In the example shown, m/z 255 is used to quantitate pregnanetriol and the other ions are used in the calculation of a confidence coefficient indicating the presence of this compound.

Reproducibility of the computer-assisted automated metabolic profiling analysis of urinary steroids using capillary column GC–MS is summarized in Table I. Values are the integrated peak areas determined by the MSSMET program of a characteristic ion for each steroid expressed as a percent of the sum of the areas for these five urinary steroids. Data are from four separate GC–MS analyses of the same sample using a 25-m SP-2100 WCOT fused silica capillary column (0.2 mm I.D.). Data are given for the earlier eluting steroids since their GC peaks are much sharper than those occurring later in the GC run (the cortols and the cortolones for example; see Fig. 5) and thus they are the most difficult to quantitate accurately by the repititive scanning technique. The overall precision was 4.8 % for these four separate GC–

TABLE I

PRECISION: CAPILLARY COLUMN GC–MS PROFILING OF URINARY STEROIDS

Values are the integrated peak areas determined by MSSMET of a characteristic ion for each steroid expressed as a percent of the sum of the areas for these five urinary steroids. Data are from four separate GC–MS analyses of the same sample using a 25-m SP-2100 WCOT fused silica capillary column (0.2 mm I.D.).

Steroid	*Run number*				*Mean ± S.D.**
	1	*2*	*3*	*4*	
Androsterone	9.4	8.6	10	10	9.50 ± 0.7
Etiocholanolone	12	12	13	13	12.5 ± 0.6
Pregnanediol	59	59	57	56	57.8 ± 1.5
Pregnanetriol**	14	16	15	15	15.0 ± 0.8
THE	5.4	5.8	5.8	5.9	5.73 ± 0.22
Etio./Andro.***	1.2	1.3	1.3	1.3	1.28 ± 0.05

* The average precision was ±4.8 % (calculated by expressing each S.D. as a % of the mean for the five steroids shown).

** A *K*-factor (refs. 37 and 39) was determined for pregnanetriol and the amount injected corresponds to 18 ng.

*** Ratio of etiocholanolone to androsterone.

MS analyses (calculated by expressing the standard deviation as a percent of the mean and averaging these values for the five steroids shown). Also shown in Table I is the ratio of etiocholanolone to androsterone as determined by MSSMET. Using a *K*-factor (calculated by knowing the ratio of the intensities of ion currents for the internal standard, cholesteryl buryrate, and pregnanetriol for equal amounts of each compound; refs. 37 and 39), the amount of pregnanetriol was calculated to be 18 ng injected (150 ng/ml urine). These results demonstrate that a 2-sec scan cycle time is sufficient to quantitate urinary steroids by capillary column GC–MS using reconstructed ion chromatograms from repetitive scanning data.

The investigations just described have led to the development of an automated GC–MS–DS procedure for reproducible quantitative analysis of complex mixtures of steroids. Important features of the system are the use of capillary column chromatography, a non-mass discriminating mass analyzer and a fully automated reverse library search procedure using methylene unit retention indices and reconstructed mass chromatograms.

ACKNOWLEDGEMENTS

The authors gratefully acknowledge the technical assistance of L. Seymore, M. McPherson, S. Johnson, L. Westover, R. Chapman and M. Martin. This work was supported in part by a research grant from the National Institutes of Health (RR00480).

REFERENCES

1 R. J. Williams, *Univ. Texas Publication*, No. 5109 (1951) 7.
2 E. C. Horning and M. G. Horning, *Clin. Chem.*, 17 (1971) 802.
3 E. C. Horning and M. G. Horning, *J. Chromatogr. Sci.*, 9 (1971) 129.
4 R. A. Hites and K. Biemann, *Anal. Chem.*, 42 (1970) 855.
5 M. Novotny, M. P. Maskarinec, A. T. G. Steverink and R. Farlow, *Anal. Chem.*, 48 (1976) 468.
6 E. C. Horning, M. G. Horning, J. Szafranek, P. Van Hout, A. L. German, J. P. Thenot and C. D. Pfaffenberger, *J. Chromatogr.*, 91 (1974) 367.
7 J. A. Luyten, and G. A. F. M. Rutten, *J. Chromatogr.*, 91 (1974) 393.
8 C. H. L. Shackelton and J. W. Honour, *Clin. Chim. Acta*, 69 (1976) 267.
9 C. D. Pfaffenberger and E. C. Horning, *J. Chromatogr.*, 112 (1975) 581.
10 G. Spiteller, *Pure Appl. Chem.*, 50 (1978) 205.
11 J. W. Honour, J. Tourniaire, E. G. Biglieri and C. H. L. Shackelton, *J. Steroid Biochem.*, 9 (1978) 495.
12 R. J. Begue, M. Moriniere and P. Padieu, *J. Steroid Biochem.*, 9 (1978) 779.
13 H. Eriksson and J.-A. Gustafsson, *Eur. J. Biochem.*, 16 (1970) 268.
14 C. H. L. Shackelton, J.-A. Gustaffsson and J. Sjövall, *Steroids*, 17 (1971) 165.
15 C. H. L. Shackelton and N. F. Taylor, *J. Steroid Biochem.*, 6 (1975) 1393.
16 C. H. L. Shackelton and F. L. Mitchell, *Steroids*, 10 (1967) 359.
17 H. Adlercreutz, F. Martin and B. Lindstrom, *J. Steroid Biochem.*, 9 (1978) 1197.
18 W. L. Gardiner and E. C. Horning, *Biochim. Biophys. Acta*, 115 (1966) 524.
19 W. J. J. Leunissen and J. H. H. Thijssen, *J. Chromatogr.*, 146 (1978) 365.
20 J. P. Thenot and E. C. Horning, *Anal. Lett.*, 5 (1972) 21.
21 C. H. L. Shackelton, J. Sjovall and O. Wisen, *Clin. Chim. Acta*, 27 (1970) 354.
22 H. L. Bradlow, *Steroids*, 11 (1968) 265.
23 J. Sjövall, *J. Steroid Biochem.*, 6 (1975) 227.
24 J. Sjövall and M. Axelson, *J. Steroid Biochem.*, 11 (1979) 129.
25 M. Novotny and A. Zlatkis, *J. Chromatogr. Sci.*, 8 (1970) 347.
26 A. L. German and E. L. Horning, *J. Chromatogr. Sci.*, 11 (1973) 76.

27 J. D. Baty and A. P. Wade, *Anal. Biochem.*, 57 (1974) 27.
28 K. D. R. Setchell, B. Alme, M. Axelson and J. Sjövall, *J. Steroid Biochem.*, 7 (1976) 615.
29 R. Reimendal and J. Sjövall, *Anal. Chem.*, 44 (1972) 21.
30 G. A. De Weerdt, R. Beke, H. Verdievel and F. Barbier, *Biomed. Mass Spectrom.*, 7 (1980) 515.
31 B. F. Maume, C. Millot, D. Mesnier, D. Patouraux, J. Doumas and E. Tomori, *J. Chromatogr.*, 186 (1979) 581.
32 M. Novotny, M. P. Maskarinec, A. T. G. Steverink and R. Farlow, *Anal. Chem.*, 48 (1976) 468.
33 M. Axelson and J. Sjövall, *J. Steroid Biochem.*, 8 (1977) 683.
34 S. L. Cohen, P. Ho, Y. Suzuki and F. E. Alspector, *Steroids*, 32 (1978) 279.
35 B. E. P. Murphy and R. C. D. D'Aux, *J. Steroid Biochem.*, 6 (1975) 233.
36 R. Reimendal and J. Sjövall, *Anal. Chem.*, 45 (1973) 1083.
37 S. C. Gates, M. J. Smisko, C. L. Ashendel, N. D. Young, J. F. Holland and C. C. Sweeley, *Anal. Chem.*, 50 (1978) 433.
38 S. C. Gates, N. Dendramis and C. C. Sweeley, *Clin. Chem.*, 24 (1978) 1674.
39 S. C. Gates, C. C. Sweeley, W. Krivit, D. DeWitt and B. E. Blaisdell, *Clin. Chem.*, 24 (1978) 1680.

Journal of Chromatography, 239 (1982) 277–286
Elsevier Scientific Publishing Company, Amsterdam — Printed in The Netherlands

CHROM. 14,551

SIMULTANEOUS DETERMINATION OF GLYCERYL TRINITRATE AND ITS PRINCIPAL METABOLITES, 1,2- AND 1,3-GLYCERYL DINITRATE, IN PLASMA BY GAS CHROMATOGRAPHY–NEGATIVE ION CHEMICAL IONIZATION–SELECTED ION MONITORING

HIROSHI MIYAZAKI*, MASATAKA ISHIBASHI, YUTAKA HASHIMOTO, GEN'ICHI IDZU and YASUHIKO FURUTA

Research Laboratories of the Pharmaceutical Division, Nippon Kayaku Co., 3-31 Shimo, Kita-ku, Tokyo 115 (Japan)

SUMMARY

A specific and sensitive method for the quantitation of glyceryl trinitrate (GTN) and its principal metabolites, 1,2- and 1,3-glyceryl dinitrate (GDN) in dog plasma by capillary gas chromatography–negative ion chemical ionization–selected ion monitoring using dichloromethane as a reagent gas and the corresponding compounds labelled with stable isotopes as internal standards. The quantitation limits of the method for GTN and the GDNs were 0.1 and 1.0 ng/ml in plasma, respectively. When GTN was administered intravenously to four anaesthetized beagle dogs at a dose of 6 μg/kg·min for 30 min, the plasma levels of GTN and 1,2- and 1,3-GDN reached a maximum at the end-point of infusion and decreased with bi-exponential decay. The half-lives of the α- and β-phases were 0.50 and 4.95 for GTN, 8.10 and 40.6 for 1,2-GDN and 8.50 and 48.5 for 1,3-GDN, respectively.

INTRODUCTION

GTN has been widely used as one of the most effective agents for decreasing peripheral vascular resistance in patients with heart failure and after myoinfarction. Recently, GTN has been tried clinically for the production of controlled hypotension during general anaesthesia in surgical operations because of the rapid appearance of its hypotensive action and its short duration, resulting in easy control of blood pressure. GTN is easily metabolized with endogenous esterase in man, and much attention has been focused on the relationship between arterial blood pressure and the plasma levels of GTN in patients receiving controlled hypotension with GTN.

We developed a specific and precise method for the quantitation of GTN in plasma by GC–NICI–SIM using [$^2H_5$,$^{15}N_3$]GTN as an internal standard, and this method was applied to the investigation of the pharmacokinetics of GTN in patients receiving it during general anaesthesia[1]. Contrary to our expectations, the study indicated that the recovery of the blood pressure to the initial value after the

0021-9673/82/0000–0000/$02.75

withdrawal of the infusion of GTN was relatively slow in some patients although its plasma levels had decreased to non-effective levels. This result led to speculation that this sustained hypotension might be caused by the action of GDNs yielded from GTN, because 1,2- and 1,3-GDNs exhibited weak hypotensive action[2].

Hence it was considered necessary to develop a specific and precise method for the quantitation of 1,2- and 1,3-GDNs in addition to GTN in plasma. This paper deals with the simultaneous determination of GTN, 1,2-GDN and 1,3-GDN in dog plasma by capillary GC–NICI–SIM using the corresponding compounds labelled with stable isotopes as internal standards.

EXPERIMENTAL

Materials

All reagents and solvents were of analytical-reagent grade and were used without further purification.

The GTN used as a standard material was obtained by several washings of the medicinal-grade product with water until nitrate ion, G, GMNs and GDNs were completely removed. GDNs were prepared as follows. GTN was moderately hydrolysed by treatment with 1 *N* sodium hydroxide solution–ethanol (9:1) for 30 min at 15°C. The reaction product was extracted with diethyl ether and the residue was concentrated under reduced pressure. The residue was dissolved in benzene–ethyl acetate (4:1) and chromatographed over a silica gel column with benzene–ethyl acetate (4:1). Each of the GDNs fractions was collected carefully and re-chromatographed over the silica gel column using the same solvent system. The purities of GTN, 1,2-GDN and 1,3-GDN were checked by TLC and HPLC[3,4]. The concentrations of working standard solutions prepared from the above standard materials were determined according to the colorimetric procedure described in Pharmacopoeia Japonica (Editio Nona).

[$^2H_5$,$^{15}N_3$]GTN was synthesized in our Explosives Research Laboratory, using [$^2H_8$]G (Merck Sharp & Dohme Canada, Quebec, Canada) and [^{15}N]nitric acid (Merck Sharp & Dohme Canada)[1]. 1,2- and 1,3-[$^2H_5$,$^{15}N_2$]GDNs were prepared from [$^2H_5$,$^{15}N_3$]GTN according to the method described above.

Sephadex LH-20 (25–100 μm) was obtained from Pharmacia (Uppsala, Sweden) and Kieselgel (70–230 mesh) from Merck (Darmstadt, G.F.R.). Extube 1003 was purchased from Analytichem International (CA, U.S.A.), BSTFA from Tokyo Kasei Kogyo (Tokyo, Japan) and CD_2Cl_2 from Merck Sharp & Dohme Canada.

Gas chromatography–mass spectrometry

A Shimadzu LKB-9000A GC–MS system modified for detection of negative ions and equipped with a data processing system was employed. The columns used were a WCOT glass capillary column coated with SE-30 (25 m × 0.35 mm I.D.; LKB, Stockholm, Sweden) for GTN and a SCOT glass capillary column coated with XE-60 (30 m × 0.30 mm I.D.; Shinwa Kako, Kyoto, Japan) for GDNs. The temperatures of the column oven were maintained at 110°C for GTN and at 150°C for GDNs. The temperature of the injection port and the separator was 180°C and the ionization source was kept at 160°C. The flow-rate of the carrier gas (helium) was 1.5 ml/min. The accelerating voltage was −3.5 kV. The ionization energy and emission current were 500 eV and 170 μA, respectively.

Selected ion monitoring

The following ions were used for monitoring GTN and 1,2- and 1,3-GDNs: *m/z* 262 (GTN), *m/z* 270 ([$^2H_5$,$^{15}N_3$]GTN), *m/z* 289 (1,2- and 1,3-GDN TMS ethers) and *m/z* 296 (1,2- and 1,3-[$^2H_5$,$^{15}N_2$]GDN TMS ethers). The ratios of the peak heights in SIR for ions of *m/z* 262 and 270 and of *m/z* 280 and 296 were calculated and compared with a calibration graph to determine the plasma levels.

Administration of GTN

Intravenous bolus injection. GTN was administrated to three conscious beagle dogs by bolus injection in a dose of 150 μg each. Blood samples were obtained 0.5, 1, 2, 3, 4, 5, 10, 15 and 30 min after the injection.

Intravenous infusion. Four beagle dogs were anaesthetized using pentobarbital and received GTN for 30 min by intravenous infusion at a dose of 6 μg/kg·min. Blood samples were obtained 15 and 30 min after the start-point of infusion and 1, 2, 5, 10, 20, 30, 45, 60 and 90 min after the withdrawal of infusion.

Sample preparation procedure

The blood samples were immediately centrifuged at 1900 *g* for 15 min at 0–4°C and the plasma was collected. An internal standard solution containing 50 ng/ml of [$^2H_5$, $^{15}N_3$]GTN and 100 ng/ml each of 1,2- and 1,3-[$^2H_5$, $^{15}N_2$]GDNs was added to 2 ml of plasma. This procedure was carried out in an ice-bath in order to avoid the enzymatic degradation of GTN in plasma[1].

The plasma sample was transferred directly on to Extube 1003 (solid-phase extraction tube). After standing for 5 min, GTN was eluted with 30 ml of *n*-hexane and subsequently GDNs were eluted with 25 ml of benzene.

GTN fraction. The eluate was transferred to a column (50 × 5 mm I.D.) packed with silica gel in *n*-hexane, washed with 15 ml of *n*-hexane and eluted with benzene–*n*-hexane (1:6). The fraction of 20–50 ml was collected and concentrated to about 0.1–0.2 ml. The residue was dissolved in 0.5 ml of *n*-hexane–chloroform–methanol (10:10:1) and applied to a column (100 × 5 mm I.D.) packed with Sephadex LH-20 in *n*-hexane–chloroform–methanol (10:10:1). The column was washed and eluted with the solvent described above. The fraction of 4–8 ml was collected and concentrated to approximately 5–10 μl. The residue was dissolved in 30 μl of benzene and an aliquot of this solution was subjected to GC–NICI–SIM using a glass capillary column coated with SE-30.

GDN fraction. The benzene eluate was evaporated at 20–25°C in a water-bath under reduced pressure. The residue was dissolved in 5 ml of *n*-hexane in an ultrasonic generator, and the solution was transferred to a column (20 × 6 mm I.D.) packed with silica gel in *n*-hexane. This step was repeated twice. The column was washed with 15 ml of *n*-hexane and eluted with a further 15 ml of *n*-hexane. The eluate was concentrated under reduced pressure and the concentrate was silylated with 20 μl of BSTFA at room temperature. An aliquot of this solution was subjected to GC–NICI–SIM using a glass capillary column coated with XE-60.

RESULTS AND DISCUSSION

GTN is metabolized to 1,2- and 1,3-GDNs; these dinitrates are further metabolized to their GMNs and ultimately to G, and a significant proportion of the GDNs

and GMNs formed is conjugated to glucuronic acid[5]. In order to separate 1,2- and 1,3-GDNs, these two isomers were silylated with BSTFA to convert them into their TMS ether derivatives without degradation. However, both TMS ether derivatives were eluted with almost the same retention times when analysed on packed columns using OV-101, OV-3 and XE-60 as the liquid stationary phase. Subsequently capillary columns coated with SE-30, OV-101, OV-17 and XE-60 were examined to achieve the separation of GDN TMS ether isomers. A baseline separation could be obtained by the use of a capillary column coated with XE-60.

NICI–MS provides negative molecular ions from compounds that possess electron-capturing ability. Contrary to our expectations, however, when methane, isobutane or ammonia was used as a reagent gas in the NICI mode, GTN and GDN TMS ethers gave rise to the negative anion (NO_3^-) as the base peak, and there were no negative ions in the high-mass regions. However, when CH_2Cl_2 was used as the reagent gas, it has been reported that the chlorinated molecular ion $[M + Cl]^-$ was often observed as a prominent ion[6]. Then, NICI–MS of GTN and 1,2- and 1,3-GDN TMS ethers using CH_2Cl_2 was examined.

Fig. 1A shows the NICI mass spectrum of GTN with CH_2Cl_2 as the reagent gas. The chlorinated molecular ion $[M + Cl]^-$ was confirmed by the presence of the doublet ion due to the characteristic intensities of the chlorine atom at *m/z* 262 and 264. The ion due to the addition of nitrate ion produced from the GTN molecule was observed at *m/z* 289. Although the NICI mass spectrum of CH_2Cl_2 was characterized by Cl^-, HCl_2^- and $CH_2Cl_2^-$ ions[7], the expected $[M + HCl_2]^-$ and $[M + CH_2Cl_3]^-$ ions could not be observed. The fragment ions appearing at *m/z* 217 and 235 were considered to be produced by the losses of $NOCl_2$ and HNO_3 from an unidentified ion of $[M + HCl_2]^-$, because when CD_2Cl_2 was used as the reagent gas, the ion of *m/z* 217 was shifted by one mass unit to *m/z* 218, whereas the ion at *m/z* 235 did not shift, and the ions corresponding to those of *m/z* 217 and 235 were observed at *m/z* 224 and 242 in the mass spectrum of $[^2H_5,^{15}N_3]$GTN (Fig. 1B).

Figs. 2A and 3A show the NICI mass spectra of the 1,2- and 1,3-GDN TMS ether derivatives. The mass spectral fragmentation of these derivatives were very

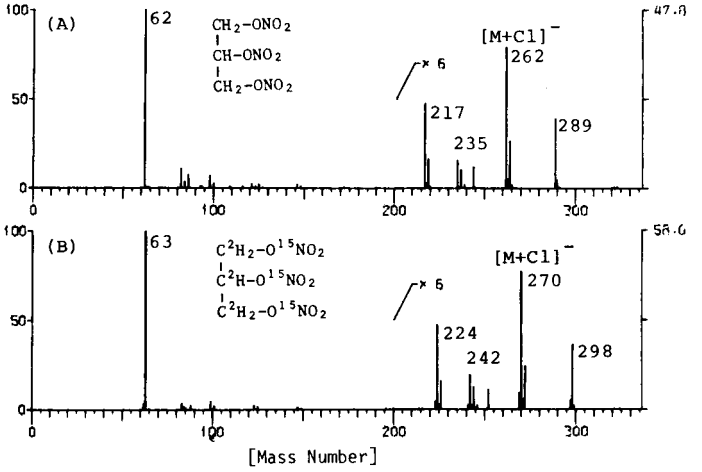

Fig. 1. NICI mass spectra of (A) GTN and (B) $[^2H_5,^{15}N_3]$GTN with dichloromethane as reagent gas.

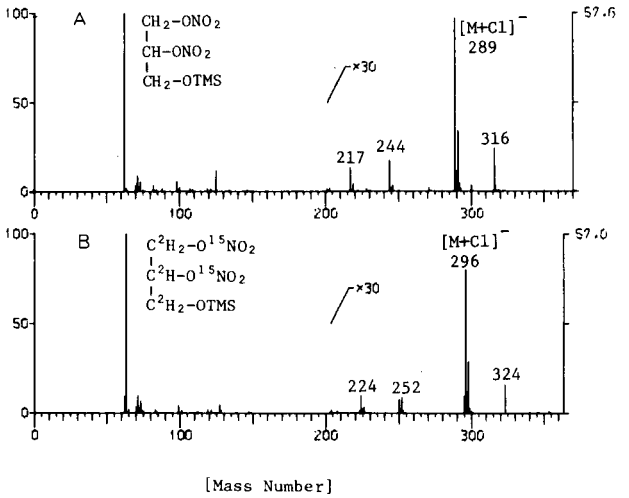

Fig. 2. NICI mass spectra of (A) 1,2-GDN and (B) 1,2-[$^2H_5$, $^{15}N_2$]GDN with dichloromethane as reagent gas.

similar to that of GTN except for a 27 mass unit shift in the ions containing the TMS ether group instead of the NO_3 group in GTN, *i.e.*, the $[M + Cl]^-$ ion was shifted from *m/z* 262 to 289 for GTN and the $[M + NO_3]^-$ ion from *m/z* 289 to 316 for GDNs.

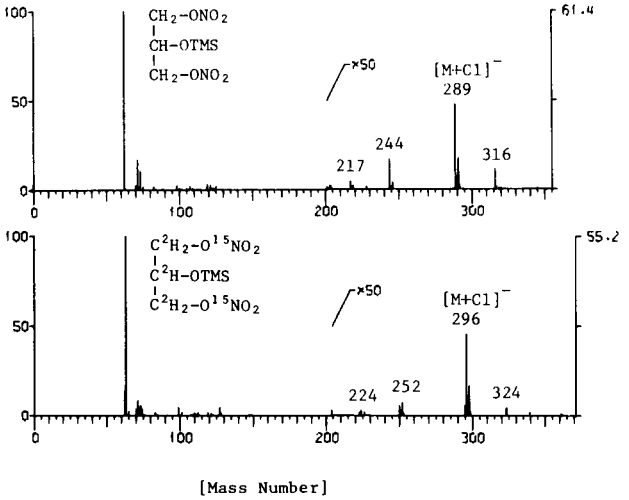

Fig. 3. NICI mass spectra of (A) 1,3-GDN and (B) 1,3-[$^2H_5$,$^{15}N_2$]GDN with dichloromethane as reagent gas.

[$^2H_5$,$^{15}N_3$]GTN and 1,2- and 1,3-[$^2H_5$,$^{15}N_2$]GDNs were synthesized as internal standards for quantitation of GTN and GDNs in plasma by GC–NICI–SIM. As shown in Figs. 1B, 2B and 3B, the NICI mass spectra of these compounds were similar to those of the corresponding non-labelled compounds except for the reasonable mass unit shift in some ions, *i.e.*, the chlorinated molecular ion $[M + Cl]^-$ of [$^2H_5$,$^{15}N_3$]GTN was observed at *m/z* 270 with an 8 mass unit shift from *m/z* 262 in

the non-labelled compound and that of $[^2H_5,^{15}N_2]$GDNs at *m/z* 296 shifted 7 mass units from that of the non-labelled compound at *m/z* 289. The relative abundance of the chlorinated molecular ion cluster agreed well with that calculated from the enrichment of [^{15}N]nitric acid (isotopic purity: 96%), suggesting that no loss of deuterium atom from the carbon–deuterium bond in $[^2H_8]$G took place during nitration. Therefore, the mass spectrometric analysis revealed that the labelled GTN synthesized as an internal standard was a mixture of $[^2H_5,^{15}N_2]$- and $[^2H_5,^{15}N_3]$GTN. Each of labelled 1,2- and 1,3-GDNs was a mixture of $[^2H_5,^{15}N]$- and $[^2H_5,^{15}N_2]$GDN. The isotopical purities of $[^2H_5,^{15}N_3]$GTN and $[^2H_5,^{15}N_2]$GDNs were estimated to be 89.6 and 91.7%, respectively.

To establish the maximum permissible amount of the internal standards added to plasma, an accurate ratio of non-labelled GTN to $[^2H_5,^{15}N_3]$GTN and that of non-labelled GDNs to $[^2H_5,^{15}N_2]$GDNs in them were determined by SIM. The recordings of ion intensities at *m/z* 262 to 270 for GTN and at *m/z* 289 to 296 for GDNs indicated that each of the ratios of non-labelled to labelled compounds was less than 0.1%. This result confirms that it is permissible to add the internal standards to plasma to the extent of 10–50 times the amounts of GTN and GDNs.

When packed columns are used for GTN analysis, GTN should be loaded prior to the analysis in order to prevent losses due to adsorption of GTN on to active sites on the column material[8–10]. On the other hand, the use of capillary columns gave a constant response with ten successive injections of 0.1 ng of GTN without preloading of GTN. This result indicates that capillary columns may have no active sites for adsorption of GTN.

A solid-phase extraction using Extube 1003 made it possible to fractionate effectively GTN and GDNs from the polar metabolites of GTN[1] such as GMNs and glucuronic acid conjugates of GDNs and GMNs. GTN and GDNs adsorbed on the Extube 1003 were eluted with an increase in the polarity of the eluents. Each of the fractions obtained was further purified in order to eliminate interfering substances and to prevent overloading of the capillary column with sample, because the signal-to-noise ratio of quantitation may be affected by coexisting amounts of endogenous

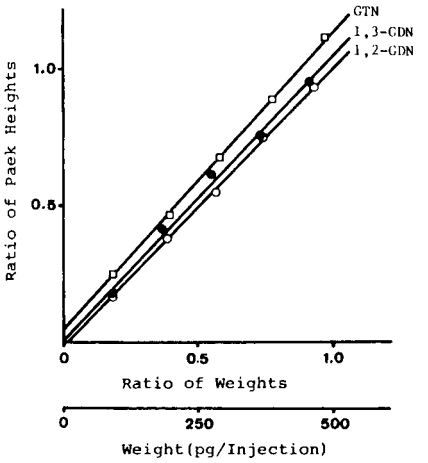

Fig. 4. Calibration graphs for GTN, 1,2-GDN and 1,3-GDN.

substances that have physico-chemical properties similar to those of the compounds of interest.

Fig. 4 shows the calibration graphs for GTN and GDNs using [$^2H_5$,$^{15}N_3$]GTN and [$^2H_5$, $^{15}N_2$]GDNs as internal standards. There were linear relationships between the peak-area ratio and the amount of GTN and GDNs in the range 50–500 pg.

Fig. 5A and B show typical SIRs obtained when 1-μl aliquots of plasma extract containing about (A) 150 pg of GTN and 1 ng of [$^2H_5$,$^{15}N_3$]GTN and (B) 500 pg each of 1,2- and 1,3-GDNs and 2.5 ng each of 1,2- and 1,3-[$^2H_5$, $^{15}N_2$]GDNs were analysed.

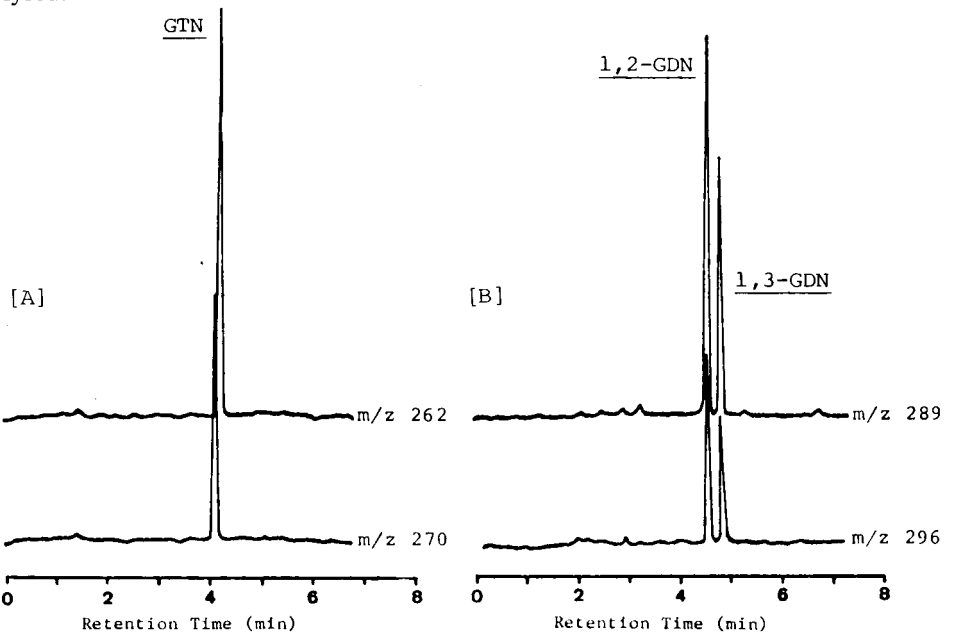

Fig. 5. Selected ion recordings of (A) GTN and (B) GDNs in extract obtained from beagle dog plasma.

Drug-free control plasma gave no interfering peaks at *m/z* 262 and 270 for GTN or at *m/z* 289 and 296 for GDNs, suggesting that the quantitation of GTN and GDNs by this method can be performed without interference from endogenous substances in plasma. Then, known amounts of GTN, 1,2-GDN and 1,3-GDN were added to the drug-free plasma together with the internal standard solution, and then extracted, purified and analysed as described. The analytical data and recoveries are shown in Table I. The recoveries of GTN and GDNs from drug-supplemented plasma were 100.4 ± 0.8% for GTN, 103.1 ± 7.2% for 1,2-GDN and 102.2 ± 8.2% for 1,3-GDN. The data in Table I were submitted to statistical analysis of one-way layout[11,12] in order to divide the total variation into those of sample preparation and measurement of SIM. As shown in the last column in Table I, the estimated standard deviations for sample preparation and SIM in this recovery experiment were calculated to be 0.48 and 0.67 for GTN, 5.73 and 4.60 for 1,2-GDN and 4.96 and 6.90 for 1,3-GDN, respectively. This result indicates that the loss of GTN and GDNs through the process of sample preparation may be compensated for completely by the use of these internal standards.

Fig. 6 shows the plasma level *vs.* time curve observed after intravenous bolus injection of GTN at a dose of 150 μg/kg to three conscious beagle dogs. The plasma

TABLE I

RECOVERY OF GTN AND GDNs FROM DRUG-SUPPLEMENTED DOG PLASMA

Compound	*Recovery (%)*			*Analysis of Variance*	
	X_1	X_2	*Mean ± S.D.*	$\hat{\sigma}_E$*	$\hat{\sigma}_S$**
	101.1	101.9			
	100.2	99.0			
GTN	99.7	100.0	100.4 ± 0.8	0.48	0.67
	100.4	100.6			
	100.9	100.6			
	113.1	107.9			
	102.2	105.9			
1,2-GDN	90.6	97.5	103.1 ± 7.2	5.73	4.60
	98.2	113.6			
	101.8	100.0			
	109.6	118.9			
	92.0	93.9			
1,3-GDN	106.3	97.1	102.2 ± 8.2	4.96	6.90
	98.6	107.0			
	99.8	98.7			

* $\hat{\sigma}_E$ = Estimated value of the standard deviation for the SIM process.
** $\hat{\sigma}_S$ = Estimated value of the standard deviation for the sample preparation process.

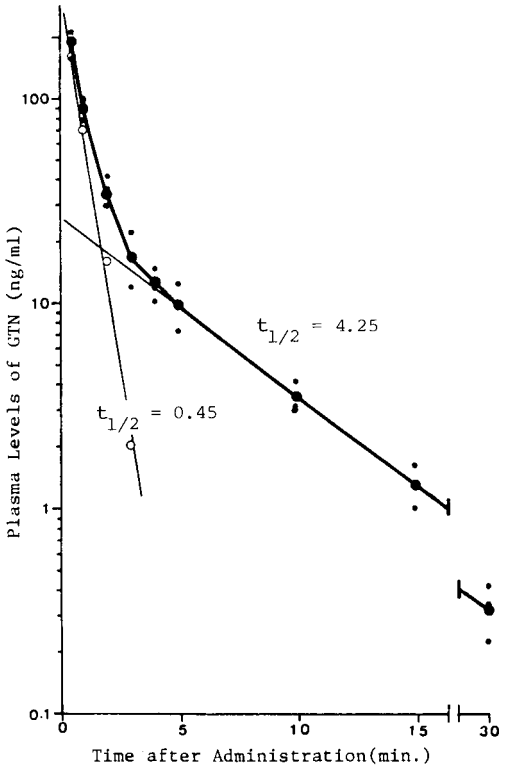

Fig. 6. Plasma GTN levels after intravenous bolus administration of GTN to three conscious beagle dogs at a dose of 150 μg each.

TABLE II

PHARMACOKINETIC PARAMETERS FOR GTN AFTER INTRAVENOUS ADMINISTRATION OF GTN TO THREE CONSCIOUS BEAGLE DOGS AT A DOSE OF 150 μg EACH

α = Elimination rate constant of the alpha phase; β = elimination rate constant of the beta phase; k_{12} = apparent first-order intercompartmental transfer rate constant from the central compartment to the peripheral compartment; k_{21} = apparent first-order intercompartmental transfer rate constant from the peripheral compartment to the central compartment; k_{10} = apparent first-order elimination rate constant from the central compartment; V_1 = apparent volume of the distribution of the central compartment; Cl = clearance.

Patient	α (min^{-1})	β (min^{-1})	k_{12} (min^{-1})	k_{21} (min^{-1})	k_{10} (min^{-1})	V_1 (*l*)	Cl (*l/min*)
A	1.40	0.14	0.53	0.26	0.75	3.63	2.72
B	1.74	0.20	0.46	0.29	1.18	3.37	3.37
C	1.55	0.16	0.60	0.24	0.88	2.99	2.63
Mean	1.56	0.16	0.53	0.26	0.94	3.33	3.11
S.D.	0.17	0.03	0.07	0.03	0.22	0.32	0.75

levels exhibited a bi-exponential decrease and this decay curve was fitted to a two-compartment open model. The pharmacokinetic parameters are listed in Table II. The average and standard deviation of the half-lives of α- and β-phases were 0.45 $\pm$ 0.05 and 4.25 $\pm$ 0.74, respectively. The half-lives of GTN in this study were in good agreement with the results of a pharmacokinetic study on patients receiving controlled hypotension during anaesthesia for surgical operation[1].

Fig. 7 shows the plasma levels of GTN, 1,2-GDN and 1,3-GDN during and after intravenous infusion of GTN (6 μg/kg · min) for 30 min into four anaesthetized beagle dogs. The plasma levels of GTN reached a maximum (57 ng/ml) at the end-point of infusion and decreased rapidly with a bi-exponential decay. The half-lives of the α- and β-phases were 0.50 and 4.95 min, respectively. Constant plasma levels were observed for 45–90 min after withdrawal of the infusion. The half-lives of GTN in intravenous infusion for 30 min were in good agreement with those in intravenous

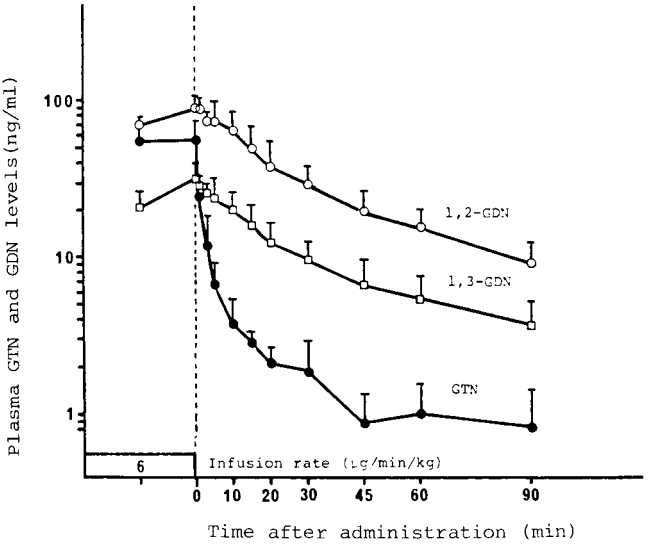

Fig. 7. Plasma levels of GTN and GDNs after intravenous infusion of GTN to four anaesthetized beagle dogs at a dose of 6 μg/kg · min.

bolus injection, suggesting that the GTN plasma levels may decrease at a definite rate regardless of the velocity of administration and/or the administered dose of GTN. The plasma levels of 1,2-GDN and 1,3-GDN also reached a maximum at the end-point of infusion, and the plasma GDN level *vs.* time curves exhibited a bi-exponential decrease. The half-lives of the α- and β-phases were 8.10 and 40.6 min for 1,2-GDN and 8.50 and 48.5 min for 1,3-GDN, respectively.

The relationship between the pharmacokinetics of GTN and GDNs and blood pressure is being investigated, and the results will be reported elsewhere.

ABBREVIATIONS

GTN	Glyceryl trinitrate
1,2-GDN	1,2-Glyceryl dinitrate
1,3-GDN	1,3-Glyceryl dinitrate
GMN	Glyceryl mononitrate
G	Glycerol
TMS	Trimethylsilyl
BSTFA	N,O-Bis(trimethylsilyl)trifluoroacetamide
CH_2Cl_2	Dichloromethane
CD_2Cl_2	[$^2H_2$]Dichloromethane
GC	Gas chromatography
MS	Mass spectrometry
NI	Negative ion
CI	Chemical ionization
SIM	Selected ion monitoring
SIR	Selected ion recording
WCOT	Wall-coated open tubular
SCOT	Support-coated open tubular
TLC	Thin-layer chromatography
HPLC	High-performance liquid chromatography

ACKNOWLEDGEMENT

The authors are grateful to Dr. W. Tanaka, Research Laboratories of the Pharmaceutical Division, Nippon Kayaku Co., for his encouragement throughout this work.

REFERENCES*

1 G. Idzu, M. Ishibashi, H. Miyazaki and K. Yamamoto, *J. Chromatogr.*, submitted for publication.
2 Y. Furuta, T. Takahira and H. Miyazaki, *Abstracts of The Eighth International Congress of Pharmacology, Tokyo, Japan, July, 1981*, Abstr. No. 1921, p. 800.
3 M. C. Crew and F. J. DiCarlo, *J. Chromatogr.*, 35 (1968) 506.
4 W. G. Grouthamel and B. Dorsch, *J. Pharm. Sci.*, 68 (1978) 237.
5 J. R. Hodgson and C.-C. Lee, *Toxicol. Appl. Pharmacol.*, 34 (1975) 449.
6 R. C. Dougherty, J. D. Roberts and H. P. Tannenbaum, *Anal. Chem.*, 47 (1975) 54.
7 H. P. Tannenbaum, J. D. Roberts and R. C. Dougherty, *Anal. Chem.*, 47 (1975) 49.
8 P. W. Armstrong, J. A. Armstrong and G. S. Marks, *Circulation*, 59 (1979) 585.
9 J. Y. Wei and P. R. Reid, *Circulation*, 59 (1979) 588.
10 H. Laufen, F. Scharpf and G. Bartsch, *J. Chromatogr.*, 146 (1978) 457.
11 W. D. Cochran and G. M. Cox, *Experimental Designs*, Wiley, New York, 1950.
12 G. Taguchi, *Experimental Designs*, Maruzen Co., Tokyo, 1962.

* *Editor's Note:* For similar work using HPLC and GC see C. C. Wu, T. D. Sokoloski, A. M. Burkman and L. S. Wu, *J. Chromatogr.*, 216 (1981) 239, and C. C. Wu, T. D. Sokoloski, A. M. Burkman, M. F. Blanford and L. S. Wu, *J. Chromatogr.*, 229 (1982) 327.

Journal of Chromatography, 239 (1982) 287–300
Elsevier Scientific Publishing Company, Amsterdam — Printed in The Netherlands

CHROM. 14,659

GAS CHROMATOGRAPHIC–MASS SPECTROMETRIC ANALYSIS OF ENDOGENOUS LEVELS OF ESTRADIOL IN PLASMA AND IN CYTOSOL FROM RAT UTERUS

M. TETSUO, H. ERIKSSON and J. SJÖVALL*
Department of Physiological Chemistry, Karolinska Institutet, S-104 01 Stockholm (Sweden)

SUMMARY

A method that permits the analysis of low levels of estradiol in plasma from women, men and rats and in cytosolic fractions of uterine tissue is described. The samples are extracted with Amberlite XAD-2 and a phenolic fraction is isolated on a lipophilic ion exchanger. Less polar contaminants in this fraction are separated from estradiol on Sephadex LH-20. Estradiol from human plasma can then be analysed by gas chromatography–mass spectrometry (GC–MS) as the trimethylsilyl ether using a capillary column and single ion monitoring of m/z 416. Samples from rat plasma and uterine cytosol require final purification by high-performance liquid chromatography prior to the GC–MS analysis. The approximate detection limits with the GC–MS instrument used were $1 \cdot 10^{-11}$–$2 \cdot 10^{-11}$ moles/l in plasma and $5 \cdot 10^{-11}$ moles/kg in the uterus. Problems in the purification procedures and the specificity and sensitivity of GC–MS analyses are discussed.

INTRODUCTION

Studies of uptake, binding, nuclear translocation and further processing of steroid hormones in target organs require simultaneous analysis of endogenous levels of steroids and their receptors in subcellular compartments. As the hormonal response is elicited by very low concentrations of steroids, highly sensitive and specific methods are needed for the analysis. At present, gas chromatography–mass spectrometry (GC–MS) and immunoassays are the only methods that possess the necessary sensitivity. The specificity of immunoassays at picogram levels is very difficult to prove, and only indirect methods of validation have been used. With GC–MS, positive proof of specificity can be obtained.

In a previous paper[1] we described a simple and relatively rapid GC–MS method for the determination of estrogens in nuclear and cytosolic fractions from rat uterus. Estrogens were isolated and purified on a lipophilic ion exchanger, and an open-tubular glass capillary column was employed in the GC–MS analysis. The method was used to study levels of estradiol in blood and uterine nuclei after injection of estradiol. When it was applied to the analysis of endogenous levels of estradiol in blood and cytosol, the method of purification was found to be insufficient to ensure specificity for all types of samples.

0021-9673/82/0000–0000/$02.75

This study was carried out in order to achieve consistent purity of extracts for GC–MS analysis. Additional steps required for the analysis of estradiol in the phenolic fraction from plasma and cytosol are described. The methods are compatible with previously developed procedures[1,2] and can be applied to different types of biological samples.

EXPERIMENTAL

Glassware, solvents, reagents

All glassware was silanized with 5% dimethyldichlorosilane in toluene. Cleaning was carried out in an ultrasonic bath.

Solvents were of reagent grade and were re-distilled twice in an all-glass system with a 1-m distillation column. Spectroscopic-grade *n*-hexane (Merck, Darmstadt, G.F.R.) was used as supplied. Methanol was purified by addition of 0.4 volumes of 1.4 *M* sodium hydroxide solution in re-distilled water, refluxing for 6–8 h and distillation twice. Hexamethyldisilazane (Fluka, Buchs, Switzerland) and trimethylchlorosilane (Applied Science Labs., State College, PA, U.S.A.) were distilled. Pyridine was refluxed for 3–4 h over calcium hydride and distilled.

To remove non-volatile interfering components formed upon mixing of the reagents, trimethylchlorosilane, hexamethyldisilazane and pyridine were mixed in the proportions 1:2:2 (v/v/v) and heated at 60°C for 30 min. The mixture was then distilled first at 60°C and then at 110°C, small portions of the distillate being discarded at the beginning and before the temperature rise. The distillates collected at the two temperatures were combined and used as the silylating reagent. When kept in a stoppered glass tube in the dark, the reagent was stable for more than 3 months.

Steroids

Unlabelled estradiol, estrone and cholestane were obtained from Steraloids (Wilton, NH, U.S.A.). Ethynylestradiol was a gift from Professor B. Högberg (Leo, Hälsingborg, Sweden). [2,3,6,7(*n*)-^{3}H]Estradiol (85 Ci/mmol) was purchased from New England Nuclear (Boston, MA, U.S.A.) and was purified on a small column of triethylaminohydroxypropyl-Sephadex LH-20 (TEAP-LH-20) and by high-performance liquid chromatography (HPLC) prior to use. Radioactivity was determined in an Minibeta Model 1211 liquid scintillation counter (LKB, Bromma, Sweden) using Instagel (Packard, Downers Grove, IL, U.S.A.) as the scintillation liquid.

Chromatographic materials

Amberlite XAD-2 (Rohm and Haas, Philadelphia, PA, U.S.A.) was extensively washed with acid, base and solvents and stored in distilled ethanol until required for use[3]. Lipidex 1000 and 5000 (Packard) were washed with aqueous and absolute ethanol at 70°C with stirring and were kept in distilled methanol until required[4]. Octadecylsilane-bonded silica (Sep-Pak C_{18}) was purchased in cartridges from Waters Assoc. (Milford, MA, U.S.A.). To eliminate contaminating compounds, the packing was removed from the cartridge and used in a glass column.

Sulphohydroxypropyl Sephadex LH-20 (SP-LH-20) (ion-exchange capacity 1.46 mequiv./g) was synthesized according to ref. 5 and stored in the Na^+ form in distilled methanol at 4°C. Before use, it was converted into the H^+ form by washing with 0.2 *M* hydrochloric acid in 72% aqueous ethanol.

TEAP-LH-20 (ref. 4) was kindly supplied by Dr. B. Egestad. It was stored in the acetate form at −20°C, and was converted into the OH^- form immediately before use by washing with 0.2 *M* sodium hydroxide in 72% ethanol.

Sephadex LH-20 (Pharmacia, Uppsala, Sweden) was sieved, and the fractions of 100–140 or 140–170 mesh were used. The material was extensively washed with dichloromethane, chloroform–methanol (1:1), ethanol and methanol with stirring at room temperature, and the moist gel was stored at 4°C until needed.

Glass columns of 8 mm I.D., having a solvent reservoir at the top and a water-jacket, were used with Amberlite XAD-2, Lipidex 1000 and Sep-Pak C_{18}. Columns without a water-jacket were used with SP-LH-20 (8 mm I.D.), SP-LH-20 and TEAP-LH-20 (4 mm I.D.). An end-piece of PTFE equipped with a stopcock was pushed into the lower end of the column. A piece of PTFE gauze (70 μm) on the end-piece supported the column bed[2].

High-performance liquid chromatography

HPLC was performed on an LDC instrument (LDC, Riviera Beach, FL, U.S.A.) using a column of LiChrosorb Diol (10 μm, 25 × 0.4 cm I.D.; Merck, Darmstadt, G.F.R.). A Rheodyne injector (Model 7125, Cotati, CA, U.S.A.) with a 1-ml sample loop was used, and the sample was injected with a 500-μl 500 A-RLC syringe (SGE, North Melbourne, Australia).

Gas–liquid chromatography (GLC)

GLC was performed on a Pye 104 gas chromatograph equipped with a flame-ionization detector and housing a 25 m × 0.2 mm I.D. open-tubular glass capillary column coated with SE-30 (ChromaChemie, Västerhaninge, Sweden). An all-glass solid injection system was used[6]. Nitrogen was used as the carrier gas at a pressure of about 50 kPa and the oven temperature was 260°C. Steroids were analysed as trimethylsilyl (TMS) ethers prepared by adding 60 μl of the distilled reagent mixture and heating at 60°C for 30 min. The sample was dried under nitrogen and dissolved in *n*-hexane.

Gas chromatography–mass spectrometry (GC–MS)

A modified LKB 9000 instrument was used with an open-tubular glass capillary column (25 m, SE-30; GC[2] Ltd., Northwich, Cheshire, Great Britain) connected to the ion source via a single-stage adjustable jet separator[2]. The column temperature was about 250°C and the temperatures of molecular separator and ion source were 250 and 290°C, respectively. The energy of the bombarding electrons was 22.5 eV, the ionizing current 120 μA and the accelerating voltage 3.5 kV.

Estradiol was determined by single-ion monitoring using the molecular ion of the derivative at *m/z* 416. Estradiol di-TMS ether, usually 8–16 pg, was used as the external standard and was injected 1–2 min before and after the injection of the sample. In this way the non-specific carrier effect of the biological sample was partly compensated for[1,7]. Cholestane (40–80 ng per injection) was added to all samples and standards, and the height of its peak in the total ion current chromatogram served to correct for differences in the aliquots injected.

Analytical procedures

In all analyses, [^{3}H]estradiol ($10 \cdot 10^3$–$25 \cdot 10^3$ dpm) was added to the samples,

and radioactivity was determined on aliquots of fractions collected during the purification procedure.

Estradiol in rat uterine nuclei. This was analysed as previously described[1].

Estradiol in human and rat plasma. Similar principles were used as in the method described previously[1]. Two adsorbents, Sep-Pak C_{18} and Amberlite XAD-2, were compared for the extraction. Plasma (2–4 ml) was diluted with one volume of physiological saline and sonicated for 5 min. The sample was applied to the columns of Sep-Pak C_{18} (10 × 8 mm) or Amberlite XAD-2 (50 × 8 mm) heated at 64°C (ref. 2) for 5 min by closing the stopcock, and was then percolated through Sep-Pak at a flow rate of 0.5 ml/min, and through Amberlite XAD-2 at a rate of 0.2 ml/min. The columns were rinsed with 10 ml of water at 64°C. The steroids were eluted with 6 ml (Sep-Pak) or 10 ml (Amberlite XAD-2) of methanol at room temperature at a flow rate of 0.5 ml/min. The Amberlite column was washed with 3 ml of *n*-hexane prior to this elution. The methanol eluate was directly passed through SP-LH-20 and TEAP-LH-20 as described previously[1]. The phenolic estrogen fraction from TEAP-LH-20[1] was taken to dryness under a stream of nitrogen. The residue was carefully dissolved in 400 μl of chloroform and 600 μl of *n*-hexane were then added. A 1-ml volume of sample was applied to a column of Sephadex LH-20 (20 × 8 mm, 0.45 g) at a flow-rate of 0.08 ml/min. The column was rinsed with 19 ml of *n*-hexane–chloroform (6:4) at a flow-rate of 0.15 ml/min. Estradiol was then eluted with *n*-hexane–chloroform–methanol (6:4:1) at the same flow-rate. The first 2 ml of the effluent were discarded and the subsequent 6–8 ml were collected and taken to dryness under a stream of nitrogen. In most analyses of human plasma the sample could then be derivatized and analysed by GC–MS.

In analyses of rat plasma, the sample had to be further purified by HPLC. The residue was dissolved in 40 μl of isopropanol by sonication, and 160 μl of *n*-hexane were added and mixed with a vortex mixer. The solution was aspirated into the 500-μl syringe and the tube was rinsed with 100 μl of 20% isopropanol in *n*-hexane, which was also aspirated into the syringe. The sample was injected and elution performed with *n*-hexane–dichloromethane–isopropanol (95:5:10) at a flow-rate of 1.2 ml/min. The volume between 11.4 and 15.3 ml of effluent was collected in a glass-stoppered centrifuge tube. Solvents were removed and the sample was derivatized and analysed by GC–MS.

Between sample applications, the column was washed with 20% methanol in dichloromethane for 10 min at a flow-rate of 3 ml/min, and was then conditioned with the mobile phase for 10 min at the same flow-rate.

Each day and when new batches of solvent were prepared, the retention time and reproducibility were checked by injection of trace amounts of [^{3}H]estradiol. Injection of estradiol for detection by UV absorption should be avoided because of the risk of memory effects in the picogram range.

Estradiol in rat uterine cytosol. A cytoplasmic fraction of uterine tissue was prepared as described previously[1] using a smaller volume of buffer. The steroids in 2–3 ml of the 0.01 *M* Tris–hydrochloric acid buffer (pH 7.9), with EDTA, were extracted with Amberlite XAD-2 or Lipidex 1000. The sample was diluted with one volume of saline and the pH was adjusted to 4 with 0.2 *M* hydrochloric acid. The extraction procedure using Amberlite XAD-2 was the same as for plasma. Lipidex 1000 (1–2 g, 70 × 8 mm in methanol) was washed with 20 ml of water before use. The diluted sample was applied to the gel bed, heated at 64°C for 5 min and passed

through the bed at a flow-rate of about 0.3 ml/min at 64°C. The bed was washed with 10 ml of water at the same flow-rate and temperature, and steroids were eluted with 8 ml of methanol at a flow-rate of 0.4–0.5 ml/min at room temperature. A phenolic fraction was isolated, and estradiol was purified by chromatography on Sephadex LH-20, and by HPLC, as described for plasma.

RESULTS AND DISCUSSION

Estradiol in uterine nuclei

The reproducibility of the method for the purification of estrogens in the nuclear fraction was assessed previously[1]. In the present study, the final recoveries of [^{3}H]estradiol added to the nulcear fractions of human endometrium and rat uterus were 87.3 ± 4.4% (mean ± S.D.; n = 23) and 89.4 ± 2.8% (n = 38), respectively, which is consistent with the previous report[1]. The purity of the samples was sufficient for the analysis of estradiol without interference by other compounds. As previously reported[1], several hundred picograms were present in the nuclear fraction from one rat uterus (Table I). These high concentrations and the relative purity of the isolated nuclei decrease the need for additional chromatographic steps to ensure specificity in the GC–MS analyses.

Estradiol in plasma and cytosol

Extraction and isolation of a phenolic fraction. In comparison with Amberlite XAD-2, Sep-Pak C_{18} has a higher capacity and extraction takes place more rapidly[8,9]. A comparison was made between the two adsorbents, particularly with respect to their influence on subsequent purification steps.

In the first experiments, pooled plasma from men was used. Labelled estradiol was extracted with Sep-Pak C_{18} at different pH values (5.5–10.5). Recoveries were 90.5 ± 3.6% (n = 6) and were not influenced by pH. Losses in the sample effluent, the water wash and on the column were 3.6 ± 0.5, 2.1 ± 0.3 and 2.3 ± 0.1%, respectively. The extracts were purified on SP-LH-20 and TEAP-LH-20 and recoveries in the

TABLE I

AMOUNTS OF ESTRADIOL IN THE NUCLEAR AND CYTOSOLIC FRACTIONS OF UTERI FROM 8 RATS IN DIFFERENT STAGES OF THE ESTRUS CYCLE

Uterine weights varied between 250 and 400 mg.

Rat No.	*Estradiol per uterus (pg)*		*Distribution ratio, nuclei/cytosol*
	Nuclei	*Cytosol*	
1	432	136	3.2
2	434	204	2.1
3	514	190	2.7
4	245	32	7.7
5	340	56	6.1
6	559	129	4.3
7	241	60	4.0
8	400	18	22.2

phenolic fraction from the latter column were 78.0 ± 7.0% (n = 6). However, this fraction was not sufficiently pure for analysis of picogram amounts of estradiol by GC–MS.

After testing the additional purification procedures as described below, attempts were made to quantitate estradiol in plasma from 19 women in different stages of the menstrual cycle. Purification steps consisted of Sep-Pak C_{18} extraction, filtration through the ion exchangers and SP-LH-20. Recoveries of ^{3}H-labelled steroids carried through the entire procedure were low and variable [45.1 ± 12.6% (n = 19)], as were recoveries in the phenolic fraction from TEAP-LH-20 [53.2 ± 5.3% (n = 4)].

These results showed that there were individual differences in recoveries, depending on the source of the sample. To investigate whether losses occurred in the Sep-Pak C_{18} extraction or in subsequent purification steps, five of the previously analysed samples from women were randomly selected for further studies. Recoveries of estradiol in the Sep-Pak C_{18} extraction were 90.0 ± 1.8% (n = 5), whereas recoveries in the phenolic fraction from TEAP-LH-20 were again low and variable [53.4 ± 24.6% (n = 4)]. The missing radioactivity was not found in any of the fractions analysed, and SP-LH-20 or glass surfaces remained the only possible sites of major loss. There appeared to be a loss associated with storage of fractions in methanol.

At this stage of the study, all glassware was not silanized, as the experiments with the pool of plasma from men indicated that this was not necessary. Following the poor results with plasma from women, all glassware was silanized, and a comparison was made between the use of this and untreated glass. Samples were studied that had previously given poor recoveries of estradiol, and both Amberlite XAD-2 and Sep-Pak C_{18} were tested. Large losses occurred with these samples when the glass was not silanized. Thus, using Sep-Pak C_{18} for extraction, recoveries were 31% and 46% for one and 36% and 65% for another sample run in duplicate through the procedure, including Sephadex LH-20. Losses increased with increasing time of storage in methanol (3–7 days). When silanized glass was used, recoveries were 73% and 69% for one sample and 71% and 66% for the other, and losses were not related to storage time (0–3 days). When Amberlite XAD-2 was used instead of Sep-Pak C_{18}, recoveries from the same samples carried through the same procedure were higher, 80% and 83%. The influence of the extraction procedure on the recoveries in subsequent purification steps cannot yet be explained, but based on these results Amberlite XAD-2 is preferred for the extraction of estradiol in plasma.

Studies of the extraction of cytosolic fractions were performed essentially as with plasma. Lipidex 1000 was tested as an alternative adsorbent[10]. The influence of the extraction method on losses in subsequent purification steps was observed as with plasma. Thus, preliminary studies using non-silanized glassware and purification including Sephadex LH-20, showed recoveries of 66, 52 and 37% in the estradiol fraction when Lipidex 1000, Amberlite XAD-2 and Sep-Pak C_{18}, respectively, were used for extraction. Losses in the aqueous phase from Amberlite XAD-2 were large (10.9 and 14.6%), possibly influenced by the high pH of 7.9. When the extractions were carried out at pH 4, losses in the aqueous phases from the columns of Lipidex 1000 and Amberlite XAD-2 were 6.0 ± 5.3% (n = 4) and 3.4 ± 1.1% (n = 4), respectively. One of the samples extracted with Lipidex was responsible for the larger loss with this method.

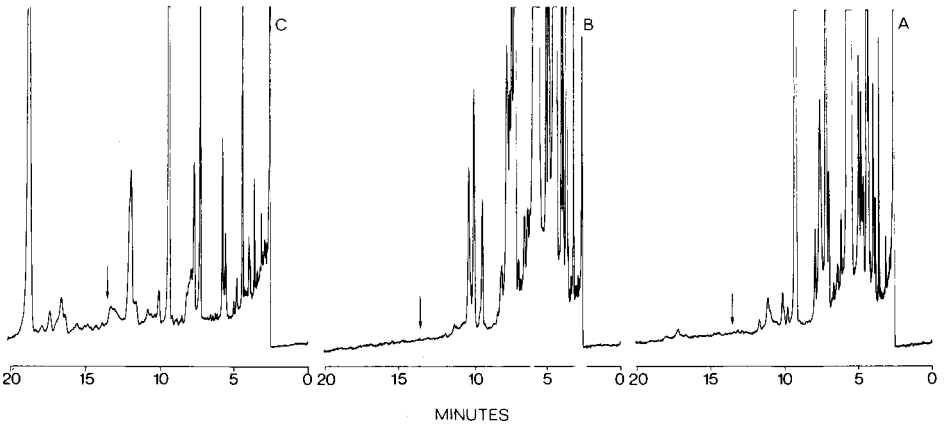

Fig. 1. GLC analyses of fractions collected from the column of Sephadex LH-20 in the purification of 4 ml of pooled plasma from men. A, 0–4 ml; B, 4–8 ml; C, 22.5–27.5 ml (estradiol fraction). Aliquots equivalent to 80 μl of plasma were injected. Cholestane was added to the estradiol fraction (peak of 20 ng at 18.5 min). The retention time of estradiol TMS ether is indicated by an arrow.

Chromatography on Sephadex LH-20. As additional purification of the phenolic fraction was needed for the analysis of low endogenous levels of estradiol, chromatography on Sephadex LH-20 was tested[11,12]. The solvent system and column dimension were optimized in terms of solubility of the sample and minimum loss of radioactivity in the fraction eluted before estradiol. *n*-Hexane–chloroform (6:4) was used for sample application and elution of less polar compounds, and *n*-hexane–chloroform–methanol (6:4:1) for elution of estradiol. Column dimensions of 20 × 8 mm I.D. were sufficient to avoid significant leakage of steroid with the void volume. As the gel swelled more in the second solvent, the column had to be wide and short in order to maintain a suitable flow-rate. To determine the minimum volume for elution with the first solvent, extracts of plasma from rats and humans were applied, and 4-ml fractions were collected. The purity of each fraction was examined by GLC (Fig. 1). Elution with 20 ml of solvent was found to be needed for the removal of less polar impurities. The recovery of estradiol was more than 96% in 4–5 ml of the second solvent. The losses in fractions collected before and after the estradiol fraction were 4.2 ± 2.3% (n = 9) and 1.7 ± 0.5% (n = 13), respectively, in analyses of plasma from women. Analyses of cytosol showed a loss of 1.5 ± 0.5% (n = 13) in the early fraction.

The purity of the estradiol fraction usually permitted solid injection of the equivalent of more than 0.4 ml of plasma (Fig. 2), which was sufficient for studies of basal levels of estradiol in plasma from women (Fig. 3). However, samples from rat plasma and cytosolic fractions required further purification (Fig. 4). Lipidex 5000 was tested in *n*-hexane–chloroform (8:2), but 10.8 ± 4.7% of [^{3}H]estradiol remained on the column following elution of the steroid with *n*-hexane–chloroform–methanol (8:2:0.5). Thus, Lipidex 5000 was inferior to Sephadex LH-20 in this purification step.

High-performance liquid chromatography. HPLC was tested as a final step in the purification procedure. Based on the studies of ethynylestradiol metabolites by Williams and Goldzieher[13], a straight-phase system using a LiChrosorb Diol column

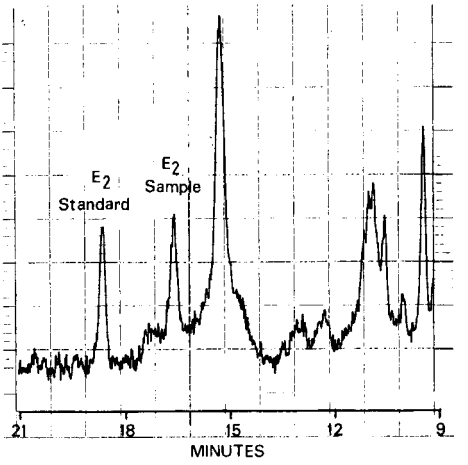

Fig. 2. GC–MS analysis of the estradiol fraction collected from Sephadex LH-20 in the analysis of 4 ml of pooled plasma from men (*cf.*, Fig. 1). The equivalent of 0.6 ml of plasma was injected and *m/z* 416 was monitored. The peaks of estradiol TMS ether from the sample and the standard (8 pg) injected 2 min later are indicated. The temperature of the capillary column was 215°C to permit separation of the steroid from contaminating compounds with shorter retention times.

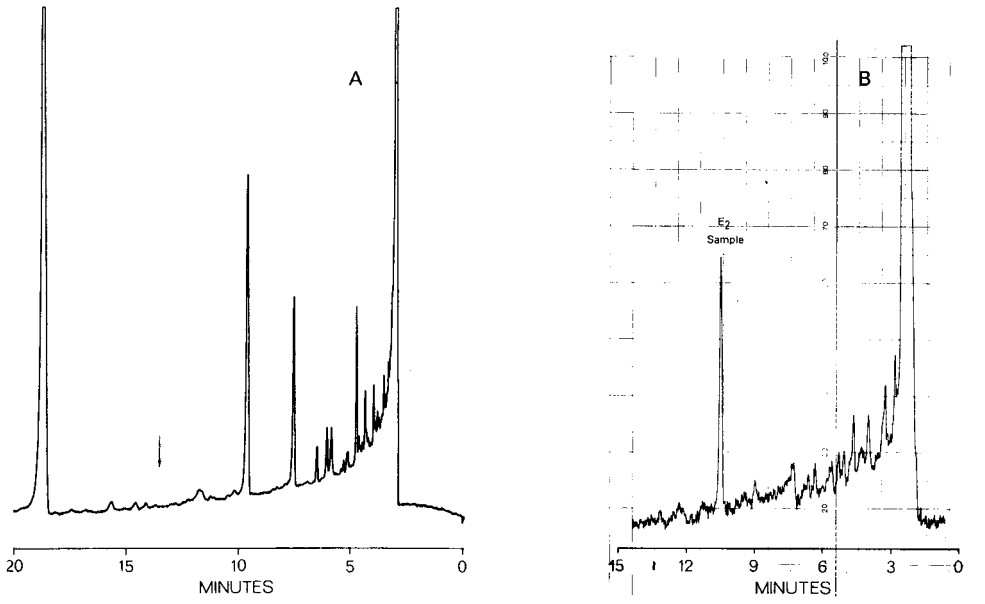

Fig. 3. (A) GLC and (B) GC–MS analyses showing purity of the estradiol fraction from Sephadex LH-20 in the analysis of plasma from a woman. The equivalents of 40 and 160 μl of plasma were injected in A and B, respectively. Cholestane was added and the peak at 19 min in A represents 20 ng. The peak of estradiol TMS ether in B represents about 14 pg.

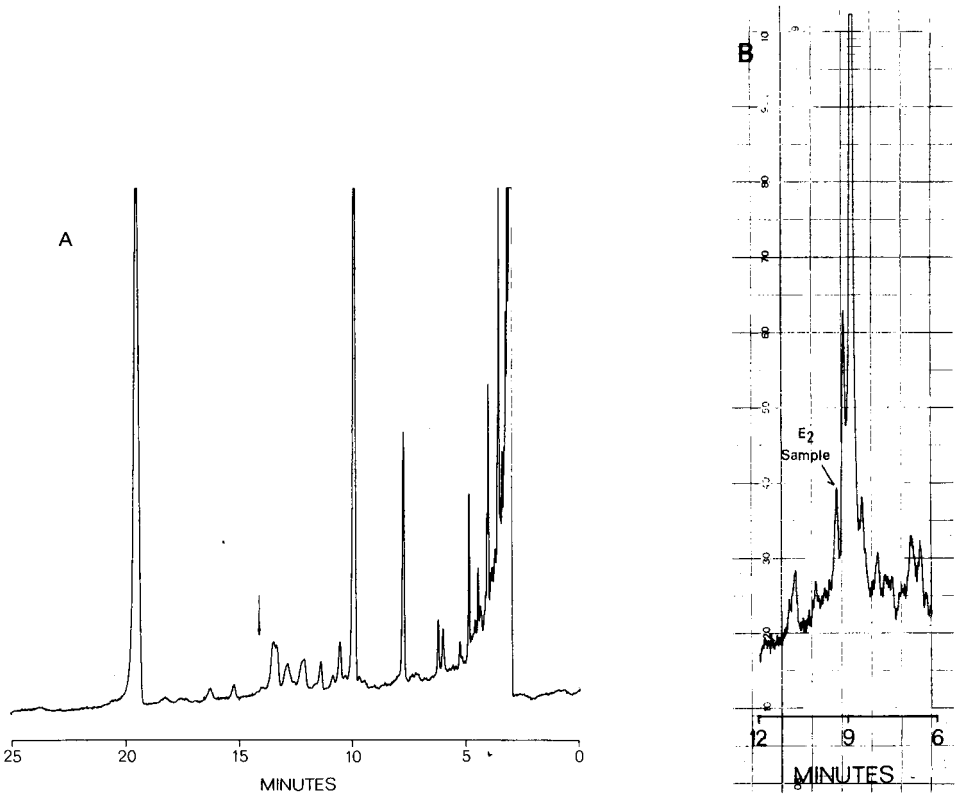

Fig. 4. (A) GLC and (B) GC–MS analyses showing insufficient purity of the estradiol fraction from Sephadex LH-20 in the analysis of a cytosol fraction from rat uterus. The equivalents of 2 and 8% of the uterus were injected in A and B, respectively. Cholestane was added and the peak at about 20 min in A represents 20 ng. The peak at the retention time of estradiol TMS ether in B might represent 6 pg of the compound.

was chosen. Solvent systems were tested for the separation of estrone, estradiol and ethynylestradiol, using UV detection. The solvent mixture *n*-hexane–dichloromethane–isopropanol (95:5:10), was optimal, with an uncorrected retention volume of estradiol of about 14 ml. Removal of polar contaminants remaining on the column required elution with 30 ml of 20% methanol in dichloromethane for 10 min. Another 10 min were required for equilibration with the mobile phase. Thus, samples could be injected at intervals of 40 min.

The volume and polarity of the solvent used for injection were important in obtaining consistent elution volumes and resolution factors. A maximum of 300 µl of 40% isopropanol in *n*-hexane could be used. Experiments with [^{3}H]estradiol showed that the steroid was quantitatively transferred to the column [1.9 ± 0.7% (n = 8) remained in the test tube]. There was no loss of estradiol on the column, 96% and 103% of the injected amount being recovered in two experiments. The degree of purity permitted solid injection of the equivalents of more than 0.2 ml of rat plasma and one third of a uterus without overloading of the capillary column.

The need for purification on Sephadex LH-20 prior to HPLC was tested. Three

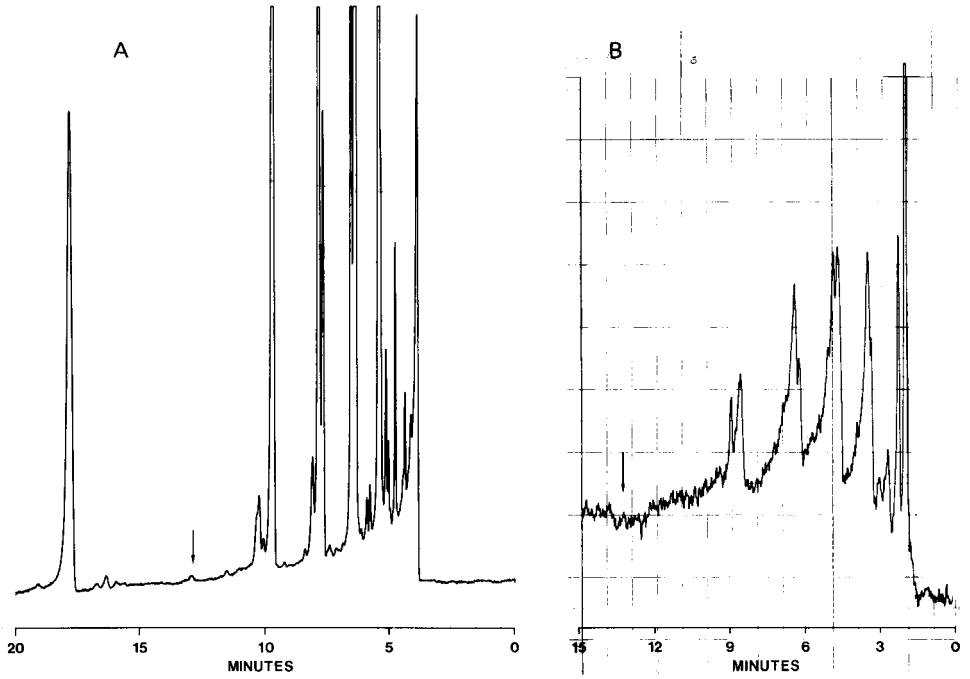

Fig. 5. (A) GLC and (B) GC–MS analyses of the effluent volume corresponding to estradiol, obtained in the HPLC separation of the non-polar contaminants from the Sephadex LH-20 column. The wide tailing peaks in B are presumably due to overloading with the four main components seen in A, resulting in increasing background from the stationary phase.

phenolic fractions from rat plasma and three from cytosol were separated on Sephadex LH-20 and the non-polar fraction (*i.e.*, before elution of estradiol) was collected. This material was subjected to HPLC and effluent corresponding to an estradiol fraction was collected. The purity of this fraction was evaluated by GLC and single-ion monitoring GC–MS. Peaks in the retention time range of estradiol TMS ether were not seen in the latter analyses but there was a marked rise of the baseline with all samples, particularly those from plasma (Fig. 5). A strong UV absorption of the effluent from the HPLC column also indicated that direct purification of the phenolic fraction from TEAP-LH-20 may lead to overloading of both the HPLC and capillary columns, with resulting rapid deterioration. Thus, purification on Sephadex LH-20 is recommended, especially when the steroid levels are close to the detection limit of the GC–MS instrument.

Evaluation of the complete method

Based on the studies described above, the original analytical procedure[1] was extended for the analysis of very low levels of estradiol. The method, including fractionation on lipophilic ion exchangers, Sephadex LH-20 and HPLC, was assessed by analysis of samples of rat plasma to which [^{3}H]estradiol was added. The final recoveries were 59.2 $\pm$ 8.9% in 12 experiments. The purity of the sample permitted the analysis of low endogenous levels of estradiol (Figs. 6 and 7). The detection limit was estimated to be 4–5 pg/ml, *i.e.*, about $1 \cdot 10^{-11}$–$2 \cdot 10^{-11}$ moles/l in plasma.

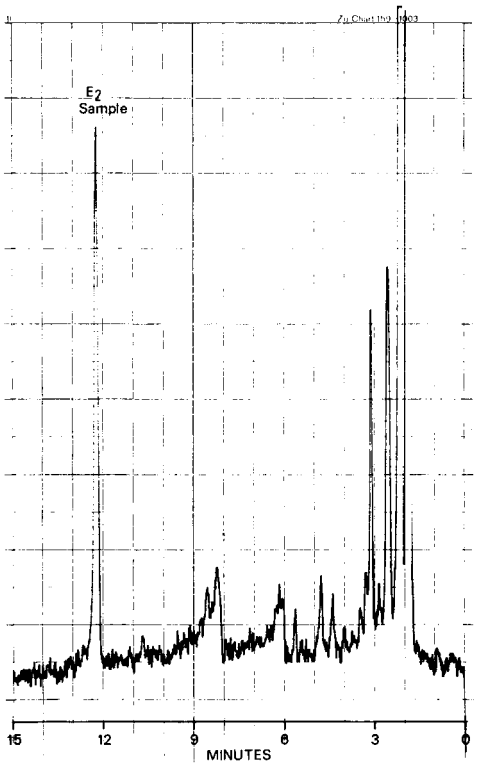

Fig. 6. GC–MS analysis of estradiol in a sample of female rat plasma showing purity of the final HPLC fraction. The equivalent of 0.12 ml of plasma was injected.

The method was tested in the same way for the analysis of estradiol in rat uterine cytosol. Final recoveries of radioactivity in the fraction from the HPLC column were 65.9 ± 13.8% (extraction with Lipidex; $n = 4$) and 74.3 ± 7.6% (extraction with Amberlite XAD-2; $n = 4$). The lower yield and higher standard deviation in the former extraction was caused by one sample.

The purity of samples carried through the entire procedure after extractions with Lipidex 1000 or Amberlite XAD-2 was evaluated by GLC and GC–MS with single-ion monitoring. The purity was sufficiently high (Figs. 8 and 9), and there was no difference between the two extraction procedures in this respect. As shown in Table I, the amount of estradiol in the cytosolic fraction from one rat uterus varied between 13 and 129 pg, which corresponds to concentrations of about $0.1 \cdot 10^{-9}$–$1 \cdot 10^{-9}$ moles/kg in tissue. The detection limit was estimated to be about 5 pg per uterus, *i.e.*, about $5 \cdot 10^{-11}$ moles/kg.

Specificity and sensitivity in steroid analysis

Specificity is the most important property of an analytical method. In this instance it is based on the selective isolation procedure and the use of a capillary column in the GC–MS analysis. Although only molecular ions were monitored, the absence of peaks in the vicinity of the estradiol derivative makes it unlikely that the

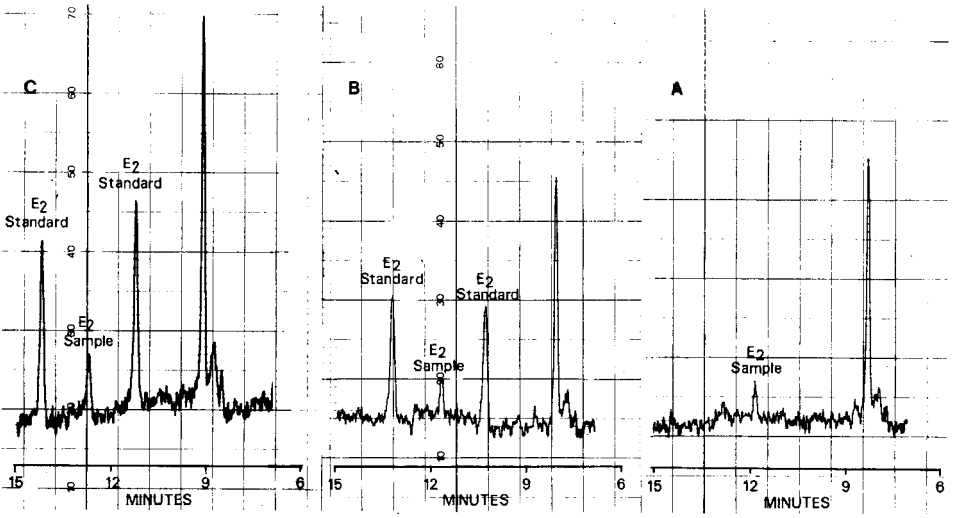

Fig. 7. GC–MS analyses of estradiol in two samples (A + B, and C), of plasma from female rats. The equivalents of 0.12 ml of plasma were injected, A without and B and C with injection of standards (8 pg) 1.5 min before and after injection of the samples.

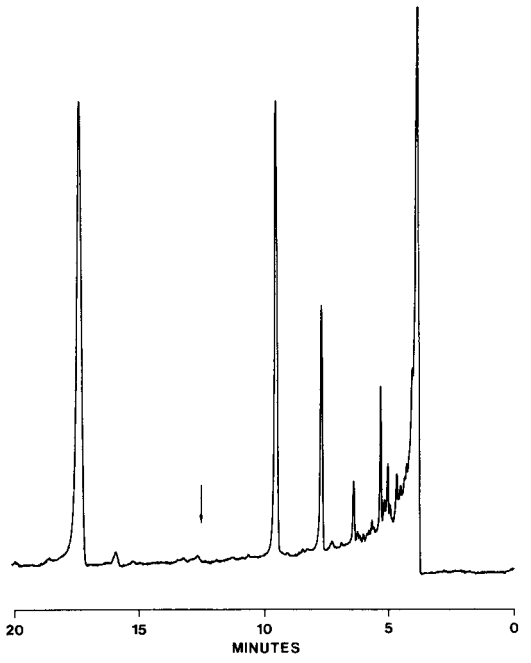

Fig. 8. GLC analysis showing the purity of the final HPLC fraction obtained in the analysis of estradiol in a sample of rat uterine cytosol. The equivalent of 8 % of the uterus was injected. Added cholestane (16 ng) is seen at 17.5 min. The peak at 9.5 min is bis-(2-ethylhexyl) phthalate. The retention time of estradiol TMS ether is indicated by an arrow.

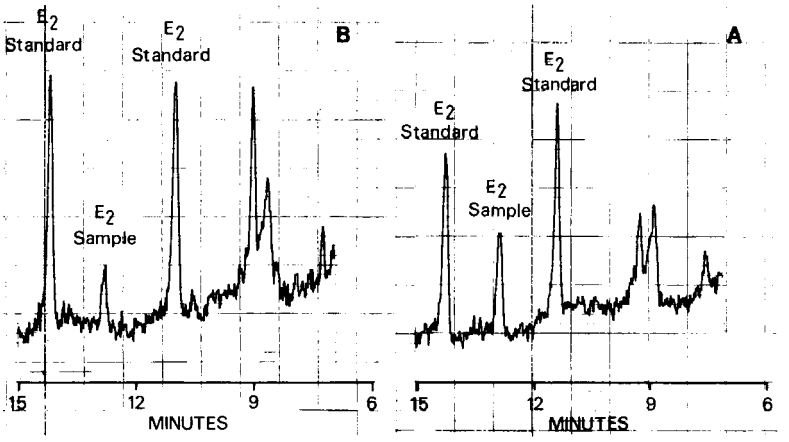

Fig. 9. GC–MS analyses of estradiol in two samples of rat uterine cytosol. The equivalents of 8% (A, same as in Fig. 8) and 12% (B) of the uterus were injected. The standards injected before and after the samples represent 16 pg of estradiol TMS ether.

peak with the appropriate retention time is due to another compound. The use of multiple ion monitoring would increase specificity at the expense of sensitivity. This method has been employed after addition of internal standards labelled with heavy isotopes in analyses of estradiol and other estrogens in plasma[14–19]. Our results indicate that packed columns used in most previous studies may not ensure sufficient specificity in many instances. However, the results of several studies indicate that loss of chromatographic resolution can be compensated for by use of derivatives that give more specific ions at high mass, *e.g.*, heptafluorobutyrates[14,16,18,19]. Another method is to use a high-resolution mass spectrometer as a detector[20–23]. Inherent in all GC–MS methods is the possibility of evaluating the specificity in each individual analysis. Immunoassays do not provide this possibility without additional analyses and considerable loss of sensitivity[24].

The purification has two objectives: to increase specificity and to permit injection of larger aliquots of sample in the capillary column. Contaminating compounds disturb the analyses even when they do not have the same retention time as the steroid being analysed. One effect seems to be on the background from the stationary phase. Thus, elution of 10–20 ng of bis-(2-ethylhexyl) phthalate results in the appearance of a peak with a sharp leading edge and a long tail. As the molecular weight of the compound is 390, this peak is probably due to increased elution of stationary phase which gives an ion of mass 415 with an isotope peak at m/z 416. The same displacement effect is noted with other contaminating compounds (*cf.*, Fig. 5). A general rise of the baseline is also seen with impure samples.

This study is part of a programme aimed at the development of generally applicable methods for the analysis of steroids[2–4] and metabolic studies using stable-isotope labelling[25]. Therefore, internal standards are not added, although this would result in considerably improved accuracy in analyses of individual steroids. This approach makes it important to achieve high recoveries in the purification procedure. The study illustrates the necessity for treating each individual sample as a separate specificity and sensitivity problem. The recovery of estradiol differed between sam-

ples. High recoveries were obtained with the sample of pooled plasma from men, irrespective of whether the glassware was silanized or not. When samples from women, rats and uterine cytosol were analysed, use of silanized glassware was essential for good recoveries in most instances. It is of interest that the losses were highest when extracts obtained with Sep-Pak C_{18} were carried through the purification procedure. Thus, the recovery is a complex function of the nature of the individual sample, the method used for extraction and the materials used in the handling of the extracts.

The combination of group separation by ion exchange[1,2] and isolation of individual steroids by partition chromatography results in highly purified samples. As more material can be analysed, sensitivity is increased. The purification procedure is relatively time consuming, 3 days being required including HPLC. Ten samples can be processed simultaneously. The advantages are that the capillary column is not overloaded and damaged by the sample injections and that a variety of steroids may be analysed with slight modifications of the final steps of the purification procedure.

REFERENCES

1 M. Axelson, J. H. Clark, H. A. Eriksson and J. Sjövall, *J. Steroid Biochem.*, 14 (1981) 1253.
2 M. Axelson and J. Sjövall, *J. Steroid Biochem.*, 8 (1977) 683.
3 K. D. R. Setchell, B. Almé, M. Axelson and J. Sjövall, *J. Steroid Biochem.*, 7 (1976) 615.
4 M. Axelson, B.-L. Sahlberg and J. Sjövall, *J. Chromatogr.*, 224 (1981) 355.
5 M. Axelson and J. Sjövall, *J. Chromatogr.*, 186 (1979) 725.
6 P. M. J. Van den Berg and T. P. H. Cox, *Chromatographia*, 5 (1972) 301.
7 M. Tetsuo, M. Axelson and J. Sjövall, *J. Steroid Biochem.*, 13 (1980) 847.
8 C. H. L. Shackleton and J. O. Whitney, *Clin. Chim. Acta*, 107 (1980) 231.
9 M. Axelson and B.-L. Sahlberg, *Anal. Lett.*, 14 (1981) 771.
10 A. Dyfverman and J. Sjövall, *Anal. Lett.*, B11 (1978) 485.
11 E. Nyström and J. Sjövall, *Ark. Kemi*, 29 (1968) 107.
12 B. P. Lisboa and M. Strassner, *J. Chromatogr.*, 111 (1975) 159.
13 M. C. Williams and J. W. Goldzieher, *Chromatogr. Sci.*, 2 (1979) 395.
14 L. Siekmann, H.-O. Hoppen and H. Breuer, *Z. Anal. Chem.*, 252 (1970) 294.
15 H. Adlercreutz, M. J. Tikkanen and D. H. Hunneman, *J. Steroid Biochem.*, 5 (1974) 211.
16 H. Breuer and L. Siekmann, *J. Steroid Biochem.*, 6 (1975) 685.
17 J. Zamecnik, D. T. Armstrong and K. Green, *Clin. Chem.*, 24 (1978) 627.
18 R. Knuppen, O. Haupt, W. Schramm and H.-O. Hoppen, *J. Steroid Biochem.*, 11 (1979) 153.
19 L. Siekmann, *J. Steroid Biochem.*, 11 (1979) 117.
20 D. Millington, D. A. Jenner, T. Jones and K. Griffiths, *Biochem. J.*, 139 (1974) 473.
21 D. S. Millington, *J. Steroid Biochem.*, 6 (1975) 239.
22 D. S. Millington, *J. Reprod. Fertil.*, 51 (1977) 303.
23 S. J. Gaskell and D. S. Millington, *Biomed. Mass Spectrom.*, 5 (1978) 557.
24 S. Z. Cekan and M. S. de Gomez, *Anal. Lett.*, 12 (1979) 589.
25 T. A. Baillie, T. Curstedt, K. Sjövall and J. Sjövall, *J. Steroid Biochem.*, 13 (1980) 1473.

Journal of Chromatography, 239 (1982) 301–322
Elsevier Scientific Publishing Company, Amsterdam — Printed in The Netherlands

CHROM. 14,532

COMPILATION OF GAS CHROMATOGRAPHIC RETENTION INDICES OF 163 METABOLICALLY IMPORTANT ORGANIC ACIDS, AND THEIR USE IN DETECTION OF PATIENTS WITH ORGANIC ACIDURIAS

KAY TANAKA* and DAVID G. HINE
Department of Human Genetics, Yale University School of Medicine, New Haven, CT 06510 (U.S.A.)

SUMMARY

Gas chromatographic retention indices have been compiled for 163 metabolically important compounds (mostly organic acids) in the form of methylene units, as trimethylsilyl derivatives, on 10% OV-1 and 10% OV-17 columns. Comprehensive references on metabolic diseases that can be diagnosed by detection of these metabolites are cross-indexed to facilitate the use of the methylene-unit list.

The gas chromatographic method, which utilizes extraction of urine with ethyl acetate and trimethylsilylations, is described. Modified methods, one for neutral compounds and one for highly polar organic acids, both of which utilize appropriate ion exchange and lyophilization, are also described. Practical applications of these methods and the use of the methylene-unit list in the diagnosis of eleven patients with various metabolic disorders are also shown.

INTRODUCTION

Since isovaleric acidemia was identified in 1966 by use of gas chromatography (GC) and mass spectrometry (MS) coupled with GC, more than 15 additional organic acidurias (acidemias) have been identified by the use of these advanced analytical techniques[1,2]. These disorders are commonly characterized either by (a) the urinary excretion of extremely large amounts of normal metabolic intermediates that are not usually detectable, or are excreted only in trace amounts in normal urine; or by (b) the excretion of unusual metabolites that are secondarily produced from the accumulated normal intermediates by alternative pathways, owing to a block in the main degradative pathway. These organic acidurias are usually the result of a genetic aberration that results in an enzyme deficiency, but some are due to an inhibition of enzymes by an environmental toxin[3,4] or by a nutritional deficiency[5].

The use of GC and GC–MS has been essential in this development in clinical chemistry during the past 15 years. GC has provided high-efficiency resolution of numerous organic acids that are present in human urines, but unknown compounds, detected by non-specific GC detectors such as the flame-ionization detector, could be identified only by the use of GC–MS, because many of the abnormal metabolites detected in urine from patients with these organic acidurias had never been identified

0021-9673/82/0000–0000/$02.75

previously from natural sources. These include several aliphatic acylglycines such as isovalerylglycine[6], 3-methylcrotonylglycine[7], tiglylglycine[8], and *n*-hexanoylglycine[9], as well as polyfunctional compounds such as methylcitric[10], ethylmalonic[11], 3-hydroxypropionic[12], 3-hydroxyisovaleric[13], and 3-hydroxy-*n*-valeric acids[14].

GC–MS requires expensive instrumentation, and maintenance, operation and data interpretation require highly specialized training and technical expertise. In addition, a computer is almost indispensible for data processing. Thus, screening for organic aciduria has been done in only a few major medical centers, where such instruments and expertise are available.

During the past 15 years most of the metabolic diseases that can be detected by these techniques appear to have been found. The unusual urinary metabolites specific to these diseases have now been well characterized. Therefore, if the retention indices for these organic acids on more than one GC column are well defined, these organic acids may be readily identified by GC alone, eliminating the need for GC–MS and for the technical expertise.

In this paper we report retention indices, in terms of methylene units (MU), on 10% OV-1 and 10% OV-17 columns of trimethylsilyl (TMS) derivatives for 163 compounds of clinical importance. The compounds listed include normal metabolic intermediates and various unusual metabolites known to accumulate in the urine of patients with organic acidurias. Because many of the diagnostic metabolites were not available from commercial sources, they were synthesized, for the most part in our laboratory. With this list of MU values, it is now possible to make diagnoses of the well-defined organic acidurias, and practical organic aciduria screening programs may be implemented in hospitals that are not equipped with GC–MS and a mass spectrometrist.

In this report, we also describe in detail a practical GC method of urinary organic acid analysis, which was designed to be used in such organic aciduria screening programs. This method involves extraction of urine with ethyl acetate, dehydration of the extract residues, trimethylsilylation, and use of the list of retention indices to identify the organic acids. We present some typical chromatograms of urines from patients with organic acidurias who have been diagnosed in our laboratory since we completed this study. Details of this work have recently been published[16,17]. Since then, we have added seven compounds to the list. Procedures for the analysis of very polar compounds and their use for detection of patients with glyceroluria and glyceric aciduria are also included.

MATERIALS AND METHODS

Organic acid standards and other chemicals

The following organic acids were synthesized by H. Ramsdell, B. Baretz and K.T. in our laboratory: 17 acylglycines[15] and ethylhydracrylic, 3-hydroxyisovaleric, 3-hydroxyvaleric, 2-hydroxyisovaleric, 2-hydroxyhexanoic, 2-hydroxyglutaric, 2-hydroxyadipic and methylcitric acids. The following compounds were the gift of other investigators: 3-hydroxyisobutyric acid (Dr. J. Craig, University of California, San Francisco, CA, U.S.A.) and 2-methyl-3-hydroxybutyric acid (Dr. O. Mamer, McGill University, Montreal, Canada). All other organic acids and hydrocarbon standards were procured from appropriate commercial sources. "TriSil-BSA formula P" was purchased from Pierce (Rockford, IL, U.S.A.).

Regular method

Urinary creatinine concentrations were first determined. Specimens were also tested for ketones and ketoacids by the dinitrophenylhydrazine–HCl (DNPH) method. When DNPH was negative, a volume of urine corresponding to 250 μg of creatinine was placed in a 110 × 13 mm screw-cap culture tube, diluted with de-ionized water to 2 ml, and the pH adjusted to 1 by dropwise addition of 6 *N* HCl. The acidified sample was extracted successively with four 2-ml aliquots of ethyl acetate, with vigorous shaking. The organic layers were combined into a second tube and 250 μg pentadecanoic acid (PDA) was added. The combined ethyl acetate layer was dried over anhydrous Na_2SO_4 and evaporated to dryness under a nitrogen stream. The evaporated residue was trimethylsilated with 100 μl TriSil-BSA Formula P (Pierce) at 60°C for 30 min.

When a specimen was positive for DNPH, an amount of the urine corresponding to 250 μg of creatinine was diluted with de-ionized water to 1 ml. After adjusting the pH to 14 with NaOH solution (30%), 1 ml of aqueous hydroxylamine–HCl (2.5%) was added and the sample was heated at 60°C for 30 min to form oximes of α-keto acids. After the sample had cooled to room temperature, the pH was adjusted to 1 by dropwise addition of 6 *N* HCl and the sample was extracted with ethyl acetate as described above.

Methods for very polar compounds

Some compounds with high polarity are of diagnostic significance. These include glycerol in glycerol kinase deficiency and L- and D-glyceric acids in L- and D-glyceric acidurias, respectively. Although these very polar compounds are not well extracted by extraction with ethyl acetate with yields ranging 3 to 8%, the amounts of these compounds which accumulate are extremely large. Therefore, small but significantly increased amounts of the polar compounds can be detected by the ethyl acetate-extraction method, indicating the underlying abnormality. When the increase of glycerol or glyceric acid is indicated, we process the sample by ion-exchange–lyophilization procedures. When a neutral compound such as glycerol is to be quantitated, urine which is equivalant to 250 μg creatinine is passed through a small column of a mixed bed resin (Bio-Rad AG 501) packed in a Pasteur pipette (2 cm height) and eluted with 5 ml water. The eluate is lyophilized and then derivatized with 0.5 ml TriSil-BSA-Formula P. When a polar acidic compound is to be quantitated, the urine specimen containing 250 μg creatinine is passed through a Dowex 50 column and eluted with 5 ml water.

RESULTS

List of methylene units of 163 compounds and its use for identification of urinary metabolites

Table I lists names of compounds and their MU values on 10% OV-1 and on 10% OV-17 columns. In the fourth column of Table I, abbreviated names of diseases in which the particular compound accumulates are listed, with pertinent references. A disease that is underlined indicates that the accompanying compound accumulates greatly and is diagnostic for the particular disease. Diseases not underlined are not specifically linked with that compound. Table II lists the abbreviated names of the diseases.

TABLE I

METHYLENE UNITS OF VARIOUS ORGANIC ACIDS

(I), (II) and (III) after acylglycines indicate mono-, di-, and tri-TMS, respectively.

Compound	*Columns used*		*Diseases to be considered*[§]
	10% OV-1	*10% OV-17*	
Propylene glycol	10.06	10.00	
Phenol	10.39	11.35	Normal, malabsorption[20]
Lactic acid	10.58	10.95	LA[2,21]
Hexanoic acid	10.63	11.24	GA II[22], JVS[3,4]
2-Hydroxyisobutyric acid	10.66	10.74	
Glycolic acid	10.70	11.27	
Oxalic acid	11.16	12.29	
o-Cresol	11.19	12.13	
Glyoxylic acid (oxime)	11.21	11.96	
2-Hydroxybutyric acid	11.30	11.61	LA[23]
p-Cresol	11.38	12.38	Normal, malabsorption[20]
3-Hydroxypropionic acid	11.40	11.94	PA[12,24]
Dipropylacetic acid (valproic acid)	11.47	11.87	Valp[25,26]
Pyruvic acid (oxime)	11.47	12.11	LA[21]
3-Hydroxybutyric acid	11.60	11.94	Ketosis
Heptanoic acid	11.62	12.19	
3-Hydroxyisobutyric acid	11.63	11.96	Ketosis[27,28]
2-Hydroxyisovaleric acid	11.70	11.88	MSUD[17,19,29]
2-Ketobutyric acid (oxime)	11.88	12.46	
Malonic acid	11.97	12.90	
Acetoacetic acid*	12.04	12.82	
2-Methyl-3-hydroxybutyric acid	12.09	12.25	KTD[30,31], PA[24]
Methylmalonic acid	12.12	12.86	MMA[32–34]
2-Ketoisovaleric acid (oxime)	12.13	12.69	MSUD[19,29,35]
3-Hydroxyisovaleric acid	12.14	12.35	MCC[7,36], MCD[17,24], IVA[13], Ketosis[27]
Urea	12.25	13.50	
Benzoic acid	12.28	13.73	Benzoic acid treatment, bacterial growth
2-Ethylhydracrylic acid	12.33	12.63	Normal***[37–39]
3-Hydroxyvaleric acid	12.39	12.70	PA[14,17,24]
2-Hydroxyisocaproic acid	12.41	12.61	
Acetoacetic acid*	12.43	13.18	Ketosis
Acetoacetic acid (oxime)	12.52	13.27	
Acetylglycine (I)[π]	12.53	14.86	
2-Ketovaleric acid (oxime)	12.55	13.05	
Octanoic acid	12.58	13.14	
4-Hydroxyisovaleric acid**	12.60	n.d.	
3-Ketovaleric acid**	12.72	13.44	PA[17,24]
2-Keto-3-methylvaleric acid (L-oxime)	12.73	13.24	MSUD[19,29,35]
Phosphoric acid	12.76	13.46	Normal***
Phenylacetic acid	12.77	14.37	PKU[17,40]
Ethylmalonic acid	12.78	13.48	GA II[22,41], EMA[42], JVS[3,11,39]
2-Hydroxyhexanoic acid	12.84	13.10	

TABLE I *(continued)*

Compound	*Columns used*		*Diseases to be considered*[§]
	10% OV-1	*10% OV-17*	
3-Ketovaleric acid	12.86	13.57	PA[17,24]
2-Keto-3-methylvaleric acid (D-oxime)	12.88	13.33	MSUD[19,29,35]
2-Ketoisocaproic acid (oxime)	12.89	13.34	MSUD[17,19,29,35]
Glycerol	12.92	12.63	GKD[43], HG[44]
Maleic acid	12.93	14.21	
trans-2-Octenoic acid	13.05	13.96	
Succinic acid	13.08	14.02	
Thymol	13.10	13.88	Sample preservative
2-Methylacetoacetic acid**	13.20	–	PA[45]
2-Methyl-3-ketovaleric acid*·**	13.20	13.76	PA[45]
Methylsuccinic acid	13.25	13.98	EMA[42]
2-Ketocaproic acid (oxime)	13.32	13.85	
Acrylylglycine (I)[π]	13.33	15.55	
Propionylglycine (I)[π]	13.34	15.37	PA[17,24,46]
Glyceric acid	13.43	13.60	Gly-L[47], Gly-D[48]
Fumaric acid	13.49	14.03	
2-Methyl-3-ketovaleric acid*·**	13.54	14.03	PA[35]
Nonanoic acid	13.55	14.16	
Acetylglycine (II)[π]	13.57	14.86	
Isobutyrylglycine (I)[π]	13.72	15.60	
Methacrylylglycine (I)[π]	13.88	15.92	
2-Propyl-3-hydroxypentanoic acid**	13.92	14.03	Valp[25,26]
Glutaric acid	13.96	14.87	GA[49,50], GA II[22,4]
Vinylacetylglycine (I)[π]	14.02	16.23	
Acrylylglycine (II)[π]	14.04	15.35	
Isobutyrylglycine (II)[π]	14.08	15.16	
n-Butyrylglycine (I)[π]	14.16	16.24	Hypoglycin intoxication in animals[39,51]
Propionylglycine (II)[π]	14.17	15.37	PA[17,24,46]
2-Propyl-3-oxopentanoic acid**	14.19	14.71	Valp[25,26]
3-Methylglutaric acid	14.19	15.01	Normal[53]
2-Propyl-3-oxopentanoic acid**	14.37	14.71	Valp[25,26]
Methacrylylglycine (II)[π]	14.42	15.52	
2-Methylbutylglycine (I)[π]	14.51	16.41	Hypoglycin intoxication in animals[39,51], PA[24]
Decanoic acid	14.53	15.06	
Isovalerylglycine (I)[π]	14.64	16.56	IVA[2,6]
Vinylacetylglycine (II)[π]	14.71	15.96	
n-Butyrylglycine (II)[π]	14.79	15.88	Hypoglycin intoxication in animals[39,51]
Crotonylglycine (I)[π]	14.82	17.18	
2-Propyl-5-hydroxypentanoic acid**	14.84	15.34	Valp[25,26]
2-Methylbutyrylglycine (II)	14.91	15.80	Hypoglycin intoxication in animals[39,51], PA[24]
Adipic acid	14.99	15.97	GA II[22,41], EMA[42], JVS[3,11,39], CD[52], Ketosis[53], food additive
Malic acid	15.01	15.39	

(Continued on p. 306)

TABLE I *(continued)*

Compound	*Columns used*		*Diseases to be considered*[§]
	10% OV-1	*10% OV-17*	
Salicylic (*o*-hydroxybenzoic) acid	15.05	16.32	SAL
trans-3-Hydromuconic acid	15.06	16.22	
Pyroglutamic acid	15.07	16.80	PGA[54,55], artificial diet[56]
Isovalerylglycine (II)[π]	15.10	16.02	IVA[2,6], GAD[22]
Crotonylglycine (II)[π]	15.13	16.52	
n-Valerylglycine (I)[π]	15.14	17.23	
2-Keto-4-methiol-butyric acid (oxime)	15.14	16.37	
trans-Cinnamic acid	15.21	17.17	
3-Methyladipic acid	15.28	16.20	
Oxalacetic acid (oxime)	15.28	16.14	
3-Methylcrotonylglycine (I)[π]	15.39	17.60	MCC[17], MCD[17,24]
2-Propylglutaric acid**	15.43	16.18	Valp[25,26]
Tiglylglycine (I)[π]	15.49	17.69	MCD[8,24], PA[57]
Tiglylglycine (II)[π]	15.49	16.76	KTD[30]
Undecanoic acid	15.49	16.04	
o-Hydroxyphenylacetic acid	15.59	16.90	
n-Valerylglycine (II)[π]	15.59	16.67	
m-Hydroxybenzoic acid	15.60	16.76	
3-Methylcrotonylglycine (II)[π]	15.63	16.97	MCC[7], MCD[17,24]
2-Hydroxyglutaric acid	15.75	16.32	
Phenyllactic acid	15.80	16.88	PKU[17,40], SBS[17]
Pimelic acid	15.91	16.93	
m-Hydroxyphenylacetic acid	15.98	17.33	
n-Hexanoylglycine (I)[π]	16.11	18.17	EMA[42], GA II[22], JVS[3,4,9]
3-Hydroxy-3-methylglutaric acid	16.12	16.48	HMG[58–60]
2-Furoylglycine (I)[π]	16.17	18.97	Dietary origin[61]
p-Hydroxybenzoic acid	16.22	17.30	
p-Hydroxyphenylacetic acid	16.25	17.66	Tyr[34], SBS[17], normal[62]
3.5-Furandicarboxylic acid	16.26	17.96	Dietary origin[61]
Phenylpyruvic acid (oxime)	16.32	17.81	PKU[17,40]
2-Ketoglutaric acid (oxime)	16.33	17.06	
2-Furoylglycine (II)[π]	16.47	18.33	Dietary origin[61]
n-Hexanoylglycine (II)[π]	16.48	17.48	EMA[42], GA II[22], JVS[3,4,9]
Dodecanoic acid	16.51	16.97	
2-Hydroxyadipic acid	16.83	17.39	KAA[62]
Octanedioic acid	16.91	17.94	EMA[42], GA II[22,41], JVS[3,4,9]
2-Ketoadipic acid (oxime)	17.21	17.98	KAA[63,64]
Orotic acid	17.49	18.59	Orotic aciduria[65]
Tridecanoic acid	17.49	17.99	
trans-Aconitic acid	17.52	18.40	
cis-Aconitic acid	17.54	18.42	
4-Hydroxy-3-methoxybenzoic acid	17.54	19.08	

TABLE I *(continued)*

Compound	*Columns used*		*Diseases to be considered*[§]
	10% OV-1	*10% OV-17*	
Homovanillic acid	17.58	19.32	
Hippuric acid (benzoylglycine) (II)[π]	17.85	20.04	Normal[17]
p-Hydroxymandelic acid	17.85	18.78	
Nonanedioic acid	17.89	18.88	
Hippuric acid (benzoylglycine) (I)[π]	17.96	21.10	Normal[17]
2,4-Dihydroxybenzoic acid	18.22	19.12	
Protocutechuic acid	18.26	19.11	
Citric acid	18.41	18.69	Normal[17]
Isocitric acid	18.41	18.86	
Phenylacetylglycine (II)[π]	18.42	21.74	
Myristic acid	18.45	18.96	
4-Decenedioic acid	18.65	19.96	Hypoglycin intoxication in animals[4,66]
Methylcitric acid	18.66	18.92	PA[10,24]
Phenylacetylglycine (I)[π]	18.66	20.67	
Decanedioic acid	18.90	19.95	GA II[22,41], EMA[42], JVS[3,11,39]
p-Hydroxyphenyllactic acid	19.09	19.93	Tyr[34], Liver failure,
p-Hydroxyphenylpyruvic acid (oxime)	19.43	20.58	SBS[17]
Pentadecanoic acid	19.44	19.95	
o-Hydroxyhippuric acid (III)[π]	19.54	21.01	SAL
Palmitic acid	20.43	20.90	JVS[3,4]
o-Hydroxyhippuric acid (II)[π]	20.47	23.03	SAL
p-Hydroxyphenylpyruvic acid	20.59	21.49	
p-Hydroxyhippuric acid (III)[π]	21.25	22.78	
Traumatic acid	21.31	22.63	
3-Indoleacetic acid	21.74	23.61	
p-Hydroxyphenylacetylglycine (II)[π]	21.82	24.72	
p-Hydroxyphenylacetylglycine (III)[π]	21.82	23.48	
5-Hydroxyindole-3-acetic acid	22.00	25.14	
Linoleic acid	22.00	23.00	
p-Hydroxyhippuric acid (II)[π]	22.02	24.56	
Oleic acid	22.08	22.87	
Stearic acid	22.39	22.90	
Tetradecanedioic acid	22.77	23.76	
Trichloroethanol glucuronide**	22.96	23.61	
Valproic acid glucuronide**	23.86	24.15	Valp[25,26]
Hexadecanedioic acid	>24.00	25.70	
Octadecanedioic acid	>24.00	27.59	

* Two isomers of 3-keto acid–TMS. These are due to *cis* and *trans* forms of enol–TMS.

** Identified in patient's urine using GC–MS.

*** Present in small amount in normal.

[§] See Table II for abbreviations.

[π] (I), (II) and (III) after acylglycines indicate mono-, di-, and tri-TMS, respectively.

As can be seen in Table I, two or more compounds may have an identical or nearly identical MU value on one column, but their MU values differ considerably on the other column, permitting identification of an organic acid with satisfactorily high probability. To identify a peak positively, the MU of the peak should match within

TABLE II

ORGANIC ACIDURIAS WHICH CAN BE DIAGNOSED BY THE USE OF TABLE I

Abbreviation	*Name of disease*	*Abbreviation*	*Name of disease*
CD	Carnitine deficiency	MSUD	Maple syrup urine disease
EMA	Ethylmalonic-adipic aciduria	MCC	3-Methylcrotonyl CoA carboxylase deficiency
GA	Glutaric aciduria	MMA	Methylmalonic acidemia
GA II	Glutaric aciduria type II	MCD	Multiple carboxylase deficiency
GKD	Glycerol kinase deficiency	N	Normal
Gly-D	D-Glyceric aciduria	PA	Propionic acidemia
Gly-L	L-Glyceric aciduria	PKU	Phenylketonuria
HG	Hyperglycerolemia	PGA	Pyroglutamic aciduria (glutathione synthetase deficiency)
HMG	3-Hydroxy-3-methylglutaric aciduria		
IVA	Isovaleric aciduria	SAL	Salicylate treatment
JVS	Jamaican vomiting sickness	SBS	Short bowel syndrome (organic aciduria due to)
KAA	2-Ketoadipic aciduria		
KTD	β-Ketothiolase deficiency	Tyr	Tyrosinemia
LA	Lactic acidosis*	Valp	Valproic acid treatment

* Several diseases due to deficiency of pyruvate carboxylase and those of E_1, E_2 and E_3 of pyruvate dehydrogenase complex are included under lactic acidosis. For details, see ref. 21.

0.03 MU on both columns unless it is overlapped with other compounds. In the event a urinary metabolite is greatly increased, the sample must be diluted with either hexane or pyridine so that the amount of metabolite in 0.5–1.0 μl would be less than 2.5 μg. If the amount of compound injected is greater than 3 μg, the columns may be overloaded and the retention time of the same compound may become larger than that listed in Table I. We noted that even with this precaution, MU of urea (di-TMS) shifted considerably, particularly on the OV-1 column, for unknown reasons. Because some important metabolites such as methylmalonic acid and 3-hydroxyisovaleric acid appear in this region, peaks in this region must be identified carefully. These metabolites can be readily distinguished from urea on the OV-17 column.

Peaks for fatty acids shorter than six carbons are eluted with or before the last solvent peak on the OV-1 column, making determination of MU values of these compounds not possible. However, in diseases such as isovaleric and propionic acidemias, in which short-chain fatty acids accumulate, these acids are converted to unusual secondary metabolites and excreted in the urine. These secondary metabolites are isovalerylglycine[6] and 3-hydroxyisovaleric acid[13] in the former and 3-hydroxypropionic[12], 3-hydroxyvaleric[14], methylcitric acids[12] and tiglylglycine[8] in the latter. These two diseases can be readily diagnosed by identifying these secondary metabolites[2].

The ethyl acetate-extraction method vs. the ion-exchange–lyophilization method

In our routine analysis, we analyze urine samples by the ethyl acetate-extraction method. Although the recovery of very polar compounds such as glyceric acid and glycerol is low, it is adequate to detect them when they are increased. When unusual compounds with high polarity are detected by this method, the urine specimen is then followed by using an appropriate ion exchange (cation exchange or mixed bed) and lyophilization which gives quantitative recovery of very polar compounds.

However, the use of the ion-exchange–lyophilization method is not utilized for routine screening for several reasons. In the cation-exchange method, huge peaks of inorganic acids such as phosphoric acid elute in the region where many important diagnostic metabolites elute (Table I). Also, this procedure is time-consuming.

Analysis of normal urines

We analyzed 50 normal urines on OV-1 and OV-17 columns according to the present method (Table III). In all of the normal chromatograms we found a urea (di-TMS) peak, usually 5–20% of that of PDA. In two samples in group I, there were numerous other small peaks, all of them less than 2% of the size of the PDA peak (Fig. 1A), and including peaks that matched exactly to succinic, adipic, *p*-hydroxyphenylacetic, hippuric, and citric acids. In the chromatograms of the six cases in group II, several peaks were somewhat more prominent than others, including succinic, adipic, *p*-hydroxyphenylacetic, hippuric and citric acids and *p*-cresol (Fig. 1B). These peaks were also detected in small amounts in normal urines from other age groups. In all age groups, compounds detectable in essentially all urines are: succinic, adipic, *p*-hydroxyphenylacetic, hippuric, and citric acids concentrations in each age group of these five compounds are listed in Table III. Other compounds were detected only in some normal urines, and the range of concentration of these compounds and the number of urines in which these compounds were detected are in Table III.

Hippuric acid was detected in virtually all urines tested but the range of its concentration varies greatly, from almost 0 to 1093 μg per mg of creatinine, which is consistent with its presumed exogenous origin (as benzoic acid). Its main source has not been fully elucidated at present.

Many other smaller peaks were detected in normal urines. However, we believe that precise quantitation and unequivocal identification of these very small peaks must be done extensively with a GC–MS–computer system and are beyond the scope of this paper, which is to present a routine screening procedure.

Typical chromatograms of urines from patients with organic acidurias

Typical chromatograms of urines from several patients with different metabolic diseases are shown in this section. Peaks that are diagnostic for these diseases are very large compared with those of other organic acids. Our routine is to analyze the samples first on the OV-1 column. When very large peaks are observed, we then analyze the sample on the OV-17 column. Because the peak size of a compound does not vary significantly on either column, peaks of the same metabolites can be readily recognized on the OV-17 column. When accurate MU values of the abnormal metabolites are necessary for identification, the sample must be appropriately diluted with pyridine so that the amount of the particular metabolite to be injected will be less than 2.5 μg per injection.

Maple syrup urine disease. When a urine from an acute ketoacidotic episode of maple syrup urine disease was analyzed without oxime-formation, branched 2-keto acids were not detectable, but two major peaks (lactic and 2-hydroxyisovaleric acids) were. 2-Hydroxyisovaleric acid, presumably formed from the reduction of 2-ketoisovaleric acid, was the most important diagnostic peak in the non-oximized sample. When the oxime–TMS derivatives were made, several additional peaks were detected, as shown in Fig. 2: 2-ketoisocaproic, 2-keto-3-methylvaleric, 2-ketoisov-

TABLE III

MAJOR ORGANIC ACIDS IN NORMAL URINE

Acid	*Excretion (μg per mg creatinine)*				
	Group I (6–24 months) n = 2 mean ± SD	*Group II (2–5 years) n = 7 mean ± SD*	*Group III (6–10 years) n = 8 mean ± SD*	*Group IV (10–15 years) n = 22 mean ± SD*	*Group V (16–20 years) n = 11 mean ± SD*
Always present					
3-Hydroxybutyric + 3-hydroxyisobutyric*	0	16 ± 3	25 ± 28	12 ± 8	12 ± 6
Succinic	10	60 ± 31	32 ± 13	19 ± 10	13 ± 8
Adipic	18	50 ± 24	43 ± 20	69 ± 50	34 ± 15
p-Hydroxyphenylacetic	21 ± 6	52 ± 17	47 ± 29	35 ± 23	23 ± 11
Hippuric	18 ± 4	284 ± 146	336 ± 189	192 ± 162	293 ± 186
Citric	14 ± 3	182 ± 152	102 ± 50	88 ± 57	78 ± 32
			Range (number of samples which contain the acid)		
Present in some samples					
Glycolic			0–59 (31/50)		
Oxalic			0–63 (13/50)		
p-Cresol			0–126 (12/50)		
Octanedioic (suberic)			0–104 (21/50)		

* These two compounds are eluted very closely from each other on both OV-1 and OV-17 columns and their separate identification was difficult.

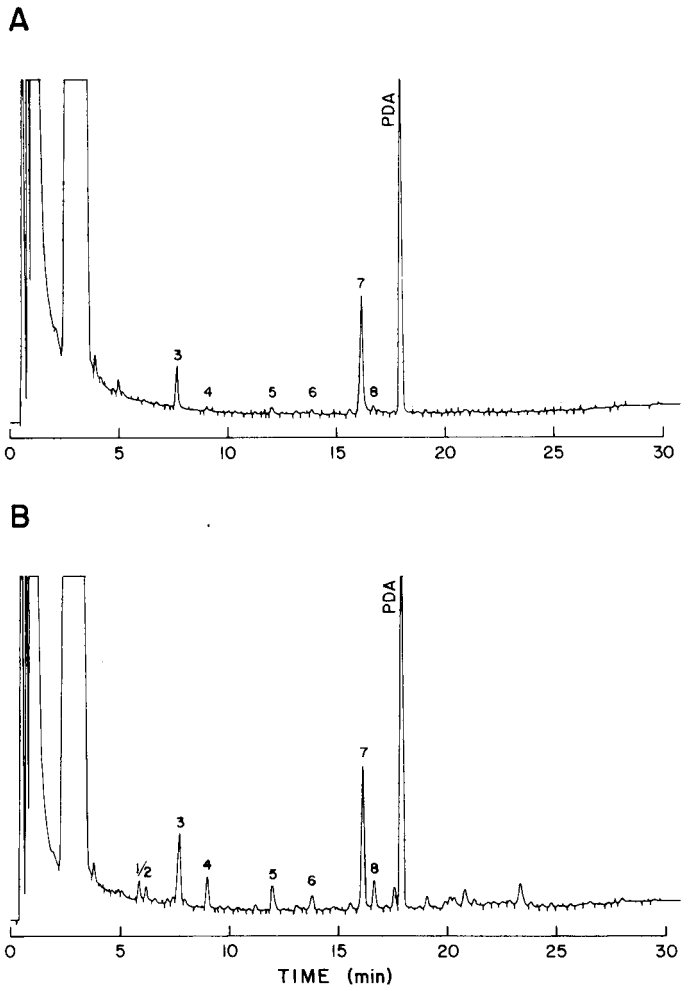

Fig. 1. Chromatograms of urinary organic acids from two normal children (A: 16 months and B: 3.5 years). A 10% OV-1 column was used for analyses. The compounds noted in the figures are TMS derivatives of the following compounds: 1 = oxalic; 2 = *p*-cresol; 3 = urea; 4 = succinic; 5 = adipic; 6 = *p*-hydroxyphenylacetic; 7 = hippuric; and 8 = citric acids. *n*-Pentadecanoic acid (PDA, 1 mg/mg creatinine) was added as an internal standard.

aleric, 2-ketoglutaric and pyruvic acids[19,29,35]. In particular, the peak sizes of the first two compounds were very large and diagnostic. In the patient we studied, these unusual 2-ketoacids all disappeared after five days of treatment with a diet low in branched-chain amino acids.

Isovaleric acidemia. When a urine was collected while the patient with isovaleric acidemia was in remission, isovalerylglycine was the only abnormal metabolite to be detected[2,6]. The amount of this metabolite was very large, far exceeding the size of the internal standard peak (PDA: 1 mg/mg creatinine; Fig. 3, top). Two peaks of isovalerylglycine were observed (the mono-TMS and di-TMS derivatives of isovaler-

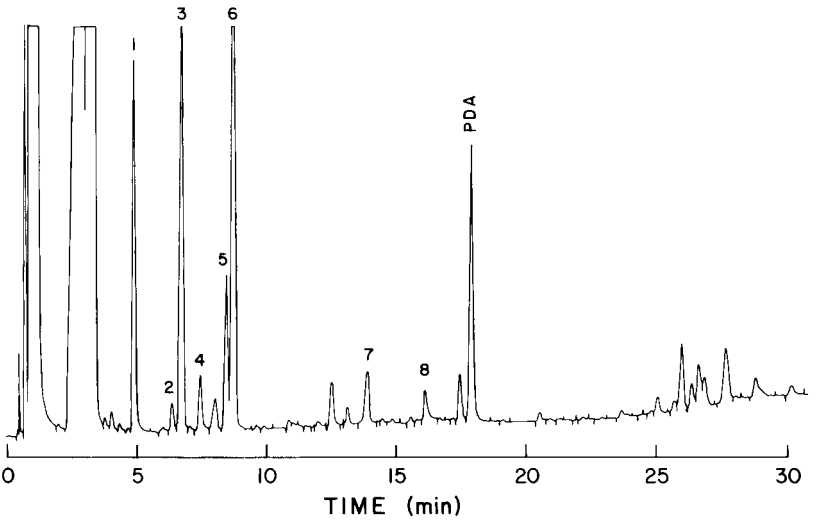

Fig. 2. Urinary organic acids from a patient with maple syrup urine disease. The column was a 10% OV-1 column. Peaks: 1 = lactic; 2 = pyruvic-oxime; 3 = 2-hydroxyisovaleric; 4 = 2-ketoisovaleric-oxime; 5 = 2-keto-3-methylvaleric-oxime; 6 = 2-ketoisocaproic-oxime, 7 = 2-ketoglutaric-oxime; 8 = hippuric acids. *n*-Pentadecanoic acid (PDA: 1 mg/mg creatinine) was added as an internal standard.

ylglycine). When urine from a ketoacidotic episode of isovaleric acidemia was analyzed, several additional large peaks were detected: lactic, 3-hydroxybutyric, acetoacetic, and 3-hydroxyisovaleric acids (Fig. 3, bottom)[2,13].

Propionic acidemia. Sometimes the only diagnostic change detectable in urinary metabolite analysis of a patient with propionic acidemia who is in stable condition is a moderate accumulation of methylcitric (homocitric) acid[10], as shown in Fig. 4 (top). This change is much less dramatic than those seen in other organic acidurias and could be easily missed unless analyses of such urines and inspection of chromatograms are carefully done. In contrast, many unusual organic acids are detectable in urines collected when the propionic acidemia patient is in an acute acidotic episode (Fig. 4, bottom). These diagnostic metabolites specific for propionic acidemia are 3-hydroxypropionic[12], 2-methyl-3-hydroxybutyric[24], 3-ketovaleric[12], 3-hydroxyvaleric[14,17,24], 3-methylacetoacetic[24], 2-methyl-3-ketovaleric[24], 2-methyl-3-hydroxyvaleric and methylcitric acids and two unusual acylglycines, propionylglycine[17,24,46] and tiglylglycine[59] (Fig. 4, bottom). However, the amounts of these diagnostic metabolites are not extremely large. In addition, large peaks of nonspecific metabolites such as 3-hydroxybutyric, acetoacetic, and *p*-hydroxphenylacetic acids are detected.

Methylmalonic acidemia. Diagnosis of methylmalonic acidemia is usually very easy; a very large amount (up to 20 mg per mg of creatinine) of methylmalonic acid is readily detectable and usually is the only abnormal peak (Fig. 5). In addition, much smaller peaks of metabolites from isoleucine, such as 2-methyl-3-hydroxyburytic acid and tiglylglycine, and the secondary metabolites of propionate (3-hydroxypropionic, 3-hydroxyvaleric, methylcitric acids) may be detected. In case a large methylmalonic acid peak is not detected in a suspected urine, one must learn whether vitamin B_{12}

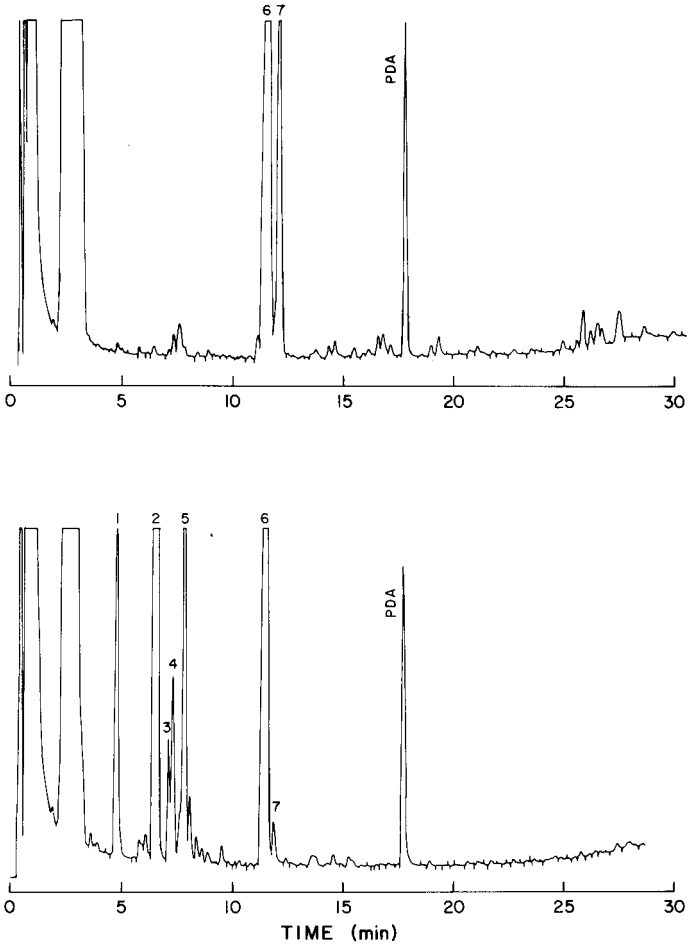

Fig. 3. Urinary organic acids from a patient with isovaleric acidemia. Top: a urine from remission. Bottom: a urine from a ketoacidotic episode. A 10% OV-1 column was used for analysis of both samples. Peaks: 1 = lactic; 2 = 3-hydroxybutyric; 3 = acetoacetic (first peak); 4 = 3-hydroxyisovaleric; 5 = acetoacetic (second (peak); 6 = isovalerylglycine (mono-TMS); 7 = isovalerylglycine (di-TMS). *n*-Pentadecanoic acid (PDA: 1 mg/mg creatinine) was added as an internal standard. 3-Ketoacids such as acetoacetic acid is detected as two peaks of di-TMS of the enol forms (*cis* and *trans*).

(cobalamin) was administered to the patient; in B_{12}-responsive methylmalonic acidemia, urinary methylmalonic acid may be decreased to a very low concentration. Several different forms of methylmalonic acidemia exist[34].

Glutaric aciduria type II (GA II) and ethylmalonic-adipic aciduria (EMA). Large amounts of ethylmalonic, glutaric, adipic, octanedioic (suberic), and decanedioic (sebacic) acids are detectable in urines from patients with GA II (Fig. 6, top)[22,41]. Although in most of the urines from patients with GA II the amount of ethylmalonic acid is larger than that shown in Fig. 6, peaks of glutaric or adipic acid are the largest. In contrast, in urines from patients with EMA, ethylmalonic or adipic acids have the largest peaks, and glutaric acid usually is detectable only in small

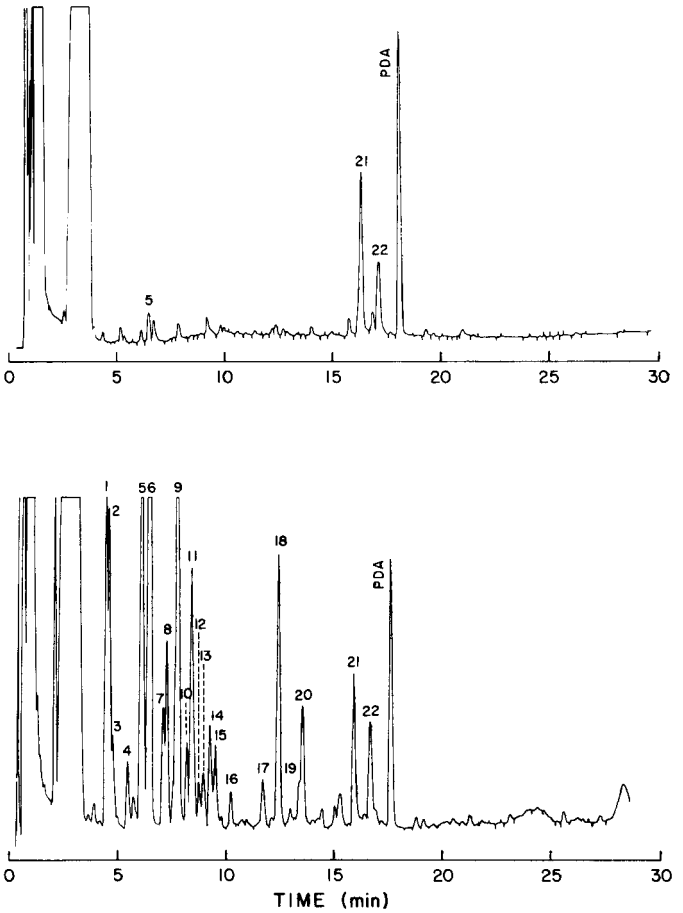

Fig. 4. Urinary organic acids from patients with propionic acidemia. Top: a urine from remission. Bottom: a urine from a ketoacidotic episode. A 10% OV-1 column was used for analyses of both samples. Peaks: 1 = oxalic; 2 = unknown; 3 = lactic; 4 = unknown; 5 = 3-hydroxypropionic; 6 = 3-hydroxybutyric; 7 = acetoacetic (first peak); 8 = 2-methyl-3-hydroxybutyric; 9 = 3-hydroxyvaleric + acetoacetic (second peak); 10 = 3-ketovaleric (first peak); 11 = 3-ketovaleric (second peak); 12 = succinic; 13 = 2-methylacetoacetic; 14 = propionylglycine; 15 = 2-methyl-3-ketovaleric; 16 = glutaric; 17 = adipic; 18 = tiglylglycine; 19 = 3-hydroxy-3-methylglutaric; 20 = *p*-hydroxyphenylacetic; 21 = hippuric; 22 = methylcitric acids. *n*-Pentadecanoic acid (PDA: 1 mg/mg creatinine) was added as an internal standard. 3-Ketoacids are detected as two peaks of di-TMS derivatives of enolic forms (*cis* and *trans*).

amounts or is undectectable (Fig. 6, bottom); large accumulations of glutaric acid may occur on rare occasions when the patient is severely acidotic[42]. GA II and EMA are both caused by a similar cellular mechanism, namely, a deficiency of multiple acyl CoA dehydrogenase activities, but the biochemical causes underlying this deficiency are still unknown. The distinct difference in urinary metabolites suggests heterogeneities of these two similar diseases. This phenotypical difference is not due to difference in severity of deficiencies of acyl CoA dehydrogenase activities, because the glutaric acid peak is as prominent in a very mild case of GA II[22] in which the

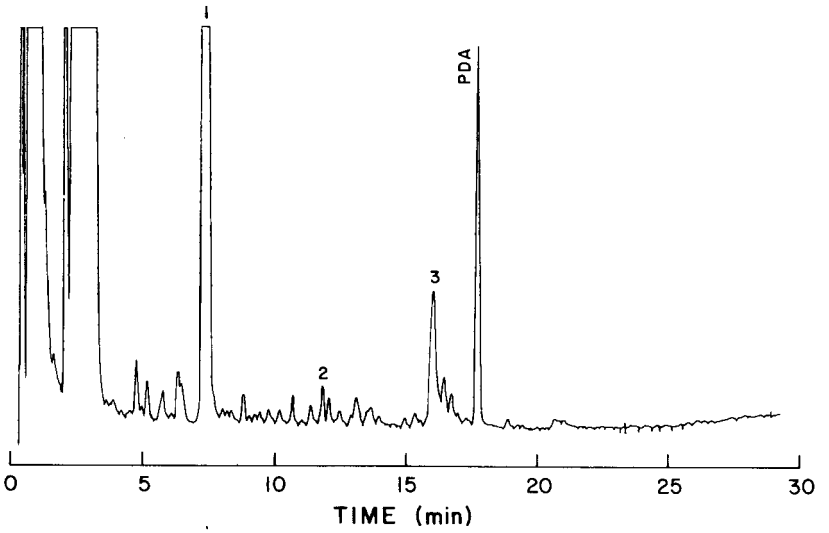

Fig. 5. Urinary organic acids from a patient with methylmalonic acidemia. A 10% OV-1 column was used for analysis. Peaks: 1 = methylmalonic; 2 = adipic; 3 = hippuric acids. *n*-Pentadecanoic acid (PDA: 1 mg/mg creatinine) was added as an internal standard.

deficiency was milder than that of the EMA patient[41]. The GA II urine in Fig. 6 (top) was from a patient with mild clinical manifestations.

Multiple carboxylase deficiency. Activities of three biotin-dependent carboxylases (propionyl CoA-, 3-methylcrotonyl CoA- and pyruvate carboxylases) are low in this disease, presumably because of a deficiency of holocarboxylase synthetase or defective biotin absorption[36]. A chromatogram of urinary organic acids from a patient with this disease, recently diagnosed in our laboratory, is shown in Fig. 7. This patient, a 28-month-old boy, had a severe episode of hypoglycemia and acidosis. Large peaks of lactic, 3-hydroxypropionic, 3-hydroxybutyric, 3-hydroxyisovaleric, and acetoacetic acids and 3-methylcrotonylglycine were detected. After two weeks of treatment with biotin (10 mg/day), these unusual urinary metabolites almost entirely disappeared except for a small amount of 3-hydroxyisovaleric acid.

Phenylketonuria. Patients with phenylketonuria are usually detected by newborn screening programs with the Guthrie test or with amino acid chromatography. However, we occasionally receive urines from undiagnosed phenylketonuria patients for analysis of urinary organic acids from such a previously undiagnosed case (four-year-old boy) is shown in Fig. 8. Large peaks of phenylacetic, phenylpyruvic, and phenyllactic acids are characteristic features of these urines.

Short bowel syndrome. Obese patients who have undergone drastic small-bowel resection may have severe acidosis. We have encountered two such cases in the past two years. In both, there was a huge lactic acid peak and moderately increased amounts of phenyllactic, *p*-hydroxyphenylacetic, and *p*-hydroxyphenyllactic acids (Fig. 9). These organic acids are presumably produced by bacteria in the colon from unabsorbed amino acids. The D-configuration of urinary lactic acid in short bowel syndrome was initially suggested by us on the basis of a discrepancy between a low serum lactate concentration, as measured enzymically with L-lactic dehydrogenase,

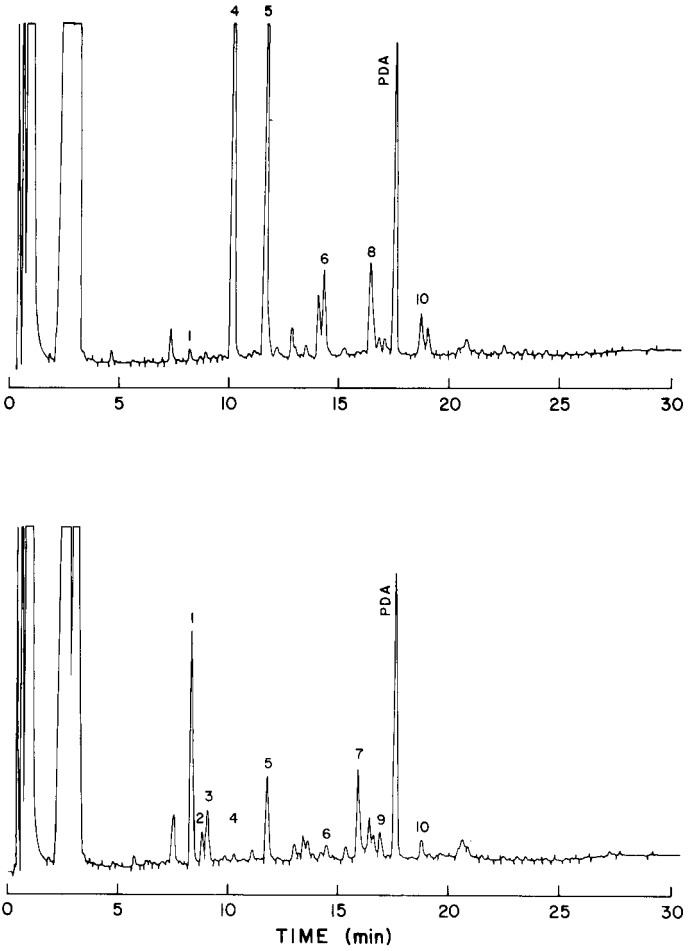

Fig. 6. Urinary organic acids from a patient with glutaric aciduria type II (acute stage) (top) and a patient with ethylmalonic aciduria (remission) (bottom). A 10% OV-1 column was used for analyses of both samples. Peaks: 1 = ethylmalonic; 2 = succinic; 3 = methylsuccinic; 4 = glutaric; 5 = adipic; 6 = octanedioic (suberic); 7 = hippuric; 8 = decenedioic; 9 = decanedioic (sebacic); 10 = palmitic acids. *n*-Pentadecanoic acid (PDA; 1 mg/mg creatinine) was added as an internal standard.

and a very large amount of urinary lactic acid, as detected by GC. It has since been confirmed.

Glyceric aciduria. In the initial sample, moderately increased amounts of lactic acid and that identified as glyceric acid were found by the ethyl acetate-extraction method (Fig. 10A). When the same sample was prepared by the Dowex-50 column method, a huge amount of glyceric acid was detected. In addition, a huge peak of phosphoric acid and those of citric acid and a few unknown compounds were detected (Fig. 10B). The stereoconfiguration of glyceric acid and the nature of the enzyme deficiency are now under investigation.

Glyceroluria. This disease is due to a deficiency of glycerol kinase activity.

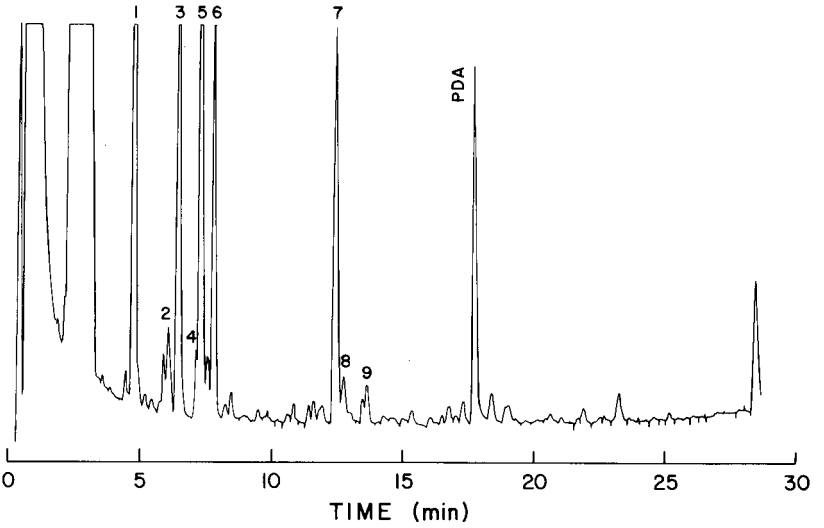

Fig. 7. Urinary organic acids from a patient with multiple carboxylase deficiency. A 10% OV-1 column was used for analysis. Peaks: 1 = lactic; 2 = 3-hydroxypropionic; 3 = 3-hydroxybutyric; 4 = 2-ethylhydracrylic; 5 = 3-hydroxyisovaleric; 6 = acetoacetic; 7 = 3-methylcrotonylglycine (mono-TMS); 8 = 3-methylcrotonylglycine (di-TMS); 9 = *p*-hydroxyphenylacetic acids. *n*-Pentadecanoic acid (PDA: 1 mg/mg creatinine) was added as an internal standard.

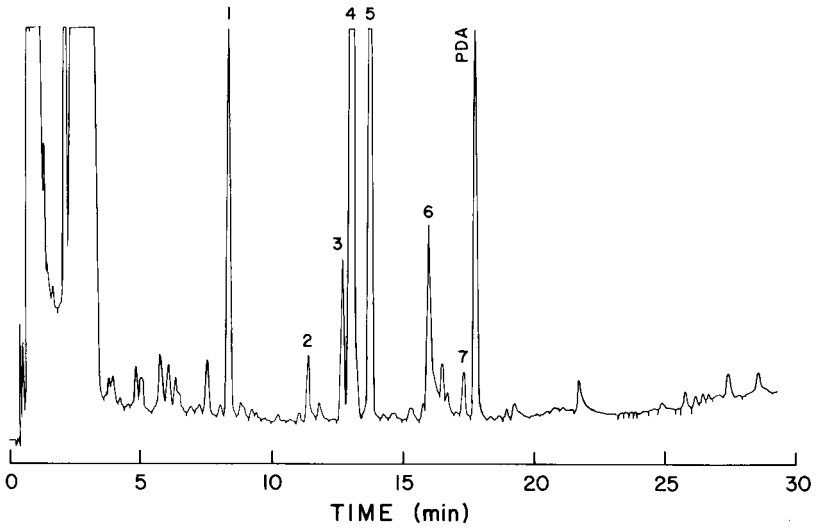

Fig. 8. Urinary organic acids from a patient with phenylketonuria. A 10% OV-1 column was used for analysis. Peaks: 1 = phenylacetate; 2 = unknown; 3 = *o*-hydroxyphenylacetic; 4 = phenyllactic; 5 = phenylpyruvic-oxime; 6 = hippuric; 7 = *p*-hydroxyphenyllactic acids. *n*-Pentadecanoic acid (PDA: 1 mg/mg creatinine) was added as an internal standard.

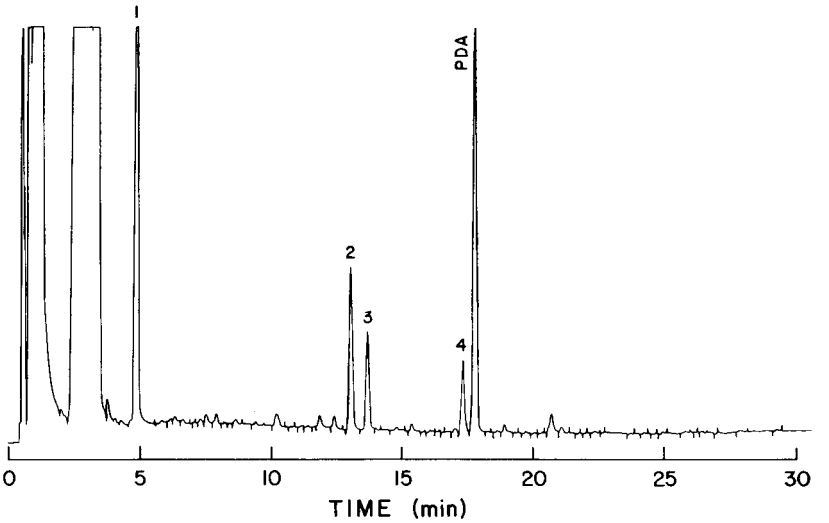

Fig. 9. Urinary organic acids from a patient with short bowel syndrome. A 10% OV-1 column was used for analysis. Peaks: 1 = lactic (D-form); 2 = phenylacetic; 3 = *p*-hydroxyphenylacetic; 4 = *p*-hydroxyphenyllactic acids. *n*-Pentadecanoic acid (PDA: 1 mg/mg creatinine) was added as an internal standard.

Although the main clinical features of the previously reported case was psychomotor retardation, spastivity, a non-specific myopathy and adrenal insufficiency[43], our patient presented severe ketoacidosis. When the first urine was analyzed using the ethyl acetate extraction, there was a large glycerol peak in addition to a huge 3-hydroxybutyric acid peak (Fig. 11A). The same urine was then fractionated by a AG 501 mixed-bed resin and the neutral fraction was trimethylsilated. A huge glycerol peak and a large urea peak were observed (Fig. 11B).

DISCUSSION

In 1966, Dalgliesh *et al.*[67] compiled an extensive list of MU values for many organic acids, pioneering in the GC analysis of urinary organic acids, but their list is now of very limited practical application in the detection of organic aciduria because of certain drawbacks. First, the stationary phase used was F-50 siloxane polymer (Dow Corning) alone, which is no longer in wide use. A more serious drawback is the fact that all compounds tested were from the shelf; thus, many diagnostic metabolites are missing from the list because this study was completed before the identification of isovaleric acidemia, the first organic aciduria to be discovered[1]. Gates *et al.*[68] recently published an extensive list of retention indices for urinary metabolites from normal adults, patients with neuroblastoma and pediatric patients with unspecified diseases, as determined by GC–MS–computer. This study also suffers from similar shortcomings in its application to the detection of patients with organic aciduria by GC alone: the use of a single stationary phase and the lack of pathological metabolites in their list. Thus, the present study represents the first comprehensive list of retention indices of organic acids that can be utilized for the diagnosis of organic acidurias.

Since completing this compilation two years ago, we have analyzed over 500

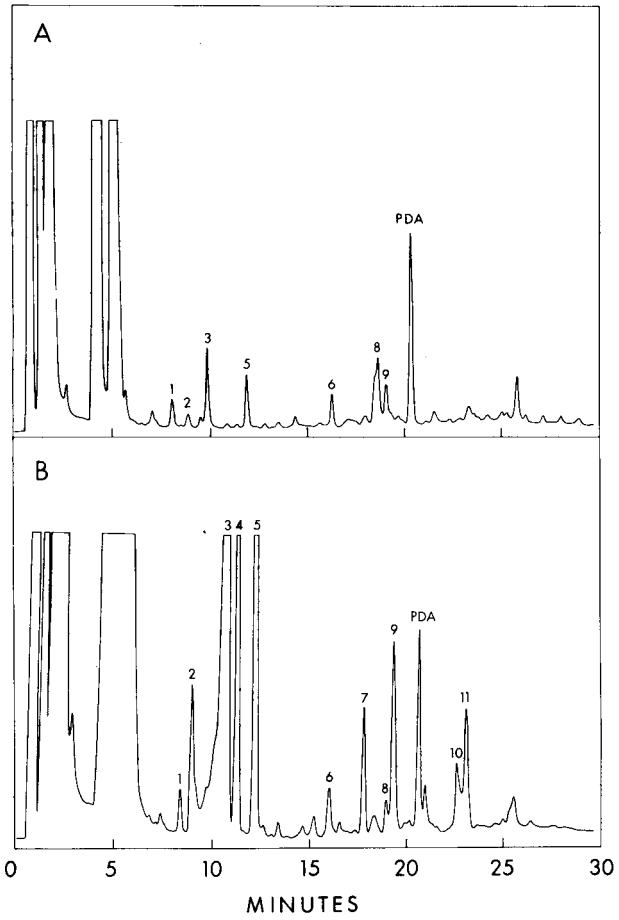

Fig. 10. Urinary organic acids from a patient with glyceric aciduria. A, ethyl acetate-extraction method; B, cation-exchange-lyophilization method. A 10% OV-1 column was used for analysis. Peaks: 1 = oxalic; 2 = 3-hydroxyisobutyric; 3 = urea; 4 = phosphoric; 5 = glyceric; 6 = *p*-hydroxyphenylacetic; 7 = unknown; 8 = hippuric; 9 = citric; 10 = unknown; 11 = unknown. PDA (1 mg/mg of creatinine) added as an internal standard.

urines by GC alone and readily identified 21 patients with well-defined organic acidurias. These include methylmalonic acidemia, isovaleric acidemia, multiple carboxylase deficiency[7,36], propionic acidemia, maple syrup urine disease, tyrosinemia[34], glyceroluria[43] and glyceric aciduria[47,48]. All of the identifications were subsequently confirmed by MS. In our experience, the diagnosis by GC alone was much easier and sometimes more convincing than with GC–MS alone, especially in a disease such as propionic acidemia, in which numerous abnormal metabolites are excreted. In these cases, interpretation of mass spectra is often obscured by overlapping peaks. For laboratories not equipped with a GC–MS, this list provides sufficient information for diagnosis of the welldefined organic acidurias listed in Table II, because we have included most of the abnormal metabolites characteristic of these diseases. For labo-

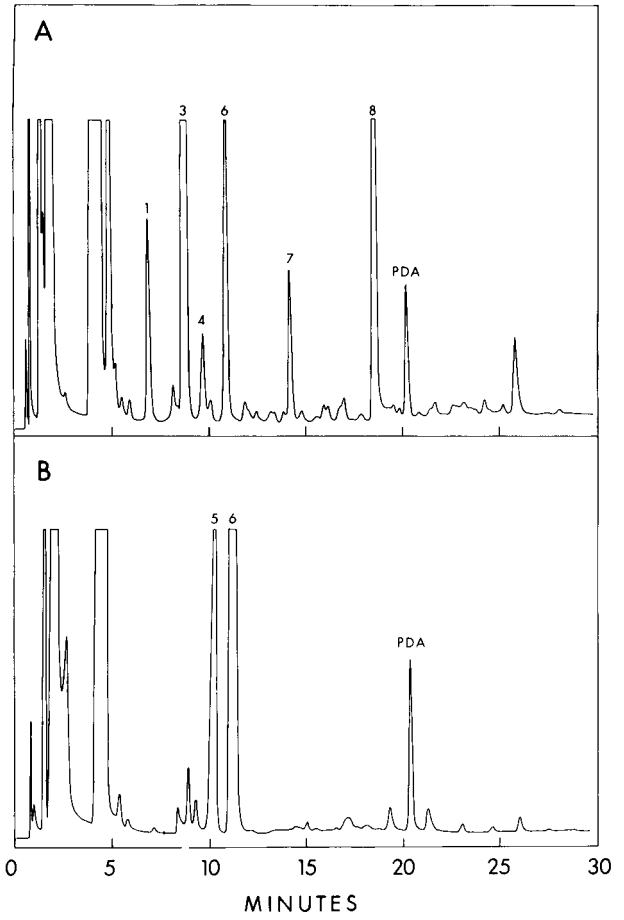

Fig. 11. Urinary organic acids from a patient with glyceroluria. A, ethyl acetate-extraction method; B, mixed-bed ion-exchange-lyophilization method. A 10% OV-1 column was used for analysis. Peaks: 1 = lactic; 2 = 2-hydroxybutyric; 3 = 3-hydroxybutyric; 4 = 3-hydroxyisovaleric; 5 = urea; 6 = glycerol; 7 = adipic; 8 = hippuric. PDA (1 mg/mg of creatinine) added as an internal standard.

ratories with a GC–MS system, use of the present MU tabulation makes it much easier to interpret mass spectra of complex urinary metabolites, by indicating possible overlapping peaks.

ACKNOWLEDGEMENTS

We thank Ms. Agnes West-Dull, Ms. Alda Saunders and Mr. Theodore Lynn for technical assistance. This study was supported in part by a NIH grant (AM 17453) and a grant from the March of Dimes-Birth Defect Foundation (1978).

REFERENCES

1 K. Tanaka, M. A. Budd, L. Efron and K. J. Isselbacher, *Proc. Nat. Acad. Sci. U.S.*, 56 (1966) 236–242.
2 K. Tanaka, in G. E. Gaull (Editor), *Biology of Brain Dysfunction, Vol. 3*, Plenum Press, New York, 1975 pp. 145–214.
3 K. Tanaka, E. A. Kean and B. Johnson, *New Engl. J. Med.*, 295 (1976) 461–467.
4 K. Tanaka, in P. J. Vinken and G. W. Bruyn (Editors), *Handbook of Clinical Neurology*, Vol. 37, North-Holland, Amsterdam 1979 pp. 511–539.
5 M. G. Hogginbottom, L. Sweetman and W. L. Nyhan, *New Engl. J. Med.*, 299 (1978) 317–323.
6 K. Tanaka and K. J. Isselbacher, *J. Biol. Chem.*, 242 (1967) 2966–2972.
7 O. Stokke, L. Eldjarn, E. Jellum, H. Pande and P. E. Waaler, *Pediatrics*, 49 (1972) 726–735.
8 D. Gompertz and G. H. Draffan, *Clin. Chim. Acta*, 37 (1972) 405–410.
9 B. H. Baretz, H. S. Ramsdell and K. Tanaka, *Clin. Chim. Acta*, 73 (1976) 199–202.
10 T. Ando, K. Rasmussen, J. M. Wright and W. L. Nyhan, *J. Biol. Chem.*, 247 (1972) 2200–2204.
11 K. Tanaka, H. S. Ramsdell, B. H. Baretz, M. B. Keefe, E. A. Kean and B. Johnson, *Clin. Chim. Acta*, 69 (1976) 105–112.
12 T. Ando, K. Rasmussen, W. L. Nyhan and D. Hull, *Proc. Nat. Acad. Sci. U.S.*, 69 (1972) 2807–2811.
13 K. Tanaka, J. C. Orr and K. J. Isselbacher, *Biochim. Biophys. Acta*, 15 (1968) 638–641.
14 O. Stokke, E. Jellum, L. Eldjarn and R. Schnittler, *Clin. Chim. Acta*, 45 (1973) 391–401.
15 H. S. Ramsdell and K. Tanaka, *Clin. Chim. Acta*, 74 (1977) 109–114.
16 K. Tanaka, D. Hine, A. West-Dull and T. H. Lynn, *Clin. Chem.*, 26 (1980) 1841–1848.
17 K. Tanaka, A. West-Dull, D. G. Hine and T. B. Lynn, *Clin. Chem.*, 26 (1980) 1849–1855.
18 O. A. Mamer, J. C. Crawhall and S. S. Tjoa, *Clin. Chim. Acta*, 32 (1971) 171–184.
19 P. Lancaster, P. Lamm and C. R. Scriver, *Clin. Chim. Acta*, 48 (1973) 279–285.
20 M. Duran, D. Ketting P. K. de Bree, C. van der Heiden and S. K. Wadman, *Clin. Chim. Acta*, 45 (1973) 341–347.
21 K. Tanaka and L. E. Rosenberg, in N. Freinkel (Editor), *Contemporary Metabolism*, Vol. 1, Plenum Press, New York, 1979 pp. 461–481.
22 G. Dusheiko, M. C. Kew, B. I. Joffe, J. R. Lewin, S. Mantagos and K. Tanaka, *New Engl. J. Med.*, 301 (1979) 1405–1409.
23 S. Landaas and J. E. Pettersen, *Scand. J. Clin. Lab. Invest.*, 35 (1975) 259–266.
24 L. Sweetman, W. Weyler, W. L. Nyhan, C. D. Cespedes, A. Rosalori and Y. Estrada, *Biomed. Mass Spec.*, 5 (1978) 198–207.
25 T. Kuhara and I. Matsumoto, *Biomed. Mass Spec.*, 1 (1974) 291–294.
26 I. Matsumoto, T. Kuhara and M. Yoshino, *Biomed. Mass Spec.*, 3 (1976) 235–240.
27 S. Landaas, *Clin. Chim. Acta*, 64 (1975) 143–154.
28 O. A. Mamer, J. A. Montgomery, S. S. Tjoa, J. C. Crawhall and C. S. Feldkamp, *Biomed. Mass Spec.*, 5 (1978) 287–290.
29 C. Jakobs, E. Solem, J. Ek, K. Halvorsen and E. Sellum, *J. Chromatogr.*, 143 (1977) 31–38.
30 R. S. Daum, C. R. Scriver, O. A. Mamer, E. Delvin, P. Lamm and H. Goldman, *Pediatr. Res.*, 7 (1973) 149–160.
31 D. Gompertz, J. M. Saudubray, C. Charpentier, K. Bartlett, P. A. Goodey and G. H. Draffan, *Clin. Chim. Acta*, 57 (1974) 269–281.
32 U. G. Oberholzer, B. Levin, E. A. Burgess and W. F. Young, *Arch. Dis. Child.*, 42 (1967) 492–504.
33 O. Stokke, L. Eldjarn, K. R. Norum, J. Steen-Johnsen and S. Halvorsen, *Scand. J. Clin. Lab. Invest.*, 20 (1967) 313–328.
34 L. E. Rosenberg and C. R. Scriver, in P. K. Bondy and L. E. Rosenberg (Editors), *Metabolic Control and Disease*, W. B. Saunders, Philadelphia, 8th ed., 1980, pp. 583–776.
35 J. Dancis and M. Levits, in J. B. Stanbury, J. B. Wyngaarden and D. S. Fredrickson (Editors), *The Metabolic Basis of Inherited Disease*, McGraw-Hill, New York, 4th ed., 1978, pp. 397–410.
36 L. Sweetman, S. Bates, D. Hull and W. L. Nyhan, *Pediat. Res.*, 11 (1977) 1144–1147.
37 O. A. Mamer and S. S. Tjoa, *Clin. Chim. Acta*, 55 (1974) 119–204.
38 O. A. Mamer, S. S. Tjoa, C. R. Scriver and G. A. Klassen, *Biochem. J.*, 160 (1976) 417–426.
39 B. H. Baretz, C. P. Lollo and K. Tanaka, *J. Biol. Chem.*, 254 (1979) 3468–3478.
40 T. Kitagawa, B. A. Smith and E. S. Brown, *Clin. Chem.*, 21 (1975) 735–740.
41 H. Przyrembel, U. Wendel, K. Becker, H. J. Bremer, L. Bruinvis, D. Ketting and S. K. Wadman, *Clin. Chim. Acta*, 66 (1976) 227–239.

42 S. Montagos, M. Genel and K. Tanaka, *J. Clin. Invest.*, 64 (1979) 1580–1589.
43 E. R. B. McCabe, P. V. Fennessey, M. A. Guggenheim, B. Miles, W. W. Bullen, D. J. Sceats and S. I. Goodman, *Biochem. Biophys. Res. Comm.*, 78 (1977) 1327–1333.
44 C. I. Rose and D. S. Haines, *J. Clin. Invest.*, 61 (1978) 163–170.
45 R. J. W. Truscott, C. J. Pullin, B. Halpern, J. Hammond, E. Haan and D. M. Danks, *Biomed. Mass Spec.*, 6 (1979) 294–300.
46 K. Rasmussen, T. Ando, W. L. Nyhan, D. Hull, D. Cottom, G. Donnell, W. Wadlington and A. W. Kilroy, *Clin. Sci.*, 42 (1972) 665–671.
47 H. E. Williams and L. H. Smith, Jr., *New Engl. J. Med.*, 278 (1968) 233–239.
48 S. K. Wadman, M. Duran, D. Ketting, L. Bruinvis, P. K. DeBree, J. B. Kamerling, B. J. Gerwig, J. F. G. Vliegenthart, B. H. Przyrembel, K. Becker and H. J. Bremer, *Clin. Chim. Acta*, 71 (1976) 477–484.
49 S. I. Goodman, S. P. Markey, P. Q. Moe, B. S. Miles and C. C. Teng, *Biochem. Med.*, 12 (1975) 12–21.
50 O. Stokke, S. I. Goodman, J. A. Thompson and B. S. Miles, *Biochem. Med.*, 12 (1975) 386–391.
51 K. Tanaka, in E. A. Kean (Editor), *Hypoglycin*, Academic Press, New York, 1975, pp. 67–92.
52 G. Karpati, S. Carpenter, A. G. Engel, G. Haltes, J. Allen, S. Rothman, G. Klassen and O. A. Mamer, *Neurology*, 25 (1975) 16–24.
53 J. E. Pettersen, E. Jellum and L. Eldjarn, *Clin. Chim. Acta*, 38 (1972) 17–24.
54 E. Jellum, T. Kluge, C. Borresen, O. Stokke and L. Eldjarn, *Scand. J. Clin. Lab. Invest.*, 26 (1970) 327–335.
55 V. P. Wellner, R. Sekura, A. Meister and A. Larsson, *Proc. Nat. Acad. Sci. U.S.* 71 (1974) 2505–2509.
56 V. G. Oberholzer, C. B. L. Wood, T. Palmer and B. M. Harrison, *Clin. Chim. Acta*, 62 (1975) 299–304.
57 K. Rasmussen, T. Ando, W. L. Nyhan, D. Hull, D. Cottom, A. W. Kilroy and W. Wadlington, *J. Pediatr.*, 81 (1972) 970–972.
58 S. J. Wysocki, S. P. Wilkinson, R. Hahnel, C. Y. B. Wong and P. K. Penegyre, *Clin. Chim. Acta*, 70 (1976) 399–406.
59 K. F. Faull, P. D. Bolton, B. Halpern, J. Hammond and D. M. Danks, *Clin. Chim. Acta*, 73 (1976) 553–559.
60 M. Duran, D. Ketting, S. K. Wadman, C. Jakobs, R. B. Schutgen and H. A. Veder, *Clin. Chim. Acta*, 90 (1978) 187–193.
61 J. E. Pettersen and E. Jellum, *Clin. Chim. Acta*, 41 (1972) 199–207.
62 J. A. Thompson, B. S. Miles and P. V. Fennessey, *Clin. Chem.*, 23 (1977) 1734–1738.
63 H. Przyrembel, D. Bachman, I. Lombeck, K. Becker, U. Wendel, S. K. Wadman and H. J. Bremer, *Clin. Chim. Acta*, 58 (1975) 257–269.
64 R. W. Wilson, C. M. Wilson, L. C. Gates and J. V. Higgins, *Pediat. Res.*, 9 (1975) 522–526.
65 W. N. Kelley and L. H. Smith Jr., in J. B. Stanbury, J. B. Wijngaarden and D. S. Fredrickson (Editors), *The Metabolic Basis of Inherited Disease*, McGraw-Hill, New York, 4th ed., 1978, pp. 1045–1071.
66 K. Tanaka, *J. Biol. Chem.*, 247 (1972) 7465–7478.
67 C. E. Dalgliesh, E. C. Horning, M. G. Horning, K. L. Knox and K. Yarger, *Biochem. J.*, 101 (1966) 792–310.
68 S. C. Gates, C. C. Sweeley, W. Kivit, D. Dewitt and B. E. Blaisdel, *Clin. Chim. Acta*, 24 (1978) 1680–1689.

Journal of Chromatography, 239 (1982) 323–334
Elsevier Scientific Publishing Company, Amsterdam — Printed in The Netherlands

CHROM. 14,512

DETERMINATION OF TOCAINIDE IN HUMAN PLASMA BY GAS CHROMATOGRAPHY WITH NITROGEN-SELECTIVE DETECTION AFTER SCHIFF BASE FORMATION

LARS JOHANSSON and JÖRGEN VESSMAN*
Analytical Chemistry, AB Hässle, S-431 83 Mölndal (Sweden)

SUMMARY

Tocainide is a primary amine with antiarrythmic properties derived from lidocaine. For biopharmaceutical and pharmacokinetic purposes an assay was developed that made use of Schiff base formation with methyl isobutyl ketone and gas chromatography with nitrogen-selective detection. The derivatization procedure was performed at 85°C for 10 min, although a longer time at this temperature caused degradation of the product. Of several structural analogues the *p*-methyl one was the internal standard of choice.

The amine was extracted from alkaline samples with dichloromethane and, after evaporation, reconstituted in methyl isobutyl ketone. From plasma the yields were lower than those from aqueous samples but the addition of hydroxylamine 30 min before the extraction process resulted in the same yields. Hydroxylamine probably acts as a competitor for carbonyl groups in the biological sample. In addition to the enhanced yields patients' samples extracted after hydroxylamine treatment were analysed with better precision.

With nitrogen-selective detection 500 nmol/l in a 0.5-ml sample could be quantified, which is well below the therapeutic levels. The method compared favourably with a liquid chromatographic assay.

INTRODUCTION

Tocainide [2-amino-N-(2,6-xylyl)propanoic acid amide], is an antiarrhythmic drug that is active after oral administration and has a suitable duration of effect. Previous bioanalytical data have been obtained with gas chromatographic methods using either flame-ionization[1] or electron-capture detection[2]. Liquid chromatography with fluorescence detection of a Dns derivative was reported to give high sensitivity[3], although methods without derivatization might suffice[4,5]. During clinical and biopharmaceutical studies of this drug large numbers of samples had to be assayed, which required a reliable and simple method that could be at least partially automated. This paper presents a gas chromatographic method based on nitrogen-selective detection of the Schiff base from tocainide and methyl isobutyl ketone. The derivatization reaction and experiences with the biological material are discussed.

0021-9673/82/0000–0000/$02.75

EXPERIMENTAL

Apparatus

A Hewlett-Packard 5730 gas chromatograph with a nitrogen-selective detector was used at 200°C with a 1 m × 2 mm I.D. glass column filled with 10% Carbowax 20M on 120–140-mesh Gas-Chrom Q. The temperatures of the detector and the injector were 300 and 200°C, respectively. The carrier gas (helium) and the detector gas (hydrogen–helium, 8:92) had flow-rates of 30 ml/min. Pre-purified air for the detector was used at 50 ml/min. A Hewlett-Packard Autoinjector was used.

Chemicals and reagents

Methylene chloride. Merck (Darmstadt, G.F.R.) p.a. (No. 6050) material was purified by distillation.

Methyl isobutyl ketone (MIBK). Merck p.a. (No. 6146) material was purified by distillation, then dried twice with and stored over molecular sieve 4A (Fluka, Buchs, Switzerland; 69834).

Tocainide standard solution. Tocainide (molecular weight 192.3) was obtained as the hydrochloride from the Department of Organic Chemistry, AB Hässle (Mölndal, Sweden). A 2.5-mg amount of tocainide hydrochloride was dissolved in and diluted to 100.0 ml with dilute hydrochloric acid (0.01 mol/l) to give a final concentration of 100 μmol/l. In this solution tocainide is stable for several months when kept in a refrigerator.

Internal standard. H 155/73 (molecular weight 206.3) was obtained as the hydrochloride from the Department of Organic Chemistry, AB Hässle. An aqueous solution was prepared in dilute hydrochloric acid (0.01 mol/l) to give a final concentration of 200 μmol/l.

Hydroxylamine solution. A 2.5-g amount of hydroxylammonium chloride (molecular weight 69.5) (Merck, p.a., No. 4619) was dissolved in 100 ml of water. This solution is stable for several months.

Glassware

All glassware was washed in a laboratory dish-washer at pH 12 (Extran AP12; Merck, No. 7563). The glassware was then rinsed at pH 2 (Extran AP21; Merck, No. 7559). The glass was finally rinsed with de-ionized water and dried at 60°C. All pipettes were silanized with dimethyldichlorosilane–toluene (1:9) overnight, washed with methanol and dried at 120°C.

Analytical procedure

The frozen sample is allowed to thaw at room temperature. After mixing, 0.5 g of plasma is transferred into a 15-ml centrifuge tube, 100 μl of the internal standard solution and 100 μl of the hydroxylamine solution are added and the sample is mixed. After standing for 30 min, 0.3 ml of sodium hydroxide solution (1 mol/l) and water to a total volume of 2.0 ml are added. This aqueous phase is extracted with 6.0 ml of dichloromethane. The tube is shaken mechanically for 10 min and centrifuged.

The organic phase is transferred into another 15-ml centrifuge tube and evaporated to dryness under a gentle stream of dry nitrogen. A 200-μl volume of MIBK is added to each tube, which is then tightly sealed with a screw-cap. The tube is placed in

a water-bath (85°C) for 10 min and then cooled with water to room temperature. A 3-μl volume of this solution is injected into the gas chromatograph.

Quantitative evaluation

A calibration graph was prepared by addition of various volumes (0, 50 and 200 μl) of the tocainide standard solution to 0.5 ml of plasma then analysing these samples according to the procedure given above. The peak-height ratios of tocainide to internal standard were calculated and the average of these values was then used for the quantitative evaluation of the samples taken for analysis.

RESULTS AND DISCUSSION

Tocainide is a primary amine (compound I in Fig. 5) that can be converted into derivatives that are more easily gas chromatographed than the free amine. Even if the primary amine itself can be chromatographed on stationary phases such as Carbowax 20M + potassium hydroxide, the handling of trace amounts of free amines can create adsorption problems in the steps before gas chromatography[6].

Primary and secondary amines can be acylated with perfluorinated reagents to give the corresponding amides, which are easily detected in picogram amounts using gas chromatography with electron-capture detection[7,8]. This approach has been reported for tocainide in small samples from rats[2]. Primary amines have also been derivatized in condensation reactions that are specific for this group of amines, *e.g.*, reaction with carbon disulphide and formation of Schiff bases with aldehydes and ketones[9]. The latter approach has mainly been used for qualitative purposes, the so-called peak shift technique[10]. Studies by Horning and co-workers[11–13] have shown the favourable gas chromatographic properties of the Schiff bases of several important amines. The separation of, *e.g.*, isomeric compounds can also be facilitated[13]. However, only a few quantitative methods have been reported. Amphetamine has been determined in dosage forms after condensation with cyclohexanone in a two-phase system[14]. Hoshika[15,16] studied the quantitative formation of Schiff bases from lower aliphatic primary amines with benzaldehyde and pentafluorobenzaldehyde.

The combination of a selective detection system such as the alkali flame-ionization detector with a simple derivatization reaction such as Schiff base formation could be used favourably for large series of samples that occur in pharmacokinetic studies.

Choice of condensing agent

Initial studies were performed with acetone as condensing agent. A single derivative was formed, which, however, co-eluted on the columns studied with a major peak originating from an endogenous plasma component. The choice then fell upon methyl isobutyl ketone, which is also available in good quality. Its volatility is lower than that of acetone, which is advantageous if the reaction mixture has to be stored for some time, such as in an auto-injector system.

Ketones were preferred to aliphatic aldehydes, which gave rapidly degrading products. As pointed out by VandenHeuvel *et al.*[13], an advantage of the stable ketones is their dual function as solvent and reagent. The reaction mixture can be injected directly into the gas chromatograph.

Reaction conditions

Schiff base formation is considered to be a two-step reaction (Fig. 1). This sequence has been suggested for the reaction between cyclohexanone and amphetamine based on infrared measurements[17].

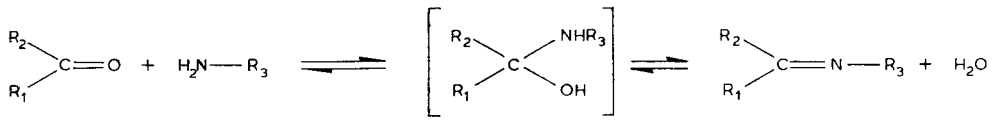

Fig. 1. Equation for the formation of a Schiff base.

Previous studies on Schiff bases (from ketones) for gas chromatography have demonstrated that the condensation reaction is a slow process[18]. With methyl isobutyl ketone the reaction at room temperature required at least 60 min for tocainide (Fig. 2A). Elevation of the reaction temperature increased the rate considerably (Fig. 2B and C). It was possible, however, even at 50°C to observe the start of degradation of the derivative formed. At 90°C the derivative was formed in apparently quantitative yield almost instantaneously (Fig. 2D), but after 120 min all of the derivative had disappeared. A number of extra peaks appeared early in the chromatograms from the

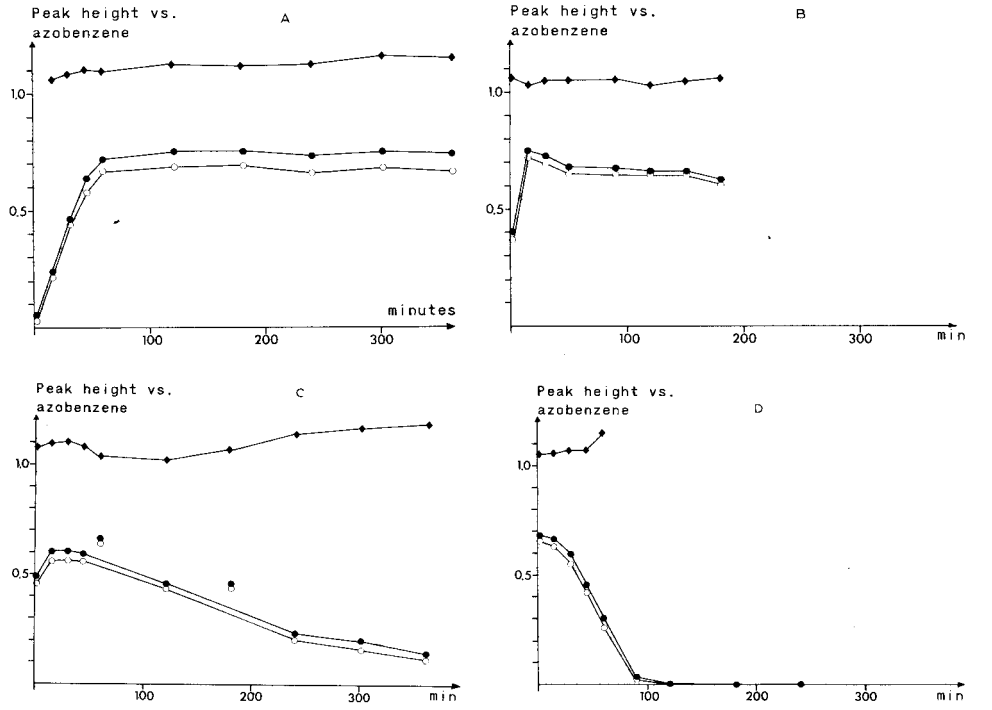

Fig. 2. Schiff base formation at (A) 22°C, (B) 50°C, (C) 70°C, (D) 90°C. ●, Tocainide Schiff base; ○, internal standard Schiff base; ◆, peak-height ratio.

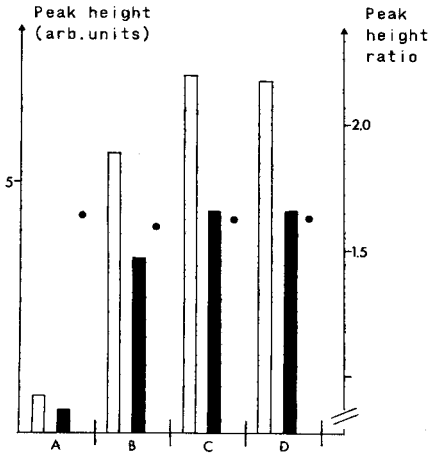

Fig. 3. Effect of pre-treatment of MIBK on peak height. (A) No treatment; (B) distillation; (C) distillation and treatment with molecular sieve; (D) as for C but with 1 % of water present. □, Tocainide Schiff base; ■, internal standard Schiff base; ●, peak-height ratio.

degraded solutions of the Schiff bases of tocainide and of the internal standard studied in parallel. Reaction at 85°C for 10 min was chosen for the method.

The formation of the derivative in the hot injector could be a possibility. This was ruled out, however, after an experiment with a so-called "sandwich" injection of methyl isobutyl ketone and tocainide dissolved in diethyl ether showed up only the free amine.

Quality of methyl isobutyl ketone

Initial studies with methyl isobutyl ketone gave high and reproducible yields of the Schiff base. It was observed, however, that single batches of the ketone gave fairly low yields, down to only 15 % of the normal values. Purification of the ketone with drying agents such as a molecular sieve and/or distillation revealed that distillation was most effective in improving the yield (Fig. 3). The derivative is apparently sensitive to impurities in the ketone, as the derivatives rapidly disappeared from the ketone solution when a small volume of the distillation residue was added to it. The nature of these components has not been studied.

The presence of water would in principle effect the reaction, as seen from the reaction formula (Fig. 1). Hwang *et al.*[19] reported for the reaction of some fluorogenic aldehydes with primary amines that it was essential to remove the water formed during the reaction. On the other hand, Schiff base formation from cyclohexanone and amphetamine in a two-phase system was possible[14]. The present Schiff base seemed to be insensitive to the presence of water up to at least 1.5 %, as the same yield was obtained as with the dried solvent (with less than 0.01 % of water (Fig. 3); see also the study of Bergel *et al.*[17] on amphetamine and acetone.

Stability of the derivative and reaction yield

As indicated above, the derivatives are prone to decomposition at elevated temperatures. At room temperature the stability was sufficient to allow storage in the

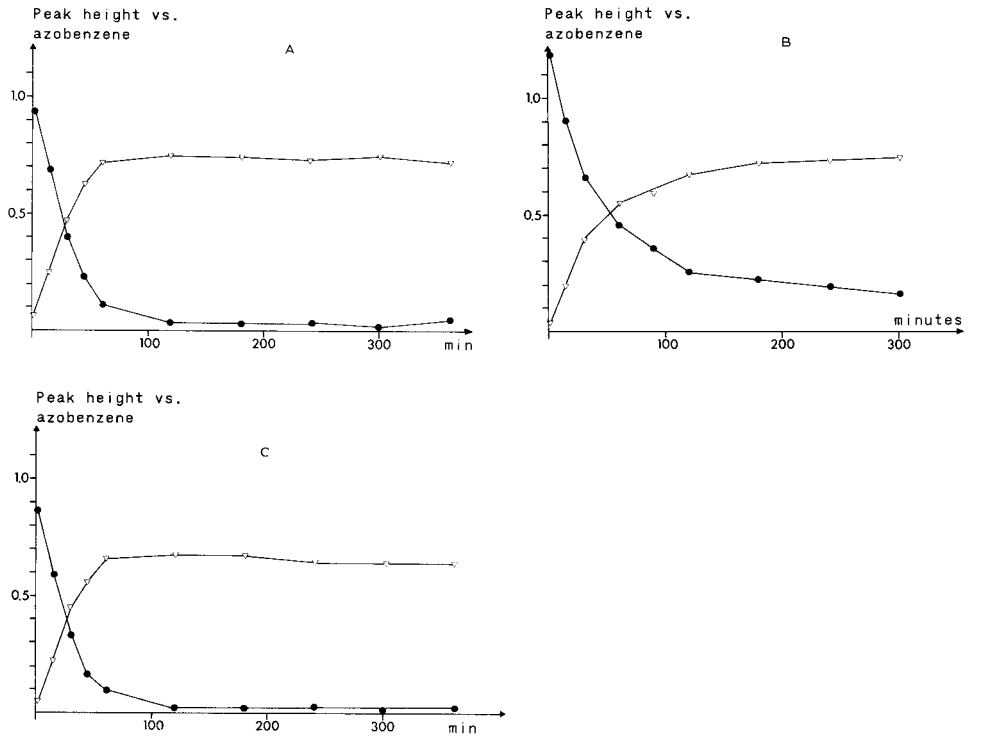

Fig. 4. Schiff base formation and disappearance of the primary amine at room temperature. (A) Tocainide (●) and its Schiff base (▽); (B) compound III (●) and its Schiff base (▽); (C) internal standard (II) (●) and its Schiff base (▽).

auto-injector cabinet for up to at least 24 h. Even if minor decomposition occurs this will not affect the quantitative evaluation as the internal standard used behaves similarly (see the peak-height ratios in Fig. 2B and C).

As soon as the ketone is removed from the reaction mixture or a dilution made with another solvent, reversal of the reaction begins[13]. The Schiff base from acetone and tocainide was available in crystalline form while the corresponding methyl isobutyl ketone derivative was an unstable oil. This makes it difficult to validate if the reaction is quantitative. A separate study (at room temperature) with some analogous compounds (see below) used chromatographic conditions more suitable for the free amine. This revealed that under the conditions employed the reaction yield is at least 95%, as less than 5% of the tocainide base was found (see Fig. 4A).

Reaction with structural analogues

Studies with four analogous compounds (Fig. 5) revealed some interesting differences (Fig. 4A–C). In these studies both the derivative and the intact primary amine were monitored. Only compound II reacted with the same profile as tocainide (I). Compound III, with an ethyl instead of a methyl group in the side-chain, reacted more slowly, whereas compound IV, lacking an alkyl substituent in that position, had a reactivity in between those of I and III. Compound V, with an additional methylene group attached to the amide carbonyl, was considerably less reactive than the other

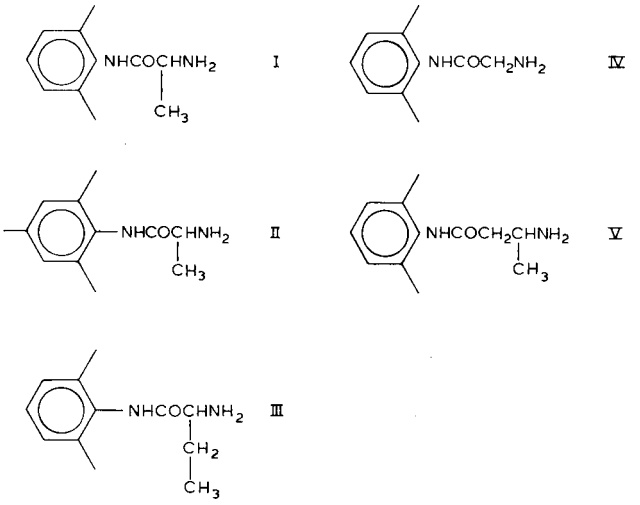

Fig. 5. Structural analogues. I, Tocainide (W 36095); II, internal standard H 155/73; III, W 36149; IV, W 49167; V, W 36196.

amines, despite its more basic nature (pK_a = 8.7) relative to tocainide (pK_a = 7.8)[19,20].

It is clear that an ideal internal standard should resemble tocainide in all respects around the functional group of interest for derivatization. Compound II, with an extra methyl group in the *p*-position, fulfilled this requirement and was the internal standard of choice. This will also be shown in other aspects below.

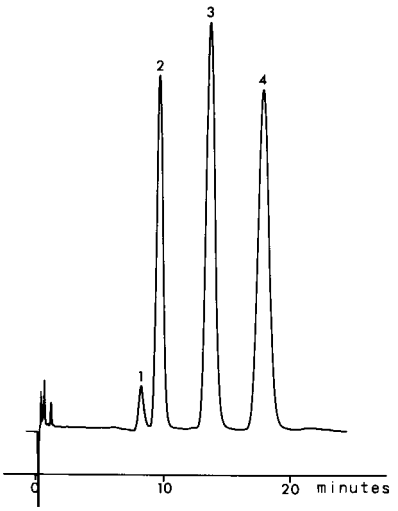

Fig. 6. Gas chromatogram from a derivatized extract of a patient's sample. 1 = Cotinine; 2 = tocainide Schiff base; 3 = internal standard Schiff base; 4 = caffeine.

TABLE I

RELATIVE RETENTIONS FOR THE COMPOUNDS STUDIED

For the structural formulas of the compounds, see Fig. 5.

Stationary phase	*Absolute retention of tocainide (min)*	*Relative retention**									
		Tocainide		*Internal standard*		*III*		*IV*		*V*	
		SB	*Base*	*SB*	*Base*	*SB*	*Base*	*SB*	*Base*	*SB*	*Base*
OV-17 (3%)	3.8	1.0	0.32	1.50	0.47	1.50	0.53	1.24	0.39	0.97	0.34
NP GSe (3%)	9.2	1.0	–**	1.29	–	2.16	–	1.40	–	1.22	–
OV-225 (3%)	5.4	1.0	0.57	1.42	0.76	1.70	0.98	1.39	0.72	0.96	0.65
Carbowax 20M (3%)	3.5	1.0	0.97	1.40	1.31	2.17	1.63	1.63	1.54	1.17	1.17
Carbowax 20M (10%)	18.9	1.0	0.92	1.42	1.29	2.03	1.57	1.52	1.43	1.10	1.14
Silar 5CP (3%)	2.6	1.0	0.77	1.42	1.04	1.88	1.46	1.58	1.12	1.00	0.92

* Relative retention *vs.* tocainide Schiff base (SB) with MIBK. All values refer to a column temperature of 190°C.

** The primary amine did not elute on this stationary phase.

TABLE II

EFFECT OF ADDITION OF HYDROXYLAMINE* TO PLASMA

Plasma sample (n = 5)	*Concentration of tocainide (μmol/l)*	*Peak height (arbitrary units)*						*Relative standard deviation of peak-height ratio (tocainide to internal standard) (%)*	
		Tocainide			*Internal standard*				
		Without hydroxylamine	*With hydroxylamine*	*Change (%)*	*Without hydroxylamine*	*With hydroxylamine*	*Change (%)*	*Without hydroxylamine*	*With hydroxylamine*
Spiked	3.4	3295	3605	+ 9	31715	35562	+12	3.1	2.3
	26.5	22954	24134	+ 5	31247	37568	+ 8	2.4	4.4
Patients' pooled	2.7	1679	1865	+11	33860	38790	+15	3.6	1.8
	25.3	20482	26413	+29	36431	43064	+18	5.3	1.4

* Final concentration of hydroxylamine in sample, 17.5 mmol/l.

Gas chromatography

The earlier documented excellent gas chromatographic performance of Schiff bases[13] was found for the derivatives in this study also (Fig. 6). Some stationary phases were studied with respect to their ability to separate tocainide, the internal standard and their Schiff bases. The results are given in Table I. Polar stationary phases are preferable to less polar ones such as OV-17, which shows some tailing of the base. Carbowax 20M (10%) was used in the method, as the other acceptable stationary phase, nitrogen-containing OV-225, used with the nitrogen-selective detector, showed much more noise. Silar 5CP did not show this behaviour. With the polyester stationary phase neopentylglycol succinate, the primary amine did not elute, probably owing to interaction with the carbonyl groups of the ester function.

The collector of the thermionic detector had a practical lifetime of about 1 month. At the end of this period the baseline began to drift and exhibited more noise.

The therapeutic levels of tocainide are within the range 10–30 μmol/l. It is possible to analyse this concentration without any difficulty with the present system as the limit of quantification is 0.5 μmol/l.

Extraction

Dichloromethane has been used as the extraction solvent in earlier studies with

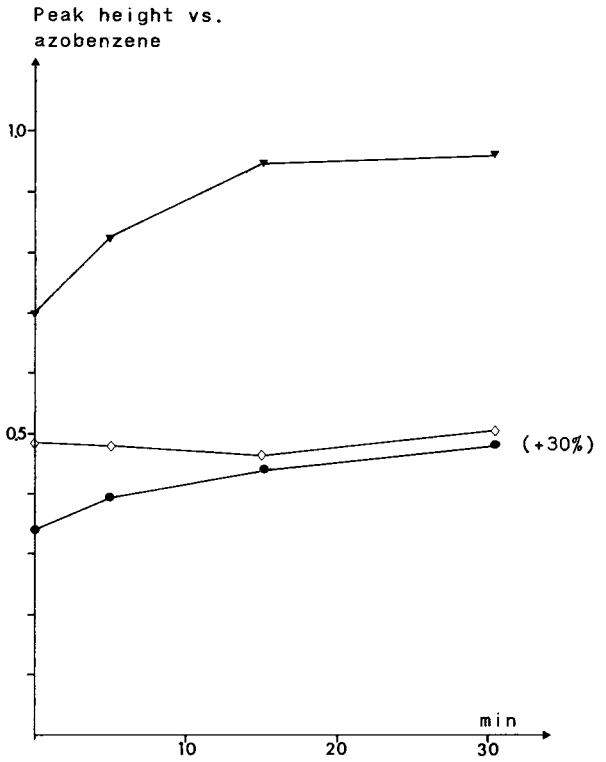

Fig. 7. Effect of time on the action of hydroxylamine. Conditions as under Experimental with 0.1 ml of hydroxylamine solution. ●, Tocainide Schiff base; ▼, internal standard Schiff base; ◇, peak-height ratio.

tocainide[2,4]. With a K_D value of 8 and a phase volume ratio (V_{org}/V_{aq}) of 3 the extraction yield is about 96%.

The quality of dichloromethane could sometimes affect the derivatization reaction in that a new compound appeared in the chromatogram. This was identified by gas chromatography–mass spectrometry as 3-(2,6-xylyl)-5-methylhydantoin. This cyclized compound, which is easily formed in a reaction with phosgene, has also been identified as a degradation product of a tocainide metabolite if the pH is raised above 12[21,22]. The presence of the extra peak was found only in dichloromethane that was not properly stabilized towards phosgene. The storage of the tocainide extracts is therefore not recommended. Smaller amounts of this by-product can be compensated for by the internal standard, which reacts in a similar way.

Applications to biological samples

The analysis of blank plasma samples spiked with tocainide differed from aqueous samples in that the recoveries were lower (80–95%). The reduction varied with samples of different origin. As the primary amine function might interact with endogenous compounds in the biological sample, the addition of a competing agent, hydroxylamine, was investigated. This resulted in recoveries that were comparable to those from pure aqueous solutions. The addition should preferably be made about 20 min before the sample is made alkaline and extracted (see Fig. 7). Again, the internal standard might compensate for minor differences between time zero and the alkalization (see the ratio of tocainide to internal standard in Fig. 7).

The results of a study of the effect of the addition of hydroxylamine to a spiked blank and to pooled patients' samples at two concentration levels are shown in Table

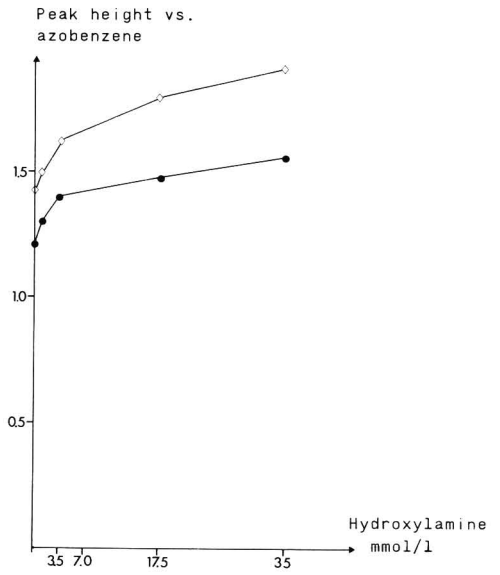

Fig. 8. Effect of final hydroxylamine concentration on the yield. Hydroxylamine acted for 30 min before extraction of the pooled patient sample. ◇, Tocainide Schiff base; ●, internal standard Schiff base.

II. The peak heights increase considerably by up to 30% for the high-level patients' samples. The amount of hydroxylamine needed was studied with a pooled patient plasma sample. From Fig. 8 it is evident that a final concentration up to 25 mmol/l increases the recoveries. In practice 17.5 mmol/l is used.

The addition of hydroxylamine also affected the repeatability of the results, especially for those from real patients' samples. Whereas aqueous and spiked samples analysed without any addition at the 25 μmol/l level had a relative standard deviation of 0.9 and 2.7%, respectively, the figure for a true biological sample at 10 μmol/l was as high as 14%. The relative standard deviation of the peak-height ratios obtained in the study shown in Table II demonstrates that the addition of hydroxylamine improves the precision for the real patients' plasma samples.

The observations on the effect of hydroxylamine imply that tocainide is present in the plasma samples not only in free form but also as a complex or a condensation product with some sample components. This resembles in a way what has been found for hydralazine, which reacts with pyruvic acid to give a hydrazone that can be co-determined under certain conditions[23,24].

With the present method the internal standard is added prior to the work-up procedure and is present during treatment with hydroxylamine. As can be seen in Fig. 7, even the absolute peak height of the internal standard increases during this treatment with the ratio between tocainide and the internal standard being almost constant. This indicates that the internal standard rapidly comes into equilibrium with the same components as tocainide and that the condensation products that they form are broken by the addition of hydroxylamine. It is not clear, however, why the patients' plasma samples differ from the spiked samples, as the latter are in fact equivalent to the way the internal standard is treated. Further studies are needed on this aspect.

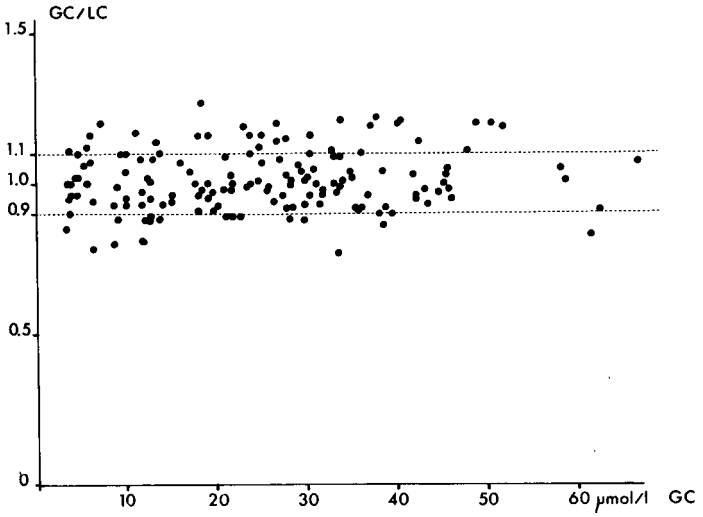

Fig. 9. Comparison of gas chromatographic (GC) and liquid chromatographic (LC) results. Mean value = 1.01; relative standard deviation = 10.1% (n = 160).

Validation of the method

The method has been used for the analysis of thousands of patients' samples with therapeutic concentrations in the range 10–30 μmol/l. The repeatability was evaluated for three levels, 50, 24 and 1.5 μmol/l, and was found to be 2.8, 3.7 and 10.7%, respectively ($n = 10$). The practical limit of quantitation for samples of 0.5 g is 500 nmol/l (corresponding to 0.1 μg/g) and one person can handle about 40 samples in a day.

The method has been compared with a liquid chromatographic assay[25]. The results agree fairly well within ±10% of the mean (see Fig. 9). The method has also been applied to urine samples.

With the use of this Schiff base no interferences were observed. However, as shown in Fig. 6, caffeine was often present in the samples, and sometimes also cotinine. The latter compound had a relative retention of 0.86 to tocainide.

ACKNOWLEDGEMENTS

We are indebted to Mr. Torsten Eklund for skilful assistance and to Dr. P.-O. Lagerström and Dr. B.-A. Persson for many stimulating discussions.

REFERENCES

1 D. Lalka, M. B. Meyer, B. R. Duce and A. T. Elvin, *Clin. Pharmacol. Ther.*, 19 (1976) 757–766.
2 R. Venkataramanan and J. F. Axelson, *J. Pharm. Sci.*, 67 (1978) 201–205.
3 P. J. Meffin, S. R. Harapat and D. C. Harrison, *J. Pharm. Sci.*, 66 (1977) 588.
4 E. M. Wolshin, M. H. Cavanaugh, C. V. Manion, M. B. Meyer, E. Milano, C. V. Reardon and S. M. Wolshin, *J. Pharm. Sci.*, 67 (1979) 1692–1695.
5 P. A. Reece and P. E. Stanley, *J. Chromatogr.*, 183 (1980) 109–114.
6 H. Brötell, *J. Chromatogr.*, 196 (1980) 489–493.
7 T. Walle and H. Ehrsson, *Acta Pharm. Suecica*, 7 (1970) 389–406.
8 T. Walle and H. Ehrsson, *Acta Pharm. Suecica*, 8 (1971) 27–38.
9 H. Brandenberger, in K. Blau and G. S. King (Editors), *Handbook of Derivatives for Chromatography*, Heyden, London, 1978, p. 234.
10 A. H. Beckett and M. Rowland, *J. Pharm. Pharmacol.*, 17 (1965) 59–60.
11 P. Capella and E. C. Horning, *Anal. Chem.*, 38 (1966) 316.
12 C. J. W. Brooks and E. C. Horning, *Anal. Chem.*, 36 (1964) 1540–1545.
13 W. J. A. VandenHeuvel, W. L. Gardiner and E. C. Horning, *Anal. Chem.*, 36 (1964) 1550–1560.
14 C. C. Clark, *J. Ass. Offic. Anal. Chem.*, 58 (1967) 1174–1177.
15 Y. Hoshika, *J. Chromatogr.*, 115 (1975) 596–601.
16 Y. Hoshika, *Anal. Chem.*, 49 (1977) 541–543.
17 F. Bergel, G. E. Lewis, S. F. D. Orr and J. Butler, *J. Chem. Soc.*, (1959) 1431.
18 E. Brochmann-Hanssen and A. Baerheim Svendsen, *J. Pharm. Sci.*, 51 (1962) 938–941.
19 T. K. Hwang, J. N. Miller, D. T. Burns and J. W. Bridges, *Anal. Chim. Acta*, 99 (1978) 305–315.
20 R. W. Layer, *Chem. Rev.*, 63 (1963) 489–510.
21 A. T. Elvin, J. B. Keenaghan, E. W. Byrnes, P. A. Tenthorey, P. D. McMaster, B. H. Takman, D. Lalka, C. V. Manion, D. T. Baer, E. M. Wolshin, M. B. Meyer and R. A. Ronfield, *J. Pharm. Sci.*, 69 (1980) 42–49.
22 R. Venkataramanan and J. E. Axelson, *Xenobiotica*, 11 (1981) 259–265.
23 S. B. Zak, G. Lukas and T. G. Gilleran, *Drug Metab. and Dispos.*, 5 (1977) 116–121.
24 K. D. Haegele, T. Talseth, H. B. Skrdlant, A. M. Shepherd and S. L. Huff, *Arzneim.-Forsch.*, 31 (1981) 357–362.
25 P.-O. Lagerström and B.-A. Persson, in preparation.

Journal of Chromatography, 239 (1982) 335–342
Elsevier Scientific Publishing Company, Amsterdam — Printed in The Netherlands

CHROM. 14,552

DETERMINATION OF PICOMOLE AMOUNTS OF CHOLINE AND ACETYLCHOLINE IN BLOOD BY GAS CHROMATOGRAPHY–MASS SPECTROMETRY EQUIPPED WITH A NEWLY IMPROVED PYROLYZER

YOSHIKAZU HASEGAWA, MINEO KUNIHARA and YUJI MARUYAMA*
Japan Upjohn Research Laboratories, 168 Ohyagi-Machi, Takasaki-Shi, Gunma 370 (Japan)

SUMMARY

Blood levels of choline (Ch) and acetylcholine (ACh) have previously not been confirmed because of the difficulty in measuring these compounds. In this paper a recently developed method for the assay of Ch and ACh, which employs a chemical ionization (isobutane) quadrupole mass spectrometer (JEOL QH 100) equipped with a new type of pyrolyzer is reported. The correlation between the mass fragmentogram peak ratios and the amounts of compounds was good from 0.5 to 4 pmol. The assay limit for quantitation was *ca.* 0.3 pmol for Ch and ACh. The values for Ch from rat whole blood, serum and red blood cells were 10.88 ± 1.46, 6.72 ± 1.02 and 4.56 ± 0.53 nmol/ml, respectively, and for ACh the respective values were 3.56 ± 0.86, 1.69 ± 0.16 and 1.87 ± 0.83 nmol/ml. In human whole blood the levels of Ch and ACh were 22.55 ± 3.97 and 3.23 ± 0.23, respectively.

INTRODUCTION

A major obstacle in clarifying the neurophysiological role of choline (Ch) and acetylcholine (ACh) has been the delay in the development of a simple assay method, even though the role of ACh as a neurotransmitter was demonstrated more than 50 years ago. Among the large number of analytical methods, gas chromatographic (GC) and GC–mass spectrometric (MS) techniques have been essential for use in the accurate estimation of neurotransmitters in biological specimens, as described in a previous report[1]. Specifically, pyrolysis–GC (Py–GC) and Py–GC–MS procedures, principally based on the method of Szilagyi *et al.*[2] and other investigators (3–6) have provided excellent accuracy, sensitivity and reproducibility for these measurements. We have been working on these assay methods for *ca.* 10 years, with the results being an improved method which has been applied to the measurement of picomole amounts of Ch and ACh in blood. The levels of these compounds in blood have previously been determined by several investigators, but the results have not been in good agreement. In this paper, this recently developed method for the assay of Ch and ACh in rat and human blood, incorporating a new type of Py–GC chemical ionization (isobutane) quadrupole MS with hyperbolic rods is reported. In addition, a newly improved type of pyrolyzer for the demethylation reaction has been used to produce the volatile derivatives.

0021-9673/82/0000–0000/$02.75

MATERIALS AND METHODS

Materials

Animals. Male Sprague-Dawley rats were obtained from Nihon Clea and housed two per cage. The lights were automatically turned on at 8:00 a.m. in a 12-h light–dark cycle.

Chemicals. All the common chemicals employed were reagent grade, obtained from either Wako (Tokyo, Japan) or Sigma (St. Louis, MO, U.S.A.). Propionyl chloride was purchased from Tokyo Kasei (Tokyo, Japan).

Apparatus

Pyrolyzer. The pyrolyzer, a Model PYR-MS, was developed as a result of cooperative efforts between Kotaki Shoji (Tokyo, Japan) and the authors' group. The pyrolyzing system consists of three parts: the filament holder, the switching connector and the power source. The pyrolyzing system is designed to be applicable to most types of gas chromatograph, and does not allow flash-back of the carrier gas to occur during the procedure of inserting or removing the filament holder. This technique is successfully carried out by means of a switching connector, as shown in Fig. 1. For this method a few microliters of sample are placed on a filament which is made of 80% platinum and 20% rhodium, as described in the previous report[1]. The filament is either V-shaped or in the form of a coil to allow the sample to be placed at the point of maximum heating. After evaporation of the solvent, using the proper conditions set on the power supply, the filament holder is attached to the switching connector using the screw holder, while keeping the switch closed. Then, the switch is opened and the filament holder is inserted into the end of the holder so that the top of the filament sits immediately in front of the column in the gas chromatograph. The duration of pyrolysis and the amount of current utilized are adjustable on the power source. The temperature of the filament at a particular setting of the power source was determined by employing a 0.3-mm chromel–alumel thermocouple welded to the filament of the pyrolyzer. The resultant electromotive force was recorded as the filament was heated and the values were converted to temperature by use of "Chart of Electromotive Force of Chromel–Alumel Thermocouple".

Mass spectrometer. Mass spectral studies were accomplished using a JMS-QH100 gas chromatograph– chemical ionization (CI) quadrupole mass spectrometer which was recently developed as a result of cooperative efforts between Japan Elec-

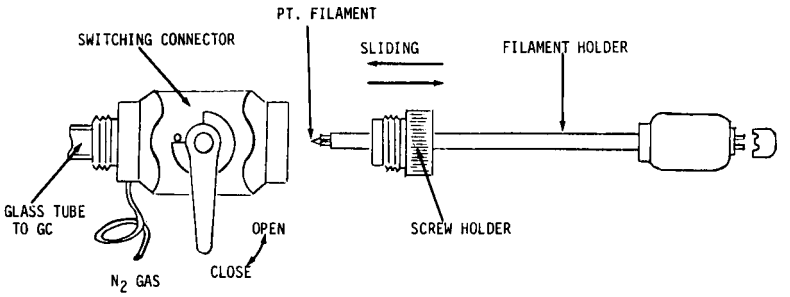

Fig. 1. Diagram of pyrolyzer showing parts of switching connector and filament holder. Explanation is given in the Materials and methods section.

tron Optics Laboratory and the authors' group. This instrument is primarily designed to provide accurate and rapid quantitation of organic compounds, particularly those derived from biological specimens. The resolution of this mass spectrometer, 1600 ($M/\Delta M_{1/2}$) at m/z 800, is accomplished by utilizing large diameter hyperbolic rods for the quadrupole mass analyzer. A single ion source for CI is used. For CI operation one of three kinds of reagent gases can be alternatively selected within 20 sec. For control of the system, three 16-bit microcomputers function in individual modes. The first one is designed to control the opening and the closing of the solvent valve and for adjusting the temperatures of the GC, the GC–MS interface and the ion source. The second computer is mainly used for monitoring ions for mass fragmentographic analyses. The last computer is designed for processing of PFK calibration, normalization of mass signals, background subtraction and quantitative calculations using peak height or peak area values from the mass fragmentograms. The analysis time is divided into three blocks for each injection, so that the four channels which are employed in each block for mass fragmentography permit the selection of twelve different ions over the entire scan. These operations are controlled by real-time dialogic communication between the computers and an operator via a display screen and keyboard. For the measurements described in this paper the ion energy was 7.5 V with an ionizing voltage of 250 eV and ionizing current of 300 μA. Isobutane was used as the reagent gas for CI and was maintained at a pressure of 0.9–1.1 Torr.

Gas chromatograph. The gas chromatograph was attached to the mass spectrometer was equipped with a glass column (1.0 m × 3 mm I.D.) packed with 5% OV-101 and 5% dodecyldimethylenetriamine succinamide (Jenden Phase) on 80–100 mesh Gas-Chrom Q (Applied Science Labs., State College, PA, U.S.A.). The carrier gas was helium for the GC–MS studies, with a flow-rate of 30 ml/min. The temperature of the column was 169°C, the injection port and the interface were 180°C and the ion source was 170°C.

Methods

Extraction procedure. Rat blood was collected from the tail vein by means of a glass pipetter. Human blood was drawn from the cephalic vein. The blood sample (200 μl) was transferred to a glass tube (100 × 15 mm) which contained 5 μl of 3 m*M* [$^2H_9$]ACh as an internal standard and 0.3 ml of 2 m*M* physostigmine. After addition of 1 ml of 0.4 *N* perchloric acid the mixture was stirred vigorously to effect protein denaturation. After centrifugation at 1500 *g* at room temperature for 10 min the supernatant was adjusted to pH 4.0 with 7.4 *N* potassium acetate. The sample was centrifuged again at 1500 *g* at room temperature for 5 min and the supernatant was washed with ether. The remaining aqueous phase was lyophilyzed. The residue was treated with propionyl chloride to form the propionyl ester of choline and further purified by the procedure which is outlined in Fig. 2. This method has previously been reported as an improved propionylation procedure for the simultaneous assay of endogenous Ch and ACh[1].

Assay for ACh-esterase activity in blood. AChE activity was measured by the spectrophotometric method of Ellman *et al.*[7].

RESULTS

Pyrolysis conditions for ACh, propionylcholine (PCh) and butyrylcholine (BCh)

In order to determine the optimum pyrolysis conditions for ACh, PCh (to be

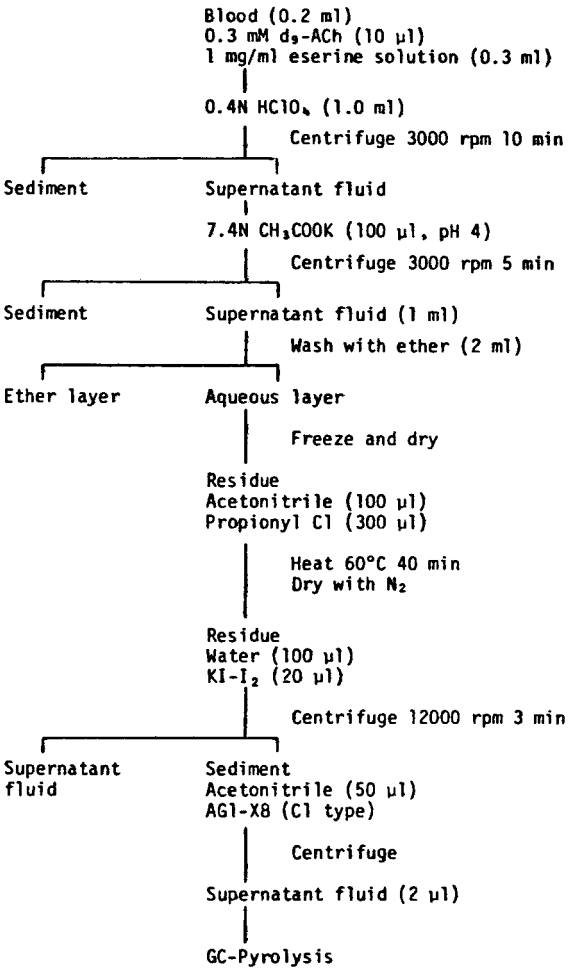

Fig. 2. Flowsheet for simultaneous extraction procedure of choline and acetylcholine from rat and human blood.

derived from Ch) and BCh (to be used as an internal standard for GC assays), the relationship between the peak heights of the pyrolyzed compounds and the filament temperature was ascertained, as shown in Fig. 3. Rapid and effective demethylation of the three compounds was accomplished by supplying 2.5 A for 7.5 sec. The temperature of the filament which produced the maximum peak height was 216°C.

Mass fragmentograms and standard curves for ACh and PCh

The ions at *m/z* 132, 138 and 146, corresponding to M + 1 for demethylated ACh, deuterated ACh ($^2H_9$, the internal standard for MS analyses) and PCh were used. As shown in Fig. 4, these substances eluted within one minute for standards and blood samples. The peak height ratios of standard ACh and PCh to [$^2H_9$] ACh were automatically calculated following the scan of the selected ions, providing the standard curves for ACh and PCh. An excellent correlation between the peak height ratio

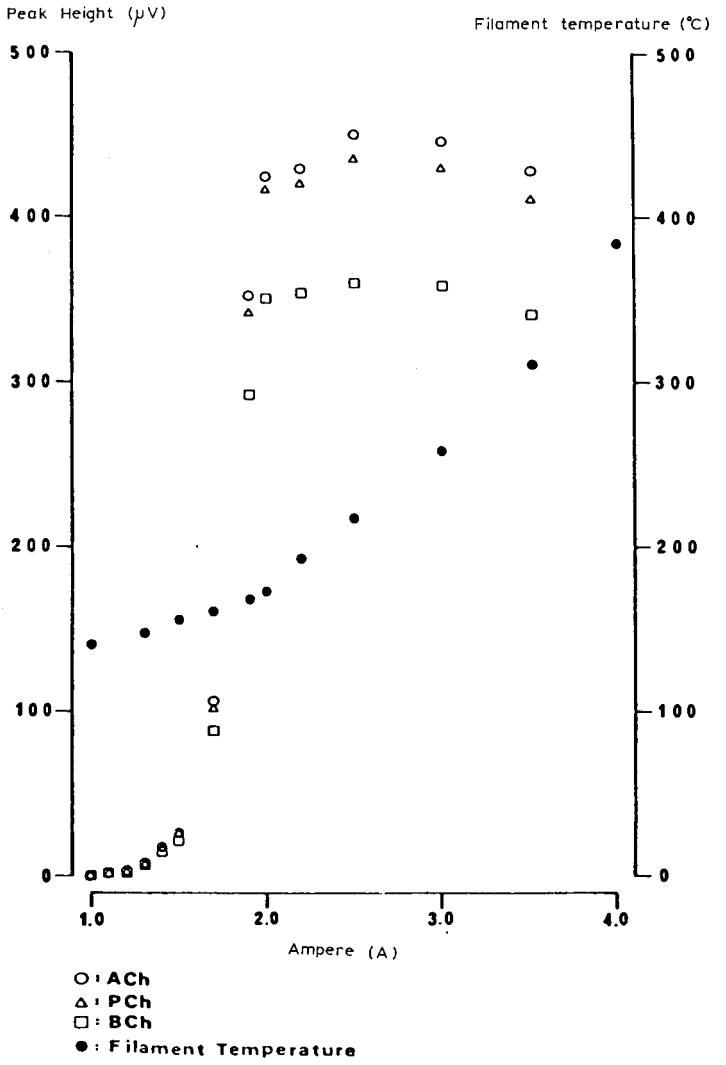

Fig. 3. Effect of temperature and current on demethylation of esters of choline.

and compound amount was obtained, with correlation coefficients of 0.9998 for ACh and 0.9991 for PCh found, as shown in Fig. 5. Linearity was seen in the range 0.5–4.0 pmol, with no significant changes in sensitivity observed for either compound. The assay limit for quantitation was *ca.* 0.3 pmol for ACh and PCh. To test the applicability of this method for assaying endogenous compounds, blood samples were spiked with various amounts of each standard and assayed by pyrolysis GC–MS. The results were parallel to the standard curves. Clear linearity was again obtained, with correlation coefficients of 0.9997 for ACh and 0.9946 for PCh being calculated.

Total recovery from rat blood

The efficiency of the assay being described was examined by studying the re-

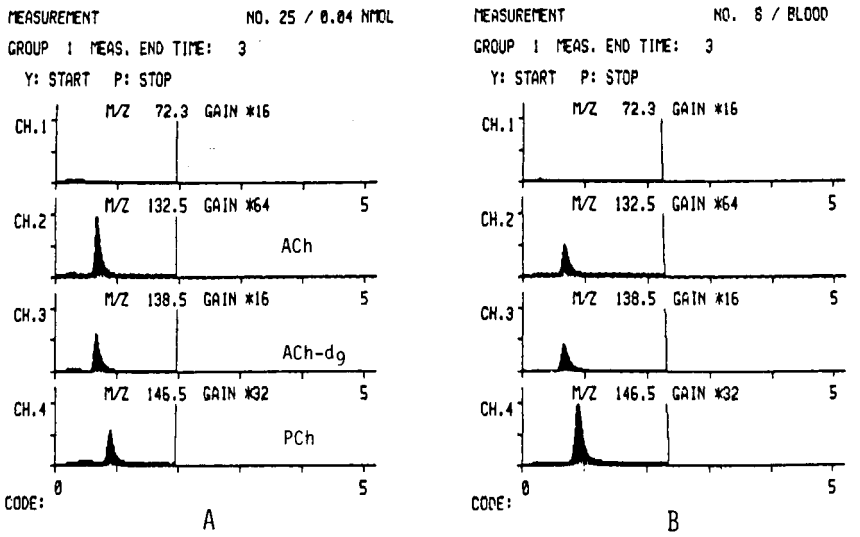

Fig. 4. Mass fragmentogram (A) of standard acetylcholine (ACh), [$^2H_9$]acetylcholine ([$^2H_9$]ACh), and propionylcholine (PCh) compared to the mass fragmentogram (B) of blood with added [$^2H_9$]ACh. The choline in the sample was propionylated.

covery of Ch and ACh added to blood. The results of the experiment are shown in Table I. The total recovery of Ch and ACh through this procedure ranged from 98.3 to 114.3%.

Levels of Ch and ACh in rat and human blood

The levels of ACh and Ch measured by this method in rat whole blood, serum and red blood cells, and in human whole blood are shown in Table II. The value of Ch and ACh in rat red blood cells was obtained by subtracting the levels found in serum from those found in whole blood.

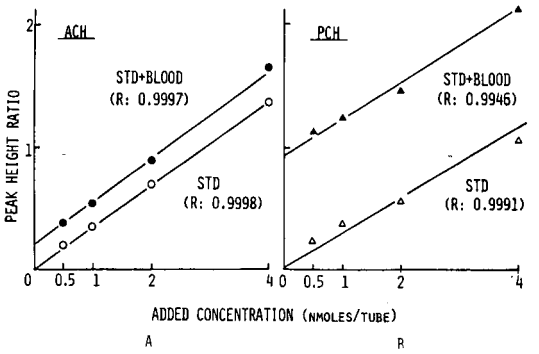

Fig. 5. (A) Calibration curves for standard ACh and standard ACh plus blood. (B) Calibration curves for standard PCh and standard PCh plus blood.

TABLE I

TOTAL RECOVERY OF CHOLINE AND ACETYLCHOLINE FROM BLOOD

Choline and acetylcholine were added to blood and extracted in the manner shown in Fig. 2. The values (nmol/ml) represent the mean ± S.E. from three determinations.

	Blood	*Std. (1 nmole)*	*Blood ± std (theorectical)*	*Blood ± std (measured)*	*Recovery (%)**
ACh/[$^2H_9$]ACh	0.119 ± 0.003	0.355 ± 0.030	0.474 ± 0.029	0.545 ± 0.041	114.3 ± 12.02
PCh/[$^2H_9$]ACh	0.973 ± 0.077	0.299 ± 0.028	1.273 ± 0.094	1.237 ± 0.017	98.3 ± 7.96

$$\star \text{ Recovery} = \frac{\text{blood + std. (measured)}}{\text{blood + std. (theoretical)}} \times 100. \quad n = 3.$$

TABLE II

CHOLINE AND ACETYLCHOLINE LEVELS IN RAT AND HUMAN BLOOD

Values expressed as mean ± S.E. and figure in parentheses shows number of animals. Results of human blood were obtained from three determinations for each sample.

		Ch (nmol/ml)	*ACh (nmol/ml)*	*Ch/Ach (nmol/ml)*
Rat (n = 3)	Whole blood	10.88 ± 1.46	3.56 ± 0.86	3.68 ± 1.29
	Serum	6.72 ± 1.02	1.69 ± 0.16	3.74 ± 0.86
	Red blood cells	4.56 ± 0.53	1.87 ± 0.83	4.56 ± 2.72
Human whole blood	1	45.95 ± 0.25	4.58 ± 0.11	10.04 ± 0.29
	2	17.97 ± 0.35	2.96 ± 0.05	6.03 ± 0.36
	3	11.11 ± 0.11	2.81 ± 0.05	3.96 ± 0.15
	4	15.16 ± 0.23	2.57 ± 0.07	5.85 ± 0.12

DISCUSSION

A newly developed pyrolyzer which prevents flash-back of carrier gas during the application of the sample on the filament has been connected to a GC–MS designed for rapid and effective measurement of relatively low molecular weight (m/z 800 maximum) organic compounds. In this study, [$^2H_9$]ACh was used as an internal standard for analysis of Ch and ACh. No transacylation was observed under the present conditions. With this equipment at least 30 samples can be processed per day by well-trained laboratory technicians.

Systematic studies have not been reported regarding changes in blood levels of Ch and ACh which occur during the isolation and purification of the samples. In our experiments there were significant changes in the blood levels of Ch and ACh when human blood was drawn from the cephalic vein and left at room temperature for 30 sec. Stavinoha *et al.*[8] have reported that an increase in ACh of up to 6.05 ± 1.36 nmol/ml was observed 1 min after intravenous infusion of the compound. The level returned to the original control value by 15 min. Unlike our assay method, Stavinoha *et al.* do not add AChE inhibitors to the blood. To examine the necessity for rapid inactivation of AChE prior to measurement of Ch and ACh in blood, the activity of

this enzyme in rat and human blood was determined and found to be 2.78 μmole/ml · min for human blood and 0.485 μmole/ml/min for rat blood. The data suggested that ACh in human blood can be hydrolyzed six times faster than in rat blood. Theoretically 465 nmole of ACh could be hydrolyzed in human blood per second at room temperature as the maximum figure from the *in vitro* study. This indicates the importance of rapid inactivation of the enzyme before assaying for Ch and ACh in blood.

The levels of Ch and ACh assayed in human blood by our method were 10–200 times higher than those given in Hanin *et al.*'s review[9]. In addition, the mean of the ratio between Ch and ACh in human blood was 57 times higher in our study than that of plasma reported in his chapter. Our measurements of Ch and ACh levels were relatively close to those in Stavinoha's recent report[10].

In summary, the presence of Ch and ACh in rat and human whole blood was clearly confirmed by a newly developed type of Py–GC–MS analysis. The levels of Ch and ACh in the blood were significantly higher than those reported by most other scientists.

REFERENCES

1 Y. Maruyama, M. Kusaka, J. Mori, A. Horikawa and Y. Hasegawa, *J. Chromatogr.*, 164 (1979) 121.
2 P. I. A. Szilagyi, D. E. Schmidt and J. P. Green, *Anal. Chem.*, 40 (1968) 2009.
3 D. J. Jenden, R. A. Booth and M. Roch, *Anal. Chem.*, 44 (1972) 1879.
4 W. B. Stavinoha and S. T. Weintraub, *Anal. Chem.*, 46 (1974) 757.
5 I. Hanin and R. F. Skinner, *Anal. Biochem.*, 66 (1975) 568.
6 Y. Maruyama, W. B. Stavinoha and E. Hosoya, *Rinshokagaku*, 4 (1975) 42.
7 G. L. Ellman, K. D. Courtney, V. Anders, Jr. and R. M. Featherstone, *Biochem. Pharmacol.*, 7 (1961) 88.
8 W. B. Stavinoha, D. Lin and T. Modak, *8th International Congress of Pharmacology, July, 1981, Tokyo*, Abstract No. 1775, p. 757.
9 I. Hanin, U. Kopp, N. R. Zahniser, T.-M. Smith, D. G. Spiker, J. R. Merikangas, D. J. Kupfer and F. H. Foster, in S. J. Jendan (Editor), *Cholinergic Mechanisms and Psychopharmacology, (Advances in Behavioral Biology*, Vol. 24), Plenum, New York, London, 1977, p. 181.
10 W. B. Stavinoha, A. T. Modak and C. L. Bowden, *17th Annual Meeting of Neuroscience, September, 1977, Anaheim, U.S.A.*, Abstract.

Journal of Chromatography, 239 (1982) 343–349
Elsevier Scientific Publishing Company, Amsterdam — Printed in The Netherlands

CHROM. 14,641

QUANTIFICATION OF ENDOGENOUS ALIPHATIC ALCOHOLS IN SERUM AND URINE

H. M. LIEBICH*, H. J. BUELOW and R. KALLMAYER
Medizinische Universitätsklinik, Otfried-Müller-Strasse 10, 7400 Tübingen (G.F.R.)

SUMMARY

The endogenous aliphatic alcohols ethanol, *n*-propanol, *n*-butanol, isobutanol and isopentanol in serum and urine were measured by gas chromatography–mass fragmentography. Whereas for the higher-molecular-weight alcohols extraction with dichloromethane is used, ethanol is determined by direct injection of serum and urine.

When zero is assigned to all values below the detection limits of the procedures (0.1 mg/l for ethanol and 2 μg/l for each of the higher-molecular-weight alcohols), the following normal ranges are found: ethanol, 0–39 mg/l in serum and 0–46 mg per 24 h in urine; *n*-propanol, 0–48 μg/l in serum and 0–300 μg per 24 h in urine; *n*-butanol, 0–20 μg/l in serum and 0–18 μg per 24 h in urine. The isobutanol and isopentanol levels in the serum and urine of normal subjects are below the detection limit. For diabetic patients, on average increased levels are found for ethanol, *n*-propanol and *n*-butanol in serum and urine.

INTRODUCTION

Primary aliphatic alcohols of endogenous origin have been detected in blood serum and urine within the gas chromatographic (GC) profile of low-molecular-weight and volatile components in these fluids[1–5]. The occurrence of endogenous ethanol in blood has long been known. Bücher and Redetzki[6] determined ethanol quantitatively in the serum of normal individuals and diabetics using the alcohol dehydrogenase method. Higher-molecular-weight endogenous alcohols have not been studied. In the presence of ethanol they cannot be quantified separately by enzymatic methods because of their cross-reactions with ethanol.

Several GC procedures have been developed for the quantitative determination of ethanol involving distillation, extraction, direct injection or headspace techniques. Of these, direct injection[7,8] and headspace analysis[9,10] are the favoured methods. In general, the GC methods are suitable for quantifying other volatile substances such as acetaldehyde, *n*-propanol and isopropanol in addition to ethanol[11,12]. However, all of the existing GC methods have been applied only to the quantification of ethanol after consumption of alcoholic beverages or to some higher-molecular-weight alcohols from exogenous sources in conjunction with intoxication.

Interferences from other constituents in serum and urine and the low concen-

0021-9673/82/0000–0000/$02.75

trations of the alcohols, especially of the higher-molecular-weight ones, are the reasons why GC methods cannot be applied satisfactorily to the quantification of endogenous alcohols. In this paper two methods are described for the quantitative determination of endogenous ethanol and endogenous higher-molecular-weight alcohols, taking advantage of the high specificity and sensitivity of mass fragmentography (MF).

EXPERIMENTAL

Serum and urine samples

Serum and urine samples were collected from normal individuals, from hospital patients without obvious metabolic defects and from diabetic patients who had abstained from drinking alcoholic beverages for 3 days before sample collection. Serum was obtained from venous blood by centrifugation for 10 min at 1600 *g*. Urine was collected for 24 h.

Apparatus

The GC–MF determinations were performed on a combination of a Model 2700 gas chromatograph and a CH 5 mass spectrometer (Varian-MAT, Bremen, G.F.R.) interfaced with a 30 cm × 0.1 mm I.D. platinum capillary.

Determination of ethanol in serum and urine

Ethanol was determined by direct injection of a serum or urine sample.

To 0.5 ml of serum or urine 2 μl of internal standard (50 μl of diethyl ether in 100 ml of distilled water) were added. The mixture was thoroughly shaken and 1 μl was analysed by GC–MF under the conditions described in Table I.

TABLE I

GAS CHROMATOGRAPHIC–MASS FRAGMENTOGRAPHIC CONDITIONS

Parameter	*Value*	*Parameter*	*Value*
Column	100 m × 0.5 mm I.D. stainless steel, coated with Emulphor ON-870	Electron energy of ion source	70 eV
		Accelerating voltage	3 kV
		Ion source temperature	220°C
Column temperature:		Interface temperature	220°C
For ethanol	65°C	Resolution	400
For higher-molecular-weight alcohols	70°C	Emission current	300 μA
		Multiplier voltage	3 kV
Injector block temperature	150°C	Specific ion	*m/e* 31
Carrier gas	Helium at 4 ml/min		

The water from the directly injected serum or urine sample was by-passed between the outlet of the GC column and the interface, *i.e.*, after its separation from the ethanol to be measured, by using a system of a T-connection and two valves (Kontron-Technik, Eching, G.F.R.), located inside but operated from outside the oven. All connections were 1/16 in. Two normal valves and a T-connection were used instead of a three-way valve because they had a low dead volume and because they

were found to perform well with respect to thermal stability and tightness. After the elution of the ethanol, the effluent of the column was by-passed by turning the valves. The gas flow into the ion source was shut off for 9 min, during which time the elution of the water was completed. Then the valves were turned back into the flow-through position, and the system was ready for the next analysis.

The calculation of the ethanol concentration was based on the ratio of the peak heights of ethanol and internal standard and on a calibration graph obtained from four aqueous standard solutions with ethanol concentrations between 0.16 and 79 mg/l.

Determination of higher-molecular-weight alcohols in serum and urine

The higher-molecular-weight alcohols *n*-propanol, *n*-butanol, isobutanol and isopentanol were determined after extraction from serum or urine.

To 1 ml of serum or urine 4 μl of internal standard (25 μl of 2-buten-1-ol in 100 ml of distilled water) were added. The mixture was extracted with 1 ml of dichloromethane by shaking for 1 min. After aspiration of the supernatant aqueous phase, the organic phase was concentrated to a volume of approximately 50 μl under a stream of nitrogen. A 1-μl volume of the concentrated extract was analysed by GC–MF under the conditions described in Table I.

The calculation of the concentrations of each alcohol was based on the ratios of the peak heights of the alcohols and the internal standard and on calibration graphs for each alcohol obtained from four aqueous standard solutions with alcohol concentrations between 10 and 320 μg/l.

RESULTS AND DISCUSSION

Specificity of the methods

The quantitative determination of ethanol, *n*-propanol, *n*-butanol, isobutanol and isopentanol by GC–MF uses the ion of *m/e* 31, corresponding to the fragment $H_2C=\overset{+}{O}H$, as the specific ion. The ion is characteristic of primary aliphatic alcohols and gives the procedure satisfactory specificity. The only endogenous substance with certain interference in the determination of ethanol is isopropanol. Under the experimental conditions described it was not separated from ethanol. However, in urine isopropanol was present in only trace amounts, and in serum its concentration was estimated to be approximately one tenth of that of ethanol. Further, because of the low intensity of the *m/e* 31 fragment in isopropanol, its detection sensitivity was only 5% of that of ethanol. For the higher-molecular-weight alcohols no interfering substances were observed.

Sensitivity and precision of the method

The detection limits of the procedures were 0.1 mg/l for ethanol and 2 μg/l for each of the higher-molecular-weight alcohols. The coefficients of variation were 5% for ethanol (at a concentration of 1.7 mg/l) and 10% for the other alcohols (at a concentration of 15 μg/l).

Practicability of the methods

Both methods are characterized by their simplicity, which is a particularly

significant factor in the quantification of ethanol. The method of direct injection of 1 μl of serum or urine after the addition of the internal standard, avoids any sample work-up procedure. The basic requirement for the method is the valve system for by-passing the water, which otherwise would cause irreproducible decreases in sensitivity.

For the higher-molecular-weight alcohols the extraction method gave better results than the direct injection procedure, because by-passing the water interferes with the elution of the alcohols, especially of *n*-propanol, and because owing to their low concentrations these alcohols require a concentration step.

For the ethanol determination the time between two injections was approximately 18 min, half of which was necessary for the elution of the water (Fig. 1). For the determination of all four higher-molecular-weight alcohols the corresponding time was only 12 min (Fig. 2) because overlapping injections were possible.

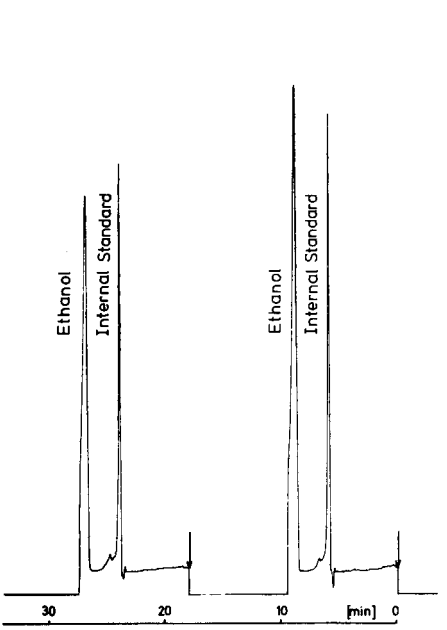

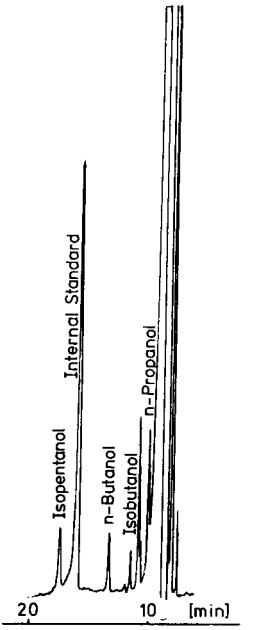

Fig. 1. Mass fragmentograms of subsequent measurements of ethanol in two urine samples, *m/e* 31. The decreases in the baseline after the ethanol peaks are caused by the by-passing of the water.

Fig. 2. Mass fragmentogram of a measurement of *n*-propanol, *n*-butanol, isobutanol and isopentanol in a diabetic urine sample, *m/e* 31.

The primary alcohol 2-buten-1-ol is a suitable internal standard for the quantification of the higher-molecular-weight alcohols. It is well separated from the four alcohols to be determined and, owing to its chemical structure, its behaviour during the work-up procedure is similar to that of the alcohols. Less similar is the structure of diethyl ether in the ethanol quantification. However, as no work-up procedure is involved, diethyl ether is acceptable as an internal standard.

TABLE II

ETHANOL IN SERUM AND URINE

Sample	*Group*	*Number of samples (n)*	*Range (mg/l)*	*Mean value (mg/l)*
Serum	Control subjects	42	0– 39	6.6
	Diabetic patients	168	0–159	10.0
			Range (mg per 24 h)	*Mean value (mg per 24 h)*
Urine	Control subjects	57	0– 46	7.2
	Diabetic patients	247	0–484	19.8

Ethanol in serum and urine

In the control group consisting of healthy individuals and hospital patients without obvious metabolic defects, the ethanol concentrations in 42 serum samples ranged from 0 to 39 mg/l and in 57 urine samples from 0 to 46 mg per 24 h. Values below the detection limit of the described quantification procedure, *i.e.*, below 0.1 mg/l, are reported as zero. By GC profile analysis[2,3,5], which uses much larger sample volumes, it has been shown that the ethanol concentration in serum and urine is always different from zero.

In the group of diabetic patients, the range of ethanol concentrations was much greater than that in the control group, in some instances by a factor of up to 10.

The results are summarized in Table II. They show that in the group of the diabetics, extreme concentrations of ethanol occurred, and that with regard to the mean values, the concentration of ethanol in serum and the excretion of ethanol in urine were increased compared with the control group. On the other hand, normal levels and levels below the detection limit were also observed in some diabetics. Fig. 3

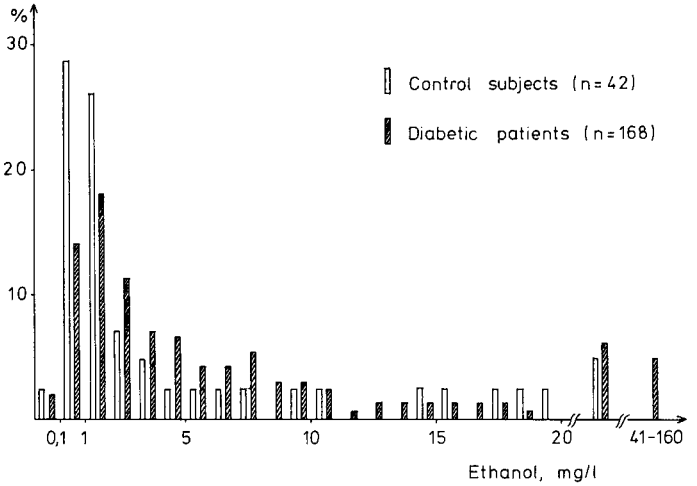

Fig. 3. Distribution curve of ethanol in sera of control subjects and diabetic patients.

shows considerable overlap of the distribution curves of the ethanol concentrations in the serum of the control subjects and the diabetic patients. A similar behaviour was observed for ethanol in urine. The highest ethanol levels observed in serum were *ca.* 160 mg/l, corresponding to 0.16 per 1000.

High-molecular-weight alcohols in serum and urine

In the control group the *n*-propanol concentrations were in the ranges 0–48 μl/l and 0–300 μg per 24 h, respectively, and the *n*-butanol concentrations were in the ranges 0–20 μg/l and 0–18 μg per 24 h, respectively. The isobutanol level was zero, *i.e.*, below the detection limit of the procedure, in all serum samples ($n = 44$) and urine samples ($n = 64$) of the control group. In the same samples the isopentanol level was found to be above the detection limit in only a few instances.

In the group of diabetic patients in many instances elevated levels of *n*-propanol (Table III) and *n*-butanol (Table IV) were found in serum and urine. Also, the mean values were increased in comparison with the control group. As with ethanol, the biological range of *n*-propanol and *n*-butanol concentrations in diabetics was very wide (Figs. 4 and 5).

TABLE III

n-PROPANOL IN SERUM AND URINE

Sample	*Group*	*Number of samples (n)*	*Range (μg/l)*	*Mean value (μg/l)*
Serum	Control subjects	43	0– 48	8
	Diabetic patients	173	0–226	17
			Range (μg per 24 h)	*Mean value (μg per 24 h)*
Urine	Control subjects	63	0–300	24
	Diabetic patients	245	0–960	47

TABLE IV

n-BUTANOL IN SERUM AND URINE

Sample	*Group*	*Number of samples (n)*	*Range (μg/l)*	*Mean value (μg/l)*
Serum	Control subjects	44	0– 20	6
	Diabetic patients	167	0–180	8
			Range (μg per 24 h)	*Mean value (μg per 24 h)*
Urine	Control subjects	64	0– 18	0
	Diabetic patients	246	0–320	10

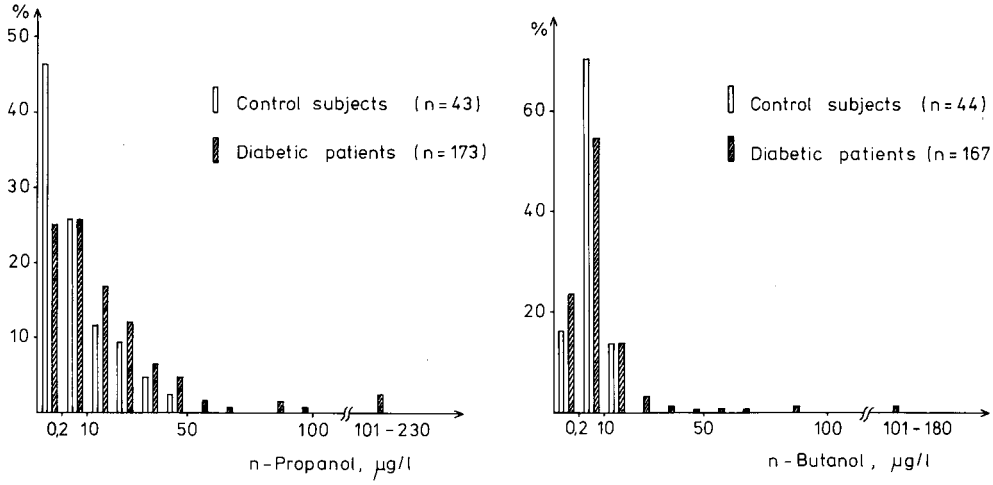

Fig. 4. Distribution curve of *n*-propanol in sera of control subjects and diabetic patients.

Fig. 5. Distribution curves of *n*-butanol in sera of control subjects and diabetic patients.

The methyl-branched alcohols isobutanol and isopentanol showed elevated levels less frequently. These alcohols were studied mainly in urine. Proceeding on the observation that in the control group the excretion of isobutanol and isopentanol was below the detection limit, in a group of 138 diabetics 45 patients (32%) showed a measurable excretion of isobutanol and 38 patients (28%) a measurable excretion of isopentanol. When, however, of the total group of diabetics only the group of patients with proved diabetic complications ($n = 37$) was considered, it was found that in 28 patients (76%) the excretion of isobutanol and in 30 patients (81%) the excretion of isopentanol were increased. When the levels of methyl-branched alcohols were high, normally also the excretion of ethanol, *n*-propanol and *n*-butanol was increased. The presence of isobutanol and isopentanol can be considered to be an indication of the existence of diabetic complications.

REFERENCES

1 A. Zlatkis, W. Bertsch, H. A. Lichtenstein, A. Tishbee, F. Shunbo, H. M. Liebich, A. M. Coscia and N. Fleischer, *Anal. Chem.*, 45 (1973) 763.
2 H. M. Liebich, O. Al-Babbili, A. Zlatkis and K. Kim, *Clin. Chem.*, 21 (1975) 1294.
3 H. M. Liebich and O. Al-Babbili, *J. Chromatogr.*, 112 (1975) 539.
4 H. M. Liebich, *J. Chromatogr.*, 112 (1975) 551.
5 H. M. Liebich and J. Wöll, *J. Chromatogr.*, 142 (1977) 505.
6 T. Bücher and H. Redetzki, *Klin. Wochenschr.*, 29 (1951) 615.
7 N. C. Jain, *Clin. Chem.*, 17 (1971) 82.
8 W. H. Swallow and P. R. Hentschel, *J. Chromatogr.*, 130 (1977) 403.
9 P. K. Gessner, *Anal. Biochem.*, 38 (1970) 499.
10 M. A. Korsten, S. Matsuzaki, L. Feinman and C. S. Lieber, *N. Eng. J. Med.*, 292 (1975) 386.
11 S. Szczepaniak, *Mikrochim. Acta*, I (1978) 513.
12 J. F. Brien and C. W. Loomis, *Clin. Chim. Acta*, 87 (1978) 175.

Journal of Chromatography, 239 (1982) 351–362
Elsevier Scientific Publishing Company, Amsterdam — Printed in The Netherlands

CHROM. 14,558

DETERMINATION OF THE PORE SIZE DISTRIBUTION, BY EXCLUSION CHROMATOGRAPHY, OF ION-EXCHANGE POLYMERS WHICH SWELL IN WATER

THOMAS CRISPIN* and ISTVÁN HALÁSZ*
Lehrstuhl für Angewandte Physikalische Chemie, Universität des Saarlandes, 6600 Saarbrücken (G.F.R.)

SUMMARY

It is shown experimentally that the partial exclusion of sugars and dextrans from the pores of a cation-exchange resin with a given counter ion is, if the eluent is 0.2 *M* sodium sulphate in deionized water, a consequence of the geometry of these standard samples alone. A method is described for determining the pore size distribution of polystyrene-based cation exchangers in aqueous systems by exclusion chromatography. A given standard sample *i* can penetrate pores of a solid with diameters smaller than $\varnothing_i$ ("exclusion value"). Some $\varnothing$-values are tabulated for standard samples as determined experimentally. Pore size distributions of cation exchangers, as measured by the exclusion chromatographic method, are described. In some applications the available pore volume of a swellable cation exchanger is of interest. This is of course, among others, a function of the counter ion, because the available pore volume for sugars and dextrans is codetermined by the solvent shell of the counter ion (Gibbs–Donnan equation). With the method described above this influence can be determined by experiments in aqueous systems. It is demonstrated that an interaction takes place between poly(ethylene glycol)s and polystyrene-based cation-exchange resins with water as the eluent. High-performance liquid chromatographic separations of amino acids and similar compounds on silica and on polystyrene-based cation exchangers are discussed.

INTRODUCTION

The morphological properties of rigid solids having pore diameters ranging from 10 to 4000 Å can be conviently determined by exclusion chromatography (EC)[1–3]. The principles and boundary conditions of the EC method for the determination of the structural data of porous rigid solids have been described in detail[2]. The pore structures of *in situ* coated stationary phases[4] and of chemically bonded stationary phases[5] have also been determined by this EC method. The mean pore diameters, $\varnothing_m$, are very similar if they are determined by classical methods (*i.e.*, nitrogen capillary condensation (*e.g.*, ref. 6) or mercury porosity[7] or by the EC

* Part of Masters Thesis, University of Saarbrücken, 1980.

0021-9673/82/0000–0000/$02.75

method. Experience has shown that, for a given solid, capillary condensation, mercury porosimetry and the EC method yield similar $\varnothing_m$ values, but increasingly broad pore size distributions. This is due to the different boundary conditions and to the wall effect in EC and has been discussed elsewhere[8]. A simple and rapid method for determining only the mean pore diameters has also been described[9]. Thus, it has been shown experimentally, that in EC the h values of a homologous series *versus* the relative molecular mass of the samples and the pore size distribution of the rigid solid determined by EC exhibit the same maximum.

The permanent porosity of "semi-rigid" gels can be determined by all of the methods discussed above. The pore structure of non-rigid solids, however, is a function of the swelling medium employed. Pore size distributions of such gels, obtained by classical methods, obviously reflect the method of sample preparation required and bear no relation to the pore size distribution when swollen in a fluid medium.

It has been shown that the exclusion method is also suitable for determining the morphological properties of swellable solids[10]. The normal standard samples (phenylalkanes and polystyrenes) are insoluble in water and in other polar eluents. The pore size distribution of swellable polymers, especially of ion exchangers, in water is of some interest. This problem is discussed in this paper.

EXCLUSION CHROMATOGRAPHIC METHOD

The principles and boundary conditions of the EC method for the determination of the structural data of porous solids have been described elsewhere[2,10]. EC calibration graphs (*i.e.*, the elution volumes as a function of the relative molecular masses of the sample) can be used to calculate the mean pore diameters and pore size distributions of solids, if one assigns $\varnothing$ (Å) to the standard samples used for calibration, where $\varnothing_i$ defines the smallest pore diameter that is accessible to a given sample of relative molecular mass M_i. The total pore volume, $V_{p,total}$, of a solid is defined as the difference between the elution volume of the smallest inert standard sample and that of the greates standard. The sum of the residues R of a given pore diameter $\varnothing_i$ is defined as the fraction of total pore volume, $V_{p\ total}$, formed by all the pores with a diameter greater than $\varnothing_i$. Usually it is assumed that the elution volume V_e in EC can be described by the equation

$$V_e = V_z + K V_p \tag{1}$$

where V_z is the interstitial volume. The numerical values of R and K are, of course, identical. All three "calibration" graphs (*i.e.*, V_e *vs.* M, R *vs.* $\varnothing$ and K *vs.* $\varnothing$) describe the pore structure of the solid stationary phase; their shapes are very similar and are interpreted as integral pore size distribution curves. Experience has shown that the pore size distribution of many rigid solids and swellable polymers can best be illustrated by a log-normal distribution curve. Consequently, these "calibration" graphs are usually plotted with V_e *vs.* log M, R *vs.* log $\varnothing$ and K *vs.* log $\varnothing$ axes.

EXPERIMENTAL AND RESULTS

Morphological properties of solids having average particle sizes up to 250 μm can be determined by the EC method. If the particle sizes are "large" the equipment

TABLE I

AVERAGE PARTICLE SIZES (d_p) OF SILICA AND CATION-EXCHANGE RESIN STATIONARY PHASES

*Type**	*Phase*	*Producer or distributor*	d_p (μm)
a	SiO_2 Kugelgel	Dynamit-Nobel (Troisdorf, G.F.R.)	10
a	Mikro H	Home-made	15
a	Nr-80-3-U	Prof. Dr. K. Unger (University of Mainz)	9
a	H-90-7	Home-made	7
a	Si 200	Merck (Darmstadt, G.F.R.)	10
a	Si 500	Merck	10
a	Si 1000	Merck	10
b	Lewatit SPC 108/H	Bayer (Leverkusen, G.F.R.)	20
b	HC-X-7	Hamilton (Bonduz, Switzerland)	25

* a = Silica; b. = cation-exchange resin.

can be simple, because the pressure drop over the column is small. As shown in Table I, the average particle size, d_p, of the stationary phases (solids) used in the following experiments was smaller than 25 μm, and consequently a typical high-performance liquid chromatographic (HPLC) apparatus was used. The following components were set up in series: a pump with a constant flow-rate (M 6000; Waters Assoc., Milford, MA, U.S.A.), a sample injector (U6K; Waters Assoc.), a stainless-steel separation column with a drilled-out[11] internal diameter of 4.2 mm and a length of 20–45 cm, a UV detector[11] of our own design (254 ± 10 nm, cell volume 8 μl) and/or a differential refractometer detector (R 401; Waters Assoc.).

All measurements were carried out at room temperature.

The silica columns were packed by a modified viscosity method[12].

The strongly acidic cation-exchange resin (–SO_3H) was regenerated with 1 *N* hydrochloric acid, washed to neutrality with 1 *N* sodium chloride solution and flushed for 1 h with deionized water. For maximum swelling it was stored for 24 h in deionized water. A slurry of 3 g of ion-exchange resin in 40 ml of water was packed into the column in the usual way. The packing pressure never exceeded 10 bars if Lewatil SPC 108/H was packed. Care was taken to prevent the columns from running dry.

Water-soluble standard samples

For the calibration graph the following samples were chosen: ribose, xylose, lactose, raffinose (Merck, Darmstadt, G.F.R.), stachyose (Südzücker, Offstein, G.F.R.) and dextrans (Pharmacia, Uppsala, Sweden). In the following a dextran with a weight-average molecular weight, for example, of 40,000 will be described as T-40. The hold-up volume of a column, with water as eluent, was always measured with D_2O, *i.e.*, it was assumed that D_2O is the smallest inert sample.

In the following, the total pore volume, V_p, of a solid will be defined as the difference between the elution volumes of D_2O ($\varnothing$ = 3.5 Å) and T-2000 ($\varnothing$ = 1500 Å). The defined total pore volume of microporous solids (*i.e.*, $\varnothing$ < 20 Å) can be an

extremely sensitive function of the arbitrarily chosen smallest inert sample. The elution volume of T-2000 was defined as the interstitial volume, V_z.

Choice of eluent

If the stationary phase is a cation-exchange resin, it is well known[13,14] that dextrans with high molecular weights are excluded from a given portion of the pore volume not only because of their geometry, but also because of the Donnan potential effect (carboxylic groups in the dextrans). Further, the dextrans tend to associate in water. This effect and the electrostratic exclusion can be minimized by the addition of inorganic salts such as sodium sulphate[13–15].

In the following it will be demonstrated that the standard samples are not adsorbed on the cation-exchange resins if the eluent is properly chosen because, if a sample is adsorbed or excluded owing to electrical fields, then its elution volume will be a function of the ionic strength of the mobile phase.

In order to alter the elution power, either sodium sulphate or acetonitrile was added to water. As shown in Table II, the elution volumes of sugars are practically constant if the concentration of sodium sulphate in deionized water is increased up to 0.3 *M*. On the other hand for dextrans a minimum concentration of 0.2 *M* sodium sulphate is required to avoid changes in their retentions. It was shown by experiments that dextran molecules will be adsorbed on the organic matrix of the ion-exchange resin if the concentration of sodium sulphate in water is 1 *M* or higher.

On the other hand, the elution volumes of the sugars and dextrans remained unchanged, to a first approximation, if the concentration of acetonitrile in water was lower than 10% (v/v), as shown in Table III. If the concentration of acetonitrile was increased to 30%, the elution volumes increased by 20% or more.

In subsequent work 0.2 *M* sodium sulphate solution was always used as the eluent when the stationary phase was a cation-exchange resin. With this system the peak symmetries were acceptable, as shown for some sugars in Fig. 1.

Calibration table for the water-soluble standard samples

The mean pore diameters of the silicas given in Table I vary between 12 Å (SiO_2 Kugelgel) and 1000 Å (Si 1000). The hydrodynamic permeability of these rigid

TABLE II

ELUTION VOLUMES OF DEXTRANS AND SUGARS AS A FUNCTION OF THE CONCENTRATION OF SODIUM SULPHATE IN WATER

Stationary phase: Lewatit SPC 108/H. L = 45 cm; I.D. = 4.0 mm; V_c = 5.54 cm^3; F = 1 cm^3/min.

Sample	V_e (cm^3)			
	M = 0*	*M = 0.1*	*M = 0.2*	*M = 0.3*
T-40	2.88	3.02	3.14	3.11
T-10	3.14	3.23	3.36	3.30
Lactose	3.84	3.89	3.91	3.85
Xylose	4.12	4.12	4.21	4.22

* M = molarity of sodium sulphate in water.

TABLE III

ELUTION VOLUMES OF DEXTRANS AND SUGARS AS A FUNCTION OF THE ACETONITRILE CONCENTRATION IN WATER

Column geometry similar to and stationary phase identical with that in Table II.

Sample	V_e (*cm*^{3})		
	0% (v/v)	*5% (v/v)*	*10% (v/v)*
T-500	2.59	2.59	2.55
T-70	2.71	2.71	2.71
T-40	2.80	2.81	2.78
T-10	3.13	3.12	3.10
Raffinose	3.67	3.67	3.60
Lactose	3.82	3.82	3.78
Xylose	4.10	4.10	4.13

solids is constant if measured in methylene chloride or water as eluent. Therefore, it is not likely that their pore structure changes with these eluents.

The integral pore size distributions of different silicas were determined with methylene chloride as the eluent and polystyrene and phenylalkane standards[2,3]. These values are marked with crosses in Figs. 2 and 3.

The column filled with methylene chloride eluent was then flushed with methanol and deionized water and equilibrated with 0.2 *M* sodium sulphate in deionized water.

The elution volumes of D_2O, sugars and dextrans were measured and their *K* (or *R*) values were calculated with the help of eqn. 1. These *K* values, determined on different silicas, were then plotted to give the calibration graph for the corresponding

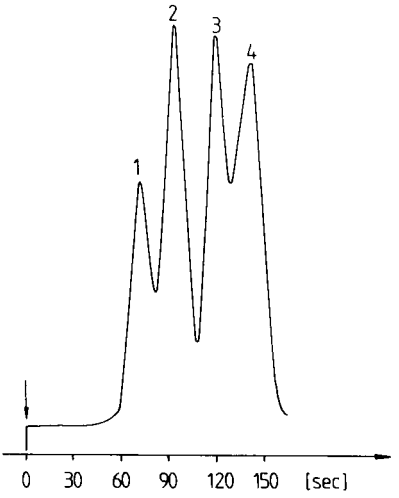

Fig. 1. Separation of sugars. Eluent: 0.2 *M* Na_2SO_4 in water. F = 1 cm^3/min. Stationary phase: HC-X-7 cation-exchange resin (d_p = 25 μm). L = 25 cm; I.D. 4.1 mm; V_c = 3.35 ml, V_p = 0.42 cm^3/cm^3 empty column volume. Packing pressure: 400 bar. Hold-up (D_2O): 166 sec. Refractive index detector. Samples: 1, stachyose; 2, lactose; 3, xylose; 4, ribose.

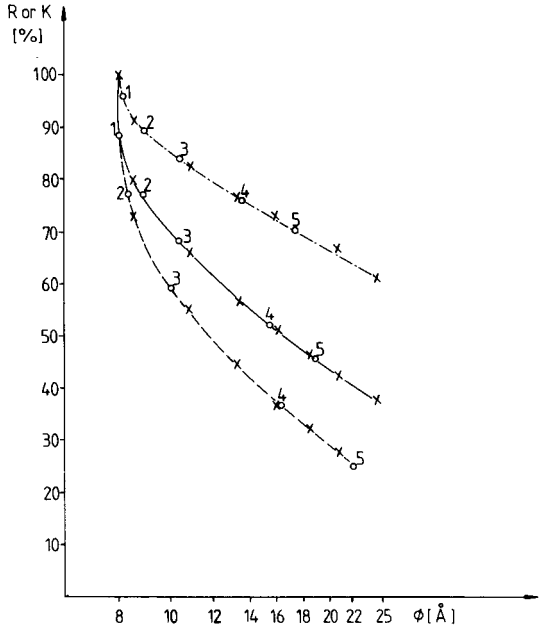

Fig. 2. Semi-logarithmic integral pore size distribution of microporous silicas and the ∅ values for water-soluble standard samples. Stationary phases: –·–·–, Mikro H silica; ——, SiO_2 Kugelgel silica; – – –, Nr-80-3-U silica. Samples: ×, phenylalkane standards (in CH_2Cl_2 eluent); 1, ribose (the eluent here and in the following is 0.2 *M* Na_2SO_4 in deionized water); 2, xylose; 3, lactose; 4, raffinose; 5, stachyose.

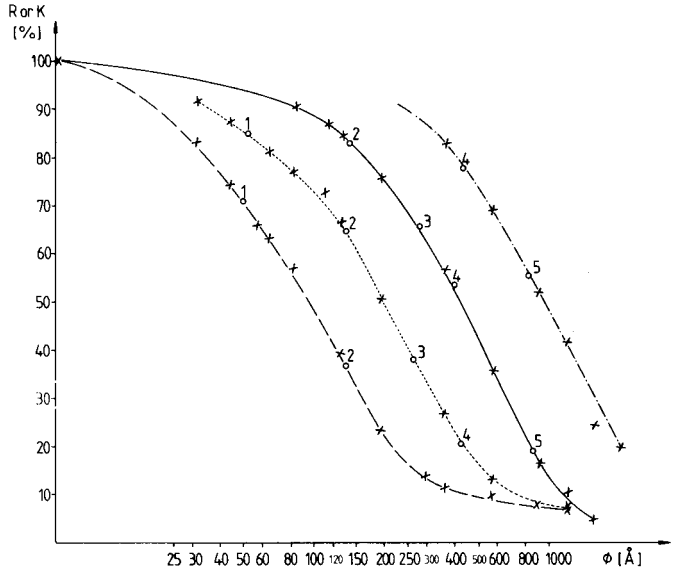

Fig. 3. Pore size distribution of silicas. Stationary phases: – – –, H-90-7 silica; ...., Si 200 silica; ——, Si 500 silica; –·–·–, Si 1000 silica. Samples: ×, polystyrene standards (in CH_2Cl_2 eluent); 1, T-4 (the eluent here and in the following is 0.2 *M* Na_2SO_4 in deionized water); 2, T-10; 3, T-40; 4, T-70; 5, T-500; 6, T-2000. F = 1 ml/min.

TABLE IV

∅ VALUES OF THE WATER SOLUBLE STANDARD SAMPLES

Eluent: 0.2 *M* Na_2SO_4 in deionized water.

Sample	$\varnothing_{average}$ (Å)	∅ (Å)	*Solid phase**
D_2O	3.5	–	–
Ribose	8	8.0	a
		8.1	b
Xylose	9	9	a
		9	b
		8.5	c
Lactose	10.5	10.5	a
		10.5	b
		10	c
Raffinose	15	15.5	a
		13.5	b
		16.0	c
Stachyose	19	18.5	a
		17.2	b
		22.0	c
T-4	51	50.5	d
		52.5	e
T-10	140	138	d
		138	e
		143	f
T-40	270	266	e
		275	f
T-70	415	427	e
		389	f
		427	g
T-500	830	841	f
		813	g
T-2000	1500	1500	g

* a, SiO_2 Kugelgel; b, Mikro H; c, Nr-80-U; d, H-90-7; e, Si 200; f, Si 500; g, Si 1000.

silica, as shown in Figs. 2 and 3. If the random condition of the pore size distribution measurements with EC are fulfilled, then the ∅ values of a given sugar or dextran, as calculated from the calibration graphs of different silicas, must be very similar.

As shown in Table IV, the scatter of the ∅ values of a given water-soluble standard sample is less than ±5% (mostly less than 3%) except for raffinose and stachyose. In the third column in Table IV, the ∅ values are given as calculated from the calibration graph for a given silica (column 4). The average calibration values as given in the second column in Table IV, will be used to determine the pore size distribution of solids with water-soluble standard samples.

For D_2O it was arbitrarily assumed that its "diameter" is its ∅-value (3.5 Å). This approach is open to discussion. The ∅ values of ribose, xylose and lactose are similar (8–10.5 Å). They are used together only if the slope of the pore size distribution curve of a solid is steep in this region. Unfortunately only one standard sample (T-4) was found in the ∅ region between 19 and 140 Å.

Coil diameter of some polymers and their ∅ values

Polystyrenes dissolved in a "good" solvent (*i.e.*, methylene chloride) may be regarded as random coils. As was previously found[2], the rotational coil diameters of polystyrenes must be about 2.5 times smaller than the diameters of the pores in the solid (*i.e.*, ∅ values) to allow the polymer unhindered access to the pores (*i.e.*, to enable "instantaneous equilibrium" to be achieved).

Kuga[16] tabulated the molecular weights and hydrodynamic ratio of equivalent spheres (r) of some polymers. The $\varnothing/r$ ratio dextrans (as given in Table IV in this paper and in Table II in ref. 16) vary for the dextrans between 2.5 (for T-500) and 3.2 (for T-70). This factor is in tolerable agreement with 2.5 as given for polystyrenes in methylene chloride[2]. However, Kuga[16] accepts, without detailed experimental argument, the simple assumption that the diameter of the smallest permeable pore ("exclusion value", ∅...) is equal to the hydrodynamic diameter ($2r$). This assumption does not seem likely, because of the experimental conditions and because of the known kinetics in a column packed with porous material.

The probability that a polymer can enter a pore, if its hydrodynamic diameter is identical with the pore "diameter", is small if a high-speed equilibration is required.

Other water-soluble standard samples

Kuga[16] proposes oligo(ethylene glycol)s (OEG) and poly(ethylene glycol)s (PEG) as standard samples. As has been shown[14,17], and as is summarized in Table V, there is unfortunately an interaction between these samples and the cation-exchange resins. If 10% (v/v) of acetonitrile is dissolved in deionized water then the elution volumes decrease, compared with water. This is probably a consequence of hydrophobic interactions between the samples and the matrix of the ion-exchange resin (reversed-phase mechanism). As will be shown, the average (*i.e.*, the most probable) pore size of HC-X-7 cation-exchange resin is around 10 Å. The decrease in the elution volumes is small if acetonitrile is added to water and the sample is PEG 500 or

TABLE V

ELUTION VOLUMES OF OLIGO(ETHYLENE GLYCOL)S AND POLY(ETHYLENE GLYCOL)S AS A FUNCTION OF THE ACETONITRILE AND SODIUM SULPHATE CONCENTRATIONS IN WATER

Stationary phase: HC-X-7. L = 25 cm; I.D. = 4.1 mm; V_c = 3.35 cm^3; F = 1 cm^3/min.

Sample	V_e (cm^3)		
	10% CH_3CN	*H_2O*	*0.2 M Na_2SO_4*
EG	2.38	2.45	2.55
DiEG	2.18	2.35	2.65
TriEG	2.04	2.31	2.61
PEG 200	1.94	2.18	2.61
PEG 300	1.47	1.84	–
PEG 400	1.27	1.51	–
PEG 600	1.11	1.14	–
PEG 1000	1.04	1.07	
PEG 40,000	1.04	1.07	

larger, because these molecules are more or less excluded. On the other hand, the elution volumes increase if the eluent is 0.2 *M* sodium sulphate in water. In this system PEG 1000 and PEG 40,000 are irreversibly adsorbed. The elution volumes for PEG 300, 400 and 600 were not measured. Because of these interactions between the OEG and PEG samples and the ion-exchange resins these samples are not proposed as standard samples and are not included in Table IV.

We did not measured the interactions between poly(ethylene oxide)s and polystyrene resins as proposed by Kuga[16]. In the absence of such interactions they could be standard samples for pore size distribution with water as the eluent and would extend the calibration values given in Table IV.

Pore size distribution of ion exchangers

Fig. 4 shows the integral pore size distribution of the cation-exchange resin Hamilton HCX-7 (Na^+). The sample T-4 ($\varnothing$ = 51 Å) is excluded. It may be that molecules with $\varnothing > 19$ Å but definitely smaller than 51 Å are also excluded. As can be seen in Fig. 4, the most probable pore diameter is around 9 Å and more than 75% of the total pore volume belongs to pores with a pore diameter smaller than 10.5 Å. The differential pore size distribution of this phase is extremely narrow. The pore volume of this cation-exchange resin, as calculated from the elution volumes of D_2O and T-2000, is high (0.55 cm^3/cm^3, empty column volume). This stationary phase can be packed using pressures of up to 700 bar.

The pore size distribution of another polystyrene-based cation-exchange resin, Lewatit SPC 108/8, is shown in Fig. 5. The distribution is much broader. About 50%

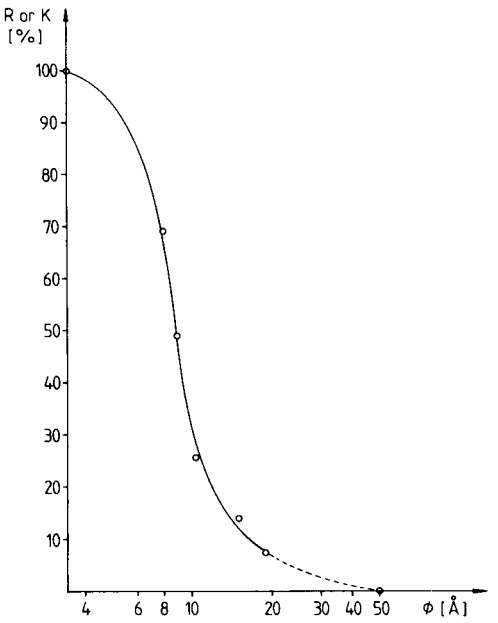

Fig. 4. Integral pore size distribution of the cation-exchange resin Hamilton HC-X-7 (Na^+). Eluent: 0.2 *M* Na_2SO_4 in deionized water. L = 25 cm; I.D. = 4.1 mm; V_p = 0.55 cm^3/cm^3; V_c = 3.35 cm^3; F = 1 ml/min. Packing pressure: 400 bar.

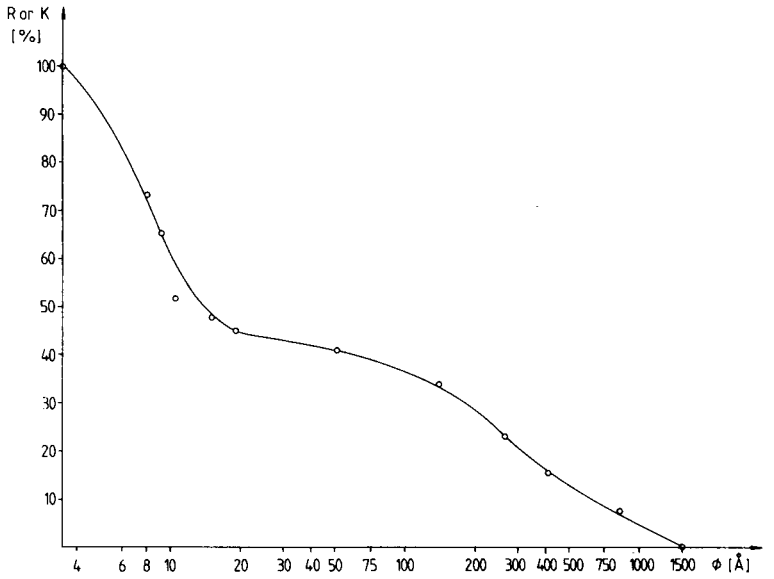

Fig. 5. Pore size distribution of the cation-exchange resin Lewatit SPC 108/8 (Na^+). Eluent: 0.2 *M* Na_2SO_4 in deionized water. L = 45 cm; I.D. = 4 mm; V_p = 0.42 cm^3/cm^3; F = 1 ml/min. Packing pressure: 5 bar.

of the total pore volume is in the micropores with $\varnothing < 10$ Å and about 20% belongs to pores with $\varnothing > 100$ Å. The pore volume is 0.42 cm^3/cm^3. Packing pressures of up to 15 bar are tolerable. The well known fact is again demonstrated that if a substantial proportion of the pores of a polystyrene resin have a diameter greater than about 15 Å, then its pressure stability decreases sharply.

Different types of cation exchangers in HPLC

The cation-exchange resin described in Fig. 4 is used as a stationary phase for the separation of amino acids and other ionic compounds. As can be seen from its pore size distribution, only a fraction of its pore volume and its surface area is available for bulky and electrostatically charged molecules. Cation-exchange stationary phases with large pore volumes and with mean pore sizes around 1000 Å can be prepared on silica bases. The integral (solid line) and the differential (broken line) pore size distributions, measured with methylene chloride as eluent and polystyrene standards[2], are shown in Fig. 6. The circles in Fig. 6 indicate the K (or R) values achieved with stachyose and dextran samples and 0.2 *M* sodium sulphate solution as eluent. It is remarkable and typical for this solid, with $\varnothing_m = 96$ Å, that the total pore volume was very similar whether it was measured with benzene ($\varnothing = 8$ Å) in methylene chloride eluent or with D_2O ($\varnothing = 3.5$ Å) in water as the smallest inert sample. Consequently, a large proportion of the total pore volume of this solid is in pores with $\varnothing > 8$ Å. Si 100 silica is a matrix with $-(CH_2)_3-SO_3H$ as the functional group[18]. Its average pore size is 96 Å with a specific surface area of about 300 m^2/g (130 m^2/cm^3) and with a specific pore volume of 0.36 cm^3/cm^3. This phase is pressure-stable up to at least 1000 bar. The ion-exchange capacity of this silica-based ion

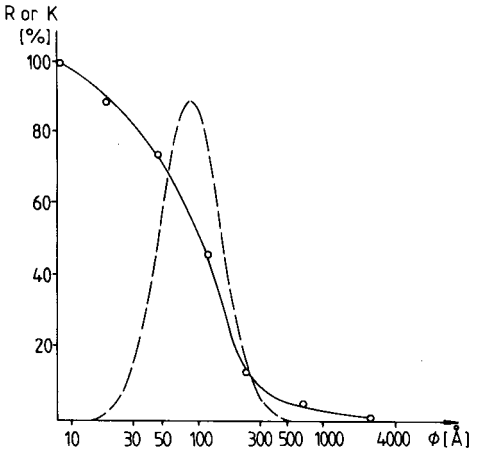

Fig. 6. Differential and integral pore size distribution of a silica-based cation exchanger. Silica base: Si 100 (10 μm). Functional group: propylphenylsulphonic acid. Packing density: 0.44 g/cm^3. Specific surface area: 300 m^2/g. Capacity: 1 mequiv./g (0.44 mequiv./cm^3). L = 25 cm; I.D. = 4.1 mm; V_c = 3.34 cm^3; V_p = 0.36 cm^3/cm^3. Solid line: the eluent is CH_2Cl_2 and the standard samples are benzene and polystyrenes. Circles: the eluent is 0.2 M Na_2SO_4 and the samples are sugar and dextrans.

exchanger is about 1 mequiv./g or 0.44 mequiv./cm^3 (ref. 18). The corresponding values for polystyrene-based cation exchangers used in HPLC are about 4–5 mequiv./g and 1–1.5 mequiv./cm^3, but with an average pore size well under 20 Å.

From the point of view of the accessibility of bulky molecules it would seem that the silica-based exchangers are superior to the polystyrene-based exchangers. On the other hand, it was shown experimentally that separations of ionic species can be effected with silica-based exchangers under identical conditions. However, these separations are only as good as those achieved with the classical polystyrene ion exchangers. Owing to the interactions with the different matrices the selectivities will vary.

ACKNOWLEDGEMENTS

We express our gratitude to the Deutsche Forschungsgemeinschaft for providing financial assistance for this work. We are especially indebted to Dr. P. M. Lange, Farbenforschung Lewatit, Bayer A.G., Leverkusen, G.F.R., for supplying some research copolymers, to Prof. Dr. K. Unger, University of Mainz, G.F.R., for supplying the microporous silica Nr-80-3-U and to Dr. F. Hampson for his help in correcting the English.

LIST OF SYMBOLS

d_p	average particle size
F	flow-rate
K	distribution coefficient in EC, as defined in eqn. 1
L	column length
M	relative molecular mass

R sum of residues
r hydrodynamic radius of equivalent sphere
V_c empty column volume
V_e elution volume
V_p total pore volume
V_z interstitial volume
$\varnothing$ pore diameter
$\varnothing_m$ mean pore diameter

REFERENCES

1 I. Halász and K. Martin, *Ber. Bunsenges. Phys. Chem.*, 79 (1975) 731.
2 I. Halász and K. Martin, *Angew. Chem.*, 90 (1978) 954; *Angew. Chem., Int. Ed. Engl.*, 17 (1978) 901.
3 I. Halász, P. Vogtel and R. Groh, *Z. Phys. Chem.*, 112 (1978) 235.
4 R. Nikolov, W. Werner and I. Halász, *J. Chromatogr. Sci.*, 18 (1980) 207.
5 W. Werner and I. Halász, *J. Chromatogr. Sci.*, 18 (1980) 277.
6 S. J. Gregg and K. S. Sing, *Adsorption Surface Area and Porosity*, Academic Press, New York, 1967, p. 162.
7 H. L. Ritter and L. C. Drake, *Ind. Eng. Chem., Anal. Ed.*, 17 (1945) 782.
8 W. Werner, *Ph.D. Thesis*, University of Saarbrücken, Saarbrücken, 1978.
9 W. Werner and I. Halász, *Chromatographia*, 13 (1980) 271.
10 I. Halász and P. Vogtel, *Angew. Chem.*, 92 (1980) 25; *Angew. Chem., Int. Ed. Engl.*, 19 (1980) 24.
11 J. Asshauer and I. Halász, *J. Chromatogr. Sci.*, 12 (1974) 139.
12 H. Elgass, H. Engelhardt and I. Halász, *Z. Anal. Chem.*, 294 (1979) 97.
13 R. A. Cooper and S. D. Derver, *J. Liquid Chromatogr.*, 1 (1978) 693.
14 H. Engelhardt and D. Mathes, *J. Chromatogr.*, 185 (1979) 305.
15 H. G. Barth and F. E. Regnier, *J. Chromatogr.*, 192 (1980) 275.
16 S. Kuga, *J. Chromatogr.*, 206 (1981) 449.
17 Th. Crispin, *Master Thesis*, University of Saarbrücken, Saarbrücken, 1980.
18 H. Engelhardt, *13th International Symposium on Chromatography, Cannes, June 30–July 4, 1980.*

Journal of Chromatography, 239 (1982) 363–376
Elsevier Scientific Publishing Company, Amsterdam — Printed in The Netherlands

CHROM. 14,639

COMPUTERIZED AUTO-CONTROL OF ON-LINE PROCESSES OR LABORATORY GAS AND LIQUID CHROMATOGRAPHS

C. L. GUILLEMIN
Direction des Recherches et du Développement, Rhône-Poulenc Industries, 12 et 14, rue des Gardinoux, 93308-Aubervilliers (France)

SUMMARY

The deferred standard concept can help the operator in controlling on-line the reliability of any process or laboratory gas or liquid chromatographic apparatus. However, more sophisticated auto-control of the chromatograph can be achieved by computerizing the interpretation of some chromatographic quantities for the deferred standard such as peak area, peak height and retention time, and can discriminate among the sample injection, the separation or the detection systems as sources of problems. This approach has been made possible owing to a commercial computing integrator which, in addition to quantitative information, displays messages about the status of the chromatograph.

This permanent auto-control suggests what the control unit of a modern process gas or liquid chromatograph, which has to be included in a closed loop control, should be.

INTRODUCTION

The concept of the deferred standard which has been published several times[1–4] has already succeeded in the on-line measurement of process chromatograph reliability and could be a real enhancement for both gas and liquid chromatographs, especially with the advent of microprocessors as control units of process or laboratory chromatographs used in routine control.

The deferred standard has three capabilities: alarm, calibration and maintenance functions. The purpose of this paper is to show how the first aspect, the alarm function, can be emphasized by using a microprocessor and what a future process gas or liquid chromatograph might look like.

DEFERRED STANDARD CONCEPT

The deferred standard (D.S.) is a pure compound, injected in each analytical sequence, the injection of which is deferred or delayed with respect to the injection of the sample to be analysed in such a way that the deferred standard elutes within the analysis time of the sample, but without interfering with any component of the mixture (Fig. 1).

0021-9673/82/0000–0000/$02.75

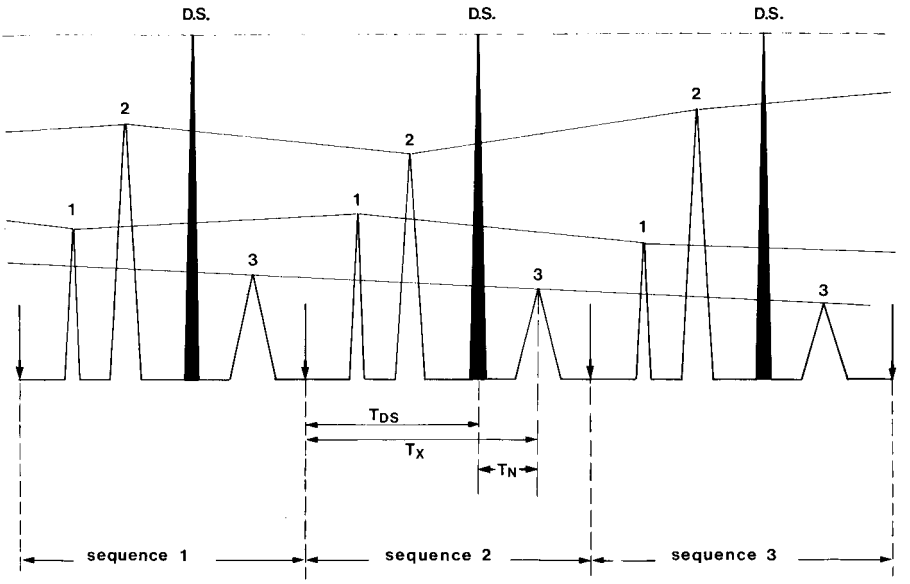

Fig. 1. Continuous checking of the reliability of a process chromatograph by the deferred standard concept.

As an alarm function, the reproducibility of the D.S. peak from one injection to the next indicates the good working order of the chromatograph, and the quantitative results for the sample to be analysed can be taken into account with confidence in the process control. In addition, this continuous checking of the reliability of the process chromatograph allows the plant operator to discriminate immediately between the analyser or the chemical process in cases of failure.

EXPERIMENTAL

This work was carried out with commercial equipment including, a Carlo Erba Model GT laboratory chromatograph automated with Spectra-Physics 4100 a computing integrator which offers, for the first time in this kind of appliance, part of the RAM memory to be programmed in modern computer language by the user himself. The interface between the chromatograph and the computing integrator was a home-made device, set up for the control of automatic injection, switching valves of the chromatographic circuit and different solenoid valves of the sampling line.

The equipment was installed on-line in a pilot plant for the continuous measurement of hydrogen in a chemical process. The chromatographic conditions were limited to a molecular-sieve column fed with argon as the carrier gas. For accuracy in quantitative measurements, pure hydrogen was choosen as the D.S., and was injected through the same injection valve as the process sample. Both the sample and the hydrogen D.S. were fed alternatively through a three-way solenoid valve and equilibrated at atmospheric pressure for 30 sec before injection.

Fig. 2 is a schematic diagram of the sampling and chromatographic circuits.

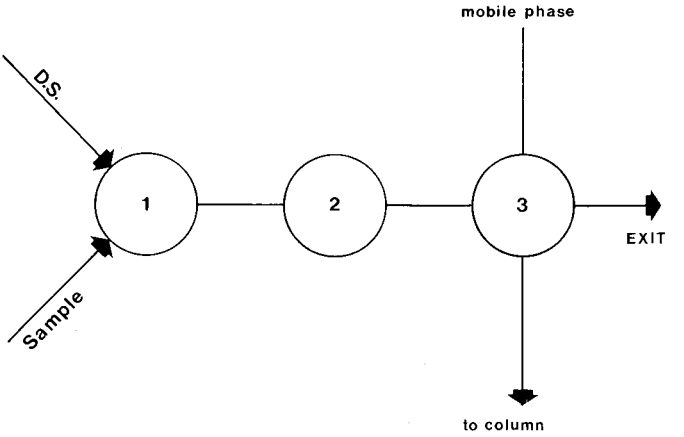

Fig. 2. Schematic diagram of sample and deferred standard circuits. 1 = Selector valve; 2 = stop-valve (atmospheric pressure); 3 = injection valve.

Primary alarm function of the deferred standard

For quantitative measurements, in which the peak area is linked to the amount of injected solute, the D.S. peak area rather than peak height is chosen as the most suitable parameter to trigger off an alarm when the value exceeds upper and lower fixed limits. These limits for the D.S. peak area are set first according to the standard deviation of the D.S. peak repeatability and second according to the requirements of the accuracy of quantitative measurements of solutes with regard to the D.S. peak.

The continuous checking of the peak area of the D.S. provides invaluable information about the overall status of the process gas chromatograph, but this permanent auto-control may be more sophisticated in order to make easier the diagnostic of any chromatographic failure and decrease the cost of maintenance.

Secondary alarm function of the deferred standard

By computerizing parameters of the D.S. peak such as peak area, peak height and retention time, discrimination between the detection, the injection and the separation systems as possible sources of problems is now possible and could be very helpful to the chromatographer searching for a malfunction or a failure of the process chromatograph. In addition to the main functions of an ordinary control unit of either a PGC and PLC, *i.e.*, timing of the analysis and chromatographic data reduction, the Spectra-Physics 4100 computing integrator also carried out the auto-control of the chromatograph and in this way acted as a modern control unit for both the PGC and the PLC.

Fig. 3 shows the algorithm built up on the three parameters peak area, peak height and retention time of the D.S. peak for failure diagnosis. The D.S. is logically identified by the absolute time from the beginning of the sample run to its peak maximum, as this deferred injection is ignored by the SP 4100. This time ($T_{D.S.}$) must be within a certain range specified by the operator; if it is outside the specified limits a "D.S. not found" message is displayed.

The next parameter checked is the peak area (S) and the peak height (H) of the

D.S. As previously pointed out, peak area depends on detection conditions, whereas peak height is related mainly to the injection conditions. To make the retention parameter more sensitive to chromatographic variations (carrier gas flow-rate,

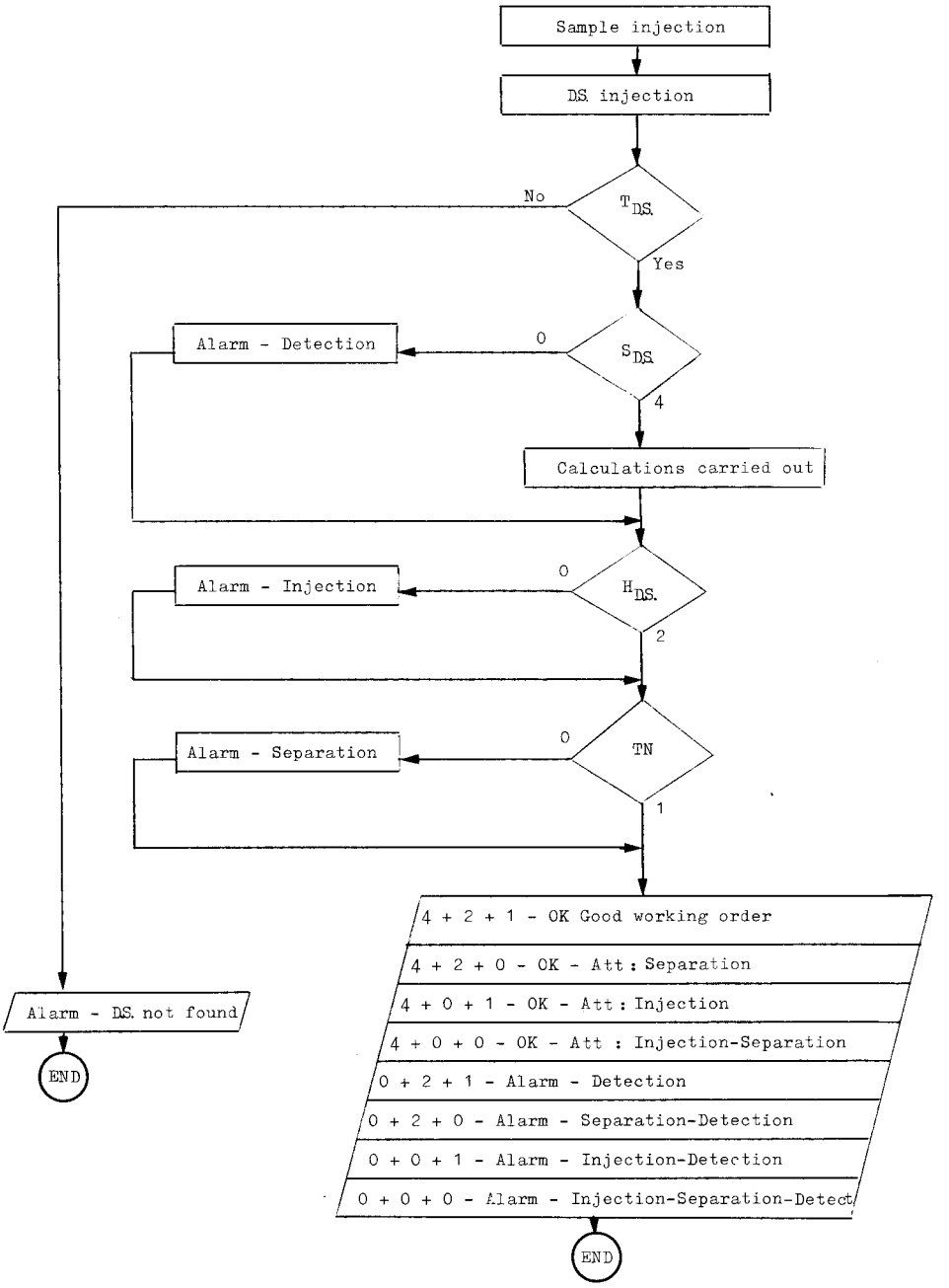

Fig. 3. Algorithm of the alarm function of the deferred standard.

column temperature, etc.), the selection of the difference in retention times between the D.S. peak and a reference peak has been chosen:

$$TN = | T_X - T_{D.S.} | \quad (1)$$

where TN is the difference between the absolute retention times as shown in Fig. 1 and T_X and $T_{D.S.}$ are the absolute retention times of peak X and D.S., respectively.

Any peak in the chromatogram may be a reference peak provided that it is always present in the sample. However, the larger the retention time of the reference peak the more sensitive it is to fluctuations in the operating conditions.

Limiting values of these parameters ($T_{D.S.}$, S, H and TN) are entered via a Basic dialogue before starting the routine analysis. To make the trouble-shooting software more understandable, values 1 and 0 have been attributed to these parameters when they are inside or outside their limits, respectively. Table I gives the various logical cases encountered when variations of these three parameters occur.

The meaning of possible variations occurring in the D.S. peak area may be some change or drift in the detector operating conditions, *i.e.*, variation of the d.c. current or block temperature for a thermal conductivity detector or variation of the flame temperature for a flame ionisation detector owing to changes in the flow-rate. Another meaning of increases in the D.S. peak area could be an unexpected peak eluting close to and interfering with the D.S. peak. In this case the D.S. injection must be delayed further so that the D.S. peak elutes at a suitable position not subject to interferences.

If the D.S. peak height is outside the specified limits, the injection function is first involved: the causes of this failure may be blockage of the injection valve, malfunction of the pneumatic actuator owing to a lack of air pressure or variation of the vaporization temperature in the case of a liquid sampling valve for PGC. Also, variation of the temperature of a gas sampling valve may cause enlargement of the peak owing to diffusion of the solute when the volumetric flow-rate of the carrier gas fluctuates. For instance, Table II and Fig. 4, show the effect on the peak height of a lack of air pressure in the actuator of a commercial liquid sampling valve for PGC. As the injection is not sufficiently instantaneous when the air pressure varies, the peak height is affected while the peak area remains constant. Halving the air pressure leads to a decrease of 13% in the peak height and 0.8% in the peak area.

Variation of TN means that some alterations in the separation conditions (column temperature, mobile phase flow-rate, elution of stationary phase, etc.) have occurred. Considering the peak area, S, the remarks made about the primary alarm function also apply here.

To illustrate the Basic program for the Spectra-Physics 4100 computing integrator, some examples are given below.

The procedure based on a conversational dialogue is as follows. Entry of PH = 1 on the SP 4100 before starting a run makes a report on peak heights while peak areas are stored. Afterwards an additional report on peak areas is obtainable for those peaks in peak storage by entering PH = 2 and pressing the REPRT key.

Entry of RUN initiates a special dialogue (see Fig. 5). The program asks for the name of the analysis, then the number of the D.S. peak as the SP 4100 identifies peaks by chronologic figures. Quantitative calculations need the D.S. concentration to be entered. Then the "windows" (limits) are requested for peak area, peak height and

TABLE I

TROUBLE-SHOOTING DIAGNOSTIC

Deferred standard parameter				*Actions*
$T_{D.S.}$	H	TN	S	
0				*Alarm:* D.S. not found. No calculation of component concentrations
1	1	1	1	Good working order. Calculation of component concentrations carried out with respect to D.S.
1	0	1	1	Calculations carried out with respect to D.S. Care of injection system
1	0	0	1	Calculations carried out with respect to D.S. Care of injection and separation systems
1	1	0	1	Calculations carried out with respect to D.S. Care of separation system
1	1	1	0	*Alarm:* No calculations reported. Care of detection system
1	1	0	0	*Alarm:* No calculations reported. Care of detection and separation systems
1	0	1	0	*Alarm:* No calculations reported. Care of detection and injection systems
1	0	0	0	*Alarm:* No calculations reported. Care of detection, separation and injection systems

retention time of the D.S. peaks, labelled as Max S, Min S, Max $T_{D.S.}$ and Min $T_{D.S.}$. A reference peak number has to be entered with the upper and lower values of TN as defined previously. Each peak whose concentration is to be calculated with respect to the D.S. peak has its number entered, then its relative response factor and name. To end the dialogue, the letter E (for END) is entered.

TABLE II

EFFECT OF VARIATIONS IN AIR PRESSURE IN THE ACTUATOR OF A PROCESS LIQUID SAMPLING VALVE ON PEAK AREAS AND PEAK HEIGHTS

Injection of 1 μl of carbon tetrachloride. Injection frequency: every 10 min. Vaporization temperature: 120°C. Peak areas and peak heights measured by computer.

Number of injections	*Air pressure on valve actuator (bar)*	*Peak area*			*Peak height*		
		S (average of last 10 runs)	σ	*Difference from previous measurement (%)*	*H (average of last 10 runs)*	σ	*Difference from previous measurement (%)*
3168	6	2655	0.009	–	15.76	0.15	–
5184	3	2676	0.008	0.8	13.90	0.3	13.4
5760	4	2679	0.009	0.1	14.40	0.1	3.5

Queries and peak height and peak area reports are displayed in Fig. 5. Fig. 6 shows several messages displayed when the parameter "window" was changed artificially to test the program. Message A indicates that D.S. has not been found, as peak 4 does not exist in the chromatogram. Message B displays the calculated concentrations for peaks X1 and X2, the values of the checked parameters, the chromatographic quantities of the D.S. and reference peaks and finally the status of the alarm function.

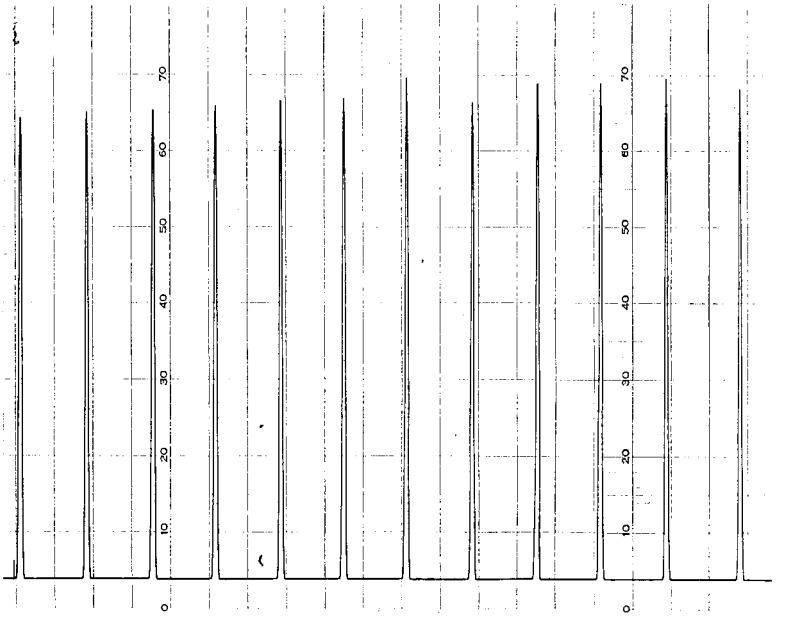

Fig. 4. Effect on peak shape of variation of air pressure in the pneumatic actuator of an automatic liquid sampling valve for a process gas chromatograph.

```
RUN
DEFERRED STANDARD - ALARM AND CALIBRATION FUNCTIONS

ANALYSE: X
PIC DS 2
Conc DS 100
MAX S DS 25000
MIN S DS 22000
MAX H DS 7000
MIN H DS 6000
MAX T DS 40
MIN T DS 33
PIC REF 3
MAX TN 17
MIN TN 13
No PIC 1
RF .5
NAME X1
No PIC 3
RF .25
NAME X2
No PIC F
END OF DIALOG
```

PH=1

```
                                        00:25:49

FILE 1      METHOD  0.      RUN   4      INDEX   4

PEAK#        HT%          RT        PK HT BC

    1       51.16       28.        12467 02
    2       28.267      36.         6888 02
    3       20.573      51.         5013 03

TOTAL       100.                    24368
```

PH=2

```
                                        00:25:49

FILE 1      METHOD  0.      RUN   4      INDEX   4

PEAK#       AREA%         RT        AREA BC

    1       38.303      28.        31954 02
    2       28.693      36.        23937 02
    3       33.004      51.        27534 03

TOTAL       100.                    83425
```

Fig. 5. Queries for the alarm function of the deferred standard.

Concentrations are calculated according to the following well known equation:

$$C_X = C_{D.S.} \cdot f_{X/D.S.} \cdot \frac{A_X}{A_{DS}} \quad (2)$$

where C_X is the concentration of solute X, $C_{D.S.}$ is the concentration of D.S., $f_{X/D.S.}$ is the relative response factor of solute X with respect to D.S., expressed in volume or weight units, and A_X and $A_{D.S.}$ are the peak areas of solute X and D.S., respectively.

To make the Basic program simpler and more elegant, a contrivance has been introduced: instead of values of 1 and 0 according to the status of the parameters, values of 4 or 0 are now attributed to *S*, 2 or 0 to *H* and 1 or 0 to *TN*, written with the

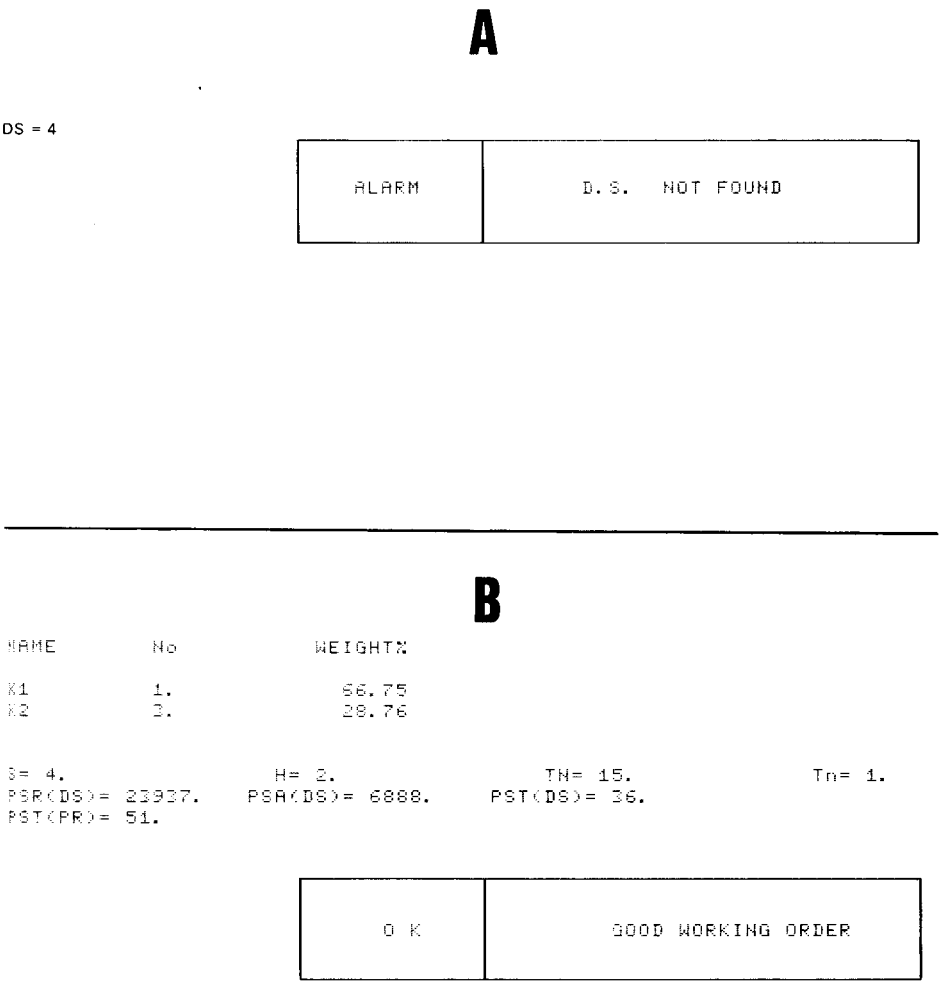

Fig. 6. Examples of displayed messages (checked parameters varied artificially, see text).

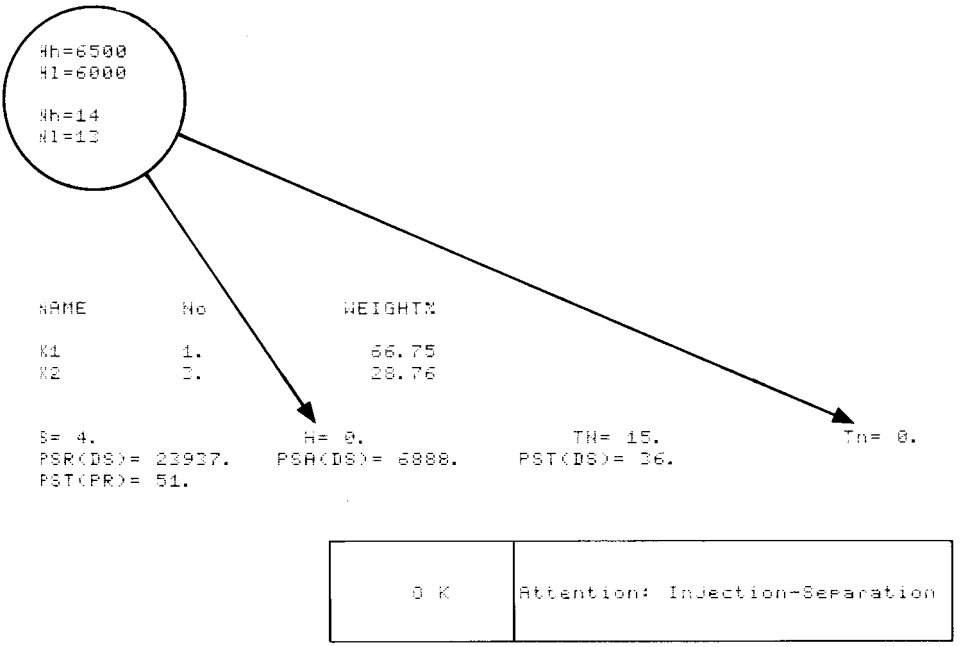

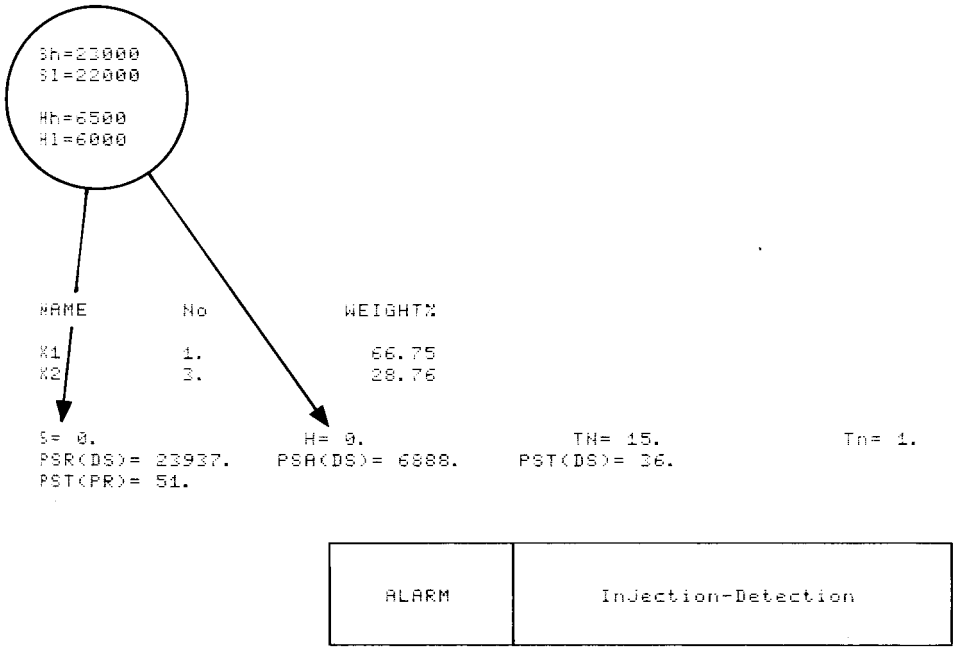

Fig. 7. Examples of reports and messages.

INJECT TIME 511:26:02

NOM	No	POIDS %
H2	2.	96.17

S= 4. H= 2. TN= 49. Tn= 1.
PSR(DS)= 3757296. PSA(DS)= 576360. PST(DS)= 113.
PST(PR)= 162.

O K	TOUT VA BIEN

INJECT TIME 511:41:02

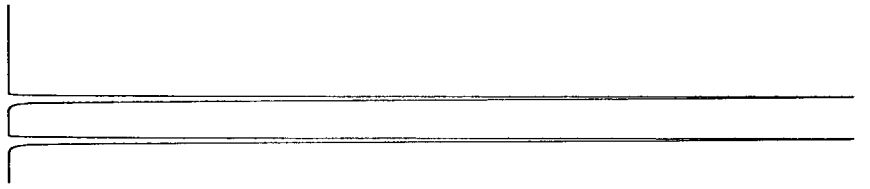

NOM	No	POIDS %
H2	2.	96.37

S= 4. H= 2. TN= 50. Tn= 1.
PSR(DS)= 3756651. PSA(DS)= 575957.33PST(DS)= 113.
PST(PR)= 163.

O K	TOUT VA BIEN

Fig. 8.

(Continued on p. 374)

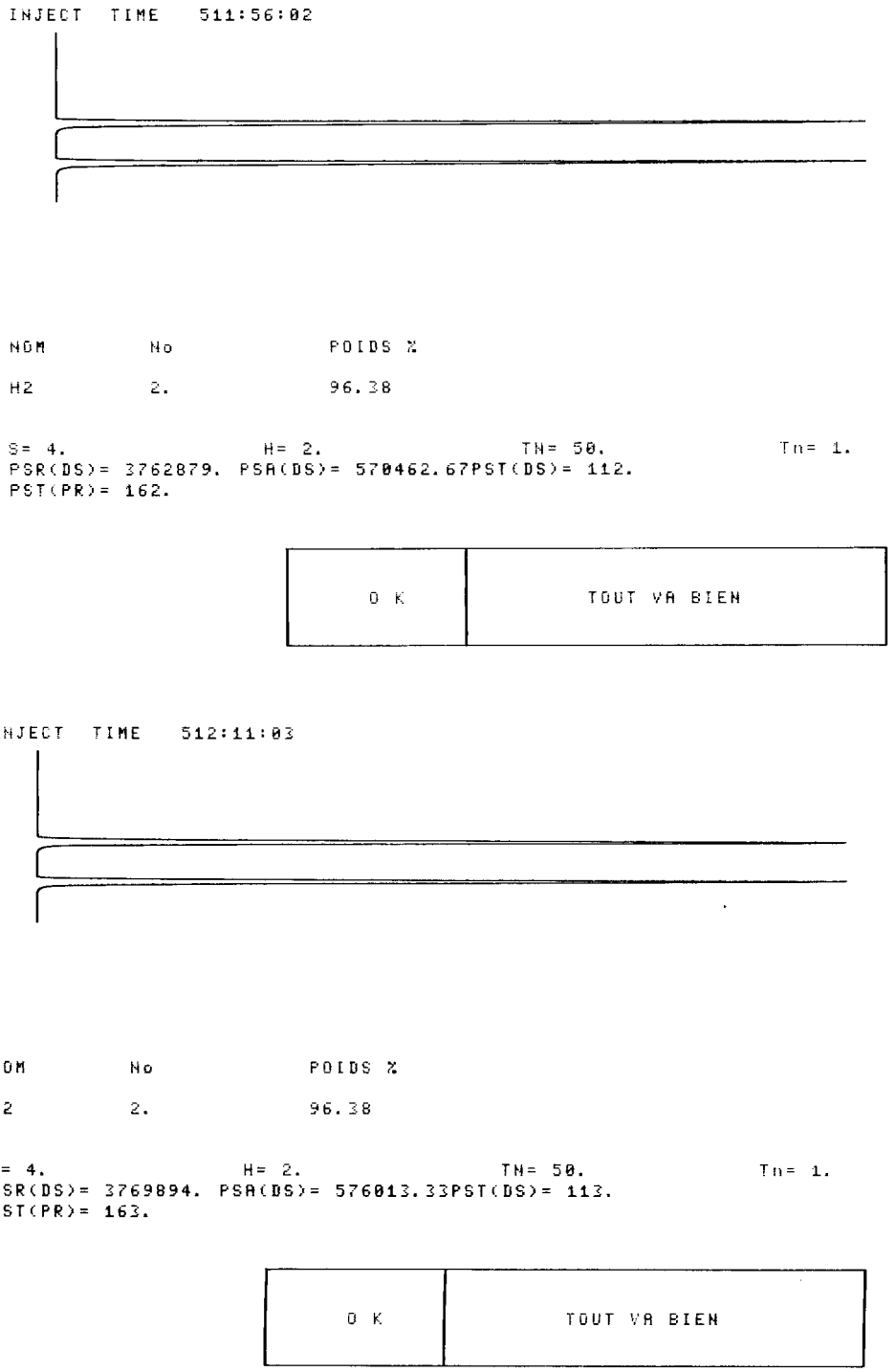

Fig. 8. Series of analytical sequences of an on-line chromatograph permanently checked with the deferred standard concept.

```
LIST

   10 !"DEFERRED STANDARD - ALARM & CALIB FUNCTIONS": !
   20 INPUT "ANALYSIS ",An
   30 INPUT "PIC DS ",DS: INPUT "Conc DS ",Cd
   40 INPUT "MAX S DS ",Sh: INPUT "MIN S DS ",Sl
   50 INPUT "MAX H DS ",Hh: INPUT "MIN H DS ",Hl
   60 INPUT "MAX T DS ",Th: INPUT "MIN T DS ",Tl
   70 INPUT "REF PIC "; PR
   80 INPUT "MAX TN ",Nh: INPUT "MIN TN ",Nl
   90 I=1
  100 INPUT "PIC No "; Xi(I)
  110 IF RXD <> 13 THEN 150
  120 INPUT "RF ",Fi(I)
  130 INPUT "NAME "; No(I)
  140 I=I+1: GOTO 100
  150 !"END OF DIALOG ": Nf=I-1: END: !!
  160 IF PST(DS)>=Th OR PST(DS)<=Tl THEN 170 ELSE 200
  170 !!
  180 GRAPH 350,350,1: !:
  190 !" ALARM            D S NOT FOUND": GOTO 600
  200 !"NAME       No          WEIGHT %": !
  210 FOR I=1 TO Nf
  220 Ci(I)=Cd*Fi(I)*(PSR(Xi(I))/PSR(DS))
  230 ! $5.02 No(I); $10.3 Xi(I);TAB20 Ci(I)
  240 NEXT
  250 !!
  260 TN=PST(DS)-PST(PR)
  270 IF PSR(DS)>=Sh OR PSR(DS)<=Sl THEN S=0 ELSE S=4
  280 IF PSA(DS)>=Hh OR PSA(DS)<=Hl THEN H=0 ELSE H=2
  290 IF TN>=Nh OR TN<=Nl THEN Tn=0 ELSE Tn=1
  300 !"S=";S;TAB20"H=";H;TAB40"TN=";TN;TAB60"Tn=";Tn
  400 !"PSR(DS)="PSR(DS);"PSA(DS)="PSA(DS)
  410 !"PST(DS)="PST(DS);"PST(PR)="PST(PR)
  420 Al=S+H+Tn
  430 !: PLOT 0
  440 GRAPH 350,350,1: !:
  450 ON Al+1 GOTO 460,470,480,490,500,510,520,530
  460 !" ALARM       Injection-Separation-Detection": GOTO 600
  470 !" ALARM            Injection-Detection": GOTO 600
  480 !" ALARM            Separation-Detection": GOTO 600
  490 !" Alarm                 Detection": GOTO 600
  500 !TAB3"O K      Attention: Injection-Separation": GOTO 600
  510 !TAB3"O K           Attention: Injection": GOTO 600
  520 !TAB3"O K           Attention: Separation": GOTO 600
  530 !TAB3"O K              GOOD WORKING ORDER": GOTO 600
  600 RESTORE 620: FOR I=1 TO 7 : READ X,Y,Z
  610 GRAPH X,Y,Z: NEXT : !&: ECHO1
  620 DATA 0,300,1.500,300,0,500,950,0,0,950,0,0,300,0
  630 DATA 0,495,1.500,495,0
  640 PLOT AUTO
  650 END
 2088 S=#C200: K=#C300: INPUT "LINE ?" L: LIST(L)
 2089 I=28+2PEEK(PEEK#C3A2+S): FOR T=S TO S+64
 2090 IF C<>13 THEN I=I+1: C=PEEK I AND #7F: POKE T,C
 2091 NEXT : POKE K,0,0,5: END
 3020 D=DT: IF D<T1 THEN D=T1 ALWAYS IF MN=0 THEN 5200
 4850 POKE #C2CD,0: DISP : GOTO 160: END
```

Fig. 9. Basic program for use with the SP 4100.

Tn label. *PSR* (D.S.), *PSA* (D.S.) and *PST* (D.S.) are the SP 4100 parameters indexed in order of detection for peak area, peak height and retention time of the D.S. peak, respectively, to access the peak storage in the core memory of the computing integrator. In the same way *PSR* (PR) is the retention time of the reference peak. All of this information is displayed in the second part of message B.

On the other hand, the first part of the framed message gives the overall status of the process chromatograph, and the second part displays the secondary alarm or diagnosis.

As can be seen in Fig. 5 or 6, the normal SP 4100 report, which is no longer useful, has been suppressed through the Basic software (see below).

Fig. 7 shows two more reports and messages in which some windows have been changed, as indicated on the left-hand side of the report, with the corresponding message.

Finally, a series of analytical sequences, reports and messages for the measurement of hydrogen in the pilot-plant process are given in Fig. 8. Reading the analytical bulletins, the plant operator and/or the control computer of the unit takes the successive calculated concentrations of hydrogen as valid and reliable for controlling the process, as the status of the on-line chromatograph remains in "good working order".

It is obvious than a more detailed and precise diagnosis might be developed to increase further the capabilities of the alarm function of the D.S. concept. For instance, in addition to the previous parameters, peak asymmetry, peak shape, etc., may reveal more about the performances of the different parts of the chromatograph.

The D.S. Basic program for use with the SP 4100, is given in Fig. 9. It should be noted that after obtaining any D.S. chromatographic quantities required for answering the program dialogue, the own SP 4100 report is no longer necessary and can be suppressed. Line 3020 of the program has to be modified as follows: instead of the number 5200 which ends the line, put 4850, as shown in the program in Fig. 9.

CONCLUSION

It is obvious that the recent advent of microprocessors in analytical instrumentation makes the operator's task easier. However, the real improvement seems to lie in the portion of the computer core memory which has been devoted to the operator for various programs or for subsequent calculations. This trend should be encouraged for the benefit of both the technique and the operator, the technique because it increases the capabilities of the apparatus and the operator because it enhances the status of his work.

The alliance of the deferred standard concept and the microprocessor is a good example of such a trend, particularly with on-line process GC or LC apparatus. On-line checking with a deferred standard, allowing any process chromatograph to fit the main criteria of process monitors (reliability, credibility and low maintenance), should allow the process gas or liquid chromatograph to be included in a closed-loop control with more confidence.

ACKNOWLEDGEMENT

The author is greatly indebted to his collegue Dr. C. Pierson for his encouraging advice in obtaining a more elegant Basic program.

REFERENCES

1 C. L. Guillemin, *Mesures*, 37 (1972) 87.
2 C. L. Guillemin, *Mesures*, 37 (1972) 99.
3 C. L. Guillemin, *Instrum. Technol.*, 4 (1975) 43.
4 C. L. Guillemin, *J. High Resolut. Chromatogr. Chromatogr. Commun.*, 3 (1980) 620.

Journal of Chromatography, 239 (1982) 377–383
Elsevier Scientific Publishing Company, Amsterdam — Printed in The Netherlands

CHROM. 14,514

CHROMATOGRAPHIC ANALYSIS OF AROMATIC POLYHYDRAZIDES, OXALYL ARYLENE POLYHYDRAZIDES AND AROMATIC POLY-(AMIDE–HYDRAZIDES) AFTER ALKALI FUSION

J. K. HAKEN* and J. A. OBITA
Department of Polymer Science, University of New South Wales, P.O. Box 1, Kensington, New South Wales 2033 (Australia)

SUMMARY

A procedure which allows rapid analysis of aromatic polyhydrazides, oxalyl arylene polyhydrazides and aromatic poly(amide–hydrazides) is reported. The various acidic and amino components are identified after derivatization following cleavage with molten potassium hydroxide rather than by prolonged hydrolysis with hydrochloric acid, as has generally been employed with nylon-type polyamides. Degradation of the poly(amide-hydrazides) produce the salt of *p*-aminobenzoic acid and the analytical scheme developed allows derivatization without an additional step. Modification of the fusion procedure previously reported is required for use with all the polyhydrazides.

INTRODUCTION

The traditional method of analysis of aliphatic polyamides of the nylon type[1] has usually employed acidic hydrolysis followed by chemical or instrumental analysis. With 6 *N* hydrochloric acid hydrolysis of Nylons 11 and 12 required a digestion period of 8 h at 130°C to effect cleavage while aromatic materials. less susceptible to hydrolysis require even longer periods of digestion.

Frankoski and Siggia[2] employed alkali fusion with amides, anilides and ureas. The procedure with Nylon 6,6 and 6,10 involves heating solid alkali with the sample in molar ratios of 50:1 or greater at 360°C of 0.5 h. The fusion was carried out in a reactor constructed from a furnace pyrolyser attached to a gas chromatograph, the liberated diamine, 1,6-diaminohexane, being determined by gas chromatography with the dicarboxylic acid remaining in the reactor as the salt. The procedure was extended for the same type of dicarboxylic acid–diamine condensate, for ω-aminoalkanoic acid-types of nylon[3] and for fatty polyamides[4] to allow examination of both the acid and the amine components.

The procedure developed (1) eliminated the restricted availability of the chromatograph and use of the cumbersome reactor; (2) allowed recovery and identifi-

0021-9673/82/0000–0000/$02.75

cation of the dicarboxylic acid as a suitable derivative; and (3) allowed recovery of the diamine, chromatography of which is often improved by examination of a derivative or by the use of liquid chromatography.

Schlueter and Siggia[5] have used a fusion reactor for the identification of aromatic diamines derived from a variety of aromatic polyamides, polyimides and poly(amide–imides) and have included a substantial bibliography of earlier analytical reports.

The examination of derivatives of amines from the same types of polymers and of the tri- and tetracarboxylic acids used has been recently reported[6].

A series of related high-modulus fibres produced by the Monsanto Company comprise both aromatic polyamides and aromatic (amide–hydrazides)[7,8]. Frazer and co-worker have described the synthesis of aromatic polyhydrazides[9,10] and alternating oxalyl/arylene polyhydrazides[11,12] prepared by low-temperature solution polycondensation of the corresponding hydrazides and the acid chlorides in hexamethylphosphoric triamide containing dissolved lithium chloride. The same condensation being subsequently reported using N,N-dimethylacetamide[13] as solvent.

The literature does not contain any procedures for the analysis of the polyhydrazides and related polymers and the procedure using alkali fusion and chemical derivatization is reported. Degradation of the poly(amide-hydrazides) produces the salt of *p*-aminobenzoic acid and an alternative reaction scheme to that previously reported is employed to allow a single derivatization step.

EXPERIMENTAL

The polymer H-22 was produced from terephthaldihydrazide (I) and terephthaloyl chloride to form poly(temphthalhydrazide) (III).

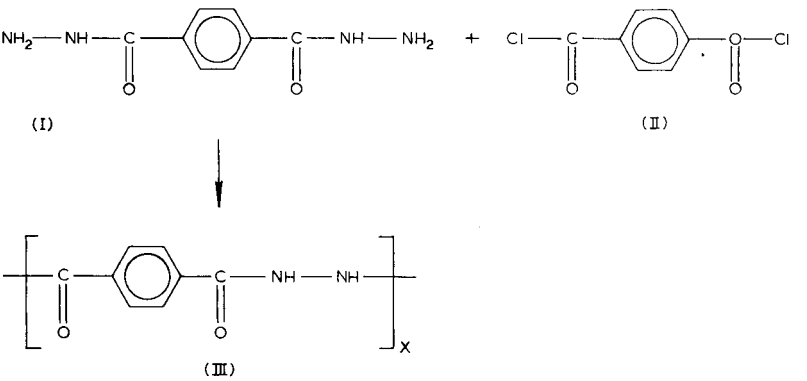

The polymer H-20 was produced from oxalic dehydrazide (IV) and terephthaloyl chloride (II) to form the alternating polyhydrazide of oxalic and terephthalic acids (V).

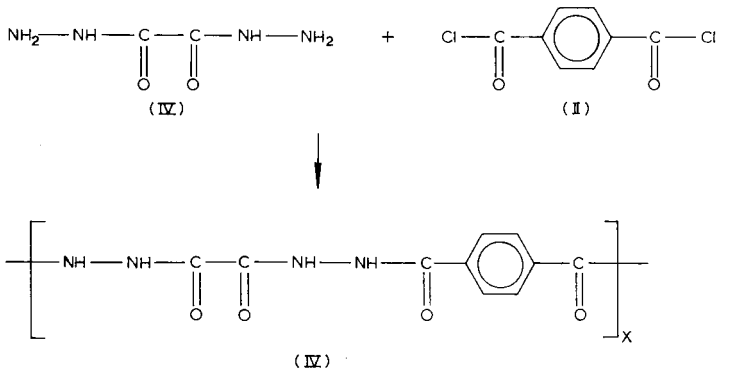

The polymer H-202 is a random copolymer produced from oxalic dihydrazide (IV), terephthaldihydrazide (I) and terephthaloyl chloride (II).

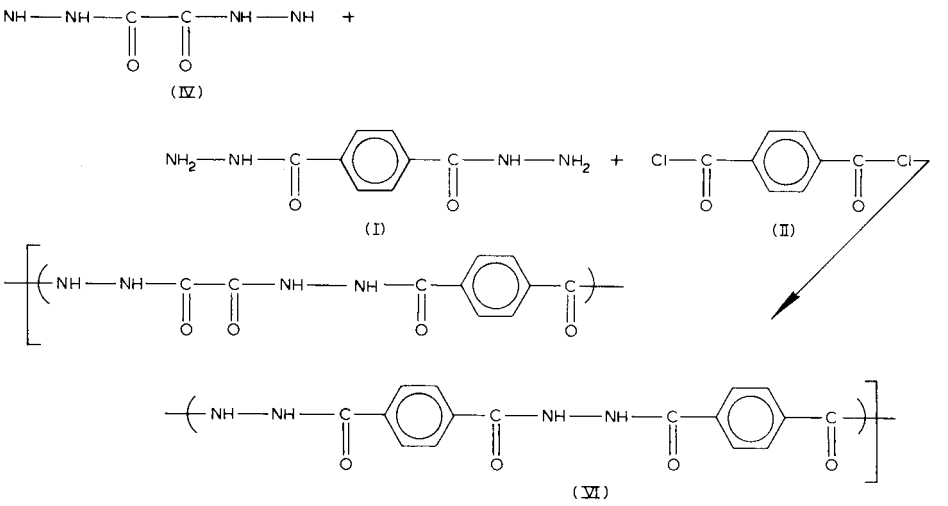

The polymer PABH-TX-500 is an ordered poly(amide-hydrazide) (VII) formed by the reaction of *p*-aminobenzhydrazide (VIII) with terephthaloyl chloride (II).

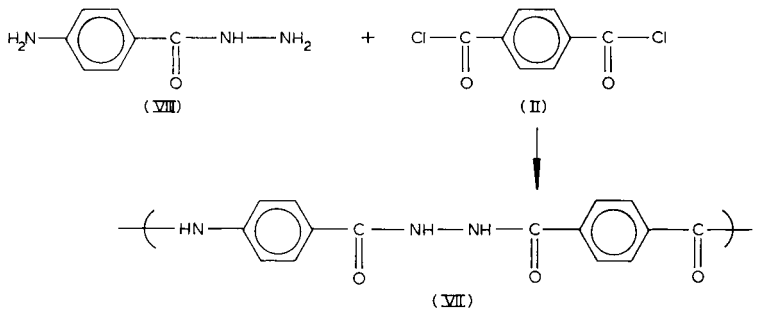

Fusion reaction

The fusion reactions carried out by Siggia and co-workers[2,5] and by Haken and co-workers[3,4,6] were performed in sealed systems. When the polyhydrazides and their copolymers were heated as in our earlier works, *i.e.* in borosilicate tubes that had been sealed under reduced pressure, violent explosions generally occurred which were due presumably to some minor degradation of the hydrazine at the high temperatures (250–300°C) used. The analyses were carried out successfully by placing the appropri-

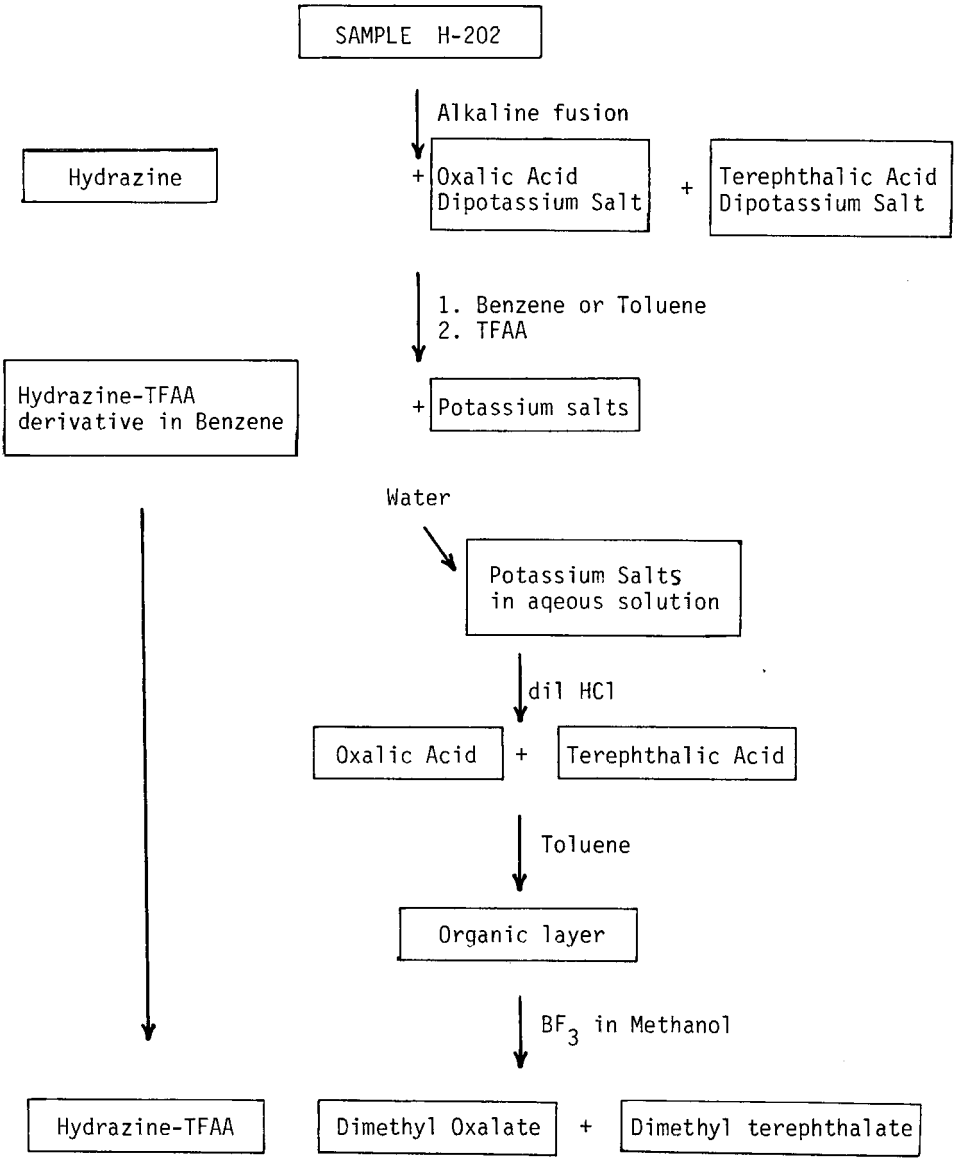

Fig. 1. Analytical scheme for H-202.

ate quantities of polymer and fusion mixture in a suitable microflask fitted with an air condenser or, alternatively, in a 25 cm × 6.0 mm borosilicate tube set in a stainless steel block heated with resistance heaters as described previously[3,4,6].

After fusion for 0.5 h at the refluxing temperature of the mixture, *i.e. ca.* 180°C, after which time all of the polymer had dissolved, the reaction mixture was cooled and separated according to the scheme shown in Fig. 1. The scheme for the copolymer H-202 was also applicable to the polymers H-20, H-22 and PABH-TX-500. With PABH-TX-500 trifluoroacetic anhydride (TFAA) reacts with the potassium salt of *p*-aminobenzoic acid to form the TFAA derivative. The derivative is water soluble and was recovered according to Fig. 1. It was identified after esterification.

Gas chromatography

An F & M 810/29 gas chromatograph fitted with flame-ionization detectors was used with columns and temperature as indicated below, and with helium as carrier gas.

Diamine TEAA derivatives. These were separated on an aluminium column (2 m × 3 mm I.D.) packed with 5% (w/w) neopentyl glycol succinate on Gas Chrom Q (100–120 mesh). The column was programmed between 180 and 22°C at 8°C/min with the final temperature being held for 3 min.

Dimethyl esters. These were separated on an aluminium column (1.2 × 6 mm O.D.) packed with 6% OV-1 silicone gum rubber on Gas-Chrom Q (100–120 mesh). The column was programmed from 160 to 240°C at 10°C/min. The initial temperature was held at 160°C for 3 min after injection.

Liquid chromatography

The liquid chromatograph was a Gowmac Model 80/20 instrument equipped with a UV detector operating at 254 nm.

A Bondapak C_{18} column (25 cm × 6 mm O.D.) was used. For elution methanol–water mixtures were used in the proportions and with the flow-rates shown in the relevant figures.

RESULTS AND DISCUSSION

The hydrazine cleaved from all four polymers was readily resolved as the TFAA derivative on the polyester column previously used for diamines. The separation gave a near-symmetrical peak (shown in Fig. 2), elution being much faster than with the corresponding derivatives of the higher-molecular-weight diphenyldiamines. The conditions selected allowed reasonably rapid elution of the higher-boiling TFA derivative of the *p*-aminobenzoic ester. Although some tailing was evident, this could be greatly reduced by starting the programme at a considerably lower temperature. Separation could also be readily achieved using liquid chromatography, as shown in Fig. 3. The derivative dissolved in methanol, was eluted methanol–water (65:35) that had been filtered and degassed.

The terephthaloyl group that is also present in all four polymers was determined as dimethylterephthalate and the separation is shown in Fig. 4. The same figure shows the separation of dimethyl oxalate produced by cleavage of the alternating polyhydrazide of oxalic and terephthalic acids (H20) and from the random copoly-

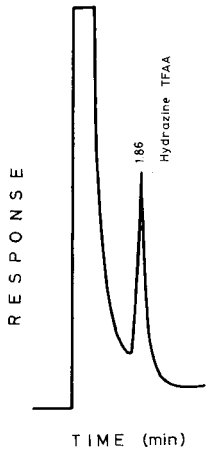

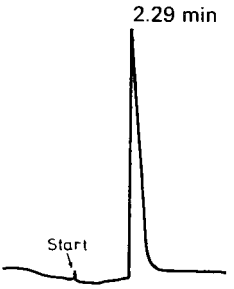

Fig. 2. Gas chromatogram showing separation of the hydrazine TFAA derivative.

Fig. 3. Liquid chromatogram showing separation of the hydrazine TFAA derivative. Eluent: methanol–water (65:35). Flow-rate: 2 ml/min. Pressure: 1500 p.s.i.

mer produced from oxalic and terephthaldihydrazides with terephthaloyl chloride (H202).

Fig. 5 shows separation of the TFAA ester derivative of *p*-aminobenzhydrazide from the poly(amide-hydrazide) PABH-TX-500.

While the separation of the TFAA derivative of hydrazine has been shown using liquid chromatography, it is apparent that the technique could also be successfully used for the other separations shown. The separation of dimethyl terephthalate by liquid chromatography has been shown previously[6] in a work which also reported separation of esters of 1,2,4-benzenetricarboxylic and 1,2,4,5-benzenetetracarboxylic

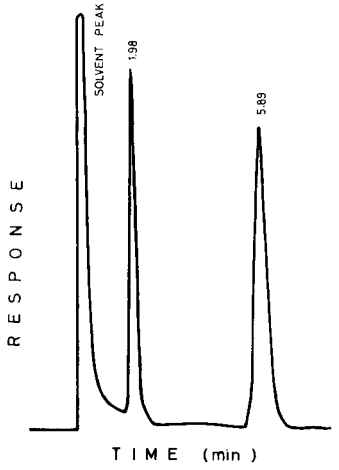

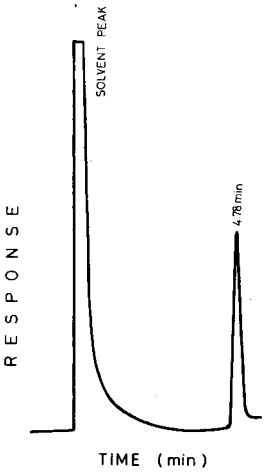

Fig. 4. Gas chromatogram showing separation of diesters of oxalic and terephthalic acids.

Fig. 5. Gas chromatogram showing separation of the TFAA ester derivative of *p*-aminobenzoic acid.

acids. The same work also reported separations of the TFAA derivatives of several 4,4′-diaminodiphenyl compounds using the same Bondapak C_{18} column.

The quantitative aspects of the method have not been definitely determined for the polyhydrazides, this being due in part to the difficulties encountered in establishing the purity of the samples. On the reasonable assumption that the samples are of high purity, near quantitative results were achieved, the error being ± 2–3% which is comparable with earlier results[3,5] from alkali-fusion analyses. Schleuter and Siggia[5] have showed some minor degradation of aromatic diamines by identifying ammonia. Using the same procedure it was evident that the hydrazides produced little ammonia, although other minor products were evident.

ACKNOWLEDGEMENT

The authors are indebted to Dr. W. B. Black for providing samples of the hydrazide polymers.

REFERENCES

1 A. Anton, *Anal. Chem.*, 40 (1968) 1116.
2 S. P. Frankoski and S. Siggia, *Anal. Chem.*, 44 (1972) 2078.
3 G. J. Glading and J. K. Haken, *J. Chromatogr.*, 157 (1978) 404.
4 J. K. Haken and J. A. Obita, *J. Chromatogr.*, 213 (1981) 55.
5 D. D. Schlueter and S. Siggia, *Anal. Chem.*, 49 (1977) 2349.
6 J. K. Haken and J. A. Obita, *J. Chromatogr.*, submitted for publication.
7 J. Preston, *U.S. Pat.* 3,376,269 (1968).
8 J. Preston, *U.S. Pat.* 3,484,407 (1969).
9 A. H. Frazer and F. T. Wallenberger, *J. Polym. Sci., Part A2*, (1964) 1147.
10 A. H. Frazer, *U.S. Pat.* 3,130,182 (1964).
11 A. H. Frazer and F. T. Wallenberger, *J. Polym. Sci., Part A2*, (1964) 1137.
12 A. H. Frazer, *U.S. Pat.* 3,130,183 (1964).
13 F. Dobinson, C. A. Pelezo, W. B. Black, K. R. Lea and J. H. Saunders, *J. Appl. Polym. Sci.*, 23 (1979) 2189.
14 J. Burke, *J. Macromol. Sci. (Chem)*, A7 (1973) 187.
15 W. B. Black, J. Preston, H. S. Morgan, G. Ruman and M. R. Lilyquist, *J. Macromol. Sci. (Chem.)*, A7 (1973) 137.
16 J. Preston, W. B. Black and W. L. Hofferbert, Jr., *J. Macromol. Sci. (Chem)*, A7 (1973) 45.

Journal of Chromatography, 239 (1982) 385–395
Elsevier Scientific Publishing Company, Amsterdam — Printed in The Netherlands

CHROM. 14,854

PREDICTION OF RETENTION TIMES FOR AROMATIC ACIDS IN LIQUID CHROMATOGRAPHY*

T. HANAI*, K. C. TRAN and J. HUBERT
Département de Chimie, Université de Montréal, Montréal, Québec H3C 3V1 (Canada)

SUMMARY

The chromatographic behaviour of 30 aromatic acids was examined in a system of fine particle macroporous polystyrene–divinylbenzene copolymers and acetonitrile–water mixtures at different pH as eluents. The acids were benzoic, phenylacetic, cinnamic, mandelic, naphthoic and hippuric acids, and their hydroxy and/or methoxy derivatives.

At low pH, the logarithm of the capacity ratios of these acids was linearly related to the logarithm of their partition coefficients in the octanol–water system calculated after Rekker. By combining the above result and the dissociation constant of the acid, it was possible to predict the retention times of the acids at a given pH of the eluent.

INTRODUCTION

The aromatic acids and their metabolites are biologically important compounds. Therefore the understanding of their chromatographic behaviour and the development of a system which allows the prediction of their retention times in liquid chromatography could improve their analyses in clinical chemistry and the study of drug metabolism.

When the retention times for the molecular and ionic forms of an ionizable compound and its dissociation constants are known, the retention time in an eluent at a given pH can be calculated in aqueous phase liquid chromatography (LC)[1] and therefore fewer experiments are needed for the rapid optimization of the chromatographic separation conditions.

It is also possible to predict retention times of non-ionic compounds in reversed-phase LC[2–4]. The retention times of aliphatic alcohols, alkyl and/or halogenated benzenes and polyaromatic hydrocarbons were related to the logarithm of their partition coefficients in the octanol–water system (log P) calculated by Rekker's method[5]. The same approach was extended[6] to aromatic acid separations on an octadecyl-bonded silica gel packing with an eluent at pH 2.

* A part of this paper was presented at the *64th Conference of the Chemical Institute of Canada, Halifax, Canada, June 1981*, and the *23rd Rocky Mountain Conference, Denver, CO, U.S.A., August 1981*.

0021-9673/82/0000–0000/$02.75

TABLE I

HYDROPHOBICITY (log P) AND LOGARITHM OF CAPACITY RATIO (log k')

Experimental conditions: column, 25 cm × 4.1 mm I.D., packed with Hitachi 3011; eluent, 0.05 M phosphoric acid in 20–50% acetonitrile in water; column temperature, 55°C.

Compound	*Abbreviation*	*log P_1**	*log P_2**	*log k'*			
				Acetonitrile (%)			
				20	*30*	*40*	*50*
3-Hydroxy-2-naphthoic acid	3(OH)NA	2.83	3.05	–	1.59	1.12	0.84
2-Naphthoic acid	NA	2.72	2.84	–	1.49	1.04	0.74
3-Methoxycinnamic acid	3MeOCA	2.33	2.37	–	1.19	0.79	0.52
Cinnamic acid	CA	2.26	2.32	–	1.10	0.75	0.49
Indole-3-propionic acid	IPA	1.99	2.20	–	1.00	0.67	0.41
2-Hydroxybenzoic acid	2(OH)BA	1.90	2.18	1.28	0.94	0.65	0.43
3-Methoxybenzoic acid	3MeOBA	1.86	1.99	1.27	0.91	0.60	0.37
3-Methoxyphenylacetic acid	3MeOPhA	1.82	1.99	1.21	0.86	0.58	0.34
4-Methoxyphenylacetic acid	4MeOPhA	1.82	1.95	1.19	0.84	0.54	0.33
Phenylacetic acid	PhA	1.75	1.94	1.11	0.81	0.55	0.33
Benzoic acid	BA	1.79	1.94	1.11	0.80	0.57	0.34
Indole-3-acetic acid	IAA	1.75	1.92	1.17	0.80	0.52	0.28

4-Hydroxy-3-methoxycinnamic acid	4(OH)3MeOCA	1.79	1.51	0.97	0.61	0.33	0.12
4-Hydroxycinnamic acid	4(OH)CA	1.72	1.46	0.81	0.50	0.23	0.049
2-Hydroxyhippuric acid	2(OH)HA	1.15	1.55	0.80	0.52	0.29	0.097
2-Hydroxyphenylacetic acid	2(OH)PhA	1.21	1.47	0.69	0.44	0.23	0.075
3-Hydroxybenzoic acid	3(OH)BA	1.25	1.37	0.60	0.37	0.17	−0.004
3-Methoxymandelic acid	3MeOMA	1.30	1.33	0.68	0.42	0.22	0.064
4-Hydroxy-3-methoxybenzoic acid	4(OH)3MeOBA	1.26	1.31	0.65	0.39	0.16	0.030
4-Hydroxybenzoic acid	4(OH)BA	1.25	1.28	0.52	0.31	0.11	−0.013
4-Hydroxyphenylacetic acid	4(OH)PhA	1.21	1.26	0.52	0.29	0.12	−0.018
Mandelic acid	MA	1.23	1.26	0.57	0.35	0.25	0.011
Hippuric acid	HA	1.04	1.25	0.56	0.32	0.19	0.000
4-Hydroxy-3-methoxyphenylacetic acid	4(OH)3MeOPhA	1.22	1.18	0.61	0.37	0.19	0.023
5-Hydroxyindole-3-acetic acid	5(OH)IAA	1.23	1.17	0.49	0.26	0.085	−0.050
3,4-Dihydroxycinnamic acid	$34(OH)_2CA$	1.12	1.15	0.52	0.28	0.076	−0.095
3,4-Dihydroxybenzoic acid	$34(OH)_2BA$	0.65	0.99	0.30	0.12	0.000	−0.16
3,4-Dihydroxyphenylacetic acid	$34(OH)_2PhA$	0.61	0.98	0.30	0.13	0.073	−0.14
3,5-Dihydroxybenzoic acid	$35(OH)_2BA$	0.65	0.94	0.22	0.084	−0.038	−0.16
2,4-Dihydroxyphenylacetic acid	$25(OH)_2PhA$	0.61	0.80	0.16	0.064	−0.058	−0.18
4-Hydroxy-3-methoxymandelic acid	4(OH)3MeOMA	0.76	0.84	0.19	0.065	−0.073	−0.17
3,4,5-Trihydroxybenzoic acid	$345(OH)_3BA$	–	0.72	0.051	−0.022	−0.092	−0.26
Uric acid	UA	–	0.18	−0.19	−0.25	−0.29	–

* log P_1 are hydrophobicity values after Rekker[5,6]; log P_2 are calculated values obtained on an octadecyl-bonded silica gel[6].

In this paper, the combination of the hydrophobicity and the acid dissociation constant K_a is used to predict the retention times of aromatic acids at a given pH and acetonitrile concentration. The retention times of *ca.* 30 aromatic acids were measured on macroporous polystyrene gels as packings with mixtures of acetonitrile and water as eluents. The ionization constants for the different acids were also measured by direct titration in different acetonitrile–water mixtures.

EXPERIMENTAL

A Waters 6000A chromatographic pump was used with a Rheodyne Model 7125 injector. A Hitachi Model 100-20 spectrophotometer with an Altex Model 155-01 8-μl flow cell was used as a detector. Perkin-Elmer Model 56 or Shimadzu Model C-R1A were used as recorder. The packings used were 5- or 10-μm macroporous polystyrene–divinylbenzene copolymers (Hitachi 3013 and 3011, respectively). The columns were slurry-packed in stainless-steel tubes (15 or 25 cm × 4.1 mm I.D.). The column was thermostated, and the temperature was controlled by a Haake F5e water bath. Analytical grade chemicals supplied by Sigma and Chem. Service were used without further purification. Burdick & Jackson glass-distilled acetonitrile UV and distilled water treated through Milli-Q system (Millipore) were used as components of the eluent. The pH was controlled with a 0.05 *M* sodium phosphate buffer. A pH meter built at Université de Montréal was used with Fisher Scientific Model 13-639-6, 13-639-56 and 13-639-92 electrodes.

RESULTS AND DISCUSSION

The logarithms of the capacity ratios (log k') of the acids in their molecular form were measured in 20–50% acetonitrile in water mixtures with 0.05 *M* phosphoric acid at 55°C. Their values and the hydrophobicity expressed as log *P* are reported in Table I.

The log k' was linearly related to log *P* in this system, and the relation is given by eqn. 1:

$$\log k' = y \cdot \log P + m \tag{1}$$

where y and m are the slope and the intercept of the least-squares straight line, respectively.

The correlation coefficients obtained when log *P* values after Rekker[5] (log P_1 in the tables) were used in eqn. 1, were 0.947 (n = 25) in acetonitrile–water (20:80), 0.973 (n = 31) in acetonitrile–water (30:70), 0.959 (n = 31) in acetonitrile–water (40:60) and 0.965 (n = 31) in acetonitrile–water (50:50) mixtures (n = the number of compounds used in the least-squares). The correlation coefficients obtained with log *P* values (log P_2 in the tables) derived from measurements in reversed-phase LC on an octadecyl-bonded silica gel[6] were 0.988 (n = 27) in acetonitrile–water (20:80), 0.996 (n = 32) in acetonitrile–water (30:70), 0.993 (n = 32) in acetonitrile–water (40:60) and 0.996 (n = 32) in acetonitrile–water (50:50) mixtures. All the lines merged at a single point and therefore the retention time in a given eluent (acetonitrile–water) for the molecular form of an acid can be predicted from its log *P* value.

TABLE II

DISSOCIATION CONSTANTS OF ACIDS (pK_a) IN WATER

The pK_a values were measured in different acetonitrile–water mixtures. They were converted into pK_a values in pure water by the experimentally derived relation:

$$pK_a \text{ (water)} = pK_a \text{ (acetonitrile–water)} - 0.022(\% \text{ acetonitrile}) \quad (7)$$

Compound	*Chromatography*		*Titration*	*Literature*
	*Method 1**	*Method 2***		
3(OH)NA	2.56	2.86	2.89	
NA	4.24	–	4.25	4.17***
3MeOCA	4.34	4.24	4.40	
CA	4.37	4.61	4.37	4.44***
IPA	4.79	4.73	4.81	
2(OH)BA	2.69	2.97	3.06	2.97***, 2.92§, 2.84§, 1.88§
3MeOBA	4.10	4.09	4.09	
3MeOPhA	4.37	4.45	4.27	
4MeOPhA	4.67	4.44	4.35	
PhA	4.43	4.58	4.29	4.25***, 4.14, 4.31, 4.10§
BA	4.18	4.20	4.19	4.19***, 3.78, 3.93§
IAA	4.68	4.60	4.65	4.75***
4(OH)3MeOCA	4.57	4.57	4.56	
4(OH)CA	4.56	4.56	4.57	
2(OH)HA	3.38	–	3.58	
2(OH)PhA	4.14	4.18	4.14	
3(OH)BA	4.12	4.15	4.16	4.06***
3MeOMA	3.28	3.36	3.47	
4(OH)3MeOBA	4.50	4.52	4.48	
4(OH)BA	4.56	4.73	4.53	4.48***
4(OH)PhA	4.43	–	4.40	4.30§
MA	3.40	3.41	3.42	3.85***, 3.37, 3.46, 3.49§
HA	3.42	–	3.58	3.80***
4(OH)3MeOPhA	4.34	4.30	4.37	4.29§
5(OH)IAA	4.61	4.65	4.57	
$34(OH)_2CA$	4.54	4.54	4.53	
$34(OH)_2BA$	4.48	4.59	4.49	4.48***
$34(OH)_2PhA$	4.37	4.38	4.34	4.20§
$35(OH)_2BA$	4.18	4.23	4.12	4.04***
$25(OH)_2PhA$	4.13	–	4.06	
4(OH)3MeOMA	3.58	3.71	3.55	3.25§
$345(OH)_3BA$	4.45	–	4.40	4.41***
UA	–	–	–	3.89***
$24(OH)_2BA$	–	–	3.32	3.20, 3.25§§
$34(OH)_2MA$	–	–	3.50	

* Experimental conditions, see Table I.

** Obtained on Hitachi 3013 packing, with a 20% acetonitrile–water mixture with 0.05 *M* sodium phosphate at 55°C.

*** Ref. 6.

§ Ref. 8.

§§ Ref. 9.

TABLE III

COMPARISON OF PREDICTED AND OBSERVED CAPACITY RATIOS FOR ACIDS

Compound	k'_m*(obs.)**	k'_m*(calc.)***	k'_i*(obs.)**	*k′ at pH 4.0*			*k′ at pH 5.09*		
				*Obs.**	*Pred.****	*Pred.* §	*Obs.**	*Pred.****	*Pred.* §
3(OH)NA	39.17	41.65	1.54	5.80	12.05	10.91	2.38	2.68	1.18
NA	30.73	29.47	1.02	24.49	26.36	26.25	11.44	12.49	11.88
3MeOCA	15.52	13.73	0.84	12.90	12.70	12.63	6.87	7.13	6.70
CA	12.67	12.60	0.78	10.90	11.56	11.53	6.13	6.35	5.93
IPA	11.10	10.38	0.70	9.92	10.06	10.04	7.64	7.60	7.40
2(OH)BA	8.76	10.02	0.68	2.20	3.90	3.45	1.01	1.07	0.41
3MeOBA	8.20	7.32	0.65	6.53	6.31	6.21	3.24	2.76	2.32
3MeOPhA	7.22	7.29	0.63	6.22	6.59	6.53	3.65	3.38	3.01
4MeOPhA	6.95	6.87	0.61	6.03	6.32	6.26	4.22	3.48	3.15
PhA	6.40	6.74	0.65	5.59	6.12	6.06	3.22	3.23	2.86
BA	6.33	6.77	0.58	5.38	6.01	5.93	2.92	2.86	2.50
IAA	6.33	6.51	0.64	5.69	6.24	6.21	3.98	4.34	4.10
4(OH)3MeOCA	4.09	3.32	0.56	3.67	3.16	3.13	2.52	2.16	1.92
4(OH)CA	3.18	3.07	0.52	2.83	2.93	2.90	1.76	2.01	1.79
	3.28	3.52	0.64	1.98	2.47	2.23	0.99	1.00	0.44

2(OH)PhA	2.77	3.08	0.68	2.38	2.75	2.66	1.38	1.50	1.05
3(OH)BA	2.35	2.64	0.50	2.01	2.36	2.29	1.12	1.25	0.93
3MeOMA	2.63	2.47	0.60	1.52	1.67	1.42	0.73	0.79	0.24
4(OH)3MeOBA	2.45	2.39	0.42	2.23	2.26	2.23	1.50	1.47	1.27
4(OH)BA	2.04	2.25	0.43	1.86	2.14	2.11	1.36	1.52	1.26
4(OH)PhA	1.95	2.18	0.51	1.75	2.04	2.00	1.22	1.32	1.06
MA	2.25	2.20	0.60	1.48	1.47	1.20	0.71	0.74	0.20
HA	2.09	2.16	0.54	1.43	1.57	1.37	0.74	0.74	0.27
4(OH)3MeOPhA	2.35	1.91	0.52	2.13	1.80	1.75	1.37	1.17	0.90
5(OH)IAA	1.81	1.90	0.52	1.73	1.82	1.79	1.28	1.32	1.11
$34(OH)_2CA$	1.90	1.84	0.35	1.69	1.75	1.73	1.23	1.19	1.03
$34(OH)_2BA$	1.33	1.40	0.44	1.23	1.34	1.31	0.91	0.96	0.75
$34(OH)_2PhA$	1.34	1.38	0.43	1.17	1.29	1.25	0.85	0.86	0.62
$35(OH)_2BA$	1.21	1.29	0.45	1.07	1.17	1.11	0.72	0.73	0.43
$25(OH)_2PhA$	1.16	1.14	0.48	1.18	1.03	0.96	0.69	0.68	0.34
4(OH)3MeOMA	1.16	1.09	0.43	0.83	0.84	0.67	0.55	0.51	0.13
$345(OH)_3BA$	0.95	0.90	0.41	0.83	0.86	0.83	0.67	0.65	0.44
UA	0.56	–	0.34	0.52	–	–	0.49	–	–

* Experimental conditions are given in Table I.
** Calculated by eqn. 1.
*** Calculated by eqn. 2 with observed k_i'.
§ Calculated by eqn. 3.

TABLE IV

COMPARISON OF PREDICTED AND OBSERVED CAPACITY RATIOS FOR ACIDS

Compound	k'_m*	k'_i**	*k′ at pH 4.26*			*k′ at pH 5.62*		
			*Obs.****	*Pred.*§	*Pred.*§§	*Obs.****	*Pred.*§	*Pred.*§§
3(OH)NA	31.72	0.72	2.93	5.78	5.18	1.35	0.98	0.27
NA	21.66	0.61	15.74	17.81	17.70	3.84	4.04	3.53
3MeOCA	9.33	0.41	8.32	8.11	8.05	2.39	2.34	2.01
CA	8.49	0.39	6.93	7.31	7.25	2.13	2.05	1.73
IPA	6.85	0.36	6.52	6.47	6.45	3.35	3.05	2.84
2(OH)BA	6.59	0.35	1.14	1.75	1.48	0.50	0.43	0.08
3MeOBA	4.66	0.30	4.03	3.59	3.52	1.34	0.82	0.55
3MeOPhA	4.64	0.30	3.88	3.88	3.83	1.38	1.04	0.79
4MeOPhA	4.35	0.29	3.76	3.74	3.69	1.67	1.09	0.86
PhA	4.26	0.29	3.95	3.58	3.53	1.67	0.99	0.75
BA	4.28	0.29	3.34	3.46	3.40	1.10	0.87	0.62
IAA	4.10	0.28	3.62	3.78	3.76	1.55	1.54	1.35
4(OH)3MeOCA	1.95	0.20	2.15	1.78	1.76	0.91	0.70	0.55
4(OH)CA	1.79	0.19	1.63	1.63	1.61	0.71	0.65	0.52
2(OH)HA	2.08	0.21	1.00	1.21	1.01	0.50	0.28	0.08
2(OH)PhA	1.79	0.19	1.27	1.43	1.39	0.55	0.40	0.23
3(OH)BA	1.51	0.18	1.09	1.23	1.19	0.31	0.36	0.21

4(OH)3MeOBA	1.36	0.17	1.27	1.22	1.20	0.50	0.47	0.34
4(OH)BA	1.27	0.17	1.00	1.15	1.14	0.49	0.46	0.34
4(OH)PhA	1.22	0.16	1.00	1.08	1.06	0.43	0.39	0.26
MA	1.24	0.16	–	0.59	0.49	0.19	0.19	0.03
HA	1.21	0.16	0.76	0.67	0.59	0.28	0.20	0.05
4(OH)3MeOPhA	1.06	0.16	1.19	0.93	0.91	0.44	0.34	0.22
5(OH)IAA	1.05	0.15	0.97	0.96	0.95	0.51	0.41	0.30
$34(OH)_2CA$	1.02	0.15	0.84	0.93	0.91	0.45	0.38	0.27
$34(OH)_2BA$	0.75	0.13	0.58	0.68	0.67	0.31	0.29	0.19
$34(OH)_2PhA$	0.74	0.13	0.60	0.65	0.63	0.30	0.25	0.14
$35(OH)_2BA$	0.69	0.12	0.55	0.56	0.53	0.18	0.20	0.09
$25(OH)_2PhA$	0.60	0.12	0.46	0.47	0.44	0.20	0.17	0.07
4(OH)3MeOMA	0.57	0.11	0.28	0.33	0.27	0.17	0.13	0.02
$345(OH)_3BA$	0.46	0.10	0.36	0.42	0.40	0.20	0.18	0.10
UA	–	–	0.09	–	–	0.09	–	–

* k'_m was calculated by eqn. 1.

** k'_i was calculated by eqn. 1.

*** The column was 15 cm long, 4.1 mm I.D. and packed with Hitachi 3013. The eluent was 30% acetonitrile–water with 0.05 *M* sodium phosphate. The column temperature was 55°C.

§ Calculated by eqn. 2.

§§ Calculated by eqn. 3.

The better correlation between the log k' and log P_2 values suggests that the log P values measured on an ODS silica gel can also be used with a different packing.

The dissociation constants K_a of the different acids were measured by chromatography in 20–50% acetonitrile–water mixtures with 0.05 M sodium phosphate (Table II). The values obtained by titration in acetonitrile–water mixtures with and without 0.1 M sodium sulfate are also given in Table II.

The dissociation constants obtained by LC were similar to those obtained by direct titration. If the dissociation constant is known, it should be possible to predict the retention times of an acid in an eluent at different pH values and/or concentrations of acetonitrile. To verify this, two eluents with different pH values were prepared in an 30% acetonitrile–water mixture with 0.05 M sodium phosphate. The capacity ratios k' of the acids at a given pH were calculated from eqns. 2 and 3:

$$k' = (k'_m + k'_i \cdot K_a/[H^+])/(1 + K_a/[H^+]) \quad (2)$$

$$k' = k'_m/(1 + K_a/[H^+]) \quad (3)$$

Eqn. 2, where k'_m is the capacity ratio of the acid in its molecular form, k'_i the capacity ratio of the acid in its ionic form and K_a the dissociation constant of the acid in the eluent, can be simplified to eqn. 3 by assuming that k'_i is negligible compared with k'_m (ref. 7).

The capacity ratio of the molecular form of an acid (k'_m calc.) in acetonitrile–water (30:70) was calculated from eqn. 1 with the log P_2 value in Table I. The y value for a given eluent was obtained from the experimental results in Table I as previously described[4].

The capacity ratio k'_i was measured in acetonitrile–water (30:70) mixtures with 0.05 M dibasic sodium phosphate, and the dissociation constants of the acids were obtained by direct titration.

The measured and calculated capacity ratios are listed in Table III. The average difference between the calculated and observed capacity ratios was *ca.* 10%. The largest differences were found for 3(OH)NA and 2(OH)BA. The main reason for such a difference was probably the poor reproducibility of the dissociation constant obtained by titration.

The capacity ratios predicted from eqn. 3 were usually found satisfactory, and this approach could be used as a first approximation for the calculation of the capacity ratios.

The agreement between the observed and the calculated capacity ratios was usually within ±10%. The compounds for which the largest deviation was found are those for which the largest error was found in K_a.

To extend the study to another system, a new column was packed with a Hitachi 3013 polystyrene gel. The eluents were 10–60% acetonitrile in water mixtures with 0.05 M sodium phosphate. Six standard* compounds were selected to characterize the system following the procedure described previously[4].

For each eluent (0.05 M phosphoric acid with acetonitrile) the capacity ratios k'_m of the standard compounds were measured and related to their hydrophobicity

* The standard compounds were: 4-hydroxy-3-methoxymandelic acid, 4-hydroxy-3-methoxybenzoic acid, 2-hydroxynippuric acid, indole-3-acetic acid, 3-methoxybenzoic acid and cinnamic acid.

(log P). From a least-squares calculation the slope y and the intercept m in eqn. 1 were obtained for each eluent. With these values the capacity ratios k'_m for all acids used previously were calculated by eqn. 1.

The same procedure was used to calculate the k'_i values of the acids. The standard compounds used were the same as previously and in addition 3,4,5-trihydroxybenzoic and 2-naphtoic acids were also used. The eluent was 0.05 M dibasic sodium phosphate in acetonitrile–water (30:70). The dissociation constants obtained by titration were used (Table II). The capacity ratios were measured and calculated by eqns. 2 and 3 in eluents with 30% acetonitrile at pH 4.26 and 5.62. All data are collected in Table IV. Here again, the agreement between the observed and predicted k' were within $\pm 10\%$. For 3-hydroxy-2-naphtoic acid an error higher than 10% was attributed mainly to the error in K_a.

CONCLUSION

The hydrophobicity calculated after Rekker can be used as a first appproach to predict retention times for both non-ionic[4] and ionic compounds on different packings (ODS, polystyrene gels) used in reversed-phase LC. The relationship between hydrophobicity (log P) and capacity ratios (log k') is linear for ionic and non-ionic compounds but different slopes were obtained. The combination of hydrophobicity and dissociation constant with solvent concentration effect also allows us to predict the retention times for acids.

ACKNOWLEDGEMENTS

The authors thank Dr. N. Takai, Tokyo University, Tokyo, Japan for his gift of the Hitachi 3011 and 3013 packings. This work was supported by the National Science and Engineering Research Council of Canada (grants RD-171 and A-0834).

REFERENCES

1 D. J. Pietrzyk and C.-H. Chu, *Anal. Chem.*, 49 (1977) 860.
2 T. Hanai, *Chromatographia*, 12 (1979) 77.
3 T. Hanai and M. D'Amboise, *Pittsburgh Conference (No. 208), Cleveland, OH, March 1979.*
4 T. Hanai, C. Tran and J. Hubert, *J. High Resolut. Chromatogr. Chromatogr. Commun.*, 4 (1981) 454.
5 R. F. Rekker, *The Hydrophobic Fragmental Constant*, Elsevier, Amsterdam, 1977.
6 T. Hanai and J. Hubert, *J. Chromatogr.*, submitted for publication.
7 T. Hanai and J. Hubert, *63rd Conference of the Chemical Institute of Canada (No. AN-108), Ottawa, Canada, June 1980.*
8 Cs. Horváth, W. Melander and I. Molnar, *Anal. Chem.*, 49 (1977) 142.
9 J. L. M. van de Venne, J. L. H. M. Hendrikx and R. S. Deelder, *J. Chromatogr.*, 167 (1978) 1.

Journal of Chromatography, 239 (1982) 397–410
Elsevier Scientific Publishing Company, Amsterdam — Printed in The Netherlands

CHROM. 14,594

SPACIAL DISTRIBUTION OF IONS AND ELECTRONS WITHIN ^{63}Ni IONIZATION CELLS

E. P. GRIMSRUD* and M. J. CONNOLLY
Department of Chemistry, Montana State University, Bozeman, MT 59717 (U.S.A.)

SUMMARY

Measurements of ion densities within a specialized ^{63}Ni ionization cell are described where the distance between a radioactive foil and the point of ion density measurement is continuously variable. Air and dichlorodifluoromethane are used as the ionizing medium. Measurements are made with an atmospheric pressure ionization mass spectrometer. The results are shown to be in excellent agreement with a simple quantitative model of the experiment. The model is then used to predict the distribution of ions throughout the active volumes of several cylindrical cells of typical dimensions.

INTRODUCTION

Radioactive beta emitters have become integral components of several important detectors for gas chromatography (GC). The electron-capture detector (ECD) is the most established among these, while the relatively newer techniques of ion mobility spectrometry (IMS) and atmospheric pressure ionization mass spectrometry (APIMS) show considerable promise. In the future development of instruments which require ionization of gases at relatively high pressures, we might expect to find beta emitters fulfilling that function.

An important characteristic of each beta source which we wish to explore here relates to their penetration into a gas and the subsequent distribution of ions and electrons throughout an ionization cell. The nature of beta penetration into GC carrier gases has been a point of continuous interest since the first uses of radiation sources for GC detection. From the known, maximum energies associated with the various beta-emitting nuclides, estimates of the "maximum" or "average" penetration depths have been made and, for the lack of more complete information, have been used as criteria for cell design. A complete description of the ionization caused by a given source is complicated by at least the following realities: a beta emitter produces beta particles of a broad range of energies; the trajectory of a beta particle through an absorbing medium is not necessarily straight; the material onto which the beta nuclide is plated will affect the energy distribution of the emitted betas due to backscattering; and the design of the cell strongly affects the net distribution of radiation and ionization. Due to these complexities, perhaps the most reliable infor-

0021-9673/82/0000–0000/$02.75

mation concerning GC beta sources obtained so far has been by measurements of cell currents under actual or simulated conditions of the ionization cell of interest. Recently, separate reports by Aue and Kapila[1] and by Ayala *et al.*[2] have described experiments in which the standing currents observed in ^{63}Ni and ^{3}H ionization cells are interpreted in terms of the probable penetration depths of the betas. Such measurements of cell current reflect an integration or sum of all ionization events occurring everywhere in the cell being examined.

The measurements to be reported here offer additional and complementary information to the subject of beta penetration into a gas in that they reflect the ion density at a specific location in an ionization cell, rather than the total cell current. An advantage of this approach is that the results obtained with our specialized cell are directly transformable to other source designs. Therefore, in this article we will describe and present evidence supporting a simple quantitative model by which radiation intensity and ion densities throughout any imagined cell can be predicted with much greater accuracy than has been previously possible. Because of its wide use in ionization cells, ^{63}Ni-on-Pt foil is the subject of this study. The method developed here for predicting the character of an ionization cell can be applied to any beta source other than ^{63}Ni, as long as the mass absorption curve of the source material is known.

EXPERIMENTAL

The APIMS system used in this study has been described previously[3,4]. Two slightly different ion source configurations have been used here. These are shown in Fig. 1. In ion source A of Fig. 1, the only piece of ^{63}Ni-on-Pt foil present is a small disk of 3.0 mm diameter and 0.20 mCi activity. It is held onto the end of a moveable pin as shown. A stainless-steel cap holds the ^{63}Ni disk in place by overlapping it slightly, so that the effective, exposed portion of the disk is then 2.8 mm in diameter. Carrier gas is passed through the source from right to left as shown in the figure at a flow-rate of *ca.* 30 ml min^{-1}. The right-side wall of the source is formed by a 5/8-in.

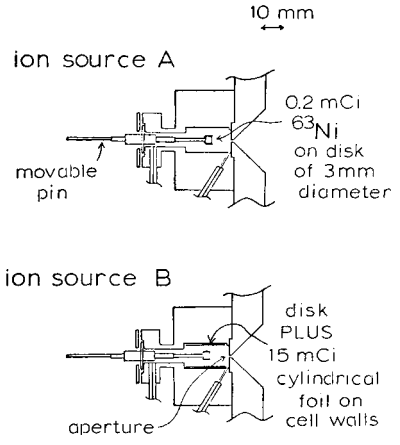

Fig. 1. Specialized atmospheric pressure ion sources in which the distance between a ^{63}Ni-on-Pt disk and the ion-sampling aperture is variable.

disk of 25-μm thick nickel with a 25-μm diameter aperture in the center. This aperture allows about 5 ml atm min^{-1} of the source contents to enter a vacuum envelope. The ion content of this gas is monitored by a quadrupole mass filter with an ion-counting detection system. In the measurements reported here, the total positive-ion signal is measured as a function of the distance between the sampling aperture and the ^{63}Ni disk on the moveable pin. For all mass spectrometry measurements, the stainless central pin is electrically grounded to the mass spectrometer ion source so that the active volume is free of applied electrical fields at all times.

Ion source B is the same one shown as source A except that the cylindrical walls of the source now are formed by a ^{63}Ni-on-Pt foil of 15 mCi activity. The cylinder is 10 mm in diameter and 18 mm in length. The moveable ^{63}Ni disk is also present in source B. The activity per unit area of the two pieces of foil present in source B is the same.

For both sources the disk-to-aperture distance was continuously variable from 0.5 mm to 22 mm. The lower limit was somewhat arbitrarily decided upon so that the ^{63}Ni disk would never come in direct contact with the gas-sampling aperture and, thereby, possibly dislodge the ^{63}Ni disk from the pin. The moveable pin can be electrically isolated from the cell block so that the cell current can be measured (as is done in one experiment here) by using the pin as an anode. Both ion sources A and B are home-built from stainless steel.

The carrier gases used are utility-grade air and CF_2Cl_2. The simultaneous presence of negative ions with positive ions was actually desirable in these experiments because better reproducibility is obtained than when purified nitrogen is used. We believe that differences in reproducibility are due to the presence of small potentials which can develop on all surfaces of the cell including areas near the ion-sampling aperture. Because the diffusion velocities of positive ions and negative ions are very similar, their rates of transport to surfaces are undoubtedly nearly equivalent in the absence of applied fields and, thus, these surface potentials do not tend to occur when air is used as the source gas. Electrons, however, having a much greater diffusion velocity, may tend to cause an unequal arrival rate of the two charge types at cell boundaries when nitrogen is used. Thus, even in a perfectly clean cell, small but significant equilibrium potentials can exist at the cell boundaries. This effect is magnified if the cell is not perfectly clean (the usual case). Then a thin layer of matter separates the point of contact of the ion or electron with the conducting walls and additional boundary potentials can be created. Since the penetration depths of the betas are determined only by the mass density of the attenuating medium, and not at all affected by the ultimate fate of the negative portion of the charge pairs created, we have used gases in which negative ions will be formed.

RESULTS AND DISCUSSION

The principle experimental results to be considered in this paper are shown in Fig. 2. The total positive-ion signal of the mass spectrometer is shown as a function of the disk-to-aperture distance, d, where air and CF_2Cl_2 were used as the carrier gas with source A and air with source B. Fig. 2 shows that each of the three experiments produced a dependence of signal on d which is unique and distinct from the other two. Of the three sets of data shown, only the magnitudes of the two sets of air

measurements can be meaningfully compared with each other, since only for these two sets could the mass spectrometer ion focusing and detector settings be unchanged without exceeding the dynamic response range of the instrument. The relative magnitude of the CF_2Cl_2 data at any value of d cannot be meaningfully compared with the air data, however, because very different mass spectrometer focusing settings where required with CF_2Cl_2 in order to keep the measurements at low disk-to-aperture distances within the dynamic response range of the instrument. Thus, in comparing the measurement of CF_2Cl_2 with those of air using source A, only the relative shapes of the two curves should be considered, and they are, indeed, seen to be distinguishably different. The CF_2Cl_2 data increases much more sharply as d is made small than does the air data.

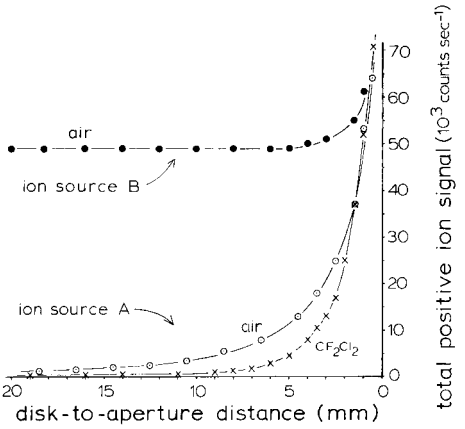

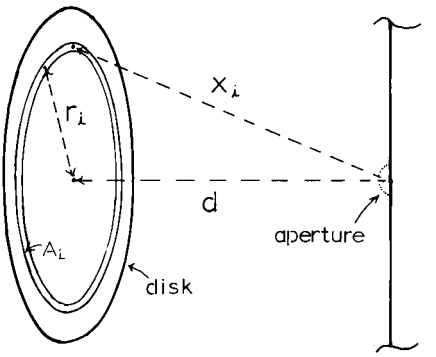

Fig. 2. Total positive-ion signals measured by mass spectrometer as a function of the disk-to-aperture distance. The source pressure and temperature are 0.85 atm and 23°C (ambient) in all cases.

Fig. 3. Representation of experiment using ion source A.

In order to develop a quantitative description of the data in Fig. 2 it is useful to consider the drawing in Fig. 3. In our experiment a signal is obtained which is proportional to the density of positive ions in a small region of space immediately adjacent to the aperture (signal = positive-ion density × flow-rate of gas through aperture × efficiency of ion transport through mass spectrometer). It is essential to the interpretation to be made here that the size of this volume being sampled by the mass spectrometer is small relative to the distances separating the ^{63}Ni disk and the aperture. We have given careful consideration to this point previously (p. 481 of ref. 4), and the conclusion is that the volume being effectively "seen" by the mass spectrometer is smaller than 0.5 mm, the distance of closest approach by the ^{63}Ni disk. The reason for this very local sampling of ion density by the mass spectrometer is that ions are rapidly destroyed in a field-free source by the recombination of opposite charge types. For ions which are formed more than 1 mm from the aperture, destruction by recombination is much faster than the rate at which they can be transported by gas flow to the aperture. Therefore, only ions which are formed very close to the aperture have a high probability of being measured by the mass spectrometer.

Again considering the drawing in Fig. 3, it is obvious that the ion density in the sampled volume will bear some type of inverse relation to the distance, d. Instead of

viewing the experiment in terms of the disk as a whole and the one value of d, however, it is useful to envision the disk as being composed of numerous concentric area units as shown, each having its own distance, x_i, to the aperture at each setting of d. The measured ion density will then be the result of a summation of contributions from the individual area elements of the disk. The very important advantage of viewing the experiment in this manner is that a generalized expression for the radiation intensity at the observation point will then result which, as will be seen, can then be used to predict the radiation intensity and ion density at any or all points in the active volume of any imagined cell design. Since we expect the contributions of each area unit, A_i, to the radiation intensity, S, at the observation point to be additive, eqn. 1 can be written

$$S = K \sum_i \mathrm{f}(x_i) \tag{1}$$

where K is a proportionality factor and $\mathrm{f}(x_i)$ is some function (not yet determined) which describes the effect of separation, x_i, of each area unit on the radiation intensity at the observation point. Eqn. 1 assumes that the total emitter surface has been partitioned into individual units, A_i, of equal area. For the experiment symbolized by Fig. 3, the symmetry accompanying this cell design makes reduction of the system into equal area units with accompanying x_i values very simple. In our calculations the disk was divided into twenty concentric rings of equal areas (rings are narrower as r_i increases), and the value of x_i associated with each is calculated from $x_i = (d^2 + r_i^2)^{1/2}$. With each setting of d, a unique combination of x_i values are set, which should alter the radiation intensity and the positive ion density at the observation point in a manner consistent with eqn. 1. Viewing the problem in this way the critical remaining task is to determine the form of the function $\mathrm{f}(x_i)$ which provides the best fit to the data.

In our initial attempts at matching the experimental data of Fig. 2 to a mathematical expression, several forms for $\mathrm{f}(x_i)$ were somewhat arbitrarily selected for trial without much consideration being given to the physical basis of each. These attempts were not successful until, upon closer consideration of the theoretically expected form of $\mathrm{f}(x_i)$, the following relationship between the mass spectrometry signal and the distances, x_i, was tested.

$$\text{signal} = K' \sqrt{\sum_i \frac{\mathrm{e}^{-ax_i}}{x_i^2}} \tag{2}$$

where K' is again simply a proportionality constant and a is a constant which was adjusted to provide the best fit to the data. By inspection of eqns. 1 and 2 and realizing that the measured signal is proportional to positive-ion density, n_+, the following relationships are then also implied.

$$\mathrm{f}(x_i) = \frac{\mathrm{e}^{-ax_i}}{x_i^2} \tag{3}$$

and

$$n_+ \propto \sqrt{S} \tag{4}$$

Eqn. 2 appears to be a valid description of the experiment for the combined reasons that (1) it works and (2) it has a plausible physical basis (which will be related below). A demonstration of the fit of eqn. 2 to the experiments using air is shown in Fig. 4. For the moment, considering the data taken with source A, the solid curve shown is obtained by eqn. 2 where $a = 0.12\ \text{mm}^{-1}$. This calculated curve has been normalized to the data at the point where the measured signal is 10,000 counts/sec. The calculation is then seen to coincide with the other experimental points reasonably well. The dashed and dotted curves are calculations where the value of a used is halved and doubled, respectively. These do not fit the data nearly as well. For the case of CF_2Cl_2 shown in Fig. 5, the solid line is again obtained from eqn. 2 but this time by using a value for a of $0.50\ \text{mm}^{-1}$. It will be shown shortly in the discussion of the physical basis of eqn. 2, that the values of the constant, a, determined for air and CF_2Cl_2 in Figs. 4 and 5 have a definite physical meaning and could, in fact, have been predicted from independent measurements of a completely different type than those reported here.

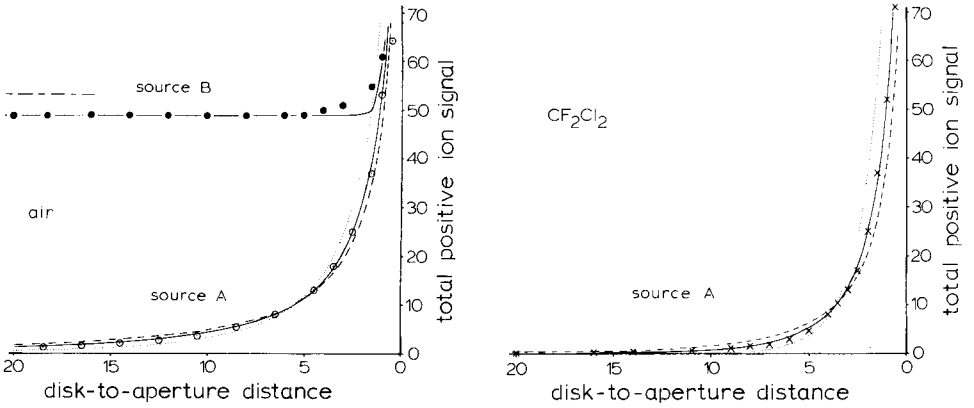

Fig. 4. Comparison of air data (dots and circles) with curves calculated from eqn. 2. For the source A curves the values of the coefficient a used are: $a = 0.12\ \text{mm}^{-1}$ (solid), $a = 0.24\ \text{mm}^{-1}$ (dotted) and $a = 0.06\ \text{mm}^{-1}$ (dashed). All curves have been normalized with respect to the data at $d_s = 5.5$ mm, where the signal is 10,000 counts/sec. For the source B calculation, the solid curve is for $a = 0.12$ with normalization with respect to the source B data at $d = 20$ mm. The short dashed line is the calculated curve in this region, normalized with respect to the source A data at 5.5 mm.

Fig. 5. Comparison of CF_2Cl_2 data (X) with curves calculated from eqn. 2. The values of the coefficient, a, used for each curve are: $a = 0.50$ (solid), $a = 1.0$ (dotted), and $a = 0.25$ (dashed). The calculations have been normalized with respect to the data at $d = 3.5$ mm where the signal is 10,000 counts/sec.

The data in Fig. 4 where ion source B was used with air carrier gas can also be compared with a prediction based on eqn. 2. This is done with the solid curve (normalized to data point at $d = 20$ mm). To obtain this calculation the contribution to ionization at the aperture from the much larger cylindrical wall was also included by dividing the cylinder into a stack of rings, each having an area equal to each other and equal to the area of the individual units defined for the disk. As the disk is moved closer to the pin in source B, two opposing effects can be expected. Radiation intensity at the observation point will tend to be increased due to a closer disk, but also will tend to be decreased due to partial blockage of radiation from the wall by the disk. This "eclipse" of wall radiation should begin at *ca.* $d = 7.5$ mm and increase

continuously with closer approach of the disk. The solid line in Fig. 4, source B, was calculated with $a = 0.12\ \text{mm}^{-1}$. The prediction is that the mass spectrometry signal will change very little with d until the last 2 mm of approach. The experimental data agrees reasonably well with this prediction, although the experimental points are observed to begin increasing measurably at *ca.* 4 mm, rather than at 2 mm. This difference is possibly due to the fact that the trajectories of betas in an attenuating medium are not necessarily straight and, therefore, the blockage of wall radiation by the disk is probably not quite as efficient as assumed in the calculation.

Just above the source B data in Fig. 4, a short dashed line is shown. This line indicates the predicted signal for source B if the calculations are normalized to the same reference point used for the source A calculation at $d = 5.5$ mm. The largest source of uncertainty in comparing the magnitudes of signals obtained by source A with those of source B results from the fact that upon changing the source a new aperture must be used. Our experience has indicated that each aperture causes a slightly different total ion signal to be observed, presumably due to slight variations in their sizes. Over the course of using about a dozen apertures in a given source, we estimate that the range of signal variations has been *ca.* 20%. Thus, it is seen that the total ion signal for source B is very adequately predicted by the source A data and eqn. 2.

Physical justification for eqn. 2

It can be shown that eqn. 2 has a physical basis from which the equation might have been suggested independent of our experiments. Furthermore it can be shown that even the correct value of the parameter, a, can be calculated from information readily available for the nuclide of interest.

We might start by explaining why n_+, the measured positive-ion density, is related to the square root of radiation intensity as stated directly in eqn. 4 and indirectly in eqn. 2. In a field-free ion source, ions are formed everywhere in the active volume in proportion to the radiation intensity, S, but are also rapidly destroyed by the recombination of the oppositely charged species. Very quickly equilibrium is established[5] and the rate of ion production equals the rate of ion loss by recombination. This is described by

$$\frac{dn_+}{dt} = 0 = \frac{S'}{V} - Rn_+n_- \tag{5}$$

where S' is the ion-pair production rate in the observation volume, V, and is proportional to radiation intensity, S. R is the positive ion–negative ion recombination rate. Since overall charge neutrality will be maintained at all points in this cell[5], $n_+ = n_-$, and eqn. 5 becomes

$$n_+ = \sqrt{\frac{S'}{VR}} \tag{6}$$

Thus, n_+ and the mass spectrometry signal should be proportional to the square root of the radiation intensity.

Having explained the square root portion of eqn. 2, we will next consider

whether eqn. 3, which expresses the critical form for $f(x_i)$, has a reasonable physical basis. The inverse square dependence on distance is to be expected to comprise a portion of $f(x_i)$ since this accounts for the well-known reduction in radiation intensity due to the effect of distance, alone, between a point source and the point of observation. It is not, however, as obvious why the simple function, e^{-ax_i}, should constitute the remainder of this function (unlike the usual visible light absorbance experiment in which monochromatic light is used, the beta radiation under consideration here consists of a wide range of energies). Nevertheless, the fact is that conventional nuclear measurements of beta emitters indicate that the attenuation of radiation intensity through a medium does, indeed, decrease linearly with the negative exponential of the absorbing mass density[6]. Taking a relevant example, the aluminum absorption curve for ^{63}Ni-on-Pt foil has been reported by Brosi *et al.*[7]. In Fig. 1 of their report, a linear relationship exists between the logarithm of counts measured by a windowless Geiger–Müller counter and the mass per unit area of the aluminum foil which separates the ^{63}Ni foil from the detector. (Since this is a parallel-plane experiment, no inverse distance squared component to the total relationship is expected or observed.) It is also important to note the magnitude of the absorption coefficient for ^{63}Ni-on-Pt deduced by Brosi *et al.* They found that an aluminum foil of mass equal to 0.6 mg/cm^2 halves the radiation intensity detected. Expressing their results in the form $S/S_0 = e^{-aM}$, where M is the mass per unit area (mg/cm^2) of the absorber, a value for a equal to 1.15 cm^2/mg is obtained. In order to compare this value for a expressed in units of cm^2/mg with the values of a obtained from the experiments reported in this study, it is necessary to convert a in the above expression to a form having units of thickness of a gaseous film. The density of a gas is given by the gas law, D (mg/cm^3) = MW $\times$ P/RT. Multiplication of D times a (cm^2/mg) yields a value for a in units of cm^{-1}. Conversion to units of mm^{-1} yields a (mm^{-1}) = 1.41 $\times$ MW $\times$ P/T, where MW, P and T are in units of g/mole, atm, and °K, respectively. With this conversion of units the equation which expresses the data of Brosi *et al.* becomes $S/S_0 = e^{-aX}$ where X is the thickness of the absorbing gas (mm). If, instead of the parallel-plane experiment by Brosi *et al.*, the absorption of betas from ^{63}Ni-on-Pt were measured using a point source emitter and a small area detector, the relationship between the measured radiation intensity and distance would be $S/S_0 = e^{-aX}/X^2$ where the value of a is the same as in the parallel-plane experiment. The similarity of this function to eqn. 3 is encouraging and becomes even more so when the value of a is predicted from the data of Brosi *et al.* As outlined above, their measurements indicate that a (mm^{-1}) = 1.41 $\times$ MW $\times$ P/T. For the conditions used in our experiments shown in Figs. 2–4, P = 0.85 atm and T = 296°K. Therefore, for air (MW$\approx$29) and CF_2Cl_2 (MW = 121) a values for these of 0.12 and 0.50, respectively, are predicted from independent experiments of a different nature than those described here. It will be recalled that these values are also the ones which gave the best fit to our measurements.

Application to any ^{63}Ni ionization cell

One can now reliably predict that the relative radiation intensity anywhere in the active volume of a ^{63}Ni-on-Pt ionization cell, will be given by

$$\text{rel } S = \sum_i \frac{e^{-ax_i}}{x_i^2} \tag{7}$$

and that the relative positive-ion density at any point in a field-free source will be given by

$$\text{rel } n_+ = \sqrt{\sum_i \frac{e^{-ax_i}}{x_i^2}} \tag{8}$$

where the summations are over all area units (of equal size) into which the total emitter is divided, and the value of a is $1.41 \times \text{MW} \times P/T$.

Several example calculations are provided below for the ^{63}Ni geometry most commonly used, the cylindrical cell. To relate the method by which this calculation has been done, consider the drawing shown in Fig. 6. The magnitude of S or n_+ expected at any volume element, V_r, located anywhere within the active volume of this cylindrical cell, is calculated using eqn. 7 or 8. The main difficulty is determining the numerous values of x_i separating each area unit, A_i, from the volume element, V_r. For the cylindrical cell these calculations are relatively straightforward if the cylinder is envisioned to be divided into a stack of rings and each ring is then divided into small rectangles (almost square) as shown in Fig. 6. The distance x_i from each area unit to any point V_r (located on a line crossing the cell and passing through its center) is obtainable by simple geometric calculations as shown. We have performed this calculation for a cylindrical cell of 10-mm diameter and 20-mm length. The cylinder is divided into 40 rings of 0.5-mm width and each ring is divided into 80 rectangles (defined by 360° of rotation about the center of a ring in increments of 4.5°). This cell then consists of 3200 area units. As each value of x_i is found, its contribution to S is added to that of the others according to eqn. 7. After completing all A_i summations, another location for V_r is chosen and the calculation is repeated. Using a handheld programmable calculator of modest capability (125 program steps were required), the magnitudes of S and n_+ at all five non-repetitious points at 1-mm intervals along the cell diameter were produced by the calculator in *ca.* 1 h. This process was repeated for intervals of 2 mm along the length of the cell, starting at the middle and continuing to 10 mm past one end of the cell. The results of these calculations are shown in Fig. 7, where the value of a chosen is 0.11. This choice for a reflects, for example, the use of argon–methane carrier gas (MW$\approx$40) at 200°C. From calculations in Fig. 7, the relative magnitudes of S and n_+ as a function of position across or along the cell are indicated. For example, at the center of this cell the positive-ion density will be 0.66 as great as the density 0.5 mm from the wall. The radiation intensity and ion-pair production rate in the center will be 0.44 as great as that 0.5 mm from the wall. (Due to the square root component of eqn. 8, the ion densities vary less with position than the radiation intensity values.) An interesting conclusion drawn from Fig. 7 is that in this field-free source, the relative ion density at positions well beyond the end of the cylinder remains surprisingly high; all along the cell cross-section at 10 mm from the end of the radioactive foil the ion density is about one-fifth (14/66) as great as at the center of the cell.

In order to demonstrate the effect of varied gas densities (which are determined experimentally by the choice of temperature, pressure, and molecular weight of the carrier gas) in the same 10-mm diameter cell, calculations were repeated using a range of a values. The results of these calculations are summarized in Figs. 8–10, where different aspects of the ionization process are shown for all points (more

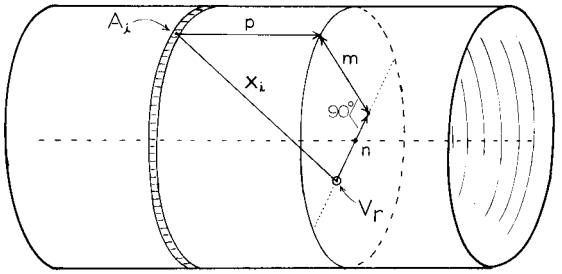

$$x_i = \sqrt{m^2 + n^2 + p^2}$$

Fig. 6. Representation of the method by which the distance, x_i, between any emitter area unit, A_i, and any volume element, V_r, of interest can be calculated. The observation element, V_r, must lie on a line running perpendicular to and passing through the axis of the cylinder.

distance from end of cell (mm)

distance from wall	(center) 10	8	6	4	2	(end) 0	2	4	6	8	10
0	100	100	98	95	87	52					
1	77	77	75	72	64	40	17	8.5	4.9	2.9	1.9
2	58	58	56	52	45	31	16	8.8	5.1	3.1	1.9
3	49	49	47	44	37	26	16	9.0	5.3	3.2	2.0
4	45	45	43	39	33	24	15	9.0	5.3	3.2	2.0
5	44	43	42	38	32	24	15	9.0	5.3	3.2	2.0
4	66	66	65	62	57	49	39	30	23	18	14
3	67	67	66	63	58	49	39	30	23	18	14
2	70	70	69	66	61	51	40	30	23	18	14
1	76	76	75	72	67	55	40	30	23	18	14
0	88	88	87	85	80	63	41	29	22	17	14
	100	100	99	97	93	72					

radiation intensity ↑ | ↓ ion density

Fig. 7. Relative magnitudes of radiation intensities and ion densities predicted throughout the active volume of a ^{63}Ni cylindrical source of 10-mm diameter and 20-mm length. Values are given at radial intervals of 1 mm and also at 0.5 mm from the cell walls. Values are given at longitudinal intervals of 2 mm and extend from the longitudinal center to 10 mm past the end of the cylinder.

than 0.5 mm from a wall) across the central diameter of the cell. Fig. 8 shows how radiation intensity varies with position and gas density. All curves have a common normalization point so that the magnitudes of the different curves are comparable with each other. Fig. 8 shows that the relative radiation intensity across the 10-mm cell with a ^{63}Ni-on-Pt source is strongly dependent on the density of the carrier gas. In all cases the radiation intensity near the walls is greater than at the center. This data should not be taken to reflect the magnitude of relative ionization at each position, because the relative ion-production rate will be proportional to the product of radiation and density at each point. Therefore, in Fig. 9 the dependence of the relative ion-production rate on position is shown, where the production rate was obtained by multiplying the radiation intensity at each point by the value of a. Fig. 9 indicates that the production rate of ions at the center of the cell changes only moderately with variation of a and passes through a maximum with $a \approx 0.2$ mm^{-1}. This maximum occurs because of the competition between gas density at the center and attenuation of radiation by intermediate layers of gas. Nearer the walls, however, the production rate is strongly dependent on gas density. It is important to point out here that the areas under each curve in Fig. 9 should provide a measure of the total ionization rate occurring throughout the cell. The maximum standing current expected for various

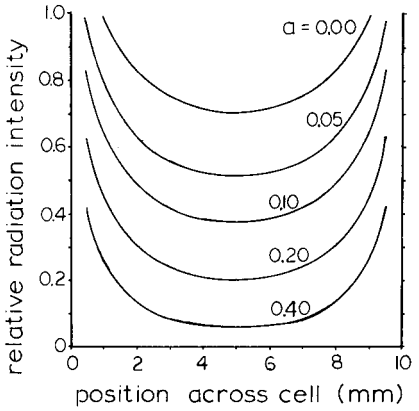

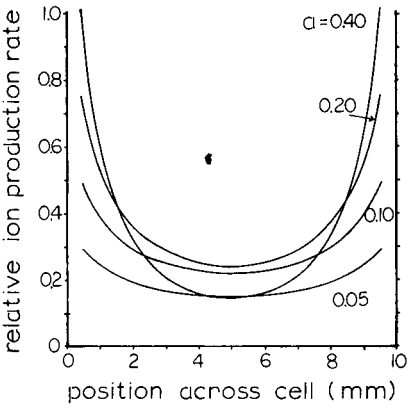

Fig. 8. Radiation intensity predicted across the center of a ^{63}Ni cylindrical cell of 10-mm diameter and 20-mm length for selected values of the gas density coefficient, a.

Fig. 9. Ion-production rates predicted for cell described in Fig. 8.

conditions of temperature, pressure, and molecular weight of the carrier gas might thereby be predicted if this cell were an ECD.

In Fig. 10 the equilibrium ion densities in this same cell in the absence of all electric fields are shown as a function of gas density. As in Fig. 7 these do not vary with position as strongly as do the ion-production rates. Normal conditions within a typical ECD are perhaps best represented by the $a = 0.1$ curve. For this gas density, the ion densities shown vary by only *ca.* 25% across the interior 9 mm of the cell's diameter. If high pressures (such as 4 atm) or high molecular weight carrier gases are used in this cell, ion densities will then become much more dependent on position within the cell. Fig. 10 should be applied to experimental conditions with caution since under typical conditions of the ECD, for example, electric fields are applied.

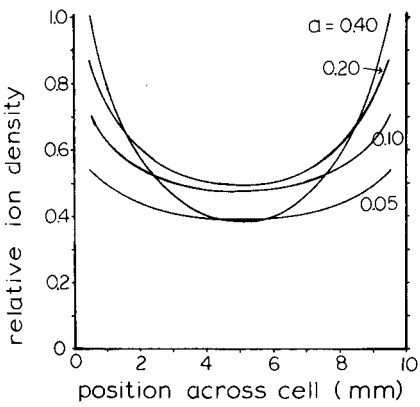

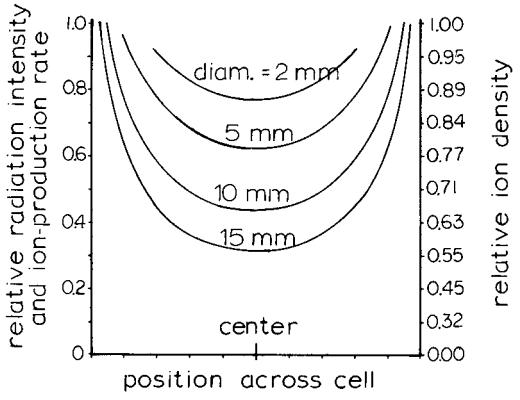

Fig. 10. Equilibrium ion densities predicted in the cell described in Fig. 8 if the cell is free of applied electric fields.

Fig. 11. Predicted effects of size of ^{63}Ni cylindrical cells on relative radiation intensity, ion-production rate and equilibrium ion density. For all cells the length is assumed to be twice the diameter. The calculations apply to positions across the longitudinal center. A gas density coefficient of $a = 0.11$ has been used.

The complete discription of ion distributions in these cases must also take into account the applied field, the resulting space–charge fields due to the separation of charge types, and the migration of electrons and ions in these fields. For the pulsed ECD we have previously done this, starting with the assumption that the ionization rate is equal everywhere in the active volume[3].

In Fig. 11, the effect of the size of the cylindrical cell is shown. Relative radiation intensity and relative ion production can now be expressed together because only one gas density ($a=0.11$) is considered. All curves terminate at a position 0.5 mm from the cell wall. Again, these calculations are all mutually comparable. Therefore it is seen that the radiation intensity, the ion-production rate and the relative ion density at the center of these cells are greatest for the smallest cell, even though the total activity of this cell will be only 1/56 as great as that of the largest cell.

CONCLUSION

We have described here a method by which ionization parameters of any imagined ^{63}Ni-on-Pt ionization cell might be calculated. The method should also be applicable to ion sources which use other beta-emitting nuclides as long as the mass absorption curve of that nuclide has been measured. With other nuclides the only alteration in the calculations described here will be in the coefficient, B, in the general expression, $a = B \times \mathrm{MW} \times P/T$.

There are a multitude of previous reports concerning the ECD, APIMS, and IMS which could be compared with the observations and predictions related in this paper. We will certainly not attempt such an ambitious task here. We will, however, comment briefly on the compatibility of our results with those of the two recent studies[1,2] referred to in the Introduction.

Aue and Kapila[1] measured direct currents in a ^{63}Ni ionization cell, where the ^{63}Ni was in the form of a small disk and was moveable relative to the counter electrode. At ambient pressure and temperatures in nitrogen gas their measurements indicated that the "center of ionization" occurs at a distance of *ca.* 1 mm from the foil. The ionization cell they used is very similar to our ion source A. Therefore, in the experiment shown in Fig. 12, in which the d.c. cell current of source A has been

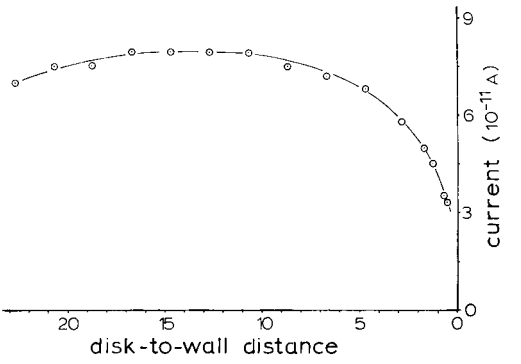

Fig. 12. Cell current measured with source A with nitrogen carrier gas at ambient temperature and pressure as a function of disk placement. This is a d.c. measurement where the pin is positively polarized by connecting a 50-V battery between the moveable pin and the electrometer.

measured as a function of distance, d, a result similar to that of Aue and Kapila might be expected. It is seen in Fig. 12 that the value of d at which the measured current decreases to 50% of the maximum value does, indeed, occur at *ca.* $d=1$ mm. Therefore, in our source, also, the "center of ionization" *for this source geometry* appears to be *ca.* 1 mm from the disk surface. Also, if one considers the mass spectrometry data from the disk experiment in air shown in Fig. 4, the experimental points and the solid curve are seen to be rising rapidly at $d = 1$ mm. Furthermore, the solid curve is for n_+, whereas to compare with a d.c. measurement a curve for ion-production rate would be more appropriate. Since ion-production rate is proportional to the square of n_+, that curve would be rising even more rapidly in the vicinity of $d = 1$ mm. From the ion measurements, also, it then seems reasonable that the "center of ionization" *for this cell design* under these conditions occurs at *ca.* 1 mm from the foil. We hasten to add, however, that this value for the "center of ionization" should be applied to other cell designs only with caution. In the experiments just described, the fall-off of radiation with distance from the foil will be reduced by some type of $1/d^2$ component (as well as the absorption component) which will be determined by the exact size of the disk. (The small-disk experiment represents neither a true parallel-plane nor point-source design, but is a composite of the two.) Recognizing this, the data of Ayala *et al.*[2] can be viewed as being consistent with and not contradictory to that of Aue and Kapila. Ayala *et al.* found that, with a cell of cylindrical geometry and a diameter of 14 mm, the ion-pair production rate increases continuously with carrier gas density (their Fig. 7). The increase in production rate with P/T is somewhat less than a proportional relation at ambient values of P/T, and the dependence becomes progressively weaker at high values of P/T. This result seems to indicate that a major portion of the ^{63}Ni betas at STP conditions of argon–methane carrier gas penetrate completely across their 14-mm cell. While this may appear inconsistent with the small-disk experiment, it can be shown that there actually is no contradiction when the total systems are considered. The calculations discussed above which supported the measurements of Aue and Kapila also lead to Fig. 9. From the data in Fig. 9, an estimate of the dependence of the ion-production rate on the gas density can be obtained by comparing the relative areas under each curve. For this 10-mm cell, it is seen that an increase in density above ambient levels (*ca.* $a = 0.1$) is expected to result in an increase in the ion-production rate. As the gas density is increased to relatively large values, an accompanying increase in production rate should continue but this dependence should become progressively weaker, as was observed by Ayala *et al.* Thus, the apparent differences between these two reports are resolved by the view provided here and are seen to result primarily from the different source geometries studied rather than the nature of ^{63}Ni beta penetration.

The objective of this study has been to describe the ionization processes occurring everywhere within the active volume of an ion source. Other parameters of general interest, such as total charge production rate, should be obtainable from these by integration over the entire volume. The results reported here and the method developed for describing any imagined beta ionization cell should be useful for future uses and studies of these devices.

ACKNOWLEDGEMENTS

This work was supported by grant number CHE-7824515 from the National Science Foundation. The authors are also indebted to Reed Howald for numerous helpful discussions.

REFERENCES

1 W. A. Aue and S. Kapila, *J. Chromatogr.*, 188 (1980) 1.
2 J. A. Ayala, W. E. Wentworth and E. C. M. Chen, *J. Chromatogr.*, 195 (1980) 1.
3 E. P. Grimsrud, S. H. Kim and P. L. Gobby, *Anal. Chem.*, 51 (1979) 223.
4 P. L. Gobby, E. P. Grimsrud and S. W. Warden, *Anal. Chem.*, 52 (1980) 473.
5 M. W. Siegel and M. C. McKeown, *J. Chromatogr.*, 122 (1976) 397.
6 G. D. Chase and J. L. Rabinowitz, *Principles of Radioisotope Methodology*, Burgess Publishing, Minneapolis, MN, 1959, p. 123.
7 A. R. Brosi, C. J. Borkowski, E. E. Conn and J. C. Griess, Jr., *Phys. Rev.*, 81 (1951) 391.

Journal of Chromatography, 239 (1982) 411–421
Elsevier Scientific Publishing Company, Amsterdam — Printed in The Netherlands

CHROM. 14,422

ADSORPTION OF POLAR SOLUTES ON LIQUID-MODIFIED SUPPORTS

MUSTAFA I. SELIM, JON F. PARCHER* and PING J. LIN
Chemistry Department, The University of Mississippi, MS 38677 (U.S.A.)

SUMMARY

The experimental technique of mass spectrometric tracer pulse chromatography was used to measure the equilibrium isotherms of acetone with *n*-hexadecane coated on different chromatographic supports. A model is proposed and shown to be accurate for these systems at three temperatures. The model is based on the assumptions that: (i) total adsorption is simply the sum of the liquid and solid contributions; (ii) these mechanisms operate independently; and (iii) there is no measurable liquid surface adsorption at the temperatures and pressures used in this investigation.

INTRODUCTION

Liquid-modified and vapor-modified adsorbents constitute a significant class of chromatographic stationary phases. Liquid-modified adsorbents include any active support, such as the diatomaceous earth and graphitized carbon black supports, coated with a non-volatile stationary liquid phase. Vapor-modified adsorbents would be those encountered in the use of steam[1], formic acid[2,3], dodecane[4], and other organic vapors[5,6] as carrier gases in gas chromatography (GC). In the particular case of the graphitized carbon blacks, many studies have shown that small amounts of either vapors[7,8] or liquids[9] can have significant, and often unpredictable, effects upon the chromatographic properties of these common adsorbents.

The mechanism for the retention of infinite dilution solutes with these "modified" adsorbents is not well understood, and little quantitative work, in the form of equilibrium isotherm measurements, has been carried out because of the experimental difficulties involved in the study of these complex, multicomponent systems. Because of the paucity of quantitative data, there are controversial, and often contradictory, reports in the literature concerning the effect of sample size and liquid surface adsorption for systems involving polar solutes and non-polar liquid phases.

The effect of these modifiers at low surface coverages is to neutralize very active adsorption sites on the adsorbent surface and, in general, to diminish the retention of any solute due to competitive adsorption. Commonly, however, the effect of increased amounts of modifier is enhanced retention of some solutes due to cooperative adsorption effects on the solid[9], liquid surface adsorption[10], or normal bulk liquid solubility effects. The effect of the solid support adsorption should be independent of

0021-9673/82/0000–0000/$02.75

the amount of modifier at surface coverages of a monolayer or more[11,12]. Solid support effects appear to diminish as the amount of modifier or liquid phase is increased because of the greater contribution from solution effects; however, the effect of the modified solid is often not negligible even at high liquid loadings.

Enhanced retention of solutes, with a maximum at some intermediate surface coverage or liquid loading, has been observed in diverse systems and attributed to equally diverse causes. Such behavior has been observed for acetone in squalane and attributed to solid support adsorption[13], for 2-butanone in octadecane and attributed to liquid surface adsorption[10], for benzene in polybutylene[14] and squalane[15] and not attributed to any cause. One of the few studies in which equilibrium isotherms were determined[12] does not really clarify the problem because the conclusion in that study was that the amount of squalane coated on Chromosorb P had little or no influence on the amount of acetone adsorbed up to 7–10% coating and that adsorption in this system was mainly solid support adsorption which was not influenced by the amount of modifier (squalane) present.

It is possible that these reports are not as contradictory as it appears. Conder[16] has proposed that the neglected parameter in these comparisons is the pressure of the solute in the gas phase or the mole fraction of the solute in the liquid phase. The suggestion is that liquid surface adsorption of polar solutes will only be observed at very low pressures and mole fractions of less than 0.02, even though Liao and Martire[17] observed liquid surface adsorption for "solution dominated" (large sample size) elution samples. Serpinet[18] has also suggested that the contradictory results concerning the existence of liquid surface adsorption for these systems is due to pooling of non-polar liquids on the surface of silanized supports which diminishes the liquid surface area. On the other hand, Mathiasson and Jönsson[10] observed significant liquid surface adsorption of ketones on octadecane coated on dimethylchlorosilane (DMCS) treated supports.

In this investigation, we have used a new experimental technique[19], called mass spectrometric tracer pulse chromatography (MSTP), to measure the equilibrium isotherms of a polar solute in a non-polar solvent coated on active and deactivated supports in an attempt to elucidate the adsorption mechanism in these complex systems.

EXPERIMENTAL

The experimental procedure, instrumentation, coating and analysis procedures were the same as described previously[8,19].

The isotope effect on the solubility of d_6-acetone in hexadecane was determined from the relative retention times of deutero- and natural acetone at three temperatures. The ratio of the solubility of acetone to that of the heavy isotope at 30, 45, and 60°C were 1.03, 1.01, and 0.98 respectively. This data was used to correct all of the isotherm data for isotope effects.

The liquid phase was *n*-hexadecane (Alltech) and the solid supports were Chromosorb P AW (Applied Science Labs.) and Chromosorb P AW DMCS (Johns-Manville). The supports were 60–80 mesh and the columns were made from 1/4 in. O.D. copper tubing in lengths from 100 to 300 cm. The percent loadings varied from 5 to 32%.

The isotopic solute was d_6-acetone (99.8%) (Commissariat Pour L'Energie Atomique, France). The gaseous mixtures used for the carrier gas were composed of the isotopic acetone in helium with mole fractions of acetone up to 0.06. The mole fractions were determined on a separate gas chromatograph with a thermal conductivity detector by comparison with the peak areas of samples of helium saturated with acetone at several temperatures lower than ambient.

RESULTS

The systems chosen for investigation were acetone with *n*-hexadecane coated on different common chromatographic supports. Acetone is a typical "polar" solute and the necessary heavy isotope is readily available as a common NMR solvent. The solvent and supports are common chromatographic systems that have been studied extensively for solid support and liquid surface adsorption. These systems with a polar solute and non-polar solvent were chosen for study because they represent a significant class of systems for which it is often difficult, if not impossible, to abstract thermodynamic solubility and adsorption data from chromatographic results because of the multiple retention mechanisms which may prevail in these systems.

The difficulties encountered with these systems are illustrated in Fig. 1 which is a plot of the specific retention volume of acetone for various sample sizes on active and deactivated supports. The plots are somewhat similar to those observed by Mathiasson and Jönsson[10] and are indicative of complex retention mechanisms, including non-ideal solution effects. The variation of the specific retention volume with sample size in these systems is significant, even for the DMCS treated support. Especially at

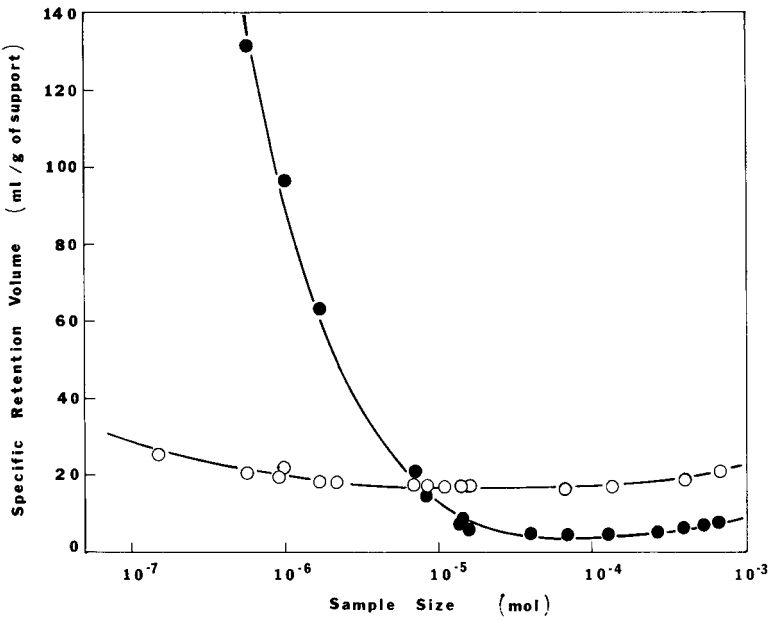

Fig. 1. Specific retention volume of acetone in *n*-hexadecane. ●, Chromosorb P AW; ○, Chromosorb P AW DMCS.

low pressures, the variation is dramatic, and there is no indication that the linear region of the adsorption isotherm, *i.e.*, infinite dilution conditions, can be attained with any practical sample size for the untreated support. However, there have been a great number of schemes suggested for abstracting the solubility data for acetone in hexadecane from this type of data. These procedures all involve the measurement of a retention parameter over a range of either sample size[10,17] or liquid loading[17,20] with an extrapolation (usually non-linear) to zero sample size and/or infinite liquid loading. These procedures have been critically reviewed and compared by several authors[10,17,20].

In an attempt to develop a model for these systems, adsorption isotherms were measured at a series of temperatures for acetone in *n*-hexadecane coated on both active and deactivated supports. The data for the deactivated (DMCS treated) supports is given in Table I and shown in Fig. 2. The variation of the activity coefficient with mole fraction was not always linear; however, the variation with pressure was linear in each case and the limiting activity coefficients obtained from a linear regression are given in Table II and compared with static literature data in Fig. 3. The agreement with literature data is good. This data was obtained from two different columns with 20 and 30% liquid coating on deactivated support, and there is no evidence of liquid surface adsorption in these systems. The DMCS support is not completely inert and the uncoated support does adsorb about 25% as much acetone

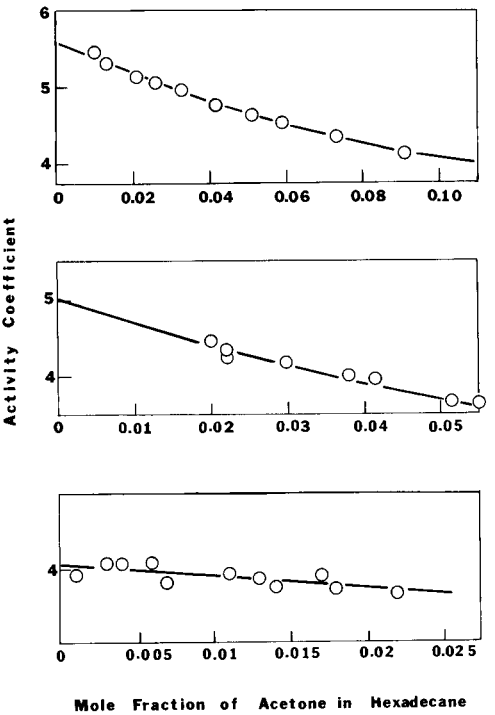

Fig. 2. Activity coefficient of acetone in *n*-hexadecane as a function of liquid phase composition. Top, 30°C; middle, 45°C; bottom, 60°C.

TABLE I

SOLUBILITY DATA FOR ACETONE IN *n*-HEXADECANE COATED ON CHROMOSORB P AW DMCS

30°C		*45°C*		*60°C*	
Liquid mole fraction	*Activity coefficient*	*Liquid mole fraction*	*Activity coefficient*	*Liquid mole fraction*	*Activity coefficient*
0.010	5.44	0.020	4.46	0.001	3.92
0.013	5.30	0.024	4.23	0.003	4.10
0.021	5.12	0.024	4.35	0.003	4.07
0.026	5.07	0.030	4.18	0.004	4.08
0.033	4.96	0.030	4.16	0.006	4.10
0.042	4.75	0.038	4.00	0.007	3.81
0.051	4.62	0.043	3.95	0.011	3.93
0.059	4.52	0.053	3.64	0.013	3.87
0.073	4.34	0.055	3.62	0.014	3.73
0.091	4.11			0.017	3.91
				0.018	3.71
				0.022	3.68

as the uncoated AW support; however, the large amounts of liquid coating used in this study effectively swamped out any residual adsorption on the DMCS supports.

Adsorption isotherms of this same system on an active support (Chromosorb P AW) were also determined under the same conditions. These results are given for 30°C in Table III and Fig. 4 as the open data points. The specific retention volume data is given per gram of solid support so there is an increase in the retention volume with liquid loading, however, the shape of the isotherm is indicative of surface adsorption, as well as, bulk liquid solubility.

In previous studies similar to this one, Urone and co-workers[11,12] proposed a model for solid support effects in which adsorption by a covered (modified) surface was shown to be independent of the liquid loading as long as the surface was covered

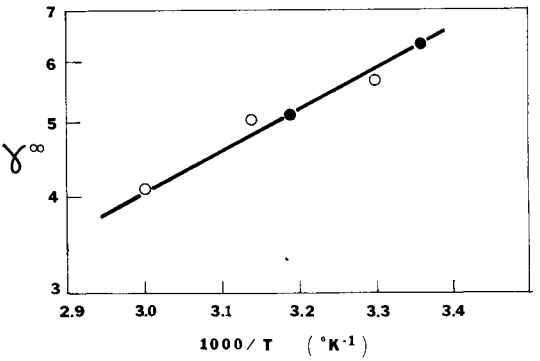

Fig. 3. Infinite dilution activity coefficients of acetone in *n*-hexadecane at various temperatures. ○, This work; ●, literature[21].

TABLE II

INFINITE DILUTION ACTIVITY COEFFICIENTS OF ACETONE IN *n*-HEXADECANE

	Temperature (°C)	*Limiting activity coefficient*
This work	30	5.6
	45	5.0
	60	4.1
Literature[21]	25	6.3
	40	5.1

by more than a monolayer of liquid. This model was tested for the present systems by substracting out the calculated liquid solubility contribution from the overall adsorption given in Table III. The liquid contribution was calculated from the pressure dependence of the activity coefficients given in Table I. The closed data points in Fig. 4 show the results of this correction for each liquid loading. The three corrected isotherms are identical, within experimental error, and independent of both liquid loading and liquid surface area (which is higher for the lowest percent coating). The solid line through this corrected data is for a Langmuir isotherm with $k_1 = 1.0$ and $k_2 = 0.07$. The adsorption isotherm of acetone on uncoated Chromosorb P AW is also shown in Fig. 4. This data is in agreement with the "corrected" isotherms showing, again, that *n*-hexadecane has little or no influence on the adsorptive properties of the solid support.

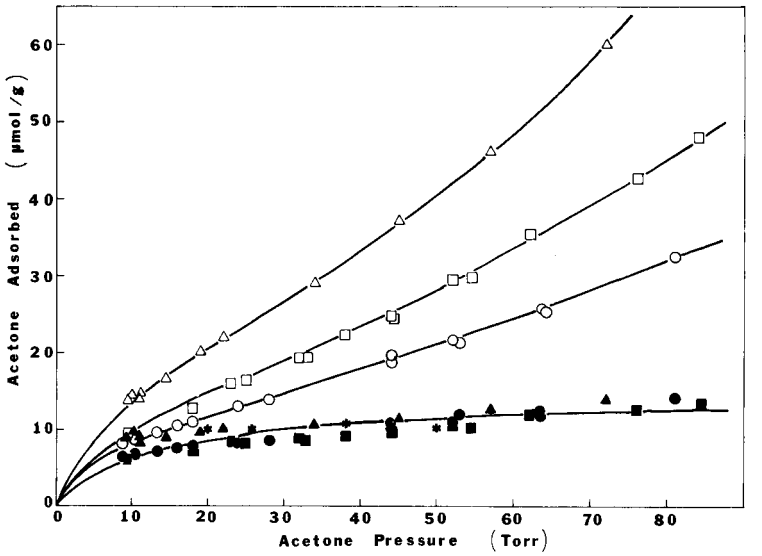

Fig. 4. Equilibrium isotherms of acetone in *n*-hexadecane on Chromosorb P AW at 30°C. Coating: ▲, △ 15%; ■, □ 10%; ●, ○ 5%; ★, 0%.

TABLE III

SORPTION ISOTHERMS FOR ACETONE AT 30°C IN *n*-HEXADECANE ON CHROMOSORB P AW

5% Coating		*10% Coating*		*15% Coating*	
Pressure (Torr)	*Acetone adsorbed (μmol/g)*	*Pressure (Torr)*	*Acetone adsorbed (μmol/g)*	*Pressure (Torr)*	*Acetone adsorbed (μmol/g)*
9.1	8.0	9.6	9.6	9.5	13.7
10.2	8.5	18.0	12.5	10.7	14.0
13.6	9.5	23.1	15.8	10.7	14.5
18.0	10.9	25.1	16.2	11.6	14.7
23.9	12.7	31.8	19.3	13.9	16.5
28.2	13.8	32.7	19.5	19.4	20.0
43.8	19.5	38.2	22.3	22.3	21.9
44.4	18.7	43.7	24.8	33.8	29.2
51.7	21.5	43.9	24.8	44.7	32.1
53.3	21.3	51.7	29.5	56.8	46.6
63.3	25.8	53.8	29.7	72.2	60.0
63.9	25.4	61.9	35.3		
81.0	32.6	75.8	42.6		
		84.1	48.0		

Similar experiments were carried out for two liquid loadings at 45 and 60°C and the results are shown in Figs. 5 and 6. The corrected isotherms for the solid supports are independent of liquid loading in each case, and there is little temperature dependence for adsorption on the liquid-modified solid surface.

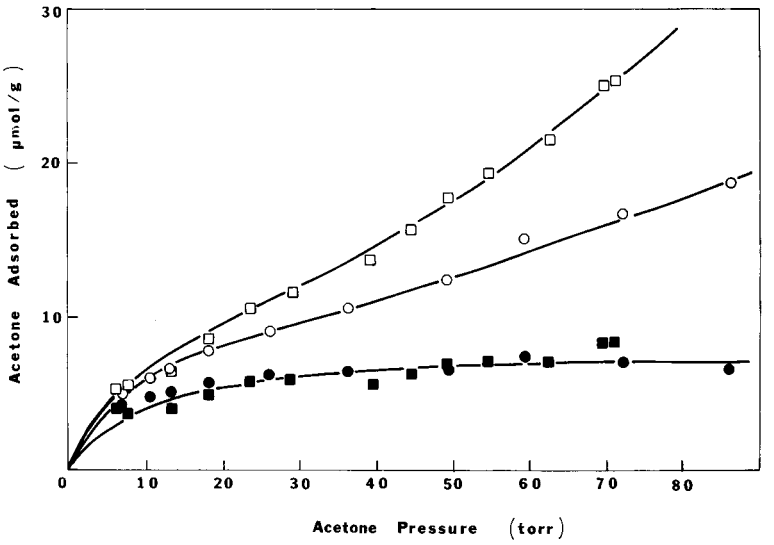

Fig. 5. Equilibrium isotherms of acetone in *n*-hexadecane on Chromosorb P AW at 45°C. Symbols as Fig. 4.

TABLE IV

RESULTS OF NON-LINEAR REGRESSION OF DATA ON CHROMOSORB P AW

Regression sets (percent coatings)	γ^{∞}			γ'			k_1			k_2		
	30°C	*45°C*	*60°C*	*30°C*	*45°C*	*60°C*	*30°C*	*45°C*	*60°C*	*30°C*	*45°C*	*60°C*
5 and 10%	7.3	4.9	3.8	−0.033	−0.017	−0.011	1.0	1.3	1.2	0.07	0.20	0.16
5 and 15%	5.4			−0.015			1.5			0.12		
10 and 15%	Program would not converge											
5, 10, and 15%	5.6			−0.018			1.5			0.12		
Data from DMCS-treated supports	5.6	5.0	4.1	−0.020	−0.013	−0.006	1.0	0.8	0.7	0.07	0.10	0.06

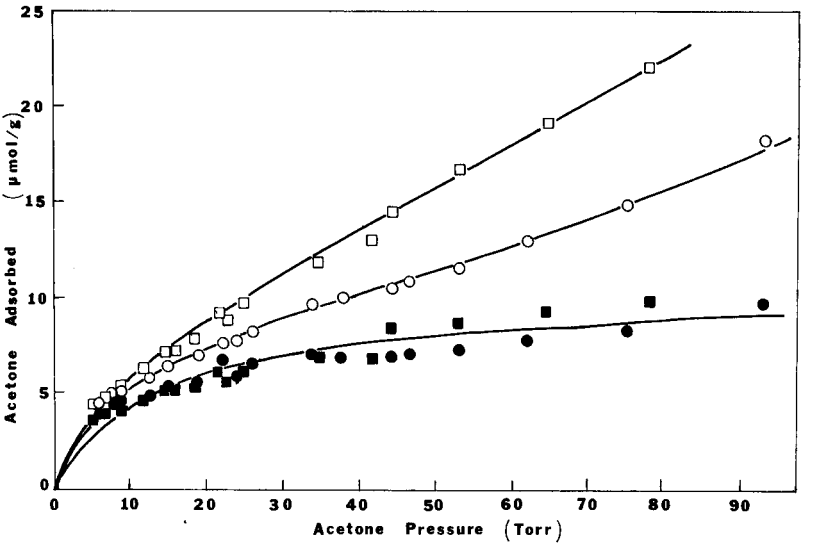

Fig. 6. Equilibrium isotherms of acetone in *n*-hexadecane on Chromosorb P AW at 60°C. Symbols as Fig. 4.

DISCUSSION

If the activity coefficient is a linear function of pressure and the modified solid adsorption follows a Langmuir isotherm, the total adsorption isotherm can be described by

$$n_T = \frac{n_{1p}P}{\gamma^\infty P^0 + (\gamma' P^0 - 1)P} + \frac{k_1 P}{1 + k_2 P} \tag{1}$$

where n_T and n_{1p} are the amount of solute and solvent in the stationary phase per gram of solid (μmol/g), P^0 is the vapor pressure of pure acetone, γ^∞ and γ' are the infinite dilution activity coefficient and the first derivative of the activity coefficient with respect to the pressure, P, and k_1 and k_2 are the constants in the Langmuir isotherm equation. This model assumes that there is no liquid surface adsorption, that the solid surface adsorption is controlled solely by the mole fraction of acetone in the liquid, and that solution and adsorption effects are mutually independent.

If this adsorption model is correct, the four adjustable parameters, γ^∞, γ', k_1 and k_2 in eqn. 1 should be attainable from a mathematical regression of the data for the total sorption isotherms on the active supports at two or more liquid loadings. These parameters were determined for the data in Table II with a general non-linear least squares computer program and the results are given in Table IV, along with the results obtained from the solvent on the deactivated support and the "corrected" solid adsorption isotherms.

These mathematical results indicate that accurate solubility and adsorption data can be obtained chromatographically for liquids coated on active supports and that the model used to derive eqn. 1 is an accurate description of these systems. There

is no evidence of liquid surface adsorption of acetone on hexadecane at the temperatures and pressures used in this investigation. This does not preclude the existence of liquid surface adsorption of polar solutes on non-polar liquids at lower pressures, however, it is more probable that solid support adsorption would dominate at lower pressure even with DMCS treated supports.

The pressure range covered in this study is larger than the pressure range normally encountered in elution GC. It was necessary to attain higher pressures in order to observe the liquid solubility contribution relative to the solid support adsorption. Urone *et al.*[12] found that the amount of acetone adsorbed by squalane coated Chromosorb P AW at a fixed pressure was independent of the amount of squalane present because the pressure used was only about 14 Torr. At this low pressure there is little liquid contribution and the solid support adsorption is not significantly affected by the amount of liquid coating as shown in Figs. 4–6. These systems with high liquid loads at low pressures are very similar to systems with low liquid loads at higher pressures. In both cases, the predominant retention mechanism is adsorption on the liquid-modified adsorbent, and the liquid coating has little or no influence on the total adsorption in either case.

Even though it is possible to evaluate the separate adsorption and solution mechanisms by frontal chromatography, as in this study, a more significant objective would be to do the same thing directly from elution experiments. The retention volume is proportional to the derivative of n_T with respect to P at each pressure, *i.e.*, the slope of the isotherm. Differentiation of eqn. 1 gives a direct relation between the specific retention volume of an elution peak and the mean pressure of the solute. The missing factor is an accurate relation between this pressure and the sample size of the elution sample. The "effective" pressure of an elution sample will likely be a complex function of several variables, such as sample size, retention volume, height equivalent to a theoretical plate (HETP), temperature, flow-rate, and liquid loading.

CONCLUSIONS

Chromatographic supports covered with more than a monolayer of a non-polar liquid or vapor will adsorb polar solutes to an extent that is determined solely by the mole fraction of the solute in the liquid and independent of the amount of liquid or vapor "modifier". The total adsorption is simply the sum of solid and liquid contributions, as first pointed out by Urone and co-workers[11,12]. The amount of solute adsorbed on the solid surface is a function of temperature and pressure, and can be adequately described by a Langmuir isotherm equation.

The simple model, represented by eqn. 1, is adequate to allow the accurate determination of activity coefficients and the composition dependence of these activity coefficients of a polar solute in a non-polar solvent coated on an untreated chromatographic support. The experiments must be carried out at relatively high pressures using frontal rather than elution techniques at present. However, this model can, hopefully, be used to develop a simple technique for correcting normal elution data for the effects of solid support adsorption.

ACKNOWLEDGEMENTS

Acknowledgement is made to the National Science Foundation and to the donors of the Petroleum Research Fund, administered by the American Chemical Society, for support of this research.

REFERENCES

1 A. Nonaka, *Advan. Chromatogr.*, 12 (1975) 223–260.
2 B. A. Rudenko, M. A. Baydarovtseva, V. A. Kuzovkin and F. Kucherov, *J. Chromatogr.*, 104 (1975) 271–275.
3 B. Pileire, Ph. Beaune, M. H. Laudat and P. Cartier, *J. Chromatogr.*, 182 (1980) 269–276.
4 K. W. M. Siu and W. A. Aue, *J. Chromatogr.*, 189 (1980) 255–258.
5 T. Tsuda, H. Yanagihara and D. Ishii, *J. Chromatogr.*, 101 (1974) 95–102.
6 T. Tsuda, T. Ichiba, H. Muramatsu and D. Ishii, *J. Chromatogr.*, 130 (1977) 87–96.
7 G. Bertoni, F. Bruner, A. Liberti and C. Perrino, *J. Chromatogr.*, 203 (1981) 263–270.
8 J. F. Parcher and P. J. Lin, *Anal. Chem.*, 53 (1981) 1889–1894.
9 A. Di Corcia and A. Liberti, *Advan. Chromatogr.*, 14 (1976) 305–366.
10 L. Mathiasson and J. Å. Jönsson, *J. Chromatogr.*, 179 (1979) 7–17.
11 P. Urone and Y. Takahashi, *Anal. Chem.*, 40 (1968) 1130–1134.
12 P. Urone, Y. Takahashi and G. H. kennedy, *J. Phys. Chem.*, 74 (1970) 2326–2333.
13 P. Urone and J. F. Parcher, *Anal. Chem.*, 38 (1966) 270–274.
14 K. Natio and S. Takei, *J. Chromatogr.*, 190 (1980) 21–34.
15 T. Komaita, K. Naito and S. Takei, *J. Chromatogr.*, 114 (1975) 1–14.
16 J. R. Conder, *Anal. Chem.*, 48 (1976) 917–918.
17 H. L. Liao and D. E. Martire, *Anal. Chem.*, 44 (1972) 498–502.
18 J. Serpinet, *Anal. Chem.*, 48 (1976) 2264–2265.
19 J. F. Parcher and M. I. Selim, *Anal. Chem.*, 51 (1979) 2154–2156.
20 J. R. Conder, *J. Chromatogr.*, 39 (1969) 273–281.
21 A. Kwantes and G. W. A. Rijnders, in D. H. Desty (Editor), *Gas Chromatography 1958*, Butterworths, London, 1958, pp. 125–135.

Journal of Chromatography, 239 (1982) 423–438
Elsevier Scientific Publishing Company, Amsterdam — Printed in The Netherlands

CHROM. 14,504

HIGH-PERFORMANCE DISPLACEMENT CHROMATOGRAPHY OF CORTICOSTEROIDS

SCOUTING FOR DISPLACER AND ANALYSIS OF THE EFFLUENT BY THIN-LAYER CHROMATOGRAPHY

HUBA KALÁSZ and CSABA HORVÁTH*
Department of Chemical Engineering, Yale University, New Haven, CT 06520 (U.S.A.)

SUMMARY

High-performance displacement chromatography was used for preparative scale separation of corticosterone, deoxycorticosterone and Reichstein's substance S with high-performance liquid chromatographic (HPLC) columns and instrumentation. Thin-layer chromatography (TLC) in the displacement mode was used to find an adequate carrier as well as a suitable displacer and its appropriate concentration. Separation of a mixture containing 60 mg of each component was carried out with a 500 × 4.6 mm column packed with 5-μm silica gel. The carrier was chloroform and the displacer was 5% (v/v) diethylethanediamine in chloroform. Regeneration of the column was carried out with alcoholic acetic acid–chloroform mixtures and checked by an HPLC test. In order to evaluate the results, fractions of the column effluent were analyzed by TLC and the results were confirmed by HPLC. TLC was found to be a sufficiently accurate and highly convenient tool to determine product distribution upon separation by displacement chromatography.

INTRODUCTION

Recent works[1,2] evinced the advantages of preparative separations by displacement chromatography with column and instrumentation generally employed in analytical high-performance liquid chromatography (HPLC). The technique called high-performance displacement chromatography (HPDC) was found, by using HPLC for analyzing fractions of the column effluent, to yield excellent separations of aromatic substances and polymyxin antibiotics with silica-bound hydrocarbonaceous stationary phases.

In this report we shall illustrate the use of HPDC for preparative separation of corticosteroid hormones with columns packed with microparticulate silica gel. Furthermore we shall demonstrate that thin-layer chromatography (TLC) can be a powerful tool to scout for a suitable displacing agent prior to fractionation and to demarcate zones of the components upon analyzing the column effluent thereafter.

0021-9673/82/0000–0000/$02.75

A variety of chromatographic methods has been described for the separation of corticosteroids[3]. Traditionally, silical gel[4-6] but frequently also Sephadex LH-20[7,8] was employed as the stationary phase in conjunction with chloroform or other chlorinated hydrocarbons as eluent. In HPLC microparticulate silica columns were first used for the analysis of corticosteroids[9-14]. Recently however reversed-phase chromatography with non-polar bonded phases and polar eluents has found increasing application in this field[15-17]. TLC with silica gel has also widely been used for steroid separation in analytical work[16-21] or in the selection of optimum eluent composition for use in HPLC[16,17].

In preparative chromatography of such steroids on silica gel the upper limit of sample loading is usually estimated as 1‰ (w/w) of dry sorbent present in the column[22-24]. In order to separate sufficiently large quantities, therefore, preparative scale chromatography usually employs columns having relatively large diameter. On the other hand, for "micropreparative" separation of 0.87 mg of corticosteroid mixture the use of a 410 × 16 mm silica gel column, which is considered small by conventional standards, has been described.

The goal of the present work is to point out and demonstrate the benefits arising from the coadjutant use of TLC with HPDC for preparative scale separation of certain corticosteroids with a microparticulate silica column. We shall see that the role of TLC as an attendant technique in HPDC is more versatile than in preparative elution chromatography where it has been employed as a scouting method for suitable eluent composition[13].

The results suggest that, with this concomitant in particular, displacement chromatography, which received great attention in early chromatographic literature[25-30] and has a well developed theoretical foundation[31], offers a powerful and convenient method for the separation of biological substances on conventional stationary phases as well.

EXPERIMENTAL

Materials, columns and reagents

Type MK6F (25 × 75 mm, 200 μm layer) and K6DF (200 × 200 mm, 250 μm layer) silica gel precoated glass TLC plates were obtained from Whatman (Clifton, NJ, U.S.A.). Partisil PXS-525 columns (250 × 4.6 mm) packed with 5-μm silica gel were obtained from Whatman. A 500 × 4.6 mm column home-packed with 5-μm Partisil (Whatman) was also employed. According to the supplier, chromatographic properties of the silicas used for manufacturing the TLC plates and HPLC columns were sufficiently similar as far as retention behaviour is concerned. Corticosterone, deoxycorticosterone and 11-desoxy-17-hydroxycorticosterone were purchased from Sigma (St. Louis, MO, U.S.A.). Chloroform, methylene chloride, carbon tetrachloride, methanol, ethanol, propanol, butanol, hexanol, octanol, cyclohexanol, benzene, tetrahydrofuran, ethylene glycol (HPLC grade), triethylamine, triethanolamine, diethylethanediamine (DEEDA) and dimethylcyclohexylamine (certified) were, unless noted otherwise, reagent grade and purchased from Fisher (Pittsburgh, PA, U.S.A.).

Apparatus

The fractionator unit used for displacement chromatography has been described in a previous report[2]. The reservoirs of chloroform used as carrier, the displacer solution, and the regenerant are connected via a four-way valve to a Model No. 110 A solvent metering pump (Altex, Berkeley, CA, U.S.A.) equipped with a 1.0-ml feed loop. The column effluent was monitored by a Model LC 55 variable-wavelength detector (Perkin Elmer, Norwalk, CT, U.S.A.) and a Model SR-206 dual-pen strip-chart recorder (Heath, Benton Harbor, MI, U.S.A.). Fractions containing 0.5 ml of the effluent were collected with an Ultrarack II, No. 2070 fraction collector (LKB, Rockville, MD, U.S.A.). In some instances eluent fractions were also analyzed by an HPLC analyzer containing the same major components as the fractionator unit. Fractionation was carried out with two Partisil PXS-525 columns in series whereas only one column was used for analytical separations. All experiments were carried out at room temperature ranging from 21 to 25°C.

Methods

Frontal TLC. Silica-coated 25 × 75 mm TLC plates were used for frontal development in a 100-ml covered beaker that held the "displacer" solution for at least 2 h prior to the beginning of the experiments to saturate the vapor phase. Upon development the distance of the solvent front and the "displacer" front from the bulk liquid level were measured. The location of the displacer front was found by direct visual observation of the plate.

Displacement TLC. Corticosteroids (5 μg in 5 μl chloroform) were spotted at a distance of 2 cm from the bottom edge of the plates having the above dimensions. Thereafter the plates were dried and placed into the beaker containing the displacer solution for development. The development was terminated when the solvent front moved a distance of 5 cm from the liquid level on the plate. Thus, the distance between the solvent front and loci of sampling was 4 cm. After development both solvent front and displacer front were marked and the plates were dried. The spots were observed under UV light at 254 nm with a Model UVS-II lamp (Ultra-violet Products, San Gabriel, CA, U.S.A.) or after they were made visible upon spraying with 50% (v/v) sulfuric acid in water and subsequent heating at 120°C for 5 min. The shape and positions of the spots relative to both the solvent and displacer fronts were recorded.

Elution TLC in scouting for suitable displacer. Under the same conditions given in the preceding section 18 neat solvents were tested as potential eluents for the three corticosterones. After development and spot visualization the R_F values were recorded.

Analytical TLC of effluent fractions. Silica-coated 200 × 200 mm plates were used in a rectangular developing tank (Fisher) having dimensions of 300 × 100 × 250 mm. A 50-ml volume of a chloroform–acetone (9:1) mixture was placed into the covered tank 2 h before the experiment. The samples were spotted at a distance of 37 mm from the bottom of the plate, the distance between the individual spots was 8 mm so that 21 samples were chromatographed simultaneously and 20-mm margins were left at both sides of the plate. The solvent front moved 180 mm from the liquid level in the tank in 50 min. Thereafter the plate was dried and the spots were made visible in the way described above.

Fractionation by displacement chromatography. The 1.0-ml loop of the feed injector valve was filled up with the feed solution of the corticosterone mixture in chloroform. At the same time, the reservoir of DEEDA solution in chloroform used as displacer was connected to the pump by turning the four-way valve. Subsequently the displacer solution was pumped into the system at a flow-rate of 0.1 ml/min and the injector valve was moved into feed position. As the displacer solution moved through the column, the three corticosterones separated into juxtaposed concentration zones and emerged from the column consecutively. Fractions of the column effluent were collected in 5-min intervals and analyzed by TLC (see above), or by HPLC (see below). The collection and numbering of fractions began upon turning the feed valve.

Column regeneration. After the displacement front emerged from the column, the four-way valve was switched to the reservoir of regenerant A which contained 20% (v/v) methanol, 10% (v/v) acetic acid and 70% (v/v) chloroform. Regenerant A was pumped through the column for 30 min at a 2 ml/min flow-rate. Thereafter regenerant B containing 30% (v/v) propanol in chloroform was pumped through the system for 30 min. Finally, the four-way valve was turned back to the original position and chloroform, the carrier used in the next chromatographic run, was pumped through the system for one hour. No attempt was made to reduce regeneration time.

Test of column regeneration. After executing the steps described for column regeneration, 20 μl of a test mixture containing *p*-cresol, benzene and phenylethylalcohol was injected by using a 20-μl loop in place of the 1.0-ml feed loop in the injection valve of the displacer unit. The eluent was chloroform, the flow-rate was 1.0 ml/min and the column effluent was monitored at 254 nm. For measurement of t_0 it was assumed that *p*-cresol is eluted in the void volume of the column under the conditions used here. Column regeneration was considered complete when the retention factors were in the range of 1.2 ± 0.12 and 1.8 ± 0.18, for benzene and phenylethylalcohol, respectively.

Analysis of the fractions by HPLC. The analyzer unit was equipped with a Partisil PXS-525 column and the eluent was 6% (v/v) propanol in chloroform. The fractions were diluted with two-fold volume of propanol containing the third component of the feed mixture which was not present in the fractions analyzed, as the internal standard and 20-μl aliquots were injected. The flow-rate was 1 ml/min and the column effluent was monitored at 254 nm.

Data evaluation

Measurement of retention in TLC. R_F values in elution chromatography were evaluated in the usual way. In both frontal and displacement TLC the front of the displacer with respect to the solvent front and the liquid level in the chamber, *viz.*, the actual starting line, was characterized by an equivalent dimensionless parameter, R_D.

Frontal chromatography of displacer with the HPLC unit. The breakthrough volume of the displacer front was measured under various conditions as far as the composition of the displacer solution is concerned. In these experiments the procedure used for the introduction of the displacer solutions was essentially the same as described for fractionation except no sample loop was employed and no sample was introduced. The fractionator unit was equipped with two Partisil PXS-525 columns and operated at a flow-rate of 1 ml/min. The carrier was chloroform and diethyleth-

anediamine solutions of different concentrations in chloroform were used as displacer. The column effluent was monitored at 300 nm and the retention volume of the displacer was measured at the inflection point of the breakthrough curve.

RESULTS AND DISCUSSION

The chemical structure of the three adrenal corticosteroids investigated here is given in Fig. 1. On the preparative scale they are most conveniently chromatographed on silica gel with chloroform containing some polar solvent such as methanol, acetone or propanol[32]. Therefore, silica gel was selected here as the stationary phase also for their separation by displacement chromatography with HPLC systems. In searching for a suitable carrier solvent and displacer we have found that TLC with silica-coated plates offers a rapid and convenient means to that end.

The criteria for an appropriate carrier with the stationary phase under investigation is that the components are strongly but selectively retarded when the carrier is

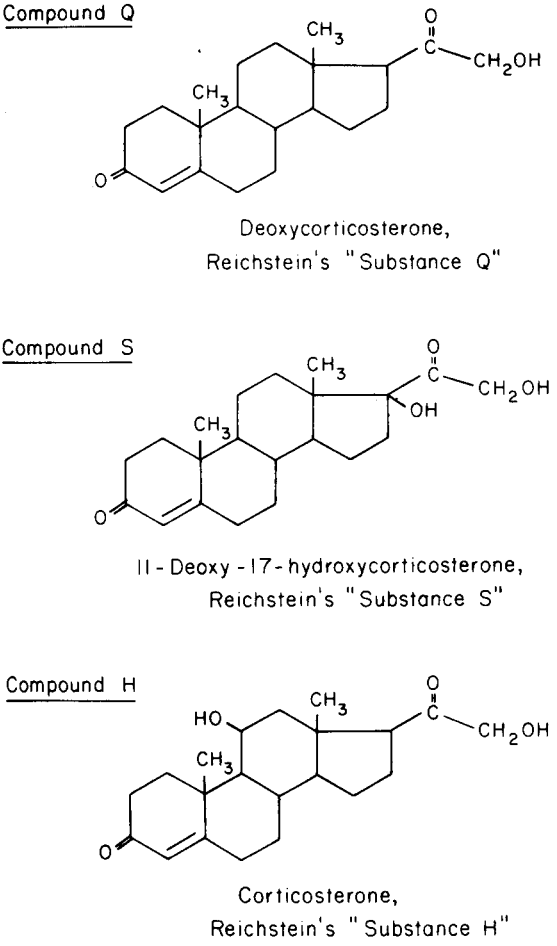

Fig. 1. Corticosteroids investigated in present study.

used as the eluent. As an arbitrary rule we consider a solvent an acceptable carrier when it yields, if used as an eluent in TLC with the same stationary phase as that present in the column, unequal R_F values smaller than 0.1 for the sample components.

In a series of screening experiments the three corticosteroids were subjected to elution development in TLC with silica gel coated plates by using a variety of neat solvents. The R_F values obtained with 18 solvents are listed in Table I. As expected the corticosteroids under investigation do not migrate upon development with non-polar solvents. Perusing the data in Table I and applying the above criteria we concluded that chloroform may be the best carrier.

TABLE I

R_F VALUES OF CORTICOSTEROIDS IN SOLVENTS EXAMINED AS POTENTIAL CARRIERS FOR DISPLACEMENT CHROMATOGRAPHY BY USING ELUTION TLC DEVELOPMENT WITH SILICA GEL COATED PLATES

Solvent	*R_F Values*		
	Corticosterone	*11-Deoxy-17-hydroxycorticosterone*	*Deoxycorticosterone*
Hexane	–*	–	–
Cyclohexane	–	–	–
Xylene	–	–	–
Carbon tetrachloride	–	–	–
Chloroform	–	0.03	0.09
Methylenechloride	0.02	0.08	0.25
Acetonitrile	0.86	0.83	0.95
Dioxane	0.90	0.90	0.98
Acetone	0.90	0.90	0.90
Tetrahydrofuran	0.95	0.95	0.99
Acetic acid	0.95	0.98	0.98
Octanol	0.65	0.70	0.85
Hexanol	0.75	0.78	0.85
Butanol	0.85	0.85	0.90
Propanol	0.85	0.85	0.90
Ethanol	0.85	0.88	0.93
Methanol	0.85	0.88	0.95

* – = Very small value: $R_F < 0.01$.

After the carrier solvent had been selected, the appropriate displacer was found in an ensuing series of experiments by using TLC in the displacement mode. Positions of both the solvent front and the displacer front were recorded upon development and the location of the displacer front was measured by its R_D value evaluated in a fashion equivalent to the measurement of R_F values. The three corticosteroids were individually spotted on silica-coated plates and the solution of a potential displacer in chloroform was used for the development of the chromatogram. The criterion for a suitable displacer was simply that all three components moved with the displacer front on the TLC plate, *i.e.*, the R_F value of each component was about the same or slightly greater than the R_D value. We have found that no displacement occurred and

the R_F value of each component was significantly smaller than R_D, when 10% (v/v) chloroform solutions of the following substances were used as developing agent: ethanol, *n*-propanol, *n*-butanol, *n*-hexanol, *n*-octanol, cyclohexanol, tetrahydrofuran, acetone, dimethylcyclohexylamine and triethylamine. On the other hand, with 10% (v/v) solutions of methanol, acetic acid, DEEDA and triethanolamine in chloroform displacement chromatography took place on the TLC plates.

Subsequently, the last four solutions described above were also used to carry out displacement chromatography with silica gel columns. We found that with 10% (v/v) methanol as the displacer corticosterone and 11-deoxy-17-hydroxycorticosterone did not separate whereas corticosterone was not displaced by 10% (v/v) acetic acid in chloroform and emerged from the column after the displacer front. However, DEEDA and triethanolamine in chloroform solution both were suitable displacers in these experiments and the results strongly advanced the notion that for our purposes chloroform solutions of these amines are the most promising displacers.

In order to investigate the effect of displacer concentration in chloroform on the migration rate of the displacer front, TLC of the three corticosteroids was performed again in the displacement mode by using amine solutions of different concentrations. Beside DEEDA and triethanolamine, dimethylcyclohexylamine and triethylamine were included in the experimental series in order to verify that indeed the first two amino compounds, and only they, are appropriate displacers in the chloroform

TABLE II

DISPLACEMENT TLC OF THE THREE CORTICOSTEROIDS ON SILICA GEL WITH VARIOUS AMINES IN CHLOROFORM SOLUTION

Positions of displacer fronts are characterized by R_D values listed here for the various displacer solutions differing in the nature and concentration of the amine. The locus of all three spots after development was at the displacer front unless otherwise indicated.

Amine in chloroform (%, v/v)	*R_D values*			
	Diethylethane-diamine	*Triethanol-amine*	*Triethyl-amine*	*Dimethylcyclo-hexylamine*
1	0.09	0.02	0.51*	<0.01
2	0.17	0.08	0.51*	0.19*
3	0.26	0.12	0.51*	0.31*
4	0.36	0.16	0.51*	0.38*
5	0.40	0.19	0.51*	0.44*
6	0.43	0.22	0.53**	0.53**
7	0.46	0.28	0.60**	0.58**
8	0.50	0.36	0.63**	0.61**
9	0.53	0.41	0.65**	0.63**
10	0.57	0.43	0.67**	0.63**
20	0.81	0.56		
30	0.91	0.86		
40	0.98	0.98		
50	1.00	1.00		

* All sample components were eluted behind the displacer front.

** Corticosterone was not displaced but eluted behind the displacer front.

carrier. The results of these experiments are displayed in Table II. In chloroform solution both DEEDA and triethanolamine were good displacers for all these corticosteroids over a concentration range from 1 to 50% (v/v), whereas the other amines were not. The R_D values, equivalent to the R_F values of the displacer front and listed in Table II, however, do not give information about the optimum concentration of the displacer solution. Evidently, too rapid migration observed at relatively high concentration of the displacer is not desirable as the displacement train may not be fully developed in a given column. Alternatively at low displacer concentrations, isotachic conditions may be reached too slowly in a given column[1,31]. According to our experience the useful range of R_D values is between 0.20 and 0.50. However, this is not a sufficient criterion for selecting the displacer concentration and therefore it was necessary to examine not only retention behavior but also the shape of the spots in actual displacement TLC development. When a suitable displacer is employed in such experiments the spots of sample component should be closely spaced at the front of the displacer and have narrow oblong shapes as shown in Fig. 2. In fact, the most effective way to use TLC in scouting for carrier solvent and displacer is to carry out TLC of the mixture to be separated in both frontal (without displacer in the prospective carrier solvent) and displacement mode and examine both the position and shape of the spots as well as the R_D value obtained for the front of the potential displacer substance.

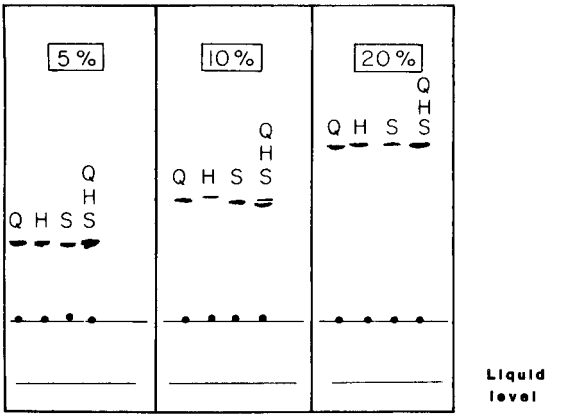

Fig. 2. Displacement TLC of the three corticosteroids by using 5, 10 and 20% (v/v) DEEDA in chloroform for development. Sample: 1 μg of each components in 10 μl of chloroform. Development time 8 min. The spot was made visible upon spraying with 50% (w/v) sulfuric acid in water and subsequent heating at 120°C for 5 min.

In our case both DEEDA and triethanolamine were found to be equally suitable displacers in chloroform solution in the concentration range from 2 to 10% (v/v). The decision to use DEEDA as the displacer in the subsequent experiments was based on its relatively low boiling point, 145°C, in comparison to 207°C the boiling point of triethanolamine. The rationale for this stems from the belief that a lower boiling displacer is easier to remove from the product if contamination occurs.

After having chosen DEEDA as the displacer we reexamined and confirmed the results of the carrier selection process. Displacement was carried out with the

three corticosteroids by using DEEDA dissolved not only in chloroform but also in carbon tetrachloride and methylene chloride, the two closest prospective carrier solvents according to Table I. The result of these experiments are presented in Fig. 3 and corroborate that chloroform is the most suitable carrier. It is seen that when carbon tetrachloride, which for all practical purposes is not an eluent for the corticosteroids, is used as the solvent DEEDA does not displace the sample components and they migrate slower than the DEEDA front. As seen in Fig. 3 they are eluted by the DEEDA solution in carbon tetrachloride and their spots are located behind the DEEDA front. On the other hand, Fig. 3 also shows that the three corticosteroids are eluted ahead of the DEEDA front by methylene chloride used as the carrier since it is a weak eluent as suggested by the R_F values of the carriers listed in Table I. Similar experiments with solutions of triethanolamine, triethylamine and dimethylcyclohexylamine in the above three solvents over a wide concentration range yielded essentially the same results. We may conclude, therefore, that the expediency of choosing chloroform and DEEDA as the carrier solvent and displacer, respectively, has been confirmed by these results.

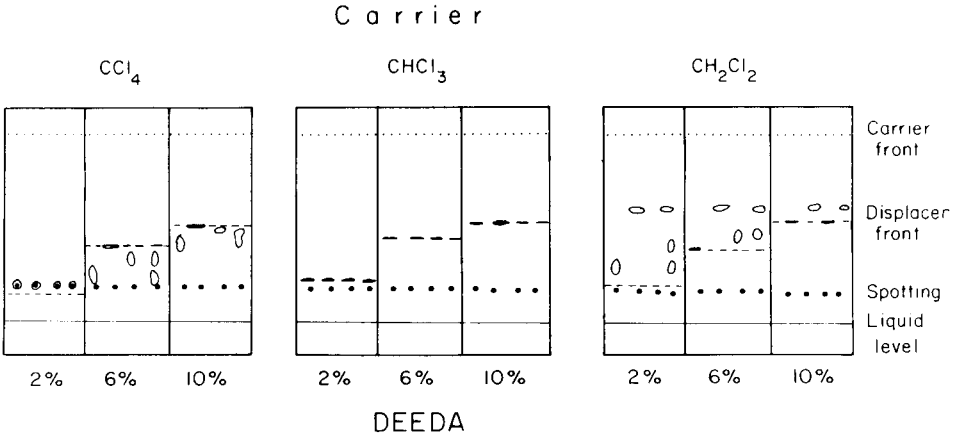

Fig. 3. Experiments with displacement TLC of corticosteroids to select the suitable carrier solvent. DEEDA was used as the displacer in carbon tetrachloride, chloroform and methylenechloride. The displacer concentration in % (v/v) is indicated at the bottom. The order of spots of sample components from left to right on each plate is the same and given by Q, S, H, Q + S + H; see Fig. 1 for symbols.

The effect of DEEDA concentration in chloroform on the migration rate of the displacer front was also investigated by using the HPDC unit in the frontal chromatographic mode. The breakthrough time of the displacer front at the inflection point was measured and the velocity of the displacer front u_D, was calculated. According to the literature[31] this velocity is given by

$$u_D = u_C/(1 + k_D^*) \quad (1)$$

where u_C is the velocity of the carrier solvent through the column and k_D^* is the "retention factor" of the displacer in the column that is given by the chord of the adsorption isotherm[1]. Fig. 4 shows the dependence of the parameter k_D^* on the con-

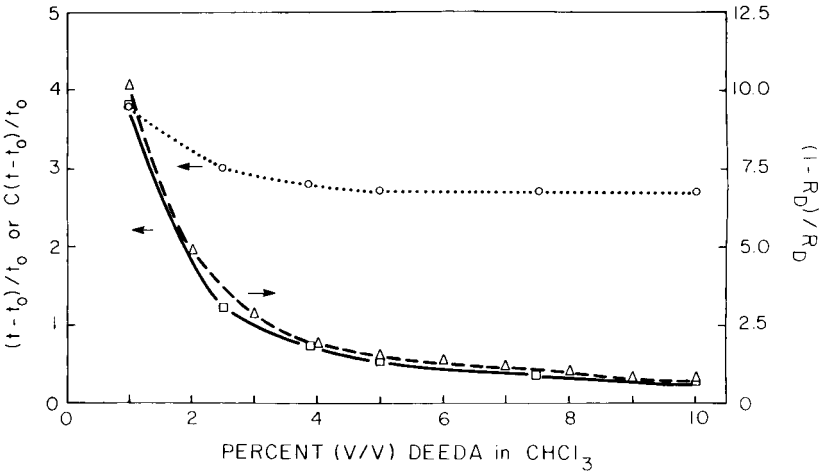

Fig. 4. Graph illustrating the dependence of frontal retention factor of DEEDA on the concentration of its solution in chloroform. Retention factors were measured with silica gel column in HPLC as $(t_D - t_0)/t_0$ where t_D is the breakthrough time of the displacer front and t_0 is the carrier hold-up time in the column, both measured at the same flow-rate. In TLC the retention factors were evaluated as $(1 - R_D)/R_D$. The dependence of $C_D(t_D - t_0)/t_0$, where C_D is the displacer concentration in the carrier, on C_D is also shown by the dotted line.

centration of DEEDA in chloroform as evaluated from frontal chromatographic experiments with both HPLC column and TLC plate. From experiments with columns k_D^* is evaluated from the carrier hold-up time, t_0, and the inflection point of the displacer front, t_D, as

$$k_D^* = (t_D - t_0)/t_0 \tag{2}$$

In planar chromatography under ideal circumstances, when uniform conditions prevail along the TLC plate, the following relationship holds

$$k_D^* = (1 - R_D)/R_D \tag{3}$$

Results obtained with both silica columns and TLC plates and shown in Fig. 4 indicate a similar dependence of k_D^* on concentration. The adsorption behavior of DEEDA on silica in both chromatographic systems, therefore, can be considered comparable. This finding supports the use of data obtained from TLC experiments in the design of displacement chromatographic systems for column chromatography. In Fig. 4, the product of the retention factor of the displacer, k_D^* and its concentration in chloroform, C_D, is also plotted against C_D. If the adsorption isotherm of DEEDA on silica has a plateau at sufficiently high value of C_D, as Langmuir isotherms do at saturation, the product $k_D^* C_D$ should reach a constant value with increasing C_D. It is seen in Fig. 4 that the value of $k_D^* C_D$ first decreases with increasing C_D and remains constant at DEEDA concentrations higher than 5% (v/v). This behavior suggests that the adsorption isotherm of DEEDA from chloroform on silica gel reaches a plateau.

Despite the conformity observed between results of experiments with columns and TLC plates, conclusions reached on the basis of TLC experiments still require confirmation by column chromatography before their applicability in the latter can be accepted. A caveat has already been implied by our experience with the selection of displacer as described above. Non-uniformity of flow in space and time as well as non-uniformity of equilibrium conditions along the migration path may give rise to deviations of TLC results from those obtained in HPLC with a homogeneous column under precisely controlled conditions.

As expected from theory[31] and shown in Fig. 4, the velocity of displacer front increases with the concentration of DEEDA. In view of these data the concentration of DEEDA in chloroform should be higher than 2% (v/v) in order to avoid lengthy development. The separation of the three corticosteroids by displacement chromato-

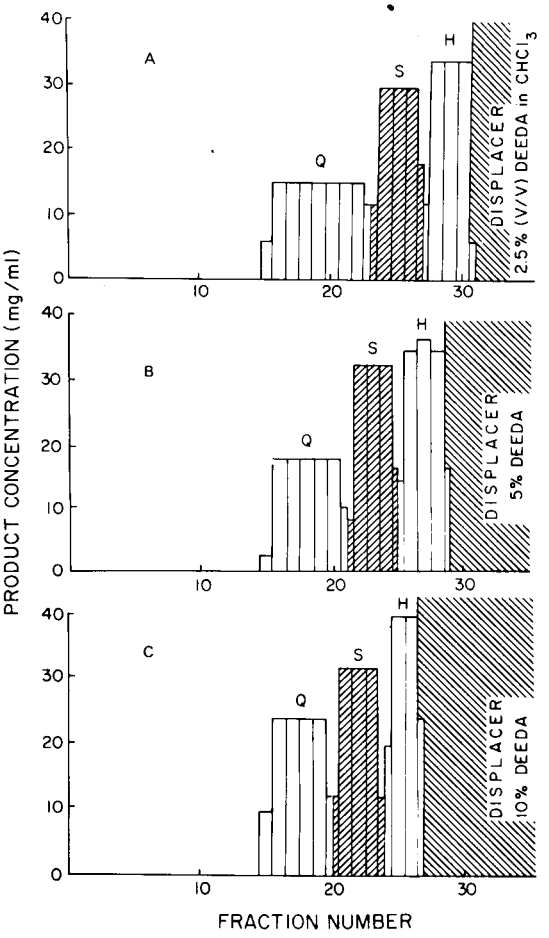

Fig. 5. Displacement diagrams of corticosterones as obtained by HPLC analysis of the effluent fractions. A, 2.5; B, 5.0 and C, 10% (v/v) DEEDA in chloroform was used as displacer. Symbols of sample components are given in Fig. 1. Column (2 × 250) × 4.6 mm, Partisil PXS-525 packed with 5 μm silica gel; feed, 60 mg of each component in 1 ml chloroform; fraction volume, 0.5 ml; flow-rate, 0.1 ml/min; temperature, 22°C.

TABLE III

RESULTS OF TLC ANALYSIS OF THE FRACTIONS OBTAINED IN DISPLACEMENT CHROMATOGRAPHY OF CORTICOSTEROIDS BY USING DIFFERENT CONCENTRATIONS OF THE DISPLACER UNDER CONDITIONS GIVEN IN FIG. 5

The symbols Q, S and H represent the three sample components, see Fig. 1, and D stands for DEEDA, the displacer. No feed component was found in fractions before No. 16.

DEEDA (%, v/v)	*Fraction number*																
	16	*17*	*18*	*19*	*20*	*21*	*22*	*23*	*24*	*25*	*26*	*27*	*28*	*29*	*30*	*31*	*32*
2.5	Q	Q	Q	Q	Q	Q Q	Q	Q S	S	S S	S	S	S H	H H	H	H	H D
5.0	Q	Q	Q	Q	Q Q	S	S	S	S S	H	H	H H	H	D			
10.0	Q	Q	Q	Q	S	S	S	S	H	H	H	D					

graphy at three different displacer concentrations, 2.5, 5 and 10% DEEDA is shown in Fig. 5. The displacement diagrams were constructed from solute concentrations found by HPLC analysis of the effluent fractions. Demarcation of the component zones does not require the use of HPLC, however. As seen in Table III analysis of the fractions by TLC offers a very simple way to identify the product and estimate its purity in each fraction. Such TLC results are eminently suitable to find zone boundaries that contain more than one component and therefore require rechromatography for their separation.

Results presented here corroborate earlier finding that the loading capacity of a column for a sample containing a few components is at least one to two order of magnitude higher when the mode of chromatography is displacement rather than elution.

Another displacement diagram illustrating the separation of the three corticosteroids is depicted in Fig. 6. The feed contained 60 mg of each component and the displacer solution was 5% (v/v) DEEDA in chloroform. However, the column was different than that used to obtain the results shown previously. In the latter experiment the volume of the fractions was 0.2 ml compared to 0.5 ml fraction volume in the previous experiments. Solute concentrations shown in the displacement diagram were determined by HPLC. For zone demarcation TLC was also used and

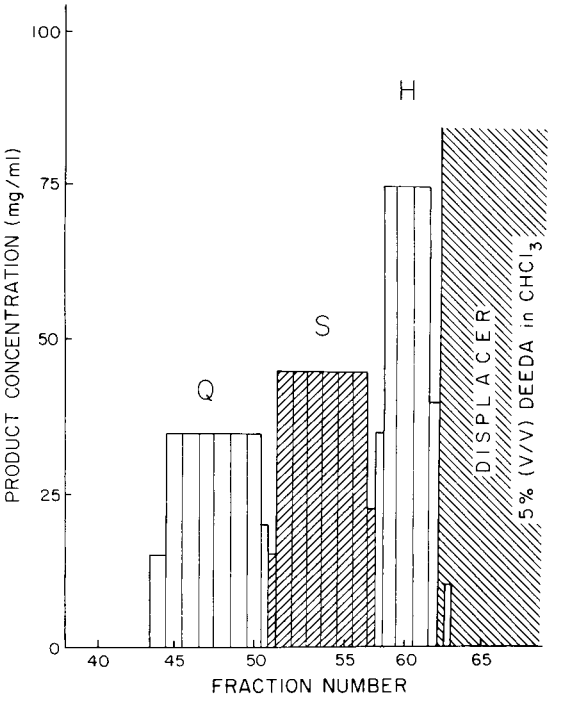

Fig. 6. Displacement diagram of three corticosterones obtained with a 500 × 4.6 mm column home packed with 5-μm Partisil silica gel by using chloroform and 5% (v/v) of DEEDA in chloroform as the carrier solvent and displacer solution, respectively. The flow-rate was 0.1 ml/min and the feed contained 30 mg of each of the three corticosterones, see Fig. 1 for symbols, in 1 ml of chloroform. Each fraction contained 0.2 ml of column effluent and was analyzed by HPLC.

typical results are shown in Fig. 7. Under conditions employed here 0.1 μg of any of the corticosteroids gives a well discernible plot. Comparison of Figs. 6 and 7 shows good agreement between the results obtained by TLC and HPLC as far as the qualitative analysis of the individual fractions is concerned. On the basis of our experience the most convenient approach to the evaluation of the results in displacement chromatography is first TLC analysis of the fraction to identify fractions containing the separated individual components and those which contain more than one component. Subsequently, the concentration of each product in the individual or combined fractions is determined by using HPLC.

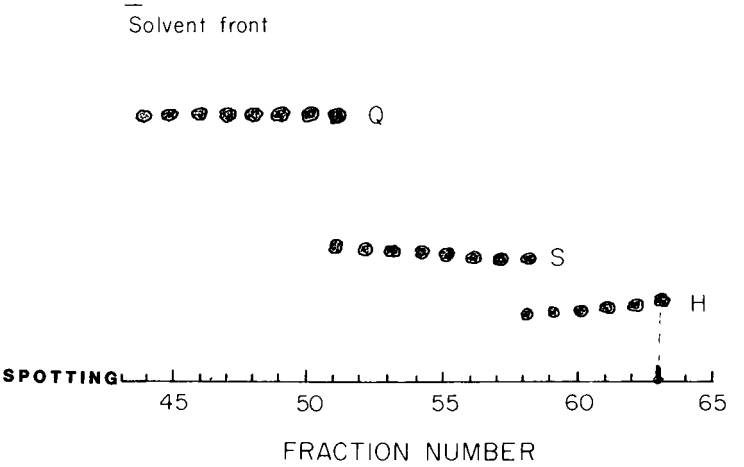

Fig. 7. TLC analysis of the fractions obtained in the displacement chromatographic separation depicted in Fig. 6.

The use of relatively high concentration of amine in the displacer solution did not impede regeneration of the column. We found that washing the column first with a mixture of acetic acid, alcohol and chloroform, then a chloroform–propanol mixture and finally with chloroform results in complete regeneration in less than 90 min. In the course of our study the "status" of the column was tested before every displacement run by using linear elution chromatography of a standard mixture as described in the experimental section. Although no particular detrimental effect of DEEDA on silica was noted, the displacer was immediately washed out from the column after each chromatographic run and after regeneration the column was filled with chloroform for storage.

CONCLUSIONS

The use of TLC for exploring optimum conditions and analyzing product fractions in displacement chromatography with HPLC columns and instrumentation greatly facilitates the exploitation of the potential of this technique for preparative scale separations. When thin-layer plates coated with the same stationary phase as that used in the column are available, scouting for appropriate carrier and displacer as well as establishing optimum displacer concentration are conveniently performed by displacement TLC.

Due to the possibility of analyzing simultaneously a large number of samples containing similar analytes, TLC is an eminently suitable technique to establish which effluent fractions contain pure product and which contain unresolved component pairs. Since the number of components to be separated by TLC is expected to be not greater than three in well-executed experiments in HPDC, TLC analysis can be performed rapidly. Of course, electrophoresis or isoelectric focussing also offer similar advantages in product analysis.

The employment of reversed-phase TLC in conventional fashion for scouting for suitable carrier and/or displacer is limited to chromatographic systems with organic rich mobile phase. On the other hand, in overpressured, *mutato nomine* "forced flow", TLC eluent flow is maintained by an external pressure gradient[33,34] that can cause even a plain aqueous eluent to migrate on a hydrophobic alkyl-silica plate. Due to the controlled conditions and relatively high speed "forced flow" TLC appears to be a particularly appropriate adjunct to displacement chromatography provided suitable instrumentation is available.

Whereas the employment of TLC greatly facilitated the selection of appropriate carrier and displacer solution, column length, sample loading, flow-rate and temperature were not optimized in the present study. We feel that such an endeavor will be more successful by taking advantage of the results of an investigation concerning the fundamentals, including the theoretical aspects, of displacement chromatography that is currently being carried out in our laboratory.

ACKNOWLEDGEMENTS

This work was supported by grants Nos. GM 20993 and CA 21948 from the National Institute for General Medical Sciences and the National Cancer Institute, U.S. Public Health Services, Department of Health and Human Services.

REFERENCES

1 Cs. Horváth, A. Nahum and J. F. Frenz, *J. Chromatogr.*, 218 (1981) 365.
2 H. Kalász and Cs. Horváth, *J. Chromatogr.*, 215 (1981) 295.
3 E. Heftmann, *Chromatography of Steroids* (*Journal of Chromatography Library*, Vol. 8), Elsevier, Amsterdam, 1976.
4 N. S. Lamontagne and D. F. Johnson, *J. Chromatogr.*, 53 (1970) 225.
5 N. S. Lamontagne and D. F. Johnson, *Steroids*, 17 (1971) 365.
6 R. Noiret and R. Davis, *Anal. Biol. Clin. (Paris)*, 21 (1963) 373.
7 A. Castro, D. Bartos, B. Jelen and M. Kutas, *Steroids*, 22 (1973) 851.
8 T. Seki and K. Matsumoto, *J. Chromatogr.*, 27 (1967) 423.
9 B. H. Shapiro and F. G. Péron, *J. Chromatogr.*, 65 (1972) 568.
10 V. Cejka and E. M. Venneman, *Clin. Chim. Acta*, 11 (1965) 188.
11 J. Q. Rose and W. J. Jusko, *J. Chromatogr.*, 162 (1979) 273.
12 N. A. Parrish, *J. Chromatogr. Sci.*, 12 (1974) 753.
13 C. Hesse, K. Pietrizik and D. Hotzel, *Z. Klin. Chem. Klin. Biochem.*, 12 (1974) 193.
14 F. K. Trefz, D. J. Byrd and W. Kochen, *J. Chromatogr.*, 107 (1975) 181.
15 M. Schöneshöffer and H. J. Dulce, *J. Chromatogr.*, 164 (1979) 17.
16 N. R. Scott and P. F. Dixon, *J. Chromatogr.*, 164 (1979) 29.
17 M. Schöneshöffer, R. Skobolo and H. J. Dulce, *J. Chromatogr.*, 222 (1981) 478.
18 S. Hara and M. Nakahata, *J. Liquid Chromatogr.*, 1 (1978) 43.
19 S. Hara, *J. Chromatogr.*, 137 (1977) 41.
20 S. Görög and G. Hajós, *J. Chromatogr.*, 43 (1969) 541.

21 B. Matkovics and G. Göndös, *Mikrochim. J.*, 13 (1968) 171.
22 E. Heftmann and I. R. Hunter, *J. Chromatogr.*, 165 (1979) 283.
23 P. Pei, S. Ramachandran and R. S. Henry, *Amer. Lab.*, 7 (1975) 37.
24 E. Godbille and P. Devaux, *J. Chromatogr.*, 122 (1976) 317.
25 A. Tiselius, *Ark.-Kemi., Minerol. Geol.*, 16A (1943) 1.
26 A. Tiselius and L. Hagdahl, *Acta Chem. Scand.*, 3 (1950) 394.
27 J. Porath, *Acta Chem. Scand.*, 6 (1952) 1237.
28 J. Porath and C. H. Li, *Biochim. Biophys. Acta*, 13 (1954) 268.
29 C. H. Li, A. Tiselius and K. O. Pedersen, *J. Biol. Chem.*, 190 (1951) 317.
30 S. Claeson, *Ark.-Kemi, Mineral. Geol.*, 23A (1947) 1.
31 F. Helfferich and G. Klein, *Multicomponent Chromatography*, Marcel Dekker, New York, 1970, pp. 225–254.
32 E. Godbille and P. Devaux, *J. Chromatogr. Sci.*, 12 (1974) 564.
33 E. Tyihák, E. Mincsovics and H. Kalász, *J. Chromatogr.*, 174 (1979) 75.
34 E. Mincsovics, E. Tyihák and H. Kalász, *J. Chromatogr.*, 191 (1980) 293.

Journal of Chromatography, 239 (1982) 439–449
Elsevier Scientific Publishing Company, Amsterdam — Printed in The Netherlands

CHROM. 14,605

QUANTITATIVE COMPUTER RESOLUTION OF SEVERELY OVERLAPPING LIQUID CHROMATOGRAPHIC PEAKS

NORMAN J. D'ALLURA and RICHARD S. JUVET, Jr.*
Department of Chemistry, Arizona State University, Tempe, AZ 85287 (U.S.A.)

SUMMARY

Severely overlapping peaks in high-performance liquid chromatography have been resolved by using a mathematical technique to extract quantitative information. This technique is applicable even in the worst situation, that in which the retention volumes of two peaks are identical, as long as the peak shapes are different. Conversely, even in the rare situation in which the peak shapes are identical, the method is applicable if the retention volumes of the peaks differ somewhat. Changes in the mobile phase flow-rate affect the chromatographic peak positions, and corrections for these variations must be made. Correction is also made for minor changes in the retentive ability of the chromatographic column as a function of aging. An accurate mobile phase flow-rate monitor and the associated computer routines were developed to make the necessary corrections. Overlapping computer-generated peaks as well as experimentally measured chromatograms have been resolved to demonstrate the applicability of this procedure to liquid chromatography. Overlapping peaks exhibiting slight shoulders were resolved with $< 13\%$ error, and quantitative information with $< 18\%$ error was obtained from completely overlapped peaks (almost identical retention times).

INTRODUCTION

The quantitative analysis of severely overlapping chromatographic peaks has been a major problem for chromatographers since chromatography was first developed. This problem continues, especially as analyses and samples become more complex, in spite of the numerous improvements that have been made in instrumentation and theory. Only two options are available for achieving quantitative information from unresolved peaks. These are: (1) to improve the resolution of the peaks by choosing an alternate column packing or mobile phase and by optimizing experimental parameters, or (2) to perform a mathematical resolution of the components of interest. In many laboratories the first approach is most often done in an empirical manner. This approach therefore generally leads to an undesirable increase in the analysis time, and, in fact, with complex mixtures it often does not succeed[1,2]. The second approach, involving mathematical resolution by such techniques as the perpendicular drop, triangulation, curve-fitting assuming a pre-defined shape, principal-

0021-9673/82/0000–0000/$02.75

component analysis and linear simultaneous equations, is successful under certain experimental conditions of resolution, but all these techniques are prone to progressively worse results as the resolution of the overlapping peaks decreases, and all these methods fail when there is complete overlap.

Lundeen and Juvet[3] recently reviewed the problems associated with previously published mathematical approaches and proposed an alternative method, which gave promising results when using computer-simulated chromatographic peaks. The present paper applies this theoretical treatment to experimental verification for the case of liquid chromatography. Pairs of chromatographic peaks with varying degrees of overlap have been evaluated for quantitative information. The detector response for each component at various times (or more exactly, at various volumes of mobile phase) throughout the peak is fitted to a second-order polynomial of each component's concentration. A series of non-linear simultaneous equations is then solved for the concentration of each component in the mixture. The complete theory for this analysis has been discussed in detail by Lundeen and Juvet[3]. The only requirement for a successful analysis is differing peaks shapes if the compounds have approximately identical retention volumes, or somewhat differing retention volumes if the components have almost identical peaks shapes. Gas chromatographic (GC) peaks obtained isothermally generally meet these requirements[3–7]. In this work it will be shown that these requirements are also met when using high-performance liquid chromatography (HPLC).

The proposed resolution method requires that parameters affecting peak position (such as mobile phase flow-rate) either be very closely controlled throughout the experiment or else these parameters must be accurately measured and the peak position corrected to what it would have been had the parameters been held constant. We chose to use the latter approach. The mobile phase flow-rate was observed to change slightly, but significantly, over the time of analysis; pump pulsations also occurred. Unless corrections were made, these changes shifted the positions of the peaks, and large errors in quantitative measurements were introduced. An accurate, computer-monitored and continuous-flow monitor was developed to record flow-rate fluctuations for the computerized correction procedure. For additional improvement in accuracy, the data may also be corrected for the slight changes in column retention behavior that are occasionally observed during an analysis. These changes may arise, for example, from the slow hydrolysis of the chemically bonded stationary phase by the mobile phase. Although this change in retention behavior is usually small, for best results it should be considered, since both the peak shapes and their positions are involved.

THEORETICAL

Fig. 1A is a series of chromatograms of 2-octanone at different concentrations. If the response at a particular mobile-phase volume is plotted *vs.* concentration, non-linear calibration curves similar to those shown in Fig. 2 are produced. These curves are linear only in the region near the peak maximum, demonstrating that peak shapes change with concentration in HPLC as has been previously demonstrated for GC[3,4,6]. The calibration curves are concave upward before the peak maximum and concave downward after the maximum. The directions of curvature can vary with the chromatographic system and experimental conditions, since opposite curvatures are

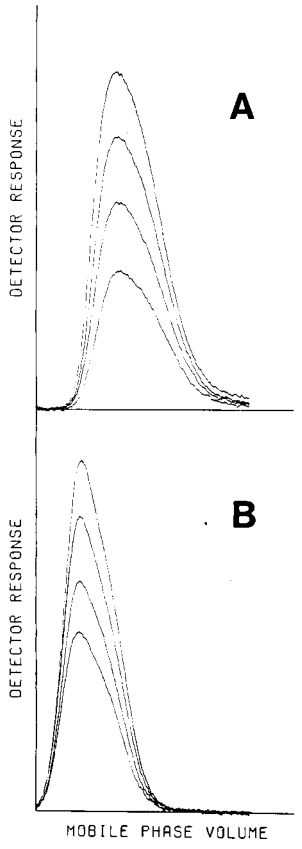

Fig. 1. A, 2-Octanone standards (5.159, 4.140, 3.132, 2.068%, w/w) in methanol–water (55:45) mobile phase. B. Toluene standards (2.133, 1.796, 1.410, 1.109%, w/w) in methanol–water (55:45) mobile phase.

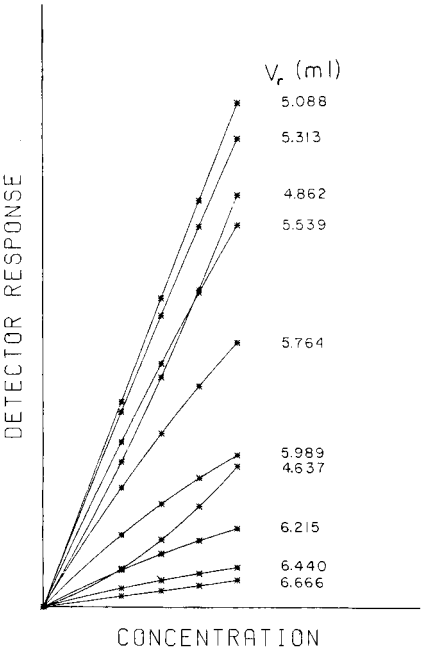

Fig. 2. Calibration curves of 2-octanone standards. V_r = Retention volume at point *i*.

generally obtained for GC systems[3]. Typically, 200–300 second-order equations relating the concentration to the detector response are utilized for the resolution calculations. A least-squares procedure is then performed on these equations in order to calculate the concentrations of each component in the unknown by minimizing the variance between the sum of the detector response of the components and that of the unknown.

When using methanol–water (55:45) mobile phase, a mixture of toluene and 2-octanone will be eluted from a Bondapak C_{18} Corasil column as an overlapping pair of peaks with a resolution of only 0.34, thus producing a single peak with a shoulder. Fig. 1B is a series of chromatograms of toluene standards at different concentrations, which have the same mobile-phase-volume axis as Fig. 1A. When comparing the two chromatograms of Fig. 1, it can be seen that both the retention time and the peak shapes differ. Thus, this pair of compounds easily meet the requirements for resolution described previously. The only basic assumption necessary for the success of this method is that the composite signal is equal to the sum of the responses of each of the

components. This implies that there is negligible interaction between the solutes at the low concentrations normally used in chromatography.

Small changes in the mobile phase flow-rate can be continuously measured with the flow monitor described below. Observed changes are caused by various factors, including pump variations and pulsations, gradual clogging of the submicron frits in the system, and build-up of particulate matter on the column. Therefore, to ensure an identical mobile-phase-volume axis for all chromatograms, the data are corrected for these perturbations.

Three different methods of flow correction were studied. The least accurate, the peak-shift method (PSM), compares the average flow-rate of the chromatogram of interest with the average for the entire data set. The chromatogram is then transposed the necessary amount along the mobile-phase-volume axis without modifying the peak shape. Thus, the new response, R_i', is,

$$R_i' = (R_{j+1} - R_j)M' + R_j \tag{1}$$

where M' is the ratio of the two flow-rate averages and R_j and R_{j+1} are the detector responses of the chromatogram that is being corrected.

In the average-volume method (AVM), the mobile phase volume corresponding to each detector response measured in the chromatogram is evaluated by summing the mobile phase volumes eluted between all previous detector response measurements. The summation is performed for both the unknown and the standards. The mobile phase volumes of the unknown are the reference volumes used when correcting all standards. The computer searches for a contiguous pair of volumes, V_j and V_{j+1}, in the standard's array, that will bracket the reference volume, V_i'. The new standard response, R_i', corresponding to the reference volume is then given by

$$R_i' = \frac{(R_{j+1} - R_j)(V_i' - V_j)}{V_{j+1} - V_j} + R_j \tag{2}$$

where R_j and R_{j+1} are the detector responses that are paired with their respective volumes. By averaging up to and including each point, this method can account for all perturbations in the mobile phase flow-rate, such as pumping pulsations, surges and dips, and it will modify the peak shape accordingly.

In the regression-volume method (RVM), the logic used is similar to that of the average volume method, but calculates the mobile phase volume in a different manner. A linear regression analysis is performed on a plot of the flow-rate as a function of time for the unknown. Knowing the slope and y-intercept of the flow-rate trend, a reference volume, V_i', can be calculated for each unknown detector response. In a similar manner, volumes are calculated for each standard sample response from its flow-rate trend. As in the AVM, the computer searches for a pair of contiguous volumes, V_j and V_{j+1}, in the standard's array that bracket the reference volume. The new standard response is calculated by using eqn. 2. This method effectively smoothes out the effect of pump pulsations and stray noise and will also modify the peak shape. Since 200–300 points per peak are used, these methods assume a straight line between successive points on the chromatographic peak with little introduction of error. Use of a second-order, least-squares fit to approximate the peak shape requires approxi-

mately twice the execution time of a straight line approximation and does not improve the results sufficiently to justify the extra computing time.

Computer measurements were accurate enough to detect a gradual loss of column efficiency and peak retention when repetitive samples were injected. This was verified by computer calculation of peak moments, which showed that the peak shape and retention volume change slightly with time, perhaps due to slow hydrolysis of the column packing material. Since peak shape and position are both important in this method, corrections for changes in column characteristics are desirable. These corrections were performed by measuring the difference in first moments (retention volume) of the first and the last chromatograms (identical samples in the scheme used) and proportioning the correction for the change in column characteristics linearly over the entire analysis run, which consists of the unknowns and calibration standards.

EXPERIMENTAL

The liquid chromatograph was built in our laboratory. All connecting tubing was 1/16-in. O.D. and either of stainless steel or PTFE (Alltech Assoc., Los Altos, CA, U.S.A.).

The mixed solvent was constantly refluxed in a 2-l, round-bottomed Pyrex flask to eliminate dissolved gases and to maintain constant composition.

Pump pulsations from a Model 396 Minipump (Laboratory Data Control, Rivera Beach, FL, U.S.A.) were easily detected with the monitor, and these fluctuations were reduced by means of a pulse dampener similar to the systems described by Nikelly and Ventura[8,9]. Acting as a bellows, a Swagelok short flexible metal hose connector (Crawford Fitting Co., Solon, OH, U.S.A.) was connected between the pump and a Li-Chroma II pulse dampener (Handy and Harman Tube Co., Norristown, PA, U.S.A.). A pressure gauge was installed before the pulse dampener to monitor the approximate pressure of the system and the pump pulsations. These modifications reduced pulsation noise by at least 50%.

An Alltech Model 9200 0.5-μm HPLC filter (Alltech Assoc.) was installed after the pulse dampener to remove any particulate matter that may have been present in the mobile phase. The flow monitor, described in detail below, was positioned after this filter.

A Rheodyne Model 7120 injector valve (Rheodyne, Berkeley, CA, U.S.A.), equipped with a 10-μl sample loop was used for reproducible sample injection. Syringe injection was not acceptable, owing to the non-uniformity of sample introduction and inaccuracies in timing encountered when injecting against a head pressure of 500 to 1000 p.s.i. The valve was so mounted that a micro switch was closed automatically at the instant of injection. This switch was monitored by software to start or stop computer sampling.

The analytical column was Bondapak C_{18} Corasil (Waters Assoc., Milford, MA, U.S.A.) contained in a 30 cm $\times$ 3.9 mm I.D. stainless-steel tube. To reduce dead volume, the 1/4- to 1/16-in. reducing unions used as end fittings were bottomed out with a 1/4-in. drill so ground that the tip was almost flat rather than cone-shaped. The fitting was then reamed through with a No. 52 drill to allow passage of 1/16-in. O.D. PTFE tubing. A 1/4,in.-diameter stainless-steel frit with 0.5-μm pores (Alltech Assoc.) was placed into the flat bottom of the fitting, and both the column tubing and the

connecting tubing (0.3 mm I.D.) were inserted into the column fittings until they butted against the frit.

A Waters Associates Model R401 refractive index detector (RID) was used to monitor the eluting peaks. An Analog Devices Model 610L instrumentation amplifier boosted the RID signal to the 0–5-V range required by the computer. Any amplification gain from 5 to 1000 could be achieved by use of a resistor bank and DIP switch arrangement. For visual monitoring of the amplified RID response, a Rikadenki Model B-181 recorder (Rikadenki Kogyo, Tokyo, Japan) and a Hewlett-Packard Model 3465A digital multimeter (Hewlett-Packard, Palo Alto, CA, U.S.A.) were used.

Earlier work in our laboratory by Werho and Juvet[10] involving the development of a streaming-potential detector for HPLC had demonstrated that the detector response changed with the flow-rate. Pursuing this observation, Werho pioneered the development of a flow monitor that produced an output voltage proportional to the flow-rate of the mobile phase with a high degree of accuracy. Modifications were made to the original design, and a monitor was built for use in this research.

The flow monitor was constructed as shown in Fig. 3. A metal box (4 × 6 × 8 in.) was used to house the flow-monitor components and to act as an electrical earth. A Swagelok 1/16-in. nut, cut such that the threaded portion was only 1 mm thick, was used to secure a 1/16-in. union to the box in bulkhead fashion, while also ensuring a good earth for the union. A Swagelok nut was ground slightly at the threaded end so that it could be used to seal PTFE tubing to the union. The PTFE support was machined into a cylindrical shape, 4 cm in diameter at the edges and center, with the remainder of the support being 3 cm in diameter. Holes were drilled and tapped to accept 10-32 screws, which held the support away from the box and were anchored to the box with nuts. In order to reduce dead volume and enable work at the high pressures necessary for acceptable flow-rates and retention times, PTFE tubing of I.D. 0.3 mm was used. The longer length (*ca.* 10 cm) of PTFE tubing was just long enough to reach from the inlet to the union secured in the PTFE support, avoiding contact with the earthed aluminium box or support screws. The shorter length of tubing was about 2.5 cm long and was connected to the outlet union with stainless-steel tubing. A multi-strand 18-gauge wire was silver-soldered to a 1/16-in. union

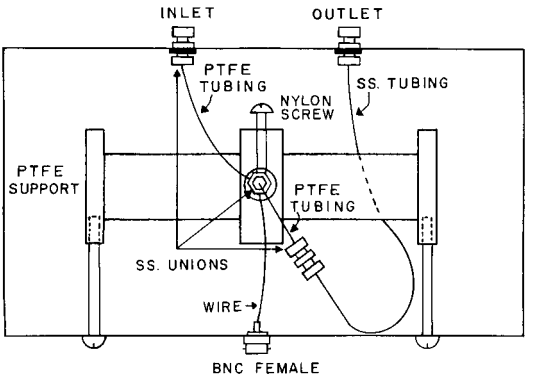

Fig. 3. The flow monitor. SS = Stainless steel.

secured inside the PTFE support. This wire conducted the voltage difference developed across the two unequal lengths of PTFE tubing inside the monitor to the BNC connector. A nylon screw was used to prevent the union inside the support from vibrating and generating electrical noise. The box, the terminating unions and the BNC female connector were earthed.

The unit was tested at 1500 p.s.i. The box was sealed by using a silicone rubber glass-and-ceramic adhesive and was repeatedly dipped into melted Parowax (Amoco Oil Co., Chicago, IL, U.S.A.) to seal any remaining leaks and to insulate the box from stray charges. This apparatus was then submerged in an aqueous constant-temperature bath controlled by a mercury thermoregulator and heated with a 50-W heater. Water was circulated constantly around the monitor by a pump. This procedure ensured constant humidity and a temperature that was held constant to within ± 0.01°C at approximately 30°C (helpful in reducing voltage fluctuations and drift).

Since the flow monitor had low output impedance, a Keithley Model 601A electrometer (Keithley Instruments, Cleveland, OH, U.S.A.) was used to measure and amplify the output voltage.

A Digital Equipment Corporation PDP-8/E computer system (Digital Equipment Corp., Maynard, MA, U.S.A.) was used for data taking and resolution calculations. The computer was equipped with 16K of memory, a KL8/E asynchronous data control board for the Teletype (Teletype Corp., Skokie, IL, U.S.A.), and a DK8-EP real-time programmable clock. An analogue-to-digital converter (ADC) (Phoenix Data, Phoenix, AZ, U.S.A.) was incorporated into a data interface. This included a multiplexer that could sample up to eight different devices at times dictated by software and convert the input voltages into binary numbers for computer utilization. A DEC RXO2 dual-density floppy-disc system fulfilled the need for a mass-storage device and a medium to run the DEC OS/8 V3D operating system.

To accomplish the resolutions presented in this paper, the minimum requirements are a 16K computer with an operating system such as the DEC OS/8 and BASIC, a mass-storage device with more than 300 free blocks for data and calculation files, a programmable clock, and an ADC–multiplexer interface. Any system with similar capability could be used to execute the BASIC programs described below.

A series of seven BASIC programs entitled RESOL was written to do the resolution calculations; these programs are modular, in order to keep the memory required by each to a minimum. This design allows large data arrays to be used, and these programs will chain to each other automatically as required. Programs for either a PDP-8/E or a PDP-11/70 are available from the authors.

Methanol and toluene were "Baker Analyzed" (J.T. Baker, Phillipsburg, NJ, U.S.A.). Other reagents were 99% pure 2-octanone and diethyl *n*-butylmalonate, and 97% *o*-xylene (Aldrich, Milwaukee, WI, U.S.A.). Methanol was used as solvent for all samples. The composition of the distilled water–methanol mobile phase was varied to change the degree of resolution between the overlapping peaks.

Since the slope of the flow monitor calibration curve changes with the mobile phase composition, it is necessary to calibrate the device each time the mobile phase composition is changed. An assembly-language program, DATATK, was written to calibrate and sample the flow monitor and RID voltages, and store the data on floppy disc. After the flow monitor was calibrated, the unknowns were injected, and the

detector-response and flow-rate pairs were stored on disc with the latter being converted from flow-monitor voltages by using the calibration curve. Eight standards were then injected in a routine fashion —four standards of varying concentrations of sample A and four of sample B. Finally, the first unknown was re-injected for later evaluation of possible changes in column retention behavior. The entire set of complete chromatograms was stored as a permanent file for calculations with the RESOL series of BASIC programs.

RESULTS AND DISCUSSION

The ADC–computer system was calibrated and found to be linear to within $\pm 0.05\%$. The electrometer, coupled with the ADC–computer system, was evaluated and found to be accurate within $\pm 0.12\%$. The reproducibility of the HPLC–ADC–computer system was $\pm 0.2\%$ in retention time and $\pm 1\%$ in area when using repetitive injections of the same sample and after correcting for flow variations by either the average volume method or the regression volume method.

With constant temperature control, the no-flow output voltage of the flow monitor varied by ± 2 mV. The calibration curve of the monitor was linear in the range used in these studies (0.5–3 ml/min) to better than $\pm 0.3\%$. With changes in the methanol–water mobile phase composition, the y-intercept of the flow calibration curve remained reproducibly at zero, while the slope varied directly with the concentration of water in the mobile phase. The output voltage was typically 6 V at a flow-rate of 1-ml/min when methanol–water (1:1) was used as mobile phase. The error introduced by digitization of the flow monitor output was small (± 0.01 to 0.05%) compared to the short- and long-term pump variability of ± 0.3 and $\pm 0.9\%$, respectively. These perturbations made flow corrections necessary.

Synthetic studies were used to evaluate the necessity for making flow corrections. Five independent studies with a random $\pm 1\%$ variation in the flow-rate and $\pm 0.3\%$ variation in pump stroke were used to simulate experimental chromatographic conditions. These five studies are shown in Fig. 4 with a line tracing the errors obtained with the three flow-correction methods. This plot demonstrates the effect that flow variations have on the results and the effectiveness of the three types of flow correction. Errors as much as 70% with no flow correction were reduced to less than 3% when flow corrections were employed. Thus, for accurate results, flow corrections to adjust the peak shapes and positions are important.

The peak-shift flow-correction method proved to be inferior to the average-volume and regression-volume methods, each of which gave comparable results. A pair of peaks showing only a slight shoulder was resolved with *no* flow correction (Fig. 5) and had an error in the quantitative results of -16% for peak A and $+19\%$ for peak B. The resultant poor fit of the peaks, as shown by the non-zero risidual plot, is due to an increase in flow-rate of 0.8% over the entire period of analysis (approximately 1.5 h). The residual was calculated by subtracting the sum of the responses of the fitted peaks from the response of the mixture at each point in the data window.

However, when flow corrections were made on the same chromatograms by using the average-volume method, the fit was markedly improved, as shown in Fig. 6A. The residual was reduced considerably, and was mostly reflective of the noise in

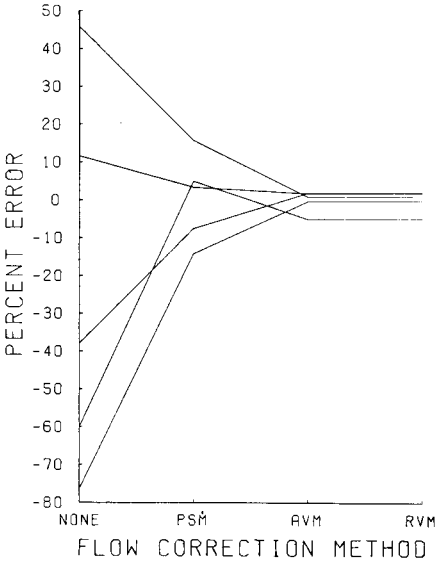

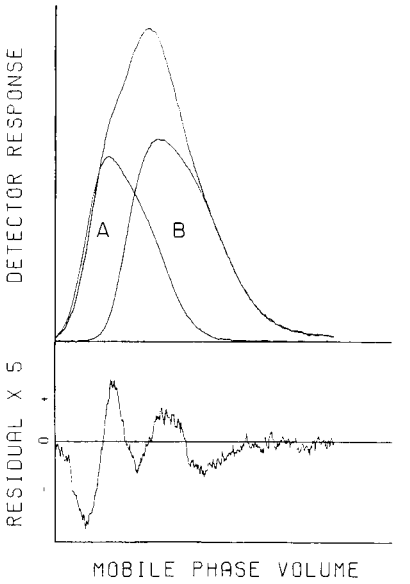

Fig. 4. Effect of flow-correction methods on synthetic data. PSM = peak-shift method; AVM = average-volume method; RVM = regression-volume method.

Fig. 5. Resolution of overlapping peaks with a shoulder with no flow correction, peak A, 1.409 % of toluene and peak B, 3.106 % of 2-octanone in methanol–water (55:45) mobile phase.

the unknown and the fitted peaks in addition to slight imperfections in the flow-correction procedures. In this analysis, results exhibited an error of only −7 % for peak A and one of +9 % for peak B, acceptable errors considering the poor resolution of the pair. Average errors encountered when resolving peaks with a similar resolution of 0.34 were −12 % for peak A and 13 % for peak B. If the flow had decreased rather than increased over the sampling interval, all positive residuals would be negative and *vice versa*. Since the average-volume method most correctly accounts for pumping pulsations and other short- and long-term variations, results obtained with use of this method are presented below. If the first moment of the unknown in the first chromatogram, and the first moment of the same mixture repeated as the last chromatogram differed by more than 0.75 %, corrections for changes in column characteristics were also made, as described under Theoretical.

Chromatographic peaks showing a valley and a resolution of 0.46 (Fig. 6B) were resolved with an average error of 7 % and 9 % for toluene (peak A) and 2-octanone (peak B), respectively. A small peak (2-octanone, peak B) overlapped by a large peak (toluene, peak A) was resolved with an average error of 1 % and 8 % for the smaller and larger components, respectively (Fig. 6C); the resolution for this pair of peaks was only 0.32. Completely overlapped peaks (resolution of 0.20), showing no shoulder, were resolved with an average error of 18 % for both diethyl *n*-butylmalonate (peak A) and *o*-xylene (peak B) as shown in Fig. 6D. Average reproducibility for all analyses was ±3.7 %. Undoubtedly, errors could be reduced by using a detector that is more sensitive and less noisy than the RID. A solvent-delivery system with less

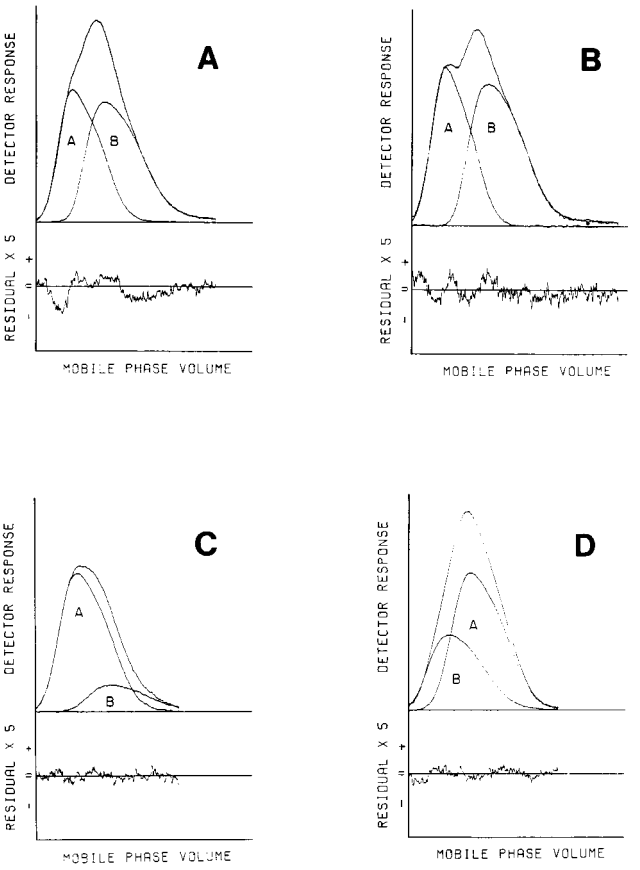

Fig. 6. Resolution of peaks with use of AVM for flow correction. A, Overlapping peaks with a shoulder: 1.409% (w/w) of toluene (peak A) and 3.106% (w/w) of 2-octanone (peak B) in methanol–water (55:45) mobile phase. B, Overlapping peaks with a valley: 1.409% (w/w) of toluene (peak A) and 3.106% (w/w) of 2-octanone (peak B) in methanol–water (50:50) mobile phase. C, Small component overlapped by a larger component: 1.780% (w/w) of toluene (peak A) and 0.6300% (w/w) of 2-octanone (peak B) in methanol–water (55:45) mobile phase. D, Completely overlapped peaks: 1.447% (w/w) of diethyl *n*-butylmalonate (peak A) and 3.629% (w/w) of *o*-xylene (peak B) in methanol–water (60:40) mobile phase.

fluctuations in the mobile phase would also be expected to improve reproducibility, although some corrections would probably still be necessary.

A good fit (small residual) does not necessarily ensure accurate results, although accurate results without a good fit are unlikely. Since this method minimizes the sum of the variance between both components and the unknown, the quantitative results will be balanced for the best fit possible. In instances in which the peaks are partially resolved, such as in Fig. 6B, there are large portions of the overlapped peak where the detector response is almost exclusively due to only one component in the mixture, which increases the probability of accurate results. However, the residual may be relatively large, as there is no other component over most of the peak to offset the detector response, which may be either too high or too low.

With completely overlapping peaks, such as in Fig. 6D, the opposite is true.

The quantitative values are the result of the best fit of the components, both of which contribute almost equally over most of the overlapped region. Therefore, errors of the size reported above should be expected, as detector response is due to one component only over a small portion of the peak. However, the residual may be small, as any positive error in the detector response of one component will be off-set by the negative error from the other. Therefore, residuals cannot strictly be compared between analyses with differing degrees of overlap. For a particular data set, of course, the best method of correction will always have the smallest residual and the most accurate results.

ACKNOWLEDGEMENT

This work was supported in part by the National Science Foundation under Grant CHE 76-81583.

REFERENCES

1 T. S. Buys and K. DeClerk, *Separ. Sci.*, 7 (1972) 527–541.
2 E. Grushka, *Chem. Technol.*, 12 (1971) 745–753.
3 J. T. Lundeen and R. S. Juvet, Jr., *Anal. Chem.*, 53 (1981) 1369–1372.
4 J. Baudisch, H. D. Papendick and V. Schloder, *Chromatographia*, 3 (1970) 469–477.
5 E. Grushka, *Methods Protein Sep.*, 1 (1975) 161–192.
6 H. M. McNair and W. M. Cooke, *J. Chromatogr. Sci.*, 10 (1972) 27–30.
7 S. D. Mott and E. Grushka, *J. Chromatogr.*, 126 (1976) 191–204.
8 J. G. Nikelly and D. A. Ventura, *Anal. Chem.*, 51 (1979) 1585–1588.
9 D. A. Ventura and J. G. Nikelly, *Anal. Chem.*, 50 (1978) 1017–1018.
10 D. Werho and R. S. Juvet, Jr., unpublished results.

Journal of Chromatography, 239 (1982) 451–462
Elsevier Scientific Publishing Company, Amsterdam — Printed in The Netherlands

CHROM. 14,550

RESOLUTION OF OPTICAL ISOMERS OF Dns-AMINO ACIDS BY HIGH-PERFORMANCE LIQUID CHROMATOGRAPHY WITH L-HISTIDINE AND ITS DERIVATIVES IN THE MOBILE PHASE

STANLEY LAM and ARTHUR KARMEN*
Albert Einstein College of Medicine, 1300 Morris Park Avenue, Bronx, NY 10461 (U.S.A.)

SUMMARY

This paper describes our continuing work in resolving the optical isomers of Dns-amino acids by high-performance liquid chromatography with mixed chelate complexation. Addition of copper(II) complexes of L-histidine to the mobile phase resulted in resolution of many D- and L-Dns-amino acids, including those with aliphatic, polar and aromatic substituents. With polar substituents, highly selective incorporation of the L-enantiomer into the ternary complex with increased retention on the column was observed. The reverse occurred with amino acids with aliphatic side chains; the D-isomers were incorporated preferentially. With aromatic substituted amino acids, the resolution was pH dependent. Substitution of copper(II) complexes of L-histidine methyl ester in the mobile phase dramatically reduced the stereoselectivity, although the isomers were still resolved. Copper(II) complexes of N-acetyl-L-histidine used in the mobile phase gave no stereoselectivity.

Excellent separations of isomers were achieved with several of these systems. Many pairs of amino acids could be separated in the same chromatographic analysis.

INTRODUCTION

A number of approaches for resolving optical isomers of amino acids have been proposed[1–3]. In most of these, resolution is generally based on the different behavior of the isomers in ligand exchange, crown ether complexation, charge transfer complexation, hydrogen bonding interaction or metal complex formation.

In this technique, a non-polar, reversed-phase column is usually used with a mobile phase containing chiral metal complexes. For example, Karger and co-workers[4,5] used L-2-alkyl-4-octyldiethylenetriamine complexes of zinc and other metals in the mobile phase to separate Dns derivatives of the amino acids. Hare and Gil-Av[6], who previously reported using Cu(II)–proline eluents to separate free D- and L-amino acids, more recently studied Cu(II)–di-N-propyl-alanine complexes[7]. Grushka and co-workers[8,9], using complexes of aspartame and derivatives of aspartic acid, resolved a number of D- and L-amino acids.

We previously reported separations accomplished with Cu(II)–L-proline and

Cu(II)–L-arginine eluents[1,10,11]. This paper describes our experience with copper(II) complexes of L-histidine and L-histidine derivatives.

Histidine forms some of the most important metal-binding sites in such proteins as carboxypeptidase A[12], thermolysin[13], carbonic anhydrase B[14]. It has also been implicated in many other enzymes and metalloproteins and in copper(II) transport in blood[15,16], although the manner in which histidine and its derivatives participate in complex formation is still uncertain.

Metal complexes of histidine and its esters form mixed complexes with other amino acids with marked stereoselectivity. The first evidence of this came from a nuclear magnetic resonance (NMR) study of Co(II)–histidine complexes[17]. Subsequently, Brookes and Pettit[18] demonstrated stereoselectivity in Cu(II) complexes of L-histidine and amino acids with a polar side group.

EXPERIMENTAL

Instrumentation

The chromatograph was a Perkin-Elmer Series 2 LC equipped with a Rheodyne 7105 injection valve, a Model LC 650-10 fluorescence spectrophotometer and a Model 56 chart recorder (Perkin Elmer, Norwalk, CT, U.S.A.). Fluorescence of the Dns derivatives at 480 nm was monitored with excitation at 340 nm. The analytical columns were 15 × 0.42 cm packed with Spherisorb® C_{18} (Phase Separations, Hauppage, NY, U.S.A.). The columns were packed by the downward slurry technique.

Reagents

Acetonitrile distilled-in-glass was bought from Burdick & Jackson Labs. (Muskegon, MI, U.S.A.), D- and L-Dns-amino acids from Sigma (St. Louis, MO, U.S.A.) and Pierce (Rockford, IL, U.S.A.). Other Dns-amino acids were prepared as previously described[1]. The mobile phases in general contained 10–20% of acetonitrile in a buffer that was $5.0 \cdot 10^{-3}$ *M* of an optically active amino acid, $2.5 \cdot 10^{-3}$ *M* copper sulfate and 2.0 g of ammonium acetate.

RESULTS

A mobile phase containing L-histidine and Cu(II) in a 2:1 molar ratio resolved Dns-amino acids with aliphatic, aromatic and polar substituents (Table I). The selectivity was excellent; low-molecular-weight amino acids were completely separated (Figs. 1–3).

As in other reversed-phase analyses, the separation depended on the acetonitrile concentration in the mobile phase (Table I). With decreasing acetonitrile concentration, solutes were retained longer, and the resolution and selectivity improved (Table II).

Esterification of the carboxylate function also had a marked effect (Table III, Figs. 4–6).

Because of competition for binding sites by hydrogen ions, the ability of the amino acid to bind Cu(II) decreased at lower pH, with an effect on both selectivity and capacity factor (Tables IV and V). With L-histidine at pH 5, there was complete

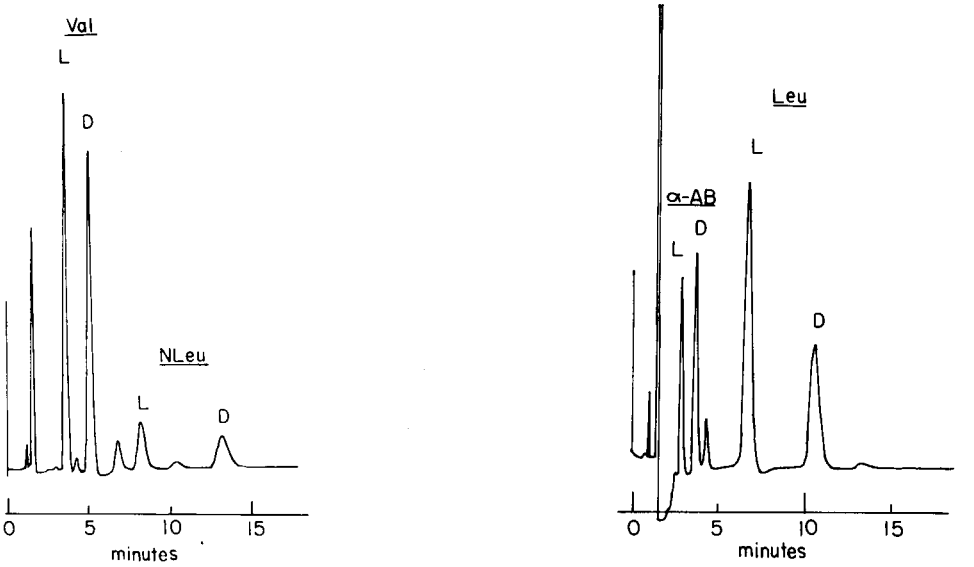

Fig. 1. Separation of D,L-Dns-valine and norleucine with L-histidine–Cu(II) eluent. Mobile phase: 17.5% acetonitrile in an aqueous solution containing 5 m*M* L-histidine, 2.5 m*M* $CuSO_4 \cdot 5H_2O$ and 2.0 g ammonium acetate, pH 7.0. Flow-rate: 2.0 ml/min.

Fig. 2. Separation of D,L-Dns-α-amino butyric acid and leucine. Conditions as in Fig. 1.

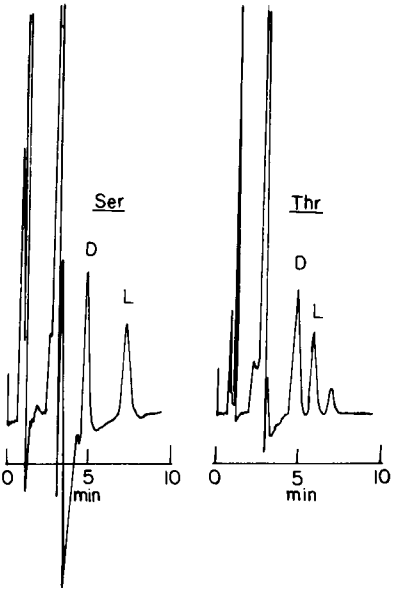

Fig. 3. Separation of D,L-Dns-serine and D,L-Dns-threonine with L-histidine–Cu(II) eluent. Mobile phase: 10% acetonitrile in an aqueous solution containing 5 m*M* L-histidine, 2.5 m*M* $CuSO_4 \cdot 5H_2O$ and 2.0 g ammonium acetate, pH 7.0. Flow-rate: 2.0 ml/min.

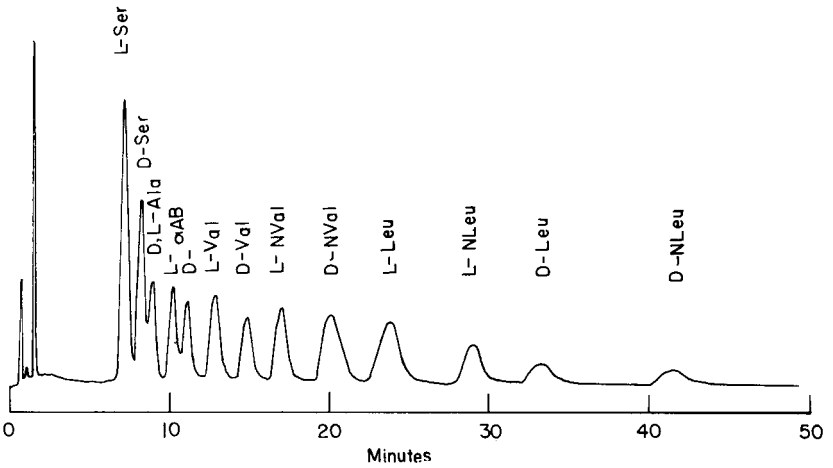

Fig. 4. Separation of D,L-Dns-amino acids with Cu(II)–L-histidine methyl ester eluent. Mobile phase: 20% acetonitrile in an aqueous solution containing 5 m*M* L-histidine methyl ester, 2.5 m*M* $CuSO_4 \cdot 5H_2O$ and 2.0 g ammonium acetate, pH 7.0. Flow-rate: 2.0 ml/min.

loss of resolution for most of the amino acids while isomers of tryptophan and phenylalanine were separated more. With the L-histidine methyl ester, there was decreased selectivity with decrease in pH, although some separation of optical isomers persisted.

TABLE I

CAPACITY RATIO (k') AND SELECTIVITY (α) OF D- AND L-Dns AMINO ACIDS

Mobile phase: aqueous solution containing 5 m*M* L-histidine, 2.5 m*M* $CuSO_4 \cdot 5H_2O$ and 2.0 g ammonium acetate/l of deionized water with the following percentage of acetonitrile: (1–3) 10%; (5–12) 15%. pH 7.0. Flow-rate: 2.0 ml/min.

No.	*Amino acid*	k'_L	k'_D	α
1	Thr	4.4	3.4	0.77
2	Ser	5.6	3.4	0.61
3	Ala	6.6	8.2	1.2
4	α-AB	2.2	3.8	1.7
5	Val	3.2	6.4	2.0
6	Met	4.4	7.8	1.8
7	NVal	3.8	9.0	2.4
8	ILeu	7.2	15.4	2.1
9	Leu	7.2	16.0	2.2
10	NLeu	9.4	22.2	2.4
11	Phe	9.0	9.0	1.0
12	Trp	7.4	7.4	1.0

TABLE II

CAPACITY RATIO (k') AND SELECTIVITY (α) AS A FUNCTION OF ACETONITRILE CONCENTRATION

Conditions as in Table I.

Amino acid	*20% Acetonitrile*			*17.5% Acetonitrile*			*15% Acetonitrile*		
	k'_L	k'_D	α	k'_L	k'_D	α	k'_L	k'_D	α
α-AB	0.6	1.2	2.0	1.8	2.6	1.4	2.2	3.8	1.7
Val	1.2	2.0	1.7	2.6	4.0	1.5	3.2	6.4	2.0
Met	1.2	2.0	1.7	3.8	5.4	1.4	4.4	7.8	1.8
NVal	1.4	2.6	1.9	3.2	5.8	1.8	3.8	9.0	2.4
ILeu	2.6	4.6	1.8	5.6	9.0	1.6	7.2	15.4	2.1
Leu	2.6	4.8	1.8	5.6	9.6	1.7	7.2	16.0	2.2
NLeu	3.0	5.8	1.9	7.0	11.8	1.7	9.4	22.2	2.4
Phe	2.6	2.6	1.0	5.4	5.4	1.0	9.0	9.0	1.0
Trp	2.2	2.2	1.0	4.8	4.8	1.0	7.4	7.4	1.0

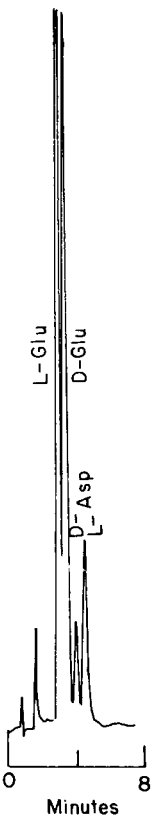

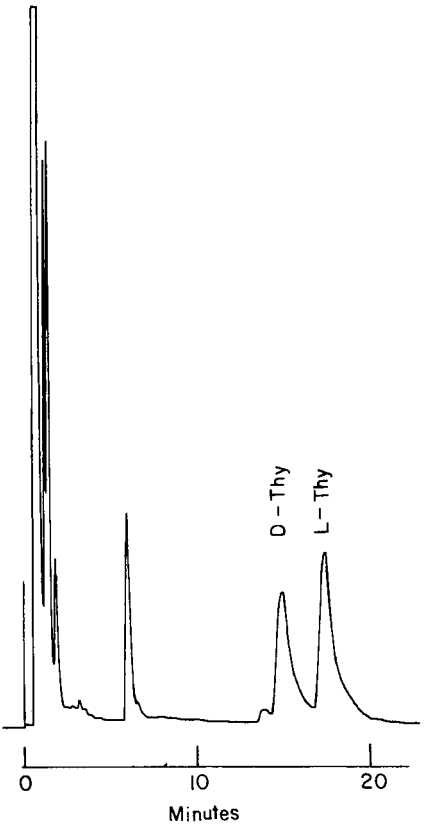

Fig. 5. Separation of D,L-Dns-glutamic acid and aspartic acids. Conditions as in Fig. 4.

Fig. 6. Separation of D,L-Dns-thyroxine with Cu(II)–L-histidine methyl ester eluent. Mobile phase: 40% acetonitrile in an aqueous solution containing 5 m*M* L-histidine methyl ester, 2.5 m*M* $CuSO_4 \cdot 5H_2O$ and 2.0 g ammonium acetate, pH 7.0. Flow-rate: 2.0 ml/min.

TABLE III

CAPACITY RATIO (k') AND SELECTIVITY (α) OF D- AND L-Dns-AMINO ACIDS

Mobile phase: 20.0% acetonitrile in an aqueous solution containing 5 m*M* L-histidine methyl ester, 2.5 m*M* $CuSO_4 \cdot 5H_2O$, and 2.0 g ammonium acetate/l of deionized water. pH 7.0. Flow-rate: 2.0 ml/min.

Amino acid	k'_L	k'_D	α
Glu	3.3	4.1	1.3
Asp	5.0	4.4	0.88
Asn	7.9	8.7	1.1
Ser	9.3	10.7	1.2
Thr	9.3	9.3	1.0
Ala	11.9	11.9	1.0
α-AB	13.6	15.0	1.1
Val	17.3	20.1	1.2
Met	27.2	30.7	1.1
NVal	23.3	27.6	1.2
ILeu	40.4	44.7	1.1
Leu	33.0	43.9	1.3
NLeu	40.4	58.4	1.5
Phe	77.9	60.4	0.78
Trp	121.8	93.3	0.77
Thy*	21.5	20.4	0.95

* 40% Acetonitrile.

TABLE IV

CAPACITY RATIO (k') AND SELECTIVITY (α) OF D- AND L-Dns-AMINO ACIDS AS A FUNCTION OF pH

Mobile phase: 15.0% acetonitrile in an aqueous solution containing 5 m*M* L-histidine, 2.5 m*M* $CuSO_4 \cdot 5H_2O$, and 2.0 g ammonium acetate/l of deionized water. Flow-rate: 2.0 ml/min.

Amino acid	*pH 7*			*pH 5*		
	k'_L	k'_D	α	k'_L	k'_D	α
α-AB	2.2	3.8	1.7	8.4	8.4	1.0
Val	3.2	6.4	2.0	13.8	13.8	1.0
Met	4.4	7.8	1.8	14.4	14.4	1.0
NVal	3.8	9.0	2.4	16.4	16.4	1.0
ILeu	7.2	15.4	2.1	30.4	30.4	1.0
Leu	7.2	16.0	2.2	31.4	31.4	1.0
NLeu	9.4	22.2	2.4	37.0	37.0	1.0
Phe	9.0	9.0	1.0	34.0	30.0	0.88
Trp	7.4	7.4	1.0	34.0	27.0	0.79

TABLE V

CAPACITY RATIO (k') AND SELECTIVITY (α) OF D- AND L-Dns-AMINO ACIDS

Mobile phase: 20.0% acetonitrile in an aqueous solution containing 5 m*M* L-histidine methyl ester, 2.5 m*M* $CuSO_4 \cdot 5H_2O$, and 2.0 g ammonium acetate/l of deionized water. pH as indicated in table. Flow-rate: 2.0 ml/min.

Amino acid	*pH 7*			*pH 5*		
	k'_L	k'_D	α	k'_L	k'_D	α
Glu	3.3	4.1	1.3	5.0	5.6	1.1
Asp	5.0	4.4	0.88	6.7	6.1	0.91
Asn	7.9	8.7	1.1	9.6	11.3	1.2
Ser	9.3	10.7	1.2	7.8	9.0	1.2
Thr	9.3	9.3	1.0	9.0	9.0	1.0
Ala	11.9	11.9	1.0	10.7	10.7	1.0
α-AB	13.6	15.0	1.1	10.7	11.3	1.1
Val	17.3	20.1	1.2	16.1	17.0	1.1
Met	27.2	30.7	1.1	20.4	22.4	1.1
NVal	23.3	27.6	1.2	19.3	21.3	1.1
Leu	33.0	43.9	1.3	31.3	34.1	1.1
NLeu	40.4	58.4	1.5	39.0	43.6	1.1
Phe	77.9	60.4	0.78	66.1	53.9	0.81
Trp	121.8	93.3	0.77	100.7	81.0	0.81

TABLE VI

COMPARISON OF SELECTIVITY (α) AND CAPACITY RATIO (k') BETWEEN FOUR ELUENT SYSTEMS CONTAINING Cu(II) COMPLEXES OF THE L-AMINO ACIDS SHOWN IN THE HEADINGS

Acetonitrile concentration was 15% for proline and histidine system and 20% for histidine methyl ester and arginine system. Other conditions as in Table I.

	Proline			*Histidine*			*Histidine methyl ester*			*Arginine (ref. 1)*		
	k'_L	k'_D	α	k'_L	k'_D	α	k'_L	k'_D	α	k'_D	k'_L	α
Ser	3.7	3.2	0.87	–	–	–	9.3	10.7	1.2	3.0	3.0	1.0
Thr	3.7	4.6	1.2	–	–	–	9.3	9.3	1.0	3.0	3.0	1.0
Ala	5.7	6.6	1.2	1.8	2.4	1.3	11.9	11.9	1.0	4.2	4.4	1.1
α-AB	7.3	9.2	1.2	2.2	3.8	1.7	13.6	15.0	1.1	5.7	6.2	1.1
Val	11.4	15.0	1.3	3.2	6.4	2.0	17.3	20.1	1.2	8.3	9.5	1.1
Met	11.4	14.8	1.3	4.4	7.8	1.8	27.2	30.7	1.1	10.3	11.7	1.1
NVal	14.6	19.0	1.3	3.8	9.0	2.4	23.3	27.6	1.2	11.0	13.0	1.2
ILeu	–	–	–	7.2	15.4	2.1	40.4	44.7	1.1	17.2	20.8	1.2
Leu	23.9	32.6	1.4	7.2	16.0	2.2	33.0	43.9	1.3	18.5	20.8	1.1
NLeu	32.6	45.7	1.4	9.4	22.2	2.4	40.4	58.4	1.5	22.3	28.2	1.3
Phe	32.6	52.8	1.6	9.0	9.0	1.0	77.9	60.4	0.78	20.3	23.0	1.1
Trp	41.2	71.2	1.7	7.4	7.4	1.0	121.8	93.3	0.77	24.8	31.2	1.3

DISCUSSION

When a divalent metal ion, M(II), is in equilibrium with 2 different amino acids, Ax and Ay, both of which can form complexes with the metal ion, the following equilibria are present:

$$M + 2Ax \rightleftharpoons M(Ax)_2$$
$$M + 2Ay \rightleftharpoons M(Ay)_2$$
$$M + Ax + Ay \rightleftharpoons M(Ax)(Ay)$$
$$M(Ax)_2 + M(Ay)_2 \rightleftharpoons 2M(Ax)(Ay)$$

The disproportionation constant K can be written as:

$$K = [M(Ax)(Ay)]^2/[M(Ax)_2][M(Ay)_2]$$

Statistically there are two ways the mixed complex M(Ax) (Ay) can be formed but only one way the binary complexes $M(Ax)_2$ and $M(Ay)_2$ can be. The expected disproportionation constant is 4.

When the stability constants for the mixed complex M(Ax)(Ay) and for the binary complexes $M(Ax)_2$ and $M(Ay)_2$ are determined, following Siegel[19], it is possible to define the stability of the ternary complex as:

$$\log K = 2 \log_{M(Ax)(Ay)} - \log_{M(Ax)_2} - \log_{M(Ay)_2}$$

Thus the tendency towards ternary complex formation can be characterized by the sign and the value of log K. The expected value of a favorable disproportionation reaction is log 4, or 0.6. A value of log K of greater than 0.6 suggests stabilization of the ternary complex.

The formation constants of some ternary complexes of Cu(II)–L-histidine and bidentate amino acids, measured by potentiometric methods[18] are as follows:

Cu(II)–L-His–L-amino acid	L-Phe	L-Try	L-Val	L-Leu	L-Thr	L-Ser
log K	2.10	2.37	2.20	2.13	2.24	1.90

The log K values greater than 0.6 suggest that histidine does indeed form ternary complexes. It has also been shown that in the Cu(II)–L-histidine–L-bidentate amino acid system over 70% of the metal complexes are ternary and with the remaining 30% distributed among the others[20].

Based on these findings, we used the binary complex of Cu(II)–L-histidine and Cu(II)–L-histidine methyl ester as the mobile phase in reversed-phase chromatography. We postulated that on the introduction of an amino acid an equilibrium of the parent complex and the ternary complex would be established; the charged species and the metal ions would remain in the aqueous phase, while the more hydrophobic and neutral binary and ternary complexes would partition into the non-polar stationary phase. Since a chiral metal complex was to be used, different disproportionation and stereoselectivity was expected with enantiomeric solutes. If one of the two

optical isomers of the solute amino acid were to displace histidine from the binary complex more strongly, separation in the high-performance liquid chromatographic (HPLC) system would have become possible.

Brookes and Pettit[18], using potentiometric measurements, demonstrated a significant degree of stereoselectivity in the formation of the ternary complex of Cu(II), L-histidine and amino acids with polar groups in the side chain. Using Cu(II)–L-histidine complexes in the mobile phase, we achieved optical resolution of Dns-amino acids with aliphatic as well as polar side-chains.

The order of elution generally was consistent with other reversed-phase separations: the higher the carbon content, the bulkier the alkyl substituent on the α-carbon (Fig. 1), the longer the retention. With isomers with equal numbers of carbons such as norleucine and leucine, the straight chain isomer was retained more, presumably because of stronger interaction with the stationary phase. The selectivity between the D- and L-pairs was also affected by the bulkiness of the alkyl substituents.

The stereoselectivity followed a defined pattern (Table I). The L-isomers of those amino acids with aliphatic side-chains eluted before the D-isomers. The D-isomers of amino acids with chelatable side chains were retarded more, yielding a greater degree of separation, while no resolution was observed with amino acids with charge transfer groups. Yamauchi *et al.*[20] showed that L-histidine and amino acids with polar, chelatable side-chains formed ternary complexes such as is shown in Fig. 7. The polar side-chain of the coordinating amino acid, represented by "X", is in the vicinity of the oxygen of the apically coordinated carboxyl group. Stabilization of the ternary complex by hydrogen bonding is probable. Hydrogen bonding is a weak but significant driving force for the stereospecific formation of the more stable L-His–L-amino acid complex with the polar side group. The retention behavior and selectivity of the polar amino acids, serine and threonine, are consistent with the above model, involving intramolecular hydrogen bonding of the terdentate histidine and bidentate amino acids coordinated around copper(II) in a *cis* configuration. With amino acids with aliphatic side-chains, hydrogen bonding interaction is not present. Instead the carboxyl group at the apical position has more steric interaction with the hydrocarbon part of the ternary complex and interferes with the approach of the carboxylate oxygen to the apical coordination site. This causes the meso complex, (L-His)–Cu(II)–(D-amino acid), to be more stable and retained longer.

Separation of the D- and L-pairs also depends on the alkyl substituent on the α-carbon. With the exception of phenylalanine and tryptophan, the bulkier the alkyl group, the higher the selectivity factor (α). Although the separation of the stereoisomers of these two amino acids was greatest in all of the other systems we

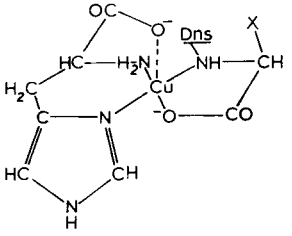

Fig. 7. Structure of L-His–Cu(II)–L-amino acid ternary complex.

studied, including the proline, arginine and histidine methyl ester systems, there was no stereoselectivity with the free histidine system at pH 7. With the Dns-derivative of phenylalanine and tryptophan, pi–pi interaction with the imidazole ring of histidine is possible. Charge transfer interaction can occur with the imidazole of histidine and the naphthyl and phenyl group of Dns-phenylalanine or the naphthyl and indole groups of Dns-tryptophan. Construction of a three-dimensional model shows that a hydrocarbon cluster is formed above the coordination plane with the amino acids bonded to the copper in the same way as is glycine; between carboxyl and α-amino nitrogen. The formation of such a complex is evidently possible with both D- and L-isomers, with no difference in the stability of the complex.

Urry and Eyring[21] have shown that histidine methyl ester would coordinate around a metal ion in a terdentate manner with the acyl oxygen at the apex. Using Cu(II)–L-histidine methyl ester as the eluent, we observed stereoselective formation of metal complexes and resolution of many pairs of Dns-amino acids (Table III, Figs. 4 and 5). The D-isomers are generally retained longer; even those such as serine with polar side-chains. The complexation mechanism in this case no longer follows the pattern of free histidine. The apical carbonyl makes no contribution to complex stability through hydrogen bonding with the weak hydrogen donors of the polar amino acids. In this case, steric interaction is more important in determining the stability of the complex. However, with the amino acids studied, reversed stereoselectivity was observed for aspartic acid, the aromatic acids, phenylalanine, thyroxine and the heterocyclic amino acid, tryptophan.

This reversed selectivity of aspartic, compared to glutamic, suggests that these two amino acids bond differently with the L-histidine methyl ester and supports the idea that glutamic acid bonds the way glycine does, while aspartic acid is terdentate[18] with hydrogen bonding of the carboxylic group of aspartic and the carbonyl group of histidine methyl ester resulting in the observed reversal in selectivity.

The Dns-phenylalanine and tryptophan optical isomers, not resolved by the free histidine system (Table I), were separated by the Cu(II)–histidine methyl ester mobile phase (Table III). The stereoselectivity, however, was not as expected from that reported for the free histidine in solution[18]. Here the ternary complex formed by the ligands of the same chirality was more stable and more strongly retained. With methylation of the carboxylate group of histidine, the histidine derivative can no longer bond as does glycine as in the free histidine system, thus preventing the formation of clusters by the naphthyl, the aromatic and the imidazole groups. Instead, the histidine methyl ester with its amine and imidazole group bonded in the *trans* manner, with the carbonyl weakly coordinated on the apical site, and the aromatic ring on the opposite side of the carbonyl. Therefore, the meso complex having both carbonyl and the ring system competing for the same coordination site is less stable. Phenylalanine and tryptophan with the aromatic ring in the side-chain have been demonstrated to undergo pi–pi interaction with the Cu(II) ion[22]. The amino acid in this case can be regarded as a terdentate ligand.

The histidine molecule offers three potential coordination sites in aqueous solution: the carboxyl group ($pK_a = 1.9$), the imidazole nitrogen ($pK_a = 6.1$) and the amino nitrogen ($pK_a = 9.1$)[23]; while the histidine methyl ester has two coordination sites, the imidazole nitrogen ($pK_a = 5.4$) and the amino nitrogen ($pK_a = 7.3$)[24] becoming available for complexation as pH increases. A change in the pH of the

mobile phase would result in a change in the equilibrium distribution of the various metal species in the solution. With the lowering of pH, the hydrogen ion would compete with the Cu(II) ion for the chelating sites. The resolution would diminish (Tables IV and V). At pH 7, more than 70% of the metal complex is present. At lower pH, this percentage decreases. It is important to note that both the amino and the imidazole nitrogen are very effective bidentate ligands at pH 5. Significant resolution of the Dns-amino acids is observed (Table V). This can be due to the fact that histidine methyl ester is more hydrophobic, as is evident from the acetonitrile concentration needed in the mobile phase to elute of the amino acids (Table III). Histidine methyl ester also has smaller dissociation constants. At pH 5 appreciable portions of the metal complexes of the L-histidine methyl ester are distributed in the stationary phase.

The free histidine system at pH 5 gave no stereoselectivity for most amino acids but resolved tryptophan and phenylalanine isomers for the first time (Table IV). At this pH, the histidine complex may have bonded in the same manner as that of the histidine methyl ester, as suggested by the similar selectivity and orders of elution. The carboxylate molecule may be involved in hydrogen bonding with H^+ or water molecules, thus rendering it unavailable for glycine-like coordination.

With copper(II) complexes of N-acetyl-L-histidine under the same mobile phase conditions, no resolution of the Dns-amino acid optical isomers was observed. As noted for the histidine methyl ester system, the amino group chelates the metal effectively. Blocking of the functional group by acylation resulted in a weaker complex and loss of stereoselectivity.

Table VI compares the selectivity and capacity factors of several systems. Even though the acetonitrile concentrations used with the four systems were different, the stereoselectivity was affected only slightly (Table II and ref. 1). Histidine differs from other amino acids in that it possesses a bulky substituent on the α-carbon. It also functions as a terdentate ligand which gives the mixed complex a rigid conformation, and thus high stereoselectivity. Histidine methyl ester gives a less rigid complex, with reduced selectivity. Proline has an intermediate selectivity because it has a ring system standing above the coordination plane, unlike the imidazole ring of histidine methyl ester which lies flat on the plane. Arginine which does not have a rigid ring structure gives selectivity similar to histidine methyl ester. Therefore, the three-dimensional conformation of the ternary complex is important in deciding stereoselectivity. Stronger spatial interaction results in better optical resolution.

Histidine methyl ester and arginine systems offer adequate stereoselectivity and excellent separation of the different Dns-amino acids while histidine offers excellent stereoselectivity for the enantiomers but poor separations of the amino acids. It is possible to optimize the histidine methyl ester or the arginine system for a one-column system in the separation of most of the amino acids into their respective isomers by some form of mobile phase gradient.

REFERENCES

1 S. Lam, F. Chow and A. Karmen, *J. Chromatogr.*, 199 (1980) 295.
2 I. S. Krull, *Advan. Chromatogr.*, 16 (1978) 175.
3 V. A. Davankov, *Advan. Chromatogr.*, 17 (1979) 139.
4 J. N. LePage, W. Lindner, G. Davies, D. E. Seitz and B. L. Karger, *Anal. Chem.*, 51 (1979) 433.

5 W. Linder, J. N. LePage, G. Davies, D. E. Seitz and B. L. Karger, *J. Chromatogr.*, 185 (1979) 323.
6 P. E. Hare and E. Gil-Av, *Science*, 204 (1979) 1226.
7 S. Weinstein, E. Gil-Av and P. E. Hare, *Pittsburgh Conference on Analytical Chemistry and Applied Spectroscopy, March 9–13, 1981*, Abstract No. 289.
8 C. Gilon, R. Leshem, Y. Tapuhi and E. Grushka, *J. Amer. Chem. Soc.*, 101 (1979) 7612.
9 C. Gilon, R. Leshem, E. Grushka, *J. Chromatogr.*, 203 (1981) 365.
10 S. Lam and F. Chow, *J. Liquid Chromatogr.*, 3 (1980) 1579.
11 S. Lam and A. Karmen, *Pittsburgh Conference on Analytical Chemistry and Applied Spectroscopy, March 9-13, 1981*, Abstract No. 768.
12 W. N. Lipscomb, *Acc. Chem. Res.*, 3 (1970) 81.
13 B. W. Matthews and L. H. Weaver, *Biochemistry*, 13 (1974) 1719.
14 K. K. Kannan, B. Notstrand, K. Fridborg, S. Lovgren, A. Ohlsson and M. Petef, *Proc. Nat. Acad. Sci. U.S.*, 72 (1975) 51.
15 B. Sarkar and T. P. A. Kruck, in J. Peisach, P. Aisen and W. E. Blumberg (Editors), *The Biochemistry of Copper*, Academic Press, New York, 1966, p. 183.
16 T. P. A. Kruck and B. Sarkar, *Can. J. Chem.*, 51 (1973) 3563.
17 C. C. McDonald and W. D. Phillips, *J. Amer. Chem. Soc.*, 85 (1963) 3736.
18 G. Brookes and L. D. Pettit, *J. Chem. Soc., Dalton*, (1977) 1918.
19 H. Sigel, in H. Sigel (Editor), *Metal Ions in Biological System, Vol. 2*, Marcel Dekker, New York, 1973, p. 63.
20 O. Yamauchi, T. Sakurai and A. Nakahara, *J. Amer. Chem. Soc.*, 101 (1979) 4164.
21 D. W. Urry and H. Eyring, *J. Amer. Chem. Soc.*, 86 (1964) 4574.
22 F. W. Wilson and R. B. Martin, *Inorg. Chem.*, 10 (1971) 1197.
23 B. Sarkar and Y. Wigfield, *J. Biol. Chem.*, 242 (1967) 5572.
24 H. K. Conley, Jr. and R. B. Martin, *J. Phys. Chem.*, 69 (1965) 2923.

Journal of Chromatography, 239 (1982) 463–474
Elsevier Scientific Publishing Company, Amsterdam — Printed in The Netherlands

CHROM. 14,631

TOTAL AMINO ACID ANALYSIS USING PRE-COLUMN FLUORESCENCE DERIVATIZATION

H. UMAGAT* and P. KUCERA
Pharmaceutical Research Products Section, Quality Control Department, Hoffmann-La Roche Inc., Nutley, NJ 07110 (U.S.A.)

and

L.-F. WEN
Diagnostic and Biological Products Section, Quality Control Department, Hoffmann-La Roche Inc., Nutley, NJ 07110 (U.S.A)

SUMMARY

An approach to total amino acid analysis utilizing off-line pre-column fluorescence derivatization is described. The full array of natural primary amino acids was treated with *o*-phthaldialdehyde (OPA) in the presence of mercaptans, and the highly fluorescent reaction products were separated on an ODS 5-μm reversed-phase column with gradient elution development. Due to their instability in solution and the relatively poor response of the OPA derivatives, cysteine and cystine were oxidized with performic acid and separated as the OPA cysteic acid reaction adduct, which is highly fluorescent.

Secondary amino acids, such as proline and hydroxyproline, were reacted with 4-chloro-7-nitrobenzofurazan, and the separation was carried out on the same column. The stability of the reaction adducts was investigated and the derivatization reactions were optimized with respect to reaction time and temperature.

It is shown that the detection limits for most amino acids are in the 0.1–1.0-pmole range. The reproducibility of the method was limited by the derivatization procedure and the gradient elution employed, but, by using an on-line computer data handling system, the retention time could be measured within $\pm$ 0.1 % relative standard deviation and the relative peak areas, based on the internal standard calculation methodology, were within $\pm$ 3 % or less. The sensitivity of lysine and hydroxylysine was improved by forming a sodium dodecylsulfate micellar solution around these amino acids to protect the fluorescent adducts from rapid decomposition. The sensitivity and separation appeared to be very much dependent on the pH of the mobile phase.

Experimental details for the determination of total amino acid residues in pharmaceutically important proteins, such as thymosin α_1 and insulin, are given. Advantages and disadvantages of the system described are discussed.

0021-9673/82/0000–0000/$02.75

INTRODUCTION

Amino acid analysis is an important technique which finds many applications in biochemistry and related fields. Determination of the primary structure of proteins[1], peptide sequencing[2], determination of completeness of solid-phase peptide synthesis, and structure elucidation[3] all require an accurate method for amino acid determination. The analysis of protein samples, however, presents a formidable problem for the practising liquid chromatographer. A very small amount of sample is usually available; trace amounts of amino acids possessing no significant fluorophores or chromophores are present in a very complex sample mixture where other substances interfere with the analysis. A substantial number of amino acids with diverse polarities and functional groups has to be quantitated. Thus, in general, the chromatographic system should exhibit high specificity, sensitivity, and chromatographic selectivity; in addition, the system should also be versatile, simple to operate, and highly reproducible.

Classical two-column amino acid analyzers[4] based on ion-exchange copolymers and operated in post-column derivatization mode utilized either ninhydrin[5] or other fluorogenic reagents[6–9]. Although the use of these instruments for amino acid analysis has been widely advocated in the past, the major shortcomings observed were long analysis times, poor chromatographic performance of ion-exchange columns, inadequate detection limits, high cost of instrumentation, and the total dedication of the system to only one type of analysis. Besides these complications, the difficulty in the detection of proline, hydroxyproline, cysteine, and cystine limited the use of these analyzers.

High-performance liquid chromatography (HPLC) as practiced in various modes has now become a common technique in the analysis of protein hydrolysates because of the tremendous advances made in the development of HPLC columns and column technology. Promising results have been obtained on the separation of dimethylaminobenzenesulfonyl[10] and phenylthiohydantoin[11,12] derivatives of the amino acids. Recent studies have demonstrated simpler and more rapid reactions with the use of *o*-phthaldialdehyde (OPA) in the presence of either ethanethiol[13] or mercaptoethanol[14–16].

The major aim of this paper was to develop an analytical method for the determination of primary and secondary amino groups containing amino acids. It was also attempted to improve the analytical technique from the point of view of separation, sensitivity, analysis time, and flexibility. Applications of total amino acid analysis to proteins of pharmaceutical importance are also demonstrated.

EXPERIMENTAL

Solvents and reagents

Methanol, acetonitrile, tetrahydrofuran, and high-purity water were obtained from Burdick & Jackson, Muskegon, MI, U.S.A. Amino acid standard H, OPA, 2-mercaptoethanol, ethanethiol, and sodium dodecylsulfate were purchased from Pierce, Rockford, IL, U.S.A. Additional amino acid standards were obtained from Sigma, Morton Grove, IL, U.S.A. and sodium acetate and boric acid were analytical-grade reagents from Mallinckrodt, St. Louis, MO, U.S.A. The sample of thymosin α_1

was obtained from Hoffmann-La Roche, Nutley, NJ, U.S.A. The insulin sample was obtained from Eli Lilly, Indianapolis, IN, U.S.A.

Chromatographic equipment

The instrument used consisted of a Spectra-Physics Model SP-8000 microprocessor-controlled liquid chromatograph coupled to a Schoeffel SF 970 fluorescence detector equipped with a deuterium lamp. The OPA derivatives were detected with the monochromator set at 330 nm and a 418-nm cut-off filter. The sensitivity was set at 1 μA full scale. The 4-chloro-7-nitrobenzofurazan (NBD) reaction adducts were monitored at an excitation wavelength of 220 nm, with a 370-nm cut-off filter, and a sensitivity setting of 0.1 μA.

The detector was connected to a Hewlett-Packard Model HP-1000 computer system with data collection and handling software provided by Computer Inquiry Systems (CIS), Allendale, NJ, U.S.A. Separations were carried out on a 25 cm × 4.6 mm I.D. Ultrasphere column packed with 5 μm ODS particles (Beckman, Berkeley, CA, U.S.A.) connected to a pre-column (5 cm × 4.6 mm I.D.) packed with the same material. The sample was introduced with a Valco air-actuated valve equipped with either a 10- or 100-μl external loop.

Hydrolysis and derivatization procedures

Acid hydrolysis. To *ca.* 100 μg of the protein sample contained in an ignition tube, 200 μl of 4 *N* methanesulfonic acid containing 0.2% of 3-(2-aminoethyl)indole were added and frozen in a slurry of carbon dioxide and isopropanol. Dissolved gases were removed by evaporating the tube by freeze-thawing twice. The tube was then sealed under vacuum and placed in a 110°C oven for 24 h.

Performic acid oxidation. Protein sample (*ca.* 100 μg) was frozen in dry ice and lyophilized. Performic acid was prepared by mixing 1 ml of 30% hydrogen peroxide with 19 ml of 97% formic acid, and allowing the mixture to stand in a closed container for 2 h at room temperature. The mixture was cooled to 0°C and used immediately: 100 μl were added to the sample; the liquid was transferred to a capped vial and was allowed to stand for 2.5 h at 0°C. The reaction was terminated by adding 0.9 ml of cold water. Then 200 μl of this sample were frozen and lyophilized. The dried sample was hydrolyzed by following the hydrolysis procedure described earlier.

Preparation of OPA derivatizing solution. To 50 mg of OPA dissolved in 1.5 ml of methanol, 50 μl of mercaptoethanol and 11 ml of 0.4 *M* borate buffer (pH adjusted to 9.5 with 4 *N* sodium hydroxide) were added. The solution was mixed and flushed with nitrogen to displace dissolved oxygen. The solution was stored in the dark and allowed to stand for 24 h before use. Every 2 days, 10 μl of 2-mercaptoethanol were added. The solution is stable for *ca.* 2 weeks. The OPA derivatizing reagent containing ethanethiol was prepared using the same procedure.

Preparation of the OPA derivatives. A sample of the protein hydrolyzate obtained from acid hydrolysis using methanesulfonic acid was neutralized with 4 *N* sodium hydroxide. For cysteine and cystine determinations, the sample was oxidized to cysteic acid with performic acid. In this case, the oxidation was carried out prior to the acid hydrolysis. The sample was diluted when necessary with 0.4 *M* borate buffer (pH 9.5) to obtain a final concentration of *ca.* 25 nmole/ml of the amino acid with the highest mole ratio in the molecule. An aliquot was withdrawn and mixed with an

equal volume of 4 μg/ml of 2-aminoethanol solution, as an internal standard. One part of this solution was combined with four parts of 1% (w/v) sodium dodecylsulfate in 0.4 *M* borate buffer and four parts of the OPA solution and mixed vigorously for 1 min using a Vortex mixer. Immediately, 5–10 μl were injected onto the column. The commercially available standard amino acid mixture was diluted appropriately to obtain a final concentration of 25 nmoles/ml for each amino acid. The derivatization procedure employed for the protein hydrolyzates was also used for the amino acid standard.

Preparation of the NBD derivatives. An aliquot of the neutralized sample used for the preparation of the OPA derivative was diluted, when necessary, to obtain a final concentration of *ca.* 20 nmoles/ml of proline. Equal volumes of the sample, 0.4 *M* borate buffer, and the NBD solution (concentration 2 mg/ml in methanol) were combined and the mixture was heated for 5 min at 60°C in a closed screw-capped vial. The reaction was stopped by cooling the mixture to 0°C. Aliquots of 100 μl were injected onto the column.

Kinetics of the derivatization reactions

The dependence of the NBD–proline reaction on time and temperature was studied. Standard proline solution (20 nmoles/ml) was treated at 50°C for 0, 1, 5, 20, and 30 min, and the reaction time necessary to reach an equilibrium state was determined from the fluorescent response. The effect of temperature on the NBD–proline reaction was also investigated at 30, 40, 50, 60, and 80°C for 5 min. Similar experiments were carried out with the OPA reaction. However, decomposition of the reaction adducts was observed at elevated temperatures. The OPA reagent is known to react within seconds to attain maximum fluorescent intensity[17], and, therefore, subsequent work with the OPA reagent was carried out using a 1-min reaction time and room temperature. Quantitative reactions with both reagents were possible only with a large excess of either reagent, which indicated that chemical equilibrium processes rather than the kinetics of the reactions were the limiting factors.

RESULTS AND DISCUSSION

Although the liquid chromatography of OPA-amino acids has been recently reported[14], the separation of complex protein hydrolyzates necessitated the development of a new HPLC method which would exhibit an improvement in selectivity, efficiency, reproducibility, speed of the analysis, resolution, and detection limits. The recent work of Jones *et al.*[16] indicated that a feasible chromatographic system consists of a 5-μm reversed-phase column operated in a gradient elution mode with a ternary tetrahydrofuran–methanol–buffer mobile phase. Throughout this work, an Ultrasphere ODS column was used.

No simple gradient could resolve all amino acids completely, and a series of isocratic elution steps coupled with gradient elution displacement effects had to be employed. Furthermore, detailed investigation of various solvent mixtures showed that the need for ternary solvent mixtures was well substantiated. Very good resolution of all primary amino acids was obtained with methanol–tetrahydrofuran–0.05 *M* sodium acetate buffer pH 6.6 (15:1:84) as a starting solvent and 80% (v/v) methanol as the final solvent. The separation obtained is illustrated in Fig. 1. Each peak cor-

responds to 20 pmoles of amino acid. For most amino acids, as shown later, the detection limit was in femtomoles. Thus, the analytical method is *ca.* 1000 times more sensitive than amino acid analyzers that employ ninhydrin for the detection. The average peak width at the base was *ca.* 400 μl. Assuming an analysis time of 45 min and a constant peak width, the maximum peak capacity calculated is *ca.* 150. This means that only *ca.* 20% of the available chromatographic peak capacity has been utilized and certainly additional amino acid-type compounds can be separated with this system. This was demonstrated for the homoserine adduct which elutes close to methionine sulfoxide; increasing the second isocratic step by 2 min resulted in total resolution between the two amino acid adducts.

The separation of the NBD derivatives was carried out on the same column, using a similar solvent system. The kinetics of the NBD–proline reaction was examined by derivatizing a standard proline solution at 50°C using different reaction times. The results can be seen in the top part of Fig. 2, where a graph relating fluorescent NBD–proline peak height to reaction time is shown. At 50°C, the reaction reaches an equilibrium state only after a relatively long time of 30 min.

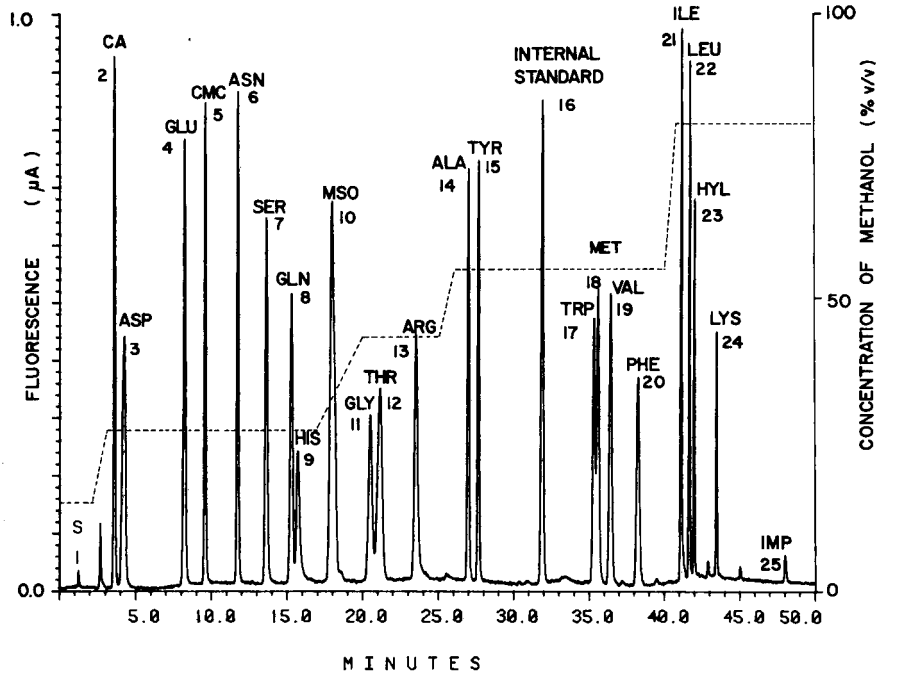

Fig. 1. Separation of OPA-amino acid standards. Operating conditions: column, Ultrasphere ODS 25 cm × 4.6 mm I.D., 5 μm particle size; flow-rate, 1.5 ml/min; solvent A, tetrahydrofuran–0.05 *M* sodium acetate pH 6.6 (1:99); solvent B, methanol; gradient program, 15% B for 2 min from the beginning of the program, linear step to 28% B for 1 min, isocratic elution step at 28% B for 14 min, linear step to 44% B in 3 min, isocratic elution step at 44% B for 5 min, linear step to 56% B in 1 min, isocratic elution step at 56% B for 9 min, linear step to 80% B in 1 min, and isocratic development at 80% B for 19 min; sample volume, 10 μl; excitation at 330 nm; emission filter 418 nm. Peaks: 1 = solvent; 2 = cysteic acid; 3 = aspartic acid; 4 = glutamic acid; 5 = carboxymethylcysteine; 6 = asparagine; 7 = serine; 8 = glutamine; 9 = histidine; 10 = methionine sulfoxide; 11 = glycine; 12 = threonine; 13 = arginine; 14 = alanine; 15 = tyrosine; 16 = 2-aminoethanol; 17 = tryptophan; 18 = methionine; 19 = valine; 20 = phenylalanine; 21 = isoleucine; 22 = leucine; 23 = hydroxylysine; 24 = lysine; 25 = unknown impurity.

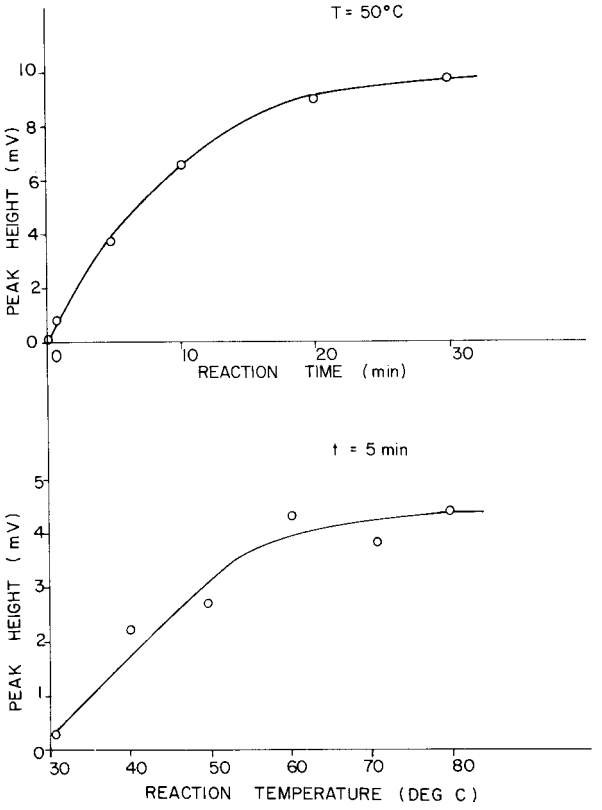

Fig. 2. Graphs relating reaction time and temperature of NBD–proline derivatization to fluorescent yield.

The effect of reaction temperature on the peak height at a constant reaction time of 5 min is shown on the bottom part of Fig. 2. The maximum fluorescent response is attained using temperatures of 60–80°C. Since the reagent blank peak increases with increasing temperature, all NBD–proline reactions were carried out at 60°C, where minimum interference from the reagent was observed. A typical separation of proline from cysteine and hydroxyproline can be seen in Fig. 3. Each peak represents 2 nmoles of amino acid, and the separation was achieved using a simple linear gradient.

Detection limits of OPA and NBD derivatized amino acids are shown in Table I. It can be noted that most amino acids exhibit detection limits below 1 pmole, except in the case of the proline derivative where the detection limit is *ca.* 6 pmoles. Since the NBD reagent peak can be separated from the NBD–proline, the reaction may be carried out at 80°C, where the detection limit for proline would also fall below 1 pmole. The much higher fluorescence response observed for secondary amino acids as compared to primary amino acids agrees well with the work of Ahnoff *et al.*[18], Krol *et al.*[19], and Roth[20], who demonstrated slower reaction kinetics for primary amino acids. The linearity of the proline derivative response was found to be excellent in the 5–25 nmoles/ml range.

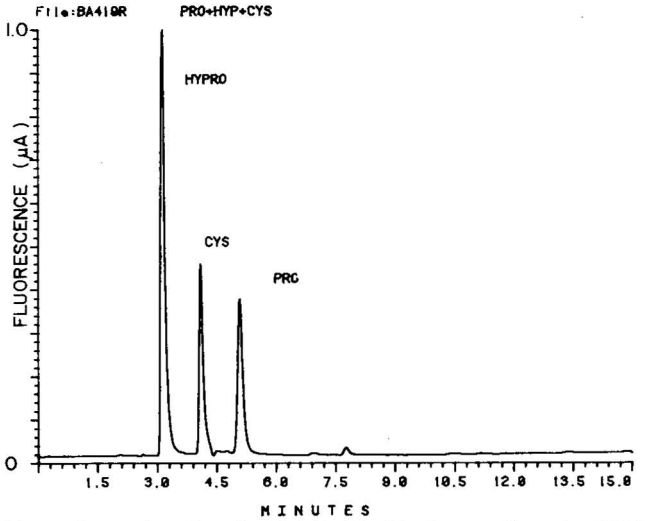

Fig. 3. Separation of proline, cysteine, and hydroxyproline using NBD derivatization. Conditions same as in Fig. 1, except for the gradient program which is linear gradient from 30% B to 45% B, rate 1.5% B per minute; flow-rate, 1.0 ml/min; sample volume, 100 μl; excitation at 220 nm; emission at 370 nm.

TABLE I

DETECTION LIMITS OF AMINO ACIDS

Sample volume, 10 μl.

Amino acid	*Peak height (mV)*	*Detection limit* (pmoles)*	*Sensitivity (relative to histidine)*
CA**	7.700	0.17	6.5
ASP	7.379	0.17	6.3
GLU	6.600	0.20	5.5
CMC**	5.408	0.24	4.5
ASN	6.233	0.21	5.2
SER	4.629	0.28	3.9
GLN	2.475	0.51	2.1
HIS	1.192	1.07	1.0
MSO**	6.692	0.19	5.6
GLY	3.025	0.42	2.5
THR	4.492	0.29	3.7
ARG	5.362	0.24	4.5
ALA	5.042	0.25	4.3
TYR	5.133	0.25	4.3
TRP	2.750	0.46	2.3
MET	4.537	0.28	3.8
VAL	5.087	0.25	4.3
PHE	3.758	0.34	3.1
ILE	6.967	0.18	5.9
LEU	5.546	0.23	4.7
HYL	2.796	0.46	2.3
LYS	1.192	1.07	1.0
PRO	1.890	5.95	–

* Detection limit given here is expressed as minimum amino acid mass placed on the column corresponding to two times signal-to-noise ratio.

** Non-standard abbreviations: CA = cysteic acid; CMC = carboxymethylcysteine; MSO = methionine sulfoxide.

The stability of the proline derivative was also found to be excellent, especially when the sample was reacted in the dark. Using the experiments described previously, no significant change in the fluorescent intensity was observed during a 5-h period. Light-exposed solutions of NBD–proline exhibited an increase in degradation, but more than 95% of the derivative remained unchanged after 5 h of light exposure. An increase in methanol concentration of the mobile phase appeared to improve the stability of all the derivatives, while a decrease in the pH of the mobile phase produced greater instability of the OPA-amino acid adducts. At pH values below 6, the detection of lysine and hydroxylysine has been a problem. To protect these derivatives from rapid decomposition, the suggestion of Jones *et al.*[16] to use sodium dodecylsulfate (SDS) in the reaction mixture was investigated. The lipophilic molecules of SDS

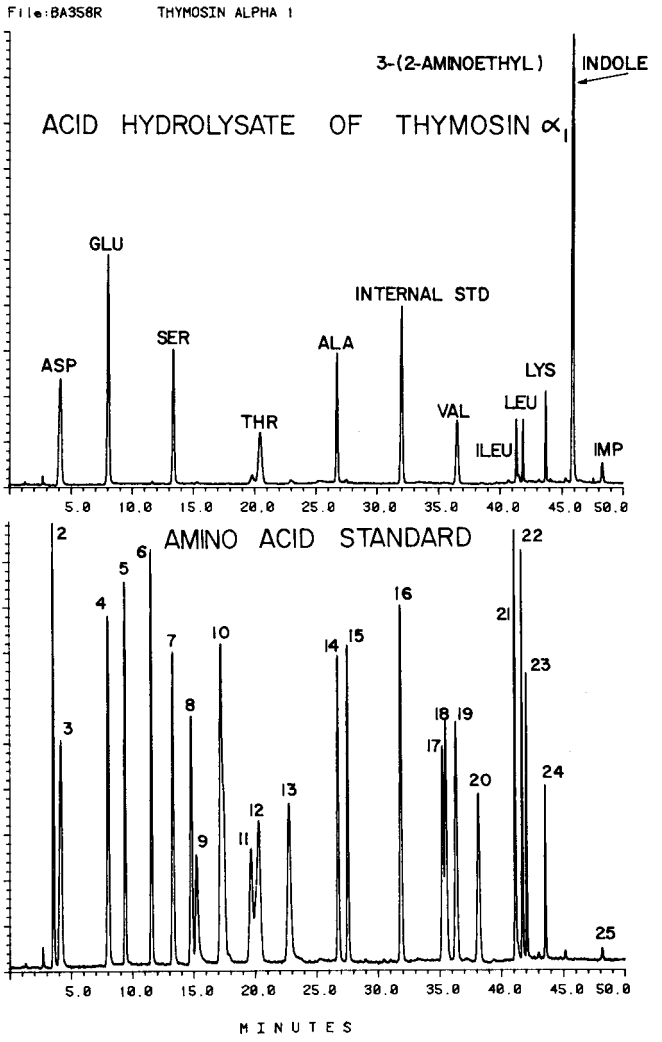

Fig. 4. Amino acid analysis of thymosin α_1. Conditions same as in Fig. 1. Top, acid hydrolysate of thymosin α_1; bottom, amino acid standard.

agglomerate to form micelles, which can entrap the decaying lysine derivative. The critical micelle concentration of SDS, determined from surface tension[21] and conductivity measurements, was found to be 0.2% (w/v). The addition of SDS improved the stability of lysine and hydroxylysine by *ca.* 30%.

The system reproducibility was determined from three replicate injections of an amino acid standard mixture using the conditions described in Figs. 1 and 3. The retention time, as determined by the CIS computer data handling system, could be measured for most amino acids within $\pm 0.2\%$ relative standard deviation (RSD).

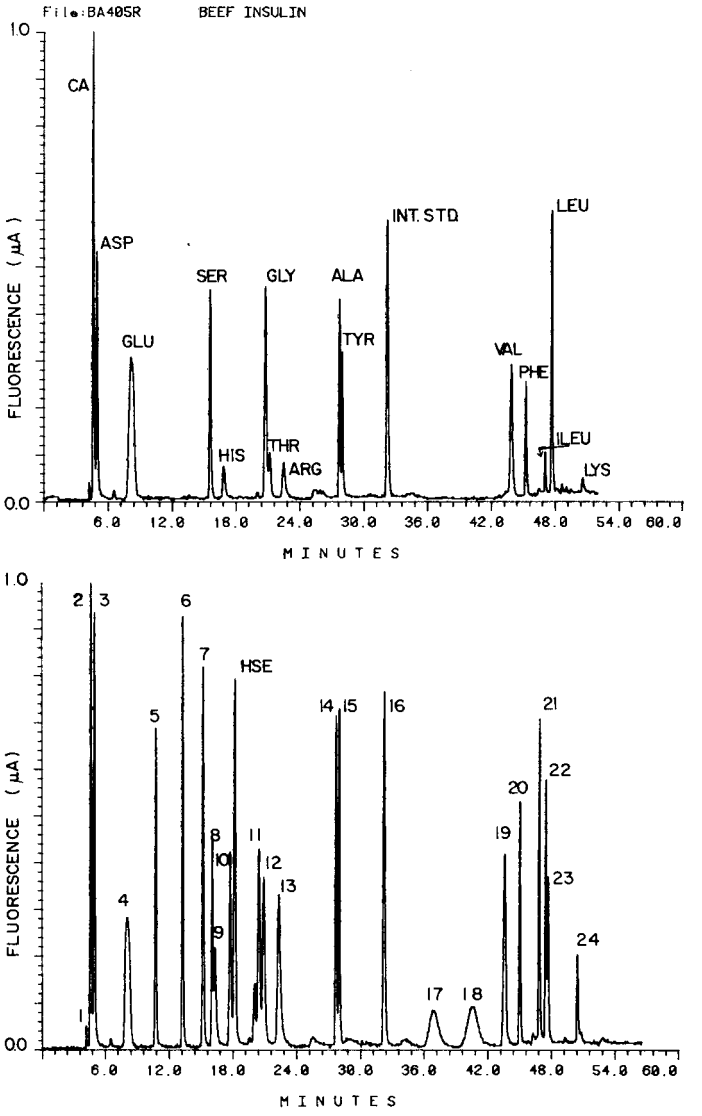

Fig. 5. Amino acid analysis of beef insulin. Conditions same as in Fig. 1. Top, acid hydrolysate of beef insulin; bottom, amino acid standard.

Even with the complex gradient elution system, the relative peak area could be reproduced within $\pm 3\%$ RSD, thus permitting the characterization and quantitation of complex amino acid mixtures.

The application of the analytical system described to the amino acid analysis of two important protein hydrolysates, thymosin α_1 and beef insulin, can be seen in Figs. 4 and 5, where chromatograms of OPA-amino acid adducts shown in comparison to the standard amino acid mixture are illustrated. The hydrolysis of beef insulin and thymosin α_1 was carried out with methanesulfonic acid. In order to quantitate cysteine in beef insulin, the sample was treated with performic acid prior to the hydrolysis which converted cysteine into cysteic acid. The fluorescent derivative of cysteic acid was then easily separated from other amino acid adducts.

A summary of the results obtained from the quantitative analysis of the above-mentioned proteins can be seen in Table II. In each case, the data obtained were consistent with the description of the protein in question. It can be observed from Table II that, after the performic acid oxidation of beef insulin, the correct mole ratio for cysteic acid was obtained. However, tyrosine and valine were partially destroyed during the oxidation. When the protein samples were hydrolyzed with 4 *N* methanesulfonic acid containing 0.2% (w/v) of 3-(2-aminoethyl)indole, very good agreement with the theoretical amino acid composition was found, and this is demon-

TABLE II
AMINO ACID COMPOSITON OF BEEF INSULIN AND THYMOSIN α_1

Amino acid	*Beef insulin mole ratio*		*Thymosin α_1 mole ratio*	
	*Found**	*Expected*	*Found***	*Expected*
CA	6.2	6	–	–
ASP	3.3	3	3.6	4
GLU	6.5	7	5.7	6
SER	3.3	2	2.9	3
HIS	1.7	2	–	–
GLY	5.5	5	–	–
THR	1.4	1	2.6	3
ARG	1.0	1	–	–
ALA	3.5	3	3.0	3
TYR	2.5	4	–	–
MET	–	–	–	–
VAL	3.8	5	2.6	3
PHE	2.7	3	–	–
ILE	1.0	1	1.1	1
LEU	7.0	6	1.1	1
LYS	0.8	1	4.2	4
PRO	1.0	1	–	–
TRP	–	–	–	–

* Sample treated with performic acid followed by hydrolysis in 4 *N* methanesulfonic acid containing 0.2% of 3-(2-aminoethyl)indole. The amino acid composition was found to be in good agreement with the predicted values except for tyrosine and valine, which are known to be partially destroyed when pretreated with performic acid.

** Sample hydrolyzed with 4 *N* methanesulfonic acid containing 0.2% (w/v) of 3-(2-aminoethyl)indole.

strated on a thymosin α_1 sample shown in Table II. Thus, the hydrolysis is an extremely important step for the correct determination of total amino acids in any given protein. The amino acid mole ratios of the above-mentioned proteins were independently checked using a post-column derivatization system based on ninhydrin[4]. In all cases, an excellent agreement between the pre-column and the post-column methods was found.

The chromatographic system designed for quantitative analysis of primary and secondary amino acids can be extended to other applications, including tryptic mapping. When hydrolyzed samples of proteins extracted from biological tissues were chromatographed, it was possible to obtain separation of the protein fragments. In the system described, these fragments eluted after the lysine peak. Because of the high selectivity and sensitivity of the system described, the qualitative and quantitative analysis of protein fragments would be quite feasible and would require only a minor change in the gradient elution program.

CONCLUSIONS

The chromatographic system for the quantitative analysis of primary and secondary amino acids described shows all the advantages of the pre-column derivatization method. Elimination of the post-column reactor yields a less expensive, more versatile system where rapid analysis and high sensitivity can be achieved. Application of gradient elution in conjunction with computer data handling gives high reproducibility of the analyses. The use of high-efficiency reversed-phase columns assures high selectivity and minimum band broadening.

The introduction of an aromatic highly fluorescent ring into the amino acid molecule not only lowers the solute detection limit, but also improves the system selectivity by increasing the dispersion forces between the solute and the hydrophobic stationary phase. The minimum solute detectability for amino acids could be improved even further by exciting the OPA-amino acid adducts at 230 nm[13]. Future improvement in the total amino acid analysis may come from the development of a detection system or a fluorogenic reagent which can achieve very high sensitivity for both primary and secondary amines.

ACKNOWLEDGEMENTS

We acknowledge the help of Drs. J. Boehlert, F. Bogdansky, and S. Moros of Hoffmann-La Roche, Quality Control Department, Nutley, NJ, U.S.A., for reviewing the manuscript and for many useful comments. Thanks are also due to Dr. B. N. Jones and Dr. S. Stein of the Institute of Molecular Biology, Hoffmann-La Roche, Nutley, NJ, U.S.A., for many valuable discussions.

REFERENCES

1 B. N. Jones, A. S. Stern, R. V. Lewis, S. Kimura, S. Stein, S. Udenfriend and J. E. Shively, *Arch. Biochem. Biophys.*, 204 (1980) 392.
2 W. W. Bromer, L. G. Sinn and O. K. Brehrens, *J. Amer. Chem.Soc.*, 79 (1957) 2807.
3 A. M. Felix and M. Jimenez, *Anal. Biochem.*, 52 (1973) 377.
4 D. H. Spackman, S. Moore and W. H. Stein, *Anal. Chem.*, 30 (1958) 1190.

5 P. B. Hamilton and R. A. Anderson, *Anal. Chem.*, 31 (1959) 1504.
6 A. M. Felix and G. Terkelsen, *Arch. Biochem. Biophys.*, 157 (1973) 177.
7 G. J. Schmidt, D. C. Olson and W. Slavin, *J. Liquid Chromatogr.*, 2 (1979) 1031.
8 M. Weigele, S. L. DeBernardo, J. P. Tengi and W. Leimgruber, *J. Amer. Chem. Soc.*, 94 (1972) 5927.
9 E. L. Johnson, *Fluorescence and Liquid Chromatography*, Varian Aerograph, Walnut Creek, CA, 1977.
10 J. M. Wilkinson, *J. Chromatogr. Sci.*, 16 (1978) 547.
11 C. L. Zimmerman, E. Apella and J. J. Pisano, *Anal. Biochem.*, 77 (1977) 569.
12 N. D. Johnson, M. W. Hunkapiller and L. E. Hood, *Anal. Biochem.*, 100 (1979) 335.
13 D. W. Hill, F. H. Walters, T. D. Wilson and J. D. Stuart, *Anal. Chem.*, 51 (1979) 1338.
14 J. P. H. Burbach, A. Prins, J. L. M. Lebouille, C. J. Verhoef and A. Witter, *J. Chromatogr.*, in press.
15 B. R. Larsen and F. G. West, *J. Chromatogr. Sci.*, 19 (1981) 259.
16 B. N. Jones, S. Päabo and S. Stein, *J. Liquid Chromatogr.*, 4 (1981) 565.
17 W. S. Gardner and W. H. Miller, *Anal. Biochem.*, 101 (1980) 61.
18 M. Ahnoff, I. Grundevik, A. Arfwidsson, J. Fonsellus and B. A. Persson, *Anal. Chem.*, 53 (1980) 485.
19 G. J. Krol, M. Banovsky, C. A. Mannan, R. E. Pickering and B. T. Kho, *J. Chromatogr.*, 163 (1979) 383.
20 M. Roth, *Clin. Chim. Acta*, 83 (1978) 273.
21 J. Pouchly and I. Vavruch, *Physical Chemistry of Colloidal Systems*, SNTL, Prague, 1959, p. 300.

Journal of Chromatography, 239 (1982) 475–482
Elsevier Scientific Publishing Company, Amsterdam — Printed in The Netherlands

CHROM. 14,673

A SIMPLE HIGH-PERFORMANCE LIQUID CHROMATOGRAPHIC PRE-COLUMN TECHNIQUE FOR INVESTIGATION OF DRUG METABOLISM IN BIOLOGICAL FLUIDS*

WOLFGANG VOELTER and THOMAS KRONBACH*
Abteilung für Organische und Physikalische Biochemie des Physiologisch-chemischen Instituts der Universität Tübingen, Hoppe-Seyler-Strasse 1, D-7400 Tübingen (G.F.R.)
and
KARL ZECH and REINHARD HUBER
Byk Gulden Lomberg, Chemische Fabrik GmbH, Byk Guldenstrasse 2, D-7750 Konstanz (G.F.R.)

SUMMARY

A simple reversed-phase high-performance liquid chromatographic pre-column technique for investigation of drug metabolism is described. This rapid method circumvents the "classical" sample purification via extraction by direct purification and enrichment of the sample on the pre-column. Almost 100% recovery of a drug (aminopyrine) and its metabolites from biological fluids is achieved. This is in strong contrast to "classical" sample preparation which allows a recovery of 30–100% depending on the polarity of the investigated compound. The procedure described has been successfully applied to the investigation of the metabolic pattern of aminopyrine in rat plasma and cell incubation media.

INTRODUCTION

For separation and isolation of drugs from biological fluids, high-performance liquid chromatography (HPLC) is often the method of choice because this technique can be applied to compounds of greatly different polarities as is often the case when comparing a drug with its metabolites[1–3]. Furthermore, semipreparative HPLC is one of the most efficient and rapid methods of isolating metabolites in amounts suitable for structure elucidation and pharmacological tests. A drug and its metabolites are often separable by reversed-phase HPLC, however, proteins (*e.g.*, from plasma, liquor or cell incubation media) and inorganic compounds have to be removed in time-consuming work-up procedures, which are the most inaccurate steps owing to the often unknown partition coefficients for all tested compounds. If these by-products are not removed, the lifetime of the column is dramatically reduced and overloading of the packing material with constituents of biological fluids causes a loss in column efficiency. In biological samples interesting compounds are often present at

* Part of the thesis of Th. Kronbach.

0021-9673/82/0000–0000/$02.75

low concentrations and may be accompanied by excessive amounts of high-molecular-weight material (*e.g.*, proteins) or salts. Therefore, both enrichment of investigated compounds and sample clean-up has to be carried out prior to analysis.

Pre-columns have been used for enrichment procedures[4–7] as well as for sample clean-up[8–11]. Recently a fully automated method was described for analysis of drugs in biological fluids using pre-columns for simultaneous sample clean-up and enrichment[12]. Unfortunately, this method requires expensive equipment such as an autosampler and time-controlled pneumatic column switching valves. Such a modified HPLC system is especially suitable for routine analysis.

In this communication a pre-column technique is described, which is accessible for manual injection, replacing the sample loop of a manual syringe-loading injector by a pre-column, filled with reversed-phase material. As mentioned above, "classical" sample pretreatment procedures often suffer from low recovery especially for polar compounds. Using the present method a mixture of a drug and its metabolites can be isolated and separated from biological fluids with almost 100% recovery.

EXPERIMENTAL

Apparatus

All separations were performed with a 1010B liquid chromatograph (Hewlett-Packard, Böblingen, G.F.R.) modified with a syringe-loading sample injector (Model 7125; Rheodyne, Berkely, CA, U.S.A.) at 40°C. The pre-column (50 × 4.6 mm I.D.; Dr. Knauer, West Berlin, G.F.R.) was dry filled with LiChroprep RP-8 (particle size 25–40 μm; E. Merck, Darmstadt, G.F.R.) and replaces the sample loop in the injection valve (see Fig. 1). The analytical column was prefilled with LiChrosorb RP-18 (particle size 5 μm, 250 × 4 mm I.D.; E. Merck). Detection was performed with a variable-wavelength detector (SpectroMonitor II; Laboratory Data Control, Riviera Beach, FL, U.S.A.) at 257 nm.

Reagents

Aminopyrine (DMAAP) and its metabolites MAAP, AAP, AcAAP and FAAP (see Table I) were supplied by Hoechst (Frankfurt/M, G.F.R.). All reagents were of research grade, except acetonitrile which was of chromatographic grade (Li-

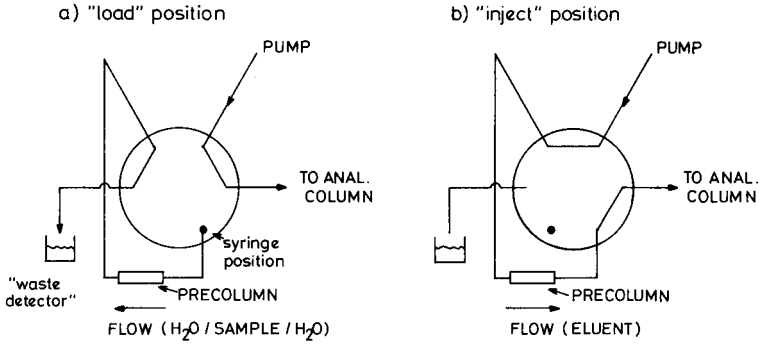

Fig. 1. Schematic flow diagram of the manual pre-column purification and enrichment system.

TABLE I

STRUCTURES AND ABBREVIATIONS OF AMINOPYRINE, SOME MAJOR METABOLITES AND THE INTERNAL STANDARD

Formula	*Abbreviation*	*Name*
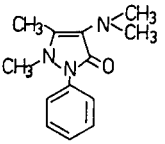	DMAAP	1-Aminopyrine (4-dimethylaminoantipyrine)
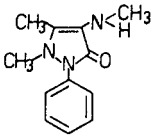	MAAP	Methylaminoantipyrine
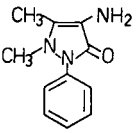	AAP	Aminoantipyrine
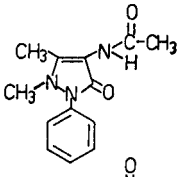	AcAAP	Acetylaminoantipyrine
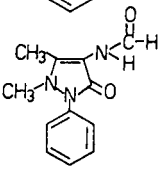	FAAP	Formylaminoantipyrine
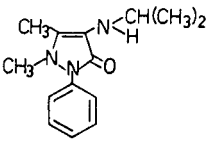	i-pAAP	Isopropylaminoantipyrine (internal standard)

Chrosolv, E. Merck) and water which was triply distilled before use. Recovery from serum was carried out with standardized serum (Biotest, Frankfurt/M, G.F.R.).

Pre-column purification and concentration

The pre-column was purged in the "load" position of the injection valve with 1 ml of water (see Fig. 1a). Then, depending on the desired enrichment factor, 50–1000 µl of sample were loaded on the pre-column and highly hydrophilic substances (*e.g.*,

salts and proteins) were washed out with another ml of water. The waste line leads to a beaker containing water–acetonitrile (50:50), to detect the proteins ("waste detector").

The sample was injected by backflushing it with the chromatographic eluent to the analytical column (see Fig. 1b), and the pre-column remains in the "inject" position until analysis is completed.

Extraction

To compare the results of pre-column sample preparation with "conventional" prepared samples, 2 ml of serum spiked with aminopyrine, its metabolites MAAP, AAP, AcAAP, FAAP and i-pAAP as internal standard were diluted with 1 ml of water, and extracted three times with 1 ml of dichloromethane–2-propanol (95:5). The extracts were dried with anhydrous sodium sulphate, filtered and the sodium sulphate was washed twice with 1.5 ml dichloromethane–2-propanol solution. The combined extracts were evaporated to dryness (rotary evaporator), the residue was dissolved in 200 μl of water and an aliquot of 50 μl was injected for analysis.

Preparation of isolated hepatocytes

The preparation technique is mainly in accordance with the method of Berry and Friend[13] as modified by Siess *et al.*[14]. Viability was checked by trypan blue exclusion 30 min after incubation.

RESULTS AND DISCUSSION

The metabolism of aminopyrine has been the subject of extensive studies (*e.g.*, refs. 15–26), however the problem of quantitative recovery of the metabolites is still not solved. Because the metabolism of drugs in isolated hepatocytes is often highly correlated with "*in vivo*" metabolism[27–29], an HPLC method was developed for separation and quantification of aminopyrine and its metabolites in biological fluids, *i.e.*, blood plasma and cell incubation media.

Aminopyrine and its major metabolites are separable from aqueous standard solutions by reversed-phase gradient elution. Therefore, we applied the pre-column technique to detect these substances in plasma and cell incubation media. Sample concentration and purification are carried out simultaneously on the pre-column. It still remains to determine whether the preconcentration is affected by polar contaminants (like salts or proteins). Drugs are also often bound to serum proteins and therefor the serum protein binding could influence their adsorption in the reversed-phase material.

The recovery of aminopyrine and its major metabolites was determined from aqueous standard solutions first, using the pre-column for concentration of the sample prior to analysis. The results are collected in Table II and the values demonstrate that the recovery of all substances is almost 100%.

The serum was spiked with the identical compounds as in the preceding experiment and due to higher background interference only a slightly lower correlation coefficient is observed. Fig. 2 shows a typical chromatogram and Fig. 4 the calibration curve for DMAAP and FAAP recovery from serum which is in the region of 100% (*cf.*, Table II). This demonstrates unequivocally that binding to the non-polar

TABLE II

REGRESSION DATA FOR THE RECOVERY OF AMINOPYRINE AND ITS METABOLITES (n = 4)

Substance	*Slope*	*Intercept*	*Correlation coefficient*
(a) From water (using pre-column sample concentration)			
DMAAP	0.9502	0.2193	0.9999
MAAP	0.9753	−0.0326	0.9995
AAP	0.9897	−0.0781	0.9988
AcAAP	0.9784	−0.0769	0.9999
FAAP	0.9176	0.7148	0.9997
(b) From spiked serum (using pre-column sample purification and concentration)			
DMAAP	0.9737	0.0813	0.9999
MAAP	0.9747	−0.2151	0.9999
AAP	0.9725	0.2608	0.9947
AcAAP	0.9872	−0.1605	0.9986
FAAP	0.9501	0.4183	0.9995
(c) From spiked serum (using "classical" extraction and direct injection)			
DMAAP	0.9865	0.4423	0.9993
MAAP	0.9962	−0.3843	0.9999
AAP	0.9763	−0.2582	0.9999
AcAAP	0.4022	0.3384	0.9952
FAAP	0.3280	0.5587	0.9969

reversed-phase material, even for the most polar compounds, is stronger than binding to the serum proteins.

One-day reproducibility of pre-column serum measurements is better than 5% in the examined concentration range (DMAAP, 1.45 ± 0.71%; MAAP, 2.55 ±

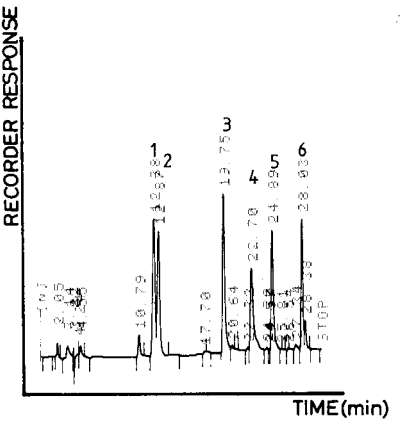

Fig. 2. Typical chromatogram of a spiked control serum sample with one-step sample purification and pre-concentration on the pre-column. Mobile phase: A, 20 mM sodium dihydrogenphosphate in water (pH 8.0, NaOH); B, acetonitrile; gradient from 0 to 8 min isocratic at 13% B, 8 to 30 min from 13 to 43% B (linear). Peaks: 1 = FAAP, 2.58 mg/l; 2 = AcAAP, 2.30 mg/l; 3 = AAP, 2.24 mg/l; 4 = MAAP, 2.16 mg/l; 5 = DMAAP, 2.22 mg/l; 6 = i-pAAP (internal standard). 1 ml water/400 µl sample/2 ml water injected subsequently on the pre-column.

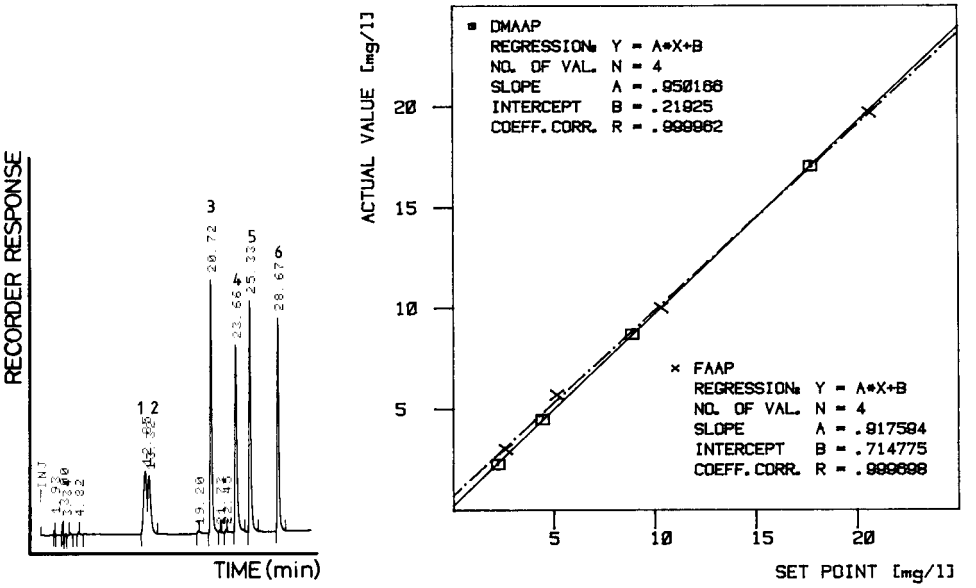

Fig. 3. Analysis of a spiked serum sample with "classical" work-up procedure and analysis by direct injection of 50 μl of extract. For experimental conditions and peak identification see Fig. 2.

Fig. 4. Calibration curves for the recovery of DMAAP and FAAP from spiked serum with pre-column sample purification and enrichment. The regression data for other investigated compounds are collected in Table II.

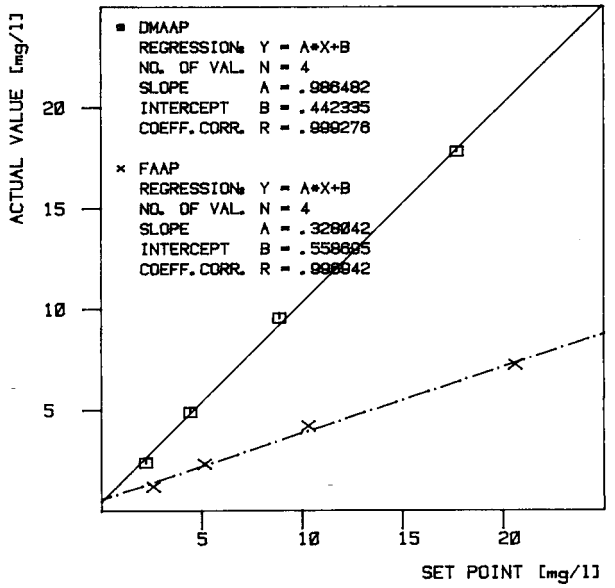

Fig. 5. Calibration curves for the recovery of DMAAP and FAAP of spiked serum obtained by "classical" sample work-up and enrichment. For regression data of other investigated compounds see Table II.

2.01%; AAP, 2.48 ± 2.49%; AcAAP, 1.38 ± 1.51%; FAAP, 2.01 ± 1.37%; $n = 12$ for each compound). Recoveries obtained with different pre-columns show no significant differences (day-to-day reproducibility). If "classical" sample preparation via extraction is used, a remarkable loss of the more polar metabolites occurs (Figs. 3 and 5) due to the change in partition coefficients. Therefore the recovery values for a drug and its metabolites obtained by the "classical" sample pretreatment procedure are often doubtful.

Because pre-column sample pre-treatment is confined to injection steps (*cf.*, water/sample/water) which are carried out during equilibration of the analytical column, no time is wasted on sample preparation. Using the classical procedure, however, the time for sample pre-treatment is as long as the analysis time in this case (about 30 min).

Consequently we used this one-step sample purification and enrichment procedure for the determination of the metabolic pattern of aminopyrine in rat plasma and isolated hepatocytes from rats and mice. Figs. 6 and 7 show typical chromatograms which demonstrate that reversed-phase HPLC combined with pre-column sample work-up is a powerful method for solving complex problems in biotransformation.

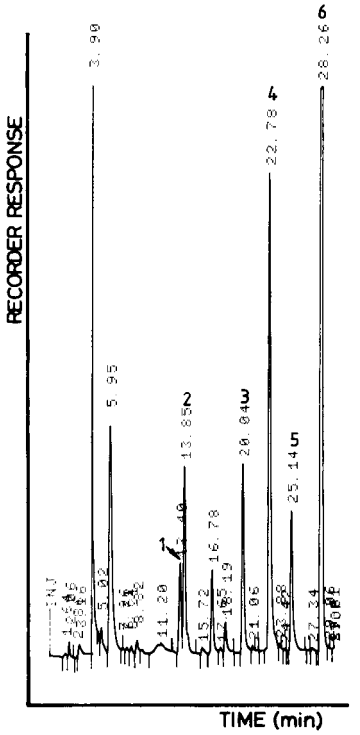

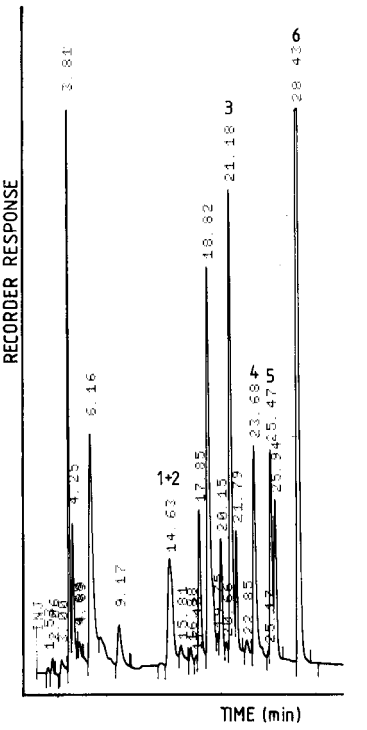

Fig. 6. Analysis of a rat plasma sample 2 h after oral administration of 20 mg/kg with the pre-column technique. Injection volume: 600 μl. For experimental conditions and peak identification see Fig. 2.

Fig. 7. Analysis of the supernatant of a 0.1 mM aminopyrine incubation of isolated rat hepatocytes after 40 min. For experimental conditions and peak identification see Fig. 2. 800 μl were purified and concentrated on the pre-column.

The difficulties of "classical" sample preparation can be easily circumvented by rapid modification of the chromatograph (replacement of the sample loop by the pre-column) and application of the pre-column sample pre-treatment method. The method is especially suitable for the analysis of drugs and metabolites in biological fluids as high recovery is obtained over a wide range of polarity.

ACKNOWLEDGEMENT

This work was supported by the Herbert Quandt Stiftung, Bad Homburg, G.F.R.

REFERENCES

1 K. Wessely and K. Zech, *High Performance Liquid Chromatography in Pharmaceutical Analyses*, Hewlett-Packard, Böblingen, 1979.
2 W. Voelter, K. Zech, P. Arnold and G. Ludwig, *J. Chromatogr.*, 199 (1980) 345–354.
3 A. Pryde and M. T. Gilbert, *Applications of High Performance Liquid Chromatography*, Chapman and Hall, London, 1979.
4 J. Lankelma and H. Poppe, *J. Chromatogr.*, 149 (1978) 587–598.
5 D. D. Koch and P. T. Kissinger, *Anal. Chem.*, 52 (1980) 27–29.
6 H. P. M. van Vliet, Th. C. Bootsman, R. W. Frei and U. A. Th. Brinkman, *J. Chromatogr.*, 185 (1979) 483–495.
7 F. Erni and R. W. Frei, *J. Chromatogr.*, 149 (1978) 561–569.
8 R. J. Dolphin, F. W. Willmott, A. D. Mills and L. P. J. Hoogeveen, *J. Chromatogr.*, 122 (1976) 259–268.
9 J. C. Gfeller and M. Stockmeyer, *J. Chromatogr.*, 198 (1980) 162–168.
10 F. F. Cantwell, *Anal. Chem.*, 48 (1976) 1854–1858.
11 G. J. de Jong, *J. Chromatogr.*, 183 (1980) 203–211.
12 W. Roth, K. Beschke, R. Jauch, A. Zimmer and F. W. Koss, *J. Chromatogr.*, 222 (1981) 13–22.
13 M. V. Berry and D. S. Friend, *J. Cell Biol.*, 43 (1969) 506–520.
14 E. A. Siess, D. G. Brocks and O. H. Wieland, *FEBS Lett.*, 69 (1976) 265.
15 B. B. Brodie and J. Axelrod, *J. Pharmacol. Exp. Ther.*, 99 (1950) 171–184.
16 B. N. La Du, L. Gaudette, N. Trousof and B. B. Brodie, *J. Biol. Chem.*, 214 (1955) 741–752.
17 F. Pechtold, *Arzneim.-Forsch.*, 14 (1964) 972–974.
18 H. Yoshimura, H. Shimeno and H. Tsakamoto, *Yakugaku Zasshi*, 90 (1970) 1406–1411.
19 E. Klug, *Arzneim.-Forsch.*, 20 (1970) 201–202.
20 B. Gradnik and L. Fleischmann, *Pharm. Acta Helv.*, 48 (1973) 144–150.
21 R. Gradnik and L. Fleischmann, *Pharm. Acta Helv.*, 48 (1973) 181–191.
22 T. Goromaru, A. Noda, K. Matsuyama and S. Iguchi, *Chem. Pharm. Bull.*, 24 (1976) 1376–1383.
23 A. Noda, N. Tsubone, M. Mihara, T. Goromaru and S. Iguchi, *Chem. Pharm. Bull.*, 24 (1976) 3229–3231.
24 D. J. Stewart and T. Inaba, *Biochem. Pharmacol.*, 28 (1979) 461–464.
25 K. Shimada and Y. Nagase, *J. Chromatogr.*, 181 (1980) 51–57.
26 A. Bast and J. Noordhoek, *J. Pharm. Pharmacol.*, 33 (1981) 14–18.
27 J. W. Bridges and L. F. Chasseaud (Editors), *Progress in Drug Metabolism*, Vol. 2, Wiley, London, New York, Sydney, Toronto, 1977, pp. 71–118.
28 R. E. Billings, R. E. McMahon, J. Ashmore and S. R. Wagle, *Drug Metab. Dispos.*, 5 (1977) 518–526.
29 Th. Kronbach, *Diplomarbeit*, Universität Tübingen, 1980.

Journal of Chromatography, 239 (1982) 483–492
Elsevier Scientific Publishing Company, Amsterdam — Printed in The Netherlands

CHROM. 14,592

PREDICTION OF MOLECULAR STRUCTURES OF THIOLS AND SULPHIDES BY RETENTION INDICES

FUJIO MORISHITA, HIROYUKI MURAKITA, YOSHIYUKI TAKEMURA and TSUGIO KOJIMA*

Department of Industrial Chemistry, Faculty of Engineering, Kyoto University, Kyoto (Japan)

SUMMARY

A method is discussed, in which the presence of thiols and sulphides is confirmed by combination of a post-column reaction and flame photometric detection. The molecular structures are determined by comparing the calculated and the observed retention indices. The retention indices of these compounds can be given in terms of the increment due to a mercapto group or a thio group and the correction values for the shielding effect of these groups by neighbouring carbon atoms.

INTRODUCTION

Recent advances in high-resolution capillary gas chromatography have made it possible to separate peaks whose retention values lie close together, thus increasing the amount of information which retention values can supply. The retention index (I) defined by Kováts[1] has a linear relationship with the free energy of solution and may be closely related to the molecular structure of the solute. It has been shown that the retention indices for several types of compounds can be accurately calculated from their molecular structures. It is, however, difficult to predict the molecular structure of compound by comparison of observed and calculated retention indices, without prior information on the type of compound or elements contained within it. In other words, if information is obtained about the unknown compound by means of a selective detector or by reaction gas chromatography, the retention index will become more useful for identification purposes. Sulphur-containing compounds are readily detected by a flame photometric detector without serious interference from coexistent substances. Furthermore, selective reactions of particular functional groups would afford information on the functional group to which the sulphur atom belongs. Fujii[2] utilized fractional extraction of sulphur-containing compounds in gasoline by silver nitrate and mercuric cyanide. Several earlier investigators[3–5] have discussed the retention index of sulphur-containing compounds. Golovnya and Garbuzov[5] have described the similarities observed in the retention behaviour of sulphur- and oxygen-containing compounds and have presented equations for estimating the retention index of the former from the latter.

In this paper, a method is reported by which (i) the presence of aliphatic thiols

0021-9673/82/0000–0000/$02.75

and sulphides is confirmed by using a combination of a post-column reaction [with silver nitrate or mercury(II) chloride] and flame photometric detection and (ii) the molecular structures are determined by comparing the calculated and the observed retention indices.

EXPERIMENTAL

The gas chromatographic separations were carried out on a Shimadzu 6A gas chromatograph equipped with a flame-ionization detector (FID) and a flame photometric detector (FPD). Three open-tubular columns were prepared. Pyrex glass capillary tubes (0.25 mm I.D.), drawn with a Shimadzu GDM-1B glass-drawing machine and on the inner wall of which was formed a layer of fine particles of barium carbonate[6], were coated with polyethylene glycol 20M (50 m length) and silicone oil DC 550 (70 m) by a dynamic technique. Glass capillary tubes of the same inner diameter were coated with silver nitrate or mercuric chloride together with polyethylene glycol 600 by a dynamic technique and were used as post-column reactors. When used for differentiation of compound types, these reactors were connected to the outlet of a separation column by a piece of thermally shrinkable PTFE and placed in the column bath. The chromatographic conditions were as follows: carrier gas, nitrogen, 1.0 ml/min; splitting ratio, 1:90; make-up gas, nitrogen, 50 ml/min; column temperature, 80°C (polyethylene glycol 20M), 70°C (silicone oil DC 550); temperatures of injection port and detector, 120 and 130°C, respectively; flow-rates of other gases, hydrogen 50 ml/min (FID) and 40 ml/min (FPD), air, 850 ml/min (FID) and 40 ml/min (FPD).

Some of the thiols and sulphides were purchased from Tokyo Chemical Industry Co. (Tokyo, Japan) and Wako (Osaka, Japan). Other thiols were prepared from the corresponding alkyl bromides and sodium hydrosulphide[7] and other sulphides were prepared from alkyl bromides and methanethiol[8] or by addition of thiols to alkenes[9]. Products were identified by their mass spectra, obtained with a Hitachi RM-50 GC gas chromatograph–mass spectrometer. Identification was also supported by the results obtained with the above-mentioned reactor.

RESULTS AND DISCUSSION

Confirmation of the presence of aliphatic thiols and sulphides by use of a combination of post-column reaction and flame photometric detection

Fig. 1 shows chromatograms obtained by use of different detection systems. Chromatograms (a) and (b) are recorded by FID and FPD, respectively. In this case, the eluted substances from the column were injected directly into the detector. Chromatograms (c), (d) and (e) were recorded by FPD after the eluted substances had been forced through 3.4 and 35 cm of silver nitrate-coated and 2 cm of mercury(II) chloride-coated reactors, respectively. All reactors captured the thiols completely and no peaks ascribed to them were obtained. Thiols are converted into non-volatile metal mercaptides within the reactors. The peaks due to aliphatic sulphides are shifted by the silver nitrate, possibly because of formation of a sulphide complex with this salt. The shorter silver nitrate reactor had little influence on the retention values of sulphides but the longer one retained these and gave broadened peaks. Thus, the silver

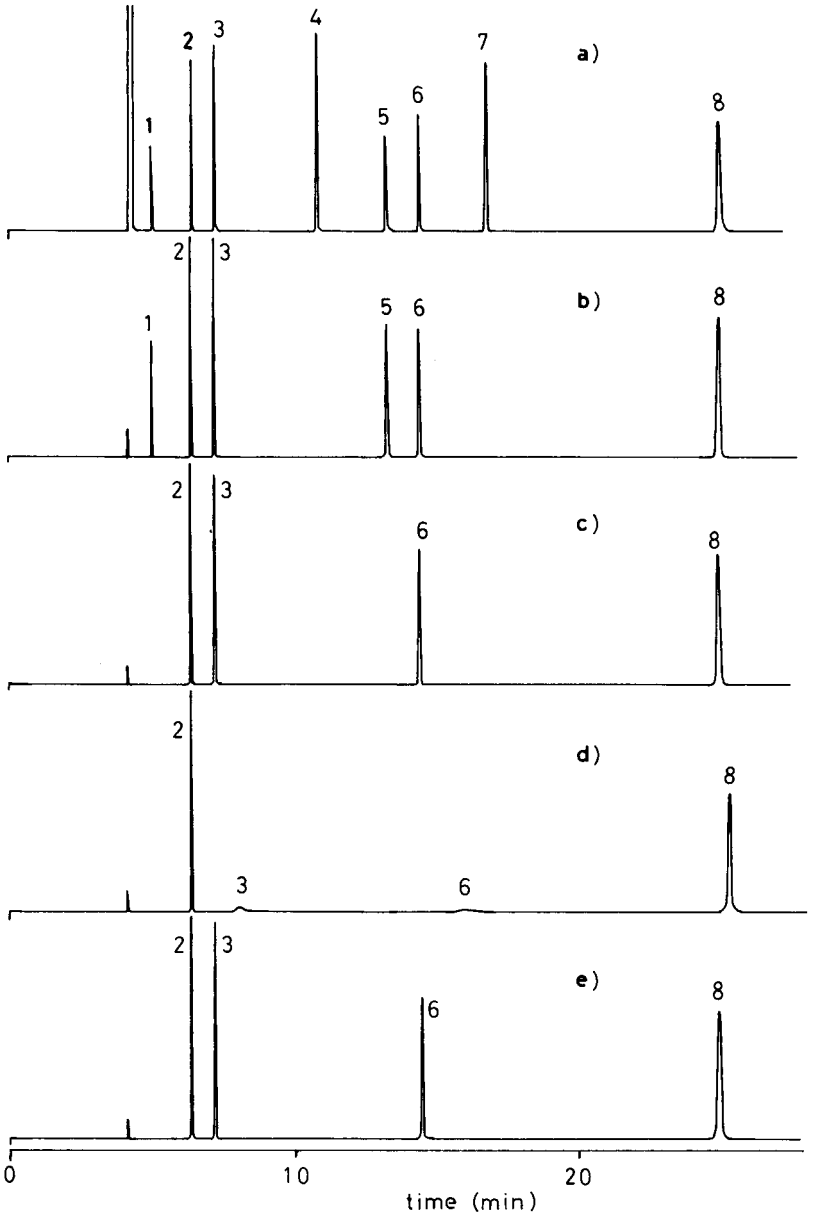

Fig. 1. Gas chromatograms obtained with different systems. (a), FID; (b) FPD; (c), post-column reactor ($AgNO_3$–PEG 600, 3.4 cm) + FPD; (d), post-column reactor ($AgNO_3$–PEG 600, 35 cm) + FPD; (e), post-column reactor ($HgCl_2$–PEG 600, 2.0 cm) + FPD. Stationary phase: polyethylene glycol 20M, 80°C. Peaks: 1 = 2-methyl-2-butanethiol; 2 = thiophene; 3 = dipropyl sulfide; 4 = *n*-dodecane; 5 = 1-heptanethiol; 6 = dibutyl sulfide; 7 = *n*-tridecane; 8 = dipropyl disulfide.

nitrate reactor may be useful for the confirmation of not only thiols but also sulfides. A longer mercury(II) chloride reactor (*ca.* 100 cm) does not retain sulfides. This reactor is useful as a thiol-specific subtractor.

Prediction of retention indices of aliphatic thiols

Table I shows the retention indices of straight-chain thiols. I^{PEG} and I^{DC550} indicate the indices on polyethylene glycol 20M and silicone oil DC 550, respectively, ΔI being the difference between them. As shown in Table I, not all the increments of I corresponding to insertion of a methylene group in a homologous series are equal to 100. The retention index is apparently affected by the length of the alkyl chain, which possibly reflects that alkyl chains hinder a mercapto group from coming close to the polar site of the solvent molecule in the stationary phase. Thus the retention index of a thiol can be represented as the sum of the increment for a mercapto group, the correction values for the shielding effect by alkyl chains and 100 × the carbon number, similar to that for a haloalkane[10]. As an example, the I value of 4-heptanethiol may be represented by the following equation:

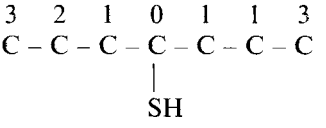

$$I\text{(4-heptanethiol)} = 700 + \delta I_{-SH} + A_0 + 2\sum_{i=1}^{3} A_i \qquad (1)$$

where δI_{-SH} is the increment of I for a mercapto group and A_i is the correction value for the shielding effect by each carbon atom; the sum of A_i therefore means the shielding effect of an alkyl chain. For all the other thiols, the additive structural

TABLE I

RETENTION INDICES OF STRAIGHT-CHAIN THIOLS ON POLYETHYLENE GLYCOL 20M AND SILICONE OIL DC 550

I^{PEG} = retention index on polyethylene glycol 20M at 80°C, I^{DC550} = retention index on silicone oil DC550 at 70°C, $\Delta I = I^{PEG} - I^{DC550}$, D_1: $I^{PEG}_{calcd.} - I^{PEG}_{obsd.}$, D_2: $\Delta I_{calcd.} - \Delta I_{obsd.}$

	Observed			*Calculated*			
Compound	I^{PEG}	I^{DC550}	ΔI	I^{PEG}	D_1	ΔI	D_2
$1C_5SH$*	1047.9	866.1	181.8	1048.1	+0.2	181.1	−0.7
$1C_6SH$	1148.0	967.2	180.8	1147.8	−0.2	181.5	+0.7
$1C_7SH$	1248.7	1068.7	180.0	1248.7	0.0	180.0	0.0
$2C_5SH$	964.9	806.3	158.6	962.8	−2.1	155.6	−3.0
$2C_6SH$	1062.1	907.8	154.3	1060.4	−1.7	154.4	+0.1
$2C_7SH$	1160.0	1004.4	155.6	1160.2	+0.2	154.9	−0.7
$3C_5SH$	973.9	815.5	158.4	971.7	−2.2	155.8	−2.6
$3C_6SH$	1058.0	906.0	152.0	1057.1	−0.9	152.5	+0.5
$3C_7SH$	1153.2	1002.5	150.7	1154.8	+1.6	151.4	+0.7
$4C_7SH$	1140.9	993.0	147.9	1142.5	+1.6	149.2	+1.3

* For example, $1C_5SH$ indicates 1-pentanethiol.

TABLE II

INCREMENTS OF I AND ΔI FOR A MERCAPTO GROUP [δI_{-SH}, $\delta(\Delta I)_{-SH}$] AND THE CORRECTION VALUES FOR HINDRANCE BY METHYLENES (A_i)

$\delta I'_{-SH} = \delta I_{-SH} + A_0$ (I), $\delta I'_{-SH} = \delta(\Delta I)_{-SH} + A_0$ (ΔI), $\delta I'_{-SH}$ (PEG 20M) = 658.3, $\delta I'_{-SH}$ (DC 550) = 443.1, $\delta(\Delta I')_{-SH}$ = 215.2.

Parameter	*i* = 1	2	3	4	5	6
A_i (PEG 20M)	−87.7	−5.6	−14.6	−2.3	−0.2	+0.5
A_i (DC550)	−61.0	−2.6	−11.3	−1.2	−0.7	+2.4
(ΔI)	−26.7	−3.0	− 3.3	−1.1	+0.5	−1.5

influence can be represented by a similar formula. The increments and the correction values were determined by the least-squares method from the observed I values and the above relationships. The values assigned are shown in Table II. As δI_{-SH} and the correction value for the carbon atom bonded to the mercapto group (A_0) cannot be determined independently, the syum of them ($\delta I'_{-SH}$) is given in Table II. In Table I, the calculated I and ΔI values are compared with the corresponding observed values.

Table III shows the retention indices of branched-chain thiols on silicone oil DC 550. The I values of these compounds cannot be predicted by using only the increment and the correction values in Table II; the effect of methyl branching must additionally be evaluated. This may be divided into two terms. (i) one is the contribution of methyl branching itself. This can be evaluated from the I value of the corresponding branched-chain alkane. It can be calculated as above by regarding a methyl branching as a functional group. Table IV shows the increment (δI_{Me}) for a methyl branching and the correction values (B_i) for the steric situation around it. As δI_{Me}, B_0 and B_1 cannot be determined independently, the sum of them is given in Table IV; $\delta I'_{Me} = \delta I_{Me} + B_0 + 2B_1$. They were determined as follows; first, a linear plot was obtained between the observed I values on silicone oil DC 550 and the published I values on squalane[11]. Secondly, I^{DC550} values for many branched-chain alkanes were evaluated from this plot. Finally, the values in Table IV were determined by expressing the structure of methyl-branched alkanes in the same way as that of linear thiols and by applying the least-squares method to the evaluated I^{DC550} values. (ii) The other term is the effect due to the positional relationship between methyl branching and a mercapto group. The calculated I^{DC550} values are shown in Table III and are obtained by taking into account only the individual contributions of a methyl branching and a mercapto group. The difference between the observed and the calculated values seems to correspond to the increment based on the positional relationship.

Prediction of retention indices of aliphatic sulphides

Table V shows the retention indices of straight-chain sulphides. The retention index of a sulphide can be represented as being based on incremental structural contributions. For example, the I value of propyl butyl sulphide is represented as follows:

$$\overset{3}{C}-\overset{2}{C}-\overset{1}{C}-S-\overset{1}{C}-\overset{2}{C}-\overset{3}{C}-\overset{4}{C}$$

$$I(C_3SC_4) = \delta I_{-S-} + \sum_{i=1}^{3} C_i + \sum_{i=1}^{4} C_i + 700 \qquad (2)$$

TABLE III

RETENTION INDICES OF BRANCHED-CHAIN THIOLS ON SILICONE OIL DC 550 AT 70°C

D: $I^{DC550}_{obsd.} - I^{DC550}_{calcd.}$

Compound	$I^{DC550}_{obsd.}$	$I^{DC550}_{calcd.}$	D
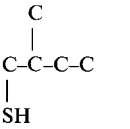	836.9	849.7	−12.8
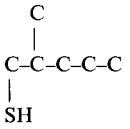	928.0	938.3	−10.3
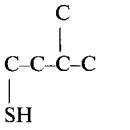	829.7	849.7	−20.0
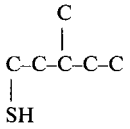	937.2	954.0	−16.8
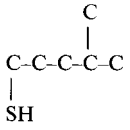	930.4	938.3	− 7.9
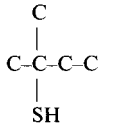	753.9	800.0	−46.1
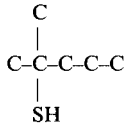	838.9	878.5	−39.6
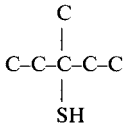	873.1	902.9	−29.8
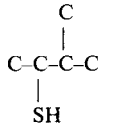	811.6	800.0	+11.6
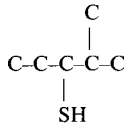	893.0	887.2	+ 5.8
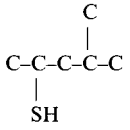	859.6	878.5	−18.9

TABLE IV

INCREMENT OF I^{DC550} FOR A METHYL BRANCHING (δI_{Me}) AND CORRECTION VALUES FOR ITS STERIC SITUATION

$\delta I'_{Me} = \delta I_{Me} + B_0 + 2B_1{}^{\star} = 76.0.$

Parameter	*i* = 2	3	4	5	6
B_i	+5.5	−10.2	−4.5	−2.6	−0.7

★ $\ldots B_2\ B_1\ B_0\ B_1\ B_2\ B_3 \ldots$
…–C–C–C–C–C–C–…
|
CH_3

where δI_{-S-} and C_i are the increment for a thiol group and the correction value for the shielding effect by each carbon atom, respectively. The values assigned to them are shown in Table VI. As δI_{-S-} and C_1 cannot be determined independently, the sum of them is given in Table VI; $\delta I'_{-S-} = \delta I_{-S-} + 2C_1$. The calculated I values are compared with the observed values in Table V. The good agreement between them indicate that the deviation from the regularities in I shown in Table VI is small. The retention index of branched-chain sulphides may be represented in the same way as that of branched-

TABLE V

RETENTION INDICES OF STRAIGHT-CHAIN SULPHIDES ON POLYETHYLENE GLYCOL 20M AND SILICONE OIL DC 550

Symbols as in Table I.

	Observed			*Calculated*			
Compound	I^{PEG}	I^{DC550}	ΔI	I^{PEG}	D_1	ΔI	D_2
C_4SC_1★	1029.3	860.8	168.5	1031.5	+2.2	167.9	−0.6
C_5SC_1	1128.1	963.0	165.1	1128.0	−0.1	165.0	−0.1
C_6SC_1	1227.0	1064.5	162.5	1226.1	−0.9	163.0	+0.5
C_7SC_1	1326.8	1164.9	161.9	1325.4	−1.4	162.0	+0.1
C_8SC_1	1426.3	1265.0	161.3	1426.3	0.0	161.3	0.0
C_9SC_1	1525.7	1364.9	160.8	1525.7	0.0	160.8	0.0
C_4SC_2	1091.1	939.7	151.4	1091.6	+0.5	151.7	+0.3
C_5SC_2	1188.6	1040.2	148.4	1188.1	−0.5	148.8	+0.4
C_6SC_2	1286.6	1139.2	147.4	1286.2	−0.4	146.8	−0.6
C_7SC_2	1385.3	1239.2	146.1	1385.5	+0.2	145.8	−0.3
C_3SC_3	1080.5	933.4	147.1	1080.6	+0.1	147.0	−0.1
C_4SC_3	1173.3	1031.2	142.1	1172.4	−0.9	142.6	+0.5
C_5SC_3	1269.7	1130.2	139.5	1268.9	−0.8	139.7	+0.2
C_6SC_3	1367.0	1228.9	138.1	1367.0	0.0	137.7	−0.4
C_7SC_3	1465.2	1328.6	136.6	1466.3	+1.1	136.7	+0.1
C_4SC_4	1265.6	1127.0	138.6	1264.2	−1.4	138.4	−0.2
C_5SC_4	1361.3	1225.6	135.7	1360.7	−0.6	135.5	−0.2
C_6SC_4	1457.8	1324.5	133.3	1458.8	+1.0	133.6	+0.3
C_5SC_5	1456.3	1323.5	132.8	1457.2	+0.9	132.6	−0.2

★ For example, C_4SC_1 indicates methyl butyl sulphide.

TABLE VI

INCREMENTS OF I AND ΔI FOR A THIO GROUP [δI_{-S-}, $\delta(\Delta I)_{-S-}$] AND CORRECTION VALUES FOR HINDRANCE BY METHYLENES (C_i)

$\delta I'_{-S-} = \delta I_{-S-} + 2C_1$ (I)*, $\delta(\Delta I)'_{-S-} = \delta(\Delta I)_{-S-} + 2C_1$ (ΔI), $\delta I'_{-S-}$ (PEG 20M) = 598.8, $\delta I'_{-S-}$ (DC 550) = 401.4, $\delta(\Delta I)'_{-S-}$ = 197.4.

Parameter	*i* = 2	3	4	5	6	7	8	9
C_i (PEG 20M)	−39.9	−19.2	−8.2	−3.5	−1.9	−0.7	+0.9	−0.6
C_i (DC 550)	−23.7	−10.1	−4.0	−0.6	+0.1	+0.3	+1.6	−0.1
(ΔI)	−16.2	− 9.1	−4.2	−2.9	−2.0	−1.0	−0.7	−0.5

* ...C_2 C_1 C_1 C_2 C_3...
...–C–C–S–C–C–C–...

TABLE VII

RETENTION INDICES OF BRANCHED-CHAIN SULPHIDES ON SILICONE OIL DC 550 AT 70°C

$D = I^{DC550}_{obsd.} - I^{DC550}_{calcd.}$

Compound	$I^{DC550}_{obsd.}$	$I^{DC550}_{calcd.}$	*D*
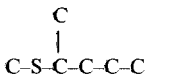	912.9	940.4	−27.5
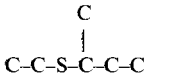	892.9	920.7	−27.8
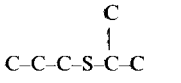	883.4	910.7	−27.3
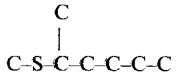	1009.8	1035.3	−25.5
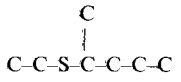	981.0	1006.5	−25.5
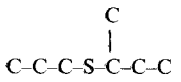	980.6	1006.1	−25.5
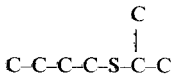	980.6	1004.1	−23.5
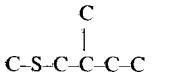	921.8	940.4	−18.6

TABLE VII *(continued)*

Compound	$I^{DC550}_{obsd.}$	$I^{DC550}_{calcd.}$	*D*
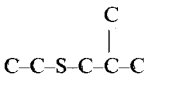	893.6	910.7	−17.1
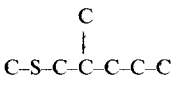	1013.5	1029.6	−16.1
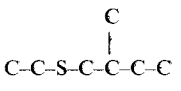	996.7	1012.2	−15.5
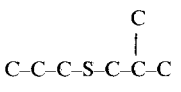	982.6	998.0	−15.4
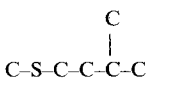	923.4	930.4	− 7.0
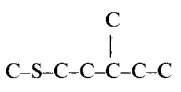	1030.7	1035.3	− 4.6
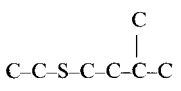	999.4	1004.1	− 4.7
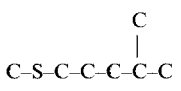	1023.7	1027.2	− 3.5

chain thiols, except that the contribution of methyl branching is evaluated from the *I* value of the branched-chain alkane whose carbon skeleton is depicted by substituting a methylene for the thio group of the original sulphide. Table VII shows the retention indices on silicone oil DC 550 for several branched-chain sulphides. The difference between the observed and the calculated values is considered to correspond to the increment based on the positional relationship between the thio group and the methyl branching, and seems to be determined by the distance between them.

CONCLUSION

The peaks due to aliphatic thiols and sulphides can be confirmed by combination of a silver nitrate or mercury(II) chloride reactor and an FPD. The retention indices of these compounds are represented in terms of the increment due to a mercapto group or a thio group and the correction values for the shielding effect of these groups by carbon atoms, and can be accurately predicted. It is suggested that the molecular structures of thiols or sulphides can be estimated by comparison of the observed *I* values with the values calculated for the expected structures.

REFERENCES

1 E. Kováts, *Helv. Chim. Acta*, 41 (1958) 1915.
2 T. Fujii, *Bunseki Kagaku (Jap. Anal)*., 25 (1976) 141.
3 V. Martinuů and J. Janák, *J. Chromatogr.*, 52 (1970) 69.
4 G. D. Gal'pern, N. T. Gollandskikh and G. N. Gordadze, *J. Chromatogr.*, 109 (1975) 119.
5 R. V. Golovnya and V. G. Garbuzov, *Chromatographia*, 8 (1975) 265.
6 K. Grob and G. Grob, *J. Chromatogr.*, 125 (1976) 471.
7 L. M. Ellis and E. E. Reid, *J. Amer. Chem. Soc.*, 54 (1932) 1674.
8 W. R. Kirner and G. H. Richter, *J. Amer. Chem. Soc.*, 51 (1929) 3135.
9 S. O. Jones and E. E. Reid, *J. Amer. Chem. Soc.*, 60 (1938) 2452.
10 F. Morishita, Y. Terashima and T. Kojima, *J. Chromatogr.*, submitted for publication.
11 R. A. Hivey and R. E. Hinton, *J. Gas Chromatogr.*, 6 (1968) 203.

Journal of Chromatography, 239 (1982) 493–498
Elsevier Scientific Publishing Company, Amsterdam — Printed in The Netherlands

CHROM. 14,627

GAS CHROMATOGRAPHIC DETERMINATION OF OPTICAL ISOMERS OF SOME CARBOXYLIC ACIDS AND AMINES WITH OPTICALLY ACTIVE STATIONARY PHASES

NAOBUMI ÔI*, TADASHI DOI, HAJIMU KITAHARA and YOKO INDA
Institute for Biological Science, Sumitomo Chemical Co., Ltd., 4-2-1 Takatsukasa, Takarazuka-shi, Hyogo-ken 665 (Japan)

SUMMARY

We recently developed some novel, optically active stationary phases (containing two asymmetric carbon atoms attached to both the nitrogen and carbon atoms of the amide group) for the gas chromatographic separation of carboxylic acid and amine enantiomers. We now report analytical methods for the determination of the optical isomers of some chiral carboxylic acids and amines with these phases. We found that (1) all four optical isomers of chrysanthemic acid [(+)-*cis*, (−)-*cis*, (+)-*trans* and (−)-*trans*] can be determined as the *tert.*-butylamide derivatives with N-(1*R*, 3*R*)-*trans*-chrysanthemoyl-(*R*)-1-(α-naphthyl)ethylamine, and (2) *R*- and *S*-isomers of 1-phenyl-2-(4-tolyl)ethylamine can be determined as the N-pentafluoropropionyl derivatives with N-lauroyl-(*S*)-proline)-(*S*)-1-(α-naphthyl)ethylamide.

INTRODUCTION

Gas chromatography is an important and convenient method for the determination of optical isomers. Generally the optical purity of enantiomeric compounds can be determined by forming derivatives with optically active reagents and analysing the resulting mixture of diasteroisomers with conventional achiral stationary phases[1]. However, in this method a standard reagent of known optical purity is required. If the optical purity of the derivative-forming reagent is less than 100%, a considerable error might be introduced in the analysis.

A more direct approach to the determination of the optical purity of a mixture of enantiomers is chromatography on optically active stationary phases, without prior conversion into diastereoisomers. This method has received considerable attention in recent years.

Many chiral phases have proved to be excellent for the separation of amino acid enantiomers since the first success by Gil-Av *et al.*[2], but they often showed lower separation factors for carboxylic acid and amine enantiomers Weinstein *et al.*[3] reported that it sufficed for a chiral stationary phase to contain an amide group and an asymmetric carbon atom, attached to the nitrogen atom [$RCONHCH(CH_3)R'$], in order to show selectivity in its interaction with the enantiomers of amides such as N-

0021-9673/82/0000–0000/$02.75

acyl amines and α-substituted carboxylic acid amides, and that the best efficiency is obtained when R′ is aromatic, particularly α-naphthyl as in N-lauroyl-(*S*)-1-(α-naphthyl)ethylamine. We prepared a *s*-triazine derivative of tripeptide ester[4] as a chiral stationary phase and accomplished the direct separation of various α-alkyl phenylacetic acid and aryl alkylamine enantiomers[5,6]. However, unfortunately, the chromatographic properties of these phases were insufficient to determine the optical purity of some chiral carboxylic acids and amines such as chrysanthemic acid and 1-phenyl-2-(4-tolyl)ethylamine.

Recently we have developed some novel amide stationary phases that contain two asymmetric carbon atoms attached to the nitrogen and carbon atoms of the amide group, respectively, and found that these phases have very excellent chromatographic properties[7,8]. In this paper, we report a method for determining the optical purity of chrysanthemic acid and 1-phenyl-2-(4-tolyl)ethylamine by gas chromatography with these novel amide stationary phases.

EXPERIMENTAL

Reagents

The optically active stationary phases, N-(1*R*,3*R*)-*trans*-chrysanthemoyl-(*R*)-1-(α-naphthyl)ethylamine[7] and N-lauroyl-(*S*)-proline (*S*)-1-(α-naphthyl)ethylamide[8], were synthesized as described previously. Optical isomers of chrysanthemic acid and 1-phenyl-2-(4-tolyl)ethylamine were prepared in our laboratory as reported by Murano[9,10]. All other reagents and solvents were of analytical- or laboratory-reagent grade.

Gas chromatography

The experiments were carried out with a Shimadzu GC-7A gas chromatograph equipped with a flame-ionization detector. The glass capillary columns were coated with an 8–10% solution of each stationary phase in chloroform.

Analytical methods

Chrysanthemic acid. To a solution of 25 mg of chrysanthemic acid in 1 ml of dry *n*-hexane, 0.25 ml of oxalyl chloride was slowly added with stirring, kept at room temperature for 30 min, then evaporated *in vacuo* at 50°C so as the remove the excess of oxalyl chloride. The residue was dissolved in a solution of *tert.*-butylamine (70 mg) in 2 ml of dry toluene. The mixture was kept at room temperature for 10 min, and acidified with 5 ml of 1 *N* hydrochloric acid. After stirring, the organic phase was dried over anhydrous sodium sulphate. A 2-μl volume of this solution was injected for gas chromatographic analysis.

The chromatographic conditions used were as follows: column, 40 m × 0.25 mm I.D. glass capillary coated with N-(1*R*,3*R*)-*trans*-chrysanthemoyl-(*R*)-1-(α-naphthyl) ethylamine; column temperature, 110°C; injector and detector temperature, 200°C; attenuation, 10 × 2; carrier gas, helium at a flow-rate of 1.0 ml/min; and splitting ratio, 1/80.

Each peak area was measured by a conventional trianguration method with approximate tangents on the chromatogram. The ratios of optical isomers were obtained from the ratios of the peak area of each isomer and the total peak area of four isomers.

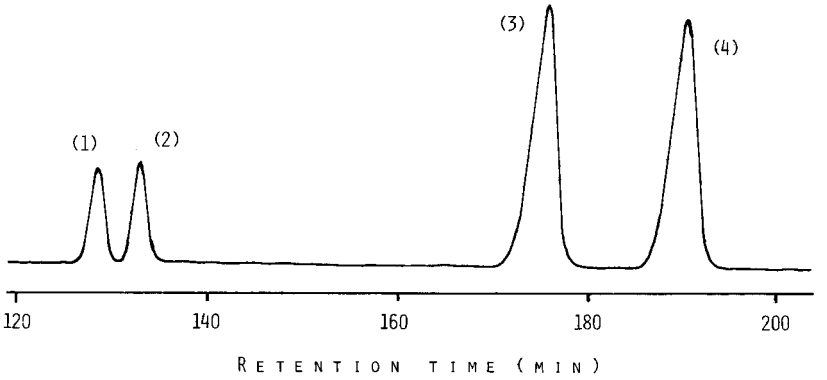

Fig. 1. Gas chromatogram of chrysanthemic acid *tert.*-butylamide. GC conditions as in Table I. (1) (−)-*cis*-isomer; (2) (+)-*cis*-isomer; (3) (+)-*trans*-isomer; (4) (−)-*trans*-isomer.

1-Phenyl-2-(4-tolyl)ethylamine. A mixture of 100 mg of 1-phenyl-2-(4-tolyl)ethylamine and 3 ml of a solution of 0.12 ml of pentafluoropropionyl anhydride in toluene containing 10% of ethyl acetate was kept at room temperature for 5 min, then 5 ml of water were added to decompose the excess of pentafluoropropionyl anhydride. The organic phase was dried over anhydrous sodium sulphate and 0.4 μl of this solution was injected for gas chromatographic analysis. The chromatographic conditions used were as follows: column, 30 m × 0.25 mm I.D. glass capillary coated with N-lauroyl-(*S*)-proline (*S*)-1-(α-naphthyl)ethylamide; column temperature, 160°C; injector and detector temperature, 220°C; attenuation, 10 × 8; carrier gas, helium at a flow-rate of 0.85 ml/min; and splitting ratio, 1/90.

Each peak area was measured by using a digital integrator (Shimadzu C-R1A). The ratios of optical isomers were obtained from the ratios of the peak area of each isomer and the total peak area of two isomers.

RESULTS AND DISCUSSION

Chrysanthemic acid, which is a very important constituent of various insecticidal pyrethroids, has four isomeric forms: (+)-*trans*, (−)-*trans*, (+)-*cis* and (−)-*cis*.

ABLE I

OMPARISON OF EXPECTED AND FOUND RATIOS OF OPTICAL ISOMERS OF CHRYSANTHEMIC CID

olumn: 40 m × 0.25 mm I.D. glass capillary coated with N-(1*R*,3*R*)-*trans*-chrysanthemoyl-(*R*)-1-(α-naphthyl)ethylamine. Column temperature: 110°C. Carrier gas (helium) flow-rate: 1.0 ml/min.

mple No.	*Expected (%)*				*Found (%)*			
	(+)-cis	*(−)-cis*	*(+)-trans*	*(−)-trans*	*(+)-cis*	*(−)-cis*	*(+)-trans*	*(−)-trans*
	20.1	0.2	78.6	1.1	19.9	0.2	78.8	1.1
	17.9	2.1	70.7	9.3	17.9	1.9	71.1	9.1
	16.5	3.4	65.5	14.6	16.5	3.2	65.8	14.5
	14.7	5.0	59.1	21.2	15.1	4.6	59.5	20.8

TABLE II

ANALYSES OF TECHNICAL GRADE-SAMPLES OF OPTICALLY ACTIVE CHRYSANTHEMIC ACID

GC conditions as in Table I.

Sample No.	*This method (%)*				*Diastereoisomer method*[9] *(%)*			
	(+)-cis	*(−)-cis*	*(+)-trans*	*(−)-trans*	*(+)-cis*	*(−)-cis*	*(+)-trans*	*(−)-tran.*
1	19.3	1.0	75.8	3.9	19.9	1.0	75.1	4.0
2	20.6	0.4	77.2	1.8	20.2	0.3	77.6	1.9
3	19.3	0.5	77.8	2.4	18.8	0.5	78.2	2.5
4	18.3	0.5	78.6	2.6	19.4	0.5	77.5	2.6
5	18.3	0.4	79.3	2.0	18.7	0.4	78.9	2.0

As is well known, optical isomers of pyrethroid esters have different toxicities for insects, depending on the configuration of the chrysanthemoyl group in the molecule, so it is important to establish the ratio of optical isomers.

Hitherto four isomers were analysed in the form of esters with (+)-2-octanol[9] or in the form of amides with (+)-α-methylbenzylamine[11]. However, as the optical purities of these derivative-forming reagents are usually less than 100%, it is necessary to correct the values obtained according to the optical purity of the chiral reagents and therefore the direct separation with optically active stationary phase was very desirable. Although we have already accomplished[12] the direct gas chromatographic separation of four isomers of chrysanthemic acid in the form of cyclohexyl-, 1,1,3,3-tetramethylbutyl-, 1-adamantyl- and α-dimethylbenzylamides on OA-300

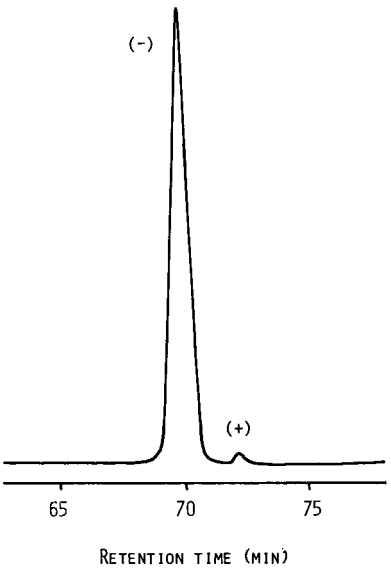

Fig. 2. Gas chromatogram of N-pentafluoropropionyl-1-phenyl-2-(4-tolyl)ethylamine showing the separation of 1% of (+)-isomer and 99% of (−)-isomer. GC conditions as in Table III.

TABLE III

COMPARISON OF EXPECTED AND FOUND RATIOS OF OPTICAL ISOMERS OF 1-PHENYL-2-(4-TOLYL)ETHYLAMINE

Column: 30 m × 0.25 mm I.D. Glass capillary coated with N-lauroyl-(*S*)-proline (*S*)-1-(α-naphthyl)ethylamide. Column temperature: 160°C. Carrier gas (helium) flow-rate: 0.85 ml/min.

Sample No.	*Expected (%)*		*Found (%)*	
	(+)-	*(−)-*	*(+)-*	*(−)-*
1	87.4	12.6	87.1	12.9
2	74.8	25.2	74.7	25.3
3	59.8	40.2	60.3	39.7
4	39.8	60.2	39.4	60.6
5	24.9	75.1	24.9	75.1
6	11.1	88.9	11.4	88.6
7*	50.0	50.0	50.0	50.0

* Racemic sample.

{N,N′-[2,4-(6-ethoxy-1,3,5-triazine)diyl]bis(L-valyl-L-valyl-L-valine isopropyl ester)}[4] as the optically active stationary phase, the separation factors were too low to determine the optical isomers accurately.

All four isomers were completely separated in the form of *tert.*-butylamide with N-(1*R*,3*R*)-*trans*-chrysanthemoyl-(*R*)-1-(α-naphthyl)ethylamine as a novel optically active stationary phase. A typical chromatogram is shown in Fig. 1. The order of elution was (−)-*cis*, (+)-*cis*, (+)-*trans*, (−)-*trans*. The ratios of the optical isomers were easily calculated by measuring peak areas. To verify that no racemization took place during the formation and analysis of the mixed amides, the expected ratios of four isomers are compared with the ratios found by analysis in Table I. Table II gives the results of analyses of some technical-grade samples. Each sample was analyzed in duplicate, and the mean value was shown in Table II. Errors were found from duplicate analyses to be ±0.3%. The precision of this methods expressed as the coefficient of variation was 0.49% (6 measurements) for the

TABLE IV

ANALYSES OF TECHNICAL-GRADE SAMPLES OF OPTICALLY ACTIVE 1-PHENYL-2-(4-TOLYL)ETHYLAMINE

GC conditions as in Table III.

Sample No.	*This method (%)*		*Diastereoisomer method*[10] *(%)*	
	(+)-	*(−)-*	*(+)-*	*(−)-*
1	98.3	1.7	98.6	1.4
2	95.0	5.0	95.7	4.3
3	95.2	4.8	95.8	4.2
4	0.1	99.9	0.2	99.8
5	17.8	82.2	17.2	82.8

(+)-*trans*-isomer of sample No. 5 in Table II. The optical isomer ratios obtained by this method were in agreement with the values obtained for the diastereoisomeric ester using (+)-2-octanol as the derivative-forming chiral reagent[9].

We have already reported[13] the gas chromatographic determination of optical isomers of 1-phenyl-2-(4-tolyl)-ethylamine, which is widely used to resolve asymmetric acids, with OA-300 as the chiral stationary phase. However, the separation (separation factor $\alpha = 1.025$, resolution $R = 1.28$) was insufficient for accurate determination. In particular, when the content of the (+)-isomer is very low, the small peak of the (+)-isomer is overlapped by the tail of the large peak of the (−)-isomer in the chromatogram and an error is often introduced. A novel optically active stationary phase, N-lauroyl-(*S*)-proline (*S*)-1-(α-naphthyl)ethylamide, has improved the separation ($\alpha = 1.038$, $R = 1.76$), as shown in Fig. 2. As both isomers were completely separated, even a small amount of the (+)-isomer can be easily determined. The results of analyses of some mixtures of (+)- and (−)-isomers are shown in Table III; the analytical values are in good agreement with the calculated values.

Table IV gives the results of the analysis of some technical-grade samples. Each sample was analyzed in duplicate, and the mean value was shown in Table IV. Errors were found from duplicate analyses to be $\pm 0.2\%$. The precision of this method expressed by coefficient of variation was 0.04% (8 measurements) for the (+)-isomer of sample No. 1 in Table IV. The optical isomer ratio determined by this method was in good agreement with the value obtained in the form of diastereoisomeric amide using (*S*)-proline as the chiral reagent[10].

We have also developed analytical methods for the determination of optical isomers of some other chiral carboxylic acids, such as 3-(2,2-dichlorovinyl)cyclopropanecarboxylic acid, and chiral amines, such as 1-(α-naphthyl)ethylamine, using these novel amide phases. Details will be reported elsewhere.

REFERENCES

1 E. Gil-Av and D. Nurok, *Advan. Chromatogr.*, 10 (1974) 99.
2 E. Gil-Av, B. Feibush and R. Charles-Sigler, *Tetrahedron Lett.*, (1966) 1009.
3 S. Weinstein, B. Feibush and E. Gil-Av, *J. Chromatogr.*, 126 (1976) 97.
4 N. Ôi, O. Hiroaki and H. Shimada, *Bunseki Kagaku (Jap. Anal.)*, 28 (1979) 125.
5 N. Ôi, M. Horiba and H. Kitahara, *Bunseki Kagaku (Jap. Anal.)*, 28 (1979) 607.
6 N. Ôi, M. Horiba and H. Kitahara, *Bunseki Kagaku (Jap. Anal.)*, 28 (1979) 482.
7 N. Ôi, H. Kitahara, Y. Inda and T. Doi, *J. Chromatogr.*, 213 (1981) 137.
8 N. Ôi, H. Kitahara, Y. Inda and T. Doi, *J. Chromatogr.*, 237 (1982) in press.
9 A. Murano, *Agr. Biol. Chem.*, 36 (1972) 2203.
10 A. Murano, *Agr. Biol. Chem.*, 37 (1973) 981.
11 F. E. Rickett, *Analyst (London)*, 98 (1973) 687.
12 N. Ôi, M. Horiba and H. Kitahara, *Agr. Biol. Chem.*, 45 (1981) 1509.
13 M. Horiba, H. Kitahara, S. Yamamoto and N. Ôi, *Agr. Biol. Chem.*, 44 (1980) 2987.

Journal of Chromatography, 239 (1982) 499–505
Elsevier Scientific Publishing Company, Amsterdam — Printed in The Netherlands

CHROM. 14,665

LIQUID CRYSTALS AS STATIONARY PHASES IN GAS CHROMATOGRAPHY

V. ADSORPTION BEHAVIOUR OF ALIPHATIC ALCOHOLS AND THEIR ESTERS ON AN ELECTRIC FIELD LIQUID CRYSTAL COLUMN

KATSUNORI WATABE*, TOSHIYUKI HOBO and SHIGETAKA SUZUKI
Department of Industrial Chemistry, Faculty of Technology, Tokyo Metropolitan University, Fukasawa, Setagaya-ku, Tokyo 158 (Japan)

SUMMARY

Previously various aspects of adsorption phenomena in electric field liquid crystal (EF–LC) columns were investigated. In this study, to establish the mechanism of the phenomenon, the amounts of C_4 and C_5 aliphatic alcohols and esters adsorbed were measured on three types of EF–LC columns, and the effects of the dielectric constants and the carbon skeleton structures of the solutes on the amounts adsorbed were determined. It was found that the amounts of isomers such as pentanols and butanols adsorbed were different from each other, although these isomers have similar dielectric constants. It was concluded that the adsorption was influenced not only by the dielectric constant, but also by the structure of the carbon skeleton. The equation proposed previously for the relationship between the field strength and the extent of adsorption was modified by introducing a structural term, f_s. Subsequently, the dielectric constants of esters were calculated from the equation by using the f_s values of the corresponding alcohols, and were compared with those found in the literature. The differences were within 10%.

INTRODUCTION

In our investigations[1–4] on liquid crystal stationary phases in gas chromatography, it was found that highly polar compounds were selectively adsorbed in the column when a d.c. electric field was applied and that when the adsorption occurred, the liquid crystals were changed to nematic mesophases by the d.c. electric field. The dielectric constants of adsorbed compounds were shown to have a close relationship with this phenomenon.

This phenomenon was utilized for the selective determination of aromatic hydrocarbons co-existing with large amounts of oxygen-containing compounds. Interfering oxygen-containing compounds were completely eliminated by application of the d.c. electric field to the liquid crystal column.

In this study, in order to clarify the mechanism of this phenomenon further, the

0021-9673/82/0000–0000/$02.75

adsorption of butanols and pentanols was investigated. By measuring the amounts of alcohols adsorbed in three kinds of electric field–liquid crystal (EF–LC) column, it was found that the amount adsorbed was affected not only by the dielectric constant, but also by the structure of carbon skeleton and the position of the functional group of the adsorbed compound. Therefore, the previously described equation which expressed the relationship between the field strength and the amount adsorbed was modified by introducing a structural term, f_s. By using the modified equation, the dielectric constants of corresponding esters were successfully calculated.

EXPERIMENTAL

Materials

Three nematic liquid crystals, 4′-ethoxybenzylidene-4-cyanoaniline (EBCA), 4′-anisal-4-acetoxyaniline (APAPA) and 4,4′-azoxydianisole (ADA), as stationary phases for the EF–LC column were obtained from Tokyo Chemical Industry (Tokyo, Japan), and were used without further purification. Butanols, pentanols, butyl acetates and amyl acetates and butyrates were of analytical-reagent grade. Diethylene glycol succinate (DEGS) polyester was obtained from Nishio Industry (Tokyo, Japan). Fine nickel wire (0.15 mm in diameter) for the inner electrode of the EF–LC column was purchased from Nippon Denkyu (Tokyo, Japan), and Sealbest P-246, an electroconductive resin, for the outer electrode from Tokuriki Kagaku (Kanagawa, Japan).

Gas chromatograph

A modified Shimadzu Model GC 6AM-Pr gas chromatograph equipped with a flame-ionization detector was used, modified as described elsewhere[4].

EF–LC column and separation column

All of the EF–LC columns were 4 m × 0.35 mm I.D. and the configuration and method of preparation were described previously[1].

A whisker-walled open-tubular glass capillary column, coated with DEGS by passing 5% methylene chloride solution through it, was employed as the separation column.

The separation column and EF–LC column were connected in series by shrinkable PTFE tubing.

d.c. generator

A high-voltage power supply for the photomultiplier (Hamamatsu TV, 1.5k-M; Hamamatsu, Shizuoka, Japan) was used.

GC conditions

Pure nitrogen gas (99.999%) was used as the carrier gas at a flow-rate of *ca.* 1 ml/min. The temperatures of the injection port and the flame-ionization detector were 150°C. The oven temperatures for DESG–ADA, DEGS–EBCA and DEGS–APAPA were 120, 120 and 90°C, respectively.

Under these conditions, an appropriate d.c. voltage was applied. Before injection, these columns must be allowed to stand for 3–4 h.

RESULTS AND DISCUSSION

Adsorption in EF–LC column

For the EF–LC column which was connected behind the separation column, three different liquid crystal stationary phases were used. The extent of adsorption in the EF–LC columns was measured by injecting ethereal solutions of the sample compounds.

The effect of the different liquid crystals on the extent of adsorption amount of each compound was studied. The amounts adsorbed and also amounts of each compound adsorbed relative to 1-pentanol are shown in Table I. The extent of adsorption of a compound varied from column to column, but the relative values were similar in all three columns. Therefore, it might be concluded that the relative amount of each compound adsorbed is independent of the liquid crystal phase used for the EF–LC column.

TABLE I

EFFECT OF LIQUID CRYSTAL IN EF–LC COLUMN ON ADSORPTION

Separation column, DEGS (30 m × 0.35 mm I.D.); EF–LC column, 4 m × 0.35 mm I.D.; applied potential, 250 V d.c. Results given are amounts adsorbed (nmol) and relative amounts adsorbed (R) (relative to 1.00 for 1-pentanol).

Compound	*ADA*		*EBCA*		*APAPA*	
	[A_s] (nmol)	*R*	*[A_s] (nmol)*	*R*	*[A_s] (nmol)*	*R*
1-Pentanol	3.64	1.00	2.58	1.00	1.86	1.00
1-Butanol	4.11	1.13	2.93	1.14	2.06	1.11
n-Butyl acetate	0.764	0.210	0.559	0.217	0.424	0.228
n-Amyl acetate	0.749	0.206	0.463	0.179	0.392	0.211
Ethyl *n*-butyrate	0.668	0.183	0.442	0.171	0.349	0.187
Column temperature (°C)	120		120		90	

Adsorption of butanols and pentanols

The amounts of butanols and pentanols adsorbed were measured in EBCA, ADA and APAPA EF–LC columns under applied voltages of 150, 100 and 150 V d.c., respectively. The results are presented in Table II. It was found that, when the number of side-chains increased, the amount of isomers adsorbed decreased, and also that the nearer the side-chain was located to the OH group the smaller was the amount adsorbed. In addition, the position of the OH group influences the amount adsorbed; Thus, 1-pentanol was adsorbed more than 2-pentanol, and 2-pentanol more than 3-pentanol. Further, it was observed that, even though these isomers had similar dielectric constants, the amounts adsorbed were different.

Amounts of the adsorbed butanol isomers decreased in the order *n-* > *iso-* > *sec.-* > *tert.-butanol.* These results obviously indicate that adsorption in the EF–LC column is influenced not only by the dielectric constant, but also by the carbon skeleton structure of the compound adsorbed.

TABLE II

AMOUNTS OF ALIPHATIC ALCOHOLS ADSORBED

Applied potential: 100 V d.c. on ADA column, 150 V d.c. on EBCA column, 150 V d.c. on APAPA column. Other conditions as in Table I.

Compound	*Amount adsorbed (nmol)*		
	ADA	*EBCA*	*APAPA*
1-Pentanol	1.46	1.53	1.09
2-Pentanol	1.02	1.00	0.733
3-Pentanol	0.765	0.867	0.550
3-Methyl-1-butanol	1.31	1.39	0.928
3-Methyl-2-butanol	0.978	0.957	0.699
2-Methyl-2-butanol	0.750	0.947	0.579
1-Butanol	1.63	1.73	1.21
2-Butanol	1.08	1.01	0.762
2-Methyl-1-propanol	1.37	1.33	0.921
2-Methyl-2-propanol	0.405	0.747	0.447

Expression of degree of adsorption

From the above results, the influence of the carbon skeleton structure on the adsorption was explained as follows. When the polar molecules were exposed to an electric field, the coulombic force between the polar molecule and the electrode played an important role in the adsorption process. This force increased as the polarization distance of the molecule increased.

Eqn. 1 was proposed previously[2] for the calculation of the dielectric constant of a solute:

$$[A_s] = k(\varepsilon - 1)E \tag{1}$$

where $[A_s]$ is the amount adsorbed (mol), E is the applied potential (V d.c.), ε is the dielectric constant of the adsorbed compound and k is a constant. As k could be considered to have a structural contribution, it was divided into a structural term of the adsorbed compound, f_s, and k'. Here, f_s could be assumed, for a straight-chain compound, to be the distance from the functional group to the terminal carbon. In this study, f_s values were expressed by the C–C bond and C–O bond numbers. Then, the resulting equation is

$$[A_s] = k(\varepsilon - 1)f_s E \tag{2}$$

The k' and f_s values of pentanols and butanols were calculated by the following procedure. For reference 1-pentanol in the DEGS–ADA EF–LC column mode, the f_s value was *ca.* 5. This value and its amount adsorbed were put into eqn. 2, and then $k' = 2.25 \cdot 10^{-4}$ was obtained. The f_s values of other isomers were calculated from eqn. 2 by substituting this k' value and using the individual amount of the isomers absorbed, $[A_s]$. By the same procedure, f_s values of butanols could be calculated. The k' and f_s values obtained are given in Table III.

TABLE III

k' AND f_s VALUES FOR ALCOHOLS CALCULATED FROM EQN. 2

Compound	*ADA*		*EBCA*		*APAPA*	
	k'	f_s	k'	f_s	k'	f_s
1-Pentanol	$2.25 \cdot 10^{-4}$	5*	$1.61 \cdot 10^{-4}$	5*	$1.14 \cdot 10^{-4}$	5*
2-Pentanol		3.45		3.23		3.55
3-Pentanol		2.84		2.99		2.85
3-Methyl-1-butanol		4.25		4.21		3.97
3-Methyl-2-butanol		3.17		2.91		2.98
2-Methyl-2-butanol		6.19		6.42		7.02
1-Butanol	$2.45 \cdot 10^{-4}$	4*	$1.65 \cdot 10^{-4}$	4*	$1.22 \cdot 10^{-4}$	4*
2-Butanol		2.89		2.64		2.69
2-Methyl-1-propanol		3.37		3.35		3.18
2-Methyl-2-propanol		1.47		1.97		2.28

* The assumed f_s values used for calculating the k' values.

The f_s values were closely, related to the chain length from the functional group to the terminal carbon, except for 2-methyl-2-butanol and 2-methyl-2-propanol, which had much larger values than expected. It was presumed that a structural interaction between the solute molecule and the long molecule of the nematic liquid existed. The k' values of the alcohols examined were similar to each other provided that the same EF–LC column was used.

Adsorption of esters

The amounts of amyl and butyl acetates, methyl and ethyl *n*-butyrates and ethyl isobutyrate adsorbed were measured under the same conditions as for alcohols in EBCA, ADA and APAPA EF–LC columns. The results are given in Table IV. The adsorption behaviour of butyl acetate isomers was similar to that of butanols, *i.e.*, *n*-butyl acetate was the most strongly adsorbed and whereas *tert.*-butyl acetate the most weakly. The amounts of butyrates adsorbed were comparable to those of *sec.*- and

TABLE IV

AMOUNTS OF ALIPHATIC ESTERS ADSORBED

Conditions as in Table II.

Compound	$[A_s]$ *(nmol)*		
	ADA	*EBCA*	*APAPA*
n-Butyl acetate	0.302	0.319	0.248
Isobutyl acetate	0.279	0.272	0.207
sec.-Butyl acetate	0.236	0.251	0.190
tert.-Butyl acetate	0.156	0.192	0.146
n-Amyl acetate	0.302	0.333	0.283
Isoamyl acetate	0.295	0.276	0.247
Ethyl isobutyrate	0.173	0.164	0.126
Methyl *n*-butyrate	0.243	0.210	0.159
Ethyl *n*-butyrate	0.254	0.233	0.176

TABLE V

COMPARISON OF CALCULATED AND LITERATURE VALUES OF DIELECTRIC CONSTANTS ON THREE EF-LC COLUMNS

ε_{calc} is the value calculated from eqn. 2; $\varepsilon_{lit.}$ is the value found in the literature.

Compound	*ADA*			*EBCA*			*APAPA*			ε_{lit}
	k'	f_s	ε_{calc}	k'	f_s	ε_{calc}	k'	f_s	ε_{calc}	
n-Butyl acetate*	$1.88 \cdot 10^{-4}$	4.00		$1.32 \cdot 10^{-4}$	4.00		$1.03 \cdot 10^{-4}$	4.00		5.01
Isobutyl acetate		3.37	5.33		3.35	5.08		3.18	5.21	5.29
sec.-Butyl acetate		2.89	5.34		2.64	5.64		2.69	5.56	–
tert.-Butyl acetate		1.47	5.65		1.97	5.86		1.28	5.14	–
n-Amyl acetate		5.00	5.42		5.00	4.36		5.00	4.66	4.75
Isoamyl acetate		4.25	4.67		4.21	4.31		3.97	5.01	4.63

* Used for calculating the k' value. The f_s values are from corresponding alcohols and were used for calculating the dielectric constant of each compound.

tert.-butyl acetates. The adsorption behaviour of these butyrates is explained by the position of the functional group, which was located in the middle of the carbon skeleton, as in *sec.*- and *tert.*-butyl acetates.

It is concluded that an almost identical structural effect of alcohols on the adsorption to that of esters exists. In order to justify this conclusion, the dielectric constants of the corresponding esters were calculated by using the f_s values of the alcohols. Thus, the k' value of *n*-butyl acetate was obtained by putting $f_s = 5$, the amount adsorbed and the dielectric constant into eqn. 2. Then, the dielectric constants of other esters were calculated by using this k' value, the amounts adsorbed and the f_s values of the corresponding alcohols. In Table V these dielectric constants calculatd are compared with those found in the literature[5,6]. Good agreement between the two values was observed each compound.

CONCLUSIONS

The adsorption behaviour of C_4 and C_5 alcohols was shown to be closely related to the structure of the carbon skeleton. When the number of side-chains in the carbon skeleton was increased the amount adsorbed decreased, and the nearer the side-chain was located to the OH group the smaller was the amount adsorbed. A compound that had the OH group at the end of the carbon skeleton was more adsorbed than one with the OH group nearer the middle.

The results indicate that the adsorption was influenced not only by the dielectric constant, but also by the structure of a compound. The equation expressing the relationship between the field strength and the amount adsorbed was modified by introducing the structural term f_s. The f_s values of alcohols calculated from this equation were shown to be closely correlated with structure, except for 2-methyl-2-butanol.

The adsorption of butyl and amyl acetates was similar to that of the corresponding alcohols. Therefore, the f_s values for alcohols were applicable to esters, and the dielectric constants of the corresponding esters were calculated. These values were compared with those found in the literature, and good agreement between the values was observed for each compound.

Additionaly, the k' values of pentanols and butanols were similar. It was found that the k' terms contained the effect of the functional group on adsorption.

Further work concerning the prediction of the amounts of ketones and aldehydes adsorbed is in progress.

REFERENCES

1 K. Watabe, S. Suziki and S. Araki, *J. Chromatogr.*, 192 (1980) 89.
2 K. Watabe, S. Suzuki and S. Araki, *Nippon Kagaku Kaishi (J. Chem. Soc. Jap.)*, (1980) 582.
3 K. Watabe, S. Suzuki and S. Araki, *Bunseki Kagaku (Jap. Anal.)*, 29 (1980) 585.
4 K. Watabe, T. Hobo and S. Suzuki, *J. Chromatogr.*, 206 (1981) 223.
5 J. A. Riddick and W. B. Bunger, *Organic Solvents*, Wiley-Interscience, New York, 1970.
6 *Kagaku Binran (Handbook of Chemistry)*, Chemical Society of Japan, Maruzen, Tokyo, 1966, p. 1163.

Journal of Chromatography, 239 (1982) 507–513
Elsevier Scientific Publishing Company, Amsterdam — Printed in The Netherlands

CHROM. 14,526

PACKED MICROCAPILLARY LIQUID CHROMATOGRAPHY WITH REDUCED I.D. COLUMNS

TAKAO TSUDA*, ISAO TANAKA and GENKICHI NAKAGAWA
Laboratory of Analytical Chemistry, Nagoya Institute of Technology, Gokiso-cho, Showa-ku, Nagoya-shi 466 (Japan)

SUMMARY

Packed microcapillary columns with internal diameters and particle size (silica gel) 30–40 μm and 10 μm, respectively, were prepared with the aim of reducing analysis time. The *h–v* relation for this microcapillary is similar to that of the microcapillary of 75 μm I.D. and particle size 30 μm, which has hitherto been thought to be the optimum. Initial results show that analysis time would be reduced to one-fifth. Applications for aromatic compounds were demonstrated. Combined loop and split injection was used. The reproducibility is good, and the operation simple.

INTRODUCTION

One of the recent topics in the field of liquid chromatography (LC) has been the development of micro columns[1–12], because they have potentially higher resolution than ordinary columns, such as 2–4 mm I.D. and 25 cm length. There are three different types of micro columns: micro-bore packed column[1,2], packed microcapillary column[3–6] and open-tubular microcapillary column[7–10]. The cross-sectional area of the micro-bore packed column is reduced to *ca.* 10% compared with that of an ordinary column, but the cross-sectional areas of microcapillary columns are even smaller, 0.1% or less.

The techniques[1,2] used for the micro-bore packed column, such as column packing method, sample introduction, detection and connection systems, are similar to those of ordinary LC. A micro-bore packed column with 250,000 plates has been demonstrated[1]. Because the column size reduction in microcapillary LC, is so striking, techniques and operational procedures are very different from ordinary LC. These have been investigated during past four years[3–10]. It is apparent from experimental results that capillary LC has the ability to give high resolution in the analysis of complex mixture[3–10].

One of the favourable characteristics of packed microcapillary LC compared with open-tubular microcapillary LC is that the sample capacity is larger because the column contains supports, such as silica gel or activated alumina, which have a large surface area. But a higher inlet pressure is necessary owing to the low permeability compared with open-tubular microcapillary LC.

0021-9673/82/0000–0000/$02.75

The most severe drawback for both packed and open-tubular microcapillary LC is that it needs a long analysis time to get a fine separation which shows a high number of theoretical plates, *e.g.*, over 100,000[5,8]. For analysis time to be reduced, the key factor might be to reduce the column I.D. as predicted theoretically[11–13]. We have attempted to reduce the I.D. of packed microcapillary column to be less than 50 μm, and we have also combined loop and split injection.

EXPERIMENTAL

Original soda-lime glass capillary tubing (0.2–0.3 mm I.D., 6 mm O.D. and 1 m length) was supplied by Ishizuka Glass (Nagoya, Japan). A glass-drawing machine (GDM-1, Shimadzu Seisakusho, Kyoto, Japan) was used to make packed microcapillaries. UV detector (UVIDEC-100II, Japan Spectroscopic) was used with a home-made microcell and connections that were same as system B of ref. 9.

Preparation of packed microcapillary columns with reduced I.D.

Original soda-lime glass was dry-packed with silica gel, Develosil[R] 10-60 (particle diameter 10 μm and pore size 60 Å) made by Nomura Kagaku (Seto, Aichi-Pref., Japan), and then drawn into packed microcapillary by the glass-drawing machine, which was place in the vertical position[3].

To obtain a good packed microcapillary column that is uniformly packed, it is essential to exclude moisture from the silica gel and the original glass capillary tubing and to prevent any access of moisture from the air throughout the whole procedure. Before dry-packing in original glass, the following procedure is necessary. After the inside wall of the original glass capillary was washed with ethanol, it was dried with dry nitrogen and then dried by a burner under flowing dry nitrogen in the original capillary, and finally dried at 500°C and a flow-rate of *ca.* 2 cm/min by passing through the oven. This was done by using the drawing machine, with the bent pipe part detached. To exclude moisture from the air, one or both ends of the original glass were closed by silicone grease or a silicone tube cap.

Silica gel should be also dried in the oven at 500–700°C for 10–60 min, or at 200°C for 2 days. The dried silica gel was dry-packed into the dried original glass capillary tubing by vibrator action. It took *ca.* 30–60 min. Then the dry-packed original glass tubing was drawn out to a packed microcapillary column. If the inside of the original glass tubing became inflated during drawing, it was because of incomplete drying.

The oven temperature for drawing was also one of the factors influencing uniform packing of the microcapillary column: lower temperatures are preferable. This may be because of the viscosity of the original glass tubing at the point of glass-stretching during drawing.

Preparation of ODS-packed microcapillary column

A microcapillary column with an octadecylsilane stationary phase[4] was prepared by the *in situ* column technique described Gilipin *et al.*[14], as follows. Several coils of microcapillary was filled hexane or toluene, and then 0.2 ml of 2% octadecyltriethoxysilane–xylene solution was passed into the capillary at 110°C. The capillary was then washed with hexane, and the process was repeated two or three

times. Then the capillary was washed with dichloromethane and methanol (or methanol alone for use in the reversed-phase mode).

Loop–split injection

In capillary LC there are currently two methods of sample introduction, namely with[3,9] or without[5,7,15] sample splitting. Although the sample introduction system is an important aspect in the construction of a capillary LC system, neither method has yet achieved predominance. Concerning split injection, the geometrical consideration was examined in a previous report[8]. Here the loop, with an inner volume of 20 μl, was combined via a six-way valve with a split injector, by using short stainless-steel tubing, 5 cm × 0.2 mm I.D.

The reproducibility of loop–split injection and the relationship of height equivalent to theoretical plate (*H*) and split ratio are show in Figs. 1 and 2, for packed and open-tubular microcapillary columns under the following conditions. The I.D. of stainless-steel tubing at the split part and the O.D. of the head of the capillary column were 0.8 mm and *ca.* 0.6 mm, respectively. The split ratio was obtained by measuring the amount of effluent by weight, which was collected both at the column outlet and as a discard flow. The experiment was performed at constant pressure to ensure a constant flow-rate in the column. The sample was 10% benzene in octane, or 0.1% N-alkylanilines, and the eluent was hexane.

The reproducibility of loop–split injection is very good. The standard deviation of the sample amount was *ca.* 2%. From Fig. 2, at lower flow-rates, *ca.* 1 cm/sec, the split ratio should be kept higher than 700, but at higher flow-rates, *ca.* 6 cm/sec, a split ratio of 100 can be used without any effect on the chromatographic peaks.

In other words, there might be necessary at some amount of effluent for clean-

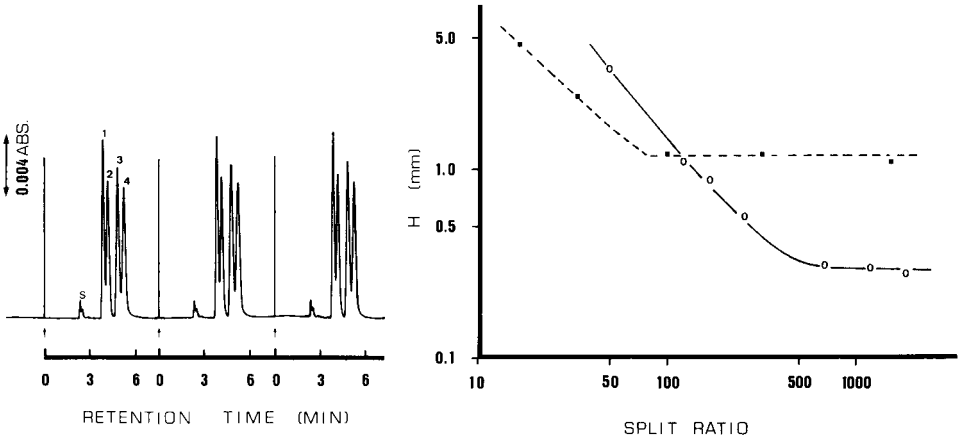

Fig. 1. Reproducibility of loop–split injection. The volume of the sample loop was 20 μl. The sample was N-substituted anilines in octane, at concentrations of 0.1% each. Peaks: S = solvent; 1 = N,N-dimethylaniline; 2 = N-butylaniline; 3 = N-ethylaniline; 4 = N-methylaniline.

Fig. 2. Split ratio *vs.* *H* for benzene, using loop–split injection method. Curves: ○, packed microcapillary column (231 cm × 53 μm I.D.); ■, open-tubular microcapillary column (10 m × 57 μm I.D.). Mobile phase, hexane. Linear velocity is 1.0 cm/sec for packed microcapillary and 6.4 cm/sec for open-tubular microcapillary column.

ing up the part of splitting. If the split ratio is over 1000, the chromatogram is not affected by sample introduction. Although this method of sample introduction requires a larger amount of sample than the direct method, it is very easy to operate.

RESULTS AND DISCUSSION

H–v relation with packed microcapillary column with reduced I.D.

Fig. 3 shows the H–v relation. The H value (height equivalent to a theoretical plate) at 1 cm/sec is nearly 0.2 mm for retained solute (capacity factor, $k' = 0.75$). This value is comparable with the H values for retained solutes in open-tubular microcapillary columns of 30–50 μm I.D.[7,8,10]. In open-tubular microcapillary columns, the mobile-phase flow is strictly laminar flow[7,10], and zone broadening due to the mobile phase can be explained by Taylor diffusion[13]. But in packed microcapillary columns, the zone broadening due to the mobile phase may originate from both Taylor diffusion and eddy diffusion.

As the packed microcapillary column has supports or adsorbents inside the capillary tubing, the inner diameter of the channel in packed microcapillary column might be reduced to one-half or one-third of that of an open-tubular microcapillary column. In the other words, a packed microcapillary column with 30 μm I.D. has almost same size of mobile phase flow channel as an open-tubular microcapillary with 10 μm I.D. From our initial results shown in Fig. 3, the H value is nearly same as that obtained with an open-butular microcapillary with 30–50 μm I.D. This suggests that there may be eddy diffusion in the mobile phase.

h–v relation

The relationship between the reduced plate height (h) and the logarithm of the reduced velocity for retained solute is shown in Fig. 4. Plots of reduced values are

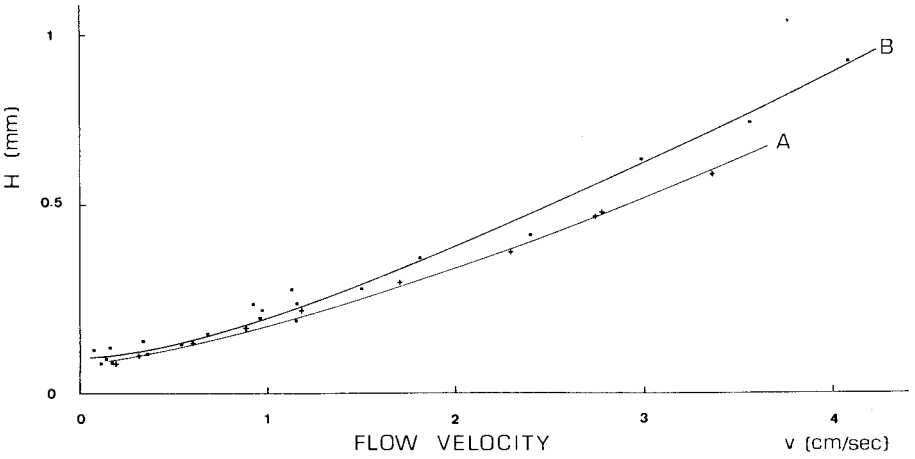

Fig. 3. H *vs.* flow velocity for packed microcapillary columns. (B) Column 2.2 m × 41 μm I.D.; adsorbent, silica gel, 10 μm particle size; samples, N,N-dimethylaniline ($k' = 0.75$); eluents, 0.12% methanol–hexane. (A) Column 450 cm × 36.5 μm I.D.; adsorbent, silica gel, 10 μm; sample, benzene; eluent as in (B).

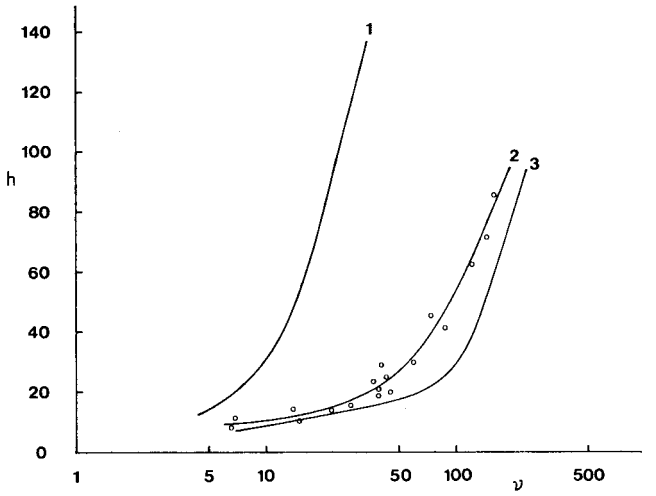

Fig. 4. h–ν relationships for different packed microcapillary columns. (1) Column, 3.6 m × 50 μm I.D.; adsorbent, alumina, 10 μm; sample, pyridine (retention relative to benzene, 0.1); eluent, 0.03% methanol–hexane. (2) Column, 2.2 m × 41 μm I.D.; conditions as in Fig. 3(A). (3) Column, 14 m × 75 μm I.D.; adsorbent, alumina, 30 μm; sample, quinoline (retention relative to benzene, 1.7); eluent, 0.03% methanol–hexane. Curves 1 and 3 quoted from ref. 3.

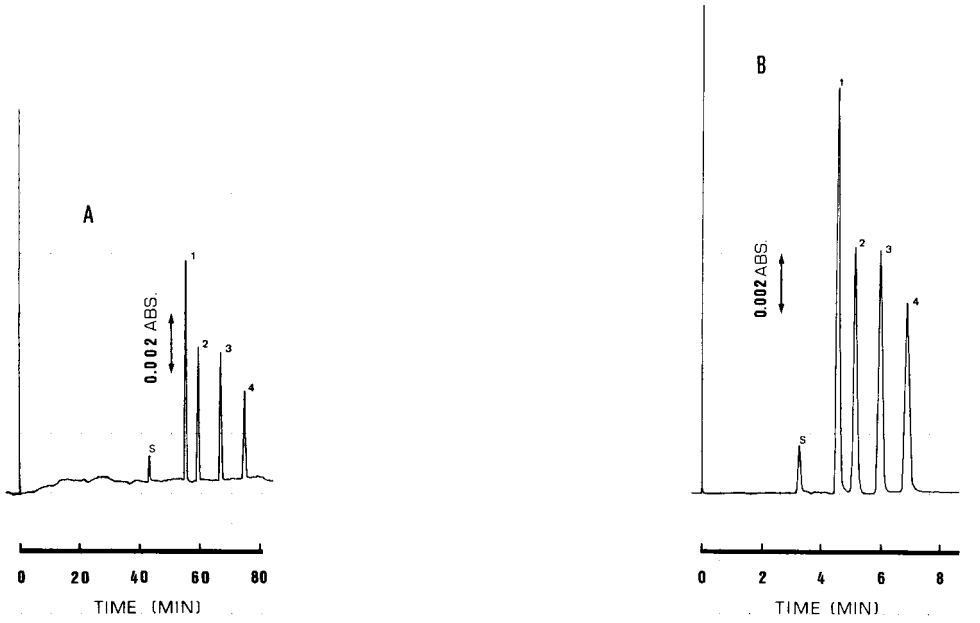

Fig. 5. Separation of N-substituted anilines on silica microcapillary columns. (A) Column, 8 m × 41 μm I.D.; adsorbent, silica gel, 10 μm; mobile phase, hexane with 0.3% methanol; linear velocity, 0.3 cm/sec; inlet pressure, 40 kg/cm^2; detection, UV at 254 nm. (B) Column same as in (A) except column length, 217 cm; mobile phase, hexane with 0.12% methanol; linear velocity, 1.1 cm/sec. Peaks as in Fig. 1.

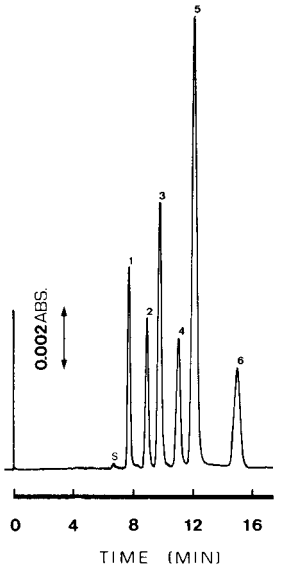

Fig. 6. Separation of model polycyclic aromatic hydrocarbons on a silica–octadecylsilane microcapillary column. Column, 232 cm × 40 μm I.D. packed with 10 μm silica gel modified to ODS; mobile phase, methanol–water (82:18); linear velocity, 0.6 cm/sec; inlet pressure, 150 kg/cm^2. Peaks: S = solvent; 1 = benzene; 2 = naphthalene; 3 = biphenyl; 4 = fluorene; 5 = anthracene; 6 = pyrene.

generally considered to be a good indication of the chromatographic quality of a column across a range of particle sizes[16]. The microcapillary of 75 μm I.D. and particle size 30 μm (curve 3) has been treated as the optimum one in previous reports[3–6]. The packed microcapillary of the present work (curve 2) shows a very similar profile. Although the initial h values of curves 1 and 2 (particle size 10 μm) are nearly the same, curve 2 is shifted generally towards a four times larger reduced velocity than curve 1. In the other words, the packed microcapillary of the present work is a considerable improvemenet on the previous (curve 1)[3]. At the same reduced velocity, curve 2 has a slightly larger h value than curve 3. But, for a given theoretical plate number, the capillary of curve 2 can be operated in an analysis time of *ca.* 20% of that of the microcapillary of curve 3.

Simple calculation of the theoretical plate numbers of 10 m and 40 m packed microcapillary columns in the present experiment gives 50,000 and 200,000 plates, respectively and the analysis times for a solute with $k' = 1$ are 33 and 133 min, respectively. These analysis times are reasonably acceptable for high-resolution LC.

Typical examples of applications are shown in Figs. 5 and 6. The theoretical plate number for N-ethylaniline ($k' = 0.56$) in Fig. 5A is almost 100,000. A fast analysis with a short microcapillary (*ca.* 2 m long) is shown in Figs. 5B and 6. Theoretical plate numbers for solutes in Figs. 5B and 6 are from 5000 to 8000. These chromatograms are very similar to those that would be obtained with a good ordinary column, *i.e.* a 2 m microcapillary column is the length that would correspond to a good ordinary column. So a long microcapillary, $2x$ m in length, would show x times larger plate numbers than an ordinary column. It should be emphasized that it is not difficult to make a microcapillary column as long as 40 m.

ACKNOWLEDGEMENT

This work was supported by a grant-in-aid for Scientific Research from the Ministry of Education of Japan (No. C56550533) and The Toyota Foundation (No. 81-1-252).

REFERENCES

1 C. E. Reese and R. P. W. Scott, *J. Chromatogr. Sci.*, 18 (1980) 479.
2 R. P. W. Scott and P. Kucera, *J. Chromatogr.*, 125 (1976) 251.
3 T. Tsuda and M. Novotny, *Anal. Chem.*, 50 (1978) 271.
4 Y. Hirata, M. Novotny, T. Tsuda and D. Ishii, *Anal. Chem.*, 51 (1979) 1807.
5 Y. Hirata and M. Novotny, *J. Chromatogr.*, 186 (1979) 521.
6 M. Novotny, *J. Chromatogr. Sci.*, 18 (1980) 473.
7 T. Tsuda, K. Hibi, T. Nakanishi, T. Takeuchi and D. Ishii, *J. Chromatogr.*, 158 (1978) 227.
8 T. Tsuda and G. Nakagawa, *J. Chromatogr.*, 199 (1980) 249.
9 T. Tsuda, K. Tsuboi and G. Nakagawa, *J. Chromatogr.*, 214 (1981) 283.
10 D. Ishii and T. Takeuchi, *J. Chromatogr. Sci.*, 18 (1980) 462.
11 J. H. Knox, *J. Chromatogr. Sci.*, 18 (1980) 453.
12 J. H. Knox and M. T. Gilbert, *J. Chromatogr.*, 186 (1979) 405.
13 G. Taylor, *Proc. Roy. Soc. London, Ser. A*, 219 (1953) 186.
14 R. K. Gilpin, J. A. Korpi and C. A. Janicki, *Anal. Chem.*, 46 (1974) 1314.
15 T. Tsuda and D. Ishii, *The 22nd Symposium on Liquid Chromatography, Kyoto, Japan, February 16, 1979.*
16 J. C. Giddings, *Dynamics of Chromatography*, Marcel Dekker, New York, 1965.

Journal of Chromatography, 239 (1982) 515–526
Elsevier Scientific Publishing Company, Amsterdam — Printed in The Netherlands

CHROM. 14,586

APPLICATION OF THE STREAMING CURRENT DETECTOR TO THE ANALYSIS OF INDIVIDUAL BILE ACIDS

SHIGERU TERABE*, KIYOSHI YAMAMOTO and TEIICHI ANDO
Department of Industrial Chemistry, Faculty of Engineering, Kyoto University, Sakyo-ku, Kyoto, 606 (Japan)

SUMMARY

The streaming current detector for high-performance liquid chromatography has been applied successfully to the analysis of human bile acids. The detector showed almost equally high sensitivities for the detection of underivatized free and conjugated bile acids and their sulphates. The detection limits were about 100 ng and linear responses were obtained for amounts injected in the range 0.1–10 μg. Reversed-phase chromatographic conditions were employed with a chemically bonded C_{18} stationary phase and a water–methanol–acetone mobile phase containing ammonium carbonate. A synthetic serum sample with bile acids added was also successfully analysed.

INTRODUCTION

The fundamental characteristics of the streaming current detector for high-performance liquid chromatography (HPLC) under reversed-phase chromatographic conditions have already been reported[1]. The operating principle of the detector is based on the measurement of the streaming current, which is produced when a liquid is forced to flow through a capillary or a packed bed[2]. The streaming current detector, which has a cell volume of about 1 μl, is structurally simple, inexpensive, practically maintenance-free and selectively sensitive to ionizable compounds in spite of being a bulk-property detector in principle.

Many HPLC studies on the analysis of individual bile acids have been made[3–13] for the purpose of diagnosing liver diseases. Most of the studies have employed reversed-phase chromatographic conditions. The difficulty of bile acid analysis by HPLC lies in achieving a high sensitivity of detection because none of the acids possesses an effective UV absorption, although the glyco- and tauro-conjugated bile acids show moderate absorptions around 200 nm[4,11,12]. The sensitivity of the differential refractometer is too low to detect the bile acids in serum[7,14]. Therefore, UV[10,11,15] or fluorimetric[16] derivatizations at the carboxyl group have been conducted in order to obtain high sensitivities of detection. Tauro-conjugated bile acids, however, must be separated from free and glyco-conjugated bile acids and hydrolysed before the derivatization[15]. This kind of procedure seems rather time consuming and

0021-9673/82/0000–0000/$02.75

unfavourable for quantitative analysis. The most sensitive method for bile acids at present is to use the reaction detector in which NADH, produced from the reaction of a bile acid with 3α-hydroxysteroid dehydrogenase, is determined fluorimetrically[3,13,17]. The sulphated bile acids at the 3α-position, however, cannot be detected by this method.

The characteristic feature of the streaming current detector strongly suggests that it is promising for use in bile acid analysis. The purpose of the present study is to explore the applicability of the detector to the HPLC analysis of individual bile acids. The separation and detection of unconjugated bile acids, glyco- and tauro-conjugated bile acids and three 3-sulphates of free and conjugated lithocholic acids is described.

EXPERIMENTAL

Reagents and materials

Methanol of HPLC quality and the other chemicals of reagent grade were purchased from Wako (Osaka, Japan) and used without further purification. Water was purified with a Milli-Q system (Millipore, Bedford, MA, U.S.A.). All of the bile acids investigated, cholic acid (C), chenodeoxycholic acid (CDC), deoxycholic acid (DC), lithocholic acid (LC), ursodeoxycholic acid (UDC), glyco(G)- and tauro(T)-conjugates of each bile acid and 3α-sulphates of LC (LC-3αS), GLC (GLC-3αS) and TLC (TLC-3αS), were kindly donated by Dr. K. Uchida of Shionogi Research Laboratory. A control serum (Control Serum I, lot no. 1890W004AA) was obtained from Hyland (Bannockburn, IL, U.S.A.).

Apparatus

The HPLC system consisted of a Jasco Tri Rotar high-pressure pump, a Jasco VL-611 sample injector and the streaming current detector described previously[1]. As the streaming current detector is very sensitive to flow-rate, a Glenco PD-3000 flow-through pulse damper and an air damper consisting of a stainless tube (50 cm × 8 mm I.D.) were used to reduce the pulsating flow, in addition to the pulse damper built in the pump. A Cecil CE212 variable-wavelength UV detector was connected in series with the streaming current detector to make a comparison of the two detectors when a human serum was analysed. The separation column (25 cm × 4.6 mm I.D.) and the pre-column (5 cm × 4.6 mm I.D.) were slurry-packed with Develosil ODS-5 (Nomura Chemical, Seto, Japan) by use of a Chemco Model 124 slurry packing apparatus.

Procedure

Each bile acid was dissolved in methanol to give a concentration of 1 mg/ml. HPLC was carried out at room temperature. A pre-column was employed only for the analysis of serum samples.

Human serum samples were pre-treated according to the method of Uemura[18]. A 1-ml volume of human serum was deproteinized by the addition of 5 ml of ethanol and heating at 80°C. The precipitates were removed by centrifugation at 1800 *g* for 5 min and washed with 5 ml of ethanol three times. The collected supernatant of total *ca.* 21 ml was evaporated to dryness. The residue was dissolved in 100 μl of the mobile phase and an aliquot was introduced into the HPLC system. The serum

sample for the recovery test was prepared by adding known amounts of four bile acids in a control serum.

RESULTS AND DISCUSSION

Effect of salt concentration on the separation and sensitivity

The separation of the bile acids was difficult when a mixture of water and methanol containing no salt was employed as the mobile phase, because the peaks were broad and unsymmetrical. This low efficiency may be attributable to the partial ionization of the carboxyl group of the bile acid.

Nambara and co-workers[4,14] reported that an alkaline buffer solution of weakly basic ammonium carbonate or ammonium phosphate is effective as a mobile phase constituent in the reversed-phase chromatographic separation of bile acids. A weakly basic solution containing ammonium carbonate was chosen as a mobile phase in this study, as it is also advantageous for the highly sensitive detection of the bile acids by the streaming current detector as ionic species.

In order to determine the optimal concentration of ammonium carbonate in the mobile phase, the dependence of the plate number of the column and the peak height of the bile acid eluted at about 4 min on the salt concentration was investigated with the flow-rate and the amount injected kept constant. The results are illustrated in Fig. 1. The evaluation of the effect of the salt concentration required that the plate number and detector response be measured for the peak at 4 min instead of the peak of a particular bile acid, because not only the response and the plate number but also the retention time of a particular bile acid depended on the concentration of the salt. The characteristic of the streaming current detector that it shows substantially equal sensitivities to all the bile acids makes this evaluation reasonable.

Fig. 1 reveals that an increase in the ammonium carbonate concentration makes the efficiency of the column higher, but the peak height lower. A compromise between the resolution and the sensitivity led to an optimal concentration of about 0.1 m*M*.

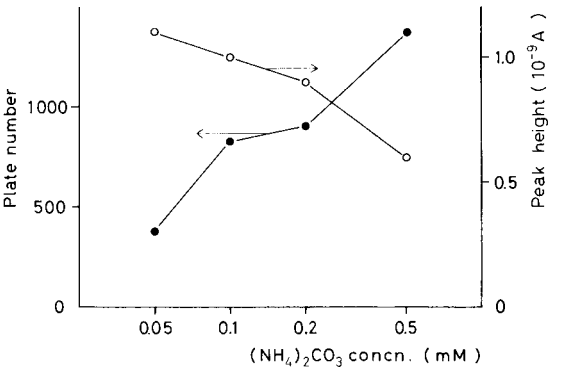

Fig. 1. Dependence of plate number and detector response of a bile acid on the concentration of ammonium carbonate in the mobile phase. The plate number and detector response were measured for a peak eluted at *ca.* 4 min. Column, Develosil ODS-5, 15 cm × 4.6 mm I.D.; mobile phase, water–methanol (30:70) containing ammonium carbonate; flow-rate, 1.0 ml/min; sample size, 2 μg.

Separation with water–methanol binary solvent

The chromatogram of ten individual bile acids shown in Fig. 2 was recorded with water–methanol containing 0.1 m*M* ammonium carbonate as the mobile phase. Each pair of glyco- and tauro-conjugated bile acids was not resolved completely under this condition.

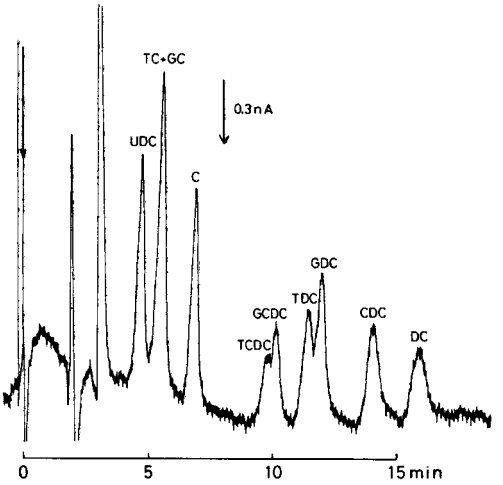

Fig. 2. Separation of individual bile acids with water–methanol (42:58) containing 0.1 m*M* ammonium carbonate as the mobile phase. Column, Develosil ODS-5, 25 cm × 4.6 mm I.D.; flow-rate, 0.8 ml/min; sample size, 1 μg each.

Periodic fluctuation observed in the baseline of the chromatogram, which is due mainly to noise from the detector, is associated with the pulsating flow by the reciprocating pump employed, because the streaming current detector is very sensitive to changes in flow-rate[1]. The baseline current was *ca.* $0.2 \cdot 10^{-7}$ A under the conditions indicated in Fig. 2. The downwards direction of the current scale drawn in Fig. 2. means that the current decreases at the peaks.

Separation with water–acetone binary solvent

Fig. 3 shows a chromatogram of individual bile acids obtained with water–acetone containing 0.1 m*M* ammonium carbonate as the mobile phase. In this chromatogram, the resolution of each pair of glyco- and tauro-conjugated bile acids was satisfactory. The glyco-conjugated acid was eluted faster than the corresponding tauro-conjugated acid, which was the reverse of the order of elution observed with water–methanol. The peaks of unconjugated acids tailed considerably and the peak of CDC partly covered that of DC. Moreover, TCDC and GDC were not separated completely.

The baseline current was *ca.* $0.4 \cdot 10^{-7}$ A under these conditions.

Separation with water–methanol–acetone ternary solvent

The results described above show that the unresolved peaks obtained with water–methanol could be separated successfully with water–acetone as the mobile

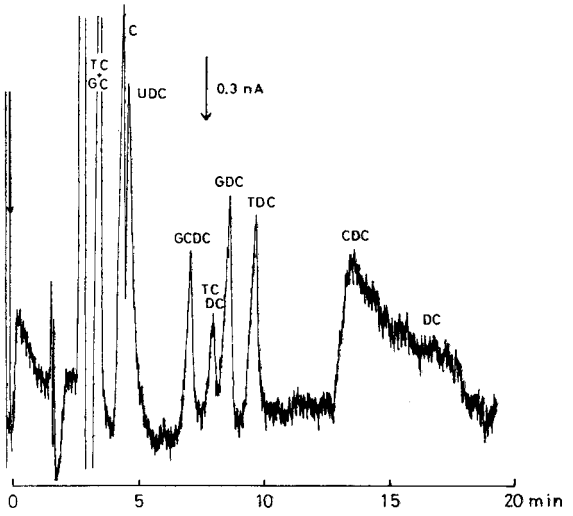

Fig. 3. Separation of individual bile acids with water–acetone (30:70) containing 0.1 m*M* ammonium carbonate as the mobile phase. Flow-rate, 0.9 ml/min; other conditions as in Fig. 2.

phase, and *vice versa*, suggesting that a water–methanol–acetone ternary solvent system might be effective for the complete separation of individual bile acids. This ternary solvent system gave successful results, as expected, but the retention times were so widely spread that the separation of all of the individual bile acids was impractical under isocratic elution conditions.

As the streaming current detector is intrinsically a bulk property detector, gradient elution methods cannot be adopted. Consequently, fifteen bile acids were divided into four groups according to their retention behaviour and each group was analysed separately. This made a sufficient resolution in a short time possible. The bile acids of each group are listed below in order of elution, together with the composition of the mobile phase employed for respective groups. Ammonium carbonate was added to the mobile phase at the concentration of 0.1 m*M*.

(i) GUDC, TUDC, GC, TC; water–acetone (77:23);

(ii) UDC, C, GCDC, TCDC, GDC, TDC, CDC, DC; water-methanol–acetone (62:18:20);

(iii) GCDC, TCDC, GDC, TDC, CDC, DC, GLC, TLC; water–methanol–acetone (62:9:29);

(iv) LC; water–methanol–acetone (30:36:34).

Chromatograms of the four groups are shown in Figs. 4–7. No significant differences among the bile acids were noticed in the detector responses. The smaller peak areas of GCDC and TCDC arose from the low purities of the samples. The baseline current was *ca.* $0.3 \cdot 10^{-7}$ A under the conditions given in Fig. 5.

Separation and detection of sulphated bile acids

The separation of monosulphated bile acids by HPLC has already been reported by Goto *et al.*[19]. The 3-sulphated bile acids cannot be detected by the reaction detector with an enzyme[3,13,17] as mentioned above, because 3α-hydroxysteroid de-

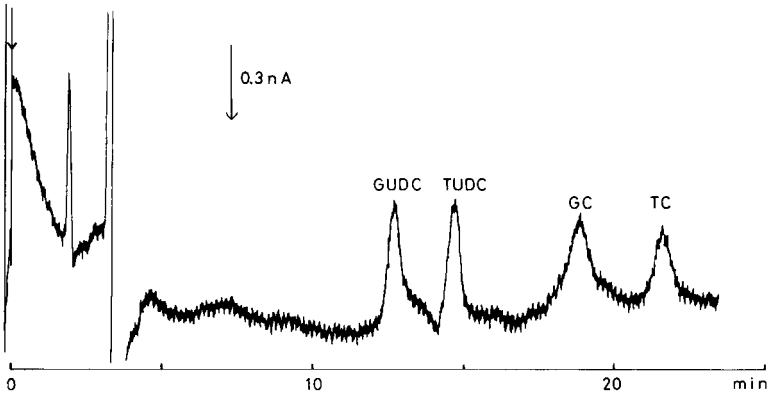

Fig. 4. Separation of four individual bile acids of group (i). Mobile phase, water–acetone (77:23) containing 0.1 m*M* ammonium carbonate; other conditions as in Fig. 2.

hydrogenase cannot oxidize these bile acids. As the streaming current detector was expected to be useful for detecting both sulphated and unsulphated bile acids, the applicability of this detector was examined for some sulphated bile acids.

Three sulphated lithocholic acids (LC) at the 3α-position, LC-3αS, GLC-3αS and TLC-3αS, were employed as samples. The optimal concentration of ammonium carbonate in the mobile phase was found to be 0.2 m*M* for the sulphated bile acids instead of 0.1 m*M* for the unsulphated acids. Concentrations of the salt lower than 0.2 m*M* gave broad, unsymmetrical peaks. A chromatogram obtained with water–methanol–acetone as the mobile phase is shown in Fig. 8. The slightly larger fluctuation in the baseline in Fig. 8 than in those in Figs. 2–7 is due to a residual pulsating

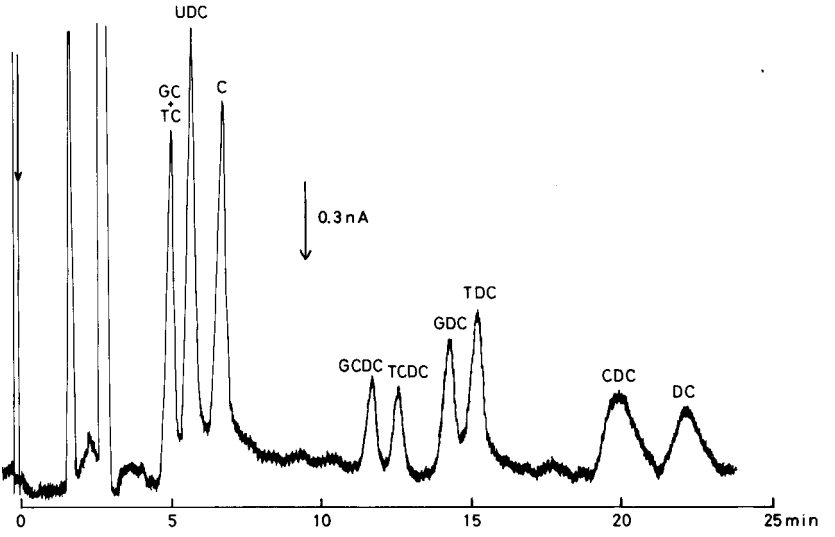

Fig. 5. Separation of eight individual bile acids of group (ii). Mobile phase, water–methanol–acetone (62:18:20) containing 0.1 m*M* ammonium carbonate; other conditions as in Fig. 3.

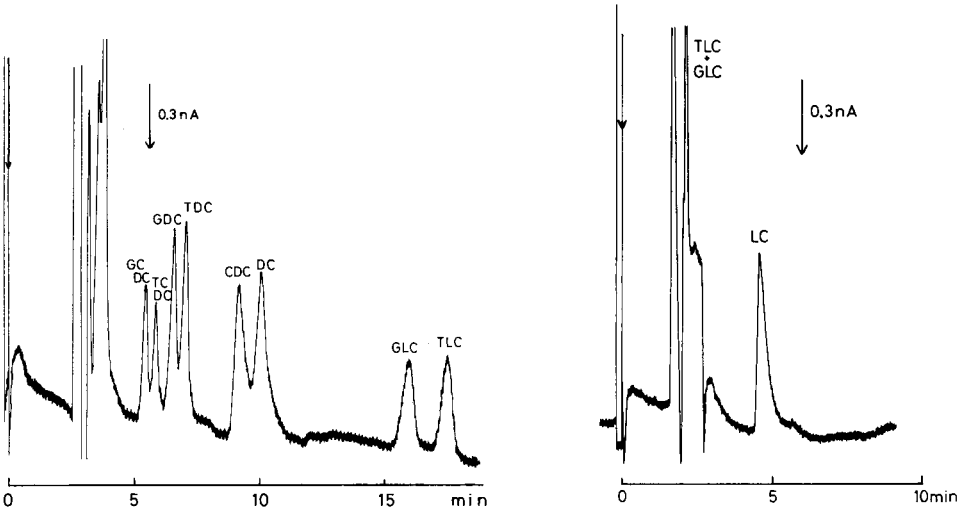

Fig. 6. Separation of eight individual bile acids of group (iii). Mobile phase, water–methanol–acetone (62:9:29) containing 0.1 m*M* ammonium carbonate; other conditions as in Fig. 3.

Fig. 7. Separation of lithocholic acid from other bile acids. Mobile phase, water–methanol–acetone (30:36:34) containing 0.1 m*M* ammonium carbonate; other conditions as in Fig. 3.

flow because of the additional flow-through damper not being used in recording the chromatogram shown in Fig. 8. These larger noises made the apparent sensitivity for sulphated bile acids lower than that for the unsulphated acids, although the actual detector response was virtually the same in spite of the increased salt concentration.

On the basis of the argument made by Goto *et al.*[19] that the order of elution of 3-sulphated bile acids is identical with that of unsulphated bile acids, LC-3αS may be

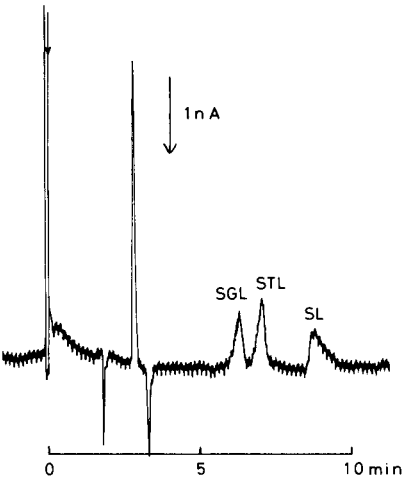

Fig. 8. Separation of three 3α-sulphates of free and conjugated lithocholic acids. Mobile phase, water–methanol–acetone (66:20:14) containing 0.2 m*M* ammonium carbonate; other conditions as in Fig. 3.

regarded as the last species eluted among all 3-sulphated bile acids under the conditions employed in this study. The retention time of GUDC, which was eluted first among the unsulphated bile acids, was 14 min and longer than that of LC-3αS by 4 min under the conditions indicated in Fig. 8. This suggests that the sulphated bile acids can be separated easily from the unsulphated bile acids.

Detector response and detection limits

An example of the dependence of the detector response on the amount of a bile acid injected is illustrated in Fig. 9. The slope of the calibration graph in Fig. 9 is nearly unity in the examined range of amounts injected of 0.1–10 μg.

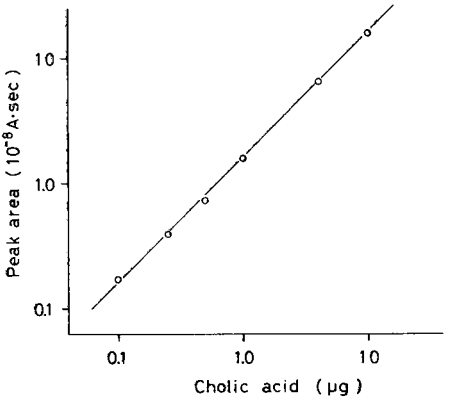

Fig. 9. Dependence of peak area on the amount of cholic acid injected. Flow-rate, 0.7 ml/min; other conditions as in Fig. 5.

The detection limit of the streaming current detector was 100 ng for the individual bile acids eluted at $k' \approx 1$. The detection limit is, as noted above, largely dependent on the concentration of ammonium carbonate in the mobile phase and the above value was determined at a concentration of 0.1 m*M*. The relationship between the concentration of ammonium carbonate and detection limit was investigated for the peak at $k' \approx 1$: for concentrations of 0, 0.1, 1 and 4 m*M*, the detection limits were 20, 100, 500 and 5000 ng, respectively. No significant differences in detector response were observed among free, glyco-conjugated, tauro-conjugated and sulphated bile acids under the condition as described above.

Application to human serum

Blank test. A control serum was deproteinized as described under Experimental and subjected to HPLC to give the chromatogram shown in Fig. 10. The only peak observed was a major one at 2–4 min, which may be assigned to inorganic ions and other ionic species such as amino acids because they are hardly retained under the reversed-phase condition employed. This result implies that the bile acids expected to be originally contained in a control serum could not be detected. That no peak was observed in the region of the bile acids means that no contaminant will interfere in the analysis of the bile acids in serum from a patient with a liver disease.

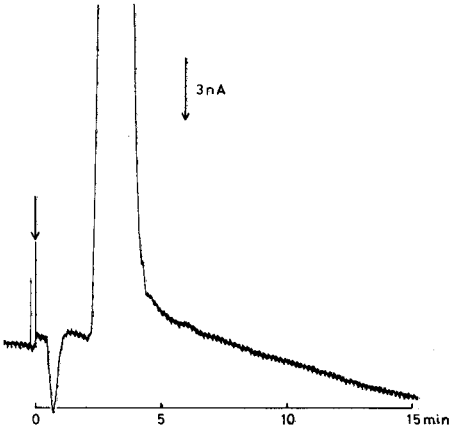

Fig. 10. Blank test of a human serum. A control serum of 1 ml was deproteinized, concentrated to 100 μl and introduced into the HPLC system. Column, Develosil ODS-5, 25 cm × 4.6 mm I.D.; pre-column, Develosil ODS-5, 5 cm × 4.6 mm I.D.; mobile phase, water–methanol–acetone (3:1:1) containing 0.1 m*M* ammonium carbonate; flow-rate, 0.8 ml/min; sample size, 25 μl.

Recovery of bile acids in serum samples. A synthetic mixture was prepared by the addition of four bile acids, 10.8 μg of GC, 38.6 μg of TC, 12.8 μg of GCDC and 36.1 μg of TCDC, to 1 ml of a control serum. It was pre-treated as described above and analysed by HPLC. A chromatogram of the synthetic serum sample is shown in Fig. 11. The recoveries were 83, 74, 97 and 100% for GC, TC, GCDC and TCDC, respectively. The recovery of cholic acid added to serum was found to be 90% by the same procedure in a separate test.

Retention behaviour of bile acids

The structure *versus* mobility relationship of bile acids in reversed-phase HPLC at pH 7.0 has been discussed in terms of the contributions of substituents to mobili-

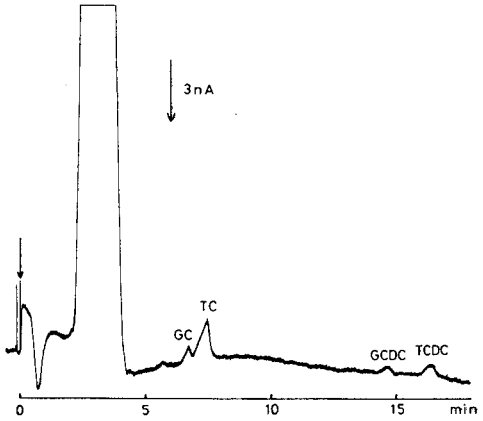

Fig. 11. Chromatogram of a synthetic serum sample. The sample, prepared by adding 10.8 μg of GC, 38.6 μg of TC, 12.8 μg of GCDC and 36.1 μg of TCDC to 1 ml of control serum, was pre-treated as described in Fig. 10. Sample size, 10 μl; other conditions as in Fig. 10.

ty[20]. Bloch and Watkins[7] found that the separation factors between glyco- and tauro-conjugates in reversed-phase HPLC at pH 4.7 are independent of the core bile acids and, therefore, the separation factors associated with differences in the parent structure are independent of the amino acid moiety. The relationship between selectivity and structure mentioned by them was confirmed for the three solvent systems employed in the present study. However, the selectivities between free and either glyco- or tauro-conjugated bile acids appear not to follow this relationship, as judged from the present results.

Five different bile acids having identical amino acid moieties were eluted in the order UDC, C, CDC, DC and LC irrespective of the carboxyl group at C-24 being unconjugated, glyco-conjugated or tauro-conjugated. This order seems general for reversed-phase HPLC regardless of pH and salt concentration in the mobile phase[3,4,7,11,12].

On the other hand, the order of elution of unconjugated, glyco-conjugated and tauro-conjugated bile acids having identical parent structures has been reported to depend on pH and salt concentration[4,14,19]. In the present study, the elution of these three types was in the order tauro-conjugated, glyco-conjugated and unconjugated bile acids with water–methanol as the mobile phase, and in the order glyco-conjugated, tauro-conjugated and unconjugated bile acids with water–acetone. A similar retention behaviour was observed between water–methanol and water–tetrahydrofuran and between water–acetone and water–acetonitrile binary mixtures containing 0.1 m*M* ammonium carbonate in a preliminary experiment.

The relative retention between unconjugated and glyco- and tauro-conjugated bile acids mentioned above was found to be reversed with concentrations of ammonium carbonate higher than 0.5 m*M* in water–methanol. No attempt was made to clarify the effect of pH on the retention behaviour of the bile acids because of the very low concentration of the salt employed. The pH measured for 0.1 m*M* ammonium carbonate was about 9.0. The life of the column was longer than 6 months, no significant decrease in efficiency being observed despite the high pH of the mobile phase.

Comparison between the streaming current detector and the UV detector

An outstanding characteristic of the streaming current detector is that it shows almost equal sensitivities to all kinds of bile acids. The sensitivity of the UV detector at about 200 nm may be slightly superior or equivalent to that of the streaming current detector for detecting glyco- and tauro-conjugated bile acids[4,12]. For the detection of unconjugated bile acids, however, the latter is about five times more sensitive than the former.

Chromatograms recorded simultaneously with both detectors are illustrated in Fig. 12 for comparison. In these chromatograms, glyco- and tauro-conjugated bile acids were not resolved because of the use of water–methanol as the mobile phase. It is evident that no appreciable unknown peaks were revealed by the streaming current detector and that in contrast, some extra peaks could seriously interfere in the detection of bile acids in serum samples using the UV detector.

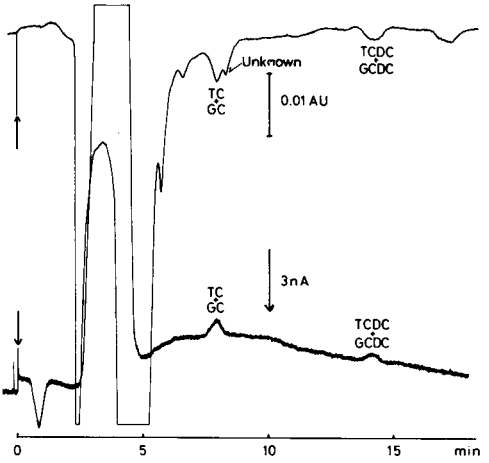

Fig. 12. Comparison of the streaming current detector (lower trace) and the UV detector (upper trace). A synthetic serum sample was prepared and pre-treated as described in Fig. 11. Mobile phase, water–methanol (42:58) containing 0.1 m*M* ammonium carbonate; detection (UV), 210 nm; sample size, 10 μl; other conditions as in Fig. 10.

CONCLUSION

Fifteen individual bile acids were separated successfully under reversed-phase chromatographic conditions, but it required the use of four mobile phases, which is impractical for routine analysis. It is desirable for the individual bile acids to be resolved completely with at most two isocratic conditions in clinical analysis. The use of a fourth organic modifier, *i.e.*, the use of a quaternary solvent system, may improve this undesirable situation, as the change of the salt concentration is fairly limited for the streaming current detector.

It is concluded that the streaming current detector is capable of detecting bile acids in amounts as low as 0.1 μg under reversed-phase chromatographic conditions. At present it is not sensitive enough to detect the bile acids contained in a control serum, but sensitive enough to detect the bile acids in bile or in serum samples from patients suffering from various hepatobiliary diseases.

ACKNOWLEDGEMENTS

The authors gratefully acknowledge the kind donation by Dr. K. Uchida of Shionogi Research Laboratory of all the bile acids employed. They also thank the Asahi Glass Foundation for Industrial Technology for financial assistance.

REFERENCES

1 S. Terabe, K. Yamamoto and T. Ando, *Can. J. Chem.*, 59 (1981) 1531.
2 K. Šlais and M. Krejčí, *J. Chromatogr.*, 148 (1978) 99.
3 S. Okuyama, N. Kokubun, S. Higashidate, D. Uemura and Y. Hirata, *Chem. Lett.*, (1979) 1443.
4 J. Goto, H. Kato, Y. Saruta and T. Nambara, *J. Liquid Chromatogr.*, 3 (1980) 991.
5 N. A. Parris, *J. Chromatogr.*, 133 (1977) 273.

6 R. Shaw, J. A. Smith and W. H. Elliott, *Anal. Biochem.*, 86 (1978) 450.
7 C. A. Bloch and J. B. Watkins, *J. Lipid Res.*, 19 (1978) 510.
8 R. W. R. Baker, J. Ferrett and G. M. Murphy, *J. Chromatogr.*, 146 (1978) 137.
9 D. Baylocq, A. Guffroy, F. Pellerin and J. P. Ferrier, *C.R. Acad. Sci., Ser. C*, 286 (1978) 71.
10 D. P. Matthees and W. C. Purdy, *Anal. Chim. Acta*, 109 (1979) 161.
11 G. Mingrone, A. V. Greco and S. Passi, *J. Chromatogr.*, 183 (1980) 277.
12 F. Nakayama and M. Nakagaki, *J. Chromatogr.*, 183 (1980) 287.
13 K. Arisue, Z. Ogawa, K. Kohda, C. Hayashi and Y. Ishida, *Jap. J. Clin. Chim.*, 9 (1980) 104.
14 K. Shimada, M. Hasegawa, J. Goto and T. Nambara, *J. Chromatogr.*, 152 (1978) 431.
15 S. Okuyama, D. Uemura and Y. Hirata, *Bull. Chem. Soc. Jap.*, 52 (1979) 124.
16 S. Okuyama, D. Uemura and Y. Hirata, *Chem. Lett.*, (1979) 461.
17 F. Takeda, K. Suminoe, R. Uenoyama, S. Baba and Y. Kameno, *Jap. J. Gastroenterol.*, 76, Suppl. (1979) 610.
18 D. Uemura, *Kagaku no Ryoiki, Zokan*, No. 133 (1981) 129.
19 J. Goto, H. Kato and T. Nambara, *J. Liquid Chromatogr.*, 3 (1980) 645.
20 R. Shaw, M. Rivetna and W. H. Elliott, *J. Chromatogr.*, 209 (1980) 347.

Journal of Chromatography, 239 (1982) 527–536
Elsevier Scientific Publishing Company, Amsterdam — Printed in the Netherlands

CHROM. 14,770

HYDROPHOBICITY AND CHROMATOGRAPHIC BEHAVIOUR OF AROMATIC ACIDS FOUND IN URINE*

T. HANAI and J. HUBERT*
Université de Montréal, Département de Chimie, C.P. 6210, Succ.A, Montréal, Québec H3C 3V1 (Canada)

SUMMARY

In reversed-phase liquid chromatography, the capacity ratios of urinary compounds were related with their hydrophobicity calculated by Rekker's hydrophobic fragmental constants. The retention behaviour of these compounds differed from that of non-ionizable compounds whose retention time can be predicted in different mixtures of acetonitrile and water as eluent and on an octadecyl silica packing from their calculated hydrophobicity. However, the calculated values for hydrophobicity and/or those derived from the results obtained for non-ionizable compounds could be useful to analyze the metabolites of acidic compounds in urine. The retention behaviour of all the compounds on gradient elution is also discussed.

INTRODUCTION

One of the challenges in liquid chromatography (LC) is the development of qualitative analyses for organic metabolites. The metabolites are usually purified by LC or gas chromatography and identified by spectrophotometric methods.

For qualitative analysis by LC, different approaches (use of resonance energy[1], delocalization energy[2], number of carbon atoms in the alkyl chain, dipole moment[3,4], Van der Waals radius or electronegativity[3]) have been used to characterize the solutes. The thermodynamic equilibrium of the solutes between mobile and stationary phases[5,6] has also been investigated and applied to the separation of catecholamine derivatives[7].

Another approach was the use of hydrophobicity for compounds in their molecular form[8–10]. The hydrophobicity of solutes was calculated with Rekker's hydrophobic fragmental constants[11], which were derived from the partition coefficients by Hansch's method. The partition coefficients for several compounds were also directly measured in LC and related to observed capacity ratios[12–14].

In order to predict the retention time of solutes in LC, different packings and organic modifiers were previously tested to find a practical system. The system formed by acetonitrile–water and a chemically bonded octadecyl packing was found to be suitable for qualitative analysis. For aliphatic alcohols and polyaromatic hydrocarbons a linear relation was found between the calculated hydrophobicity and the

* Part of this paper was presented at the *63rd Conference of the Chemical Institute of Canada, Ottawa, June 1980.*

0021-9673/82/0000–0000/$02.75

TABLE I

HYDROPHOBICITY OF URINARY AND STANDARD COMPOUNDS

No.	*Compound*	*log* P_c*	*k'*			
			% Acetonitrile			
			90	*80*	*70*	*60*
1	Benzoic acid	1.79	0.512	0.581	0.702	0.890
2	2-Hydroxybenzoic acid	1.90	0.558	0.644	0.777	1.066
3	3-Hydroxybenzoic acid	1.25	0.402	0.414	0.445	0.575
4	4-Hydroxybenzoic acid	1.25	0.393	0.405	0.443	0.541
5	2,4-Dihydroxybenzoic acid	1.30	0.391	0.414	0.486	0.647
6	3,4-Dihydroxybenzoic acid	0.65	0.370	0.365	0.376	0.471
7	3.5-Dihydroxybenzoic acid	0.65	0.350	0.327	0.362	0.434
8	3,4,5-Trihydroxybenzoic acid	−0.011	0.333	0.356	0.333	0.373
9	3-Methoxybenzoic acid	1.86	–	–	–	–
10	4-Hydroxy-3-methoxybenzoic acid	1.26	0.419	0.431	0.454	0.558
11	Cyclohexanecarboxylic acid	1.93	0.529	0.595	0.725	0.887
12	Phenylacetic acid	1.75	0.417	0.538	0.673	0.864
13	2-Hydroxyphenylacetic acid	1.21	0.402	0.434	0.486	0.607
14	4-Hydroxyphenylacetic acid	1.21	0.385	0.396	0.443	0.529
15	2,5-Dihydroxyphenylacetic acid	0.61	–	–	–	–
16	3,4-Dihydroxyphenylacetic acid	0.61	0.368	0.342	0.382	0.434
17	3-Methoxyphenylacetic acid	1.82	0.477	0.520	0.665	0.884
18	4-Methoxyphenylacetic acid	1.82	0.466	0.532	0.639	0.858
19	4-Hydroxy-3-methoxyphenylacetic acid	1.22	–	–	–	–
20	Indoleacetic acid	1.75	–	–	–	–
21	Indolepropionic acid	1.99	0.469	0.523	0.673	0.904
22	5-Hydroxyindoleacetic acid	1.23	–	–	–	–
23	Tryptophan	1.13	1.181	0.751	0.694	0.541
24	5-Hydroxytryptophan	0.61	–	–	–	–
25	Cinnamic acid	2.26	0.541	0.624	0.800	1.037
26	4-Hydroxycinnamic acid	1.72	–	–	–	–
27	3,4-Dihydroxycinnamic acid	1.12	0.370	0.365	–	0.443
28	3-Methoxycinnamic acid	2.33	–	–	–	–
29	4-Hydroxy-3-methoxycinnamic acid	1.79	–	–	–	–
30	Hydrocinnamic acid	1.99	0.552	0.616	0.780	1.043
31	Mandelic acid	1.23	0.402	0.428	0.486	0.515
32	3-Methoxymandelic acid	1.30	0.411	0.425	0.486	0.529
33	4-Hydroxy-3-methoxymandelic acid	0.76	–	–	–	–
34	2-Naphthoic acid	2.72	0.673	0.881	1.424	1.559
35	3-Hydroxy-2-naphthoic acid	2.83	0.691	0.884	1.212	1.902
36	Hippuric acid	1.04	0.411	0.379	0.437	0.544
37	2-Hydroxyhippuric acid	1.15	–	–	–	–
38	Nicotinic acid	0.43	0.999	0.682	0.500	0.443
39	Uric acid	–	0.310	0.269	0.229	0.212
40	Caffeine	–	0.639	0.558	0.543	0.587
41	Theobromine	–	0.460	0.399	0.369	0.362
42	Xanthine	–	0.333	0.298	0.248	0.249
43	Phenacetin	1.62	0.613	0.653	0.774	1.020
44	Uracil	–	0.396	0.327	0.304	0.307
45	Benzylalcohol	0.93	0.569	0.616	0.694	0.846

						*log P_m***	*log P_r****
50	*40*	*30*	*20*	*10*	*0*		
1.175	1.732	3.132	6.934	–	–	1.94	1.86, 1.87 (11)
1.522	2.280	4.424	10.05	–	–	2.18	2.26, 2.31 (11)
0.725	0.875	1.382	2.667	8.752	–	1.37	1.32, 1.36, 1.50 (11)
0.659	0.795	1.224	2.116	6.527	–	1.28	1.31, 1.36, 1.58 (11)
0.789	1.054	1.750	3.299	10.71	–	1.51	
0.494	0.564	0.763	1.193	3.440	18.45	0.99	
0.471	0.541	0.760	1.35	3.345	25.06	0.94	
0.393	0.443	0.535	0.699	1.634	9.03	0.72	
1.193	1.937	3.789	–	–	–	1.99	2.02 (11)
0.659	0.844	1.268	2.384	8.735	–	1.31	
1.279	1.787	3.045	7.050	–	–	1.96	
1.230	1.741	3.160	6.882	–	–	1.94	1.41, 1.42, 1.45, 1.96 (11)
0.797	1.011	1.556	3.065	9.127	–	1.47	
0.692	0.795	1.135	2.009	5.953	–	1.26	0.85 (11)§
–	–	0.673	0.916	1.949	10.86	0.86	
0.538	0.558	9.751	1.184	3.147	22.08	0.98	
1.222	1.827	3.466	8.550	–	–	1.99	1.46, 1.50 (11)
1.187	1.729	3.305	8.108	–	–	1.95	1.42, 1.46 (11)
0.569	0.777	1.147	–	–	–	1.18	
–	1.637	3.287	8.342	–	–	1.92	1.39, 1.41 (11)
1.366	2.370	5.544	17.34	–	–	2.20	
–	0.702	1.121	1.822	6.363	–	1.17	
0.515	0.607	0.815	1.545	6.184	–	1.09	
–	0.365	0.483	0.656	1.885	23.23	0.62	
1.606	2.647	6.103	18.89	–	–	2.32	2.13, 2.25 (11)
0.720	1.043	1.891	–	–	–	1.46	
0.544	0.691	1.155	2.381	10.72	–	1.15	
1.608	2.976	7.223	–	–	–	2.37	
0.731	1.118	2.087	–	–	–	1.51	
1.562	2.405	5.174	13.89	–	–	2.25	1.84 (11)
0.665	0.789	1.230	2.061	4.724	–	1.26	
0.694	0.846	1.380	2.635	7.482	–	1.33	
–	–	0.670	0.832	1.692	7.03	0.84	
2.503	4.995	13.02	–	–	–	2.84	
3.077	5.463	18.45	–	–	–	3.05	
0.639	0.722	1.184	2.125	5.818	–	1.25	
–	–	1.738	3.830	13.23	–	1.55	
0.492	0.379	0.431	0.443	0.558	2.26	0.66	
0.180	0.209	0.321	0.359	0.561	4.83	0.18	
0.636	0.668	0.994	1.920	8.645	–	0.59	−0.07 (13)
0.376	0.368	0.558	0.771	2.381	–	0.69	
0.255	0.232	0.385	0.428	0.844	6.32	0.30	
1.351	1.986	3.942	9.828	–	–	1.47	
0.258	0.298	0.422	0.443	0.616	2.36	0.42	
1.161	1.764	2.332	3.821	–	–	1.19	

(Continued on p. 530)

TABLE I *(continued)*

No.	*Compound*	*log P_c**	*k'*			
			% Acetonitrile			
			90	*80*	*70*	*60*
46	Cinnaminal	1.49	0.621	0.699	0.864	1.129
47	Indole	2.06	0.644	0.783	1.100	1.654
48	Phenol	1.54	0.523	0.595	0.720	0.921
49	Naphthalene	3.21	0.985	1.424	2.185	3.850
50	Butylophenone	2.81	0.870	1.158	1.706	2.681
51	Propiophenone	2.28	0.754	0.971	1.363	1.960
52	Acetophenone	1.75	0.679	0.803	1.051	1.398
53	2-Hydroxyacetophenone	1.21	0.581	0.616	0.708	0.774
54	Isopentylbenzoate	4.15	1.305	2.087	3.564	6.897
55	Butylbenzoate	3.74	1.141	1.741	2.837	5.145
56	Isopropylbenzoate	3.09	0.962	1.380	2.087	3.432
57	Methylbenzoate	2.15	0.771	0.962	1.317	1.926
58	4-Hydroxypropylbenzoate	2.72	0.630	0.740	1.010	1.525

* log P_c values were calculated by Rekker's hydrophobic fragmental constants.
** log P_m values are mean values of observed data in 20–60% acetonitrile in water with 0.04 *M* phosphoric acid.
*** log P_r values are mainly collected from ref. 11.
§ This value is the one of 3-hydroxyphenylacetic acid.

logarithm of the capacity ratios[9]. It was not necessary to classify the solutes in different categories, including the ones with a surface of covalently bonded hydrogen atoms and the others with a surface of non-covalently bonded electrons[15].

In this article, a liquid chromatographic system was used for the separation of aromatic acids. Compounds found in urine (urinary compounds) were selected as solutes and their calculated hydrophobicity was related with their capacity ratios in reversed-phase LC separation with acetonitrile–water mixtures as eluents. The results obtained were compared with those of non-ionizable compounds.

EXPERIMENTAL AND RESULTS

The solutes listed in Table I were supplied from Sigma and Chem. Service. The instruments and solvents were used as previously described[9,10]. The capacity ratios obtained in the system of a 5 μm octadecyl silica packing (Chromosorb LC-7 from Johns Manville) and different acetonitrile–water mixtures with 0.04 *M* phosphoric acid are also listed in Table I.

The linear relations between log *k'* and the hydrophobicity log P_c (calculated after Rekker) for non-ionizable compounds (Nos. 49–57 in Table I) in 30–90% acetonitrile–water mixtures at pH 2 were obtained with correlation coefficients higher than 0.995. All the straight lines merged at a single point. This fact allows the prediction of the retention times of non-ionizable compounds in a system with an octadecyl bonded silica as packing and a known concentration of acetonitrile in the eluent[8]. The slopes of the lines obtained in 70, 80 and 90% acetonitrile–water mixtures with phosphoric acid are identical to those of eluents without acid. Thus, the

						*log P_m***	*log P_r****
50	*40*	*30*	*20*	*10*	*0*		
1.631	2.606	5.394	13.81	–	–	1.67	1.95, 2.03 (11)
2.765	4.909	10.64	–	–	–	2.17	2.00, 2.06, 2.13, 2.14, 2.25 (11)
1.334	1.467	3.039	4.810	–	–	1.28	1.46, 1.48, 1.54 (11)
7.275	14.74	–	–	–	–	3.21	3.01, 3.18, 3.30, 3.37, 3.48, 3.59 (11)
4.877	9.828	–	–	–	–	2.77	
3.290	5.832	12.26	–	–	–	2.30	
2.125	3.299	5.924	–	–	–	1.83	1.58, 1.70, 1.73 (11)
1.034	1.372	2.024	–	–	–	1.07	
15.45	–	–	–	–	–	4.10	
10.68	–	–	–	–	–	3.68	
6.501	14.67	–	–	–	–	3.11	
3.031	5.391	10.98	–	–	–	2.24	2.12, 2.17 (11)
2.508	4.967	12.49	–	–	–	2.15	

retention behaviour of non-ionizable compounds was not influenced by addition of the acid in the eluents. From the least-square lines the hydrophobicities log P_0 of the different compounds were calculated using the experimental values of log k'. The mean value log P_m of the hydrophobicities log P_0 obtained for different eluents are also given in Table I.

The same approach was applied to study the retention behaviour of aromatic acids. The correlation coefficients between log k' and log P_c of aromatic acids were not as good as those of non-ionizable compounds and the values in 80, 70, 60, 50, 40, 30, 20 and 10% acetonitrile in water at pH 2 were 0.857 (n = 26), 0.939 (n = 25), 0.960 (n = 26), 0.942 (n = 31), 0.957 (n = 34), 0.964 (n = 37), 0.954 (n = 30) and 0.848 (n = 20) respectively (n is the number of compounds which were studied).

The hydrophobicities log P_0 for these compounds were calculated with the results obtained for the non-ionizable compounds and examples of the variation of log P_0 with the acetonitrile concentration are reported in Figs. 1 and 2.

For the analysis of compounds in urine, an elution gradient was required and the influence of the gradient length on the relative retention defined as $(V_r - V_0)/V_0$ is shown in Fig. 3. The relationships between the relative retention and log P_c or log P_m are shown in Figs. 4 and 5.

DISCUSSION

In Fig. 1, we can notice that the log P_0 values of non-ionizable compounds are not influenced by the acetonitrile concentration with the exception of phenolic compounds. An example of the behaviour of phenols is given (No. 58) in Fig. 1. In a water rich eluent, the log k' and consequently log P_0 increased for phenols and therefore the

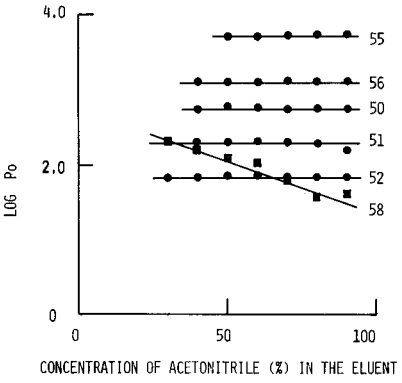

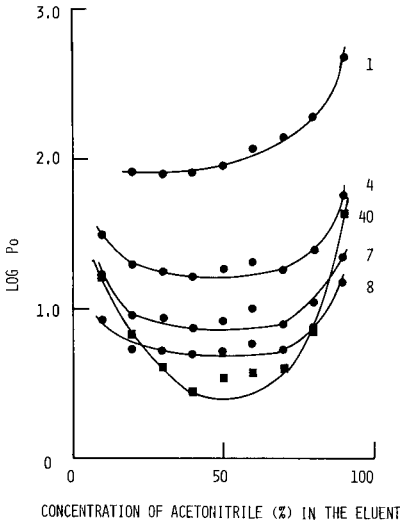

Fig. 1. Relation between log P_0 of non-ionizable compounds and concentration of acetonitrile in water. The column was an octadecyl silica packing (Chromosorb LC-7) and the eluents were acetonitrile–water mixtures with 0.04 *M* phosphoric acid. The numbers after the symbols refer to the compounds listed in Table I.

Fig. 2. Relation between log P_0 of ionizable compounds and concentration of acetonitrile in water. The experimental conditions are the same as in Fig. 1.

prediction of retention time for phenols will be discussed separately in a future paper.

For acidic compounds, the hydrophobicity increases in eluents with acetonitrile concentration higher than 70% (Nos. 1, 4, 7 and 8). Only the hydrophobicities log P_0 obtained for acetonitrile–water mixtures up to 60% acetonitrile were used for the calculation of log P_m in Table I.

The large capacity ratios and hence the high hydrophobicities for ionizable compounds in acetonitrile–water mixtures with a large proportion of acetonitrile could be explained by the poor solvation of these compounds in acetonitrile or by the direct adsorption on the surface of the packing.

The mean value log P_m obtained for the hydrophobicities in different eluent mixtures is usually similar to the values obtained with Rekker's hydrophobic fragmental constants (log P_c). The largest discrepancies were observed for 3,4,5-trihydroxybenzoic acid and nitrogen heterocyclic compounds.

The change of hydrophobicity for nitrogen containing heterocycles was important and irregular, especially for caffeine, theobromine, xanthine and tryptophan (Nos. 23, 40, 41 and 42). The behaviour of these nitrogen heterocycles is still unexplained in separation on bonded phase silica packings. One possible explanation could be the existence of unreacted silanol groups on the packing and therefore the interaction should not be only hydrophobic in nature[16].

From the above results it can be concluded that for eluents with acetonitrile concentrations between 20 and 60% the differences between log P_c and log P_m are small, the correlation between log P_c and log k' is good and it is therefore possible to predict the retention times from the values of log P_c. Better prediction for retention times can be made with the log P_m values.

The different chromatographic behaviour for polar and non-polar compounds made the discussion of the retention mechanism difficult. The change of the ratio of acetonitrile to water affects only slightly the dipole moment. This phenomenon differs from the one observed in mixtures of water and methanol or tetrahydrofuran, whereas the hydrogen bonding is more changed[24]. However, a preclassification of solutes according to their nature may allow the development of qualitative analysis in reversed-phase LC from the hydrophobicity log P or related values.

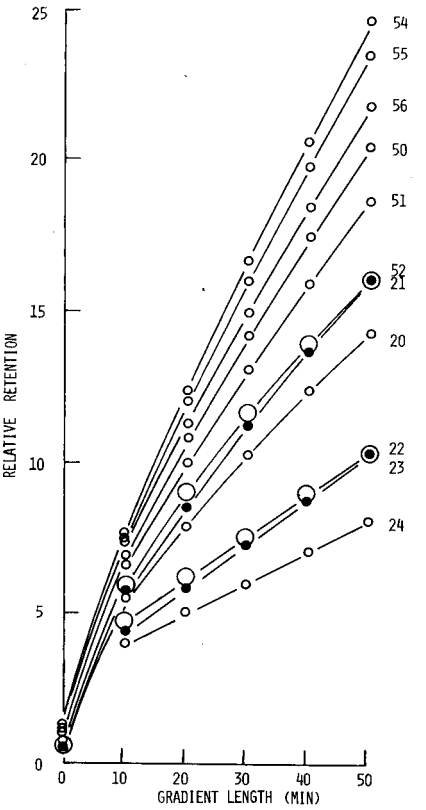

Fig. 3. Influence of the gradient length on relative retentions. The packing was Chromosorb LC-7, the flow-rate was 1ml/min. The linear gradient elution was from 0.04 M phosphoric acid to 90% acetonitrile–water with 0.04 M phosphoric acid. The detection was done at 254 nm. The numbers after symbols indicate the compounds listed in Table I.

Effect of hydroxylation on retention

The differences between the hydrophobicity of hydroxy-substituted compounds and the hydrophobicity of the unsubstituted parent compounds were calculated for both the observed and calculated values of log P. The values of the differences (Δ log P) are summarized in Table II.

The *ortho*-monosubstituted compounds for which an intramolecular hydrogen bond exists were more retained than their parent compounds (Δ log $P > 0$). The *meta*- and *para*-monohydroxy compounds were less retained than the parent com-

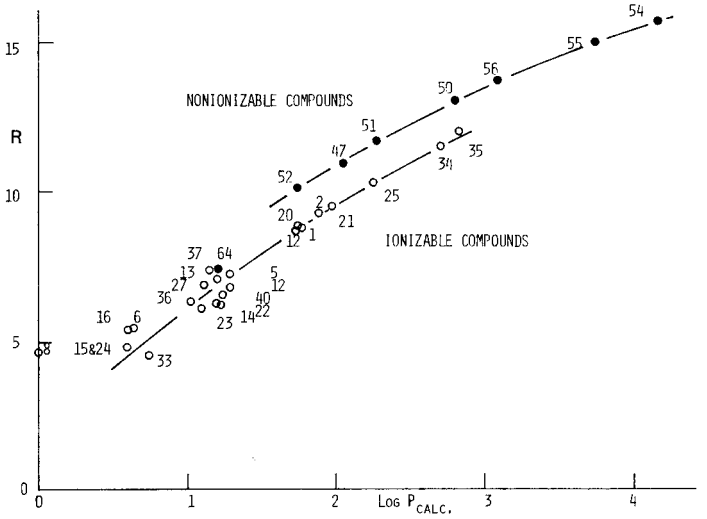

Fig. 4. Relation between log P_c and relative retention in a linear gradient elution. A 30-min gradient was used. For experimental conditions, see Fig. 3. R = relative retention.

pounds (Δ log $P < 0$). The di- and trisubstituted compounds were also less retained than their parent compounds.

For the di- and tri-substituted compounds in which intramolecular bonding can be expected (2-hydroxyphenylacetic acid, No. 13, and 2,4-dihydroxybenzoic acid, No. 5) the log P_m value and hence the retention was higher than for compounds with the same degree of substitution on the parent molecule (4-hydroxyphenylacetic acid, No. 14, and 3,4-dihydroxybenzoic acid, No. 6, respectively).

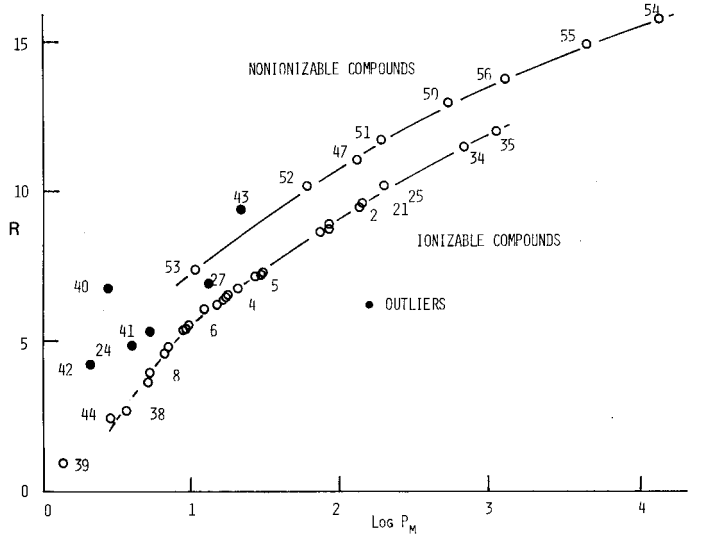

Fig. 5. Relation between log P_m and relative retention on a linear gradient. For experimental conditions, see Fig. 4. R = relative retention.

It is therefore important to introduce correcting factors based on the number and position of substituents for a more accurate calculation of hydrophobicity and hence a better prediction of retention times.

Effect of gradient

For practical analyses of urine samples, a gradient has to be used for fast separation, and it is therefore important to examine the change of the retention time (or volume) with the gradient length on one hand, and on the other hand, the change of the retention time (or volume) with the log P_0 for a given gradient. The relative retention was calculated from $(V_r - V_0)/V_0$. A linear gradient with a starting eluent of 0 or 10% acetonitrile in water mixture with 0.04 *M* phosphoric acid and a final eluent of 90% acetonitrile in water with 0.04 *M* phosphoric acid was used. The variation of the relative retention with the length of the gradient is shown in Fig. 3.

TABLE II

Δ log *P* FOR HYDROXYLATION*

Type of compounds	*Number of the compound*	Δ log P_{calc}	Δ log P_{obs}
Monosubstituted with intra-molecular bonding	2,35,37	0.11	0.23 ± 0.03
Monosubstituted	3,4,10,14,19,22,26,53	−0.54	−0.70 ± 0.11
Disubstituted	6,7,15,16,27	−1.14	−1.03 ± 0.12
Trisubstituted	8	−1.80	−1.20

* Δ log *P* is the difference between log *P* of the hydroxy-substituted compound and log *P* of the parent compound.

The relative retention of different types of compounds were affected by the gradient length and no linear relation was observed. The examples are separation of No. 21 from No. 52 and No. 23 from No. 22. These compounds are indicated as fused circles and large circles in Fig. 3. Even if the column efficiency was good, some separation became difficult in longer gradient length due to the change of selectivity. This phenomenon was expected from the results in Figs. 1 and 2. Such selectivity change was also seen in the separation of caffeine and phenacetin. The elution order was reversed in different mixtures of methanol and water[23] and therefore, in discussion of selectivity, the compounds have to be carefully selected.

In Figs. 4 and 5, the relations between the relative retention and log P_c (or log P_m) of the standard compounds are shown. The chromatography was done with a 30-min linear gradient.

The behaviour of the two classes of compounds, *i.e.* ionizable and non-ionizable, is more apparent in Fig. 5. Most compounds in each class were located on the same curve. As mentioned before, even by using log P_m instead of log P_c, some compounds, especially nitrogen heterocyclic compounds showed a different chromatographic behaviour in this system.

CONCLUSION

The qualitative analysis in reversed-phase liquid chromatography is different from that with an organic solvent as eluent[17–22]. The selection of the organic modifier is limited, hence the main solubility parameter could be the hydrophobicity. The use of Rekker's hydrophobic fragmental constants was shown to be a simple and useful approach to qualitative analysis.

The retention times for aromatic acids were related with their log P values even with gradient elution. Regular changes were found for log P on hydroxylation of aromatic acids. Further studies are still required to understand the different steric effects and to introduce correction factors for the calculation. Nevertheless the log P can be used as a first approach to qualitative analysis. The log k' values differ from column to column, but the log P values are relatively constant.

ACKNOWLEDGEMENTS

The authors thank the National Sciences and Engineering Research Council of Canada for its financial support (grants RD-171 and A-0834).

REFERENCES

1 C. A. Streuli, *J. Chromatogr.*, 56 (1971) 219 and 225.
2 C. A. Streuli, *J. Chromatogr.*, 62 (1971) 73.
3 M. Yamada, N. Nomura and D.-I. Shiho, *J. Chromatogr.*, 64 (1972) 253.
4 J. F. Schabron, R. J. Hurtubise and H. F. Silver, *Anal. Chem.*, 50 (1978) 1911.
5 R. Tijssen, H. A. H. Billiet and P. J. Schoenmakers, *J. Chromatogr.*, 122 (1976) 185.
6 W. Melander, D. E. Campbell and Cs. Horváth, *J. Chromatogr.*, 158 (1978) 215.
7 B.-K. Chen and Cs. Horváth, *J. Chromatogr.*, 171 (1979) 15.
8 T. Hanai, *Chromatographia*, 12 (1979) 77.
9 T. Hanai and M. D'Amboise, *Pittsburgh Conference, Cleveland, March 1979.*
10 T. Hanai and J. Hubert, *6th FACSS Meeting, Philadelphia, September 1979.*
11 R. F. Rekker, *The Hydrophobic Fragmental Constant*, Elsevier, Amsterdam, 1977.
12 D. Henry, J. H. Block, J. L. Anderson and G. R. Carson, *J. Med. Chem.*, 19 (1976) 619.
13 M. S. Mirrles, S. J. Moulton, C. T. Murphy and P. J. Tayler, *J. Med. Chem.*, 19 (1976) 615.
14 K. Miyake and H. Terada, *J. Chromatogr.*, 157 (1978) 386.
15 A. Leo, C. Hansch and P. Y. C. Jow, *J. Med. Chem.*, 19 (1976) 611.
16 R. P. W. Scott and P. Kucera, *J. Chromatogr.*, 142 (1977) 213.
17 T. Hanai and K. Fujimara, *J. Chromatogr. Sci.*, 14 (1976) 140.
18 T. Hanai, in H. Hatano (Editor), *Shin kosoku ekitai kuromatogurafi (New developments in High-Performance Liquid Chromatography)*, Nankodo, Tokyo, 1978, p. 35.
19 S. Hara, *J. Chromatogr.*, 137 (1977) 41.
20 S. Hara, Y. Fujii, M. Hirasawa and S. Miyamoto, *J. Chromatogr.*, 149 (1978) 143.
21 S. Hara, M. Hirasawa, S. Miyajima and A. Oshawa, *J. Chromatogr.*, 169 (1978) 117.
22 G. Matysik and E. Soczewinski, *J. Chromatogr.*, 160 (1978) 29.
23 T. Hanai, in H. Hatano (Editor), *New Developments in High-Performance Liquid Chromatography*, Nankodo, Tokyo, 1978, p. 36.
24 L. R. Snyder, *J. Chromatogr. Sci.*, 16 (1978) 223.

Journal of Chromatography, 239 (1982) 537–548
Elsevier Scientific Publishing Company, Amsterdam — Printed in The Netherlands

CHROM. 14,525

ION CHROMATOGRAPHY WITH AN ION-EXCHANGE MEMBRANE SUPPRESSOR

YUZURU HANAOKA, TAKESHI MURAYAMA, SETSUO MURAMOTO*, TAMIZO MATSUURA and AKINORI NANBA

Analytical Instruments Center, Yokogawa Electric Works, Ltd., 9-32, Naka-cho 2-chome, Musashino-shi, Tokyo 180 (Japan)

SUMMARY

Suppressor and separator column packings for ion chromatography are described. The suppressor consists of fine cation-exchange membrane tubing and an outer plastic tubing, which allow continuous operation with minimum peak broadening without peak height changes or varying water-dip interference.

The separator packing uses small-anion latex-bonded styrene–divinylbenzene copolymer, which gives a high resolution because of a thin superficial macroporous construction. It is also mechanically rigid and chemically extremely stable.

INTRODUCTION

Ion chromatography, first introduced in 1975 by Small *et al.*[1], is a unique combination of a separator with low ion-exchange capacity, a suppressor to remove most of the background conductance of the eluent, and a conductivity detector to locate the peaks. Since its introduction, ion chromatography has become popular and is widely used for the analysis of inorganic anions (and certain cations), because of its fine resolution and high sensitivity.

Although the adoption of a suppressor column enables superior ion-chromatographic performance, it also causes the following problems.

(1) The suppressor column must be regenerated periodically to remove the accumulated ions from the eluent stream. As the separated species are re-mixed in the void volume of the suppressor, a loss of resolution (peak broadening) occurs. The suppressor volume is always a compromise between regeneration frequency and chromatogram resolution.

(2) Owing to interaction with the suppressor column, the peak height of the nitrite drastically changes as a function of suppressor exhaustion[2]. Retention time of "water dip" also changes accordingly.

For the reasons mentioned above, Gjerde *et al.*[3] proposed to eliminate the suppressor by using an anion-exchange resin of very low capacity, and by adopting an eluent having a very low conductivity. This approach is of limited use, however, because of its low sensitivity and narrow useful concentration range[2].

This paper describes a new type of ion-chromatographic system for the separa-

0021-9673/82/0000–0000/$02.75

tion and quantitative determination of anions. Instead of a suppressor column filled with cation-exchange resin, a new type of suppressor using a cation-exchange membrane tubing was developed, which enables an uninterrupted analysis and lessens the band broadening effect. For the separator column packing, a small-anion latex was bonded to styrene–divinylbenzene copolymer. With this separator and suppressor combination, very sharp anion separations could be achieved and changes of nitrite peak heights proved to be minimal.

EXPERIMENTAL

Suppressor

A diagrammatic view of a suppressor is presented in Fig. 1. It consists of two coaxial tubes. The inner tube is made of perfluorosulphonic acid cation-exchange membrane (Dupont Nafion type 811X), which was heated to 150°C, and stretched to lengthen it 3.75 times to make a fine tubing of 0.4 mm I.D. and 0.55 mm O.D. A 5-m length of this resultant tubing was inserted coaxially into a PTFE tube of 1.0 mm I.D.

Eluent and separated ionic species flow inside the inner tubing while a so-called scavenger (aqueous acid) flows outside. As the cation-exchange membrane is per-

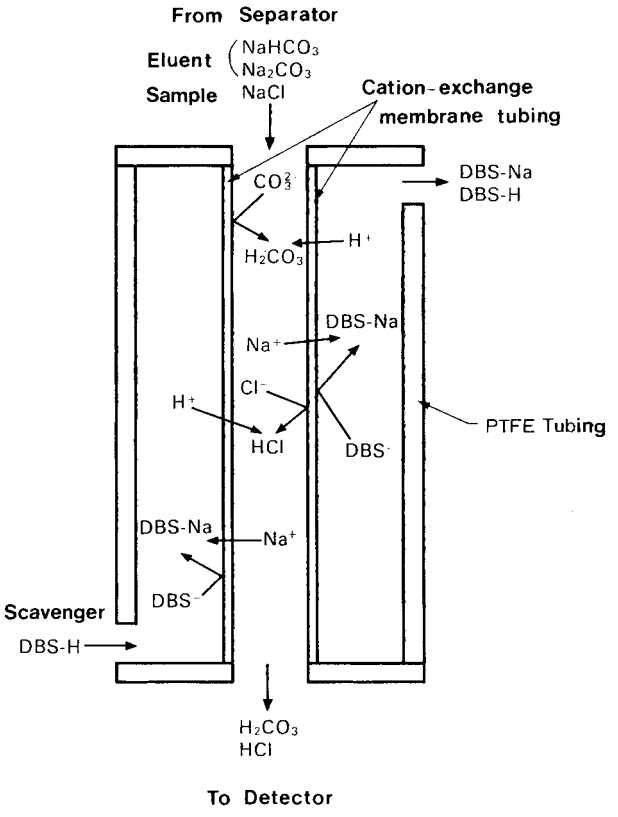

Fig. 1. Theory of operation of a cation-exchange membrane tubing suppressor. DBS-H = dodecylbenzenesulfonic acid; DBS-Na = sodium dodecylbenzenesulphonate.

meable to cations but is impermeable to anions, cations in the eluent and samples are exchanged with hydrogen ions in the scavenger.

Separator resin

A strong base anion-exchange resin AG 1-X8 (200–400 mesh, chloride form, Bio-Rad) was ground and a 0.6 g fraction was suspended in 300 ml of methanol and centrifuged. The resultant ion-exchange resin latex was added to 5 g of styrene–divinylbenzene copolymer MCIGEL CHP-3C (10 μm, Mitsubishi), and the methanol was evaporated in a 60°C hot bath. Just before all the methanol had evaporated, 0.25 g of a mixture of chloromethylstyrene and divinylbenzene (95:5) with 1% of α,α'-azobis-isobutyronitrile as a catalyst was added and stirred thoroughly. Polymerization then proceeded for an hour in a 80°C drying oven followed by cooling at room temperature. After the beads had been separated, they were aminated with trimethylamine.

The final product was washed with methanol, water, 1 *M* HCl, and water.

Flow system

The chromatographic system used is shown in Fig. 2. The separator, suppressor and detector are enclosed in a temperature-controlled oven at 40°C to prevent temperature fluctuations.

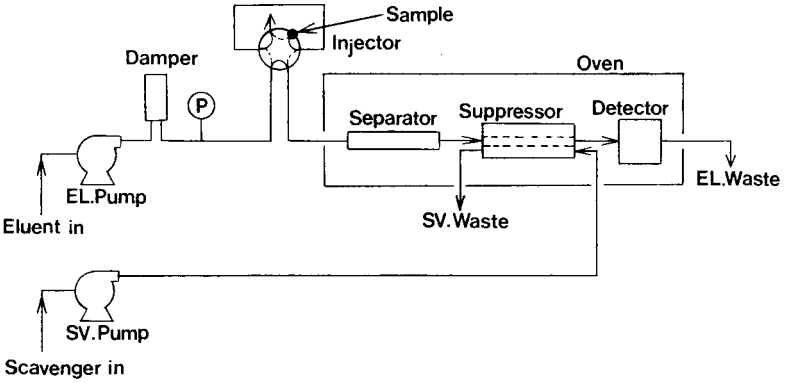

Fig. 2. Flow diagram. Eluent pump, LDC Model 396 Minipump; damper, Waters low-pressure filter; injector, rheodyne 7125; scavenger pump, Iwaki EP diaphragm pump; detector, YEW conductivity detector; oven temperature, 40°C.

Unless otherwise noted, the eluent used is 0.004 *M* Na_2CO_3 and 0.004 *M* $NaHCO_3$, and the scavenger is 0.05 *M* dodecylbenzenesulphonic acid (DBS). The flow-rate is 2 ml/min for both eluent and scavenger.

Standard sample solutions were prepared from reagent grade sodium salts containing 5 ppm fluoride, 10 ppm chloride, 15 ppm nitrite, 30 ppm phosphate, 10 ppm bromide, 30 ppm nitrate, and 40 ppm sulphate.

A conventional Dionex 30829 (100 × 9 mm I.D.) suppressor column packed with cation-exchange resin was used for comparison.

RESULTS AND DISCUSSION

Suppressor

The effect of the suppressor was examined without a separator column by injecting 100 μl of 200 ppm chloride ion, first with water flowing instead of scavenger and then with 0.05 *M* DBS as scavenger. Background conductance decreased significantly from 1.5 mS/cm to 30 μS/cm as soon as the scavenger was used, because sodium carbonate and sodium bicarbonate were converted into carbonic acid which has low conductivity. At the same time, the peak height of the chloride ion increased 2.5 times because sodium chloride was transformed into hydrochloric acid (see Fig. 3).

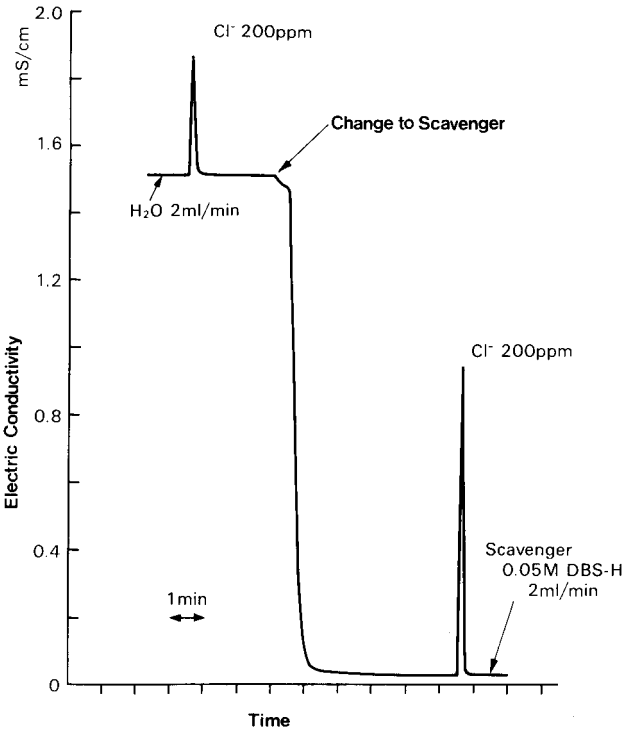

Fig. 3. Effect of the tubing suppressor.

The dependence of the peak height on the tubing length was investigated by injecting 100 μl of 10 ppm chloride ion with a scavenber flow-rate of 2 ml/min. The results (Fig. 4) reveal that 5 m of tubing are sufficient for an eluent with a flow-rate of 2 ml/min and that peak broadening occurs with longer tubing lengths. For an eluent with higher flow-rate or higher concentration, the flow-rate of the scavenger should be changed accordingly.

The scavenger used can be any aqueous acid as long as an ideal cation-exchange membrane is used. But, in practice, the leakage of scavenger into the eluent is inevitable, and therefore the molecular weight of the scavenger should be as large as possible. At the same time, it should not be corrosive, toxic, or dangerous.

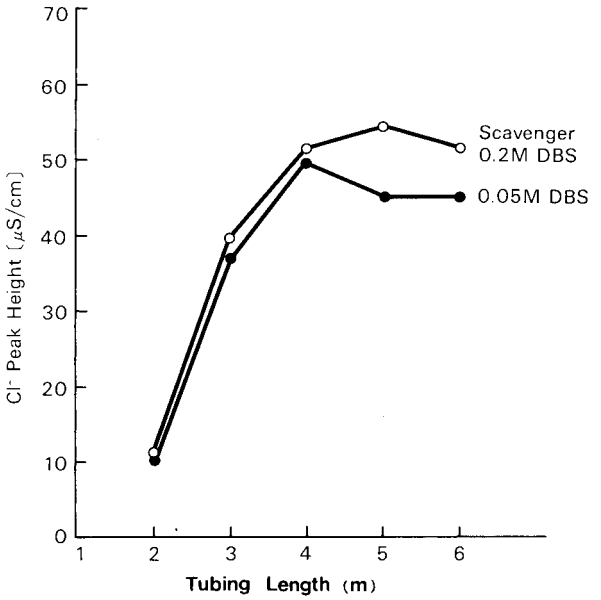

Fig. 4. Relationship of peak height to tubing length following injection of 100 μl of 10 ppm chloride.

DBS and nitric acid were compared as scavengers in regard to background conductance and peak height by injecting 100 μl of 10 ppm chloride ion. Fig. 5 illustrates the changes in peak height and background conductance as a function of scavenger concentration. For the same concentration level, nitric acid has higher background conductance than DBS. Another experiment showed that hydrochloric acid acts the same as nitric acid as a scavenger.

Separator

The ion-exchange capacity of the separator resin was found to be 0.035 mequiv./g. This can be easily adjusted by changing the amount of latex. The resin was washed several times with 1 *M* HCl, 1 *M* NaOH, methanol, and acetone, but no change in ion-exchange capacity was found. The resin was packed into a column and then removed. The procedure was repeated three times but no change in ion-exchange capacity was observed. Thus, the packing resin for a separator column proved to be chemically stable and mechanically rigid.

The resin was packed into a stainless steel column (250 × 4.6 mm I.D.) with a dynamic packing technique. A chromatogram combining the separator and suppressor is shown in Fig. 6. The seven anions were separated within 10 min. Theoretical plate numbers including suppressor, are 1800 for chloride and 1100 for sulphate. Fig. 7 illustrates the relationship between HETP and eluent flow-rate. The HETP value includes the suppressor for experimental and practical reasons. The HETP change of the sulphate when the eluent flow-rate changes from 2 to 4 ml/min is *ca.* 25%. This enables fast analysis (7 anions within 5 min) with minimum chromatogram deterioration.

Fig. 8 illustrates a chromatogram for seven anions at low concentrations. The

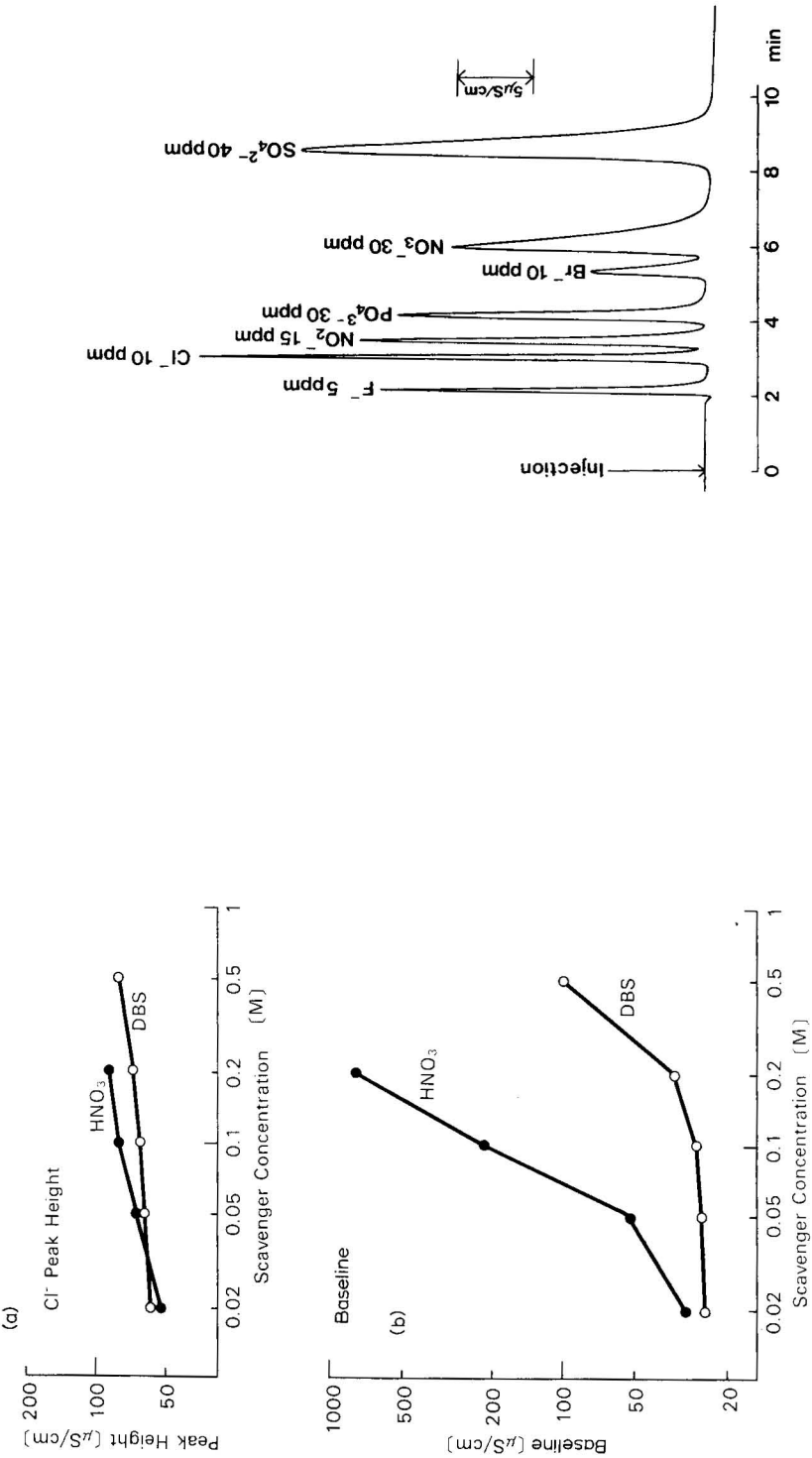

Fig. 5. (a) Change of peak height as a function of scavenger and concentration. (b) Background conductivity as a function of scavenger and concentration.

Fig. 6. Chromatogram of seven anions using a tubing suppressor. Injection volume, 100 μl.

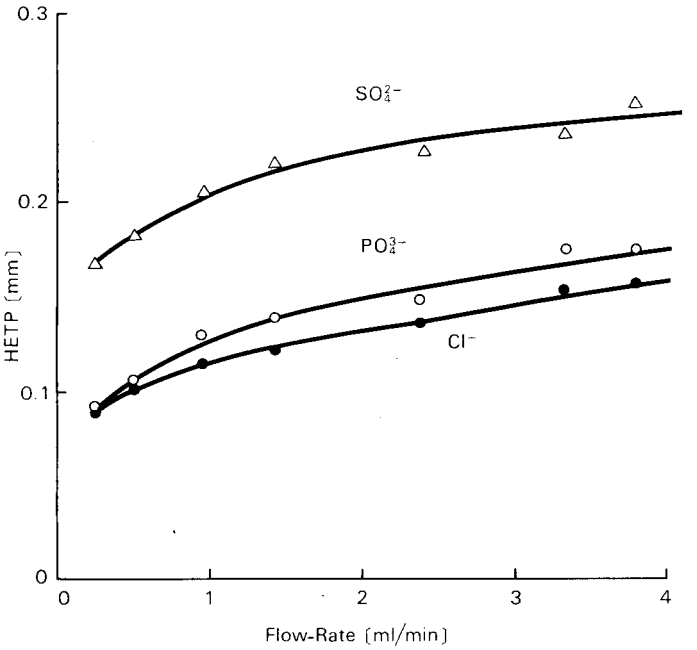

Fig. 7. Relationships between height equivalent to a theoretical plate (HETP) and eluent flow-rate. Measurements include tubing suppressor.

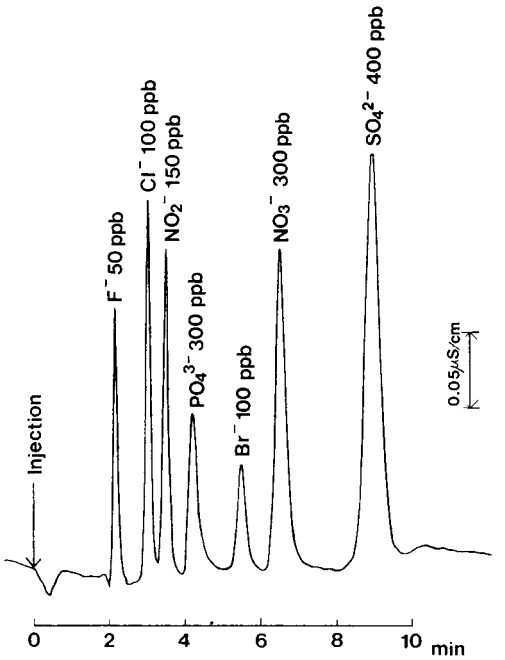

Fig. 8. Chromatogram with low concentrations of anions. Injection volume, 100 μl.

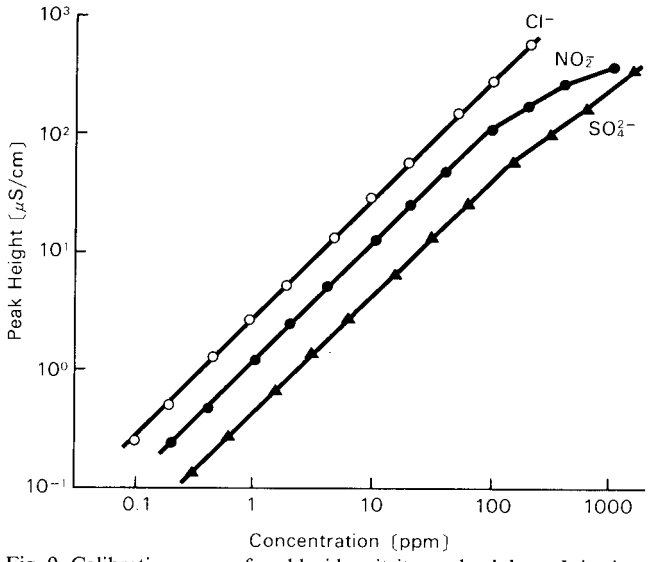

Fig. 9. Calibration curves for chloride, nitrite, and sulphate. Injection volume, 100 μl.

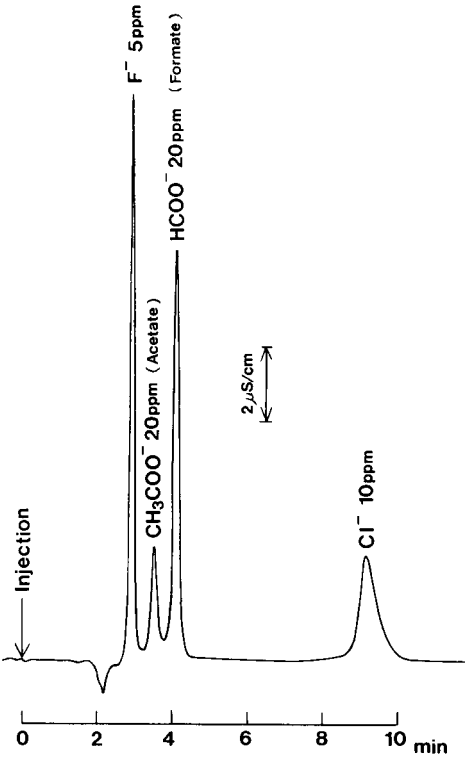

Fig. 10. Chromatogram for acetate and formate. Eluent, 0.015 *M* $Ba_2B_4O_7$; flow-rate 2 ml/min; injection volume, 100 μl.

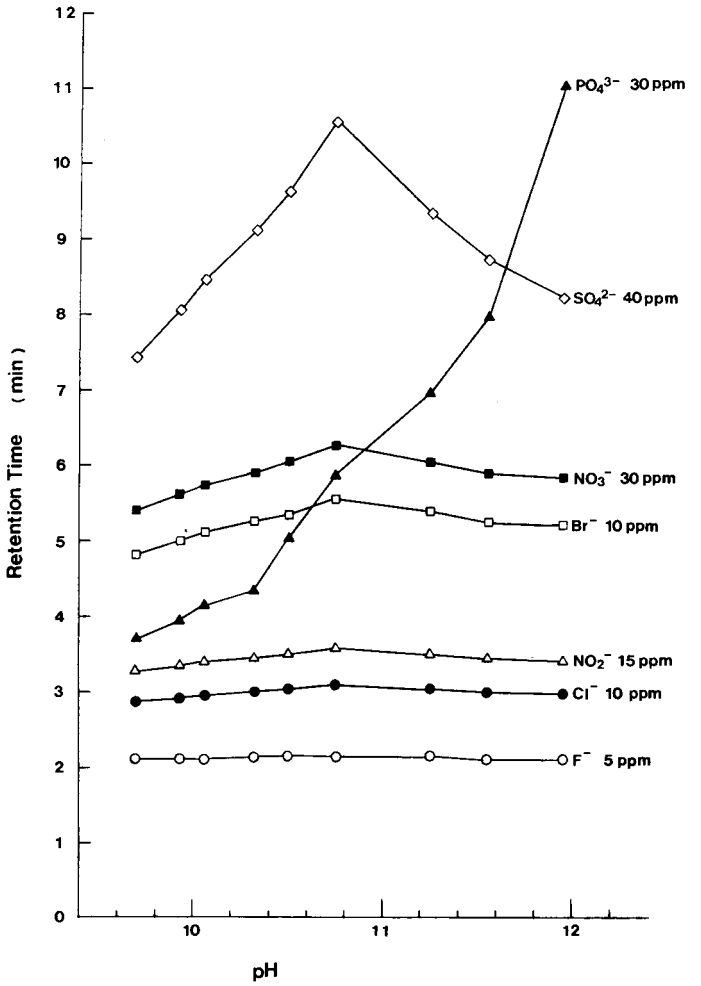

Fig. 11. Change of retention times with eluent pH. The pH of the eluent was adjusted by adding sodium bicarbonate or sodium hydroxide to 0.004 *M* Na_2CO_3.

sample was diluted with an eluent to avoid a "water dip". Detection limits are 5 ppb* for chloride and 20 ppb for sulphate, when the signal-to-noise ratio is set to 2. Fig. 9 shows the linearity and dynamic range of some typical anions.

Eluents

Eluent with 0.004 *M* Na_2CO_3 and 0.004 *M* $NaHCO_3$ was used under standard conditions because of its intermediate affinity for the separator resin and safety aspects. For species with high affinity such as chromate or iodide, the eluent concentration was increased by a factor between 2 and 10 with increased scavenger flow-rate. Organic anions with low affinity that elute between fluoride and chloride can be

* Throughout this article, the American billion (10^9) is meant.

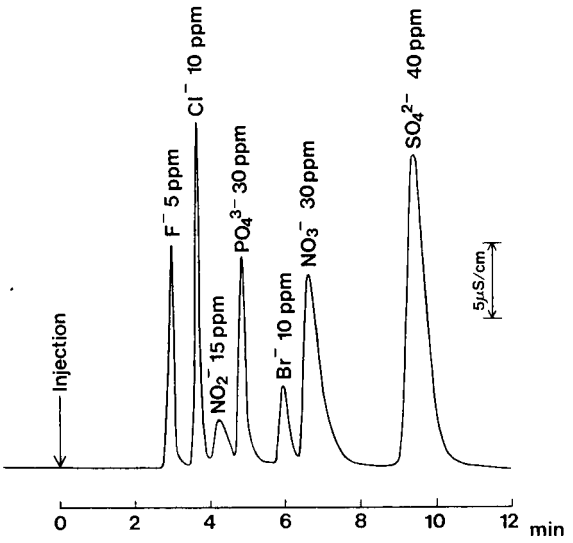

Fig. 12. Chromatogram of seven anions using a conventional packed suppressor just after regeneration. Conditions are the same as Fig. 6 except the suppressor.

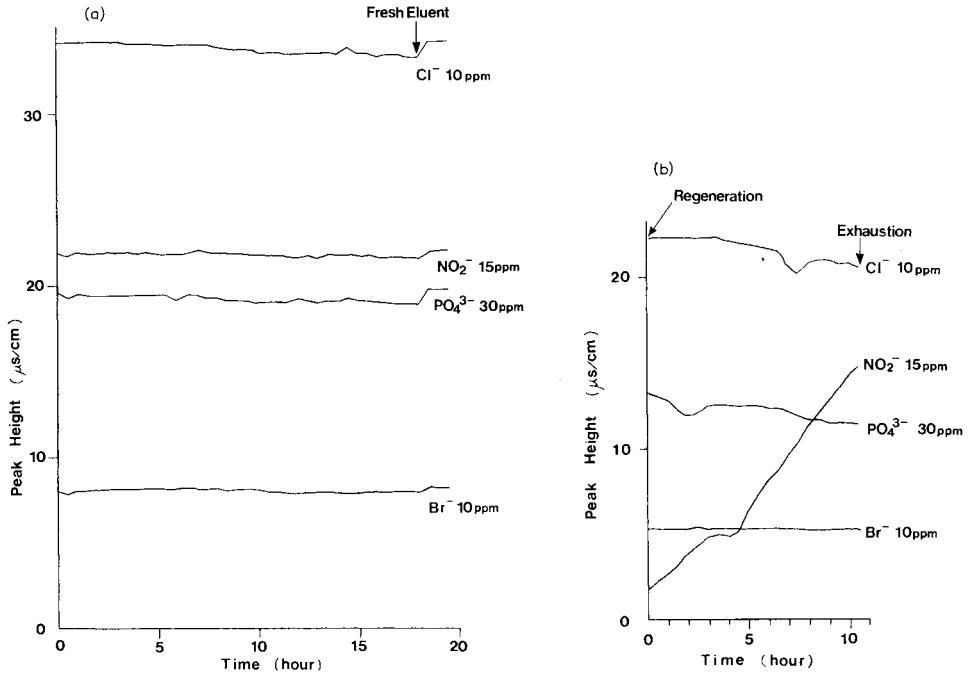

Fig. 13. (a) Changes of peak heights of chloride, nitrite, phosphate, and sulphate with the tubing suppressor. Injection volume, 100 μl. (b) Changes of peak heights of the same four anions with a conventional suppressor from regeneration to full exhaustion. (Full exhaustion occurs only with the conventional suppressor.)

separated with eluents of low eluting power. Fig. 10 shows the separation of acetate and formate using 0.015 *M* $Na_2B_4O_7$ as an eluent.

The effect of retention time changes were investigated by varying the pH of the eluent (Fig. 11). The pH was adjusted using NaOH and $NaHCO_3$ while the concentration of Na_2CO_3 was held constant.

Comparison with conventional suppressor

A comparison was made between an ion-exchange membrane tubing suppressor and a conventional suppressor packed with cation-exchange resin, while using the same separator, eluent, standard sample solution, and flow system. Chromatograms are shown in Fig. 6 for a tubing suppressor and in Fig. 12 for a conventional packed suppressor. Note that peak broadening with a tubing suppressor is minimal while peak heights showed a 50% increase.

Fig. 13 illustrates the change in peak heights for each suppressor under identical conditions. The change of nitrite peak with a conventional packed suppressor is so large that it is almost impossible to quantify the nitrite ions. This phenomenon is due to interaction of the sample with cation-exchange resin in the unexhausted portion of the suppressor column. This interaction is a function of suppressor exhaustion. In a tubing suppressor, equilibrium between exhaustion and regeneration is established and peak heights remain resonably constant for a considerable time.

Changes in retention time of the water dip (negative peak against a baseline of carbonic acid) are plotted in Fig. 14 for a conventional and a tubing suppressor. With a conventional suppressor, the water dip moves and interfere with nitrite, chloride and fluoride peaks as a function of suppressor exhaustion. This upsets the quantification of those ions especially when the concentration is low. In a tubing suppressor the water dip interferes with the fluoride peak but this interference remains constant. In both cases, the water dip can be avoided by adding the same amount of sodium bicarbonate and sodium carbonate as eluent to the sample solution.

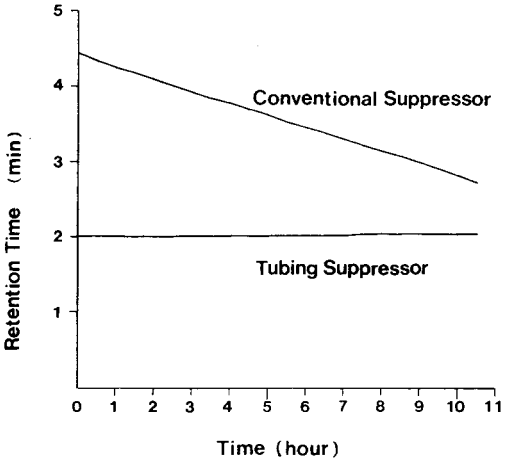

Fig. 14. Change of conventional suppressor water-dip retention time in relation to tubing suppressor.

CONCLUSION

An ion-exchange membrane suppressor enables continuous chromatogram operation. Wide choice of eluent, eluent concentration and eluent flow-rate become possible without the annoying problems related to regeneration such as time dependence of water dip and nitrite peak height changes.

The thin superficial macroporous packing resin combined with a tubing suppressor allows fast analysis.

An anion suppressor for cation analysis is now under development.

REFERENCES

1 H. Small, T. S. Stevens and W. C. Bauman, *Anal. Chem.*, 47 (1975) 1801.
2 C. A. Pohl and E. L. Johnson, *J. Chromatogr. Sci.*, 18 (1980) 442.
3 D. T. Gjerde, J. S. Fritz and G. Schmuckler, *J. Chromatogr.*, 186 (1979) 509.

Journal of Chromatography, 239 (1982) 549–557
Elsevier Scientific Publishing Company, Amsterdam — Printed in The Netherlands

CHROM. 14,541

HIGH-PERFORMANCE LIQUID CHROMATOGRAPHY OF HUMAN SERUM LIPOPROTEINS

SELECTIVE DETECTION OF TRIGLYCERIDES BY ENZYMATIC REACTION

ICHIRO HARA*, KEIKO SHIRAISHI* and MITSUYO OKAZAKI
Laboratory of Chemistry, Department of General Education, Tokyo Medical and Dental University, Kohnodai, Ichikawashi, Chiba prefecture 272 (Japan)

SUMMARY

A simple and convenient method for detection and quantitation of triglycerides in each lipoprotein fraction (chylomicron, VLDL, LDL and HDL) has been developed by high-performance liquid chromatography followed by enzymatic reaction using a high-speed reaction type chromatograph.

Triglycerides in serum lipoproteins eluted from the gel permeation column (TSK GEL) could be sensitively and selectively detected by the absorbance at 550 nm using a commercial enzyme reagent kit.

The distribution of triglycerides in each lipoprotein fraction could be examined with a small amount of serum (10–50 μl) in less than 50 min by this method. Moreover, free glycerol could be detected as a sharp peak at the elution volume of total permeation of the column.

This technique was found to be suitable for the study of triglyceride-rich lipoproteins such as chylomicron and VLDL.

INTRODUCTION

Serum lipoproteins are usually defined according to their density: very-low-density lipoprotein (VLDL), low-density lipoprotein (LDL) and high-density lipoprotein (HDL_2 and HDL_3). However, it is well known that there is a high correlation between lipoprotein density and particle size, owing to their chemical composition and structure.

We have succeeded in applying high-performance liquid chromatography (HPLC) with gel permeation columns for serum lipoprotein analysis[1,2]. The direct quantitation method for cholesterol in each lipoprotein fraction from a small amount of serum (10–20 μl) was developed by combining two methods: separation by HPLC with gel permeation columns and selective detection of cholesterol by enzymatic

* Present address: Research Laboratory, Morishita Pharmaceutical Co., Ltd., Oshinohara, Yasu-cho, Yasu-gun, Shiga prefecture 520-23, Japan).

0021-9673/82/0000–0000/$02.75

reaction[3,4]. This technique can be applied to the selective detection of other lipid components, such as triglycerides and phospholipids, using an appropriate reagent. In fact, we have established the quantitation method of choline-containing phospholipids in serum lipoproteins using a commercial enzyme reagent kit[5].

In this paper, we describe a procedure of selective detection for triglycerides by a method combining HPLC and enzymatic reaction in post-column effluent. Elution patterns of triglyceride are examined for human sera from normal and pathological subjects. A few examples of monitoring a change of lipoprotein distribution are also reported. Evaluation of the gel permeation column for lipoprotein analysis and the effect of elongation of the column on the separation are also investigated.

EXPERIMENTAL

Apparatus

HPLC was carried out using the high-speed chemical derivatization chromatograph (HLC 805, Toyo Soda, Yamaguchi, Japan), as described previously[3,4] except that the enzymatic reaction was done by using a stainless-steel tube (20 m × 0.5 mm I.D.) in a thermostatted water bath (Thermo Mini TM-100, Tokyo Rikakikai, Tokyo Japan).

Ultracentrifugation for the separation of the standard lipoprotein fractions from human serum was carried out using an RP 55 rotor in an Hitachi 55P-2 ultracentrifuge. After centrifugation, lipoproteins in the top layer were collected with an Hitachi tube slicer (Model TSU2, Hitachi, Tokyo, Japan).

Materials and methods

Samples. Human sera used in this experiment were obtained from normolipidemia, hyperlipidemia and patients with various diseases after 12–16 h of fasting. Standard lipoprotein fractions for analysis by HPLC were prepared from the serum by the sequential flotation method of Havel *et al.*[6]. Ascitic chylomicron was prepared from abdominal ascites as the $d < 1.006$ fraction after centrifugation at 10.500 *g* for 24 h.

Standard proteins (thyroglobulin, γ-globulin, β-lactoglobulin, cytochrome *c* and albumin) dissolved in 0.15 *M* NaCl at a concentration of 0.1–1.0% were used to obtain the relationship between molecular weight and elution volume for the gel permeation column.

Reagents. The concentration of triglycerides in the samples subjected to HPLC or in the fraction separated by HPLC was enzymatically determined using a commercially available reagent kit (Determiner TG, Kyowa Medex, Tokyo, Japan). This reagent was obtained in premixed lyophilized vials together with buffer solution. When reconstituted with (per vial) 85 ml of 0.1 *M* Good buffer (pH 6.75) containing detergents and aldehyde trapping reagent, the individual components were present in the following concentrations: lipoprotein lipase, 1 unit/ml; glycerol oxidase, 33.4 units/ml; peroxidase, 10 units/ml; 4-am8in 4-aminoantipyrine, 0.5 m*M*; N-ethyl-N-(3-methylphenyl)-N′-acetylethylendiamine, 0.9 m*M*. The concentration of cholesterol in the loaded samples or in the fraction separated by HPLC was determined using a commercial enzyme reagent kit (Determiner TC"555", Kyowa Medex) as described previously[3,4].

Separation of lipoproteins by HPLC. The separation of lipoproteins was performed by HPLC with gel permeation columns (TSK GEL, G5000PW and G4000PW; Toyo Soda). Experimental conditions were as follows: column, G5000PW, G4000PW, G5000PW + G5000PW (each column, 600 × 7.5 mm I.D.); eluent, 0.15 *M* NaCl; flow-rate, 0.50 ml/min.

Detection of triglycerides in flow diagram. Triglycerides were detected by measuring the A_{550} of the post-column effluent, described previously for cholesterol quantitation[3,4]. The A_{550} of the mixed eluate and enzyme solution (Determiner TG kit) was monitored after passage through a stainless steel reaction tube (20 m × 0.5 mm I.D.) at 45°C using the high-speed chemical derivatization chromatograph. The flow-rate of the enzyme solution (Determiner TG) was 0.40 ml/min.

RESULTS AND DISCUSSION

Recently, highly sensitive and simple quantitation methods for serum triglycerides have been developed using various enzymatic reaction systems[7–10], and the determination of triglycerides can be precisely and reproducibly performed with a very small amount of serum (20 μl) in an aqueous system.

For the detection of triglycerides in the eluate from the gel permeation column, we used a commercial enzyme reagent kit (Determiner TG), which had been developed using a new enzyme, glycerol oxidase[11,12]. The enzymatic reaction schemes for the selective detection of triglycerides are as follows:

$$\text{triglycerides} + H_2O \xrightarrow[\text{lipoprotein lipase}]{} \text{free glycerol} + \text{fatty acid}$$

$$\text{free glycerol} + O_2 \xrightarrow[\text{glycerol oxidase}]{} \text{glyceraldehyde} + H_2O_2$$

$$\text{4-aminoantipyrine} + \text{EMAE} + 2H_2O_2 \xrightarrow[\text{peroxidase}]{} \text{quinone diimine dye} + 4H_2O$$

where EMAE is N-ethyl-N-(3-methylphenyl)-N′-acetylethylendiamine.

Triglycerides can be measured by the A_{550} of the quinonediimine dye (λ_{max} = 555 nm) which is produced by the above reaction schemes using this reagent kit. The end-point of this reaction can be obtained within 5 min after incubation at 37°C in a test-tube. We successfully applied this reagent kit for the detection of triglycerides in the flow diagram by HPLC using the following experimental conditions: temperature of the reaction bath, 45°C; dimensions of the reactor, 20 m × 0.5 mm I.D.; flow-rate of the main path (*i.e.* the pathway of the eluate from the column), 0.50 ml/min; flow-rate of the enzyme solution (Determiner TG), 0.40 ml/min. The A_{550} of the mixed eluate and enzyme solution was monitored after passage through the reactor.

The elution patterns monitored by the A_{550} using the G5000PW column are

shown in Fig. 1 for the standard lipoprotein fractions (chylomicron, VLDL, LDL, HDL_2 and HDL_3) which were prepared by the sequential flotation methods[6]. The elution profile of free glycerol is also presented in the same figure (Fig. 1j). Free glycerol in the applied samples to HPLC was detected as a sharp peak at the elution volume of total permeation of the column.

The relationship of the molecular weights of proteins and lipoproteins to elution volumes was investigated by monitoring the A_{280} using the standard proteins and lipoproteins. The results for the G5000PW column are shown in Fig. 2. All the plots for proteins and lipoproteins in the molecular weight range from 10^4 to 10^6 are almost on the straight line.

Fig. 3 presents typical elution patterns monitored by the A_{550} for various amounts of human serum applied to the HPLC apparatus. Sample is the whole serum from the patient with primary biliary cirrhosis, which contains 173 mg/dl of triglycerides. A very small amount of serum (5 μl) gave five clearly separated peaks: chylo-

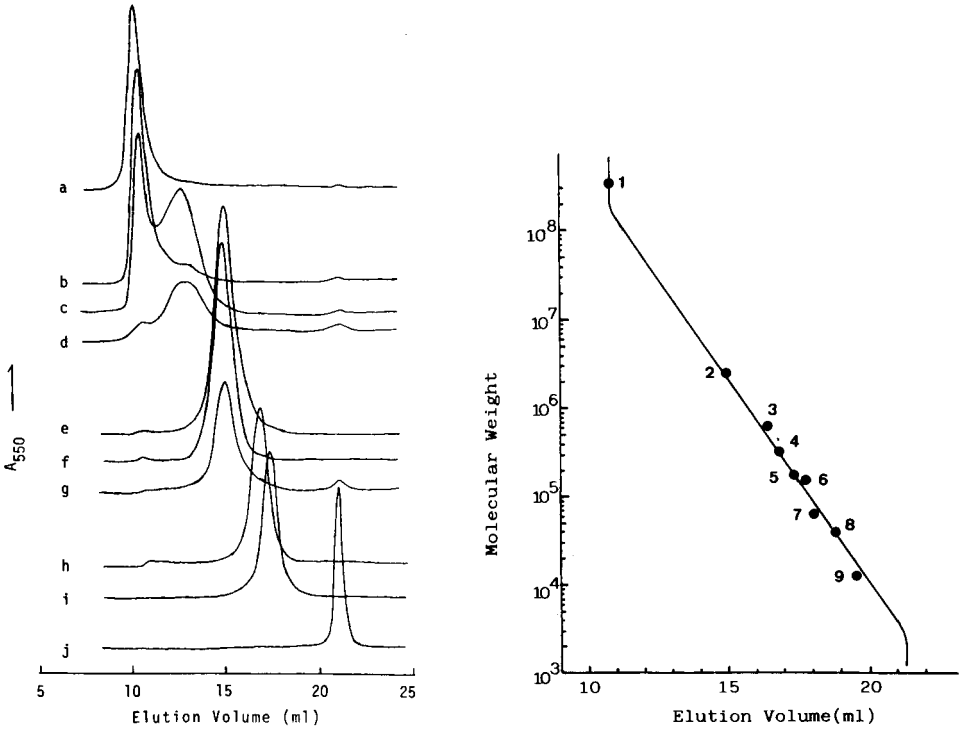

Fig. 1. Elution patterns of the A_{550} for standard samples. Column, G5000PW (600 × 7.5 mm I.D.); eluent, 0.15 *M* NaCl; flow-rate, 0.50 ml/min (main path), 0.40 ml/min (enzyme solution, Determiner TG kit); temperature of the reactor (20 m × 0.5 mm I.D., stainless steel tube), 45°C. Samples: a, ascitic chylomicron; b–d, chylomicron + VLDL fraction (*d* < 1.006); e–g, LDL (*d* 1.006–1.063); h, HDL_2 (*d* 1.063–1.125); i, HDL_3 (*d* 1.125–1.210); j, free glycerol.

Fig. 2. Relationship between molecular weight and elution volume for G5000PW column. Column, G5000PW (600 × 7.5 mm I.D.); eluent, 0.15 *M* NaCl; flow-rate, 0.50 ml/min; detector, A_{280}. Samples: 1, ascitic chylomicron; 2, LDL; 3, thyroglobulin (bovine); 4, HDL_2; 5, HDL_3; 6, γ-globulin (human); 7, albumin (human); 8, β-lactoglobulin (bovine); 9, cytochrome *c*.

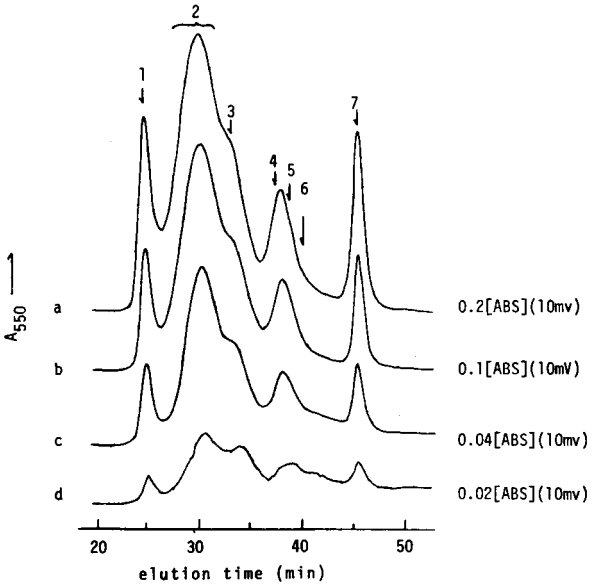

Fig. 3. Elution curves monitored by the A_{550} for various amounts of human serum applied to HPLC. Sample: serum of patient with primary biliary cirrhosis (173 mg/dl of triglycerides). Loaded volume: a, 40 μl; b, 20 μl; c, 10 μl; d, 5 μl. Elution position: 1 = chylomicron; 2 = VLDL; 3 = LDL; 4 = HDL_2; 5 = HDL_3; 6 = albumin; 7 = free glycerol. HPLC conditions as in Fig. 1.

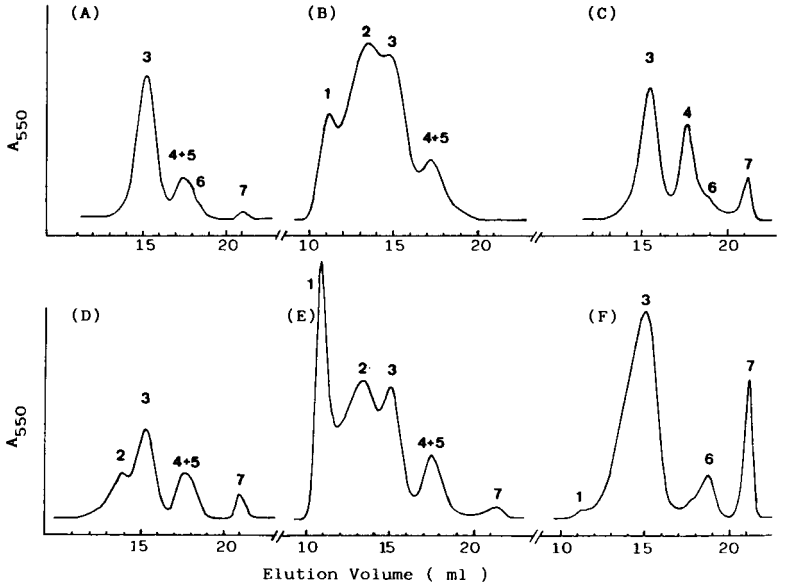

Fig. 4. Elution patterns of the A_{550} for various human sera. Sample: A, normal male; B, hyperlipidemia; C, liver cirrhosis; D, normal child; E, fatty child; F, baby one day after birth. Loaded volume: 10–50 μl. Peaks: 1 = chylomicron; 2 = VLDL; 3 = LDL; 4 = HDL_2; 5 = HDL_3; 6 = bilirubin; 7 = free glycerol. HPLC conditions as in Fig. 1.

micron, VLDL, LDL, HDL and free glycerol. The arrow in Fig. 3 indicates the elution position of each lipoprotein fraction, serum albumin and free glycerol. The elution positions were determined from the results shown in Fig. 1 and Fig. 2. These fractions are designated by the numbers: 1, chylomicron; 2, VLDL; 3, LDL; 4, HDL_2; 5, HDL_3; 6, albumin; 7, free glycerol. As shown in Fig. 3, the G5000PW column was found to be useful for the separation of the large-particle-size fractions of serum lipoproteins such as chylomicron, VLDL and LDL. On the other hand, small-particle-size fractions, such as HDL_2 and HDL_3, eluted as one peak.

The detection limit for triglycerides by this method was found to be 1 μg per one separated peak (see Fig. 3d). This indicates that *ca.* 50 μg of triglycerides per millilitre of serum can be detected when 20 μl of serum is analysed. Although the peak responce of the A_{550} increased slightly with increased serum volume, the elution patterns obtained for serum volumes from 10 to 40 μl were very similar. This shows that the quantitation of triglycerides in each lipoprotein and that of free glycerol can be performed from the peak area of the A_{550} and the concentration of triglycerides in applied samples with use of 10–40 μl of whole serum.

In Fig. 4, typical elution patterns monitored by the A_{550} are presented for six examples of human sera: A, normal male; B, hyperlipidemia; C, liver cirrhosis; D, normal child; E, fatty child; F, baby one day after birth. Six distinct peaks of the A_{550} were observed. They were identified from the results shown in Fig. 1 and Fig. 2 as follows: 1, chylomicron; 2, VLDL; 3, LDL; 4, HDL_2; 5, HDL_3; 6, pigments such as bilirubin which adsorb to serum albumin; 7, free glycerol. Among these peaks, the elution position of VLDL (peak 2) varied with the individual subjects. This result is consistent with the fact that the VLDL fraction has a wide distribution of particle size and has many subclasses[13–17]. The hyperlipidemic sera (subjects B and E) present a larger amount of large-particle-size lipoprotein fractions, such as chylomicron and VLDL, than that of normolipidemic sera (subjects A, C and D). This method was found to give much information about large-particle-size lipoproteins that contained a high amount of triglycerides.

In the case of liver cirrhosis (subject C), a sharp peak of HDL_2 and a shoulder peak of bilirubin are observed. We have reported the decrease in serum HDL_3-cholesterol level in the case of liver cirrhosis using our HPLC method[18]. In the case of the one-day-old baby (subject F), which contains a high amount of bilirubin, a large peak is detected at the elution position of serum albumin (peak 6). These results indicate that this method can give qualitative data about small-particle-size fractions.

It is well known that there is an appropriate amount of free glycerol in human serum[19,20]. By our HPLC method, free glycerol can be detected as a sharp peak at the elution volume of total permeation as shown in Fig. 1. The content of free glycerol was found to vary with the individual subjects (see peak 7 of Fig. 4).

Fig. 5 shows two examples of the application of this method for monitoring a change of lipoprotein distribution. One is a change of elution patterns due to fasting time in the case of an obese woman (Fig. 5A). The other is the comparison of lipoprotein distribution between the fresh serum and the freezing–thawing serum for a triglyceride-rich subject (Fig. 5B) and a triglyceride-poor subject (Fig. 5C). The latter example indicates that large-particle-size fractions, such as chylomicron and VLDL, increase on freezing–thawing. On the other hand, in the case of the subject containing a very low level of VLDL, no change was observed as shown in Fig. 5C.

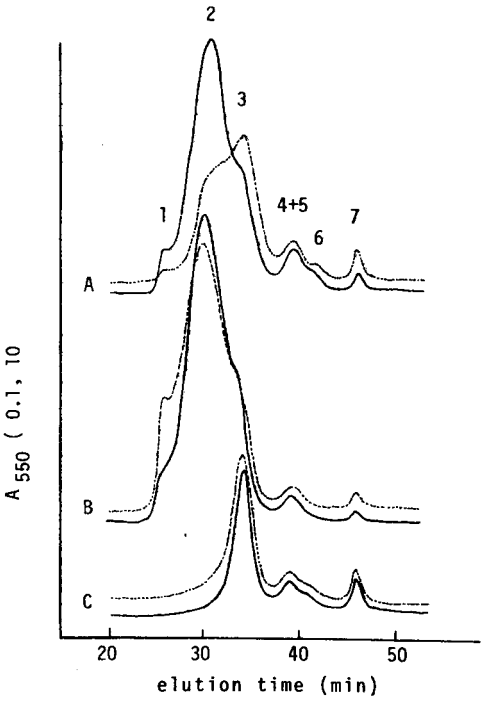

Fig. 5. Elution patterns of the A_{550} for human sera: examples of monitoring pattern change. Samples: A, serum of obese woman, ——— (6 h of fasting), --------- (16 h of fasting); B, hyperlipidemia, ——— (fresh serum), --------- (freezing–thawing serum); C, normolipidemia, ——— (fresh serum), --------- (freezing–thawing serum). Loaded volume: A, 30 μl; B, 10 μl; C, 30 μl. Peaks as in Fig. 4. HPLC conditions as in Fig. 1.

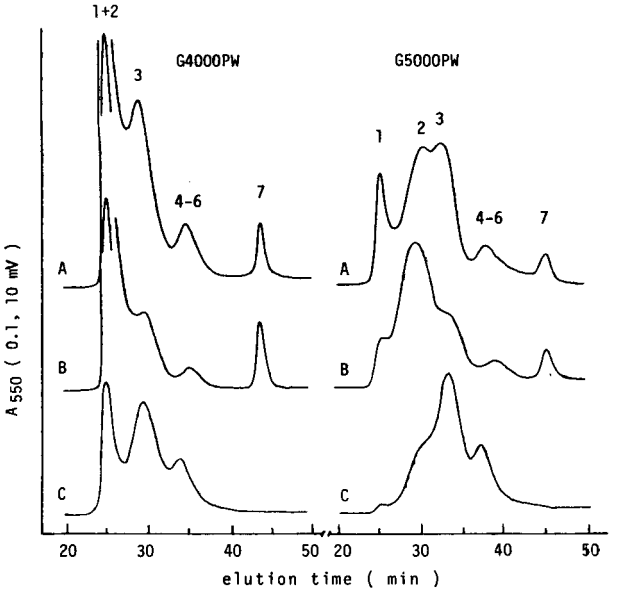

Fig. 6. Comparison of elution pattern of the A_{550} between G4000PW and G5000PW columns. Samples: human serum (A, acute liver hepatitis; B and C, hyperlipidemia). Loaded volume: A, 30 μl; B, 10 μl; C, 30 μl. Peaks as in Fig. 4. HPLC conditions as in Fig. 1.

Thus our results are consistent with the fact that evaluation of lipoproteins of frozen serum by electrophoretic procedures is possible only for the subject of a very low level of VLDL[21,22].

Elution patterns of the A_{550} for the same subject were compared on the G4000PW and G5000PW columns (see Fig. 6). In the case of G4000PW, chylomicron and VLDL elute as one peak at the void volume, and LDL is completely separated from VLDL. Therefore, the G4000PW column is preferable for evaluating the level of LDL.

Lastly, the effect of elongation of the column on the separation was examined using a single column of G5000PW and a combined column of G5000PW + G5000PW. Elongation of the column was found to increase the resolution of the separation for all lipoprotein fractions, as shown in Fig. 7. Detailed examination of subclasses of the VLDL fraction can be performed by using the G5000PW + G5000PW system (see peak 2 of Fig. 7A). The elution patterns of cholesterol monitored by the A_{550} using Determiner TC"555" are also presented in the same Figure for reference. From these experiments, it can be seen that the combination of the elution patterns of triglycerides and cholesterol give much information on the nature of serum lipoproteins in normal and pathological subjects.

The establishment of the selective detection method for triglycerides in serum lipoproteins by HPLC should help to make progress rapid in the study of lipoprotein metabolism and diagnosis of the various diseases. We are now examining the pattern analysis of the Fredrickson *et al.* typing system for familial hyperlipidemia[23] using our HPLC method.

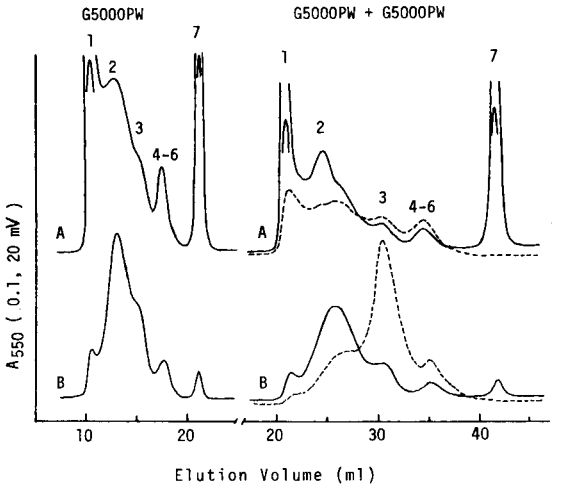

Fig. 7. Elution patterns of triglycerides (———) and cholesterol (---------) for human serum. Columns, G5000PW, G5000PW + G5000PW (each column, 600 × 7.5 mm I.D.); sample, human serum of hyperlipidemia; loaded volumes, 20 μl HPLC conditions for triglyceride monitor as in Fig. 1. HPLC conditions for cholesterol monitor: flow-rate, 0.50 ml/min (main path) and 0.20 ml/min (enzyme solution, Determiner TC"555"); temperature of the reactor (20 m × 0.25 mm I.D., stainless steel tube), 40°C. Peaks as in Fig. 4.

ACKNOWLEDGEMENTS

The authors acknowledge the gifts of serum by Dr. H. Itakura and Dr. T. Kodama of Tokyo University Hospital and Dr. C. Naito of Tokyo Teishin Hospital. This work was supported by a research grant from Nissan Science Foundation.

REFERENCES

1 M. Okazaki, Y. Ohno and I. Hara, *J. Chromatogr.*, 221 (1980) 257.
2 Y. Ohno, M. Okazaki and I. Hara, *J. Biochem.*, 89 (1981) 1675.
3 M. Okazaki, Y. Ohno and I. Hara, *J. Biochem.*, 89 (1981) 879.
4 M. Okazaki, K. Shiraishi, Y. Ohno and I. Hara, *J. Chromatogr.*, 223 (1981) 285.
5 M. Okazaki, N. Hagiwara and I. Hara, *J. Biochem.*, 91 (1982) 1381–1389.
6 R. J. Havel, H. A. Eder and J. H. Bragden, *J. Clin. Invest.*, 34 (1955) 1345.
7 G. Bucolo and H. David, *Clin. Chem.*, 19 (1973) 476.
8 K. Whitlow and N. Gochman, *Clin. Chem.*, 24 (1978) 2018.
9 R. E. Megraw, D. E. Dunn and H. G. Biggs, *Clin. Chem.*, 25 (1979) 273.
10 H. Winaltasaputla, V. N. Mallet, S. S. Kuan and G. G. Guilhault, *Clin. Chem.*, 26 (1980) 613.
11 T. Uwajima, H. Akita, K. Ito, A. Mihara, K. Aisaka and O. Terada, *Agr. Biol. Chem.*, 43 (1979) 2633.
12 T. Uwajima, H. Akita, K. Ito, A. Mihara, K. Aisaka and O. Terada, *Agr. Biol. Chem.*, 44 (1980) 399.
13 S. H. Quarfordt, A. Nathans, M. Dowdee and H. L. Hilderman, *J. Lipid Res.*, 13 (1972) 435.
14 T. Sata, R. J. Havel and A. L. Jones, *J. Lipid Res.*, 13 (1972) 757.
15 W. R. Hazzard, F. T. Lindgren and E. L. Bierman, *Biochim. Biophys. Acta*, 202 (1970) 517.
16 C. J. Packard, J. Shepherd, S. Jones, A. M. Gotto and D. Taunton, *Biochim. Biophys. Acta*, 572 (1979) 269.
17 A. Pagnan, R. J. Havel, J. P. Kane and L. Kotite, *J. Lipid Res.*, 18 (1977) 613.
18 M. Okazaki, I. Hara, A. Tanaka, T. Kodama and S. Yokoyama, *New Eng. J. Med.*, 304 (1981) 1608.
19 K. Stinshoff, D. Weisshaar, F. Staeler, D. Hesse, W. Gruber and E. Steier, *Clin. Chem.*, 23 (1977) 1029.
20 H. A. Schwertner, R. C. McLaren and E. L. Arnold, *Clin. Chem.*, 25 (1979) 520.
21 F. T. Hatch, F. T. Lindgren, G. L. Adamson, L. C. Jensen, A. W. Wong and R. I. Levy, *J. Lab. Clin. Med.*, 81 (1973) 946.
22 F. T. Lindgren, A. Silvers, R. Jutagir, L. Layshot and D. D. Bradley, *Lipids*, 12 (1977) 278.
23 D. S. Fredrickson, R. I. Levy and R. S. Lees, *New Eng. J. Med.*, 276 (1967) 148.

Journal of Chromatography, 239 (1982) 559–564
Elsevier Scientific Publishing Company, Amsterdam — Printed in The Netherlands

CHROM. 14,544

SEPARATION AND DETERMINATION OF NAPROXEN ENANTIOMERS IN SERUM BY HIGH-PERFORMANCE LIQUID CHROMATOGRAPHY

JUNICHI GOTO, NOBUHARU GOTO and TOSHIO NAMBARA*
Pharmaceutical Institute, Tohoku University, Sendai 980 (Japan)

SUMMARY

The separation and determination of *d*- and *l*-naproxen in serum by high-performance liquid chromatography (HPLC) is described. The method is based on pre-column derivatization with a newly developed chiral reagent, *l*-1-(4-dimethylamino-1-naphthyl)ethylamine (DANE) to form the diastereoisomeric amides. The diastereoisomers were separated on a normal-phase column by HPLC with fluorescence detection employing *n*-hexane–tetrahydrofuran (80:26) as the mobile phase. The clean-up of naproxen in serum was efficiently attained by the use of a Sep-Pak C_{18} cartridge. The quantitation limit of naproxen by this method was 100 pg. The serum levels of naproxen enantiomers after administration of the racemate or each enantiomer to rabbits were determined by the proposed method.

INTRODUCTION

A reliable method for the simultaneous determination of each enantiomeric drug in biological fluids is a prerequisite for pharmacokinetic studies of the racemate. In previous papers we reported the preparation of chiral derivatization reagents for the resolution of enantiomeric amines[1,2] and their use for the determination of 2,4-dimethoxy-4-methylamphetamine enantiomers in plasma by high-performance liquid chromatography (HPLC)[3]. We also synthesized chiral derivatization reagents, *d*- and *l*-1-(4-dimethylamino-1-naphthyl)ethylamine (DANE), which have a fluorophore that is highly responsive to a fluorescence detector, and demonstrated their applicability to the resolution of carboxylic acid enantiomers by HPLC[4]. This paper deals with the use of these pre-column derivatization reagents for the separation and determination of naproxen enantiomers in serum by HPLC on a normal-phase column.

EXPERIMENTAL

High-performance liquid chromatography

The apparatus was a Waters 6000A solvent delivery system (Waters Assoc., Milford, MA, U.S.A.) equipped with a Hitachi Model 650-10LC fluorescence spectrophotometer (excitation wavelength 320 nm; emission wavelength 410 nm). The test samples were applied to the chromatograph by a Waters U6K sample loop injector

0021-9673/82/0000–0000/$02.75

(Waters Assoc.) with an effective volume of 2 ml. A μPorasil column (1 ft. × 1/4 in. I.D.) was used under ambient conditions. *n*-Hexane–tetrahydrofuran (80:26) was employed as mobile phase at a flow-rate of 0.6 ml/min.

Materials

All of the chemicals employed were of analytical-reagent grade. *dl*-Naproxen was obtained by the known method[5]. The racemate was resolved by fractionally crystallizing the *d*- or *l*-α-methylbenzylamine salt from ethyl acetate. The optical purity of each enantiomer thus obtained was over 99.0% as judged by HPLC. *l*-DANE hydrochloride was synthesized by the method previously reported[4] and its optical purity was determined to be over 99.5%. 3,5-*tert*.-Butyl-4-hydroxybenzaldehyde O-(methoxycarbonylmethyl)oxime, used as the internal standard (IS), was prepared in these laboratories. Solvents were purified by distillation prior to use. A Sep-Pak C_{18} cartridge (Waters Assoc.) was washed thoroughly with ethanol and water before use.

Sample preparation

A serum sample (20–100 μl) was diluted with 0.1 *M* phosphate buffer (pH 2.0, 2 ml) and passed through a Sep-Pak C_{18} cartridge. After successive washing with water (10 ml) and 70% ethanol (0.5 ml), the desired fraction was obtained by elution with 70% ethanol (2 ml). After evaporation of the solvent, the residue was dissolved in 0.05 *M* sodium carbonate buffer (pH 10, 1 ml) and washed with *n*-hexane (three 2-ml volumes). The aqueous layer was acidified with 1 *N* hydrochloric acid (200 μl) and then extracted with ethyl acetate (three 2-ml volumes). After addition of 1-hydroxybenzotriazole (HOBT) (5 μg) and IS (300 ng), the solution was evaporated under a stream of nitrogen. To the residue were added *l*-DANE hydrochloride (30 μg) in pyridine (20 μl) and 1-ethyl-3-(3-dimethylaminopropyl)carbodiimide hydrochloride (WSC) (100 μg) in dichloromethane (200 μl), and the solution was allowed to stand at 4°C for 45 min. After removal of the solvent under a stream of nitrogen, the residue was dissolved in *n*-hexane–ethyl acetate (3:1) (500 μl). The solution was washed with 5% sodium hydrogen carbonate solution and then applied to a silica gel column (3 cm × 4 mm I.D.). After washing with *n*-hexane–ethyl acetate (3:1) (700 μl), the desired fraction was obtained by elution with ethyl acetate (2 ml). The eluate was dried and dissolved in the mobile phase (400 μl), and a 5–10-μl aliquot of the solution was injected into the HPLC system.

Recovery test for naproxen added to human serum

The test samples were prepared by dissolving 25, 50, 100 or 250 ng of *d*- and *l*-naproxen in human serum (0.1 ml). Clean-up by the use of a Sep-Pak C_{18} cartridge and derivatization with *l*-DANE followed by determination of each enantiomer by HPLC were carried out according to the procedure described above.

Administration of naproxen to rabbits

d- or *l*-naproxen (5 mg/kg each) or *dl*-naproxen (10 mg/kg) was dissolved in 0.05 *M* sodium carbonate buffer (pH 10, 1.3 ml) and saline (0.7 ml), and the solution was injected intravenously into a male albino rabbit weighing 3–4 kg. The blood was withdrawn at 5, 10, 20 and 40 min and 1, 2, 3, 4, 5, 6 and 8 h after administration and centrifuged for 20 min at 1500 *g* to separate serum.

RESULTS AND DISCUSSION

Derivatization of naproxen to diastereoisomers with l-DANE

Resolution of the enantiomers by liquid chromatography has been developed in two ways: introduction of an asymmetric environment intramolecularly by conversion to diastereoisomers[6,7] and intermolecularly by the use of a chiral stationary or mobile phase[8-11]. The former method is more favourable for pharmacokinetic studies of a racemic drug with respect to resolution and sensitivity. In a previous paper, we reported the preparation of *d*- and *l*-DANE as derivatization reagents and their utility for the resolution of carboxylic acid enantiomers by HPLC[4].

In this study, suitable conditions were first investigated for the coupling of *l*-DANE with naproxen through its carboxylic acid function. There are several methods available for the formation of a peptide bond, but most are not necessarily suitable for the quantitative derivatization of carboxylic acid groups owing to the lack of reproducibility. The combined use of WSC and HOBT was chosen for condensation of naproxen with *l*-DANE. Initially, the effects of the concentrations of these two reagents on the formation of diastereoisomeric amides were examined. *dl*-Naproxen, *l*-DANE and various amounts of HOBT and WSC were dissolved in dichloromethane–pyridine (200:20), and the reaction mixture was allowed to stand at 4°C for 45 min. A portion of the resulting solution was then used for HPLC. As shown in Fig. 1, the concentrations of HOBT and WSC exerted a significant influence on the reaction rate. When naproxen was treated with these reagents at 4 or 50°C, the yield of the diastereoisomeric amide increased with increasing reaction time up to 30 min and reached a plateau as illustrated in Fig. 2. The quantitative formation of a peptide bond was attained at 4°C, but a lower reaction rate was observed at 50°C. In addition, without HOBT the reaction rate was depressed to 60% and hence HOBT was concluded to be a useful catalyst for amide formation. No racemization of naproxen or *l*-DANE took place during the condensation reaction.

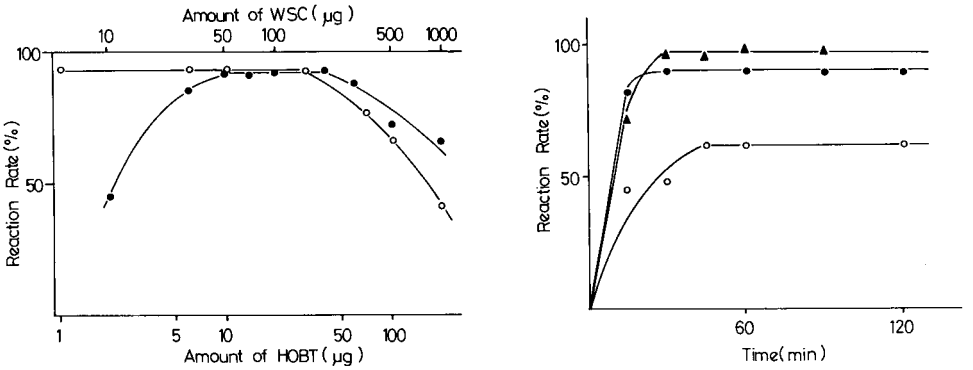

Fig. 1. Effects of concentrations of HOBT and WSC on the formation of diastereomeric amides. ○, HOBT; ●, WSC.

Fig. 2. Time course for derivatization of naproxen with *l*-DANE. ▲, At 4°C with HOBT; ●, at 50°C with HOBT; ○, at 50°C without HOBT.

Clean-up of naproxen in serum

The recovery of a drug in blood is significantly influenced by the clean-up procedure employed. For this purpose, deproteinization with an alcohol or acid and extraction with the organic solvent are widely used prior to HPLC. These procedures, however, proved not to be applicable to serum naproxen owing to the insufficient recovery rate and the occurrence of interfering peaks on the chromatogram. In previous papers, we demonstrated the utility of a Sep-Pak C_{18} cartridge for the clean-up of 2,5-dimethoxy-4-methylamphetamine[3], bile acids[12] and their sulphates[13] in biological fluids. Therefore, the use of this cartridge was attempted for the purification of naproxen in serum. Naproxen was readily adsorbed on Sep-Pak C_{18} and quantitatively recovered by elution with 70% ethanol. This procedure was found to be effective for the removal of co-existing polar substances in serum. Elimination of the neutral materials in biological fluids was then carried out. The eluate was dissolved in alkali and the resulting solution was washed with *n*-hexane. The aqueous layer was then acidified and extracted with ethyl acetate, providing the desired naproxen quantitatively. The efficient clean-up procedure for HPLC of naproxen enantiomers in serum gave an excellent chromatogram without any interfering peaks (Fig. 3). No racemization of naproxen occurred during this clean-up.

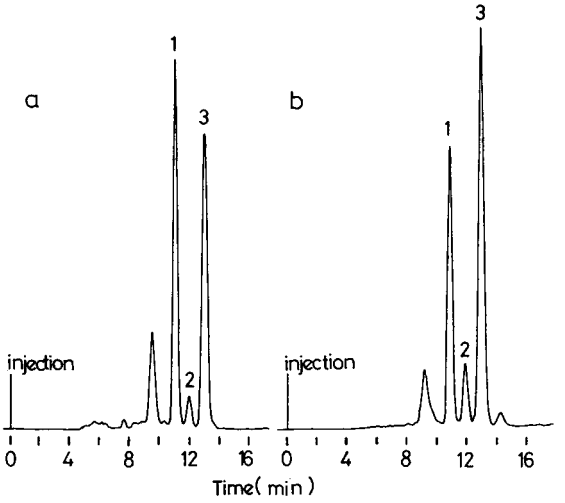

Fig. 3. Chromatogram of *d*- and *l*-naproxen. (a) Standard sample; (b) serum sample obtained 2 h after administration of *dl*-naproxen. 1, *l*-Enantiomer; 2, IS; 3, *d*-enantiomer.

Detection of diastereoisomers formed from naproxen with l-DANE

Elution of the diastereoisomeric amides in HPLC was monitored by fluorescence detection at 320 nm, the limit of quantitation being 100 pg. A calibration graph was constructed by plotting the ratio of the peak area of *d*- or *l*-naproxen to that of 3,5-*tert*.-butyl-4-hydroxybenzaldehyde O-(methoxycarbonylmethyl)oxime against the amount of naproxen enantiomers, a linear response to each enantiomer being observed in the range 5–2000 ng.

Determination of d- and l-naproxen in serum

The applicability of the method to the simultaneous determination of *d*- and *l*-

TABLE I

RECOVERY OF *d*- AND *l*-NAPROXEN ADDED TO HUMAN SERUM

Enantiomer	*Naproxen (ng)*		*Recovery ± S.D. (%)**
	Added	*Found*	
d	25	24.5	97.8 ± 3.4
	50	49.0	98.0 ± 3.8
	100	95.7	95.7 ± 3.2
	250	249.5	99.8 ± 2.4
l	25	23.9	95.7 ± 4.2
	50	47.7	95.3 ± 4.3
	100	95.3	95.3 ± 2.5
	250	242.5	97.0 ± 3.4

* $n = 8$.

naproxen in serum was examined. Known amounts (25–250 ng) of *d*- and *l*-naproxen was added to human serum and the recoveries were determined. As shown in Table I, the recoveries of *d*- and *l*-naproxen were 95–100% with a standard deviation of 2.4–4.3%. It is evident that the proposed method is applicable to the quantitation of naproxen enantiomers in serum with satisfactory accuracy and precision.

The simultaneous determination of serum levels of the enantiomers was carried out according to the procedure thus established. Blood specimens were collected at 5, 10, 20 and 40 min and 1, 2, 3, 4, 5, 6 and 8 h following intravenous injection of *d*-, *l*- or *dl*-naproxen to rabbits. A typical chromatogram of naproxen enantiomers in serum obtained at 2 h is shown in Fig. 3. The half-life of *d*-naproxen was found to be longer than that of *l*-enantiomer when *dl*-naproxen was injected intravenously (Fig. 4). Moreover, the formation of a significant amount of the *d*-enantiomer was recognized after administration of *l*-naproxen. On the other hand, the *l*-enantiomer was not detected when *d*-naproxen was administered in a similar manner (Fig. 5). The stereo-

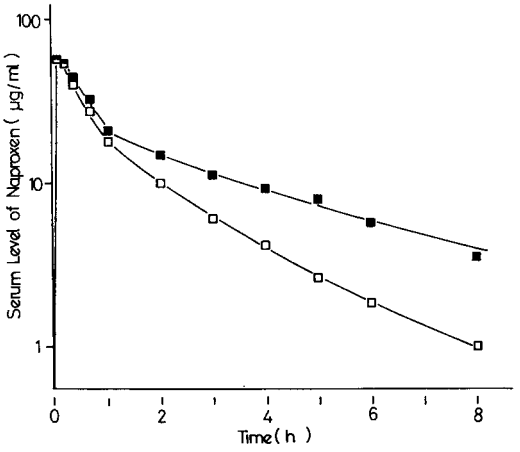

Fig. 4. Serum levels of *d*- and *l*-naproxen after administration of the racemate. ■, *d*-Naproxen; □, *l*-naproxen.

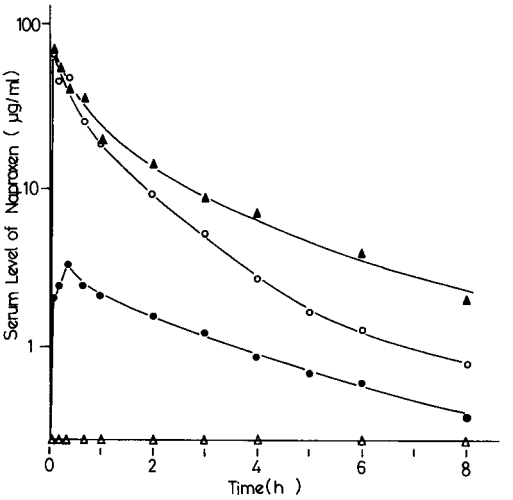

Fig. 5. Serum levels of *d*- and *l*-naproxen after administration of each enantiomer. ▲, *d*-Naproxen after administration of *d*-enantiomer; △, *l*-naproxen after administration of *d*-enantiomer; ●, *d*-naproxen after administration of *l*-enantiomer; ○, *l*-naproxen after administration of *l*-enantiomer.

specific inversion of *l*-naproxen to the *d*-enantiomer in living animals has been unequivocally demonstrated. These results are in good accord with the findings reported in previous papers[14–16].

It is hoped that the availability of a new method for the simultaneous determination of enantiomeric drugs in biological fluids with satisfactory reliability and sensitivity may provide more precise information on the pharmacokinetics of α-arylpropionic acid anti-inflammatory drugs.

ACKNOWLEDGEMENTS

This work was supported in part by a grant from the Ministry of Education, Science and Culture of Japan.

REFERENCES

1 J. Goto, M. Hasegawa, S. Nakamura, K. Shimada and T. Nambara, *J. Chromatogr.*, 152 (1978) 413.
2 T. Nambara, S. Ikegawa, M. Hasegawa and J. Goto, *Anal. Chim. Acta*, 101 (1978) 111.
3 J. Goto, N. Goto, A. Hikichi and T. Nambara, *J. Liquid Chromatogr.*, 2 (1979) 1179.
4 J. Goto, N. Goto, A. Hikichi, T. Nishimaki and T. Nambara, *Anal. Chim. Acta*, 120 (1980) 187.
5 I. T. Harrison, B. Lewis, P. Nelson, W. Rooks, A. Roszkowski, A. Tomolonis and J. H. Fried, *J. Med. Chem.*, 13 (1970) 203.
6 T. Tamegai, M. Ohmae, K. Kawabe and M. Tomoeda, *J. Liquid Chromatogr.*, 2 (1979) 1229.
7 T. Kinoshita, Y. Kasahara and N. Nimura, *J. Chromatogr.*, 210 (1981) 77.
8 P. E. Hare and E. Gil-Av, *Science*, 204 (1979) 1226.
9 B. Lefebvre, R. Audebert and C. Quivoron, *J. Liquid Chromatogr.*, 1 (1978) 761.
10 S. Hara and A. Dobashi, *J. Chromatogr.*, 186 (1979) 543.
11 C. Gilon, R. Leshem and E. Grushka, *Anal. Chem.*, 52 (1980) 1206.
12 J. Goto, H. Kato, Y. Saruta and T. Nambara, *J. Liquid Chromatogr.*, 3 (1980) 991.
13 J. Goto, H. Kato, Y. Saruta and T. Nambara, *J. Chromatogr.*, 226 (1981) 13.
14 D. G. Kaiser, G. J. Vangiessen, R. J. Reischer and W. J. Wechter, *J. Pharm. Sci.*, 65 (1976) 269.
15 T. Tamegai, T. Tanaka, T. Kaneko, S. Ozaki, M. Ohmae and K. Kawabe, *J. Liquid Chromatogr.*, 2 (1979) 551.
16 J. M. Kemmerer, F. A. Rubio, R. M. McClain and B. A. Koechlin, *J. Pharm. Sci.*, 68 (1979) 1274.

Journal of Chromatography, 239 (1982) 565–570
Elsevier Scientific Publishing Company, Amsterdam — Printed in The Netherlands

CHROM. 14,608

TWO-DIMENSIONAL SEPARATION SYSTEM FOR ANALYSIS OF PROTEINS EMPLOYING ISOELECTRIC FOCUSING AND HIGH-PERFORMANCE LIQUID CHROMATOGRAPHY

KIYOTSUGU KOJIMA*, TAKASHI MANABE and TSUNEO OKUYAMA
Department of Chemistry, Faculty of Science, Tokyo Metropolitan University, Setagaya-ku, Tokyo 158 (Japan)
and
TSUGIKAZU TOMONO, TOHRU SUZUKI and EIICHI TOKUNAGA
The Japanese Red Cross Central Blood Center, Shibuya-ku, Tokyo 150 (Japan)

SUMMARY

A new type of separation system, which combined isoelectric focusing with high-performance liquid chromatography, was designed for the analysis and fractionation of serum proteins. For the first dimensional separation, carrier-free isoelectric focusing was used to separate proteins according to their electric charge. For the isoelectric focusing, an instrument which consisted of multiple chambers was deviced. For the second dimensional separation, high-performance gel permeation chromatography was used to separate proteins according to their molecular size. Human serum was subjected to analysis with this two-dimensional system, and separation of serum proteins according to their p*I* and molecular size was demonstrated.

INTRODUCTION

Two-dimensional separation methods, which combine two methods of different separation principles, are widely used for the separation of complex mixtures of proteins. In 1965, Moore and McGregor[1] separated soluble proteins from bovine brain by DEAE-cellulose chromatography, and each fraction was then subjected to starch gel electrophoresis. Two-dimensional electrophoretic techniques, employing polyacrylamide gel isoelectric focusing in the first dimension and polyacrylamide gradient gel electrophoresis[2] (or polyacrylamide slab gel electrophoresis in the presence of sodium dodecyl sulphate[3]) in the second dimension, offer the highest resolution of proteins at the present stage. However, when separation is performed employing starch gels or polyacrylamide gels as carriers, procedures for staining and destaining are necessary to detect proteins, and troublesome procedures are required to extract stained proteins from the gel matrix.

In this report, we describe a new type of separation system that combines carrier-free isoelectric focusing and high-performance gel permeation chromatography. In this system, proteins were separated by their electric charge in the first dimen-

0021-9673/82/0000–0000/$02.75

sion and by their molecular size in the second dimension. Applications of this system to the separation of human serum proteins are described.

EXPERIMENTAL

Reagents

Ampholine (pH 3.5–10, Lot No. 56) was obtained from LKB (Stockholm, Sweden). Other reagents were obtained from Wako (Osaka, Japan). Human albumin, transferrin, and immunoglobulin G (IgG) were industrially prepared in the Japanese Red Cross Central Blood Centre.

Preparation of serum samples

Fresh human blood (10 ml) was centrifuged at 800 *g* for 10 min. Sucrose was added to the serum up to 10% (w/v), and the serum was stored at −20°C and thawed at room temperature before use.

Apparatus

For the first dimension (carrier-free isoelectric focusing), an apparatus (side view shown in Fig. 1A) was constructed that consists of three parts: a column to be filled with cathode solution (Fig. 1A-a), a separation column to be filled with ampholine solution (Fig. 1A-b), and a column to be filled with anode solution (Fig. 1A-c); the total column length is 130 mm. The separation column consisted of seventeen acrylic unit plates with holes (4 mm diameter) (one of these is shown in Fig. 1B). These holes form a line during isoelectric focusing, and after isoelectric focusing the odd-numbered plates are shifted, so that the solution is separated in seventeen closed, small cells. The surfaces of the unit plates are coated with vaseline for water-sealing and then the unit plates are piled up. All parts are pressed together by nuts and bolts with springs inserted. The procedure for the fractionation of samples with this apparatus is shown in Fig. 2. Each fraction is taken out with a syringe (2-ml tuberculin syringe) equipped with a long needle (120 × 0.6 mm O.D.) and either injected into a chromatographic column or transferred to a small vial and stored in a refrigerator.

For the second dimension (gel permeation chromatography), a Model HLC-802 UR HPLC system (Toyo Soda, Yamaguchi, Japan) equipped with a UV spectrophotometer UVIDEC-100-II (JASCO, Tokyo, Japan) is used. For chromatography, a tandem column (two 600 × 7.5 mm stainless-steel columns) packed with G 3000 SW is used.

Isoelectric focusing

Carrier-free isoelectric focusing was performed as follows. On the bottom of the reservoir of the anode solution, a piece of dialysis membrane (3 cm × 3 cm) was attached and fixed with an O-ring. By a syringe equipped with a long needle, 0.75 ml of the anode solution (0.03 *M* phosphoric acid–40% sucrose) was poured into the anode reservoir (Fig. 1A-c), 0.43 ml of the ampholine solution (2% ampholine–20% sucrose) into the electrophoresis column (Fig. 1A-b), and 0.5 ml of the cathode solution (0.1 *M* sodium hydroxide) into the cathode reservoir (Fig. 1A-a), in that order. Sample solution (10 μl) was added at the top of the ampholine solution with a microsyringe. Then the apparatus was put in a polyethylene vessel (120 mm × 80 mm

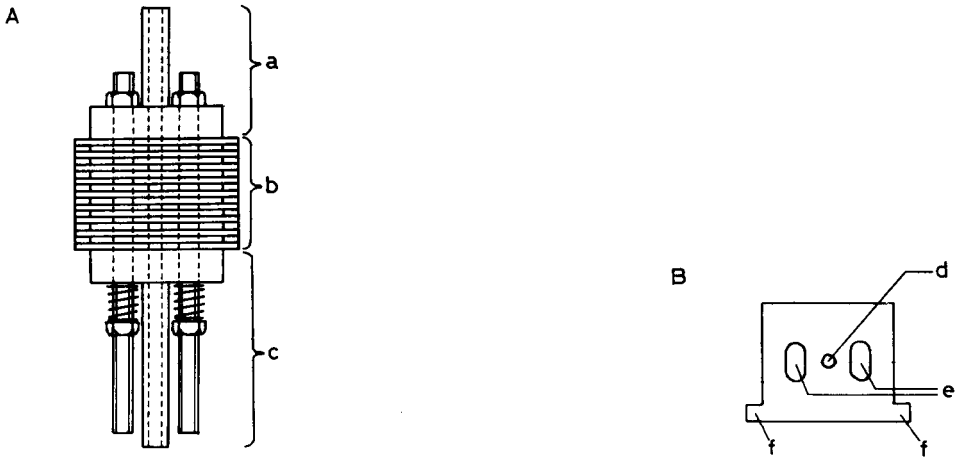

Fig. 1. Carrier-free isoelectric focusing apparatus. (A) Side view of the apparatus: a, column to be filled with cathode solution; b, column to be filled with 2% ampholine solution; c, column to be filled with anode solution; the total column length is 130 mm. B, Top view of a unit plate of column b (50 × 40 × 2 mm): d, hole (all holes together form the electrophoretic column for isoelectric focusing); e, holes for bolts; f, notches for shifting the unit plate.

I.D.) and the vessel was filled with the anode solution so that the electrophoretic column was completely dipped in the anode solution. The vessel was cooled with ice-water. Isoelectric focusing was run at a constant current of 2 mA for 20 min and then at a constant voltage of 460 V for 17 h.

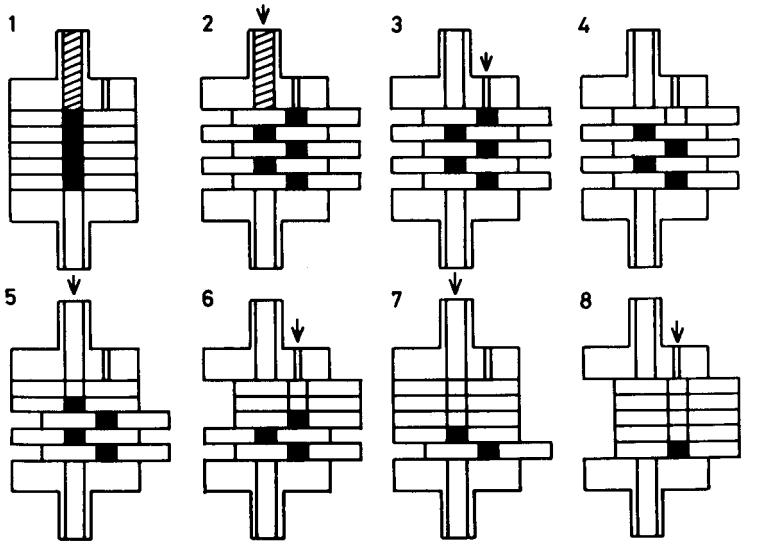

Fig. 2. Method for the fractionation of protein bands after isoelectric focusing. (1) Position of unit plates during isoelectric focusing. (2) Position of unit plates after isoelectric focusing. Odd-numbered unit plates were shifted to fractionate protein bands. The needle of a syringe was inserted as shown by an arrow to take out the solution in the top cell. (3–8) The process of taking the solution out of the cells.

High-performance liquid chromatography

After isoelectric focusing, each fraction was subjected to high-performance gel permeation chromatography. A 25-μl volume of each fraction was introduced into the column and developed with an elution buffer (0.05 *M* sodium acetate containing 0.2 *M* sodium sulphate, pH 5.0). The flow-rate was 1 ml/min at room temperature. The absorbance of the eluate was monitored at 230 nm. The time necessary for the separation of one sample was *ca.* 50 min.

RESULTS

Separation of serum proteins by carrier-free isoelectric focusing

Fig. 3 shows an example of the separation of a serum sample. The pH values and the protein contents in the seventeen fractions obtained by the carrier-free isoelectric focusing apparatus are shown. The pH range of the fractions was from 7.08 (fraction 1) to 4.90 (fraction 17). Protein content is shown as a percentage of the total protein.

Separation of IEF-fractionated serum proteins by HPLC system

Fig. 4 shows HPLC elution patterns of the IEF fractions 1–10. Fraction 1 was the most alkaline fraction (pH 7.1). Arrows under the elution patterns show the peak positions of purified proteins.

As shown in the elution patterns of fractions 1–3 (the pH values of the three fractions were 7.1, 6.8 and 6.7 respectively), IgG in these fractions showed a symmetrical peak, suggesting the absence of other protein species in the peak. This implies that IgG in a serum sample could be purified by this IEF–HPLC system. Fraction 10 also had a peak close to the peak position of IgG. However, this peak should represent a protein species other than IgG, because fraction 10 contained proteins of p*I* 6.0, which is outside the p*I* range of IgG. Seventy-five peaks were counted in the seventeen elution patterns of a serum sample, excluding the peaks of ampholine.

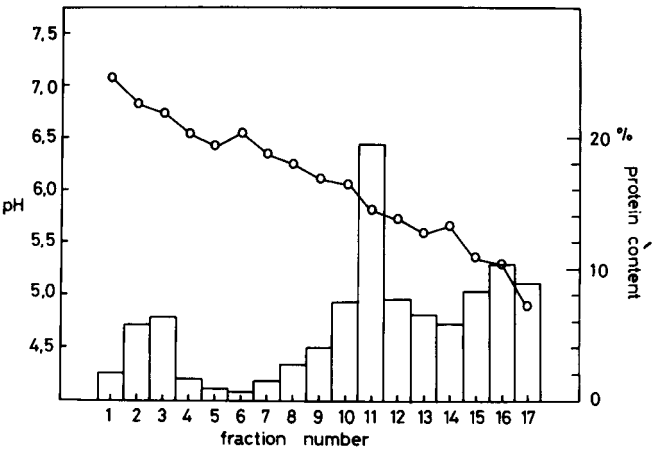

Fig. 3. Separation of human proteins with the carrier-free isoelectric focusing apparatus. The pH gradient and the protein contents (bars, % of total protein) of the seventeen fractions are shown. The most alkaline fraction was fraction 1 and the most acidic one was fraction 17.

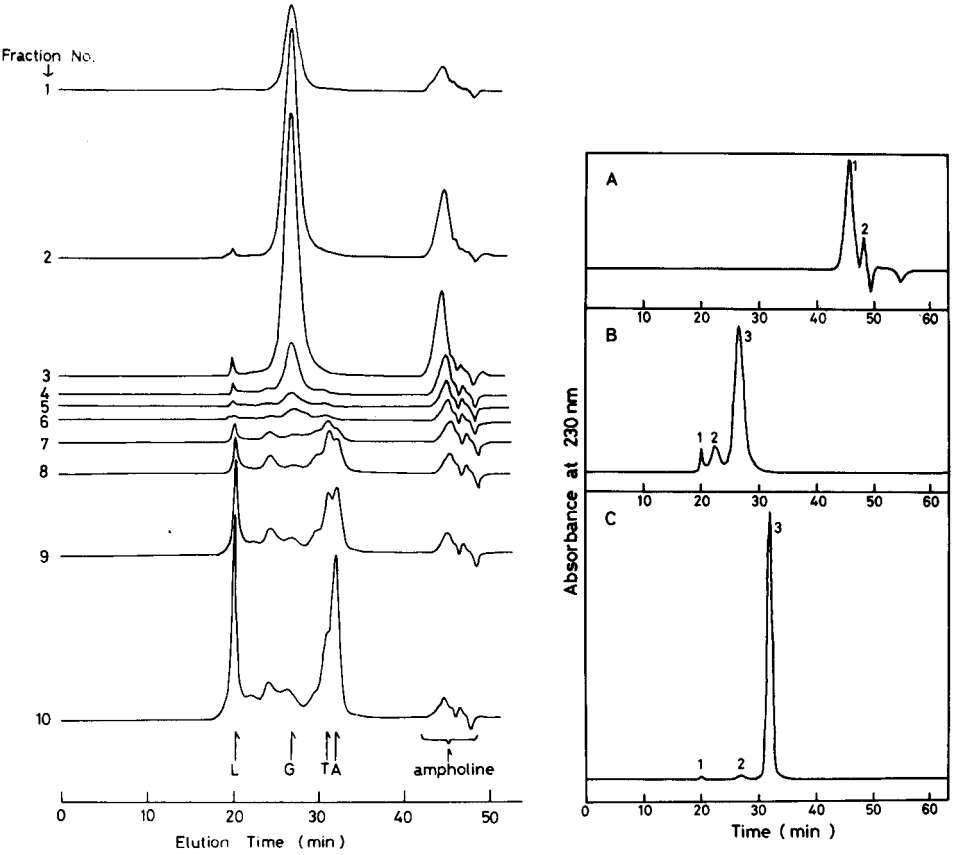

Fig. 4. High-performance gel permeation chromatograms of fractions (fractions 1–10) obtained by the carrier-free isoelectric focusing apparatus. Buffer, 0.05 *M* sodium acetate containing 0.2 *M* sodium sulphate, pH 5.0; flow-rate, 1 ml/min; detection, UV (230 nm). Arrows indicate the elution time of: L, lipoprotein; G, IgG; T, transferrin; A, albumin.

Fig. 5. Elution patterns of ampholine and purified proteins. (A) 2% Ampholine (pH 3.5–10)–20% sucrose, 20 μl. (B) Human serum IgG (0.15%), 20 μl. (C) Human serum albumin (0.2%), 20 μl. Buffer, 0.05 *M* sodium acetate containing 0.2 *M* sodium sulphate, pH 5.0; flow-rate, 1 ml/min; detection, UV (230 nm).

Elutions of purified serum proteins and ampholine by HPLC

Fig. 5A shows an elution pattern of ampholine by HPLC. When 20 μl of 2% ampholine (pH 3.5–10)–20% sucrose was applied, two peaks appeared (1 and 2 in Fig. 5A) and their elution times were between 40 min and 50 min.

Fig. 5B shows an elution pattern of human serum IgG (0.15%, 20 μl). Peaks 3, 2, and 1 were identified from a molecular weight standard curve[4] to be monomer, dimer, and other polymers of IgG, respectively. Elution time of the monomer was 27 min.

Fig. 5C shows an elution pattern of human serum albumin (0.2%, 20 μl). Peak 3, 2, and 1 were identified to be albumin monomer, dimer, and polymers, respectively. Elution time of the monomer was 32 min.

DISCUSSION

Two-dimensional separation is a feasible method for analysis of complex mixtures of proteins such as serum proteins. Various combinations of different techniques have been used for two-dimensional separation[5–7]. Combination of carrier-free isoelectric focusing and high-performance gel permeation chromatography was chosen for the following reasons. (1) This system separates proteins by two independent factors, p*I* in the carrier-free isoelectric focusing and molecular weight in the high-performance gel permeation chromatography. The p*I* values in each fraction obtained by carrier-free isoelectric focusing and the molecular weight of proteins separated by HPLC can be measured. Thus, proteins separated by this system can be assigned by p*I* and molecular weight. (2) Proteins can be separated without using a gel matrix. Therefore, no troublesome procedures to extract proteins from the gel matrix are necessary, and the processes of staining and destaining are not required to detect proteins because they can be detected by UV absorbance.

Automatic separation will become easy in this system because proteins are separated in solution and no operation to extract proteins from the gel matrix is necessary. Construction of an automatic sample take-out device is in progress.

REFERENCES

1 B. W. Moore and D. McGregor, *J. Biol. Chem.*, 240 (1965) 1647.
2 T. Manabe, K. Kojima and T. Okuyama, *J. Biochem.*, 85 (1979) 649.
3 P. O'Farrell, *J. Biol. Chem.*, 250 (1975) 4007.
4 T. Hashimoto, H. Sasaki, M. Aiura and Y. Kato, *J. Chromatogr.*, 160 (1978) 301.
5 K. S. Bloom and J. N. Anderson, *Anal. Biochem.*, 98 (1979) 410.
6 L. Anderson and N. G. Anderson, *Proc. Nat. Acad. Sci. U.S.*, 74 (1977) 5421.
7 F. Erni and R. W. Frei, *J. Chromatogr.*, 149 (1978) 561.
8 T. Manabe, K. Kojima, S. Jitsukawa, T. Hoshino and T. Okuyama, *J. Biochem.*, 89 (1981) 841.

Journal of Chromatography, 239 (1982) 571–583
Elsevier Scientific Publishing Company, Amsterdam — Printed in The Netherlands

CHROM. 14,690

CHARACTERIZATION OF BILE ACID METHYL ESTER ACETATE DERIVATIVES OF RAT BILE USING SOLVENTLESS GLASS CAPILLARY GAS CHROMATOGRAPHY AND ELECTRON IMPACT AND AMMONIA CHEMICAL IONIZATION MASS SPECTROMETRY

TAKESHI MURATA*, SEJI TAKAHASHI, SHOZO OHNISHI and KIYOSHI HOSOI
Analytical Application Laboratory, Shimadzu Corporation, Nakagyo-ku, Kyoto 604 (Japan)
and
TOSHIAKI NAKASHIMA, YASUCHIKA BAN and KINYA KURIYAMA
Department of Pharmacology, Kyoto Prefectural University of Medicine, Kyoto (Japan)

SUMMARY

Methyl ester acetate derivatives of rat bile acids were analysed by a combined technique of solventless glass capillary gas chromatography and electron impact and ammonia chemical ionization mass spectrometry. Glass capillary columns ensure an excellent separating efficiency and effectiveness in detailed studies of many kinds of bile acid components. We found that the ammonia chemical ionization mass spectrometry gave $(M+NH_4)^+$ ions for all the methyl ester acetate derivatives of bile acids, and that these ions had intensities equal, or almost equal, to that of the base peak. This indicates that the technique is useful for the identification of unknown components, especially at trace levels. The results of electron impact and ammonia chemical ionization mass spectrometry of the major compound and the product obtained by catalytic hydrogenation of the compound indicated that this bile acid was a derivative of $\Delta\beta$-muricholic acid having a double bond in the side-chain. We also found that most components had one double bond in their side-chain.

INTRODUCTION

Bergström *et al.*[1], Eneroth and co-workers[2,3], Sjövall and co-workers[4,5] and Miyazaki and co-workers[6,7] have presented reports on the gas chromatography (GC)–mass spectrometry (MS) of bile acids. Using electron impact ionization mass spectrometry (EI-MS), they made detailed study of the method of derivatization and fragmentation and succeeded in obtaining useful information on the structures of bile acids.

Chemical ionization mass spectrometry (CI-MS)[8,9], which has the advantages that fewer fragment ions are produced and that the molecular ion intensities are higher, has been used for the analysis of bile acids, in addition to EI-MS.

Szczepanic *et al.*[10] analysed bile acid methyl ester derivatives by isobutane CI-MS, and found that only keto bile acids gave MH^+ ions, that monohydroxy, dihydroxy and trihydroxy bile acids gave no MH^+ ions, and that, although these bile acids

0021-9673/82/0000–0000/$02.75

gave $MH^+ - 60$, $MH^+ - 60 \times 2$, and $MH^+ - 60 \times 3$ ions (which are molecular ions without the acetic acid groups), these ions were not very useful for the qualitative analysis of multi-component samples.

Muschik *et al.*[11] analysed bile acid methyl esters by GC–CI (CH_4)-MS with methane as the reagent gas, and found that only keto bile acids gave MH^+ ions, and that all the other components gave fragment ions which were $(M \pm H)^+$ ions from which methanol, water or methane groups were lost.

Kuriyama and co-workers[12,13] analysed bile acid methyl ester acetate derivatives by GC–CI (NH_3)-MS, and found that the $(M + NH_4)^+$ ions which are the QM^+ ions were detected at intensities almost equal to that of the base peak. They succeeded in identifying an unknown component as β-muricholic acid having a double bond in its side-chain. A. Maquestion *et al.*[14] reported the formation of some cation to aliphatic and aromatic ketones using ammonia chemical ionization mass analyzed ion kinetic energy spectrometry, and Carroll *et al.*[15] also reported the adduct ion formation in ammonia chemical ionization mass spectrometry.

Various column packings, such as OV-1, OV-17, OV-225, QF-1, AN-600 and SP-525, were tried in this analysis, but none gave satisfactory separations. Although glass capillary columns ensure for better separations, there have been few reports on their application in GC–MS analysis. Among the few examples of the reports are the following: Yanagisawa *et al.*[16] carried out trace quantitative analyses of bile acids in human liver tissue by the selected ion monitoring method, using an SE-30 wall-coated open tubular (WCOT) column (25 m × 0.35 mm I.D.); Barnes[17] used an SP-225 WCOT column (30 m × 0.2 mm I.D.) for studying the permethylation of bile acids.

We reported[12,13] that, in GC–CI (NH_3)-MS analysis of bile acid methyl ester acetate derivatives, all the bile acids gave $(M + NH_4)^+$ ions. Our recent experiments showed that the solventless glass capillary GC-CI (NH_3)-MS method is effective for the identification of so far unknown peaks and minor peaks.

EXPERIMENTAL

Materials

The authentic bile acids and cholylglycine hydrolase (*Clostridium welchii* acetone powder, type IV) were purchased from Sigma (St. Louis, MO, U.S.A.). Amberlite XAD-2 and Amberlyst A-15 (H^+) resins were supplied by Rohm and Haas (Philadelphia, PA, U.S.A.). The XAD-2 resin was treated as follows prior to use. A suspension of resin in 3–5 volumes of methanol containing 0.5% hydrochloric acid was heated for 1 h under gentle refluxing, then washed successively with methanol and water. The column used was a WCOT type (20 m × 0.36 mm I.D.), coated with SE-30 (LKB, Stockholm, Sweden).

Preparation of bile

Male Wistar rats (200–250 g) were fasted for 24 h before the analysis, then anaesthetized with pentobarbital (50 mg/kg, i.p.). Bile samples were collected for 30 min after inserting a bile duct cannula. The collected samples were stored at −15°C until the chemical treatments for GC–MS analysis.

The collected bile sample was added dropwise to 50 ml of ethanol and agitated in an ultrasonic bath, then the solution was heated under refluxing for 10 min. After

cooling to room temperature, the insoluble materials were filtered off and the filtrate was concentrated under reduced pressure. A solution of the residue in 50 ml of 72% ethanol was passed through a column of Amberlyst A-15 (H^+) (50 × 16 mm I.D.) followed by the elution with 10 ml of 72% ethanol. The effluent from this column was concentrated *in vacuo* and the residue was dissolved in 50 ml of 90% ethanol.

A sample containing unconjugated and glycine- and taurine-conjugated bile acids was dissolved in 8 ml of 0.2 *M* acetate buffer (pH 5.6) and then hydrolysed with cholylglycine hydrolase[18]. After acidifying and extracting with diethyl ether, the unconjugated and hydrolysed bile acids were methylated with diazomethane and then acetylated by heating with 2 ml of acetic anhydride at 140°C for 4 h[19]. Each methylated and acetylated sample was evaporated to dryness and the residue was dissolved in 0.2 ml of acetone.

Catalytic hydrogenation of the methyl ester acetate of bile acids was performed at room temperature in 5 ml of 90% ethanol using 3 mg of platinum oxide.

Gas chromatograph–mass spectrometer

GC–EI/CI-MS analyses were performed on LKB-2091 and Shimadzu AUTO GCMS-6020 instruments equipped with an EI/CI dual ion source using an all-glass, solventless injector constructed according to Van den Berg and Cox[20], mounted in the heated injector block of the column oven.

Open-tubular glass capillary columns (20 m × 0.36 mm I.D.) coated with SE-30, were held in aluminium column holders. The column temperature was programmed from 250 to 290°C at 2°C/min and kept isothermal at 290°C until the last peak had been recorded.

The mass spectrometric conditions for EI-MS were as follows: the ion source temperature was held at 310°C; the mass spectra were all obtained at an electron energy of 20 eV, an emission current of 60 μA and an accelerating voltage of 3.5 kV. In the CI-MS the ion source temperature was held at 230°C, the mass spectra were all obtained at an electron energy of 500 eV, an emission current of 500 μA and of an accelerating voltage of 3.5 kV. Ammonia was used as the reagent gas and the pressure in the ion source was adjusted to 0.9 Torr.

The data processing system included a GCMS-PAC 500 FDG consisting of an OKITAC 4300C minicomputer with 16K core, a printer–plotter and a magnetic disk. The mass spectra were stored in a magnetic disk at 3-sec intervals and the mass chromatograms of desired *m/z* values were recorded.

RESULTS AND DISCUSSION

Gas chromatography–ammonia chemical ionization mass spectrometry

In the GC–EI-MS analysis of bile acids, keto bile acids were the only compounds that gave molecular ions; no other bile acids gave molecular ions in any derivative form. If isobutane of methane was used as the reagent gas in the CI-MS of bile acids, as used by Szczepanik *et al.* and Muschik *et al.*, QM^+ ions were given only by keto bile acids.

We found in analyses of sugars[21] and triglycerides[22] that, although QM^+ ions are not given when isobutane or methane is used as the reagent gas, the molecular ions are seen if ammonia is used. We applied this method to the analysis of bile acids.

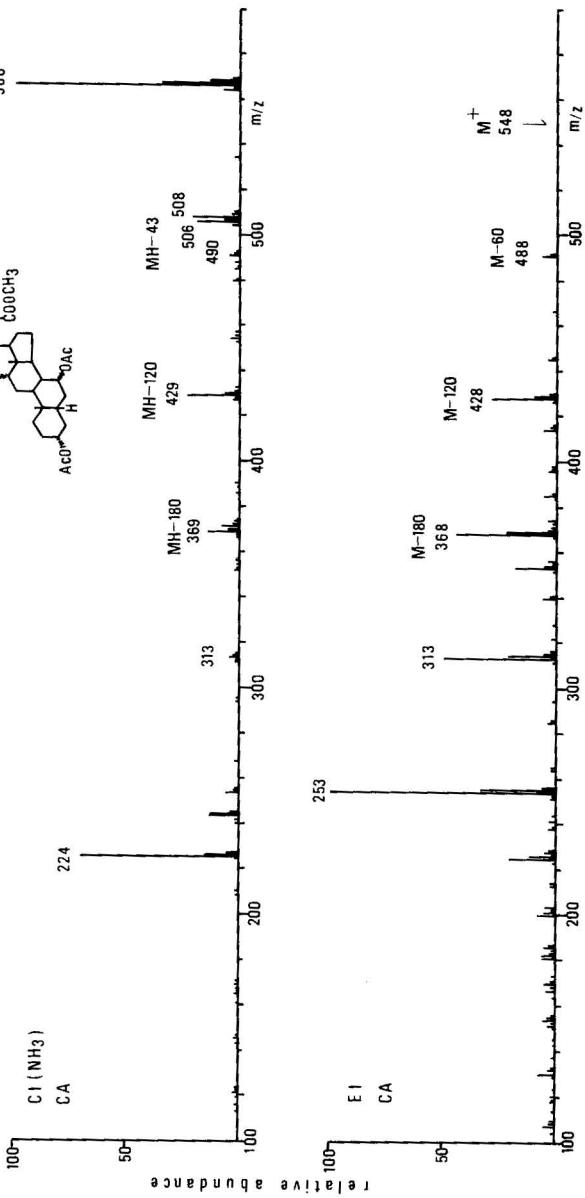

Fig. 1. CI(NH_3) and EI mass spectra of cholic acid methyl ester acetate. The $(M + NH_4)^+$ ion is recorded at *m/z* 566 as the base peak in the CI(NH_3) mass spectrum, but is not recorded in the EI mass spectrum.

We found that in the CI (NH_3)-MS analysis of bile acid methylester acetate derivatives, all of the keto bile acids, dihydroxy bile acids and trihydroxy bile acids gave $(M+NH_4)^+$ ions. However, if the bile acids were derivatized into methyl ester trimethylsilylated derivatives, none of them gave $(M+NH_4)^+$ ions even when ammonia was used as the reagent gas.

Figs. 1 and 2 show the CI(NH_3) and EI-MS spectra of cholic acid methyl ester derivatives (CA) and β-murucholic acid methyl ester acetate (β-MCA). These mass spectra are presumed that the high intensity of the $(M + NH_4)^+$ ions is attributable to the bonding of the basic NH_4^+ ion in the molecule. This intramolecular bonding occurs in CA at the 3α-OAc, 7α-OAc and 12α-OAc, and in β-MCA of 3α-OAc, 6β-OAc and 7β-OAc positions. The $-COOCH_3$ group hardly combines with NH_4^+ ion in the molecule. This can be seen from the CI(NH_3)-MS spectra of the methyl ester trimethylsilylated derivatives. In these derivatives, the only position where intramolecular bonding with NH_4^+ ion can possibly occur is the $-COOCH_3$ group, but in fact this group does not give any $(M+NH_4)^+$ ion. It is known that $(M+NH_4)^+$ ions are seen in the CI(NH_3)-MS spectra of fatty acid methyl esters. The fact that the $-COOCH_3$ group of some compounds gives $(M+NH_4)^+$ ions and that of other compounds does not may be explained by the influence of the stereoscopic conformation of the molecules concerned.

In the CI(NH_3) mass spectrum, the $(M+NH_4)^+$ ion is recorded at m/z 566 as the base peak. In the EI-mass spectrum, the peak of the largest mass number is the M – 60 (CH_3COOH) peak recorded at a low intensity at m/z 488. The CI(NH_3) mass spectrum always has a peak at m/z 224, probably given by the steroid skeleton. The EI mass spectra give more information on chemical structures. In Figs. 1 and 2, for example, CA and β-MCA, which are both trihydroxy bile acids, can be easily differentiated in the EI mass spectrum, while they are hardly differentiated in the CI(NH_3) mass spectrum.

Some components cannot be separated by either a packed column or a capillary column. Fig. 3 shows the CI(NH_3) and the EI mass spectra of hyodeoxycholic acid methyl ester acetate (HDCA) and 7-ketodeoxycholic acid methyl ester acetate (7-keto-DCA), which cannot be separated even with a capillary column. In the EI mass spectrum, these two compounds, which are recorded as main peaks, or peaks as intense as the main peaks, on the chromatogram can be identified from the fragment ion peaks, but they cannot be identified from the fragment peaks if they are not so intense on the chromatogram and, moreover, are overlapped by intenser peaks. In the CI(NH_3) mass spectrum, the QM^+ ions of HDCA and 7-keto-DCA are recorded at m/z 508 and 522, respectively. These two peaks show that dihydroxy and keto bile acids coexist. The EI mass spectrum is informative about chemical structure only when the information about molecular weight is given. The three ions at m/z 444 (M – 60), m/z 426 (M – 60 – 18) and m/z 384 (M – 120 – 18), which are fragment ions of 7-keto-DCA, cannot be distinguished from the fragment ions of m/z 444 (M-60-42), m/z 426 (M – 120) and m/z 384 (M – 180 – 42) of trihydroxy bile acids, which are given when one double bond exists in the molecules.

Fig. 4 shows the CI(NH_3) and EI mass spectra of the main peak of $\Delta\beta$-muricholic acid methyl ester acetate. In the CI(NH_3) mass spectrum, the QM^+ ion was recorded at m/z 564. In the spectra of CA and β-MCA shown in Figs. 1 and 2, the QM^+ ions were recorded at m/z 566. Compared with these spectra, that in Fig. 4 gives

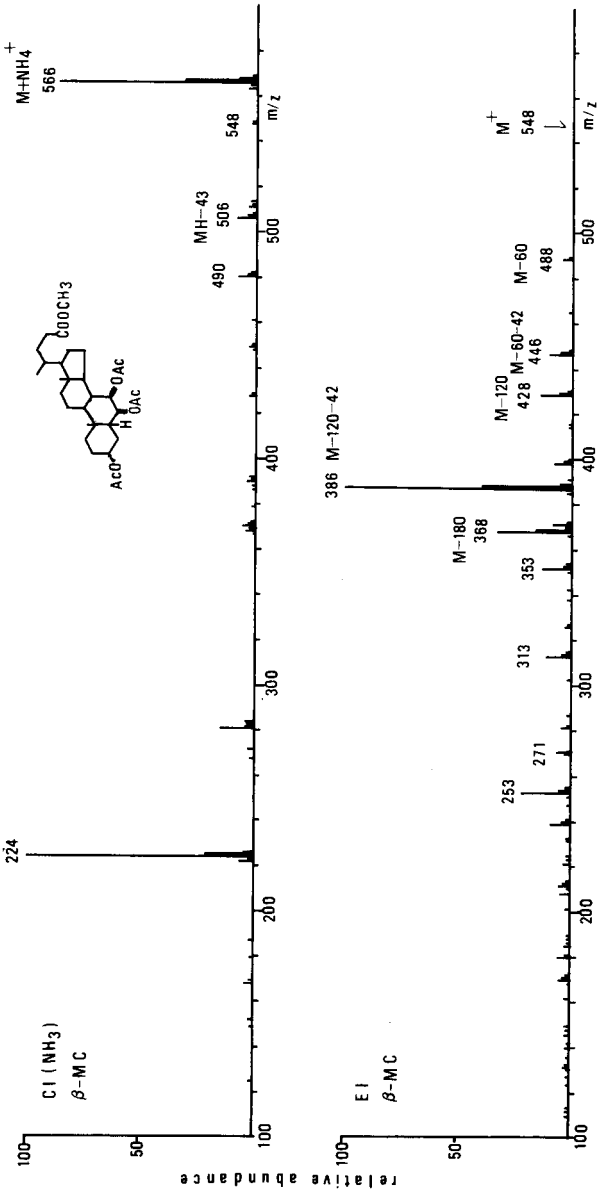

Fig. 2. CI(NH_3) and EI mass spectra of β-muricholic acid methyl acetate.

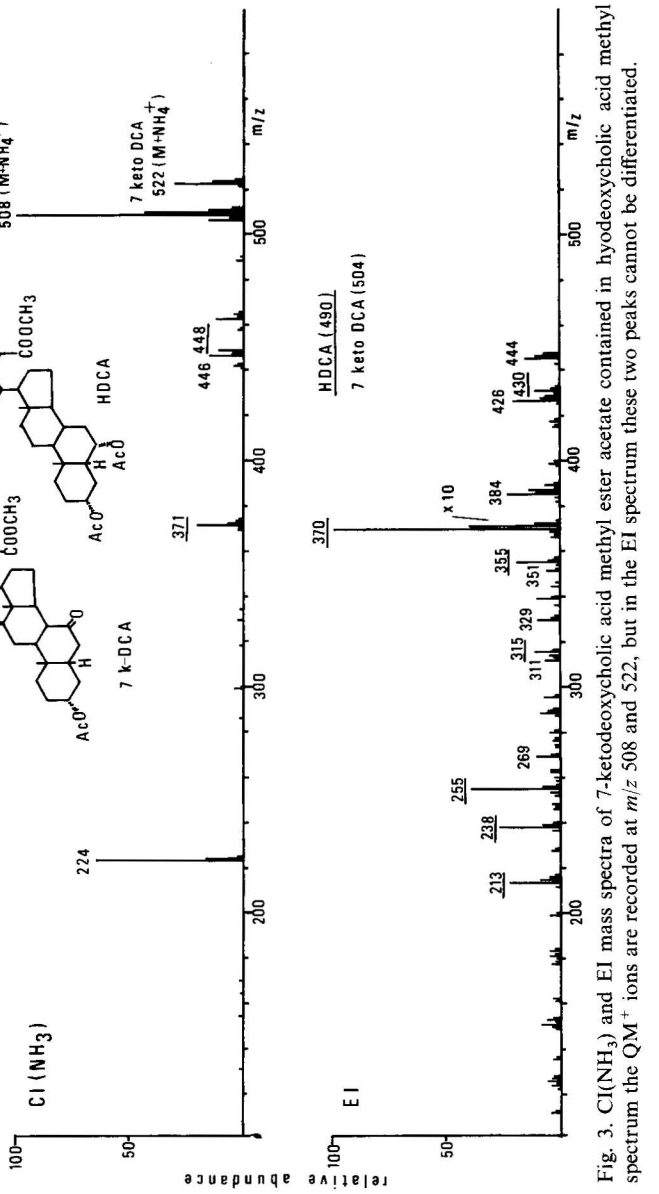

Fig. 3. CI(NH_3) and EI mass spectra of 7-ketodeoxycholic acid methyl ester acetate contained in hyodeoxycholic acid methyl acetate. In the CI(NH_3) mass spectrum the QM^+ ions are recorded at m/z 508 and 522, but in the EI spectrum these two peaks cannot be differentiated.

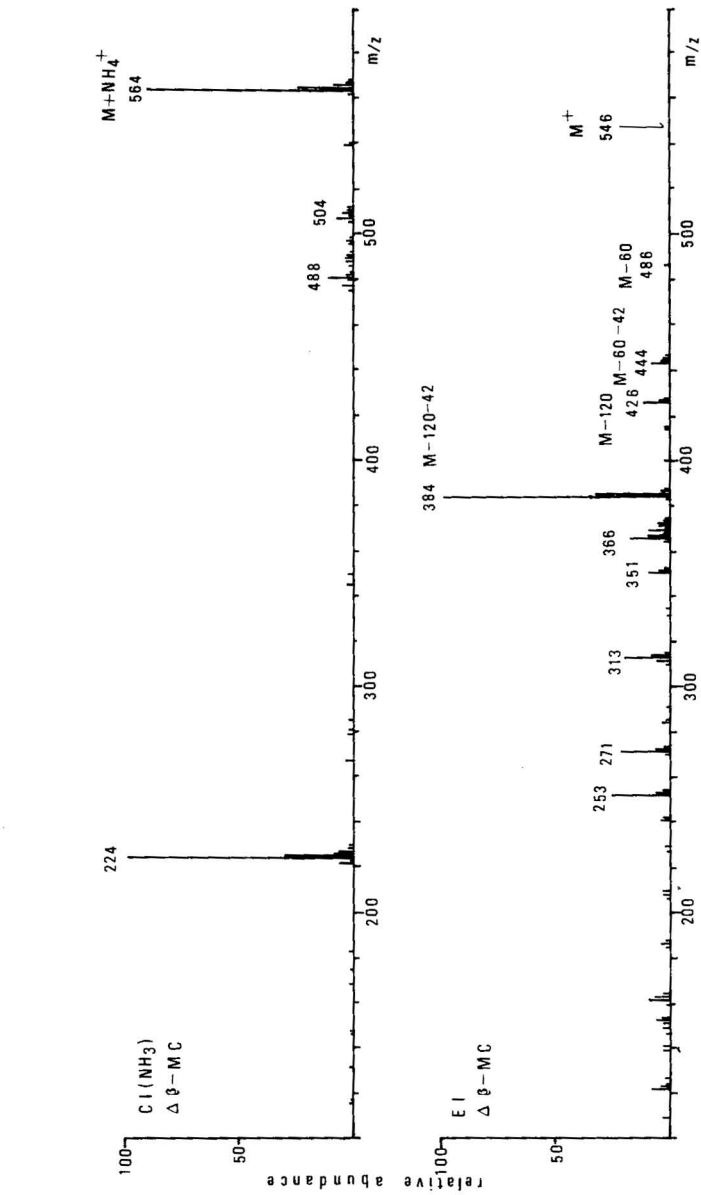

Fig. 4. CI(NH_3) and EI mass spectra of $\Delta\beta$-muricholic acid methyl ester acetate. The pattern is similar to that of β-MCA shown in Fig. 2, but the fragment ions M^+, M − 60, M − 60 − 42, M − 120, M − 120 − 42 and M − 180 and the ions below *m/z* 351 are recorded 2 a.m.u. lower.

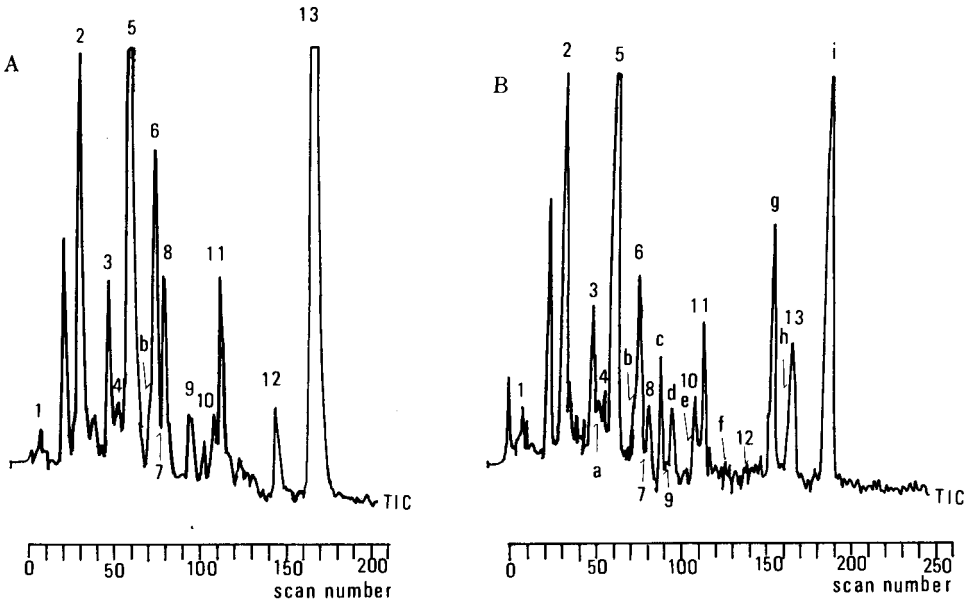

Fig. 5. Total ion chromatogram obtained by glass capillary column GC–EI-MS. (A) After catalytic hydrogenation; (B) before catalytic hydrogenation.

the QM^+ ion at a position lower by 2 a.m.u. This shows the presence of one double bond in the molecule. The combination of the $CI(NH_3)$ and EI mass spectra shows that this compound is $\Delta\beta$-MCA, which is β-MCA having a double bond in the molecule. Also, the data provided by the $CI(NH_3)$ mass spectrum on the QM^+ ion show that the molecules of dihydroxy and trihydroxy bile acids, as well as $\Delta\beta$-MCA, have double bonds in their molecules. The EI mass spectra were further studied to determine the positions of double bonds. Not only the molecular ion but also the fragment ions such as M − 60, M − 60 − 42, M − 120, M − 120 − 42 and M − 180 and the ion of *m/z* 351 of trihydroxy bile acids were recorded at positions 2 a.m.u. lower than the ions having no double bonds. In other words, the fragment ions produced in the process in which the hydroxy groups are cleaved off one by one are recorded at positions 2 a.m.u. lower. The *m/z* 313 and 253 ions produced when the side-chains are cleaved off are given by both compounds having double bonds and those having no double bonds (dihydroxy groups commonly give *m/z* 315 and 255 ions).

We can conclude from these facts that the double bond is present in the side-chains. We could not obtain the fragment ions that indicate the position of the double bond in the side-chains, but it is probable that it occurs at one of the positions between the 20th and 21st, 20th and 22nd and 22nd and 23rd positions.

Further, the sample was treated by catalytic hydrogenation, and analysed by $CI(NH_3)$-MS and EI-MS. None of the compounds that we presumed to have a double bond was detected.

Glass capillary column GC–electron impact ionization mass chromatography

As described earlier, the technique using $CI(NH_3)$-MS is effective for determining molecular weights but is not very effective for structural studies. We identified the

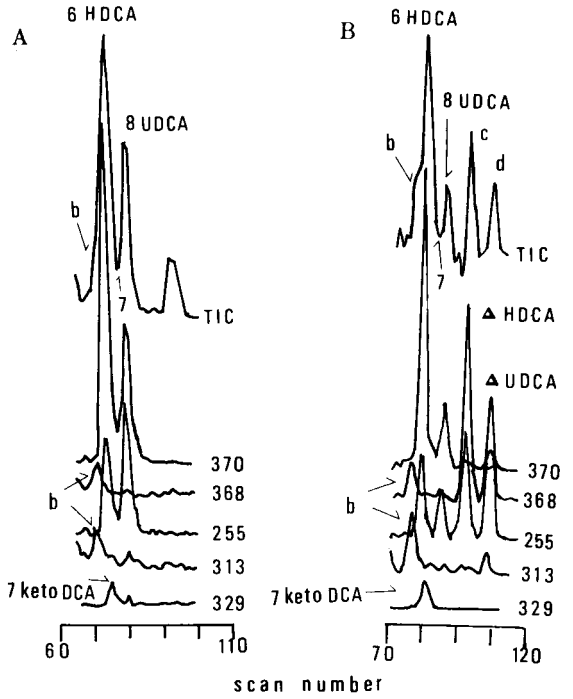

Fig. 6. Mass chromatograms from scans 60–110 (A) and from scans 70–120 (B). (A) is the MC of the *m/z* 370 ion, and gives the peaks for HDCA and UDCA. (B) is the MC of the *m/z* 370 and ions and gives the peaks for HDCA, UDCA, ΔHDCA and ΔUDCA. The MC of the *m/z* 255 ion formed when two acetic acid groups and side-chains are cleaved off is common to HDCA, UDCA, ΔHDCA and ΔUDCA. This shows the presence of double bond in the side-chains. The MC of the *m/z* 329 ion shows the presence of 7-keto-DCA. The ion at *m/z* 313 is not influenced by catalytic hydrogenation. The EI mass spectrum shows that it is trihydroxy bile acid.

components by electron impact ionization mass chromatography (MC). Fig. 5 shows the total ion chromatograms (TIC) of samples before (B) and after catalytic hydrogenation (A). Of the many components detected, those marked with numerals and letters were identified; those marked with numerals correspond to representative bile acid components, and those with letters were identified in our experiments.

The peaks a–h, except for b, in the chromatogram B are not seen in chromatogram A. This indicates that all of these peaks have double bonds.

Fig. 6 shows the data obtained by MC. The ion at *m/z* 370 ($M - CH_3COOH \times 2$) is seen on both chromatograms A and B as HDCA and UDCA. The ion at *m/z* 368 ($M - CH_3COOH \times 2$), lower than *m/z* 370 by 2 a.m.u., is seen only on chromatogram B. This shows that sample B contains ΔHDCA and ΔUDCA.

The ion at *m/z* 255 corresponds to the dihydroxy bile acid from which two acetic acid groups and side-chains have been removed by cleavage. This ion is seen in HDCA, UDCA, ΔHDCA and ΔUDCA, which indicates that the double bond is present in the side-chains. If the double bond were to be present in the steroid skeleton, ΔHDCA and ΔUDCA would give an MC peak at *m/z* 253. ΔCDCA is also present in dihydroxy bile acid.

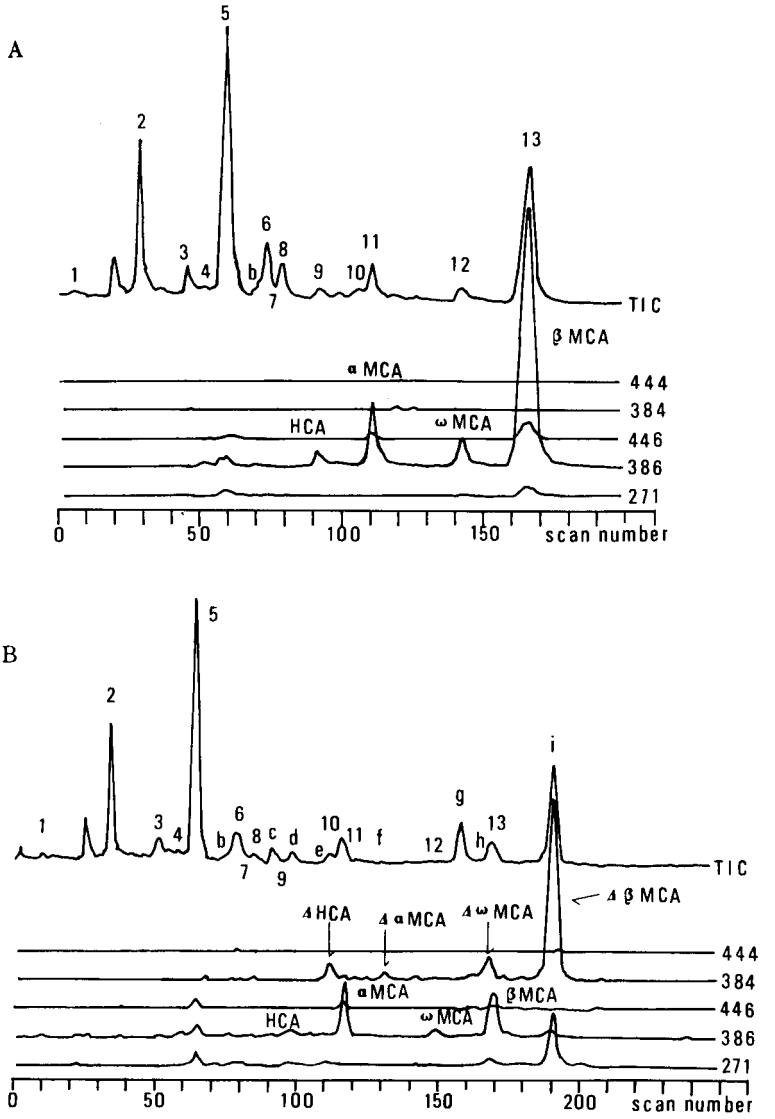

Fig. 7. MC of 3,6,7-trihydroxy bile component. In (A), HCA, α-MCA, ω-MCA and β-MCA are seen. In (B), ΔHCA, Δα-MCA, Δω-MCA and Δβ-MCA are seen in addition to these components.

The ion at *m/z* 329 corresponds to 7-keto-DCA from which one acetic acid group and side-chain have been cleaved off. It is the MC of the mass spectra of HDCA and 7-keto-DCA shown in Fig. 3.

Only component b gives the $(M+NH_4)^+$ ion at *m/z* 566 (molecular weight 548), is not influenced by catalytic hydrogenation and gives an EI mass spectrum similar to that of CA and allo-CA: the base peak is recorded at *m/z* 253 and the main fragment peaks at *m/z* 313, 368 and 428. This indicates that the component b is 3,7,12-trihydroxy bile acid. We presumed it to be $C_{24}5\beta3\beta OAc7\alpha OAc12\alpha OAc$.

TABLE I

IDENTIFICATION OF BILE ACIDS BY GLASS CAPILLARY COLUMN GAS CHROMATOGRAPHY–ELECTRON IMPACT, CHEMICAL IONIZATION MASS SPECTROMETRY

Peak	*Compound*	M^+	$M + NH_4^+$
1	Lithocholate (C_{24} 5β3αOAc)	432	450
2	Deoxycholate (C_{24}5β3αOAc12αOAc)	490	508
3	Chenodeoxycholate (C_{24}5β3αOAc7αOAc)	490	508
4	7-Ketolithocholate (C_{24}5β3αOAc7C=O)	446	464
5	Cholate (C_{24}5β3αOAc7αOAc12αOAc)	548	566
6	Hyodeoxycholate (C_{24}5β3αOAc6αOAc)	490	508
7	7-Ketodeoxycholate (C_{24}5β3αOAc7C=O12αOAc)	504	522
8	Ursodeoxycholate (C_{24}5β3αOAc7βOAc)	490	508
9	Hyocholate (C_{24}5β3αOAc6αOAc7αOAc)	548	566
10	Allo-cholate (C_{24}5α3αOAc7αOAc12αOAc)	548	566
11	α-Muricholate (C_{24}5β3αOAc6βOAc7αOAc)	548	566
12	ω-Muricholate (C_{24}5β3αOAc6αOAc7βOAc)	548	566
13	β-Muricholate (C_{24}5β3αOAc6βOAc7βOAc)	548	566
a	Δ-Chenodeoxycholate (C_{24}5β3αOAc7αOAc)	488	506
b	– (C_{24}5β3βOAc7αOAc12αOAc)	548	566
c	Δ-Hyodeoxycholate (ΔC_{24}5β3αOAc6αOAc)	488	506
d	Δ-Ursodioxycholate (ΔC_{24}5β3αOAc7βOAc)	488	506
e	Δ-Hyocholate (C_{24}5β3αOAc6αOAc7αOAc)	546	564
f	$\Delta\alpha$-Murichole (C_{24}5β3αOAc6βOAc7αOAc)	546	564
g	Unidentified (not bile acid)	368	369
h	$\Delta\omega$-Muricholate (ΔC_{24}5β3αOAc6αOAc7βOAc)	546	564
i	$\Delta\beta$-Muricholate (ΔC_{24}5β3αOAc6βOAc7βOAc)	546	564

3,6,7-Trihydroxy bile acid gives the base peak at *m/z* 386 and main fragment peaks at *m/z* 368, 428 and 446. Fig. 7 shows the mass chromatograms of the base peak (*m/z* 386) and of the peak at *m/z* 384. Sample A gives the MC peaks of HCA, α-MCA, ω-MCA and β-MCA attributable to the *m/z* 386 ion. Sample B gives, in addition to all of these peaks, the MC peaks of ΔHCA, $\Delta\alpha$-MCA, $\Delta\omega$-MCA, and $\Delta\beta$-MCA.

The MC of the ion at *m/z* 253 shows that 3,6,7-trihydroxy bile acid has a double bond in its side-chains. 3,7,12-Trihydroxy bile acid has no components that have a double bond.

Table I shows the identification results.

REFERENCES

1 S. Bergström, R. Ryhage and E. Stenhagen, *Sv. Kem. Tidskr.*, 73 (1961) 566.
2 P. Eneroth, B. Gorden, R. Ryhage and J. Sjövall, *J. Lipid Res.*, 7 (1966) 511.
3 P. Eneroth, B. Gordon and J. Sjövall, *J. Lipid Res.*, 7 (1966) 524.
4 J. Sjövall, *Application of Gas Chromatography–Mass Spectrometry to the Analysis of Bile Acids in Biological Materials*, Cambridge University Press, London, 1967, p. 243.
5 J. Sjövall, P. Eneroth and R. Ryhage, *Mass Spectra of Bile Acids, Vol. I, Chemistry*, Plenum Press, New York, 1971, p. 209.
6 H. Miyazaki, M. Ishibashi, M. Inoue, M. Itoh and T. Kubodera, *J. Chromatogr.*, 99 (1974) 553.
7 H. Miyazaki, M. Ishibashi and K. Yamashita, *Biomed. Mass Spectrom.*, 5 (1978) 469.
8 B. Munson and F. H. Field, *J. Amer. Chem. Soc.*, 88 (1966) 2621.

9 B. Munson, *Anal. Chem.*, 43 (1971) 28A.
10 P. A. Szczepanik, D. L. Hacheg and P. D. Klein, *J. Lipid Res.*, 17 (1976) 314.
11 G. M. Muschik, L. H. Wright and J. A. Schroer, *Biomed. Mass Spectrom.*, 6 (1979) 266.
12 K. Kuriyama, Y. Ban, T. Nakashima and T. Murata, *Steroids*, 34 (1980).
13 T. Murata, T. Takahashi, T. Takeda, S. Onishi, T. Nakashima, Y. Ban and K. Kuriyama, *Proceedings of the Fifth Meeting of the Japanese Society for Medical Mass Spectrometry*, Japanese Society for Medical Mass Spectrometry, Kurume, 1980, p. 205.
14 A. Maquestion, R. Flammang and L. Nielson, *Org. Mass Spectrom.*, 15 (1980) 379.
15 D. I. Carroll, J. G. Nowlin, R. N. Stillwell and E. C. Horning, *Anal. Chem.*, 53 (1981) 2007.
16 J. Yanagisawa, M. Itoh, M. Ishibashi, H. Miyazaki and F. Nakayama, *Anal. Biochem.*, 104 (1980) 75.
17 S. Barnes, D. G. Pritchard, R. L. Settine and M. Geckle, *J. Chromatogr.*, 183 (1980) 269.
18 O. J. Roseleurand and C. M. van Gent, *Clin. Chim. Acta*, 66 (1976) 269.
19 K. Tsuda, Y. Sato, N. Ikekawa, S. Tanaka, H. Higasshikuze and R. Ohsawa, *Chem. Pharm. Bull.*, 13 (1965) 720.
20 P. N. J. van den Berg and Th. P. H. Cox, *Chromatographia*, 5 (1972) 301.
21 T. Murata and S. Takahashi, *Carbohydr. Res.*, 62 (1978) 1.
22 T. Murata and S. Takahashi, *Anal. Chem.*, 49 (1977) 728.

Journal of Chromatography, 239 (1982) 585–594
Elsevier Scientific Publishing Company, Amsterdam — Printed in The Netherlands

CHROM. 14,545

DETERMINATION OF CAPTOPRIL AND ITS DISULPHIDE IN BIOLOGICAL FLUIDS

YASUHIKO MATSUKI*, TOMIHARU ITO, KATSUHARU FUKUHARA, TETSUYA NAKAMURA, MICHIKO KIMURA and HIROSHI ONO
Hatano Research Institute, Food and Drug Safety Centre, Hadano, Kanagawa (Japan)
and
TOSHIO NAMBARA
Pharmaceutical Institute, Tohoku University, Aobayama, Sendai (Japan)

SUMMARY

A gas chromatographic–mass spectrometric method for the simultaneous determination of captopril (SQ 14,225) and its disulphide (SQ 14,551) in biological fluids by means of selected ion monitoring is described. In order to prevent oxidative degradation, captopril was treated with N-ethylmaleimide (NEM). The captopril–NEM adduct and the disulphide were converted into the hexafluoroisopropyl esters, which were separated on a 10% Dexsil 300GC column and determined by employing the captopril–N-butylmaleimide adducts as an internal standard. The blood and urine levels of captopril and its disulphide in dogs to which captopril had been administered orally were measured by the proposed method. The urinary excretion of these two substances in rats was also determined in a similar manner.

INTRODUCTION

Captopril [1-(D-3-mercapto-2-methyl-1-oxopropyl)-L-proline] (SQ 14,225) is a potent inhibitor of angiotensin-converting enzyme, one of the most important components in the renin–angiotensin system[1–4]. It was demonstrated that the disulphide is a major urinary metabolite in living animals[5,6] and exhibits pharmacological activity in the dog[7]. Both *in vitro* and *in vivo* experiments revealed that captopril is readily converted into the disulphide and unknown sulphur-containing metabolites[8]. A simple method for the gas chromatographic determination of captopril in blood and urine using a flame photometric detector has previously been reported[9]. However, suitable conditions for quantitative derivatization of captopril into the N-ethylmaleimide (NEM) adduct still remain to be established. The methods so far available for the determination of captopril in biological fluids involve thin-layer chromatography (TLC) using a radioactive substrate[5,6,8] and gas chroamtography–mass spectrometry (GC–MS)[10]. These methods, however, are not necessarily satisfactory with respect to feasibility, reliability and sensitivity. An urgent need to investigate the metabolic fate and pharmacokinetics of captopril and its disulphide administered

0021-9673/82/0000–0000/$02.75

orally to dogs and rats prompted us to develop a method for their simultaneous determination.

This paper describes a GC–MS method for the determination of captopril and its disulphide in blood and urine by means of selected ion monitoring.

EXPERIMENTAL

Gas chromatography–mass spectrometry

A Shimadzu Model LKB-9000B gas chromatograph–mass spectrometer was used. A coiled glass column (1 m × 3 mm I.D.) was packed with 10% Dexsil 300GC on Gas-Chrom Q (80–100 mesh). The flow-rate of the carrier gas (helium) was 30 ml/min. The temperature of the column was 258°C, and the injection port and ion source were kept at 270°C. The accelerating voltage, ionization voltage and trap current were 3.5 kV, 70 eV and 60 μA, respectively.

Materials

Captopril (SQ 14,225) and its disulphide (SQ 14,551) were kindly donated by Sankyo Co. (Tokyo, Japan). Hexafluoroisopropanol (HFIP), trifluoroacetic anhydride (TFAA), N-ethylmaleimide (NEM) and other chemicals were of analytical-reagent grade. Piperidinohydroxypropyl Sephadex LH-20 (PHP-LH-20) was prepared in these laboratories by a previously reported method[11]. Amberlite XAD-2 resin was purified prior to use. The resin was stirred with 0.6% hydrochloric acid in 70% ethanol at 70°C for 24 h and washed successively with water, 0.6% sodium hydroxide in 70% ethanol, water, acetone and ethanol. The purified resin was further washed with water and stored in a refrigerator. When used for blood and plasma specimens, the resin should first be washed with ethanol.

Synthesis of captopril–N-butylmaleimide adduct

A solution of maleic anhydride (60 mmol) in chloroform (60 ml) was added dropwise to a stirred solution of *n*-butylamine (50 mmol) in chloroform (50 ml) at 0°C, and the resulting solution was evaporated to dryness. The residue was dissolved in acetic anhydride (125 ml) and the solution heated with anhydrous sodium acetate (6.0 g) at 100°C for 1 h and then at 120°C for 10 h. The reaction mixture was poured into ice–water to decompose the excess of the reagent, and the resulting solution was adjusted to pH 8–9 with 30% sodium hydroxide and 5% sodium hydrogen carbonate. After removal of the precipitate by filtration, the filtrate was extracted twice with 100-ml volumes of *n*-hexane. The organic layer was evaporated and the oily residue was chromatographed on silica gel (50 g) using *n*-hexane–benzene (9:1) as eluent. The eluate was subjected to preparative TLC using chloroform–benzene (9:1) as developing solvent. Elution of the area corresponding to the spot gave N-butylmaleimide (NBM) (1.2 g) as a colourless oil (Mass spectrum: m/z 153, $[M]^+$). The product was homogeneous as judged by TLC.

The captopril–NBM adduct was prepared from captopril and NBM as described in a previous paper[9]. The desired compound was not obtained in the crystalline state but was substantially homogeneous as judged by TLC; mass spectrum (HFIP derivative), m/z 520 ($[M]^+$); TLC [chloroform–methanol–acetic acid (30:8:0.5)], R_F 0.68.

Derivatization into hexafluoroisopropyl ester

Captopril and its disulphide were dissolved in HFIP (0.3 ml) and TFAA (0.6–60 μl) and the solution was heated at 50°C for 60 min. After removal of the excess of reagents with aid of a stream of nitrogen, the residue was dissolved in ethyl acetate (100 μl) and a 1-μl aliquot of this solution was subjected to GC–MS.

Assay of captopril and its disulphide in blood, plasma and urine

A 1-ml volume of blood was diluted with 0.5% NEM in 0.2 *M* phosphate buffer (2 ml) containing an internal standard and washed twice with 10-ml volumes of benzene. The aqueous layer was treated with 20 ml of ethanol for deproteinization. The precipitate was removed by centrifugation at 1600 *g* for 15 min and the supernatant was evaporated to dryness. The residue was dissolved in 5 ml of ethanol and percolated through an Amberlite XAD-2 resin column (15 cm × 10 mm I.D.). The desired fraction was obtained by elution with 45 ml of ethanol, and the eluate was evaporated to dryness. The residue was dissolved in 1 ml of 90% ethanol and an aliquot of the solution (0.8 ml) was applied gently to a PHP-LH-20 column (20 mm × 5 mm I.D.). After washing with 15 ml of 90% ethanol, captopril and its disulphide were eluted with 15 ml of 7% acetic acid in ethanol. The two compounds were converted into the hexafluoroisopropyl esters with HFIP (0.3 ml) and TFAA (0.03 ml) and then subjected to GC–MS. Clean-up of a plasma sample (0.5 ml) was carried out in a similar manner.

With urine, 0.1 ml of a specimen was treated with 0.5% NEM in 0.2 *M* phosphate buffer (2 ml) and washed twice with 5-ml volumes of *n*-hexane. After complete removal of *n*-hexane with the aid of a stream of nitrogen the aqueous phase was adjusted to pH < 2 with 0.5 *N* hydrochloric acid. The resulting solution was percolated through an Amberlite XAD-2 resin column (15 cm × 10 mm I.D.) for removal of water-soluble compounds. After washing with 200 ml of water, captopril and its disulphide were eluted with 50 ml of 90% ethanol, and the eluate was evaporated to dryness. The subsequent procedure was carried out as described above.

Stability of NEM in phosphate buffer solution

To a canine urine specimen (0.1 ml) was added 0.5% NEM in phosphate buffer (2 ml) which had previously been left at room temperature for 3 or 24 h. The determination of captopril and its disulphide was carried out according to the procedure described above.

Effect of the amount of NEM on the formation of captopril–NEM adduct

To a canine urine specimen (0.1 ml) was added freshly prepared 0.01–1.0% NEM in 0.1 *M* phosphate (2 ml). The determination of captopril and its disulphide was carried out according to the procedure described above.

Stability of captopril and its disulphide in blood, plasma and urine

A canine blood specimen was divided into two portions. The plasma was obtained from one of these by centrifugation at 1600 *g* for 10 min. To the blood specimen (1.0 ml) was added freshly prepared 0.5% NEM in 0.1 *M* phosphate buffer at intervals of 15, 30 or 60 min. To the plasma specimen was also added freshly prepared 0.5% NEM in 0.1 *M* phosphate buffer at intervals of 1 or 3 h. The determi-

nation of captopril and its disulphide was carried out according to the procedure described above.

Recovery tests on captopril and its disulphide added to blood, plasma and urine

The test samples were prepared by dissolving *ca* 100 ng of captopril–NEM, 1000 ng of the disulphide and 100 ng of internal standard in canine blood (1 ml), plasma (0.5 ml) and urine (0.1 ml). Each sample was diluted with 2 ml of 0.5% NEM in 0.2 *M* phosphate buffer. The determination of captopril and its disulphide was carried out according to the procedure described above.

Determination of captopril and its disulphide in blood and urine

Female CSK strain beagle dogs (body weight 11.2–12.3 kg) were orally given a single dose of 10 mg/kg of captopril in a gelatine capsule. The blood was withdrawn from a superficial vein, and urine specimens were collected at several intervals through a catheter inserted into the bladder. To the blood (1.0 ml) or urine (0.1 ml) specimen was added 2 ml of freshly prepared 0.5% NEM in 0.2 *M* phosphate buffer.

Sprague Dawley rats (body weight 277–318 g) were orally given through a catheter a single dose of 10 mg/kg each of captopril and its disulphide suspended with 1% carboxymethylcellulose solution. The urine was collected for 24 h throught the metabolic cage into the beaker containing 12.5 ml of 1% NEM in 0.2 *M* phosphate buffer. The determination of captopril and its disulphide was carried out according to the procedure described above.

RESULTS AND DISCUSSION

It has previously been demonstrated that significant amounts of oxidation products are formed from captopril in blood unless it is immediately derivatized[10]. Therefore, initial efforts were directed to establishing suitable conditions for derivatization into the captopril–NEM adduct in the assay procedure.

First, the stability of an NEM solution in phosphate buffer against oxidative decomposition was examined. The urine captopril and its disulphide in dogs administered captopril were determined. The use of NEM reagents that had been left at room temperature for 3 or 24 h after preparation gave the values corresponding to 89% and 84% of the control, respectively. In contrast, there was observed no substantial change in the value for the disulphide (Table I). The immediate treatment of a urine specimen with freshly prepared reagent containing NEM in the range 0.2–20 mg

TABLE I

STABILITY OF NEM IN PHOSPHATE BUFFER

A urine specimen from a dog administered captopril was used for the test.

Time after administration (h)	*Captopril (μg/ml)*	*Disulphide (μg/ml)*
0	175.34	332.44
3	152.68	340.03
24	148.39	342.62

TABLE II

STABILITY OF CAPTOPRIL AND ITS DISULPHIDE IN BLOOD AND PLASMA

Blood (1.0 ml) and plasma (0.5 ml) specimens from a dog administered captopril were used for the test.

Time after administration (min)	*Blood*		*Plasma*	
	Captopril (ng)	*Disulphide (ng)*	*Captopril (ng)*	*Disulphide (ng)*
0	943.8	222.8	–	–
15	825.7	190.6	654.5	428.7
30	684.6	194.9	381.9	475.6
60	587.4	207.0	144.7	443.5

gave substantially identical values for captopril. The use of NEM in these amounts was sufficient to provide the captopril–NEM adduct quantitatively.

The stability of captopril and its disulphide in blood, plasma and urine was also examined (Tables II and III). Employing freshly prepared NEM solution, captopril and its disulphide were determined in blood and plasma specimens left for 15, 30 and 60 min and urine pooled for 1 and 3 h at room temperature. It is evident from the results that a considerable decrease in the level of captopril in plasma was observed as compared with that in blood, although no plausible explanation can be given at present. On the other hand, there was no difference in the disulphide levels in blood and plasma. These results indicated that captopril underwent no oxidation into the disulphide in biological fluids.

TABLE III

STABILITY OF CAPTOPRIL AND ITS DISULPHIDE IN URINE

Urine specimens from a dog administered captopril were used for the test.

Time after administration (h)	*Captopril (μg/ml)*	*Disulphide (μg/ml)*
0	175.34	332.44
1	113.09	336.88
3	66.77	330.80

The utility of the hexafluoroisopropyl ester as a derivative for the GC of captopril has been demonstrated in a previous paper[9]. The disulphide and captopril–NEM were simultaneously derivatized with TFAA and HFIP in various proportions. When treated with these two reagents at 50°C for 60 min, the disulphide was converted into the bis(hexafluoroisopropyl) ester (Fig. 1). The esterification rate was plotted against the ratio of the two reagents in the range 0.002–0.2 as illustrated in Fig. 2. Based on these data, TFAA and HFIP in a ratio of 0.1 was used for derivatization.

The structure of the derivatized disulphide was characterized by GC–MS (Fig. 3). The molecular ion ($[M]^{\ddagger}$) and fragment ion ($[M-366]^{+}$) formed by cleavage of the disulfide bond appeared at m/z 732 and 366, respectively. The base peak at m/z

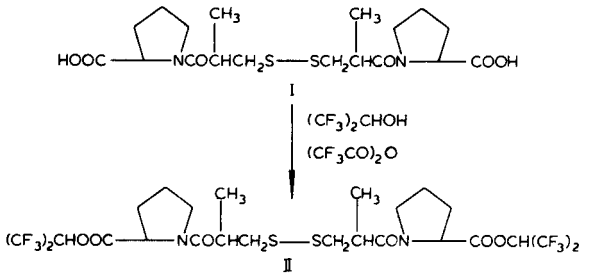

Fig. 1. Derivatization of the disulphide (I) into the bis(hexafluoroisopropyl) ester (II).

264 was assignable to the hexafluoroisopropyl ester of proline produced by the fission of the amide linkage[9]. Among the closely related compounds prepared in these laboratories, the captopril–NEM adduct was chosen as a pertinent internal standard. Dexsil 300GC was the most suitable stationary phase for the separation of captopril–NEM, the disulphide and internal standard. A typical chromatogram obtained by selected ion monitoring is illustrated in Fig. 4. These compounds gave a single peak of the correct theoretical shape.

Calibration graphs were constructed by plotting the ratio of the peak of captopril and its disulphide to that of the internal standard against the amount of the former two. Satisfactory linearity was observed in the range 2.5–10 ng of captopril and its disulphide (Fig. 5). The detection limits of these two were calculated to be 0.5 and 1 ng, respectively.

The utility of the present method for the quantitation of captopril and its disulphide in blood and urine was tested. Clean-up of a blood specimen was readily achieved by extraction with benzene for removal of lipids followed by deproteinization with ethanol. Without the extraction step, captopril and its disulphide were recovered at unsatisfactory levels. The separation of water-soluble compounds in blood, plasma and urine was effected by the use of Amberlite XAD-2 resin. Efficient purification of captopril–NEM and the disulphide was attained by chromatography on PHP-LH-20. Captopril–NEM, the disulphide and the internal standard were simultaneously eluted with 7% acetic acid in ethanol. In order to check the validity of the

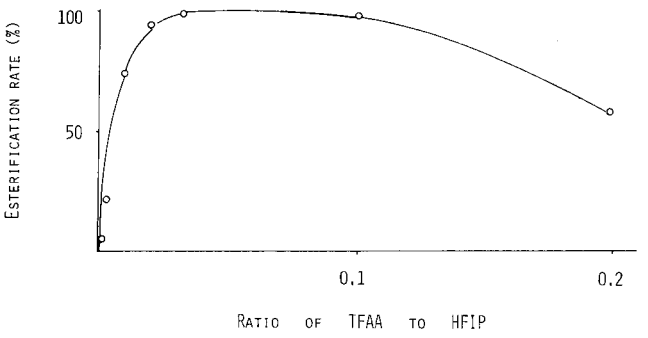

Fig. 2. Effect of TFAA on esterification of the disulphide. The reaction was carried out with hexafluoroisopropanol (0.3 ml) and trifluoroacetic anhydride (0.6–60 μl) at 50°C for 60 min.

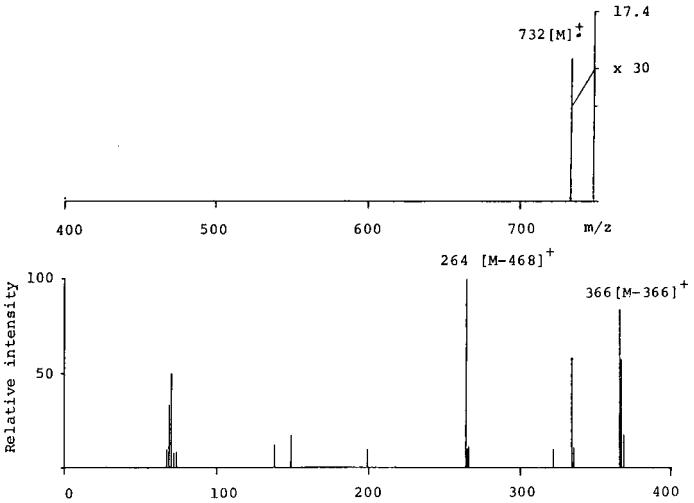

Fig. 3. Mass spectrum of the disulphide bis(hexafluoroisopropyl) ester.

proposed method, known amounts of captopril–NEM and the disulphide were added to biological fluids and their recovery rates were determined by the proposed method. The results obtained with blood, plasma and urine specimens are given in Table IV.

The blood and urine levels of captopril and its disulphide were determined after oral administration of captopril (10 mg/kg) to two dogs. The changes in blood levels of these two are illustrated in Fig. 6. The maximum blood levels of captopril and its disulphide were observed at 1 and 1.5 h, respectively. A significant difference in the change of the disulphide level was observed between the two dogs.

The data for cumulative urinary excretion in dogs are given in Table V. The

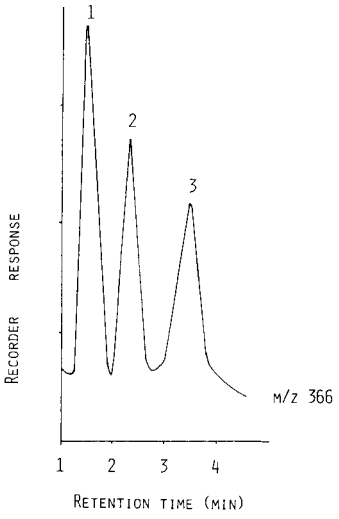

Fig. 4. Chromatogram of captopril (1), internal standard (2) and the disulphide (3) obtained by selected ion monitoring.

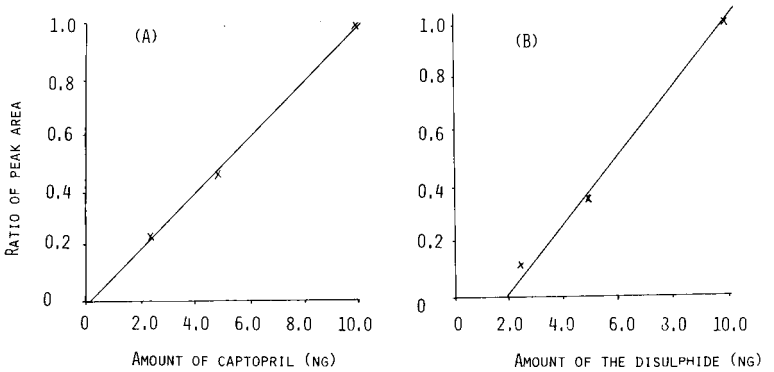

Fig. 5. Calibration graphs for captopril (A) and its disulphide (B).

TABLE IV

RECOVERY OF CAPTOPRIL AND ITS DISULPHIDE ADDED TO BLOOD, PLASMA AND URINE SPECIMENS FROM A DOG

Compound	*Added (μg)*	*Blood**		*Plasma***		*Urine***	
		Found (μg)	*Recovery (%)*	*Found (μg)*	*Recovery (%)*	*Found (μg)*	*Recovery (%)*
Captopril	0.10	0.098	98	0.086	86	0.092	92
Disulphide	1.00	0.85	85	0.88	88	0.87	87

* $n = 5$.
** $n = 6$.

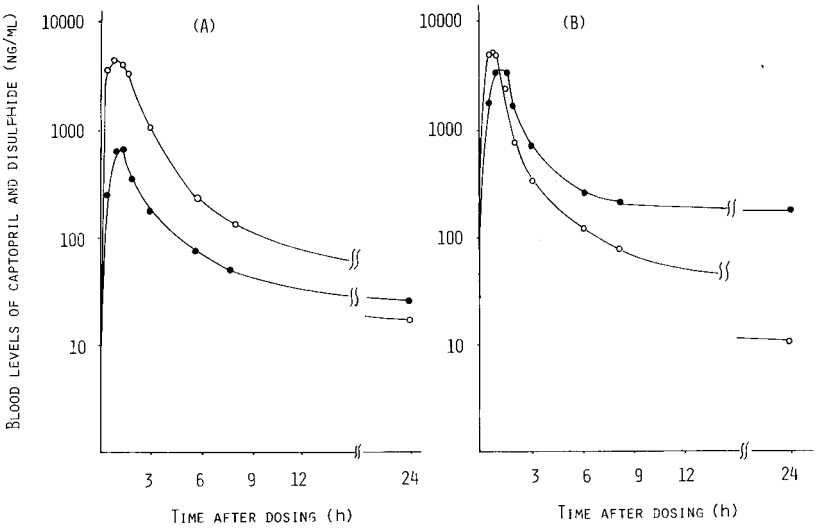

Fig. 6. Change in blood levels of captopril (○) and its disulphide (●) in dog 1 (A) and dog 2 (B). A single dose of captopril (10 mg/kg) was given orally to each dog.

TABLE V

CUMULATIVE URINARY EXCRETION OF CAPTOPRIL AND ITS DISULPHIDE IN DOGS

A single dose of captopril (10 mg/kg) was given orally to each dog.

Time after administration (h)	*Amount excreted (% of dose)*			
	Dog 1		*Dog 2*	
	Captopril	*Disulphide*	*Captopril*	*Disulphide*
0– 1	17.7	n.d.*	15.5	2.7
1– 2	7.4	n.d.*	19.9	3.7
2– 3	1.5	2.8	6.1	0.9
3– 6	0.7	2.9	5.1	0.7
6– 8	0.2	1.3	1.1	0.2
8–24	0.4	0.3	0.1	0.1
0–24 (total)	27.9	7.3	47.8	8.3

* Not detectable.

cumulative amounts of captopril and its disulphide excreted in 24 h were calculated to be 37.8% and 7.8% of the dose, respectively.

The data for urinary excretion of captopril and its disulphide in rats to which the compounds had been administered are given in Table VI. These results indicate that the disulphide was absorbed from the intestine to a lesser extent than captopril in the rat. The *in vivo* formation of captopril from the disulphide lent support to previous work[6]. The amount of captopril excreted in urine after administration of captopril was less than that reported by Ikeda *et al.*[5].

The proposed method for the determination of captopril and its disulfide in biological fluids is satisfactory with respect to sensitivity and reliability. It should be noted that solutions of NEM in phosphate buffer should be prepared freshly prior to use.

It is hoped that the availability of a satisfactory method for the determination of captopril and its disulphide will provide more precise knowledge of the relationship between the pharmacological activities and pharmacokinetics of these drugs. Further studies on the pharmacodynamics of captopril and its disulphide in man and experimental animals are being conducted and details will be reported elsewhere.

TABLE VI

URINARY EXCRETION OF CAPTOPRIL AND ITS DISULPHIDE IN RATS FOR 24 h

A single dose of 10 mg/kg of captopril and its disulphide was given orally to each of three rats. Results are means obtained with the three rats.

Drug	*Amount excreted (% of dose)*		
	Captopril	*Disulphide*	*Total*
Captopril	20.9	5.4	26.3
Disulphide	2.6	2.8	5.4

ACKNOWLEDGEMENTS

The authors are grateful to Dr. K. Hashimoto, Director of the Hatano Research Institute, for his support and encouragement throughout this work. They are indebted to Sankyo Co. Ltd. for the generous supply of captopril and its disulphide.

REFERENCES

1 R. R. Vollmer, J. A. Boccagno, D. N. Harris and V. S. Murthy, *Eur. J. Pharmacol.*, 51 (1978) 39.
2 B. Rubin, R. J. Laffan, D. G. Kotler, E. H. O,Keefe, D. A. DeMaio and M. E. Goldberg, *J. Pharmacol. Exp. Ther.*, 204 (1978) 271.
3 D. N. Harris, C. L. Heran, H. J. Goldberg, *Fed. Proc., Fed. Amer. Soc. Exp. Biol.*, 37 (1978) 718.
4 D. W. Cushman, H. S. Cheung, E. F. Sabo and M. A. Ondetti, *Biochemistry*, 16 (1977) 5484.
5 T. Ikeda, T. Komai, K. Kawai and H. Shindo, *Chem. Pharm. Bull.*, 29 (1981) 1416.
6 T. Komai, T. Ikeda, K. Kawai, E. Kameyama and H. Shindo, *J. Pharm. Dynam.*, 4 (1981) 677.
7 N. O'Hara, H. Ono and K. Hashimoto, *Jap. J. Pharmacol.*, 29, Suppl. (1979) 102.
8 K. K. Wong and J. Dreyfuss, *Pharmacologist*, 20 (1978) 213.
9 Y. Matsuki, K. Fukuhara, T. Ito, H. Ono, N. O'hara, T. Yui and T. Nambara, *J. Chromatogr.*, 188 (1980) 177.
10 P. T. Funke, E. Ivashkive, M. F. Malley and A. I. Cohen, *Anal. Chem.*, 52 (1980) 1086.
11 J. Goto, M. Hasegawa, H. Kato and T. Nambara, *Clin. Chim. Acta*, 87 (1978) 141.

Journal of Chromatography, 239 (1982) 595–608
Elsevier Scientific Publishing Company, Amsterdam — Printed in The Netherlands

CHROM. 14,572

MICRODETERMINATION OF PROSTAGLANDINS AND THROMBOXANE B_2 BY GAS CHROMATOGRAPHY USING AN ELECTRON-CAPTURE DETECTOR

HIROSHI MIYAZAKI*, MASATAKA ISHIBASHI, KOUWA YAMASHITA and IZUMI OHGUCHI

Research Laboratories, Pharmaceutical Division, Nippon Kayaku Co., 3-31 Shimo, Kita-ku, Tokyo 115 (Japan)

HISASHI SAITOH, HIROSHI KURONO and MASAO SHIMONO

Analytical Application Laboratories, Shimadzu Corporation, 1-Nishinokyo Kuwabara-cho, Kyoto 904 (Japan)

and

MAKOTO KATORI

Department of Pharmacology, Kitazato University School of Medicine, 1 Asamizodani, Sagamihara, Kanagawa 228 (Japan)

SUMMARY

The separation of the dimethylethylsilyl, dimethyl-*n*-propylsilyl (DMnPS) and dimethylisopropylsilyl ether derivatives of pentafluorobenzyl (PFB) esters of $PGF_{1\alpha}$ and $PGF_{2\alpha}$ and methoxime-PFB esters of PGE_1, PGE_2, 6-keto-$PGF_{1\alpha}$ and TXB_2 was investigated by gas chromatography using an electron-capture detector. Of these silyl ether derivatives, the DMnPS ether derivatives gave the best separation when analysed with the use of a high-performance fused silica capillary column coated with OV-101.

The stability of the DMnPS ether derivative of $PGF_{2\alpha}$ PFB ester was compared with that of the trimethylsilyl (TMS) ether derivative. The recovery of the DMnPS ether derivative of $PGF_{2\alpha}$ PFB ester in the eluate from a silica gel column was more than 95%, whereas the corresponding TMS ether derivative was partially decomposed and adsorbed on the silica gel column. In addition, the DMnPS ether derivative of $PGF_{2\alpha}$ PFB ester was stable for at least 1 week during storage in *n*-hexane solution (10 ng ml^{-1}) at room temperature.

The method was applied to the quantitation of PGs in extracts obtained from the urine of spontaneous hypertensive rats. The amounts of PGE_2 and $PGF_{2\alpha}$ in the urine were calculated to be 92 ± 30 and 29 ± 7 ng ml^{-1}, respectively, when analysed using the orthogonal polynomial equation.

INTRODUCTION

Much attention has been focused on the elucidation of the physiological role of prostaglandins (PGs), which exhibit diverse physiological activity because of the different positions of the functional groups in the molecule. A number of methods for the microdetermination of PGs have been investigated in order to elucidate the rela-

0021-9673/82/0000–0000/$02.75

tionship between the pharmacological activity and metabolic profile of PGs and thromboxanes (TXs).

As gas chromatography with electron-capture detection (GC–ECD) has a sensitivity comparable to those of radioimmunoassay[1,2] and gas chromatography–mass spectrometry (GC–MS)[3–5], it has been widely used for the analysis of PGs in biological fluids[6,7]. On the other hand, the capillary column technique makes it possible to perform the profile analysis of biologically important substances in a complicated mixture obtained from biological fluids as a result of a great improvement in the GC separation[8–10].

In conventional methods, the trimethylsilyl (TMS) ether derivatives of pentafluorobenzyl (PFB) esters of PGs have been used to enhance their sensitivities in GC–ECD[11–13]. However, it has been suggested that the profile analysis of PGs using the TMS ether derivatives of PFB esters might be difficult owing to their incomplete separation even if an open-tubular glass capillary column is used.

In previous work, it was found that the dimethylethylsilyl (DMES), dimethyl-*n*-propylsilyl (DMnPS) and dimethylisopropylsilyl (DMiPs) ether derivatives gave a better GC separations than the corresponding TMS ether derivatives[14–16]. This paper describes the GC separation of these silyl ether derivatives of PG PFB esters or MO-PFB esters suitable for GC–ECD and a biomedical application of the method to the quantitation of PGE_2 and $PGF_{2\alpha}$ in rat urine.

EXPERIMENTAL

Gas chromatography

A Shimadzu GC-7A gas chromatograph equipped with a 10-mCi ^{63}Ni electron-capture detector was employed. A thermostable open-tubular fused silica capillary column coated with OV-101 (25 m × 0.25 mm I.D.) was prepared in our laboratories using a dynamic coating method as described by Schomburg and Hasman[17]. An all-glass solventless injector constructed according to the method of Van den Berg and Cox[18] was mounted horizontally on the heated injector block of the gas chromatograph. Helium was used as the carrier gas and nitrogen make-up gas was introduced at the end of the column to keep the flow-rate through the detector at 40 ml min^{-1}. An inlet pressure of 0.4 kg cm^{-1} produced a linear gas velocity of 25 cm sec^{-1}. The gas inlet pressure was adjusted to obtain maximum column efficiency with respect to the TMS ether derivative of $PGF_{2\alpha}$ PFB ester as a representative sample. The temperature of the column oven was maintained at 270–280°C. The temperature of the injection heating block and detector was 290°C.

Gas chromatography–mass spectrometry

An LKB 2091 gas chromatograph–mass spectrometer equipped with a data processing system was employed. The column was a 2 m × 2.5 mm I.D. glass coil packed with 1.5% OV-101 (Ohio Valley Co., Marietta, OH, U.S.A.) on Chromosorb W HP (80–100 mesh) (Applied Science, U.S.A.). The temperature of the column oven was maintained at 250–270°C. The flow-rate of the carrier gas (helium) was 20 ml min^{-1}. The temperature of the injection heating block and separator was kept at 290°C and that of the ionization source at 280°C. The ionization energy and trap current were 22.5 eV and 100 μA, respectively. The accelerating voltage was 2.33 kV.

Materials

PGE_1, PGE_2, $PGF_{1\alpha}$ and $PGF_{2\alpha}$ were purchased from Fuji Chemical Industry (Takaoka, Japan). TXB_2 and 6-keto-$PGF_{1\alpha}$ were kindly supplied by Ono Pharmaceutical Co. (Osaka, Japan). TMS-imidazole, DMES-imidazole, DMnPS-imidazole, methoxyamine hydrochloride and pentafluorobenzyl (PFB) bromide were purchased from Tokyo Kasei Kogyo (Tokyo, Japan). DMiPS-imidazole was synthesized in our laboratories as previously reported[19].

Sephadex LH-20 (25–100 μm) and silica gel (Kieselgel 60, 70–230 mesh) were obtained from Pharmacia (Uppsala, Sweden) and Merk (Darmstadt, G.F.R.), respectively. Extube® 1003 was purchased from Analytichem International (CA, U.S.A.). Other reagents were of the highest purity available.

Extraction of PGs from rat urine

After PGE_1 (100 ng) and $PGF_{1\alpha}$ (50 ng) had been added to the rat urine (1.0 ml) as internal standards, the urine was acidified to pH 3.0 with 0.2 *N* hydrochloric acid and the resulting solution was transfered on to Extube 1003. After being allowed to stand for 5 min, PGs were eluted with 30 ml of benzene–ethyl acetate (90:10). The organic layer was then evaporated under reduced pressure below 40°C and the residue was treated with methoxyamine hydrochloride and PFB bromide, followed by reaction with silylating agents.

Derivatization

Authentic $PGF_{1\alpha}$ and $PGF_{2\alpha}$ were converted directly into their PFB esters by treatment with PFB bromide and diisopropylethylamine in acetonitrile at 40°C for 1 h according to the method of Wickramasinghe and Shaw[20]. The resulting mixture was diluted with benzene and extracted. The organic layer was washed with water, dried over anhydrous sodium sulphate and then introduced into a microcolumn of silica gel (5 cm × 0.8 cm I.D.). PG PFB esters were eluted with ethyl acetate–methanol (99:1) (25 ml). The solution of the eluate was evaporated and the resulting PFB ester was treated with TMS-imidazole, DMES-imidazole, DMnPS-imidazole and DMiPS-imidazole (100 μl) at room temperature for 30 min. Ketonic PGs were converted into methoxime derivative by treatment with a saturated solution of methoxyamine hydrochloride in dry pyridine at 60°C for 1 h prior to esterification.

In order remove the excess of silylating reagents, the reaction mixture was chromatographed over Sephadex LH-20 (5 cm × 0.8 cm I.D.) with chloroform–*n*-hexane–methanol (10:10:1). After evaporation of the solvent the residue was dissolved in *n*-hexane containing 1% (v/v) pyridine and used for GC analysis. The extract obtained from rat urine was treated in the same manner as ketonic PGs.

RESULTS AND DISCUSSION

The DMES, DMnPS and DMiPS ether derivatives of PGs and thromboxane B_2 (TXB_2) PFB esters or methoxime(MO)–PFB esters were prepared and used for the investigation of derivatization and GC separation conditions.

$PGF_{1\alpha}$ and $PGF_{2\alpha}$ were smoothly converted into their PFB esters by treatment with PFB bromide in acetonitrile in the presence of diisopropylethylamine according to the procedure of Wickramasinghe and Shaw[20]. On being treated under the above

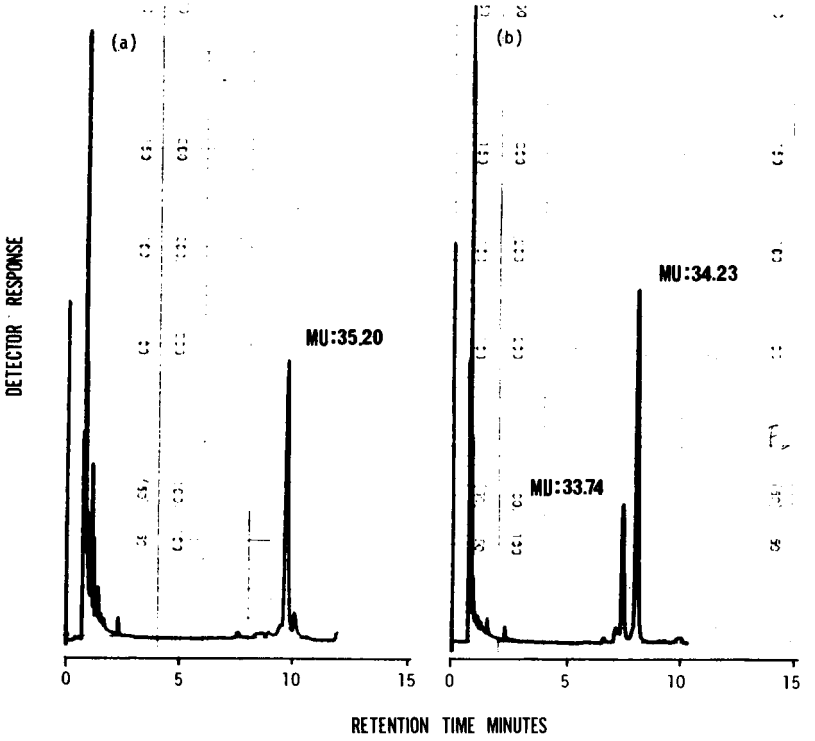

Fig. 1. ECD gas chromatograms of the reaction products of (a) $PGF_{2\alpha}$ PFB ester and (b) PGE_2 MO-PFB ester with DMnPS-imidazole by the use of a fused silica capillary column coated with OV-101 (25 m × 0.25 mm I.D.) at 280°C.

esterification conditions using a basic catalyst, PGE_1 and PGE_2, which contain a β-ketol system, were partially dehydrated and converted into α,β-unsaturated ketones such as the PGA or PGB series. Ketonic samples should initially be converted into the MO derivatives prior to esterification in order to prevent the above undesirable side-reaction. The PG and TXB_2 PFB esters or MO–PFB esters were then silylated with trimethylsilyl(TMS)-, DMES-, DMnPS- or DMiPS-imidazole at room temperature and the resulting derivatives gave well shaped GC peaks, suggesting that the stepwise derivatization proceeded smoothly and quantitatively.

Fig. 1 shows the gas chromatograms with electron-capture detection of the reaction products of $PGF_{2\alpha}$ PFB ester (a) and PGE_2 MO-PFB ester (b) with DMnPS-imidazole obtained with the use of an open-tubular fused silica capillary column coated with OV-101 (25 m × 0.25 mm I.D.). Each of the silyl ether derivatives of PG MO-PFB esters except TXB_2 provided two well resolved peaks owing to the formation of *syn*- and *anti*-isomers, as in the case of PG MO-methyl ester (ME) reported by Gréen[21].

Table I lists the methylene unit (*MU*) values of the resulting TMS, DMES, DMnPS and DMiPS ether derivatives when analysed using the fused silica capillary column. Although the TMS ether derivatives were eluted in the order $PGF_{2\alpha}$, $PGF_{1\alpha}$, PGE_2, PGE_1, TXB_2 and 6-keto-$PGF_{1\alpha}$, the individual PGs could not be separated

TABLE I

GC DATA FOR THE TMS, DMES, DMnPS AND DMiPS ETHER DERIVATIVES OF PGs AND TXB_2 PFB ESTERS OR MO-PFB ESTERS

Compound	*MU values*				*Δ[Um] values*		
	TMS	*DMES*	*DMnPS*	*DMiPS*	$\Delta[Um]_E$	$\Delta[Um]_{nP}$	$\Delta[Um]_{iP}$
PGE_1	31.66*	33.62	34.03	34.89	1.96	2.37	3.23
	32.15**	34.10	34.59	35.39	1.95	2.44	3.24
PGE_2	31.40*	33.32	33.74	34.61	1.92	2.34	3.21
	31.86**	33.79	34.23	35.06	1.93	2.44	3.20
$PGF_{1\alpha}$	31.70	34.79	35.70	36.67	3.09	4.00	4.97
$PGF_{2\alpha}$	31.34	34.28	35.20	36.18	2.94	3.86	4.84
6-Keto-$PGF_{1\alpha}$	32.35	35.21	36.28	37.00*	2.86	3.93	4.65
				37.10**			4.75
TXB_2	32.11	34.92	35.89	36.95	2.81	3.78	4.84

* The minor isomer of the methoxime derivative.
** The major isomer of the methoxime derivative.

completely with these TMS ether derivatives, as shown in Table I. On the other hand, the DMES ether derivatives were eluted in the order PGE_2, PGE_1, $PGF_{2\alpha}$, $PGF_{1\alpha}$, TXB_2 and 6-keto-$PGF_{1\alpha}$. The separation of the DMES ether derivatives of PGs and TXB_2 PFB esters or MO-PFB esters was better than that of the TMS ether derivatives. However, the major isomer of PGE_1 and the peak of $PGF_{2\alpha}$ overlapped completely and were observed as a single peak.

The DMES, DMnPS and DMiPS ether derivatives of hydroxysteroids gave larger *MU* values than the TMS ether derivatives, and this was multiplied in proportion to the number of hydroxyl group in the molecule[22–25]. The separation of PGE and PGF series was improved with an increase in the carbon number in the silyl ether derivatives[14,19]. Particularly when PGs and TXB_2 were analysed as their DMiPS and DMnPS ether derivatives the peaks of the PGF series were well separated from those of the PGE series.

Table I also shows the $\Delta[Um]$ values, which are defined as the difference between the *MU* values of the TMS ether and the DMES ($\Delta[Um]_E$), DMnPS ($\Delta[Um]_{nP}$) or DMiPS ($\Delta[Um]_{iP}$) ether derivatives. The average and standard deviations of the $\Delta[Um]_E$ values were 1.94 ± 0.02 for dihydroxy compounds and 2.93 ± 0.12 for trihydroxy compounds, and those of the $\Delta[Um]_{nP}$ values were 2.40 ± 0.05 and 3.89 ± 0.09, respectively. The $\Delta[Um]_{iP}$ values of these compounds were larger than the corresponding $\Delta[Um]_{nP}$ values. The $\Delta[Um]$ values of the silyl ether derivatives of PGs and TXB_2 PFB esters or MO-PFB esters were in agreement with those of di- and trihydroxysteroids[22,23] bile acids[15,24] and PG ME derivatives[14,19].

The DMES, DMnPS and DMiPS ether derivatives permitted the PGs and TXB_2 to be classified into two distinct groups of di- and trihydroxy compounds and greatly enhanced the separation of the individual PGs and TXB_2 in comparison with the corresponding TMS ether derivatives.

Fig. 2 shows the GC separation of the standard mixture of PGs and TXB_2 as their DMnPS ether derivatives of PFB esters or MO-PFB esters by the use of the

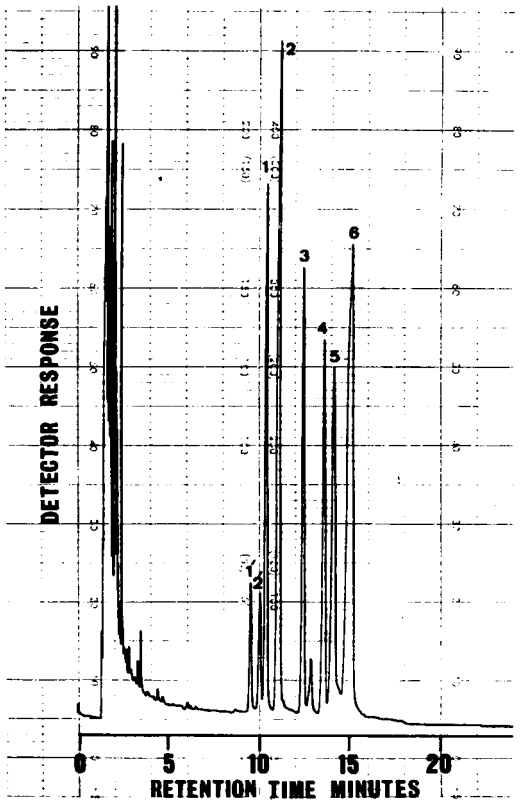

Fig. 2. GC–ECD separation of the DMnPS ether derivatives of five kinds of PGs and TXB_2 PFB esters or MO-PFB esters by the use of fused silica capillary column at 280°C: (1′, 1) PGE_2; (2′, 2) PGE_1; (3) $PGF_{2\alpha}$; (4) $PGF_{1\alpha}$; (5) TXB_2; (6) 6-keto-$PGF_{1\alpha}$.

fused silica capillary column as described above. Complete separation of the DMnPS of PFB esters or MO-PFB esters could be achieved within 20 min.

Fig. 3 shows the mass spectra of the TMS and DMnPS ether derivatives of $PGF_{2\alpha}$ PFB ester. The appearance of the molecular ion, although in low abundance, was sufficient to confirm the structure of the expected derivative. The shift of the molecular ion from m/z 750 to 834 indicated the incorporation of the DMnPS group into the PFB ester. When the mass spectrum of the DMnPS ether derivative was compared with that of the TMS ether derivative, the mass spectral fragmentation patterns were closely related except for 28 mass unit shift per silanoxy group. For instance, the [M − 71] ion produced by the cleavage of the C_{15}–C_{16} bond implied the presence of three silanoxy groups by the shift from m/z 679 in the TMS ether derivative to m/z 763 ($679 + 28 \times 3$) in the DMnPS ether derivative.

With hydroxysteroids, the mass spectra of the DMES and DMnPS ether derivatives were characterized by their inherent [M − alkyl] ion. Contrary to our expectation, the intensity of this inherent ion in the DMES and DMnPS ether derivatives of PGs and TXB_2 PFB ester or MO-PFB ester was not enhanced to that of the correspond-

ing TMS ether derivative as in the ME or MO-ME derivatives of PGs previously reported[14,19].

The ion of *m/z* 763 produced by the loss of 71 mass units (C_5H_{11}) from the molecular ion was typical of a β-chain. Successive elimination of three dimethyl-*n*-propylsilanol (DMnPSOH) groups from the molecule gave rise to ions of *m/z* 716, 598 and 480 from the molecular ion and the ions of *m/z* 645, 527 and 409 from the [M − 71] ion. The ion of *m/z* 247 was a constituent with an F prostaglandin ring system, which was assigned as the structure corresponding to the ion of *m/z* 191 in the TMS ether derivative of $PGF_{2\alpha}$ ME. The ion of *m/z* 265 which was observed as a base peak was characterized and assigned as the ion corresponding to the ion of *m/z* 237 in the TMS ether derivative.

Fig. 4 shows the mass spectrum of the DMnPS ether derivative of the major isomer of PGE_2 MO-PFB ester. The ions of $[M]^{+\cdot}$ and $[M-43]^+$ were observed in low abundance, but the appearance of the molecular ion was sufficient to confirm the structure of the expected derivative. The ion of *m/z* 688 which was produced by the loss of C_5H_{11} from the molecular ion was typical of a β-chain as in the DMnPS ether derivative of $PGF_{2\alpha}$ PFB ester. The mass spectrum of the major isomer of the DMnPS ether derivative of PGE_2 MO-PFB ester was dominated by the ions of *m/z* 489 and 253. The ion of *m/z* 489 was considered to be formed by the cleavage of the E prostaglandin ring system, which was assigned as the structure corresponding to the analogous ion of *m/z* 323 in the DMnPS ether derivative of MO-ME. The shift of the ion of *m/z* 323 to *m/z* 489 indicated the incorporation of a PFB moiety in the DMnPS ether of PGE_2 MO. The ion of *m/z* 253 was produced by the cleavage of the C_{10}–C_{11} bond, as deduced from a comparison with the mass spectra of the corresponding TMS and DMnPS ether derivative of PGE_2 MO-ME[14,19].

Table II summarizes the mass spectral data of PGs and TXB_2 as their DMnPS ether derivatives of the PFB esters or MO-PFB esters. The appearance of the molecular ion was sufficient to confirm the structural elucidation of the expected derivatives. The elimination of the appropriate silanol and production of the subsequent characteristic fragment ion were observed in all PGs except TXB_2.

The storage stability of the DMnPS ether derivative of $PGF_{2\alpha}$ PFB ester in *n*-hexane solution was compared with that of the corresponding TMS ether derivative. The DMnPS ether derivative of $PGF_{2\alpha}$ PFB ester was diluted with *n*-hexane to 10 ng/ml and the residual amount of the derivative in the solution was determined by GC–ECD using the PFB ester of 5β-cholanic acid as an internal standard. The results are shown in Fig. 5. The DMnPS ether derivative of $PGF_{2\alpha}$ PFB ester was stable in *n*-hexane solution for at least 7 days at room temperature, whereas the corresponding TMS ether derivative was decomposed to the extent of more than 30%. This observation was in good agreement with the storage stability of the DMnPS ether derivatives of catecholamine trifluoroacetamides[16] and the DMES ether derivative of $PGF_{2\alpha}$ ME[14].

Further, the DMnPS ether derivative of $PGF_{2\alpha}$ PFB ester was chromatographed over a silica gel column and eluted with benzene–diethyl ether (95:5). When [^{14}C]$PGF_{2\alpha}$ was used as a marker, the recovery of the DMnPS ether derivative of $PGF_{2\alpha}$ PFB ester (10 ng) in the eluate from the column was more than 95%. On the other hand, the recovery of the corresponding TMS ether derivative was found to be 75% owing to decomposition and adsorption onto the column. The DMnPS ether

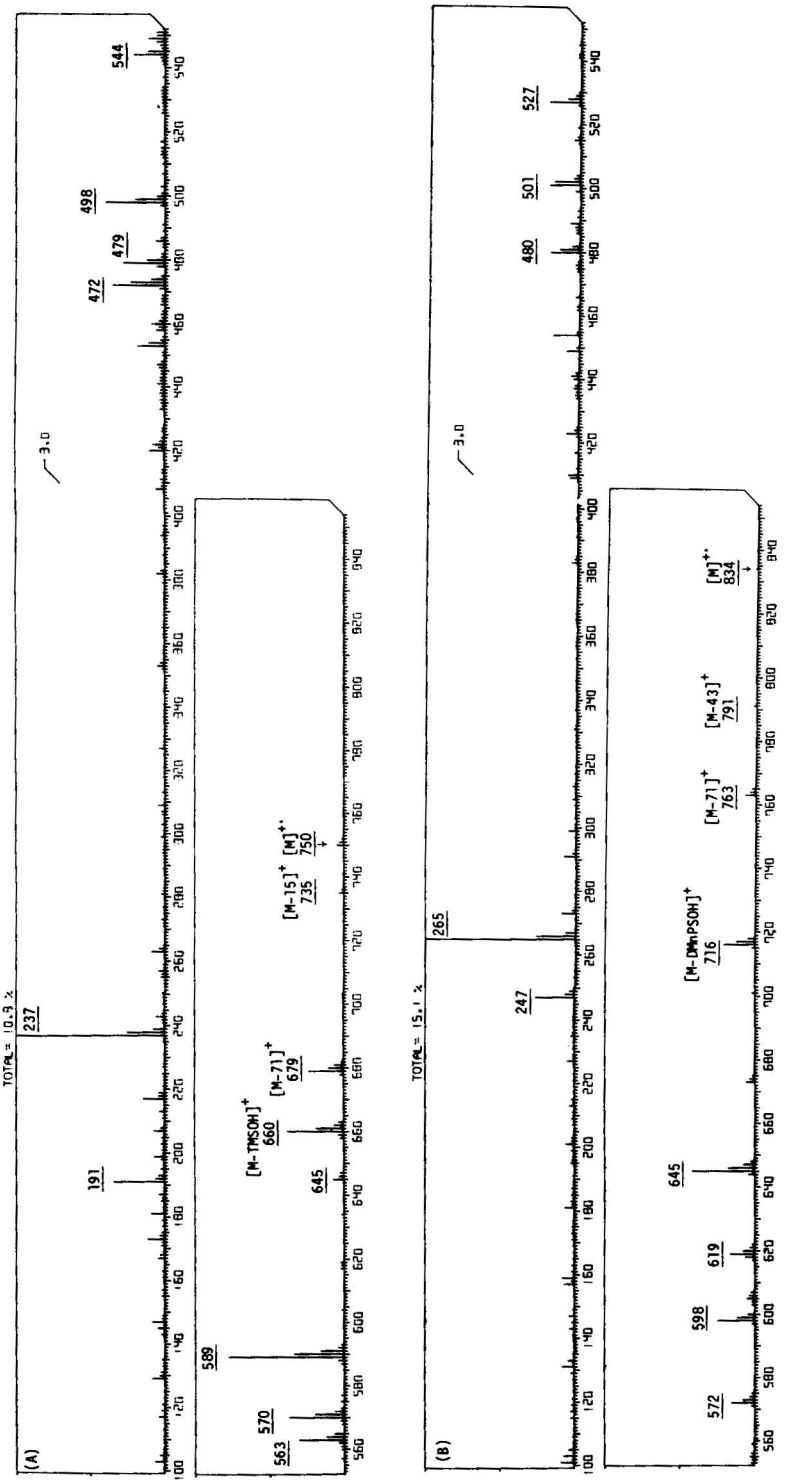

Fig. 3. Mass spectra of (A) TMS and (B) DMnPS ether derivative of $PGF_{2\alpha}$ PFB ester.

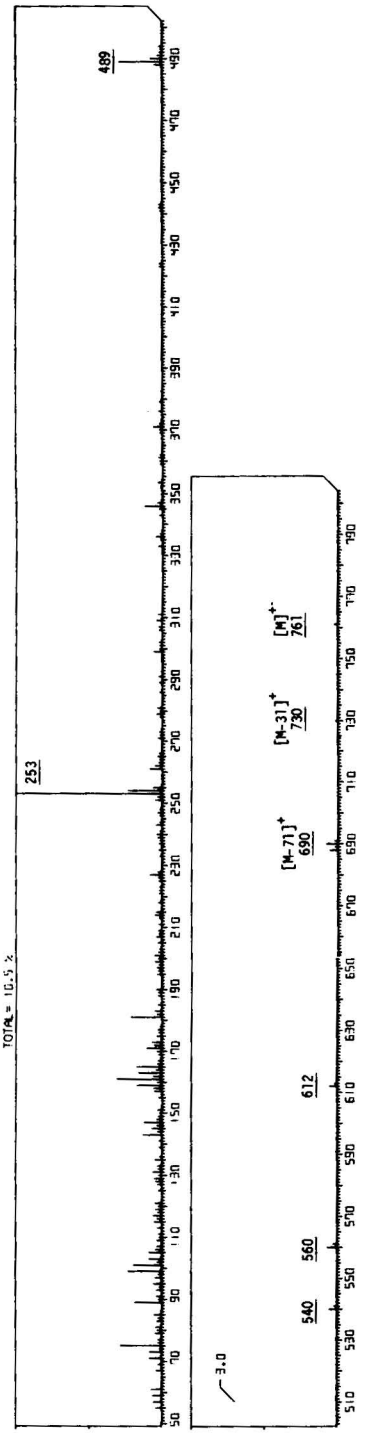

Fig. 4. Mass spectrum of the DMnPS ether derivative of the major isomer of PGE_2 MO-PFB ester.

TABLE II

MASS SPECTRAL DATA FOR THE DMnPS ETHER DERIVATIVES OF PGs AND TXB_2 PFB OR MO-PFB ESTERS

Compound	*Mol. wt.*	*Relative intensity (%)*								
		$M^{+\cdot}$	*M − 31*	*M − 43*	*M − 71*	*M − 118*	*Other ions*			
PGE_1	763	1.2★	22.5	8.8	100	10.5	614 (34)★★★	574 (90)§	491 (23)	227 (98)
		1.0★★	2.5	2.0	5.0	2.3	614 (3)★★★	562 (24)	491 (100)	253 (25)
PGE_2	761	1.0★	15.0	7.0	43.0	10.0	612 (26)★★★	572 (54)§	489 (10)	75 (100)
		0.8★★	1.0	0.5	7.5	0.2	612 (2)★★★	560 (2)	489 (29)	253 (100)
$PGF_{1\alpha}$	836	0.2	–	3.8	20.1	28.8	647 (98)§	600 (16)§§	265 (35)	247 (100)
$PGF_{2\alpha}$	834	0.4	–	1.0	2.5	7.1	645 (14)§	598 (9)§§	265 (100)	247 (26)
6-Keto-$PGF_{1\alpha}$	879	5.0	40.1	17.5	12.5	10.0	730 (63)★★★	690 (25)	612 (70)§§§	572 (100)†
TXB_2	879	0.2	2.0	0.5	0.2	0.3	730 (5)★★★	690 (4)	612 (6)§§§	308 (100)

★ The minor isomer of the methoxime derivative.
★★ The major isomer of the methoxime derivative.
★★★ $[M - (31 + 118(DMnPSOH))]^+$.
§ $[M - (71 + 118)]^+$.
§§ $[M - (2 \times 118)]^+$.
§§§ $[M - (31 + (2 \times 118))]^+$.
† $[M - (71 + (2 \times 118))]^+$.

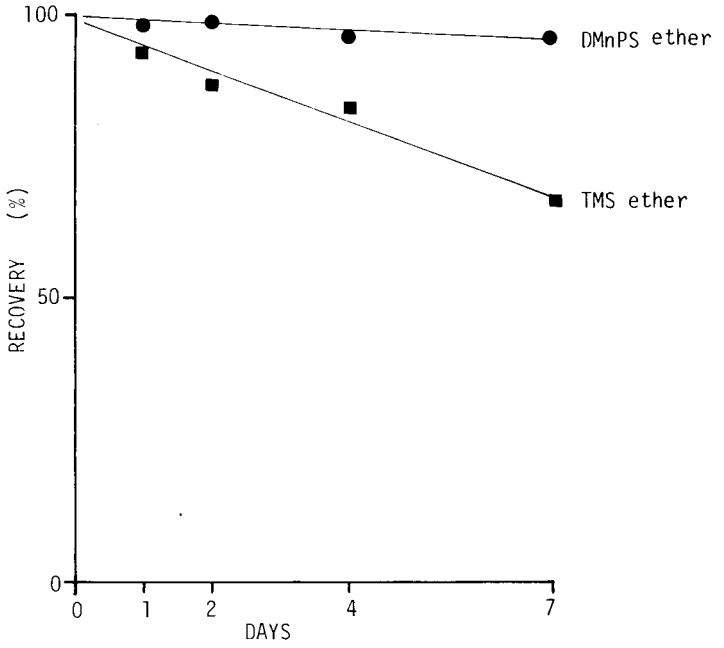

Fig. 5. Storage stability of the TMS and DMnPS ether derivatives of $PGF_{2\alpha}$ PFB ester in *n*-hexane solution.

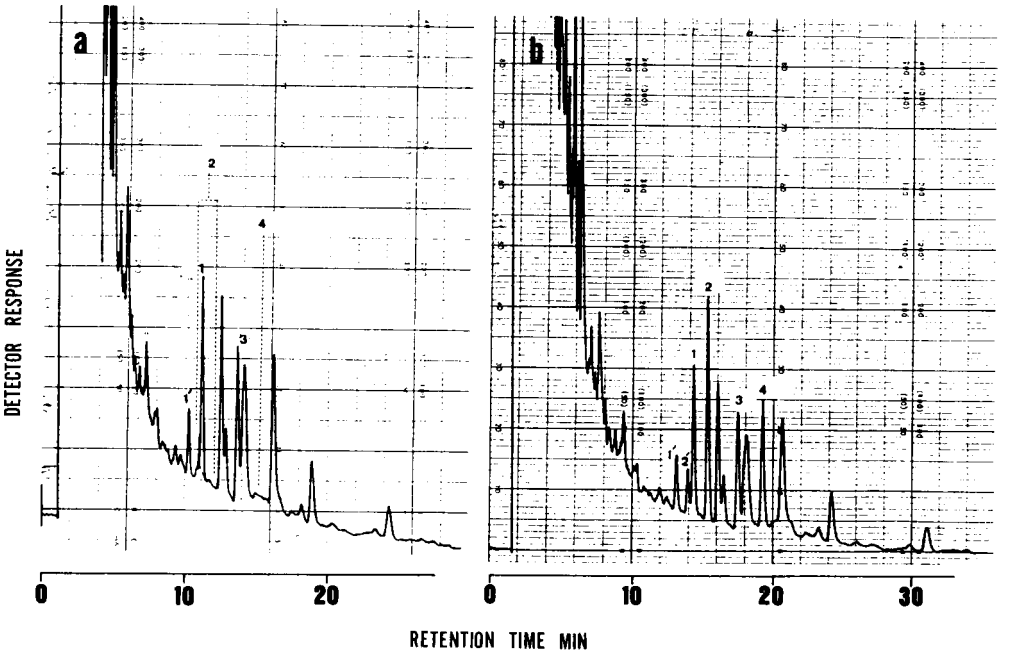

Fig. 6. ECD gas chromatograms of the DMnPS ether derivatives of PG PFB esters and MO-PFB esters (a) in the extracts from the urine of SH rats and (b) after addition of PGE_1 and $PGF_{1\alpha}$ as internal standards by the use of a fused silica capillary column at (a) 285°C and (b) 280°C: (1′, 1) PGE_2; (2′, 2) PGE_1; (3) $PGF_{2\alpha}$; (4) $PGF_{1\alpha}$.

derivative may be very useful for the further purification of PGs and TXB_2 in extracts of biological samples with a silica gel column.

The present method, based on the combination of the DMnPS ether derivatives and fused silica capillary GC–ECD, was applied to the determination of primary PGs in the urine of spontaneous hypertensive (SH) rats. Fig. 6 shows typical ECD gas chromatograms of the DMnPS ether derivatives of PGs PFB esters or MO-PFB esters in the extract of urine. As shown in Fig. 6a, the peaks with *MU* values of 34.23 and 35.20 were identified as PGE_2 and $PGF_{2\alpha}$, by comparison with the mass spectra of the authentic compounds. Several unidentified peaks were observed in addition to PGE_2 and $PGF_{2\alpha}$. Fortunately, the *MU* values of these unidentified peaks did not overlap those of the peaks corresponding to the DMnPS ether derivatives of PGE_2, PGE_1, $PGF_{2\alpha}$ and $PGF_{1\alpha}$. This fact indicated that the interfering substances coexisting in the urine could be eliminated completely by this sample preparation using Extube® and silica gel column chromatography.

It was essential to add an internal standard to the urine prior to extraction in order to compensate for the losses during the extraction and derivatization process. PGE_1 and $PGF_{1\alpha}$ could be utilized as internal standards for the quantitation of PGE_2 and $PGF_{2\alpha}$ in the urine of SH rats.

Fig. 7. shows the calibration graphs for PGE_2 and $PGF_{2\alpha}$ as their DMnPS ether derivatives using PGE_1 and $PGF_{1\alpha}$ as internal standards. Good linearity was

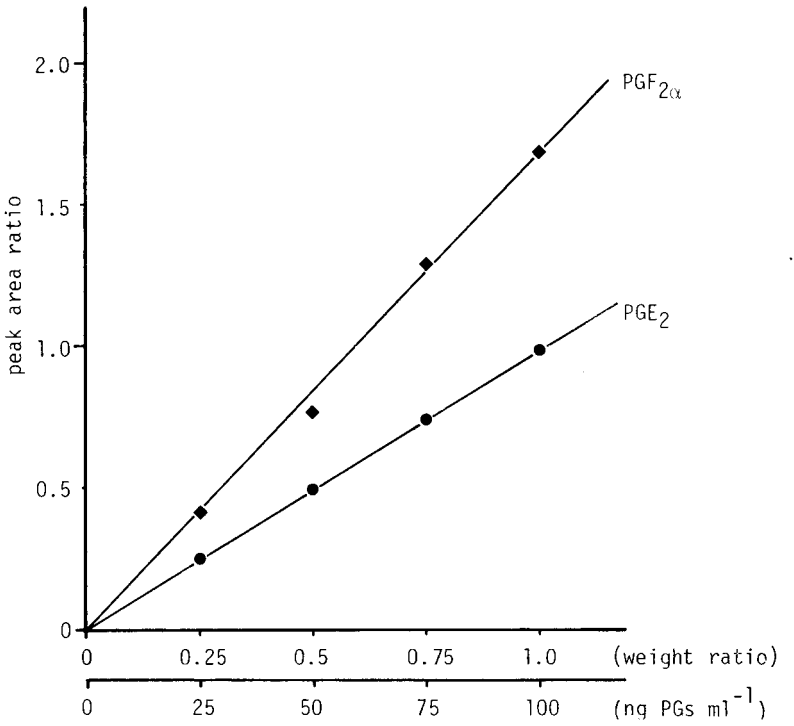

Fig. 7. Calibration graphs for PGE_2 and $PGF_{2\alpha}$ obtained by plotting the weight ratio (PGE_2/PGE_1 or $PGF_{2\alpha}/PGF_{1\alpha}$) *versus* the peak-area ratio.

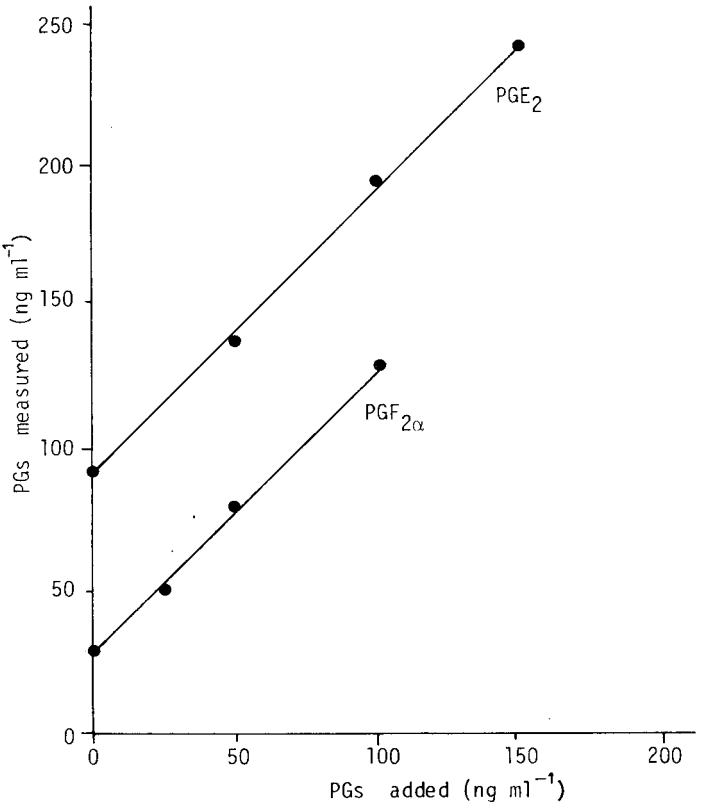

Fig. 8. Determination of PGE_2 and $PGF_{2\alpha}$ in the extracts obtained from the urine of SH rats by statistical analysis using the orthogonal polynomial equation after addition of known amounts of PGE_2 and $PGF_{2\alpha}$ to the urine.

obtained for concentrations of PGE_2 and $PGF_{2\alpha}$ in the range from 25–100 ng ml^{-1} in urine.

To obtain a more accurate determination of PGE_2 and $PGF_{2\alpha}$ in the urine of SH rats, we applied the orthogonal polynomial equation[26] with addition of known amounts of authentic PGE_2 and $PGF_{2\alpha}$. Fig. 8 shows the plots of amounts of PGs measured *versus* known amounts of PGs added before extraction. The exact amounts of PGE_2 and $PGF_{2\alpha}$ in the extracts obtained from the urine of SH rats were calculated to be 92 ± 30 and 29 ± 7 ng ml^{-1} respectively, from the orthogonal polynomial equation.

In conclusion, the microdetermination based on the capillary GC–ECD using the DMnPS ether derivatives was very useful for the analysis of PGs and TXB_2 in biological fluids without any interference from endogeneous substances. This method may be useful for the elucidation of the relationship between the pharmacological activity and metabolic profile of PGs and TXB_2 in biological fluids.

ACKNOWLEDGEMENTS

The authors are grateful to Dr. W. Tanaka, Research Laboratories, Nippon Kayaku Co., for his encouragement throughout this work. They express their sincere thanks to Dr. M. Hayashi, Ono Pharmaceutical Co., for his generous gift of the samples.

REFERENCES

1 R. M. Gutierrez-Cernosek, L. Levin and H. Gujika, *Methods Enzymol.*, 35 (1975) 287.
2 E. Granström, H. Kindahl and B. Samuelsson, *Anal. Lett.*, 9 (1976) 611.
3 U. Axén, K. Gréen, D. Holin and B. Samuelsson, *Biochem. Biophys. Res. Commun.*, 45 (1969) 519.
4 L. Baczynskj, D. J. Duchamp, J. F. Fieserl and U. Axen, *Anal. Chem.*, 45 (1973) 479.
5 J. Rosello, J. Tusell and E. Gelpi, *J. Chromatogr.*, 130 (1977) 65.
6 B. S. Middledich and D. M. Desiderio, *Prostaglandins*, 2 (1972) 195.
7 F. A. Fitzpatrick, M. A. Wynalda and D. G. Keiser, *Anal. Chem.*, 49 (1977) 1032.
8 J. Yanagisawa, M. Itoh, M. Ishibashi, H. Miyazaki and F. Nakayama, *Anal. Biochem.*, 104 (1980) 75.
9 F. A. Fitzpatrick, *Anal. Chem.*, 50 (1978) 47.
10 J. Maclouf, M. Rigaude, J. Durand and P. Chebroux, *Prostaglandins*, 11 (1976) 999.
11 M. Kortwez, G. Verdonk, P. Sandra and M. Verzele, *Prostaglandins*, 13 (1977) 1221.
12 F. A. Fitzpatrick, D. A. Stringfellow, M. Maclouf and M. Rigaude, *J. Chromatogr.*, 177 (1979) 51.
13 F. A. Fitzpatrick, R. R. Gorman and M. A. Wynalda, *Prostaglandins*, 13 (1977) 201.
14 H. Miyazaki, M. Ishibashi, K. Yamashita and M. Katori, *J. Chromatogr.*, 153 (1978) 83.
15 H. Miyazaki, M. Ishibashi and K. Yamashita, *Biomed. Mass Spectrom.*, 5 (1978) 469.
16 H. Miyazaki, M. Ishibashi, K. Yamashita and M. Yakushiji, *Chem. Pharm. Bull.*, 26 (1981) 796.
17 G. Schomburg and H. Hasman, *Chromatographia*, 8 (1975) 517.
18 P. M. J. van den Berg and T. P. Cox, *Chromatographia*, 5 (1972) 301.
19 H. Miyazaki, M. Ishibashi, K. Yamashita and M. Katori, *Biomed. Mass Spectrom.*, 8 (1981) 521.
20 J. A. Wickramasinghe and R. S. Shaw, *Biochem. J.*, 141 (1974) 179.
21 K. Gréen, *Chem. Phys. Lipids*, 3 (1968) 254.
22 H. Miyazaki, M. Ishibashi, M. Itoh and T. Nambara, *Biomed. Mass Spectrom.*, 4 (1977) 23.
23 H. Miyazaki, M. Ishibashi and K. Yamashita, *Biomed. Mass Spectrom.*, 6 (1979) 57.
24 H. Miyazaki, M. Ishibashi, M. Itoh, K. Yamashita and T. Nambara, *J. Chromatogr.*, 133 (1977) 311.
25 A. Fukunaga, Y. Hatta, M. Ishibashi and H. Miyazaki, *J. Chromatogr.*, 190 (1980) 339.
26 G. Taguchi, *Statistical Analysis*, Maruzen, Tokyo, 1972, p. 197.

Journal of Chromatography, 239 (1982) 609–615
Elsevier Scientific Publishing Company, Amsterdam — Printed in The Netherlands

CHROM. 14,671

DETERMINATION OF β-ADRENERGIC BLOCKING DRUGS AS CYCLIC BORONATES BY GAS CHROMATOGRAPHY WITH NITROGEN-SELECTIVE DETECTION

TOSHIKAZU YAMAGUCHI*, YOKO MORIMOTO, YUTAKA SEKINE and MASAHISA HASHIMOTO

Department of Drug Metabolism, Research Laboratories, Dainippon Pharmaceutical Co., Ltd., 33-94, Enoki-cho, Suita, Osaka 564 (Japan)

SUMMARY

A gas chromatographic method with nitrogen-selective detection has been developed that permits the sensitive and simple determination of β-adrenergic blocking drugs, including alprenolol, bufetolol, bupranolol, carteolol, nadolol, oxprenolol, pindolol and propranolol. The drugs were derivatized with *n*-butylboronic acid or phenylboronic acid to form their cyclic boronates. The derivatives were readily formed at room temperature, and were stable for at least 3 days. The cyclic boronates formed gave symmetrical peaks, and showed high responses with minimum detectable amounts in the range 1.5–4 pg, corresponding to $6–14 \cdot 10^{-16}$ mol/sec.

Propranolol was extracted with *n*-hexane containing 1.5% of isoamyl alcohol from alkaline plasma by a single-extraction procedure, with bufetolol as the internal standard, and derivatized with phenylboronic acid. Accurate determinations were possible in the concentration range 1–500 ng/ml, and the minimum detectable concentration in plasma was 0.5 ng/ml, permitting the pharmacokinetic study of propranolol under therapy. Pindolol was also determined in the range 2–500 ng/ml, and the minimum detectable concentration was 1 ng/ml.

These results suggest the general applicability of the method to the determination of the unchanged β-blocking drugs in plasma and other biological samples.

INTRODUCTION

The β-adrenergic blocking drugs are in clinical use in the treatment of angina and hypertension. It has been observed for several of these drugs that the response of individuals to the same dose varies considerably, which is attributed in part to individual differences in the pharmacokinetic properties of these drugs. In order to achieve a better understanding of the pharmacokinetics of these drugs, a sensitive and simple assay method for the unchanged drug in plasma is necessary.

The β-blocking drugs have been determined by several analytical methods, of which fluorometric[1,2] and electron-capture gas chromatographic (GC–ECD)[3–5] methods are generally used. The former is limited by specificity[5], sensitivity and a highly

0021-9673/82/0000–0000/$02.75

variable assay blank[4]. The latter, consisting of the formation of perfluoroacyl derivatives, is highly sensitive and specific but involves tedious procedures, including a back-extraction and chemical derivatization. Recently, another GC–ECD method for the determination of alprenolol has been reported, with the 2,3-dichlorophenylboronate of propane-1,3-diamine as the reagent[6]. The method utilizes the selective reaction of boronic acid with the side-chain of the drug to form cyclic boronate. The procedure is simple and the cyclic boronate has good GC properties, but the chromatographic separation requires a very long time (more than 25 min) because of the presence of thermal decomposition products of the reagent.

For practical performance of the pharmacokinetic study, a simple assay procedure would be preferable. This paper describes a GC method with nitrogen-selective detection. The method, based on a single-extraction procedure and the formation of cyclic boronates with *n*-butylboronic acid (BBA) and phenylboronic acid (PBA), is reproducible and sensitive for the determination of β-blocking drugs.

EXPERIMENTAL

Chemicals and reagents

Alprenolol, bufetolol, bupranolol, carteolol, oxprenolol and propranolol were obtained as their hydrochlorides, and pindolol was obtained as the free base from commercial sources. Nadolol was the free base was a gift from Squibb Institute (Princeton, NJ, U.S.A.). Their purity was checked by thin-layer chromatography. The molecular structures are shown in Table I.

BBA and PBA were purchased from Aldrich (Milwaukee, WI, U.S.A.). All other chemicals used were of analytical reagent grade.

The BBA or PBA solution was prepared by dissolving 100 mg of the boronic acid in a mixture of 95 ml of ethyl acetate and 5 ml of anhydrous sodium sulphoxide.

All centrifuge tubes, pipetes and flasks were silanized as described previously[7].

Instrument

GC was carried out using a Hewlett-Packard Model 5840A gas chromatograph equipped with a nitrogen–phosphorus selective detector (NPD). A silanized glass column (1.2 m × 2 mm I.D.) was packed with 2% OV-17 on Gas-Chrom Q (80–100 mesh). Helium was used as carrier gas at a flow-rate of 30 ml/min, and air and hydrogen as detector gases at 70 and 3 ml/min, respectively. The voltage applied to the NP collector was 18–19 V which was about 2–3 V higher than the usual operating voltage. The column, injector and detector temperatures were 265, 320 and 300°C, respectively.

For the determination of pindolol, a glass column packed with 2% Dexsil 410GC was used and operated at 260°C. Other conditions were the same as described above.

Preparation of derivatives

Pindolol and nadolol were dissolved in ethyl acetate, and other drugs were extracted with ethyl acetate from their hydrochlorides and dried with anhydrous sodium sulphate. The drug solution was mixed with BBA or PBA solution, and dilutions in reagent solution were analysed in triplicate by GC–NPD to determine the detector responses of the drugs.

TABLE I

STRUCTURES RETENTION INDICES AND NPD RESPONSES FOR CYCLIC BORONATES OF β-ADRENERGIC BLOCKING DRUGS

A glass column (1.2 m × 2 mm I.D.) packed with 2% OV-17 on Gas-Chrom Q, 80–100 mesh, was used.

Generic	*Structure*	*Retention index*		*Minimum detectable amount**	
		*BBA***	*PBA****	*pg*	*Mol/sec* ($\cdot 10^{-16}$)
Propranolol	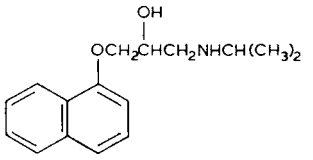	2706	3238	1.9	7.1
Alprenolol	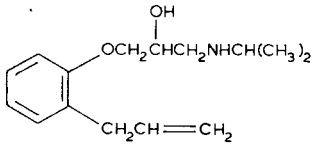	2303	2749	2.0	8.1
Bufetolol	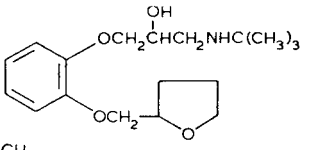	2935	3408	3.7	11.5
Bupuranolol	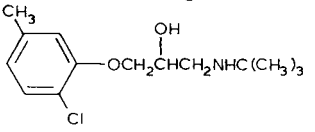	2455	2870	2.4	9.0
Carteolol	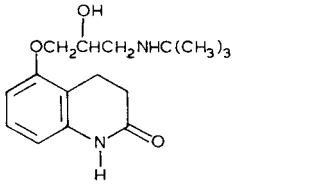	3275	3759	4.0	13.7
Nadolol	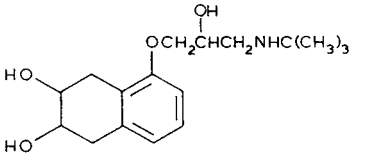	3171	4167	3.2	10.4
Oxprenolol	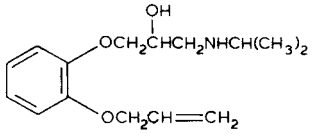	2426	2876	2.3	8.6

(Continued on p. 612)

TABLE I *(continued)*

Generic	*Structure*	*Retention index*		*Minimum detectable amount**	
		*BBA***	*PBA****	*pg*	*Mol/sec* ($\cdot 10^{-16}$)
Pindolol	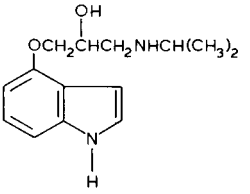	2896	3447	1.5	6.1

* Minimum detectable amount expressed in picograms is valid at t_R = 1–2 min.
** *n*-Butylboronic acid.
*** Phenylboronic acid.

Determination of propranolol in plasma

To 1 ml of plasma sample was added 0.2 ml of an aqueous solution of the internal standard (bufetolol, 1 μg/ml) and 2 ml of 1 *N* sodium hydroxide solution in a glass-stoppered 15-ml centrifuge tube. The tube was shaken with 5 ml of *n*-hexane containing 1.5% of isoamyl alcohol for 10 min and centrifuged for 5 min. The organic layer (4 ml) was transferred into another tube and evaporated to dryness under a gentle stream of air at 50°C. The residue was dissolved in 50 μl of PBA solution, and a 2-μl aliquot of the solution was injected into the column.

Samples (1 ml) of the control plasma containing 1–500 ng of propranolol were treated as described above. Peak-area ratios of propranolol to the internal standard (bufetolol) were measured and plotted against the amount of propranolol added.

Determination of pindolol in plasma

The procedure was essentially the same as for propranolol but the extraction was with ether. Propanolol was used as the internal standard.

RESULTS AND DISCUSSION

Cyclic boronates of β-blocking drugs

The β-blocking drugs were readily derivatized at room temperature with BBA or PBA to form their cyclic boronates (Fig. 1). The reaction was not affected by temperature (20–60°C) or time (0–2 h) under excess boronic acid.

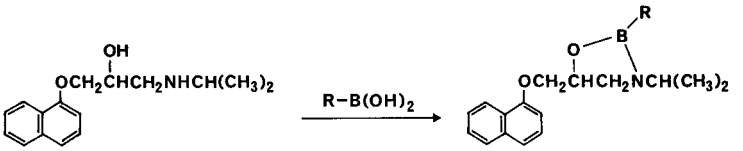

Fig. 1. Reaction of β-blocking drug, propranolol, with boronic acid. R = n-C_4H_9: *n*-butylboronic acid; R = C_6H_5: phenylboronic acid.

The retention indices for BBA and PBA derivatives of eight β-blocking drugs examined are shown in Table I. The PBA derivatives have larger retention indices than the BBA derivatives (*ca.* 400–500 units). Only nadolol showed prolongation of retention index (*ca.* 1000 units) because of the introduction of two cyclic boronate groups into the molecule, at the hydroxyamine and diol sites. The results permit the choice of most suitable derivative for GC analysis in order to obtain the well separated peaks of interest with regard to biological samples.

It is well known that the cyclic boronate derivatives are readily hydrolysed or solvolysed[8,9]. In the case of β-blocking drugs, the derivatives were stable at room temperature for at least 3 days. However, 7 days after derivative formation, the PBA derivatives were almost decomposed but BBA derivatives were not.

The cyclic boronates of the drugs have good GC properties and give high responses on NPD. The detector responses of BBA and PBA derivatives were almost the same, and the minimum detectable amount, givings a signal three times greater than the background noise level, were in the range $6–14 \cdot 10^{-16}$ mol/sec, corresponding to 1.5–4 pg under the GC conditions used (Table I). The described valves were about 10–30 times more sensitive than those of NPD when operated as usual, because of the higher collector voltage.

Determination of propranolol in plasma

Propranolol was extracted from plasma by a single-extraction procedure and derivatized with PBA, as described in the Experimental section. Bufetolol, used as the internal standard, was added to plasma before extraction. The procedure permits analysis of 30 or more samples per day on an instrument. The calibration graph obtained with 1–500 ng of propranolol in 1 ml of plasma is shown in Fig. 2. The graph is rectilinear within a 500-fold range and passed through the origin. The minimum detectable concentration was *ca.* 0.5 ng/ml. The relative standard deviation after eight

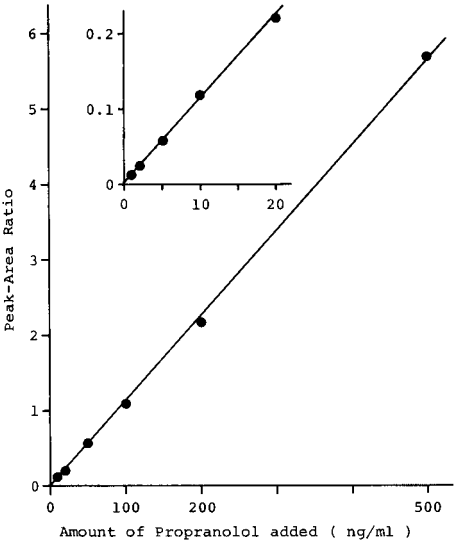

Fig. 2. Calibration graph for propranolol in plasma. Plots are means of three determinations.

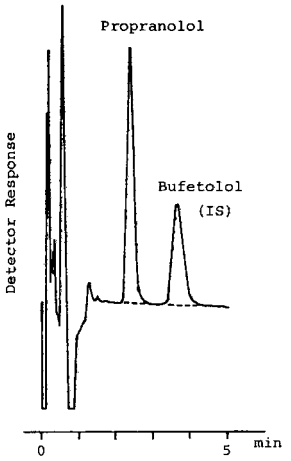

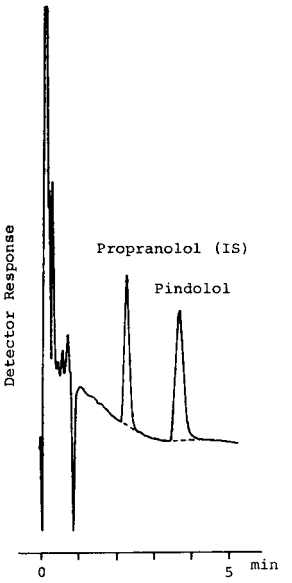

Fig. 3. A typical chromatogram of propranolol in plasma, propranolol corresponding to a plasma concentration of 100 ng/ml. Broken lines represent the background from control plasma. Gas chromatographic conditions as described in the text.

Fig. 4. A typical chromatogram of pindolol in plasma, pindolol corresponding to a plasma concentration of 100 ng/ml. Broken lines represent the background from control plasma. Gas chromatographic conditions as described in the text.

determinations was 6.6 % at the 10 ng/ml level and 4.1 % at the 100 ng/ml level. Fig. 3 shows a typical chromatogram of a plasma sample containing 100 ng of propranolol.

Compared with other methods for the determination of propranolol, the described method was 10–20 times more sensitive than the fluorometric method[1]. This method was simpler and speedier than the GC–ECD method[4,5], which includes a back-extraction procedure and derivatization with trifluoroacetic or heptafluorobutyric anhydride, and the sensitivity was about the same. The results indicate that the proposed method would permit the pharmacokinetic study of propranolol under therapy.

Determination of pindolol in plasma

Pindolol was also determined by the same method but the extraction was with ether. The calibration graph obtained with 2–500 ng of pindolol was rectilinear and passed through the origin. The minimum detectable concentration was 1 ng/ml. A typical chromatogram containing 100 ng of pindolol is shown in Fig. 4. The method was about three times more sensitive than the fluorometric method[2].

CONCLUSION

The results indicate that the described method is generally applicable for the determination of the unchanged β-blocking drugs in plasma and other biological samples. The high sensitivity and relative simplicity of the method would permit

analysis of small samples, and permit pharmacokinetic studies, particularly after low doses, resulting a better understanding of the therapeutic effects of β-blocking drugs.

ACKNOWLEDGEMENT

The authors are grateful to Dr. H. Nishimura, director of their laboratory, for his support of this work.

REFERENCES

1 D. G. Shand, E. M. Nuckolls and F. A. Oates, *Clin. Pharmacol. Ther.*, 11 (1970) 112.
2 W. L. Pacha, *Experientia*, 25 (1969) 802.
3 M. Ervik, *Acta Pharm. Suecica*, 6 (1969) 393.
4 E. Di Salle, K. M. Baker, S. R. Bareggi, W. D. Watkins, C. A. Chidsey, A. Frigerio and P. L. Morselli, *J. Chromatogr.*, 84 (1973) 347.
5 T. Walle, *J. Pharm. Sci.*, 63 (1974) 1885.
6 C. F. Poole, L. Johansson and J. Vessman, *J. Chromatogr.*, 194 (1980) 365.
7 T. Yamaguchi, Y. Utsui and M. Hashimoto, *J. Chromatogr.*, 150 (1978) 147.
8 C. J. W. Brooks and D. J. Harvey, *J. Chromatogr.*, 54 (1971) 193.
9 C. F. Poole and A. Zlatkis, *J. Chromatogr.*, 184 (1980) 99.

Journal of Chromatography, 239 (1982) 617–624
Elsevier Scientific Publishing Company, Amsterdam — Printed in The Netherlands

CHROM. 14,616

CHEMILUMINESCENT NITROGEN DETECTOR–GAS CHROMATOGRAPHY AND ITS APPLICATION TO MEASUREMENT OF ATMOSPHERIC AMMONIA AND AMINES

NOBUYUKI KASHIHIRA*, KAZUO MAKINO, KUWAKO KIRITA and YOSHICHIKA WATANABE

Training Institute for Environmental Pollution Control, 3-3 Namiki, Tokorozawa 359 (Japan)

SUMMARY

A nitrogen-sensitive detector for gas chromatography was constructed by utilizing a commercial chemiluminescent nitrogen oxide analyser in conjunction with formation of nitrogen monoxide from nitrogen-containing compounds by pyrolysis on the hot platinum catalyst. The detector is very specific and quite sensitive to nitrogen compounds. There is no interference from other hydrocarbons. The collection ability of the adsorbents for ammonia and amines was determined in terms of (1) breakthrough volume and/or (2) collection efficiency. The maximum loading capacities of the adsorbents are 3.0 μg/g for ammonia on alkalized Porasil A, more than 2 μg/g for amines on all adsorbents studied. The recoveries of adsorbed compounds were measured by gas chromatographic analysis after thermal injection and almost 100% of ammonia and amines were recovered from Tenax-GC and alkalized Porasil A, but less quantitative from Porapak T and Chromosorb T. The present method was successfully applied for a determination of atmospheric ammonia and trimethylamine.

INTRODUCTION

In order to determine minor constituents in air, they have to be pre-concentrated by a proper collection method. Ambient temperature adsorption and thermal desorption techniques have advantages over collection on a filter paper or in solution, such as (i) no reagent blank, (ii) an ease of handling, and (iii) small sample size due to injection of whole amounts collected to gas chromatography. Ambient temperature collection of ammonia and amines is not get popular[1,2], though they are one of the major nuisances as offensive odour. This is because of severe interference from hydrocarbons in gas chromatography with a flame ionization detector (GC–FID), the detection is not selective to nitrogen compounds. In order to avoid this problem, the selective detector must be used.

Recently, the performance of the flame thermionic detector (FTD) which is very specific to nitrogen and phosphorus compounds has been improved sufficiently to detect picogram levels of these compounds[3]. Chemiluminescence from a reaction

0021-9673/82/0000–0000/$02.75

between nitrogen monoxide and ozone can be also used for specific detection of N-nitrosamines after thermal cleavage of N–NO bond, and a detector based on this principle is called a thermal energy analyser (TEA)[4].

We constructed a nitrogen-selective detector by employing a commercial nitrogen oxide analyser in conjunction with pyrolysis of nitrogen-containing compounds[5], and applied gas chromatography with a chemiluminescent nitrogen detector (GC–CLD) for measurement of ammonia[6] and trimethylamine (TMA)[7] in air. The present paper deals with the performance of the chemiluminescent nitrogen detector and the adsorption behaviour of ammonia and amines to some adsorbents.

EXPERIMENTAL

Apparatus

The GC–CLD system consisted of a chromatograph, a pyrolyser, and a CL-NO_x analyser (Fig. 1). A Shimadzu 4BM-GC chromatograph was used, and a column separation was done with a glass column (3m × 3 mm I.D.) packed with either 5% squalane + 2% KOH on Chromosorb 104 (80–100 mesh) or on Chromosorb 103 (80–100 mesh) isothermally at 130°C with nitrogen carrier gas at a flow-rate of 50 ml/min. The pyrolyser was a quartz tube (20 cm × 6 mm I.D.) packed with platinum net in 10 cm long heated at 900°C, and the detector was a chemiluminescent nitrogen oxide analyser (Bendix Model 8101-C) with 0.5, 1.0, and 2.0 ppm full scale range.

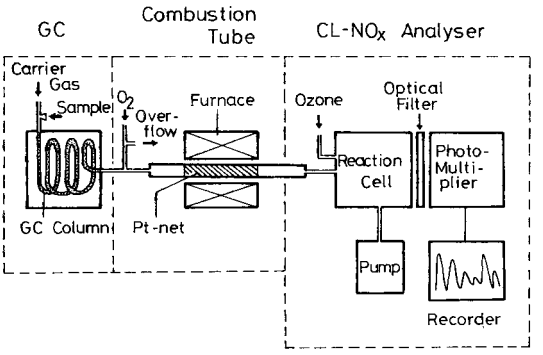

Fig. 1. Schematic view of GC–CLD.

Materials

Standard solutions for ammonia, methylamine (MMA), dimethylamine (DMA), and TMA were prepared by diluting aqueous solutions (30%) of each compound (Wako, Osaka, Japan, "S" grade) with water and standardized by the titrimetric method with hydrochloric acid.

Standard gases for each compound were made by vapourizing *ca.* 1 μl of aqueous solution in a nitrogen-filled sampling bottle (1 l) and further diluted with nitrogen gas in another bottle (DMA). Its concentration was calibrated with the standard solution by GC. The sample gas stream with a constant concentration at ppb*levels was prepared by diluting a vapour permeating through a permeation tube

* Throughout this article, the American billion (10^9) is meant.

wall with air compressed from a laboratory room with an air pump. The dilutant air was desiccated with silica gel but not purified further. The permeation tube was prepared by filling concentrated aqueous solution for each compound, instead of liquefied gas[8], into a PTFE tube (FEP, 4 cm × 7 mm O.D. × 6 mm I.D.) with both ends plugged with glass stoppers[9]. The concentration of the diluted sample gas was determined either by colorimetry or by GC after collection in an acidic solution.

The collection tubes for Porapak T, Chromosorb T, and Porasil A were of glass (10 cm × 6 mm I.D.), and the tube for Tenax-GC was longer (18 cm). One end of the tube was plugged with silicone rubber and the other was attached to a syringe needle. Porasil A was coated with 5% KOH. They were conditioned according to refs. 2 and 10.

RESULTS AND DISCUSSION

Response of the chemiluminescent nitrogen detector to nitrogen compounds

The chemiluminescent nitrogen oxide analyser is based on measurement of the light emitted by the relaxation of excited-state NO_2*, which is produced in a reaction of nitrogen monoxide with ozone, to ground-state NO_2. Therfore, the sensitivity of CLD towards nitrogen compounds is governed by the effectiveness of the conversion from nitrogen compounds into nitrogen monoxide. Nitrogen-containing compounds decompose stoichiometrically to yield NO by combustion in an oxygen stream with a proper catalyst[11].

The response of nitrogen compounds to the CLD was measured by injecting *ca.* 40 ng of each compound into a pyrolyser directly without a column separation. The result is shown in Fig. 2, in which the ordinate is the intensity of nitrogen monoxide on the CLD and the abscissa represents the number of moles corresponding to 10 ng for each compound. From Fig. 2 it is clear that the CLD has a good response to nitrogen compounds. Particularly ammonia, acetonitrile and nitromethane have a higher sensitivity than amines by a factor of *ca.* 1.5.

Raising the temperature of the pyrolyser gave a steady increase of CLD signal up to 900°C. A peak height at 500°C is *ca.* 80% of that at 900°C with a large peak

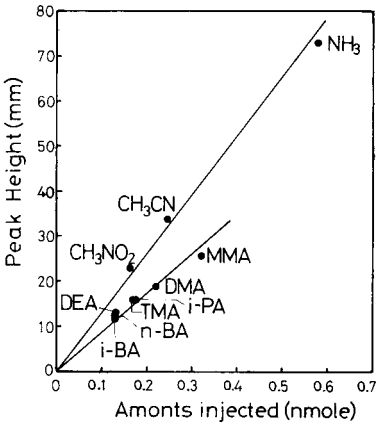

Fig. 2. Response of the CLD to various nitrogen compounds.

tailing. There is no significant interference from other hydrocarbons, and 1 μl of solvents such as ethanol, acetone, hexane, benzene gave a small peak equivalent to a new nanograms of TMA. As shown in Fig. 3, with GC–CLD it is possible to determine even diethylamine (DEA), which is hidden in the solvent peak in GC–FID.

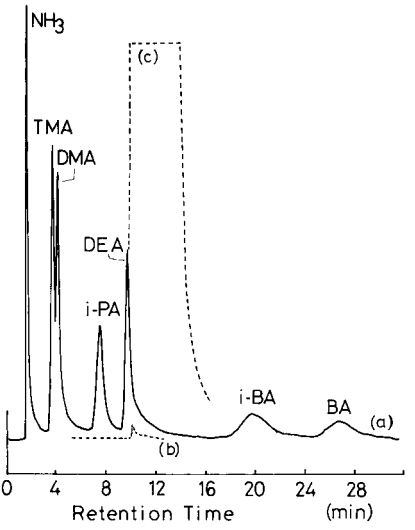

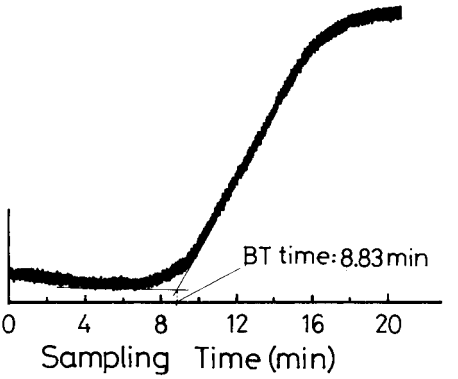

Fig. 3. Gas chromatogram of amines with GC–CLD. Conditions: 5% squalane plus 2% KOH/Chromosorb 104 (80–100 mesh) in a glass column (2 m × 3 mm I.D.), isothermally at 130°C with nitrogen flow-rate of 60 ml/min. (a) Mixed standard sample in ethanol solution. (b) Ethanol only. (c) Ethanol with GC–FID.

Fig. 4. Break-through curve of TMA (0.28 ppm) on Chromosorb T sampled with 0.6 l/min at 18°C.

Collection capacity of adsorbent tube

The collection tube must have a large capacity at ambient temperature (large adsorbing constant). The capacity of the collection tubes was measured by two methods: (1) from the collection efficiency and (2) from the breakthrough volume. The collection efficiency of the adsorbent was measured by either connecting two collection tubes in series or using a cryogenic trap as the backup. Measurements were carried out by sampling the sample gas in low concentrations through the adsorbent tube by the air pump. Results for TMA with Tenax-GC are shown as a function of sampling rate in Table I. For ammonia with alkalized Porasil A, no ammonia was observed in the backup tube at flow-rates of up to 0.8 l/min, indicating almost 100% collection efficiency for the front tube.

The breakthrough volume was determined by drawing the sample gas through the collection tube in a thermostat with a fixed sampling rate. A fraction (about 100 ml/min) of the exit air stream from the tube was monitored continuously by CLD without a column separation. A typical breakthrough curve is shown in Fig. 4. The breakthrough volume was calculated from the breakthrough time of the signal multiplied by the fixed sampling rate at the given temperature. The change in breakthrough volume as a function of temperature is shown in Fig. 5 for ammonia and in Fig. 6 for TMA*.

* Similar behaviours to TMA were also obtained for DMA and MMA.

TABLE I

COLLECTION EFFICIENCY OF TMA WITH TENAX-GC AT 20°C

Sampling rate (l/min)	*Collection efficiency (%)*
0.29	100
0.54	100
0.78	90.1
1.05	93.8
1.41	88.4

The variation of breakthrough volumes with temperature follows two different curves, a steep line at higher temperatures and nearly constant value at lower collection temperatures. The line at high temperatures is insensitive to the concentration of sample gas, and all amines lie on almost the same line for a given adsorbent. This indicates that retention volume is dependent on temperature[12], and also a tendency to thermal release and easier desorption by heating. On the other hand, the constant line at lower temperatures went up and down depending on the gas concentration. However, almost constant values were obtained by multipling the gas concentration by the breakthrough volume. This is the maximum amount of substance that can be adsorbed on the given adsorbent and is called the maximum loading capacity ($^{m}L_{c}$) of the adsorbent. For ammonia no distinct saturation was observed at lower temperatures. This may be due to very fast transfer of ammonia through the tube, as observed by McClenny[1].

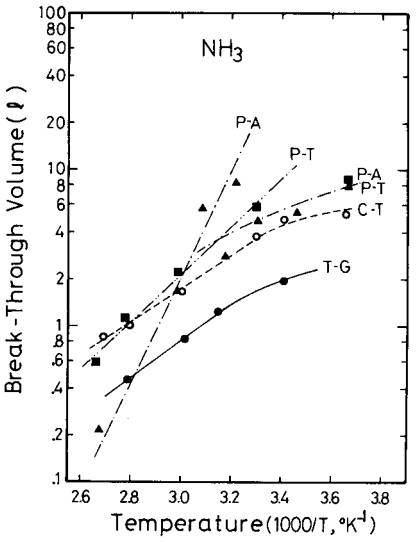

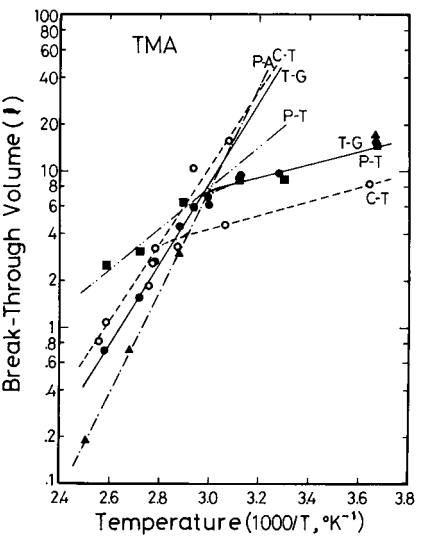

Fig. 5. Temperature dependence of breakthrough volumes for ammonia with adsorbents used. ●—●, Tenax-GC (0.3 ppm); ■—■, Porapak T (0.3 ppm); ○—○, Chromosorb T (0.2 ppm); ▲—▲, Porasil A (*ca.* 1 ppm).

Fig. 6. Temperature dependence of breakthrough volumes for TMA with adsorbents used. ●—●, Tenax-GC (0.10 ppm); ■—■, Porapak T (0.13 ppm); ○—○, Chromosorb T (0.18 ppm); ▲—▲, Porasil A (> 2 ppm).

Table II shows the maximum loading capacities of adsorbents used for ammonia and amines at 18°C. For alkalized Porasil A, the breakthrough phenomena could not observed after passage of 60 l of the sample gas (2 ppm), but a strong odour was detected and a very large peak of TMA was obtained by injection on to the gas chromatograph.

TABLE II

MAXIMUM LOADINGS CAPACITIES (^mL_c) OF ADSORBENTS USED AT 18°C

Adsorbent	*Amounts packed (g)*	^mL_c *(μg/g)*			
		NH_3	*MMA*	*DMA*	*TMA*
Tenax-GC	0.6	0.7	3.2	5.7	4.5
Porapak T	0.8	2.1	3.6	8.4	4.8
Chromosorb T	0.9	0.6	>2	4.7	4.0
Porasil A	1.0	3.0			>18

From Table II, Porapak T and alkalized Porasil A have a sufficiently large capacity to adsorb both ammonia and amines in air. Chromosorb T and Tenax-GC can also be used as adsorbent for amines at low ppb levels. By stepwise sampling of the gas in a low concentration with Tenax-GC, the amount of TMA was determined by GC–FID and the corresponding concentrations of the gas were calculated for each measurement. From the results shown in Fig. 7 along with the breakthrough curve for the gas it can be concluded that the maximum sampling volume is *ca.* 1.5 times larger than the breakthrough volume for the same gas. This indicates that the breakthrough volume can be used as a measure of the sample size for each adsorbent tube.

Recovery of adsorbates from adsorbents

A good collection tube for GC must have not only a large collection capacity but also a quantitative recovery of adsorbates by thermal desorption. The recovery of ammonia and amines from the collection tube was measured with the standard gases and was almost 100% for TMA from Tenax-GC[7] and ammonia[6] and DMA from alkalized Porasil A.

Porapak T and Chromosorb T gave a poor recovery due to the low temperature allowable, particularly for DMA. Overall recovery for the whole procedure was

TABLE III

RECOVERIES OF ADSORBATES FROM COLLECTION TUBE WITH 8 l OF THE MIXED GAS

Adsorbent	*Recoveries (%)*		
	NH_3 (130 ppb)	*DMA (70 ppb)*	*TMA (23 ppb)*
Tenax-GC	20.0	80.3	100*
Porasil A	100*	100*	104.6
Chromosorb T	91	74.2	85.2
Porapak T	–	–	76.3

measured by sampling 8 l of a mixed gas at ppb level with the collection tube. The results shown in Table III are expressed by comparing the values to those marked (*) which were considered as 100%. It was not possible to achieve a satisfactory recovery for ammonia and DMA from Porapak T. Recovery of MMA was not reproducible, even with the standard gas.

Application

We applied ambient temperature preconcentration and GC–CLD to the determination of atmospheric ammonia and amines. TMA in freezer air was analysed with GC–CLD after preconcentration with a Tenax-GC tube. The gas chromatogram for 6 l of the freezer air is shown in Fig. 8, and the amount of TMA was 35 ng, corresponding to 2.4 ppb, whereas a 0.1 N H_2SO_4 collection cryogenic trap and GC–FID gave 5.8 ppb and 1.3 ppb with 15 l of the same gas. Both results can be said to be in relatively good agreement.

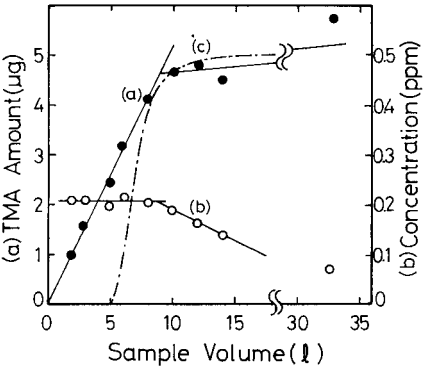

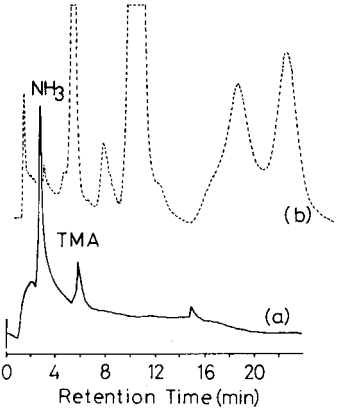

Fig. 7. Relation between TMA amounts collected and sample volumes with Tenax-GC at 22°C. (a) ●—●, Amount of TMA collected; (b) ○—○, TMA concentration; (c) break-through curve.

Fig. 8. Gas chromatogram of 6 l of freezer air with Tenax-GC: (a) GC–CLD; (b) GC–FID. GC conditions as in Fig. 3.

Ammonia in air around the boundary zone of a cattle farm was also measured by collecting with alkalized Porasil A, and 129 ppb was obtained with 0.4 l of sample gas.

REFERENCES

1 M. A. McClenny and C. A. Benett, Jr., *Atmos. Environ.*, 14 (1980) 641.
2 K. Kuwata, Y. Yamazaki and M. Uehori, *Bunseki Kagaku (Jap. Anal.)*, 29 (1980) 170.
3 B. Kolb and J. Bischoff, *J. Chromatogr. Sci.*, 12 (1974) 625.
4 D. H. Fine, F. Rufeh, D. Lieb and D. P. Roubekler, *Anal. Chem.*, 47 (1973) 1188.
5 N. Kashihira, K. Tanaka, K. Kirita and Y. Watanabe, *Bunseki Kagaku (Jap. Anal.)*, 29 (1980) 35.
6 N. Kashihira, K. Makino, K. Kirita and Y. Watanabe, *Bunseki Kagaku (Jap. Anal.)*, 31 (1982) E13.
7 N. Kashihira, K. Kirita, Y. Watanabe and K. Tanaka, *Bunseki Kagaku (Jap. Anal.)*, 29 (1980) 853.
8 F. P. Scaringelli, A. E. O'Keefe, E. Rosenberg and J. P. Bell, *Anal. Chem.*, 42 (1970) 871.
9 N. Kashihira, *J. Jap. Soc. Air Pollut.*, 15 (1980) 275.

10 *Measuring Method for Offensive Odor Substances*, Kankyo-cho Kokuji 47, Chuo-Hoki Shuppan, Tokyo, 1976, Appendix 5.
11 H. Yoshimi, K. Oka, T. Nozaki, H. Makino, M. Tohyama, S. Ohmori and S. Fukui, *Gesuido-Kyokai-shi*, 12 (1975) 1.
12 W. Funasaka and N. Ikekawa (Editors), *Modern Gas Chromatography*, Vol. 1, Hirokawa Publ. Co., Tokyo, 1979.

Journal of Chromatography, 239 (1982) 625–632
Elsevier Scientific Publishing Company, Amsterdam — Printed in The Netherlands

CHROM. 14,517

"BUFFER MEMORY" TECHNIQUE FOR THE COMBINATION OF MICRO-HIGH-PERFORMANCE LIQUID CHROMATOGRAPHY AND INFRARED SPECTROMETRY

KIYOKATSU JINNO* and CHUZO FUJIMOTO
School of Materials Science, Toyohashi University of Technology, Toyohashi 440 (Japan)
and
DAIDO ISHII
Faculty of Engineering, Nagoya University, Nagoya 464 (Japan)

SUMMARY

The buffer memory technique was applied to the combination of micro-high-performance size-exclusion chromatography and Fourier transform infrared spectrometry. A series of polystyrene standards with known molecular weights was studied and the molecular weight calibration was established. Polyethylene glycol of unknown molecular weight was determined from the calibration. The utility of the technique is discussed.

INTRODUCTION

The combination of high-performance liquid chromatography (HPLC) and infrared (IR) spectrometry has so far been accomplished via two approaches, the automated diffuse reflectance–solvent elimination technique[1–3] and the direct flow cell technique[4–7]. With these techniques a number of compounds isolated by HPLC have been successfully detected. However, both techniques have involved some intrinsic problems, as described by Kuehl and Griffiths[2] and Vidrine[8].

Recently, we proposed the novel potassium bromide buffer memory technique[9,10] which has been used to couple conventional dispersive IR with micro-HPLC (MHPLC). The technique was applied to the detection of sample components separated in the normal-phase mode. In this technique, the effluent from the MHPLC column is deposited via a UV flow-cell on a potassium bromide plate as a narrow, continuous band (about 1.5 mm wide) with instantaneous elimination of the carrier solvent. After collecting all the solutes, the "memorized" plate, the "buffer memory", is automatically brought into the optical path of the IR spectrometer and IR chromatograms are measured at fixed wavenumbers.

This technique offers several advantages over conventional HPLC–IR techniques; most important is that completely continuous chromatograms can be obtained without interference from the mobile phase.

0021-9673/82/0000–0000/$02.75

In this paper, the applicability of the buffer memory technique to size-exclusion chromatography (SEC) is demonstrated, and the analytical potential of this technique is discussed.

Previous work from this laboratory[11] has generally shown that a miniaturized SEC column can be used for the determination of the components of polymer materials.

EXPERIMENTAL

Spectrometer

The IR instrument employed was a JEOL JIR-40X Fourier transform (FT) spectrometer with a 3 × beam condenser. The system used a TGS pyroelectric bolometer, a potassium bromide–germanium beam splitter and a water-cooled Globar source. All spectra were measured at 8 cm^{-1} resolution in the double-precision mode. The operating software was that normally supplied by JEOL.

Chromatographic system

The micro-high-performance liquid chromatograph was a JASCO Familic 100N system equipped with a Uvidec-100 II UV detector. A TSK GEL 3000 H column of (22 cm × 1 mm I.D.) (excluded molecular weight $6 \cdot 10^4$) was used for the SEC separations. Tetrahydrofuran was used as the mobile phase at a flow-rate of 8 μl/min.

Procedure

The interfacing device developed[10] was simply placed in the sample chamber of the FT-IR spectrometer. With the device, the effluent from the MHPLC column is deposited on to a potassium bromide plate as a narrow, continuous band; the carrier solvent is instantaneously evaporated with a gently warmed stream of dry nitrogen. After collecting all the solutes, the "memorized" plate is automatically brought into the IR beam of the FT-IR spectrometer, and interferograms are sequentially measured and stored in the data system. At the end of the chromatogram, each stored interferogram is recalled and transformed. Then, absorbances in the selected regions are integrated and plotted in a recorder. Subtraction of the absorption bands due to water retained on the plate was performed by using the initial file in which no solutes were memorized. A potassium bromide plate, on which only the mobile phase is memorized, is placed in the reference beam. The transfer line between a column and a plate is designated not to cause the extra-column broadening. More details have been described elsewhere[12].

Chemicals

Three polystyrenes of molecular weight 37,000, 10,200 and 2800 were purchased from Toyo Soda (Tokyo, Japan). Polystyrene with a wider molecular weight distribution (average molecular weight about 500) and Carbowax 6000 were kindly supplied by Dr. Hirata (Toyohashi University of Technology). The chromatographic solvent used was tetrahydrofuran of HPLC grade (Kanto Chemicals). A large single crystal of potassium bromide (35 × 35 × 3 mm) was obtained from JASCO. The crystal was cut into four equal pieces and used as a buffer memory substrate.

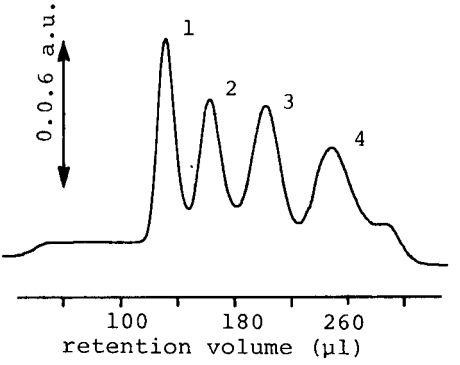

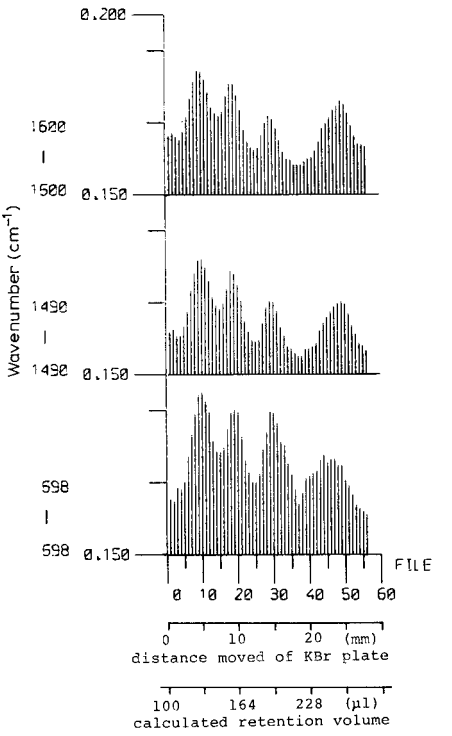

Fig. 1. SEC chromatogram of polystyrene standards measured with a UV detector at 254 nm. MHPLC conditions: column, 22 cm × 0.1 cm I.D. PTFE tube; packing, TSK GEL G-3000 H; mobile phase, tetrahydrofuran, 8 µl/min. Peaks: 1 = mol.wt 37,000 (8.8 µg); 2 = mol.wt. 10,200 (7.2 µg); 3 = mol.wt. 2800 (7.7 µg); 4 = mol.wt. 500 (28.7 µg).

Fig. 2. FT-IR chromatograms at various wavenumbers. Spectrometer: JEOL JIR-40X. Mirror rate: 1.6 mm/sec. Detector: TGS. Accumulation: 64 × times. Resolution: 8 cm^{-1}. Peak maxima of PS 37,000, 10,200, 2800 and 500 appear at 130, 159, 192 and 254 µl, respectively.

RESULTS

SEC has a unique separation mechanism based on differences in the molecular size of the components of a sample. Its chromatograms are usually evaluated by determining the molecular weights corresponding to a given retention volume, with help of pre-determined calibration graphs. For this purpose, a mixture of polystyrene standards was eluted through a micro-SEC column. The resulting UV chromatogram and FT-IR chromatograms at characteristic absorption bands of the solutes are shown in Figs. 1 and 2, respectively. It can be seen that the FT-IR chromatograms obtained by the buffer memory technique reflect the original chromatographic separation without a decrease in resolution. In the present work, interferometric data are collected every 0.5 mm on the plate. The flow-rate of the mobile phase is 8 µl/min and the deposition rate of the effluent is 1.25 mm/min. Hence the elution volume between each file corresponds to 3.2 µl. The calculated elution volumes at each peak maximum are indicated in the figures, with file numbers and distances on the plate.

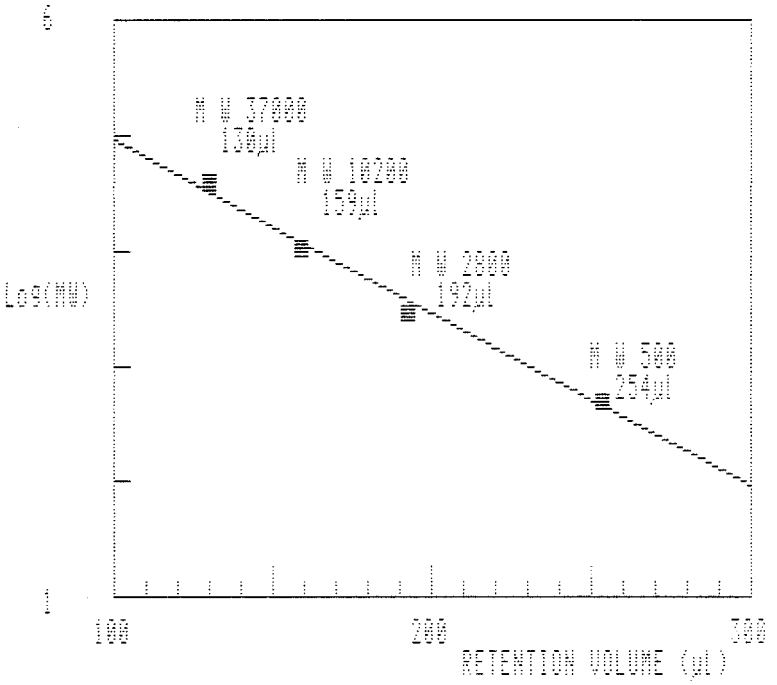

Fig. 3. Peak position calibration graph for a series of polystyrene standards obtained by the potassium bromide buffer memory technique. MW = Molecular weight.

Fig. 3 shows the peak position calibration graph obtained by plotting the retention volumes for each peak against the logarithms of the corresponding molecular weights.

Carbowax 6000 was analysed under the same conditions (the molecular weight was expected to be about 6000). This sample is of interest because it is a high-molecular-weight polymer of polyethylene glycol that has been widely used as a stationary phase in gas chromatography. Naturally, it cannot be analysed by gas chromatography. In addition, it has no absorption in the UV region so that it is impossible to detect it on a UV detector.

The FT-IR chromatograms of the compound are shown in Fig. 4. Its peak maximum appears at a retention volume of 161 µl, which corresponds to a molecular weight of 10,800 on the calibration graph established above. However, this value is greater than expected value. This is due to the fact that, in general, different types of molecules give different calibration graphs because of their characteristic molecular configurations. According to Mori and Yamamoto[13], the reduced molecular weight of polyethylene glycol is given by

$$M = 1.21 \cdot M_S^{0.916} \tag{1}$$

for $M < 10000$, where M_S is the molecular weight of polyethylene glycol obtained from the peak position on the polystyrene calibration graph. Utilizing this equation, the molecular weight of Carbowax 6000 is calculated to be 5990. The transmittance

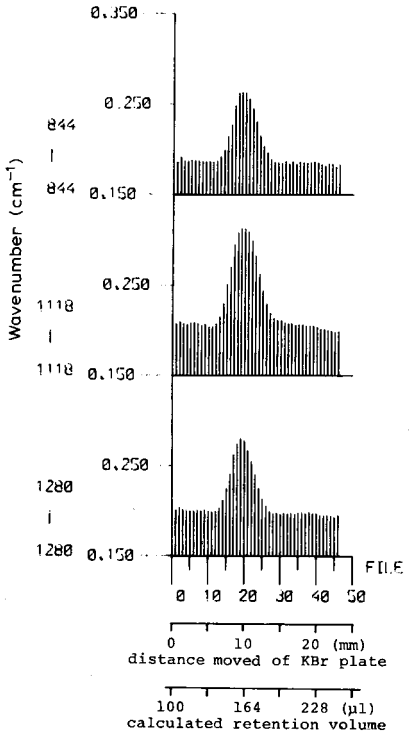

Fig. 4. FT-IR chromatograms of Carbowax 6000 at various wavenumbers. Sample weight: 15.7 μg. Other conditions as in Fig. 2.

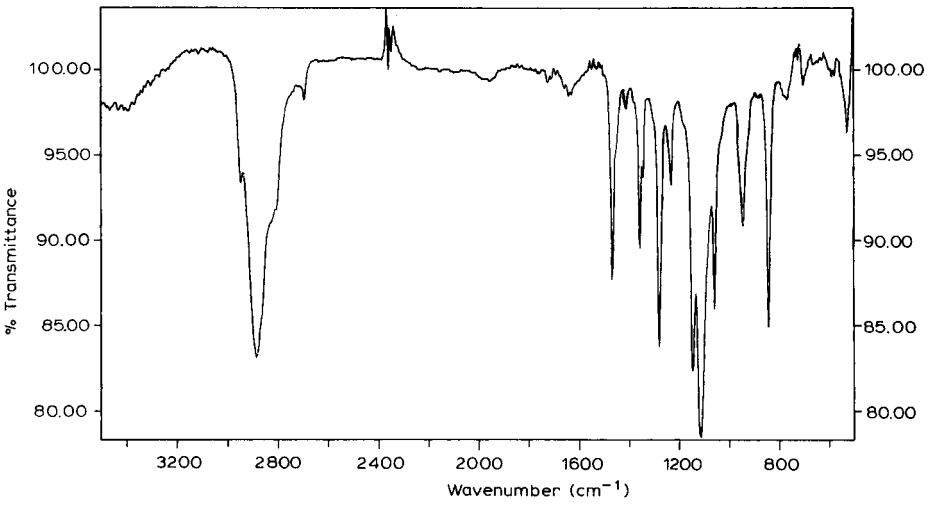

Fig. 5. IR spectrum of Carbowax 6000 obtained from file no. 19 in Fig. 4.

spectrum of file No. 19 in Fig. 4 is shown in Fig. 5. This is just spectrum of polyethylene glycol.

DISCUSSION

This work was intended to obtain good chromatograms, rather than a high sensitivity of the technique. We regard these experiments as preliminary in terms of sensitivity and FT-IR system parameters. In fact, the width of the IR beam focus of the FT-IR spectrometer equipped with the 3 × beam condenser was about 2.5 mm, while that of the solute-deposited band was about 1.5 mm. In order to improve the signal-to-noise ratio, a small aperture (4 × 1 mm) was placed in front of the memorized plate in this experiment. The use of this aperture resulted in a significant reduction in the measurement efficiency. Moreover, an MCT detector would have been desirable but was not used here. We plan to optimize these parameters in the future.

The buffer memory technique investigated here has several advantageous features, outlined below.

Use of MHPLC

For the separation, this technique utilizes MHPLC, developed by Ishii and coworkers[14–17]. Its separation ability is comparable to that of conventional HPLC. One of the principal advantages of using MHPLC is that the flow-rate of the mobile phase is extremely low, compared with that of conventional HPLC. Hence it is easy to eliminate solvents and interference from the mobile phase in the spectrum. In the flow-cell technique, the interference caused by the strong IR absorption of the mobile phase solvent is serious, especially when gradient elution is needed for chromatography. Lack of interference from the mobile phase also enables the total absorbance to be measured in a wide wavenumber range provided that absorption due to the

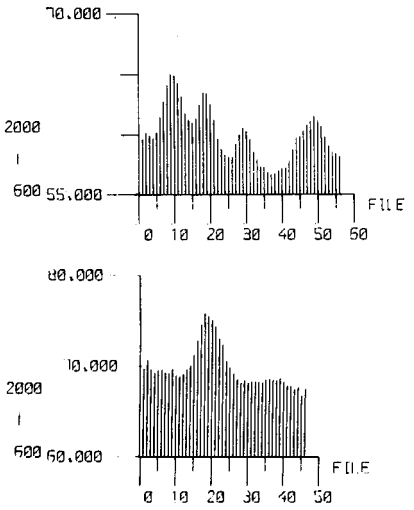

Fig. 6. FT-IR chromatograms of polystyrene standards and Carbowax 6000 for a wide wavenumber range of 600–2000 cm^{-1}. (A) Polystyrene standards; (B) Carbowax 6000. Conditions as in Fig. 2.

background is kept constant in every part of the plate. Fig. 6 shows the chromatograms of polystyrenes and Carbowax 6000 measured at 600–2000 cm^{-1}. It is important to note that the absorbance values obtained in this way are much higher than those in Figs. 2 and 4. The FT-IR chromatograms obtained with a wide wavenumber range seem to be similar to those at fixed wavenumbers. This result gives us the important information that IR can be used as an MHPLC detector by measuring the total absorbance over a wide wavenumber range even if the characteristic absorption wavenumbers of the sample are unknown. Actually, this is not the best way to obtain highly sensitive detection with a low signal-to-noise ratio, but IR can be useful as a universal detector in LC based on this non-dispersive[18] concept using the potassium bromide buffer memory technique.

Perfectly continuous chromatogram

Because the effluent is deposited continuously on the potassium bromide plate, a perfectly continuous chromatogram is obtained, whereas chromatograms obtained by the automated diffuse reflectance–solvent removal technique are only collections of absorbance values for each fraction.

Further characterization

The sample deposited on the plate remains as the "chromatogram". This permits subsequent detailed characterization by other instrumental techniques.

Mechanical simplicity

As the buffer memory technique utilizes the well established IR absorption method, there is no need for a sophiscated system and auxiliary instruments. The technique requires only a simple interface and it is very easy to set up and operate the interface for a particular analysis.

However, there is one drawback to this technique. It is not suitable for solutes that are more volatile than the mobile phase used. Although this is a serious problem common to solvent removal techniques, such solutes can be separated by gas chromatography.

In summary, the buffer memory technique enables completely continuous chromatograms to be measured without any interference from the mobile phase solvents.

ACKNOWLEDGEMENTS

We thank Dr. Hirata for supplying polystyrene and Carbowax 6000. Thanks are also due to M. Nakano for his assistance with the experimental work.

REFERENCES

1 M. P. Fuller and P. R. Griffiths, *Amer. Lab.*, 10 (1978) 69.
2 D. Kuehl and P. R. Griffiths, *J. Chromatogr. Sci.*, 17 (1979) 471.
3 D. T. Kuehl and P. R. Griffiths, *Anal. Chem.*, 52 (1980) 1394.
4 M. M. Gomez-Taylor, D. Kuehl and P. R. Griffiths, *Int. J. Environ. Anal. Chem.*, 5 (1978) 103.
5 K. L. Kizer, A. W. Mantz and L. C. Bonar, *Amer. Lab.*, 7 (1975) 85.
6 D. W. Vidrine and D. R. Mattson, *Appl. Spectrosc.*, 32 (1978) 502.

7 D. W. Vidrine, *J. Chromatogr. Sci.*, 17 (1979) 477.
8 D. W. Vidrine, in J. R. Ferraro (Editor), *Fourier Transform Infrared Spectroscopy*, Vol. 1, Academic Press, New York, London, 1978, p. 129.
9 K. Jinno, C. Fujimoto, M. Ideriha, T. Takeuchi and D. Ishii, *Bunseki Kagaku (Jap. Anal.)*, 29 (1980) 612.
10 K. Jinno, C. Fijimoto and Y. Hirata, *Appl. Spectrosc.*, 36 (1982) in press.
11 K. Jinno and M. Nishihara, *Anal. Lett.*, 13 (B8) (1980) 673.
12 K. Jinno and C. Fujimoto, *J. High Resolut. Chromatogr. Chromatogr. Commun.*, 3 (1980) 313.
13 S. Mori and N. Yamamoto, in *Proceedings of 41st Symposium on Analytical Chemistry*, The Japan Society for Analytical Chemistry, Kochi, 1980, p. 232.
14 D. Ishii, K. Asai, K. Hibi, T. Jonokuchi and M. Nagaya, *J. Chromatogr.*, 144 (1977) 157.
15 D. Ishii, A. Hirose, K. Hibi and Y. Iwasaki, *J. Chromatogr.*, 157 (1978) 43.
16 D. Ishii, K. Hibi, K. Asai and T. Jonokuchi, *J. Chromatogr.*, 151 (1978) 147.
17 D. Ishii, A. Hirose and I. Horiuchi, *J. Radioanal. Chem.*, 45 (1978) 7.
18 K. Jinno, *Spectrosc. Lett.*, 14 (1981).

Journal of Chromatography, 239 (1982) 633–641
Elsevier Scientific Publishing Company, Amsterdam — Printed in The Netherlands

CHROM. 14,535

HIGH-BACK-PRESSURE LIQUID CHROMATOGRAPHY

II. DEVELOPMENT OF A POST-COLUMN-CONTROLLED FLOW SYSTEM

TOYOHIDE TAKEUCHI* and DAIDO ISHII
Department of Applied Chemistry, Faculty of Engineering, Nagoya University, Chikusa-ku, Nagoya-shi 464 (Japan)

SUMMARY

A liquid chromatograph including three pumps for use in micro-high-performance liquid chromatography was examined. The flow-rate of the mobile phase was controlled by a constant-flow pump located downstream of the detector. Mobile phases were supplied from two pumps, a constant-flow and a constant-pressure pump, and mixed through a T-piece. The mixing ratio could be varied stepwise by changing the flow-rate of the forward constant-flow pump. An inlet pressure required was applied in excess by the constant-pressure pump, consisting of a gas-tight syringe and a weight. This flow system permitted both stepwise gradient elution and isocratic elution. Some typical stepwise gradient separations are demonstrated.

INTRODUCTION

In modern high-performance liquid chromatography (HPLC), solvent gradient elution is a highly promising technique that reduces the analysis time or improves the selectivity. At present, various types of chromatographs equipped with gradient system are commercially available, with which both complex ternary and binary-solvent gradient elution can easily be performed.

On the other hand, micro-HPLC lacks a gradient system at present; when gradient elution is necessary simple gradient elution techniques[1,2] have been adopted as follows. For stepwise gradient elution, an eluent that had been prepared previously was stored in a capillary tube prior to a chromatographic run and was forwarded on to the column by feeding the last solvent from a syringe-type pump[2]. For linear or continuous gradient elution, the eluent was stored in a capillary tube while being prepared[1]. These techniques are simple but require expert manipulation.

Recently, high-back-pressure liquid chromatography has been developed[3] and the employment of low-boiling solvents such as butane or propane as the mobile phase in micro-HPLC has been examined. The chromatograph was a closed system and the pressure was kept sufficiently high to exceed the vapor pressure of the now liquid mobile phase by a back-pressure pump in order to prevent vaporization of the mobile phase in the whole system. This technique was also effective for operation at

0021-9673/82/0000–0000/$02.75

elevated temperature[4]. These advances have been possible owing to the development of a micro valve injector.

The above closed-system chromatograph was modified and a new flow system employing three pumps was developed in this work, with which both stepwise gradient elution and isocratic elution were performed *in situ*.

EXPERIMENTAL

The liquid chromatograph developed in this work included a constant-pressure pump, two constant-flow pumps, a T-piece, three-way valves (JASCO, Japan Spectroscopic Co., Tokyo, Japan), a micro valve injector (JASCO), a micro column, a UVIDEC-100 UV spectrophotometer (JASCO) and a pressure gauge (JASCO). The apparatus is illustrated in Fig. 1.

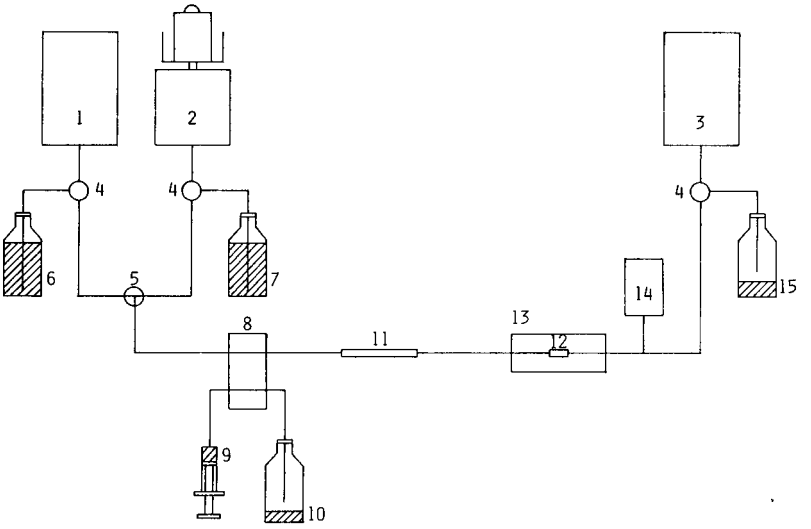

Fig. 1. Diagram of the apparatus. 1 = Constant-flow pump (Familic 100N); 2 = constant-pressure pump; 3 = constant-flow pump (Micro Feeder); 4 = three-way valve; 5 = T-piece; 6 = solvent reservoir; 7 = solvent reservoir; 8 = micro valve injector; 9 = sample; 10 = waste reservoir; 11 = column; 12 = micro flow cell; 13 = UV detector; 14 = pressure gauge; 15 = waste reservoir.

Two kinds of solutions were supplied from two pumps, a constant-pressure and a constant-flow pump, located upstream of the column and mixed through a T-piece. The flow-rates of the mobile phase were controlled by another constant-flow pump located downstream of the detector. The inlet pressure required to feed the mobile phase was applied by the constant-pressure pump, consisting of a gas-tight syringe [1710-N (100 μl) (Hamilton, Reno, NV, U.S.A.), MS-GAN 025 (250 μl) (Terumo Co., Tokyo, Japan) or MS-GAN 050 (500 μl) (Terumo)] and a weight. The pressure was controlled so as to exceed the pressure drops across the separation column and capillary connecting tubing by changing the weight. The forward constant-flow pump was a Familic 100N (JASCO), altering the flow-rate stepwise instantaneously. The flow-rates depend on the dimensions of the gas-tight syringe em-

ployed. When using an MS-GAN 025 250-μl gas-tight syringe, flow-rates of 0.5–14.5 μl/min can be selected at 0.5 μl/min intervals. The backward constant-flow pump was a Micro Feeder (Azumadenki Kogyo Co., Tokyo, Japan) equipped with an MS-GAN 050 gas-tight syringe, generating ten different flow-rates between 0.69 and 16.7 μl/min stepwise. The mixing ratio of two solutions was varied by changing the flow-rate of the forward constant-flow pump, with which stepwise gradient elution was performed, keeping flow-rate of the mobile phase constant.

A home-made T-piece was employed as the mixing joint, consisting of stainless-steel tubing of 0.33 mm I.D. and 0.63 mm O.D. connected by silver solder as shown in Fig. 2. Prior to silver-soldering, one of the stainless-steel tubes was filed and a hole was opened in the middle of the tube so as to fit the cross-section of the other tube. Both tubes were packed with silica gel in order to prevent the silver solder entering the tubes during soldering. The connecting volume between the separation column and the T-piece was about 18 μl.

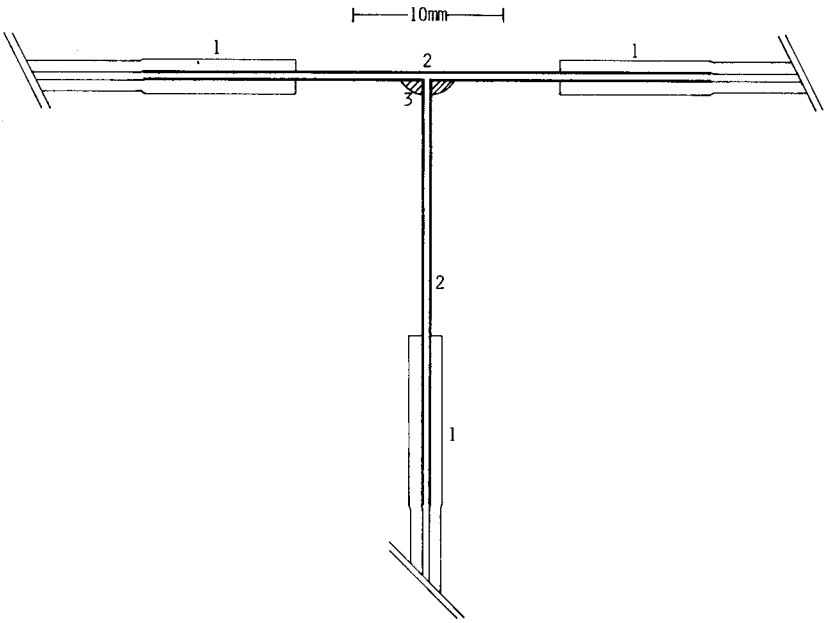

Fig. 2. Schematic diagram of T-piece. 1 = PTFE tubing (0.5 mm I.D., 2 mm O.D.); 2 = stainless-steel tubing (0.33 mm I.D., 0.63 mm O.D.); 3 = silver solder.

A small volume (0.02 μl) of sample solution was loaded by employing a micro valve injector. The reproducibility of the sample amounts injected was good, as reported previously[5].

A fused silica tube (0.35 mm I.D.) (Gasukuro Kogyo Co., Tokyo, Japan) was used as the micro column and was packed with ODS SC-01 silica (5 μm) (JASCO).

The flow cell of the UV detector should withstand high pressures. The flow cell shown in Fig. 3 was resistant to about 40 atm. A fused silica tube of 57 μm I.D. and 0.31 mm O.D. (Scientific Glass Engineering, Victoria, Australia) was inserted in a

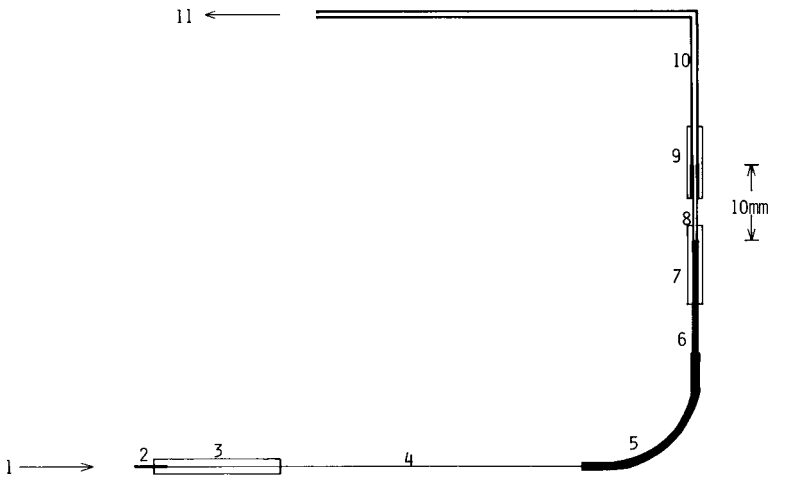

Fig. 3. Schematic diagram of the modified micro flow cell for UV detector. 1 = Eluent; 2 = stainless-steel tubing (0.13 mm I.D., 0.31 mm O.D., 4 mm long); 3 = PTFE tubing (0.2 mm I.D., 2 mm O.D.); 4 = fused-silica tubing (57 μm I.D., 0.31 mm O.D., 9 cm long); 5 = stainless-steel tubing (0.41 mm I.D., 0.71 mm O.D., *ca.* 2.5 cm long); 6 = stainless-steel tubing (0.33 mm I.D., 0.63 mm O.D., *ca.* 1.5 cm long); 7 = PTFE tubing (0.5 mm I.D., 2 mm O.D.); 8 = quartz tubing (0.3 mm I.D., 0.6 mm O.D.); 9 = PTFE tubing (1 mm I.D., 2 mm O.D.); 10 = PTFE tubing (0.5 mm I.D., 1 mm O.D.); 11 = to downstream constant-flow pump.

stainless-steel tube of 0.33 mm I.D. and 0.63 mm O.D. with adhesive. The slit was 0.3 mm wide and 1.5 mm long. The detection volume and dead volume between the column and the flow cell were 0.1 and 0.6 μl, respectively.

RESULTS AND DISCUSSION

The pressure attained by the constant-pressure pump depended on both the weight and the dimensions of the gas-tight syringe employed, as shown in Fig. 4. The smaller the inner volume of the gas-tight syringe, the larger was the pressure attained with constant weight. Nearly linear relationships between weight and pressure attained were observed. Each pressure attained was about 80% of the calculated value, owing to the friction between the plunger and the inner wall of the gas-tight syringe, as shown in Table I. In addition, the gas-tight syringes employed withstood about 70 atm pressure.

The flow-rate of the mobile phase could be controlled by the downstream constant-flow pump if a pressure exceeding the pressure drop across the system, including the column and capillary connecting tubing, was applied by the constant-pressure pump. Otherwise, bubbles were generated in the detector. It was desirable to keep the pressure of the downstream constant-flow pump at 10–30 atm, nearly the same as that of the detector. On the other hand, if leakage of the mobile phase occurred at the connections between the column and the downstream constant-flow pump, the mobile phase composition changed, leading to variations in the retention time of the solute.

It should be noted that mixing of two solutions in a T-piece plays a significant

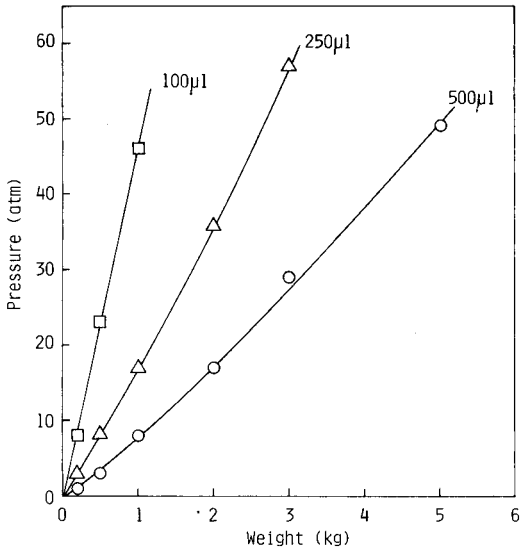

Fig. 4. Relationship between weight and attained pressure.

TABLE I

COMPARISON OF ATTAINED PRESSURES AND CALCULATED VALUES

Weight (kg)	*Pressure (atm)*					
	1710-N (100 µl, 0.0167 cm²)		*MS-GAN 025 (250 µl, 0.0417 cm²)*		*MS-GAN 050 (500 µl, 0.0833 cm²)*	
	Observed	*Calculated*	*Observed*	*Calculated*	*Observed*	*Calculated*
0.2	8	12	3	4.8	1	2.4
0.5	23	30	8	12	3	6
1	46	60	17	24	8	12
2			36	48	17	24
3			57	72	29	36
5					49	60

role in this new flow system. Fig. 5 illustrates baselines for stepwise gradient elution using the MS-GAN 025 as the constant-flow pump. Water and acetonitrile–water (1:1) were supplied from the constant-flow and the constant-pressure pump, respectively. The mixing direction is also indicated in Fig. 5. The upper trace was obtained by employing a T-piece packed with Develosil ODS (15–30 μm) (Nomura Chemical Co., Seto-shi, Japan) in order to perform the mixing effectively. The noise of the baseline is slightly reduced compared with the lower trace, obtained by employing an unmodified T-piece. In both instances stable baselines were observed when the flow-rate of the constant-pressure pump (V_{cp}) was dominant. However, the drift or the noise of the baselines was noticeable when the flow-rate of the constant-flow pump

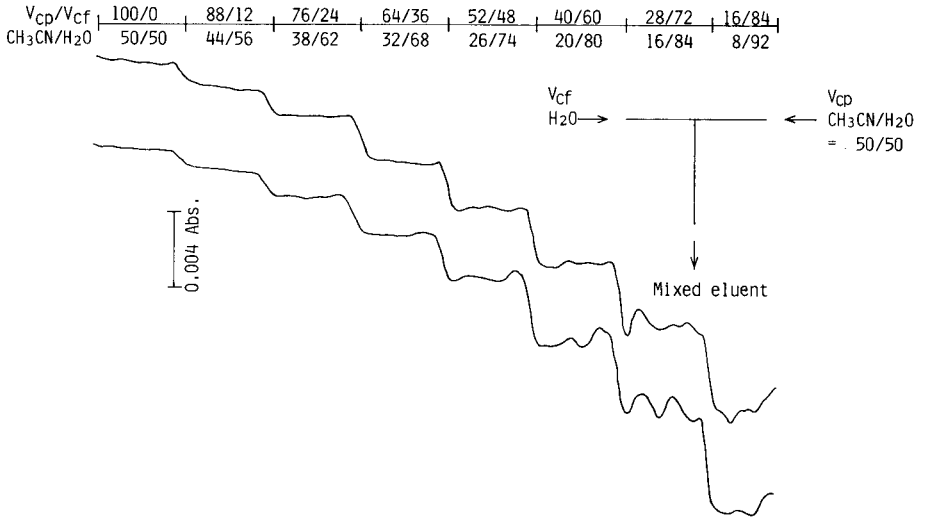

Fig. 5. Baselines for stepwise gradient elutions. Upper trace: obtained with a T-piece packed with Develosil ODS (15–30 μm). Lower trace: obtained with an unmodified T-piece. Wavelength of UV detection: 240 nm. V_{cp}: flow-rate of water with the constant-pressure pump. V_{cf}: flow-rate of acetonitrile–water (1:1) with the constant-flow pump.

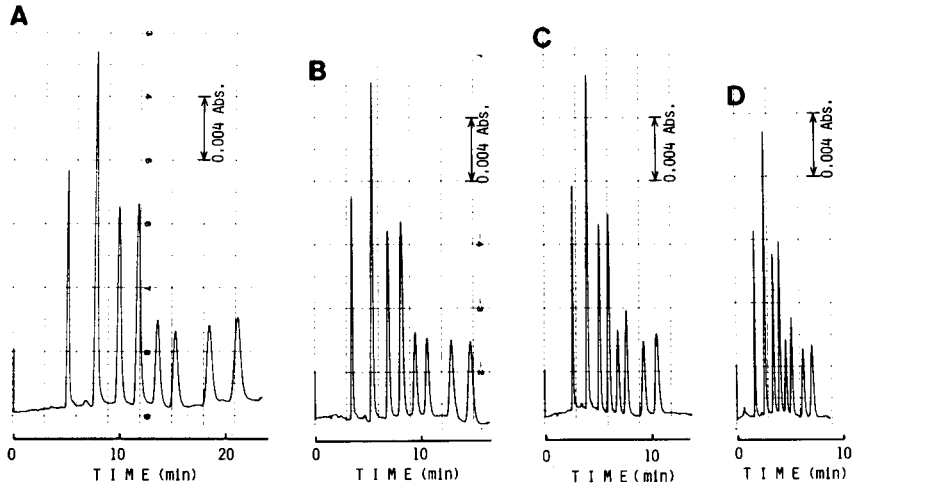

Fig. 6. Isocratic separations of aromatic hydrocarbons at various flow-rates. Column: 10.1 cm × 0.35 mm I.D., packed with SC-01. Mobile phase: acetonitrile–water (64:36). Flow-rates: (A) 2.8 μl/min, V_{cp} = 1.8 μl/min (acetonitrile) and V_{cf} = 1.0 μl/min (water); (B) 4.2 μl/min, V_{cp} = 2.7 μl/min and V_{cf} = 1.5 μl/min; (C) 5.6 μl/min, V_{cp} = 3.6 μl/min and V_{cf} = 2.0 μl/min, and (D) 8.3 μl/min, V_{cp} = 5.3 μl/min and V_{cf} = 3.0 μl/min. Samples: 1.8% (w/w) of benzene, 0.20% of naphthalene, 0.038% of biphenyl, 0.040% of fluorene, 0.0098% of phenanthrene, 0.0078% of anthracene, 0.040% of fluoranthene and 0.040% of pyrene, eluted in that order. Sample size: 0.02 μl. Wavelength of UV detection: 254 nm.

(V_{cf}) was dominant, which may be attributed to the pulsation of the constant-pressure pump. The baseline obtained with the 1710-N as the constant-flow pump was wavy owing to the pulsation of the constant-flow pump even when V_{cp} was larger than V_{cf}.

Fig. 6 demonstrates isocratic separations of aromatic hydrocarbons at various flow-rates. The total flow-rate of the mobile phase was varied by the downstream constant-flow pump. The flow-rate of the upstream constant-flow pump should be changed so as to keep the mobile phase composition constant. The baselines and peak shapes of the chromatograms were as good as those obtained with the one-pump system, indicating that the two solutions were mixed well. The reproducibility of the retention volume of each solute was good; the relative standard deviation of the retention volume of each solute for five measurements was 0.6–0.8%.

Column efficiencies obtained with this flow system are shown in Fig. 7. The dependence of the height equivalent to a theoretical plate (HETP) on the linear velocity of the mobile phase is small, which is characteristic of a fused silica flexible micro column[6]. The operating conditions are the same as those in Fig. 6.

Fig. 8 shows isocratic and stepwise gradient separations of polynuclear aromatic hydrocarbons on an ODS column. In the latter instance the analysis time is reduced and the resolution of 1,3,5-triphenylbenzene and 3,4-benzopyrene is increased. Gradient elution was attained by changing the flow-rate of the upstream constant-flow pump containing water.

Stepwise gradient separations of phthalates and typical components of a cold medicine are shown in Figs. 9 and 10, respectively. The relative standard deviation of the retention of phthalates for ten measurements (Fig. 9) was a few percent. In both

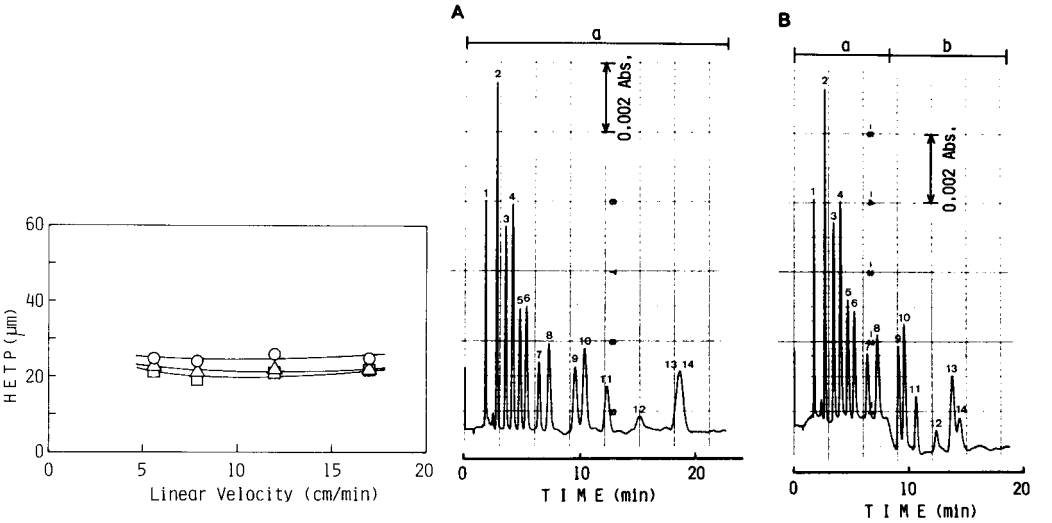

Fig. 7. Relationship between linear velocity and HETP. Operating conditions as in Fig. 6. Samples: ○, naphthalene; △, anthacene; and □, pyrene.

Fig. 8. Isocratic and stepwise gradient separations of polynuclear aromatic hydrocarbons. Column: 10.1 cm × 0.35 mm I.D., packed with SC-01. Mobile phases: (A) acetonitrile–water (64:36) (a); (B) acetonitrile–water [64:36 (a) + 70:30 (b)]. Flow-rate: 8.3 μl/min. Samples: 1 = 1.0% (w/w) of benzene; 2 = 0.097% of naphthalene; 3 = 0.019% of biphenyl; 4 = 0.022% of fluorene; 5 = 0.0076% of phenanthrene; 6 = 0.0058% of anthracene; 7 = 0.017% of fluoranthene; 8 = 0.020% of pyrene; 9 = 0.020% of *p*-terphenyl; 10 = 0.0074% of chrysene; 11 = 0.0061% of 9-phenylanthracene; 12 = 0.0025% of perylene; 13 = 0.011% of 1,3,5-triphenylbenzene; 14 = 0.0058% of 3,4-benzopyrene. Sample size: 0.02 μl. Wavelength of UV detection: 254 nm. Temperature: 32°C.

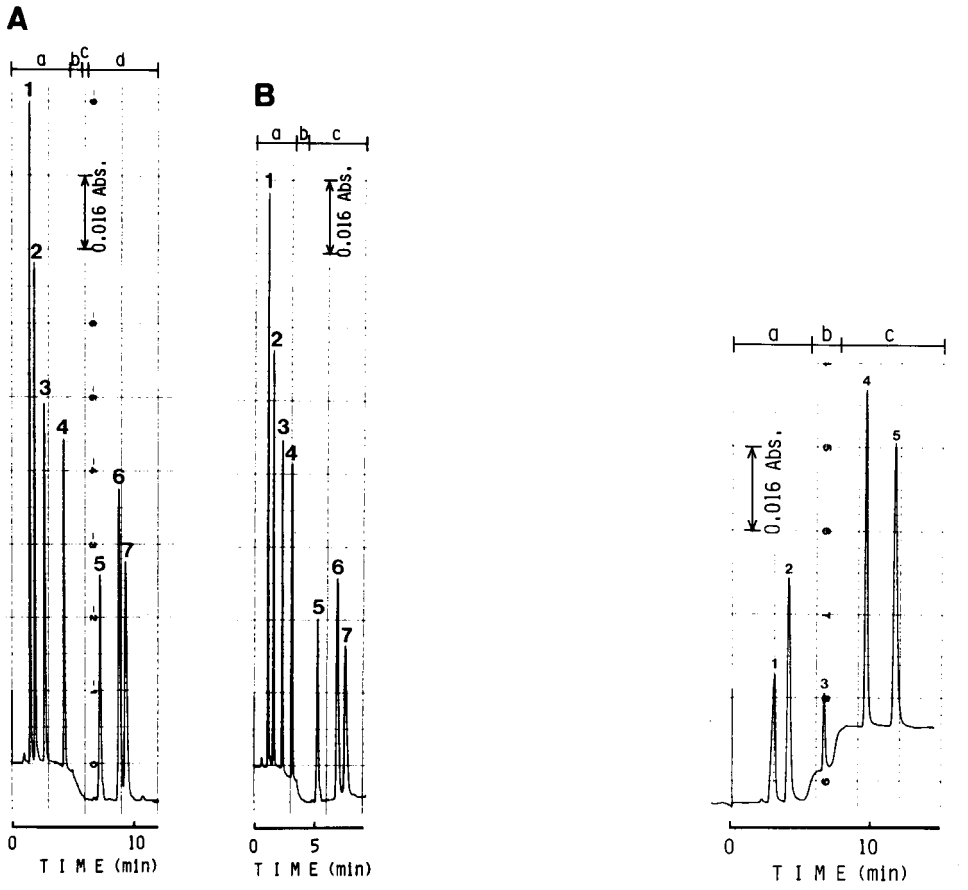

Fig. 9. Stepwise gradient separations of phthalates. Column: 10.3 cm × 0.35 mm I.D., packed with SC-01. Mobile phases: (A) acetonitrile–water [64:36 (a) + 73:27 (b) + 82:18 (c) + 91:9 (d)]; (B) acetonitrile–water [64:36 (a) + 76:24 (b) + 88:12 (c)]. Flow-rates: (A) 5.6 μl/min; (B) 8.3 μl/min. Samples: 1 = 0.81% (w/w) of dimethyl; 2 = 0.76% of diethyl; 3 = 0.74% of diisopropyl; 4 = 0.78% of di-*n*-butyl; 5 = 1.09% of diheptyl; 6 = 1.38% of di-2-ethylhexyl; 7 = 1.46% of dinonyl phthalate. Sample size: 0.02 μl. Wavelength of UV detection: 235 nm. Temperature: 29°C.

Fig. 10. Stepwise gradient separation of typical components in a cold medicine. Column: 10.1 cm × 0.35 mm I.D., packed with SC-01. Mobile phases: acetonitrile–water [7.5:92.5 (a) + 15:85 (b) + 30:70 (c)], each containing 0.05% (w/v) of ammonium carbonate. Flow-rate: 4.2 μl/min. Samples: 1 = 0.15% (w/v) of barbital; 2 = 0.14% of acetoaminophenol; 3 = 0.14% of caffeine; 4 = 0.14% of phenacetin; 5 = 0.13% of *p*-chloroacetanilide. Sample size: 0.02 μl. Wavelength of UV detection: 240 nm. Temperature: 26°C.

instance a pressure of *ca.* 50 atm was applied by the constant-pressure pump. Stepwise gradient elutions are satisfactorily carried out with this new flow system as shown in Fig. 8B.

CONCLUSION

The new flow system employing three pumps permitted both stepwise gradient

elution and isocratic elution *in situ*, and it should be possible to perform continuous or linear gradient elution if a constant-flow pump altering the flow-rate continuously is developed for micro-HPLC.

REFERENCES

1 D. Ishii, K. Asai, K. Hibi, T. Jonokuchi and M. Nagaya, *J. Chromatogr.*, 144 (1977) 157.
2 T. Takeuchi and D. Ishii, *J. Chromatogr.*, 218 (1981) 199.
3 T. Takeuchi, Y. Watanabe, K. Matsuoka and D. Ishii, *J. Chromatogr.*, 216 (1981) 153.
4 T. Takeuchi, Y. Watanabe and D. Ishii, *J. High Resolut. Chromatogr. Chromatogr. Commun.*, 4 (1981) 300.
5 T. Takeuchi and D. Ishii, *J. High Resolut. Chromatogr. Chromatogr. Commun.*, 4 (1981) 469.
6 T. Takeuchi and D. Ishii, *J. Chromatogr.*, 213 (1981) 25.

Journal of Chromatography, 239 (1982) 643–649
Elsevier Scientific Publishing Company, Amsterdam — Printed in The Netherlands

CHROM. 14,626

A NEW CENTRIFUGAL COUNTER-CURRENT CHROMATOGRAPH AND ITS APPLICATION

WATARU MURAYAMA*, TETSUYA KOBAYASHI, YASUTAKA KOSUGE, HIDEKI YANO*, YOSHIAKI NUNOGAKI and KANICHI NUNOGAKI
Sanki Engineering, Ltd., 2-16-10 Imazato, Nagaokakyo, Kyoto (Japan)

SUMMARY

A centrifugal counter-current chromatograph with a rotary seal joint has been developed. The capability of the apparatus was demonstrated on separations of a set of dinitrophenyl amino acids and application examples of the method to the separation of some biological materials are presented.

INTRODUCTION

Counter-current chromatography (CCC) is defined as liquid–liquid chromatography without solid support and it has many advantages in the separation and purification of a wide variety of compounds. The classical counter-current distribution method using Craig's apparatus is very complicated to operate and types of continuous-flow counter-current chromatography such as droplet counter-current chromatography (DCCC)[1] and coil planet centrifugation (CPC)[2–6] have been developed.

We have developed another kind of centrifugal partition chromatography which employs a rotary seal joint (CCCC–RJ). The apparatus is of simple construction and is suitable for the fractionation of materials on a preparative scale in short reaction times.

The key point of the apparatus is the construction of the rotary seal joint which enables the solvents to be pumped into the rotating separation columns in the centrifuge at a continuous high pressure.

Partition efficiency of CCCC–RJ has been tested using some 2,4-dinitrophenyl (DNP) amino acids as test samples, and some examples of its application in the separation of some biological materials are reported.

APPARATUS

The principle of the separation in CCCC-RJ is similar to that for DCCC and is shown in Fig. 1. The separation columns, arranged on the rotor of a centrifuge with

* Present address; Central Research Laboratories, Unichica Co. Ltd., 23 Kozakura, Uji, Kyoto, Japan.

0021-9673/82/0000–0000/$02.75

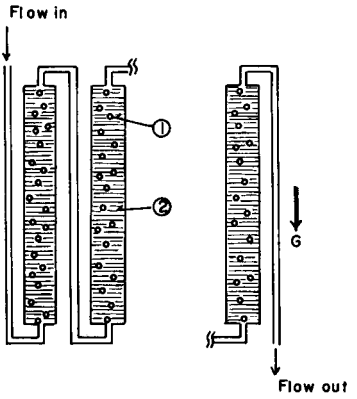

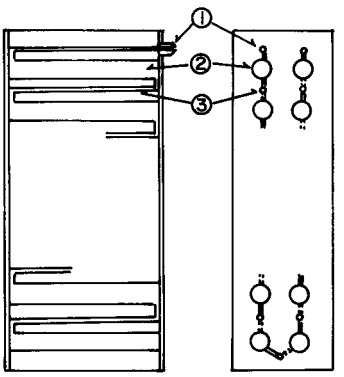

Fig. 1. Separation columns: 1 = mobile phase; 2 = stationary phase.

Fig. 2. Separation column cartridge: 1 = connectors for solvent inlet and outlet; 2 = separation columns; 3 = connecting tubes.

their longitudinal axes parallel to the direction of the centrifugal force, are connected to each other by fine tubes. The separation columns are filled with stationary liquid phase (lower phase in the case shown in Fig. 1) prior to the experiment. While the rotor of the centrifuge is in motion, the mobile liquid phase (upper phase in this case) is pumped into the separation columns and bubbles up through the stationary phase in the columns by the action of centrifugal force.

The separation columns and connecting tubes are actually arranged in the form of column cartridges (Fig. 2). The polytrifluoroethylene resin block (150 × 40 × 40 mm) has drilled in it fifty holes for the separation columns (40 × 3 mm)

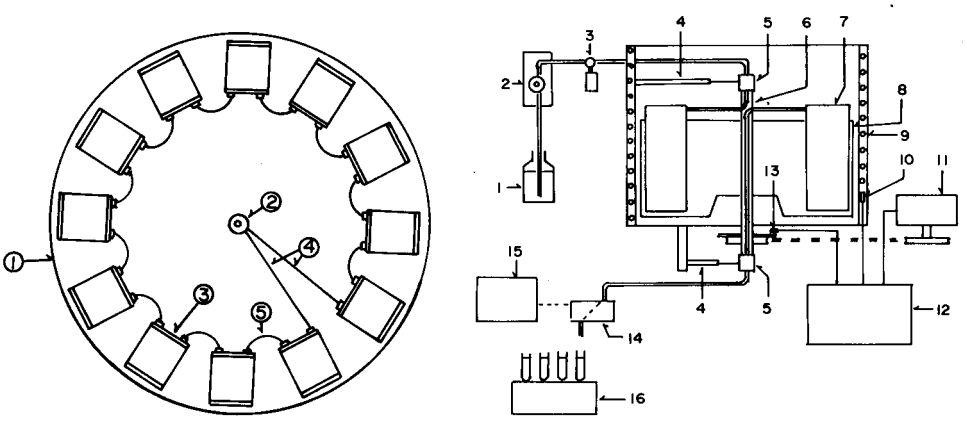

Fig. 3. Rotor of the centrifugal partition chromatograph: 1 = rotor of the centrifuge; 2 = rotary seal joint; 3 = column cartridge; 4 = connecting tubes between rotary seal joint and column cartridges; 5 = connecting tubes between column cartridges.

Fig. 4. Centrifugal partition chromatograph system: 1 = Solvent reservoir; 2 = high-pressure constant flow pump; 3 = sample injector; 4 = rotary seal joint stopper; 5 = rotary seal joint; 6 = rotor axis; 7 = column cartridge; 8 = rotor; 9 = heater and cooler; 10 = temperature-control sensor; 11 = motor; 12 = temperature and rotational-speed control unit; 13 = rotational-speed control sensor; 14 = monitor; 15 = recorder; 16 = fraction collector.

alternating with fifty holes for the connecting tubes (1 mm diameter). The holes are connected by fine troughs on both sides of the block, and are sealed by polytetrafluoroethylene sheets which are pressed tightly on both sides by metal plates and screws. The inlet and outlet for the solvents are attached to one end of the column cartridge. The inner volume for each column cartridge is *ca.* 15 ml.

Twelve column cartridges are arranged around the rotor of the centrifuge and are connected to each other by fine tubes as shown in Fig. 3. Solvents are pumped into the column cartridges through the rotary seal joint attached at the upper end of the rotor axis of the centrifuge, and collected through the rotary seal joint at the lower end. A clockwise flow of the mobile phase corresponds to the cases where a heavier phase of the two-phase solvent system is used as the stationary phase, and a counter-clockwise flow corresponds to the opposite case.

Fig. 4 shows the complete chromatographic system of the chromatograph; a photograph of the system is shown in Fig. 5.

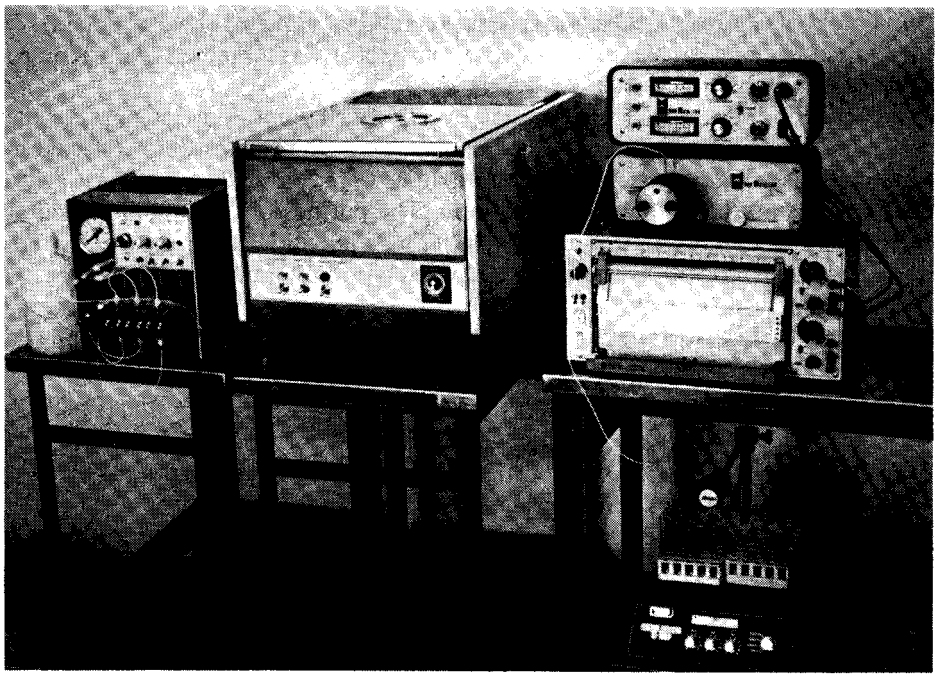

Fig. 5. Photograph of the centrifugal counter-current chromatograph system.

The rotary seal joint consists of two discs, one of which is fixed and the other which rotates with the axis of the centrifuge. The two discs are pressed against each other by a spring so that they provide a leak-free seal under a high-pressure pumping of the solvents into the separation column cartridges. The faces of the two discs, one of which is made from graphite and the other from ceramics, are highly polished. This rotary seal joint enables the apparatus to be operated continuously under high pressures for long periods of time.

TABLE I

RESOLUTION OF DNP-AMINO ACIDS

Flow-rate (ml/min)	*Resolution ($R_{s_{i,j}}$)*		
	$R_{s_{1,2}}$	$R_{s_{2,3}}$	$R_{s_{3,4}}$
4.0	2.8	2.0	2.5
1.9	3.8	2.3	2.6
1.2	4.1	2.3	3.1
0.50	4.1	2.2	2.9
0.28	4.2	2.3	–

EXPERIMENTAL

The solvents used for the preparation of the two phase partitioning solutions are of reagent grade. DNP-amino acids were purchased from Sigma (St. Louis, MO, U.S.A.), fatty acids from Tokyo Kasei and sugars from Nakarai (Kyoto, Japan). A crude extract of *Bepleurum falcatum* (Mishima Saiko) was obtained from Kotaro Shoten (Osaka, Japan).

The DNP-amino acids were detected by a flow-cell monitor at 350 nm. For the experiments involving separation of sugars or saponins the eluates were collected in 1–5 ml fractions using a fraction collector; fractions were coloured by sulphuric acid–phenol to measure the absorbance at 490 nm. The purities of the saponin fraction were checked by thin-layer chromatography (TLC) on silica gel. Fatty acids were detected gravimetrically and were checked by gas chromatography.

RESULTS AND DISCUSSION

Resolution of the centrifugal counter-current chromatograph was tested by

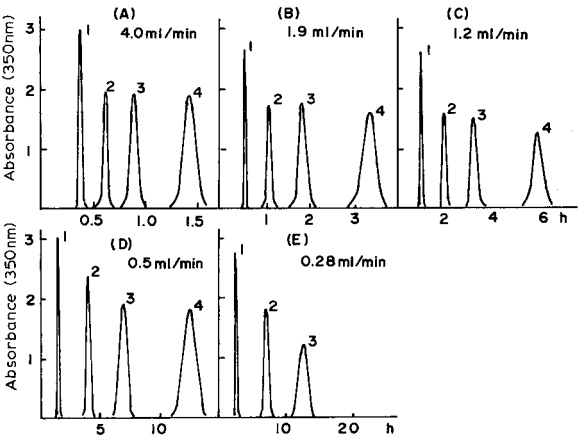

Fig. 6. Separation of DNP-amino acids. Solvent system: chloroform–0.1 *M* hydrochloric acid–acetic acid (2:1:2). Stationary phase: lower. Peaks: 1 = N^{δ}-DNP-L-Ornithine HCl, 4.0 mg, K = 50; 2 = DNP-L-Threonine, 4.0 mg, K = 2.0; 3 = N,N′-di-DNP-L-Cystine, 8.0 mg, K = 0.92; 4 = DNP-L-Proline, 12.0 mg, K = 0.54. Rotational speed, 700 rpm.

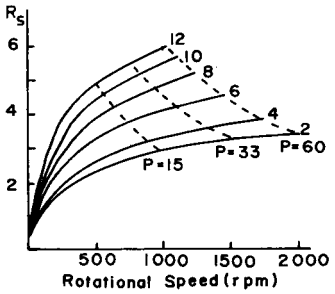

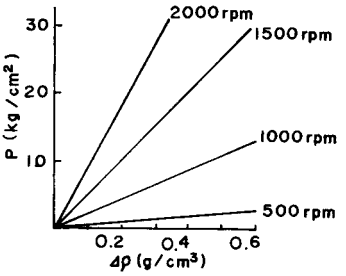

Fig. 7. Rotational speed *vs.* resolution (R_s). The numbers denoted at solid lines indicate the numbers of column cartridges used, and the values denoted at dotted lines indicate the pumping pressure.

Fig. 8. Density difference between upper and lower phase *vs.* pumping pressure.

separation of mixed DNP-amino acids (N^{δ}-DNP-L-ornithine, N,N′-di-DNP-L-cystine, DNP-L-threonine and DNP-L-proline). The solvent system reported by Tanimura *et al.*[1] was used. The rotational speed of the centrifuge was 700 rpm and the flow-rate of the mobile phase varied from 0.28 to 4.0 ml/min. The resultant chromatogram is shown in Fig. 6. Resolution (R_s) between two adjacent peaks, defined by eqn. 1, were calculated from the chromatogram and are shown in Table I.

$$R_s = \frac{L_{ij}}{\frac{1}{2}(W_i + W_j)} \tag{1}$$

where L_{ij} = peak to peak distance between component i and component j, W_i = peak width of component i, and W_j = peak width of component j.

No significant changes were observed in resolution when the flow-rate of the mobile phase was increased to 1.9 ml/min, and slight decreases in R_s values was observed when the flow-rate was raised to 4.0 ml/min.

These results indicate that the "true" flow-rate of the bubbles of the mobile phase through the stationary phase is determined by the strength of the applied centrifugal force. As long as the pumping rate (the apparent flow-rate) does not exceed the "true" flow-rate, it does not effect the resolution of the peaks. This means that the separation can be completed in a short time provided a sufficient centrifugal force is applied.

Resolution between DNP-L-threonine and N,N′-di-DNP-L-cystine were measured at a constant pumping rate by varying the speed of rotation of the centrifuge and the numbers of column cartridges used (Fig. 7). The results show that a high rotational speed gives better peak resolution.

The pumping pressure necessary for injecting the mobile phase into the separation columns during the centrifuge run is proportional to the differences in density between the upper and lower phases of the partitioning solvent system, and to the strength of the centrifugal force applied. The relationship between the density difference ($\Delta\varrho$) of the two phases in the solvent system and the pumping pressure is shown in Fig. 8. For density differences of 0.10–0.25 the solvent system used was *n*-butanol–ethanol–water and for differences of 0.25–0.60 chloroform–methanol–water

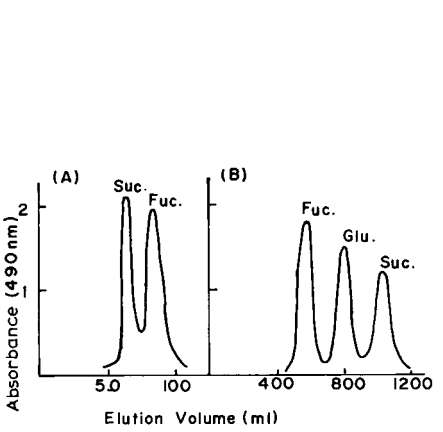

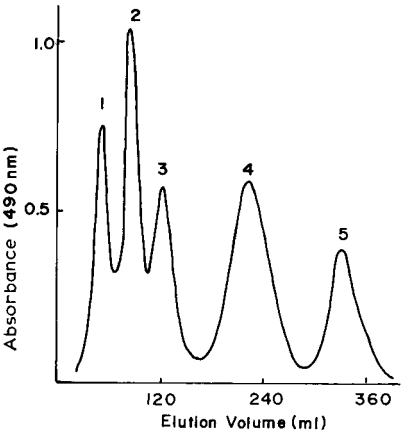

Fig. 9. Separation of sugars. Solvent system: *n*-butanol–ethanol–water (10:2.5:10). Sample: 100 mg of each sugar. A, Stationary phase = upper, flow-rate = 1.0 ml/min. B, Stationary phase = lower, flow-rate = 4.0 ml/min. Rotational speed, 1500 rpm.

Fig. 10. Separation of saponins from extracts of *Bepleurum falcatum* (Mishima Saiko). Solvent system: chloroform–methanol–water–benzene–ethyl acetate (45:60:40:2:3). Stationary phase = lower. Sample = 20 mg. Flow-rate = 2.0 ml/min. Rotational speed = 1000 rpm.

was used. Because of instrumental limitations, all the experiments were carried out at a rotational speed of the centrifuge at which the pumping pressure did not exceed 60 kg/cm^2. It is important to select the appropriate rotational speed for the solvent systems employed when using the CCCC–RJ system.

The separation of a mixture of sugars was performed using an *n*-butanol–ethanol–water (10:2.5:10) solvent system (Fig. 9). Sugars have a tendency to partition into the aqueous layer of a solvent mixture. When the aqueous phase was used as the mobile phase, two components, sucrose and fucose, were separated, while in the opposite case three components, fucose, glucose and sucrose, were resolved.

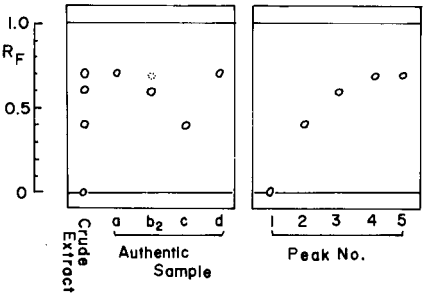

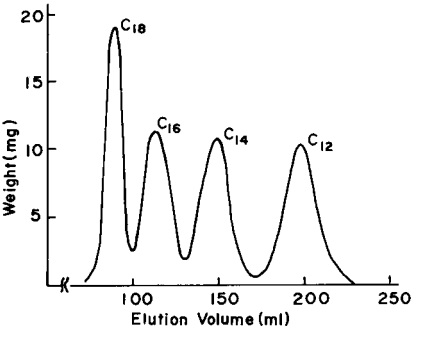

Fig. 11. TLC of peak fractions in Fig. 10. Elution: chloroform–methanol–water = (30:10:1). Detection: Sulphuric acid.

Fig. 12. Separation of saturated fatty acids. Solvent system: *n*-heptane–methanol–acetic acid (1:1:1). Sample: C_{18}, stearic acid; C_{16}, palmitic acid; C_{14}, myristic acid; C_{12}, lauric acid. Flow-rate = 1.0 ml/min. Rotational speed = 1000 rpm.

Separation of saponins from *Bepleurum falcatum* (Mishima saiko) have been reported by Ogiwara *et al.*[7] using DCCC. A crude extract from the root of Mishima Saiko, which was known to contain Saiko saponins a, b_2, c and d, was fractionated using CCCC–RJ with the same solvent system as reported. Four saponin components were completely resolved within 3 h (Fig. 10) and were identified by TLC (Fig. 11).

Separation of saturated fatty acids was also demonstrated using a non-aqueous two-phase solvent (*n*-heptane–acetic acid–methanol, 1:1:1) (Fig. 12).

It has been reported that in DCCC there are limitations on the solvent systems that can form stable droplets during the experiments[8]. In CCCC–RJ separations have been achieved when sufficient amounts of the stationary phase solution (usually 70–80% of the column volume) were retained in the column cartridges while the mobile phase solution was continuously eluted through the columns. This state of dynamic equilibrium could be achieved by selection of suitable speeds for rotation of the centrifuge and for pumping; we have encountered few cases which do not have a solvent system suitable for the present method.

Centrifugal counter-current chromatography may have many uses in the fields of normal- or reversed-phase partition chromatography. Improvements of the apparatus are now in progress and results of its application will be published later.

REFERENCES

1 T. Tanimura, J. J. Pisano, Y. Ito and R. L. Bowman, *Science*, 169 (1970) 54.
2 Y. Ito, M. A. Weinstein, I. Aoki, R. Harada, E. Kimura and K. Nunogaki, *Nature (London)*, 212 (1966) 985.
3 Y. Ito, I. Aoki and E. Kimura, *Anal. Chem.*, 41 (1969) 1579.
4 Y. Ito and R. L. Bowman, *J. Chromatogr. Sci.*, 8 (1970) 315.
5 Y. Ito, *Protein, Nucl. Acid Enzyme*, 26 (1981) 1020.
6 Y. Ito, *J. Biochem. Biophys. Methods*, 5 (1981) 105.
7 Y. Ogihara, O. Inoue, H. Otsuka, K.-I. Kawai, T. Tanimura and S. Shibata, *J. Chromatogr.*, 128 (1976) 218.
8 K. Hostettmann, M. Hostettmann-Kaldas and K. Nakanishi, *J. Chromatogr.*, 170 (1979) 355.

Journal of Chromatography, 239 (1982) 651–659
Elsevier Scientific Publishing Company, Amsterdam — Printed in The Netherlands

CHROM. 14,628

HIGH-SPEED HIGH-RESOLUTION GEL PERMEATION CHROMATOGRAPHY OF SMALL MOLECULES AND OLIGOMERS

SUSUMU ISHIGURO*, YOSHINORI INOUE and TADAYUKI HOSOGANE
Instruments Research Laboratory, Showa Denko K.K., 24–25, Tamagawa 2-chome, Ohta-ku, Tokyo 146 (Japan)

SUMMARY

High-speed high-resolution gel permeation chromatography of small molecules and oligomers was performed, using Shodex GPC KF-800 series columns packed with porous styrene–divinylbenzene copolymers of particle size 4–8 μm. The number of theoretical plates of 30-cm columns ranged from 19,800 to 23,000 when propylbenzene was used as a test sample with a mobile phase velocity of 0.09 cm/sec. The characteristics of the columns and some applications to small molecules and oligomers are reported.

INTRODUCTION

Gel permeation chromatography (GPC) employing organic solvents introduced by Moore[9] in 1964, is now applied not only to determine the molecular-weight distribution of polymers but also to separate small molecules and oligomers[1,2].

When measuring low-molecular-weight compounds, a complete separation of the individual components is often desired. It is, however, difficult with conventional long GPC columns to attain satisfactory separations in short periods of time[3]. With the development of microparticulate columns for liquid–solid and bonded-phase chromatography in the early 1970s, microparticles have also been available for GPC. However, only one report[4] has so far been published which uses packing materials of 5 μm in diameter for the separation of small molecules and oligomers. Although many other reports have been published, they refer only to the use of porous silica[5] of 10 μm in diameter and cross-linked polystyrene gel[6].

In GPC, separation is performed in the distribution constant range 0–1. The limited peak capacity n is expressed as in the following equation[7]:

$$n = (1 + 0.2N^{\frac{1}{2}}) \quad (1)$$

where N = number of theoretical plates. A column possessing a large number of theoretical plates is necessary to attain a large peak capacity in a short time. A large number of theoretical plates can be obtained by packing a column with gel of a small diameter.

0021-9673/82/0000–0000/$02.75

Showa Denko K.K. (Tokyo, Japan) recently made available on a commercial basis high-performance GPC columns packed with styrene–divinylbenzene copolymer gel of 4–8 μm in diameter (Shodex GPC KF-800-series high-performance columns). This paper reports their characteristics and their applications to the separation of small molecules and oligomers.

EXPERIMENTAL

Apparatus

The liquid chromatograph employed was assembled in the authors' laboratory, and consisted of a high-pressure pump (Milton-Roy), high-pressure sample valves (Rheodyne, Model 7125 with 100-μl sample loop), a UV detector (JASCO, UVIDEC-100) and a refractive index detector (Showa Denko, Shodex RI SE-11).

Columns

GPC was performed, using Shodex GPC KF-800-series columns packed with 4–8-μm particle size polystyrene gels of four different pore sizes. Technical data for the columns are given in Table I. The columns are made of seamless 316 stainless-steel tubing of 30 cm length, 10 mm O.D. and 8 mm I.D. Both ends of the column are packed with stainless steel frits of mean porosity 2 μm manufactured by Shoketsu Kinzoku, Japan, to keep the packing material firmly in place.

Reagents

Reagent-grade tetrahydrofuran (THF) (Wako, Osaka, Japan) was used as mobile phase. Standard polystyrene (Toyo Soda, Tokyo, Japan) shown in Table II was also used.

Calculations

The number of theoretical plates (N) was calculated according to the following equation:

$$N = 5.54\,(t_R/W_{\frac{1}{2}})^2 \qquad (2)$$

where t_R = retention time and $W_{\frac{1}{2}}$ = peak width at half-height.

The distribution of V_0, V_i and V_s was obtained according to the method developed by Pfannkoch *et al.*[8]: thus, the sum of the interstitial volume (V_0), pore volume (V_i) and support volume (V_s) is equal to the total internal column volume (V_c).

TABLE I

CHARACTERISTICS OF PS GEL

Column	*Particle size (μm)*	*Excluded mol. wt.*	*Linear fraction range*
Shodex GPC			
KF-801	6 ± 2	$1.5 \cdot 10^3$	50–1500
KF-802	6 ± 2	$5 \cdot 10^3$	100–5000
KF-802.5	6 ± 2	$2 \cdot 10^4$	100–20,000
KF-803	6 ± 2	$7 \cdot 10^4$	100–70,000

TABLE II

STANDARD POLYSTYRENE

Grade	*Mean molecular weight*	M_w/M_n	*Lot No.*
F-40	422,000	1.04	TS-6
F-10	107,000	1.01	TS-20
F-4	42,800	1.01	TS-19
F-2	16,700	1.02	TS-18
A-5000	6200	1.04	TS-24
A-2500	2800	1.05	TS-23
A-1000	890	*ca.* 1.1	TS-25
A-500	474	*ca.* 1.2	TS-26
A-300	370	*ca.* 1.2	TS-28

$$V_c = V_0 + V_i + V_s \tag{3}$$

The fractional pore volume (E_i), fractional void volume (E_0) and fractional support volume (E_s) were calculated according to the following equations:

$$E_i = V_i/V_c \tag{4}$$
$$E_0 = V_0/C_c \tag{5}$$
$$E_s = V_s/V_c \tag{6}$$

The following equations were used to calculate the fractional pore (E_{pv}) and fractional solid volumes (E_{sv}) of packing material.

$$E_{pv} = V_i/(V_i + V_s) \tag{7}$$
$$E_{sv} = V_s/(V_i + V_s) \tag{8}$$

RESULTS AND DISCUSSION

Characteristics of column

Fig. 1 shows the molecular weight calibration curves for standard polystyrene obtained with Shodex GPC KF-801, -802, -802.5 and -803, each packed with polystyrene gel of a different pore size. A column packed with polystyrene gel of a suitable pore size can be selected according to the molecular weight of the test sample. All curves are almost linear. Polystyrene gel is different from packing materials of the porous silica group, being is characterized by pores of a suitable sizes for separating organic compounds with lower molecular weights. It excels particularly in the separation of substances with molecular weights of 1000 or less.

Table III indicates the distribution of V_0, V_i and V_s in the four columns. V_0 is nearly constant regardless of the pore size, accounting for 35–36% of V_c. The E_0 values of columns packed with spherical silica gel[8] are reported to range from 35 to 39% and that of Shodex GPC KF-800-series columns was close to the E_0 of columns packed with rigid silica. This signifies that polystyrene gel is properly packed in the Shodex columns. The effective pore volume for separation ranged from 31 to 44% of the total internal column volume. The percentage of the pore volume ($\%E_{pv}$) was in

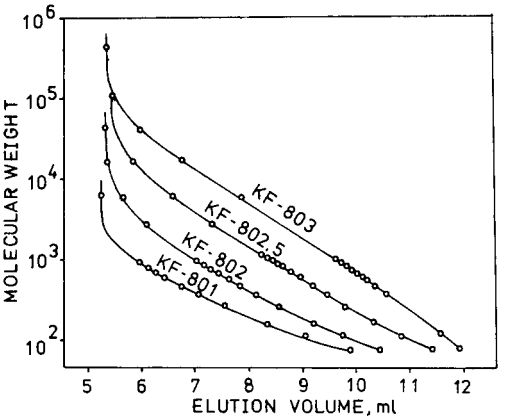

Fig. 1. Molecular weight calibration plots for Shodex GPC KF columns. Standard polystyrene; mobile phase, THF; 25°C; flow-rate, 1.0 ml/min; UV detector.

the range 48–69%. There was a tendency for the percentage to increase as the pore size becomes larger. The $\%E_{pv}$ of the Shodex columns, except for KF-803, was somewhat smaller than that of porous silica-packed columns. Although the $\%E_{pv}$ of polystyrene gel can be increased by polymerization formulation, the mechanical strength of the gel decreases with increasing $\%E_{pv}$ of polystyrene gel to such an extent that it cannot be used as the packing material for high-speed GPC.

The separation capacity of packed columns for GPC depends on the number of theoretical plates. A large number of theoretical plates can be obtained by using packing material of particle size 10 μm or less. Table IV gives the characteristics of the Shodex columns packed with polystyrene gel of 4–8 μm in particle size. The number of theoretical plates was measured at a flow-rate of 1 ml/min with propylbenzene used as a test sample and THF as the mobile phase. The guaranteed number of plates for Shodex GPC KF-800-series columns is 16,000 plates/30 cm. Kirkland and Antle[5] reported that a reduced plate height of a well made column does not exceed the range 2.0–3.5. Judging from his report, Shodex GPC KF-type columns can be recognized as being well made since their reduced plate heights are in the range 2.2–2.5.

Fig. 2 shows a plot of mobile phase velocity *vs.* the plate heights for three columns packed with Shodex GPC gels of different particle sizes. Benzene was used for measurement of the plate heights, and it was shown that the smaller the mean particle size, the lower the plate height, thereby enabling a high-performance column

TABLE III

DISTRIBUTION OF TOTAL INTERNAL COLUMN VOLUME AMONG INTERSTITIAL VOLUME (V_0), PORE VOLUME (V_i) AND SUPPORT VOLUME (V_s)

Column	V_i/V_0	V_0	V_i	V_s	E_0 (%)	E_i (%)	E_t (%)	E_{pv} (%)	E_{sv} (%)
KF-801	0.90	5.25	4.69	5.14	34.8	31.1	34.1	47.7	52.3
KF-802	0.99	5.29	5.22	4.57	35.1	34.6	30.3	53.3	46.7
KF-802.5	0.99	5.44	5.40	4.27	36.1	35.8	28.1	56.0	44.0
KF-803	1.25	5.33	6.68	3.07	35.3	44.3	20.4	68.5	31.5

TABLE IV

CHROMATOGRAPHIC EFFICIENCY OF COLUMN

Mobile phase, tetrahydrofuran; 24°C; 1.0 ml/min.

Column	*Pressure drop (kg/cm²)*	*Plate count (propylbenzene)*	*H (cm) (propylbenzene)*	*h* (H/d_p)
KF-801	21	23,000	0.00130	2.2
KF-802	17	21,100	0.00142	2.4
KF-802.5	15	19,800	0.00151	2.5
KF-803	15	21,100	0.00141	2.4

to be obtained. The minimum plate height can be observed for each curve and that for curve C occurs at a higher point on the mobile phase velocity axis than those for the other curves.

Fig. 3 shows the relationship of the plate heights and mobile phase velocity measured with four test samples of different molecular weights. The higher the molecular weight, the further down the mobile phase velocity axis the minimum plate height moves. Thus, when benzene (molecular weight 78) was used as a test sample, the minimum plate height was obtained at a velocity of 0.13 cm/sec; for dimethyl phthalate (DMP) (194), it was 0.065 cm/sec, with dibutyl phthalate (DBP) (278), 0.05 cm/sec and with dioctyl phthalate (DOP) (309), it was 0.04 cm/sec. Columns packed with polystyrene gel are usually used with a flow-rate of 1 ml/min. The velocity at which the minimum plate height was obtained when benzene was used as a test sample was 0.13 cm/sec, which corresponds to a flow-rate of 1.4 ml/min. Use of Shodex GPC KF-802 with a flow-rate of 1 ml/min (corresponding to a velocity of

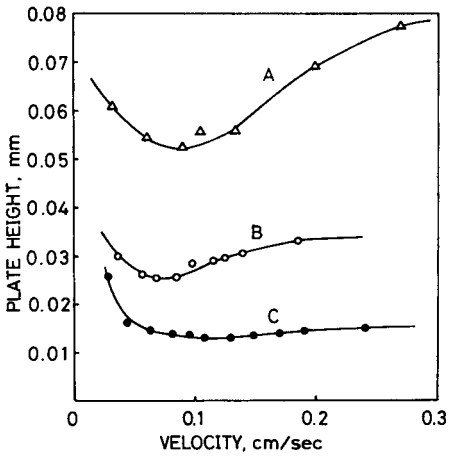

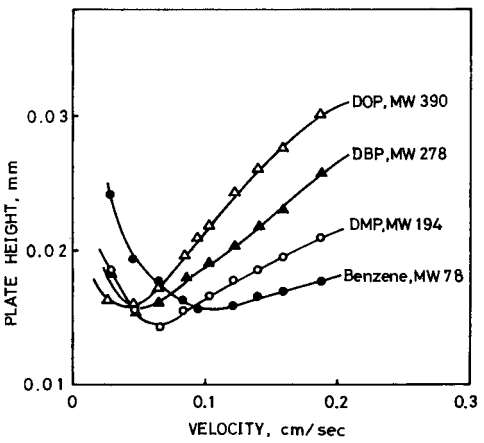

Fig. 2. Effect of particle size (d_p) of Shodex GPC gel on column efficiency. Solute, benzene; mobile phase, THF; column dimensions 30 cm × 8 mm I.D.; (A) d_p = 14–18 μm; (B) d_p = 8–12 μm; (C) d_p = 4–8 μm.

Fig. 3. Effect of velocity on plate height (H) for different molecular weight solutes. Column, Shodex GPC KF-802; mobile phase, THF; 24°C; detection UV: sample size, 10 μl.

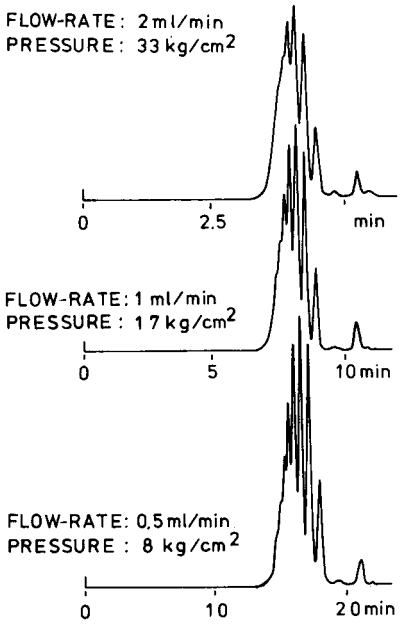

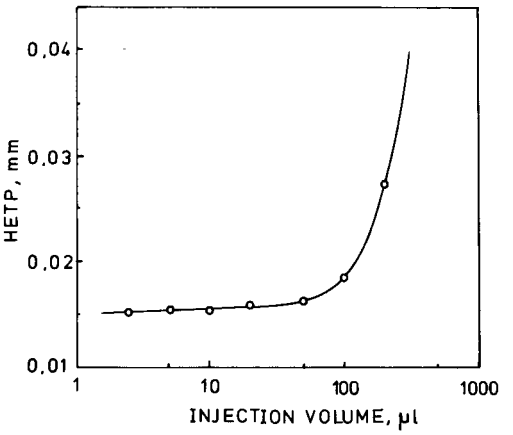

Fig. 4. Effect of flow-rate on elution patterns of polystyrene oligomers. Column: Shodex GPC KF-802, 30 cm × 8 mm I.D.; mobile phase, THF; detector, UV, 0.32 A.U.F.S. at 254 nm; sample size, 20 µl; sample, 0.5% MW 474 polystyrene; temperature, 25°C.

Fig. 5. Effect of injection volume on plate height (H). Column, Shodex GPC KF-803, 30 cm × 8 mm I.D.; mobile phase, THF; flow-rate, 1.0 ml/min; sample, benzene, 0.05 mg.

0.09 cm/sec), slightly increases the plate height for compounds of low molecular weight (such as benzene which elutes at the total permeation volume). Separation of compounds which are eluted in the vicinity of the exclusion volume, however, is more difficult than that of material which is eluted in the vicinity of the total permeation volume. A flow rate of 1 ml/min, therefore, appears appropriate for columns packed with polystyrene gel of particle size 4–8 µm in view of the relationship of the analytical time and resolution.

Fig. 4 shows chromatograms of styrene oligomers with an average molecular weight of 474. These were obtained with flow rates of 0.5, 1 and 2 ml/min.

Fig. 5 shows the effect of an injection volume of a test sample on the plate height, indicating that the volume of 50 µl maximum does not produce any effect.

APPLICATIONS

For the separation of small molecules or oligomers, GPC is advantageous in the following respects when compared with other methods of adsorption or partition chromatography. First, as long as it is soluble in the eluent, any test sample can be injected and the setting of the analytical conditions is easy. Secondly, all the components of the test sample are eluted within a certain time without adsorption onto

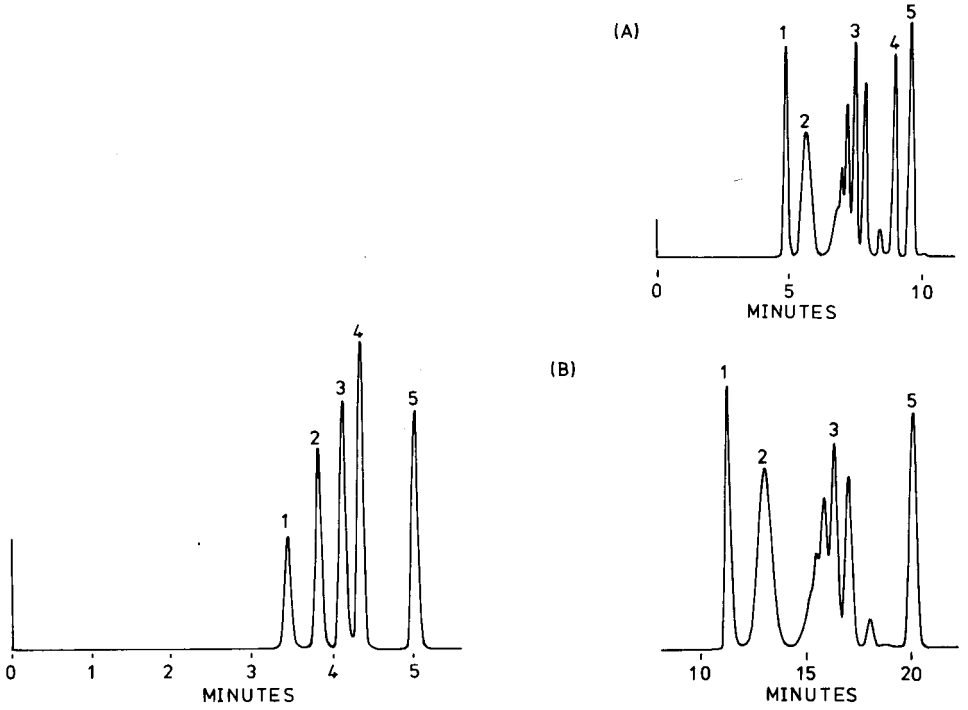

Fig. 6. Separation of mixture of DOP, DBP, DEP, DMP and benzene. Peaks: 1 = DOP, 2 = DBP, 3 = DEP, 4 = DMP, 5 = benzene; column, Shodex GPC KF-801, 30 cm × 8 mm I.D.; sample, 0.07% DOP, DBP, DEP, DMP and 0.35% benzene in THF; sample size, 10 μl; mobile phase, THF; flow-rate, 1.95 ml/min; pressure, 40 kg/cm^2.

Fig. 7. Comparison of analysis times between 4–8-μm (A) and 8–12-μm (B) PS gel-packed columns. Peaks: 1 = polystyrene MW 42,800, 2 = polystyrene MW 2,800, 3 = polystyrene MW 370, 4 = *n*-propylbenzene; 5 = benzene. (A) Column, Shodex GPC KF-802, 30 cm × 8 mm I.D.; mobile phase, THF; flow-rate, 1.1 ml/min. (B) Column, Shodex GPC A-802, 50 cm × 8 mm I.D.; mobile phase, THF; flow-rate, 1.0 ml/min.

the packing materials. The third advantage is that the molecular size of the test sample can be estimated from the elution volume.

Fig. 6 shows the separation of a mixture of DOP, DBP, diethyl phthalate (DEP), DMP and benzene. These phthalic esters are often used as plasticizers. The separation was performed at a flow rate of 2 ml/min with Shodex GPC KF-801 (30 cm × 8 mm I.D.). The esters and benzene were separated satisfactorily within 5 min.

Fig. 7 shows a comparison of the separation capacity of Shodex GPC KF-802 (30 cm × 8 mm I.D.) packed with polystyrene gel of particle size 4–8 μm with that of conventional Shodex GPC A-802 (50 cm × 8 mm I.D.) packed with polystyrene gel of particle size 8–12 μm. A mixture of standard polystyrene and benzene was used for the comparison, in which KF-802 completed separation within 10 min and A-802 within 20. KF-802 packed with polystyrene gel of particle size 4–8 μm separates twice as fast as A-802 packed with particle sizes of 10 μm yet attains the same resolution.

A satisfactory separation of oligomers over a short period of time is not easy to

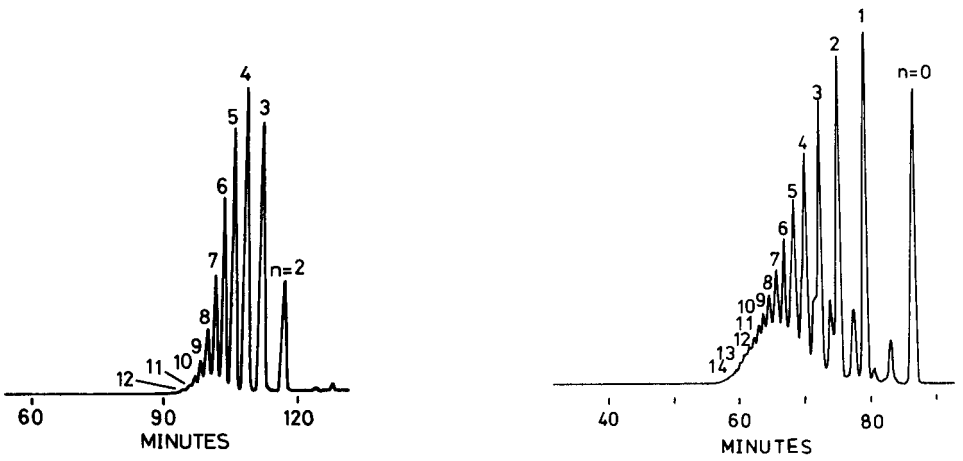

Fig. 8. Separation of polystyrene oligomers. Column, Shodex GPC KF-802.5, 4 × (30 cm × 8 mm I.D.) + KF-802, 4 × (30 cm × 8 mm I.D.); mobile phase, THF; flow-rate, 0.6 ml/min; pressure, 73 kg/cm^2; sample, 0.5% polystyrene MW 474; sample size, 100 μl.

Fig. 9. Separation of epoxy oligomers. Column, Shodex GPC KF-803, 4 × (30 cm × 8 mm I.D.) + KF-802.5, 4 × (30 cm × 8 mm I.D.); mobile phase, THF; flow-rate, 0.96 ml/min; pressure, 104 kg/cm^2; detector, UV, 254 nm; sample, 0.5% Epikote 1001; sample size, 100 μl.

achieve with conventional columns. Extremely long columns or recycle systems[2] are therefore employed for the analyses of oligomers, and these require long separation times. However, columns packed with polystyrene gel of particle size 4–8 μm have enabled short-time analyses with high resolution to be achieved.

Fig. 8 shows the separation of standard polystyrene with a molecular weight of

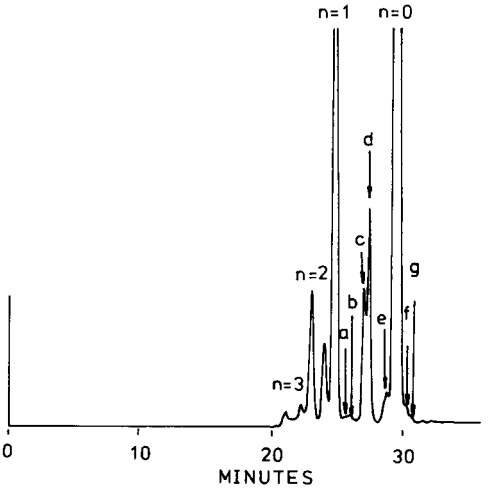

Fig. 10. Separation of epoxy oligomers. Column, Shodex GPC KF-801, 4 × (30 cm × 8 mm I.D.); sample, 0.5% Epikote 828 in THF; sample size, 15 μl; mobile phase, THF; flow-rate, 1.0 ml/min; pressure, 76 kg/cm^2.

474. The chromatogram was obtained with a flow-rate of 0.62 ml/min and four columns each of KF-802 and KF-802.5 connected in series. A low flow rate was effective in separating the test samples which were otherwise difficult to separate. The chromatogram shows good separation up to $n = 12$ within 2 h.

Fig. 9 shows a chromatogram of Epikote 1001, an epoxy oligomer. Four columns each of KF-803 and KF-802.5 were used in series and the flow rate was set to 0.96 ml/min. Peaks corresponding to the degree of polymerization ranging from $n = 0$ to $n = 14$ can be observed. Epoxy resin is used as coating material, as an electrical insulating material, as a constructional or building material and as an adhesive. When used as such, its molecular weight distribution as well as impurities formed by secondary reactions changes its performance and characteristics. Fig. 10 shows the separation of the impurities in epoxy resin. With a view to detecting traces of the impurities, the sensitivity of the dectector was amplified to such an extent that the peaks of the main components went off the recording range. Five impurities were detected between the $n = 0$ and $n = 1$ peaks. A few small peaks can also be observed at the bottom right of the $n = 0$ peak, indicating the inclusion of some other impurities. Use of high-resolution columns has made it possible to obtain peaks with narrow bases and has also improved the sensitivity of detection, thereby facilitating detection of trace impurities contained in epoxy resin.

CONCLUSION

High-speed and high-resolution GPC has become possible with the use of columns packed with polystyrene gel of particle size 4–8 μm. Small molecules or oligomers can be quickly separated with an optimum column selected from four columns each of which is packed with gel of a different pore size.

REFERENCES

1 J. M. Howard, III, *J. Chromatogr.*, 55 (1971) 15.
2 S. Nakamura, S. Ishiguro, T. Yamada and S. Moriizumi, *J. Chromatogr.*, 83 (1973) 297.
3 W. Heitz, B. Boemer and U. Ullner, *Makromol. Chem.*, 121 (1969) 102.
4 Y. Kato, S. Kido, H. Watanabe, M. Yamamoto and T. Hashimoto, *J. Appl. Polym. Sci.*, 19 (1975) 629.
5 J. J. Kirkland and P. E. Antle, *J. Chromatogr. Sci.*, 15 (1977) 137.
6 R. E. Majors and E. L. Johnson, *J. Chromatogr.*, 167 (1978) 17.
7 J. C. Giddings, *Anal. Chem.*, 39 (1967) 1027.
8 E. Pfannkoch, K. C. Lu, F. E. Regnier and H. G. Barth, *J. Chromatogr. Sci.*, 18 (1980) 430.
9 J. C. Moore, *J. Polymer Sci., Part A*, 2 (1964) 835.

Journal of Chromatography, 239 (1982) 661–670
Elsevier Scientific Publishing Company, Amsterdam — Printed in The Netherlands

CHROM. 14,664

SOLVENT DEPENDENCE OF GEL CHROMATOGRAPHIC RETENTION OF LOW-MOLECULAR-WEIGHT COMPOUNDS ON POLYSTYRENE–DIVINYLBENZENE GEL

KOICHI SAITOH*, ETSUO OZAKI and NOBUO SUZUKI
Department of Chemistry, Faculty of Science, Tohoku University, Sendai, Miyagi 980 (Japan)

SUMMARY

Chromatographic distribution coefficients, K_{av}, of small solute molecules on a polystyrene–divinylbenzene gel were measured with five different solvents, *viz.*, benzene, toluene, chlorobenzene, *o*-dichlorobenzene and tetrahydrofuran. Various types of compounds, such as alkanes, ethers, esters, ketones and alcohols, were selected as model solutes. The K_{av} values are well correlated with the molar volumes, V_m, of compounds within every homologous series. The retention sequence depends on the solvent used; in toluene it is alkanes < ethers < esters < ketones < alcohols, even if the molar volumes of the compounds are identical. The reverse sequence, except for alcohols, is observed in tetrahydrofuran, chlorobenzene and *o*-dichlorobenzene. In benzene, compounds other than alcohols share an identical relationship between K_{av} and log V_m. The solvent effects on the retention behaviour are well explained for the compounds other than alcohols by introducing a partition concept into gel chromatography.

INTRODUCTION

The solvent systems used in gel chromatography are relatively simple compared with those used in adsorption and partition chromatography. Binary or more complex solvent mixtures are requently required in the latter two techniques, whereas single component solvents are generally satisfactory in gel chromatography. This is one of the practical merits of gel chromatography as a laboratory technique with respect to the preparation, recovery and re-preparation of eluents. An important problem is the selection of a suitable solvent for the eluent.

Most reported gel chromatographic experiments involve the use of only a few limited kinds of solvents as eluents, in contrast to the variety of solvents used in adsorption and partition chromatographies. This suggests that little attention has been paid to solvent dependence in gel chromatography. However, the importance of the solvent effects in gel chromatography was pointed out in several studies with Sephadex LH-20 gel[1,2] and polystyrene–divinylbenzene gel[3,4].

There are two directions in which investigations of solvent effects in gel chromatography are focused. One is to find the optimum solvent with which pure steric

0021-9673/82/0000–0000/$02.75

exclusion process can be realized. When the chromatographic process is governed only by the steric exclusion effect, *i.e.*, free from any additional effects (so-called "secondary effects"), the determination of molecular weight or size of a sample can be made with accuracy. The other direction is to clarify the solvent dependence of additional effects concurring with the steric exclusion process, in order to utilize these effects actively to improve the resolution of the compounds to be separated. With much attention to both of these aspects, we have made systematic investigations of solvent dependence in the gel chromatographic behaviour of small molecules. Various alkanes and metal chelates of β-diketones were selected as model compounds, and the retention behaviour of these compounds was investigated in various organic solvent systems on poly(vinyl acetate) gels[5–8] or polystyrene gels[9,10]. One of the important results was that the secondary effects in gel chromatography could be interpreted by introducing the solubility concept into the chromatographic process[11].

This paper describes a systematic study of the retention behaviour of small molecules on a polystyrene gel with several solvents. The compounds investigated include alkanes, ethers, esters, ketones and alcohols. Four aromatic solvents, *viz.*, benzene, toluene, chlorobenzene and *o*-dichlorobenzene, and tetrahydrofuran were selected as eluents.

EXPERIMENTAL

Apparatus

A JASCO (Japan Spectroscopic Co., Tokyo, Japan) FLC-350 high-performance liquid chromatograph was used with a Laboratory Data Control (Riviera Beach, FL, U.S.A.) Model 1107L refractometric detector. A glass column (100 cm × 5 mm I.D.) was used with a constant-temperature water-jacket. A sample injection valve with a sample loop of 40-μl capacity was arranged in the flow system between the pump and the column.

Materials and reagents

Six *n*-alkanes, viz., pentane, hexane, octane, decane, dodecane and hexadecane, were standard-grade materials (Standard Kit NP A-1, Tokyo Chemical Industry, Tokyo, Japan). All other compounds used as solutes (samples) were reagent-grade materials purchased from several sources. They were diethyl, dipropyl, dibutyl and dihexyl ethers, ethyl, butyl and isoamyl acetates, acetone, methyl ethyl, diethyl, methyl isobutyl and dibutyl ketones and ethyl, propyl, butyl, hexyl, isoamyl, octyl and decyl alcohols.

Benzene, toluene, chlorobenzene (CB), *o*-dichlorobenzene (DCB) and tetrahydrofuran (THF) were carefully distilled prior to use as eluents.

The column packing material was Styragel 60A (< 37 μm) (Waters Assoc., Milford, MA, U.S.A.) (cross-linked polystyrene). The gel beads, after being swollen overnight in the solvent to be used, were packed into the column by the slurry packing procedure.

Procedure

The column was thermostated at 25 $\pm$ 0.1°C by circulating water through the column jacket from a constant-temperature water bath. The solvent flow-rates were adjusted to 1.0 ml/min.

Sample solutions were prepared by dissolving the compound of interest in the same solvent as the eluent. Sample concentrations were selected between 10 and 30 mg/ml so as to obtain a suitable response from the detector. The sample injection volume was 40 μl. The measurement of the retention time of each sample in a given column system was carried out at least in triplicate.

The dead volume between the sample injection valve and the detector was estimated by injecting an air bubble into the flow system from which the column had been omitted.

In order to determine the column void volume, mono disperse polystyrene standard with of molecular weight 200,000 (Pressure Chemical Co., Pittsburg, PA, U.S.A.) was used as a reference sample.

RESULTS AND DISCUSSION

In order to characterize a solute substance in gel chromatography, the distribution coefficient, K_d, derived from the following equation is frequently used:

$$V_e = V_0 + K_d V_i \tag{1}$$

where V_e, V_0 and V_i are the elution volume of the solute, the volume of the interstitial solvent (column void volume) and the volume of the solvent imbibed in the pores of the gel (pore volume), respectively. The solvent in the pores corresponds to the stationary phase in the column, and the gel matrix polymer is simply regarded as supporting material. Therefore, K_d is apparently independent of the physical properties of the gel matrix polymer.

When chromatographic behaviour is governed not only by pure steric exclusion but also by additional effects due to the interactions among the solute, solvent and gel matrix polymer, the whole gel phase, that is, the gel in the swollen state with the solvent, has to be taken into account as the practical stationary phase. Therefore, in this work, the distribution coefficient, K_{av}, derived from eqn. 2 was used.

$$V_e = V_0 + K_{av} V_x \tag{2}$$

where V_x is the volume of the gel swollen by the solvent (gel phase). By introducing the total column volume, V_t ($= V_0 + V_x$), eqn. 2 can be rearranged to give

$$K_{av} = (V_e - V_0)/(V_t - V_0) \tag{3}$$

In this work, the V_0 value of the Styragel 60A column conditioned with a given solvent was assumed to be equal to the V_e value of the monodisperse polystyrene standard of molecular weight 200,000, which was regarded as a large molecule enough to be completely excluded from the gel network. The V_t value was determined to be 19.24 ml in any solvent system. The value of V_e for a compound was calculated from the elution time and the solvent flow-rate. The K_{av} values were thus determined for a series of alkanes, ethers, esters, ketones and alcohols, on Styragel 60A with benzene, toluene, CB, DCB and THF. The results are summarized in Table I together with molar volumes, V_m, and solubility parameters, δ, of the compounds. The solvents are arranged in this table in increasing order of their δ values.

TABLE I

K_{av} VALUES OF LOW-MOLECULAR-WEIGHT COMPOUNDS ON STYRAGEL 60A WITH DIFFERENT SOLVENTS

Compound	V_m*	δ*	K_{av}**				
			Toluene (δ = 8.9)	*THF* (δ = 9.1)	*Benzene* (δ = 9.2)	*CB* (δ = 9.5)	*DCB* (δ = 10.0)
Pentane	116.6	7.0	0.467	0.441	0.518	0.487	0.554
Hexane	131.6	7.3	0.433	0.417	0.480	0.455	0.526
Octane	163.5	7.6	0.384	0.363	0.426	0.399	0.458
Decane	194.9 §		0.328	–	0.373	0.341	0.407
Dodecane	228.6	7.9	0.293	0.283	0.335	0.311	0.362
Hexadecane	295***	8.0***	0.235	0.230	0.264	0.244	0.289
Diethyl ether	104.8	7.4	0.510	0.469	0.537	0.485	0.545
Dipropyl ether	138.8 §		0.440	0.407	0.466	0.428	0.488
Dibutyl ether	169.0 §		0.385	0.359	0.411	0.378	0.435
Dihexyl ether	234.8 §		0.299	0.280	0.324	0.296	0.344
Ethyl acetate	98.5	9.1	0.544	0.465	0.545	0.493	0.561
Butyl acetate	132.5	8.5	0.466	0.407	0.474	0.428	0.487
Isoamyl acetate	148.8	7.8	0.436	0.373	0.443	0.403	0.460
Acetone	74.0	9.0	0.611	0.487	0.608	0.533	0.598
Methyl ethyl ketone	90.1	9.3	0.565	0.467	0.568	0.496	0.558
Diethyl ketone	106.4	8.8	0.525	0.449	0.532	0.464	0.519
Methyl isobutyl ketone	125.8***	8.5***	0.477	0.409	0.490	0.428	0.479
Diisobutyl ketone	177.1	7.8	0.385	0.331	0.401	0.354	0.403
Ethyl alcohol	58.5	12.7	0.713	0.429	0.718	0.662	0.773
Propyl alcohol	75.2	11.9	0.645	0.405	0.658	0.606	0.701
Butyl alcohol	91.5	11.4	0.594	0.380	0.617	0.563	0.647
Isoamyl alcohol	108.9 §		0.548	–	0.577	0.521	0.602
Hexyl alcohol	124.8 §		0.508	0.338	0.540	0.483	0.562
Octyl alcohol	157.7	10.3	0.440	0.298	0.468	0.426	0.489
Decyl alcohol	190.5 §		0.392	0.267	0.416	0.373	0.432

* Data from ref. 12, except where indicated otherwise. (a) From ref. 15.
** The relative standard deviation in each instance is less than 0.7%.
*** Data from ref. 15.
§ Data calculated from molecular weight and density.

The gel chromatographic behavior of a solute is, in general, closely correlated with the size of the solute molecule. For large molecules such as polymers, molecular weight or chain length is frequently used as an effective size parameter for discussing the solute retention in gel chromatography, whereas for small molecules, such as those of molecular weight less than 1000, V_m is superior to the above two parameters[13]. The relationships between K_{av} and log V_m prepared from the data in Table I are shown in Fig. 1a–e. It is obvious that the K_{av} *versus* log V_m plot is approximately linear within every homologous series of compounds, and also that the arrangement of such plots for five different series of compounds depends on the solvent used. Even

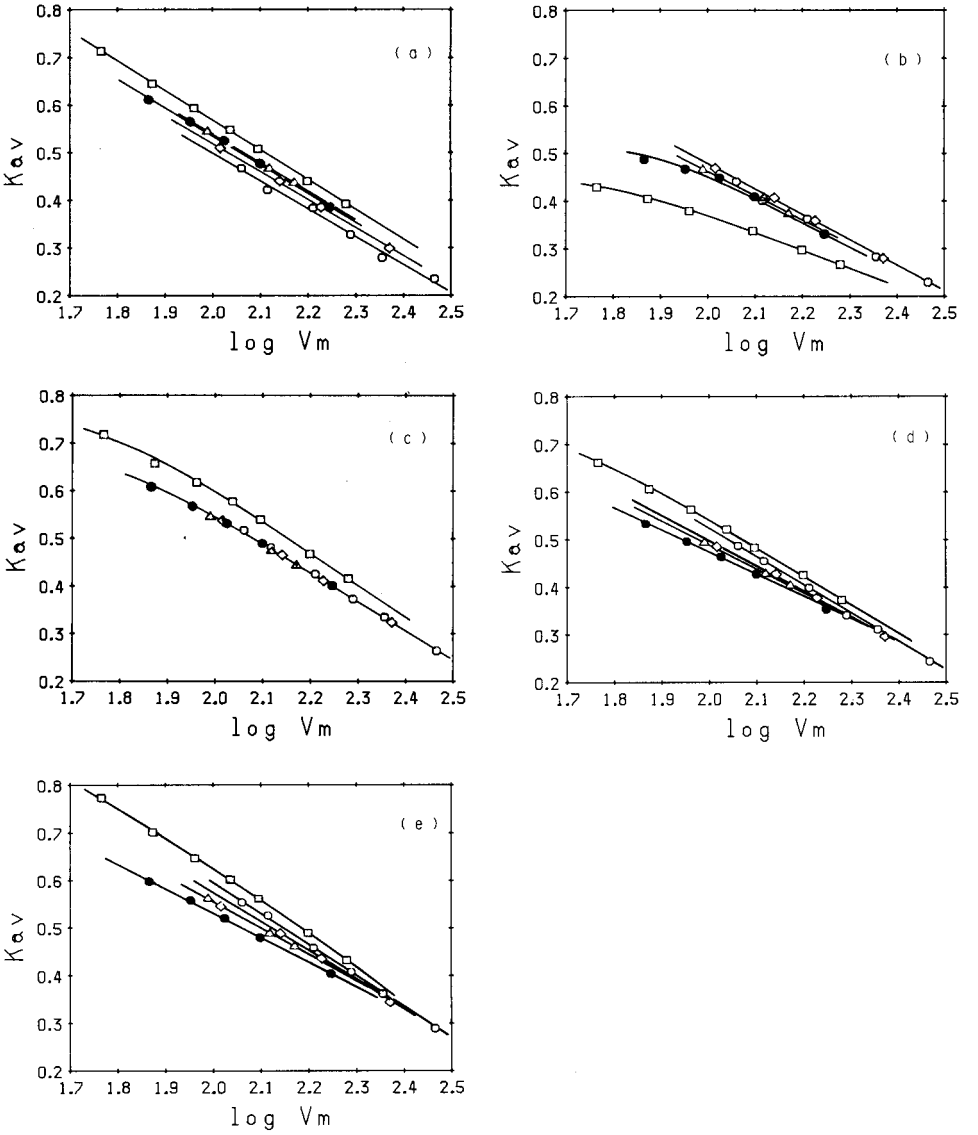

Fig. 1. Relationship between K_{av} values and molar volume, V_m, for alkanes (○), ethers (◇), esters (△), ketones (●) and alcohols (□) in toluene (a), THF (b), benzene (c), CB (d) and DCB (e) systems. Column: Styragel 60A; 25°C.

if the compounds with equal V_m values are not identical, the K_{av} value tends to increase in the following orders of compounds:

(a) in toluene, alkanes < ethers < esters < ketones < alcohols;
(b) in THF, alcohols < ketones < esters < ethers ≈ alkanes;
(c) in benzene, ketones = esters = ethers = alkanes < alcohols;
(d) in CB or DCB, ketones < esters < ethers < alkanes < alcohols.

These facts can not be explained simply in terms of steric exclusion. The solute distribution process has to be discussed, taking additional effects into consideration.

Solute distribution in gel chromatography was previously discussed on the assumption that practical gel chromatography was based on a combination of steric exclusion and partition effects[11]. On such an assumption, the V_e value of a solute S is expressed as

$$V_e = V_0 + K_{part.} K_{size} V_x \tag{4}$$

where $K_{part.}$ is the partition coefficient, defined as the concentration of S in the gel phase divided by the concentration of S in the solvent phase. The effective volume of the gel phase to the solute partition is not V_x, but rather only a certain fraction, K_{size}, of V_x is available for S owing to the steric exclusion effect. According to the theoretical treatment by Laurent and Killander[14], K_{size} is expressed by the equation

$$K_{size} = \exp[-\pi L(r_r + r_s)^2] \tag{5}$$

where r_s is the radius of the solute molecule, r_r is the radius of the polymer chain of gel matrix and L is the concentration of the polymer chain in the gel phase. Both r_r and L are constant in a combination of the gel matrix and a solvent. If the molecular dimensions (r_s) of various compounds are identical, the compounds have the same K_{size} value. It is obvious from eqn. 4 that solute retention on the basis of pure steric exclusion can be realized under the condition $K_{part} = 1$. In other words, even if the molecular dimensions of different compounds are identical, the V_e values of the compounds can be made to differ by controlling the $K_{part.}$ fractions so as to be different to each other.

According to the solubility parameter theory[15], the partition of S between the solvent and the gel phases is given by the solubility parameters, δ, of S, the solvent and the gel phase (indicated by subscripts s, o and x, respectively), the molar volume of S, $V_{m,s}$, the gas constant, R, and temperature, T:

$$\log K^x_{part.} = V_{m,s}[(\delta_0 - \delta_s)^2 - (\delta_x - \delta_s)^2]/2.3RT \tag{6}$$

where $K^x_{part.}$ is the partition coefficient defined as the molar fraction of S in the gel phase divided by that in the solvent phase. $K_{part.}$ in eqn. 4 is related to $K^x_{part.}$ by the equation

$$K_{part.} = K^x_{part.}(V_{m,0}/\bar{V}_{m,x}) \tag{7}$$

where $V_{m,0}$ and $\bar{V}_{m,x}$ are the molar volume of the solvent and the average molar volume of the gel phase. As the gel phase consists of gel matrix polymer substance and solvent, δ_x is, in general, not equal to the δ value of the gel matrix polymer, δ_g, but to the δ of the mixture of the above two components, approximately expressed by

$$\delta_X = \varphi_g\delta_g + (1 - \varphi_g)\delta_0 \tag{8}$$

where φ_g is the volume fraction of the gel-matrix polymer in the gel phase.

From eqns. 2, 4 and 6–8, the following equation[11] is derived:

$$\log K_{av} = \log K_{size} + V_{m,s}[2(\delta_s - \delta_0)(\delta_g - \delta_0)\varphi_g - (\delta_g - \delta_0)^2\varphi_g^2]/2.3RT + \log (V_{m,o}/\bar{V}_{m,x}) \quad (9)$$

The last term of the above equation is constant in a given solvent system.

We assume here that different compounds have the same K_{size} value in a given gel chromatographic column if the V_m values of the compounds are identical. When two different compounds, S_1 and S_2, with molar volumes equal to $V_{m,s}$ are chromatographed in a column, the relative retention, R_{s_1/s_2}, of S_1, compared with S_2, is given by the following equation:

$$\begin{aligned} \log R_{s_1/s_2} &= \log (K_{av,s_1}/K_{av,s_2}) \\ &= \log (K_{part.,s_1}/K_{part.,s_2}) \\ &= 2V_{m,s}(\delta_{s_1} - \delta_{s_2})(\delta_g - \delta_0)\varphi_g/2.3RT \end{aligned} \quad (10)$$

It is difficult to evaluate the fraction of $K_{part.}$ directly in the experimentally available distribution coefficient, K_{av}. However, by comparing the K_{av} values of two compounds, the contribution of the partition effect in gel chromatography can be discussed quantitatively by using known or measurable physical properties of the solvent, gel and solute, as shown in eqn. 10. Eqn. 10 predicts that R_{s_1/s_2} depends on the solvent used. Log R_{s_1/s_2} decreases with increase in δ_0, provided that δ_{s_1} is larger than δ_{s_2}. As φ_g, in general, depends on the solvent[11,16], log R_{s_1/s_2} does not always bear in a linear relationship to δ_0. Under the condition $\delta_0 = \delta_g$, log R_{s_1/s_2} is always zero, which means the absence of the partition effect from the solute distribution process in the column.

We assume here an imaginary alkane, ester, ketone and alcohol with V_m values equal to 100, a value selected for convenience. The K_{av} values of these imaginary

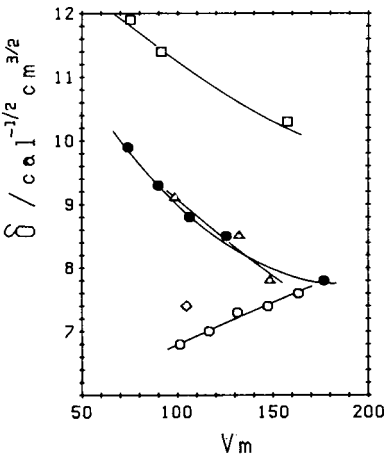

Fig. 2. Relationship between solubility parameter, δ, and molar volume, V_m, for alkanes (○), ether (◇), esters (△), ketones (●) and alcohols (□). The data[12] for butane (V_m = 101.4, δ = 6.8) and heptane (V_m = 147.4, δ = 7.4) are used in addition to those in Table I.

TABLE II

ESTIMATED VALUES OF δ AND K_{av} FOR IMAGINARY COMPOUNDS WITH $V_m = 100$

Compound	δ	K_{av}*				
		Toluene	*THF*	*Benzene*	*CB*	*DCB*
Alkane	6.8	0.50	0.48	0.54	0.52	0.60
		(1.00)	(1.00)	(1.00)	(1.00)	(1.00)
Ether	7.4	0.52	0.48	0.54	0.50	0.57
		(1.04)	(1.00)	(1.00)	(0.96)	(0.95)
Ester	9.1	0.54	0.46	0.54	0.49	0.56
		(1.08)	(0.96)	(1.00)	(0.94)	(0.93)
Ketone	9.0	0.54	0.45	0.54	0.47	0.53
		(1.08)	(0.94)	(1.00)	(0.90)	(0.88)
Alcohol	11.2	0.57	0.37	0.59	0.54	0.62
		(1.14)	(0.77)	(1.09)	(1.04)	(1.03)

* Values in parentheses are relative retentions, R, taking the K_{av} value of the alkane as unity.

compounds are estimated by reading off the corresponding values at log $V_m = 2.0$ from the K_{av} *versus* log V_m plots shown in Fig. 1. A rough estimate of the δ values of these imaginary compounds is made from the δ *versus* V_m plots shown in Fig. 2. The results of these estimations are summarized in Table II.

When the relative retention, R, is calculated for each compound, taking the K_{av} value of the imaginary alkane as unity, the relationship between log R and δ_0 of the solvent prepared for each compound is as shown in Fig. 3. The log R value of every compound tends to decrease with increase in δ_0. The plots for compounds other than alcohols intersect each other in benzene ($\delta_o = 9.2$). This suggests that the δ_g value of

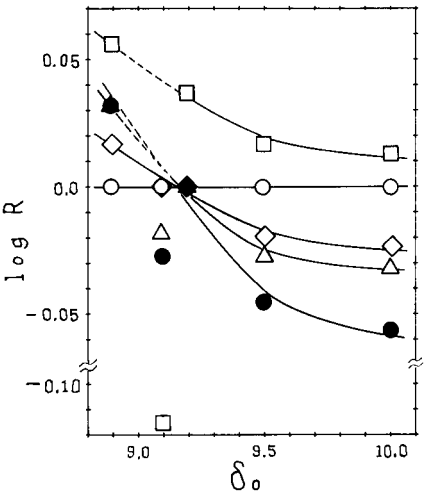

Fig. 3. Relationship between the relative retention, R, of an imaginary compound with $V_m = 100$ and solubility parameter, δ_0, of solvent. The K_{av} value of an imaginary alkane is taken as unity. Compounds: ○, alkane; ◇, ether; △, ester; ●, ketone; □, alcohol.

the gel matrix polymer used (Styragel 60A) is about 9.2. The δ value range for polystyrene is 9.1–9.4[12]. The imaginary alcohol shows log R values larger than zero in all solvents except THF. In contrast, the log R value of this compound observed in THF is the smallest of all.

The relationship between log R and δ_s for the imaginary compounds is shown in Fig. 4. With the exception of alcohol, an increasing tendency of log R with increasing δ_s is observed in solvents with δ_0 smaller than δ_g (=9.2), such as toluene. The reverse tendency is observed in solvents with δ_0 larger than δ_g, such as CB (δ_0 = 9.5) and DCB (δ_0 = 10.0). A similar tendency to the latter is also observed in THF, although the δ value of THF (δ_0 = 9.1) is close to δ_g. In benzene (δ_0 = 9.2), log R is always zero.

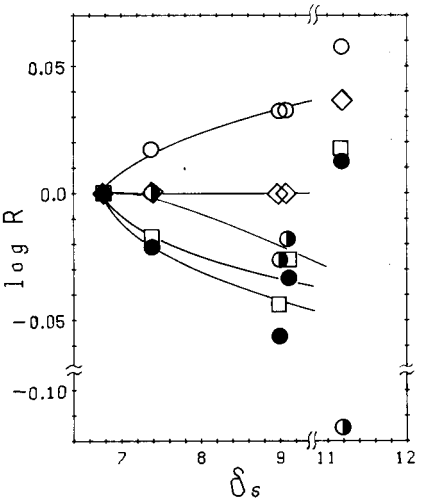

Fig. 4. Relationship between the relative retention, R, and solubility parameter, δ_s, for imaginary compounds with V_m = 100 in toluene (○), THF (◑), benzene (◇), CB (□) and DCB (●).

These facts are consistent with the prediction made from eqn. 10. The poor linearity of each plot is presumably caused by errors in the estimations of δ_s and R.

The retention behaviour of alcohols exhibited in Figs. 1a–e, 3 and 4 is so anomalous that the behaviour can no longer be explained on the basis of eqn. 9. Alcohols, compared with other compounds, show relatively large K_{av} values in all solvents other than THF. The interaction between the alcohol molecule and the π-electrons on the benzene ring in polystyrene is presumably one of the factors that lead to the high retention of alcohols. However, no clear evidence has been obtained. On the other hand, alcohols have very small K_{av} value in THF (see Fig. 1b). This is considered to be a result of the increase in the effective molecular size of alcohols due to solvation[17].

It is concluded that the solvent effect in gel chromatography on polystyrene gel can be interpreted by the theory in which the solubility concept is introduced. Benzene is a suitable solvent for achieving a pure size exclusion process for alkanes, ethers, esters and ketones in a Styragel 60A column. So-called secondary effects in gel chromatography can be controlled by using a carefully selected solvent.

REFERENCES

1 C. A. Streuli, *J. Chromatogr.*, 56 (1971) 225.
2 M. Wilk, J. Rochlitz and H. Bende, *J. Chromatogr.*, 24 (1966) 414.
3 J. G. Bergman, L. J. Duffy and R. B. Stevenson, *Anal. Chem.*, 43 (1971) 131.
4 H. Noda, K. Saitoh and N. Suzuki, *J. Chromatogr.*, 168 (1979) 250.
5 K. Saitoh and N. Suzuki, *J. Chromatogr.*, 109 (1975) 333.
6 K. Saitoh and N. Suzuki, *J. Chromatogr.*, 111 (1975) 29.
7 N. Suzuki and K. Saitoh, *Bull. Chem. Soc. Jap.*, 50 (1977) 2907.
8 K. Saitoh and N. Suzuki, *Anal. Chem.*, 52 (1980) 30.
9 N. Suzuki, K. Saitoh and M. Shibukawa, *J. Chromatogr.*, 138 (1977) 79.
10 E. Ozaki, K. Saitoh and N. Suzuki, *J. Chromatogr.*, 177 (1979) 122.
11 K. Saitoh and N. Suzuki, *Bull. Chem. Soc. Jap.*, 51 (1978) 116.
12 A. F. M. Barton, *Chem. Rev.*, 75 (1975) 731.
13 W. B. Smith and A. Kollmansberger, *J. Phys. Chem.*, 67 (1965) 4157.
14 T. C. Laurent and J. Killander, *J. Chromatogr.*, 14 (1964) 317.
15 J. H. Hildebrand and R. S. Scott, *The Solubility of Nonelectrolytes*, Dover, New York, 1964.
16 K. Saitoh, T. Ozawa and N. Suzuki, *J. Chromatogr.*, 124 (1976) 231.
17 J. G. Hendrickson and J. C. Moore, *J. Polym. Sci., Part A-1*, (1966) 167.

Journal of Chromatography, 239 (1982) 671–675
Elsevier Scientific Publishing Company, Amsterdam — Printed in The Netherlands

CHROM. 14,519

REVERSED-PHASE LIQUID CHROMATOGRAPHIC RESOLUTION OF UNDERIVATIZED D,L-AMINO ACIDS USING CHIRAL ELUENTS

NORIYUKI NIMURA*, ATSUKO TOYAMA, YOKO KASAHARA and TOSHIO KINOSHITA
School of Pharmaceutical Sciences, Kitasato University, 9-1 Shirokane-5, Minato-ku, Tokyo 108 (Japan)

SUMMARY

Resolution of underivatized amino acid enantiomers by reversed-phase liquid chromatography is described using chiral eluents containing the copper(II) complexes of the chiral chelates N-(*p*-toluenesulfonyl)-L-phenylalanine and N-(*p*-toluenesulfonyl)-D-phenylglycine. Resolution of the enantiomers of neutral, basic and acidic amino acids and their amides was accomplished on a octadecylsilyl bonded silica gel column. A chromatographic model is proposed that is based on dynamic ligand-exchange mechanism of D,L-amino acid with tosylated amino acid–copper(II) complex on the chemically bonded phase.

INTRODUCTION

High-performance liquid chromatographic (HPLC) resolution of amino acid enantiomers has been developed by using chiral derivatization reagents[1–3], chiral eluent[4] or chiral stationary phases[5]. Resolution utilizing a mobile phase containing a chiral additive is simple and furnishes the sensitive detection of enantiomeric amino acids by post-column derivatization with various reagents. We have recently reported[6] direct resolution methods for underivatized D,L-amino acids using a chiral mobile phase containing the copper(II) complex of N-(*p*-toluenesulfonyl)-L-phenylalanine (TosPhe) by reversed-phase HPLC on an *n*-octylsilyl (OS) bonded phase. This method provided excellent resolution of each of the amino acids, which were sensitively detected using *o*-phthalaldehyde (OPTA) reagent. D,L-Proline, which could not be detected by the resolution method using proline as the chiral additive[7], were detected by post-column derivatization with 7-chloro-4-nitrobenzofrazan (NBD-Cl) in this method[8].

In the present study, the copper(II) complex of N-(*p*-toluenesulfonyl)-L-phenylglycine (TosPhG) was found to be applicable to the resolution of the widest range of amino acids among the chiral additives so far reported.

MATERIALS AND METHODS

Amino acids and other reagents were purchased from Wako (Osaka, Japan) and Tokyo Chemical Indsutry (Tokyo, Japan). Chemically bonded octadecylsilyl

0021-9673/82/0000–0000/$02.75

(ODS) silica gel, Develosil ODS (particle size 5 μm) was obtained from Nomura Chemical (Seto-shi, Japan). OPTA was purchased from Funakoshi Pharmaceutical (Tokyo, Japan). Water and acetonitrile were distilled using glass apparatus before use. TosPhe and TosPhG were prepared as described by Theodoropoulos and Craig[9].

The mobile phase consisted of acetonitrile–water containing 1 m*M* TosPhe (or TosPhG) and 0.5 m*M* $CuSO_4 \cdot 5H_2O$. The pH of the mobile phase was adjusted to 6.0 with 5% aqueous sodium carbonate solution. The OPTA reagent was prepared by dissolving the following materials in 500 ml of the water and de-gassing: 17 g of boric acid, 15 g of potassium hydroxide, 2 ml of mercaptoethanol, 400 mg of OPTA dissolved in 5 ml of methanol and 1.5 g of EDTA2Na. Develosil ODS was packed in the stainless-steel column tube (10 cm × 4.0 mm I.D.) in our laboratory by the conventional slurry-packing technique. Other chromatographic apparatus and conditions were similar to those previously described[6].

RESULTS AND DISCUSSION

The concentrations of hydrogen ion and TosPhe–copper(II) complex or TosPhG–copper(II) complex in the mobile phase were set according to the basic approach described previously[6], except for ODS silica gel as the reversed-phase packing which showed better reproducibility of the retention time than the OS column. because the separation of amino acids was dependent on the acetonitrile concentration in the mobile phase, the pertinent concentration was chosen for each amino acid enantiomer.

Several methods[10–12] have been reported for the resolution of enantiomeric amino acids using chiral additives such as L-proline–copper(II)[4,7]. However, no conventional method has achieved the resolution of all of the neutral, basic and acidic amino acids together with their amides. Table I lists the capacity ratio (k'), separation factor (α), and difference in the free energies ($\Delta\Delta G^\circ = -RT \ln \alpha$) of D.L-amino acids resolved using TosPhe–copper(II) and TosPhG–copper(II) as chiral additives. All the amino acids tested, except glutamine, were resolved by the TosPhe–copper(II) system. Neutral amino acids were eluted in the order of L before D. On the other hand, basic and acidic amino acids and serine were eluted in the order D before L. D,L-Phenylglycine (D,L-PhG) showed the largest α value on the ODS column, suggesting that the stereoselectivity of the D,L-PhG–copper(II)–TosPhe complex is higher than those of other amino acids in the ligand-exchange reaction. This fact prompted us to develop TosPhG, which was expected to give better resolution than TosPhe owing to its sterically favored structure. In the present study, the α values of many amino acids were shown to increase by the use of TosPhG–copper(II) in place of TosPhe–copper(II) (Table I). The elution orders were reversed for all pairs of enantiomers compared with those observed for the TosPhe–copper(II) system. A typical resolution was observed for D,L-glutamine, which was not clearly separated with the TosPhe–copper(II) system as displayed in Fig. 1. Although the TosPhG–copper(II) system showed a slightly smaller separation factor in the limited case, it facilitated complete resolution of neutral, basic, and acidic amino acids and their amides.

Karger *et al.*[13] reported the resolution method for D,L-Dns-amino acids using L-prolyl-*n*-dodecylamide–nickel(II) as the chiral additive in reversed-phase HPLC. They have obtained data indicating that their chiral additive is distributed on the

TABLE I

CAPACITY RATIOS (k'), SEPARATION FACTORS (α), AND DIFFERENTIAL GIBBS FREE ENERGIES ($\Delta\Delta G^{\circ}$) OF D,L-AMINO ACIDS

Mobile phase, aqueous solution containing 1 m*M* TosPhe (or TosPhG), 0.5 m*M* $CuSO_4 \cdot 5H_2O$ and acetonitrile (percentage indicated in the table); pH 6.0; column, Develosil ODS-5 (10 cm × 4.0 mm I.D.)

Amino acid		*TosPhe*			*TosPhG*			*Acetonitrile (%)*
		k'	α	$\Delta\Delta G^0$	k'	α	$\Delta\Delta G^0$	
Serine	L	5.50	1.10	57	4.40	1.34	176	0
	D	5.00			5.90			
Aspartic acid	L	6.20	1.24	130	2.30	1.13	74	0
	D	5.00			2.60			
Asparagine	L	6.40	1.08	46	5.50	1.12	68	0
	D	5.90			6.14			
Glutamic acid	L	8.60	1.30	158	5.60	1.21	115	0
	D	6.60			6.80			
Glutamine	L	7.40	1.00	0	6.20	1.29	153	0
	D	7.40			8.00			
Alanine	L	5.50	1.31	163	7.60	1.10	57	0
	D	7.20			6.88			
Valine	L	7.80	1.77	344	14.10	1.34	176	10
	D	13.80			10.55			
Norvaline	L	2.70	1.48	236	4.40	1.73	330	15
	D	4.00			2.55			
Tyrosine	L	2.50	1.44	220	3.09	1.67	309	15
	D	3.60			1.85			
Phenylglycine	L	4.90	2.04	429	10.08	2.58	571	15
	D	10.00			3.90			
Isoleucine	L	4.80	1.71	323	8.12	2.08	441	15
	D	8.20			3.90			
Leucine	L	7.20	1.44	220	9.40	1.68	312	15
	D	10.40			5.60			
Norleucine	L	7.60	1.62	290	11.40	1.90	386	15
	D	12.30			6.00			
Phenylalanine	L	16.00	1.63	294	24.71	2.03	426	15
	D	26.00			12.19			
Tryptophan	L	22.00	1.64	298	34.20	1.93	396	15
	D	36.10			17.70			
Histidine	L	6.00	1.76	340	1.64	1.25	134	15
	D	3.40			2.05			
Lysine	L	11.60	1.09	52	6.05	1.31	163	15
	D	10.60			7.90			
Arginine	L	14.00	1.11	63	6.34	1.32	167	15
	D	12.60			8.38			

surface of an *n*-alkyl-bonded stationary phase and may act as an immobilized chiral phase. The copper(II) complexes of tosylated amino acid (TosAA) herein described may also exert a similar effect. The reversed-phase column, previously equilibrated by passing TosAA–copper(II) solution through it, retained the resolution power against amino acid enantiomers for more than 5 h when eluted with an aqueous solution containing only 0.5 m*M* copper sulfate, as depicted in Fig. 2. This indicates that

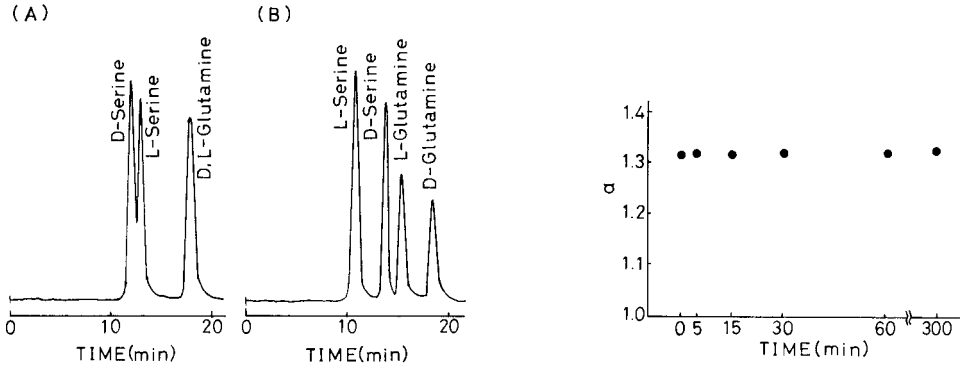

Fig. 1. Separation of D,L-glutamine and D,L-serine with (A) TosPhe–copper(II) and (B) TosPhG–copper(II) eluent system. Mobile phase, aqueous solution containing 1 m*M* TosPhe (or TosPhG) and 0.5 m*M* $CuSO_4 \cdot 5H_2O$; pH 6.0; *ca.* 0.25 nmol of each amino acid was injected.

Fig. 2. Change in α of D,L-alanine as a function of the time when eluted with an aqueous solution containing only 0.5 m*M* $CuSO_4 \cdot 5H_2O$. At zero time, the mobile phase is switched to one containing no chiral chelate (TosPhe).

TosPhe adheres to the surface of the ODS phase. Fig. 3 demonstrates the proposed resolution model based on the dynamic ligand-exchange mechanism for the stereoselective retention involving the labile immobilization of TosAA on the stationary phase. First the binary complex, $(TosAA)_2Cu$, in the mobile phase is adsorbed on the surface of the chemically bonded phase through hydrophobic interaction, and equilibrium is attained between the free and immobilized chelate complexes. Then the D- or L-amino acid injected into the column shifts in the column and triggers the ligand exchange with the immobilized chiral chelate. At this stage, an enantiomeric pair of amino acids may form ternary complexes of different conformation. The relationship between the resolution and the structure of the complex was explained in the preceding paper[6] as follows. The ternary complex of the D-amino acid may assume a *trans* conformation around the copper(II) ion and that of L-isomer a *cis* conformation. Molecular models support the fact that L-amino acid was eluted before the D-isomer because the *trans* isomer is thermodynamically more stable than the *cis* one[14]. However, the resolution may actually be influenced by the varying degree of hydrophobic interaction between the side-chain of the amino acids and the tosyl residue of the chiral additive and between the ternary complex of varying struc-

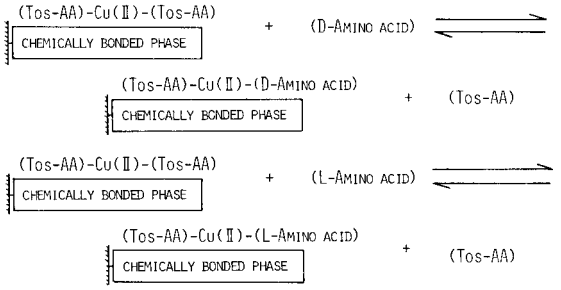

Fig. 3. Model of ligand-exchange mechanism of D,L-amino acid with TosAA–copper(II) complex on the stationary phase.

ture and the alkyl chain on the silica support. This may be the cause of the fact that some enantiomers are resolved in the order contrary to the above expectations, and that the separation factors of some amino acids in the TosPhG–copper(II) method are somewhat smaller than those in the TosPhe–copper(II) method.

The TosPhG–copper(II) system is expected to be suitable for the simultaneous resolution of amino acid enantiomers.

REFERENCES

1 T. Tamegai, M. Ohmae, K. Kawabe and M. Tomoeda, *J. Liquid Chromatogr.*, 2 (1979) 1229.
2 N. Nimura, H. Ogura and T. Kinoshita, *J. Chromatogr.*, 202 (1980) 375.
3 T. Kinoshita, Y. Kasahara and N. Nimura, *J. Chromatogr.*, 210 (1981) 77.
4 P. E. Hare and E. Gil-Av, *Science*, 204 (1979) 1226.
5 V. A. Davankov and S. V. Rogozhin, *J. Chromatogr.*, 60 (1971) 280.
6 N. Nimura, T. Suzuki, Y. Kasahara and T. Kinoshita, *Anal. Chem.*, 53 (1981) 1380.
7 E. Gil-Av, A. Tishbee and P. E. Hare, *J. Amer. Chem. Soc.*, 102 (1980) 5115.
8 N. Nimura, A. Toyama and T. Kinoshita, *J. Chromatogr.*, 234 (1982) 482.
9 D. Theodoropoulos and L. C. Craig, *J. Org. Chem.*, 21 (1956) 1376.
10 E. Oelrich, H. Preusch and E. Wilhelm, *J. High Resolut. Chromatogr. Chromatogr. Commun.*, 3 (1980) 269.
11 C. Gilon, R. Leshem and E. Grushka, *Anal. Chem.*, 52 (1980) 1206.
12 J. N. LePage, W. Lindner, G. Davies, D. E. Seitz and B. L. Karger, *Anal. Chem.*, 51 (1979) 433.
13 Y. Tapuhi, N. Miller and B. L. Karger, *J. Chromatogr.*, 205 (1981) 325.
14 J. Jozefonvidz, D. Muller and M. A. Petit, *J. Chem. Soc., Dalton Trans.*, (1980) 76.

Journal of Chromatography, 239 (1982) 677–685
Elsevier Scientific Publishing Company, Amsterdam — Printed in The Netherlands

CHROM. 14,747

SILICA GEL LIQUID–LIQUID CHROMATOGRAPHY USING AQUEOUS BINARY PHASE SYSTEMS

HIGH-EFFICIENCY EXTRACTION AND RESOLUTION OF PHENOLS AND CARBOXYLIC ACIDS

SHOJI HARA*, YASUO DOBASHI and KITARO OKA
Tokyo College of Pharmacy, Horinouchi, Hachioji, Tokyo 192-03 (Japan)

SUMMARY

An investigation was made of silica gel liquid–liquid partition chromatographic systems incorporating aqueous phases in order to provide a highly efficient solvent extraction procedure. By employing a simple aqueous binary solvent system containing diethyl ether and/or *n*-hexane and a droplet current pre-equilibration device, an instrumental aqueous two-phase distribution chromatographic system was constructed. Hydrophilic solutes such as polyhydroxybenzene derivatives and free carboxylic acids were separated by using silica gel columns treated with mineral acids. The capacity ratios of the solutes were found to be proportional to the distribution ratios of the samples, and therefore the resolution mechanism of this system can be assumed to be a liquid–liquid distribution.

INTRODUCTION

The use of organic solvents for the extraction of solutes in aqueous solutions has been widely applied in preparative processes in analytical and synthetic chemistry. Although manual batch experiments are commonly carried out in these fields, mechanical multi-step methods such as counter-current distribution and liquid–liquid partition chromatography (LLC) are often adopted in order to improve the efficiency of the separation process as alternative techniques.

LLC separation involving an aqueous stationary phase was achieved by employing cellulose or silica gel as a support material. Hydrophilic organic substances such as α-amino acid derivatives and carbohydrates were resolved by applying the classical LLC system from which the concepts and technology of today's chromatography were originally developed[1].

Several contributions by Huber's and Karger's groups incorporating modern technology showed the usueful selectivities and the high separation power of the LLC system[2–5]; however, high-performance aqueous-phase LLC has not been accepted for routine analysis, probably because the selection procedure for the phase system is always troublesome and the pre-conditioning of LLC columns is time consuming. For

0021-9673/82/0000–0000/$02.75

instance, phase liquids are commonly prepared by using ternary solvents obtained by the addition of a third solvent that is miscible with both of the components of the two-phase system. Therefore, in recent years, reversed-phase chromatography incorporating chemically bonded lipophilic phases and aqueous binary solvents has been commonly adopted for the routine analysis of water-soluble substances. LLC involving two aqueous phases has been replaced by more stable and convenient techniques for these practical reasons.

Highly efficient solvent extraction procedures were required in our laboratory for the development of a "programmed flow preparation" system[6] which permits continuous fractionation and separation. Such a process would contribute to the improvement of clean-up techniques used in the analysis of biological fluids. Therefore, the aqueous-phase LLC system was re-examined as an organic solvent multi-extraction process having high efficiency. In order to construct the aqueous-phase LLC system, we first tried to simplify the phase systems by removing the third solvent that is miscible with water and to use solvents that are commonly applied for the extraction procedure. Second, we designed dynamic pre-conditioning equipment for the carrier to accomplish the equilibration of the system and to obtain the stable analytical column rapidly. Lacking a pre-column, which is commonly required in LLC, the system was instrumentalized by using a UV detector.

Silica gel columns having a high theoretical plate number were incorporated to extract and separate water-soluble solutes, such as polyhydroxybenzene derivatives and free carboxylic acids, which were selected as model compounds for our basic study. Even water-coated silica gel showed an adsorption activity for polar substances such as hydroxycarboxylic acids; however, it was found that deactivation of the silica gel was achieved by treating the surface with mineral acids. In this paper, high-efficiency extraction and resolution of hydrophilic solutes in an aqueous two-phase partition system were accomplished by using acid-treated silica gel columns.

EXPERIMENTAL

Apparatus

The chromatographic apparatus is shown in Fig. 1. The droplet current equilibration system consisted of three stainless-steel tubes (250 × 10 mm I.D.). Each tube contained 16 ml of water saturated with a carrier solvent. The equilibration between the solvent and water was achieved during passage of droplets of a carrier solvent through the three tubes.

Packing material and column

Spherical silica gel with a pore size of 95 Å, particle size 10 μm and specific surface area 380 m^2/g (Kusano Scientific Co., Tokyo, Japan) was packed into stainless-steel tubes (200 × 4.6 mm I.D.) by the high-pressure slurry procedure.

Preparation of liquid–liquid partition column

Treatment with mineral acid. The packed column was washed with 20 ml of methanol and 100 ml of distilled water, and then treated with 20 ml of 20% sulphuric acid. The acid-treated column was washed with distilled water until the effluent gave no precipitate of barium sulphate on addition of saturated barium nitrate solution. The column was then further washed with 60 ml of distilled water.

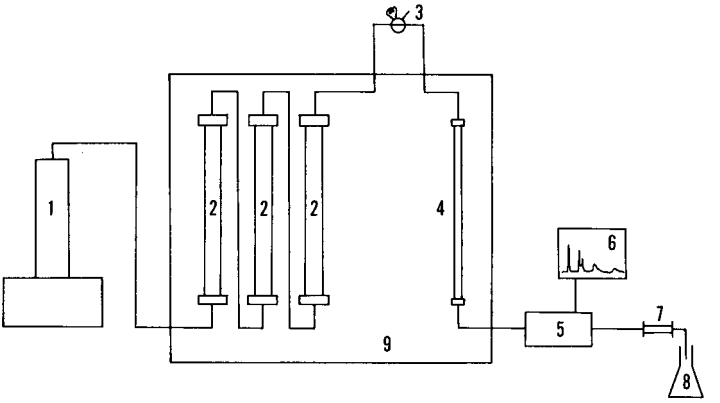

Fig. 1. Schematic diagram of the apparatus. 1 = High-pressure syringe-type pump (LCP-150; Japan Spectroscopic Co., Tokyo, Japan); 2 = droplet current equilibration system (250 × 10 mm I.D.); 3 = loop injector (Rheodyne Model 7125); 4 = separation column (200 × 4.6 mm I.D.); 5 = UV detector (UVIDEC 100-II; Japan Spectroscopic Co.); 6 = recorder; 7 = back-pressure column; 8 = waste reservoir; 9 = column oven (TU-100; Japan Spectroscopic Co.).

Column conditioning. The resulting column was connected to the chromatographic apparatus shown in Fig. 1 and purged with diethyl ether saturated with water at a flow-rate of 3 ml/min until a stable baseline was obtained.

Samples

All samples except Bz-DL-serine were commercially available (Wako, Osaka, Japan). Bz-DL-serine was prepared by the usual Schotten–Baumann procedure, and identified from IR spectral data. All samples and chromatographic solvents were of reagent grade (Wako).

Chromatographic procedure

The flow-rate of the eluent was 1 ml/min. The hold-up volume, V_0, was measured by injecting benzene as a standard sample. The ratio of stationary phase to mobile phase was calculated with the equation

$$V_s/V_m = (V_{oi} - V_{oc})/V_{oc}$$

where V_s is the volume of stationary phase, V_m is the volume of mobile phase, V_{oi} is the hold-up volume of the column containing no liquid stationary phase and V_{oc} is the hold-up volume of the column containing liquid stationary phase.

The droplet current equilibration system and separation column were maintained at 20°C. The capacity ratio, k', was calculated by the equation $k' = (V_r - V_0)/V_0$, where V_r is the retention volume.

The sample (0.1–1 μg) in diethyl ether (*ca.* 5 μl) was injected. The sample eluate was detected by UV absorbance at 254 nm.

Measurement of distribution ratio

The distribution ratios of solutes between water and diethyl ether were calcu-

lated with the equation $D = C_s/C_m$, where, D is the distribution ratio, C_s is the concentration of solute in the aqueous phase (stationary phase) and C_m is the concentration of solute in the diethyl ether phase (mobile phase).

C_s and C_m were obtained by the usual batch procedure in which the distribution process was carried out at 20°C and concentrations of solutes were determined by calibration graphs using UV absorbance.

RESULTS AND DISCUSSION

Several problems were encountered in an attempt to improve the performance and the instrumentalization of aqueous-phase LLC systems. These problems included the selection of a fine porous support material for coating the aqueous stationary phase, elimination of the adsorption activity for the packing surface and the preparation of high-efficiency columns supporting the aqueous stationary phase having sufficient stability for monitoring the solute elution. For realization of the system, we examined a silica gel column prepared by the common slurry packing procedure to support the aqueous stationary phase. As an alternative to the pre-column, which is normally required to obtain a stable analytical system for LLC, droplet current liquid columns were used.

Equipment for pre-equilibrating the carrier by passing water as droplets was constructed from empty HPLC tubes made of glass or stainless steel. Several tubes containing water were connected in a series using a pump. The flow-chart of this system is illustrated in Fig. 1. The droplet current conditioning device provided an efficient dynamic equilibration on the phase system without a pre-column and also avoided the preparation of excessive amounts of mixed solvents as carriers. This

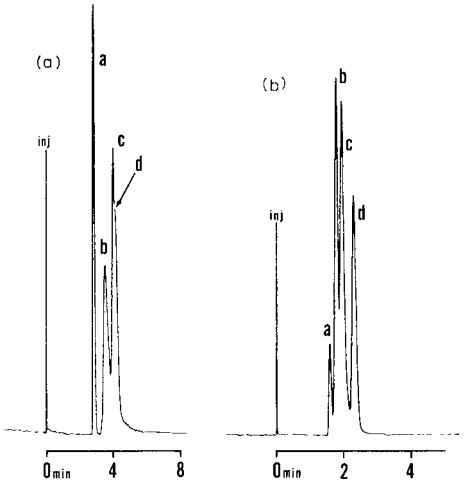

Fig. 2. (a) Separation of dihydroxybenzene isomers by adsorption chromatography. (a) Benzene; (b) catechol; (c) resorcinol; (d) hydroquinone. Packing: spherical silica gel (pore size 95 Å, particle size 10 μm). Eluent: diethyl ether. Flow-rate: 1 ml/min. Column temperature: 20°C. Detection: UV absorbance at 254 nm. (b) Separation of dihydroxybenzene isomers by LLC using an aqueous binary phase system. (a) Benzene; (b) catechol; (c) resorcinol; (d) hydroquinone. Support: spherical silica gel (pore size 95 Å, particle size 10 μm) (not treated with acid). Phase system: diethyl ether–water. Phase ratio (V_s/V_m): 0.70. Flow-rate: 1 ml/min. Column temperature; 20°C. Detection: UV absorbance at 254 nm.

system and separation column were allowed to equilibrate in a temperature-controlled chamber. A stable analytical system was constructed using a UV detector.

Diethyl ether, which is widely utilized for the extraction of solutes in aqueous solution, was selected as an organic solvent. *n*-Hexane was additionally employed to control the retention of the solutes. Hydrophilic samples such as phenols and carboxylic acids were used as samples. The retention behaviour of homologous compounds were examined in this phase system.

Before testing water-coated silica gel columns, we first examined the retention characteristics of three isomeric dihydroxybenzene derivatives in adsorption chromatography by using diethyl ether as the eluent on a bare silica gel (pore size 95 Å) column. The chromatogram is shown in Fig. 2a. Three peaks appeared; however, the resolution of resorcinol and hydroquinone was incomplete.

Next, the column was coated with water. Although three peaks were also obtained with the same elution order, the resolution of the first two peaks was incomplete. The result is shown in Fig. 2b. The decrease of the hold-up volume for the water-coated column clearly suggested that the aqueous phase was tightly retained on the surface of the packing material. To increase the retention of the solutes, *n*-hexane was added to the carrier.

The retention of the solutes was examined using *n*-hexane–diethyl ether (1:1) as the eluent. The resulting adsorption chromatogram is depicted in Fig. 3a. The resolution of the three isomers was not improved by tailing phenomena. On the other hand, a partition chromatogram (Fig. 3b) indicated that the LLC mode is very suitable for the resolution of the given sample mixture.

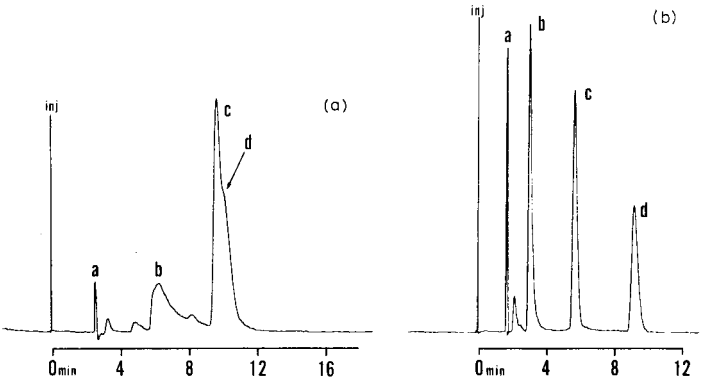

Fig. 3. (a) Separation of dihydroxybenzene isomers by adsorption chromatography. (a) Benzene; (b) catechol; (c) resorcinol; (d) hydroquinone. Separation conditions as in Fig. 2a except for the eluent: *n*-hexane–diethyl ether (1:1). (b) Separation of dihydroxybenzene isomers by LLC using *n*–hexane-diethyl ether/aqueous phase system. (a) Benzene; (b) catechol; (c) resorcinol; (d) hydroquinone. Separation conditions as in Fig. 2b except for the phase system: *n*-hexane–diethyl ether (1:1)/water. Phase ratio (V_s/V_m): 0.60.

Trihydroxybenzene and carboxylic acids that are more soluble in water were then injected into the aqueous-phase LLC columns. These solutes were eluted using diethyl ether as the eluent; however, some polar compounds such as gallic acid and vanilylmandelic acid gave tailing peaks. This phenomenon was interpreted as a stronger interaction between polar functional groups in the solutes and the active sites

of the silica gel surface. Elimination of such interactions required the elimination of the adsorption activity on the silica gel surface. Various methods for treating the silica gel were examined and washing with mineral acids such as 20% hydrochloric or sulphuric acids was found to be a suitable means of deactivating the sites. To eliminate excess of acids, the acid-treated columns were washed with water until the carrier was free of acid. A trace amount of acid was localized on the active sites of the support; however, peak tailing decreased and the resolution of the polar solute mix-

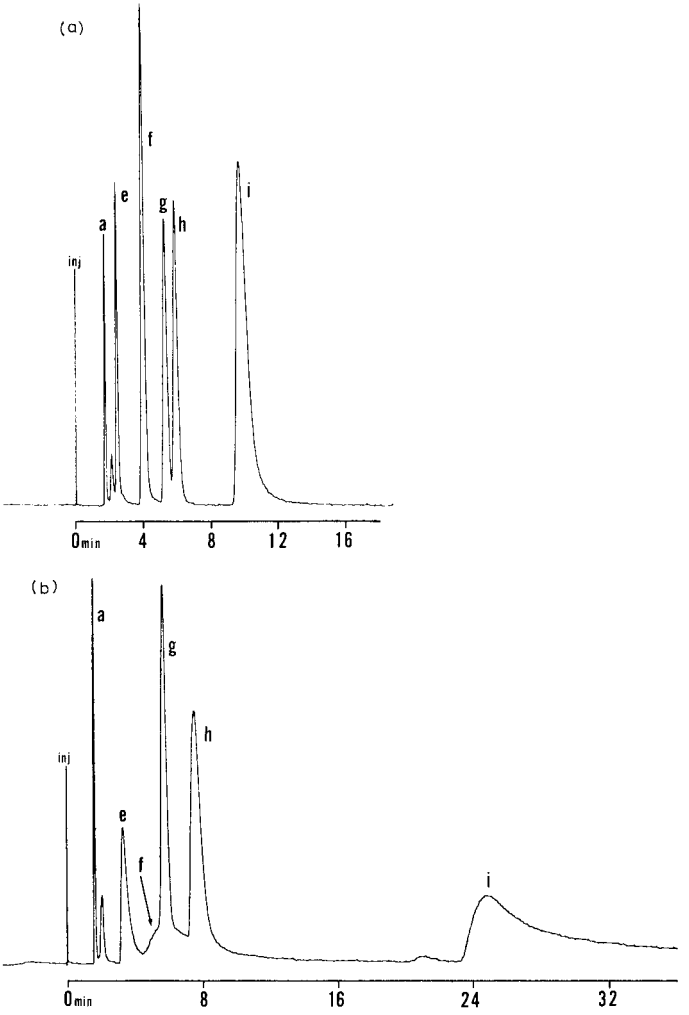

Fig. 4. (a) Separation of a mixture of trihydroxybenzenes and a group of carboxylic acids by LLC using an acid-treated support. (a) Benzene; (e) fumaric acid; (f) gallic acid; (g) phloroglucinol; (h) hippuric acid; (i) 4-hydroxy-3-methoxymandelic acid (VMA). Support: acid-treated spherical silica gel (pore size 95 Å, particle size 10 μm). Phase system: diethyl ether–water. Phase ratio (V_s/V_m): 0.60. Flow-rate: 1 ml/min. Column temperature: 20° C. Detection: UV absorbance at 254 nm. (b) Separation of a mixture of trihydroxybenzenes and a group of carboxylic acids in LLC using a support not treated with acid. (a) Benzene; (e) fumaric acid; (f) gallic acid; (g) phloroglucinol; (h) hippuric acid; (i) 4-hydroxy-3-methoxymandelic acid (VMA). Separation conditions as in Fig. 2b.

ture was improved. Continuous analysis over a period of several weeks was possible by employing the acid-treated columns. If the treated surface of the support in the column showed deterioration, for example if the carrier component or carrier composition changed considerably, the columns were regenerated by washing successively with methanol and acid *in situ*.

A mixture of trihydroxybenzene and a group of carboxylic acids were separated by using acid-treated columns and aqueous diethyl ether as the eluent. Chromatograms are illustrated in Fig. 4a. Fig. 4b shows a chromatogram obtained by using a non-acid-treated column, long tailing peaks being observed for gallic and vanilylmandelic acid.

Salicylic acid, gentisic acid and salicyluric acid are known as the main metabolites of aspirin[7,8]. A mixture of these metabolites was resolved by using an acid-treated column and *n*-hexane–diethyl ether (1:1)/aqueous phase system. The chromatogram is depicted in Fig. 5. The capacity ratios of phenols and carboxylic acid derivatives in *n*-hexane–diethyl ether or diethyl ether/aqueous phase systems are summarized in Table I. In these separations, an aqueous phase-supported silica gel column showed approximately 10,000 plates/m.

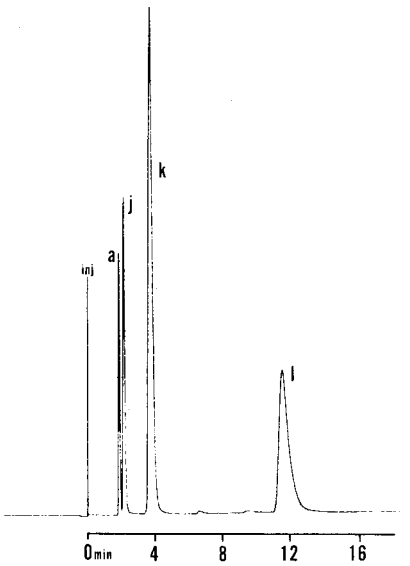

Fig. 5. Separation of the main metabolites of asparin by LLC. (a) Benzene (internal standard for V_0); (j) salicylic acid; (k) gentisic acid; (l) salicyluric acid. Separation conditions as in Fig. 4a except for the phase system: *n*-hexane–diethyl ether (1:1). Phase ratio (V_s/V_m): 0.53.

To confirm the separation mechanism of the column, the capacity ratios of the solutes obtained by using an acid-treated column in the present study were compared with the distribution ratios of the same samples in the phase system of diethyl ether and pure water, which were measured by a common batch procedure. Later ratios were determined by using the UV absorbance of solutes in the two equilibrated phases. If the retention mechanism is attributed to liquid–liquid distribution, the

TABLE I

CAPACITY RATIOS (k') OF PHENOLS AND CARBOXYLIC ACIDS IN VARIOUS PHASE SYSTEMS USING AN ACID-TREATED SUPPORT

Sample	*Phase system**			
	1	*2*	*3*	*4*
Catechol	0.13	0.32	0.89	2.73
Resorcinol	0.25	0.74	2.54	10.42
Hydroquinone	0.42	1.22	4.12	16.41
Pyrogallol	0.36	–	–	–
Phloroglucinol	2.11	–	–	–
Salicylic acid	–	0.06	0.15	0.33
Gentisic acid	–	0.32	0.97	3.98
Salicyluric acid	–	1.34	5.19	–
p-Hydroxybenzoic acid	0.18	0.52	1.76	7.35
Protocatechuic acid	0.41	1.56	7.42	–
Fumaric acid	0.43	1.48	5.50	–
Gallic acid	1.35	–	–	–
Hippuric acid	2.46	–	–	–
4-Hydroxy-3-methoxymandelic acid	4.70	–	–	–
N-Benzoylserine	8.47	–	–	–
3,4-Dihydroxymandelic acid	11.04	–	–	–
Maleic acid	13.54	–	–	–

* Phase systems: 1, diethyl ether–water (phase ratio, $V_0/V_m = 0.58$); 2, *n*-hexane–diethyl ether (1:3)/water ($V_0/V_m = 0.58$); 3, *n*-hexane–diethyl ether (1:1)/water ($V_0/V_m = 0.54$); 4, *n*-hexane–diethyl ether (7:3)/water ($V_0/V_m = 0.52$).

following relationship should hold:

$$k' = DV_s/V_m$$

where D is the distribution ratio, k' is the capacity ratio, V_s is the volume of the stationary phase and V_m is the volume of the mobile phase.

The correlation between the capacity ratios and distribution ratios of a group of solutes is shown in Fig. 6. The linear relationship was indicated with a correlation coefficient of 0.978 and a slope of 0.69. This slope represents the phase ratio (V_s/V_m) of the column. The phase ratio can also be calculated from the following equation:

$$V_s/V_m = (V_{oi} - V_{oc})/V_{oc}$$

where V_{oi} is the hold-up volume of columns containing no stationary phase and V_{oc} is the hold-up volume of columns containing an aqueous stationary phase.

The phase ratio obtained from the above equation is 0.60 and is consistent with the slope of the k' *versus* D plot. These results suggest that the retention mechanism of this system depends on a liquid–liquid distribution and that the acid on the surface of the support doses not affect the distribution process.

From the value of V_s/V_m, the hold-up volume of the column, V_o, and the

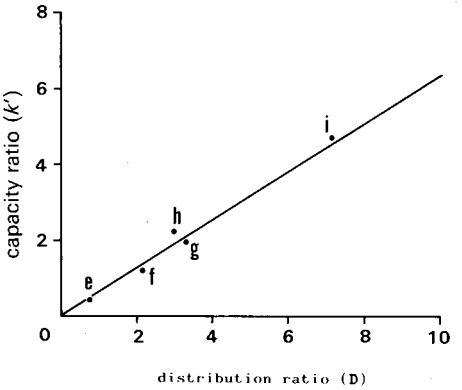

Fig. 6. Correlation of distribution ratios (D) and capacity ratios (k'). The correlation coefficient is 0.978 and the slope is 0.69 (this represents the phase ratio, V_s/V_m). The phase ratio calculated from V_0 is 0.6. Phase system: diethyl ether–water. Capacity ratios were obtained by using an acid-treated column. Samples: (e) fumaric acid; (f) gallic acid; (g) phloroglucinol; (h) hippuric acid; (i) 4-hydroxy-3-methoxymandelic acid (VMA).

specific surface area of support, it is assumed that about ten water molecules are layered on the support surface.

CONCLUSION

Aqueous binary-phase LLC systems using silica gel columns and acid-treated silica gel columns proved to be useful for the simultaneous extraction of water-soluble solutes such as phenols and free carboxylic acids and possibly other water-soluble materials from aqueous solutions and the resolution of the mixture. High-efficiency columns and pre-equilibration systems allowed the construction of an instrumentalized aqueous-phase HPLC system. In this paper preliminary results have been described; however, it must be ensured that the system has a high resolution power permitting to be applied to wide range of analytical and preparative chemistry research problems.

REFERENCES

1 A. J. P. Martin and R. L. M. Synge, *Biochem. J.*, 35 (1941) 1358.
2 J. F. K. Huber, *J. Chromatogr. Sci.*, 9 (1971) 72.
3 J. F. K. Huber, D. A. M. Meijiers and J. A. R. J. Hulsman, *Anal. Chem.*, 44 (1972) 111.
4 B.-A. Persson and B. L. Karger, *J. Chromatogr. Sci.*, 12 (1974) 521.
5 B.-L. Karger, S. C. Su, S. Marchese and B.-A. Persson, *J. Chromatogr. Sci.*, 12 (1974) 678.
6 K. Oka, Y. Dobashi, T. Ohkuma and S. Hara, *J. Chromatogr.*, 217 (1981) 387.
7 K. Hartialand and H. Kriger, *Acta Chem. Scand.*, 17 (1963) 62.
8 A. J. Cummings and M. L. Kings, *Nature (London)*, 209 (1966) 620.

Journal of Chromatography, 239 (1982) 687–694
Elsevier Scientific Publishing Company, Amsterdam — Printed in The Netherlands

CHROM. 14,762

TERNARY SOLVENT SYSTEM DESIGN FOR LIQUID–SOLID CHROMATOGRAPHY

SHOJI HARA*
Tokyo College of Pharmacy, Horinouchi, Hachioji, Tokyo 192-03 (Japan)
KAZUO KUNIHIRO and HIROYUKI YAMAGUCHI
Central Research Laboratory, Wakunaga Pharmaceutical Co., Hiroshima 729-64 (Japan)
and
EDWARD SOCZEWIŃSKI
Department of Inorganic and Analytical Chemistry, Medical Academy, Lublin (Poland)

SUMMARY

The linear relationship between the logarithmic values of capacity ratio and the molar fraction of one or two stronger solvents (S or $S_1 + S_2$) in ternary eluent systems containing two or one diluents, respectively ($S + W_1 + W_2$ or $S_1 + S_2 + W$), was determined by using steroid sapogenins as solutes in silica gel liquid–solid chromatography. The linear relationship was found to be reliable for concentrations of the S component as high as 100%. On the basis of this, an optimization procedure was established for a pair of model compounds in a ternary eluent by employing the retention–eluent composition correlation in two corresponding binary solvent systems.

INTRODUCTION

In the process of optimization in liquid–solid chromatography, binary eluents composed of a diluent and a stronger solvent have commonly been utilized. In ternary solvent systems made by adding one more component to a binary solvent system, the solvent strength and the selectivity for given samples can be more closely controlled and better resolution of the mixture can be achieved[1–3]. However, such systems are not commonly used, because the adaptation and design of the system is more troublesome than for corresponding binary systems.

Soczewiński and Jusiak[4,5] and Hara and co-workers[6–13] have systematically investigated the correlation between eluent composition and retention in binary solvent liquid–solid chromatography. They found in numerous instances a linear, theoretically expected relationship between the logarithm of the capacity ratio and the logarithm of the molar fraction of the stronger component for chromatographic systems of the silica–diluent + stronger solvent type. Such a relationship was found to be useful in the optimization of chromatographic systems. On the basis of these results, a rational method for the design of ternary solvent systems was established and is presented in this paper.

0021-9673/82/0000–0000/$02.75

EXPERIMENTAL

Samples and columns

Sapogenins and derivatives were prepared in Kunihiro's laboratory[14,15] and cholesterol was purchased from Wako (Osaka, Japan). Radialpack silica plastic cartridges (10 cm × 10 mm I.D.) (Waters Assoc., Milford, MA, U.S.A.) were used.

Chromatography

Model 7125 injector (Rheodyne, Berkeley, CA, U.S.A.) and a Model 45 pump (Waters Assoc.) were linked to a Model 401 differential refractometer (Waters Assoc.). Technical-grade solvents (Wako) were used. The flow-rates were 2.0 ml/min under a pressure drop of 500 p.s.i. An amount of 1 mg of sample was dissolved in 1 ml of eluent. A volume of 5 μl of sample solution was injected into the column. The hold-up volume was measured by using *n*-hexane as a sample, and the capacity ratio, k', was obtained with the equation $k' = t_s/t_m$, where t_s is adjusted retention time and t_m is dead time. The results were obtained at ambient temperature (23 ± 2°C) and at a relative humidity of 60 ± 5%.

RESULTS AND DISCUSSION

A binary eluent in liquid–solid chromatography consists of a diluent (W) and a stronger solvent (S). When a ternary solvent system is prepared, a third component (W or S) is added to the binary system, W + S. As a result, the ternary eluents can be classified into two groups. The first contains two diluents and a stronger solvent, *i.e.*, $W_1 + W_2 + S$ (solvent strength of the diluents defined as $W_2 > W_1$) and the other contains a single diluent and two stronger solvents, *i.e.*, $W + S_1 + S_2$ (similary, the eluent strength of the stronger solvents is defined as $S_2 > S_1$.

A linear relationship between the logarithm of the capacity ratio and the logarithm of the molar fraction of the stronger solvent in the binary system had been found for numerous systems[4–13].

When the content of polar component is higher than 5–10%, this relationship is represented by the equation

$$\log k' = c - n \log X_s \tag{1}$$

where k' is the capacity ratio, X_s is the molar fraction of the stronger solvent and c and n are constants ($c = \log k'$ for a pure stronger solvent, *i.e.*, $X_s = 1$). To examine the correlation between the retention of a solute and the composition of the ternary solvent system, we simplified the ternary system to a two-component system such as a binary (W + S) plus W or S. The correlation between the capacity ratio and the solvent composition of $S/(W_1 + W_2)$ or $(S_1 + S_2)/W$ was examined for various proportions of W_1/W_2 or S_1/S_2, respectively.

n-Hexane (O) and benzene (P) were used as diluents and ethyl acetate (B_2) and acetone (B_3) were added as stronger solvents. The solvent codes used in this paper are those suggested by Hara *et al.*[6,7].

The solvent strength of the ternary system must, in general, be greater than that of the corresponding binary system. Triterpenoid sapogenins obtained from ginseng were chosen as solutes, because they have three or more functions and exhibit

stronger adsorption activity than the mono- and disubstituted steroid derivatives that were used in earlier work on the systematic design of binary solvent systems[6–10]. Such functional groups contain an oxygen atom, together with acyloxy, keto carbonyl and hydroxy groups. Structural formulae of these substances are shown in Fig. 1.

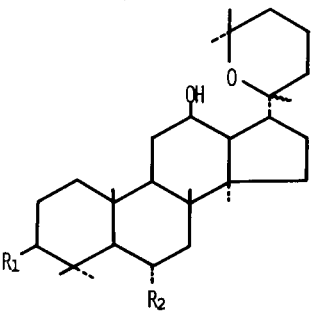

R1 = OH , R2 = H (PD)
R1 = OAc , R2 = H (PDA)
R1 = OH , R2 = OH (PT)

Fig. 1. Structural formulae of triterpenoid sapogenin and its derivatives.

W_1 + W_2 + S system

n-Hexane (O) and benzene (P) were used as diluents of W_1 and W_2. The diluent molar ratios were 1:0, 2:1, 1:1, 1:2 and 0:1. Ethyl acetate (B_2) was added to the diluent binary W_1 + W_2. The capacity ratio, k', of panaxadiol (PD) and panaxatriol (PT) was determined for various compositions of the stronger component, $X_{s/(w_1+w_2)}$. The data obtained were plotted as a log–log graph. The results are illustrated in Fig. 2.

A linear relationship between the logarithm of k' and the logarithm of $X_{s/(w_1+w_2)}$ was found, with a correlation coefficient of 0.9981–0.9998. All lines merged to a point on the vertical axis when the ratio of the stronger eluent (S) was increased to 100%.

These results indicate that the linear relationship discussed above was achieved at high concentrations of the S component. Therefore, it became possible to predict the capacity ratio of a solute in a pure stronger solvent by extrapolating the plots obtained for moderate concentrations of the S solvent. Based on these results, the retention in a ternary solvent system can be expressed as follows:

$$\log k'(W_1 + S) = c - n_1 \log X_s \tag{2a}$$

$$\log k'(W_2 + S) = c - n_2 \log X_s \tag{2b}$$

$$\log k'(W_1 + W_2 + S) = c - n_{12} \log X_{s/(w_1+w_2)} \tag{2c}$$

where c and n_1, n_2 and n_{12} are constants given by the systems: W_1 + S, W_2 + S and W_1 + W_2 + S, respectively. It is assumed that the value of constant n_{12} is intermediate between n_1 and n_2, because the constant n is considered to be an exchange ratio between solvent molecules and a solute on the active site of the adsorbent surface[16]. On the basis of such a concept, the constant n_{12} can be calculated approxi-

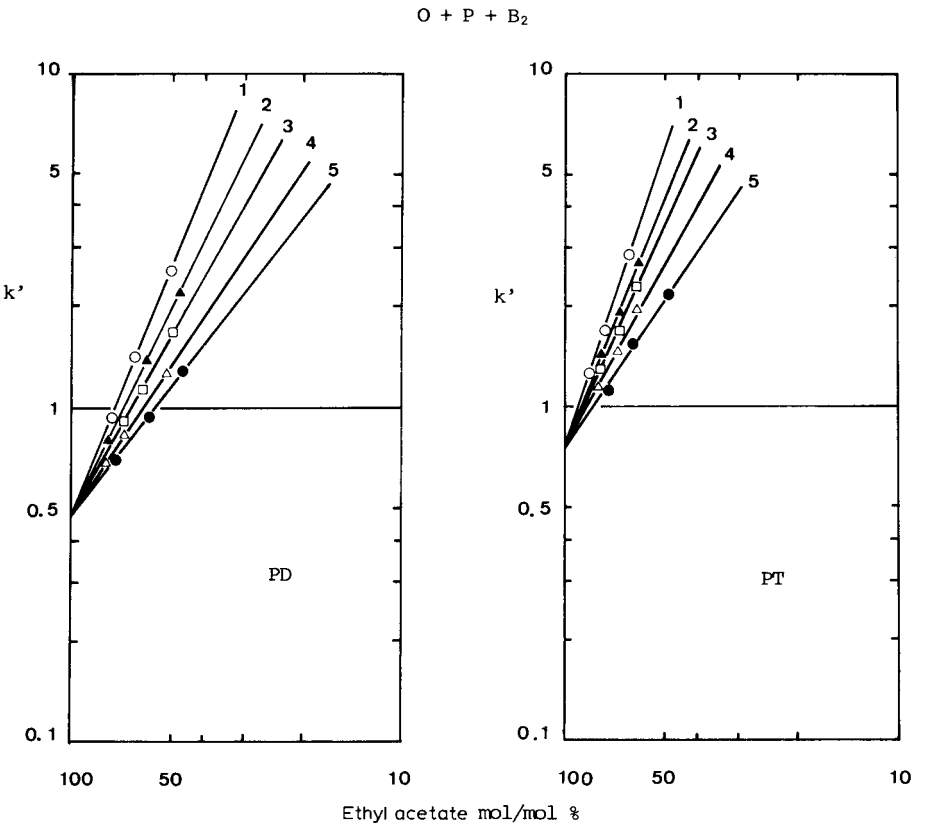

Fig. 2. Correlation between the logarithm of the capacity ratio (k') and the logarithm of the stronger solvent composition $X_s/(w_1 + w_2)$ in a ternary eluent system. Samples: PD = panaxadiol; PT = panaxatriol. Solvents: O = *n*-hexane; P = benzene; B_2 = ethyl acetate. Eluent systems: 1 = O + B_2; 2 = O + P + B_2 (O/P = 2); 3 = O + P + B_2 (O/P = 1); 4 = O + P + B_2 (O/P = 1/2); 5 = P + B_2.

mately from the additivity principle

$$n_{12} = X_{w_1} n_1 + X_{w_2} n_2 \tag{2d}$$

It was found that the calculated value of n_{12} was very close to the experimentally obtained value of n_{12}

$W + S_1 + S_2$ system

Ethyl acetate (B_2) and acetone (B_3), which were selected as two stronger solvents, S_1 and S_2 were added to the diluent *n*-hexane (O). Stronger solvent binary systems, $S_1 + S_2$, were composed using molar ratios of 1:0, 2:1, 1:1, 1:2 or 0:1. The capacity ratios of PD and PT in various compositions of the stronger solvents, $X(s_1 + s_2)/w$ were determined. The retention of the solutes and the composition of the ternary solvent were plotted on a log–log scale and the results are illustrated in Fig. 3. A linear relationship was obtained with a correlation coefficient of 0.9930–0.9996. The experimental results can be expressed as follows:

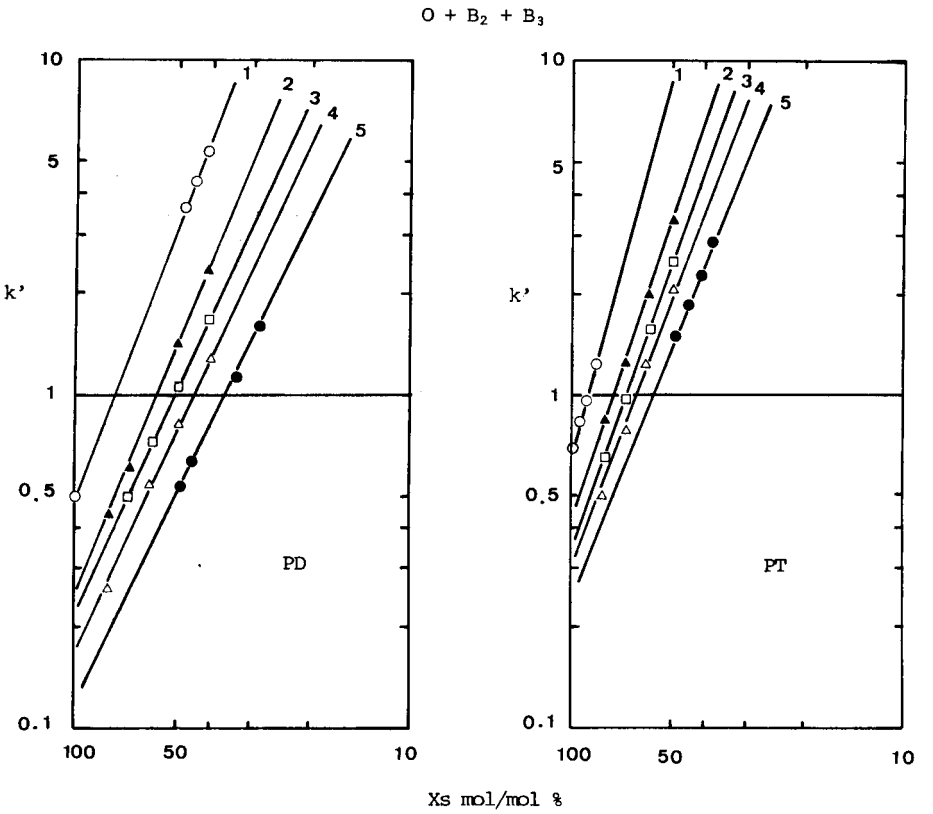

Fig. 3. Correlation between the logarithm of the capacity ratio (k') and the logarithm of the stronger solvent composition X (s_1 + s_2)/w in a ternary eluent system. Samples as in Fig. 2. Solvents: O = *n*-hexane; B_2 = ethyl acetate; B_3 = acetone. Eluent systems: 1 = O + B_2; 2 = O + B_2 + B_3 (B_2/B_3 = 2); 3 = O + B_2 + B_3 (B_2/B_3 = 1); 4 = O + B_2 + B_3 (B_2/B_3 = 1/2); 5 = O + B_3.

$$\log k'(W + S_1) = c_1 - n_1 \log X_{s_1} \tag{3a}$$

$$\log k'(W + S_2) = c_2 - n_2 \log X_{s_2} \tag{3b}$$

$$\log k'(W + S_1 + S_2) = c_{12} - n_{12} \log X(s_1 + s_2)/w \tag{3c}$$

where c_1, n_1; c_2, n_2 and c_{12}, n_{12} are the intercepts and slopes corresponding to the solvent systems: W + S_1; W + S_2 and W + S_1 + S_2, respectively.

Constants c_{12} and n_{12} were found to have intermediate values between c_1, c_2 and n_1, n_2, respectively; the n_{12} value could be calculated from eqn. 2d and the c_{12} value from eqn. 3d:

$$c_{12} = X_{S_1} c_1 + X_{S_2} c_2 \tag{3d}$$

Although a slight difference was observed between the calculated values and the experimental values, it seems possible to predict the retention for a given ternary solvent

system on the basis of the retention behaviour for a pair of corresponding binary systems.

In previous papers[7–9], commonly available volatile solvents that are used for the preparative research work in liquid–solid chromatography were classified in several types and the strength of the solvents in the binary systems was evaluated. By considering such a classification and a relative strength, a solvent for the ternary system can be defined as one of the components in the system; $W_1 + W_2 + S$ or $W + S_1 + S_2$ due to the sequence of the solvent strength ($W_1 < W_2 < S$ or $W < S_1 < S_2$). Additionally, the solvent composition of the ternary system can readily be optimized by adapting the given sample mixture according to the linear relationships expressed by eqns. 2a–c and 3a–c. The procedure described in this report seems to be especially useful for controlling the retention of the weak polar compounds such as steroid and terpenoid mixtures by employing weak polar solvent systems.

An example of controlling the resolution of a pair of solutes

Based on the correlation between the retention and the composition of the ternary solvent system discussed above, optimization of the resolution of a pair of solutes was attempted.

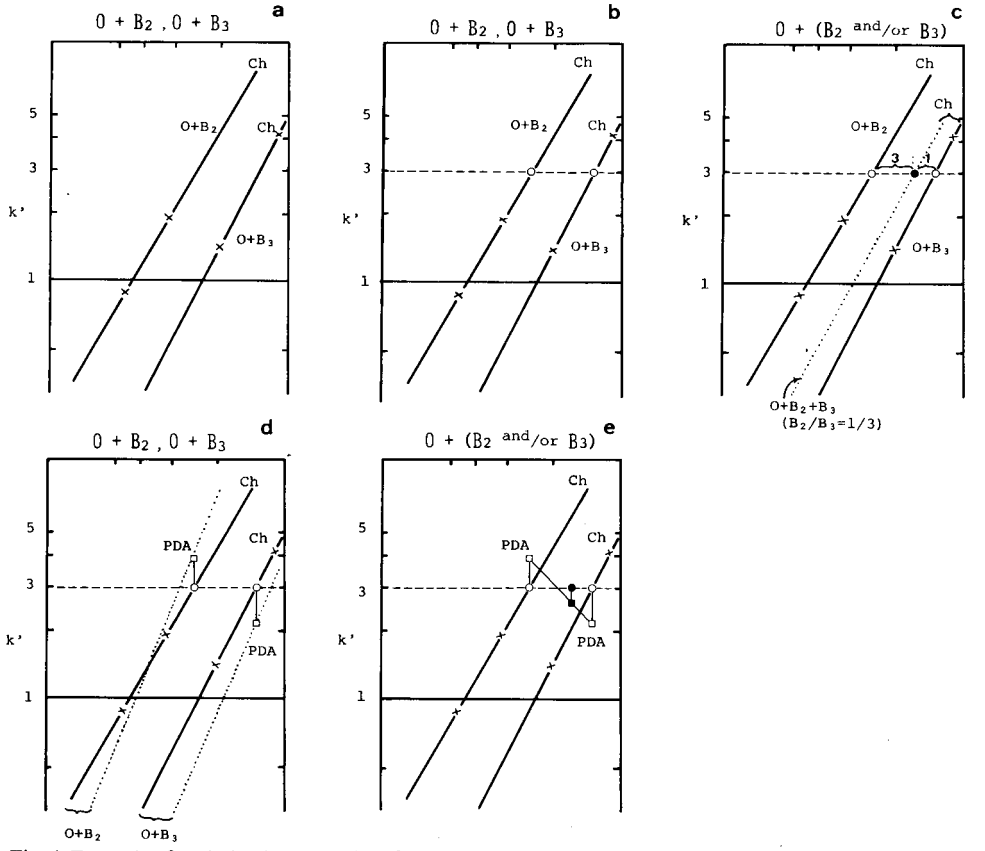

Fig. 4. Example of optimization procedure for the resolution of a pair of solutes. Model compounds: Ch = cholesterol; PDA = panaxadiol 3-acetate. Solvent components: *n*-hexane (O), ethyl acetate (B_2), acetone (B_3). For details see text.

Cholesterol (Ch) and panaxiadiol acetate (PDA) were selected as a pair of model compounds and a ternary mixture consisting of *n*-hexane (O), ethyl acetate (B_2) and acetone (B_3) was adapted. First, the retention behaviour of Ch as a standard solute was determined by two binary eluents containing the same diluent. A pair of capacity ratios obtained by applying binaries of the type O + B_2 and O + B_3 is plotted in Fig. 4a (crosses). On the basis of eqn. 1, the correlation between the retention and the composition of the binary solvents can be quantitatively expressed as two straight lines. The proper composition of the binary systems O + B_2 and O + B_3 can be predicted by determining the points where these lines intersect with a horizontal line drawn to represent the capacity ratio ($k' = 3$, see broken line and open circles in Fig. 4b).

According to a model experiment described in the section on the W + S_1 + S_2 system, it is possible to control the retention directly by adjusting the solvent composition of the ternary solvent system. When a stronger eluent binary B_2 + B_3 is prepared with a composition ratio of 1:3, the molar ratio of the ternary system O + B_2 + B_3 with a capacity ratio of 3 for Ch can be found at the intersection with the horizontal broken line in Fig. 4c. This point was determined by proportional division of a segment of the dotted line according to the ratio of S_1 *versus* S_2. This is represented by the closed circles.

To control the separation of a pair of solutes, the retention behaviour of PDA as a second compound was then determined. Two capacity ratios for PDA were obtained by using two binaries, O + B_2 and O + B_3, which provide a capacity ratio of 3 for Ch. These points are indicated by open squares in Fig. 4d. In this instance, elution sequences of a pair of solutes in the O + B_2 and O + B_3 systems were reversed. The chromatograms obtained in this experiment are illustrated in Fig. 5a and c.

The distance between two points indicated by the open squares and open

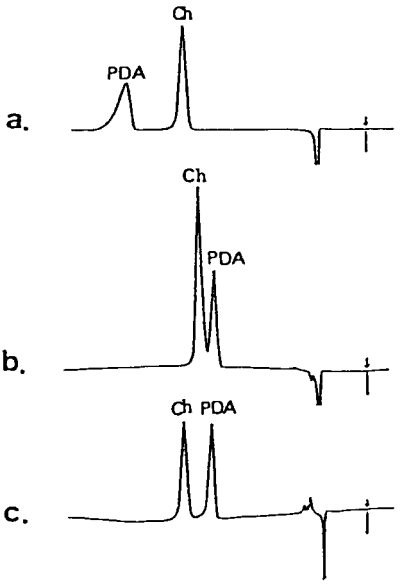

Fig. 5. Chromatograms showing the controlling process for the resolution of a pair of model compounds. Solvent components as in Fig. 4. (a) O + B_2 (B_2: 24.5%); (b) O + B_2 + B_3 (X_S: 15%), B_2:B_3 = 1:3; (c) O + B_3 (B_3: 12.6%).

circles in Fig. 4d is directly related to the logarithm of the separation factor. The resolution of a mixture can be controlled by adjusting the solvent system and the solvent composition.

The retention of PDA and the resolution of a mixture of Ch and PDA for the ternary solvent O + B_2 + B_3 which corresponded to a k' value of 3 for Ch were directly predicted by determining the point indicated by the closed square in Fig. 4e. Such an assumption was confirmed experimentally and the chromatogram obtained is shown in Fig. 5b.

As shown above, the optimization process for the ternary solvent system was elaborated systematically. First, a standard solute was selected and the retention behaviour of the solute was quantitatively determined by using a pair of binary solvent systems. Capacity ratios of the second solute are determined by using the same binaries. From these experimental data, ternary solvent systems, for which the separation factor is an average of the values obtained for the two corresponding binary systems, can be directly prepared. The systematic design of ternary solvent systems described in this paper can be applied effectively to control the retention and to optimize the separation of complex mixtures. The limitations of the method are due to the assumptions relating to the additivity of the slopes (n) of log k' *vs.* log X_S plots as well as of the intercepts c (Eqns. 2d and 3d). The assumptions are realistic for limited differences in the solvent strengths of the components of the binary diluent W_1 + W_2 or of the binary polar solvent S_1 + S_2. For larger differences in ε^0 values the log k' *vs.* X_S plot becomes concave (*cf.*, corresponding plots for eluent strength of binary eluents[17]. As stated earlier, the linear log k' *vs.* log X_S relationship which follows from the Snyder–Soczewiński displacement model, does not apply to dilute solutions of polar solvents ($X_S < 0.05$). The approach is thus based on semi-empirical equations and although simpler, is less general than that proposed recently by Glajch and Snyder[3] for multi-component eluents.

For larger differences in ε^0 values the linear equations 2d and 3d could probably be substituted by quadratic equations.

A microcomputer program for control of the resolution and the separation described in this report has been developed in Hara's laboratory. The program was found to be useful and reliable in analytical and synthetic chemistry research.

REFERENCES

1 E. Soczewiński and W. Maciejewicz, *J. Chromatogr.*, 22 (1966) 176.
2 S. R. Bakalyar, R. McIlwrick and E. Roggendorf, *J. Chromatogr.*, 142 (1977) 353.
3 J. L. Glajch and L. R. Snyder, *J. Chromatogr.*, 214 (1981) 21.
4 E. Soczewiński, *Anal. Chem.*, 41 (1969) 179.
5 E. Soczewiński and J. Jusiak, *Chromatographia*, 14 (1981) 23.
6 S. Hara, *J. Chromatogr.*, 137 (1977) 41.
7 S. Hara, Y. Fujii, M. Hirasawa and S. Miyamoto, *J. Chromatogr.*, 149 (1978) 143.
8 S. Hara, M. Hirasawa, S. Miyamoto and A. Ohsawa, *J. Chromatogr.*, 169 (1979) 117.
9 S. Hara and A. Ohsawa, *J. Chromatogr.*, 200 (1980) 85.
10 S. Hara and S. Miyamoto, *Anal. Chem.*, 53 (1981) 1365.
11 S. Hara, N. Yamauchi, C. Nakae and S. Sakai, *Anal. Chem.*, 52 (1980) 33.
12 K. Oka and S. Hara, *J. Chromatogr.*, 202 (1980) 187.
13 S. Hara, A. Ohsawa and A. Dobashi, *J. Liquid Chromatogr.*, 4 (1981) 409.
14 M. Fujita, H. Itokawa and S. Shibata, *Yakugaku Zasshi*, 82 (1962) 1634.
15 S. Shibata, O. Tanaka, K. Soma, Y. Iida, T. Ando and H. Nakamura, *Tetrahedron Lett.*, (1965) 207.
16 L. R. Snyder, *Anal. Chem.*, 46 (1974) 1384.
17 L. R. Snyder and J. J. Kirkland, *Introduction to Modern Liquid Chromatography*, Wiley, New York, 1979, 2nd ed., p. 369.

Journal of Chromatography, 239 (1982) 695–706
Elsevier Scientific Publishing Company, Amsterdam — Printed in The Netherlands

CHROM. 14,510

LIQUID CHROMATOGRAPHY WITH CROWN ETHER-CONTAINING MOBILE PHASES

II. RETENTION BEHAVIOUR OF β-LACTAM ANTIBIOTICS IN REVERSED-PHASE HIGH-PERFORMANCE LIQUID CHROMATOGRAPHY

TERUMICHI NAKAGAWA*, AKIMASA SHIBUKAWA and TOYOZO UNO
Faculty of Pharmaceutical Sciences, Kyoto University, Sakyo-ku, Kyoto 606 (Japan)

SUMMARY

The retention behaviour of several β-lactam antibiotics in reversed-phase liquid chromatography with mobile phases containing crown ether(18-crown-6 or dicyclohexyl-18-crown-6) has been investigated. The capacity factors were determined with various concentrations of crown ether and methanol in the aqueous mobile phase at different pH values. The observed profiles of capacity factor, k, *vs.* crown ether concentration and k *vs.* pH are discussed with reference to an equation derived from a chromatographic model involving association of β-lactam antibiotics with crown ethers and bindings of free and associated species to the hydrophobic stationary phase. The effect of ionic salts on the capacity factor is also discussed. The applicability of the method is demonstrated by specific separations of ampicillin in urine and cephalexin in plasma.

INTRODUCTION

The specific cation-anchoring ability of crown ethers has been utilized in liquid chromatography of various inorganic and organic ions. Cram and co-workers demonstrated the optical resolution of amino acids and their ester salts through chiral recognition by a crown ether which was contained in the mobile phase[1] or immobilized on silica gel[2] or on macroreticular cross-linked polystyrene *p*-divinylbenzene resin[3]. Blasius and co-workers separated enantiomers of amino acids[4], alkali and alkaline-earth metals[5–7] and several ammonium cations[5,7] using crown ether-based ion exchangers as the stationary phase. Delphin and Horwitz[8] also investigated the effects of crown ethers on the ion exchange behaviour of alkali metals. The associations of metals with several host substances were investigated by Horváth *et al.*[9], and metal–crown ether association constants were measured by using an aqueous cation-containing solution as mobile phase and a non-polar bonded stationary phase.

Anions can also be separated using a common cation associated with a crown ether as a counter ion. Blasius and co-workers[5,7,10,11] demonstrated the separation of various anions with a common cation as well as of various cations with a common

0021-9673/82/0000–0000/$02.75

TABLE I

STRUCTURES AND ABBREVIATIONS OF β-LACTAM ANTIBIOTICS

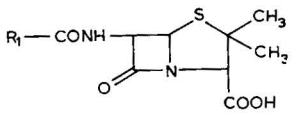

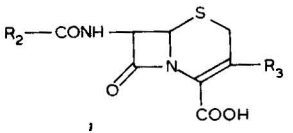

Penicillins	R_1	*Cephalosporins*	R_2	R_3
Ampicillin (ABPC)	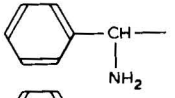	Cephalexin (CEX)	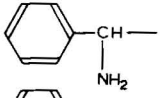	$-CH_3$
Amoxicillin (AMPC)	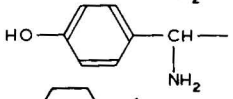	Cephaloglycin (CEG)	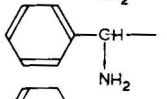	$-CH_2OCOCH_3$
Ciclacillin (ACPC)	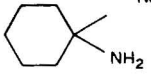	Cefradine (CED)	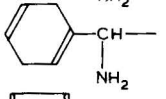	$-CH_3$
Benzylpenicillin (PCG)	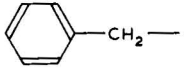	Cephaloridine (CER)	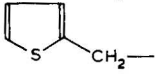	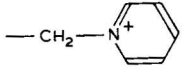
Carbenicillin (CBPC)	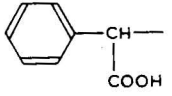			
Oxacillin (MPIPC)	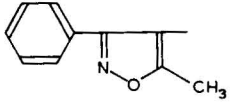			
Cloxacillin (MCIPC)	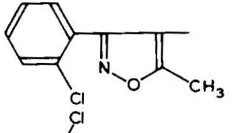			
Dicloxacillin (MDIPC)	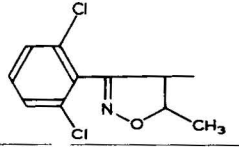			

anion. Brugman and Kraak[12] achieved normal phase separation of sulphonic acids using potassium associated with a crown ether as a common cation. Recent developments have included the use of crown ether polymers immobilized on silica[13,14] and polyamide crown resin[15,16] for the specific separation of alkali and alkaline-earth metals and various organic ions.

In a previous paper[17], we described the retention behaviour of various amino compounds in reversed-phase liquid chromatography with crown ethers in the aqueous mobile phase.

β-Lactam antibiotics such as penicillins and cephalosporins are widely used in clinical chemotherapy. In investigations of the *in vitro* and *in vivo* properties of these drugs, high-performance liquid chromatography (HPLC) has proved to be a facile assay method. The aim of the present study was to investigate the retention behaviour of β-lactam antibiotics in reversed-phase liquid chromatography with mobile phases containing crown ethers, and to demonstrate the applicability of the method to the analysis of biological samples.

EXPERIMENTAL

Reagents and materials

The β-lactam antibiotics were commercial products available for clinical use. Their structures and abbreviations are shown in Table I. 18-crown-6(18-C-6) and dicyclohexyl-18-crown-6(DC-18-C-6) were products of Nippon Soda Co. (Tokyo, Japan). DC-18-C-6 was used without separation of A,B-isomers. Glass-distilled water and methanol were used to prepare the mobile phases after degassing. Hydrochloric acid of analytical reagent grade was used to adjust the pH of the mobile phase.

Liquid chromatography

Liquid chromatographs (TWINCLE and TRIROTAR-III; Jasco, Tokyo, Japan) each equipped with a variable-wavelength detector (UVIDEC-100 III, Jasco) were used for the measurements of capacity factors. The experimental conditions employed are summarized in Table II. The β-lactam antibiotics were dissolved in water and the minimal amounts required for UV detection (at 220 nm for penicillins and 254 nm for cephalosporins) were used. The flow-rate of the mobile phase was 1.0 ml/min. The capacity factors were calculated according to $k = (t_R - t_0)/t_0$, where t_R is the average retention time of a solute measured repeatedly at the peak of the elution curve and t_0 is that of a non-absorbed substance.

Analysis of experimental data

The non-linear least squares fittings were carried out on a microcomputer (PET 2001, Commodore Co.) specially programmed in BASIC.

THEORETICAL

The β-lactam antibiotics used each have a carboxyl group on the skeletal structure and also in some cases, another carboxyl group or amino group on the lateral chain (see Table I). Therefore, those having an amino group exhibit amphoteric behaviour in their retention on a hydrophobic stationary phase. Since it is known that

TABLE II

HPLC CONDITIONS

Experiment	*Stationary phase*	*Mobile phase*
k vs. [18-C-6]	Develosil ODS-10 packed in stainless-steel tube (25 cm × 4 mm I.D.)	Water–methanol (55:45 v/v), pH 2.5 [18-C-6] = 0–45 m*M*
k vs. [DC-18-C-6]	Develosil ODS-10 packed in stainless-steel tube (25 cm × 4 mm I.D.)	Water–methanol (1:1 v/v), pH 2.5 [DC-18-C-6] = 0–25 m*M*
k vs. pH	Nucleosil 10 C_{18} packed in stainless-steel tube (15 cm × 4 mm I.D.)	Water–methanol (1:1 v/v), pH 2.2–4.4 [18-C-6] = 20 m*M*
k vs. % methanol	Develosil ODS-10 packed in stainless-steel tube (20 cm × 4 mm I.D.)	Water–methanol (3:7–7:3 v/v), pH 4.5 [18-C-6] = 20 m*M*
k vs. [KCl]	Nucleosil 10 C_{18} packed in stainless-steel tube (15 cm × 4 mm I.D.)	Water–methanol (1:1 v/v), pH 4.2 [18-C-6] = 20 m*M* [KCl] = 0–25 m*M*

a solute without an ionized amino group shows no apparent association with crown ethers and the association of an ionized amino group with a crown ether is expected to exhibit 1:1 stoichiometry, the chromatographic processes involved in the present system are as depicted in Fig. 1. The equilibria indicated by the broken lines involve the anionic form of the amphoteric β-lactam antibiotics and are not taken into account in deriving the capacity factor equation since they are not significant in the pH region employed in the present experiments. Thus, the capacity factor of amphoteric β-lactam antibiotics is given by

$$k = \phi \cdot \frac{[LS^+]_s + [LS^\pm]_s + [LCS^+]_s + [LCS^\pm]_s}{[S^+]_m + [S^\pm]_m + [CS^+]_m + [CS^\pm]_m} \quad (1)$$

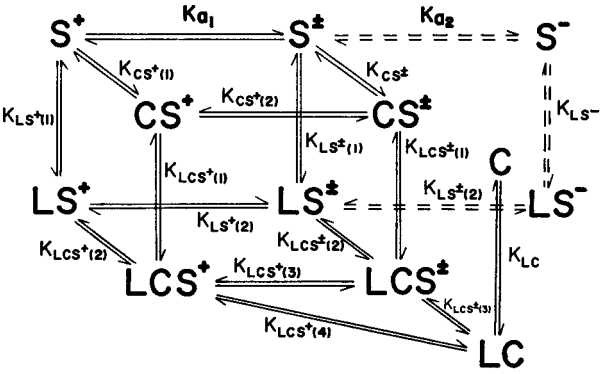

Fig. 1. The equilibria involved in reversed-phase liquid chromatography with a crown ether-containing mobile phase. C = Crown ether; S^+, $S^\pm$, S^- = cationic, zwitterionic and anionic forms of amphoteric β-lactam antibiotics; L = hydrophobic stationary phase.

where the subscripts m and s specify the mobile and stationary phases, respectively, and ϕ denotes the phase ratio. Introducing the equilibrium constants, K, in Fig. 1 we obtain

$$k = \phi[L]_s \cdot \frac{(A + B[C]) + (D + E[C])[H^+]}{(1 + K_{CS^\pm}[C])K_{a_1} + (1 + F[C])[H^+]} \quad (2)$$

where [C] is the concentration of crown ether in the mobile phase and $A = K_{LS^\pm(1)}K_{a_1}$, $B = K_{LCS^\pm(1)}K_{CS^\pm}K_{a_1} = AK_{LCS^\pm(2)} = K_{LCS^\pm(3)}K_{LC}K_a$, $D = K_{LS^+(1)} = AK_{LS^+(2)}$, $E = FK_{LCS^+(1)} = DK_{LCS^+(2)} = BK_{LCS^+(3)} = K_{LC}K_{LCS^+(4)}$ and $F = K_{CS^+(1)} = K_{CS^+(2)}K_{CS^\pm}K_{a_1}$. Since the amount of stationary phase bound to the solute represents only a small part of the total, $[L_t]$:

$$[L_t] = [L]_s + [LC]_s \quad (3)$$

Introducing K_{LC} into eqn. 3:

$$[L]_s = \frac{[L_t]}{1 + K_{LC}[C]} \quad (4)$$

Substituting for $[L]_s$ in eqn. 2, we finally obtain:

$$k = \phi \cdot \frac{[L_t]}{1 + K_{LC}[C]} \cdot \frac{(A + B[C]) + (D + E[C])[H^+]}{(1 + K_{CS^\pm}[C])K_{a_1} + (1 + F[C])[H^+]} \quad (5)$$

Eqn. 5 yields several expressions for the capacity factor depending on the choice of the constants B to F. These constants reflect the processes of crown ether–cation complexation and of binding of the complex with the hydrophobic stationary phase. Eqn. 5 predicts that the k *vs.* $[H^+]$ profile is rectangular hyperbolic at a constant concentration of crown ether. When the pH of the mobile phase is low enough for the amphoteric β-lactam antibiotics to be in the cationic form, the capacity factor is expressed by

$$k = \frac{k_0 + \phi[L_t]G[C]}{(1 + K_{LC}[C])(1 + K_{CS^+(1)}[C])} \quad (6)$$

where k_0 is the capacity factor for $[C] = 0$ and $G = K_{LCS^+(1)}K_{CS^+(1)} = K_{LCS^+(2)}K_{LS^+(1)} = K_{LCS^+(4)}K_{LC}$. Eqn. 6 indicates that the capacity factor at low pH initially increases with increase in the concentration of crown ether, reaches a maximum and then decreases at higher concentrations. For a small value of K_{LC}, *i.e.*, weak retention of the crown ether on the hydrophobic stationary phase

$$k = \frac{k_0 + k_{CS^+}K_{CS^+(1)}[C]}{1 + K_{CS^+(1)}[C]} \quad (7)$$

where k_{CS^+} is the capacity factor of the cationic form of the amphoteric β-lactam antibiotics, which is equal to $\phi[L_t]K_{LCS^+(1)}$.

RESULTS AND DISCUSSION

Effect of crown ether concentration

The dependence of capacity factor on the concentration of crown ether was investigated by using mobile phases containing 0–45 m*M* 18-C-6 or 0–25 m*M* DC-18-C-6 at pH 2.5. Figs. 2 and 3 show the *k vs.* [18-C-6] profiles for β-lactam antibiotics with and without an amino group, respectively. Figs. 4 and 5 show the *k vs.* [DC-18-C-6] profiles for the same substances. The capacity factors of β-lactam antibiotics without an amino group remained constant despite the addition of 18-C-6 (Fig. 3), but decreased significantly upon addition of DC-18-C-6 (Fig. 5). On the contrary, the capacity factors of amphoteric β-lactam antibiotics initially increased markedly with increase in the concentrations of both crown ethers followed by a gradual approach to a maximum (Figs. 2 and 4), and then decreased with further increase in the concentration of DC-18-C-6 (Fig. 4).

These results suggest that crown ethers exert different effects on the retention of β-lactam antibiotics on the hydrophobic stationary phase; an increase in the capacity factor by complex formation with the amino group, and a decrease in the capacity factor by competing with β-lactam antibiotics in binding to the stationary phase. The former effect is predominant in the retention of amphoteric β-lactam antibiotics, resulting in the enhancement of the hydrophobicity of the cation. β-Lactam antibiotics without an amino group are subject solely to the latter effect. Figs. 2–5 indicate that degree of such effects depends on the hydrophobicity of the crown ether, that is, an increase in the hydrophobicity results in an increase in the capacity factors of amphoteric β-lactam antibiotics, but a decrease in those of β-lactam antibiotics

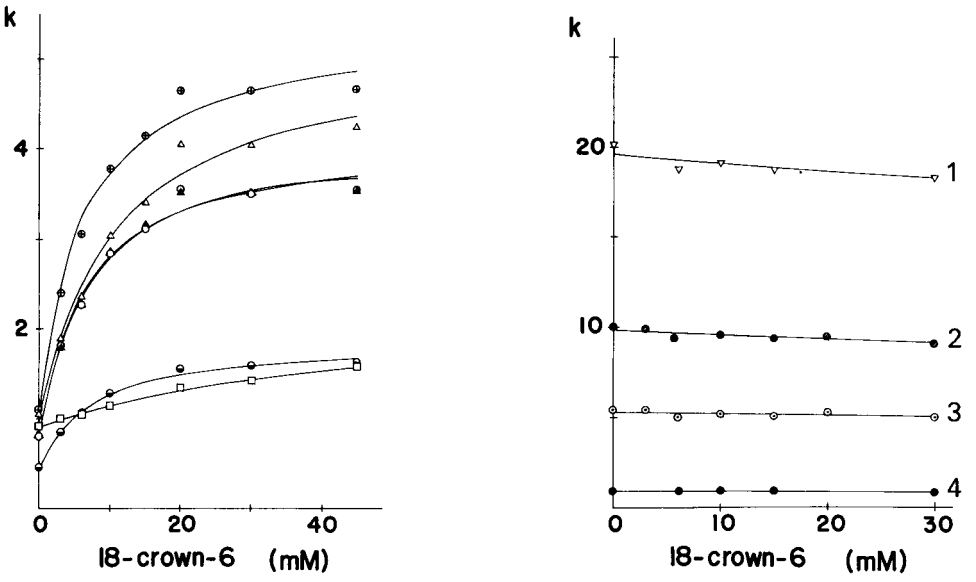

Fig. 2. Effect of 18-crown-6 concentration on the capacity factor of amphoteric β-lactam antibiotics (pH 2.5). Key: ⊕, ABPC; △, CED; ○, CEX; ▲, CEG; ◒, AMPC; □, ACPC.

Fig. 3. Effect of 18-crown-6 concentration on the capacity factor of β-lactam antibiotics without an amino group (pH 2.5). Key: 1, MPIPC; 2, PCG; 3, CBPC; 4, CER.

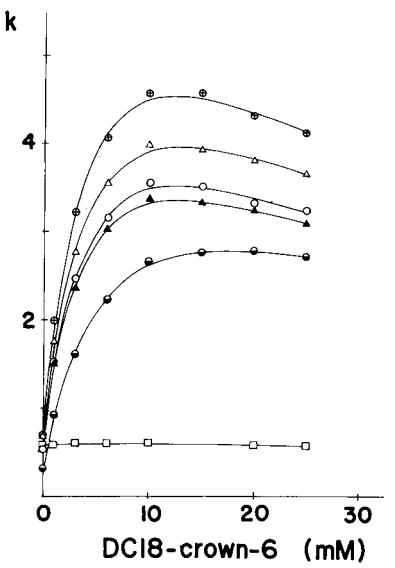

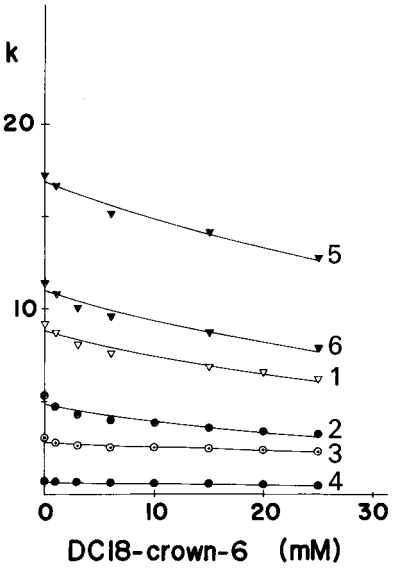

Fig. 4. Effect of dicyclohexyl-18-crown-6 concentration on the capacity factor of amphoteric β-lactam antibiotics (pH 2.5). For key see Fig. 2.

Fig. 5. Effect of dicyclohexyl-18-crown-6 concentration on the capacity factor of β-lactam antibiotics without an amino group (pH 2.5). Key: 5, MDIPC; 6, MCIPC; others, see Fig. 3.

without an amino group. The decrease in the capacity factor shown in Fig. 5 is ascribable to the stronger hydrophobicity of DC-18-C-6 than 18-C-6. Therefore, the *k vs.* crown ether concentration profiles in Fig. 5 can be expressed by

$$k = \phi[L_t] \cdot \frac{K_{LS}}{1 + K_{LC}[C]} \tag{8}$$

where K_{LS} is the equilibrium constant for β-lactam antibiotics without an amino group to bind to the stationary phase. The values of K_{LC} were estimated by non-linear least squares fittings of the *k vs.* [DC-18-C-6] data using eqn. 8. The curves in Fig. 5 are those best fitted thereby. The results for K_{LC} of DC-18-C-6 given in Table III, which are essentially independent of the β-lactam antibiotics, are scattered in a relatively narrow range with an average value of 15.3 M^{-1}.

The decrease in the capacity factor at higher concentrations as shown in Fig. 4 may also be due to the strong hydrophobicity of DC-18-C-6, since the capacity

TABLE III

PARAMETERS IN EQN. 8 FOR *k vs.* [DC-18-CROWN-6] OF β-LACTAM ANTIBIOTICS WITHOUT AN AMINO GROUP

	PCG	*CBPC*	*CER*	*MPIPC*	*MCIPC*	*MDIPC*
$\phi[L_t]K_{LS}$	4.87	2.81	0.634	8.81	11.0	16.8
K_{LC} (M^{-1})	23.3	9.06	11.7	17.7	17.0	13.1

TABLE IV

PARAMETERS IN EQN. 7 FOR k vs. [18-CROWN-6] OF AMPHOTERIC β-LACTAM ANTIBIOTICS

	ABPC	*AMPC*	*ACPC*	*CEX*	*CEG*	*CED*
k_0	1.06	0.444	0.909	0.781	0.775	1.00
k_{CS^+}	5.42	1.87	2.36	4.17	4.11	5.18
k_{CS^+}/k_0	5.11	4.21	2.60	5.34	5.30	5.18
$K_{CS^+(1)}$ (M^{-1})	158	138	19.0	148	158	94.3

factors of the same substances in the corresponding concentration range of 18-C-6 (Fig. 2) increase gradually toward a maximum. Thus, the k *vs.* [DC-18-C-6] profiles in Fig. 4 were approximated by eqn. 6 and the k *vs.* [18-C-6] profiles in Fig. 2 by eqn. 7. The computer fittings obtained using these equations are also shown in Figs. 2 and 4, and the parameters derived therefrom are listed in Tables IV and V, respectively. Although the average value of K_{LC} in Table V is a little larger than that in Table III, the computer fitting achieved by putting the latter value (15.3 M^{-1}) into eqn. 6 gave almost the same results as those in Table V.

It is notable in Figs. 2 and 4 that ACPC exhibits a peculiar behaviour upon addition of crown ether. The slight increase in the capacity factor in Fig. 2 suggests weak association with 18-C-6. This is possibly due to a steric effect of the amino group of ACPC, which unlike the others is located at a quaternary carbon atom on a cyclohexyl ring (see Table I). The stronger hydrophobic effect of DC-18-C-6, as mentioned above, compensates this effect, resulting in no apparent change in the capacity factor (Fig. 4).

Effect of pH

The dependence of capacity factor on pH between 2.2 and 4.4 was investigated using a mobile phase containing a constant concentration (20 mM) of 18-C-6. The results are shown in Fig. 6. The initial increase in proton concentration gave rise to a marked decrease in the capacity factors of amphoteric β-lactam antibiotics, and to a slight increase in those antibiotics without an amino group. Further increase in

TABLE V

PARAMETERS IN EQN. 6 FOR k *vs.* [DC-18-CROWN-6] OF AMPHOTERIC β-LACTAM ANTIBIOTICS

	ABPC	*AMPC*	*ACPC*	*CEX*	*CEG*	*CED*
k_0	0.721	0.323	0.580	0.547	0.547	0.702
$\phi[L_t]G$ (M^{-1})	1600	689	30.6	1240	1220	1330
K_{LC} (M^{-1})	29.5	23.1	19.4	28.5	24.8	27.1
$K_{CS^+(1)}$ (M^{-1})	185	123	23.1	188	206	180
k_{CS^+}*	8.65	5.60	1.32	6.60	5.92	7.39
k_{CS^+}/k_0	12.0	17.3	2.28	12.1	10.8	10.5

* Calculated from $\phi[L_t]G/K_{CS^+(1)}$.

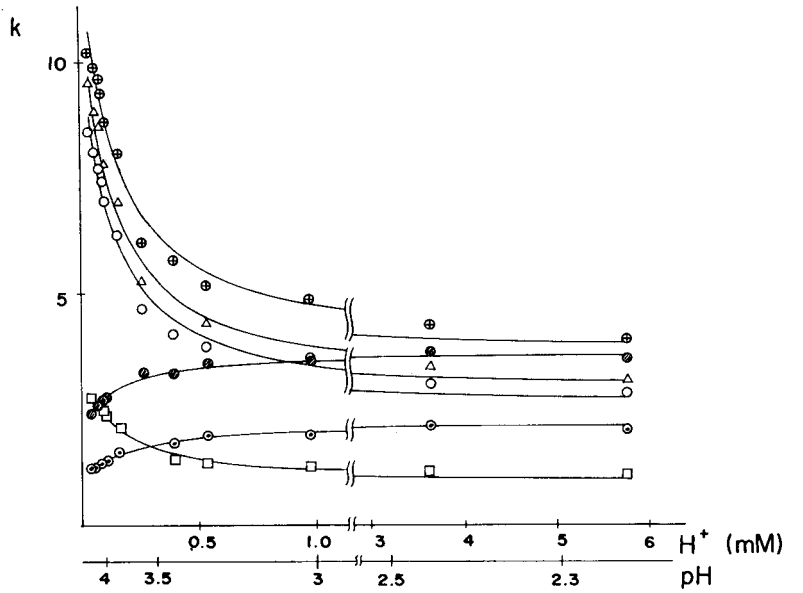

Fig. 6. Effect of proton concentration on the capacity factor of β-lactam antibiotics ([18-C-6] = 20 m*M*). Key: see Figs. 2 and 3.

proton concentration (pH < 3.3), however, had no effect in both cases. The behaviour of the β-lactam antibiotics without an amino group is similar to the pH dependence of the capacity factor of carboxylic acids in reversed-phase systems.

The *k vs.* pH profiles of amphoteric β-lactam antibiotics in Fig. 6 were analyzed according to

$$k = \frac{P_2 + P_3[H^+]}{P_1 + [H^+]} \tag{9}$$

which is the simplified form of eqn. 5 for a constant concentration of crown ether, where:

$$P_1 = \frac{1 + K_{CS^\pm}[C]}{1 + F[C]} \cdot K_{a_1} \tag{10}$$

Assuming that association of the protonated amino group with the crown ether is not affected by the dissociation of the carboxyl group, *i.e.*, $K_{CS^\pm} = K_{CS^+(1)}$, P_1 approximates to K_{a_1}. The non-linear least squares fittings of the *k vs.* pH data in Fig. 6 using eqn. 9 allowed the estimation of K_{a_1} values. The pK_{a_1} values thus obtained are 3.89(3.93) for ABPC, 3.94(4.02) for CEX, 3.98(4.37) for CED and 3.87 for ACPC, the values in parentheses being measured potentiometrically by Salto *et al.*[18] in 30% aqueous methanol with ionic strength 0.15 at 20°C. It is seen that these values are similar and also to the literature values.

It is interesting to compare the *k vs.* pH profiles of the amphoteric β-lactam antibiotics in Fig. 6 with those given by Salto *et al.*[18], who found that the capacity

factors of the zwitterion forms of amphoteric β-lactam antibiotics in a reversed-phase system (*i.e.*, stationary phase of ODS and mobile phase of phosphate buffer–methanol) were consistently lower than those of the cationic and anionic forms. Thus, the *k vs.* pH curves shown therein are convex toward the pH axis with minimal *k* values at around pH 5–6. This is in contrast to the *k vs.* pH profiles of ABPC, CEX and CED shown in Fig. 6. However, the profile of ACPC exhibits a slight decrease in the capacity factor. This suggests that the weaker association of the amino group with the crown ether is less dependent on proton concentration.

Effect of solvent

The solvent effect on capacity factor was investigated using mobile phases of water–methanol (7:3 to 3:7 v/v) containing 20 m*M* 18-C-6 at pH 4.5. The results are shown in Fig. 7, where it is seen that β-lactam antibiotics with and without an amino group exhibit linear decreases in log *k* values with similar slopes upon increasing concentration of methanol expressed in volume percent. This result is consistent with those found in other reversed-phase systems without crown ethers.

Effect of salt

The effect of inorganic electrolyte added to the crown ether-containing mobile phase is expected to be quite different from that in usual reversed-phase systems, because alkali metal cation from the salt associates with the crown ether more strongly than does the cationic amino group. As a result, the capacity factors of amphoteric β-lactam antibiotics in the present system must be decreased upon addition of such a salt. Fig. 8 shows the dependences of the capacity factors of several β-

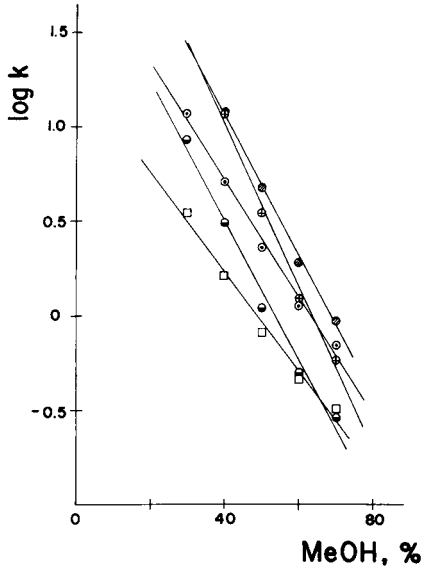

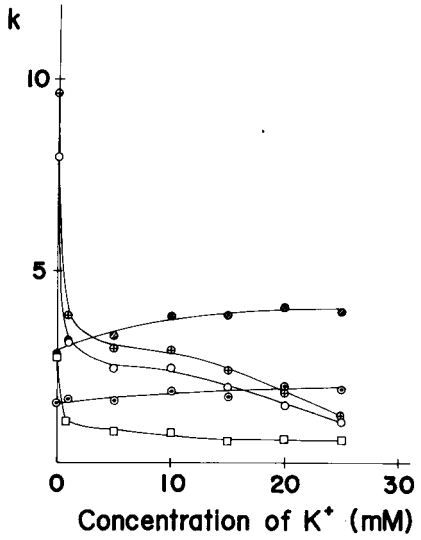

Fig. 7. Effect of methanol (MeOH) concentration on the capacity factor of β-lactam antibiotics (pH 4.5, [18-C-6] = 20 m*M*). Key: see Figs. 2 and 3.

Fig. 8. Effect of KCl concentration on the capacity factor of β-lactam antibiotics (pH 4.2, [18-C-6] = 20 m*M*). Key: see Figs. 2 and 3.

lactam antibiotics on the concentration of KCl dissolved in a mobile phase containing 20 m*M* 18-C-6 at pH 4.2. It is seen that the capacity factors of amphoteric β-lactam antibiotics initially decrease markedly with increasing KCl concentration followed by a gentle decline at higher concentrations. In contrast, the capacity factors of PCG and CBPC show a slight increase over the whole [KCl] region, in accord with previous results in reversed-phase systems. The profiles of the amphoteric β-lactam antibiotics, as expected, differ from those in usual reversed-phase systems, where an increase of ionic strength increases the retention of charged species on a hydrophobic stationary phase.

Anions are also expected to affect the retention of cationic substances in the present system, since the crown ether–ammonium complex can associate with the counter anion to form an ion pair. The degree of ion pairing and consequent enhancement of the capacity factor are dependent on the dielectric constant of the medium and on the hydrophobicity of the counter ion. The mobile phase used in this experiment includes Cl^- as a common anion in 50% aqueous methanol. However, the solvation of chloride ion in this medium, although perhaps weaker than in aqueous solution, seems unlikely to favour the formation of a hydrophobic ion pair with amphoteric β-lactam antibiotics. The addition of organic acid to the crown ether-containing mobile phase may further enhance the capacity factor.

Application

In order to demonstrate the applicability of the present method, biological samples were chromatographed on an ODS stationary phase. Fig. 9 shows chromato-

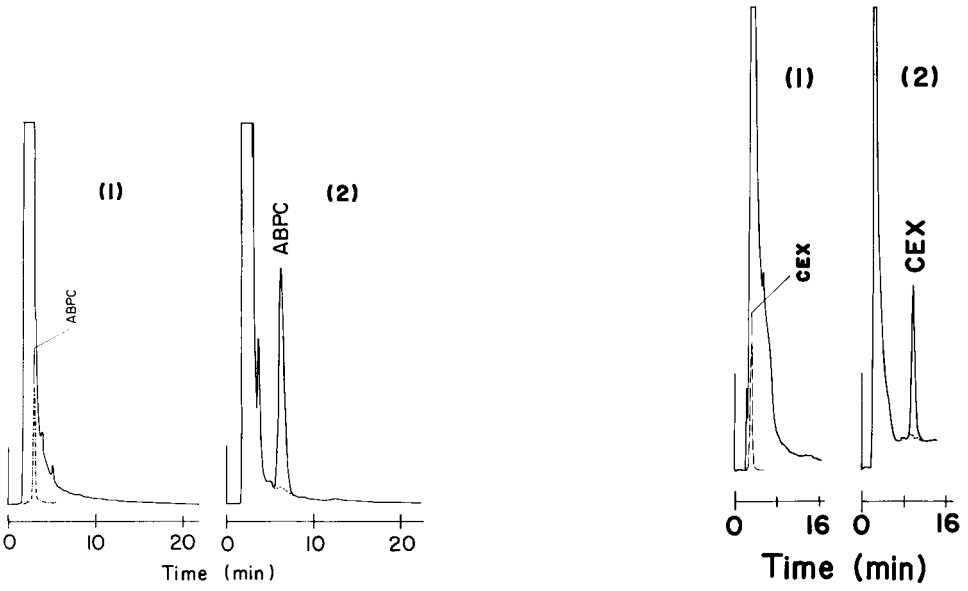

Fig. 9. Separation of ampicillin in human urine. HPLC conditions: stationary phase, Develosil ODS-10 (20 cm × 4 mm I.D.); mobile phase, (1) methanol–water (1:1 v/v), pH 5.2, (2) methanol–water (1:1) containing 20 m*M* 18-crown-6, pH 5.2; flow-rate, 1.0 ml/min; detection, UV 220 nm.

Fig. 10. Separation of cephalexin in human plasma. HPLC conditions: stationary phase, Develosil ODS-10 (20 cm × 4 mm I.D.); mobile phase, (1) methanol–water (1:1), pH 4.7, (2) methanol–water (1:1) containing 6 m*M* dicyclohexyl-18-crown-6, pH 4.7; flow-rate, 1.0 ml/min; detection, UV 254 nm.

grams of urine excreted after oral administration of ABPC to a man, and Fig. 10 indicates the separation of CEX from regular plasma components. Compared with the chromatograms obtained by using a mobile phase without crown ether, the elutions of these amphoteric β-lactam antibiotics are markedly delayed by addition of crown ether with complete separation from endogenous substances, while the retention times of the background peaks remained amost unchanged.

The present method is easily accessible by a simple modification of the mobile phase in conventional reversed-phase HPLC, although special care should be taken because of the toxicity of the crown ether monomer.

REFERENCES

1 L. R. Sousa, D. H. Hoffman, L. Kaplan and D. J. Cram, *J. Amer. Chem. Soc.*, 96 (1974) 7100.
2 G. Dotsevi, Y. Sogah and D. J. Cram, *J. Amer. Chem. Soc.*, 97 (1975) 1259.
3 G. Dotsevi, Y. Sogah and D. J. Cram, *J. Amer. Chem. Soc.*, 98 (1976) 3038.
4 E. Blasius, K.-P. Janzen and G. Klautke, *Z. Anal. Chem.*, 277 (1975) 374.
5 E. Blasius, W. Adrian, K.-P. Janzen and G. Klautke, *J. Chromatogr.*, 96 (1974) 89.
6 E. Blasius and P. G. Maurer, *J. Chromatogr.*, 125 (1976) 511.
7 E. Blasius, K.-P. Janzen, W. Adrian, G. Klautke, R. Lorscheider, P.-G. Maurer, V. B. Nguyen, T. Nguyen Tien, G. Scholten and J. Stockemer, *Z. Anal. Chem.*, 284 (1977) 337.
8 W. H. Delphin and E. P. Horwitz, *Anal. Chem.*, 50 (1978) 843.
9 C. Horváth, W. Melander and A. Nahum, *J. Chromatogr.*, 186 (1979) 371.
10 E. Blasius, K.-P. Janzen, H. Luxenburger, V. B. Nguyen, H. Klotz and J. Stockemer, *J. Chromatogr.*, 167 (1978) 307.
11 E. Blasius, K.-P. Janzen, W. Adrian, W. Klein, H. Klotz, H. Luxenburger, E. Mernke, V. B. Nguyen, T. Nguyen-Tien, R. Rausch, J. Stockemer and A. Toussaint, *Talanta*, 27 (1980) 127.
12 W. J. T. Brugman and J. C. Kraak, *J. Chromatogr.*, 205 (1981) 170.
13 K. Kimura, M. Nakajima and T. Shono, *Anal. Lett.*, 13 (1980) 741.
14 E. Blasius, K.-P. Janzen, M. Keller, H. Lander, T. Nguyen-Tien and G. Scholten, *Talanta*, 27 (1980) 107.
15 M. Igawa, M. Tanaka, Y. Abe, M. Yamaguchi and T. Yamabe, *Nippon Kaisui Gakkaishi*, 33 (1980) 331.
16 M. Igawa, I. Itoh and M. Tanaka, *Bunseki Kagaku (Jap. Anal.)*, 29 (1980) 580.
17 T. Nakagawa, H. Mizunuma, A. Shibukawa and T. Uno, *J. Chromatogr.*, 211 (1981) 1.
18 F. Salto, J. G. Prieto and M. T. Alemany, *J. Pharm. Sci.*, 69 (1980) 501.

Journal of Chromatography, 239 (1982) 707–710
Elsevier Scientific Publishing Company, Amsterdam — Printed in The Netherlands

CHROM. 14,536

Note

Determination of blood transketolase by high-performance liquid chromatography (a preliminary note)

MIEKO KIMURA* and YOSHINORI ITOKAWA
Department of Hygiene, Faculty of Medicine, Kyoto University, Kyoto (Japan)

The technique of high-performance liquid chromatography (HPLC) is utilized in various analytical methods for diagnostic purposes, because of its sensitivity and rapidity.

In order to diagnose the nutritional status of thiamin, total thiamin level in blood and erythrocyte transketolase activity are considered to be the most sensitive measures. Recently we have explored a liquid chromatographic method for the determination of the total thiamin content in blood, which evaluates the nutritional status of thiamin in clinical studies[1].

However, a liquid chromatographic method has not yet been utilized for the assay of transketolase activity in blood, another useful diagnostic measure for thiamin. Under these circumstances, we have contrived a new analytical method to determine the amount of transketolase in blood using HPLC.

EXPERIMENTAL

Apparatus

The system consists of a LC-3A pump for liquid chromatography, a SIL-1A injector, a TSK-Gel G-3000 SW column, a SPD-2A UV detector, a PRR-2A proportioning pump, a RF-500 LCA spectrofluorophotometer and a strip chart recorder. The TSK-Gel column was purchased from Toyo Soda (Tokyo, Japan), and all other equipment was purchased from Shimadzu (Kyoto, Japan).

Preparation of samples

Blood (100 μl) was put in a polypropylene centrifuge tube with 400 μl of 0.05 *M* sodium acetate (pH 7.5) and mixed vigorously with a vortex mixer. The sample was then centrifuged at 33,000 *g* for 60 min. The supernatant solution was used as the sample.

Procedures

Fig. 1 shows the schematic diagram of this system. The mobile phase (0.05 *M* sodium acetate (pH 7.5)) was pumped at a flow-rate of 0.5 ml/min into the HPLC column. An aliquot (200 μl) of the sample was injected onto the column. The absorbance at 280 nm was monitored continuously with a UV detector. A solution containing 0.01 % potassium hexacyanoferrate(III) and 15 % sodium hydroxide was applied

0021-9673/82/0000–0000/$02.75

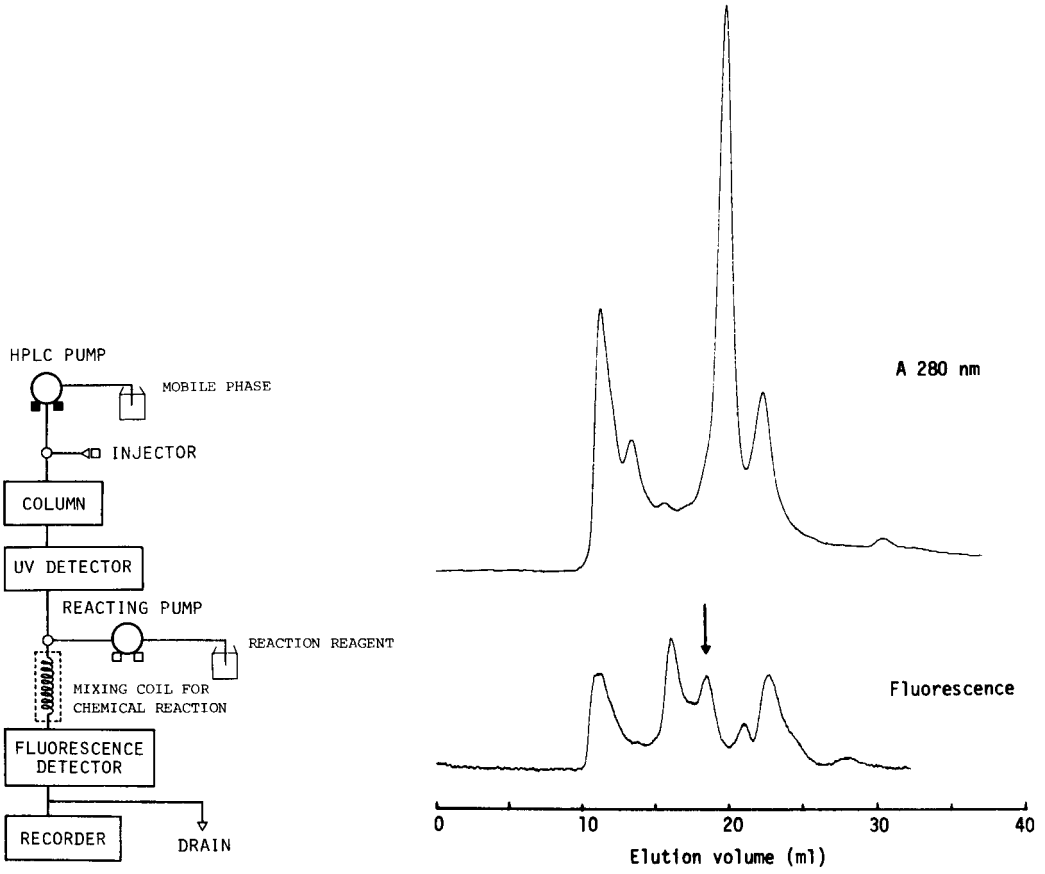

Fig. 1. Schematic diagram of transketolase analyzing system.

Fig. 2. Elution profiles of transketolase in rat blood.

and mixed with the column eluate at a flow-rate of 0.5 ml/min with a proportioning pump (thiochrome reaction). By this procedure, transketolase and other thiamin-binding proteins are converted into fluorophores. The fluorescence was measured using a 12-μl flow-cell with a spectrofluorimeter (excitation, 375 nm; emission, 450 nm) and recorded graphically.

RESULTS AND DISCUSSION

Fig. 2 shows elution profiles of transketolase in normal rat blood. Six peaks each were observed with UV absorption and with fluorescence. Each peak was collected fractionally before the thiochrome reaction and transketolase activity was assayed by the conventional method[2]. The transketolase activity was observed only in the third fluorescent peak.

Elution profiles of blood samples taken from a normal and a thiamin-deficient rat (fed a thiamin-deficient diet for 4 weeks) are shown in Fig. 3. In blood of the thiamin-deficient rat, the peak of transketolase was not detected.

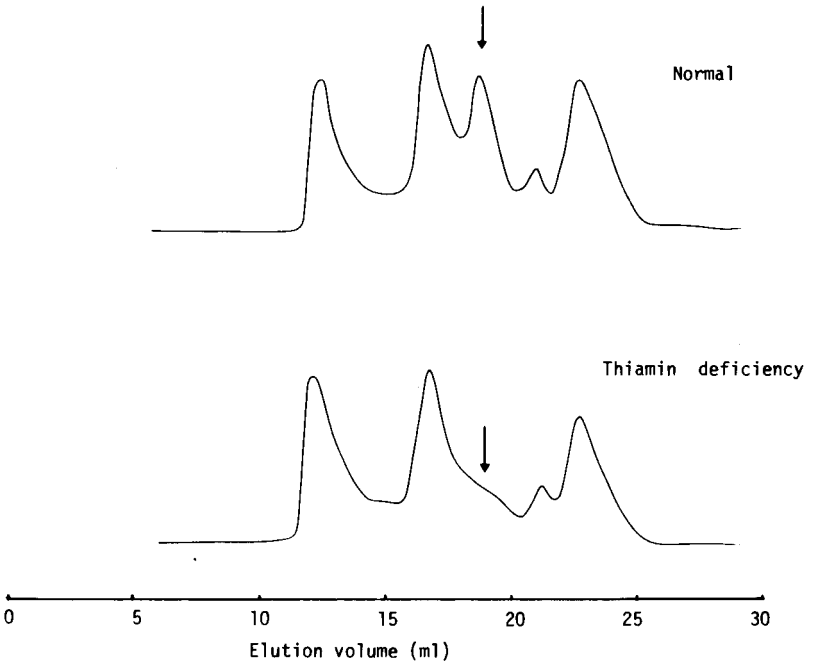

Fig. 3. Elution profiles of transketolase from blood in normal and thiamin-deficient rats.

Fig. 4 shows elution profiles of blood from a normal person and a beriberi patient with fluorescence. The decrease in the peak height of transketolase in the beriberi patient is significant when compared with the normal person. Erythrocyte transketolase activity in these persons determined by the conventional method[2] were

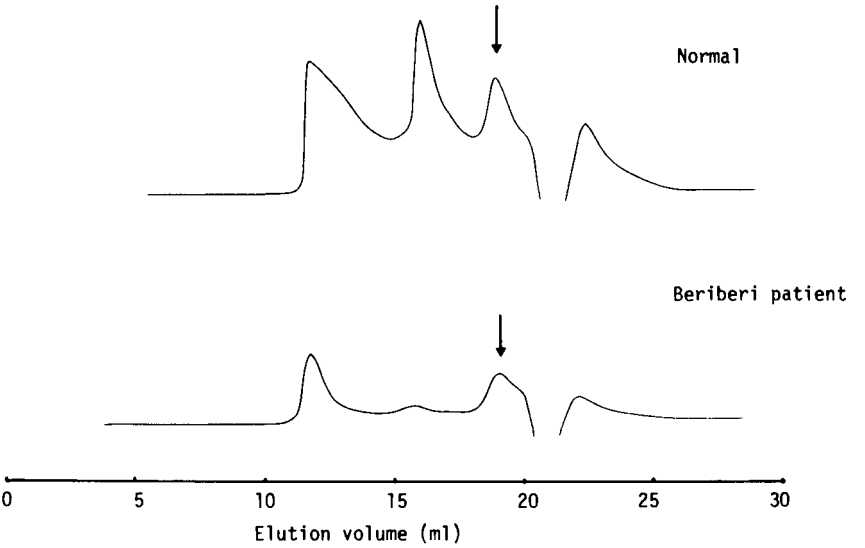

Fig. 4. Elution profiles of transketolase from blood in normal person and beriberi patient.

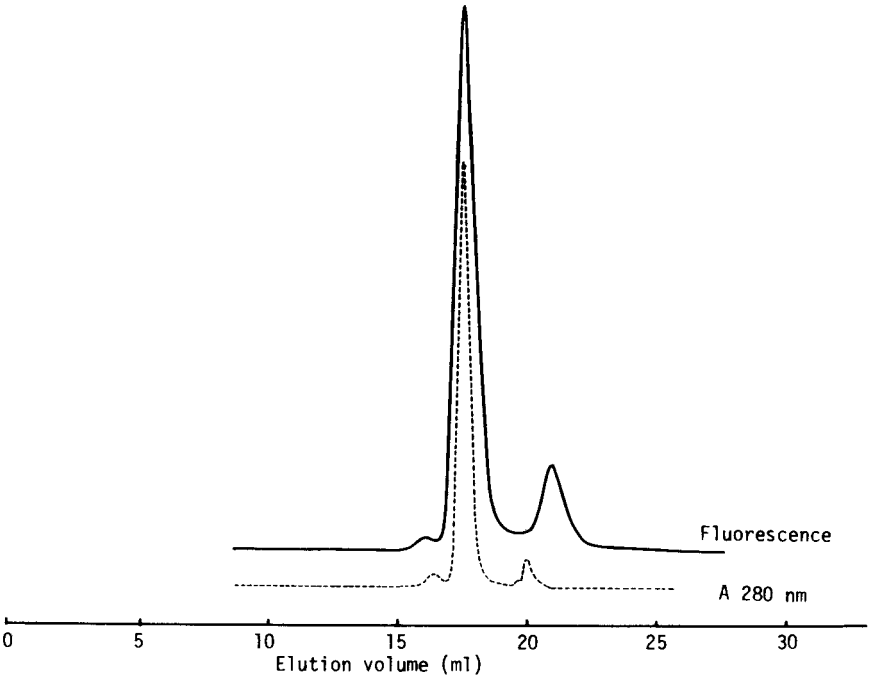

Fig. 5. Elution profiles of crystalline transketolase from baker's yeast.

found to be 656 (μg sedoheptulose produced per ml erythrocytes per h) for the normal person and 324 for the beriberi patient.

Fig. 5 shows the elution profiles of crystalline transketolase from baker's yeast (Sigma, St. Louis, MO, U.S.A.) determined by UV absorption and fluorescence. The elution volume in crystalline transketolase was the same as in blood transketolase.

Although this method is convenient for evaluating the transketolase content of blood, further studies to determine possible discrepancies between this and the conventional method are necessary before utilizing this method in clinical studies. Note that this method does not determine the activity of transketolase but rather the amount of this enzyme. The relationship between the amount and activity of transketolase remains to be clarified.

REFERENCES

1 M. Kimura, T. Fujita and Y. Itokawa, *Clin. Chem.*, 27 (1981) in press.
2 Y. Itokawa, *Brain Res.*, 94 (1975) 475.

Journal of Chromatography, 239 (1982) 711–716
Elsevier Scientific Publishing Company, Amsterdam — Printed in The Netherlands

CHROM. 14,647

DETERMINATION OF PREDNISONE AND PREDNISOLONE IN HUMAN SERUM BY HIGH-PERFORMANCE LIQUID CHROMATOGRAPHY —ESPECIALLY ON IMPAIRED CONVERSION OF CORTICOSTEROIDS IN PATIENTS WITH CHRONIC LIVER DISEASE

TADAHIRO UI*, MASAYUKI MITSUNAGA, TERUJI TANAKA and MASAHARU HORIGUCHI
Department of Medicine, The Third Hospital, Jikei University School of Medicine, 4-11-1 Izumihoncho Komae, Tokyo (Japan)

SUMMARY

A reliable and rapid method is described for the determination of prednisone and prednisolone in human serum by high-performance liquid chromatography, using a Zorbax-SIL column with dichloromethane–ethanol (92.5:7.5) as eluent, with UV detection at 254 nm.

Metabolites and endogenous hydrocortisone did not interfere with the determination of prednisone and prednisolone. The alteration of corticosteroid concentrations in serum from patients with chronic liver diseases was studied following a single oral administration of prednisone or prednisolone (30 mg).

The proposed method showed good separation of several corticosteroids and was time-saving, suitable and reliable for the routine analysis of corticosteroids in human serum.

INTRODUCTION

The application of high-performance liquid chromatography (HPLC) to the determination of human serum concentrations of synthetic corticosteroids has been reported by several researchers[1–4].

Determination of corticosteroids in human serum requires specificity and high sensitivity, two demands that can be satisfied by using suitable phase systems and efficient columns in HPLC. At the same time, chromatographic parameters and extraction methods should be optimized to determine low concentrations (200–500 pg) with reasonable reliability.

HPLC is very effective for the separation of synthetic corticosteroids, either singly or as a group[5–8]. The practical application for the routine determination of serum prednisone and prednisolone has been studied, and this paper describes an HPLC method that is sufficiently sensitive and specific for the determination of serum prednisone and prednisolone in order to study the dynamic metabolism of synthetic corticosteroids in liver diseases.

0021-9673/82/0000–0000/$02.75

EXPERIMENTAL

Materials

Prednisone and prednisolone (Sigma, St. Louis, MO, U.S.A.) were used for the preparation of standard solutions. Δ^4-Pregnene-17α, 20β, 21-triol-3,11-dione (Sigma) was used as internal standard. Solvents used for mobile phase were dichloromethane (Wako, Osaka, Japan) and ethanol (Kanto, Tokyo, Japan).

Chromatographic conditions

A constant-volume HPLC Shimadzu Model LC-1 type with SIL-injector, and Shimadzu Model UVD-2 UV detector (254 nm), were used. The column Zorbax-SIL (25 cm × 4.6 mm I.D.) containing 5-μm spherical silica gel was packed in the stainless-steel tube purchased from Shimadzu Corporation.

The mobile phase was dichloromethane–ethanol (92.5:7.5) at a flow-rate of 1 ml/min.

Reagent solutions

Prednisone and prednisolone, accurately weighed, were dissolved in dichloromethane–ethanol (9:1) in a 100-ml volumetric flask. An aliquot of this solution was diluted with dichloromethane–ethanol (9:1) to produce a final solution of the desired concentration.

A solution of the internal standard, Δ^4-pregnene-17α,20β,21-triol-3,11-dione, was prepared by a similar procedure.

Procedure

The extraction procedure for prednisone and prednisolone from serum is as follows.

To 0.5 ml of serum, 100 μl of internal standard solution (corresponding to 250 ng of Δ^4-pregnene-17α,20β,21-triol-3,11-dione, 0.2 ml of 1.25 *M* sodium hydroxide and 10 ml of dichloromethane were added. The solution was shaken for 10 min in a triturium, and stored at room temperature for 30 min. The upper phase of the extracted solution was aspirated off, and 1 ml of distilled water was added to 10 ml of the lower phase, then stored for 30 min at room temperature. The 10 ml of the lower phase was evaporated to dryness in a rotary evaporator at 40°C. The residue was dissolved in 100 μl of dichloromethane–ethanol (9:1), and 10 μl of this was injected on to the chromatograph using a SGE 10-μl syringe (North Melbourne, Australia).

Subjects

In order to study the dynamic metabolism of synthetic corticosteroids (prednisone and prednisolone) in liver diseases, rapid prednisone or prednisolone tests were performed on five healthy volunteers and seven patients with decompensated liver cirrhosis. Diagnosis of liver cirrhosis was confirmed by needle biopsy under laparoscopic observation. None of the patients had previously been treated with glucocorticoids. None had been taking drugs believed to induce microsomal enzymes.

After preload blood had been sampled, all subjects orally received (on randomised days) 30 mg of prednisone or prednisolone with 120 ml of water. Peripheral

venous blood samples were drawn after 15, 30, 60, 120, 180, 240 and 360 min, under fasting conditions. The serum was stored at −20°C until analysis.

RESULTS AND DISCUSSION

The chromatogram recorded at 254 nm (Fig. 1) showed satisfactory separation of the steroids, and the following retention times were obtained: prednisone, 4 min 40 sec; cortisol (F), 6 min; prednisolone, 7 min; internal standard, 9 min. It is worthy of note that prednisolone was clearly separated from its metabolites, prednisone and endogenous hydrocortisone.

Fig. 2 shows a chromatogram of a serum blank and HPLC pattern after addition of three standard steroids to serum sample. It is evident that no interfering compounds were extracted from serum and that any endogenous substances did not interfere with simultaneous analysis of prednisone and prednisolone.

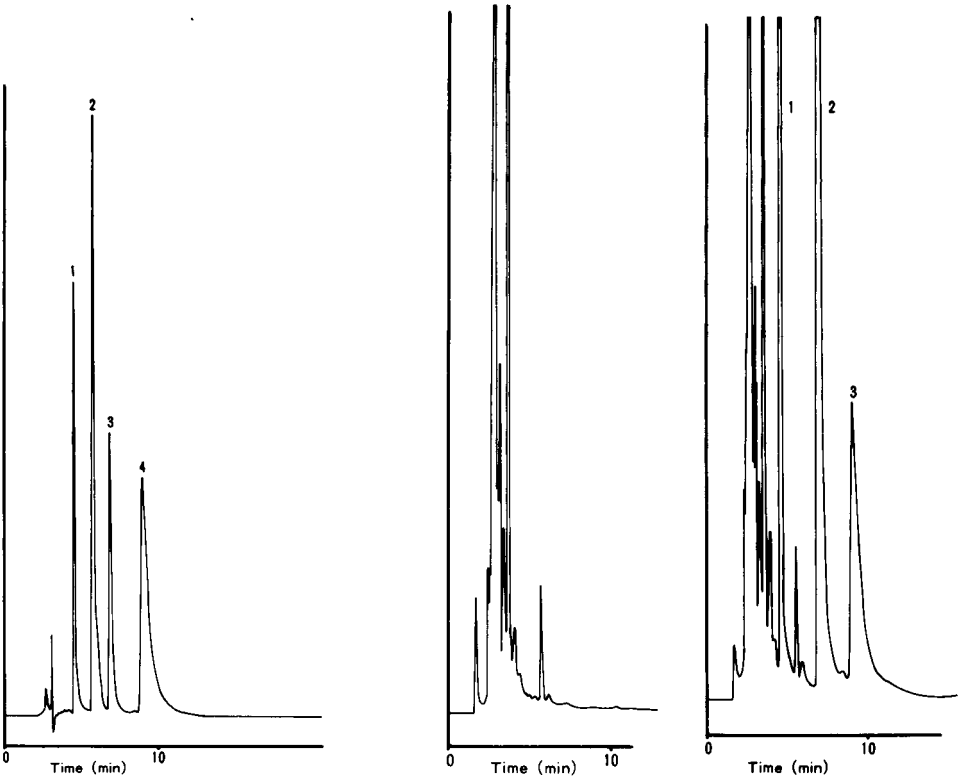

Fig. 1. HPLC profile of four standard steroids added to dichloromethane–ethanol (90:10). Peaks: 1 = prednisone; 2 = hydrocortisone; 3 = prednisolone; 4 = Δ^4-pregnene-17α,20β-21-triol-3,11-dione.

Fig. 2. HPLC profile of serum in patient with liver cirrhosis before addition of prednisone (left). HPLC profile of three standard steroids added to serum sample. Peaks: 1 = prednisone; 2 = prednisolone; 3 = internal standard (right).

The calibration curves for the synthetic corticosteroids are showed in Fig. 3.

The coefficients of variation (C.V.), derived from using spiked serum samples were, at the lowest quantifiable limits: prednisone, 1.0%; hydrocortisone, 0.9% prednisolone, 1.2%; internal standard, 1.2%.

The recoveries of prednisone, prednisolone and internal standard from a pooled serum samples were calculated by chromatographing extracts before and after adding known amounts of these steroids. Constant recovery of 83.4% was observed for each of steroids.

Rapid prednisolone test

A rapid prednisolone test was performed in order to elucidate the reserve function of corticosteroid metabolism in liver disease. Fig. 4 shows the serum concentration of prednisolone after oral administration of prednisolone. There was no significant difference between controls and cirrhosis patients with the respect to the maximal concentrations or to the concentration of prednisolone.

A rapid prednisone test

In the same way, a rapid prednisone test was performed. Fig. 5 shows the HPLC pattern of serum prednisone and prednisolone in patients with liver cirrhosis. The time course of changes in the amount of each of these steroids varied. In the control group, the average maximal concentrations of prednisone and prednisolone were usually identified at 60 min (prednisone, 23.7 ng/ml; prednisolone, 171 ng/ml), then decreased. In the group with chronic liver diseases, the average maximal concentrations of these steroids were identified at 30 min (prednisone, 332 ng/ml; prednisolone, 113 ng/ml), then gradually decreased during 6 h (Fig. 6).

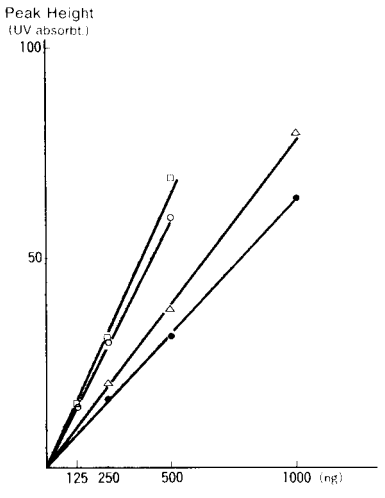

Fig. 3. Calibration curves for the determination of steroids. ●, Hydrocortisone; ○, prednisone; △, prednisolone; □, Δ^4-pregnene-17α,20β,21-triol-3,11-dione.

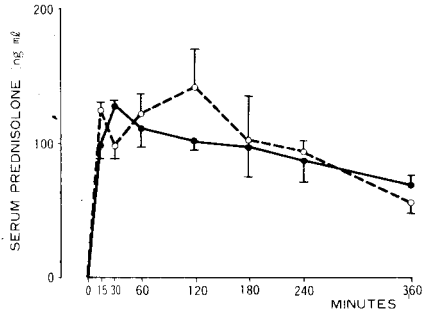

Fig. 4. Serum concentration of prednisolone after oral administration of prednisolone in patients with liver cirrhosis, and in controls. Mean ± S.E.M. (n = 4). ○ – – – ○, control; ●—●, liver cirrhosis.

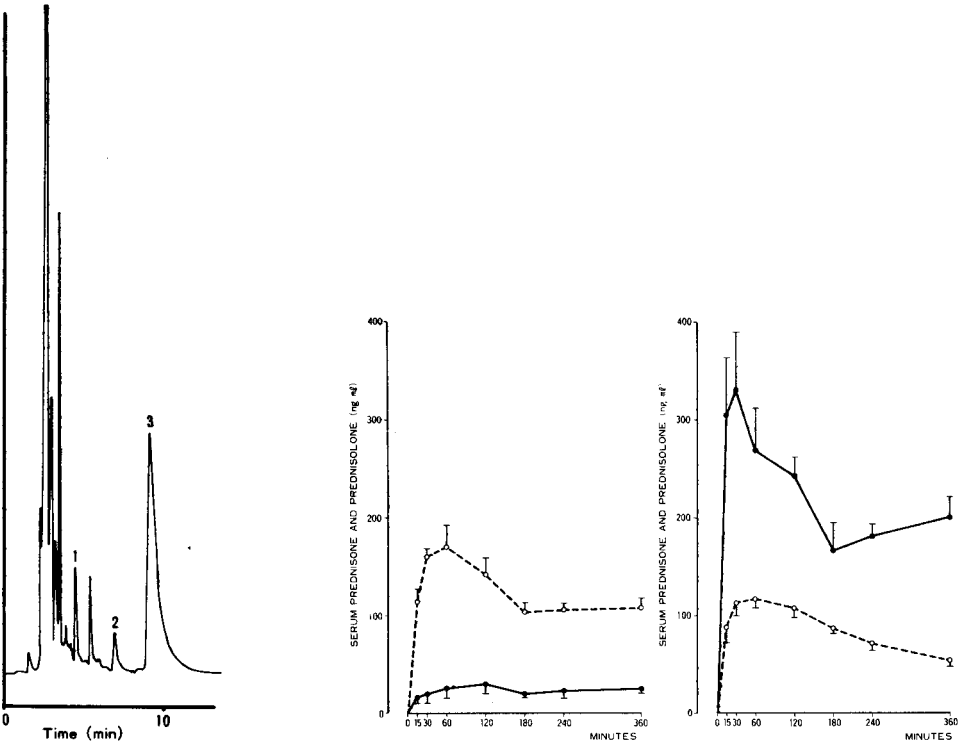

Fig. 5. HPLC profile of serum prednisone and prednisolone in patients with liver cirrhosis given 30 mg of prednisone. Peaks: 1 = prednisone; 2 = prednisolone; 3 = internal standard.

Fig. 6. Serum concentration of prednisone (●— ●) and prednisolone (○ – – – ○) after oral administration of prednisone to patients with liver cirrhosis (right) and controls (left). Mean ± S.E.M.; controls: $n = 5$, patients with liver cirrhosis; $n = 7$.

CONCLUSION

Several methods have been described for the determination of prednisone and prednisolone in human serum[1–4,9]. These methods were sensitive, specific and reproducible; however, long retention times and comparatively complex procedures of extraction effectively prevent their use in a bioavailability trial. The simultaneous determination of prednisone and prednisolone by the present method proved to be sensitive, specific, efficient, reproducible and clinically useful. It has proved robust in use with fast analysis time, less than 12 min for each sample, and no significant problems of late eluting peaks. It is possible to perform more than 20 samples by this method in one day. The procedure described in this paper also facilitates the characterization of prednisone and its pharmacologically active metabolite, prednisolone. The simple procedure described is likely to be available in any laboratory practising HPLC and is cheap and easy to run and maintain.

Prednisone is frequently prescribed for the treatment of chronic active liver disease in western countries, and must be reduced at the 11β-keto group for conversion into its active therapeutic derivative, prednisolone[10]. This conversion depends on an 11β-dehydrogenase, mainly located in the liver[11].

A few studies have been reported of impaired conversion of prednisone into prednisolone in patients with liver cirrhosis[12,13] by means of radioimmunoassay. But this method is not attractive for bioavailability trials, because of cross-reactivity with endogenous cortisone and cortisol[14].

On the basis of the HPLC method described in this paper, it can be concluded that the present method is superior to other techniques for the analysis of corticosteroids, and that simultaneous determination of prednisone and prednisolone by HPLC shows that conversion of prednisone into prednisolone is impaired in patients with liver cirrhosis.

ACKNOWLEDGEMENT

We acknowledge beneficial discussions with Dr. E. Okada and Dr. K. Kitsuwa.

REFERENCES

1 W. Wortmann, C. Schnabel and J. C. Touchstone, *J. Chromatogr.*, 84 (1973) 396.
2 J. C. K. Loo, A. G. Butterfield, J. Moffatt and N. Jordan, *J. Chromatogr.*, 143 (1977) 275.
3 P. de Moor, O. Steeno, M. Raskin and A. Hendrikx, *Acta Endocrinol.*, 33 (1960) 297.
4 N. R. Scott, J. Chakraborty and V. Marks, *Anal. Biochem.*, 108 (1980) 266.
5 F. K. Trefz, D. J. Byrd and W. Kochen, *J. Chromatogr.*, 107 (1975) 181.
6 J. C. Touchstone and W. Wortmann, *J. Chromatogr.*, 76 (1973) 244.
7 N. R. Scott and P. F. Dixon, *J. Chromatogr.*, 164 (1979) 29.
8 J. H. M. Van den Berg, C. H. R. Mol, R. S. Deelder and J. H. H. Thijssen, *Clin. Chim. Acta*, 78 (1977) 165.
9 Z. Saito, E. Amatsu, T. Ono, S. Hihumi, T. Mimou, T. Hashiba, S. Sakato, M. Miyamoto and R. Takeda, *Folia Endocrinol. Jap.*, 55 (1979) 1296.
10 J. S. Jenkins and P. A. Sampson, *Brit. Med. J.*, 2 (1967) 205.
11 I. E. Bush and V. B. Mahesh, *Biochem. J.*, 93 (1964) 236.
12 M. Uribe, S. W. Schalm, W. H. J. Summerskill and V. L. W. Go, *Gut*, 19 (1978) 1131.
13 S. Madsbad, B. Bjerregaard, J. H. Henriksen, E. Juhl and H. Kehlet, *Gut*, 21 (1980) 52.
14 W. A. Colburn, *Steroids*, 24 (1974) 95.

Journal of Chromatography, 239 (1982) 717–721
Elsevier Scientific Publishing Company, Amsterdam — Printed in The Netherlands

CHROM. 14,624

DETERMINATION OF 5′-NUCLEOTIDASE ACTIVITY IN HUMAN ERYTHROCYTES AND PLASMA USING HIGH-PERFORMANCE LIQUID CHROMATOGRAPHY

TADASHI SAKAI*, SUSUMU YANAGIHARA and KOICHI USHIO
Centre of Occupational Medicine, Tokyo Labour Accident Hospital, 13-21, Omoriminami-4-Chome, Ota-Ku, Tokyo 143 (Japan)

SUMMARY

A method is described for the determination of 5′-nucleotidase activity in human erythrocytes and plasma. Using reversed-phase high-performance liquid chromatography; the product (uridine) was separated from the substrate (uridine-5′-monophosphate) in less than 4 min. The activity determined closely agreed with that determined by the conventional method, in which the inorganic phosphate released is measured. The present method eliminates the need for dialysis of enzyme solution prior to the assay, and offers several advantages over other assay methods, including high sensitivity.

INTRODUCTION

5′-Nucleotidase is widespread in various animal tissues and determinations of the activity in human erythrocytes and serum have diagnostic value for some disorders. The enzyme activity in erythrocytes (pyrimidine 5′-nucleotidase) is deficient in hereditary haemolytic anaemia and is inhibited in lead poisoning[1–5]. Serum 5′-nucleotidase activity is increased in diseases of the liver and bilary tract[6,7].

High-performance liquid chromatography (HPLC) has been utilized for the assay of several enzymes[8–12]. This paper describes an HPLC method for the determination of the activity in human erythrocytes and in plasma. Uridine 5′-monophosphate (UMP) is used as the substrate and the product (uridine) formed is separated by automated reversed-phase chromatography.

EXPERIMENTAL

Materials

UMP, uridine and tris(hydroxymethyl)aminomethane (Tris) were obtained from Sigma (St. Louis, MO, U.S.A.). Methanol, potassium dihydrogen phosphate, hydrochloric acid, and magnesium chloride were purchased from Wako (Osaka, Japan) and 1-decanesulphonic acid from Tokyo Kasei Kogyo (Tokyo, Japan).

0021-9673/82/0000–0000/$02.75

Preparation of buffered substrate

For low blank values to be obtained in the assay, commercially available UMP was purified by ion-exchange chromatography[13]. All procedures for purification were carried out at 4°C. A 25-ml volume of 50 m*M* UMP was applied to a 3 × 4 cm column of 400 mesh Dowex 1-X8 (Cl^-). The column was washed with 1 l of water to remove uridine. Subsequent elution with 20 m*M* HCl gave UMP free from uridine. Peak fractions (about 160 ml) were pooled and the concentration of UMP was determined from the absorbance at 262 nm in 10 m*M* HCl, with an extinction coefficient of $10.0 \cdot 10^3$ (ref. 14). A 160-ml volume of purified UMP (the pooled fractions) was added to 10 ml of 1 *M* Tris, and carefully adjusted the pH to 7.7 with 1.5 *M* HCl. After adjusting the volume to 200 ml by adding water, the concentration of UMP was also adjusted to 3.12 m*M* with 50 m*M* Tris–HCl buffer pH 7.7. Thus prepared Tris-buffered UMP was stored at −20°C.

Enzyme solution and incubation procedure

Heparinized venous blood from normal subjects was the enzyme source. Erythrocytes were washed twice with a 10-fold volume of saline (0.9%), and then suspended in the saline (about 50% suspension). The enzyme solution was prepared by diluting 50 µl of erythrocyte suspension or 100 µl of plasma to 300 µl with distilled water. The standard assay mixture contained 300 µl of the enzyme solution, 400 µl of Tris-buffered UMP, and 50 µl of 150 m*M* $MgCl_2$. The incubation was carried out at 37°C for 60 min, and the reaction was terminated by placing tubes in boiling water for 3 min. The mixture was diluted 2-fold with distilled water and then centrifuged. The resulting supernatant was used for the HPLC analysis.

Automated HPLC

The chromatographic system employed was a Shimazu LC-3A (Shimazu, Kyoto, Japan), consisting of a Model LC-3A pump, an automatic sample injector (SIL-2AS), a column oven (CTO-2AS), a variable-wavelength spectrophotometer (SPD-1) and an integrator (C-R1A). A disposable MPLC guard column (RP-18 cartridge, 30 × 4.6 mm; Brownlee Labs., CA, U.S.A.) and a 5-µm reversed-phase column (Shodex ODSpak, 150 × 4.6 mm; Showa Denko, Tokyo, Japan) were used for the separations. The mobile phase was 5% methanol containing 5 m*M* potassium dihydrogen phosphate and 0.25 m*M* 1-decanesulphonic acid. The flow-rate, column temperature, and wavelength were set at 1.0 ml/min, 40°C and 254 nm, respectively. Samples were cooled to 4°C during a series of analyses, and 10 or 20 µl were injected at 7-min intervals.

Other analyses

The pyrimidine 5′-nucleotidase activity of erythrocyte lysate dialysed was also determined by the method of Valentine *et al.*[1]. Hb concentrations in erythrocyte suspension and lysate were determined using a haemoglobin counter (TOA Medical Electronic Co., Tokyo, Japan), which directly measured Hb concentrations spectrophotometrically as cyanmethaemoglobin.

RESULTS AND DISCUSSION

In the present system, the desired separation of the product (uridine) from the substrate (UMP) and blood components was achieved in less than 4 min (Fig. 1). The substrate used here was almost free from uridine. In the blank with no added UMP no uridine peak was found in either erythrocytes or plasma, from normal and abnormal subjects. There was also no detectable peak of uridine even if the samples stored at 4°C for 2 weeks were incubated without UMP, although two or three other peaks that were completely separated from the uridine peak appeared in the chromatogram. Hence the blank for each sample can be omitted in routine analysis.

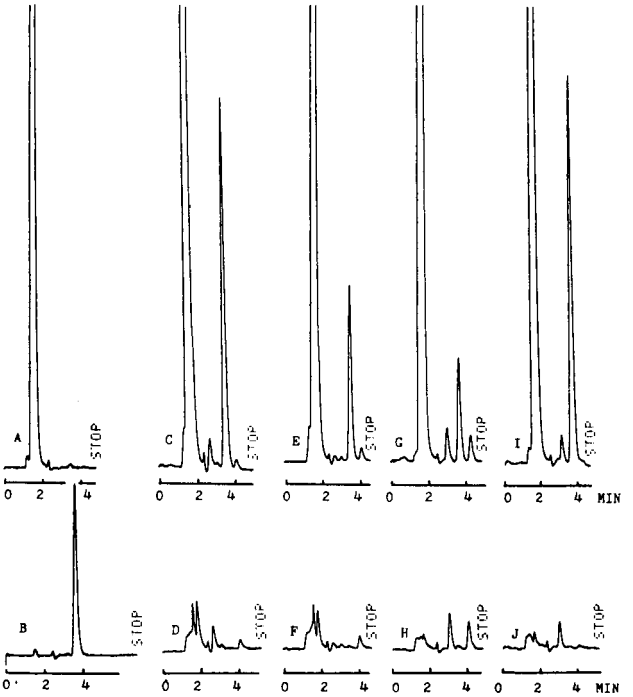

Fig. 1. Separations of uridine from UMP and blood components. A and B were the chromatogram of UMP in the reaction mixture without enzyme, and uridine standard (50 μM), respectively. Samples were incubated with (C, E, G and I) or without UMP (D, F, H and J). C and D: erythrocytes from a normal subject; E and F: erythrocytes from a lead-poisoned subject; G and H: plasma from a normal subject; I and J: plasma from a person suffering from hepatobiliary disease.

There was no effect of boiling on the uridine level in the reaction mixture. The reaction of both enzymes was linear over a broad range with respect to the amount of enzyme added (less than 100 μl).

Fig. 2 indicates the relationship between reaction time and the activity. A reaction time of 60 min was adopted because it seemed to be sufficiently long for the decreased activity to be detected. In the present method measuring uridine with high sensitivity, the reaction time was shortened for erythrocyte enzyme. In the conven-

TABLE I

PRECISION OF THE ASSAY

	Mean ± S.D. (n = 10)	*C.V. (%)*
Erythrocytes		
normal	16.0 ± 0.342 μmol/h/g Hb	2.14
abnormal*	7.28 ± 0.376 μmol/h/g Hb	5.16
Plasma		
normal	13.3 ± 0.299 μmol/min/l	2.25
abnormal**	43.2 ± 0.879 μmol/min/l	2.03

* Lead poisoning.
** Hepatobiliary disease.

tional method it is incubated for 2 h for enough amount of phosphate to be released[1]. Michaelis constants for UMP in normal erythrocyte enzyme were 0.154 m*M*.

To evaluate the precision of the method, we calculated within-run coefficients of variation for normal and abnormal samples (Table I). We assayed 10 replicates for each sample in a single analytical run. The results indicate that the method is sufficiently accurate to detect the abnormal activity.

The enzyme activity in erythrocyte lysate that had been dialysed overnight was measured both by the method of Valentine *et al.*[1] and by the present method (Table II). The data for the uridine formed measured by the present method agreed well with those obtained by the conventional method, measuring inorganic phosphate released. This suggests that all of the uridine formed from UMP can be measured by the present method. The S.D. shown in Table II included both the biological variation

TABLE II

COMPARISON OF THE HPLC METHOD WITH THE METHOD OF VALENTINE *ET AL.*[1]

Sample No.	*Pyrimidine 5'-nucleotidase activity (μmole/h · g Hb)*	
	HPLC method	*Method of Valentine et al.*[1]
1	14.6	15.2
2	11.7	12.1
3	14.4	14.7
4	12.9	13.2
5	13.6	14.8
6	15.3	15.9
7	12.6	12.2
8	10.8	11.1
9	11.4	12.0
10	13.3	13.0
Mean ± S.D.	13.1 ± 1.40	13.5 ± 1.54

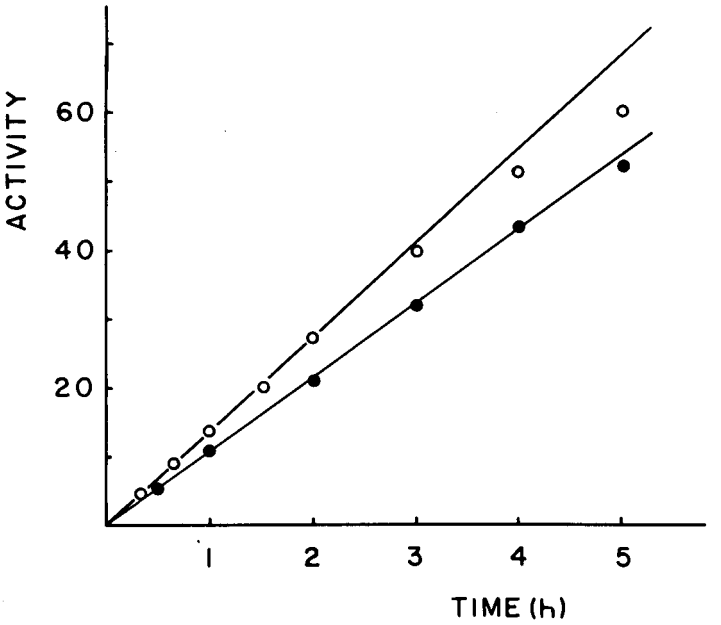

Fig. 2. Relationship between time of incubation and the activity. ○, Erythrocyte enzyme (μmol/h/g Hb); ●, plasma enzyme (μmol/min/l).

and the S.D. of the method mentioned above. The biological one or the normal limit of the activity remains to be determined.

The method of Valentine *et al.*[1] requires dialysis of erythrocyte lysate prior to enzyme assay, to remove inorganic phosphate that is already present in erythrocytes. It is also necessary to incubate the samples for relatively long periods of time for enough phosphate to be released. In our method, in contrast, dialysis of the samples is not necessary and the incubation time is shortened, because of the negligible amount of endogenous uridine and the high intensity of the absorption of uridine at 254 nm. Hence the present method should be more useful for routine analysis in clinical laboratories and for biochemical research on the enzyme.

REFERENCES

1 W. N. Valentine, K. Fink, D. E. Paglia, S. R. Harris and W. S. Adams, *J. Clin. Invest.*, 54 (1974) 866.
2 D. E. Paglia, W. N. Valentine and J. G. Dahlgren, *J. Clin. Invest.*, 56 (1975) 1164.
3 I. Ben-Bassat, F. Brok-Simoni, G. Kende, F. Holtzmann and B. Ramot, *Blood*, 47 (1976) 919.
4 W. N. Valentine, D. E. Paglia, K. Fink and G. Madokoro, *J. Clin. Invest.*, 58 (1976) 926.
5 D. E. Paglia, W. N. Valentine and K. Fink, *J. Clin. Invest.*, 60 (1977) 1362.
6 T. F. Dixon and M. Purdom, *J. Clin. Pathol.*, 7 (1954) 341.
7 A. Belfield and D. M. Goldberg, *J. Clin. Pathol.*, 22 (1969) 144.
8 S. N. Pennington, *Anal. Chem.*, 43 (1971) 1701.
9 J. Uberti, J. J. Lightbody and R. M. Johnson, *Anal. Chem.*, 80 (1977) 1.
10 R. Hartwick, A. Jeffries, A. Krstulovic and P. R. Brown, *J. Chromatogr. Sci.*, 16 (1978) 427.
11 N. D. Danielson and J. A. Huth, *J. Chromatogr.*, 221 (1980) 39.
12 S. S. Chen and D. Hsu, *J. Chromatogr.*, 210 (1981) 186.
13 M. Smith and H. G. Khorana, *Methods Enzymol.*, 6 (1963) 645.
14 R. M. Bock and N.-S. Ling, *Arch. Biochem. Biophys.*, 62 (1956) 253.

Journal of Chromatography, 239 (1982) 723–732
Elsevier Scientific Publishing Company, Amsterdam — Printed in The Netherlands

CHROM. 14,672

PRE-COLUMN LABELLING FOR HIGH-PERFORMANCE LIQUID CHROMATOGRAPHY OF AMINO ACIDS WITH 7-FLUORO-4-NITROBENZO-2-OXA-1,3-DIAZOLE AND ITS APPLICATION TO PROTEIN HYDROLYSATES*

YOSHIHIKO WATANABE and KAZUHIRO IMAI*
Department of Analytical Chemistry, Faculty of Pharmaceutical Sciences, University of Tokyo, 7-3-1, Hongo, Bunkyo-ku, Tokyo 113 (Japan)

SUMMARY

A high-performance liquid chromatographic (HPLC) method for the determination for minute amounts of eighteen amino acids of the presumed components of protein hydrolysates is presented. The method consists of derivatization of the amino acids with a new fluorigenic reagent, 7-fluoro-4-nitrobenzo-2-oxa-1,3-diazole (NBD-F), in ethanol–0.1 *M* phosphate buffer (pH 8.0) (50:50) at 60°C for 1 min, separation of the resultant fluorophores, including ε-aminocaproic acid as an internal standard, on a reversed-phase column (μBondapak C_{18}) by (i) isocratic elution by solvent A [methanol–tetrahydrofuran (THF) in 0.1 *M* phosphate buffer (pH 6.0) (3.75:1.6:94.65)] for 24 min, (ii) a linear gradient of 100% solvent A to 100% solvent B [methanol–THF in 0.1 *M* phosphate buffer (pH 6.0) (25:15:60)] over 30 min, (iii) isocratic elution using solvent B for 6 min and (iv) an isocratic elution by solvent C [methanol–water (40:60)] for 12 min, and detection at 530 nm with excitation at 470 nm. The detection limit for each amino acid is *ca.* 10 fmol. Profile analysis was achieved for *ca.* 1.5 μg of protein hydrolysates (rabbit pyruvate kinase-M_1, rabbit aldolase A and papain) in the final pre-column labelling reaction mixture for HPLC.

INTRODUCTION

In order to determine small amounts of amino acids, such as in protein or peptide hydrolysates, a sensitive method is mandatory. Fluorimetry is valid for such a use. However, the popular fluorigenic reagents, fluorescamine[1] and *o*-phthalaldehyde (OPA)[2], are not suitable for such a purpose because they are not reactive to secondary amino acids such as Pro and Hyp. Although conversion of secondary amino acids into primary amines using N-chlorosuccinimide prior to the fluorigenic reaction has been developed[3], the excess of the latter reagent required obstructs the fluorescence yield of the generated fluorophores.

* Presented in part at the *1981 Pittsburgh Conference on Analytical Chemistry and Applied Spectroscopy, March 10–13*, Abstracts, p. 647.

0021-9673/82/0000–0000/$02.75

7-Chloro-4-nitrobenzo-2-oxa-1,3-diazole (NBD-Cl)[4] has recently been extensively used for the detection and determination of secondary amino acids by pre-column labelling[5,6] or a post-column reaction technique[7]. Ahnoff *et al.*[6] showed that NBD-Cl is less reactive to amino acids having primary amino groups than hydroxide or methoxide anions in the reaction medium, so that solvolysis occurred before the reaction with the amino acids having primary amino groups was complete. In the case of Lys, which has an α-amino group plus ε-amino group, the reaction process is rather complex. Thus two fluorescent products for Lys were obtained which might be mono- and bis-derivatives.

Previously[8,9], we reported that 7-fluoro-4-nitrobenzo-2-oxa-1,3-diazole (NBD-F), presumably a more reactive homologue of NBD-Cl, proved to be more reactive to the secondary amino acids than NBD-Cl or NBD-Br, so that even amino acids having primary amino groups, such as Asp, Glu, Ser, Gly, Thr and Ala, could be derivatized simultaneously with Pro and Hyp at pH 8.0 at 60°C for 2.5 min. The derivatives were separated and detected at 1 pmol level in high-performance liquid chromatography (HPLC).

In this paper, we describe HPLC separation and determination of eighteen, rather than eight in the previous paper[9], amino acid standards derivatized with NBD-F. A profile analysis of amino acids in protein hydrolysates is also reported.

EXPERIMENTAL

Materials

NBD-F was synthesized by the method of Nunno *et al.*[10]. Amino acids were purchased from Kyowa Hakko Co., Tokyo, Japan. All other chemicals were of analytical reagent grade. Methanol and tetrahydrofuran (THF) were of HPLC grade (Nakarai Kagaku Co., Tokyo, Japan). Water was deionized and doubly distilled. The pH of the borate buffer (Na^+, 0.1 *M*, pH 8.0) was adjusted with 0.1 *M* hydrochloric acid. The phosphate buffers (pH 6.0–7.5) used as mobile phases, prepared with 0.1 *M* NaH_2PO_4 and 0.1 *M* Na_2HPO_4, were filtered through Toyo No. 6 filter-paper (Toyo Roshi, Tokyo) prior to use.

Rabbit pyruvate kinase-M_1 (E.C. 2.7.1.40), rabbit aldolase A and papain (E.C. 3.4.22.2) which were used as standard proteins were hydrolysed in the usual way with 6 *M* hydrochloric acid at 110°C for 24 h in evacuated sealed tubes. The lyophilysed hydrolysates were kindly donated by Dr. Noboru Nakai of Fukui Medical School.

HPLC

For the isocratic elution studies, a Model 6000A pump equipped with a U6K Universal Injector (Waters Assoc., Milford, MA, U.S.A.) was employed. For the gradient elution studies, two Model 6000A pumps, controlled by a Model 660 solvent programmer (Waters Assoc.) were used. A guard column of Bondapak C_{18}–Corasil (20 × 3.9 mm) and a main column of μBondapak C_{18} (300 × 3.9 mm, 10 μm) connected to the former column were used. All eluting solvents were filtered and degassed prior to use. The flow-rate was 2.0 ml/min. The column temperature was ambient. The void volume of the column was measured with NBD–Asp as a marker under elution with 100% methanol. A Hitachi 560-10S spectrofluorimeter equipped with a 18 μl flow cell was used with an excitation wavelength of 470 nm and an emission at 530 nm.

Derivatization procedure

To a 500-μl conical tube were added 10 μl of a mixed amino acid standards solution (500 pmol each) and 10 μl of borate buffer (0.1 *M*, pH 8.0). To this solution 20 μl of NBD-F (50 m*M* in ethanol, freshly prepared) were added and the tube was capped and covered with aluminium foil. The vessel was then heated at 60°C for 1 min. After cooling on ice–water, 460 μl of 0.005 *M* hydrochloric acid were added to the reaction mixture. A 10-μl volume of the solution was injected onto the column. Ten 1-μl aliquots of protein hydrolysates (*ca.* 15 μg each) mentioned under *Materials*, dissolved in 100 μl of water containing ε-aminocaproic acid (10 nmol), were derivatized and treated as for the standard amino acids.

RESULTS

Optimization of the derivatization

In the preceding paper[8], we reported that the rate of formation of the fluorophores derived from the reaction of amino acids with NBD-F increased with increasing volume of organic solvents, pH of buffer and reaction temperature. Therefore, in a previous paper[9], the reaction for derivatization prior to HPLC was performed in 50% ethanol at pH 8.0 and 60°C for 2.5 min. In this experiment, to prevent degradation of the fluorophores and to decrease the rate of hydrolysis of NBD-F to 7-hydroxy-4-nitrobenzo-2-oxa-1,3-diazole (NBD-OH), which interferes with the peaks of NBD–Gly and –Arg, milder conditions (in 50% ethanol at pH 8.0 and 60°C for 1 min) were selected.

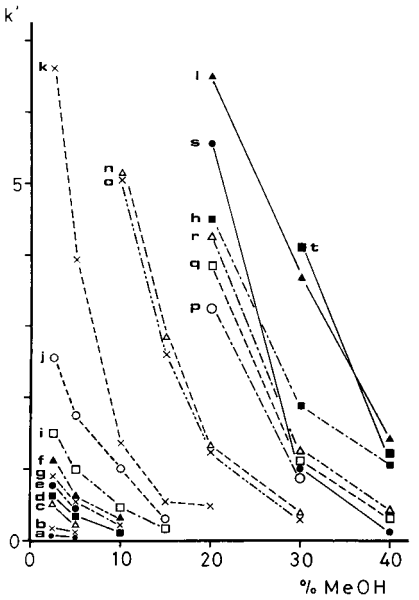

Fig. 1. Plots of *k'* *vs.* concentration of methanol (MeOH) for isocratic elution: a = NBD–Asp; b = NBD–Glu; c = NBD–Hyp; d = NBD–Ser; e = NBD–His; f = NBD–Gly; g = NBD-OH; h = NBD–Arg; i = NBD–Thr; j = NBD–Ala; k = NBD–Pro; l = NBD-NH_2; n = NBD–Val; o = NBD–Met; p = NBD–Ile; q = NBD–Leu; r = NBD–Phe; s = NBD–Lys; t = NBD–Tyr.

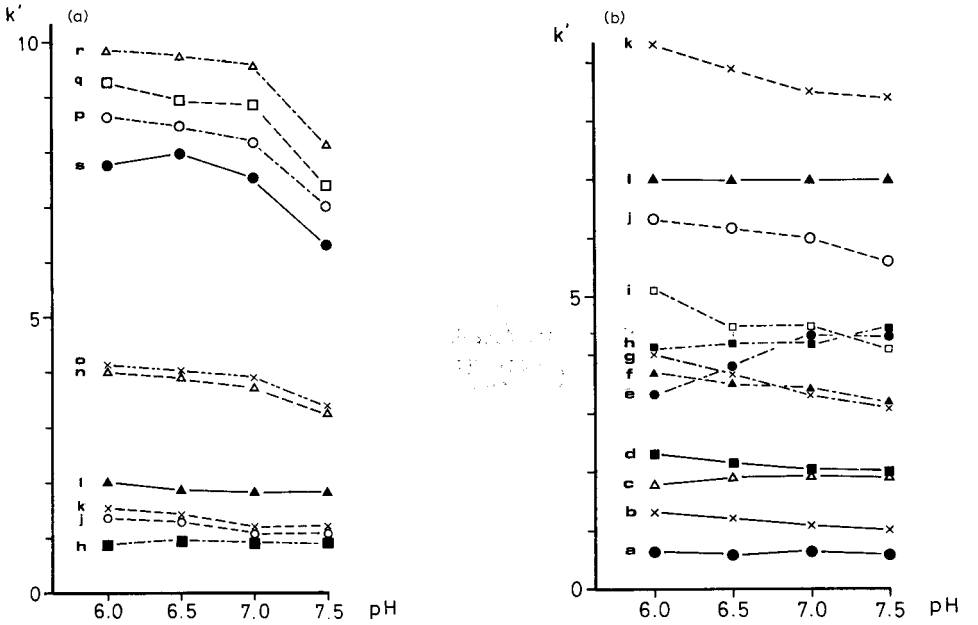

Fig. 2. Plots of k' *vs.* pH of a 0.1 *M* phosphate buffer for isocratic elution with 40% (a) or 20% (b) methanol. Abbreviations are as in Fig. 1.

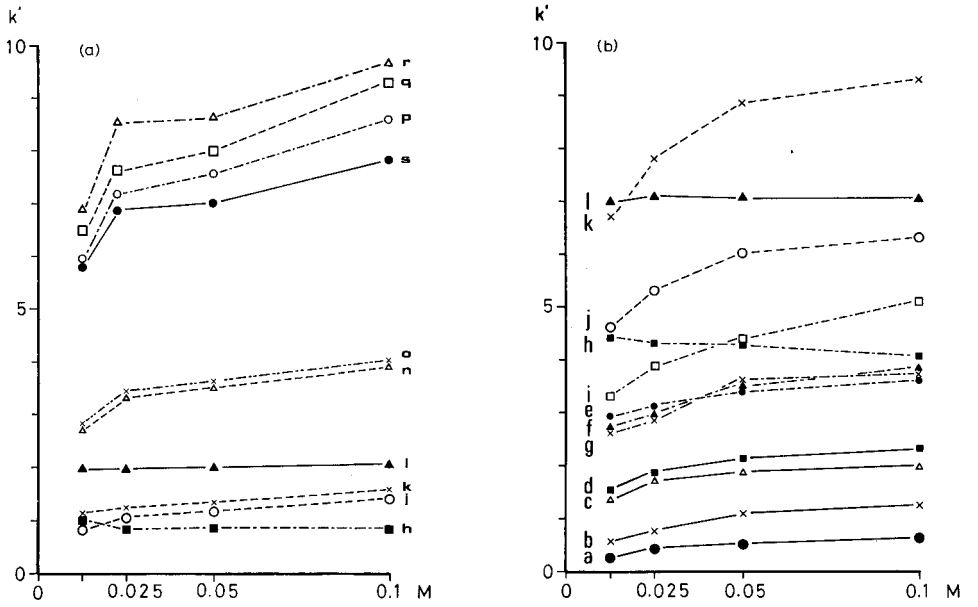

Fig. 3. Plot of k' *vs.* concentration of the phosphate buffer at pH 6.0 for isocratic elution with 40% (a) or 20% (b) methanol. Abbreviations are as in Fig. 1.

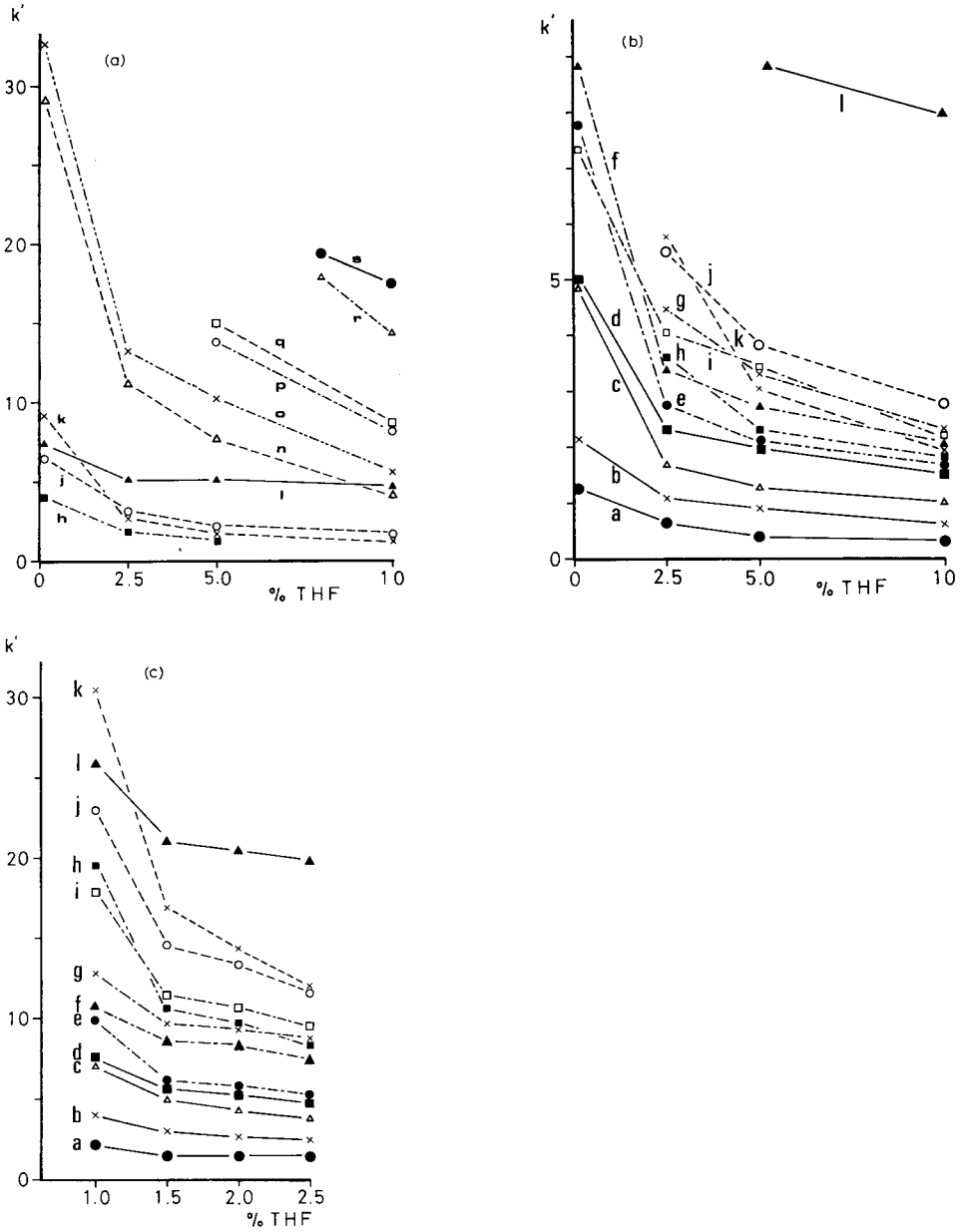

Fig. 4. Plots of k' *vs.* concentration of tetrahydrofuran for isocratic elution with 20% (a), 10% (b) or 3.75% (c) methanol in 0.1 *M* phosphate buffer at pH 6.0. Abbreviations are as in Fig. 1.

Separation of NBD–amino acid derivatives

In reversed-phase HPLC, methanol is commonly used as an eluent. In this experiment, separation of NBD–amino acids was also studied using various concentrations of methanol in water. As expected, the capacity factor (k') of all the amino acid derivatives increased as the concentration of methanol decreased (Fig. 1). How-

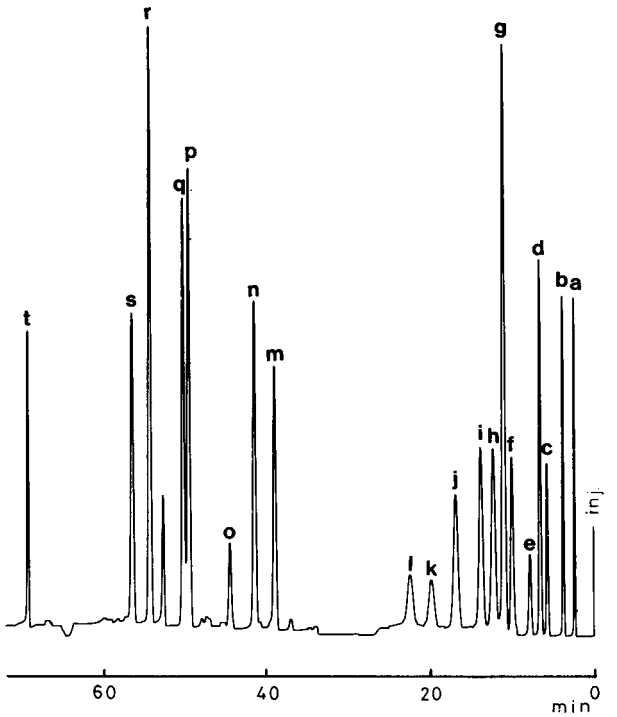

Fig. 5. Elution profile of amino acid standards derivatized by reaction with NBD-F. Each peak represents 10 pmoles. Conditions: solvent A, methanol–THF–0.1 *M* phosphate buffer (pH 6.0) (3.75:1.6:94.65); solvent B, methanol–THF–0.1 *M* phosphate buffer (pH 6.0) (25:15:60); solvent C, 40% methanol in water; gradient programme, 100% A for 24 min, linear step to 100% B over 30 min, 100% B for 6 min, 100% C for 12 min; flow-rate, 2.0 ml/min. Abbreviations are as for Fig. 1, except for (m) NBD–ε-aminocaproic acid.

ever, in this simple binary mixture of solvents, the NBD–amino acid derivatives eluted earlier, such as Asp, Glu, Hyp, Ser, His, Gly and Thr, were not well separated and some tailing of peaks was also observed. In order to retain more of the fluorophores the use of buffers (pH 6.0–7.5) containing 40 (Fig. 2a) or 20% methanol (Fig. 2b) was examined. The k' values of almost all the NBD–amino acid derivatives decreased with increasing pH while the k' of NBD–Arg increased and the k' of 7-amino-4-nitrobenzo-2-oxa-1,3-diazole (NBD-NH_2), NBD–Hyp and NBD–Asp remained approximately constant over this pH range. The effect of buffer ion concentration (phosphate buffer, pH 6.0) was examined from 0.0125 to 0.10 *M* with 40 and 20% methanol (Figs. 3a and b). The k' values increased with increasing ion concentration. The effect was greater compared to that observed with change of pH. However, the k' value of NBD-NH_2 was not affected and that of NBD–Arg decreased. Curiously, NBD–Tyr would not elute using mobile phases containing buffers, while use of simple binary mixtures of methanol–water caused elution as shown in Fig. 1 (line t). Since complete separation was difficult using the binary solvent systems examined, a ternary solvent system using THF as a third modifier[11] was investigated where an efficient separation was achieved. As shown in Figs. 4a–c, THF (1.0–10%) reduced remarkably the retentions of amino acid derivatives, especially those with large k' values. On the basis of the results obtained above, the ternary solvent system with gradient elution was se-

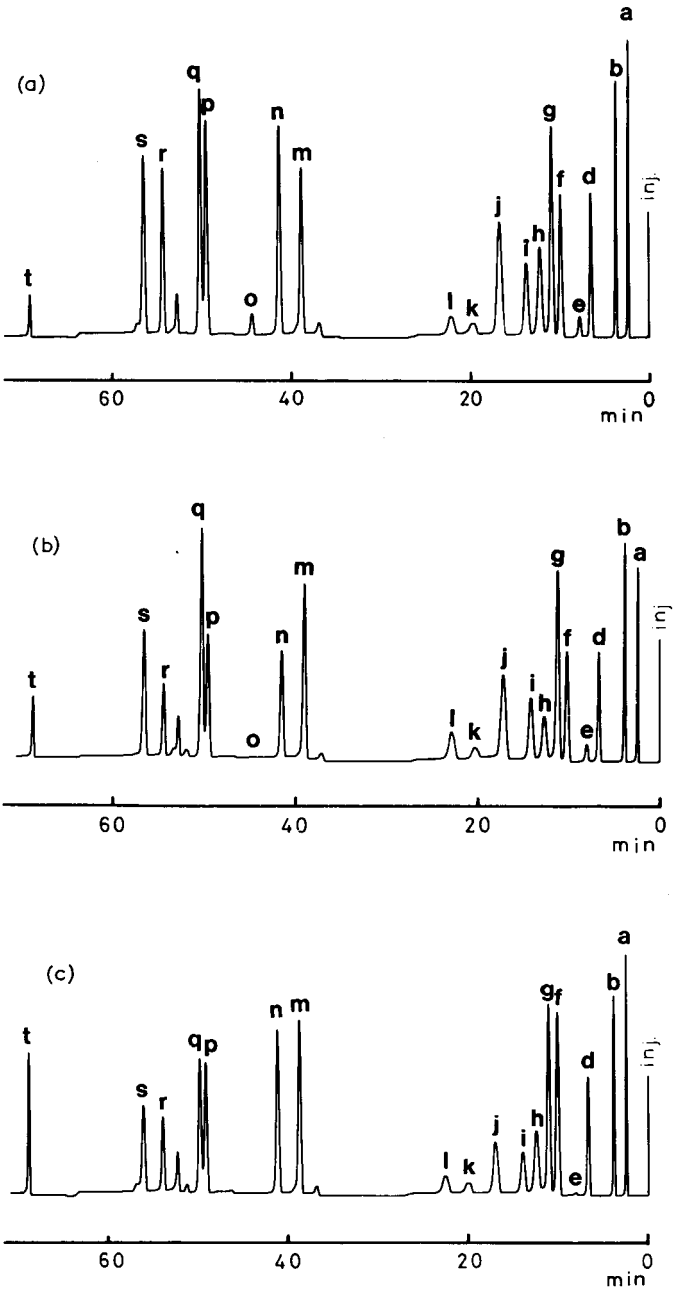

Fig. 6. Elution profiles for hydrolysates of rabbit pyruvate-M_1. (a), rabbit aldolase A (b) and papain (c). The protein (1.435 mg for a, 0.82 mg for b, 0.82 mg for c), hydrolysed with 6 *M* hydrochloric acid was diluted to a concentration of 0.146 μg/μl with an internal standard solution (100 pmol/μl). Aliquots (10 μl) of the hydrolysate were derivatized and 2% of the resulting mixture was applied onto the HPLC column. Conditions were as in Fig. 5. Abbreviations are as in Figs. 1 and 5.

TABLE I

RATIO OF AMINO ACID COMPOSITIONS OF PROTEIN HYDROLYSATES

Ratio of Ala is tentatively fixed as 1.00.

Amino acid	*Rabbit pyruvate kinase-M_1*		*Rabbit aldolase A*		*Papain*	
	NBD-F method	*Ref. 15*	*NBD-F method*	*Ref. 16*	*NBD-F method*	*Ref. 17*
Asp (+Asn)	0.71	0.83	0.63	0.67	1.22	1.34
Glu (+Gln)	0.82	0.92	0.91	0.96	1.37	1.42
Ser	0.45	0.47	0.45	0.50	0.81	0.92
His	0.21	0.21	0.27	0.26	*	0.14
Gly	0.73	0.70	0.74	0.72	1.99	2.00
Arg	0.61	0.57	0.37	0.36	0.63	0.85
Thr	0.42	0.40	0.53	0.53	0.56	0.56
Ala	1.00	1.00	1.00	1.00	1.00	1.00
Pro	0.25	0.37	0.37	0.46	0.54	0.72
Val	0.77	0.76	0.51	0.50	1.28	1.28
Met	0.29	0.29	*	0.07	0	0
Ile	0.58	0.61	0.46	0.46	0.76	0.86
Leu	0.71	0.73	0.85	0.81	0.82	0.78
Phe	0.29	0.26	0.17	0.17	0.29	0.28
Lys	0.62	0.61	0.58	0.62	0.63	0.72
Tyr	0.17	0.17	0.30	0.29	1.18	1.36

* Not determined as a measurable peak was not obtained.

lected for the separation of the NBD–amino acid derivatives. Of the several gradient shapes available, linear gradient elution proved most effective. The eluting solvents for all the NBD–amino acids were as follows; (A) 3.75% methanol–1.6% THF in 0.1 *M* phosphate buffer (pH 6.0), (B) 25% methanol–15% THF in 0.1 *M* phosphate buffer (pH 6.0), (C) 40% methanol in water. Isocratic elution with A for 24 min, a linear gradient of 100% A to 100% B over 30 min, isocratic elution with B for 6 min and isocratic elution with C for 12 min were performed successively. Fig. 5 shows that all the derivatives are eluted with reasonably good separation except NBD–Ile (peak p) and NBD–Leu (peak q). The average deviation of retention times for the eighteen amino acid derivatives was 1.35% (n = 5), the largest being 5.37% (for Asp) and the lowest 0.19% (for Leu). This deviation might be caused by evaporation of THF at room temperature (*ca.* 25°C). Fig. 5 shows that NBD–ε-aminocaproic acid (peak m) was a good internal standard. A linear relationship was obtained for the peak-height ratio of NBD–ε-aminocaproic acid from 0.5 to 100 pmol for each NBD–amino acid. The average deviation of 10 pmol of each amino acid was 2.78% (n = 5); the largest was 5.60% for NBD–Pro and the lowest was 0.57% for NBD–Glu. The detection limits (signal-to-noise ratio 2) for each amino acid were over a range of 10 fmol except for His, Pro and Met, for which they were *ca.* 100 fmol.

Application to protein hydrolysates

The protein hydrolysates of rabbit pyruvate kinase-M_1, rabbit aldolase A and papain were examined by this method. Fig. 6a–c illustrate the amino acid profiles of each protein hydrolysate. Table I summarizes the results of the intercalibration in terms of ratios of amino acid residues, with the amount of Ala fixed as 1.00. The

composition ratios were almost the same as those in the literature[15–17] except those for Pro which were lower.

DISCUSSION

According to Ahnoff *et al.*[6] a reaction time of 3 min at pH 9.5 and 60°C is required for derivatization of Hyp with NBD-Cl. A longer reaction time may be required to derivatize other amino acids, especially amino acids having primary amino groups since the two amino groups of Lys partially reacted to give two peaks[6] presumably of mono- and bis-derivatives. As reported previously[8], NBD-F reacts faster than NBD-Cl with amino acids. Thus, a reaction time of 1 min at pH 8.0 and 60°C is enough for derivatization of the eighteen amino acids, the presumed components of the protein hydrolysates, plus ε-aminocaproic acid to give one peak for each amino acid as shown in Fig. 5.

Contrary to the fact that OPA derivatives of amino acids, especially Lys and Gly, are less stable and for HPLC must be injected at exactly the same time after reaction[12]. Our data (unpublished) that the NBD derivatives are stable for 2 days when stored in the absence of light in a refrigerator might be advantageous for the analysis of amino acids. The third organic modifier in the eluting solvent, THF, suggested for the efficient elution of ethereal compounds[11], is also favourable for the efficient separation of all the NBD derivatives of the amino acids tested except for NBD–Tyr. The reason why NBD–Tyr is difficult to be eluted by the solvent containing salt is not clear. However, in our preliminary results, NBD–Tyr is converted to a N,O-bis-NBD derivative. It might be a reason for strong affinity of NBD–Tyr to the gel.

Since the effect of ion concentration on the elution of NBD–Arg is not great, the guanidino group in the molecule may not be derivatized. The same phenomena were observed as suggested for OPA–[13] and PTH–Arg[14]. The relatively poorer reproducibility of the retention time of NBD–Asp may be ascribed to the volatility of THF present in the eluting solvent in small amounts. Therefore, the eluting solvents should be prepared freshly before use.

The sensitivity of the present NBD method for amino acids is almost the same as for the OPA method[12], excluding Pro and Hyp to which OPA is not reactive, and might be advantageous for NBD-F against OPA.

Since the NBD-OH peak interferes with the baseline separation of NBD–Gly and NBD–Arg, the final dilution ratio in the reaction solution with 0.005 *M* hydrochloric acid cannot be reduced in our present experiment. However, the intensity of the NBD-OH peak could be lowered by changing the pH of the buffer in the eluting solvent to *ca.* 1 (ref. 8). Thus, under such conditions the dilution ratio with hydrochloric acid may be lowered and a greater quantity of sample can be injected without loss of separation.

When the proposed method was applied to the protein hydrolysates, the amounts of Pro gave a lower value compared to that in the literature[15–17] (Table I) for reasons unknown. However, in a trial experiment the values for the other amino acids are in reasonably good agreement with those in the literature[15–17]. Our results suggest that *ca.* 1–1.5 μg of protein hydrolysates in 10 μl of final sample solution prior to derivatization are appropriate for one experiment. It means, occasionally, even a protein band on a polyacrylamide gel could be supplied for the study of the amino

acid composition. The difficulty which might be encountered is how to avoid interference between the amino acids, ascribed to the solvents used for extraction from the gel and hydrolysis of the protein. We are currently investigating this matter.

ACKNOWLEDGEMENT

The authors express their thanks to Professor Z. Tamura, University of Tokyo, for his interest and support. Thanks are also due to Dr. N. Nakai of Fukui Medical School for his donation of protein hydrolyzates. This work was supported in part by a grant from Tokyo Biochemical Research Foundation.

REFERENCES

1 S. Udenfriend, S. Stein, P. Bohlen, W. Dairman, W. Leimgruber and M. Weigele, *Science*, 178 (1972) 871–872.
2 M. Roth, *Anal. Chem.*, 43 (1971) 880–882.
3 M. Weigele, S. DeBernado and W. Leimgruber, *Biochem. Biophys. Res. Commun.*, 50 (1973) 352–356.
4 P. B. Ghosh, M. W. Whitehouse, *Biochem. J.*, 108 (1968) 155–156.
5 J. H. Wolfram, J. I. Feinberg, R. C. Doerr and W. Fiddler, *J. Chromatogr.*, 132 (1977) 37–43.
6 M. Ahnoff, I. Grundavik, A. Arfwidsson, J. Fonselius and B. Persson, *Anal. Chem.*, 53 (1981) 484–489.
7 M. Roth, *Clin. Chim. Acta*, 83 (1978) 273–277.
8 K. Imai and Y. Watanabe, *Anal. Chim. Acta*, 130 (1981) 377–383.
9 Y. Watanabe and K. Imai, *Anal. Biochem.*, 116 (1981) 471–472.
10 L. D. Nunno, S. Florio and P. E. Todesco, *J. Chem. Soc. C*, (1970) 1433–1434.
11 E. Roggendorf and R. Spatz, *J. Chromatogr.*, 204 (1981) 263–268.
12 B. N. Jones, S. Paabo and S. Stein, *J. Liquid Chromatogr.*, 4 (1981) 565–586.
13 P. Lindroth and K. Mopper, *Anal. Chem.*, 51 (1979) 1667–1674.
14 S. J. Dimari, J. P. Robinson and J. H. Hash, *J. Chromatogr.*, 213 (1981) 91–97.
15 K. Harada, S. Saeki, K. Wada and T. Tanaka, *Biochim. Biophys. Acta*, 524 (1978) 327–339.
16 C. Y. Lai, N. Nakai and D. Chang, *Science*, 183 (1974) 1204–1206.
17 R. E. Michel, I. M. Chaiken and E. L. Smith, *J. Biol. Chem.*, 245 (1970) 3485–3492.

Journal of Chromatography, 239 (1982) 733–745
Elsevier Scientific Publishing Company, Amsterdam — Printed in The Netherlands

CHROM. 14,670

ANALYSIS OF BODY FUNCTIONS USING A CLINICAL LIQUID CHROMATOGRAPH

HIROYUKI MIYAGI*, JUNKICHI MIURA and YOSHINORI TAKATA
Branch Laboratory at Hitachi Research Laboratory, Central Research Laboratory, Hitachi Ltd., 4026 Kujimachi, Hitachi-shi, Ibaraki, 319-12 (Japan)
SEIGO KAMITAKE and SHIGETAKE GANNO
Naka Works, Hitachi Ltd., 882 Ichige, Katsuta-shi, Ibaraki, 312 (Japan)
and
YOH YAMAGATA
Hitachi General Hospital, Hitachi Ltd., 2-1-1 Jonan-cho, Hitachi-shi, Ibaraki, 317 (Japan)

SUMMARY

A clinical liquid chromatograph, which consists of a completely automated liquid chromatograph combined with a microcomputer for diagnosis, and its application to body function analyses are described. The analytical rate for urinary ultraviolet-absorbing constituents using anion-exchange chromatography was 12 samples per day, and the reproducibilities for retention time and peak area were less than 3% and 4%, respectively. Diagnostic methods for kidney functions using the chromatograms are discussed.

INTRODUCTION

It has been reported that much useful information on body functions can be obtained by the chromatographic analysis of components in physiological fluids[1]. Scott[2] demonstrated that an anion-exchange chromatographic system for ultraviolet-absorbing constituents in human urine had potential for diagnostic purposes, and he and his co-workers[3] developed an automated instrument for urine analysis. Although the analysis time was reduced to 8 h by using sequential columns of microreticular and pellicular resins[4], it was prohibitive for routine clinical use. Seta *et al.*[5] proposed a high-speed liquid chromatographic system with a macroreticular anion-exchange resin, by which 100 ultraviolet-absorbing constituents in human urine could be separated within 2 h.

In order to explore the potentialities of such systems, we have investigated the chromatography of urinary ultraviolet-absorbing constituents in human urine and its application to analyses of body functions. Since Scott[2] developed a linear gradient elution system with acetate buffer solution (pH 4.4) for chromatographing urinary ultraviolet-absorbing constituents, it has been used even for high-speed analysis using a macroreticular resin[5]. As described in a previous paper[6], we found that acetate

0021-9673/82/0000–0000/$02.75

buffer could not be used with a stepwise elution system because of the significant ultraviolet absorption of the eluents at 254 nm, resulting in baseline drift during the stepwise elution.

We developed a high-performance liquid chromatographic system, using stepwise elution with ammonium chloride–acetonitrile eluents, by which the analysis time was reduced to 90 min. Detection at 220–280 nm was possible with the system, so that ultraviolet absorption of the eluents was minimized. However, the eluent system needs a high concentration of ammonium chloride (2 mol/l) in the final eluent, which resulted in corrosion of the stainless-steel tubing and the separation column used in the chromatograph. Therefore, our later efforts were directed towards searching for a new eluent system, and finally it was found that addition of ammonium dihydrogen phosphate was effective in reducing the chloride concentration[7].

We report in this paper an automated apparatus for body function analyses,

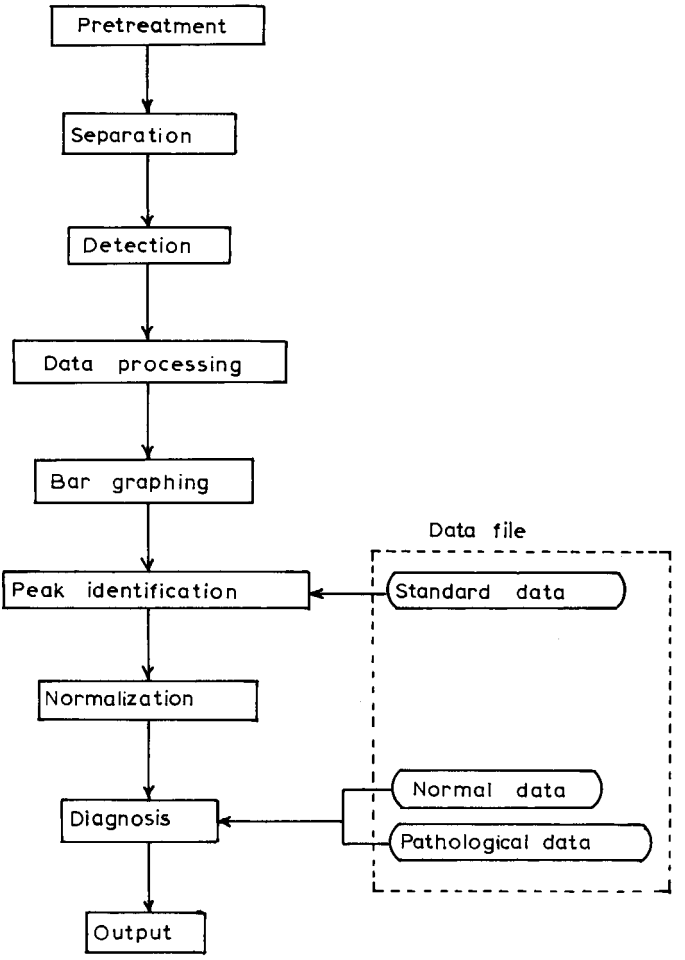

Fig. 1. General procedure for body function analysis.

which we call a clinical liquid chromatograph, based on a high-performance liquid chromatograph combined with a microcomputer for diagnosis.

PRINCIPLE

General procedure for body function analysis is illustrated in Fig. 1. After pretreatment to remove suspended or precipitated material, a urine sample is analysed with the liquid chromatograph, and ultraviolet-absorbing constituents are detected with a dual-wavelength ultraviolet monitor. The detected signals are digitized with a data processor, transferring the output signals to a microcomputer.

In order to effect peak matching, the peaks in the chromatogram are identified using the retention time and the absorbance ratio detected at two different wavelengths. Peak heights or peak areas of the identified peaks are normalized with respect to an appropriate peak to correct urine concentrations. Subsequently, diagnosis of the body functions is performed by several dignostic algorithms, for example, comparing total chromatographic profiles or comparing the ratio of the areas of two appropriate peaks. The diagnostic data are displayed on a screen or printed out.

EXPERIMENTAL

Apparatus

A schematic diagram of the clinical liquid chromatograph is shown in Fig. 2. An automated liquid chromatograph was constructed for the purpose described above, in which a dual-column system with two Model 835 pumps and a Model 635-0900 multiple wavelength ultraviolet monitor (Hitachi, Tokyo, Japan) were mounted. Seventy-two samples can be set simultaneously on the auto-sampler, which is cooled

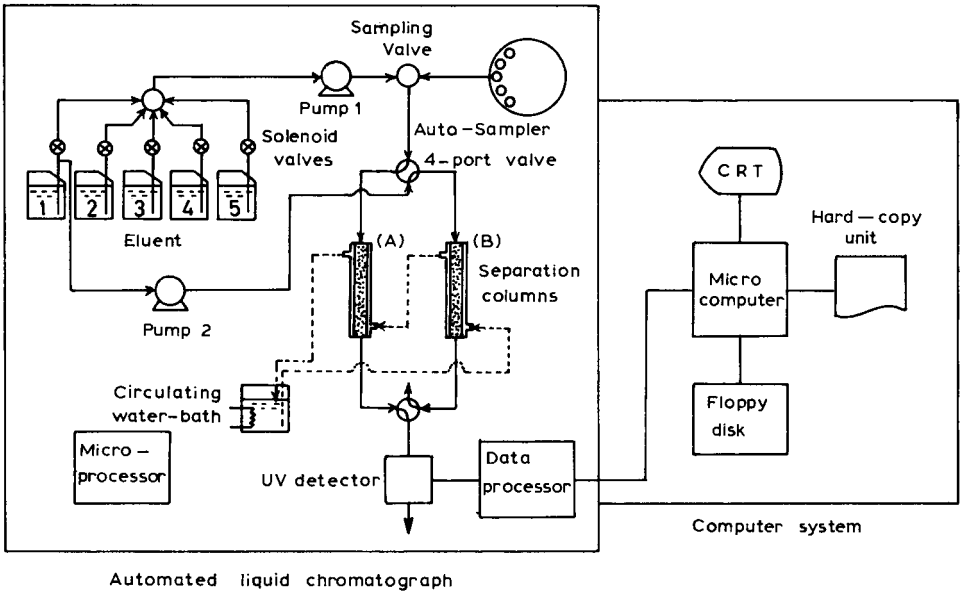

Fig. 2. Schematic diagram of clinical liquid chromatograph.

to 4°C with circulating water supplied by a Model BL-11 water cooling unit (Yamato, Tokyo, Japan). The eluent delivery system was based on stepwise elution, five or six consecutive eluents being supplied successively to the columns. A dual-column system was used to increase the analytical speed. Columns were switched with 4-port valves such that when one was used for the analysis, the other was used for re-equilibration with the first eluent. The column temperature was controlled by a constant-temperature circulating water-bath, and temperature programming was also possible. The detection wavelengths of the ultraviolet monitor can be chosen every 10 nm from 210 to 280 nm for each channel.

All of the analytical operation can be performed automatically by means of a microprocessor with respect to selection of eluent, column temperature, sample loading, column switching, etc.

The output signals of the data processor, which was mounted in the liquid chromatograph, were transferred to a microcomputer Model 9845 B/T with a graphic display and a hard-copy unit (Hewlett-Packard, Fort Collins, CO, U.S.A.). The chromatographic data were stored on a Hewlett-Packard Model 9845M floppy disk.

Anion-exchange chromatography

Stainless-steel columns of 250 × 4.6 mm I.D. packed with Hitachi Gel No. 3013-N macroreticular anion-exchange resin[6] were used for the separation of ultraviolet-absorbing constituents in urine. The resin was packed into the column by the slurry packing method. A new eluent system was developed for routine chromatographic analysis, consisting of ammonium chloride, ammonium dihydrogen phosphate and acetonitrile[7]. Under optimized conditions, the concentration of the final eluent was 0.3 mol/l ammonium chloride–0.05 mol/l ammonium dihydrogen phosphate–30 vol.-% acetonitrile (pH 4.8), and the eluents for the other steps, except for the first step (water), were prepared by dilution of the final eluent with water.

The column temperature was programed from 30 to 60°C synchronized with the eluent switching. The detection wavelengths of the ultraviolet monitor were selected at 230 and 250 nm.

Peak identification and diagnostic procedure

The chromatographic data digitized by the data processor were used for the diagnosis of body functions. First, peaks in the individual chromatograms were identified using the retention time and the absorbance ratio at 230 and 250 nm. The allowed variability of the identification parameters were fixed at ±1 min for the retention time and ±15% for the absorbance ratio. A commercially available chemical control urine was used to obtain a standard chromatogram.

Four kinds of diagnostic procedure were examined, the key parameters being (a) the chromatographic profile, (b) the normal range for an individual peak, (c) the peak height or peak area of an appropriate peak which is closely related to the traditional diagnostic parameter and (d) the relationship between two different peaks.

These diagnostic approaches were evaluated for the analysis of kidney functions.

Chemicals

Water and acetonitrile were purchased from Wako (Osaka, Japan) and were

purified for liquid chromatography. All other chemicals were of analytical-reagent grade. Reference urine was Q-PAK Chemical Control Urine (Hyland, Costa Mesa, CA, U.S.A.).

Urine samples were centrifuged with a Model 05RP-22 centrifuge (Hitachi, Tokyo, Japan) for 10 min at 3000 r.p.m., then the supernatant was pressure-filtered through a 0.1-μm pore size filter (Millipore, Bedford, MA, U.S.A.) before analysis.

RESULTS AND DISCUSSION

Anion-exchange chromatography of urine samples

A typical chromatogram of the reference urine obtained by stepwise elution with ammonium chloride–ammonium dihydrogen phosphate–acetonitrile is shown in Fig. 3. More than 80 peaks are separated within a 100 min under the conditions specified. The peak resolution and the analysis time are comparable to those obtained with the ammonium chloride–acetonitrile elution system[6]. As the eluent components have low ultraviolet absorption at wavelengths shorter than 250 nm, detection at 230 nm is possible without any baseline drift, as shown in Fig. 4.

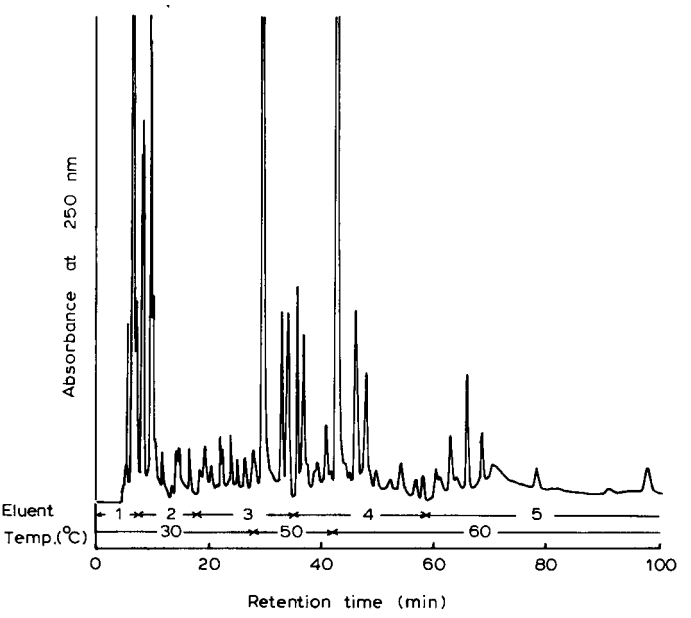

Fig. 3. Chromatogram of chemical control urine detected at 250 nm. Sample volume, 50 μl; column, Hitachi Gel 3013-N (250 × 4.6 mm I.D.). Eluent: (1) water; (2) 1/6 × (5); (3) 1/3 × (5); (4) 2/3 × (5); (5) 0.3 mol/l NH_4Cl–0.05 mol/l $NH_4H_2PO_4$–30% (v/v) acetonitrile (pH 4.8). Flow-rate, 0.8 ml/min; detector sensitivity, 0.32 full-scale.

We did not observe any corrosion problems with the eluents during 18 months' operation, because the chloride concentration was low, being one tenth of that in previous eluents.

The reproducibilities of the retention time, peak height and peak area are shown in Table I. A better reproducibility of the retention time was obtained for the

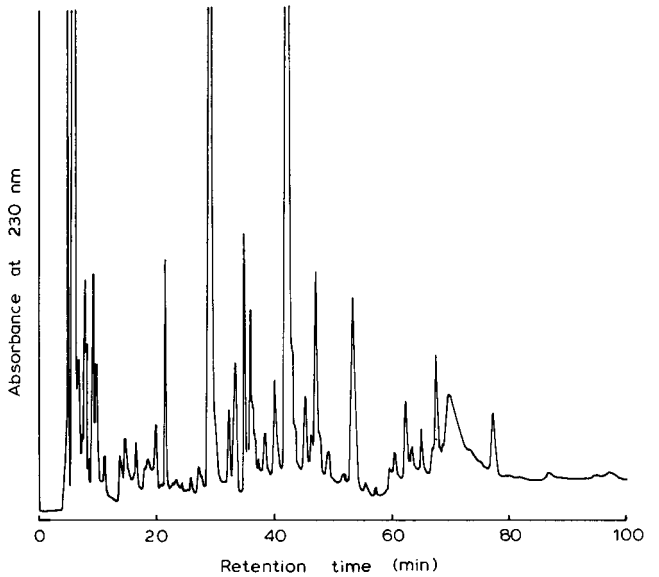

Fig. 4. Chromatogram of chemical control urine detected at 230 nm. Conditions as in Fig. 3.

peaks that were separated perfectly from neighbouring peaks (peaks 1 and 4) than for unseparated peaks (peaks 2 and 3). Instability of the baseline gave a lower reproducibility for peak height than peak area.

As would be expected, the long-term stability of the separation column depends on the number of samples loaded. It could be prolonged to more than 100 urine analyses by using a pre-column (10 × 4 mm I.D.) packed with the same packing material as the separation column.

The overall analytical rate with the apparatus was about twelve samples per day.

Peak identification

We examined the possibility of automatic peak identification with the microcomputer using the retention time and the absorbance ratio. The term "identification" is defined in this paper as discrimination of a peak in one chromatogram that is identical with a peak in a standard chromatogram.

TABLE I

REPRODUCIBILITY OF THE LIQUID CHROMATOGRAPH

No.	*Retention time (min)*	*Coefficient of variation (%) (n = 11)*		
		Retention time	*Peak height*	*Peak area*
1	5.32	0.82	0.78	2.27
2	18.40	1.92	7.27	3.23
3	33.80	2.70	8.38	3.32
4	74.20	0.89	8.12	2.80

Forty urine samples from normal subjects and a reference chemical control urine, used to obtain a standard chromatogram, were analyzed. Fifty peaks in the individual chromatograms were examined for identification with the criteria described above, and it was found that 25–35 of the 50 peaks could be identified. The reason why this number is lower than expected might be non-coincidence of the compounds involved in the reference urine and in the human urine, or the criteria used for the automatic identification, which did not allow for slight changes in the selectivity of the separation column.

Therefore, we checked the data for the chromatograms (retention times, peak heights, peak areas and absorbance ratios), then we numbered the peaks manually and input the peak numbers into the computer, these being used for diagnoses.

The peak identification process might be automated by increasing qualitative information such as the ultraviolet absorbance detected at 250–280 nm (ref. 3) or the intensity of fluorescence[8].

Diagnostic functions

In order to utilize the chromatographic data for diagnostic purposes, the chro-

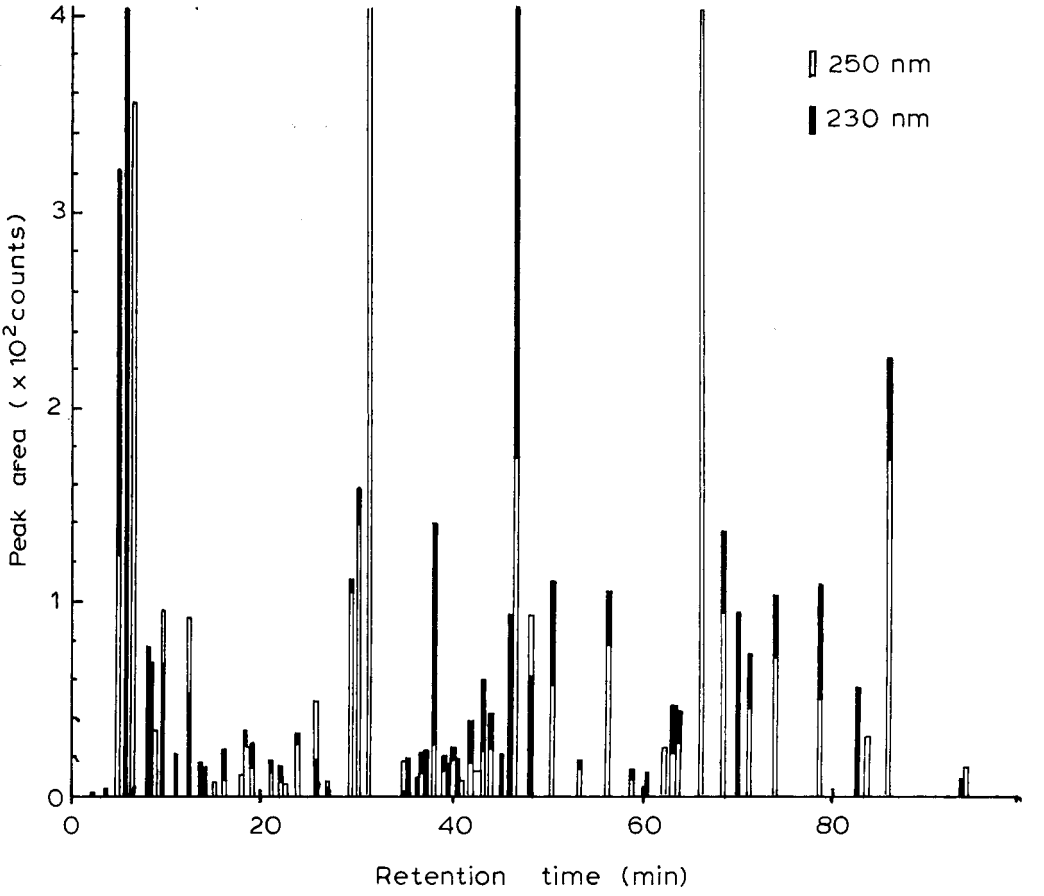

Fig. 5. Bar graph for urine of normal subjects reconstructed for body function analysis.

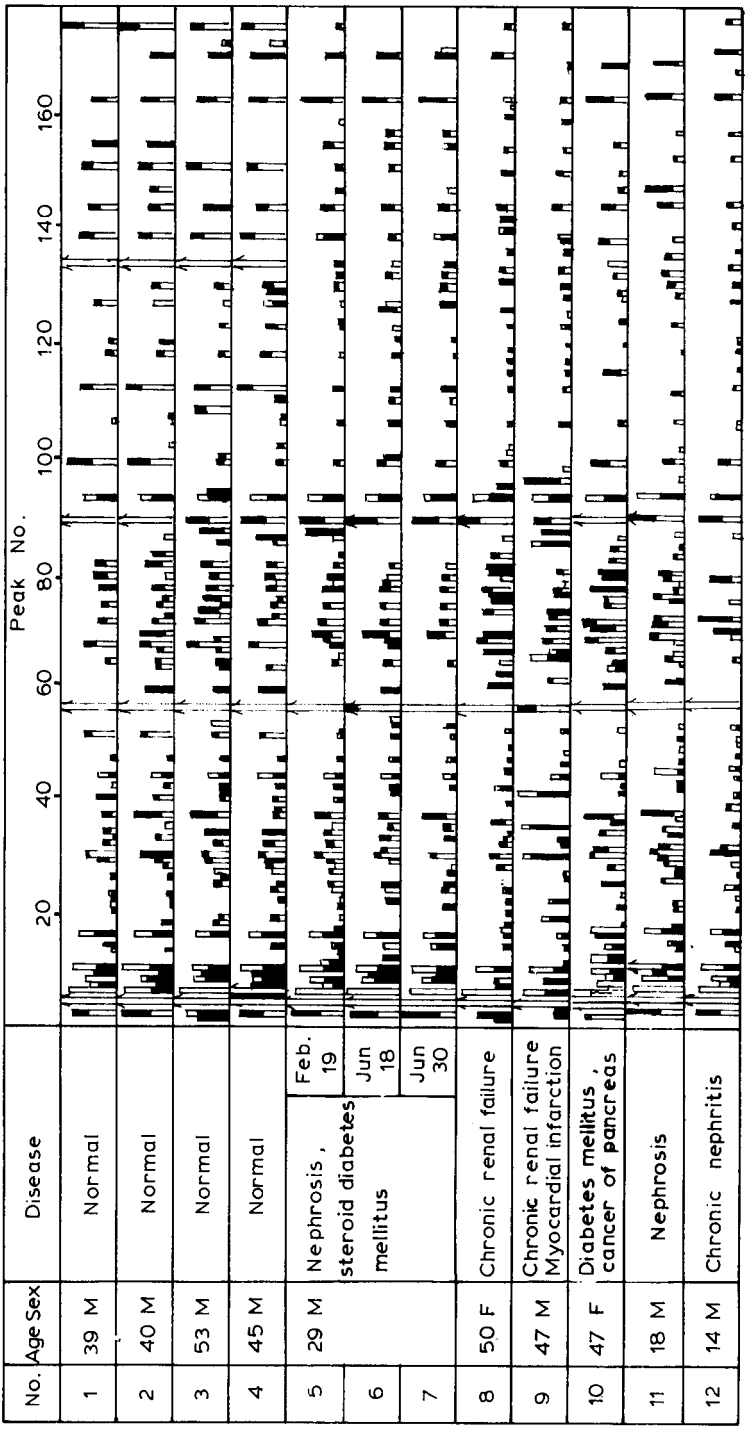

Fig. 6. Comparison of chromatographic profiles for various diseases.

matographic profiles[9,10] or concentrations of individual peaks calculated from the calibration graph or molar absorbance were used[11,12]. However, it is not so easy to make calibrations for many compounds using standard materials, because of a lack of pure standard compounds in some instances. Therefore, it is necessary to establish a diagnostic procedure using the chromatographic data without calibration.

We investigated such a diagnostic procedure, especially for the diagnosis of kidney functions, and found that the methods described below were promising.

All approaches tried in this work started from compiling a bar graph such as that shown in Fig. 5, which was composed automatically by the computer. Although the graph is simplified comparing with the original two chromatograms, sufficient data are included, namely retention time and peak area or peak height detected at 230 and 250 nm.

We analysed more than 300 urine samples, including 40 from normal subjects and 250 from patients with kidney disorders.

It is obvious that much useful information could be obtained by comparing the chromatographic profiles as shown in Fig. 6. For example, it was found that similar patterns were observed for normal subjects, samples 1–4; on the other hand, differences between normal and pathological patterns were observed for the region between peaks 100 and 180. We analysed urines from patients with nephrosis during five months (samples 5–7) and very similar chromatographic patterns were obtained, except for a slight difference in the region of peaks 110–150, which suggests a variation in the pathological situation.

It is very useful to compare chromatographic profiles such as those shown in Fig. 6 for diagnoses of body functions as described above. However, it is difficult to automate the process, because we cannot establish a normal pattern. Therefore, we tried to establish the normal range for individual peaks, instead of a normal pattern.

Urine samples from 40 normal subjects collected after dieting for 1 day were chromatographed, then the normal range was decided as ± 2 standard deviations of the mean value from the distribution graph of the peak area for each peak. In this instance, peak identification was performed automatically using a reference chemical control urine as a standard chromatogram, as described above.

Typical diagnostic graphs for a normal subject and a patient with chronic nephritis are shown in Figs. 7 and 8, respectively. Whereas seventeen peaks were identified and compared with the normal range in Fig. 7, only six peaks were identified in the patient's urine. In the pathological data, peaks which are out of the normal range are indicated by AAA (greatest), AA and A (smallest) according to the degree of shift from the normal range. It was again considered that the small numbers of peaks identified for the pathological urine might be due to the standard chromatogram.

It was felt that the automated diagnosis described above might provide a useful screening test if the probability of peak identification could be increased.

The urinary excretion rate of several compounds was examined by anion-exchange chromatography of ultraviolet-absorbing constituents in human urine[12,13]. Concerning to the diagnosis of kidney function, creatinine clearance is a most popular traditional diagnostic parameter. We tried to obtain information on creatinine clearance by using the liquid chromatographic system. In order to find the peak providing this information, correlations between the peak area of each peak and creatinine clearance were examined. Eventually, we found that peak 17 had the best

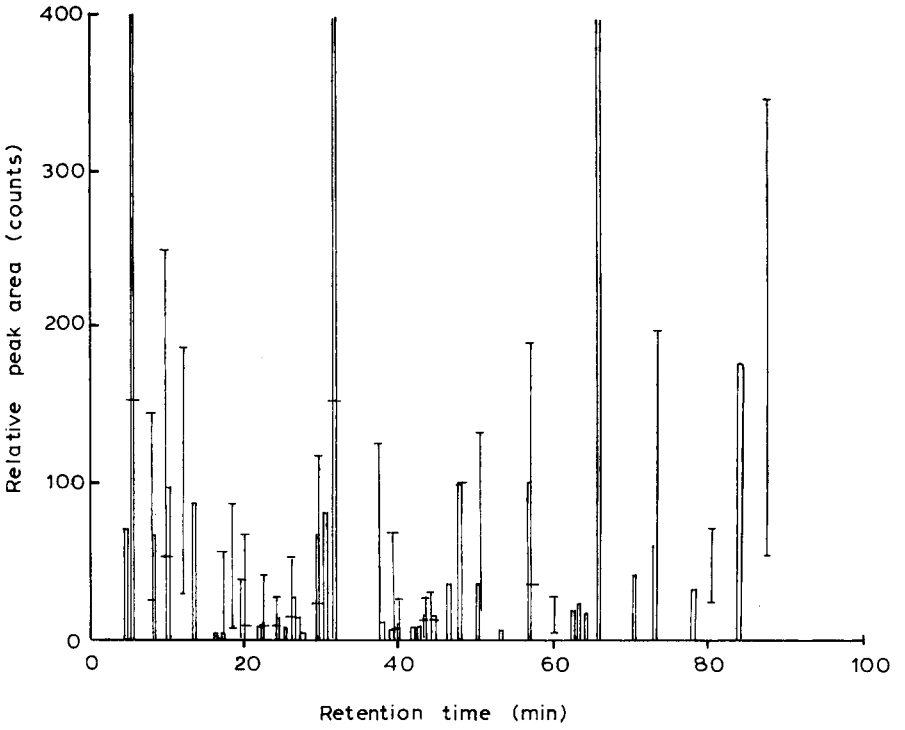

Fig. 7. Diagnostic data for a normal subject.

No.	*Time*	*Height*	*Normal range*	*Remarks*
1	5.59	833.34	152.88–2247.39	N
2	8.46	67.54	24.90– 143.84	N
3	10.20	97.02	53.52– 248.66	N
7	19.91	39.92	– 66.56	N
8	22.87	4.91	– 40.76	N
9	24.44	13.51	8.37– 27.09	N
10	26.56	27.46	14.36– 52.31	N
12	30.73	82.02	22.79– 116.78	N
13	31.76	576.16	152.97–1552.82	N
15	40.08	10.64	6.90– 24.97	N
17	44.69	15.92	10.95– 27.70	N
18	43.62	18.12	11.72– 30.39	N
19	46.45	36.50	– 589.80	N
21	50.41	37.41	– 134.01	N
22	57.16	102.16	33.97– 190.90	N
24	66.04	682.96	– 969.98	N
35	73.41	61.48	– 196.68	N

correlation, as shown in Fig. 9. Consequently, it is felt that the creatinine clearance can be determined by the chromatographic analysis of urine, without collection of blood, which is advantageous with children and serious cases.

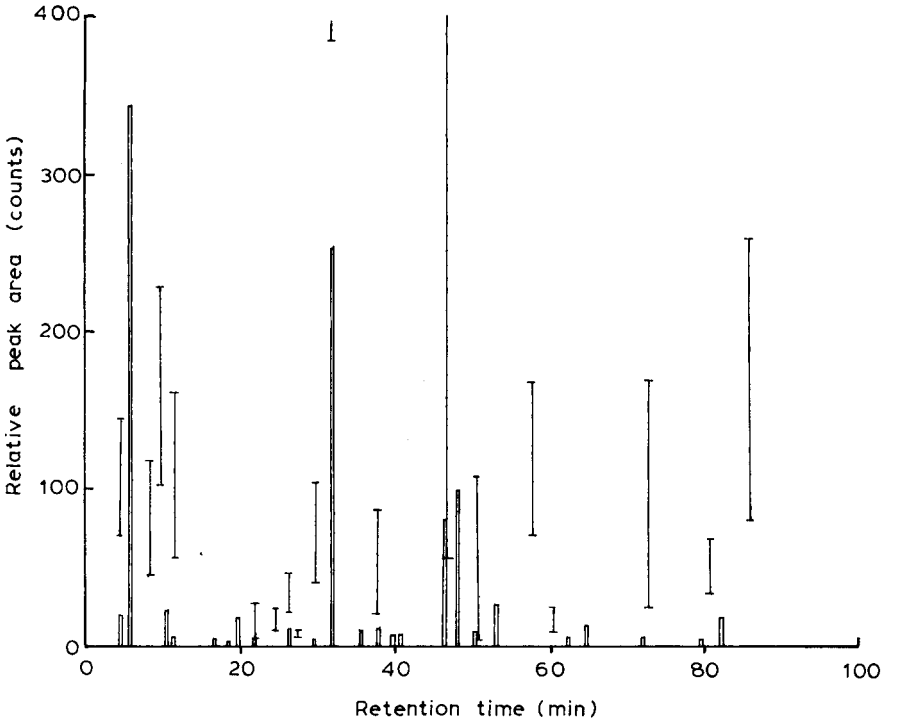

Fig. 8. Diagnostic data for a kidney patient.

No.	*Time*	*Height*	*Normal range*	*Remarks*
4	10.31	22.52	101.79– 228.32	–AA
8	26.29	11.26	20.68– 45.98	–A
11	31.76	254.33	386.28–1319.51	–A
13	46.32	81.31	56.24– 492.47	N
19	71.86	5.25	23.83– 169.94	–A
20	79.35	3.39	33.39– 68.75	–AA

Correlations of peak area between two different peaks are shown in Fig. 10. Whereas a very good correlation between peaks 11 and 135 was obtained for normal subjects (correlation factor 0.955), patients with kidney disorders, such as chronic nephritis, renal insufficiency and diabetes mellites did not conform to this relationship.

Beardmore and Kelley[12] reported that metabolic processes could be estimated by the anion-exchange chromatography of urinary ultraviolet-absorbing compounds. According to their proposals, two constituents shown in Fig. 10 might be metabolically related compounds excreted in urine. Finally, it is felt that diagnosis based on the correlation between two appropriate peaks is most promising for analysis of kidney functions.

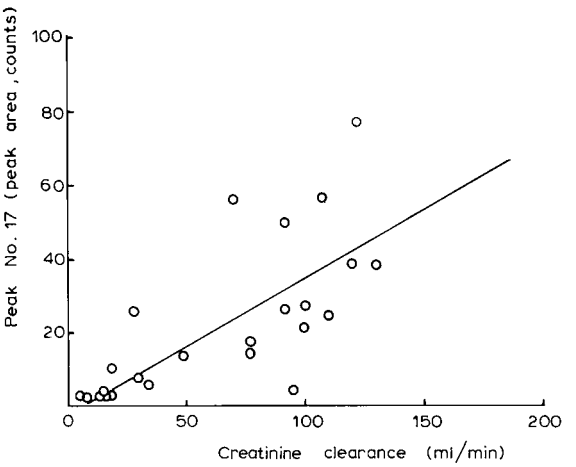

Fig. 9. Correlation between creatinine clearance and chromatographic peak (peak 17). $y = 0.372x - 2.42$; $r = 0.753$; $n = 24$.

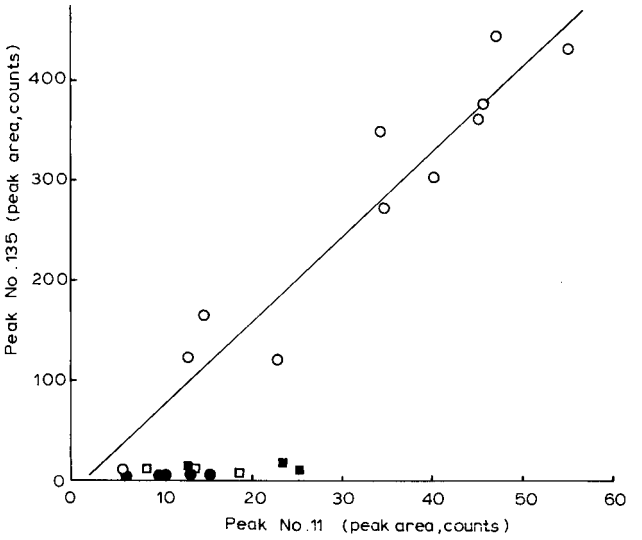

Fig. 10. Correlation between peaks 11 and 135. ○, Normal subject; ■, diabetes mellitus; □, renal insufficiency; ●, chronic nephritis. $y = 8.59x - 12.23$; $r = 0.955$; $n = 11$ (for normal subject).

CONCLUSION

We have demonstrated the performance of a clinical liquid chromatograph consisting of an automated liquid chromatograph combined with a computer for diagnosis. This on-line type of apparatus has potential applications in routine clinical analysis, because of the short analysis time, high resolution and automated diagnostic functions. Variations of the apparatus are possible. Although only a small range of application with respect to diagnostic power was described in this paper, much useful information on body function could be obtained with the apparatus. Its capabilities will be extended further by accumulating pathological data.

REFERENCES

1 L. Pauling, *Science*, 160 (1968) 268.
2 C. D. Scott, *Clin. Chem.*, 14 (1968) 521.
3 C. D. Scott, J. E. Attril and N. G. Anderson, *Proc. Soc. Exp. Biol. Med.*, 125 (1967) 181.
4 S. Katz, W. W. Pritt, Jr. and J. E. Mrochek, *J. Chromatogr.*, 104 (1975) 303.
5 K. Seta, M. Washitake, T. Anmo, N. Takai and T. Okuyama, *Bunseki Kagaku (Jap. Anal.)*, 27 (1978) 73.
6 H. Miyagi, J. Miura, Y. Takata and S. Ganno, *Clin. Chem.*, 25 (1979) 1617.
7 H. Miyagi, J. Miura, Y. Takata and S. Ganno, *Pittsburgh Conference on Analytical Chemistry and Applied Spectroscopy, Atlantic City, N.J., 1980.*
8 S. Katz, W. W. Pritt, Jr. and G. Jones, Jr., *Clin. Chem.*, 19 (1973) 817.
9 A. B. Robinson and L. Pauling, *Clin. Chem.*, 20 (1974) 961.
10 G. K. Brown, O. Stokke and E. Jellum, *J. Chromatogr.*, 145 (1978) 177.
11 R. L. Jolley and C. D. Scott, *Clin. Chem.*, 16 (1970) 687.
12 T. D. Beardmore and W. N. Kelley, *Clin. Chem.*, 17 (1971) 795.
13 D. S. Young, *Clin. Chem.*, 16 (1970) 681.

Journal of Chromatography, 239 (1982) 747–754
Elsevier Scientific Publishing Company, Amsterdam — Printed in The Netherlands

CHROM. 14,611

PREPARATION OF AFFINITY ADSORBENTS WITH TOYOPEARL GELS

ISAMU MATSUMOTO*, YUKI ITO and NOBUKO SENO
Department of Chemistry, Faculty of Science, Ochanomizu University, 2-1-1 Otsuka, Bunkyo-ku, Tokyo 112 (Japan)

SUMMARY

The optimal conditions for the activation of Toyopearl by epichlorohydrin and subsequent immobilization of ligands were investigated. The optimal conditions for the activation were very different from those for agarose gel. The concentration of epoxy groups introduced was as high as 330 μmole per gram of wet gel for Toyopearl HW-55 and 150 μmole per gram of wet gel for Toyopearl HW-65 (diol type). Epoxy-activated Toyopearl was converted into amino and carboxyl derivatives and was subsequently coupled with various ligands. Glycamyl Toyopearl was prepared in a much shorter time (6 h) than agarose gel (800 h), because a higher reaction temperature could be used. The adsorbents obtained were successfully used for the affinity chromatography of lectin and trypsin. However, their adsorption capacities were lower than those of the agarose adsorbents prepared by the same methods.

INTRODUCTION

The preparation of adsorbents for affinity chromatography requires suitable matrices and effective coupling methods for attachment of ligands. Beaded agarose gel has been most widely used as a carrier because of its porous, hydrophilic properties and abundance of hydroxyl groups that can be activated by the CNBr method or the epoxy method. Though the CNBr method discovered by Axén *et al.*[1] has contributed greatly to the recent development of affinity chromatography, it does not completely satisfy demands such as the formation of stable linkages between ligands and matrix[2,3], no introduction of charged groups in the linkage region[4,5] and high yield. The epoxy method, in which a ligand or a spacer having an amino group or a hydroxyl group is readily coupled to epoxy-activated agarose[6,7], gives adsorbents with better properties in these respects[7,8]. Though the epoxy method has other disadvantages, such as the requirements of high temperature[6], high pH[6,7] and a large excess of ligand during coupling step[7], these problems were circumvented by derivatizing epoxy groups of activated agarose into more reactive groups, which are able to react with ligands under mild conditions[9].

However, agarose gel is not a completely satisfactory carrier especially for an industrial use, because it has several unfavourable properties: instability to high temperature and organic solvents that are useful for derivatization reactions; poor

0021-9673/82/0000–0000/$02.75

mechanical strength; inability to give a high flow-rate on the column; and sensitivity to degradation by micro-organisms. On the other hand, a hydrophilic vinyl polymer Toyopearl[10], which is now available as a carrier for gel filtration and high-performance liquid chromatography, does not have these disadvantages. In this paper, we report an investigation of the optimal conditions for the activation of Toyopearl by the epoxy method, the subsequent derivatization and the immobilization of various ligands. The affinity adsorbents obtained were successfully used for the affinity chromatography of lectin and trypsin.

EXPERIMENTAL

Materials

Toyopearls HW-55, -65, -65 (diol type) and -75 were obtained from Toyo Soda, epichlorohydrin, succinic anhydride, lactose, trypsin and 2,4,6-trinitrobenzene sulfonate (TNBS) from Wako, D-galactosamine hydrochloride (GalNHCl) from Seikagaku Kogyo, and sodium cyanoborohydride ($NaCNBH_3$), 1-ethyl-3-(3-dimethylaminopropyl)carbodi-imide (EDC) from Nakarai Chemicals. Galactose oxidase was purchased from Sigma, soybean trypsin inhibitor (STI) from Miles Chemicals and benzoyl L-arginine ethylester (BAEE) from Fluka. Crude soybean agglutinin (SBA) and *Ricinus communis* agglutinin (RCA) were prepared by the method of Allen and Johnson[11].

Epoxy activation of Toyopearl

The activation of Toyopearl with epichlorohydrin was performed as follows. A 1-ml volume of 15 *M* NaOH and 2.5 ml of epichlorohydrin were added to 1.3 g of Toyopearl HW-55. The final concentrations were as follows: 50% (v/v) epichlorohydrin, 3 *M* NaOH. The suspension was incubated at 50°C for 2 h with shaking. The gel was then washed extensively with water. To 1.3 g of Toyopearl HW-65 (diol type) suspended in 1 ml of water, 1 ml of 10 *M* NaOH solution and 1.5 ml of epichlorohydrin were added. The final concentrations were 30% (v/v) epichlorohydrin, 2 *M* NaOH. The suspension was incubated at 50°C for 1 h with shaking. To find the optimal conditions, a series of experiments were carried out with one of the parameters modified in each experiment. The content of epoxy groups in the gel was determined according to the method of Sundberg and Porath[6] and expressed as μmoles per gram of wet gel. The volume per gram of wet Toyopearl gels was 1.1–1.2 ml.

Amination and succinylation of epoxy-activated Toyopearl

Amino Toyopearl was prepared by the same method for the preparation of amino Sepharose described previously[9]. The epoxy-activated Toyopearl was suspended in 1.5 volumes of concentrated ammonia solution. The suspension was incubated at 40°C for 1.5 h with shaking. Determination of amino groups introduced into the gel was performed with respect to the nitrogen content by the micro Kjeldahl method[12].

Succinyl Toyopearl was prepared by the same method for preparing succinyl Sepharose described previously[9]. Amino Toyopearl was washed with 0.1 *M* NaCl and suspended in 1.5 volumes of 0.1 *M* NaCl. Small portions of powdered succinic anhydride (0.08 g per gram of wet amino Toyopearl) were added gradually. The pH

of the suspension was maintained at 6 by the addition of 20% NaOH. The suspension was allowed to stand at room temperature overnight. The substitution of free amino groups was ascertained by the negative result of the TNBS colour test. To remove labile carboxyl groups, the washed succinyl Toyopearl was incubated with 0.1 *M* NaOH for 30 min at room temperature.

Coupling of lactose by reductive amination with amino Toyopearl

First, 2 g of suction-dried amino Toyopearl HW-65 (diol type) were suspended in 1.25 ml of 0.2 *M* K_2HPO_4 containing 0.2 g of lactose and 0.2 g of $NaCNBH_3$. The suspension was refluxed for 6 h. Then the free amino groups that remained in the gel were acetylated by the method previously described[9]. The amounts of lactose immobilized on the gel were determined as galactose liberated after hydrolysis with 0.5 *M* H_2SO_4 at 100°C for 4 h by the galactose oxidase method[13].

Coupling of GalNHCl with succinyl Toyopearl

First, 3 g of suction-dried succinyl Toyopearl HW-65 (diol type) was mixed with 6 ml of 0.5 *M* NaCl containing 0.2 g of GalNHCl. Then, after the pH had been adjusted to 5, the suspension was mixed with 0.1 g of EDC and was incubated at room temperature. After 24 h, another 0.1 g of EDC was added and the incubation was continued for 3 days. To determine the amounts of GalN immobilized on the gel, a part of the gel was hydrolysed with 3 *M* HCl at 100°C for 16 h and then the concentration of GalN in the hydrolysate was determined by the Elson–Morgan method[14].

Coupling of STI with succinyl Toyopearl

First, 8 g of suction-dried succinyl Toyopearl HW-55 was mixed with 16 ml of 0.5 *M* NaCl containing 0.4 g of STI. Then, after the pH had been adjusted to 5, the suspension was mixed with 0.25 g of EDC and was incubated at room temperature for more than 2 days. The gel thus obtained was then washed with water, 0.1 *M* sodium carbonate buffer (pH 9.5), water, 0.1 *M* glycine buffer (pH 3.0), and 0.05 *M* Tris–HCl buffer (pH 7.8). The amount of immobilized STI was estimated from the absorbance of the supernatant at 280 nm, using $A_{280}^{1\%} = 20.5$.

RESULTS

Optimal conditions for the activation of Toyopearl by epichlorohydrin

Effect of the concentrations of NaOH and epichlorohydrin. Samples of suction-dried Toyopearl were mixed in a round-bottomed flask with water and NaOH solution of various molarities. The reaction was started in an incubator with shaking by the addition of various amounts of epichlorohydrin. After 2 h the gel was washed on a glass filter with 50 ml of water, the amount of epoxy groups in the gel was then determined. The maximum amount of epoxy groups introduced into Toyopearl HW-55 was found at an initial concentration of 3 *M* NaOH and that of 30% epichlorohydrin as shown in Fig. 1, and that for Toyopearl HW-65 (diol type) was found at initial concentrations of 2 *M* NaOH (Fig. 2A) and of 30% epichlorohydrin (Fig. 2B).

Effect of reaction time and temperature. The time course of activation was studied at four different temperatures: 30, 40, 50 and 60°C, as shown in Figs. 3 and 4.

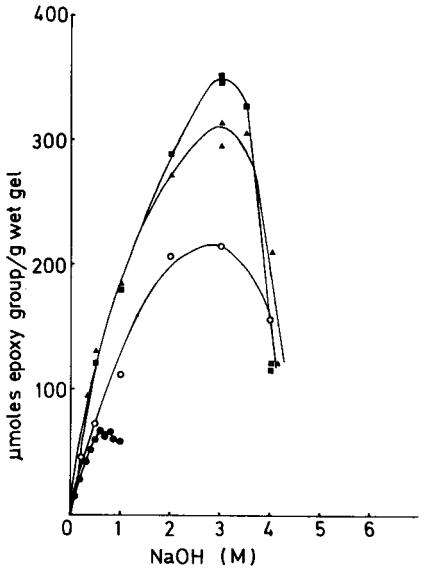

Fig. 1. Effect of the concentrations of NaOH and epichlorohydrin (ECH) on the incorporation of epoxy groups into Toyopearl HW-55. Curves: ■, 50% ECH, 50°C, 2 h; ▲, 50% ECH, 40°C, 2 h; ○, 20% ECH, 50°C, 2 h; ●, 5% ECH, 40°C, 2 h.

The higher the reaction temperature, the quicker was the time for maximum incorporation and for degradation. At 30°C the reactions were slow; the maximum was reached after 20 h for both carriers. At 60°C the maximum was reached in less than 1 h and then the epoxy groups introduced were hydrolysed quickly. At 50°C the highest amount of epoxy groups was introduced in 2 h for Toyopearl HW-55 (330 μmole per gram of wet gel) and in 1 h for Toyopearl HW-65 (diol type) (160 μmole per gram of wet gel).

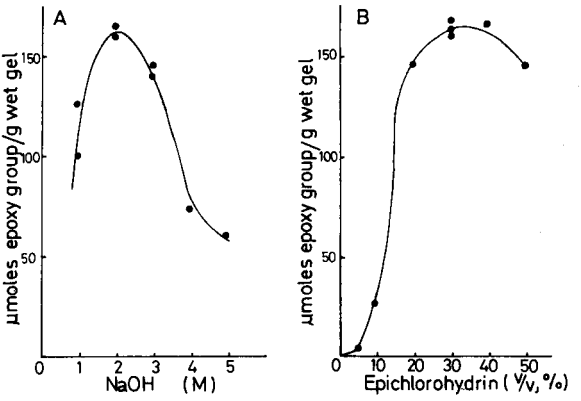

Fig. 2. Effect of the concentrations of NaOH (A) and epichlorohydrin (B) on the incorporation of epoxy groups into Toyopearl HW-65 (diol type). (A), 30% epichlorohydrin, at 50°C for 2 h; (B), 2 *M* NaOH, at 50°C for 2 h.

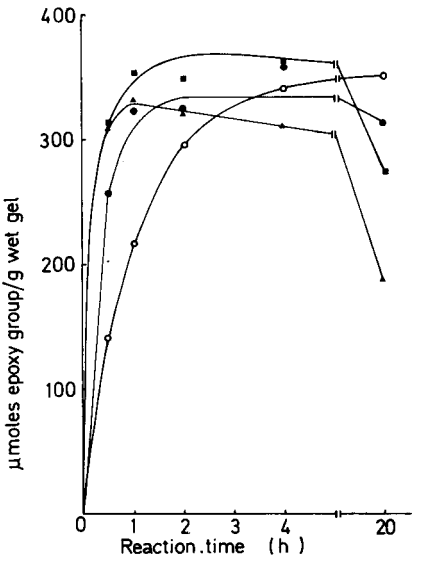

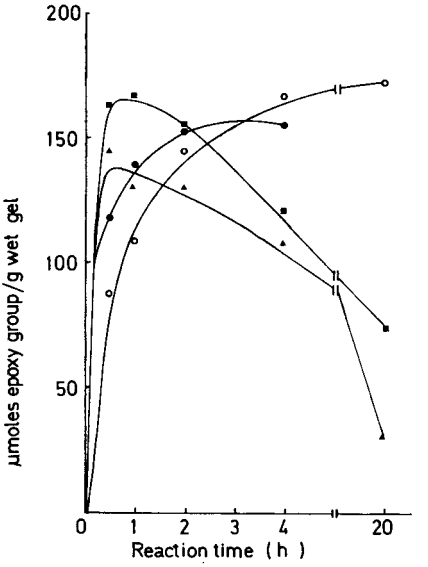

Fig. 3. Effect of reaction time and temperature on the incorporation of epoxy groups into Toyopearl HW-55. Curves: ○, at 30°C; ●, at 40°C; ■, at 50°C; ▲, at 60°C.

Fig. 4. Effect of reaction time and temperature on the incorporation of epoxy groups into Toyopearl HW-65 (diol type). Curves: ○. at 30°C; ●, at 40°C; ■, at 50°C; ▲, at 60°C.

Derivatization of epoxy-activated Toyopearl

The amination of epoxy-activated Toyopearl was performed in concentrated ammonia solution at 40°C for 1.5 h. The introduction of amino groups into the gel was detected by the TNBS colour test, and the content of amino groups was determined by the micro Kjeldahl method. The content of amino groups introduced was 200 μmole per gram of wet gel for Toyopearl HW-55 and 100 μmole per gram of wet gel for Toyopearl HW-65 (diol type). The conversion of epoxy groups into amino groups was not complete and some epoxy groups remained, as was observed in case of agarose gel. The remaining epoxy groups may be less reactive and should not covalently adsorb the solute non-specifically during the course of affinity chromatography[7].

Coupling of ligands with derivatized Toyopearl

Direct reductive amination of lactose and amino Toyopearl HW-65 (diol type) with sodium cyanoborohydride was performed in 6 h because the gel could be boiled. The content of lactose immobilized on the gel was 30 μmole per gram of wet gel, which was comparable with that in the agarose gel obtained by the same reaction at room temperature for 800 h (ref. 15). Couplings of STI and GalN with Toyopearls were performed by the aid of water-soluble carbodiimide, EDC. Some 40 mg of STI and 24 μmole of GalN were immobilized per gram of wet gel.

Affinity chromatography of lectins on Toyopearl adsorbents

Affinity chromatograms of lectins from castor bean and soybean are shown in Figs. 5 and 6. Crude lectin solution was applied to the affinity column, and effluents

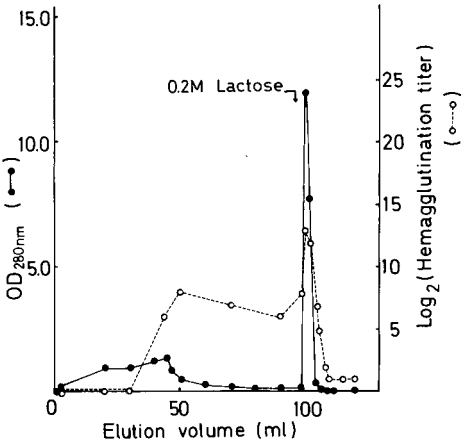

Fig. 5. Affinity chromatography of *Ricinus communis* agglutinins on a lactamyl Toyopearl HW-65 (diol type) column. Crude agglutinins (200 mg) were loaded on a column (2.4 × 1.3 cm I.D.) and washed with phosphate-buffered saline. The adsorbed agglutinins were then eluted with 0.2 *M* lactose. Fractions of 2 ml were collected at a flow-rate of 6 ml/h at 4°C. The absorption at 280 nm (●) and hemagglutinating activity (○) of eluted fractions were measured.

were assayed for absorbance at 280 nm (protein) and for hemagglutinating activity. After the hemagglutinating activity of the effluent became as high as that of the original lectin solution, each column was washed with PBS to remove unbound proteins and then elution was started with 0.2 *M* lactose. Fractions were assayed for protein, and the hemagglutinating activity of each fraction was determined after exhaustive dialysis against PBS to remove lactose. The adsorption capacities of lactamyl Toyopearl HW-65 (diol type) and GalN-Toyopearl HW-65 (diol type) were 3.7 mg RCAs and 2.4 mg SBA per ml of gel, respectively. The purity of the lectins ob-

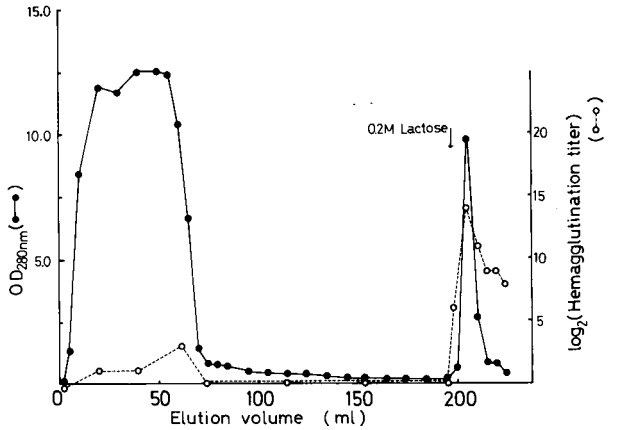

Fig. 6. Affinity chromatography of soybean agglutinin on a GalN-Toyopearl HW-65 (diol type) column (10.4 × 1.0 cm I.D.). A solution of crude soybean agglutinin (50 mg/ml) was applied to the column until the hemagglutinating activity became as high as that of the original solution. Hemagglutination titer was measured using trypsin-treated human erythrocytes.

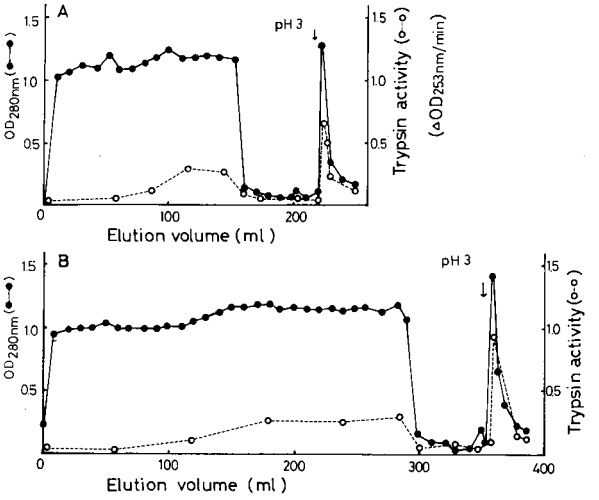

Fig. 7. Affinity chromatography of trypsin on an STI-Toyopearl HW-55 column (2.1 × 1.25 cm I.D.) (A) and an STI-Sepharose 4B column (2.8 × 1.25 cm I.D.) (B). A solution of crude trypsin (16.7 mg/ml 0.05 *M* Tris–HCl–0.5 *M* NaCl, pH 7.8) was applied to both columns until the trypsin activity of the effluent became as high as that of the original trypsin solution. The columns were then washed with 0.05 *M* Tris–HCl–0.5 *M* NaCl, pH 7.8, and citrate-phosphate buffer (pH 3) was started. Fractions of 3 ml were collected at a flow-rate of 10 ml/h at 4°C. The absorption at 280 nm (●) and the trypsin activity (○) were measured.

tained was examined by polyacrylamide gel electrophoresis[16]. Purified SBA gave a single band, whereas purified RCA gave two bands as had been expected[17].

Affinity chromatography of trypsin on STI-Toyopearl

As shown in Figs. 7A and 7B, affinity chromatography of trypsin was performed on STI-Toyopearl HW-55 (described in the section on coupling of ligands) and STI-Sepharose 4B prepared by the same procedures as STI-Toyopearl except the conditions for epoxy activation. A solution of crude trypsin was continuously applied to the affinity columns until the trypsin activity of the effluent reached that level of the original solution. Enzyme activity was determined with BAEE as substrate, the change in absorption at 253 nm being measured. After the column had been washed, the adsorbed trypsin was eluted with citrate–phosphate buffer (pH 3). STI-Toyopearl had a lower adsorption capacity for trypsin than STI-Sepharose containing almost the same amount of STI.

DISCUSSION

The optimal conditions for the epoxy activation of Toyopearls were very different from those for agarose gels. Under the optimal conditions for Sepharose 6B gel (5% epichlorohydrin, 0.4 *M* NaOH, 40°C, 2 h)[7], only a low amount of epoxy groups (67 μmole per gram of wet gel) was introduced on Toyopearl HW-55, as shown in Fig. 1. Because Toyopearl gel can withstand stronger conditions (higher temperature and higher concentrations of NaOH and epichlorohydrin) a sufficient amount of epoxy groups was introduced into the gel.

The optimal conditions for epoxy activation varied with the pore size of the Toyopearl. Toyopearls HW-65 and HW-75 were activated with epichlorohydrin under the optimal conditions for Toyopearls HW-65 (diol type), and 51 and 36 μmole per gram of wet gel of epoxy groups were introduced into Toyopearls HW-65 and HW-75, respectively. As the pore size increased, the amount of epoxy groups introduced decreased. It may be due to a lower amount of hydroxyl groups in Toyopearls with a large pore size.

Because Toyopearl gels withstand higher temperatures than agarose gel, it was also possible to perform reductive amination of lactose and amino-Toyopearl in a far shorter time. However, because Toyopearl gels were not solubilized by 70% acetic acid at 100°C or even by 6 *M* HCl at 100°C overnight, it was impossible to determine the content of amino groups introduced in the gel by the TNBS method. The micro Kjeldahl method was used, but a very long degradation time was required.

As had been expected, the affinity adsorbents obtained with Toyopearl gel were very stable, and a flow-rate of the columns was maintained under the increased pressure. The adsorption capacities of these columns, however, were lower than those of extremely high capacity agarose adsorbents[15] prepared by the same method and with the same amount of ligand. It is well known that affinity adsorbents prepared with BioGel also have lower binding capacities than those prepared with agarose gel[15,18,19]. It may be due to the less hydrophilic properties of Toyopearl and BioGel.

REFERENCES

1 R. Axén, J. Porath and S. Ernback, *Nature*, 215 (1967) 1302.
2 J. Ludens, I. R. De Vries and D. D. Fanstiel, *J. Biol. Chem.*, 247 (1972) 7533.
3 V. Sica, E. Nola, I. Parikh, G. A. Puca and P. Cuatrecasas, *J. Biol. Chem.*, 248 (1973) 6543.
4 R. Lamed, Y. Levin and A. Oplatka, *Biochim. Biophys. Acta*, 305 (1973) 163.
5 A. H. Nishikawa and P. Bailon, *Arch. Biochem. Biophys.*, 168 (1975) 576.
6 L. Sundberg and J. Porath, *J. Chromatogr.*, 90 (1974) 87.
7 I. Matsumoto, Y. Mizuno and N. Seno, *J. Biochem.*, 85 (1979) 1091.
8 R. F. Murphy, J. M. Conlon, A. Imam and G. J. C. Kelly, *J. Chromatogr.*, 135 (1977) 427.
9 I. Matsumoto, N. Seno, A. M. Golovtchenko-Matsumoto and T. Osawa, *J. Biochem.*, 87 (1980) 535.
10 Y. Kato, K. Komiya, T. Iwaeda, H. Sasaki and T. Hashimoto, *J. Chromatogr.*, 211 (1981) 383.
11 H. J. Allen and E. A. Z. Johnson, *Carbohydr. Res.*, 50 (1976) 121.
12 Y. Nagai, *Seikagaku Kenkyuho* (in Japanese), Asakura Shoten, Tokyo, 1976, pp. 444–445.
13 H. Roth, S. Segal and D. Bertoli, *Anal. Biochem.*, 10 (1965) 32.
14 S. Gardell, *Acta Chem. Scand.*, 7 (1953) 207.
15 I. Matsumoto, H. Kitagaki, Y. Akai, Y. Ito and N. Seno, *Anal. Biochem.*, 116 (1981) 103.
16 R. A. Reisfeld, U. J. Lewis and D. E. Williams, *Nature*, 195 (1962) 281.
17 G. L. Nicolson, J. Blaustein and M. E. Etzler, *Biochemistry*, 13 (1974) 196.
18 P. Cuatrecasas, *J. Biol. Chem.*, 245 (1970) 3059.
19 R. J. Baues and G. R. Gray, *J. Biol. Chem.*, 252 (1977) 57.

Journal of Chromatography, 239 (1982) 755–760
Elsevier Scientific Publishing Company, Amsterdam — Printed in The Netherlands

CHROM. 14,649

ADSORPTION CHROMATOGRAPHY OF PROTEINS ON SILICONIZED POROUS GLASS

TAKAHARU MIZUTANI* and TAKAHIKO NARIHARA
Faculty of Pharmaceutical Sciences, Nagoya City University, Tanabe-dori, Mizuho-ku, Nagoya 467 (Japan)

SUMMARY

Conditions of adsorption chromatography on silicone-coated porous glass were studied using standard proteins and rabbit serum. By elution at a high flow-rate, identical with that used in high-performance liquid chromatography, protein separation on silicone-coated glass was better using an acetonitrile elution system than one containing cholate detergent.

INTRODUCTION

We have developed adsorption chromatography of proteins on porous glass[1–3], which adsorbs approximately 5 μmol of cationic materials and proteins per gram[4,5]. Recently, the porous glass was siliconized to prevent protein adsorption[6]. However, this silicone-coated porous glass still adsorbed proteins well at high concentrations of salts (about 50 mg/g)[7,8], and was used as an adsorbent for protein separation[9].

Chromatography of proteins on hydrophobic media can be performed in two ways. The first, reversed-phase high-performance liquid chromatography (HPLC) on μBondapak C_{18}, uses acetonitrile or methanol as mobile phases[10,11]. The second, affinity chromatography of active proteins on alkyl-Sepharose, uses solvent systems containing detergents, such as cholate or Triton X-100[12,13]. In this work, we report adsorption chromatography of standard proteins or rabbit serum on siliconized porous glass using both acetonitrile and detergent systems (described above), and achieve a separation of some microsomal proteins, which are hydrophobic proteins, on silicone-coated glass.

MATERIALS AND METHODS

Porous glass (1 g, CPG-10 240 Å), coated with 200 μl of silicone oil as previously reported[6], was packed into a column (30 × 0.26 cm I.D.). The standard proteins used were haemoglobin (Hb), bovine serum albumin (BSA), and peroxidase (1 mg of each in 0.5 ml of 0.9 *M* sodium chloride). Rabbit serum (0.1 ml) was mixed with 1 *M* sodium chloride (0.4 ml) and applied on to the column. In order to elute, two solvent systems were used. The detergent solvent system was composed of a

0021-9673/82/0000–0000/$02.75

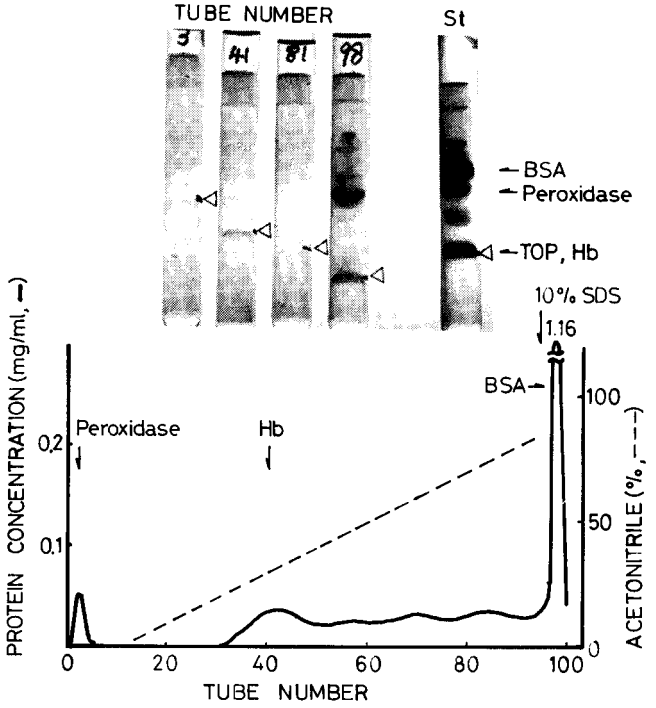

Fig. 1. Elution pattern of standard proteins using the acetonitrile system. Elution was carried out at room temperature and a flow-rate of 1 ml per 0.05 cm^2 per min with a linear gradient of 0.01 *M* ammonium acetate at pH 5.6 to 100% acetonitrile (total 100 ml). Standard proteins (each 1 mg) were BSA, peroxidase and haemoglobin. The column size of the silicone-coated porous glass was 30 × 0.26 cm I.D. Fraction volumes were 1 ml. In the gel patterns, the position of marker dye BPB by electrophoresis is indicated by a triangle (TOP) and St is the pattern of the standard protein mixture.

linear gradient from 0 to 100% or from 30 to 100% (total volume 60 ml) of 0.5% sodium cholate to 0.5% deoxycholate in 0.01 *M* Tris–HCl at pH 7.6. A second solvent system was a linear gradient of acetonitrile. After elution was complete, the column was regenerated by elution with 10% sodium dodecyl sulphate (SDS) and then thoroughly washed with distilled water. The flow-rate was 1 ml per column diameter (0.05 cm^2) per min, which is identical with that used for HPLC of proteins. The fraction volumes were 1 ml. Protein was determined by the absorbance at 280 nm or by the Lowry method. The fractions containing proteins were analysed by SDS disc electrophoresis[14].

Mammalian microsomes contain many membrane-bound, hydrophobic, and water-insoluble proteins. With this hydrophobic media of siliconised CPG, separation of these microsomal proteins was attempted.

Chromatography of microsomal proteins (precipitates at 105,000 *g*) was performed as follows. Rat liver microsomes (0.1 ml, 1.1 mg total protein) were mixed with 0.9 ml of 1 *M* sodium chloride and applied on to a silicone-coated glass column (5.2 × 0.65 cm). The column was eluted stepwise with several buffers containing cholate or Triton X-100 at a flow-rate of 0.5 ml/cm^2 · min. The 1-acylGP acyltransferase activity, as one typical enzyme in microsomes, in the eluates was measured at 412 nm by addition of oleoyl–CoA (12 μmol) in a reaction mixture (1 ml) containing 1 m*M* 5,5′-dithiobis(2-nitrobenzoic acid), 20 μM 1-acylglycerophosphate, 1 *M* Tris–HCl at pH 7.2 and 20 μl of eluate.

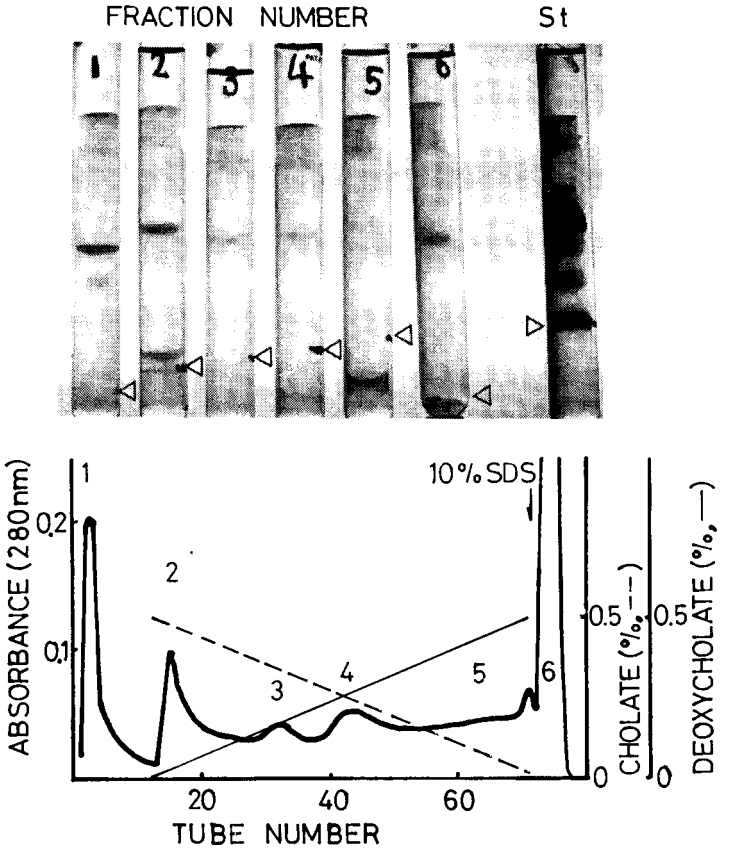

Fig. 2. Elution pattern of standard proteins using the cholate–doxycholate system. Elution was carried out with a linear gradient of 0.5% cholate to 0.5% deoxycholate in ;.01 *M* Tris–HCl at pH 7.6 (total volume 60 ml). Other conditions as in Fig. 1. The gel pattern of the standard proteins is identical with that in Fig. 1.

RESULTS AND DISCUSSION

Fig. 1 shows the elution pattern for standard proteins using acetonitrile as mobile phase together with stained gel patterns of some fractions. The gel patterns show that tube 3 contains peroxidase and tubes 41–81 contain haemoglobin. Elution of haemoglobin was also confirmed by the absorbance at 400 nm in Fig. 1. BSA was eluted with 10% SDS (tube 98) as shown in Fig. 1; tube 98 also contained haemoglobin.

In a buffer of high concentration of salt, peroxidase was not adsorbed onto the siliconized CPG column, so it was passed through the column as shown in Fig. 1. We also obtained similar results from adsorption pattern of a mixture of peroxidase and BSA[7]. The order of affinities onto the coated glass surfaces were haemoglobin > albumin > peroxidase[7]. The order of affinities of haemoglobin and BSA was incompatible with the eluting order of those proteins on adsorption chromatography (haemoglobin was eluted faster than BSA). This discrepancy might be due to the kind of solvent (acetonitrile).

Fig. 2 shows the elution pattern for standard proteins using a detergent system together with stained gel patterns of the fractions. Fraction 1 contains BSA and

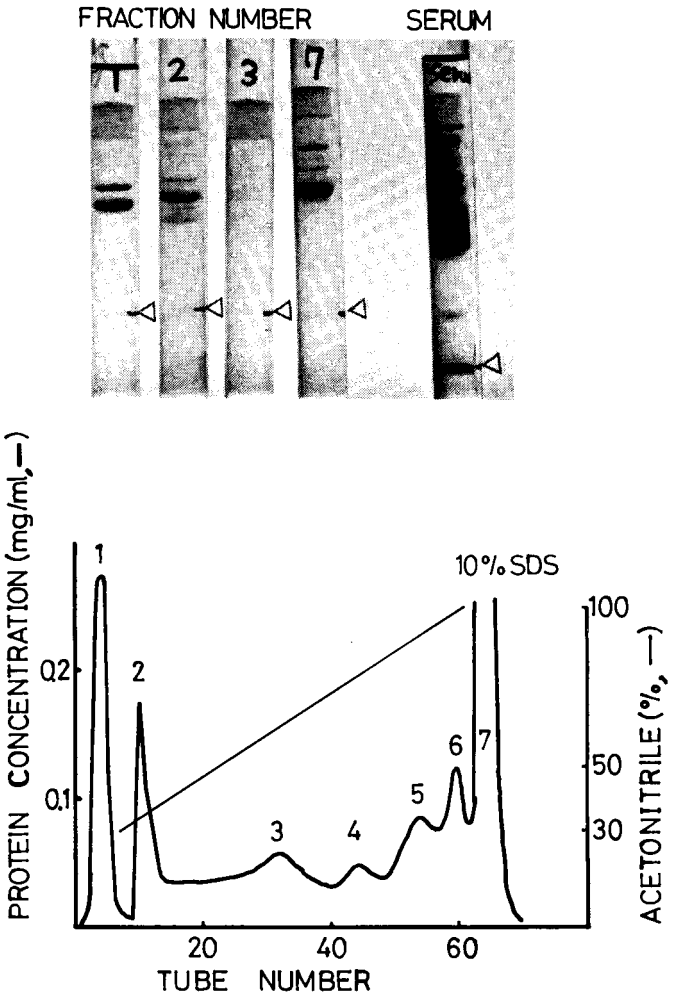

Fig. 3. Elution pattern of rabbit serum (0.1 ml) using the acetonitrile system. Elution was carried out with a linear gradient of 30% acetonitrile in 0.01 *M* Tris–HCl at pH 7.6 to 100% acetonitrile (total volume 60 ml). Other conditions as in Fig. 1.

peroxidase and fraction 2 contains BSA and haemoglobin; fractions 1–6 all contain BSA. Comparison of Figs. 1 and 2 shows that protein separation was better using the acetonitrile system and protein recovery was with the detergent system, even though the orders of elution of the proteins from the columns are similar.

Fig. 3 shows the elution pattern of rabbit serum using an acetonitrile elution system together with stained gel patterns. The gel patterns show fraction 1 to contain albumin and fraction 2 to contain some globulins with albumin. Protein bands were not found in fractions 4–6. Fraction 7 contains different globulins to those in fraction 2 as shown in the gel patterns.

Fig. 4 shows the elution patterns of serum with cholate and deoxycholate. The gel patterns show that the fractions contain albumin. Protein separation in Fig. 3 is better than that in Fig. 4. These results show silicone-coated porous glass to be useful for protein separation at a high flow-rate, similar to that used in HPLC. The aceto-

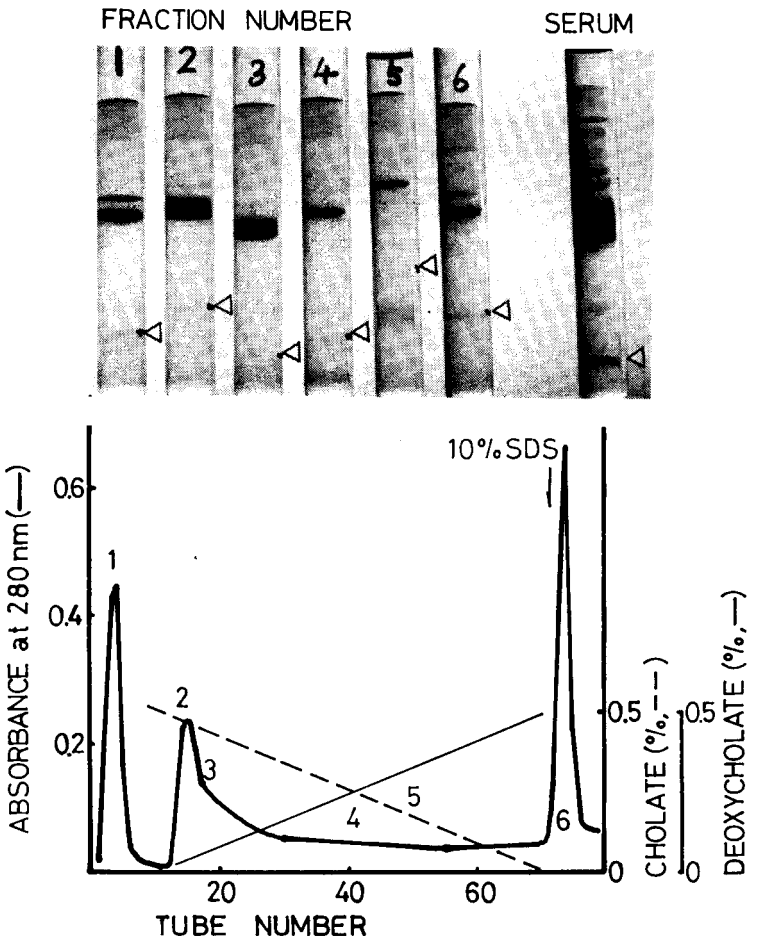

Fig. 4. Elution pattern of serum with a detergent elution system. Rabbit serum (0.1 ml) was used; other conditions as in Fig. 2.

nitrile elution system is slightly better than that containing cholate and deoxycholate.

As affinity chromatography for purification of active proteins, hydrophobic ligand-coupled Sepharose is used by elution with detergents. Meanwhile, as HPLC, hydrophobic adsorbents, such as μBondapak C_{18}, are used for analysis of peptides with polar solvent (methanol or acetonitrile). These two systems of affinity chromatography and reversed-phase HPLC should be fused and developed to new systems. As one of the new systems, we showed adsorption chromatography of proteins on siliconised porous glass at a high flow-rate under atmospheric pressure.

Fig. 5 shows the elution pattern of microsomal proteins on silicone-coated glass. As shown in the schematic gel patterns, some proteins were separated with the cholate elution system. Microsomes are composed of many hydrophobic membrane proteins as well as ribosomal proteins. We could not attribute the band on the gel as that of a specific protein, but the results showed that adsorption chromatography on siliconized porous glass was effective for separation of hydrophobic microsomal proteins. Recovery of proteins was better and the activity of 1-acylglycerophosphate acyltransferase was retained after chromatography on siliconized glass.

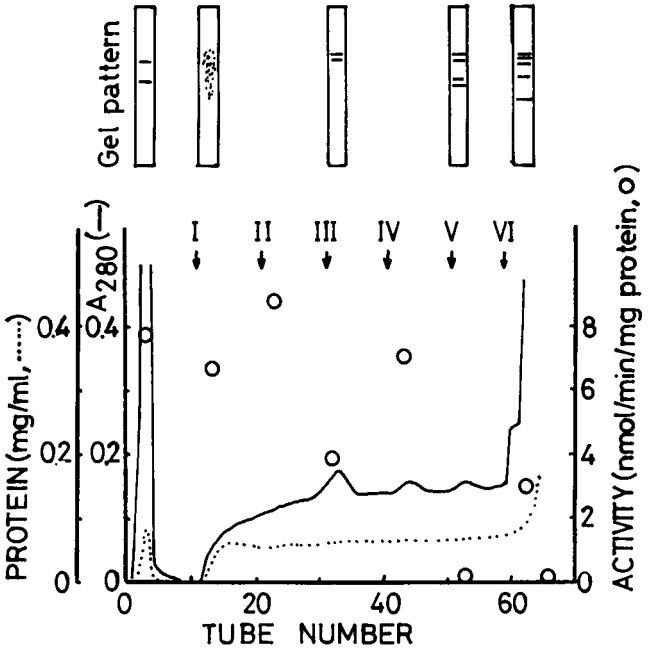

Fig. 5. Adsorption chromatography and disc gel patterns of microsomal proteins on siliconized porous glass. Buffers for elution are as follows: I, 0.05 *M* Tris–HCl–20% glycerol (pH 7.6); II, 0.125% sodium cholate in I; III, 0.25% sodium cholate in I; IV, 0.375% sodium cholate in I; V, 0.5% cholate in I; VI, 1% Triton X-100 in I. Activity is that of 1-acylglycerophosphate acyltransferase.

CONCLUSION

Adsorption chromatography on silicone-coated porous glass at a high flow-rate, that was identical to that used in HPLC, was studied using standard proteins (peroxidase, albumin, and haemoglobin) or rabbit serum. Proteins were separated by both the eluting system with acetonitrile and by that with cholate. Therefore, siliconized porous glass is useful for hydrophobic adsorption chromatography of proteins at high flow-rate under atmospheric pressure. Separation of microsomal proteins on the glass was attempted.

REFERENCES

1 T. Mizutani and A. Mizutani, *J. Chromatogr.*, 120 (1976) 206.
2 T. Mizutani and A. Mizutani, *J. Chromatogr.*, 168 (1979) 143.
3 T. Mizutani, *J. Colloid Interface Sci.*, 79 (1981) 284.
4 T. Mizutani and A. Mizutani, *Anal. Biochem.*, 83 (1977) 216.
5 T. Mizutani and A. Mizutani, *J. Pharm. Sci.*, 67 (1978) 1102.
6 T. Mizutani, *J. Chromatogr.*, 196 (1980) 485.
7 T. Mizutani, *J. Pharm. Sci.*, 70 (1981) 493.
8 T. Mizutani, *J. Colloid Interface Sci.*, 82 (1981) 162.
9 T. Mizutani, *J. Chromatogr.*, 207 (1981) 276.
10 F. E. Regnier and K. M. Gooding, *Anal. Biochem.*, 103 (1980) 1.
11 M. T. W. Hearn, B. Grego and W. S. Hancock, *J. Chromatogr.*, 183 (1979) 429.
12 S. Hjertén, J. Rosengren and S. Påhlman, *J. Chromatogr.*, 101 (1974) 281.
13 Y. Imai, *J. Biochem.*, 80 (1976) 267.
14 U. K. Laemmli, *Nature (London)*, 227 (1970) 680.

Journal of Chromatography, 239 (1982) 761–772
Elsevier Scientific Publishing Company, Amsterdam — Printed in The Netherlands

CHROM. 14,625

EFFECT OF STATIONARY PHASE STRUCTURE ON RETENTION AND SELECTIVITY IN REVERSED-PHASE LIQUID CHROMATOGRAPHY

NOBUO TANAKA*, YASUYUKI TOKUDA, KAZUFUSA IWAGUCHI and MIKIO ARAKI
Faculty of Textile Science, Kyoto Technical University, Matsugasaki, Sakyo-ku, Kyoto 606 (Japan)

SUMMARY

The effect of the structure of the stationary phase on retention and selectivity in reversed-phase liquid chromatography was studied, using chemically bonded stationary phases on silica gel. Nine stationary phases with various size, rigidity and degree of unsaturation were prepared, including alkyl, aryl, aralkyl and alicyclic structures. In addition to the solvophobic interaction and the solvation of the solutes in the mobile phase, stationary phase effects such as steric recognition and π–π interaction between solutes and the stationary phase, and the effect of solvent molecules bound to the stationary phase, were found to be important in determining retention in reversed-phase liquid chromatography. Planar solutes were preferentially retained by the stationary phases of planar structure and rejected by the non-planar stationary phases. Extended octadecyl groups and large aromatic rings in the stationary phase contributed to the preferential retention of planar solutes. The aromatic stationary phases showed greater retention for aromatic and polar solutes and lesser retention for saturated hydrocarbons than the saturated stationary phases. Retention and selectivity on stationary phases with aryl or aralkyl functionality were found to be more sensitive to solvent changes than on saturated stationary phases. The results suggest the possibility of controlling the magnitude of the stationary phase effects by selecting a stationary phase structure that can enhance the separation capability of reversed-phase liquid chromatography. The versatility of stationary phases with large aromatic groups was shown, and the complementary use of stationary phases of widely different nature was suggested to provide maximum selectivity.

INTRODUCTION

In a previous paper[1], we reported the effect of the alkyl chain length of the stationary phase in reversed-phase liquid chromatography (RPLC). We showed that the appearance of the chain-length effect was strongly influenced by the structure of the solutes and the type of organic solvent used in the mobile phase, both of which affect the extent of interaction associated with the stationary phase. The results implied that it was possible to vary the magnitude of these stationary phase effects by selecting the structure of the hydrocarbon moiety of the stationary phase. This is expected to increase the versatility of RPLC. The examination of the retention characteristics of stationary phases with various structures may lead to new stationary phases with greater separation capability, and at the same time provide information on the retention mechanism in RPLC.

0021-9673/82/0000–0000/$02.75

There have been some reports in this respect in the past. Little *et al.*[2] tried to increase the selectivity of the stationary phase by using a very long alkyl chain in the stationary phase. Attempts to control selectivity in RPLC by the use of various stationary phase structures have been popular[3–5], but the role of the stationary phase in RPLC is not yet fully understood.

Although RPLC is more widely used than normal-phase chromatography and improvements are still being made, the former has generally been considered to be less selective than the latter with respect to changes in retention due to steric factors associated with the solutes and changes in the type of solvents in the mobile phase. The major factor in retention in RPLC is the solvophobic interaction[6], which has less polar and steric selectivity compared with polar adsorption in normal-phase chromatography.

The present practice in RPLC is that a preliminary attempt at separation on a C_{18} stationary phase with a certain composition of the aqueous mobile phase is followed by a change in the eluent composition in order to adjust k' values and the separation. The use of tetrahydrofuran and solvents other than methanol or acetonitrile was shown to be useful[7–9]. If the desired separation is not obtained, one can try other stationary phases, such as C_8 or phenyl, which are commercially available. Several manufacturers offer instruments that can accomodate up to three or four solvents and carry out systematic development of the mobile phase[10].

A few points can be made on this approach of the development of the chromatographic system. First, this approach assumes the superiority of the C_{18} phase. Second, the selection of the alternative stationary phase is largely based on personal experience. Third, the search for suitable solvents with a single column can be time consuming, and some organic solvents for high-performance liquid chromatography (HPLC) are very expensive.

Another possible approach of attaining separations is to employ well characterized columns with widely different nature and to use simpler mobile phases and less time to develop the system. Thorough understanding of the interrelation between the solute structure, stationary phase structure and the retention seems to be very valuable in this regard, and the development of a stationary phase superior to the C_{18} phase, or a good alternative to the C_{18} phase, will greatly enhance the versatility of RPLC.

EXPERIMENTAL

Equipment

An HPLC system was constructed with an LC-3A pumping system (Shimadzu, Kyoto, Japan), a 7125 valve loop injector (Rheodyne, Berkeley, CA, U.S.A.) and M440 UV and R401 refractive index detectors (Waters Assoc., Milford, MA, U.S.A.). A thermostated bath was used to maintain the column temperature at 30 $\pm$ 0.1°C.

Materials

Spherical silica gel (Develosil; Nomura Chem., Seto, Japan) of average particle diameter 5 μm (surface area *ca.* 330 m^2/g) was used. Silylating reagents were either purchased from Petrarch System (Levittown, PA, U.S.A.) or prepared from corresponding olefins by standard methods. Chemical bonding reactions including end capping and column packing were carried out as described previously[7]. Mobile

phases were made up by volume from LC-grade solvents (Nakarai Chem., Kyoto, Japan) and distilled water. Absolute methanol and absolute acetonitrile were obtained by standard methods[1].

Sample substances were either purchased or prepared by standard methods. Some polar compounds, including *n*-alkyl alcohols, *n*-alkyl carboxylic acid methyl esters and aromatic nitro compounds, were used in addition to hydrocarbons with various structures as follows: toluene (1), ethylbenzene (2), *n*-propylbenzene (3), *n*-butylbenzene (4), *n*-pentane (5), *n*-hexane (6), *n*-heptane (7), *n*-octane (8), naphthalene (9), anthracene (10), pyrene (11), 3,4-benzpyrene (12), cyclohexane (13), *trans*-decahydronaphthalene (14), adamantane (15), *n*-decane (16), diphenylmethane (17), 1,2-diphenylethane (18), triphenylmethane (19), tetraphenylethylene (20), fluorene (21), bidiphenyleneethylene (22), *o*-terphenyl (23), triphenylene (24), triptycene (25), tetrahydronaphthalene (26), *n*-dodecane (27), *n*-tetradecane (28) and *n*-hexadecane (29). Samples were made up in the mobile phase in most instances.

Chromatographic measurement

Chromatographic runs were carried out in duplicate. The reproducibility between the runs was better than $\pm$ 0.5%. The void volume (t_0) was obtained by the injection of water and glycerine. The outer column dead volumes in the connecting tubing and detectors were corrected.

RESULTS AND DISCUSSION

The structures of the organic silyl groups of the stationary phases differing in size, rigidity, planarity and degree of unsaturation are shown in Scheme 1. They include trimethylsilyl (C_1), *n*-octyldimethylsilyl (C_8), *n*-octadecyldimethylsilyl (C_{18}), 2-cyclohexylethyldimethylsilyl (CHE), 2-(3-cyclohexenyl)ethyldimethylsilyl (CHNE), phenyldimethylsilyl (Ph), 2-phenylethyldimethylsilyl (PE), 2-(2-naphthyl)ethyldimethylsilyl (NE) and 2-(3-pyrenyl)ethyldimethylsilyl (PYE). As shown in Table I, surface coverages are considered to be maximum for each bonded phase[11]. The stationary phases were treated with trimethylsilylating reagents to reduce the number of residual silanols. Maximum coverages are desirable when comparing the retention characteristics of the stationary phases.

The four types of hydrocarbons which visualized the difference in chainlength of the stationary phases[1] were used to study the nine stationary phases in 80% methanol. The solutes included *n*-alkanes, planar polynuclear aromatic hydrocarbons (PAHs), aromatic compounds that cannot adopt a planar structure owing to steric repulsion within the molecule, and alicyclic compounds. The three pairs of solutes,

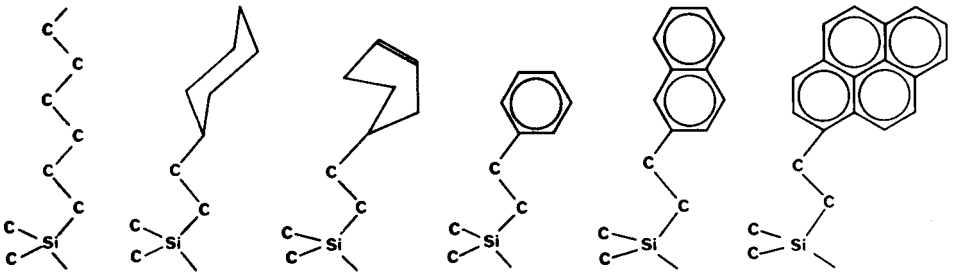

Scheme I

TABLE I

SURFACE COVERAGES OF THE STATIONARY PHASES

Parameter	*Stationary phase*								
	C_1	C_8	C_{18}	*CHE*	*CHNE*	*Ph*	*PE*	*NE*	*PYE*
Carbon content (%)*	5.3	12.2	20.8	11.7	12.0	9.8	13.1	15.5	20.0
Surface coverage (μmol/m^2)	4.9	3.7	3.6	3.5	3.6	3.6	4.0	3.5	3.4

* From elemental analysis, prior to trimethylsilylation, except for the C_1 phase.

17 and 21, 20 and 22, and 23 and 24, have the same number of carbon atoms and π-electrons. Steric repulsion between the phenyl rings in 17, 20 and 23, makes these molecules non-planar. This type of analysis is expected to provide clues to the problems of why the C_{18} phase preferentially retains planar hydrocarbons[1] compared to the C_1 or C_8 phases and how the planarity, rigidity and degree of unsaturation of the stationary phase affects retention and selectivity in RPLC. The results are shown in the form of log k' *versus* log k' plots in Fig. 1–3.

Fig. 1 shows a comparison of four stationary phases with eight carbon atoms in the major hydrocarbon part. Although straight lines are expected only for *n*-alkanes, the groups of solutes are located very close to straight lines, and it is convenient to show the retention characteristics of each stationary phase in this way. The solutes used to construct these lines were *n*-alkanes from C_5 to C_{10}, PAHs from naphthalene (9) to benzpyrene (12), alicyclic compounds from cyclohexane (13) to adamantane (15) and the non-planar aromatic compounds diphenylmethane (17), triphenylmethane (19), tetraphenylethylene (20) and *o*-terphenyl (23).

In these log k' *versus* log k' plots, the *n*-alkanes can be taken as the solutes with a minimum degree of specific interactions with the stationary phase. When a

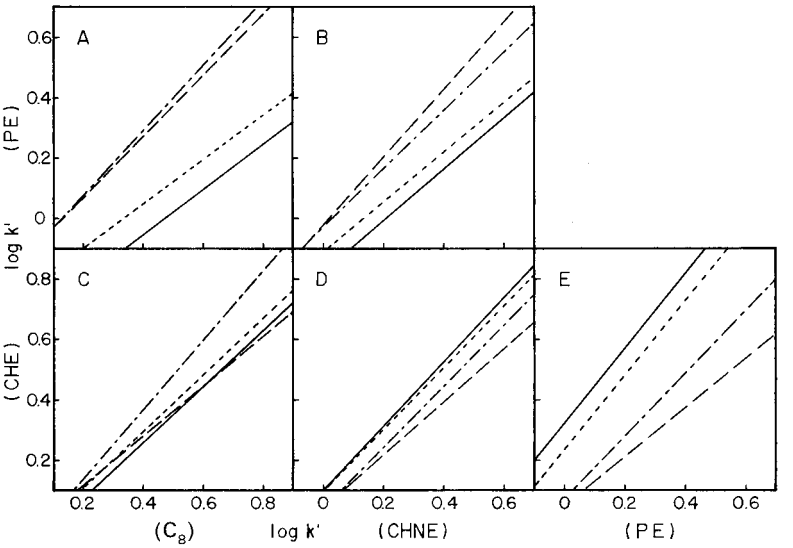

Fig. 1. Plots of log k' values on CHE and PE phases against log k' values on C_8, CHNE and PE phases in 80% methanol. ——, *n*-Alkanes; – – –, PAHs; – · – · –, non-planar aromatics; - - - - -, alicyclics.

group of solutes behaved differently from *n*-alkanes in the plots, the solutes were preferentially retained by the stationary phase whose axis is closer to the line compared to the line for *n*-alkanes. When the straight lines were well separated in the plots, there is a difference in selectivity between the two stationary phases toward the different type of compounds. In other words, if two solutes belonging to different groups gave similar k' values or no separation on one stationary phase, they can be easily separated on the other stationary phase with the same mobile phase. Thus a pair of columns which give the most scattered plot can provide maximum selectivity difference. The difference in selectivity is large between aromatic and aliphatic stationary phases, and also significant between straight chain and cyclic stationary phases as shown.

In Fig. 1C, two saturated stationary phases, CHE and C_8, are compared. The difference in the retention behaviour is relatively minor between these two phases, but the non-planar aromatic compounds showed significantly larger retentions compared with other types of hydrocarbons on the cyclic CHE phase than the C_8 phase. This suggests that the non-planar aromatic compounds were either favoured by the CHE phase or disfavoured by the C_8 phase compared with planar PAHs and saturated hydrocarbons. The results shown later indicate there seem to be no positive effects by the CHE phase. The apparent preference of non-planar aromatic compounds by the CHE phase was caused by the fact that the straight chain C_8 phase disfavors these hydrocarbons. The results obtained by Řehák and Smolková[5] can also be explained by similar shape compatibility.

Fig. 1D, the plot between the CHE phase and the CHNE phase, shows the influence of a double bond in the stationary phase structure. As can be seen, only one double bond significantly affected the retention, favouring the aromatic compounds, particularly the planar PAHs. The introduction of a double bond increases the planarity and rigidity of six-membered ring while increasing the extent of electronic interactions. In the comparison of the two stationary phases having six-membered rings, in Fig. 1E, the PE phase showed preferential retention for aromatic compounds, as expected. Similarly, the PE phase showed a larger retention for aromatic compounds than saturated compounds when compared to the C_8 phase, as shown in Fig. 1A. The two phases did not differentiate the aromatic compounds based on their planarity. Among the four stationary phases examined in Fig. 1, the largest difference was seen between the CHE and PE phases with respect to the retention of the four types of the hydrocarbon solutes.

In Fig. 2, the C_1 phase, which had been thought to have unusual characteristics as an RPLC stationary phase, was compared with three other phases. Fig. 2A suggests that the two alkyl phases, C_1 and C_8, are very similar with respect to the retention of these hydrocarbons. The difference between the two was close to that between the Ph and the PE phase. Fig. 2B indicates that the CHE phase favours non-planar aromatic compounds and disfavours planar PAHs in comparison with the shortest C_1 phase. In other words, the CHE phase, which cannot take a planar structure, rejects planar hydrocarbons even in comparison with the C_1 phase. This emphasizes the importance of the planar structure of the stationary phase to show preferential retention of planar solutes. The plot between the C_1 and the Ph phase is similar to that between the C_8 and the PE phase in Fig. 1A. This implies that the stationary phases having one phenyl ring did not show much preference toward planar PAHs over non-planar aromatic compounds. A phenyl ring seems to be insufficient to show much planarity.

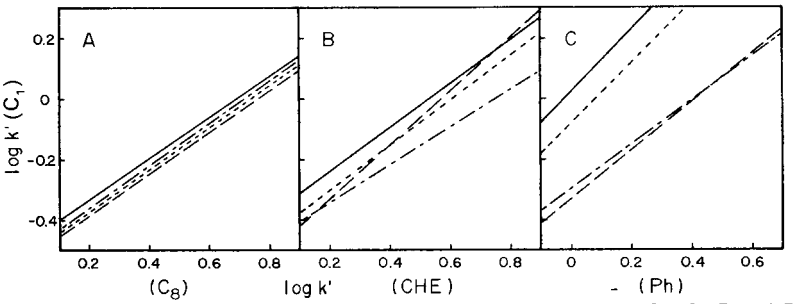

Fig. 2. Plots of log k' values on C_1 phase against log k' values on C_8, CHE and Ph phases in 80% methanol. See Fig. 1 for the solute identification.

Fig. 3 shows a comparison between the C_{18} phase, the most commonly used stationary phase in RPLC, and five stationary phases that be used as complementary stationary phases owing to their differing retention characteristics from the C_{18} phase. As shown in Fig. 3A, the difference between the C_{18} and the C_8 phase is not particularly great, especially for non-planar aromatic compounds and saturated compounds, although the C_8 phase is commonly used as an alternative to obtain separations which are not possible with the C_{18} phase. The largest difference in retention between the PAHs and non-planar aromatic compounds is seen in Fig. 3B, which compares the C_{18} and CHE phases. The planarity of the stationary phase is the factor to give such a difference. Figs. 3C–E show plots between the C_{18} and the three aromatic stationary phases. Large differences in retention behaviour between aromatic compounds and saturated compounds were observed, which was not the case with the C_8 phase. Aromatic compounds were preferentially retained by the aromatic stationary phase, and saturated compounds by the C_{18} phase. Any of these three combinations can also provide different selectivity between alicyclic compounds and *n*-alkanes. The largest increase in retention was seen for PAHs with an increase in the size of the aromatic ring system in the stationary phase, as with increase in alkyl chain length in the stationary phase from the C_1 to the C_{18} phase[1].

The PE phase could be a possible choice as a complementary stationary phase to the C_{18} phase in Fig. 3. When considering the versatility of a stationary phase, however, the absolute retention of the stationary phase has to be taken into account. The retention times of hydrocarbons on the PE phase were three to six times smaller than on the C_{18} phase. The commercially available Ph phase showed even smaller retention. Thus the solvent strength has to be lowered when these stationary phases are used instead of the C_{18} phase. Large retention times are also preferable with preparative separations, because they allow the use of stronger eluents. Large sample volumes and higher elution strengths of the sample solvents often cause a decrease in column performance in preparative separations[12,13] and the undesirable effect can be minimized by the use of stronger mobile phases. The PYE phase is more retentive, and is considered to be better in this respect.

The stationary phase still needs improvement to provide a greater selectivity difference to the C_{18} phase as the PAHs and non-planar aromatic compounds behaved very similarly on both the C_{18} phase and the PYE phase in this mobile phase. The PAHs and the non-planar aromatic compounds behaved differently on the two stationary phases in other mobile phases such as 80% acetonitrile and absolute methanol. This is probably due to the change in the alkyl chain structure of the C_{18}

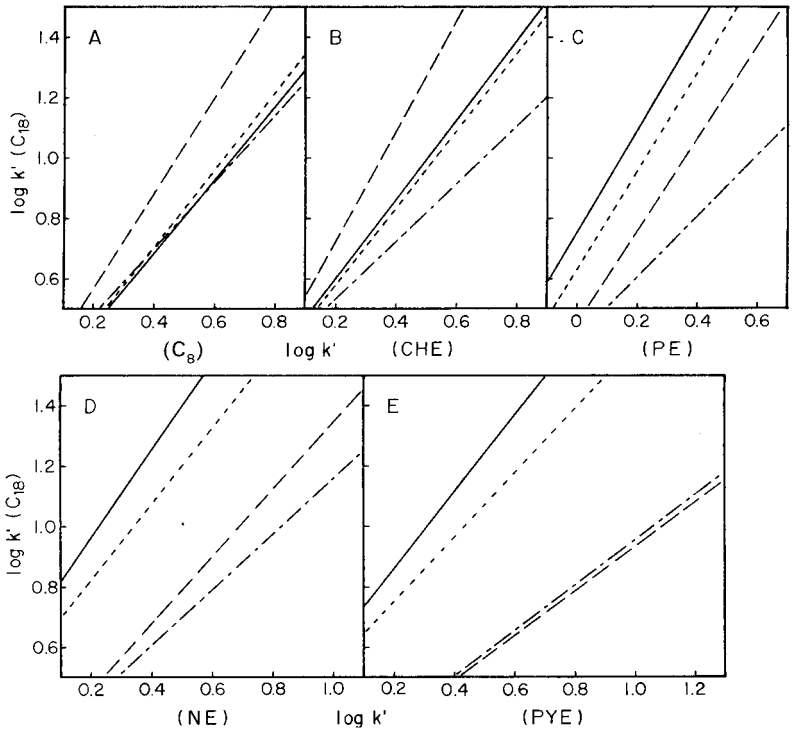

Fig. 3. Plots of log k' values on C_{18} phase against log k' values on C_8, CHE, PE, NE and PYE phases in 80% methanol. See Fig. 1 for the solute identification.

phase and the extent of solvation of the PYE phase. The more extended C_{18} chains seem to favour the planar PAHs in stronger mobile phases than the PYE phase, which is expected to show little structural change with change in the mobile phase.

There is no doubt that any of the five stationary phases in Fig. 3 can enhance the capability of RPLC, as the C_8 phase, which showed a relatively small difference from the C_{18} phase, has proved useful. If one considers an alternative stationary phase to the C_{18} phase which can provide a greater separation capability and versatility in RPLC, it will be a stationary phase with large aromatic groups such as the PYE phase used in this study. Some advantages of such a phase over other phases are mentioned below.

First, the PYE phase gave the greatest retention among the five stationary phases in Fig. 3, almost similar to the C_{18} phase for aromatic compounds and slightly less for aliphatic polar compounds, as shown in Fig. 4. Large k' values, which enable the use of strong solvents, are needed with preparative separations, as mentioned before, to allow large sample volumes and strong sample solvents to be used, because large aromatic compounds sometimes have limited solubility in aqueous solvents. Second, a large difference in the retention characteristics was seen between the PYE phase and the C_{18} phase with respect to the degree of unsaturation of the solutes. Aromatic and polar compounds, especially aromatic nitro compounds, were selectively retained by the PYE phase. The chromatograms in Fig. 5 show a difference in selectivity between the two phases. Peak reversal can be seen in the same k' range in the same mobile phase. Selectivity difference of this magnitude for hydrocarbons in the

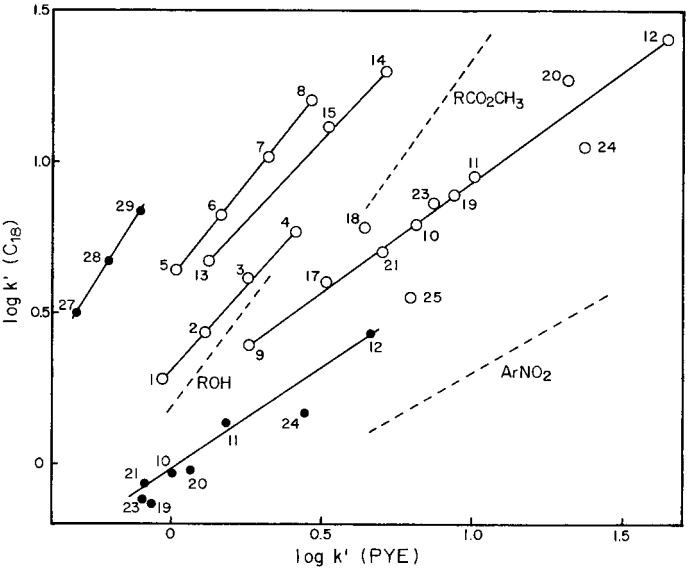

Fig. 4. Plots of log k' values on C_{18} phase against log k' values on PYE phase. The numbers indicate the compounds listed in the Experimental section. ○, 80% methanol; ●, absolute methanol.

same mobile phase is unprecedented. As seen in Fig. 4, an increase in retention on the PYE phase relative to the C_{18} phase is seen with increase in the rigidity and the extent of interaction with the aromatic stationary phase. The preference by the PYE phase decreases in the following order: aromatic nitro compounds, aromatic hydrocarbons, aliphatic esters, aliphatic alcohols, alkylbenzenes and alicyclic compounds. The scattered plot in Fig. 4 illustrates the large difference in selectivity in the similar k' range in the same mobile phase. The comparison between the two stationary phases in absolute methanol is also shown in Fig. 4. The difference in selectivity is even larger in this mobile phase, and planar PAHs showed a slightly different behaviour to non-planar aromatic compounds. The third point of the versatility of aromatic stationary phases is that a change in the mobile phase causes more variation of retention and selectivity on the PYE phase than on the C_{18} phase. As shown in Table II, a change in the mobile phase from 80% methanol to 80% acetonitrile did not affect the relative retention between pyrene and triphenylmethane on the C_{18} phase, whereas the same change in the mobile phase gave a significant difference in selectivity on the PYE phase. Triptycene, a rigid non-planar aromatic compound, was selectively retained by the PYE phase relative to triphenylmethane, which also has three phenyl rings in its structure. These facts imply that, in addition to the effect of solvents in the stationary phase[1], some other factors that depend on the orientation of aromatic rings of solutes in the stationary phase, such as π–π interaction, are responsible. The magnitude of the solvent effect on k' was strongly dependent on solute structure, providing the sensitivity towards a change of solvents. This can be an advantage, as the greater solvent effect may allow the use of less complicated and less expensive solvents.

There are cases where a very slight change in a particular portion of a chromatogram is desirable. There are other cases, however, where transfer of a group of peaks to another region of the chromatogram to prevent overlap with interfering

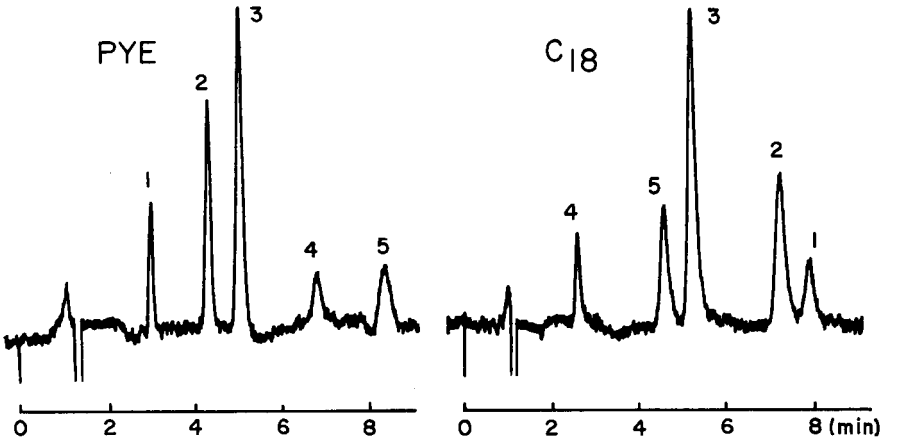

Fig. 5. Chromatograms of *n*-hexane (1), *n*-butylbenzene (2), diphenylmethane (3), 1-nitronaphthalene (4) and triptycene (5) on PYE and C_{18} phases in 80% methanol. Flow-rate: 1 ml/min. Detector sensitivity: ×2 on the R401 RI detector. Column: 10 cm × 4.6 mm I.D.

peaks is needed. Complementary use of the C_{18} and the PYE phases may make this kind of operation possible.

Another interesting point is that a group of compounds with the same carbon skeleton with different functional groups, *e.g.*, C_8H_{18}, $C_8H_{17}OH$ and $C_7H_{15}CO_2CH_3$, were eluted closer to each other on the PYE phase than on the C_{18} phase, making the analysis time shorter. The k' of *n*-octane was nine times greater than that of 1-octanol on the C_{18} phase, but the difference was less than three-fold on the PYE phase in 80% methanol.

In order to understand the difference among the stationary phases in more detail, separation factors generated by changes in solute structure were plotted against the retention increase caused by one additional methylene group derived from *n*-alkanes on each stationary phase in Fig. 6. As a very small specific interaction is expected with a methylene group, the line representing the methylene group increment with the slope of unity follows the contribution of simple solvophobic interaction on these stationary phases. Aromatic stationary phases showed much smaller hydro-

TABLE II

EFFECT OF MOBILE PHASE ON k' VALUES ON C_{18} AND PYE PHASES

Solute	k'					
	C_{18} *phase*			*PYE phase*		
	*I**	*II**	k'_I/k'_{II}	*I**	*II**	k'_I/k'_{II}
n-C_8H_{18}	16.0	12.9	1.24	2.93	1.97	1.49
Pyrene	8.95	4.80	1.86	10.2	3.22	3.17
Triphenylmethane	7.82	4.15	1.88	8.74	3.20	2.73
1-Nitronaphthalene	1.34	1.30	1.03	4.90	1.51	3.25
Triphenylcarbinol	2.46	1.78	1.38	3.24	1.61	2.01
n-$C_{12}H_{25}OH$	9.35	6.26	1.49	3.72	1.57	2.37
n-$C_9H_{19}CO_2CH_3$	7.24	5.66	1.28	4.54	1.82	2.49

* Mobile phases: I, 80% methanol; II, 80% acetonitrile.

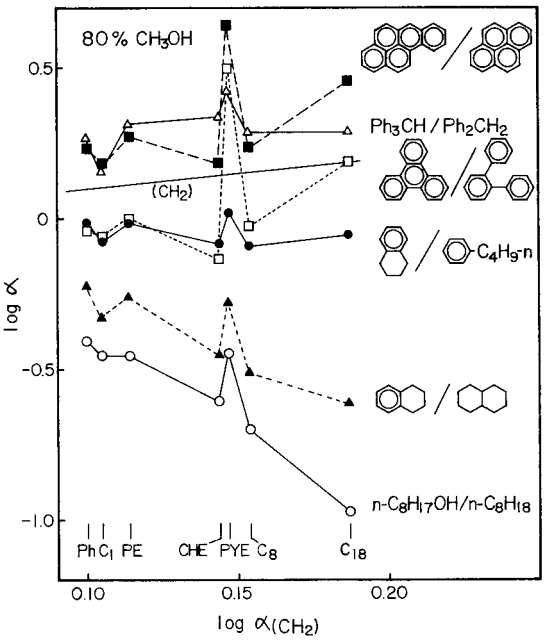

Fig. 6. Plots of separation factors (log α) for the pair of compounds shown on the right against the separation factor caused by one methylene group (log α_{CH_2}) on each stationary phase in 80% methanol.

phobicity than saturated stationary phases having the same carbon numbers. As can be seen in Fig. 6, no other change follows the tendency of the methylene group increment. The measurements were made in the same mobile phase throughout, and therefore the difference was attributed to the stationary phase effects. An increase of one fused aromatic ring from pyrene to 3,4-benzpyrene caused a large increase in retention on the PYE and aromatic stationary phases as well as on the C_{18} phase. A similar tendency was observed for the change from *o*-terphenyl to triphenylene, with an increase in planarity and rigidity. An increase of one phenyl ring in non-planar aromatic compounds, however, produced a relatively small retention increase with the PYE and C_{18} phases, and a large increase on stationary phases with one six-membered ring. Cyclization within a molecule or a change from *n*-butylbenzene to tetrahydronaphthalene caused a decrease in retention on small saturated stationary phases. However, aromatic stationary phases and the C_{18} phase showed a slight upward shift in the plot. This was also the case with aromatization, *i.e.*, a change from decahydronaphthalene to tetrahydronaphthalene, which makes the solute more rigid and planar. Addition of a hydroxyl group produced a smaller retention decrease on aromatic stationary phases than on saturated stationary phases. The conclusion from Fig. 6 is that the C_{18} phase has the characteristics of a planar aromatic stationary phase with respect to selectivity based on steric recognition toward the solutes, only slightly less in magnitude than the PYE phase. This suggests the contribution of the aligned alkyl chains in the C_{18} phase for its preference toward planar solutes.

A test of RPLC stationary phases using a non-polar eluent such as *n*-heptane has been recommended for characterizing chemically bonded phase[14]. Table III shows the k' values obtained in *n*-hexane containing *ca.* 28 ppm of water at 30°C. We

TABLE III

k' VALUES IN *n*-HEXANE (30°C)

The solvent contained *ca.* 28 ppm of water. The elution time of *n*-dodecane was used as t_0.

Solute	*Stationary phase*				
	C_1	C_{18}	*CHE*	*PE*	*PYE*
1-Nitronaphthalene	0.52	0.31	0.11	0.46	2.2
Ethyl benzoate	1.3	0.35	0.14	0.26	0.87
Acetophenone	4.9	2.0	0.80	0.91	6.3
n-$C_{12}H_{25}OH$	~16	2.0	1.5	1.6	6.0
Benzene	0.04	0.04	0.03	0.10	0.06
Pyrene	0.07	0.22	0.06	0.25	0.76
Triphenylene	0.14	0.29	0.04	0.30	1.5
3,4-Benzpyrene	0.15	0.50	0.06	0.34	2.1
Triphenylmethane	0.09	<0.01	0.02	0.20	0.62
Triptycene	0.22	<0.01	0.03	0.25	0.88
Tetraphenylethylene	0.15	<0.01	0.06	0.20	0.88

used a single batch of *n*-hexane and measured the retention after constant k' values were attained with a minimum amount of sample. The magnitude of the k' values for polar compounds gave an estimate of how much silanol groups was left and accessible to the solutes. Although similar reaction conditions were used throughout the bonding reaction and the end capping, considerable differences were found among the five stationary phases. The C_1 phase allows the polar solutes to come close to the silanols easily, as expected. The PYE phase showed considerable retention of polar solutes. Specific retention of aromatic nitro compounds on the PYE phase was seen, as noted in aqueous methanol. Hemetsberger *et al.*[15] proposed the use of this type of interaction in normal-phase chromatography.

The results with aromatic hydrocarbons as solutes gave useful information on the mechanism of retention in RPLC. The C_1 and PE phases showed significant retentions for these aromatic compounds regardless of planarity, probably owing to accessible silanols and π–π interaction in the latter. The CHE phase showed very small retentions for all of the hydrocarbons tested. On the C_{18} phase, considerable retention was seen only for large PAHs. The PYE phase showed significant retention for both types of aromatic compounds, but a preference was seen for the PAHs. This observation is very similar to that in RPLC. The results with the PYE phase are understandable on the basis of the residual silanols and π–π interaction. As the only driving force of retention in the non-polar eluent with the C_{18} phase is the affinity to silanols, supposedly extended C_{18} chains in hexane seem positively to assist the adsorption of PAHs on to the silanols. The location of the PAHs in the C_{18} stationary phase must be close to the bottom of the brush-type structure between the long chains. The common observation of the steric recognition provided by the C_{18} chains in both polar and non-polar mobile phases is indicative of the similar retention scheme under RPLC conditions, as suggested before. The driving force of retention is different, but the steric interaction between the solutes and stationary phases seems to be common. With the PYE phase, the planar PAHs are accomodated in the slots made by pyrenyl groups just like slides in slide trays. The preference of planar compounds over non-polar ones is easily understood. The results with the CHE phase suggest that the non-

planar stationary phase does not have a positive effect on the preferred retention of non-planar aromatic compounds, which was seen in Fig. 3B. The different behavior between PAHs and non-planar aromatic compounds in Fig. 3B was probably due to the fact that non-planar compounds are rejected by the C_{18} phase. Although a significant retention was seen for many compounds in *n*-hexane, the retention is much less in 10% benzene in *n*-hexane, and almost no retention was seen in tetrahydrofuran. Hence the effect of silanols on the retention of these hydrocarbons in RPLC is considered to be very small.

CONCLUSION

The stationary phase effects such as steric recognition and π–π interactions between solutes and stationary phases and the solvent effect were found to be important in determining the retention and selectivity in RPLC, in addition to the solvophobic interaction. Unsaturated compounds were selectively retained by aromatic stationary phases. Rigid solutes were favoured by rigid stationary phases. Planar solutes were preferentially retained under both reversed-phase and normal-phase condition by stationary phases such as C_{18} and PYE, which are assumed to have a planar structure and to accommodate easily planar molecules between the bonded hydrocarbon moieties. It was shown to be possible to control the magnitude of the stationary phase effects by selecting the structure of the stationary phase to make it more sensitive to specific interactions. Stationary phases with a large aromatic functionality were shown to have some merits such as the good retentivity, widely different selectivity from the C_{18} phase and the large solvent effect on retention and selectivity. They can be a good alternative for the C_{18} phase, and the complementary use of such stationary phases with the C_{18} phase will increase the capability of RPLC.

ACKNOWLEDGEMENT

Financial support by a grant from the Ministry of Education is gratefully acknowledged.

REFERENCES

1 N. Tanaka, K. Sakagami and M. Araki, *J. Chromatogr.*, 199 (1980) 327.
2 C. J. Little, A. D. Dale and M. B. Evans, *J. Chromatogr.*, 153 (1978) 543.
3 C. J. Little, A. D. Dale and M. B. Evans, *J. Chromatogr.*, 153 (1978) 381.
4 H. Hemetsberger, P. Behrensmeyer, J. Henning and H. Ricken, *Chromatographia*, 12 (1979) 71.
5 V. Řehák and E. Smolková, *J. Chromatogr.*, 191 (1980) 71.
6 C. Horváth, W. Melander and I. Molnár, *J. Chromatogr.*, 125 (1976) 129.
7 N. Tanaka, H. Goodell and B. L. Karger, *J. Chromatogr.*, 158 (1978) 233.
8 R. M. McCormick and B. L. Karger, *J. Chromatogr.*, 199 (1980) 259.
9 E. Roggendorf and R. Spatz, *J. Chromatogr.*, 204 (1981) 263.
10 J. L. Glajch, J. J. Kirkland, K. M. Squire and J. M. Minor, *J. Chromatogr.*, 199 (1980) 57.
11 G. E. Berendsen and L. de Galan, *J. Liq. Chromatogr.*, 1 (1978) 561.
12 K. J. Williams, A. Li Wan Po and W. J. Irwin, *J. Chromatogr.*, 194 (1980) 217.
13 R. A. Barford, R. McGraw and H. L. Rothbart, *J. Chromatogr.*, 166 (1978) 365.
14 P. Roumeliotis and K. K. Unger, *J. Chromatogr.*, 149 (1978) 211.
15 H. Hemetsberger, H. Klar and H. Ricken, *Chromatographia*, 13 (1980) 277.

Journal of Chromatography, 239 (1982) 773–783
Elsevier Scientific Publishing Company, Amsterdam — Printed in The Netherlands

CHROM. 14,539

SEPARATION AND DETERMINATION OF BILE ACIDS BY HIGH-PERFORMANCE LIQUID CHROMATOGRAPHY USING IMMOBILIZED 3α-HYDROXYSTEROID DEHYDROGENASE AND AN ELECTROCHEMICAL DETECTOR

SATORU KAMADA, MASAKO MAEDA and AKIO TSUJI*
School of Pharmaceutical Sciences, Showa University, 1-5-8, Hatanodai, Shinagawa, Tokyo (Japan)
YOSHIO UMEZAWA
Department of Chemistry, Faculty of Sciences, Tokyo University, 7-3, Hongo, Tokyo (Japan)
and
TATSUO KURAHASHI
Yanagimoto Seisakusho, Fushimi, Kyoto (Japan)

SUMMARY

A high-performance liquid chromatographic method using an immobilized 3α-hydroxysteroid dehydrogenase column and an electrochemical detector was developed for the determination of individual bile acids in serum and bile. Bile acids in the eluate from a Radial-Pak A column reacted with NAD in the enzyme column to generate NADH, which was monitored by a voltammetric detector after mixing with phenazine methosulphate solution. Each bile acid was measurable at the 20 pmole level at the highest sensitivity of the detector. The mean recoveries and reproducibilities of bile acids were 86.7–104.6% [coefficient of variation (C.V.) = 0.3–8.7%] within-assay and 83.8–103.4% (C.V. = 1.6–7.0%) between-assay.

INTRODUCTION

Methods for the simultaneous determination of individual free and conjugated bile acids in serum and bile have usually been based on gas–liquid chromatography[1], gas chromatography–mass spectrometry[2,3], mass fragmentography[4] or thin-layer chromatography[5,6]. In recent years, high-performance liquid chromatography (HPLC)[7–12] has been developed, but the most common bile acids have no ultraviolet light-absorbing properties, which are necessary with the photometric detector of the liquid chromatograph. Therefore, bile acids have to be derivatized before column separation with a UV-absorbing reagent[13–16]. A fluorescence derivatizing reagent, 4-bromomethyl-7-methoxycoumarin[17], has also been used in the fluorescent liquid chromatography of bile acids in order to improve their detectability.

Baba and co-workers[18,19] reported a highly sensitive and selective fluorescence HPLC determination of bile acids and their conjugates using 3α-hydroxysteroid de-

0021-9673/82/0000–0000/$02.75

hydrogenase and cofactor. However, this method consumes considerable amounts of expensive enzyme. Okuyama *et al.*[20] and Arisue *et al.*[21] developed a modified method using an immobilized enzyme column instead of the enzyme solution. Since an electrochemical detector was used in the HPLC analysis of catecholamines by Kissinger *et al.*[22], this novel detector has been widely applied in the HPLC analysis of biological substances. Although this type of detection is more selective than UV detection, non-redox compounds not be detected.

Recently, derivatization to an electrochemically active form was reported by Shimada *et al.*[23] and Ikenoya *et al.*[24]. In this work, we have attempted to develop a method for the determination of bile acids and their conjugates using immobilized 3α-hydroxysteroid dehydrogenase combined with an electrochemical detector.

EXPERIMENTAL

Materials

Cholic acid, chenodeoxycholic acid, deoxycholic acid, ursodeoxycholic acid, lithocholic acid, glycine conjugates and taurine conjugates were purchased from Sigma (U.S.A.), Wako (Japan) and PL Biochemical Co. (U.S.A.), respectively. NAD, NADH, phenazine metosulphate and sodium pyrophosphate were obtained from Wako and 3α-hydroxysteroid dehydrogenase (grade II) from Sigma. Amino glass beads used as the solid phase of the immobilized enzyme were Amino Propyl-CPG 180 Å from Electro-Nucleonics (U.S.A.). PHP-LH-20 was a gift from Professor T. Nambara (Pharmaceutical Institute, Tohoku University, Sendai, Japan).

Reagent solutions

Bile acid stock solutions. Each bile acid was dissolved in methanol and made up to 10 μmol/ml with methanol.

Bile acid mixture solutions. Each mixture of free bile acids, glycine conjugates and taurine conjugates was prepared by mixing the bile acid stock solutions.

NAD solution. A 0.5 m*M* NAD solution was prepared by dissolving NAD in 0.1 *M* pyrophosphate buffer (pH 9.0).

Phenazine methosulphate solution. 1.0 m*M* phenazine methosulphate solution was prepared by dissolving phenazine methosulphate in 0.1 *M* pyrophosphate buffer (pH 7.0).

Immobilized 3α-HSD column. 3α-hydroxysteroid dehydrogenase was coupled to amino glass beads (120–200 mesh) by the glutaraldehyde method[25] and packed in a stainless-steel tube (25 × 4.6 mm I.D.).

Apparatus

The apparatus consisted of a Model LC-3A chromatograph (Shimadzu, Kyoto, Japan), a Waters Radial-Pak A column (10 μm, 5 × 100 mm) (Waters Assoc., Milford, MA, U.S.A.), a Model VMD-101 voltammetric detector (Yanagimoto Seisakusho, Japan), a solvent exchanger (Kyowaseimitsu Co., Japan), a Model KSU-16 reciprocating pump (Kyowaseimitus Co.) and a Model M-4 thermostated water bath (Thermonics Co., Japan).

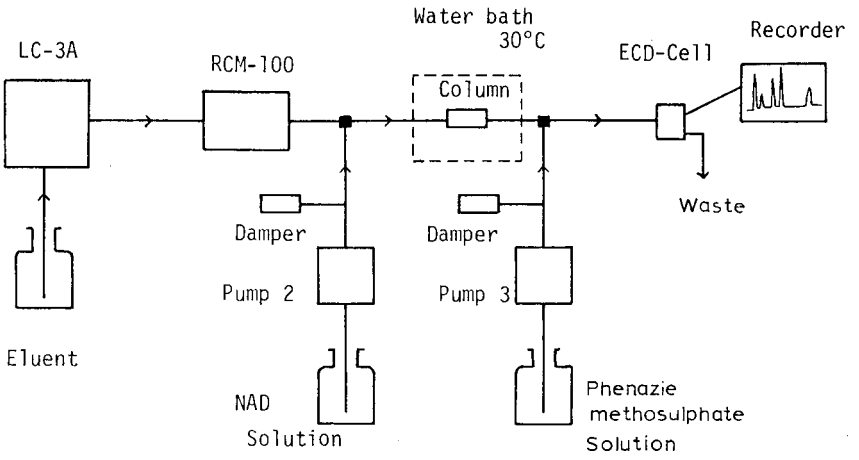

Fig. 1. Flow diagram of the HPLC system.

Chromatographic conditions

The HPLC system shown in Fig. 1 was used. The separation of individual bile acids was carried out on a Radial-Pak A column at room temperature using 0.3% ammonium phosphate (pH 7.3)–acetonitrile–methanol [100:35:15 (A) and 100:45:15 (B)] as the mobile phase at a flow-rate of 1 ml/min. The mobile phase was changed by a solvent exchanger from A to B 4 min after injection of the sample solution. The eluate from the column was mixed with the NAD solution pumped at the rate of 0.64 ml/min just before the enzyme reactor column maintained at 30°C. After the enzyme reaction in column, the eluate was mixed with the phenazine methosulphate solution delivered with a pump at the rate of 0.42 ml/min. The mixture was monitored by using a Model VMD-101 voltammetric detector, the potential of which was set at +0.10 V *vs.* a silver–silver chloride reference electrode.

Assay procedure

Extraction of free and conjugated bile acids from serum. A 0.5-ml serum sample was mixed with 2.5 ml of methanol and ultrasonicated for 15 min. A 1.5-ml volume of the supernatant was transferred into a test-tube and evaporated to dryness under nitrogen. The residue was dissolved in 1.0 ml of 0.05 *M* phosphate buffer (pH 7.0) and applied to a Sep-Pak C_{18} column. After washing the column with 2 ml of 2% methanol, bile acids were eluted with 4 ml of 80% methanol, and evaporated under reduced pressure at 40°C.

Extraction of free and conjugated bile acids from bile. A 20-μl bile sample was diluted with 5.0 ml of 0.05 *M* phosphate buffer (pH 7.0). A 1-ml volume of the diluted bile sample was applied to a Sep-Pak C_{18} column and extracted as described above.

Fractionation of free and conjugated bile acids. The fractionation of bile acids was carried out as described by Goto *et al.*[26]. The bile acids and their conjugates extracted from serum or bile were dissolved in 1 ml of 90% ethanol and applied to a PHP-LH-20 column (13 × 7.5 mm I.D.). After washing the column with 3 ml of 90% ethanol, free acids, glycine conjugates and taurine conjugates were fractioned by stepwise elution with 4-ml volumes of 0.1 *M* acetic acid, 0.2 *M* formic acid and 0.3 *M*

acetic acid–potassium acetate buffer (pH 6.3) in 90% ethanol solution. Each fraction was evaporated to dryness under reduced pressure. In order to remove salts, the taurine fraction was redissolved in 1 ml of water, applied to a Sep-Pak C_{18} column, eluted with 4 ml of 80% methanol and then re-evaporated to dryness under nitrogen.

The residues were dissolved in 50–100 μl of methanol and applied to the HPLC system mentioned above.

RESULTS AND DISCUSSION

Several parameters were examined in order to determine the optimum conditions for the enzymatic reaction of bile acids by using the system without a separation column shown in Fig. 1.

Type of buffer

Various buffers, such as Tris–HCl, phosphate and pyrophosphate, were used for the reaction of 3α-hydroxysteroid dehydrogenase. The pyrophosphate buffer gave the highest response in this system and was therefore used for the following experiments and the assay procedure.

Concentration and pH of buffer

Fig. 2 depicts the peak heights plotted *versus* the concentration and pH of the pyrophosphate buffer. When the concentration of the buffer (pH 9.0) was increased from 0.01 to 0.05 *M*, the peak height reached plateaux at a concentration of buffer of 0.025 *M* and at pH of the buffer of 9.0.

Concentration of phenazine methosulphate and NAD solutions

Oxidation of NADH occurs only at high potentials, which considerably decreases the selectivity of the assay in eluates that contain other electrochemically

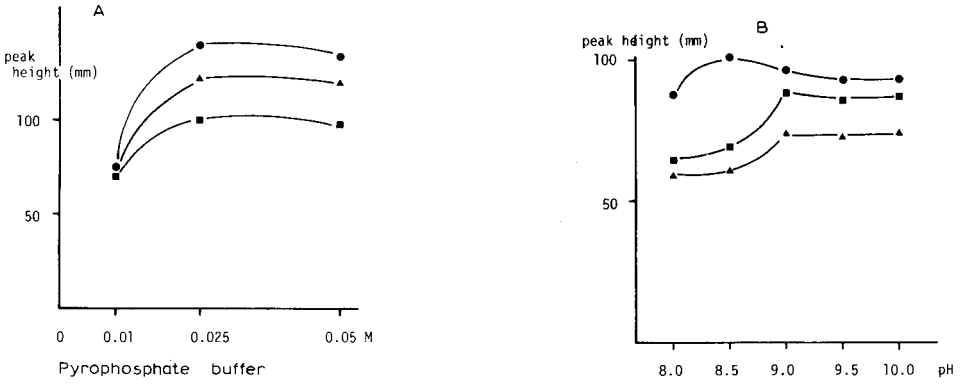

Fig. 2. (A) Peak height of 2-nmol samples of bile acids plotted against concentration of pyrophosphate buffer (pH 9.0). NAD, 0.2 m*M* (1 ml/min); phenazine methosulphate, 1.0 m*M* (0.3 ml/ml); detector potential, +0.1 V, 200 nA full-scale. (B) Peak height of 1-nmol samples of bile acids plotted against the pH of pyrophosphate buffer (0.05 *M*). NAD, 0.1 m*M* (1 ml/min); phenazine methosulphate, 0.5 m*M* (0.3 ml/min); detector potential, +0.32 V, 200 nA full-scale. ●, Cholic acid; ■, taurinecholic acid; ▲, glycinecholic acid.

active compounds. The rate of oxidation of NADH is slow and consequently electro-oxidation of NADH can limit the entire conjugated enzyme reaction process. To eliminate these problems, phenazine methosulphate was used as an electron-transfer intermediate in the enzyme electrode using oxidoreductase[27]. In absence of phenazine methosulphate in the present system, the potential of detector should be set at +0.33 V and the responses of all bile acids were low compared with those obtained by using the phenazine methosulphate solution. Therefore, phenazine methosulphate was used as a mediator for electrochemical regeneration of coenzyme in this system. The sequence of conjugated enzyme reactions occurring at the detection part in the system may be illustrated as follows:

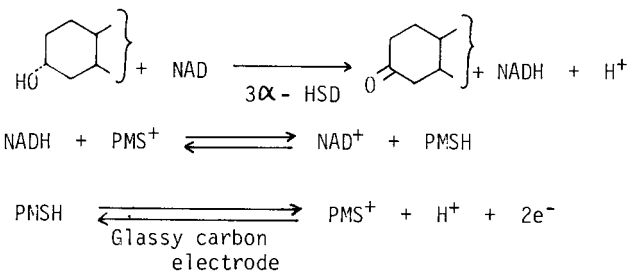

(where PMS = phenazine methosulphate and 3α-HSD = 3α-hydroxysteroid dehydrogenase).

As shown in Fig. 3, the peak height increased with increasing concentration of phenazine methosulphate, whereas the peak height reached a maximum at a concentration of NAD of 0.2 m*M*.

From the above results and the mixing ratio of the reagent to the eluate from

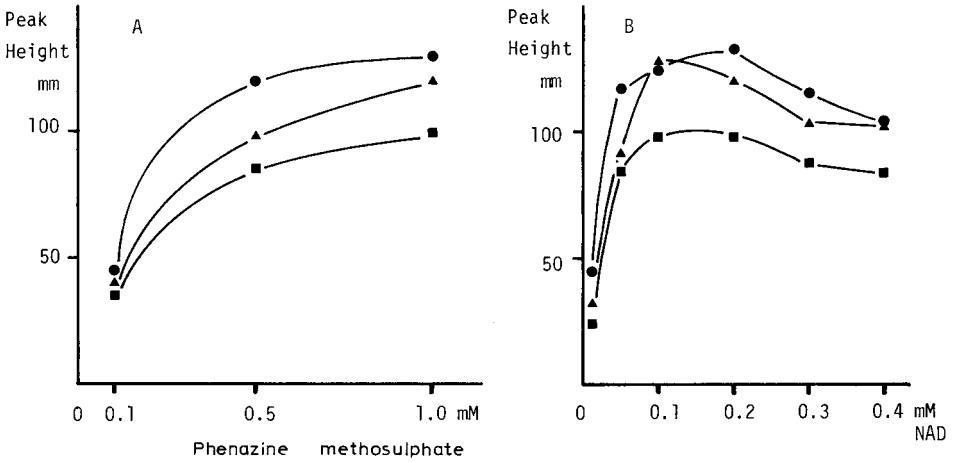

Fig. 3. Effects of phenazine methosulphate and NAD concentration on the enzymatic reaction (0.05 *M* pyrophosphate buffer, pH 9.0). Detector potential, +0.1 V, 100 nA full-scale. (A) 0.2 m*M* NAD (1 ml/min); (B) 1.0 m*M* phenazine methosulphate (0.3 ml/min). ●, Cholic acid; ■, glycinecholic acid; ▲, taurinecholic acid.

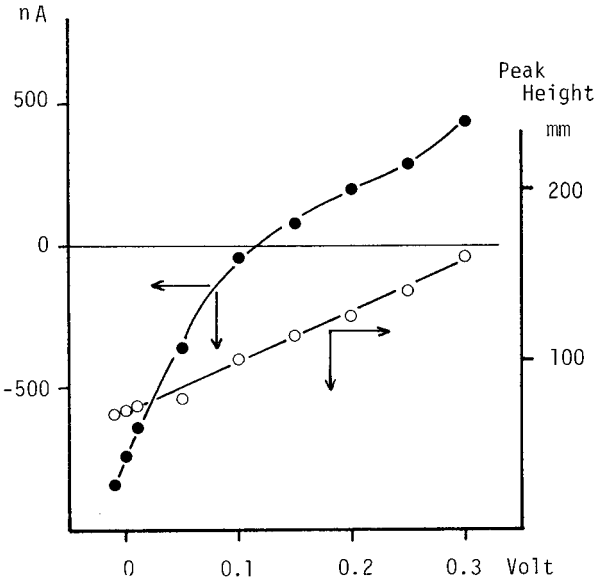

Fig. 4. Background current and peak height *versus* detector potential. NAD, 0.1 m*M* (1 ml/min); phenazine methosulphate, 0.5 m*M* (0.3 ml/min).

the column in the HPLC system, the concentration of phenazine methosulphate, NAD and pyrophosphate buffer were fixed at 1.0 m*M*, 0.5 m*M* and 0.1 *M*, respectively.

Potential of the detector

The peak height and background currents were in the potential range from −0.10 to +0.30 V using NADH solution (2.0 nmol/ml), 0.1 m*M* NAD solution (flow-rate 1 ml/min) and 0.5 m*M* phenazine methosulphate solution (flow-rate 0.3 ml/min). As the potential of the detector increased, the peak height increased and the background current also increased (Fig. 4). Therefore, the potential was fixed at +0.10 V, at which the background current was nearly zero.

Chromatographic separation

Various solvent systems for the separation of bile acids and their conjugates have been reported. In this study, the separation of bile acids should be carried out under nearly neutral conditions because enzymatic reaction was used in the detection system. On the basis of the separation system reported by Goto *et al.*[26], we examined a range of solvent systems using a Waters Radial-Pak A separation column. It was difficult to separate completely ursodeoxycholic acid from cholic acid or chenodeoxycholic acid from deoxycholic acid with 0.3% ammonium phosphate–acetonitrile as the solvent system. Addition of methanol to the above solvent system was effective for the separation of bile acids. Finally, two solvent systems, 0.3% ammonium phosphate (pH 7.3)–acetonitrile–methanol [100:35:15 (A) and 100:45:15 (B)] were found to be suitable for the separation of all of the bile acids in each group (free acids, glycine conjugates and taurine conjugates), but ursodeoxycholic acid and

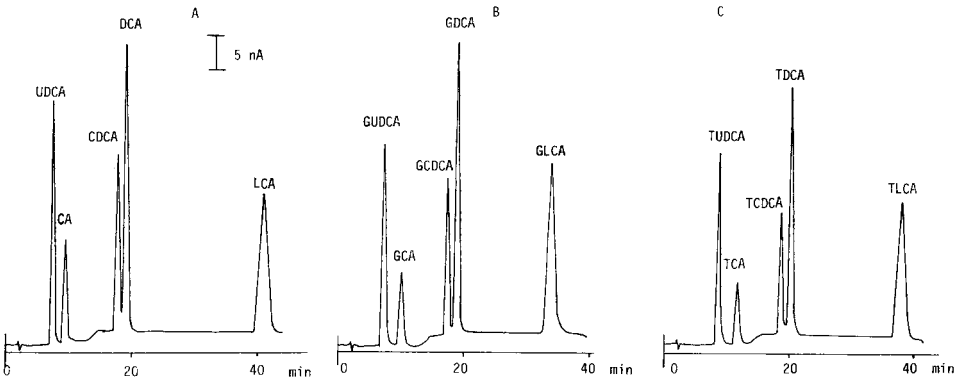

Fig. 5. Typical chromatograms of standard mixture of bile acids (1 nmol). (A) Free bile acids: UDCA = ursodeoxycholic acid, CA = cholic acid, CDCA = chenodeoxycholic acid, DCA = deoxycholic acid, LCA = lithocholic acid; (B) glycine (G) conjugates; (C) taurine (T) conjugates.

chenodeoxycholic acid could not be separated as their conjugates. Therefore, bile acids extracted from serum by Sep-Pak C_{18} were fractionated into three groups by using a PHP-LH-20 column[26] and then each fraction was subjected separately to the HPLC system. Stepwise elution using solvent systems A and B was adopted to shorten the retention times of lithocholic acid, glycinelithocholic acid and taurinelithocholic acid.

Calibration graphs

Typical chromatograms of bile acids and their conjugates obtained by using standard mixtures of free and conjugated bile acids in methanol are shown in Fig. 5. Calibration graphs were constructed from the chromatograms obtained by injecting 2, 4, 6, 8 and 10 μl of the standard mixtures of free bile acids and their conjugates (250 nmol/ml) in methanol.

Typical calibration graphs are shown in Fig. 6. Linearity of the relationship

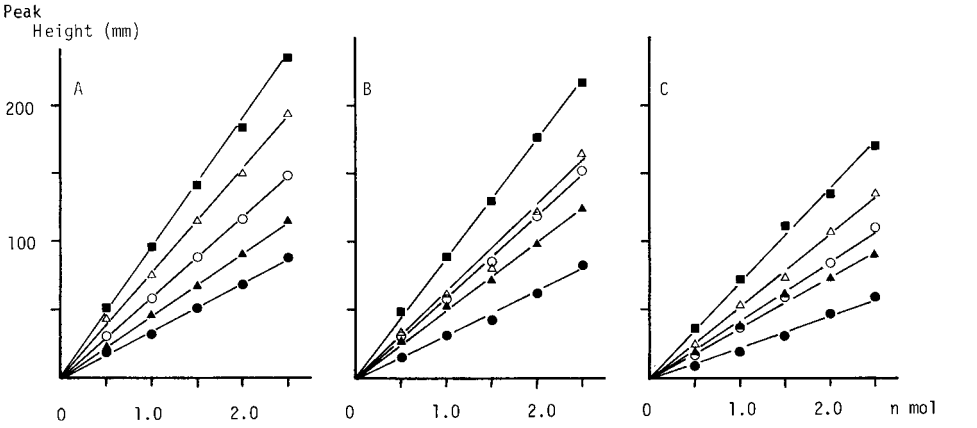

Fig. 6. Calibration graphs for bile acids. (A) Free bile acids; (B) glycine conjugates; (C) taurine conjugates. ●, Cholic acid; ▲, lithocholic acid; ○, chenodeoxycholic acid; △, ursodeoxycholic acid; ■, deoxycholic acid.

TABLE I

RECOVERY AND REPRODUCIBILITY OF INDIVIDUAL BILE ACIDS IN HUMAN SERUM (WITHIN-ASSAY) (n = 5)

Compound	*Added (nmol)*	*Free*		*Glycine*		*Taurine*	
		Mean recovery (%)	*C.V. (%)*	*Mean recovery (%)*	*C.V. (%)*	*Mean recovery (%)*	*C.V. (%)*
Ursodeoxycholic acid	20	104.6	4.8	88.0	2.8	92.9	2.2
	200	102.1	2.9	90.4	1.9	93.6	3.6
Cholic acid	20	94.6	8.7	91.0	7.5	94.4	2.0
	200	98.6	0.3	93.5	1.4	94.9	3.9
Chenodeoxycholic acid	20	99.3	1.5	86.7	6.6	92.6	2.3
	200	90.5	4.8	94.4	1.4	97.9	1.4
Deoxycholic acid	20	99.7	2.4	90.0	4.5	93.0	1.2
	200	98.1	4.6	95.1	2.0	93.4	1.2
Lithocholic acid	20	98.2	2.0	88.5	2.8	88.4	1.8
	200	100.6	3.8	95.5	2.5	97.3	1.1

between peak height and amount of bile acids injected was obtained between 0.5 and 2.5 nmol. The detection limit for bile acids was about 0.2 nmol, depending on the efficiency of the detector and the final volume of sample. The lowest detection limit was 20 pmol, achieved by adjusting the detector sensitivity to 20 nA full-scale.

Recovery and reproducibility

In order to determine the recovery and reproducibility for each bile acid, standard bile acids (20 or 200 nmol) were added to 1.0 ml of human serum and assayed with the HPLC system after extraction and fractionation as described under Experimental. The results are summarized in Tables I and II. The mean recoveries and

TABLE II

RECOVERY AND REPRODUCIBILITY OF INDIVIDUAL BILE ACIDS IN HUMAN SERUM (BETWEEN-ASSAY) (n = 5)

Compound	*Added (nmol)*	*Free*		*Glycine*		*Taurine*	
		Mean recovery (%)	*C.V. (%)*	*Mean recovery (%)*	*C.V. (%)*	*Mean recovery (%)*	*C.V. (%)*
Ursodeoxycholic acid	20	94.7	2.3	96.2	6.7	92.1	3.1
Cholic acid	20	94.2	3.1	98.0	3.1	94.5	3.4
Chenodeoxycholic acid	20	92.1	4.0	103.4	2.7	93.3	5.8
Deoxycholic acid	20	90.9	4.2	95.7	3.0	90.3	3.6
Lithocholic acid	20	92.3	7.0	92.2	1.6	83.8	2.2

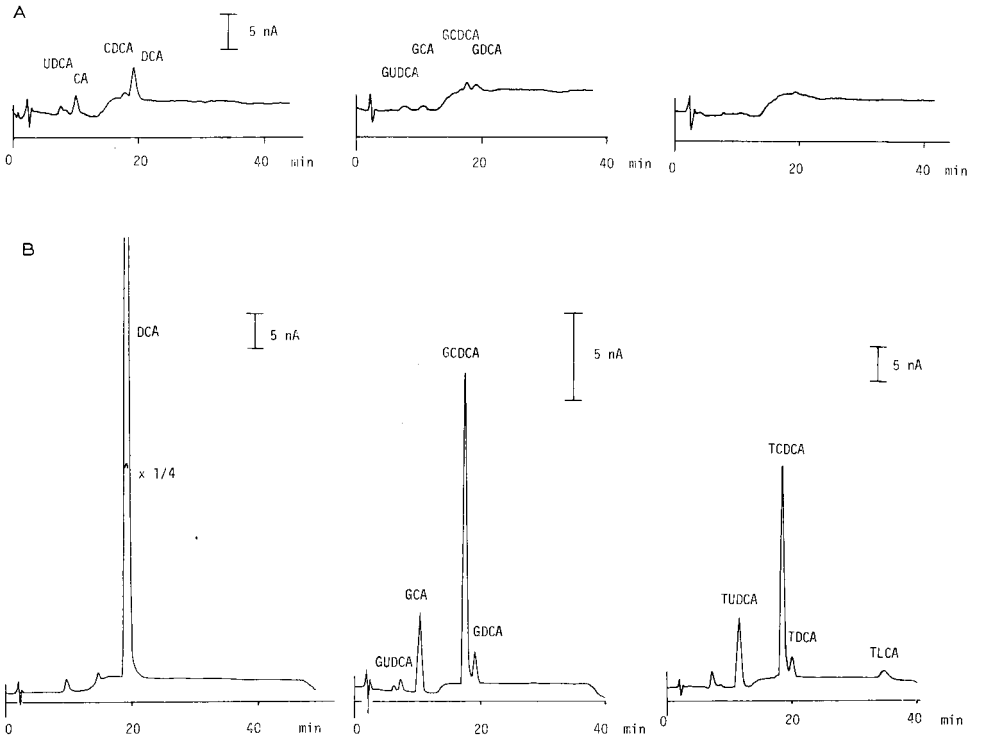

Fig. 7. Typical chromatograms obtained from sera of (A) a normal healthy male and (B) a patient with acute hepatitis. For abbreviations, see Fig. 5.

coefficients of variation, within-assay and between-assay, ranged from 86.7 to 104.6 % [coefficient of variation (C.V.) = 0.3–8.7 %) and from 83.8 to 103.4 % (C.V. = 1.6–7.0 %), respectively.

Application

In order to investigate the applicability of the present method, the simultaneous determination of free and conjugated bile acids in serum and bile was carried out for 11 patients with various diseases and a healthy volunteer. The results are given in Table III and the typical chromatograms of a healthy male and a patient with liver cirrhosis are shown in Fig. 7. Although taurine conjugates, lithocholic acid and glycinelithocholic acid could not be detected in the case of Fig. 7, using 100 μl of serum sample, all other bile acids were detected in normal serum. Characteristic patterns of individual serum bile acids were observed in patients with various diseases. Free, conjugated cholic acid and chenodeoxycholic acid were significally elevated in patients with liver cirrhosis and hepatitis and liver carcinoma. It is also of particular interest that cholic acid, deoxycholic acid and taurinedeoxycholic acid in two breast-cancer patients showed a significant increase compared with normal serum, and a large unknown peak appeared near the peak of taurinedeoxycholic acid in serum of patients with breast cancer and lung cancer. The results suggest that the method may provide more precise information on the meta-

TABLE III

INDIVIDUAL BILE ACIDS IN SERUM AND BILE OF A HEALTHY SUBJECT AND PATIENTS

UDCA = Ursodeoxycholic acid; CA = cholic acid; CDCA = chenodeoxycholic acid; DCA = deoxycholic acid; LCA = lithocholic acid. 0 = No peak observed.

Sample	*Disease*	*Free*					*Glycine*					*Taurine*				
		UDCA	*CA*	*CDCA*	*DCA*	*LCA*	*UDCA*	*CA*	*CDCA*	*DCA*	*LCA*	*UDCA*	*CA*	*CDCA*	*DCA*	*LCA*
Serum*	Normal	0.03	0.08	0.02	0.10	0	0.02	0.02	0.03	0.02	0	0	0	0	0	0
	Hepatitis	0.04	0.55	0.13	0.97	0	0.08	0.18	0.13	0.07	0	0.02	0.55	ND	0.59	0
	Liver cirrhosis	ND***	0.27	ND	6.59	ND	0.07	1.03	1.79	0.13	0	0.01	1.12	1.72	0.08	0.05
	Liver cancer:															
	1	ND	0.13	0.02	0.10	0	0.04	13.30	0.29	13.85	0	ND	0.18	0.39	0.61	0
	2	0	0.07	0.10	0.10	0	0.02	0.36	0.13	0.09	0	ND	0.18	0.11	0.13	ND
	3	0.10	0.39	0.48	0.25	0	0.17	0.27	1.24	0.16	0.03	6.38	1.21	ND	1.79	ND
	Pancreas cancer	0.01	0.26	0	0.50	0	0.02	0.04	0.05	0	0	ND	ND	ND	0.25	0
	Breast cancer:															
	1	0.09	6.13	ND	7.80	0	0.13	2.36	1.69	0.13	0.08	0.09	6.82	4.46	1.79	0
	2	0.03	1.45	ND	1.48	0	0.02	0.09	0.02	0.78	0	ND	UP§	ND	4.62	0
	3	ND	0.52	0.02	0.31	0	0	0	0.05	0.03	0	ND	UP	0	1.39	0
	4	0	0.42	0.04	0.20	0	0.04	0.04	0.25	0.13	0	ND	UP	0.04	4.30	0
	Lung cancer	0	3.77	ND	2.42	0	0.04	0.44	0.05	0.24	0	0.02	UP	0.04	0.36	ND
Bile**	Normal	0.03	0.09	ND	1.18	0.07	1.00	8.71	10.00	7.28	0.66	0.26	5.30	6.49	3.90	0.49

* Serum: μmol/dl.
** Bile: μmol/ml.
*** ND = Non-detectable (peak height < 1 mm).
§ UP = Unknown peak.

bolic profile of bile acids in patients with various diseases, including hepatobiliary diseases.

ACKNOWLEDGEMENTS

The authors are indebted to Professor T. Nambara, Pharmaceutical Institute of Tohoku University, for a gift of PHP-LH-20, and also to Dr. E. Araki, National Central Cancer Hospital, for supplying serum samples from patients. This work was supported in part by a Grant-in-Aid for Scientific Research from the Ministry of Education, Science and Culture of Japan, which is gratefully acknowledged.

REFERENCES

1 P. P. Nair and C. Garcia, *Anal. Biochem.*, 29 (1969) 164.
2 G. Karlaganis and G. Paumgartner, *Clin. Chim. Acta*, 92 (1979) 19.
3 J. Yanagisawa, M. Itoh, M. Ishibashi, H. Miyazaki and F. Nakayama, *Anal. Biochem.*, 104 (1980) 75.
4 M. Shino, Y. Nezu, T. Tateyama, K. Sakaguchi, K. Katayama, J. Tsutsumi and K. Kawabe, *Yakugaku Zasshi*, 99 (1979) 421.
5 A. K. Batta, G. Salen and S. Sarah, *J. Chromatogr.*, 168 (1979) 557.
6 R. W. Shepherd, *Clin. Biochem.*, 11 (1978) 106.
7 K. Shimada, M. Hasegawa, J. Goto and T. Nambara, *J. Chromatogr.*, 152 (1978) 431.
8 H. Kimura, N. Suzuki, T. Sato, J. Goto and T. Nambara, *Japan J. Clin. Chem.*, 81 (1979) 126.
9 J. Goto, M. Hasegawa, H. Kato and T. Nambara, *Clin. Chim. Acta*, 87 (1978) 141.
10 N. Parris, *Anal. Biochem.*, 100 (1979) 260.
11 M. S. Sian and A. J. Harding Ranis, *Clin. Chim. Acta*, 98 (1979) 243.
12 S. Miyazaki, H. Tanaka, R. Horikawa, H. Tsuchiya and K. Imai, *J. Chromatogr.*, 181 (1980) 177.
13 F. Stellaard, D. L. Hachey and P. D. Klein, *Anal. Biochem.*, 87 (1978) 359.
14 B. Shaikh, N. J. Pontzen, J. E. Molina and M. I. Kelsey, *Anal. Biochem.*, 85 (1978) 47.
15 S. Okuyama, D. Uemura and Y. Hirata, *Bull. Chem. Soc. Jap.*, 52 (1979) 124.
16 D. P. Mattees, *Anal. Chim. Acta*, 109 (1979) 161.
17 S. Okuyama, D. Uemura and Y. Hirata, *Chem. Lett.*, (1979) 461.
18 F. Takeda, K. Suminoe, R. Uenoyama, S. Baba and Y. Kameno, *Jap. J. Gastroenterol.*, 76, *Suppl.*, (1979) 610.
19 S. Baba, R. Uenoyama, K. Suminoe, F. Takeda, S. Hasegawa and Y. Kameno, *Kobe J. Med. Sci.*, 26 (1980) 89.
20 S. Okuyama, N. Kokubun, S. Higashidate, D. Uemura and Y. Hirata, *Chem. Lett.*, (1979) 1443.
21 K. Arisue, Z. Ogawa, K. Kohda, C. Hayashi and Y. Ishida, *Jap. J. Clin. Chem.*, 9 (1980) 104.
22 P. T. Kissinger, R. M. Alcorn and L. D. Rart, *Biochem. Med.*, 13 (1975) 299.
23 K. Shimada, M. Tanaka and T. Nambara, *Anal. Lett.*, 13 (1980) 1129.
24 S. Ikenoya, O. Hiroshima, M. Ohmae and K. Kawabe, *Chem. Pharm. Bull*, 28 (1980) 2941.
25 H. H. Weetall, *Methods Enzymol.*, 44 (1976) 104.
26 J. Goto, H. Kato, Y. Saruta and T. Nambara, *J. Liquid Chromatogr.*, 3 (1980) 991.
27 A. Malinuskas and J. Kulys, *Anal. Chim. Acta*, 98 (1978) 31.

Author Index

Ando, T., see Terabe, S. 515
Araki, M., see Tanaka, N. 761
Aue, W. A.
—— and Siu, K. W. M.
Evidence for more than one response mechanism in pulsed electron-capture detectors 127
Ban, Y., see Murata, T. 571
Barkley, R. M., see Wizner, M. A. 145
Barnes, R. M., see Estes, S. A. 181
Barrow, S. E.
——, Waddell, K. A., Ennis, M., Dollery, C. T. and Blair, I. A.
Analysis of picomolar concentrations of 6-oxo-prostaglandin $F_{1\alpha}$ in biological fluids 71
Benecke, I., see König, W. A. 227
Blair, I. A., see Barrow, S. E. 71
Blomberg, L.
——, Buijten, J., Markides, K. and Wännman, T.
Peroxide-initiated *in situ* curing of silicone gums for capillary column gas chromatography 51
Borthwick, J. H., see Brooks, C. J. W. 191
Braselton, Jr. W. E., see Vrbanac, J. J. 265
Brien, J. F., see Nakatsu, K. 97
Brooks, C. J. W.
——, Cole, W. J., Borthwick, J. H. and Brown, G. M.
Characterization of dihydroarenediols and related compounds by gas chromatography–mass spectrometry: Comparison of derivatives 191
Brown, G. M., see Brooks, C. J. W. 191
Buelow, H. J., see Liebich, H. M. 343
Buijten, J., see Blomberg, L. 51
Clement, R. E., see Karasek, F. W. 173
Cole, W. J., see Brooks, C. J. W. 191
Connolly, M. J., see Grimsrud, E. P. 397
Craig, J. C.
——, Gruenke, L. D. and Nguyen, T.-L.
Simultaneous analysis of imipramine and its metabolite desipramine in biological fluids 81
Crispin, T.
—— and Halász, I.
Determination of the pore size distribution, by exclusion chromatography, of ion-exchange polymers which swell in water 351
Curtius, H.-Ch., see Wetzel, E. 107
D'Allura, N. J.
—— and Juvet, Jr., R. S.
Quantitative computer resolution of severely overlapping liquid chromatographic peaks 439
Desiderio, D. M.
—— and Yamada, S.
Measurement of endogenous leucine enkephalin in canine thalamus by high-performance liquid chromatography and field desorption mass spectrometry 87
Dobashi, Y., see Hara, S. 677
Doi, T., see Ôi, N. 493
Dollery, C. T., see Barrow, S. E. 71
Ennis, M., see Barrow, S. E. 71
Eriksson, H., see Tetsuo, M. 287
Estes, S. A.
——, Uden, P. C. and Barnes, R. M.
Plasma emission spectral detection for high-resolution gas chromatographic study of group IV organometallic compounds 181
Fehsenfeld, F. C., see Goldan, P. D. 115
Francke, W., see König, W. A. 227
Fujimoto, C., see Jinno, K. 625
Fukuhara, K., see Matsuki, Y. 585
Furuta, Y., see Miyazaki, H. 277
Ganno, S., see Miyagi, H. 733
Goldan, P. D.
——, Fehsenfeld, F. C. and Phillips, M. P.
Detection of carbon monoxide at ambient levels with an N_2O-sensitized electron-capture detector 115
Goto, J.
——, Goto, N. and Nambara, T.
Separation and determination of naproxen enantiomers in serum by high-performance liquid chromatography 559
Goto, N., see Goto, J. 559
Grimsrud, E. P.
—— and Connolly, M. J.
Spacial distribution of ions and electrons within ^{63}Ni ionization cells 397
Gruenke, L. D., see Craig, J. C. 81
Guillemin, C. L.
Computerized auto-control of on-line processes or laboratory gas and liquid chromatographs 363
Haken, J. K.
—— and Obita, J. A.
Chromatographic analysis of aromatic polyhydrazides, oxalyl arylene polyhydrazides and aromatic poly(amide–hydrazides) after alkali fusion 377
Halász, I., see Crispin, T. 351

Hanai, T.
—— and Hubert, J.
Hydrophobicity and chromatographic behaviour of aromatic acids found in urine 527
——, Tran, K. C. and Hubert, J.
Prediction of retention times for aromatic acids in liquid chromatography 385
Hanaoka, Y.
——, Murayama, T., Muramoto, S., Matsuura, T. and Nanba, A.
Ion chromatography with an ion-exchange membrane suppressor 537
Hara, I.
——, Shiraishi, K. and Okazaki, M.
High-performance liquid chromatography of human serum lipoproteins. Selective detection of triglycerides by enzymatic reaction 549
Hara, S.
——, Dobashi, Y. and Oka, K.
Silica gel liquid–liquid chromatography using aqueous binary phase systems. High-efficiency extraction and resolution of phenols and carboxylic acids 677
——, Kunihiro, K., Yamaguchi, H. and Soczewiński, E.
Ternary solvent system design for liquid–solid chromatography 687
Harvey, D. J.
——, Leuschner, J. T. A. and Paton, W. D. M.
Gas chromatographic and mass spectrometric studies on the metabolism and pharmacokinetics of Δ^1-tetrahydrocannabinol in the rabbit 243
Hasegawa, Y.
——, Kunihara, M. and Maruyama, Y.
Determination of picomole amounts of choline and acetylcholine in blood by gas chromatography–mass spectrometry equipped with a newly improved pyrolyzer 335
Hashimoto, M., see Yamaguchi, T. 609
Hashimoto, Y., see Miyazaki, H. 277
Hine, D. G., see Tanaka, K. 301
Hobo, T., see Watabe, K. 499
Holland, J. F., see Vrbanac, J. J. 265
Horiguchi, M., see Ui, T. 711
Horváth, Cs., see Kalász, H. 423
Hosogane, T., see Ishiguro, S. 651
Hosoi, K., see Murata, T. 571
Huber, R., see Zech, K. 475
Hubert, J., see Hanai, T. 385, 527
Idzu, G., see Miyazaki, H. 277
Ikekawa, N., see Takatsuto, S. 233
Imai, K., see Watanabe, Y. 723
Inda, Y., see Ôi, N. 493
Ingraham, D. F.
——, Shoemaker, C. F. and Jennings, W.
Optimization of liquid phase mixtures 39
Inoue, Y., see Ishiguro, S. 651
Ishibashi, M., see Miyazaki, H. 277, 595
Ishiguro, S.
——, Inoue, Y. and Hosogane, T.
High-speed high-resolution gel permeation chromatography of small molecules and oligomers 651
Ishii, D., see Jinno, K. 625
——, see Takeuchi, T. 633
Ito, T., see Matsuki, Y. 585
Ito, Y., see Matsumoto, I. 747
Itokawa, Y., see Kimura, M. 707
Iwaguchi, K., see Tanaka, N. 761
Jellum, E.
Multi-component analyses of human body fluids and tissues in health and disease using capillary gas chromatography–mass spectrometry and high-resolution two-dimensional electrophoresis 29
Jennings, W., see Ingraham, D. F. 39
Jinno, K.
——, Fujimoto, C. and Ishii, D.
"Buffer memory" technique for the combination of micro-high-performance liquid chromatography and infrared spectrometry 625
Johansson, L.
—— and Vessman, J.
Determination of tocainide in human plasma by gas chromatography with nitrogen-selective detection after Schiff base formation 323
Juvet, Jr., R. S., see D'Allura, N. J. 439
Kalász, H.
—— and Horváth, Cs.
High-performance displacement chromatography of corticosteroids. Scouting for displacer and analysis of the effluent by thin-layer chromatography 423
Kallmayer, R., see Liebich, H. M. 343
Kamada, S.
——, Maeda, M., Tsuji, A., Umezawa, Y. and Kurahashi, T.
Separation and determination of bile acids by high-performance liquid chromatography using immobilized 3α-hydroxysteroid dehydrogenase and an electrochemical detector 773
Kamitake, S., see Miyagi, H. 733
Karasek, F. W.
——, Clement, R. E. and Viau, A. C.
Distribution of PCDDs and other toxic compounds generated on fly ash particulates in municipal incinerators 173
Karmen, A., see Lam, S. 451
Kasahara, Y., see Nimura, N. 671

Kashihira, N.
——, Makino, K., Kirita, K. and Watanabe, Y.
Chemiluminescent nitrogen detector–gas chromatography and its application to measurement of atmospheric ammonia and amines 617
Katori, M., see Miyazaki, H. 595
Kimura, M.
—— and Itokawa, Y.
Determination of blood transketolase by high-performance liquid chromatography (a preliminary note) 707
——, see Matsuki, Y. 585
Kinoshita, T., see Nimura, N. 671
Kirita, K., see Kashihira, N. 617
Kitahara, H., see Ôi, N. 493
Kobayashi, T., see Murayama, W. 643
König, W. A.
——, Francke, W. and Benecke, I.
Gas chromatographic enantiomer separation of chiral alcohols 227
Kojima, K.
——, Manabe, T., Okuyama, T., Tomono, T., Suzuki, T. and Tokunaga, E.
Two-dimensional separation system for analysis of proteins employing isoelectric focusing and high-performance liquid chromatography 565
Kojima, T., see Morishita, F. 483
Kosuge, Y., see Murayama, W. 643
Kováts, E. sz., see Riedo, F. 1
Kronbach, T., see Voelter, W. 475
Kucera, P., see Umagat, H. 463
Kunihara, M., see Hasegawa, Y. 335
Kunihiro, K., see Hara, S. 687
Kurahashi, T., see Kamada, S. 773
Kuriyama, K., see Murata, T. 571
Kurono, H., see Miyazaki, H. 595
Kuster, Th., see Wetzel, E. 107
Lam, S.
—— and Karmen, A.
Resolution of optical isomers of Dns-amino acids by high-performance liquid chromatography with L-histidine and its derivatives in the mobile phase 451
Leuschner, J. T. A., see Harvey, D. J. 243
Liebich, H. M.
——, Buelow, H. J. and Kallmayer, R.
Quantification of endogenous aliphatic alcohols in serum and urine 343
Lin, P. J., see Selim, M. I. 411
Lipsky, S. R.
—— and McMurray, W. J.
Performance of different types of cross-linked methyl polysiloxane stationary phases on fused-silica glass capillary columns 61
McMurray, W. J., see Lipsky, S. R. 61
Maeda, M., see Kamada, S. 773
Makino, K., see Kashihira, N. 617
Manabe, T., see Kojima, K. 565
Markides, K., see Blomberg, L. 51
Marks, G. S., see Nakatsu, K. 97
Maruyama, Y., see Hasegawa, Y. 335
Matsuki, Y.
——, Ito, T., Fukuhara, K., Nakamura, T., Kimura, M., Ono, H. and Nambara, T.
Determination of captopril and its disulphide in biological fluids 585
Matsumoto, I.
——, Ito, Y. and Seno, N.
Preparation of affinity adsorbents with Toyopearl gels 747
Matsuura, T., see Hanaoka, Y. 537
Middleditch, B. S.
Volatile constituents of the produced water effluent from the Buccaneer Gas and Oil Field 159
Mitsunaga, M., see Ui, T. 711
Miura, J., see Miyagi, H. 733
Miyagi, H.
——, Miura, J., Takata, Y., Kamitake, S., Ganno, S. and Yamagata, H.
Analysis of body functions using a clinical liquid chromatograph 733
Miyazaki, H.
——, Ishibashi, M., Hashimoto, Y., Idzu, G. and Furuta, Y.
Simultaneous determination of glyceryl trinitrate and its principal metabolites, 1,2- and 1,3-glyceryl dinitrate, in plasma by gas chromatography–negative ion chemical ionization–selected ion monitoring 277
——, Ishibashi, M., Yamashita, K., Ohguchi, I., Saitoh, H., Kurono, H., Shimono, M. and Katori, M.
Microdetermination of prostaglandins and thromboxane B_2 by gas chromatography using an electron-capture detector 595
Mizutani, T.
—— and Narihara, T.
Adsorption chromatography of proteins on siliconized porous glass 755
Morimoto, Y., see Yamaguchi, T. 609
Morisaki, M., see Takatsuto, S. 233
Morishita, F.
——, Murakita, H., Takemura, Y. and Kojima, T.
Prediction of molecular structures of thiols and sulphides by retention indices 483
Murakita, H., see Morishita, F. 483
Muramoto, S., see Hanaoka, Y. 537

Murata, T.
——, Takahashi, S., Ohnishi, S., Hosoi, K., Nakashima, T., Ban, Y. and Kuriyama, K.
Characterization of bile acid methyl ester acetate derivatives of rat bile using solventless glass capillary gas chromatography and electron impact and ammonia chemical ionization mass spectrometry 571
Murayama, T., see Hanaoka, Y. 537
Murayama, W.
——, Kobayashi, T., Kosuge, Y., Yano, H., Nunogaki, Y. and Nunogaki, K.
A new centrifugal counter-current chromatograph and its application 643
Nakagawa, G., see Tsuda, T. 507
Nakagawa, T.
——, Shibukawa, A. and Uno, T.
Liquid chromatography with crown ether-containing mobile phases. II. Retention behaviour of β-lactam antibiotics in reversed-phase high-performance liquid chromatography 695
Nakamura, T., see Matsuki, Y. 585
Nakashima, T., see Murata, T. 571
Nakatsu, K.
——, Brien, J. F., Taub, H., Racz, W. J. and Marks, G. S.
Gram quantity synthesis and chromatographic assessment of 3,3′,4,4′-tetrachlorobiphenyl 97
Nambara, T., see Goto, J. 559
——, see Matsuki, Y. 585
Nanba, A., see Hanaoka, Y. 537
Narihara, T., see Mizutani, T. 755
Nguyen, T.-L., see Craig, J. C. 81
Nimura, N.
——, Toyama, A., Kasahara, Y. and Kinoshita, T.
Reversed-phase liquid chromatographic resolution of underivatized D,L-amino acids using chiral eluents 671
Nunogaki, K., see Murayama, W. 643
Nunogaki, Y., see Murayama, W. 643
Obita, J. A., see Haken, J. K. 377
Ohguchi, I., see Miyazaki, H. 595
Ohnishi, S., see Murata, T. 571
Ôi, N.
——, Doi, T., Kitahara, H. and Inda, Y.
Gas chromatographic determination of optical isomers of some carboxylic acids and amines with optically active stationary phases 493
Oka, K., see Hara, S. 677
Okazaki, M., see Hara, I. 549
Okuyama, T., see Kojima, K. 565
Ono, H., see Matsuki, Y. 585
Ozaki, E., see Saitoh, K. 661
Parcher, J. F., see Selim, M. I. 411
Paton, W. D. M., see Harvey, D. J. 243
Peoples, A. J., see Pfaffenberger, C. D. 217
Pfaffenberger, C. D.
—— and Peoples, A. J.
Long-term variation study of blood plasma levels of chloroform and related purgeable compounds 217
Phillips, M. P., see Goldan, P. D. 115
Poole, C. F., see Schuette, S. A. 251
Racz, W. J., see Nakatsu, K. 97
Riedo, F.
—— and Kováts, E. sz.
Adsorption from liquid mixtures and liquid chromatography 1
Saitoh, H., see Miyazaki, H. 595
Saitoh, K.
——, Ozaki, E. and Suzuki, N.
Solvent dependence of gel chromatographic retention of low-molecular-weight compounds on polystyrene–divinylbenzene gel 661
Sakai, T.
——, Yanagihara, S. and Ushio, K.
Determination of 5′-nucleotidase activity in human erythrocytes and plasma using high-performance liquid chromatography 717
Schuette, S. A.
—— and Poole, C. F.
Unidimensional, sequential separation of PTH-amino acids by high-performance thin-layer chromatography 251
Sekine, Y., see Yamaguchi, T. 609
Selim, M. I.
——, Parcher, J. F. and Lin, P. J.
Adsorption of polar solutes on liquid-modified supports 411
Seno, N., see Matsumoto, I. 747
Shanfield, H., see Zhou, L. 259
Shibukawa, A., see Nakagawa, T. 695
Shimono, M., see Miyazaki, H. 595
Shiraishi, K., see Hara, I. 549
Shoemaker, C. F., see Ingraham, D. F. 39
Sievers, R. E., see Wizner, M. A. 145
Singhawangcha, S., see Wizner, M. A. 145
Siu, K. W. M., see Aue, W. A. 127
Sjövall, J., see Tetsuo, M. 287
Soczewiński, E., see Hara, S. 687
Suzuki, N., see Saitoh, K. 661
Suzuki, S., see Watabe, K. 499
Suzuki, T., see Kojima, K. 565
Sweeley, C. C., see Vrbanac, J. J. 265
Takahashi, S., see Murata, T. 571
Takata, Y., see Miyagi, H. 733
Takatsuto, S.
——, Ying, B., Morisaki, M. and Ikekawa, N.
Microanalysis of brassinolide and its analogues by gas chromatography and gas chromatography–mass spectrometry 233
Takemura, Y., see Morishita, F. 483

Takeuchi, T.
—— and Ishii, D.
High-back-pressure liquid chromatography. II. Development of a post-column-controlled flow system 633
Tanaka, I., see Tsuda, T. 507
Tanaka, K.
—— and Hine, D. G.
Compolation of gas chromatographic retention indices of 163 metabolically important organic acids, and their use in detection of patients with organic acidurias 301
Tanaka, N.
——, Tokuda, Y., Iwaguchi, K. and Araki, M.
Effect of stationary phase structure on retention and selectivity in reversed-phase liquid chromatography 761
Tanaka, T., see Ui, T. 711
Taub,-H., see Nakatsu, K. 97
Terabe, S.
——, Yamamoto, K. and Ando, T.
Application of the streaming current detector to the analysis of individual bile acids 515
Tetsuo, M.
——, Eriksson, H. and Sjövall, J.
Gas chromatographic–mass spectrometric analysis of endogenous levels of estradiol in plasma and in cytosol from rat uterus 287
Tokuda, Y., see Tanaka, N. 761
Tokunaga, E., see Kojima, K. 565
Tomono, T., see Kojima, K. 565
Toyama, A., see Nimura, N. 671
Tran, K. C., see Hanai, T. 385
Tsuda, T.
——, Tanaka, I. and Nakagawa, G.
Packed microcapillary liquid chromatography with reduced I.D. columns 507
Tsuji, A., see Kamada, S. 773
Uden, P. C., see Estes, S. A. 181
Ui, T.
——, Mitsunaga, M., Tanaka, T. and Horiguchi, M.
Determination of prednisone and prednisolone in human serum by high-performance liquid chromatography—especially on impaired conversion of corticosteroids in patients with chronic liver disease 711
Umagat, H.
——, Kucera, P. and Wen, L.-F.
Total amino acid analysis using pre-column fluorescence derivatization 463
Umezawa, Y., see Kamada, S. 773
Uno, T., see Nakagawa, T. 695
Ushio, K., see Sakai, T. 717
Vessman, J., see Johansson, L. 323
Viau, A. C., see Karasek, F. W. 173
Voelter, W.
——, Kronbach, T., Zech, K. and Huber, R.
A simple high-performance liquid chromatographic pre-column technique for investigation of drug metabolism in biological fluids 475
Vrbanac, J. J.
——, Braselton, Jr., W. E., Holland, J. F. and Sweeley, C. C.
Automated qualitative and quantitative metabolic profiling analysis of urinary steroids by a gas chromatography–mass spectrometry–data system 265
Waddell, K. A., see Barrow, S. E. 71
Wännman, T., see Blomberg, L. 51
Watabe, K.
——, Hobo, T. and Suzuki, S.
Liquid crystals as stationary phases in gas chromatography. V. Adsorption behaviour of aliphatic alcohols and their esters on an electric field liquid crystal column 499
Watanabe, Y.
—— and Imai, K.
Pre-column labelling for high-performance liquid chromatography of amino acids with 7-fluoro-4-nitrobenzo-2-oxa-1,3-diazole and its application to protein hydrolysates 723
——, see Kashihira, N. 617
Wen, L.-F., see Umagat, H. 463
Wetzel, E.
——, Kuster, Th. and Curtius, H.-Ch.
A split system applicable as a gas chromatographic–mass spectrometric interface and as effluent splitter for specific gas chromatographic detectors 107
Wizner, M. A.
——, Singhawangcha, S., Barkley, R. M. and Sievers, R. E.
Selective electron-capture sensitization of water, phenols, amines and aromatic and heterocyclic compounds 145
Yamada, S., see Desiderio, D. M. 87
Yamaguchi, H., see Hara, S. 687
Yamaguchi, T.
——, Morimoto, Y., Sekine, Y., Hashimoto, M.
Determination of β-adrenergic blocking drugs as cyclic boronates by gas chromatography with nitrogen-selective detection 609
Yamagata, Y., see Miyagi, H. 733
Yamamoto, K., see Terabe, S. 515
Yamashita, K., see Miyazaki, H. 595
Yanagihara, S., see Sakai, T. 717
Yano, H., see Murayama, W. 643
Ying, B., see Takatsuto, S. 233
Zech, K., see Kronbach, T. 475

Zhou, L.
——, Shanfield, H. and Zlatkis, A.
Quantitative determination of lecithin and sphingomyelin at nanogram levels by high-performance thin-layer chromatography using fluorescence. Preliminary results 259
Zlatkis, A., see Zhou, L. 259

PUBLICATION SCHEDULE FOR 1982

Journal of Chromatography (incorporating *Chromatographic Reviews*) and *Journal of Chromatography, Biomedical Applications*

MONTH	J	F	M	A	M	J	J	A	S	O	N	D
Journal of Chromatography	234/1 234/2 235/1 235/2	236/1 236/2	237/1 237/2 237/3	238/1 238/2 239	240/1 240/2 241/1	The publication schedule for further issues will be published later.						
Chromatographic Reviews		251/1		251/2								
Biomedical Applications	227/1	227/2	228	229/1	229/2							

INFORMATION FOR AUTHORS

(Detailed *Instructions to Authors* were published in Vol. 209, No. 3, pp. 501-504. A free reprint can be obtained by application to the publisher.)

Types of Contributions. The following types of papers are published in the *Journal of Chromatography* and the section on *Biomedical Applications:* Regular research papers (Full-length papers), Short communications and Notes: Short communications are preliminary announcements of important new developments and will, whenever possible, be published with maximum speed. Notes are usually descriptions of short investigations and reflect the same quality of research as Full-length papers, but should preferably not exceed four printed pages. For review articles, see page 2 of cover under Submission of Papers.

Submission. Every paper must be accompanied by a letter from the senior author, stating that he is submitting the paper for publication in the *Journal of Chromatography*. Please do not send a letter signed by the director of the institute or the professor unless he is one of the authors.

Manuscripts. Manuscripts should be typed in double spacing on consecutively numbered pages of uniform size. The manuscript should be preceded by a sheet of manuscript paper carrying the title of the paper and the name and full postal address of the person to whom the proofs are to be sent. Authors of papers in French or German are requested to supply an English translation of the title of the paper. As a rule, papers should be divided into sections, headed by a caption (*e.g.*, Summary, Introduction, Experimental, Results, Discussion, etc.). All illustrations, photographs, tables, etc., should be on separate sheets.

Introduction. Every paper must have a concise introduction mentioning what has been done before on the topic described, and stating clearly what is new in the paper now submitted.

Summary. Full-length papers and Review articles should have a summary of 50–100 words which clearly and briefly indicates what is new, different and significant. In the case of French or German articles an additional summary in English, headed by an English translation of the title, should also be provided. (Short communications and Notes are published without a summary.)

Illustrations. The figures should be submitted in a form suitable for reproduction, drawn in Indian ink on drawing or tracing paper. Each illustration should have a legend, all the *legends* being typed (with double spacing) together on a *separate sheet*. If structures are given in the text, the original drawings should be supplied. Coloured illustrations are reproduced at the author's expense, the cost being determined by the number of pages and by the number of colours needed. The written permission of the author and publisher must be obtained for the use of any figure already published. Its source must be indicated in the legend.

References. References should be numbered in the order in which they are cited in the text, and listed in numerical sequence on a separate sheet at the end of the article. Please check a recent issue for the lay-out of the reference list. Abbreviations for the titles of journals should follow the system used by *Chemical Abstracts*. Articles not yet published should be given as "in press", "submitted for publication", "in preparation" or "personal communication".

Proofs. One set of proofs will be sent to the author to be carefully checked for printer's errors. Corrections must be restricted to instances in which the proof is at variance with the manuscript. "Extra corrections" will be inserted at the author's expense.

Reprints. Fifty reprints of Full-length papers, Short communications and Notes will be supplied free of charge. Additional reprints can be ordered by the authors. An order form containing price quotations will be sent to the authors together with the proofs of their article.

News. News releases of new products and developments, and information leaflets of meetings should be addressed to: The Editor of the News Section, Journal of Chromatography/Journal of Chromatography, Biomedical Applications, Elsevier Scientific Publishing Company, P.O. Box 330, 1000 AH Amsterdam, The Netherlands.

Advertisements. Advertisement rates are available from the publisher on request. The Editors of the journal accept no responsibility for the contents of the advertisements.